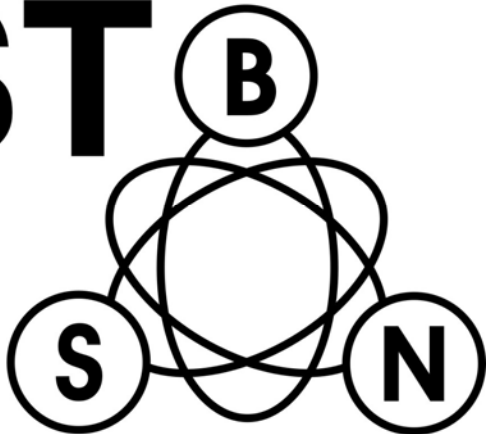


XLVIII INTERNATIONAL SCIENTIFIC CONFERENCE ON  
INFORMATION, COMMUNICATION  
AND ENERGY SYSTEMS AND TECHNOLOGIES

**iCEST**  
**2013**

[www.icestconf.org](http://www.icestconf.org)



26 - 29 June 2013, Ohrid, Macedonia



Proceedings of Papers

---

---

VOLUME 2

---

---

Bitola, 2013

**XLVIII INTERNATIONAL SCIENTIFIC CONFERENCE ON INFORMATION,  
COMMUNICATION AND ENERGY SYSTEMS AND TECHNOLOGIES**

**- ICEST 2013 -**

**Proceedings of Papers - Volume 2 of 2 volumes**

**Editor:** Prof.Dr. Cvetko Mitrovski

**Technical Editor:** Jove Pargovski

**Published by:** Faculty of Technical Sciences - Bitola

**Printed by:** OFFICE 1 - BITOLA

**Print run:** 50

**ISBN:** 978-9989-786-89-1

CIP - Каталогизација во публикација

Национална и универзитетска библиотека "Св. Климент Охридски", Скопје

004(062)

620.9(062)

621.3(062)

XLV International Scientific Conference on Information,  
Communication and Energy Systems and Technologies (45 ; 2010 ; Ohrid)

ICEST 2013 : proceedings of papers / XLVIII International  
Scientific Conference on information, communication and energy  
systems and technologies, 26-29 Juni, Ohrid, Macedonia ; [editor  
Cvetko Mitrovski]. - Bitola : Faculty of Technical Sciences, 2013. -  
2 св. (862 стр.) : илустр. ; 30 см

Фусноти кон текстот. - Библиографија кон трудовите. - Регистри

ISBN 978-9989-786-90-7 (вол. И)

ISBN 978-9989-786-89-1 (вол. ИИ)

1. Mitrovski, Cvetko [уредник]

а) Информатика - Собира б) Енергетика - Собира в) Електротехника -  
Собира

COBISS.MK-ID 94746890

---

# TABLE OF CONTENTS

---

---

## VOLUME 1

---

<b>PLENARY SESSION - Paraconsistent Annotated Logic Program and its Application to Intelligent Control .....</b>	<b>23</b>
Kazumi Nakamatsu	

### Radio Communications, Microwaves, Antennas

<b>1.Investigation of Second and Third Order Distortions Influence in the CATV/HFC .....</b>	<b>33</b>
Oleg Panagiev	
<b>2.Experimental study on availability of FSO system under a heavy snowfall .....</b>	<b>37</b>
Nikolay Kolev and Tsvetan Mitsev	
<b>3.Design of Cross Coupled Meander Folded Hairpin Resonator Filters .....</b>	<b>41</b>
Marin Nedelchev	
<b>4.For certain problems with DVB-T reception.....</b>	<b>45</b>
Oleg Panagiev	
<b>5.Comparative Performance Studies of Laboratory WPA IEEE 802.11b,g Point-to-Multipoint Links .....</b>	<b>49</b>
José A. R. Pacheco de Carvalho, Cláudia F. F. P. Ribeiro Pacheco, Hugo Veiga, António D. Reis	
<b>6.Two-way Doherty amplifier – asymmetry analysis and linearization.....</b>	<b>53</b>
Aleksandar Atanasković, Kurt Blau, Nataša Maleš-Ilić, Aleksandra Đorić	
<b>7.Environmental wireless sensor node .....</b>	<b>57</b>
Vladimir Smiljaković, Siniša Randić, Uroš Pešović	
<b>8.Effectiveness of Reed-Solomon and Convolutional Codes used in Digital Video Broadcasting....</b>	<b>61</b>
Lidia Jordanova, Lyubomir Laskov and Dobri Dobrev	
<b>9.Linearization of microwave power amplifier for broadband applications.....</b>	<b>65</b>
Aleksandra Đorić, Aleksandar Atanasković, Nataša Maleš-Ilić, Bratislav Milovanović	
<b>10.Modelling of a Coaxially Loaded Probe-Coupled Cylindrical Cavity using the Cylindrical TLM Method.....</b>	<b>69</b>
Tijana Dimitrijević, Jugoslav Joković, Bratislav Milovanović	
<b>11.Analysis of Electromagnetic Emissions from Printed Circuit Board in Enclosure Using TLM Method.....</b>	<b>73</b>
Jugoslav Joković, Nebojša Dončov and Tijana Dimitrijević	

### Telecommunication Systems and Technology

<b>1.The level crossing rate of the ratio of product of two k-<math>\mu</math> random variables and k-<math>\mu</math> random variable .....</b>	<b>79</b>
Časlav Stefanović, Danijel Đošić, Dušan Stefanović, Miloš Perić, Mihajlo Stefanović, Srđan Maričić	
<b>2.Second order statistics of MRC receiver over <math>\alpha</math>-<math>\mu</math> multipath fading channels .....</b>	<b>83</b>
Danijel Đošić, Časlav Stefanović, Stefan Panić, Nataša Kontrec, Petar Spalević, Negovan Stamenković	
<b>3.Development of Mobile Backhaul and Transport Demands .....</b>	<b>87</b>
Maja Kukulovska and Liljana Gavrilovska	

<b>4.Active Time-slot Extension in Wireless Sensor Networks.....</b>	<b>91</b>
Mirko Kosanovic, Mile Stojcev	
<b>5.Modeling and Analyzing LTE Networks with EstiNet Network Simulator and Emulator.....</b>	<b>95</b>
Stojan Kitanov and Toni Janevski	
<b>6.BER Performance of IM/DD FSO System with PIN Photodiode Receiver over Gamma-Gamma Atmospheric Turbulence Channel.....</b>	<b>99</b>
Milica Petković, Nemanja Zdravković, Bata Vasić and Goran Đorđević	
<b>7.Preemptive and Non-preemptive Service of IoT Traffic Flows .....</b>	<b>103</b>
Dimitar Atamian and Boris Tsankov	
<b>8.Carrier Frequency Offset Problem Solving in the OFDM/MDPSK System .....</b>	<b>107</b>
Slavimir Stošović, Nenad Milošević, Bojan Dimitrijević and Zorica Nikolić	
<b>9.Overview of current trends in IPTV related FP7 projects.....</b>	<b>111</b>
Biljana Veselinovska, Marjan Gusev, Toni Janevski	

## Signal Processing

<b>1.Dynamic compensation of the gyroscope bias offset .....</b>	<b>117</b>
Rosen Miletiev, Radostin Kenov, Ivaylo Simeonov, Emil Iontchev	
<b>2.Simulation of Codec for Adaptive Delta Modulation .....</b>	<b>121</b>
Rumen Mironov	
<b>3.Omnidirectional Sound Sources for Usage in a Small Anechoic Chamber .....</b>	<b>125</b>
Dejan Ćirić, Marko Janković and Aleksandar Pantić	
<b>4.Practical realization and analysis of shotgun microphone prototype .....</b>	<b>129</b>
Marko Janković, Dejan Ćirić and Marko Stamenković	
<b>5.EEG Sleep Spindles Identification Using Empirical Mode Decomposition and Morphological Operations .....</b>	<b>133</b>
Yuliyan Velchev, Deyan Milev and Kalin Dimitrov	
<b>6.A Wavelet Based Approach for K-complexes Identification for Automated EEG Sleep Staging</b>	<b>137</b>
Deyan Milev, Yuliyan Velchev and Kalin Dimitrov	
<b>7.Inharmonicity of Two-Tones In Contra Octave of Upright Piano .....</b>	<b>141</b>
Zoran Milivojević, Milena Rajković and Dragan Milosavljević	
<b>8.Tempo Map Retrieval from the MIDI Clock Stream .....</b>	<b>145</b>
Lutshayzar Gueorguieff and Peter Antonov	
<b>9.Customization of software for sound insulation prediction in buildings to national legislations – Case study: Slovenia .....</b>	<b>149</b>
Draško Mašović, Nikola Arsić, Dragana Šumarac Pavlović and Miomir Mijić	
<b>10.The influence of less available physical parameters on the sound insulation calculation according to EN 12354.....</b>	<b>153</b>
Draško Mašović, Dragana Šumarac Pavlović and Miomir Mijić	

## Digital Image Processing

<b>1.Content-Based Facial Image Retrieval Using SIFT Descriptor with Reduced Number of Matched Keypoints.....</b>	<b>159</b>
Nikolay Neshov	
<b>2.Text Extraction from Complex Background Images.....</b>	<b>161</b>
Nikolay Neshov, Ivo Draganov, Darko Brodić	
<b>3.Estimination of the Global and Local Text Skew in the Old Printed Documents .....</b>	<b>165</b>
Darko Brodić, Ivo Draganov, Dragan Milivojević, Viša Tasić	

<b>4.New and advantageous approach for lossless compression of computer tomography image sequences .....</b>	<b>169</b>
Peter Ivanov, Agata Manolova, Roumen Kountchev	

## Computer Systems and Internet Technologies

<b>1.Comparison of Open Source Cloud Platforms.....</b>	<b>175</b>
Aleksandar Donevski, Sasko Ristov and Marjan Gusev	
<b>2.Interactive Environment for Solving Multiple Objective Programming Problems GENS-IM ....</b>	<b>179</b>
Leonid Kirilov, Krasimira Genova, Vassil Guliashki and Peter Zhivkov	
<b>3.Managing Risk In Transmission System With Implemented Service Oriented Arhitecture .....</b>	<b>183</b>
Nevenka Kiteva Rogleva, Vladimir Trajkovik, Vangel Fustik, Atanas Iliev and Dimitar Dimitrov	
<b>4.Performance Analysis of Different Queuing Scheduling Disciplines for Internet Applications ...</b>	<b>187</b>
Sarhan M. Musa, Mahamadou Tembely, Matthew N. O. Sadiku, and J. D. Oliver	
<b>5.A study of open source PKI systems applicable into INDECT project.....</b>	<b>191</b>
Nikolai Stoianov and Emil Altimirski	
<b>6.Implementation of the Objects Queue of 20 elements for the File Cabinet Memory Method .....</b>	<b>195</b>
Vladimir Stankovic and Kristina Stanisavljevic	
<b>7.Implementation of Parallel LFSR for BIST .....</b>	<b>199</b>
M. K. Stojčev, I. Ž. Milovanović, E. I. Milovanović, T. R. Nikolić	
<b>8.Improving performance of geospatial data processing using OpenMP .....</b>	<b>203</b>
Natalija Stojanović, Dragan Stojanović	
<b>9.Acquiring Performability Metrics of e-Commerce Systems .....</b>	<b>207</b>
Pece Mitrevski and Ilija Hristoski	
<b>10.Web Services Performance on Commercial Virtual Environment (VMware ESX).....</b>	<b>211</b>
Goran Velkoski, Sasko Ristov and Marjan Gusev	
<b>11.Using Petri Nets to Capture Search Behavior Patterns in the Context of Query Reformulation .....</b>	<b>215</b>
Vesna Gega and Pece Mitrevski	
<b>12.Dataflow Computing: Trend in HPC.....</b>	<b>219</b>
Nenad Anchev, Blagoj Atanasovski, Sasko Ristov and Marjan Gusev	
<b>13.QoS Routing Models in Mobile Applications that Implement Ad-Hoc Networking.....</b>	<b>223</b>
Trajche Kocev, Pece Mitrevski and Tome Dimovski	
<b>14.Cloud Solutions for Bug Reporting .....</b>	<b>227</b>
Pano Gushev, Ana Guseva, Sasko Ristov and Marjan Gusev	
<b>15.Optimization of DC/AC inverter driving.....</b>	<b>231</b>
Goran Nikolić, Tatjana Nikolić, Branislav Petrović and Mile Stojčev	
<b>16.A 900 MHz Self-Tunable Narrowband Low-Noise Amplifier.....</b>	<b>235</b>
Goran Jovanovic, Darko Mitić, Mile Stojcev and Tatjana Nikolic	

## Informatics and Computer Science

<b>1.Evaluation of smartphone capabilities for efficient physical activity recognition.....</b>	<b>241</b>
Nikola Jajac, Bratislav Predic and Dragan Stojanovic	
<b>2.A Method for Estimation Camera Georeference in GIS-based Video Surveillance .....</b>	<b>245</b>
Aleksandar Milosavljević, Dejan Rančić and Aleksandar Dimitrijević	
<b>3.Computation of Best Fixed Polarity Reed-Muller Transform on Multicore CPU Platform.....</b>	<b>249</b>
Miloš Radmanović	
<b>4.Hybrid Evolutionary Algorithm for Integer Multiple-Objective Optimization Problems.....</b>	<b>253</b>
Vassil Guliashki, Krasimira Genova, Leoneed Kirilov	

<b>5.Reasoning-enabled Semantic E-Learning Approach.....</b>	<b>257</b>
Martin Jovanović and Dejan Todosijević	
<b>6.Efficient Parallel Computation of the Galois Field Expressions for Ternary Logic Functions ....</b>	<b>261</b>
Dušan Gajić and Radomir Stanković	
<b>7.Calculation and Visualization of Electromagnetic Field Strength Estimate using Real Terrain Model .....</b>	<b>265</b>
Vladan Mihajlović, Marko Kovačević, Aleksandar Milosavljević and Dejan Rančić	
<b>8.Solving Kakuro puzzle – comparison of deterministic approaches.....</b>	<b>269</b>
Stojanche Panov and Saso Koceski	
<b>9.Cache Misses Challenge to Modern Processor Architectures.....</b>	<b>273</b>
Milco Prisaganec and Pece Mitrevski	
<b>10.Machine Learning Based Classification of Multitenant Configurations in the Cloud.....</b>	<b>277</b>
Monika Simjanoska, Goran Velkoski, Sasko Ristov and Marjan Gusev	
<b>11.Buffer Management in High-performance Routers.....</b>	<b>281</b>
Dragi Kimovski and Atanas Hristov	

## Electronics

<b>1.VHDL-AMS Description of Digitally Programmable Gain Amplifiers through SPI .....</b>	<b>287</b>
Marieta Kovacheva and Ivailo Pandiev	
<b>2.Concurrent X-fault simulator – problems and decision .....</b>	<b>291</b>
Pavlinka Radoyska and Kamen Fillyov	
<b>3. Design of GPS-based Wild Animal's Tracking System with Reduced Size and Weight .....</b>	<b>295</b>
Eltimir Stoimenov, Tsvetan Shoshkov, Rosen Miletiev, Ivailo Pandiev	
<b>4.Finite Element Analysis for Multiconductor in Non-Homogenous Multilayered Dielectric Media .....</b>	<b>299</b>
Sarhan M. Musa, Matthew N. O. Sadiku, and J. D. Oliver	
<b>5.Computer-Aided Parameter Extraction of Behavioral RF Inductor Models.....</b>	<b>303</b>
Elissaveta Gadjeva	
<b>6.Effectiveness of the Verilog-A Noise Macromodel of Current Feedback Operational Amplifier</b>	<b>307</b>
Georgi Valkov and Elissaveta Gadjeva	

## Energy Systems and Efficiency

<b>1.Optimal experiment for determination of the thermo physical properties on materials with low thermal conductivity .....</b>	<b>313</b>
Zore Angelevski, Cvete Dimitrieska, Silvana Angelevska and Ivo Kuzmanov	
<b>2.Daily Optimal Operation of Cascade Hydro Power Plants With Small Storage Capacities .....</b>	<b>317</b>
Anton Causevski and Sofija Nikolova-Poceva	
<b>3.Distributed Renewable Energy and Conviviality.....</b>	<b>321</b>
Aleksandar Malecic	
<b>4.Probabilistic Assessment of the Impact of Renewable Energy Sources on the Power Flows of Medium Voltage Grids .....</b>	<b>325</b>
Nikolay Nikolaev	
<b>5.Optimal Modules Deployment in Large-Scale Photovoltaic Plants.....</b>	<b>329</b>
Dimitar Dimitrov, Atanas Iliev and Nevenka Kiteva Rogleva	
<b>6.Benefits of 6 kV Smart Grid Implementation in Open Cast Coal Mine Suvodol - REK Bitola....</b>	<b>333</b>
Ljupco Trpezanovski and Jove Gjorgijovski	
<b>7.Analysis of the Grounding System of the Thermal Power Plant Oslomej .....</b>	<b>337</b>
Nikolce Acevski, Elena Stojkoska	

<b>8.The State of Renewable Electricity – Worldwide, in EU and in R.Macedonia.....</b>	<b>341</b>
Gordana Janevska	

## Control Systems

<b>1.Analyzing the number and the nature of the injuries in a industrial system from Bitola, R. Macedonia .....</b>	<b>347</b>
Ivo Kuzmanov, Silvana Angelevska and Zore Angelevski	
<b>2.Trajectory Tracking Control for the Slew Motion of a Dragline Excavator .....</b>	<b>351</b>
Rosen Mitrev and Plamen Petrov	
<b>3.Global path planning algorithm for mobile robots .....</b>	<b>355</b>
Stojanche Panov and Saso Koceski	
<b>4.Efficient RF voltage transformer with bandpass filter characteristics .....</b>	<b>359</b>
M.Moreira, J.Bjurström, I.Katardjiev and V.Yantchev	
<b>5.Dynamic Models for Induction Motor Drives for Heavy Duty Regimes.....</b>	<b>361</b>
Dragan Vidanovski and Slobodan Mirčevski	

## Measurement Science and Technology

<b>1.Investigation of Memory Effect by Measurement of Time Delay of Electrical Breakdown in Commercial Gas-filled Surge Arresters.....</b>	<b>367</b>
Momčilo Pejović, Nikola Nešić, Milić Pejović and Nataša Bogdanović	
<b>2.Smart sensor network for ergonomic evaluation of working environment .....</b>	<b>371</b>
Teodora Trifonova, Valentina Markova, Ventseslav Draganov, Krasimira Angelova and Vasil Dimitrov	
<b>3.Measurements and Test Performance for Integrated Digital Loop Carrier for White Noise Impairment with Fast Mode .....</b>	<b>375</b>
Sarhan M. Musa, Mohammed A. Shayib, Matthew N. O. Sadiku and J. D. Oliver	
<b>4.Testing Procedure applied to Virtual Instrument for Analysis of the Power Quality Disturbances.....</b>	<b>379</b>
Milan Simić, Dragan Živanović, Dragan Denić and Goran Miljković	
<b>5.Improved Pseudorandom Absolute Position Encoder.....</b>	<b>383</b>
Goran Miljković, Dragan Denić, Milan Simić, Aleksandar Jocić, Jelena Lukić	

## Engineering Education

<b>1.Trends in Increasing the Channel Capacity of FSO Systems .....</b>	<b>389</b>
Yordan Kovachev and Tsvetan Mitsev	
<b>2.A New Curriculum Design for an Engineer-Constructor Study Program .....</b>	<b>393</b>
Tale Geramitcioski, Cvetanka Mitrevska, Vangelce Mitrevski and Pece Mitrevski	

## Poster 1 - Radio Communications, Microwaves, Antennas

<b>1.Topologies of Wireless Sensor Networks .....</b>	<b>399</b>
Zlatan Ganev	
<b>2.QWS Surge Protectors Testing Using Random High-Voltage Pulses Modeling .....</b>	<b>403</b>
Kliment Angelov and Miroslav Gechev	
<b>3.Impact of Laser Beam Divergence on Power Design of Free Space Optics Communication Systems .....</b>	<b>407</b>
Boncho Bonev	

<b>4.Methods of Coordinates Determination in Wireless Sensor Networks .....</b>	<b>409</b>
Zlatan Ganev	
<b>5.Statistical study of dispersion properties of the CATV reverse channel.....</b>	<b>413</b>
Ilia Iliev and Marin Nedelchev	
<b>6.System for monitoring and management of energy efficiency in public buildings .....</b>	<b>417</b>
Emil Altimirski, Nicola Kaloyanov, Plamen Vichev, Veselin Plamenov	
<b>7.Methods for Determination of Coordinates in Two-Dimensional Navigation System by Measuring the Delay of the Signal.....</b>	<b>421</b>
Emil Altimirski, Petko Simeonov	
<b>8.Efficient Neural Model for Estimation of the Microwave Antenna Noise Temperature.....</b>	<b>425</b>
Ivan Milovanovic, Zoran Stankovic, Marija Agatonovic and Marija Milijic	
<b>9.2D DOA Estimation of Two Coherent Sources based on RBF Neural Networks .....</b>	<b>429</b>
Marija Agatonovic, Zoran Stankovic, Bratislav Milovanovic, Ivan Milovanovic and Nebojsa Doncov	
<b>10.Statistical analysis of multiple reflections in single mode waveguides .....</b>	<b>433</b>
András Fehér and Szilvia Nagy	
<b>AUTHOR INDEX .....</b>	<b>437</b>

## VOLUME 2

### Poster 2 - Telecommunications Systems and Technology

<b>1.Investigate common work of IP software phone systems and PSTN equipment.....</b>	<b>455</b>
Todorka Georgieva and Borislav Necov	
<b>2.Integration of optical and wireless networks under the Radio-over-Fiber concept.....</b>	<b>459</b>
Suzana Miladic	
<b>3.Optical Line Terminal Process modeling.....</b>	<b>463</b>
Stela Kostadinova and Rozalina Dimova	
<b>4.Development of algorithm and simulation program for audio and video information quality estimation in multimedia systems.....</b>	<b>467</b>
Kalina Peeva, Aleksander Bekiarski and Snejana Pleshkova	
<b>5.Comparative Analysis of Modern Wireless Communication Systems Relevant to Smart Metering .....</b>	<b>471</b>
Mariana Shotova, Georgi Nikolov and Vencislav Valchev	
<b>6.Mobile Wireless Sensor Networks Localization .....</b>	<b>475</b>
Vasil Dimitrov, Rozalina Dimova and Teodora Trifonova	
<b>7.Laboratory SCADA – System for Control on Railway Traffic.....</b>	<b>479</b>
Emiliya Dimitrova	
<b>8.Channel Capacity of Dual SC Diversity System Based on Desired Signal Decision Algorithm in Microcell.....</b>	<b>483</b>
Aleksandra Panajotović, Mihajlo Stefanović, Dragan Drača and Nikola Sekulović	
<b>9.Simulation of Effects of Group Velocity Dispersion on Gaussian Pulse Propagation through Optical Fiber .....</b>	<b>487</b>
Petar Spalević, Branimir Jakšić, Aleksandar Marković, Zoran Todorović and Vladislav Simić	
<b>10.Algorithm for modular exponentiation in public key cryptosystems .....</b>	<b>491</b>
Plamen Stoianov	
<b>11.Energy Efficient Add/Drop Approach for Heterogeneous Networks.....</b>	<b>495</b>
Oleg Asenov, Pavlina Koleva, Vladimir Poukov	

## Poster 3 - Signal Processing

<b>1.A Variational Approach of Optimization the Signal Form in the Radio Communication Systems .....</b>	<b>501</b>
Galina Cherneva, Elena Dimkina	
<b>2.Synchronization in Radio Communication Systems with Pseudo Random Restructuring Operation.....</b>	<b>503</b>
Antonio Andonov and Filip Iliev	
<b>3.The Reduction of Rotating Element Noise Using Active Noise Control.....</b>	<b>505</b>
Zoran Milivojević and Violeta Stojanović	
<b>4.Investigation of second-order digital filter structures having low sensitivity to parasitic effects.</b>	<b>509</b>
Maria Nenova	

## Poster 4 - Computer Systems and Internet Technologies

<b>1.A Methodology of Developing Interoperable Electronic Business in the Transport Sector.....</b>	<b>515</b>
Sladana Janković, Snežana Mladenović, Marko Vasiljević, Irina Branović, Slavko Veskovčić	
<b>2.Recommendation in E-Learning Based On Learning Style.....</b>	<b>519</b>
Aleksandar Kotevski, Gjorgi Mikarovski and Ivo Kuzmanov	
<b>3.Analysis and Classification of Robot Control Algorithms .....</b>	<b>523</b>
Maya Todorova	
<b>4.Elaboration of Internet of Things Security Functional Model .....</b>	<b>527</b>
Evelina Pencheva	
<b>5.Internet of Things in Healthcare Applications.....</b>	<b>531</b>
Evelina Pencheva, Ivaylo Atanasov, Raycho Dobrev	
<b>6.Determining the importance of the usability attributes of Web-based GIS applications.....</b>	<b>535</b>
Nebojša Djordjević, Dejan Rančić	
<b>7.Implementation of LMS in the Education in the Field of Programming .....</b>	<b>539</b>
Niko Naka, Snezana Savoska and Josif Petrovski	
<b>8.Adaptive vs. Non-adaptive e-Learning Systems – a Petri Net-based Evaluation Approach .....</b>	<b>543</b>
Emilija Spasova Kamceva and Pece Mitrevski	
<b>9.Content Management Systems – Unleashed Possibilities .....</b>	<b>547</b>
Jove Jankulovski, Mimoza Anastoska-Jankulovska and Pece Mitrevski	
<b>10.Appropriate Learning Tools and Approaches According to the Different Learning Styles and Collaboration Skills of the Students.....</b>	<b>551</b>
Donika Valcheva and Margarita Todorova	
<b>11.Optimal Design of Elements in Confirmation of Panel Buildings .....</b>	<b>555</b>
Vassil Guliashki, Chavdar Korsemov, Hristo Toshev, Leoneed Kirilov and Krassimira Genova	
<b>12.Modification of Algorithms to Control of Mobile Object.....</b>	<b>559</b>
Maya Todorova	
<b>13.Creating a virtual reality application from Memorial Museum “11th October” – Prilep .....</b>	<b>563</b>
Boban Mircheski, Igor Nedelkovski, Aleksandra Lozanovska and Jove Pargovski	
<b>14.Improved Data Transfer for Wireless Meteorological Stations.....</b>	<b>567</b>
Orlin Stanchev, Emilian Bekov and Vencislav Valchev	
<b>15.Interoperability of Cloud and Mobile Services .....</b>	<b>571</b>
Aleksandar Bahtovski and Marjan Gusev	

## Poster 5 - Digital Image Processing

<b>1.Adaptive Vision System.....</b>	<b>577</b>
Rosen Spirov and Neli Grancharova	
<b>2.An Approach for Position Detection of Industrial Objects.....</b>	<b>581</b>
Veska Georgieva and Plamen Petrov	
<b>3.Approaches for Texture Image Creation.....</b>	<b>585</b>
Daniela Ilieva	
<b>4.Coding of a Video with the Inserted Watermark using H.264/AVC Coder .....</b>	<b>589</b>
Zoran Veličković and Zoran Milivojević	
<b>5.3D Modelling from video.....</b>	<b>593</b>
Svetlana Mijakovska, Igor Nedelkovski	
<b>6.Automated Vegetation Classification for LANDSAT 7 Multispectral Images .....</b>	<b>597</b>
Dragan Stevic, Igor Hut, Nikola Dojčinović and Jugoslav Joković	

## Poster 6 - Informatics and Computer Science

<b>1.Numerical Experiments for the Study of the Influence of Wavelength in Laser Impact onto Metals and Alloys.....</b>	<b>603</b>
Nikolay Angelov	
<b>2.Similarity search in text data for Serbian language.....</b>	<b>607</b>
Ulfeta Marovac, Adela Crnisanin, Aldina Pljaskovic, Ejub Kajan	
<b>3.Optimization of Vehicle Maintenance Concept Using Simulation .....</b>	<b>611</b>
Ivan Djokic, Ljubomir Lazic, Aldina Pljaskovic, Aleksandra Pavlovic	
<b>4.Use of genetic algorithms for optimal design of electrical resistive furnaces insulation.....</b>	<b>615</b>
Hristo Nenov and Borislav Dimitrov	
<b>5.Communications in Realized Industrial Computer Networks.....</b>	<b>619</b>
Viša Tasić, Dragan R.Milivojević, Vladimir Despotović, Darko Brodić, Marijana Pavlov, Ivana Stojković	
<b>6.Information technology to calculate energy savings using solar panels and home appliances .....</b>	<b>623</b>
Nanko Bozukov, Tanya Titova and Veselin Nachev	
<b>7.Using Dashboards as tools to improve the process of decision making in heathcare.....</b>	<b>625</b>
Jasmina Nedelkoska, Snezana Savoska and Emilija Taleska	
<b>8.Preparation of data for visualization using SQL Server 2008 .....</b>	<b>629</b>
Emilija Taleska, Snezana Savoska, Jasmina Nedelkoska	
<b>9.Statistical parameters of the first order for Rayleigh Fading with EGC Diversity combiner using MATLAB.....</b>	<b>633</b>
Borivoje Milosevic, Mihajlo Stefanovic, Slobodan Obradovic and Srdjan Jovković	
<b>10.Expert systems for managing asbestos in premises .....</b>	<b>637</b>
Igor Nedelkovski, Boban Mircheski and Aleksandra Lozanovska	
<b>11. Ontology-based Personalization and Recommender System in Digital Libraries .....</b>	<b>641</b>
Daniela Kjurchievska	

## Poster 7 - Electronics

<b>1.Autonomous Inverters With Energy Dosing For Ultrasonic Applications .....</b>	<b>647</b>
Nikolay Dimitrov Madzharov	
<b>2.Virtual System for Magnetic Field Measurement.....</b>	<b>651</b>
Nikola Draganov, Totka Draganova, Anatolii Aleksandrov	

<b>3.Based on AMR Sensor Device for Contactless Measurement of AC Current.....</b>	<b>655</b>
Nikola Draganov	
<b>4.Design and Signal Processing Techniques on 0.18<math>\mu</math>m CMOS Hall Microsensors.....</b>	<b>659</b>
Tihomir Takov, Ivelina Cholakova and Yavor Georgiev	
<b>5.Investigation of the Defects Formation in Flexible Organic Light Emitting Devices by Thermal Activated Currents.....</b>	<b>663</b>
Mariya Aleksandrova	
<b>6.Incremental Encoder Macromodel for Educational Purpose .....</b>	<b>667</b>
Marieta Kovacheva and Peter Yakimov	
<b>7.Electrical Properties of Poly(Vinylidene Fluoride-COHexafluoropropylene) Nanocomposites with Nanoclays .....</b>	<b>671</b>
Pavlik Rahnev, Dimitrina Kiryakova, Lyudmila Borisova and Atanas Atanassov	
<b>8.Metal – Polymer Based Power Bulk Resistors .....</b>	<b>675</b>
Pavlik Rahnev and Silvija Letskovska	
<b>9.Modeling of high voltage periodically attenuating discharge in liquid with controllable high voltage switch thyratron.....</b>	<b>677</b>
Milena Ivanova and Stefan Barudov	
<b>10.Analysis and Design of Instrumentation Amplifiers.....</b>	<b>681</b>
Ivailo Pandiev	
<b>11.Pspice Simulation of Optoelectronic Circuits of Detectors .....</b>	<b>685</b>
Hristo Sabev and Tsanko Karadzhov	
<b>12.Subtraction Procedure for Removing the Baseline Drift from ECG Signals: Adaptation For Real Time Operation With Programmable Devices .....</b>	<b>687</b>
Tsvetan Shoshkov and Georgy Mihov	
<b>13.Investigation of Thin PZT and ZnO Piezoelectric Layers in Dynamic Mode for Application in MEMS .....</b>	<b>691</b>
Georgi Kolev, Krassimir Denishev, Mariya Aleksandrova and Yordanka Dutsolova	
<b>14.Sputtering of Thin Films on Flexible Substrates.....</b>	<b>695</b>
Pavlik Rahnev, Silvija Letskovska, Dimitar Parachkevov and Kamen Seymenliyski	
<b>15.Design and Realization of a small 10 Watt Forward Converter .....</b>	<b>699</b>
Zoran Zivanovic and Vladimir Smiljakovic	

## Poster 8 - Measurement Science and Technology

<b>1.Vibration Measurement with Piezoelectric Transducer.....</b>	<b>705</b>
Bozhidar Dzhudzhev, Veselka Ivancheva, Silviya Kachulkova and Ekaterina Gospodinova	
<b>2.Examination of capacitive transducers and their use for measurement of small linear displacements .....</b>	<b>709</b>
Veselka Ivancheva, Silvia Kachulkova, Bozhidar Dzhudzhev and Vladislav Slavov	
<b>3.RADFET as a sensor and dosimeter of gamma-ray irradiation .....</b>	<b>713</b>
Milić Pejović, Momčilo Pejović and Nikola Nešić	
<b>4.New approach for designing high-performance controllers in electrical drives systems using Programmable Logic Devices .....</b>	<b>717</b>
Vladimir Karailiev and Valentina Rankovska	

## Poster 9 - Energy Systems and Efficiency

<b>1.Analysis of the Mesh Voltage Calculation Method in the Presence of a Two-Layer Soil.....</b>	<b>723</b>
Marinela Yordanova, Margreta Vasileva and Rositsa Dimitrova	

<b>2.Design, Construction, Calibration and Use of A New Type of Electromagnetic Brake.....</b>	<b>727</b>
Miroslav Bjekic, Milos Bozic, Marko Rosic, Marko Popovic, Dragisa Petkovic	
<b>3.Energy Capability of Metal-Oxide Surge Arresters in Electric Power Lines 20 kV.....</b>	<b>731</b>
Margreta Vasileva and Marinela Yordanova	
<b>4.Model-experiment comparative analysis of roof type photovoltaic generator .....</b>	<b>735</b>
Bohos Aprahamian and Milena Goranova	
<b>5.Renewable Energy Sources and Tariffng of Electrical Power .....</b>	<b>739</b>
Silvija Letskovska and Kamen Seymenliyski	
<b>6.Experimental Verification of Algorithm for Indirect Domestic Load Recognition .....</b>	<b>743</b>
Konstantin Gerasimov, Julian Rangelov and Nikolay Nikolaev	
<b>7.Functionalities Extension of the NASAVR Software For Small-Signal Stability of Electric Power Systems.....</b>	<b>747</b>
Julian Rangelov, Konstantin Gerasimov, Yoncho Kamenov and Krum Gerasimov	
<b>8.Mechanical Design of High Voltage Overhead Transmission Lines With Thermal-Resistant Aluminum Alloy Conductors Considering the Heating From The Electrical Current .....</b>	<b>751</b>
Yoncho Kamenov, Julian Rangelov and Angel Varangov	
<b>9.Optimization of Electric Resistance Furnace Using Backtracking Algorithm .....</b>	<b>755</b>
Borislav Dimitrov, Marinela Yordanova and Hristo Nenov	
<b>10.Heat-accumulation system powered by photovoltaic modules.....</b>	<b>759</b>
Milena Goranova and Bohos Aprahamian	
<b>11.Model Study of the Processes In Current Instrument Transformers For The Purposes of Relay Protection.....</b>	<b>763</b>
Krum Gerasimov, Mediha Hamza, Margreta Vasileva and Anton Filipov	
<b>12.Design of Photovoltaic plant for research purposes in University of Transport – Sofia .....</b>	<b>767</b>
Ivan Milenov and Vasil Dimitrov	
<b>13.Vector Analysis and Comparative Valuation of Precise and Approximate Non-Linear Models of Discrete Regulator with Reducing Input AC Voltage.....</b>	<b>771</b>
Emil Panov, Emil Barudov and Stefan Barudov	
<b>14.LED Technology in public lighting installations – facts or fiction.....</b>	<b>775</b>
Andrej Djuretic, Nebojsa Arsic and Mile Petrovic	
<b>15.Daily Load Curves for Different Months of Commercial Load Excluding Craft Stores and Shops .....</b>	<b>779</b>
Lidija Korunovic and Marko Vuckovic	
<b>16.Electromagnetic field analysis on salient poles synchronous motor in 3D.....</b>	<b>783</b>
Blagoja Arapinoski, Mirka Popnikolova Radevska, Milan Cundev, Vesna Ceselkoska	
<b>17.Numerical analysis and calculation of parameters of Three-Phase Induction Motor with Double Squirrel Cage .....</b>	<b>787</b>
Blagoja Arapinoski, Milan Cundev and Mirka Popnikolova Radevska	

## Poster 10 - Control Systems

<b>1.Development of a system for power supply monitoring and autonomous ignition of gasoline generator.....</b>	<b>793</b>
Goran Goranov and Iskren Kandov	
<b>2.Bondsim Modeling and Simulation of Chaos in Cascade Connected Nonlinear Electrical Systems .....</b>	<b>797</b>
Bojana M. Zlatkovic and Biljana Samardzic	
<b>3.Further results on integer and non-integer order PID control of robotic system .....</b>	<b>801</b>
Mihailo Lazarević, Srećko Batalov, Milan Cajić and Petar Mandić	

<b>4.Investigating the behaviour of the welding manipulator tip .....</b>	<b>805</b>
Svetlana Gerganova-Savova	
<b>5.Neuro-Genetic Algorithm for Non-Destructive Food Quality Determination.....</b>	<b>809</b>
Tanya Titova, Veselin Nachev, Chavdar Damyanov and Nanko Bozukov	
<b>6.11DoF inertial system for dynamics analysis of moving objects.....</b>	<b>813</b>
Rosen Miletiev, Emil Iontchev, Ivaylo Simeonov, Rumen Yordanov	
<b>7.Principles and Methods of Data Models Creation Within Automated Control Systems.....</b>	<b>817</b>
Zoya Hubenova, Antonio Andonov, Vladimir Gergov	
<b>8.Bond Graph Modelling and Simulation of the 3D Crane System Using Dymola.....</b>	<b>821</b>
Dragan Antić, Dragana Trajković, Saša Nikolić, Staniša Perić and Marko Milojković	
<b>9.Identification of Dynamic Processes with Artificial Neural Networks.....</b>	<b>825</b>
Jordan Badev and Ivan Maslinkov	
<b>10.AGV Guidance System Simulation with Lego Mindstorm NXT and RobotC .....</b>	<b>829</b>
Violeta Kostova, Ramona Markoska and Mitko Kostov	

## Poster 11 - Engineering Education

<b>1.Teaching FPGA-Based CPU Cores and Microcontrollers .....</b>	<b>835</b>
Valentina Rankovska	
<b>2.Interactive Learning Module Implementing "Divide and Search" Procedure in Convolutional Encoders Analysis .....</b>	<b>839</b>
Adriana Borodzhieva, Galia Marinova and Tzvetomir Vassilev	
<b>3.GUI for Properties Measurement of Medical Images.....</b>	<b>843</b>
Veska Georgieva and Olga Valchkova	
<b>4.Realization of flying shear for laboratory experiments.....</b>	<b>847</b>
Božić Miloš, Nebojša Mitrović and Marko Rosić	
<b>5.Curricula Innovation of the Study Program in Environmental Protection Engineering .....</b>	<b>851</b>
Tale Geramitcioski, Vangelce Mitrevski, Ilios Vilos and Pece Mitrevski	
<b>6.English for specific purposes on Cloud Platform.....</b>	<b>855</b>
Danica Milosevic and Borivoje Milosevic	
<b>7.Online simulation of nonlinearity limitations in a single mode optical fiber .....</b>	<b>859</b>
Kalin Dimitrov and Lidia Jordanova	
<b>AUTHOR INDEX.....</b>	<b>861</b>



---

---

## **Poster 2 - Telecommunications Systems and Technology**

---

---



# Investigate common work of IP software phone systems and PSTN equipment

Todorka Georgieva<sup>1</sup> and Borislav Necov<sup>2</sup>

**Abstract** - This paper discusses common work between PSTN and software – based VoIP phone systems. The experimental part is based on real working system including specialized interface modules and gateways.

**Keywords**– VoIP, FXO, FXS , Phone systems,SIP signalizations

## I. INTRODUCTION

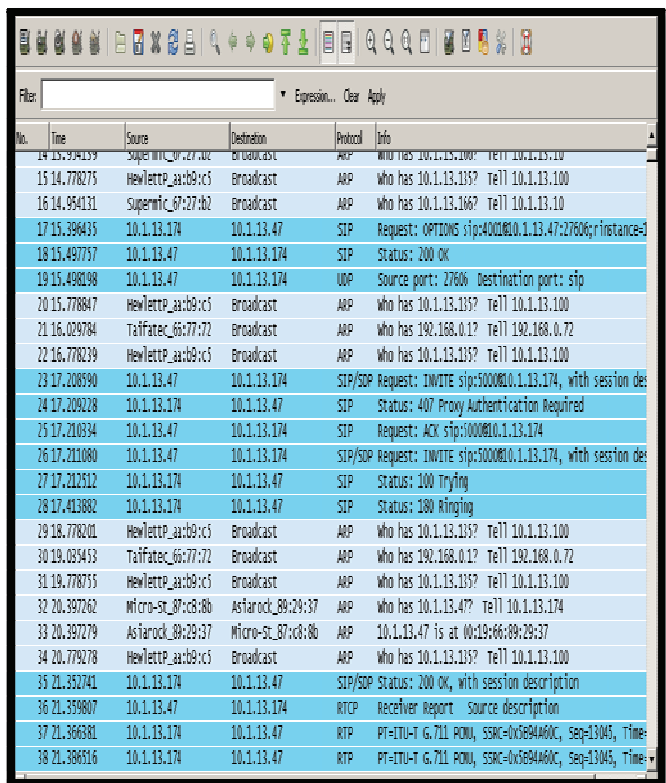
The purpose of this experiment is to create a interconnection of IP-based phone systems with conventional telephone equipment in already build telecommunication network. Investigated system allows connection to various outside PSTN, ISDN and other networks. IP telephone systems like TRIXBOX and ELASTIX are used. The Network consists various conventional and IP, software and hardware phones[1].

For realization of channelswitching commutation and packet switching commutation two methods are applied: using a hybrid interface card with four FXO ports and one FXS port and by connecting input-output device (gateway)[2].

## II. EXPERIMENTAL RESULTS

2.1. Investigate and analyze the common work of conventional telephone equipment with IP software telephone system "Elastix"[3].

When initially connect two phones stream of packets contains not only conversation of the subscribers, but different SIP signalizations between them (Fig.2.1).



The screenshot shows a packet capture interface with a list of network frames. The columns include No., Time, Source, Destination, Protocol, and Info. The protocol column shows mostly ARP and SIP, while the Info column provides detailed SIP message details. Key messages visible include SIP Request: OPTIONS, SIP Status: 200 OK, SIP/SDP Request: INVITE, and SIP Status: 407 Proxy Authentication Required. The SIP messages are exchanged between two hosts with IP addresses 10.1.13.174 and 10.1.13.100.

Fig.2.1. SIP signalizations between subscribers in VoIP conversation

VoIP signal recorded in this study is presented with VoIP analyzer (Fig.2.2)[4].

<sup>1</sup>Todorka Georgieva, teacher in . KTT in FE of TU-Varna „Studentska” № 1 str, e-mail: banki4@abv.bg

<sup>2</sup>Borislav Rozenov Necov, eng. in . KTT in FE of TU-Varna, „Studentska” № 1 str, e-mail: sharkiller@mail.bg

For normal use of the system a phone number is necessary to be created. This number is part of the phone system and is responsible to port on the interface module.

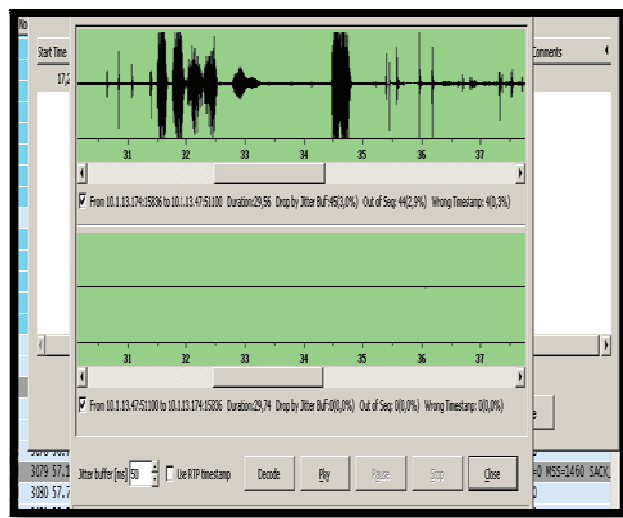


Fig.2.2. Realized VoIP call

RTP, TCP, and SIP protocols are monitored in the study (fig.2.3).

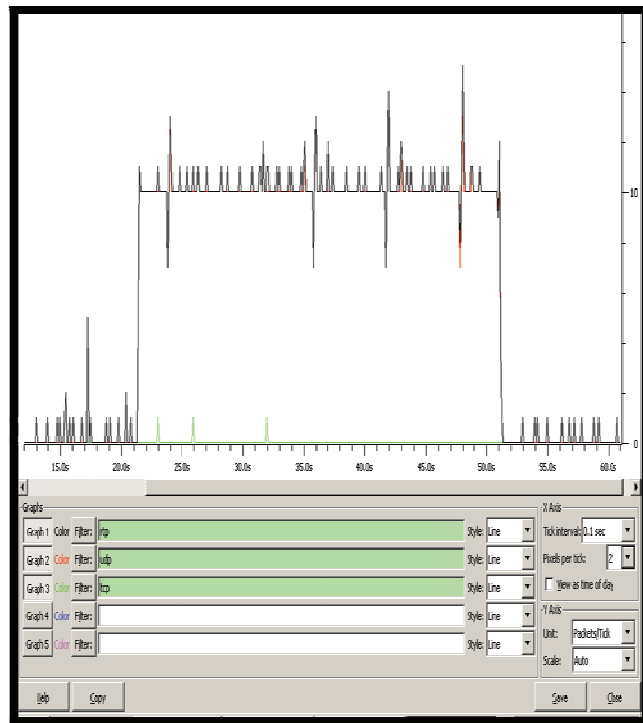


Fig.2.3. Time dependence of VoIP protocols

Main parameters of the conversation like network activity by category, bandwidth consumption by category, network activity by protocol and bandwidth consumption by protocol are shown in Fig. 2.4

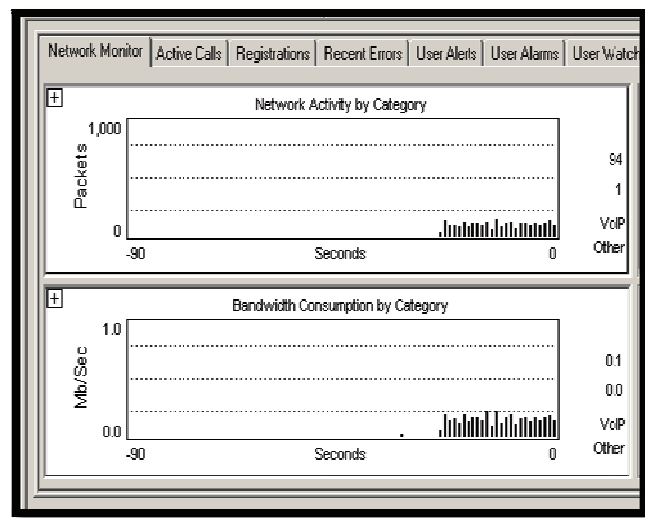


Fig.2.4. Parameters of the conversation

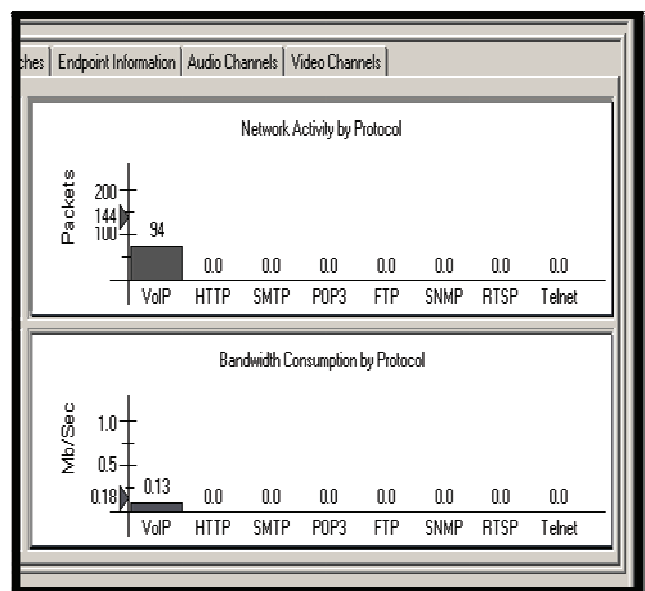


Fig.2.5 Parameters of the conversation part 2

Along with that the status of the investigated system is monitored. Fig.2.5 shows profiles of the network, which tracks current employment of bandwidth and the packet employment of the network.

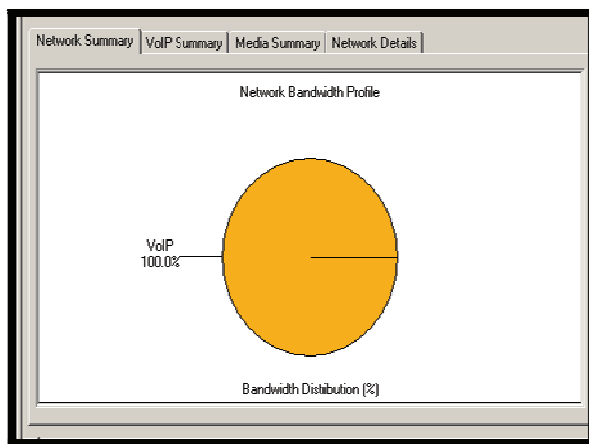


Fig.2.6 Parameters of the network

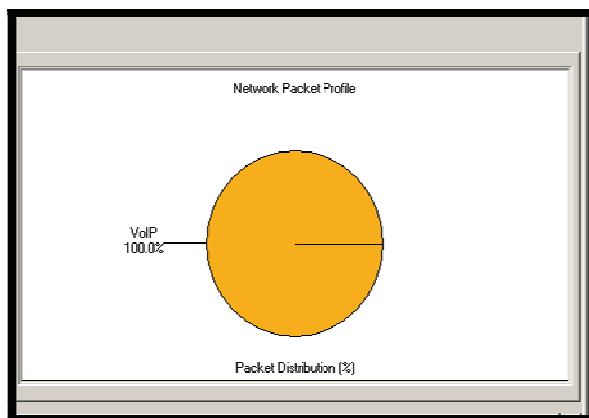


Fig.2.7Parameters of the network part 2

Information about ongoing conversations in the study is shown in fig.2.6:

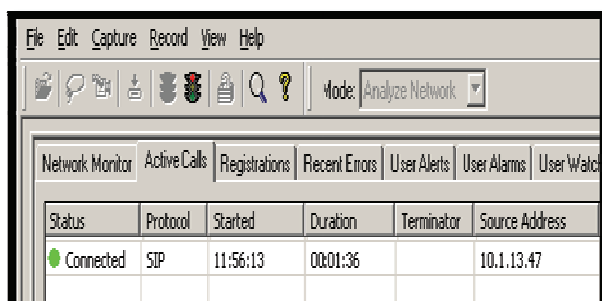


Fig.2.8Information for current conversations

Endpoint Information			
Source ID/E.164	Source Name/H.323 ID	Destination Address	Destination ID/E.164
4001	"4001"	10.1.13.174	5000

Fig.2.9 Information for current conversations

2.2. Investigate and analyze the common work of interface commutation modules and PSTN network

In this study connections are created between PSTN network, interface hybrid card and the input-output module (Sangoma B600 and Micronet SP5014)[5].

In the first case, the Sangoma card is part of Elastix phone system, therefore it is necessary some important settings to be configured in the phone system for the proper functioning of the module[6].

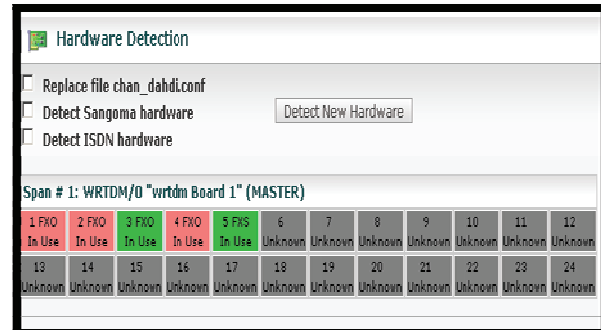


Fig.2.10. FXOport configuration

The second way of connection to the PSTN network in this experiment is using the gateway.

The device is connected to one of the telephone systems with IP address: 10.1.13.100. Phone numbers are chosen for the ports (two FXO and two FXS ports) and the relevant settings are applied (fig.2.8 and fig. 2.9):



Mode:	<input type="radio"/> Peer-to-Peer <input checked="" type="radio"/> Proxy
Primary Proxy IP Address:	10.1.13.100
Primary Proxy port:	5060
Secondary Proxy IP Address:	null
Secondary Proxy port:	5060
Outbound Proxy:	null
Outbound Proxy port:	5060
Prefix String:	null
Line1 Number:	2001
Line2 Number:	2002
Line3 Number:	2003
Line4 Number:	2004
SIP port:	5060
RTP Port:	16384
Expire:	60

Fig.2.11.Sip configuration

Line Configuration						
Line (TEL 1):	Type:	Bunting Group:	Hot Line:	No Answer Fwd.:	Registration:	Status:
Line 1(LINE 1):	FXS	1	x	x	Not Registered	Ready
Line 2(LINE 1):	FXO	2	x	x	Not Registered	Ready
Line 3(TEL 2):	FXS	3	x	x	Not Registered	Ready
Line 4(LINE 2):	FXO	4	x	x	Not Registered	Ready
<b>OK</b>						

Fig.2.12. Ports settings

External connections are provided through one of the FXO entrances of the device and thereby a connection is created between PSTN and IP telephone systems.

### III.CONCLUSION

The conducted experiments show successful collaboration of IP-based systems, PSTN networks and the connected to them hardware and software communication devices. The results confirm the effectiveness of the established communication connections and ensure the quality of conversations. The realized system requires further study in obtaining parameters to ensure quality teletrafficparameters and QoS.

### REFERENCES

- [1]David Kelly, Cullen Jennings, LaanDang, Practical VoIP Using Vocal, 2010
- [2]Ted Uelingford, VoIP Hacks - Tips & Tools for Internet Telephony, 2005
- [3]Kerry Garrison, Trixbox CE 2.6: Implementing, managing, and maintaining an Asterisk-based telephony system, Packt Publishing, 2009
- [4]Bruce Stuart, Speaking about VoIP, 2011
- [5]Тед Уелингфорд, Преход към VoIP, 2006
- [6]Ben Sharifeh Шариф, Elastix Without Tears, 2010

# Integration of optical and wireless networks under the Radio-over-Fiber concept

Suzana Miladic<sup>1</sup>

**Abstract –** Combination of high bandwidth of optical fiber networks with the mobility of wireless networks is the main characteristic of the hybrid concept known as FiWi (Fiber-Wireless) and it is considered as a realistic concept for the implementation of broadband fixed and mobile wireless access. Towards the technical evolution of fiber-wireless access networks and the seamless coexistence of both technologies, this paper provides a review of advantages of the integration of optical and wireless networks under the FiWi concept with emphasis on Radio-over-Fiber (RoF) approach.

**Keywords –** Optical-wireless integration, FiWi, RoF

## I. INTRODUCTION

To meet the demands of high-capacity and broadband wireless access for future services and applications such as High Definition IPTV (HD IPTV), Video-On-Demand (VoD) and Online Interactive Gaming, the next-generation access networks are driving the needs for the convergence of wired and wireless services. Hybrid fiber-wireless networks for fixed wireless access operating in the sub-millimeter-wave and millimeter-wave (mm-wave) frequency regions are being actively pursued to provide untethered connectivity for ultrahigh bandwidth communications [1]. Therefore, authors of that paper focused on the subsystem and interface designs for WDM-based mm-wave fiber-wireless networks.

Newer standards such as WiMAX and LTE extend the capabilities of existing (WiFi, UMTS) but they are also based on using a lower microwave range which will further increase the occupancy of microwave part of the RF (Radio Frequency) spectrum. The particular area of interest is the unlicensed 60 GHz frequency band, which has 5-mm wavelengths but it is not without challenges, either, which is mentioned at [2]. The advantage of bimodal FiWi systems is that they can enjoy the strength of both optical and wireless technologies.

In recent years significant researches were made focused on the implementation of these systems. Therefore, fixed mobile convergence architectures for broadband access are proposed at [3]. Various challenges and opportunities of FiWi networks are discussed in [4]. This paper deals only with RoF architectures, an approach that is different compared to the R&F (Radio-and-Fiber) network integration mainly because of its use in the indoor environment and outdoor zones for the needs of communication systems.

The paper is organized as follows. Section II presents an overview of the structure and the main elements of FiWi

networks under the RoF concept. Optical and wireless technologies and their latest developments are presented in section III. Section IV introduces advantages of the integration of these two technologies and often combined optical and wireless technologies in RoF approach while section V concludes the paper.

## II. RADIO-OVER-FIBER CONCEPT

Radio-over-Fiber is a communication technology for broadband access network where radio signals sent by equipment to Base Stations (BS) modulate a light, transmitting optical data. RF signals that modulate an optical carrier in a Central Station (CS) are being propagated over an analog fiber link to Remote Antenna Units (RAUs) and are then transmitted to clients through the air [5].

RF signal processing, which includes modulation, frequency conversion and multiplexing in conventional wireless communication systems is done on the side of each base station. In RoF systems network complexity is moved to a central base station where all demultiplexing and signal processing are done. Using this architecture each RAU contains a fewer components what reduces the implementation costs. Each base station is adapted to communicate over a radio link with at least one user's mobile station located within the radio range of said base station. Basic architecture of RoF technology is shown at Fig.1 which can be used to distribute the GSM signal at 900 MHz [6]. The RF signal modulates the laser diode in the central site (headend). Modulated optical signal is then transported over the fiber to the BS where transmitted RF signal is recovered by detection in the photodetector. The signal is then amplified and radiated by the antenna. The uplink signal from the mobile units is transported from the RAU to the headend in the same way.

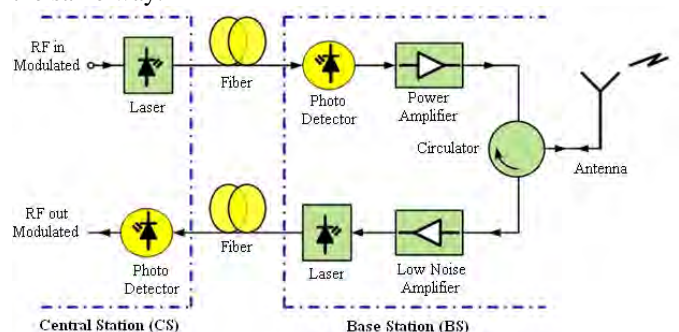


Fig. 1. Basic RoF architecture

Applying this concept of FiWi systems the complexity of the equipment at the base stations is reduced because they only perform optoelectronic conversion and signal amplification before the signal is brought to the transmitting antenna. This is opposed to the traditional way where each

<sup>1</sup>Suzana Miladic is with the Faculty of Traffic and Transport Engineering Doboј at University of East Sarajevo, E-mail: miladics@hotmail.com

protocol type requires separate equipment at the location of the antenna.

Depending on the frequency range of the radio signal is transported, RoF transmission systems are usually classified into two main categories: RF-over-Fiber and IF-over-Fiber.

In RF-over-Fiber architecture (RFoF), a data-carrying RF signal with a high frequency (usually greater than 10 GHz) is imposed on a lightwave signal before being transported over the optical link. Therefore, wireless signals are optically distributed to base stations directly at high frequencies and converted from the optical to electrical (O/E) domain at the base stations before being amplified and radiated by an antenna. As a result, no frequency up/down conversion is required at the various base stations, thereby resulting in simple and rather cost-effective implementation is enabled at the base stations.

In IF-over-Fiber architecture (IFoF), an IF (Intermediate Frequency) radio signal with a lower frequency (less than 10 GHz) is used for modulating light before being transported over the optical link. Therefore, before radiation through the air, the signal must be up-converted to RF at the base station. The lowest complexity is achieved by applying the RFoF technique but it requires the solution of other challenges such as chromatic dispersion, spectral efficiency, modulation of the optical carrier, what can significantly affect the overall system performance.

An important application of RoF systems is their use for in-building (indoor) distribution of wireless signals of both mobile and data communication systems and its use to provide wireless coverage in the area where wireless backhaul link is not possible. These zones can be areas inside a structure such as a tunnel, areas behind buildings, mountainous places etc. In China, for example, systems are being widely deployed in industrial zones, harbors, hospitals and supermarkets [6]. Plans are in place to expand into rural zones along rail lines, and in new residential and commercial construction spaces. It is believed China will be the leading user of the technology and this will bring down the cost of equipment.

Vehicle Communication and control is also a potential application of RoF technology. Frequencies between 63-64 GHz have already been allocated for this service within Europe. The objective is to provide continuous mobile communication coverage on major roads for the purpose of Intelligent Transport Systems (ITS) such as Road-to-Vehicle Communication (RVC) and Inter-Vehicle Communication (IVC). In the USA RoF systems are deployed in places like stadiums, shopping malls and inside buildings, but their important application is in the satellite communications and beam handling/processing. It involves the remoting of antennas to suitable locations at satellite earth stations.

### III. OPTICAL AND WIRELESS TECHNOLOGIES AND THEIR DEVELOPMENTS

#### A. Optical technologies and standards

The purity of today's glass fiber, combined with improved system electronics, enables fiber to transmit digitized light

signals hundreds of kilometers without amplification. Fiber access systems are also referred to as fiber-to-the-x (FTTx) system, where "x" can be "home," "building," "curb," "premises," etc., depending on how deep in the field fiber is deployed or how close it is to the user. FTTx is considered as an ideal solution for access networks because of the inherent advantages of optical fiber in terms of huge capacity, small size and weight, and its immunity to electromagnetic interference and crosstalk [7]. For safety reasons fiber should be installed underground and therefore its deployment involves costs so such systems probably will be limited to core and backbone networks. However these systems are well suited to support integrated high bandwidth digital services, and can alleviate bandwidth bottlenecks.

Passive Optical Network (PON) became a solution for "last mile" access, since the "last mile" is the most expensive part of the network because there are far more end users than backbone nodes. The optical elements used in such networks are only passive components, such as fibers, splitters/couplers and connectors. A PON is formed by an Optical Line Terminal (OLT), located at the CO (Central Office), and a set of Optical Network Units (ONUs) located at or in the neighbourhood of subscribers' premises. Downstream traffic is broadcast by the OLT to all ONUs and Time Division Multiplexing (TDM) is used for sending data. Upstream traffic uses Time Division Multiple Access (TDMA), under control of the OLT located at the CO, which assigns time slots to each ONU for synchronized transmission of its data bursts (Fig.2).

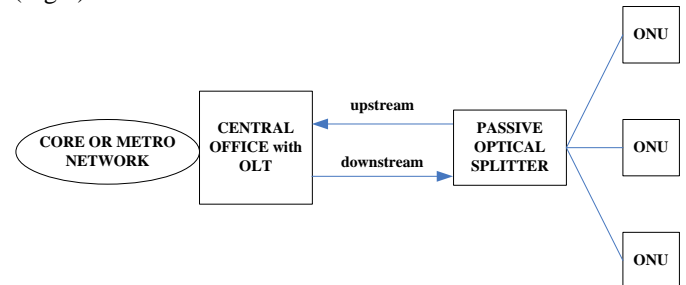


Fig. 2. PON access networks

Today, the development of PON is based on two main standards: ITU-T G.984 Gigabit PON (GPON) and IEEE 802.3ah Ethernet PON (EPON). GPON carries different data types including voice, Ethernet, ATM, leased lines and wireless extension by using a convergence protocol layer designated GFP (Generic Framing Procedure) [8] while EPON carries Ethernet frames with symmetric rates equal to 1.25 Gbit/s. Some characteristics of the GPON standard are: physical reach of at least 20 km, with support for logical reach up to 60 km, support of several data rate options, using the same protocol, including a symmetrical link at 622 Mbit/s or 1.25 Gbit/s, or 2.5 Gbit/s downstream with 1.25 Gbit/s upstream. Future developments of GPON and EPON are related to capacity increase through combinations of TDM with WDM (Wavelength Division Multiplexing), then increase of data rates, with faster lasers and more sensitive burst-mode receivers.

#### B. Wireless technologies and standards

The IEEE 802.11x ( $x = a, b, g$ ) family of standards also known as Wi-Fi is the technology that has dominated the wireless local area networking (WLAN) market worldwide in the last decade. These standards support the WLAN functionality where one Access Point (AP) is able to serve several users in a range of 100 m indoor to 400 m outdoor with rates up to 54 Mbit/s (802.11g) [5].

IEEE 802.16 otherwise known as WiMAX is another type of access technology which uses radio waves for last-mile connectivity. WiMAX seeks to provide high-bit rate mobile services using frequencies between 2–11 GHz and aims to provide Fixed Wireless Access (FWA) at bit-rates in the excess of 100 Mbit/s and at higher frequencies between 10–66 GHz [9]. WiMAX can provide at-home or mobile Internet access across whole cities or countries and it's bandwidth and range make it suitable for the following potential applications: providing portable mobile broadband connectivity across cities and countries through a variety of devices, providing a wireless alternative to cable and digital subscriber line (DSL) for "last mile" broadband access and providing data, telecommunications (VoIP) and IPTV services. WiMAX cannot deliver 70 Mbit/s over 50 kilometers. Like all wireless technologies, WiMAX can operate at higher bitrates or over longer distances but not both. Operating at the maximum range of 50 km increases bit error rate and thus results in a much lower bitrate. Conversely, reducing the range (to under 1 km) allows a device to operate at higher bitrates. One way to increase capacity of wireless communication systems is to deploy smaller cells (micro- and pico-cells) or to increase the carrier frequencies. But, at the same time, smaller cell sizes mean that large numbers of BSs in order to achieve the wide coverage required of ubiquitous communication systems.

IEEE works on the new 802.16m amendment which adds many enhancements while being backward compatible with previous WiMAX standards. It will support various MIMO schemes, QoS, Multi-hop Relaying, which allows for range extension and avoidance of coverage holes and Multi-Carrier Aggregation where one or more clients may use more than one channels, depending on channel availability, increasing in this way the data rates up to 100 Mbit/s for mobile clients and 1 Gbit/s for fixed clients [5].

#### IV. ADVANTAGES AND BENEFITS OF THE ROF TECHNOLOGY

Integration of optical and wireless technologies under the Radio-over-Fiber concept has some advantages compared with conventional optical and wireless signal distribution, where it is obviously that combining these two technologies we get the new one with better performances, in order to achieve efficiency of the telecommunications services market.

These performances are related to: ability to transport long distance with high fidelity, modulation format transparent, centralized control of electronic circuitry, compact and reliable. More detailed form of the RoF system and its central base station is shown at Fig.3. The possibility of integration of different wireless systems, including Wi-Fi and WiMAX with PON technology in the future Fi-Wi systems is proposed at [7] while combination of different WLAN and Wireless Mesh

Networks (WMN) with optical access architectures based on PON technology (EPON) are demonstrated at [2,10].

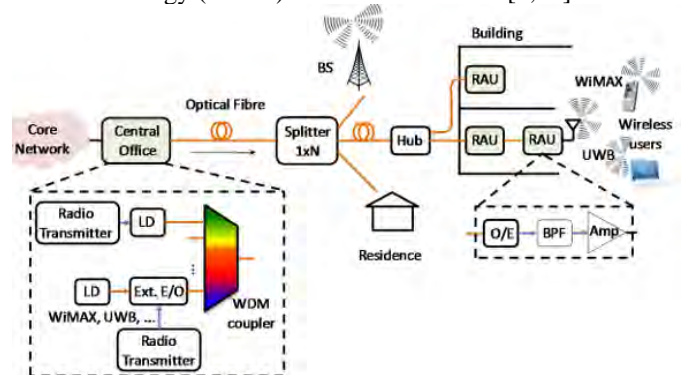


Fig.3. The complex form of the RoF technology and its central base station

#### C. Low attenuation loss and huge bandwidth of optical fiber

Attenuation is the progressive loss of signal strength as the signal propagates along the cable. The effective resistance of a cable increases with frequency because of the so-called skin effect. The skin effect is strongly dependent on frequency, rising rapidly with increased frequency. Electrical distribution of high frequency microwave signals either in free space or through transmission lines is problematic and costly [6]. Signals transmitted on optical fiber attenuate much less than through other media, especially when compared to wireless medium. By using optical fiber, the signal will travel further, reducing the need of repeaters. Optical fiber communications bounces light around inside a fiber and the result is no crosstalk and less attenuation because optical fibers don't suffer from the skin effect. You can back hundreds of fibers together and it would not make a difference. In transmission lines and in free space higher frequency means higher impedance and increasing of absorption and reflection respectively which includes more expensive equipment. The potential solution for this problem is to distribute signals at low intermediate frequencies from the switching centre to the base station. The baseband or IF signals are up-converted to the required microwave or mm-wave frequency at each base station, amplified and then radiated. There are three main transmission windows, which offer low attenuation, namely the 850 nm, 1310 nm, and 1550 nm wavelengths. Attenuation of the RF signal transmitted optically are below 0.2 dB/km and 0.5 dB/km in the 1550 nm and the 1300 nm windows, respectively what is much lower than those in coaxial cable.

Because of operating at higher frequencies, optical fibers offer enormous bandwidth. The high optical bandwidth enables faster transmission and high speed signal processing which can be implemented in the optical domain. Since the microwave functions such as filtering, mixing, up- and down-conversion are implemented in the optical domain it is possible to use cheaper low bandwidth optical components such as laser diodes and modulators, and still be able to handle high bandwidth signals. The capacity of the fiber optic networks in mm-wave fiber-radio systems can be increased by applying WDM technology. In analogue optical systems

including RoF technology, Sub-Carrier Multiplexing (SCM) is used where a large number of mm-wave channels, each carried by a separate wavelength, are transmitted to/from the BSs via the CO through a single fiber.

#### D. Immunity to radio frequency interference

This advantage is consequence of the fact that fiber optic carries signals as light waves instead of electrical impulses and therefore it is immune to EMI (Electromagnetic Interference) and does not create its own EMI. Also, it is immune to RFI, or Radio Frequency Interference and emit no radiation. Since fiber optic systems do not emit RF signals, they are difficult to tap into without being detected what provides privacy and security.

#### E. Centralized control and reduced power consumption

To make the base station compact and cost-effective it has been proposed that RoF technique be used to transfer the complicated RF modem and signal processing functions from the base station to a centralized control station where all signal processing are done. The typical distances between the CO and the BSs are 5-50 km, where each of the BS serves a microcell or picocell covering the distances of few ten's to few 100's metres. Centralised network arrangement allows easy installation and maintenance and simplifies the BSs to having transmitter and receiver with additional optoelectronic & electrooptic (O/E) interface to detect and transmit optical mm-wave signals. It also allows securing the sensitive and delicate equipment in a central location, in addition to enabling them to be shared between a larger numbers of customers.

As the complexity of each base station is reduced and their large numbers are required the costs of system installation and maintenance are much smaller. The much lower power level eliminates the needs for expensive frequency multiplexes and high power amplifiers currently employed at base stations so the consequence of having simple RAUs with reduced equipment is reduced power consumption. Reducing the cell size the radiated power at the antenna is reduced to.

#### F. Modulation format transparency and compactness

The RoF distribution system can be made signal-format transparent. For instance the Intensity Modulation and Direct Detection (IM-DD) technique can be made to operate as a linear system and therefore as a transparent system [6]. Using low dispersion fiber in combination with pre-modulated RF subcarriers the same RoF network can be used to distribute multi-operator and multi-service traffic, resulting in huge economic saving. Since RF functions are performed at a centralized station, there is the possibility of dynamic capacity allocation to individual BS. For example more capacity can be allocated to an area in accordance with the needs and then re-allocated to other areas when off-peak because allocating constant capacity would be a waste of resources. This can be

done by allocating optical wavelengths through WDM as need arises.

## V. CONCLUSIONS

This paper has reviewed the current advantages of using Radio-over-Fiber technology. Despite of these advantages it is also important to mention its limitations which are related to noise and distortion since RoF involves analogue modulation, and detection of light. So, fundamentally, it is an analogue transmission system. In analogue optical fibre links the noise sources include the laser's Relative Intensity Noise (RIN), the laser's phase noise, the photodiode's shot noise, the amplifier's thermal noise, and the fibre's dispersion so Bit Error Rate (BER) may be affected by transmission channel noise, interference and distortion. The BER may be improved by choosing strong signal strength or choosing a slow and robust modulation scheme. Also, because all the processing in RoF is moved towards the CS a possible failure inside the CS will endanger overall service availability.

As a new research topic, FiWi broadband access network is a promising "last mile" access technology, because it integrates wireless and optical access technologies in terms of their respective merits and it should be more explored before commercial deployment, so many issues must be considered such as peer-to-peer communication, multicasting, which are also significant and can be the subject of further researches.

## REFERENCES

- [1] C. Lim et al., „Fiber-Wireless networks and subsystem technologies“, Journal of Lightwave Technology, vol. 28 (4), pp. 390-414, 2010.
- [2] G. Markovic and V. Radojicic, „Hybrid Fiber Wireless next generation networks“, PostTel 2011, Proceedings vol. 1, pp. 268-278, 06-07 December 2011, Belgrade.
- [3] G. Shen et al., „Fixed mobile convergence architectures for broadband access: Integration of EPON and WiMAX“, IEEE Communications Magazine, vol. 45 (8), pp. 44-50, 2005.
- [4] N. Ghazisaidi and M. Maier, „Fiber-Wireless (FiWi) networks: Challenges and Opportunities“, IEEE Network, vol. 25 (1), pp. 36-42, 2011.
- [5] T. Tsagklas and F. N. Pavlidou, „A survey on Radio-and-Fiber FiWi network architectures“, Journal of Selected Areas in Telecommunications (JSAT), march edition, 2011.
- [6] A. Ng'oma, „Radio-over-Fiber technology for broadband wireless communication systems“, The faculty of Electrical Engineering of the Eindhoven University of Technology, Ph.D, Thesis, ISBN: 90-386-1723-2, 2005, Netherlands.
- [7] P. Chowdhury et al., „Hybrid Wireless-Optical Broadband Access Network WOBAN: Prototype development and research challenges“, IEEE Network, vol. 23 (3), pp. 41-48, 2009.
- [8] H. J. A. da Silva, „Optical access networks“, available at web: [www.co.it.pt](http://www.co.it.pt) (09.03.2005).
- [9] G. Aditya and Er. R. K. Sethi, „Integrated optical wireless network for next generation wireless systems“, Signal Processing: An International Journal (SPIJ), vol. 3 (1), pp. 1-13, 2009.
- [10] X. Wang and A. Lim, „IEEE 802.11s Wireless Mesh Networks: Framework and Challenges,“ Ad Hoc Networks, vol. 6 (6), pp. 970-84, 2008.

# Optical Line Terminal Process modeling

Stela Kostadinova<sup>1</sup> and Rozalina Dimova<sup>2</sup>

**Abstract –** The paper presents a mathematical modelling of the processes in an element of passive optical access network – Optical Lime Terminal (OLT) using queuing theory. Based on a mathematical model, utilizing MATLAB, we study the process in OLT and the dependence of traffic characteristics from input streams (coming flow) parameters.

**Keywords -** Traffic modelling, PON, Pareto distribution, OLT.

## I. INTRODUCTION

With the development of many advanced multimedia applications, there is a massive increase in bandwidth demand. Passive optical network (PON) technology is emerging as the key access technology, as it has a scalable and cost-effective architecture to satisfy the ever-growing bandwidth requirements generated by advanced applications.[1] To meet the requirements of users and for obtaining acceptable precise predictions of performance of the system, system models must be developed taking into account the characteristics of the actual network load. The integrated nature of the multi-service networks with a wide range services determines the diversity of traffic, which greatly changes its parameters and the mathematical model.

The most performance studies, dealt with simulation without mathematical approaches, or used the queuing model traffic models, without considering self similarity and long range dependence of the traffic. In our paper we present analytical model using Bounded Pareto Distribution for network traffic modeling.

An important task in building a modern network is to provide an appropriate quality of service for all types of traffic. The main reason for the degradation of the quality of service in multiservice networks, and subsequently access networks of next generation, is the packet delay caused by queues in the buffers of network devices. This is why we utilize a queuing model for process modeling in Optical Line Terminal (OLT) equipment, integrating switching and routing function in PON systems. The model will be used in the future state for system analysis and prediction of the QoS characteristics, like packet transfer delay and packet delay variation on network planning stage.

## II. TRAFFIC MODELING

### A. Traffic flow

An important task in the description of a queuing system is to describe the flow of arrival and service requests. As arrival requests, in the study of our OLT model we considered the beginning of Ethernet frames entering the system. Intervals between incoming requests, one after another, create random input streams that can be described by the distribution of the time between receipts of the neighboring requests.

The mathematical model of traffic is a probability distribution function of random number of requests for mean service time.

There is an extensive study showing that most network traffic flows in today's multiservice networks can be characterized by self-similarity and long-range dependence (LRD). [2-5] The measure of self-similarity is the Hurst parameter ( $H$ ). For Short Range Dependence (SRD):  $0 < H < 0,5$ , for Long Range Dependence (LRD):  $0,5 < H < 1$ . [4]

An analytical description of network traffic does not exist, because we cannot predict the size and arrival time of the next packets. Therefore, we can only describe network traffic as a stochastic process. Hence, we can describe two stochastic processes - arrival time and packet size; with the use of Hurst parameter and probability distributions. [6]

All processes are usually described by probability distributions. Self-similar process can be described by heavy tailed distributions. [4-5]. The main task for modeling the stochastic process with probability distribution is to choose the right distribution, which would be a fair representation of our network traffic stochastic process. In case of high speed networks with unexpected demand on packet transfers, Pareto based traffic models are excellent candidates since the model takes into the consideration the long-term correlation in packet arrival times [7]. The main property of heavy-tailed distributions is that they decay hyperbolically, which is opposite to the light-tailed distributions, which decay exponentially. The probability density function of Pareto distribution is given by [8] where parameter  $\alpha$  represents the shape parameter, and  $k$  represents the minimum possible positive value of the random variable  $x$ . The mean value -  $M$ , variance -  $\sigma^2$  and coefficient of variation -  $v$  of the Pareto distribution are:

$$M = \frac{\alpha k}{\alpha - 1} \quad (2.1)$$

<sup>1</sup>Stela Kostadinova is with the Faculty of Electronic at Technical University of Varna, 1 Studentska Str., Varna 9000, Bulgaria, E-mail: stela.kostadinova@tu-varna.bg.

<sup>2</sup>Rozalina Dimova is with the Faculty of Electronic at Technical University of Varna, 1 Studentska Str., Varna 9000, Bulgaria, E-mail: rdim@abv.bg

$$\sigma^2 = D = \frac{\alpha k}{(\alpha-1)^2(\alpha-2)} \quad (2.2)$$

$$v^2 = \frac{\sqrt{D}}{M} = \frac{1}{\alpha(\alpha-2)} \quad (2.3)$$

The relationship between the Hurst parameter  $H$  and the shape parameter  $\alpha$  is  $H = (3-\alpha)/2$  [9]. Thus if for LRD  $0,7 \leq H \leq 0,9$ , it should result in  $1,6 \geq \alpha \geq 1,2$ , but Pareto distribution has a finite mean and an infinite variance for  $1 \leq \alpha \leq 2$ .

For real systems, the values of random variables are limited. For a description of self-similar processes, limited (bounded) distribution can be introduced. This limited distribution allows, without changing the shape of the tail of the distribution, to set the maximum value of the random variable. Limited distribution differs from the normal in that there is not one, but two boundaries [10]. The bounded (or truncated) Pareto distribution has three parameters  $\alpha$ ,  $L$  and  $k$ . As in the standard Pareto distribution  $\alpha$  determines the shape.  $k$  denotes the minimal value, and  $L$  denotes the maximal value. [8]

$$M = \frac{\alpha(kL^\alpha - Lk^\alpha)}{(\alpha-1)(L^\alpha - k^\alpha)} \quad \alpha \neq 1 \quad (2.4)$$

$$\sigma^2 = \frac{\alpha}{(\alpha-2)} \left( \frac{k^2 L^\alpha - k^\alpha L^2}{(L^\alpha - k^\alpha)} \right) \quad (2.5)$$

$$v^2 = \frac{(\alpha-1)^2(L^\alpha - k^\alpha)(k^2 L^\alpha - k^\alpha L^2)}{\alpha(\alpha-2)(k L^\alpha - L k^\alpha)} \quad (2.6)$$

### B. PON systems

The PONs are designed to deliver multiple services and applications, such as voice communications, standard and high-definition video (STV and HDTV), video conferencing (interactive video), real-time and near-real-time transactions, and data traffic. A PON is a point-to-multipoint (PtMP) optical network with no active elements in the signals' path from source to destination. The only interior elements used in a PON are passive optical components, such as optical fiber, splices, and splitters. All transmissions in a PON are performed between an optical line terminal (OLT) and optical network units (ONUs) (Fig.1). The OLT resides in the telecom central office (CO) and connects the optical access network to the metropolitan-area network (MAN) or wide-area network (WAN). The ONU is located either at the end-user location fiber-to-the-home (FTTH) and fiber-to-the-business (FTTB) configurations, or at the curb, resulting in fiber-to-the-curb (FTTC) architecture. In the downstream direction, PON is a broadcasting media; Ethernet packets transmitted by the OLT pass through a 1:N passive splitter and reach each ONU. OLT provides dynamic bandwidth allocation and prioritization between services using a MAC

(Media Access Control) protocol. Packets are broadcasted by the OLT and extracted by their destination ONU based on their media-access control (MAC) address [11]. The main functions on a PON OLT line card can be divided into four categories: physical layer, MAC layer, packet processing, and traffic management. The MAC layer functions mainly include framing, media access control, operations, administration and maintenance (OAM), dynamic bandwidth allocation (DBA), forward error correction (FEC), and security. In terms of framing, GEPON (Gigabit Ethernet PON) standards are based on Ethernet. In GEPON, Ethernet frames are carried in their native format on the PON system. Services are all mapped over Ethernet (either directly or via Internet Protocol) (fig.2).

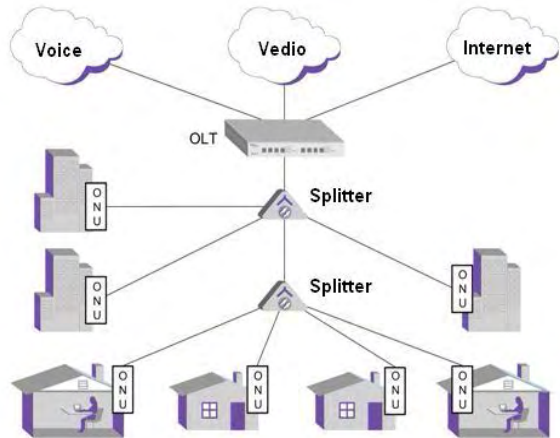


Fig.1. GEPON System Network

### III. MATHEMATICAL MODELING AND RESULTS

We consider OLT device that is part of PON network. In the input on the system we have three types of traffic flows VoIP, Data and IPTV.

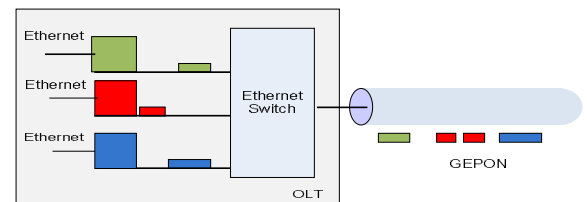


Fig. 2. Framing in GEPON [13]

A separate queue for each subscriber and for each traffic flow in the system is created (fig. 3). The queue for video flow is one for all subscribers. We consider each traffic flow as a G/G/1 queuing system with Pareto arrival process and Pareto service times, one server, full accessibility, and an infinite number of waiting positions. We have three priority classes and service discipline is FIFO (First In – First Out). Voice traffic flow has highest priority and means arrival rate  $\lambda_{v1}, \dots, \lambda_{v32}$ , Data traffic flow has lowest priority and mean arrival rate  $\lambda_{D1}, \dots, \lambda_{D32}$ . Number of subscribers in the

network is  $N=32$ . We assume that the system is in steady state. All streams are composed of Ethernet frames with variable length from 64 bytes to 1580 bytes. Their speed depends on the type of traffic. We assume that  $k$  is the minimal time interval between two adjacent Ethernet frames with a minimum duration and  $L$  is the interval between two Ethernet frames one of which is in the final in the packet burst and another is first in the next packet burst.

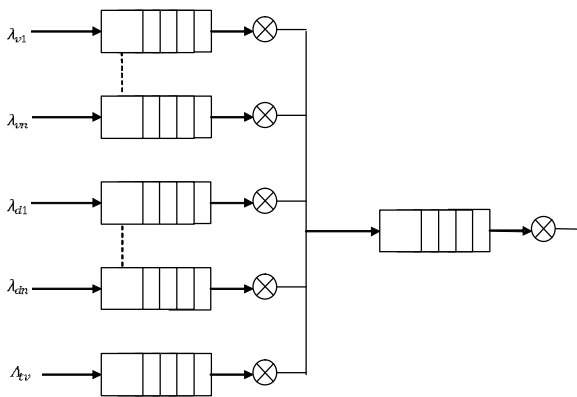


Fig. 3. Multiple -priority queues at an OLT

For arrival and service process modeling we use bounded Pareto distribution. Calculations were done for different values for  $\alpha$ :  $\alpha = 1.1$ ;  $\alpha = 1.3$ ;  $\alpha = 1.6$ . Coefficient of variation  $v$  were calculated for each type of traffic

$L_{aHi}$  – Maximum value of interval time between incoming requests

$k_{aHi}$  - Minimum value of interval time between incoming requests

$L_{bHi}$  - Maximum value of interval time between service requests

$k_{bHi}$  - Minimum value of interval time between service requests

$$i = (0, 1, 2, \dots, N)$$

$$H = (0, 1, 2, \dots, j)$$

In the input buffers of the OLT enters 3 classes traffic flow ( $H=0, 1, 2$ ), each with a minimum length  $n_{\min Hi}$  and a maximum speed  $R_{\max Hi}$ . The minimum transmission interval can be presented:

$$k_{Hi} = \frac{n_{\min Hi}}{R_{\max Hi}} \quad i = (1, 2, \dots, N) ; \quad H = (0, 1, 2)$$

$$\lambda_{Hi} = M_{aHi}^{-1} \quad i = (1, 2, \dots, N) ; \quad H = (0, 1, 2)$$

$$\mu_{Hi} = M_{bHi}^{-1}$$

$$\rho_{HN} = \frac{\lambda_{HN}}{\mu_{HN}}$$

Where,  $\lambda$  is mean arrival rate,  $\mu$  -mean rate of service time and  $\rho$  - the traffic intensity parameter.

Figure 4, shows the IPTV traffic intensity as a function of maximum value of interval time between incoming requests (upper Pareto boundary) for:  $\alpha = 1.1$ ;  $\alpha = 1.3$ ;  $\alpha = 1.6$ . Figure

5, shows coefficient of variation of intervals in the output streams as a function of the upper limit of the Pareto distribution for VoIP traffic flow, calculated in accordance (2.6), for:  $\alpha = 1.1$ ;  $\alpha = 1.3$ ;  $\alpha = 1.6$ . Figure 6, shows coefficient of variation of intervals in the output streams as a function of the upper limit of the Pareto distribution for Data traffic flow. Figure 7, shows coefficient of variation of intervals in the output stream as a function of the upper limit of the Pareto distribution for IPTV traffic flow.

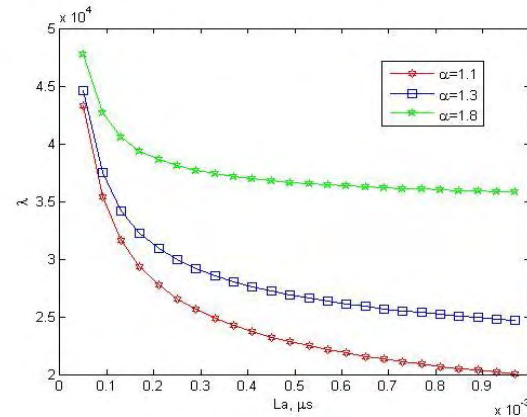


Fig. 4. IPTV traffic intensity parameter as a function of upper Pareto boundary

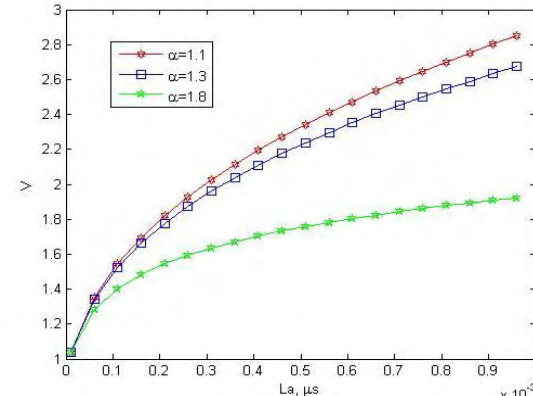


Fig. 5. coefficient of variation of intervals in the output stream as a function of the upper limit of the Pareto distribution for VoIP traffic flow

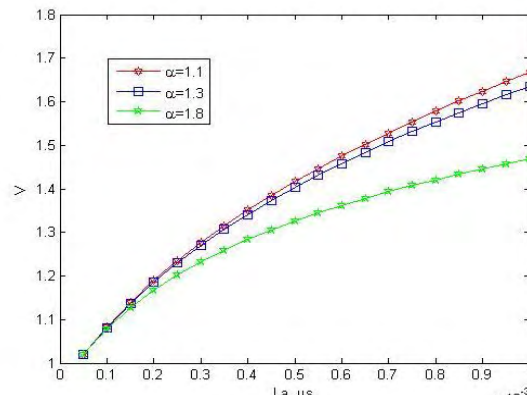
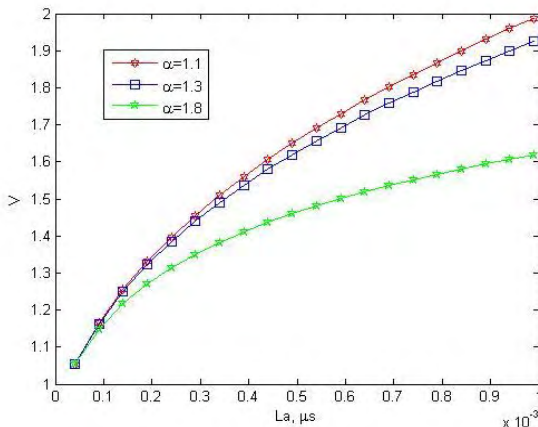
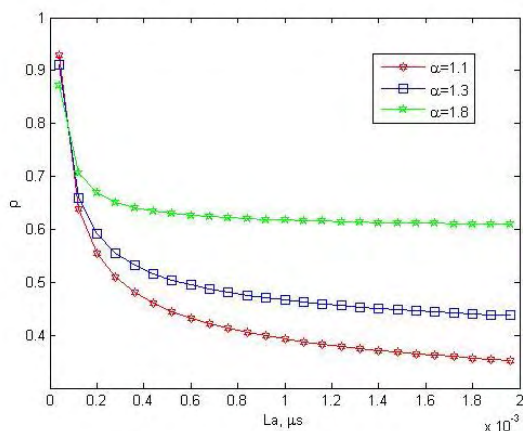


Fig. 6. Coefficient of variation of intervals in the output stream as a function of the upper limit of the Pareto distribution for Data traffic flow



**Fig. 7.** Coefficient of variation of intervals in the output stream as a function of the upper limit of the Pareto distribution for IPTV traffic flow



**Fig. 8.** Traffic intensity parameter as a function of maximum value of interval time between incoming requests for IPTV traffic flow

#### IV. CONCLUSION

The scope of this paper focused on the creation of an analytical model which describes traffic flow processes in a part of PON network, like OLT. Bounded Pareto Distribution was chosen and substantiated for representation of network traffic stochastic process modeling. General queuing model G/G/1 was chosen for presentation of the mathematical model. All calculations were carried out utilizing MATLAB.

The results present coefficient of intervals variation in the output streams as a function of the upper limit of the Pareto distribution for different traffic flow. Traffic intensity parameter has been received as a function of maximum value of interval time between incoming requests for IPTV traffic flow and for different shape parameters.

The preliminary obtained results can be used for prediction of OLT processes on depends of traffic flow parameters.

#### ACKNOWLEDGEMENT

The work is conducted under the grant of the Project BG051PO001-3.3.06-0005, Program ‘Human Resources Development’.

#### REFERENCES

- [1] Altera corporation, Implementing Next-Generation Passive Optical Network Designs with FPGAs, White Paper, 2010.
- [2] W. E. Leland, M. S. Taqqu, W. Willinger and D. V. Wilson, On the self-similar nature of Ethernet traffic, IEEE/ACM Transactions on Networking, Vol.2, pp. 1-15, 1994.
- [3] M. E. Crovella and A. Bestavros, Self-Similarity in World Wide Web Traffic Evidence and Possible Causes, IEEE/ACM Transactions on Networking, 1997.
- [4] O. Sheluhin, S. Smolskiy and A. Osin, Self-Similar Processes in Telecommunications, John Wiley & Sons, 2007.
- [5] K. Park and W. Willinger, Self-Similar Network Traffic and Performance Evaluation, John Wiley & Sons, 2000.
- [6] Matjaž Fras, Jože Mohorko and Žarko Čučej Modeling and Simulating the Self-Similar Network Traffic in Simulation Tool, Telecommunications Networks - Current Status and Future Trends, Dr. Jesús Ortiz (Ed.), ISBN: 978-953-51-0341-7, InTech, pp. 354, 2012.
- [7] Abdelnaser Adas, “Traffic Models in Broadband Networks”, IEEE Communications Magazine, pp. 82-89, Jul. 1997.
- [8] [http://en.wikipedia.org/wiki/Pareto\\_distribution](http://en.wikipedia.org/wiki/Pareto_distribution).
- [9] Jingjing Zhang and Nirwan Ansari, Yuanqiu Luo, Frank Effenberger, and Fei Ye, “Next generation PONs: A Performance investigation of candidate architectures for Next-Generation Access Stage 1”, IEEE Communications Magazine • pp. 49-57, August 2009.
- [10] Galkin A.M., Simonina O.A, Yanovsky G.G. Analysis of IP-oriented multiservice networks characteristics with consideration of traffic's self-similarity properties, IEEE Russia Northwest section: proceedings. St-Petersburg, V. 2. C, pp. 155-158, 2005.
- [11] L G. Kazovsky, N. Cheng, Wei-Tao Shaw, D Gutierrez, Shing-wa Wong, “Broadband Access Networks”, John Wiley & Sons, 2011.
- [12] Commscope, “EPON-GPON comparison”, White Paper, 2012 [www.commscope.com](http://www.commscope.com)

# Development of algorithm and simulation program for audio and video information quality estimation in multimedia systems

Kalina Peeva<sup>1</sup>, Aleksander Bekiarski<sup>2</sup> and Snejana Pleshkova<sup>3</sup>

**Abstract –** This paper examine the use of program system Matlab, as a tool for creating an algorithm and a program for analysis and quality estimation of the reproduced video and audio information in multimedia systems. As a basis of development in this paper is the widespread standard for digital television (DTV). The purpose of this article is to create a simple simulation model of the DTV standard, for transmission of video and audio information. The developed algorithm and simulation program can be used for simulations of professional measurements or in students education to study the transmission of digital multimedia content with DTV standard, for additionally protected terrestrial channel, intended to secure the information against the possible existence of negative factors such as the occurrence of interference and noise in the communication channel within a chosen type of digital television system with DTV standard. Presented are the experimental results of the analysis for the reliability and the effectiveness of the applied algorithm, obtained during the simulation program.

**Keywords –** Digital television, DVB standard, Digital image, Communication channel model, Quality of video and audio information.

## I. INTRODUCTION

In the past few years the international approved standard DVB for digital broadcasting in television and video multimedia systems is successfully found wide continuity in number of areas and is earned popularity especially in the countries from EU zone [1, 2]. Depending on the signals propagation mode there are tree existing paths – terrestrial, cable and satellite – which shall comply with the technical capabilities and the audience needs. In this paper when developing an algorithm and simulation program will be use the following generalized block (Fig. 1), including the basic for the DVB system functional blocks [3], regardless of the type of transmitting channel terrestrial, cable or satellite [4, 5].

The specific characteristics of these types of video communication systems will be reflected in the simulation model by specifying the relevant parameters of the communication channel (terrestrial, cable or satellite) during

<sup>1</sup>Kalina Peeva is with the Faculty of French Education in Electrical Engineering at Technical University of Sofia, 8 Kl. Ohridski Blvd, Sofia 1000, Bulgaria. E-mail: [kala\\_peeva@yahoo.com](mailto:kala_peeva@yahoo.com)

<sup>2</sup>Aleksander Bekiarski is with the Faculty of Telecommunications at Technical University of Sofia, 8 Kl. Ohridski Blvd, Sofia 1000, Bulgaria. E-mail: [aabbv@tu-sofia.bg](mailto:aabbv@tu-sofia.bg)

<sup>3</sup>Snejana Pleshkova is with the Faculty of Telecommunications at Technical University of Sofia, 8 Kl. Ohridski Blvd, Sofia 1000, Bulgaria. E-mail: [snegpl@tu-sofia.bg](mailto:snegpl@tu-sofia.bg)

the experimental verification of the proposed model of algorithm and simulation program of DVB system.

The goal of this article is to develop algorithm and simulation program for the presented in Fig. 1 the main blocks, which formed the transmitter and the receiver parts of the DVB system and to use for simulations of professional measurements or in students education to study the transmission of digital multimedia content with DTV standard.

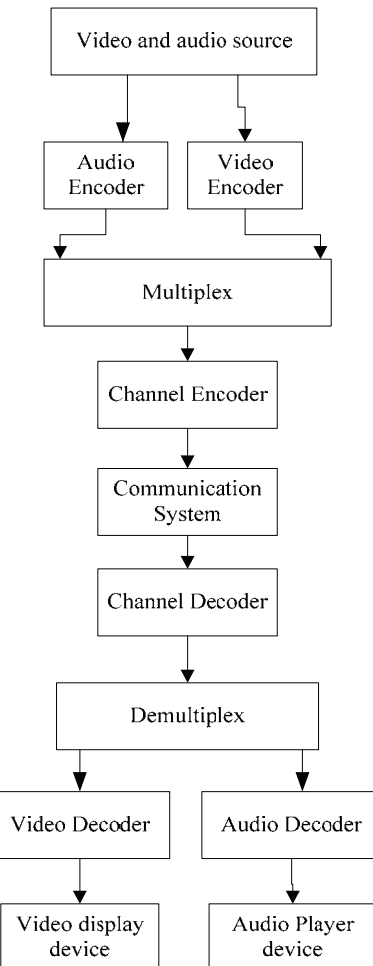


Fig. 1 Functional block scheme of DVB system

## II. APPROACH TO THE DEVELOPED ALGORITHM

The developed algorithm is focused and describes the preparation of simulation model and analysis for digital video transmission and reproduction of informational signals, which meets the established standard DTV. The given test signals

represent the consistent data, contained in the information. Because of the requirements in the DVB standard, they are initially digitally converted in most appropriate color space YCbCr, then compressed, multiplexed together, interleaved and finally shaped by a channel coding in an output binary stream form, ready for submission in the communication channel model. All actions, support by the decoder devices in the receiver performs an opposite order, ensuring a quality video display.

The main milestones and key moments ensuring the multimedia data processing are illustrated at the main block diagram at Fig. 2. Here for the simplicity is presented only the video part of the appropriate multimedia information, assuming the similarity of the algorithm if the video information is with the accompanied audio information.

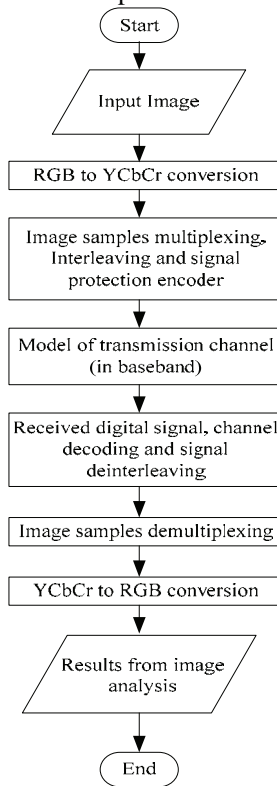


Fig. 2 Functional block scheme of processing, transmission and receiving the informational signals in multimedia system at DVB standard

One of the goals of the simulation program is the creation of a suitable functional scheme for simulation model, which will be applicable for practical realization in the specific science-oriented Simulink space.

### III. SIMULATION MODEL, IMPLEMENTED ON MATLAB PROGRAM SYSTEM

#### A. Block scheme

The original input image could be selected from a file and saved in Matlab Workspace like digital uncompress content in

true RGB colors as required the main resolution of DVB standard.

Fig. 3 shows the general simulation program model, developed by Matlab program Simulink system and includes the transmitter, a communication channel model and the receiver part, as follows.

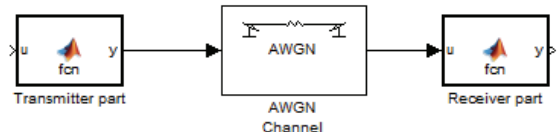


Fig. 3 Block scheme of the simulation program model for video transmission by DVB standard

The digital RGB image shall be subjected to color space conversion, which results in yielding the three separate Y, Cb and Cr components of transmission signal.

As the DVB standard supports color sub-sampling, in the simulation model has been added a bloc for color sub-sampling, which compress the two color components Cb and Cr and reduce the redundant color information. Therefore the both signals Cb and Cr for transmission are presented in color formats (like MPEG1 or MPEG2) for images, specified by the operator. Generating the multiplexed digital data sequence is individual and depends from the chosen color sub-sampling format and its application in particular case. The processed digital signals are submitted in communication channel for distribution. The output signals are recorded in Matlab Workspace as variables or matrices with names *Yout*, *Cbout* and *Crout*. The digital sequence is standardized and meets the ITU-R 601 Recommendations and generates multiplex successive frames of image. The output signals *Yout*, *Cbout* and *Crout* are multiplexed to form a completed binary signal, which is protected against transmission errors by cascade coding with Error Correction Codes and subsequent interleaves.

The described above preprocessing processes as appropriated operations in the transmitting part of the general Simulink model (Fig. 3.) are illustrated on Fig. 4.

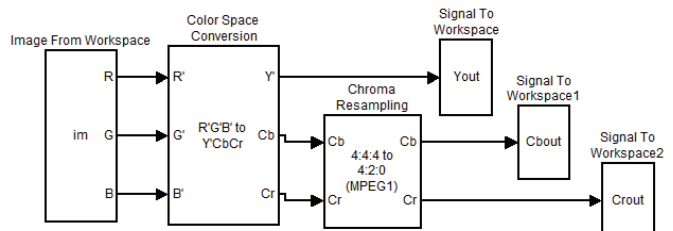


Fig. 4 Block scheme of input image preprocessing levels, composed in Simulink space

The performed in the receiving part actions (Fig. 5.) follow a reverse order to those, described in the transmission part of the DVB system. The only difference is the interpolation of video data, which depends of the used color sub-sampled format and is final step of analysis. As shown on Fig. 5, the three components of the signal are taken from the Matlab Workspace, where they are previously recorded after the signal transmission. The two color components *Cb* and *Cr* are reconstructed with the same, but opposite, values for color up-

sample format, as those performed by the color sub-sample format in the transmission part. After decoding, the three signal components are converted back into the original RGB color space and the received reconstructed image sequences are reproduced on video viewer.

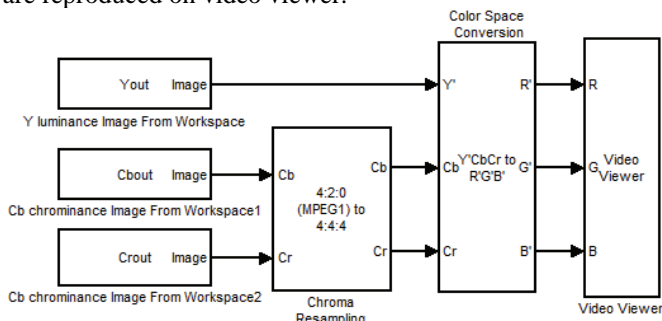


Fig. 5 Block scheme of image reconstruction levels, composed in Simulink space

#### B. Digital image, chosen for the developed simulation

The uncompressed digital image used in DVB model consists of three components, indicated as  $Y$  - component of luminance signal,  $Cb$  and  $Cr$  – sub-sampled components of color signals (Table I) with standard sampling frequency  $F_s$  (Table II) :

$$Y = 0.257R + 0.504G + 0.098B + 16 \quad (1)$$

$$Cb = -0.148R - 0.291G + 0.439B + 128 \quad (2)$$

$$Cr = 0.439R + 0.368G + 0.071B + 128 \quad (3)$$

TABLE I

COLOR SUBSAMPLING FORMATS AND ACHIEVED IMAGE RESOLUTIONS

Format	Resolution Y		Resolution CbCr	
	horizontal [pixels]	vertical [pixels]	horizontal [pixels]	vertical [pixel]
4:4:4	720	576	720	576
4:2:2	720	576	360	576
4:2:0	720	288	360	288

TABLE II

SAMPLING FREQUENCIES AND ACHIEVED DATA RATES

Signal	4:4:4		4:2:2		4:2:0	
	$F_s$ [MHz]	H [Mbps]	$F_s$ [MHz]	H [Mbps]	$F_s$ [MHz]	H [Mbps]
Y	13.5	108	13.50	108	13.50	108
Cb	13.5	108	6.75	54	6.75	27
Cr	13.5	108	6.75	54	6.75	27
MUX	40.5	324	27.00	216	27.00	162

#### C. Error Protection Coding in DVB

The principle of digital broadcasting, with coding against errors, in digital TV is determined by adding some extra information to the coded digital signal in the channel. Adding

more information leads to increase the volume of information and requires the presence of specific channel decoder device in the receiving part. The decoder finds the position of each incorrect bit by evaluation of the extra information, which is also possibly affected by transmission errors. Two relevant methods for providing an error protection are applied, under the common name Forward Error Correction. The first is by Reed-Solomon encoding (FEC1) and the second - by convolution encoding with interleaving (FEC2) [6].

#### IV. EXPERIMENTAL RESULTS

The experimental results from the analysis of digital signal transmission over a communication channel model, affected by different levels of transmission errors, are briefly illustrated below. In this article only the results for video part of multimedia information are presented in form of original and received images. The results for audio part of multimedia information are also tested but are not presented here because they usually are estimated with precisely with different subjective and objective methods, which are object of another article.

The original images are submitted using the communication channel with known error to noise ratio value defined as the ratio of bit energy to noise power spectral density  $E_b/N_0$  (dB). It is possible to set and change the error levels, in order to follow different scenarios. Here are presented the results using two different values error to noise ratio small ( $E_b/N_0 = 2, dB$ ) and large ( $E_b/N_0 = 12, dB$ ). The received color image quality is affected by the corresponding transmission errors. Fig. 6 shows the original color image, Fig. 7.a and Fig. 7.b displays the received color images for chosen values of error to noise ratio small ( $E_b/N_0 = 2, dB$ ) and large ( $E_b/N_0 = 12, dB$ ), respectively and Fig. 8 presents the absolute difference between the two images (original and received), where black pixels mean the full accordance, and white regions indicate the transmission errors.

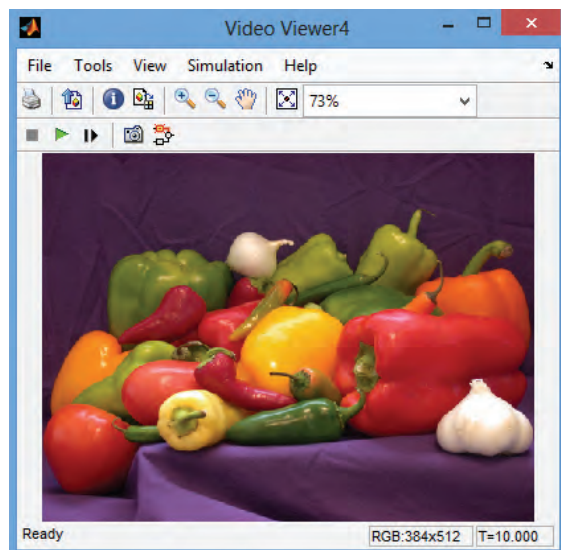
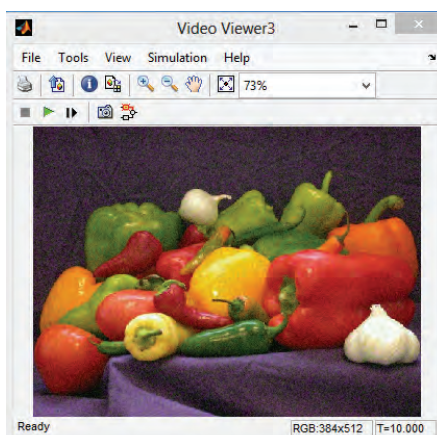


Fig. 6 Original color image before transmission over a noisy communication channel



(a)



(b)

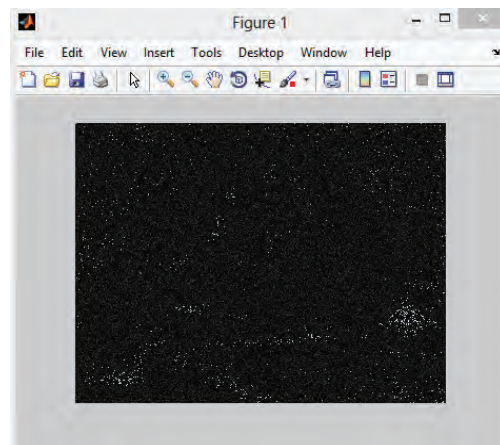
Fig. 7 Received color images, affected by transmission channel errors and noise distortions for two different values error to noise ratio (a) small ( $Eb/No = 2, dB$ ) and (b) large ( $Eb/No = 12, dB$ )

## V. CONCLUSION

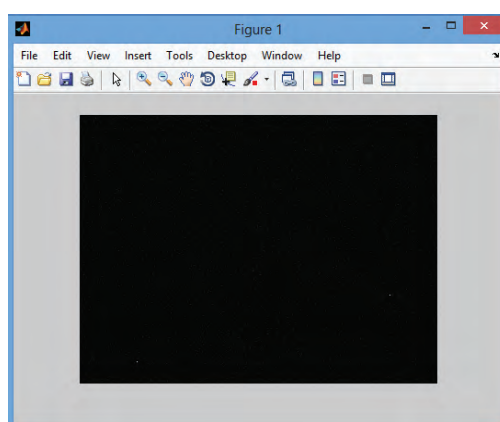
From Fig. 8 is seen that visual observation and estimation of received image quality from images of the absolute difference between the original and received images can be used because for small values ( $Eb/No = 2, dB$ ) of error to noise ratio (Fig. 7.a.) the white regions, which indicate the transmission errors are more visible compared with the same white regions for large values ( $Eb/No = 12, dB$ ) of error to noise ratio (Fig. 7.b.), where black pixels, which mean the full accordance with of received to the original images are dominated.

## ACKNOWLEDGEMENT

This paper was supported by Technical University – Sofia inner program to support PhD research projects under Contract 132 PD0025-07: "Development of algorithms for quality estimation of audio-visual information in multimedia computer systems and networks".



(a)



(b)

Fig. 8 Image of the absolute difference between the original and the error-affected image for two different values error to noise ratio (a) small ( $Eb/No = 2, dB$ ) and (b) large ( $Eb/No = 12, dB$ )

## REFERENCES

- [1] Michael Robin, Michel Poulin. Digital Television Fundamentals (Hardcover). McGraw-Hill, 2000.
- [2] Digital Video Broadcasting (DVB); A Guideline for the Use of DVB Specifications and Standards. DVB Document A020 Rev. 1, May 2000.
- [3] Al. BekiarSKI, Television Systems, Technical University – Sofia Press, Sofia, 2009.
- [4] Dimitrov D., Velchev Y., "Communication Protocol for Medical Mobile Network" 48 Internationales Wissenschaftliches Kolloquium, Ilmenau, Germany, 2001.
- [5] Dimitrov D., Y. Velchev, St. Kolev, Kl. Angelov, "Infrared Measurements Signal Processing", TELECOM'2009, 8-9 October, St. Constantine, Varna, BULGARIA, 2009.
- [6] Tomáš KRATOCHVÍL, Utilization of MATLAB for Digital Image Transmission Simulation Using the DVB Error Correction Codes, RADIOENGINEERING, VOL. 12, NO. 4, DECEMBER 2003.

# Comparative Analysis of Modern Wireless Communication Systems Relevant to Smart Metering

Mariana Shotova<sup>1</sup>, Georgi Nikolov<sup>2</sup> and Vencislav Valchev<sup>3</sup>

**Abstract –** In this paper a comparative analysis of modern wireless communication systems relevant to smart metering is presented. Several of the most widely used standards are compared and their advantages towards the smart metering system are presented. Electrical parameters of possible protocol implementation using readily available modules are given as well.

**Keywords –** wireless communication system, Zigbee, WiFi, bluetooth, smart metering.

Experiments with a four modules were conducted. Some of the electrical parameter of the modules are given in Section III of the current article.

## II. WIRELESS COMMUNICATION PROTOCOLS USED IN THE SMART METERING

### A. WiFi (802.11)

Smart Grid solutions are being driven by the desire for more efficient energy usage worldwide. The Smart Grid communications network will be a heterogeneous network based on many different standards. Wi-Fi® technology will certainly be part of any future Smart Grid. [1].

Wi-Fi offers many benefits for Smart Grid applications:

- Mature technology with an established worldwide testing network
- Suitable for personal-area, home-area, and even wide-area networking
- Government-grade WPA2™ security
- Portfolio includes low bandwidth/low power designs, high-gain/high performance systems and points in between – all can interoperate
- Advanced mechanisms for reliability, robustness and manageability
- Continued technology innovation now and in the future, leveraging an interoperable set of baseline standards
- Economies of scale drive cost effectiveness

A key advantage of Wi-Fi for the WAN Smart Grid is its use of free, unlicensed spectrum. This makes it practical for a city or utility to own and operate a large private wireless network for Smart Grid. Cellular data networks can provide the required service, but are usually owned and operated by large carriers who pay for the frequency licenses.

The Smart Energy Profile helps build a framework for Smart Grid Applications. Version 2.0 of the Smart Energy Profile was specified by NIST as a PHY independent protocol, which therefore could be implemented in Wi-Fi systems. The only work required for an implementer would be to port SEP 2.0 software to Wi-Fi-based devices.



Fig. 2. Tested Wi-Fi module

Fig. 1. Smart meters communication technology evolution

There are many different smart meters on the market today, and most of them use some kind of proprietary protocol to communicate with the service provider. The current trend however is to standardise the communication. Which communication protocol the future smart meters will use is still not decided. The scope of the article is to present some of the possible communication systems that has high probability to win the contest.

<sup>1</sup>Mariana Shotova is with the Faculty of Electronics at Technical University - Varna, 1 Studentska st, Varna 9010, Bulgaria, E-mail: mshotova@tu-varna.bg.

<sup>2</sup>Georgi Nikolov is with the Faculty of Electronics at Technical University - Varna, 1 Studentska st, Varna 9010, Bulgaria, E-mail: mshotova@tu-varna.bg.

<sup>3</sup>Vencislav Valchev is with the Faculty of Electronics at Technical University - Varna, 1 Studentska st, Varna 9010, Bulgaria, E-mail: mshotova@tu-varna.bg.

### B. Bluetooth (802.15.1)

Until recently, Bluetooth was used mainly for connecting mobile /personal/ devices (mobile phones, mice and keyboards, barcode scanners and so on.). However in 2010 the Bluetooth Special Interest Group has formed a Smart Energy Study Group to explore application in smart electric grids. CSR, Broadcom and Emerson Electric are the initial members of the group.

The Bluetooth technology continues to evolve, building on its inherent strengths—small-form factor radio, low power, low cost, built-in security, robustness, ease-of-use, and ad hoc networking abilities. This evolution now provides manufacturers and consumers with three options for connecting wirelessly – Classic Bluetooth technology for use in a wide range of consumer electronics; Bluetooth high speed technology for the transfer of video, music and photos between phones, cameras, camcorders, PCs and TVs; and Bluetooth low energy for low power sensor devices and new web services within the healthcare, fitness, security, home entertainment, automotive and automation industries [5].

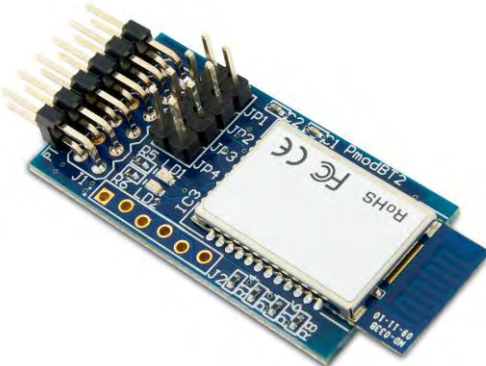


Fig. 3. Tested Bluetooth module

### C. ZigBee (802.15.4)

ZigBee is a low-power wireless communications technology designed for monitoring and control of devices, and is maintained and published by the ZigBee Alliance [7]. Home automation is one of the key market areas. Zigbee works on top of the IEEE 802.15.4 standard [8], in the unlicensed 2.4 GHz or 915/868 MHz bands. An important feature of ZigBee is the possibility to handle mesh-networking, thereby extending the range and making a Zigbee network self-healing. The Zigbee Smart Energy Profile [9] (numbered 0x0109) was defined in cooperation with the Homeplug Alliance in order to further enhance earlier HAN (Home Area Network) specifications. The profile defines device descriptions for simple meter reading, demand response, PEV charging, meter prepayment, etc. Recently a collaborative effort between the Zigbee Alliance and the DLMS UA was announced to define a method to tunnel standard DLMS/COSEM messages with metering data through ZigBee Smart Energy networks. Considering the low

power requirements, robustness, availability of cheap Zigbee “kits” and the specific profile for metering applications, Zigbee has a lot of potential in home area networks.

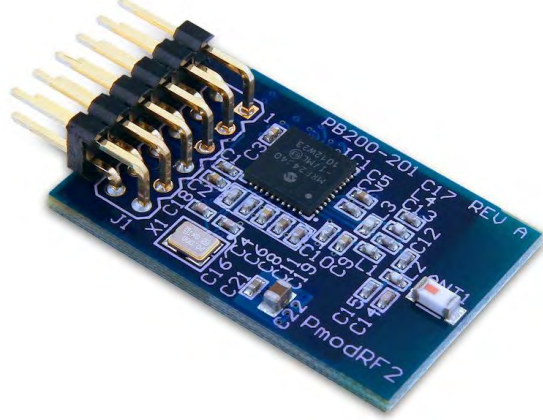


Fig. 4. Tested ZigBee module

#### D. KNX

KNX [6] is the result of the joint effort of three European consortia working on home and building control, namely Batibus, EIB and EHS. KNX was made into standard ISO/IEC 14543-3-x in November 2006. KNX provides application models for distributed automation, configuration and management schemes, device profiles and a communication system (media and protocol stack). Possible communication media are twisted pair cabling, RF, IP/Ethernet or sometimes PLC. Each bus device has some sort of certified BCU (Bus coupler unit) that is typically flush mounted for switches, displays and sensors. To manage network resources, KNX uses both point-to-point and multicast communication. When a device publishes a data-point (an input, output or parameter), it is assigned a multicast group address. A data-point in another device having the same address will then receive updates and be able to notify the local application. Thus all local applications in a group form a so-called “distributed application”. KNX aims to provide a complete solution for home and building automation and is backed by a lot of manufacturers worldwide.



Fig. 5. Tested KNX module

#### E. EN 13757 / M-Bus

EN 13757 (Meter bus) is an European standard [4] for the remote interaction with utility meters and various sensors and actuators which was developed at the University of Paderborn. M-Bus uses a reduced OSI layer stack. Several physical media are supported including twisted pair and wireless M-Bus (in the ISM band). Primary focus of the standard is on simple, low-cost, battery powered devices. As this standard is already widely used in meters and reasonably future proof it is a good contender for local data exchange in the smart grid.

### III. COMPARISON BETWEEN PROTOCOLS

Comparison of some parameters for the discussed protocols is presented in Table 1, while some electrical parameters of modules used to realize the communication is given in Table 2.

TABLE I  
COMPARISON OF THE DIFFERENT WIRELESS STANDARDS

standard	WiFi	Bluetooth	ZigBee	KNX
Frequency band	2.4GHz	2.4 ÷ 2.48GHz	868MHz	868.0 ÷ 870.0
Serial data rate	56Mbps	1Mbps	250kbps	32kbps
Number of RF channels	13	79	16	1
Channel bandwidth	22MHz	1MHz	0.3/0.6MHz	2MHz
Interference immunity	FHSS	DSSS, OFDM, CCK	DSSS	-
Nominal range	10m	10-100m	100m	10-100m

TABLE II  
COMPARISON OF THE POWER CHARACTERISTICS OF DIFFERENT WIRELESS STANDARDS

standard	WiFi [10]	Bluetooth [11]	ZigBee [12]	RC1180-KNX [13]
Supply voltage	3.3V	3.3V	2.1 ÷ 3.6 V	2.0 ÷ 3.9 V
Output power	+10dBm	+4dBm	+3dBm	+10dBm
Power consumption	Standby/Idle	250 µA	25 mA	5.7 mA
	Normal mode	80mA	3 mA	14.3mA
	Low power	10mA	8 mA	0.4 mA

Sniff					
Deep sleep	0.1 µA	26 µA	0.02 µA	-	-
Operating temperature range	-40C to +85C				

### IV. CONCLUSION

In this paper, an overview was given of communication standards relevant to the smart grid and smart house concepts. Of course, many more technologies are out there, but most of them lack wide acceptance, flexibility, or are still nascent or vendor-controlled. The latter is especially true in the home and building automation space.

### ACKNOWLEDGEMENT

This paper is prepared in the frames of Project MU03/164 - "Intelligent systems for energy management and control of consumer expenses", Ministry of Education Youth and Science, Bulgarian National Science Fund.

### REFERENCES

- [1] Wi-Fi® for the Smart Grid Mature, Interoperable, Secure Technology for Advanced Smart Energy Management Communications, 2010 Wi-Fi Alliance.
- [2] Open Public Extended Network Metering. [Online]. Available: [www.openmeter.com](http://www.openmeter.com)
- [3] Kema Consulting, "Smart Meter Requirements - Dutch Smart Meter specification and tender dossier V2.31," Jan. 2009.
- [4] EN 13757 Communication systems for remote reading of meters, European Committee for Standardization (CEN) Std.
- [5] Bluetooth SIG Brings Bluetooth to the Smart Grid, Sensors magazine, February 2010
- [6] IEC 14543-3 Information technology - Home electronic system (HES) architecture, International Electrotechnical Commission Std
- [7] The ZigBee Alliance. [Online]. Available: [www.zigbee.org](http://www.zigbee.org)
- [8] IEEE 802.15.4-2006 Telecommunications and information exchange between systems - Local and metropolitan area networks – Specific requirements Part 15.4: Wireless Medium Access Control (MAC) and Physical Layer (PHY) Specifications for Low Rate Wireless Personal Area Networks (LR-WPANs), IEEE Std.
- [9] Zigbee Standards Organisation, "Zigbee smart energy profile specification," Dec. 2008. [Online]. Available: [www.zigbee.org/Products/DownloadTechnicalDocuments/tabid/465/Default.aspx](http://www.zigbee.org/Products/DownloadTechnicalDocuments/tabid/465/Default.aspx)
- [10] PmodWiFi™ Reference Manual
- [11] PmodBT2™ Reference Manual
- [12] PmodRF2™ Reference Manual
- [13] RC1180-KNX, KNX® RF Transceiver Module with Embedded protocol datasheet
- [14] V. C. Güngör, D. Sahin, T. Kocak, S. Ergüt, C. Buccella, C. Cecati, G. P. Hancke, "Smart Grid Technologies: Communication Technologies and Standards", IEEE Transactions on Industrial Informatics, vol. 7, no. 4, pp. 529-539, November 2011.

**This Page Intentionally Left Blank**

# Mobile Wireless Sensor Networks Localization

Vasil Dimitrov<sup>1</sup>, Rozalina Dimova<sup>2</sup> and Teodora Trifonova<sup>3</sup>

**Abstract –** The paper presents mobility influence to wireless sensor network(WSN) applications monitoring, requiring information on the location of the sensor node. Although the deployment of WSN never predicts full static, the mobility is faced range of challenges, which should be overcome.

In this paper we simulate the mobility of the wireless sensor network using the help of MatLab 7.13 on the different types of movement of the nodes - constant speed and constant speed with random walk. Results improve the accuracy of localization using an algorithm to predict the unknown position. Evaluating error in localization is performed based on the mean square error.

**Keywords –** Wireless sensor, Localization, Mobile WSN

## I. INTRODUCTION

Wireless Sensor Networks (WSN) are a technology which allows observing some natural phenomena in time and space. At first the wireless sensor networks were used mostly for military applications, but in time they started to come in applications, comprehending all different areas, including observation, chemical and biological monitoring of the locations, etc. Some of these applications comprehend a wide specter of goals. For example the function of observation goes from finding intruders to watching patients in old age in their homes [1]. For environmental applications include monitoring on the ground [2], tracing the populations of amphibians [3], and even the early detecting underwater sea earthquakes that form tsunami [4]. Other advanced applications of the WSN include identification and applying of chemical, biological, radiological, nuclear and explosive phenomena and infrastructural monitoring [5]. The technological restrictions imposed by the nature of WSN with the increased need in many applications are fertile soil for research.

Wireless Sensor Networks are built from large number of separate devices (sensors) capable of tracking signals from the environment [6]. The sensors have limited potential when it comes to communication, processing and storage of information.

Each sensor node contains four basic components: power supply that supports all sensor operations; sensitive unit to collect measurements in the environment and translates the analog signal of the observed phenomena (energy) into a

<sup>1</sup>V.Dimitrov is with the Technical University of Varna, ul. Studentska 1, 9010 Varna, Bulgaria (phone: +359-52-383350; e-mail: v\_1986@abv.bg).

<sup>2</sup>R.Dimova is with the Technical University of Varna, ul. Studentska 1, 9010 Varna, Bulgaria; (phone: +359-52-383350, e-mail: rdim@abv.bg).

<sup>3</sup>T. Trifonova is with the Technical University of Varna, ul. Studentska 1, 9010 Varna, Bulgaria (phone: +359-52-383350; e-mail: t\_t\_trifonova@abv.bg ).

digital signal by an analog-digital converter (ADC), a processor to processes digital signal, and transceiver, which is responsible for all sensor communications [7].

## II. ISSUES ASSOCIATED WITH THE DESIGN OF SENSOR NETWORKS

The technological restrictions of the sensors, combined with the area of application, largely determine the design of WSN. In industrial applications, the sensors are located on specific places compared to interest; the same goes for structural monitoring. In different applications the sensors often combine in one-dimensional array or even relatively network [8]. In many other situations, depending on the situation and equitable relief deployment is neither feasible nor practical. In such cases, methods of deployment are often equivalent to the random placement of sensors. For example, inaccessible area as contaminated land or battlefield requires tracking of mobile sensor nodes, which leads to random distribution of sensor locations. In underwater WSN, nodes are usually anchored to the seabed and associated floating buoy, which regulates their positions. The inaccuracy of this method is close to that of the random distribution. Another example for mobile sensor networks is the integration of sensor nodes in order to monitor and measure the properties of materials such as polymeric structures, rock landslides, avalanches, etc..

In general, the sensor network under any distribution must satisfy the two constraints [9]: coverage (all or most of the region of interest to be within the scope of observation and at least one sensor) and coherence (each sensor can communicate with each other directly or through sensor information transmission in neighboring nodes). These restrictions are crucial to wireless sensor networks to be able to perform functional tasks

In this paper we explore issues related to the localization of mobile sensor nodes .

## III. NETWORK MODEL

In our analysis we assume that the system is a set of sensors S on an unknown area randomly distributed with density  $\rho_s$  within a zone A, and a set of specially equipped nodes L, which we call beacons, and a certain guidance randomly distributed with density  $\rho_L$ .

Sensors are equipped with omnidirectional antennas and transmit power  $P_s$  and the beacons are equipped with M omnidirectional antennas by the factor of amplification  $G > 1$  and can transmit with power  $P_L > P_s$ . Attenuation of the signal is proportional to the exponent ( $\gamma$ ) the distance between two nodes d.

$$G=1 \text{ in omnidirectional antennas and } \frac{P_r}{P_s} = cG^2d^{-\gamma} \text{ at}$$

$2 \leq \gamma \leq 5$ , where  $c$  is proportional constant and  $P_r$  is the minimum power required for communication. If  $r_{ss}$  denotes the communication range between two sensors and  $r_{sL}$  denotes the communication range between sensor unit and a beacon then:

$$\frac{P_r}{P_s} = c(r_{ss})^{-\gamma}, \quad \frac{P_r}{P_s} = cG(r_{sL})^{-\gamma} \quad (1)$$

It follows that  $r_{sL} = r_{ss}G^{1/\gamma}$ . In the same way if  $r_{ls}$  assigns the communication between beacon and sensor node and  $r_{LL}$  is the range between the thrust bearing unit and another unit has the following relationship  $r_{LL} = r_{ls}G^{2/\gamma}$ . For short we assign  $r_{ss}$  as  $r$  and  $r_{ls}$  as  $R$ . Table 1 summarizes the four possible ways of communication.

TABLE 1  
COMMUNICATIONS BETWEEN SENSOR AND A BEACON

Sender	Receiver	
	Sensor	Beacon
Sensor	$r$	$rG^{1/\gamma}$
Beacon	$R$	$RG^{2/\gamma}$

In order to achieve the ratio  $\frac{R}{r}$  the communication range the beacons must have to transmit power  $P_L = \left(\frac{R}{r}\right)^\gamma (P_s / G)$ .

Bearing in mind that the sensors are devices with low power transmitters and supporting units with larger capacities are known following communication options. A typical sensor node has range between 3 to 30 m with a maximum power of transmission  $P_s=0.75$  mW. Hence the beacons have to transmit with power  $P_g=75$  mW. To achieve communication range  $\frac{R}{r}=10$  where  $\gamma=2$  without even using an omnidirectional

antennas. Having in mind that the omnidirectional antenna is important for the operating frequency of the sensor, if the design of sensor networks to provide high operating frequency, it will greatly easier to use the directional antennas in the core nodes. At a frequency 2.4 GHz and half-wavelength the size of the cylindrical antenna element 8 will have a radius 8 cm at a frequency of 5 GHz the size of an antenna will be the same tap having a radius of 3.3 cm. As for beacons are allowed more glam dimensions of the sensors, equipping them with directional antennas is possible decision to increase the communication range.

#### IV. SIMULATION STUDIES OF MOBILE WSN LOCALIZATION

Let's take a look at L beacon with coordinates  $(x_i, y_i)$  when  $i=1, \dots, L$  which are randomly arranged in two-dimensional plane (2D) of dimensions  $(x_{max}, y_{max})$ . The coordinates of the beacons are well known. During each simulation position K of the support node is a constant. In this valley are also randomly spaced S unknown nodes with coordinates  $(x_{0i}, y_{0i})$   $i=1, \dots, S$ . From the standpoint of the distribution measurements were

made in the condition of direct visibility. The actual distance between a beacon and an unknown node is  $d_i$  and it may be defined as:

$$d_i = \sqrt{(x_0 - x_i)^2 + (y_0 - y_i)^2} \quad (2)$$

Measured distance is:

$$r_{di} = d_i + \varepsilon_i \quad (3)$$

where  $\varepsilon_i \sim N(0, \sigma_i^2)$   $\varepsilon$  is the zero mean Gaussian noise with variance  $\sigma_i^2$

##### A. Algorithm for tracking the position in the WSN

Our research is based on the following algorithm :

- Step 1: determine the position of each unknown node based on the fixed bearing assemblies.
- Step 2: for all unknown items determining the distance between nodes:

for node  $i : (\hat{x}_{(i)}^0, \hat{y}_{(i)}^0)$ , for node  $j : (\hat{x}_{(j)}^0, \hat{y}_{(j)}^0)$

$$\hat{d}_{i,j}^0 = \sqrt{(\hat{x}_{(i)}^0 - \hat{x}_{(j)}^0)^2 + (\hat{y}_{(i)}^0 - \hat{y}_{(j)}^0)^2} + noise_{i,j}^0 \quad (4)$$

- Step 3: For each unknown movable unit determining the distance to the distance L to S

d- for fixed beacons

$d_{i,j}^{(0)}$  - for unknown nodes

- Step 4: Repeat Steps 2-3 S times - reps to refresh the calculation

$$\hat{d}_{i,j}^\alpha = \sqrt{(\hat{x}_{(i)}^\alpha - \hat{x}_{(j)}^\alpha)^2 + (\hat{y}_{(i)}^\alpha - \hat{y}_{(j)}^\alpha)^2} + noise_{i,j}^{(\alpha)} \quad (5)$$

In this case, the mean square error MSE [10] for the node  $i$  is:

$$MSE_i = \frac{1}{K} \sum_{j=1}^K \left[ \left( x_0 - \hat{x}_{(i,j)} \right)^2 + \left( y_0 - \hat{y}_{(i,j)} \right)^2 \right] \quad (6)$$

$$\text{and } MSE = \frac{1}{S} \sum_{m=1}^{S+1} MSE_j \quad (7)$$

The Cramer-Rao lower bound CRB [11] in this case is:

$$CRB = \frac{4\sigma^2}{L+S} \quad (8)$$

Determine the position of the unknown mobile node will be:

$$\hat{x}(t), \hat{x}(t+1), \dots, \hat{x}(t+10),$$

$$\hat{y}(t), \hat{y}(t+1), \dots, \hat{y}(t+10)$$

The next step can be predicted. In this case, the speed for the next step cannot be determined by these equations:

$$\hat{v}_x T(i) = \frac{1}{i} \sum_{i=1}^i (\hat{x}(i) - \hat{x}(i-1)),$$

$$\hat{v}_y T(i) = \frac{1}{i} \sum_{i=1}^i (\hat{y}(i) - \hat{y}(i-1)),$$

which are used to predict the next position of the unknown node  $\tilde{x}(i+1)$  и  $\tilde{y}(i+1)$ .

$$\tilde{x}(i+1) = \tilde{x}(i) + \hat{v}_x T(i)$$

$$\tilde{y}(i+1) = \tilde{y}(i) + \hat{v}_y T(i)$$

So the next step can be predicted with some accuracy. This algorithm can improve performance of the method of steepest descent, and also the accuracy of the system.

### *E. Simulation results*

In a real environment the unknown node changes its position and having to track the position. Mobility of sensors can be considered as: constant speed and constant speed and random walk. The movement may be divided into ten steps ( $t=1, \dots, 10$ ). The first position is  $t = 1$ . Therefore, each new step may be represented as:  $x(t+1) = x(t) + v_x T$  and  $y(t+1) = y(t) + v_y T$ , where  $v_x T$  and  $v_y T$  is the speed on axis X and the speed on axis y. According to  $v_x T$  and  $v_y T$  the movement is separated in two types:

- Constant speed -  $v_x T = \text{const}$  and  $v_y T = \text{const}$

In this case the velocity of the unknown node is constant for the simulation:  $v=0.1$  ( $v_x=0.1$  and  $v_y=0.1$ ). The movement is divided in ten steps. MSE for each step is calculated and shown in Figure 1. Unknown position cannot be determined with sufficient accuracy. There is one peak. As can be seen in Figure 2, where is a predictive algorithm, unknown position can be determined with sufficient accuracy and lines for each step are too close.

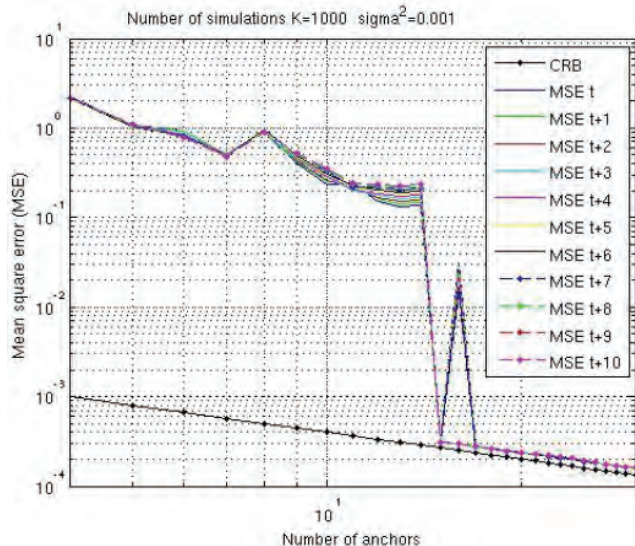


Fig.1. MSE on constant speed.

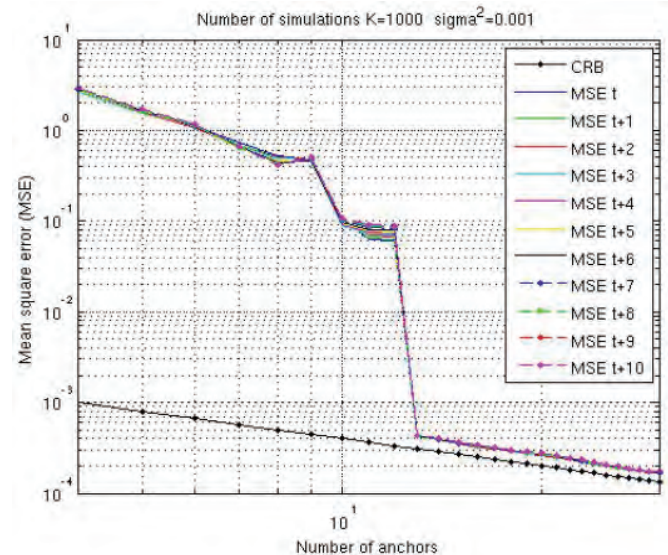


Fig.2. MSE with prediction.

- Constant speed and random walk -  $v_x T = \text{const} + \text{random}$  and  $v_y T = \text{const} + \text{random}$

This is the most realistic movement, because the path from point A to point B doesn't always a straight line. Figure 3 shows a simulation of this case, without prediction, and the necessary support nodes here is about 19-20. By using the predictive algorithm, shown in Figure 4, the number of abutment assemblies for sufficient accuracy has been reduced to 11, and the position of the unknown node is set at approximately the same accuracy for each step.

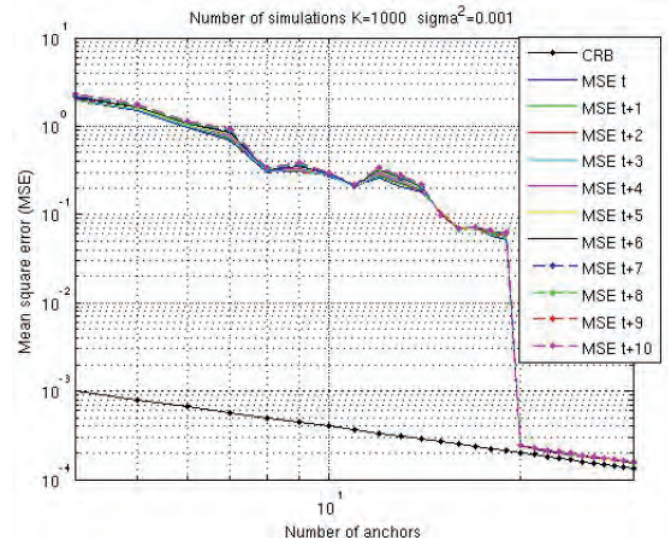


Fig.3. MSE on constant speed and random walk

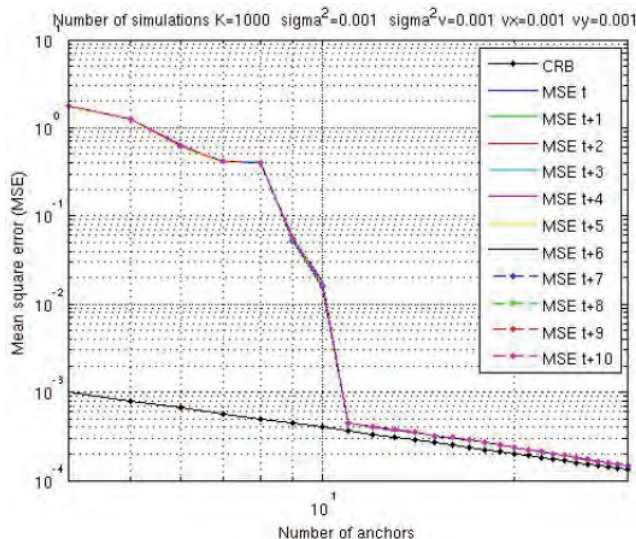


Fig.4. MSE on constant speed and random walk with prediction

## V. CONCLUSION

The mobility of sensor networks helps in monitoring the large number of processes and phenomena. The advantages of mobile WSN over static WSN are better coverage, enhanced target tracking and superior channel capacity.

We examined the localization of the mobile sensor nodes using MatLab 7.13, simulating motion of the nodes - Constant speed and Constant speed with random walk. The algorithm is presented to predict the next position of the sensor node.

The performed tests show that achieved geometric method for determining the position is relatively conveniently locate. The results of the simulations are as follows:

- the number of supporting units for obtaining sufficient accuracy is higher than the theoretical number ;
- increase the number of repetitions to refresh the calculations do not improve accuracy ;
- the prediction algorithm may be applied to improve the localization of unknown nodes .

Future studies, based on these results are to improve communication between mobile sensor nodes and to reduce the cost of the system.

## ACKNOWLEDGEMENT

This paper is conducted under the grant of the Project BG051PO001-3.3.06-0005, Program ‘Human Resources Development’ and scientific project NP 6, supported by FNI-TU-Varna.

## REFERENCES

- [1] R. Steele, C. Secombe, and W. Brookes. Using wireless sensor networks for aged care: the patient's perspective. In Proceedings of Pervasive Health Conference, pages 1-10, 2006.
- [2] A. Mainwaring, J. Polastre, R. Szewczyk, D. Culler, and J. Anderson. Wireless sensor networks for habitat monitoring. In Proceedings of the 1st ACM international workshop on Wireless sensor networks and applications, pages 88-97, New York, NY, USA, 2002.
- [3] Wen Hu, Van Nghia Tran, Nirupama Bulusu, Chun Tung Chou, Sanjay Jha, and Andrew Taylor. The design and evaluation of a hybrid sensor network for cane-toad monitoring. In Proceedings of the 4th international symposium on Information processing in sensor networks (IPSN 2005), page 71. IEEE Press, 2005.
- [4] I.F. Akyildiz, D. Pompili, and T. Melodia. Underwater acoustic sensor networks:research challenges. Ad Hoc Networks Jounal (Elsevier), 18:257{279, March 2005.
- [5] N. Xu, S. Rangwala, K. Chintalapudi, D. Ganesan, A. Broad, R. Govindan, and D. Estrin. A wireless sensor network for structural monitoring. In *Proceedings of the 4th international conference on Embedded networked sensor systems*, New York, NY, USA, November 2004.
- [6] K. J. Bahi, A. Makhoul, and A. Mostefaoui. Localization and coverage for high density sensor networks. In *Proceedings of the 5th Annual IEEE International Conference on Pervasive Computing and Communications Workshops*, pages 295-300, 2007.
- [7] V. Raghunathan, C. Schurgers, Park.S, and M.B. Srivastava, “Energy-aware wireless microsensor networks,” *IEEE Signal Processing Magazine*, Volume: 19 Issue: 2 , March 2002.
- [8] Katenka, E. Levina, and G. Michailidis. Robust target localization from binary decisions in wireless sensor networks. *Technometrics: A journal of statistics for the physical, chemical and engineering sciences*, 50(4):448{461, November 2008.
- [9] J. Bahi, A. Makhoul, and A. Mostefaoui. Localization and coverage for high density sensor networks. In *Proceedings of the 5th Annual IEEE International Conference on Pervasive Computing and Communications Workshops*, pages 295{300, 2007.
- [10] Y. C. Eldar, A. Ben-Tal, and A. Nemirovski, “Robust mean-squared error estimation in the presence of model uncertainties,” *IEEE Trans. Signal Process.*, vol. 53, pp. 168–181, Jan. 2005.
- [11] C. R. Rao, *Linear Statistical Inference and Its Applications*, second ed. New York: Wiley, 1973.

# Laboratory SCADA – System for Control on Railway Traffic

Emiliya Dimitrova<sup>1</sup>

**Abstract –** Supervisory Control and Data Acquisition systems (SCADA) in some important industry sectors, such as production and distribution of electricity, transport management, etc., are crucial for their correct and reliable functioning. The purpose of these systems is centralized data acquisition for remote geographical sites, information processing and generation of managerial impacts.

**Keywords –** SCADA - systems, Railway traffic control.

## I. INTRODUCTION

Scientific and technical revolution, especially in the last two decades, has led to fast development and improvement of technological processes in all sectors of the economy, transport, energy, education etc.

Efficiency of technological processes in industry, transport, energy and communications cannot be achieved without the use of appropriate methods and systems for its control, which are also developing and growing at an exponential pace.

The technical literature is full with reports of specialized automated operational dispatch control on complex objects, and lately with reports of applications of the most modern SCADA – systems [1].

The fast industrial progress set up higher requirements of education quality. The power engineering and the transport are attractive areas for Bulgarian and foreign investment for progress, modernization and expert education. The training under the Bachelor and Master programmes in Telecommunications and Signaling at the Todor Kableshkov University of Transport (VTU) prepares highly qualified experts in telecommunications and signaling in railway and underground transport. A special place is given on the study of remote monitoring and control systems in transport. The VTU's lecturers realize the necessity to train skilled workers for transport needs. A modern laboratory simulator representing SCADA - system will be built.

## II. PURPOSE AND NATURE OF SCADA - SYSTEMS

Automated systems of control and SCADA - systems have the same purpose, namely to remotely control on technological objects without or with as little as possible human involvement. Although somewhat SCADA – systems

<sup>1</sup> Emiliya Dimitrova is with Faculty of Communications and Electrical Equipment at the Todor Kableshkov University of Transport-Sofia, 158 Geo Milev Str., Sofia 1574, Bulgaria,

E-mail: edimitrova@bitex.bg, web page: <http://vtu.bg>.

appears to be a natural development of automated systems of control, there is a significant difference between these two types of systems.

As a rule, both kinds of systems are a product of engineering activity. They are configurable technical software project complexes and have a unique character for each case of application. This difference is in the way of implementation of the management process. In automated systems, the attention of the designers is directed to the technical part – selection of the most appropriate technical devices. However, SCADA - systems appear when the abundance and diversity of electronic computing on the market is rich and the design is only reduced to selecting technical devices, which satisfy the amount of memory, performance and other technical parameters according to the specific requirements of the process. Here the attention of designers is drawn to the creation of the maximal operator's comfort, so that he/she will not think of what to do at the same point but how to deal better with the situation.

## III. STRUCTURE OF SCADA - SYSTEMS

Each SCADA - system consists of three formal levels:

- Dispatching (upper) level;
- Communication level;
- Object (lower) level.

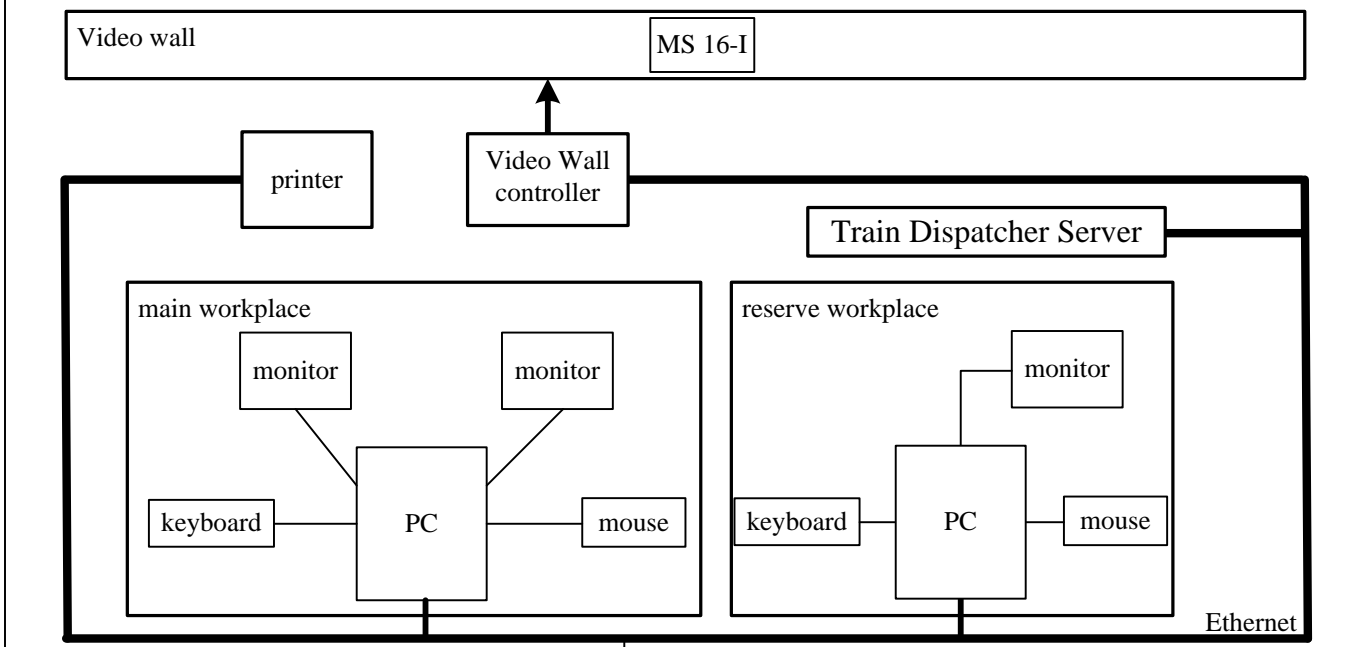
A SCADA – system is implemented for dispatching and control on the train traffic in the Sofia underground. A simplified structural scheme of this SCADA – system DISIM-V is shown in Fig. 1. The object level covers only one object such as one underground station. Dispatching and communication levels are the same regardless of the number of stations on the object level.

The system is a complex structure of technical, software and organizational resources related to certain rules, providing control and operating on the train traffic process. In general, the control is performed automatically, while operating is done either automatically or through operator commands submitted by the train dispatcher of the Central Dispatcher Post (CDP).

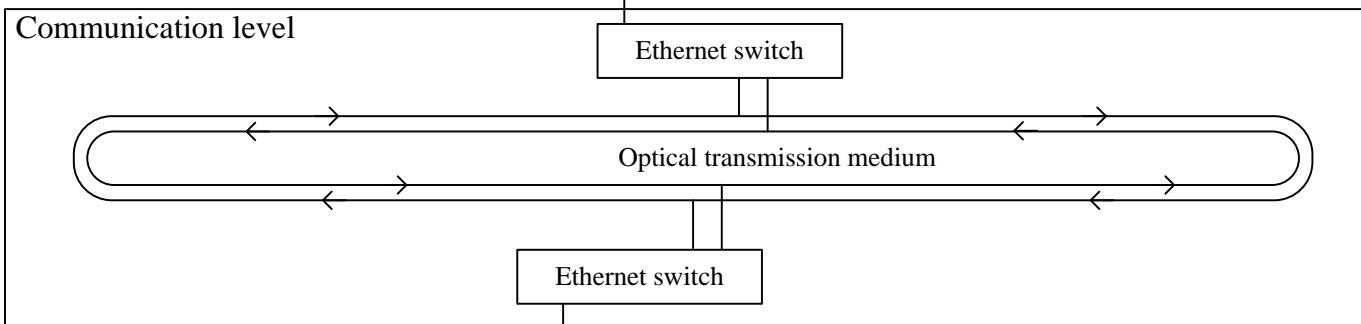
The connection between CDP and the underground station is realized by a programmable logic controller (PLC) situated in the object level. It has a modular structure that allows easy configuration and reconfiguration if necessary (e.g. when there are changes at the object). The PLC is connected to the electrical interlocking devices. The data on the track circuits state and the current status of the station are translated by the PLC to the CDP. The main controlled elements are points, traffic lights, track circuits and general alarm and signaling.

Normally trains run on automatic locomotive signaling indications for automatic speed regulation (ALS-ASR) in the

### Dispatcher level



### Communication level



### Object level

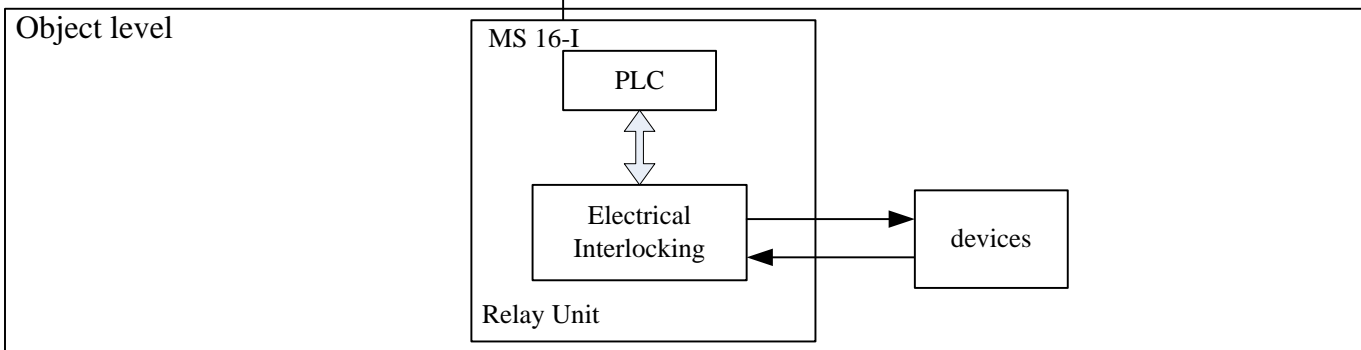


Fig. 1. SCADA - system DISIM-V

cab. In case of failure of one of the elements of ALS-ASR trains run on automatic block system signals.

The communication level realizes the connection between object level PLC and computers situated in the CDP. Ethernet network of the CDP is also part of this level.

The data received from the object enter in "Train Dispatcher Server" where according to the system algorithm their treatment is carried out. This process includes functions of displaying the information and human-system dialogue.

The main components of this SCADA - system are PCs and specialized and custom-developed software. The system works in a Linux environment. All menus in the system, as well as event logs and printed reports are in Bulgarian language, in line with the industry-accepted terminology. The system provides a comfortable and simple dialogue and an opportunity for easy manipulation. Dialogue with the system is in Bulgarian and performed via keyboard and mouse – standard peripherals of computers. DISIM is running under control of a complex program structure, which consists of

high standard software package and applications developed by the company DISSI - LTD. The standard software used in the system is:

- OS LINUX;
- Graphics upgrade X-Window System;
- X.org server;
- Package management windows - Metacity;
- Software to work with a video wall controller;
- Software for use with a programmable controllers' object level;
- Standard Java Virtual Machine;
- Implementation of the CORBA specification TAO / ACE, omniORB;
- Management System database - PostgreSQL.

#### IV. FUNCTIONS OF SCADA - SYSTEMS

SCADA - systems perform basic technological functions (monitoring functions and process control functions), system functions and additional functions.

##### A. Technological functions

The functions of monitoring on the technological processes ensure:

- Permanently and automatically collecting of data about the current state of equipment in the area;
- Continuously automatically sending of the collected data to the CDP;
- Analysis and processing of the data received in the CDP;
- Visualization of the received information on the system screens and on the video wall (with the existing subway system);
- Printing the current information or different pieces of the past tense, if necessary, by a command of the operator;
- Automatic backup in chronological order of the events that occurred.

The functions of control on the technological processes must provide:

- Reliable sending of operator's dispatching commands to the objects and their implementation;
- Reliable protection and prevention against improper and wrong manipulation (password, incorrectly set command, nonexistent command, inability to execute the command, etc.).

##### B. System functions

The system functions include the control function, internal control and diagnostics of the system and all its facilities, including software. The system functions provide also interconnection to all other systems in the SCADA - complex, including:

- Maintenance the system time and date;
- Internal automatic control and diagnostics of the successful operation of the system individual devices;
- Exchange of information with other SCADA - systems in a common computer network;

- Monitoring on the successful operation of communication between stations and the control center;
- Location of place and type of the damage;
- Monitoring and diagnostics of the software.

##### C. Additional functions

The additional functions are related to data archiving events, data analysis, generating various types of reports, including:

- Record of events;
- List of executed and outstanding commands;
- Data records and lists storing for time that is set by the operator;
- providing an opportunity to review the data in reports and lists and printing if necessary;
- printing the current information or stored information about various pieces in the past;
- testing the equipment for control on the video wall;
- testing hardware and application software at all levels of the system;
- testing the condition of communication channels.

#### V. LABORATORY SCADA - SYSTEM

##### A. Description

A simplified structural scheme of the laboratory SCADA - system is shown in Fig. 2. The object level will be presented by special software. The train traffic will be simulated by the lecturer. The communication level consists of only Ethernet network. The students will be able to watch train traffic in one or more stations as well as the status of the points, traffic lights, track circuits and general alarm and signaling. The train traffic schedule will also be displayed.

The main window of the laboratory SCADA - system will act as a control panel. This will be a group of buttons that run separate software modules with the following meaning: Stations, Schedule, Train number, Track circuits out of dispatcher monitoring, Records, etc. The menu for selecting the station will be displayed by pressing the button of Stations. The status of the selected station will be displayed on the monitor and all status changes could be monitored in real time. The student – Dispatcher could control on the electrical interlocking devices by the mouse. Two stations could be displayed simultaneously on the two monitors.

Information for registered alarms and messages, as well as the actions of the dispatcher for a specified period of time could be made by pressing the button of Records.

##### B. Benefit to the students training

The uniqueness of each SCADA - system makes the access to the information about the system very difficult, simply because if such information is available, it is primarily commercial and advertising. On the other hand, a contemporary, modern and efficient SCADA - system is in operation in the underground and covers all the technological

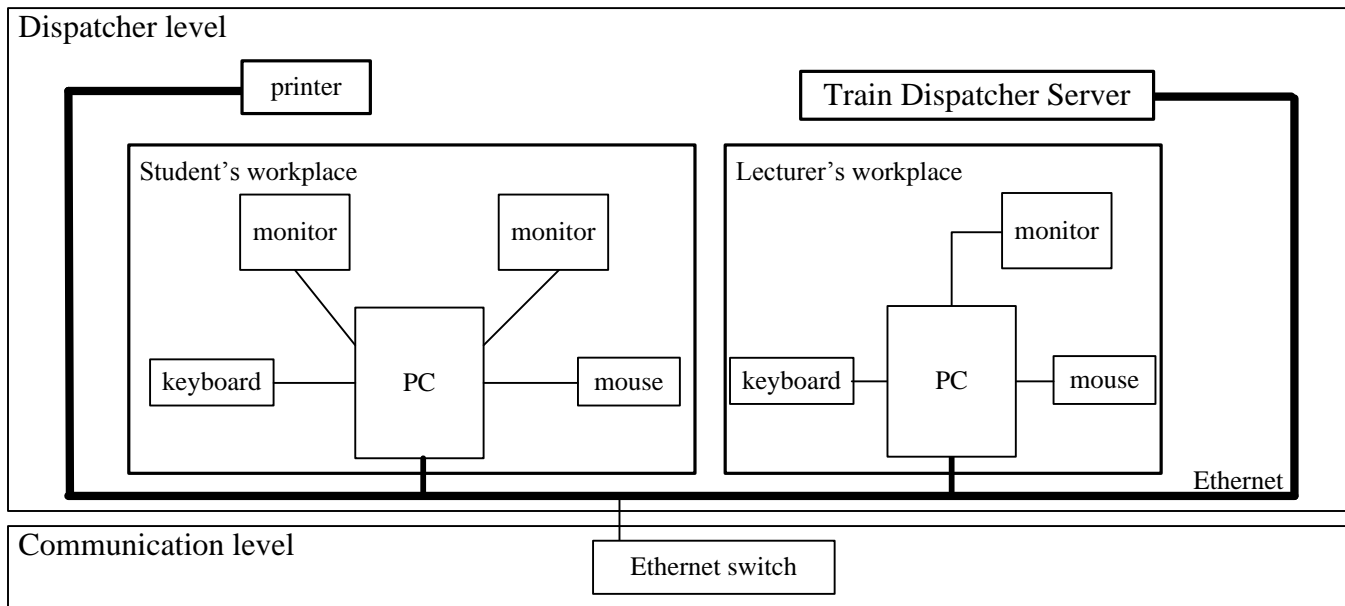


Fig. 2. Laboratory SCADA - system

processes. Its extensive study is not possible due to the special mode and permission of access. Therefore, the presence of upgraded laboratory models of SCADA - system in the Todor Kableshkov University of Transport will be extremely useful for students in the learning process and will enable them to deepen their knowledge in the core of modern SCADA - technology.

## REFERENCES

- [1] Е. Горанов, Е. Димитрова, “Системи за дистанционен контрол и управление в транспорта”, ВТУ „Тодор Каблешков, София, 2010
- [2] G. Cherneva, E. Dimitrova, “Применение интеллигентных технологий при управлении кризисными ситуациями в энергетике”, 17. medzinárodná veddecká konferencia Riešenie krízových situácií v špecifickom prostredí, Fakulta špeciálneho inžinierstva ŽU, Žilina, 30. - 31. máj 2012.

# Channel Capacity of Dual SC Diversity System Based on Desired Signal Decision Algorithm in Microcell

Aleksandra Panajotović<sup>1</sup>, Mihajlo Stefanović<sup>2</sup>, Dragan Drača<sup>3</sup> and Nikola Sekulović<sup>4</sup>

**Abstract –** Average channel capacity of selection combining (SC) diversity system based on desired signal decision algorithm operating in microcell interference-limited environment is evaluated in this paper. Numerical results are presented graphically and used to examine the effects of channel and systems parameters on concerned quantity. In addition, desired signal decision algorithm advantage to signal-to-interference ratio (SIR) decision algorithm is presented by way of obtained average channel capacity.

**Keywords –** Average channel capacity, Cochannel interference, Correlation, Fading, SC system.

## I. INTRODUCTION

In designing a cellular mobile system, a fundamental requirement is to provide specified quality-of-service (QoS) in combination with high system capacity. Cochannel interference (CCI), as a result of frequency reuse and multipath fading due to multipath propagation, are the main factors limiting system's performance [1]. Upgrading transmission reliability and increasing system's capacity without increasing transmission power and bandwidth can be achieved by using some of diversity techniques. Space diversity technique combines inputs signals from multiple receive antennas [2]. Three the most popular space diversity techniques are maximal ratio combining (MRC), equal gain combining (EGC) and selection combining (SC). Among them, SC is widely accepted because of its simple realization. Actually, it processes only one of the diversity branches, i.e. chooses the branch with largest signal-to-noise ratio (SNR) [3]. In interference-limited environment, environment where the level of CCI is much higher as compared to thermal noise, SC receiver can employ one of following decision power algorithms: the desired signal power algorithm, the total signal power algorithm and the signal-to-interference power ratio (SIR) algorithm [4].

The continued rising of demands for multimedial services and products lead to increasing needs for radio channel

<sup>1</sup>Aleksandra Panajotović is with the Faculty of Electronic Engineering, University of Niš, Aleksandra Medvedeva 14, 18000 Niš, Serbia, E-mail: [aleksandra.panajotovic@elfak.ni.ac.rs](mailto:aleksandra.panajotovic@elfak.ni.ac.rs)

<sup>2</sup>Mihajlo Stefanović is with the Faculty of Electronic Engineering, University of Niš, Aleksandra Medvedeva 14, 18000 Niš, Serbia, E-mail: [mihajlo.stefanovic@elfak.ni.ac.rs](mailto:mihajlo.stefanovic@elfak.ni.ac.rs)

<sup>3</sup>Dragan Drača is with the Faculty of Electronic Engineering, University of Niš, Aleksandra Medvedeva 14, 18000 Niš, Serbia, E-mail: [dragan.draca@elfak.ni.ac.rs](mailto:dragan.draca@elfak.ni.ac.rs)

<sup>4</sup>Nikola Sekulović is with the School of Higher Technical Professional Education, Aleksandra Medvedeva 20, 18000 Nis, Serbia, E-mail: [sekulani@gmail.com](mailto:sekulani@gmail.com)

spectrum and information data rate. Therefore, the channel capacity would be concerned in the future wireless systems as the primary performance metric. All of these is the reason for great number of the papers in the open technical literature that consider the channel capacity of diversity systems over the different fading channels [5-9].

Several statistical models are used in communication system analysis to describe fading. The most frequently used distributions are Nakagami, Rayleigh, Rician and Weibull. For example, in a microcellular environment, an undesired signal from distant cochannel cells may well be modeled by Rayleigh statistics, but Rayleigh fading is not good assumption for desired signal since a line-of-sight (LoS) path may exists within microcell. Actually, in such situation Rician statistic is acceptable solution for modeling desired signal. The channel capacity of dual SC diversity system over correlated fading channels is analyzed in this paper in the case when the receiver applies desired signal power decision algorithm. The influence of fading severity and branch correlation on the channel capacity are investigated through obtained results. Moreover, those results are compared with previous published [10] in order to reveal the best decision algorithm for SC system operating in the microcell environment.

## II. CHANNEL AND SYSTEM MODEL

Due to insufficient antenna spacing, when diversity system is applied on small terminal, desired signal envelopes,  $r_1$  and  $r_2$ , experience correlated Rician distribution whose probability density function (PDF) is given as [11]

$$p_{r_1 r_2}(r_1, r_2) = \frac{r_1 r_2}{\sigma^4(1-\rho^2)} \exp\left(-\frac{r_1^2 + r_2^2 + 2b^2(1-\rho)}{2\sigma^2(1-\rho^2)}\right) \times \sum_{k=0}^{\infty} \varepsilon_k I_k\left(\frac{r_1 r_2 \rho}{\sigma^2(1-\rho^2)}\right) I_k\left(\frac{b r_1}{\sigma^2(1+\rho)}\right) I_k\left(\frac{b r_2}{\sigma^2(1+\rho)}\right), \quad (1)$$

$$\varepsilon_k = \begin{cases} 1, & k=0 \\ 2, & k \neq 0 \end{cases}$$

where  $\rho$  is branch correlation coefficient and  $I_k(\cdot)$  is modified Bessel function of the first kind and  $k$ -th order. Rician factor and average desired signal power are defined as  $K = b^2/(2\sigma^2)$  and  $\beta = \sigma^2(1+K)$ , respectively.

The single dominant interference signal in microcell environment is subjected to Rayleigh fading [12]. The PDF of its envelope is expressed by

$$p_a(a) = \frac{a}{\sigma_a^2} \exp\left(-\frac{a^2}{2\sigma_a^2}\right), \quad (2)$$

where  $\sigma_a^2$  is average CCI power.

In this paper, SC diversity system applying desired signal decision algorithm is considered since it provides the same

performance as total signal decision algorithm, but it is easier to be modeled. Such diversity system selects the branch with the largest instantaneous desired signal power, i.e.  $r^2 = \max\{r_1^2, r_2^2\}$ . The instantaneous SIR at the output of SC receiver is given by  $\eta = \max\{r_1^2, r_2^2\} / a^2 = r^2 / a^2$ . Applying [13, Eq. (4.10)] on [14, Eq. (6)], the PDF of output SIR is obtained in following form

$$p_\eta(\eta) = \exp\left(-\frac{2K}{1+\rho}\right) \sum_{k,p,n,l=0}^{\infty} \varepsilon_k \frac{\rho^{2p+k} K^{n+l+k} (1+K)^{p+k+1}}{n!l!p!\Gamma(p+k+1)\Gamma(l+k+1)} \\ \times \frac{S\eta^{p+k}}{\Gamma(n+k+1)(1-\rho)^p(1+\rho)^{2k+p+n+l}} \\ \times \left\{ \frac{(p+n+k)!(1+K)^l \eta^l (1-\rho)^n}{(1+\rho)^l} \left[ \left( \frac{(p+k+l+1)!}{\left(S + \frac{(1+K)\eta}{1-\rho^2}\right)^{p+k+l+2}} \right. \right. \right. \\ \left. \left. \left. - \sum_{i=0}^{p+n+k} \frac{(p+l+k+i+1)!(1+K)^i \eta^i}{2^{p+k+l+i+2} i! (1-\rho^2)^i \left(S + \frac{(1+K)\eta}{1-\rho^2}\right)^{p+k+l+i+2}} \right] \right. \\ \left. + \frac{(p+l+k)!(1+K)^n \eta^n (1-\rho)^l}{(1+\rho)^n} \left[ \left( \frac{(p+k+n+1)!}{\left(S + \frac{(1+K)\eta}{1-\rho^2}\right)^{p+k+n+2}} \right. \right. \right. \\ \left. \left. \left. - \sum_{j=0}^{p+l+k} \frac{(p+n+k+j+1)!(1+K)^j \eta^j}{2^{p+k+l+j+2} j! (1-\rho^2)^j \left(S + \frac{(1+K)\eta}{1-\rho^2}\right)^{p+k+n+j+2}} \right] \right\}, \quad (3)$$

where  $S$  is average input SIR defined as  $S = \beta/\sigma_a^2$ .

### III. CHANNEL CAPACITY

The channel capacity in fading environment has to be calculated in average sense due to variation of signal in time caused by the fading. The average channel capacity then, can be defined as [15]

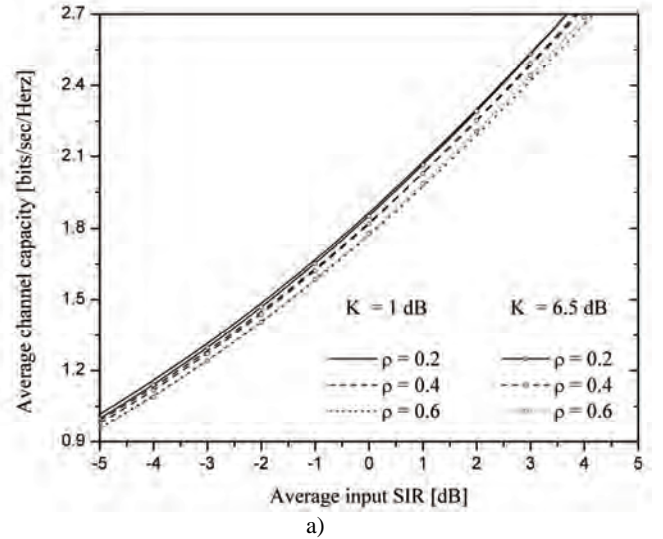
$$\bar{C} = BW \int_0^\infty \log_2(1+\eta) p_\eta(\eta) d\eta, \quad (4)$$

where  $BW$  is signal's transmission bandwidth. The program package *Mathematica 7* can be used for numerical evaluation of previous integral after substitution Eq. (3) into Eq. (4).

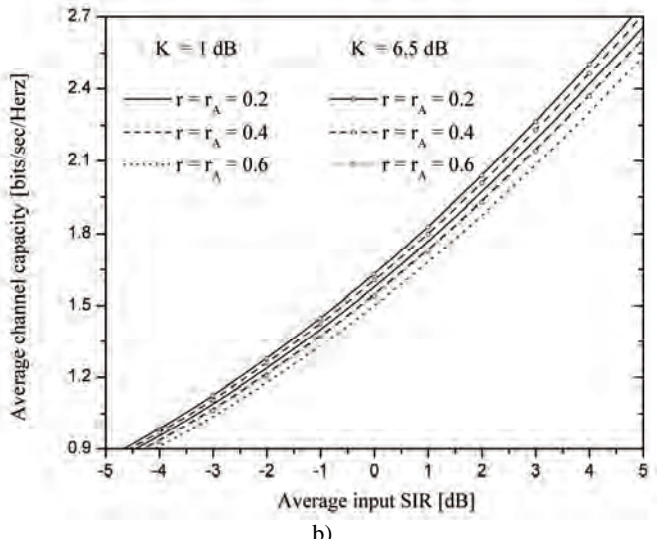
### IV. NUMERICAL RESULTS

Normalized to  $BW$  the average channel capacity of SC system ( $\bar{C} / BW$ ) versus average input SIR is depicted in Fig. 1. Actually, channel capacity of two SC systems with different decision algorithms is analyzed in this Section. Results from Fig. 1 (a) are obtained solving integral in (4) and represent average channel capacity of diversity system applying desired

signal decision algorithm. Results in Fig. 1 (b) have already been published in [10] and they are presented for comparison purpose. Namely, they present channel capacity of diversity system using SIR decision algorithm. As it is expected, regardless of applied decision algorithm channel capacity of SC system increases with increase of Rician factor (decrease of fading severity) and decrease of branch correlation coefficient (increase of distance between diversity branches). It can be concluded from comparison between Figs. 1 (a) and 1 (b), that for same system and channel parameters SC system considered in this paper guarantees higher channel capacity than SC system with SIR decision algorithm. Also, it shows greater resistance to variation of both Rician factor and correlation coefficient. Having in the mind previous exposed facts, it is obvious that SC system using desired signal decision algorithm has priority, especially if we know that it is easier to realize such SC system.



a)



b)

Fig. 1. Normalized channel capacity of SC systems with different decision algorithms  
(a) desired signal decision algorithm; (b) SIR decision algorithm

## V. CONCLUSION

In this paper, the performance of dual SC system operating in interference-limited microcell environment has been investigated. Actually, channel capacity, as widely accepted performance criterion, has been obtained for the case when SC system using desired signal power decision algorithm. Presented numerical results have described influence of fading severity and correlation coefficient on considered performance criterion. Moreover, evaluated results have been compared with results obtained for SIR decision algorithm. The general conclusion of this paper is that SC diversity system with desired signal decision algorithm provides higher channel capacity regardless of working conditions.

## ACKNOWLEDGEMENT

This work has been funded by Serbian Ministry for Education and Science under the projects TR-32052, III-44006, TR-33035.

## REFERENCES

- [1] J. D. Parsons, *The Mobile Radio Propagation Channels*, 2<sup>nd</sup> ed, New York: Willey, 2000.
- [2] A. Goldsmith, *Wireless Communications*, New York: Cambridge University, 2005.
- [3] M. K. Simon and M. -S. Alouini, *Digital Communications over Fading Channels*, 2<sup>nd</sup> ed, New York: Willey, 2005.
- [4] L. Yang and M. -S. Alouini, "Average outage duration of wireless communications systems", ch. 8, *Wireless Communications Systems and Networks*, Springer, 2004.
- [5] N. C. Sagias, D. A. Zogas, G. K. Karagiannidis and G. S. Tombras, "Channel capacity and second-order statistics in Weibull fading", *IEEE Commun. Lett.*, vol. 8, no. 6, pp. 377-379, 2004.
- [6] N. C. Sagias, G. S. Tombras and G. K. Karagiannidis, "New results for the Shannon capacity in generalized fading channel", *IEEE Commun. Lett.*, vol. 9, no. 2, pp. 97-99, 2005.
- [7] N. C. Sagias, D. A. Zogas and G. K. Karagiannidis, "Selection diversity receivers over nonidentical Weibull fading channels", *IEEE Trans. Veh. Technol.*, vol. 54, no. 6, pp. 2146-2154, 2005.
- [8] P. S. Bithas and P. T. Mathiopoulos, "Performance analysis of SSC diversity receivers over correlated Ricean fading satellite channels", *EURASIP J. Wireless Commun. Netw.*, vol. 2007, doi: 10.1155/2007/25361, 2007.
- [9] N. M. Sekulović, M. Č. Stefanović, D. Lj. Drača, A. S. Panajotović and D. M. Stefanović, "Performance analysis of microcellular mobile radio systems with selection combining in the presence of arbitrary number of cochannel interferences", *Advan. Elect. Comp. Eng.*, vol. 10, no. 4, pp. 3-8, 2010.
- [10] A. Panajotović, D. Stefanović, D. Drača, M. Stefanović and D. Milović, "Channel capacity of SC diversity system over Ricean fading channel in the presence of interference" ("Kapacitet kanala SC diverziteta sistema sa Rajsovim fedingom u prisustvu kanalne interferencije"), Conference Proceedings ETRAN 2008, TE 1.3, Palić, Serbia, 2008.
- [11] M. K. Simon, *Probability Distributions Involving Gaussian Random Variables – a Handbook for Engineers, Scientists and Mathematicians*, New York: Springer, 2002.
- [12] H. Yang and M. -S. Alouini, "Outage probability of dual-branch diversity systems in the presence of co-channel interference", *IEEE Trans. Wireless Commun.*, vol. 2, no. 2, pp. 310-319, 2003.
- [13] D. Zwillinger and S. Kokoska, *Standard Probability and Statistics, Tables and Formulae*, Boca Raton: Chapman-Hall/CRC, 2000.
- [14] A. Panajotović, N. Sekulović, M. Stefanović and D. Drača, "BEP comparison for dual SC system using different decision algorithm in the presence of interference", Conference Proceedings TELSIKS 2011, vol. 2, pp. 467-470, Niš, Serbia, 2011.
- [15] W. C. Y. Lee, "Estimate of channel capacity in Rayleigh fading environment", *IEEE Trans. Veh. Tech.*, vol. 39, no. 3, pp. 187-189, 1990.

**This Page Intentionally Left Blank**

# Simulation of Effects of Group Velocity Dispersion on Gaussian Pulse Propagation through Optical Fiber

Petar Spalević<sup>1</sup>, Branimir Jakšić<sup>1</sup>, Aleksandar Marković<sup>2</sup>, Zoran Todorović<sup>1</sup>  
and Vladislav Simić<sup>3</sup>

**Abstract –** In this paper, using a software package OptiSystem is designed system with optical fiber in a linear regime. Analyzed the Gaussian pulse propagation through the fiber under the influence of group velocity dispersion and chirp. Shows the Gaussian pulse shapes in characteristic sections under the influence of group velocity dispersion with and without initial chirp. Shows the compensation group velocity dispersion and dispersion induced chirp.

**Keywords –** Gaussian pulse, Group velocity dispersion (GVD), Chirp, Pulse width, Peak power.

## I. INTRODUCTION

An optical signal will be degraded by attenuation and dispersion as it propagates through the fiber optics. Dispersion can sometime be compensated or eliminated through an excellent design, but attenuation simply leads to a loss of signal [1]. Many optical fiber properties increase signal loss and reduce system bandwidth. Eventually the energy in the signal becomes weaker and weaker so that it cannot be distinguished with sufficient reliability from the noise that always present in the system, then an error may occur. Attenuation therefore determines the maximum distance that optical links can be operated without amplification. There are several component options available in fiber optic technologies that lead to particular system configurations. For longer distance optical amplifiers are needed. In general, when a system has a very wide-bandwidth used over a long distance, a single-mode fiber is used [2-4].

There are two different types of dispersion in optical fibers. The first type is intermodal, or modal, dispersion occurs only in multimode fibers. The second type is intramodal, or chromatic, dispersion occurs in all types of fibers. Each type of dispersion mechanism leads to pulse spreading. As a pulse spreads, energy is overlapped [5].

There are two types of intramodal dispersion. The first type is material dispersion. The second type is waveguide dispersion. Intramodal dispersion occurs because different colors of light travel through different materials and different waveguide structures at different speeds. Material dispersion

<sup>1</sup>Petar Spalević, Branimir Jakšić and Zoran Todorović are with the Faculty of Technical Sciences at University of Pristina, Kneza Miloša 7, Kosovska Mitrovica 38200, Serbia, E-mail: petarspalevic@yahoo.com.

<sup>2</sup>Aleksandar Marković is with the Faculty of Electronic at University of Niš, A. Medvedeva 14, Niš 18000, Serbia.

<sup>3</sup>Vladislav Simić is with the Telekom Srbija, Takovska 2, Beograd 11100, Serbia.

occurs because the spreading of a light pulse is dependent on the wavelengths' interaction with the refractive index of the fiber core. Different wavelengths travel at different speeds in the fiber material. Different wavelengths of a light pulse that enter a fiber at one time exit the fiber at different times [3], [4], [6].

Material dispersion is a function of the source spectral width. The spectral width specifies the range of wavelengths that can propagate in the fiber. Material dispersion is less at longer wavelengths. Waveguide dispersion occurs because the mode propagation constant is a function of the size of the fiber's core relative to the wavelength of operation. Waveguide dispersion also occurs because light propagates differently in the core than in the cladding [7].

The main advantage of single-mode fibers is that intermodal dispersion is absent simply because the energy of the injected pulse is transported by a single mode. However, pulse broadening does not disappear altogether. The group velocity associated with the fundamental mode is frequency dependent because of chromatic dispersion. As a result, different spectral components of the pulse travel at slightly different group velocities, a phenomenon referred to as group velocity dispersion (GVD), intramodal dispersion, or simply fiber dispersion. Intramodal dispersion has two contributions, material dispersion and waveguide dispersion. We consider both of them and discuss how GVD limits the performance of lightwave systems employing single-mode fibers [8-11].

## II. EFFECT OF GROUP VELOCITY DISPERSION

The equation, which describes the effect of group velocity dispersion (GVD) on optical pulse propagation neglecting the losses and nonlinearities, is [4]:

$$i \frac{\partial E}{\partial z} = \frac{\beta_2}{2} \frac{\partial^2 E}{\partial t^2} \quad (1)$$

where  $z$  is the propagation direction,  $t$  is the time,  $E$  is the electric field envelope, and  $\beta_2 = \frac{\partial^2 \beta}{\partial \omega^2}$  is the GVD parameter, defined as the second derivative of the fiber mode propagation constant with respect to frequency.

For an input pulse with a Gaussian shape

$$E(z=0, t) = \sqrt{P_0} \exp\left(-\frac{t^2}{2T_0^2}\right) \quad (2)$$

the pulse width  $T_0$ , related to the pulse full width at half maximum by

$$T_{FWHM} \approx 1.665T_0 \quad (3)$$

increases with  $z$  (the pulse broadens) according to [4]:

$$T(z) = \left[ 1 + \left( \frac{z}{L_D} \right)^2 \right]^{1/2} T_0 \quad (4)$$

and, consequently, the peak power changes, due to GVD, are given by:

$$P(z) = \frac{P_0}{\left[ 1 + \left( \frac{z}{L_D} \right)^2 \right]^{1/2}} \quad (5)$$

In Eqs. (4) and (5):

$$L_D = \frac{T_0^2}{|\beta_2|} \quad (6)$$

is the dispersion length. Its meaning is quite straightforward: after propagating a distance equal to  $L_D$ , the pulse broadens by a factor of  $\sqrt{2}$ .

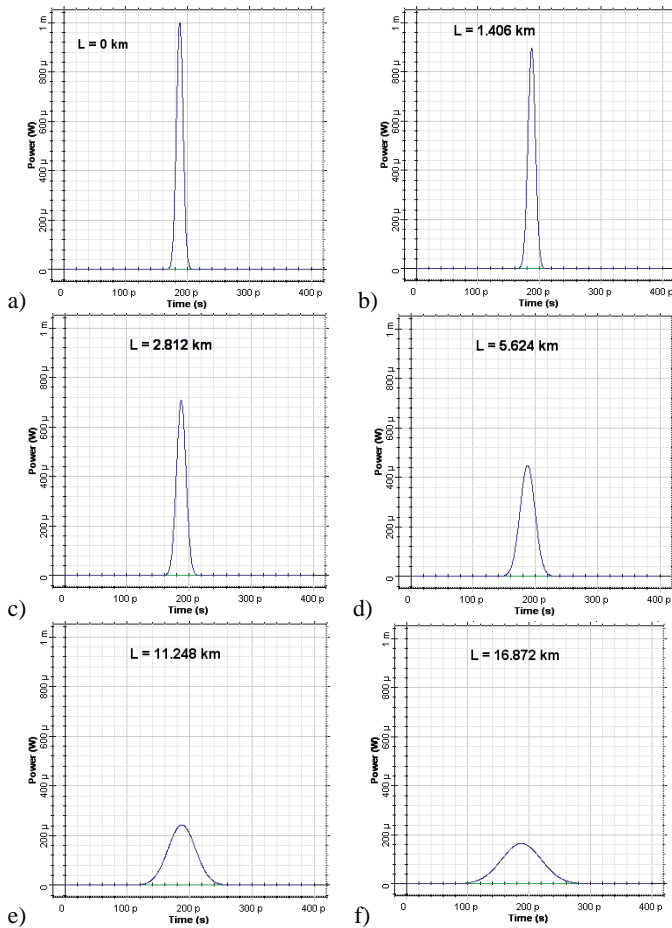


Fig. 1. Gaussian pulse on optical fiber length of: a)  $L=0$ , b)  $L=0.5L_D$ , c)  $L=L_D$ , d)  $L=2L_D$ , e)  $L=4L_D$ , f)  $L=6L_D$

Effect of GVD on the Gaussian pulse is analyzed in the software OptiSystem [12]. Characteristics of the system include: bit rate signal is 40 Gb/s, bit duration 25 ps, the width of the Gaussian pulse is 0.5, and the power of 0 dBm (1 mW). The system is observed at wavelengths 1.55  $\mu$ m. Value of GVD parameter is  $\beta_2 \approx -20(ps)^2/km$  on 1.55  $\mu$ m for single-mode fiber.

Based on Eqs (3) and (6) and the values of the parameters observable system we obtain values  $T_0 = 7.5$  ps and  $L_D = 2.812$  km.

Fig. 1 shows the Gaussian pulse at the output of the transmitter ( $L=0$ ) and after transmission through an optical fiber length  $L=nL_D$ ,  $n=0.5, 1, 2, 4, 6$ .

From Fig. 1 we can see that with the increase of the length of the distance is to spread the impulse and to reduce its power. The peak power decreases in accordance with Eq. (5). The origin of pulse broadening can be understood be looking at the instant frequency of the pulse, namely the chirp.

Whereas the input pulse is chirpless, the instantaneous frequency of the output pulse decreases from the leading to the trailing edge of the pulse. The reason for this is GVD. In the case of anomalous GVD ( $\beta_2 < 0$ ), the higher frequency components of the pulse travel faster than the lower frequency.

### III. EFFECT OF INITIAL CHIRP WITH GROUP VELOCITY DISPERSION

If the input pulse is frequency modulated (i.e. chirped), Eq. (2) is replaced by:

$$E(z=0, t) = \sqrt{P_0} \exp\left(-\frac{1+iC}{2} \frac{t^2}{T_0^2}\right) \quad (7)$$

and the expression for the dependence of the pulse width on  $z$  is:

$$T(z) = T_0 \left[ \left( 1 + \frac{C\beta_2 z}{T_0^2} \right)^2 + \left( \frac{\beta_2 z}{T_0^2} \right)^2 \right]^{1/2} \quad (8)$$

The pulse broadens monotonically with  $z$  if  $\beta_2 C > 0$ , however, it goes through initial narrowing when  $\beta_2 C < 0$ . In the latter case, the pulse width becomes minimum at distance [4]:

$$z_{min} = \frac{|C|}{1+C^2} L_D \quad (9)$$

and is given by:

$$T(z_{min}) = \frac{T_0}{(1+C^2)^{1/2}} \quad (10)$$

where  $C$  is chirp parameter.

The peak power of the pulse in this case is:

$$P(z_{min}) = P_0 (1+C^2)^{1/2} \quad (11)$$

Table 1 provides the values of the length of the optical fiber in which the minimum pulse width and peak power at that point for different values of the chirp parameter.

TABLE I  
VALUES OF  $Z_{\text{MIN}}$  AND  $P(Z_{\text{MIN}})$  FOR DIFFERENT CHIRP PARAMETER

C	$Z_{\text{min}}$ [km]	$P(Z_{\text{min}})$ [mW]
1	1.406	1.414
2	1.125	2.236
3	0.844	3.162
4	0.662	4.123
5	0.541	5.099
6	0.456	6.083
7	0.394	7.071
8	0.346	8.062
9	0.309	9.055
10	0.278	10.05

Figs. 2 and 3 shows the Gaussian pulse in the characteristic points for chirp parameter  $C=1$  and  $C=5$ , respectively.

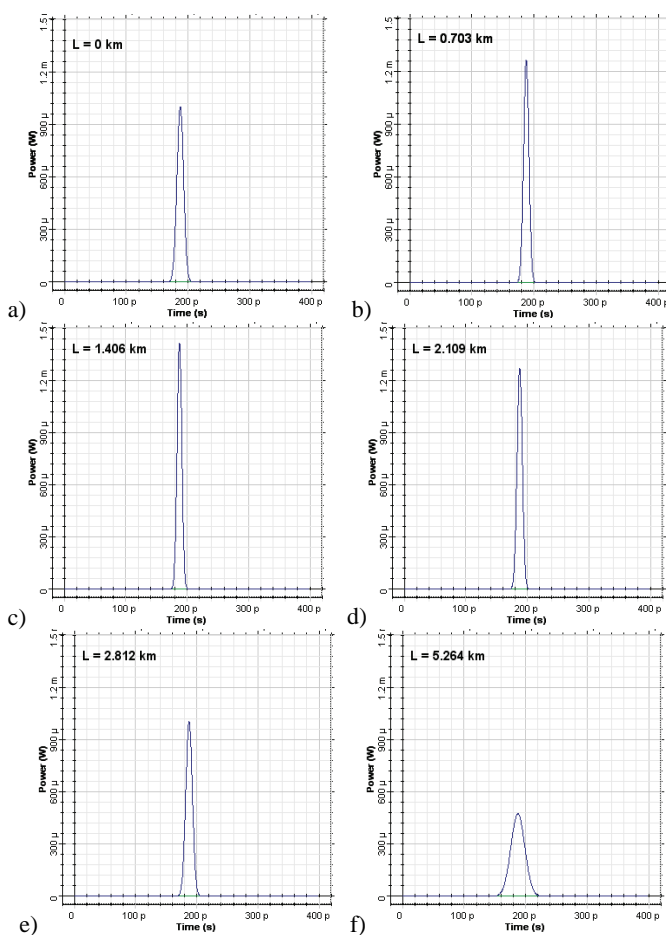


Fig. 2. Gaussian pulse for  $C=1$  at distance: a)  $L=0$ , b)  $L=0.5z_{\text{min}}$ , c)  $L=z_{\text{min}}$ , d)  $L=2z_{\text{min}}$ , e)  $L=L_D$ , f)  $L=2L_D$

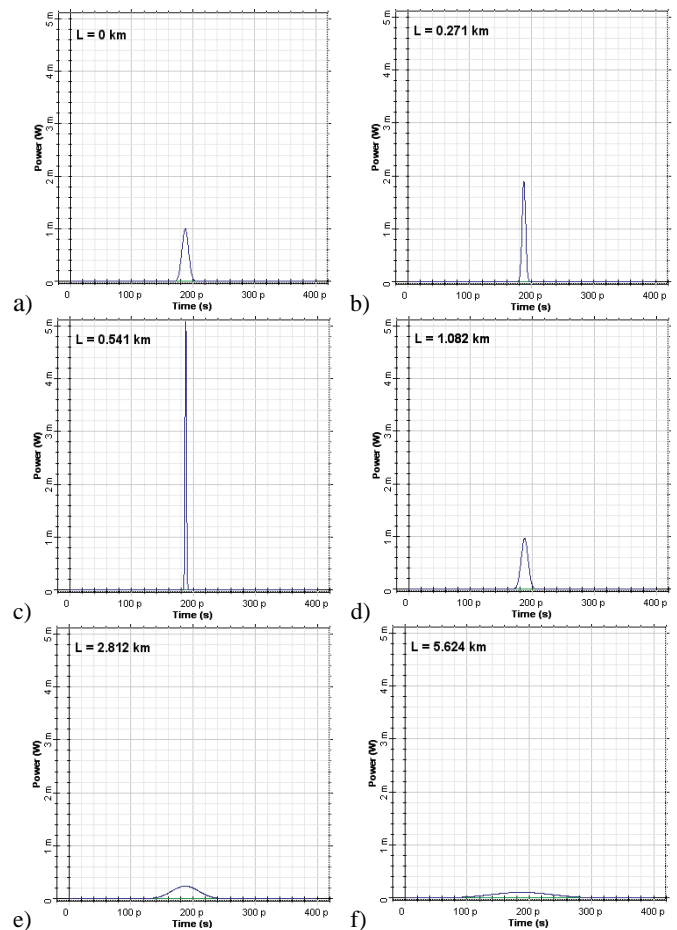


Fig. 3. Gaussian pulse for  $C=5$  at distance: a)  $L=0$ , b)  $L=0.5z_{\text{min}}$ , c)  $L=z_{\text{min}}$ , d)  $L=2z_{\text{min}}$ , e)  $L=L_D$ , f)  $L=2L_D$

With the given figure can be seen under the influence of chirp leads to increase peak power and reduce the pulse width to the point  $L=z_{\text{min}}$ , where it reaches its maximum power and a minimum width. After a distance  $z_{\text{min}}$  comes to a sharp decline of peak power and a significant expansion of impulse. These effects are much more expressed for higher values of chirp parameter  $C$ .

#### IV. CONCLUSION

Initial narrowing of the pulse for the case  $\beta_2 C < 0$  can be explained by noticing that in this case the frequency modulation (or "chirp") is such that the faster frequency components are in the trailing edge, and the slower in the leading edge of the pulse. As the pulse propagates, the faster components will overtake the slower ones, leading to pulse narrowing. At the same time, the dispersion induced chirp will compensate for the initial one. At  $L=z_{\text{min}}$ , full compensation between both will occur. With further propagation, the fast and the slow frequency components will tend to separate in time from each other and, consequently, pulse broadening will be observed.

## ACKNOWLEDGEMENT

This work was done within the research project TR32023 and TR35026 of the Ministry of Science and Technological Development of Republic Serbia.

## REFERENCES

- [1] S. Nilsson-Gistoik, *Optical Fiber Theory for Communication Networks*, Ericsson, Sweden, 1994.
- [2] L. Harte, D. Eckard, *Fiber Optic Basics, Technology, Systems and Installation*, Athos Publishing, USA, 2006.
- [3] E. G. Sauter, *Nonlinear Optics*, New York, Wiley, 1996.
- [4] G. P. Agrawal, *Nonlinear Fiber Optics*, Academic Press, 2nd Ed., 2001.
- [5] F. Yaman, Q. Lin, S. Radic, G. P. Agrawal, "Impact of Dispersion Fluctuations on Dual-Pump Fiber-Optic Parametric Amplifiers", *Photonics Technology Letters*, IEEE vol. 16, no. 5, pp. 1292 – 1294, May 2004.
- [6] M. Stefanovic, D. Draca, P. Spalevic, A. Panajotovic: "The influence of crosstalk signal interference to signal propagation along nonlinear and dispersive fiber", *Journal of Optical Communications*, vol. 26, no. 1, pp. 9-12, 2005.
- [7] V. B. Katok, M. Kotenko, O. Kotenko, "Features of Calculation of Wideband Dispersion Compensator for Fiber-Optic Transmission System", 3rd International Workshop on Laser and Fiber-Optical Networks Modeling, Proceedings of LFNM 2001, pp. 88 – 91, 2001.
- [8] G. P. Agrawal, *Fiber-Optic Comunication Systems*, New York, Wiley, 3nd Ed., 2002.
- [9] P. Lekić, B. Jakšić, P. Spalević, S. Milosavljević, "Analysis of the Interaction of two Solitons and Violation of Their Linear Superposition in the Transmission Path", UNITECH conference, vol. 1, pp. 307–311, Gabrovo, Bulgaria, 2010.
- [10] M. Stefanović, P. Spalević, D. Martinovic, M. Petrović, "Comparison of Chirped Interference Influence on Propagation Gaussian and Super Gaussian Pulse along the Optical Fiber", *Journal of Optical Communications* vol. 28, no. 1, 2007.
- [11] M. Stefanovic, D. Draca, P. Spalevic, A. Panajotovic, "Performance of IM-DD Optical System in the Presence of Interference at Input of the Fiber", *Nonlinear Phenomena in Complex System*, vol. 6, no. 4, pp. 870-878, 2003.
- [12] [www.optiwave.com](http://www.optiwave.com).

# Algorithm for modular exponentiation in public key cryptosystems

Plamen Stoianov<sup>1</sup>

**Abstract** – The operational speed of most public key cryptosystems is largely determined by the modular exponentiation operation. The required modular exponentiation is computed by a series of modular multiplications. Optimized algorithms are required for various platforms, especially for lower-end platforms. These require the algorithms to be efficient and consume as little resources as possible. This article presents algorithm for calculating modular exponentiation using less precomputation without division. The aim is to improve computational efficiency of modular exponentiation based public key cryptosystems.

**Keywords** – Cryptography, modular reduction, modular exponentiation, long integers.

## I. INTRODUCTION

The word cryptography comes from the Greek words crypto (hidden) and graphy (writing), hence cryptography is the art of secret writing. More formally cryptography is the study of mathematical techniques related to the security services of information security. The ITU-T X.800 standard defines the security services provided by a system to give a specific kind of protection to system resources. The standard divides security services into the following four categories:

- Confidentiality is a service used to keep the content of information accessible to only those authorized to have it. This service includes both of protection of all user data transmitted between two points over a period of time as well as protection of traffic flow from analysis.
- Integrity is a service that requires that computer system assets and transmitted information be capable of modification only by authorized users. Modification includes writing, changing, changing the status, deleting, creating, and the delaying or replaying of transmitted messages. It is important to point out that integrity relates to active attacks and therefore, it is concerned with detection rather than prevention. Moreover, integrity can be provided with or without recovery, the first option being the more attractive alternative.
- Authentication is a service that is concerned with assuring that the origin of a message is correctly identified. That is, information delivered over a channel should be authenticated as to the origin, date of origin, data content, time sent, etc. For

<sup>1</sup>Plamen Stoianov is with the Electronic Engineering Faculty at Technical University of Varna, Communications Equipment and Technology Department, Studentska 1, Varna , Bulgaria,

E-mail: pl\_stoianov@tu-varna.bg.

these reasons this service is subdivided into two major classes: entity authentication and data origin authentication. Notice that the second class of authentication implicitly provides data integrity. An important part of almost all modern security protocols is public-key algorithms.

- Non-repudiation is a service which prevents both the sender and the receiver of a transmission from denying previous commitments or actions. When disputes arise due to an entity denying that certain actions were taken, a means to resolve the situation is necessary. A procedure involving a trusted third party is needed to resolve the dispute.

Specifically, unauthorized access to information must be prevented, privacy must be protected, and the authenticity of electronic documents must be established. Cryptography, or the art and science of keeping messages secure, allows us to solve these problems.

These security services are provided by using cryptographic algorithms. There are two major classes of algorithms in cryptography: Symmetric algorithms and Public-Key algorithms.

Symmetric algorithms are algorithms where the encryption and decryption key is the same, or where the decryption key can easily be calculated from the encryption key. The main function of these algorithms, which are also called secret-key algorithms, is encryption of data, often at high speeds. Private-key algorithms require the sender and the receiver to agree on the key prior to the communication taking place. The security of private-key algorithms rests in the key; divulging the key means that anyone can encrypt and decrypt messages. Therefore, as long as the communication needs to remain secret, the key must remain secret.

There are two types of symmetric-key algorithms: block ciphers and stream ciphers. Block ciphers are a function which maps n-bit plaintext to n-bit ciphertext blocks (n is called the blocklength). The most used secret-key algorithms are DES, 3DES, AES, RC5 etc. Stream ciphers operate on a single bit of plaintext at a time. They are useful because the encryption transformation can change for each symbol of the message being encrypted. They can be used when the data must be processed one symbol at a time because of lack of equipment memory or limited buffering.

One of the major issues with symmetric key systems is the need to find an efficient method to agree on and exchange the secret keys securely. This is known as the key distribution problem.

A major advance in cryptography came in 1976 with the publication by Diffie and Hellman (New Directions of Cryptography) [1] of a new concept of cryptography. This new concept was called public-key cryptography. Public-Key Cryptography (PKC) is based on the idea of separating the key used to encrypt a message from the one used to decrypt it. Pair of matched keys is used, termed “public” and “private”

keys. Anyone that wants to send a message to party A can encrypt that message using A's public key but only A can decrypt the message using her private key. In implementing a public-key cryptosystem, it is understood that A's private key should be kept secret at all times. Furthermore, even though A's public key is publicly available to everyone, including A's adversaries, it is impossible for anyone, except A, to derive the private key.

In general, one can divide practical public-key algorithms into three families [2]:

- Algorithms based on the integer factorization problem: given a positive integer  $n$ , find its prime factorization. RSA [3], the most widely used public-key encryption algorithm, is based on the difficulty of solving this problem. RSA problem: given a positive integer  $n$  that is a two distinct odd primes  $p$  and  $q$ , a positive integer  $e$  such that  $\gcd(e, (p-1)(q-1))=1$ , and an integer  $c$ , find an integer  $m$  such that  $m^e \equiv c \pmod{n}$ .
- Algorithms based on the discrete logarithm problem: given  $\alpha$  and  $\beta$  find the integer  $x$  such that  $\alpha^x \equiv \beta \pmod{p}$ . The Diffie-Hellman key exchange protocol is based on this problem: given a prime  $p$ , a generator  $\alpha$  and elements  $\alpha^a \pmod{p}$  and  $\alpha^b \pmod{p}$ , find  $\alpha^{ab} \pmod{p}$ .
- Algorithms based on Elliptic Curves. Elliptic curve cryptosystems are the most recent family of practical public-key algorithms, but are rapidly gaining acceptance. Due to their reduced processing needs, elliptic curves are especially attractive for embedded applications. Despite the differences between these mathematical problems, all three algorithm families have something in common: they all perform complex operations on very large numbers, typically 1024 bits in length for the RSA and discrete logarithm systems or 160 bits in length for the elliptic curve systems.

## II. OVERVIEW OF ALGORITHMS FOR MODULAR REDUCTION AND EXPONENTIATION

The most common operation performed in public-key schemes is modular exponentiation, i.e., the operation  $A^E \pmod{M}$ . Performing computation of numbers of this large size (e.g., 2048 bit) with multiple precisions is not easy or fast to implement. Modular exponentiations are typically calculated using repeated square-and-multiply algorithms with modular reductions in between. In [2] this method is called binary exponentiation. A similar algorithm is also used for point multiplication in ECC. The basic idea of binary method is to compute modular exponentiation using the binary expression of exponent  $E$ . The exponentiation operation is broken into a series of squaring and multiplication operations by the use of the binary method. There are two variations of the algorithm: left to right (LRB) and right to left binary exponentiation (RLB). LRB algorithm computes the exponentiation starting from the most significant bit position of the exponent  $E$  and proceeding to the right, which is depicted as follows.

Input : integers  $A, M, E = (e_n e_{n-1} \dots e_1 e_0)_2$

Output:  $X = A^E \pmod{M}$

1.  $X \leftarrow 1$
2. for  $i = n$  to 0 do
- $X \leftarrow X^2 \pmod{M}$
- If  $e_i = 1$ , then  $X \leftarrow X \cdot A \pmod{M}$
3. Return ( $X$ )

Let  $n + 1$  be the bitlength of the binary representation of  $E$ , and let  $w(e)$  be the number of 1's in this representation.

Algorithm LRB performs  $t + 1$  modular squarings and  $w(e) - 1$  modular multiplications by  $A$ . Different from the LRB, the RLB algorithm computes the exponentiation starting from the last significant bit position of the exponent  $E$  and proceeding to the left. Each multiplication (or squaring) operation requires a large number of clock cycles due to the long operand length depending on the implementation. The binary method is frequently used in smartcards and embedded devices, due to its simplicity and low resource consumption.

Mostly mentioned are various windowing techniques as a generalization of the basic algorithm in which more than one bit of the exponent is processed per iteration. The basic idea is as follows: the exponent is divided into digits (windows). Algorithm LRB can thus be considered as a special case where the window size is equal to 1.

The k-ary method (fixed window) is an optimization of the binary method. Bits of the exponent are scanned in groups as against the binary method in which a bit is scanned per iteration. The algorithm for this technique is shown below.

Input : integers  $A, M, E = (e_n e_{n-1} \dots e_1 e_0)_b$  where

$$b = 2^k \text{ for } k \geq 1$$

Output:  $X = A^E \pmod{M}$

1. precomputation
  - 1.1  $a_0 \leftarrow 1$
  - 1.2 for  $i = 1$  to  $2^k - 1$  do :  $a_i \leftarrow a_{i-1} \cdot A \pmod{M}$
2.  $X \leftarrow 1$
3. for  $i = n$  down to 0 do
  - 3.1  $X \leftarrow X^{2^k} \pmod{M}$
  - 3.2  $X \leftarrow X \cdot a_{e_i} \pmod{M}$
4. return ( $X$ )

Most methods rely on modular reduction algorithm functions to reduce the size and complexity of the required arithmetic operations to carry out their public-key cryptosystem implementations more efficiently [4] [5]. The Classical, Barrett, and Montgomery algorithms are well-known modular reduction algorithms for large integers used in public-key cryptosystems

Montgomery Reduction can be implemented in two ways: word-serial and bit-serial. For a software implementation, the bit-serial algorithm becomes too slow because the processor is built on word-level arithmetic. Therefore, software implementations typically utilize the word-level Montgomery Reduction algorithm. If we assume a word-level length of  $n$ ,

to reduce a  $2n$ -bit number to an  $n$ -bit number, 2 full multiplications and 2 full addition operations are required. Thus, a full modular multiplication requires 3 multiplication and 2 addition operations [2]. This also applies to large digit approaches such as ours, where the multiplication/addition operations on large digits are further decomposed into word-size operations. The approach of Montgomery avoids the time consuming trial division that is the common bottleneck of other algorithms. His method is proven to be very efficient and is the basis of many implementations of modular multiplication in hardware as well as software such as high-radix design [6][7], scalable design [8], parallel calculation quotient and partial result and signed-digit recoding [9].

The notation is as follows:  $\text{MONT}(X, Y) = XY R^{-1} \bmod N$

For a word base  $b = 2^a$ ,  $R$  is usually chosen such that  $R = 2^r = (2^a)^l > N$ .

To compute  $Z = xyR \bmod N$ , one first has to compute the Montgomery function of  $x$  and  $R^2 \bmod M$  to get  $Z' = xR \bmod M$ .  $\text{Mont}(Z', y)$  gives the desired result. When computing the Montgomery product  $T = XY R^{-1} \bmod M$ , the following procedure was proposed:

**INPUT:** Integers  $M$  (odd),  $x \subset [0, M-1]$ ,  $y \subset [0, M-1]$ ,

$$R = 2^r,$$

$$\text{and } M' = -M^{-1} \bmod 2^r$$

**OUTPUT:**  $xyR^{-1} \bmod M$

1.  $T \leftarrow 0$
2. For  $i$  from 0 to  $(l-1)$  do:

$$2.1 m_i \leftarrow (t_0 + x_i y)M' \bmod 2^a$$

$$2.2 T \leftarrow (T + x_i y + m_i M)/2^a$$

3. If  $T \geq M$ , then  $T \leftarrow T - M$
4. Return ( $T$ )

An architecture based on Montgomery's algorithm[10] is probably the best studied architecture in hardware. Differences appeared because of a different approach for avoiding long carry chains.

The Barrett reduction [11] requires the pre-computation of

$$\text{one parameter, } \mu = \left\lfloor \frac{b^{2k}}{M} \right\rfloor, \text{ where } M \text{ is the modulus of the}$$

multiplication operation. Since this is a parameter that only depends on the modulus, it remains unchanged throughout the entire exponentiation operation, thus the calculation time of this parameter is not significant. If the number to be reduced is  $N$ , the reduction then takes the form

$Q = \left\lfloor (A/b^{2k-l}) \cdot \mu / b^l \right\rfloor$  by integer division which requires two  $n$ -bit multiplies and one  $n$ -bit subtract, leaving the total at three multiplications and one subtraction. In [12], the authors proposed a method called folding to reduce the amount of computations for a Barrett's reduction scheme. Their method relies on the precomputation of the constant  $M' = 2^{3s} \bmod M$ .

### III. PROPOSED ALGORITHM

The algorithm proposed related to computing  $A^E \bmod M$  uses a combination between sliding windows exponentiation and an improvement of the reduction method for moduli of special form  $b^n - c$  [2][13]. By reduction method for moduli of special form the time of execution depends on the value of the radix. Before involution the radix is being checked first. If  $A > M/2$ , the modular operation calculates by

$$\begin{aligned} & (M-A)^l \bmod M, (M-A)^2 \bmod M = \\ & = M^2 \bmod M - 2M \cdot A \bmod M + A^2 \bmod M = \\ & = A^2 \bmod M \end{aligned} \quad (1)$$

Equation (1) is valid for all the even powers

$$(M-A)^{2n} \bmod M = A^{2n} \bmod M \text{ for } n \geq 1.$$

By odd powers a correction

$$(M-A)^{2n+1} \bmod M = M - A^{2n+1} \bmod M \quad (2)$$

(1) and (2) could be used by modular multiplication of two integers :  $AB \bmod M$ .

By  $A > M/2$  and  $B > M/2$   $(M-A)(M-B) \bmod M = AB \bmod M$ .

By  $A > M/2$  and  $B < M/2$   $(M-A)B \bmod M = M-AB \bmod M$ .

The modular squaring algorithm is described in Algorithm 1. Algorithm 1 . EXPMOD(A,M)

**Input :** Integers  $A, M = (m_{n-1} \dots m_1 m_0)$ ,  $m_{n-1} = 1$

**Output:**  $Y = A^2 \bmod M$

1. if  $A > M/2$  then  $A \leftarrow M-A$
2.  $P \leftarrow 2^n \cdot M$ ,  $Y \leftarrow A^2$
3. while  $Q > 0$  do  
 $Q \leftarrow \lfloor Y/2^n \rfloor$   
 $Y \leftarrow Q \cdot P + Y \bmod 2^n$
4. if  $Y \geq M$  then  $X \leftarrow Y-M$
5. Return ( $Y$ )

The modular multiplication algorithm is presented in Algorithm 2.

Algorithm 2 . MULMOD(A,B,M)

**Input :** Integers  $A, B, M = (m_{n-1} \dots m_1 m_0)$ ,  $m_{n-1} = 1$

**Output:**  $Y = AB \bmod M$

1.  $0 \leftarrow j$  if  $A > M/2$  then  $A \leftarrow M-A$ ,  $j \leftarrow j+1$   
if  $B > M/2$  then  $A \leftarrow M-B$ ,  $j \leftarrow j+1$
2.  $P \leftarrow 2^n \cdot M$ ,  $Y \leftarrow A \cdot B$
3. while  $Q > 0$  do
  - a.  $Q \leftarrow \lfloor Y/2^n \rfloor$   
 $b. X \leftarrow Q \cdot P + Y \bmod 2^n$
4. if  $Y \geq M$  then  $Y \leftarrow Y-M$
5. if  $j=1$  then  $X \leftarrow M-Y$
6. Return ( $Y$ )

For the sliding window algorithm the window size may be of variable length and hence the partitioning may be performed so that the number of zero-windows is as large as possible, thus reducing the number of modular multiplication

necessary in the squaring and multiplication phases. Furthermore, as all possible partitions have to start (i.e. in the right side) with digit 1, the pre-processing step needs to be performed for odd values only.

Algorithm 3. Sliding window with EXPMOD and MULMOD

Input: Integers A, M, E=(e<sub>t</sub> e<sub>t-1</sub>...e<sub>1</sub> e<sub>0</sub>)<sub>2</sub>, k≥1

k is called window size

Output: X=A<sup>E</sup> mod M

1. precomputation : compute and store A<sub>i</sub>

A<sub>1</sub> ← A, EXPMOD(A,M), A<sub>2</sub> ← Y

for i=1 to 2<sup>k-1</sup>-1 do MULMOD(A<sub>2i-1</sub>,A<sub>2</sub>,M),

A<sub>2i+1</sub> ← Y

for i = 0 to p, decompose E into zero and nonzero windows f<sub>i</sub> of length L(f<sub>i</sub>)≤k

2. X←A<sub>f<sub>p</sub></sub>

3. for i = p-1 down to 0 do

for j=1 to L(f<sub>i</sub>) do EXPMOD(X,M), X ← Y ; X<sup>2<sup>L(f<sub>i</sub>)</sup></sup>

if f<sub>i</sub> ≠ 0 then MULMOD(X,A<sub>f<sub>i</sub></sub>,M), X ← Y

4. Return (X)

- [5] B. Moller, "Improved Techniques for Fast Exponentiation", Information Security and Cryptology-ICIST 2002, Springer-Verlag LNCS 2587, pp.298-312, 2003.
- [6] N. Pinckney, D. Harris, "Parralelized radix-4 scalable Montgomery multipliers", Journal of Integrated Circuits and Systems, vol.3, no.1, pp.39-45, 2008.
- [7] L. Tawalbeh, A. Tenca and C. Koc, "A radix-4 scalable design", IEEE Potentials, vol.24, pp.16-18, 2005.
- [8] A. Tenca, C. Koc, "A scalable architecture for modular multiplication based on Montgomery's algorithm, IEEE Trans. On computer, vol.52, no.9, pp.1215-1221, 2003.
- [9] N. Pinckney, P. Amberg and D. Harris, "Parallelized Booth-encoded radix-4 Montgomery multipliers", proceeding of 16<sup>th</sup> IFIP/IEEE International Conference on Very Large Scale Integration, 2008.
- [10] P. Montgomery, "Modular multiplication without trial division", Mathematics of Computation, vol.44, pp.519-521, 1985.
- [11] P. Barrett, "Implementing the Rivest Shamir and Adleman public key encryption algorithm on a standard digital signal processor", Advances in Cryptology- CRYPTO'86, pp.313-323, 1987.
- [12] W. Hasenplaugh, G. Gaubatz and V. Gopal, "Fast Modular Reduction", 18<sup>th</sup> IEEE Symposium on Computer Arithmetic (ARITH'07), pp.225-229, 2007.
- [13] П.Стоянов, В.Димов, "Модулна редукция за криптографски алгоритми без предварителни изчисления", Научни трудове на Русенски университет, том 47, серия 3.2, стр.80-83, 2008.

#### IV. CONCLUSION

Modular exponentiation is the main operation to RSA-based public-key cryptosystems. It is performed using successive modular multiplications. This operation is time consuming for large operands, which is always the case in cryptography. For software or hardware fast cryptosystems, one needs thus reducing the total number of modular multiplications required. The proposed algorithm for modular exponentiation is effective by transmission of short messages. It is faster then the classical algorithm why because it does not use integer division. The check in step 1 of EXPMOD and MULMOD reduces the execution time, because always A<M/2. The execution time for step 3 is less, as smaller is the value of  $\lfloor X / 2^n \rfloor$ . With multiplicity of the modulus different than 8 is selected n=8k and step 2 is being executed while P<M. This permits canceling of rotation within steps 3.1 и 3.2 and operating with bytes only.

#### REFERENCES

- [1] W. Diffie, M. Hellman, "New direction in cryptography", IEEE Trans., Inform. Theory IT-22, pp. 644-654, Nov.1976.
- [2] A. Menezes, P. van Oorschot and S. Vanstone, "Handbook of Applied Cryptography", CRC Press, first ed. 1997.
- [3] R. Rivest, A. Shamir and L. Adleman, "A method for obtaining digital signatures and public-key cryptosystems", Communications of the ACM, 21(2), pp. 120-126, 1978.
- [4] C. Koc, "Analysis of Sliding Window Techniques for Exponentiation", Computers and Mathematics with Applications, 30(10), pp.17-24, 1995.

# Energy Efficient Add/Drop Approach for Pico-Cells in Heterogeneous Networks

Oleg Asenov<sup>1</sup>, Pavlina Koleva<sup>2</sup> and Vladimir Pulkov<sup>3</sup>

**Abstract –** In this paper we propose an approach for finding a Heterogeneous Networks (HetNet) Long Term Evolution (LTE) operation scenario which leads to minimization of both the overall downlink power of the Base Stations (BS) in the cell and uplink power of the users. The approach is based on the facts that the transmitted downlink power of a BS is dependent on their load and the uplink power is dependent on the distance of the users from the serving BS. The development of an energy efficient operating solution from both base station and user point of view introduced in this paper is based on a power model for the LTE HetNet and an add/drop heuristic activating procedure for different operation modes of pico BS located in the serving area of the LTE evolved Node Base (eNB).

**Keywords –** Heterogeneous Networks, Long Term Evolution, Pico Cells, Add/Drop Heuristics.

## I. INTRODUCTION

Heterogeneous scenarios in LTE with macro cells and pico cell deployments besides increasing coverage and throughput in many cases can optimize the energy efficiency of a cellular network. Deploying pico cells is expected to make the cellular networks more power efficient due to the reduction of the transmission power as a consequence of the decrease of the distance between the serving nodes and smaller serving areas. In such cases the energy efficiency of the wireless network is mainly dependent on the overall power consumption of the macro and pico base stations, their transmission power and load. The energy efficiency of such scenarios is investigated in many papers. The analyses consider mainly the deployment phase in order to find the best deployment architectures and scenarios for quantifying the potential macro-offloading benefits in terms of higher date rates and reduction of the energy consumption [1], [2], [3], [4], [5], [6].

Energy consumption of the Macro Base Station (eNB in LTE) and Pico Base Stations (PBSs) is traffic dependent and thus dependent on the number of their associated User Equipments (UEs), or UEs served by the corresponding base station. In 3GPP LTE, an UE is associated with the node from which it receives the highest SINR (Signal to Interference plus Noise Ratio). Sometimes this could result in a load imbalance between the eNB and PBSs in the serving area, thus limiting

<sup>1</sup>Oleg Asenov is with the Faculty of Mathematics and Informatics, St.Kiril and St.Metodius University of Veliko Tarnovo, 5003 Veliko Tarnovo, 2 T. Tarnovski str., Bulgaria, e-mail: olegasenov@abv.bg.

<sup>2</sup>Pavlina Koleva is with the Faculty of Telecommunications, Technical University of Sofia, Sofia 1756, 8 Kl. Ohridski Blvd., Bulgaria, e-mail: p\_koleva@tu-sofia.bg.

<sup>3</sup>Vladimir Pulkov is with the Faculty of Telecommunications, Technical University of Sofia, Sofia 1756, 8 Kl. Ohridski Blvd., Bulgaria, e-mail: vkp@tu-sofia.bg.

the user throughput and practically not contributing to the overall energy efficiency. On the other hand energy efficiency is considered in relation with the downlink emitted power from the serving Base Station (BS) and in most cases the uplink power from the UEs is not taken under consideration.

In this paper we propose a dynamic add/drop approach for finding an operation scenario of a LTE cell with PBSs which has an optimum in relation to the energy efficiency of both the overall downlink power of the Base Stations (BS) and uplink power of the users in the cell. This could also be reviewed as a trade-off between the power consumption of the access BSs and UEs.

In the next section we describe the power model for the HetNet scenario, the add/drop approach is explained in section III, in section IV we present some numerical results and the last section concludes this paper.

## II. POWER MODEL FOR HETNET SCENARIO

A typical LTE heterogeneous network scenario is shown in Fig. 1. In the serving area of the eNB are deployed several pico cells. The pico cell in a mobile phone network is served by a low power cellular PBS that covers a smaller area usually deployed in places with dense traffic.

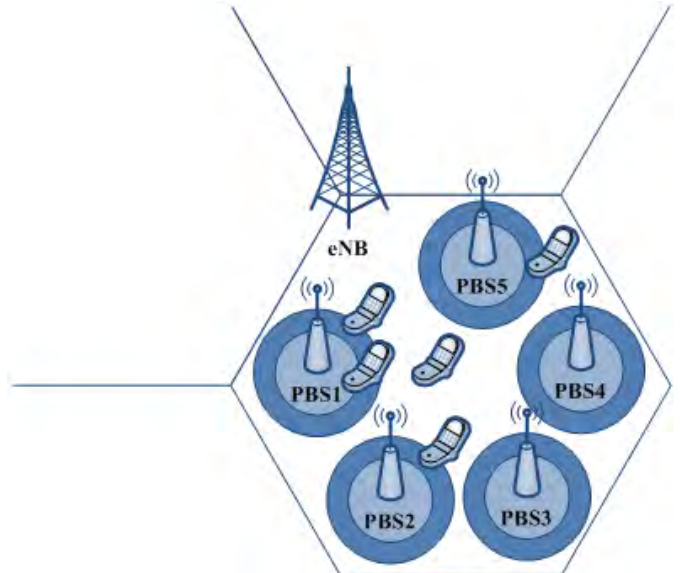


Fig. 1. HetNet scenario

The power models used in this paper are adopted from [7]. The power models of the eNB and PBS are described by a downlink static and a dynamic part as follows:

$$P_{\text{downlink\_one}} = (P_{\text{static}} + P_{\text{dynamic}}) \quad (1)$$

The eNB static part for one sector is defined as 40% of the maximum downlink power:

$$P_{eNB\_static} = 0.4 * P_{eNB} = N_{PA} * \left( \frac{P_{Tx}}{\mu_{PA}} + P_{SP} \right) * (1 + C_C) * (1 + C_{PSBB}) \quad (2)$$

and the dynamic:

$$P_{eNB\_dynamic} = C_{Tx,N_L} * N_L \quad (3)$$

The PBS downlink static part is described as:

$$P_{PBS\_static} = \left( \frac{P_{Tx}}{\mu_{PA}} * C_{Tx,static} + P_{SP,static} \right) * (1 + C_{PS}) \quad (4)$$

and the dynamic:

$$P_{PBS\_dynamic} = P_{PBS\_dynamic\_link} * N_L, \quad (5)$$

where

$$P_{PBS\_dynamic\_link} = \left( \frac{P_{Tx}}{\mu_{PA}} * (1 - C_{Tx,static}) * C_{Tx,N_L} + P_{SP,N_L} \right) * (1 + C_{PS}) \quad (6)$$

The power model parameters are shown in Table I.

TABLE I  
POWER MODEL PARAMETERS

Parameters	Descriptions	Values	
		eNB	PBS
$N_{PA}$	# of power amplifiers per sector	2	2
$\mu_{PA}$	Power amplifiers efficiency	0.38	0.20
$P_{Tx}$	Maximum transmit power	39.81	1
$P_{SP} [W]$	Signal processing overhead	58	-
$P_{SP,static} [W]$	Static signal processing overhead	-	15
$P_{SP,NL} [W]$	Dynamic signal processing per link	-	0.55
$C_C$	Cooling loss	0.29	-
$C_{PSBB}$	Battery backup & power supply loss	0.11	-
$N_L$	# of active links	-	50
$C_{Tx,NL}$	Dynamic transmit power per link	1	0.04
$C_{Tx,static}$	Static transmit power	-	0.80
$C_{PS}$	Power supply loss	-	0.11

Each PBS can operate in the modes off (stand by), active - normal range and active - extended range, the latter being function of the radius of the normal or extended serving area of the PBS.

The uplink power of an UE associated to an eNB or PBS station is defined as:

$$P_{uplink} = \sum_{j=1}^U MA_j * P_{tx,j}. \quad (7)$$

Here  $U$  is the number of UEs,  $MA_j$  are the elements of the matrix of associations  $MA$  with values:

$$M_j = \begin{cases} 1; & \text{if } UE_j \text{ is associated to a BS} \\ 0; & \text{if } UE_j \text{ is not associated to a BS} \end{cases} \quad (8)$$

and the transmit power  $P_{tx}$  is calculated from the following equation:

$$P_{tx} = \min\{P_{max}, P_0 + 10 * \log_{10} M + \alpha * PL\} \quad (9)$$

Here  $P_{max}$  is the maximum allowed transmit power which has an upper limit of 23 dBm for UE power class 3,  $P_0$  is the power offset comprising cell-specific and UE specific components,  $M$  is the number of physical resource blocks (PRBs) allocated to the UE,  $\alpha$  is a cell-specific path loss compensation factor,  $PL$  is the path loss estimate calculated at the UE.

For the UEs served by the eNB the path loss is determined in the following way:

$$PL_{eNB} = 131.1 + 42.8 * \log_{10} R \quad (10)$$

For the UEs served by the PBSs the path loss is:

$$PL_{PBS} = 145.4 + 37.5 * \log_{10} R \quad (11)$$

where  $R$  is the distance in kilometers.

The total power for the cell (eNB and PBSs) including uplink and downlink is given as:

$$P_{system} = P_{downlink} + P_{uplink} \quad (12)$$

where:

$$P_{downlink} = \sum_{i=1}^{N+1} P_{static,i} + P_{dynamic,i} \quad (13)$$

$$P_{uplink} = \sum_{i=1}^{N+1} \sum_{j=1}^U MA_{ij} * P_{tx,ij} \quad (14)$$

### III. ENERGY DEPENDENT ADD/DROP ALGORITHM TO USER ASSOCIATION IN HETNET

To determine an optimal energy efficient operating solution from both BS and UE point of view we use add/drop heuristics [8]. The task is to find such an operating scenario (operating modes of the PBSs) which will lead to minimization of the overall downlink power of the eNB and PBSs in the cell and the uplink power of the UE. Practically we propose an algorithm to find the set of active PBSs, which will lead to minimum overall power balance in the cell, based on the assumption that the set is formed through a heuristic activation/deactivation PBSs procedure.

In each step of the algorithm, based on the power model described in section II, we determine the operating mode of the PBS for which  $P_{system}$  has minimum:

$$\text{MIN}\{P_{system}\} \quad (15)$$

Depending on the radius of the serving area of the PBS (a function of the operating mode – active normal or active

extended) a corresponding number of users are served (associated). After determining the PBS mode we apply the add/drop procedure for activating the PBSs and for each case calculate a power parameter reflecting the changes of the overall uplink and downlink power in the cell which we call “power balance”, given as:

$$PowerBalance = abs(\Delta P_{uplink} + \Delta P_{downlink}) \quad (16)$$

where

$$\Delta P_{uplink} = \left( 1 - \frac{P_{uplink}}{P_{uplink\_eNB}} \right) \quad (17)$$

$$\Delta P_{downlink} = \left( 1 - \frac{P_{downlink}}{P_{downlink\_eNB}} \right) \quad (18)$$

At the end of each step we choose the case which gives:

$$MIN\{PowerBalance\} \quad (19)$$

To find the most efficient solution and giving the trade-off between the changes of the overall downlink and uplink power in the cell we compare the chosen minimum power balances from each step of the add/drop algorithm and choose for operation scenario the step in which the power balance is minimum. Looking at the matrix of associations for this step we can see the operating mode for each of the PBSs in the cell and its user associations. Based on the MA the corresponding PBSs are activated.

In the case of a number of N pico base stations in the serving area of the eNB the add/drop algorithm is realized in the following steps:

### **Input calculations:**

- Input calculations:**

  - a) Determination of the elements of the Distant Matrix (Floyd matrix). The Distant Matrix (DM) gives the distance of each UE to the eNB and all of the PBSs in the cell.
  - b) Calculation of  $P_{uplink\_eNB}$  and  $P_{downlink\_eNB}$  in the case of all PBSs being in mode “OFF” and all UEs being served by the eNB.

### **PBS Add/Drop procedure:**

### Step 1:

- Step 1:

  - Based on the DM, a matrix of associations ( $MA$ ) is determined in the case when the first PBS is in mode “ACTIVE-NORMAL”. All UEs that are not in the normal serving range of this PBS are associated to (served by) the eNB.  $P_{uplink}$ ,  $P_{downlink}$ ,  $P_{system}$  and the  $PowerBalance$  are calculated.
  - Based on the DM, a matrix of associations ( $MA$ ) is determined in the case when the same PBS is in mode “ACTIVE-EXTENDED”. All UEs that are not in the extended serving range of this PBS are associated to the eNB.  $P_{uplink}$ ,  $P_{downlink}$ ,  $P_{system}$  and the  $PowerBalance$  are calculated.
  - For this PBS the active mode with less  $P_{system}$  is chosen to be operating.
  - The calculations of  $P_{uplink}$ ,  $P_{downlink}$ ,  $P_{system}$  and  $PowerBalance$  are done in the cases of sequentially

activating and turning off the rest of the PBSs in the eNB serving area.

- e) Based on the results of the calculations above the case with the minimum *PowerBalance* (Eq.19) is chosen, thus determining which PBS will be considered as active for this step.

### **Step 2:**

- a) The PBS in the previous step is in active (normal or extended) operating mode thus associating the UEs located in its serving area.
  - b) Based on the DM, a matrix of associations is determined ( $MA$ ) in the case when one of the rest ( $N-1$ ) of the PBSs is in mode “ACTIVE-NORMAL”. The rest of the UEs that are not in the normal serving range of this PBS are associated to the eNB.  $P_{uplink}$ ,  $P_{downlink}$ ,  $P_{system}$  and the  $PowerBalance$  are calculated.
  - c) Based on the DM, a matrix of associations ( $MA$ ) is determined in the case when the same PBS is in mode “ACTIVE-EXTENDED”. The rest of the UEs that are not in the extended serving range of this PBS are associated to the eNB.  $P_{uplink}$ ,  $P_{downlink}$ ,  $P_{system}$  and the  $PowerBalance$  are calculated.
  - d) For this PBS the active mode with minimum  $P_{system}$  is chosen to be operating.
  - e) The calculations of  $P_{uplink}$ ,  $P_{downlink}$ ,  $P_{system}$  and  $PowerBalance$  are done in the cases of sequentially activating and turning off the other PBSs in the eNB serving area.
  - f) Based on the results of the calculations above the case with the minimum  $PowerBalance$  (Eq.19) is chosen, thus determining the next PBS that will be considered as active for this step.

### **Steps 3 to N:**

These steps are repeated until reaching the value of  $N$ , which is the number of the PBSs in the cell.

### **Output:**

The algorithm compares the results for the minimum *PowerBalance* (Eq.19) for each step and gives as output the step with least value. Based on the MA for this step the corresponding PBSs are activated.

The advantage of the proposed algorithm is that in each step the number of calculations decreases with  $N-p$ , where  $p$  is current step of the algorithm. This actually determines it heuristic nature.

#### IV. SIMULATION RESULTS

TABLE II  
SIMULATION INPUT DATA

Number of users	50
Number of PBSs	5
PBS operating modes: Active-normal	20 m coverage
Active-extended	30 m coverage
Static eNB downlink power – Eq. (2)	186.45 W
Static PBS downlink power – Eq. (4)	21.09 W
Dynamic downlink eNB power per link	1 W
Dynamic downlink PBS power per link – Eq. (6)	0.655 W

To illustrate the algorithm we have developed a simulation scenario. The input data is given in Table II and the

simulation results are given in Tables III, IV, V, VI and Fig. 2. From the calculations and the results it could be seen that the power balance is minimum in the third step where active are PBS1, PBS2 and PBS5 in active-extended mode. The associated UEs to each base station are given in Table VI.

TABLE III  
DISTANCE MATRIX

	UE1	UE2	UE3	...	UE48	UE49	UE50
eNB	124.93	110.29	128.61	...	58.32	118.83	94.37
PBS1	16.35	8.82	8.11	...	103.46	163.97	139.51
PBS2	165.83	173.7	169.75	...	262.1	322.62	298.16
PBS3	194.46	200.3	197.15	...	268.93	329.45	304.99
PBS4	307.85	291.18	299.94	...	217.38	205.57	200.11
PBS5	155.95	139.28	148.04	...	50.62	13.15	18.62

TABLE IV  
RESULTS FOR THE ASSOCIATION MATRIX FOR STEP 3

Step 3	UE1	UE2	...	UE11	...	UE48	UE49	UE50
eNB	0	0	...	0	...	1	0	0
PBS1	1	1	...	0	...	0	0	0
PBS2	0	0	...	1	...	0	0	0
PBS5	0	0	...	0	...	0	1	1

TABLE V  
ACTIVE PBSS AND ASSOCIATED UEs FOR STEP 3

Base Station	Mode	Associated UEs
eNB	-	UE5, UE17, UE18, UE20-UE40, UE46-UE48
PBS1	Active-extended	UE1-UE4, UE6-UE10
PBS2	Active-extended	UE11-UE16, UE19
PBS5	Active-extended	UE41-UE45, UE49, UE50

TABLE VI  
POWER BALANCE RESULTS FOR EACH STEP OF THE ALGORITHM

Step	$\Delta P_{uplink}$	$\Delta P_{downlink}$	PowerBalance
1	-10.72%	7.61%	3.12%
2	-17.63%	15.50%	2.13%
3	<b>-22.74%</b>	<b>23.40%</b>	<b>0.66%</b>
4	-27.47%	31.30%	3.83%
5	-31.29%	39.34%	8.05%

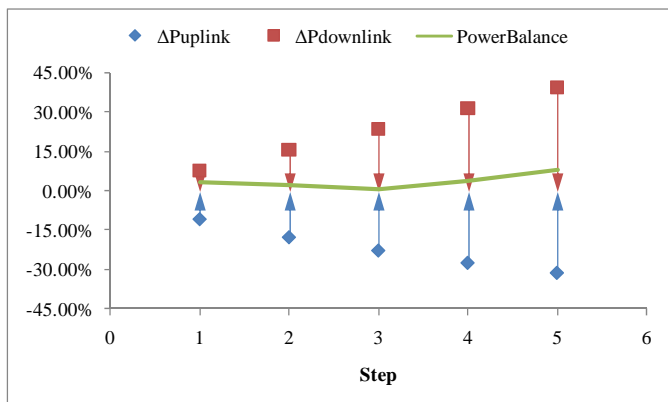


Fig. 2. Power Balance Results for each Step of the Algorithm

## V. CONCLUSION

In this paper we propose an approach for finding an operation scenario of a LTE HetNet cell with pico cells which has an optimum in relation to the energy efficiency of both the overall downlink power of the Base Stations (BS) and uplink power of the users in the cell. We introduced a parameter reflecting the changes in the downlink and uplink power in the cell when the pico base stations operate in different modes. The determination of an energy efficient operating solution from both base station and user point of view is based on an appropriate power model for the heterogeneous network and an add/drop heuristic procedure for putting into operation (activating) the pico base stations. The advantage of the proposed algorithm is that it is with low complexity as the number of calculations decreases with each step of the algorithm.

Future work in the aspect of this approach is related to the further development of the algorithm in order to reflect the dynamic changes in the user associations to the different pico base stations, i.e. mobility and activity of the users in the cell. A change of the user location or state will lead to change of the elements of the distance matrix and matrix of associations. Such cases must be analyzed and a proper solution must be proposed in order to avoid distortion of the power balance of the system and frequent and adverse changes of the operating conditions of the pico base stations. A throughput analysis together with the power efficiency is also foreseen.

## ACKNOWLEDGEMENT

This work was supported in part by the Grant DDVU02/13/17.12.2010 "Public and Private Multimedia Network Throughput Increase by Creating Methods for Assessment, Control and Traffic Optimization" of the Bulgarian Science Fund.

## REFERENCES

- [1] D. Calin, H. Claussen, and H. Uzunalioglu, "On femto deployment architectures and macrocell offloading benefits in joint macro-femto deployments", IEEE Communications Magazine, vol. 48, no. 1, pp. 26-32, 2010.
- [2] F. Richter, A. J. Fehske, and G. P Fettweis, "Energy Efficiency Aspects of Base Station Deployment Strategies for Cellular Networks", Proc. of IEEE VTC2009-Fall, pp.1-5, 2009.
- [3] A. J Fehske, F. Richter, and G. P Fettweis, "Energy Efficiency Improvements through Micro Sites in Cellular Mobile Radio Networks", Proc. of IEEE GLOBECOM 2009, pp.1-5, 2009.
- [4] I. Ashraf, L.T.W. Ho, H. Claussen, "Improving Energy Efficiency of Femtocell Base Stations Via User Activity Detection", Proc. of IEEE WCNC'10, pp.1-5, 2010.
- [5] J. Hoydis, M. Kobayashi, and M. Debbah, "Green Small-Cell Networks", IEEE Vehicular Technology Magazine, vol. 6, no. 1, pp. 37-43, 2011.
- [6] O.-E., Barbu, O. Fratu, "An enabler of interoperability in heterogeneous wireless networks", Proc. of Wireless VITAE, pp. 1-5, 2011.
- [7] A. B. Saleh, O. Bulakci, S. Redana, B. Raaf, J. Hamalainen, "Evaluating the energy Efficiency of LTE-Advanced Relay and Picocell Deployments", Proc. of IEEE WCNC'12, pp. 2335-2340, 2012.
- [8] R. Rardin, R. Uzoy, "Experimental Evaluation of Heuristic Optimization Algorithms: A Tutorial", Journal of Heuristics, vol. 7, pp. 261-304, 2001.

---

---

## Poster 3 - Signal Processing

---

---



# A Variational Approach of Optimization the Signal Form in the Radio Communication Systems

Galina Cherneva<sup>1</sup>, Elena Dimkina<sup>2</sup>

**Abstract –** The paper presents the criteria of quality of optimization the signal form, the general kind of the functional and the complementary conditions as well as the methods of its examination.

**Keywords –** Variational approach, optimal signals synthesis quality

## I. INTRODUCTION

The signals transmitting information along the channels of connection are a function of the real time defining their forms and of the message characterizing the type of modulation [1]. To define the form, it is necessary to know the signal coordinates in the signal space. In that sense the form is an individual feature of the signal.

In cases when there is signal receiving at noise background it asymmetrical and non-monotonous probability of density [1], it is possible to assign the task of optimization: to define those signals, which, passing through the channel of connection, would create fluctuations at its output maximally far away from one to another.

Optimization tasks are of extreme nature that predetermines the variation approach [3] for solving them.

The paper presents the results of defining the criteria of quality of optimal signals synthesis quality, the general kind of the functional and the complementary conditions as well as the methods of its examination.

## II. FORMULATION OF THE PROBLEM OF OPTIMIZATION THE TRANSMISSION SIGNALS

The channel of connection is described by an “input-output” integral-and-differential equation in the kind of:

$$s(t) = \sum_{r=-q}^l \alpha_r(t) x^{(r)}(t), \quad (1)$$

where  $s(t)$  is the input signal,

$x(t)$  is the output signal,

$\alpha_r(t)$ - coefficients before  $x(t)$  and its derivatives from “ $r$ ”-

<sup>1</sup>Galina Cherneva is with the Faculty of Telecommunications and Electrical Equipment in Transport at T. Kableshkov University of Transport Sofia, 158 Geo Milev Blvd, Sofia 1574, Bulgaria, E-mail: cherneva@vtu.bg.

<sup>2</sup>Elena Dimkina is PhD Student with the Faculty of Telecommunications and Electrical Equipment in Transport at T. Kableshkov University of Transport Sofia, 158 Geo Milev Blvd, Sofia 1574, Bulgaria, E-mail: elena.dimkina@abv.bg.

th order,  $r = -q \dots 0 \dots l$ .

The functional of the quality can be definite as [3,4]:

$$I = \sum_{i=1}^n \sum_{j=1}^n \left[ \frac{1}{\Delta\tau} \int_{\tau_1}^{\tau_2} f_{ij}[x_i(t), x_j(t), V(t), t] dt \right] \quad (2)$$

where  $V(t)$  is the vector function of the disturbing signals,

$[\tau_1, \tau_2]$  is the interval of examination of the output signal.

The function  $f_{ij}[\cdot]$  is the distance between the  $i$ -th and  $j$ -th signals at the output of the channel of connection and the functional (2) takes the kind of:

$$I = \left[ \frac{1}{\Delta\tau} \int_{\tau_1}^{\tau_2} |x_i(t)|^m dt \right]^{1/m}, \quad (3)$$

where  $|x_i(t)|^m$  is the norm of  $m$ - order of the output signal  $i=1,2,\dots,n$ .

When  $m=1$ , the functional of the quality is commensurable to the average rectified value of the output signal  $x(t)$ .

When  $m \rightarrow \infty$  - the functional is commensurable to the crest value of the output signal.

When  $m=2$  - the functional of the quality is commensurable to the energy of the output signal.

A characteristic peculiarity of the form optimization problem is that it is a problem of limitations . They determine a close area in the signal space where the signals searched for are found.

The most spread limitation in practice is that of the average value of  $p$ - th order of the signal being optimized [5]:

$$\left[ \frac{1}{\Delta T} \int_{\tau_1}^{\tau_2} |s_j(t)|^p dt \right]^{1/p} \leq S_p, \quad (4)$$

he value of  $p$  in equation (4) depends on the kind of limitation imposed by the transmitter. The possible cases are as follows:

- limitation of the peak value of the signal ( $p \rightarrow \infty$ ).
  - limitation of the average rectified value of the signal ( $p=1$ ).
  - limitation of the average square value of the signal ( $p=2$ ).
- So the problem of optimization the transmission signals can be formulated in such a way: within the class of signals  $L_p[\tau_1, \tau_2]$  determined by limitations of (4) to find those  $s_j(t)$ , that maximize the functional of the quality (3).

It is assumed that the most common case in practice is the one with coincidence of the intervals of examination  $[\tau_1, \tau_2]$  and signal existence  $[t_1, t_2]$ .

Expressing the output signal by the input one, the functional, which has to be maximized, takes the kind of:

$$I = \int_{t_1}^{t_2} \dots \int_{t_1}^{t_2} s(t_1) \dots s(t_v) H_v(t_1 \dots t_v) dt_1 \dots dt_v . \quad (5)$$

where  $H_v(t_1, \dots, t_v)$  is the kernel of the functional.

When the model of channel of connection is linear (Fig.1), the kernel of the functional depends on the channel pulse characteristics  $h(t)$ :

$$H_v(t_1, \dots, t_v) = \frac{\int_{\max(t_1, t_2, \tau_1)}^{\tau_2} m_1[h(t, t_1) \dots h(t, t_v)] dt}{\tau_2 - \max(t_1, t_2, \tau_1)} . \quad (6)$$

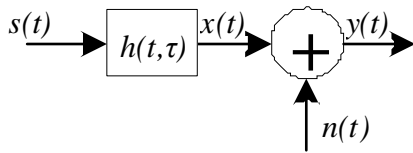


Fig. 1 A linear model of communication channel

The solution of this optimization task is carried out according to the method of double-sided variations of searching signals. This method consists in substituting the functional argument by an argument in the kind of a real variable and obtaining a homogeneous differential equation of

boundary conditions at the end points of the harmonized signal localization interval, i.e. it is a boundary problem.

#### IV.CONCLUSION

The paper presents a variational approach in the purpose of optimization of the transmitted signal form in the connection channel. The approach is based on the definition of a functional that is used to describe the quality criteria of synthesis and to determine the kernel of the optimal operator operating on the input signal with which the functional reaches its extreme. The functional of the quality depends on an integral operator connected with a defined function in the linear standardized signal area. The kernel of the functional is determined by the necessary and sufficient conditions of the functional extreme. Thus the signals searched for are obtained as a solution of a system of integral equations.

#### REFERENCES

- [1] Haykin S. *Communication Systems* - 4th ed. - John Wiley & Sons, 2001.
- [2] Hutson V. *Applications of Functional Analysis and Operator Theory*. London, 1980.
- [3] Cherneva G. Generation and Examination on Signals, Harmonized with Communication Channels. PhD Dissertation. S. 2007.
- [4] Cherneva G., Setting the Problem of Synthesis of Signals Coordinated with the Cannel of Connection, Mechanics, Transport, Communications, Vol. 2/2004, pp.8.1-8.8
- [5] A.Andonov , G.Cherneva Formation of Signals Harmonized with the Linear Channel of Connection with Limitation of their Average Rectified Values, XLI iCEST, 29.06-01.07.06, TU-Sofia, pp.129-131.

# Synchronization in Radio Communication Systems with Pseudo Random Restructuring Operation

Antonio Andonov<sup>1</sup> and Filip Iliev<sup>2</sup>

**Abstract –** On the basis of Markov theory for optimal nonlinear filtration a problem is set and being researched for the estimation and maintenance of autonomous synchronization in the system for radio communication among remote moving objects.

**Keywords –** radio communication systems, synchronization.

The analysis of systems using pseudo-mode with frequency hopping has specific characteristics determined by the need for joint evaluation of discrete and continuous processes. Estimation error of filtration can be carried out in accordance with methods of Markov theory [1].

If applied common description of the useful signal in the form of known function of a discrete data parameter  $d(t)$  and random delay  $\tau(t)$  can be written as follows:

$$s(t, dt) = s[(t - \tau(t)), d(t - \tau(t))] \quad (1)$$

The transmitted signal in the analyzed case of the proposed work is the sum of  $n$  elementary signals, each of which with duration of  $T_s$  seconds, i.e.  $s(t) = \sum_{k=0}^{\infty} s_k(t - kT_s)$ .

Then in the presence of random delays, adopted useful signal is:

$$s(t, \tau(t)) = s(t - \tau(t)) = \sum_{k=0}^{\infty} s_k(t - kT_s - \tau(t)).$$

The values of the information parameter of the respective clock intervals  $T_s$  form a simple homogeneous Markov chain  $d_k$ ,  $k = 0, 1, \dots$  with  $n$  states. The accidental time delay, which is a consequence of the relative movement between the receiver and transmitter, in the general case can be considered as a first component of a diffusion Markov process  $\lambda(t)$ , i.e.  $\tau(t) = \lambda_1(t)$ . In the theory of nonlinear filtering [1], process  $\lambda(t)$  satisfies the system stochastic differential equations containing a' priori information about the signal:

$$\frac{d\lambda_i(t)}{dt} = K_i(\lambda, t) + n_i(t), \quad i = 1, m \quad (2)$$

Here  $\lambda_i = \lambda_i(t)$  are components of multidimensional Markov random vector  $\lambda(t)$ ,  $n_i(t)$  is independent of the white noise.

A' priori probabilistic density  $W_{pr}(\lambda, t)$  of random vector  $\lambda(t)$  is described by the equation of Fokker-Planck-Kolmogorov:

<sup>1</sup>Antonio Andonov is with the Faculty of Telecommunications and Electrical Equipment in Transport at Higher School of Transport of Sofia, 158 Geo Milev Str., Bulgaria, E-mail: andonov@vtu.bg.

<sup>2</sup>Filip Iliev is with the Faculty of Telecommunications and Electrical Equipment in Transport at Higher School of Transport of Sofia, 158 Geo Milev Str., Bulgaria, E-mail: fgi@mail.bg.

$$\begin{aligned} \frac{\partial W_{pr}(\lambda, t)}{\partial t} &= -\sum_{i=1}^m \frac{\partial}{\partial \lambda_i} [K_i(\lambda, t) W_{pr}(\lambda, t)] + \\ &+ \frac{1}{4} \sum_{i,j=1}^m \frac{\partial^2}{\partial \lambda_i \partial \lambda_j} [N_{ij} W_{pr}(\lambda, t)] \equiv L_{pr} W_{pr}(\lambda, t) \end{aligned} \quad (3)$$

where  $K_i$  is a deterministic function (transmission coefficient).

Equation (3) characterizes the behaviour of the probabilistic density  $W_{pr}(\lambda, t)$  at any point in time. All available information on the parameters of the useful signal is contained in the final a' posteriori probabilistic density  $W(\lambda, t) = W_{pr}(\lambda, t | r_o^i)$  of the vector  $\lambda(t)$ , which satisfies the following integro differential equation:

$$\frac{\partial W(\lambda, t)}{\partial t} = L_{pr} W(\lambda, t) + F(\lambda, t) - \langle F(\lambda, t) \rangle W(\lambda, t), \quad (4)$$

wherein:

$$\begin{aligned} F(\lambda, t) &= \frac{1}{N_0} [2r(t)s(t, \lambda) - s^2(t, \lambda)], \\ \langle F(\lambda, t) \rangle &= \int_{-\infty}^{\infty} F(\lambda, t) W(\lambda, t) d\lambda, \end{aligned}$$

$r_0^t$  is adopted to implement interval  $[0, t]$ ,  $N_0$  – one-sided spectral density of white noise.

Equation (4) describes the evolution of a' posteriori probabilistic density. At the initial moment of time, a' posteriori density coincides with the a' priori. In the process of monitoring the implementation  $r(t)$  is accumulating information about the filtered parameters and a' posteriori probabilistic density is concentrated in the vicinity of the assessed values of the parameters of the useful signal. Solving equation (4), and its modeling, is a complex task. Therefore, for practical purposes is assumed, that the a' posteriori density  $W(\lambda, t)$  at sufficiently high signal/noise ratio is close to normal. Then it is enough to estimate the value  $\lambda_i^*(t) \equiv \lambda_i^*$  of the components of a vector  $\lambda$ , and cumulants  $h_{ij}(t) = h_{ij}$  (Gaussian approximation in the theory of nonlinear filtration [1]), satisfying the following equations:

$$\frac{d\lambda_i^*}{dt} = K_i(\lambda^*) + \sum_{j=1}^m h_{ij} \frac{\partial F(\lambda^*, t)}{\partial \lambda_j^*} \quad (5)$$

$$\begin{aligned} \frac{dh_{ij}}{dt} &= \frac{1}{2} N_{ij} + \sum_{\mu=1}^m \left[ \frac{\partial K_i(\lambda^*)}{\partial \lambda_\mu^*} h_{\mu j} + \frac{\partial K_i(\lambda^*)}{\partial \lambda_\mu^*} h_{i\mu} \right] + \\ &+ \sum_{\mu, v=1}^m h_{i\mu} h_{vj} \frac{\partial^2 F(\lambda^*, t)}{\partial \lambda_\mu^* \partial \lambda_v^*} \end{aligned} \quad (6)$$

Equations (2) and (6) are equations for quasi optimal (quasi-linear) filtration, in accordance with which it can construct a device for filtration. These devices ensure minimum errors in filtration, characterized by the dispersions

$\sigma_a^2 = h_{aa}(t)$  and the correlation moments  $h_{ij}(t)$ . In this case  $\frac{dh_{ij}}{dt} = 0$  and by the function  $F(\lambda^*, t)$  is passing to its average value at the time  $F(\lambda^*)$ . As a result, the equations (5), (6) can be written in the form:

$$\frac{\partial \lambda_i^*}{\partial t} = K_i(\lambda^*) + \sum_{j=1}^m \bar{h}_{ij} F_{ij} F_j(\lambda^*, t) \quad (7)$$

$$\frac{1}{2} N_{ij} + \sum_{\mu=1}^m \left[ \frac{\partial K_i(\lambda^*)}{\partial \lambda_\mu^*} \bar{h}_{i\mu} + \frac{\partial K_i(\lambda^*)}{\partial \lambda_\mu^*} \bar{h}_{i\mu} \right] + \sum_{\mu, \nu=1}^m \bar{F}_{\mu\nu}(\lambda^*) \bar{h}_{i\mu} \bar{h}_{i\nu} = 0 \quad (8)$$

Here:  $F_j(\lambda^*, t) = \frac{\partial F(\lambda^*, t)}{\partial \lambda_j^*}$ ,  $\bar{F}_{\mu\nu}(\lambda^*) = \frac{\partial^2 \bar{F}(\lambda^*)}{\partial \lambda_\mu^* \partial \lambda_\nu^*}$ ,

$\sigma_j^2 = h_{jj}$  is independent of  $t$  stationary value of the a' posteriori dispersion of estimation of parameter  $\lambda_j(t)$ ;  $h_{ij}$  characterized the degree of correlation of the parameter estimates, respectively to  $\lambda_i(t)$  and  $\lambda_j(t)$  at steady-state.

In order compensation of the delay  $\tau(t)$  in the transmission medium of the signal  $s(t)$ , the same should be broadcast with overtaken in time  $y(t)$ , i.e. be of the form:  $s_y(t) = s[t + y(t)]$ . In case of delay  $\tau(t)$  the useful signal at the input of the receiver will be:

$$s_y[t - \tau(t)] = s_y[t - \tau(t) + y(t - \tau(t))] \quad (9)$$

Problem whose solution is the purpose of this study is to determine the value of  $y(t)$ , at which is providing minimum mean square value of the offset  $\varepsilon(\tau)$  in the time of reception of the signals at the input of the receiver in case of accidental delay  $\tau(t)$ , i.e.:

$$\varepsilon(t) = \tau(t) - y[t - \tau(t)] \quad (10)$$

For the determination of  $y(t)$  can be used all the current information about the random delay, which is contained in the realized oscillation  $r(t)$  for the interval  $[0, t]$  at the input of receiver, whereupon this oscillation is the sum of the useful signal and the noise:

$$r(t) = s_y[t - \tau(t)] + n(t).$$

The signal emitted by the transmitter in random moment of time  $t_0$ , enters at the input of the receiver in a channel with a random delay time point  $t_1$ , so that the equality obviously is met:  $t_0 = t_1 - \tau(t)$ . The raised problem can be reduced, so that based on the monitoring of implementation  $r(t)$  until the time of transmission of the signal  $r_0^{t_0} = \{r(t), 0 \leq t \leq t_0\}$  to determine the overtaking  $y(t_0)$ , which is providing minimum mean square value of the offset  $\varepsilon(t_1)$  of the signal, taken at the moment of time  $t_1$ . As is known, the optimal mean square assessment coincides with the conditional mathematical expectation, i.e.:

$$y(t_0) = M\{\tau(t_1) | r_0^{t_0}\} = \int_{-\infty}^{\infty} \tau p_1(\tau | t_0) d\tau \cdot p_1(\tau | t_0) = p\{\tau(t_1) | r_0^{t_0}\} \quad (11)$$

is a' posteriori, i.e. the conditional at monitoring of implementation  $r_0^{t_0}$  density of the probabilities of the random process  $\tau(t)$  at the moment  $t_1$ . At a fixed time of signal broadcasting  $t_0$ , the time of its occurrence at the input of the receiver  $t_1$ , determining according to equality (10) is random. To avoid examining of the process in random moments of time may be introduced process:

$$\tau_1(t_0) = \tau(t_1). \quad (12)$$

From (10) it follows that:

$$\tau_1(t_0) = \tau[t_0 + \tau(t_1)] = \tau[t_0 + \tau_1(t_0)]. \quad (13)$$

So  $p_1(\tau | t_0)$  is the current a posteriori probabilistic density of the process  $\tau_1(t)$ :  $p_1(\tau | t_0) = p\{\tau(t_1) | r_0^{t_0}\} = p\{\tau_1(t_0) | r_0^{t_0}\}$ .

In its physical sense  $\tau_1(t)$  is the magnitude of delaying of emitted signal at the moment  $t$ .

Ratio (12) is a transcendental equation on the basis of which it is possible to determine the  $\tau_1(t)$  at given process. From formula (13) can be obtained an equation defining the relationship between  $p_1(\tau | t)$  and  $p(\tau, l | t) = p\{\tau(t+l) | r_0^{t_0}\}$ , i.e. with a' posteriori probabilistic density of the random delay at some point of the time  $\tau(t+l)$ . When  $l$  considering as a random variable with probabilistic density  $p(l)$ , and  $\tau(t+l)$  as a function of this value, then on the basis of (12) is satisfied:

$$p\{\tau_1(t) = \tau | r_0^{t_0}\} = \int_{-\infty}^{\infty} p\{\tau(t+l) = \tau | r_0^{t_0}\} p(l) dl. \quad (14)$$

From equation (3.13) follows that:  $l = \tau_1(t)$ , i.e.  $p(l) = p_1(l | t)$ , from where follows the ratio determining  $p_1(\tau, t)$  at a set probabilistic density  $p(\tau, l | t)$ :

$$p_1(\tau | t) = \int_{-\infty}^{\infty} p(\tau, l | t) p_1(l | t) dl. \quad (15)$$

Equation (15) connects the probabilistic characteristics of the process  $\tau_1(t)$  with the characteristics of process  $\tau(t)$ . The algorithm for calculation of the  $p(\tau, l | t)$ , follows from the results of the theory of optimal nonlinear filtration. The accidental delay may accept non-negative values, i.e.  $\tau_1(t) \geq 0$ ,  $p_1(t | \tau) = 0$  to  $\tau < 0$ . Therefore, in equation (15) is only used  $p(\tau, l | t)$  to  $l \geq 0$ , i.e. only the extrapolated density of probability. Monitoring  $r(t)$  is determined by the formula (9).

Therefore, the determination of the a' posteriori probability density  $p(\tau, l | t)$  based on the monitoring of  $r^{t_0}$  is solvable task of Markov theory for optimal nonlinear filtration.

## References

- [1] B. Sklar, "DIGITAL COMMUNICATIONS – Fundamental and Applications", Prentice Hall P T R, 2003

# The Reduction of Rotating Element Noise Using Active Noise Control

Zoran Milivojević<sup>1</sup> and Violeta Stojanović<sup>2</sup>

**Abstract** –In this study we are dealing with the presentation of simulative results of noise reduction generated by a rotating element within the meeting room in The Technical College of Professional Studies in Nis. The results are obtained using ANC system. The operating principle of ANC system is first described and subsequently the results along with their analysis.

**Keywords** – Noise reduction, ANC system, acoustic impulse response.

## I. INTRODUCTION

The conventional method of noise reduction using passive acoustic absorbers is slightly efficient at frequencies below 500Hz. It is because the fact that at low frequencies the wavelength of acoustic signal becomes higher comparing to acoustic absorber. The Active Noise Control gives good results while minimizing the acoustic disturbance at low frequencies. The Active Noise Control operates on the principle of destructive interference of sound fields [1]. The destructive interference implies the superposition of two sound waves with phase shift of  $\pi$ . In a specific case, one sound wave is generated by a fan and therefore causes a nuisance, while other sound wave is generated by ANC system using loudspeakers and it is called a anti noise. The resulting sound wave at the place of receipt is considerably weakened or even annulated owing to the phase difference between these two waves. The resulting sound wave at the place of receipt is measured by an error sensor, i.e. by a microphone [1-2].

The basic ideas of the active control were first established by Paul Lueg in his patent published in The United States of America in 1936 [3]. In 1953 Harry Olson and Everett May discussed the active noise control system within both plane cockpits and car cabs [4]. In 1956 William Conover analysed the use of noise reduction active control for distributive transformators [5]. The intensive development in this field is highly contributed by the use of digital techniques for signal processing. By construction of adequate devices in the field of digital signal processing the production of practical systems with the active noise control is enabled.

In this study a simulative model of ANC system for noise reduction generated by a element rotating fan is applied in the meeting room. The acoustic impulse response is determined at the point where a microphone is set (where an error is minimised) and at some points of the room which are set at the level of the microphones. The image method is used for

<sup>1</sup>Zoran Milivojević works at The Technical College of Professional Studies in Nis, 20. Aleksandra Medvedeva, St, 18000 Nis, Serbia, e-mail: zoran.milivojevic@vtsnis.edu.rs

<sup>2</sup>Violeta Stojanović works at The Technical College of Professional Studies in Nis, 20 Aleksandra Medvedeva, St, 18000 Nis, Serbia, e-mail: violeta.stojanovic@vtsnis.edu.rs

determination of acoustic impusle response in meeting premises [6]. The implementation of this method is described in [7]. The simulation is carried out in case that the above described system is applied in a room using a sinusoidal arousal.

The organization of this study is as follows. In the section II the working principle of ANC system for noise reduction of fans and the adaptive algorithm of ANC system are described. In the section III the simulative results are shown along with the analysis of the results. The conclusion is in the section IV.

## II. ANC SYSTEMS

Three requirements can be achieved using the ANC system: a) reaching a minimum of total acoustic power of a sound source, b) forming “silence zone” and c) realization of a system which would operate as a side signal absorber. Two basic control strategies are used: a) Feedback ANC, where ANC system generates signal based on the electric signal obtained by a microphone at the point where the noise elimination is wanted and b) Feedforward ANC where a coherent electric signal of a noise is generated from acoustic noise before the acoustic noise reaches the loudspeakers for the elimination.

### A. Operating Principle and Adaptive Algorithm

The acoustic-electric equivalent scheme of ANC system for noise reduction of fan is shown in Fig 1 [8].

The sinusoidal signal with frequency which is equal to fundamental frequency of noise is generated in block OSC. The information about fundamental frequency of noise is given by a tachometer. The parameters of ANC system are changed by the adaptive algorithm LMS which also processes both sinusoidal signal and a signal from a microphone. An electric signal for the loudspeaker arousal is generated on the outlet of the ANC system. The acoustic signal out of a loudspeaker should have such an amplitude and a phase, so that after superposition with an acoustic noise signal of a fan at the point where a microphone is placed, obtains a minimal acoustic signal which represents the acoustic error signal. The electric signal on the outlet of a microphone is the electric error signal,  $e(n)$ , and it is led to ANC system.

The adaptive algorithm LMS should adjust the parameters of ANC system so that after several iterative procedures the error signal equals zero. There is a fan, a loudspeaker and a microphone in the room where the simulative model is applied. We are observing: a) the primary path of the acoustic signal of noise from a fan to a microphone and b) the secondary path of the acoustic signal of noise from a loudspeaker to a microphone. The characteristics of these path are described

by acoustic impulse response  $h(n)$  and subsequently by using Z-transformation of the transfer functions can be determined.

$P(z)$  is the transfer function of a primary path, while  $S(z)$  is a transfer function of a secondary path. The effect of a secondary path model on the system characteristics is analysed in [9-12].

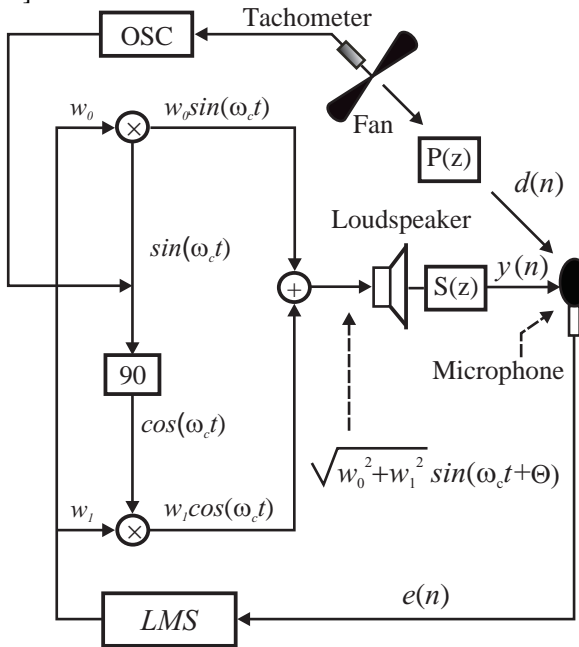


**Fig. 1.** Acoustic-electric block scheme of the system for noise reduction for the fan.

Reference signal is  $x(n) = \cos(\omega_0 n)$ . Owing to its simplicity  $A=1$  is taken. For  $n$ -th iteration results as follows [7]:

$$w_0(n+1) = w_0(n) + \mu e(n)[S(z)\cos(\omega_0 n)], \quad (1)$$

$$w_1(n+1) = w_1(n) + \mu e(n)[S(z)\sin(\omega_0 n)], \quad (2)$$

where  $\mu$  is a step size of iteration, while  $\omega_0$  is a normalised circular frequency:

$$\omega_0 = 2\pi \frac{f_0}{f_s}, \quad (3)$$

where  $f_s$  is a sampling frequency. Having in mind that the objective of this system is minimising the difference  $e(n)$  between a primary noise  $d(n)$  and a generated noise  $y(n)$ , a transfer function is here [13]:

$$H(z) = \frac{z^2 - 2z \cos \omega_0 + 1}{z^2 - 2z \cos \omega_0 + 1 + \beta S(z)[z \cos(\omega_0 - \phi_s) - \cos \phi_s]}, \quad (4)$$

where is  $\beta = \mu A^2 A_s$ ,  $A_s$  i  $\phi_s$  are the amplitude and the phase function  $S(z)$ .

$$A_e(\omega_0, \omega_1) = \frac{2A_d |\cos \omega_1 - \cos \omega_0|}{\sqrt{(2 - \beta)(\cos \omega_1 - \cos \omega_0)^2 + (\beta \sin \omega_1)^2}}, \quad (5)$$

Where is  $\omega_1$  normalized circular frequency:

$$\omega_1 = 2\pi \frac{f_1}{f_s}. \quad (6)$$

The error signal is:

$$e(n) = A_e(\omega_0, \omega_1) \cos(\omega_1 n + \phi), \quad (7)$$

where  $\phi$  is a phase angle. For the same frequencies is get:

$$A_e(\omega_0, \omega_1)|_{\omega_0=\omega_1} = 0. \quad (8)$$

Accordingly, when the frequency of a referent signal  $\omega_0$  is strictly equal to the primary frequency  $\omega_1$  a remaining signal equals 0.

### III. SIMULATION AND RESULTS ANALYSIS

#### A. Simulation

The ANC system model for noise reduction is defined by the acoustic-electric block scheme shown in the Fig. 1.

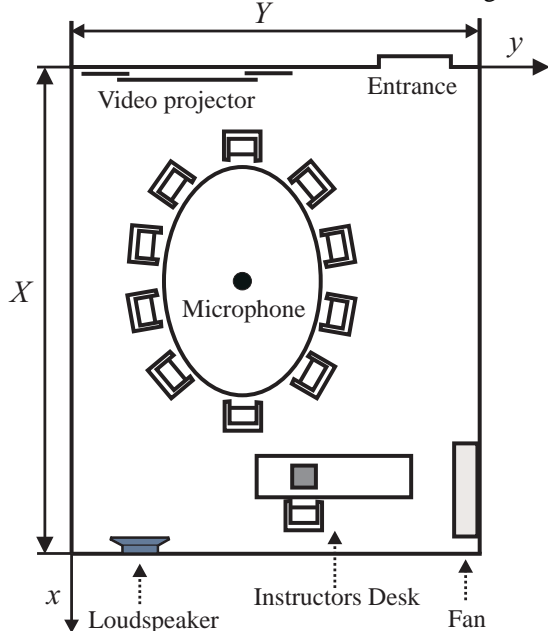


**Fig. 2.** The image of the room.

The acoustic impulse responses between the loudspeaker ( $k_L$ ,  $l_L$ ) and the positions of noise minimization ( $k_0$ ,  $l_0$ ) are determined. The characteristics of the transfer function  $S(z)$  and the characteristics of transfer functions between the loudspeakers and some points within the room ( $k$ ,  $l$ ),  $S_{kl}(z)$  are also established. The transfer function from the noise source ( $k_F$ ,  $l_F$ ) and point ( $k_0$ ,  $l_0$ ),  $P(z)$  is determined, as well as the transfer function from the noise source ( $k_F$ ,  $l_F$ ) and point ( $k$ ,  $l$ ),  $P_{kl}(z)$ .

The simulation model of the ANC system for noise reduction is applied on the meeting room, with dimensions  $X=8m$ ,  $Y=3m$ ,  $H=3.5m$ . The image of the room is given in the Fig. 2.

The noise level in whole room is calculated in  $K \times L = 33 \times 13 = 429$  points. The indexes  $k=(0-32)$  i  $l=(0-12)$  are

chosen within the grid. The distances along the  $x$ -axis and  $y$ -axis between adjacent points of a grid are  $d_x=d_y=0.25\text{m}$ . The ANC system of noise reduction from a fan ( $k_F, l_F$ ) is consisted of a microphone which is set in the points ( $k_{LS}, l_{LS}$ ) and ( $k_0, l_0$ ), respectively. The valid values are:  $0 \leq x_0, x_{LS}, x_F \leq X; 0 \leq y_0, y_{LS}, y_F \leq Y$ . The following locations are included: ( $k_F, l_F, h_F$ )=(7.25, 3, 3), ( $k_{LS}, l_{LS}, h_{LS}$ )=(8, 0.5, 3) i ( $k_0, l_0, h_0$ )=(3.25, 1.5, 0.75). The simulation is implemented for a sinusoidal arousal at point M ( $k_0, l_0, h_0$ ), where a micophone is location and also at points which are set in the plane of the microphone (points ( $k, l, h_0$ )). For the calculation of an impulse response of the room [7], the real reflection coefficients of the walls, the floor and the ceiling are as follows: 0.95, 0.95, 0.95, 0.85, 0.85 i 0.88. The algorithm includes the following parametres: a number of iterative steps  $N=2000$ , a number of steps during the analysed  $T=400$ , a size of iteration steps  $\mu=0.1$ , referent frequency  $f_0=15.097\text{Hz}$ , sampling frequency  $f_s=4\text{kHz}$ , amplitude  $A=1$ , amplitude of the fuction  $S(z)$   $A_S=2.5$ , and  $\beta=0.25$ .

The effectiveness of ANC system effect on noise reduction within the meeting room is characterized by a mean absolute value of the signal at a specific point of the room  $E_{k,l}$  and a mean absolute value of the signal for the whole room  $\bar{E}$ . At a referent point in the room ( $k_0, l_0$ ), the effectiveness of the effect is characterized by two values: the relation between a mean absolute value for noise level of the fan before the effect of the ANC system and a mean absolute value for noise level at the measured point during the ANC operation,  $\eta_{k_0,l_0}$ , and its logarithmic function,  $\varepsilon_{k_0,l_0}$  (dB).

### B. Simulation Results

The results obtained using the simulative model of ANC system for the sinusoidal arousal are as follows:  $\overline{E_{F_{k_0,l_0}}}=1.8\times10^{-3}$ ,  $\overline{E_{LS_{k_0,l_0}}}=1.8\times10^{-3}$ ,  $\overline{E_{k_0,l_0}}=0.37\times10^{-7}$ ,  $\eta_{k_0,l_0}=4.92\times10^4$ ,  $\varepsilon_{k_0,l_0}=93.84\text{dB}$ ,  $\overline{E_F}=2.1\cdot10^{-3}$ ,  $\overline{E_{LS}}=2.1\cdot10^{-3}$ ,  $\overline{E}=0.08\cdot10^{-3}$ .

In the Fig. 3 the time diagram of noise signal  $d(n)$  and compensational signal  $y(n)$  is shown. In the Fig. 4. the time diagram of an error signal is shown. In the Fig. 5 and Fig. 6 the spatial distribution of noise level signal for the fan  $E_F$  and the loudspeaker  $E_{LS}$  is shown. In the Fig. 7 the distribution of a noise level for the superposed signal  $E$  is shown. The Fig. 8 shows the equal-loudness contours of the room. The room area with compensational noise is shown in the Fig. 9.

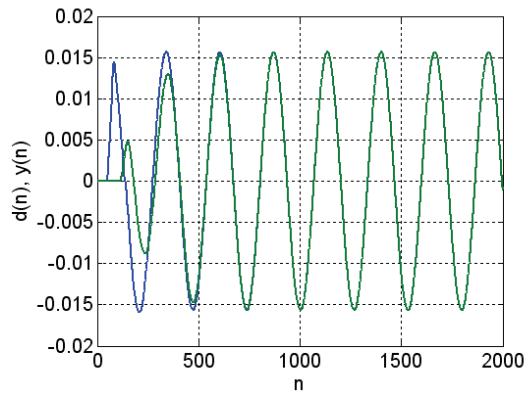


Fig. 3. Noise signal  $d(n)$  and compensational signal  $y(n)$ image of the room.

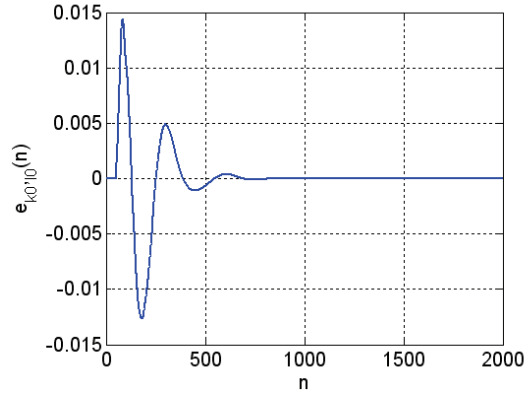


Fig. 4. The compensation of noise error signal image of the room.

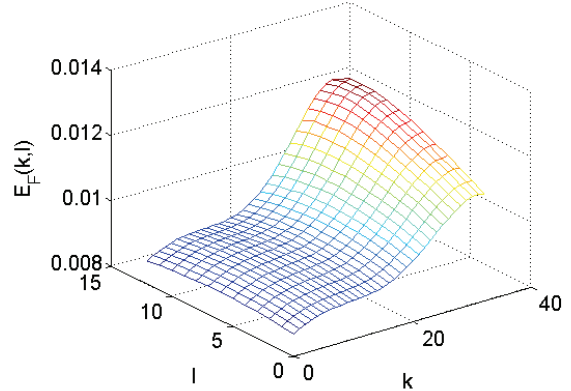


Fig.5. Noise level signal for the fan image of the room.

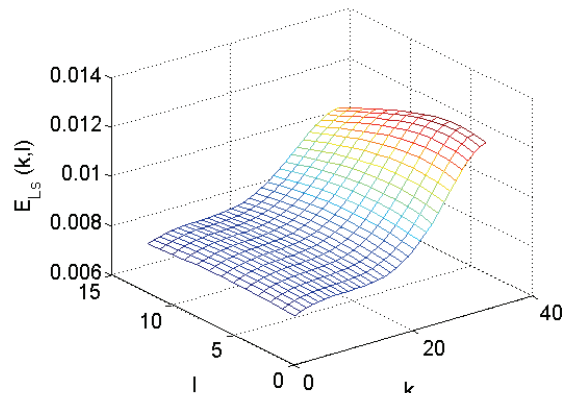


Fig. 6. Signal of loudspeaker noise level example.

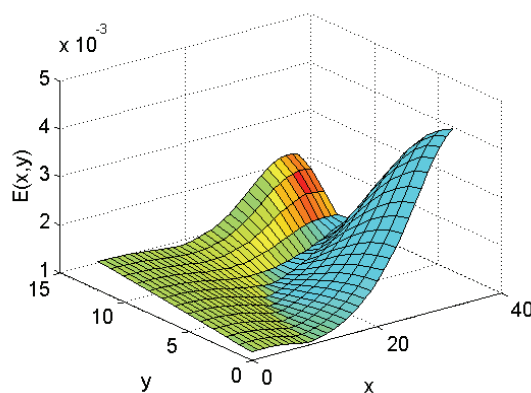


Fig. 7. Noise level of the superimposed signal example.

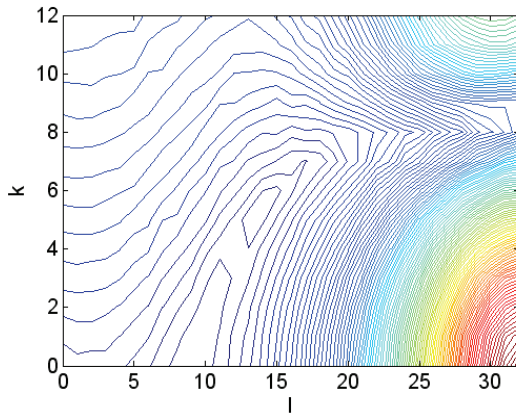


Fig. 8. Equal-Loudness contours of the room.

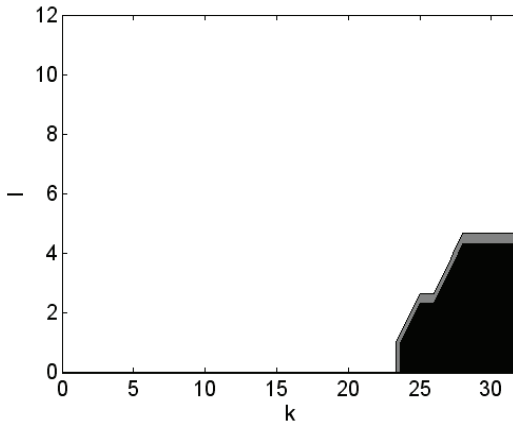


Fig. 9. The room area with compensated noise.

#### IV. CONCLUSION

The results obtained by applying simulative model of the ANC system for noise reduction, which comes from the rotating element, on the meeting premises, show that the noise reduction is not achieved for only 8.63% of the room area. Such results indicate a possibility to investigate the use of this model on an operating system in real time.

#### REFERENCES

- [1] J. Elliott and P. A. Nelson, "Active noise control", IEEE Signal Processing, Mag., vol. 10, pp. 12–35, Oct. 1993.
- [2] Martin Bouchard and Stephan Quednau, "Multichannel Recursive-Least-Squares Algorithms and Fast-Transversal-Filter Algorithms for Active Noise Control and Sound Reproduction Systems", IEEE Trans. Acoust., Speech, Signal Processing, vol. 8, no.5, pp. 606-618, Sept. 2000.
- [3] P. Lueg, "Process of silencing sound oscillator", U.S.Patent No. 2043416, 1936.
- [4] H. F. Olson and A. H. May, "Electronic sound absorber", Journal of the Acoustical Society of America, vol. 25, pp.1130-1136, 1953.
- [5] W. B. Conover, "Fighting noise with noise", Noise Control, vol. 2, pp. 78-82, 1956.
- [6] J.B.Allen and Berkley, "Image method for efficiently simulating small-room acoustics", Journal of the Acoustical Society of America, vol 65, no. 4, pp. 943-950, Apr. 1979.
- [7] E. A. P. Habets,"Room Impulse Response Generator", internal report, Sept. 2010.
- [8] X. Sun, N. Liu, G. Meng, "Adaptive frequency tuner for active narrowband noise control systems", Mechanical Systems and Signal Processing, Vol. 23 (2009), pp. 845–854.
- [9] J. Glover, "Adaptive noise cancellation applied to sinusoidal interfaces", IEEE Transactionson Acoustics, Speech and Signal Processing ASSP-25 (1977) 484–491.
- [10] D. Morgan, "An analysis of multiple correlation cancellation loops with a filter in the auxiliary path", IEEE Transactions on Acoustics, Speech and Signal Processing ASSP-28 (1980) 454–467.
- [11] C. Boucher, S. Elliott, P. Nelson, "Effect of errors in the plant model on the performance of algorithms for adaptive feedforward control", IEE Proceedings - F 138 (4) (1991).
- [12] S. Snyder, C. Hansen, "The effects of transfer function estimation errors on the filtered - x LMS algorithm", IEEE Transactions on Signal Processing 48 (4) (1994) 950–953.
- [13] S.J. Elliott, I.M. Stothers, P.A. Nelson, "A multiple error LMS algorithm and its application to the active control of sound and vibration", IEEE Transactions on Acoustics, Speech, and Signal Processing ASSP-35 (10) (1987) 1423–1434.

#### C. Results Analysis

The average noise level is reduced, which can be seen according to both numeric and graphic results. The mean noise level for the whole room before the effect of the ANC system was  $\bar{E}_F = 2.1 \cdot 10^{-3}$ , but during the effect of the ANC system  $\bar{E} = 0.08 \cdot 10^{-3}$ . The compensation of noise for the fan at the microphone location is 93.84dB. The compensation success rate is 91.37% (Fig. 9).

# Investigation of second-order digital filter structures having low sensitivity to parasitic effects

Maria Nenova<sup>1</sup>

**Abstract** –The errors occurring after the process of representation of digital filter coefficients with a finite word length registers are sometimes crucial for the communication equipment. In the present paper an investigation and analysis of structures having improved low sensitivity characteristics to parasitic effects is performed. The different types of criterion for sensitivity measure are presented. Then according to them is performed analysis of a low sensitivity structures. The impact of the pole distribution after quantization is shown for different number of bits.

**Keywords** – sensitivity, quantization effects, IIR (infinite impulse response) low sensitivity structure.

## I. INTRODUCTION

The evaluation of sensitivity is the main factor to measure the effects occurring after the process of quantization. The analogue or digital circuit's characteristics depend on the values of their components. The characteristics sometimes are different from the specified value, because the elements are not ideal. They can also vary over time and environmental conditions.

The sensitivity is one of the most important features investigated when digital filters are implemented. If the digital filter structure is sensitive to parasitic effects then it worsens the characteristics.

The researchers aim for the past few decades is the reducing of quantization errors. One of the first structures published in the literature [1] with low pass-band sensitivity is based on all-pass sections. The desire in general is the structure having low sensitivity also in the band-stop. One more section with improved low-sensitivity is discussed in [2] which show very low sensitivity for transfer function poles.

Usually the infinite impulse response (IIR) filters are very sensitive to the quantization effects. The recursive also show large round off noise. One of the big problems is the behavior of the filters with poles located near the  $z=1$ . In this area the parasitic effects become more severe.

The authors in [3] developed a new second-order digital filter structure with good low sensitivity properties. Their section has a low sensitivity for values for the specific pole radius  $[0.8 - 0.99]$ .

In [4] are presented three different structures which in the present paper are investigated and compared according to the

<sup>1</sup>Maria Nenova is with the Faculty of Telecommunications at Technical University of Sofia, 8 Kl. Ohridski Blvd, Sofia 1000, Bulgaria, E-mail: mvn@tu-sofia.bg.

effects arising after the quantization process. All those structures realize different transfer function (TF).

The first one called BQ1 is based on the lattice structure. The structure does not realize polynomial LP and HP output. Later the same author presented one more second-order section - BQ2 good for realizations in the low frequency band, which realizes all possible second-order transfer functions. A third section called BQ3 presented in [5] also has good sensitivity properties and provides full number of outputs.

The adaptive realization of the first two structures is presented in [6] and the third one is in [7].

During the years many authors have shown interesting and very useful implementations of such types of low sensitivity filters is presented in [8], [9]. In [8] is presented the design and implementation of allpass filter sections with low sensitivity near the area of  $z=1$  with high accuracy in the process of design.

The application of low sensitivity second-order filter sections is proposed in [9], where the authors uses such type filters in the sound model for tracing or extraction of sound sources.

## II. SENSITIVITY CHARACTERISTICS – GENERAL OVERVIEW

The sensitivity of the frequency characteristics – magnitude and phase response, group delay time are functions of the frequency, which must be considered when comparing different schemes. The sensitivity is different in the transition band and in the passband of one and the same structure.

This work considers infinite impulse response (IIR) digital filters with poles near the unit circle and deals with coefficient sensitivity as a criterion for comparing filter structures with each other.

Magnitude and phase sensitivity functions have to be considered in a reasonably wide range when different recursive digital filter realizations are compared to each other.

The worst-case sensitivity (WS) is also called maximum sensitivity can be evaluated according to [10] as:

$$WS_{a_i}^{H(e^{jw})} = \sum_i \left| S_{a_i}^{H(e^{jw})} \right|, \quad (1)$$

In the WS (1) criterion are taken into account only the absolute values of the partial sensitivities. This type of sensitivity of the three sections is investigated in this paper.

## III. SECOND-ORDER STRUCTURES

Figure 1 - a) b) c) shows three examined in this paper biquadratic sections. They realize on their outputs full number of transfer function - LP, HP, BP and BS. The section BQ1 realizes elliptic LP/HP TF and for the BP and BS the equations are [4]:

$$H_{BP}(z) = \frac{0.5(1-\alpha)(1-z^{-2})}{1-\beta(1+\alpha)z^{-1}+z^{-2}} \quad (2)$$

$$H_{BS}(z) = \frac{(1+\alpha)(1-2\beta z^{-1}+z^{-2})}{1-\beta(1+\alpha)z^{-1}+z^{-2}} \quad (3)$$

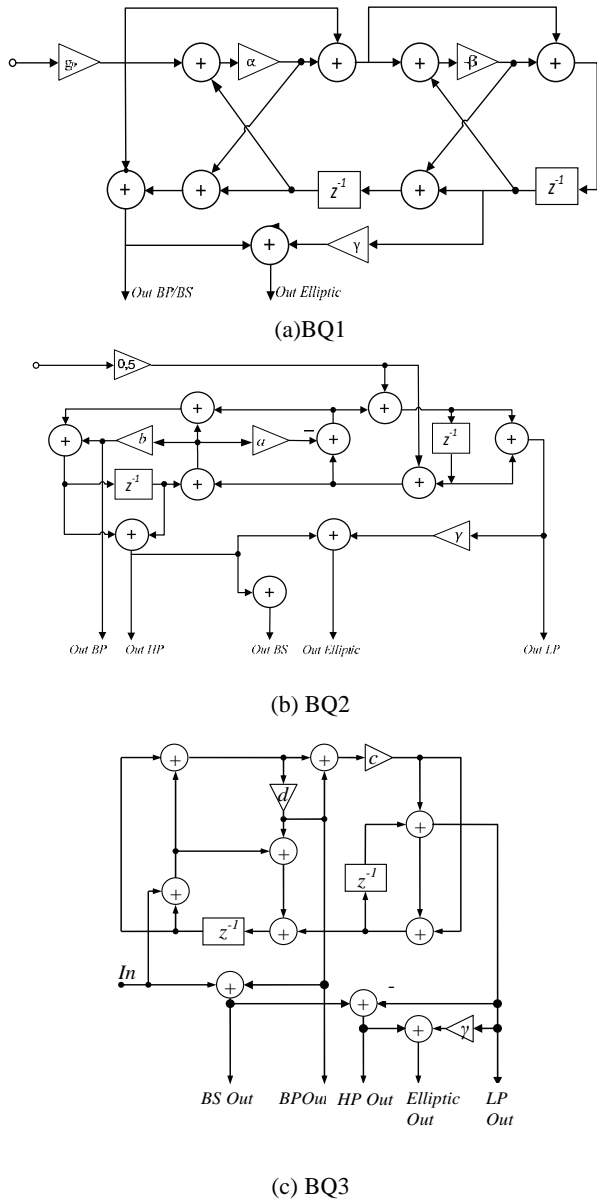


Fig. 1. Biquad sections

The BQ1 is based on lattice structure Fig.1. It is presented in [11], and in [12] the authors approved that this biquad is not universal, because of the lack of polynomial low and high frequency outputs.

This is the main reason for development of the next two sections – BQ2 и BQ3 [11], [12], [13] и [5]. Those structures

are the basis for cascade realizations of identical second-order structures.

The BQ2 – Fig. 1 b) presents a full amount of possible realizations of transfer functions [4].

$$H_{BP}(z) = \frac{-0.5b(1-z^{-2})}{1+(-2+b+2a)z^{-1}+(1-b)z^{-2}}; \quad (4)$$

$$H_{BS} = \frac{0.5(2-b)\left[1+\frac{-2+2a+b}{2-b}z^{-1}+z^{-2}\right]}{1+(-2+b+2a)z^{-1}+(1-b)z^{-2}}$$

The BQ3 section releases on the outputs all possible types of second-order TFs. In addition, as one of its biggest advantages over other implementations considered is the realization of Band Pass and Notch outputs independently (4).

This feature of the section gives possibility of extraction or elimination of different frequencies.

The structure depicted on Fig.1c), has only two multipliers denoted with  $d$  and  $c$  (the small number of multipliers leads to decreasing in parasitic effects, arising due to the quantization of the coefficients). The BP and BS TFs are:

$$H_{BS}(z) = \frac{(1-d)[1-2(1-2c)z^{-1}+z^{-2}]}{1+(-2+4c+2d-4cd)z^{-1}+(1-2d)z^{-2}} \quad (5)$$

$$H_{BP}(z) = \frac{d(1-z^{-2})}{1+(-2+4c+2d-4cd)z^{-1}+(1-2d)z^{-2}} \quad (6)$$

All tree structures have almost the same complexity, because they have two delays and two multipliers for the polynomial TFs and three for the elliptic one. The adders are 8 for BQ1 and 10 for BQ2 and BQ3. One of the biggest advantages of the three investigated structures is the possibility of independent tuning of the pole radii  $r_p$ , the angle of the poles  $\Theta_z$ ,  $\Theta_p$  and zeros of the elliptic TF, and the central frequency and bandpass of the BP and BS TFs [4].

Another advantage of BQ1 and BQ3 is the tuning of  $r_p$ , which is performed by coefficients  $\alpha$  for BQ1 and  $d$  for BQ3, will not affect  $\Theta_z$ . Setting the radius of the poles is mostly used in bandpass and notch realizations and less frequently in elliptical ones.

The turning into adaptive of these three sections is desirable to be implemented without any changes in the radius of the poles, because this can lead to possible instability.

#### IV. POLE LOCATION DENSITY

An indirect criterion for the sensitivity evaluation of a transfer function in a particular frequency band is the pole location density. In the corresponding area of the unit circle

for a given word-length is different the amount of possible pole locations.

The poles in the denominator of the TF have the possibility to take place only in a limited number of points within the unit circle. This is due to the position of the coefficients of the TF and the limitation in the registers in which the multipliers are stored. This two limits leads to non-desirable effects. It is important to be noted that as the number of the possible pole locations increases, as uniformly they are distributed. The quantization error of the TF coefficients will become smaller when the distribution is uniform. If the size of the register increases then higher pole density will be observed. The pole location for the BQ3 is presented in simulation results.

## V. SIMULATION RESULTS

When a quantization of the coefficients is performed, the coefficients of the TF become with a finite and shorter word length. Then the poles of the TF can be positioned on a certain finite number of places. If a binary word with length  $B$  in bits is implemented, then in each quadrant of the unit circle will result [14]:

$$L_{\max} = (2^B - 1)^2 \quad (7)$$

Number of poles for a TF of second-order with coefficients in the denominator  $a_1 \neq 0$  and  $a_2 \neq 0$ . The number of the positions increases as the error due to the quantization decreases, instead of the non uniform placement.

Digital filters give the possibility of changes in the pole density for a specific frequency area instead of another area. The number of poles remains constant.

The poles sensitivities of the BQ1, BQ2 and BQ3 are compared.

On Fig. 2 can be observed the result of simulations performed on digital filter structure BQ3. The density of poles situated near the unit circle increases with the increase of number of bits for quantization.

The control of pole location is often employed technique in variable and adaptive filtering. In the areas where the poles are densest can be performed precise tuning of the frequency. In this type of areas the sensitivity is low.

The analysis of sensitivity is important because structures having higher density and more uniform distribution of poles for a given transfer function and the same word-length can be compared. The low sensitivity leads to structures represented with shorter word-length. This will also decrease the calculation complexity.

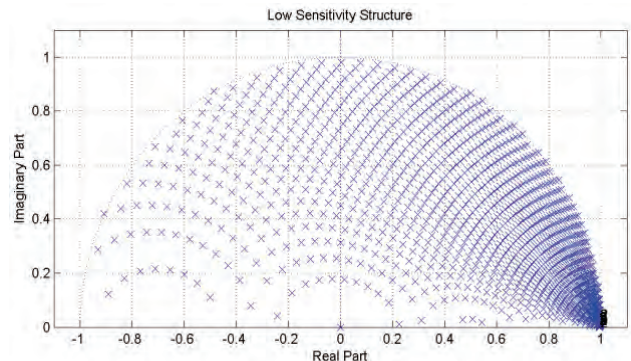


Fig. 2. Possible pole location density of BQ3

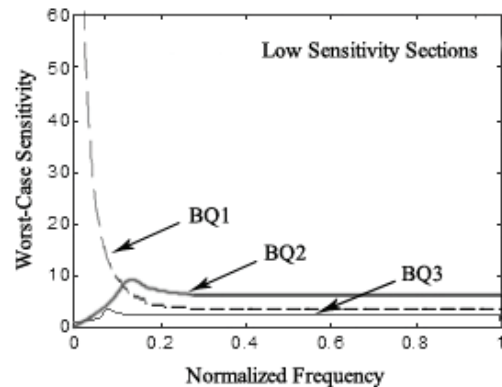


Fig. 3. Worst-case sensitivity investigation of three different low frequency structures

Fig. 3 shows the results of the experiments for three different structures suitable for use in the low frequency band. It is investigated the sensitivity of the multiplier coefficients. A feature which is similar for the three structures is the minimized sensitivity to non-desirable effects. All digital structures – BQ1, BQ2 and BQ3 are of second order. The BQ1 and BQ2 are low frequency digital filter structures.

The overall sensitivity to all multiplier coefficients is evaluated using the worst-case sensitivity.

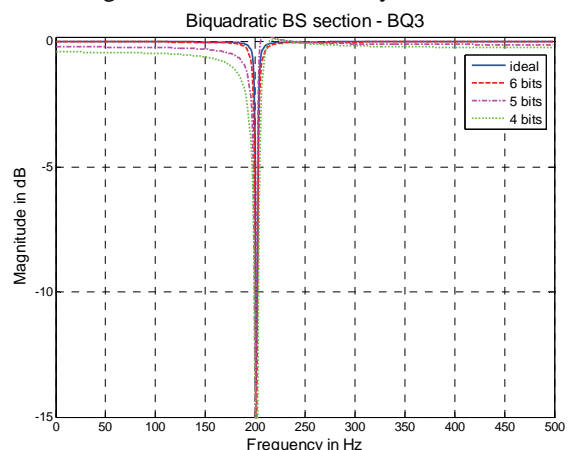


Fig. 4. Sensitivity investigation of low sensitivity structure

On Fig. 4 are the curves of simulation results after the experiments for quantization with different number of bits (b=4,5,6 bits) performed on the structure BQ3.

In order to be compared with the ideal characteristic it is also presented. It is obvious that with increase of the number of bits it gets closer to the ideal one. Even the quantizing is performed with less bits the characteristics are very close to the desirable.

The BQ3 structure is suitable for noise cancelation in the low frequency band, because it presents very narrow and sharp magnitude response.

## VI. CONCLUSION

Frequency-dependent sensitivities allow different digital filter realizations to be compared to each other in a wide frequency range. For this reason, worst-case sensitivity (1) is considered in this work.

An overview of the various types of evaluations of sensitivity of structures suitable for implementation with digital filters is presented. The impact of the change in the number of quantization bits with which are quantized the coefficients in different type realizations is shown. The use of low-sensitive to parasitic effects structures leads to improvements in the realization. The sections that have been investigated were in the worst-case sensitivity. All analyzed structures are suitable for the low-frequency band and the BQ3 section as expected has shown the lowest sensitivity characteristics with comparison to the other structures. All experiments were conducted in one and the same poles location and the conditions were equal.

All three investigated here sections are suitable for cascade realizations of identical sub filters.

The section BQ3 has shown the lowest sensitivity according to the graphical results and has also presented very good properties during the process of quantization.

All the sections presented here can be also realized as adaptive digital filters.

## REFERENCES

- [1] Agarwal, Ramesh C., Burrus, C. Sidney, "New recursive digital filter structures having very low sensitivity and roundoff noise", IEEE Transactions on Circuits and Systems, Volume: 22 , Issue: 12, Page(s): 921 – 927, Dec 1975.
- [2] Nishihara, A. and K. Sugahara, A synthesis of digital filters with minimum pole sensitivity, Trans. Of the IEICE of Japan, vol. E65-A, No. 5, pp. 234-240, May 1982.
- [3] Jovanovic D.G. and Mitra S.K. A new low sensitivity second-order bandpass digital filter structure. Electronics Letters, 38 (16):858–860. August 2002.
- [4] Stoyanov, G., "A comparative study of variable biquadratic digital filter sections sensitivities and tuning accuracy", Proc. Int. Conference "Telecom2002", pp. 674-681, 2002.
- [5] Stoyanov G., "A new digital biquadratic section with pole and zero frequencies tuned by a single parameter", Proc. 37th International Sc. Conf. on Information, Communication and Energy Systems, "iCEST'2002", Nis, Yugoslavia, Oct. 2-4, 2002.

- [6] Z. Nikolova, G. Stoyanov, G. Iliev, V. Pulkov, "Complex Coefficient IIR Digital Filters", Chapter 9 of "Digital filters", Fausto Pedro García Márquez (Ed.), ISBN: 978-953-307-190-9, Intech, pp. 209–239, Apr. 2011.
- [7] Maria Nenova, Georgi Stoyanov, Georgi Iliev, "Investigation of least-squares algorithm based adaptive digital filter section for detection/ suppression of a single sinusoidal signal", National Conference with Foreign Participation Telecom'2005, Varna, Bulgaria, pp. 370-375, October 6-7, 2005
- [8] G. Stoyanov, K. Nikolova, High-accuracy design and implementation of allpass-based Hilbert transformers and fractional delay filters, Proc. 5th International Symp. IGNOIE&SOIM (System Const. Global-Oriented Inf. Electronics), Sendai, Japan, Vol. 1, pp. 418-423, Feb. 22-24, 2012.
- [9] Pleshkova-Bekiarska Sn., Al. Bekiarski, Sound Propagation Model for Sound Source Localization in Area of Observation of an Audio Robot, International Journal of Neural Networks and Application, 2(1), Januare-June 2009, International Science Press, India, pp.1-4.
- [10] Sugino N. and A. Nishihara, Frequency-Domain Simulator of Digital Networks from the Structural Description, IEEE Transactions of the IEICE, Vol. E-73, No.11, November 1990.
- [11] Stoyanov G. and Uzunov I., " A new variable digital second-order elliptic low-pass filter section", Proc. 9th Sc. Conference "Electronics'2000", Sozopol, Bulgaria, Vol. 1, pp. 21-26, Sept. 20-22, 2000.
- [12] Stoyanov G., I. Uzunov and M. Kawamata, "Design of variable IIR digital filters using equal subfilters", Proc. 2000 IEEE Inetrnational Symp. Intelligent Signal Processing and Communications Systems (ISPACS'2000), Honolulu, Hawaii, vol. 1, pp. 141-146, Nov. 5-8, 2000.
- [13] Stoyanov G., I. Uzunov and M. Kawamata, "Design and realization of variable IIR digital filters as a cascade of identical sub-filters", IEICE Trans. Fundamentals, vol. E84-A, No. 8, pp. 1831-1839, August 2001.
- [14] Proakis, J. and D. Manolakis, *Digital signal processing, algorithms and applications*, Third edition, Prentice-Hall, 1996

---

---

## Poster 4 - Computer Systems and Internet Technologies

---

---



# A Methodology of Developing Interoperable Electronic Business in the Transport Sector

Sladana Janković<sup>1</sup>, Snežana Mladenović<sup>2</sup>, Marko Vasiljević<sup>3</sup>, Irina Branović<sup>4</sup>, Slavko Vesković<sup>5</sup>

**Abstract –** In this paper, we describe a development methodology to achieve interoperability in e-business for different entities in the transport sector. Interoperable e-business is achieved by combining the following methods of B2B (Business-to-Business) integration: information integration, service-based integration and portal integration. The methodology respects diversity of business requirements and constraints in the implementation.

**Keywords –** E-business, B2B integration, Interoperability.

## I. INTRODUCTION

The notion of interoperability, in general, refers to the possibility of two systems to exchange information, as well as to make use of the exchanged information [1]. Traffic and transport systems are heterogeneous systems which share information in their operation. The subject of research in this paper is the definition of the methodology of interoperable electronic business of traffic business systems. The methodology has been based on the combination of the known methods of Business-to-Business (B2B) integration: integration of information, integration on the basis of services and portal integration. The methods of B2B integration have been implemented within the cloud computing environment.

## II. THE FRAMEWORK OF ELECTRONIC BUSINESS IN TRAFFIC SECTOR

Electronic business of subjects in the area of traffic should be realized on the following types of relations:

- commercial sector – commercial sector (C-C),
- commercial sector – public sector (C-P),
- commercial sector – Government sector (C-G),

<sup>1</sup>Sladana Janković is with the Faculty of Transport and Traffic Engineering University of Belgrade, Vojvode Stepe 305, 11000 Belgrade, Republic of Serbia, E-mail: s.jankovic@sf.bg.ac.rs.

<sup>2</sup>Snežana Mladenović is with the Faculty of Transport and Traffic Engineering University of Belgrade, Vojvode Stepe 305, 11000 Belgrade, Republic of Serbia, E-mail: snezanam@sf.bg.ac.rs.

<sup>3</sup>Marko Vasiljević is with the Saobraćajni fakultet Dobojski University of East Sarajevo, Vojvode Mišića 52, 74000 Dobojski, Republika Srpska, Bosnia and Herzegovina, E-mail:..

<sup>4</sup>Irina Branović is with the Faculty of Informatics and Computing Singidunum University, Danijelova 32, 11000 Belgrade, Republic of Serbia, E-mail: ibranovic@singidunum.ac.rs.

<sup>5</sup>Slavko Vesković is with the Faculty of Transport and Traffic Engineering University of Belgrade, Vojvode Stepe 305, 11000 Belgrade, Republic of Serbia, E-mail: veskos@sf.bg.ac.rs.

- public sector – public sector (P-P),
- public sector – Government sector (P-G),
- Government sector – Government sector (G-G).

Fig. 1 shows the frame of B2B integrations in the traffic and transportation sector.

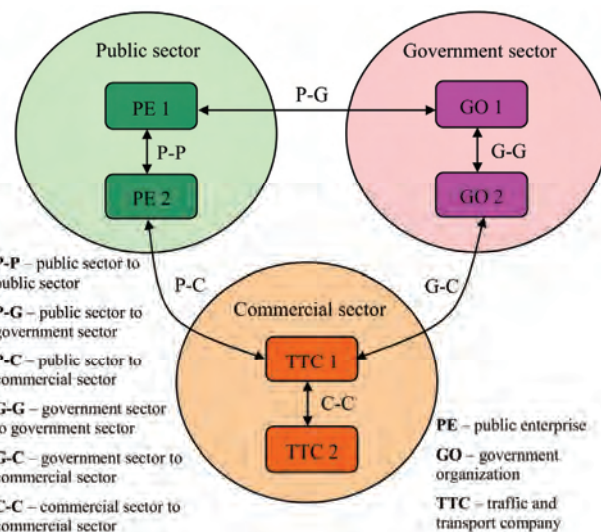


Fig. 1: Frame of B2B integrations in the transport sector

In defining the legal and institutional frames of integration, two basic types of B2B integrations are distinguished:

- horizontal B2B integrations – integrations of entities which consider the common domain with approximately equal level of abstraction,
- vertical B2B integrations – integrations of entities which consider the common domain with significantly different levels of abstraction.

In practice, during B2B integration of two organizations usually the horizontal and the vertical integration are combined [2]. Depending on whether pure horizontal integration, pure vertical integration, or combined – hybrid integration is meant, also the frames of B2B integration are distinguished.

Horizontal B2B integration is suitable in case of:

- integration of organizations that belong to the same level within the same sector;
- integration of organizations that belong to the same level, within different sectors.

Vertical B2B integration is suitable in case of integration of organizations that belong to different levels within the same sector. Hybrid B2B integration is suitable in case of integration of organizations that belong to different levels within different sectors.

### III. APPROACHES IN THE DEVELOPMENT OF B2B INTEGRATION SOLUTIONS

All the solutions of the B2B integration of traffic-transport business subjects can be classified into three big classes:

- solutions based on the integration of the existing information and applications,
- solutions based on the development of new databases and applications,
- solutions based on the integration of the existing and new applications.

For the solutions based on the integration of the existing information and applications, the “bottom-up” approach is suitable (Fig. 2). The integration of the existing applications requires the development of Web services as required. Therefore, the development of this category of solutions begins with the analysis of the application services. The modelling of application services should result in the definition of the requirements by the applications that can be fulfilled by using Web services.

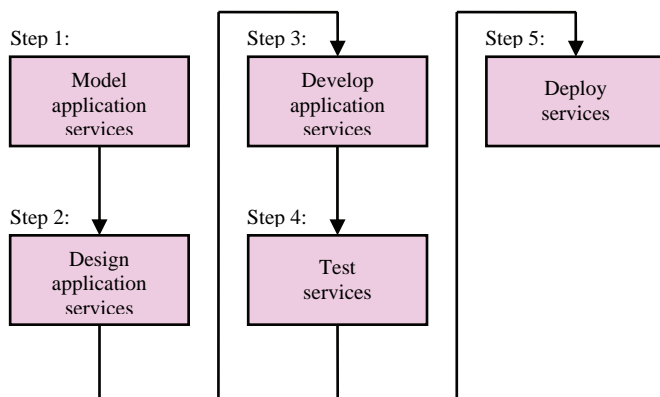


Fig. 2: “Bottom-up” approach

For the solutions based on the development of new databases and applications the “top-down” approach is suitable (Fig. 3).

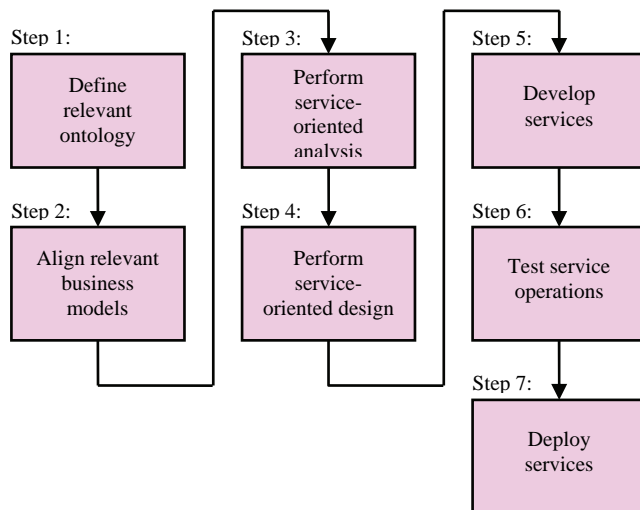


Fig. 3: “Top-down” approach

In this approach, first comes the analysis of the requests and business models of B2B integration subjects. It promotes not only the service-oriented development of the business processes, but also the creation (or harmonization) of the overall business organization model.

This process has been derived from the existing business organization logics, and it results in the creation of a large number of business and application services. The part of the process that has the formation of ontology as consequence, represents the classification of the sets of information processed by one organization. This results in the creation of a common glossary, as well as in defining the relations existing between certain groups of data.

After having established the ontology, the existing business models have to be adapted and harmonized with ontology, and in many cases completely new business models need to be created, for the glossary defined by ontology to be validly represented by the business modelling terminology.

The solutions of B2B integration based on the integration of the existing and new applications are the most complicated ones. For the solutions based on the integration of the existing and new applications the agile strategy is suitable (Fig. 4).

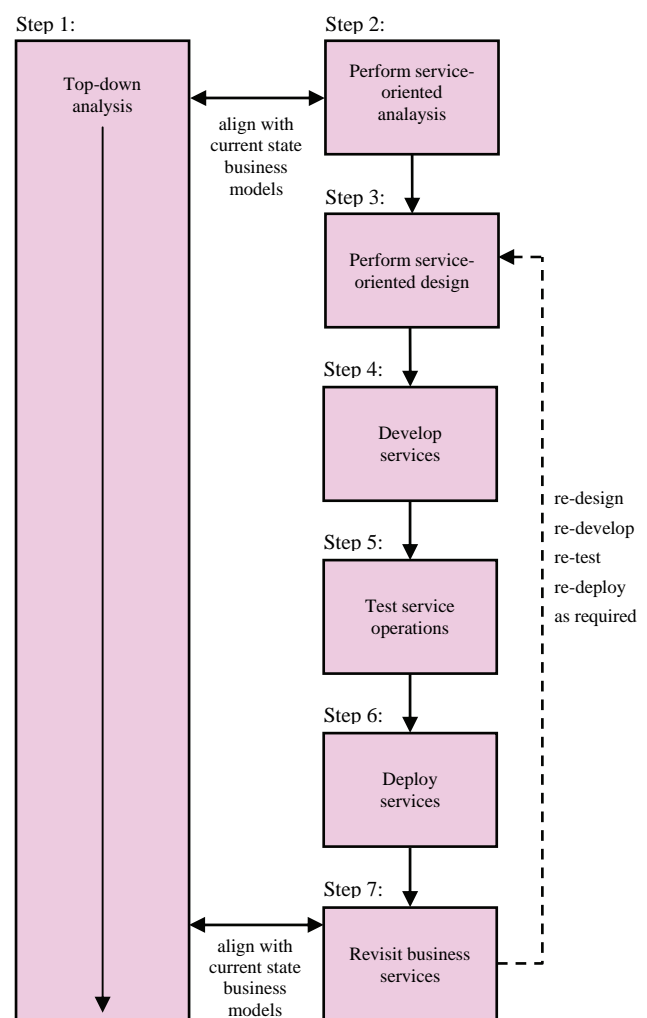


Fig. 4: Agile strategy

In comparison with the previous two approaches, this approach is the most complex one since it has the task to fulfil two sets of opposed requirements. The agile strategy is based on the parallel analysis of the business processes and service development. The biggest challenge is to find the balance in the implementation of the principle of service-oriented design in the business analysis environment. This strategy is also called "meeting-in-the-middle" approach.

The approaches to solving and the development phases are different for the three classes of solutions. Regardless of the class to which the solution belongs, the proposed model of B2B integration means the development of the service-oriented solution in the cloud computing environment.

#### IV. DEVELOPMENT OF B2B INTEGRATION SOLUTION IN TRANSPORT SECTOR

The essence of the proposed solution lies in the fact that every pair of business systems should select the scenario, or those scenarios of B2B integration which best satisfy their needs, and which are realized on the basis of the following principles:

- the existing databases that are used by the studied business systems, which have a similar structure and purpose, will be integrated into one common base located on the cloud computing platform;
- the Web portal is set on the cloud computing platform and it contains the user interface for updating the common base and for setting the queries over it. The tasks of updating the base will be divided among the studied business systems, in compliance with their jurisdiction and competence;
- the existing applications that are used by the studied business systems, currently operate over local databases set on their servers and generate diverse reports that represent the decision-making support. The proposed solution plans for some of these applications to download in the future the necessary data from the common database from the cloud;
- the existing local applications will download data from the common database which is located in the cloud, using the WCF (Windows Communication Foundation) Data services hosted in the cloud;
- the local databases that have not been integrated in the common base, and whose data the business systems want to share, will be accessed by means of the Web portal hosted on the cloud computing platform;
- the local application of one business system will use the data from the local database of another business system, by calling WCF Data services hosted in the cloud;
- the local applications will be improved by the development of the user interface for accessing the common database in the cloud.

WCF Data services are elegant Microsoft technology for data publishing, either from the database from the local servers or from the databases in the cloud [3]. They may be hosted on local Web servers or on the servers from the cloud. The application which uses the WCF Data service can be

Desktop application, Web application hosted on the local Web server, or Web application hosted as a service in the cloud [4].

The phases in the development of the solution of the B2B integration of traffic business systems:

- identification of business subjects that need to be included in the B2B integrations;
- analysis of institutional and business relations between the selected subjects;
- defining of the solution requirement of the B2B integration for every pair of traffic systems that needs to realize the integration;
- development of local ontologies that represent the business domain of every single organization;
- development of the common domain ontology;
- defining of one or several scenarios of B2B integration for every pair of the traffic systems that need to realize the integration;
- defining of mechanisms for the realization of the selected scenarios of B2B integration for every pair of traffic business systems;
- implementation of components that allow the realization of the selected mechanisms of B2B integration;
- analysis of the realization effects of B2B integration for every single traffic business system;
- analysis of the realization effects of B2B integration for the entire safety domain in traffic.

We propose the B2B integration model of traffic business systems which consists of the following components:

- C1 – B2B integration system architecture;
- C2 – development activities of B2B integration systems;
- C3 – software architecture of B2B integration systems;
- C4 – scenarios of B2B integration of traffic systems;
- C5 – methods of B2B integration of traffic systems;
- C6 – time planning of model realization.

Scenarios of B2B integration:

- Scenario 1: local application of one traffic system downloads data from the local base of another traffic business system by calling the service from the cloud;
- Scenario 2: local application of traffic system downloads data from the common database by calling the service;
- Scenario 3: the user accesses data from the common base via user interface of the local application;
- Scenario 4: the user accesses data from the local base via common user interface - Web portal in the cloud;
- Scenario 5: the user accesses data from the common base via Web portal in the cloud;
- Scenario 6: using Web portal in the cloud the user creates queries that are executed over the integrated data which originate from several local databases (Fig. 5).

Two traffic business systems can select even several scenarios of B2B integration [5]. The selection of the integration scenario depends on the nature of the business relations and interdependence of two traffic business subjects, i.e. on the defined requirements of the B2B integration. If there are several B2B integration requirements between two traffic business subjects, the most favourable integration scenario will be selected for each requirement.

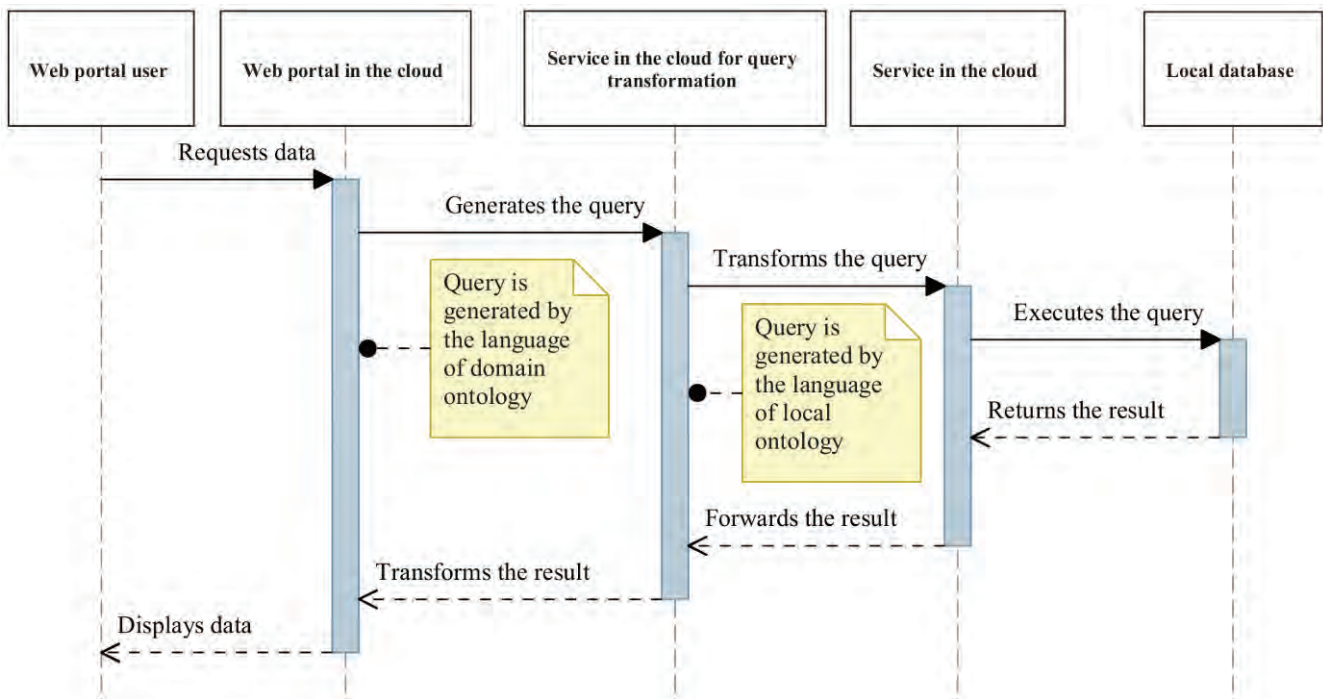


Fig. 5: Diagram of sequences: Scenario 6 of B2B integration of traffic business systems

## V. CONCLUSION

The implementation of the proposed solution of B2B integration allows interoperability of the traffic business systems at the level of: data, services, business processes, and operation. The interoperability of data is realized by sharing the information from the heterogeneous sources of data, stored on different machines, under different operating systems, and in different database management systems. The interoperability of the services is enabled by composing different applicative functions to work together, although they had been designed and implemented independently. The interoperability of the business processes has been realized by unifying the service sequences in order to realize a certain business activity. The interoperability of operation has been enabled by the harmonization of cooperation of organizations in the domain of traffic, regardless of the differences in: the decision-making method, working methods, legal acts etc.

The proposed solution exceeds all three categories of barriers to business system interoperability: conceptual, technological, and organizational barriers. The conceptual barriers refer to the syntactic and semantic differences of information that are being exchanged. These problems have been solved by unifying different models of data, used by the studied traffic business systems, into a unique domain data model. The technological barriers refer to the impossibility to connect the information technologies. These problems have been solved by using common standards for presenting, storing, exchange, and processing of data. The organizational barriers refer to the definition of responsibilities and authorities, and they are solved by defining the legal and contractual frame. The common database and the services in the cloud are used in accordance with the pre-determined user

authorities. The service-oriented architecture, which is the basis of the methodology, allows the integration of the applications developed on different platforms. It may be concluded that the proposed solution does not require development of new local applications and databases, but rather allows the usage of the existing information systems.

## ACKNOWLEDGEMENT

This work has been partially supported by the Ministry of Education, Science and Technological Development of the Republic of Serbia under No. 036012.

## REFERENCES

- [1] S. Janković, "Interoperability of Transport Business Systems Based on the Integration of Service-Oriented B2B Applications", University of Belgrade Faculty of Organizational Sciences, Info M, vol 36, pp. 4-12, 2010.
- [2] S. Janković, S. Mladenović, "B2B Integration Models in Cloud Computing Environment", University of Belgrade Faculty of Organizational Sciences, Info M, vol. 43, pp. 26-32, 2012.
- [3] D. Betts, S. Densmore, R. Dunn, M. Narumoto, E. Pace, M. Woloski, *Developing Applications for the Cloud on the Microsoft® Windows Azure™ Platform*, Microsoft, 2010.
- [4] S. Janković, J. Milojković, S. Mladenović, M. Despotović-Zrakić, Z. Bogdanović, "Cloud Computing Framework for B2B Integrations in the Traffic Safety Area", Romanian Metallurgical Foundation, Metalurgia International, vol. 17 no. 9, pp. 166-173, 2012.
- [5] S. Janković, S. Mladenović, S. Mitrović, N. Pavlović, S. Aćimović, "A model for integration of railway information systems based on cloud computing technology", iCEST 2011, Conference Proceedings, pp. 833-836, Nis, Serbia, 2011.

# Recommendation in E-Learning Based On Learning Style

Aleksandar Kotevski<sup>1</sup>, Gjorgi Mikarovski<sup>2</sup> and Ivo Kuzmanov<sup>3</sup>

**Abstract –** This paper proposes a prototype of intelligent system for recommendation and delivering learning material to students in format and design that is adequate to students learning style. On the other words, the system should meet the needs of students, showing learning materials in acceptable format and style to the user. In order to make decision about the most adequate learning style, system is going to using VART classification to detect the student learning style. Furthermore, teachers can post learning materials in the system. They are going to receive suggestion for the most adequate category by using Vector-space models for information retrieval.

**Keywords –** VARK, e-learning, learning style, learning material, data mining.

## I. INTRODUCTION

Intelligent web-based learning systems aim to improve the quality of services and applications in e-learning systems. In this context, they deliver the most adequate content to users, based on their requirements and learning styles. Moreover in intelligent systems, users not searching through a large repository of learning materials – they search in smaller set of materials, that are most adequate for the users, based on their experience, previous content and needs. Also, the data is supplied in a form acceptable to the user, and in the course of using the system user often receives advice and guidance for its next action.

## II. LEARNING STYLES

Individual learning styles differ, and these individual differences become even more important in the area of education[1]. Therefore, the real challenge in e-learning is keeping the people it is designed for in mind (Canavan, 2004). Individual learning style refers to style or learning methods used in the process of learning. According to Jantan and Razali (2002), psychologically, learning style is the way the student concentrate, and their method in processing and obtaining information, knowledge, or experience. On the other hand, from the cognitive aspect, learning style can be referred to various methods in perception creation and information

processing to form concepts and principles (Fleming & Baume 2006) [1].

Learning style is a cognitive composite, affective, and psychological factor which act as an indicator on how individuals interact and respond to learning environment (Duff 2000).

There are many models on learning styles that can be identified from earlier studies, but according to the Malaysian Education Ministry (2008), there are two learning style models that are commonly used; Dunn & Dunn and VARK. In this paper we are going to using VARK model for determination of student learning style.

## III. VARK

The VARK (stands for Visual, Aural, Read/Write, Kinesthetic) is model for detecting learning styles by providing questionnaires with 16 questions. It's authored by Fleming and Mills and has been used as a guide to help people learn more effectively. It is VAK modification and includes a systematic presentation of questions to identify preferences for the ways information and ideas can be taken in or put out [4].

### A. What is VARK

The VARK model is based on principles of sensory perception so the instructional methods must be a stimulus for the student to gain any understanding of the subject [2]. It makes students classifying to four different modes (aural, reading, visual, kinesthetic), based on different senses, namely visual, aural, reading, and kinesthetic, and the name of the model itself.

Based on Fleming (2006), aural mode students tend to attain information by discussion and listening. For reading mode, these students have the ability to accept and interpret printed information. For visual mode, the students are more prone to accept learning through interpreting charts, graph figures, and pictures. While kinesthetic mode leans more towards accepting learning based on behavior such as touch, feel, see, and listen. Based on each mode's tendency, researcher hopes to conduct a study to obtain students' feedback on computer based learning [4].

Users complete the questionnaire online or on paper. They can have more than one answer per question, so they get a profile of four scores - one for each modality. That begins a process of thinking about how they prefer to learn. VARK is a catalyst for meta cognition, not a diagnostic or a measure. The questionnaire is deliberately kept short in order to prevent student survey fatigue.

<sup>1</sup>Aleksandar Kotevski is with the Faculty of Law, University St. Kliment Ohridski – Bitola, R.Macedonia, e-mail:aleksandar.kotevski@uklo.edu.mk

<sup>2</sup>Gjorgi Mikarovski is with the Faculty of Technical Sciences Bitola,University St.Kliment Ohridski – Bitola, R.Macedonia, email:gjorgi.mikarovski@tfb.uklo.edu.mk

<sup>3</sup>Ivo Kuzmanov is with the Faculty of Technical Sciences Bitola,University St.Kliment Ohridski – Bitola, R.Macedonia, email:ivo.kuzmanov@tfb.uklo.edu.mk

### B. Related works

There are many authors that were using VARK to identify the most adequate student learning style. Based on Murphy et al. (2004), learning based on VARK learning style model provides a medium for self-knowledge and exploring opportunities in classrooms, thus, making a more productive learning experience and enjoyment among students. According to Drago and Wagner (2004) it has been proven that students possess diversity in learning styles, which has become their priority, and teachers should effectively deliver the course according to the students' needs. Research by Bachok et al. (2000) discovers that students have different learning style practice, in which unsuitable lessons and learning style usage can effect to students' learning and behavior quality in class.

### C. Using VARK in the proposed system

Students have to complete the online questionnaire. They can have more than one answer per question, so they get a profile of four scores - one for each modality. That begins a process of thinking about how they prefer to learn. The questionnaire is deliberately kept short in order to prevent student survey fatigue. It also tries to encourage respondents to reflect and answer from within their experience, rather than from hypothetical situations.

System is going to provide online questionnaire with 16 questions. To be more reachable, questions will be shown in text and audio format. After passing the questionnaire, based on the student answers, system is going to set adequate learning style to the student.

## IV. PROPOSED SYSTEM

The proposed intelligent system is going to deliver learning material to students in format and design based on students learning style. The student learning style is going to be detected via VARK questionnaire. In additional, teachers are going to receive suggestion for the most adequate category while they are posting new learning materials in the system, by using Vector-space models.

### A. System architecture

The general architecture of the proposed system contains three main units:

- Student unit
- Teachers and system administrator unit
- Hardware and software

Fist, student need to be registered to be able to read learning materials that are post from the teachers. In the process of registering, student has to go through 16 questions from VARK questionnaires. As a result, VARK will give the most adequate learning style for the student, based on his answers.

Then, learning material will be delivering in format that is predicted with selected learning style for the student. Teachers, as a separate unit of this system, can upload learning materials. For each learning material, teachers have to add abstract first. Then, in manner to deliver the learning materials in the most adequate format, teachers need to post learning materials in few formats:

- Visual format (using shapes and the different formats that are used to highlight and convey information)
- Aural format (audio materials, providing materials in group discussion boards, sending learning content to email while it is upload to server)
- Read/write format (providing some additional links, dictionaries, quotations and words)
- Kinesthetic format (simulations, videos and movies of "real" things, as well as case studies, practice and applications)

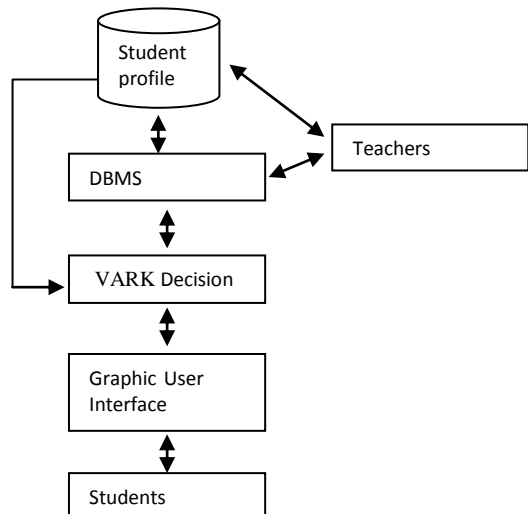


Figure 1: System architecture

The abstract of all learning materials in the proposed system will be saved in textual files.

The system is going to have several defined categories. Each of them has keywords that are using in the process of determination and proposing the most adequate category for the learning material.

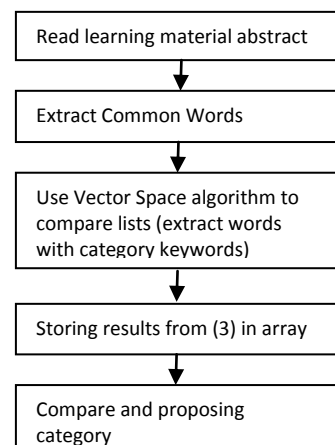


Figure 2: Process of category detection

Category detection will be made by vector space models, with searching through learning articles abstract that are published by teacher. The result of text mining process will be proposing the most relevant category for learning material. Category list is dynamically and editable by system administrator. This technique mainly relies on the analysis of keyword in the learning content abstract.

In order to make the process of information retrieval efficient, each category contains a list of synonyms and keywords, and the categories are manageable by administrator and users

The vector-space models for information retrieval are just one subclass of retrieval techniques that have been studied in recent years. Although the vector-space techniques share common characteristics with other techniques in the information retrieval hierarchy, they all share a core set of similarities that justify their own class [2]. The Vector Space Model (VSM) is probably the most widely used model for retrieving information from text collections [3].

#### *B. System functionality*

The main idea of this paper is proposing system that will detect the most adequate student learning style and delivering learning material based on VARK questionnaire results. For better understanding the proposed system, we are going to review one process of using the system:

##### *1) Students:*

- A student visit application URL
- Students need to go through questionnaire to be determinate his learning style. In this step, student have to select questions format type: textual or audio format
- After completing the questionnaire, system is going to check student answers and generate final results. There are 4 possible results:
  - o Visual
  - o Aural
  - o Read/Write
  - o Kinesthetic
- System will insert new record in student table (will create student model)
- System is going to set learning style for that student model
- Students login to application
- Select category (learning area)
- System is going to delivery learning material in format based on his learning style

##### *2) Teachers*

- Teacher is login to application
- Teacher can manage his learning materials
  - o Add new learning material – he has to select category (to accept proposed or select new one) and upload learning material in four formats (Visual, Aural, Read/Write and Kinesthetic)
  - o Change or delete his learning materials

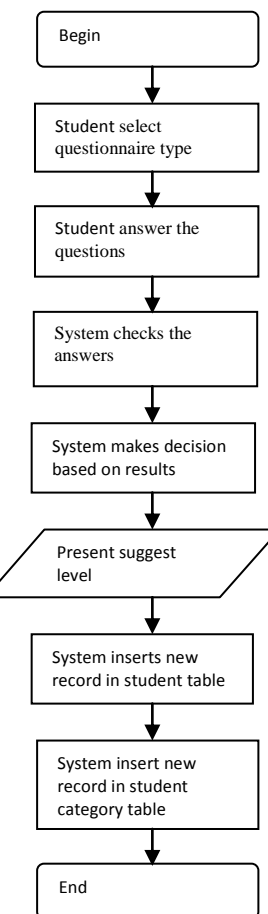


Figure 3: Creating new student model

#### *C. System monitoring and improvement*

In order to be the proposed system more efficient (learning materials to be delivered to students in the most acceptable form for them), system is going to check for students activity. When a student receive a learning material, the system will check if the student uses the format set by the system (according to the learning style determinate by VARK) or student chose a different format to display the learning material.

On certain period of time, the system is going to check this statistics. There are two possible situations:

- 1) The student is satisfied - use the format suggested by the system. It means that his learning style, determinate by VARK is adequate for the student.
- 2) The student often changes the format of the delivery of learning content. It means that his learning style, determinate by VARK is not adequate for the student. In this case, the system will change the selected student learning style. The new learning style will be selected based on the most chosen learning style from the student.

## V. CONCLUSION

The main goal of this system is to provide the learner with suitable learning material thus possibly enhancing their potential for learning. There are a lot of models for determination of learning style, but we propose using a VARK. It was selected for determination student learning style due to the fact that it seemed to be the most concise tool and had the most relevant questions. On the other hand, it does not contain too many questions, so student will give answers to all of them without problems. Also, it gives clear results, so the proposed system can make decision about format of learning materials, based on questionnaires results. This paper shows how the VARK learning style can be incorporated into the e-learning system and thus shows how it will be used to provide the relevant learning material for the learner based on their learner type.

Except determination of student learning style, proposed system is going to propose the most adequate category for learning material, while teacher post new learning article.

## VI. REFERENCES

- [1] K - Naser-Nick Manochehr, The Influence of Learning Styles on Learners in E-Learning Environments, Information Systems Department, Qatar University
- [2] J. Clerk Maxwell, A Treatise on Electricity and Magnetism, 3rd ed., vol. 2. Oxford: Clarendon, 1892, pp.68–73.
- [3] I. S. Jacobs and C. P. Bean, “Fine particles, thin films and exchange anisotropy,” in Magnetism, vol. III, G. T. Rado and H. Suhl, Eds. New York: Academic, 1963, pp. 271–350.
- [4] K. Elissa, “Title of paper if known,” unpublished.
- [5] R. Nicole, “Title of paper with only first word capitalized,” J. Name Stand. Abbrev., in press.
- [6] Y. Yorozu, M. Hirano, K. Oka, and Y. Tagawa, “Electron spectroscopy studies on magneto-optical media and plastic substrate interface,” IEEE Transl. J. Magn. Japan, vol. 2, pp. 740–741, August 1987 [Digests 9th Annual Conf. Magnetics Japan, p. 301, 1982].
- [7] M. Young, The Technical Writer’s Handbook. Mill Valley, CA: University Science, 1989.
- [8] Khribi, M. K., Jemni, M., & Nasraoui, O. (2009). Automatic Recommendations for E-Learning Personalization Based on Web Usage Mining Techniques and Information Retrieval. Educational Technology & Society, 12 (4), 30–42
- [9] Tiffany Ya TANG and Gordon MCCALLA. Dept. of Computer Science, University of Saskatchewan 57 Campus Drive, Saskatoon, Smart Recommendation for an Evolving E-Learning System
- [10] Olga C. Santos, Jesus G. Boticario, Recommendation Strategies for Promoting eLearning Performance Factors for All

# Analysis and Classification of Robot Control Algorithms

M. Todorova<sup>1</sup>

**Abstract –** The paper introduces a classification of the main categories of object movement algorithms in a maze. The paper also presents a brief description and a comparative analysis of the basic types of algorithms. A movement algorithm of a linear robot on a preset trajectory is outlined. The results are analysed and the necessary corrections are made in order to improve the control of the robot.

**Keywords –** robot, robot control algorithms, random mouse algorithm, Pledge algorithm, recursive algorithm, shortest path algorithm.

## I. INTRODUCTION

The automated control systems as whole are widely implemented in various industries, medicine, households, etc. The main goal of robotics is designing and putting into effect a mobile robot movement and control algorithm. An algorithm is a finite sequence of actions carried out in succession in order to solve a given problem. The problem might be related to calculations or data processing [1]. For the programming of algorithms, information from the environment is needed. The robot cannot be analysed and evaluated separately from its environment and the tasks to be fulfilled. The robot as a device, the environment and the tasks of the robot are entwined. The relationship is shown in Fig 1. [2].

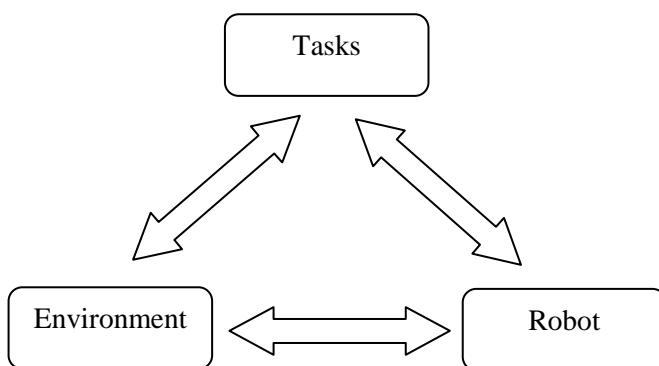


Fig 1. Tasks, Robot and Environment

<sup>1</sup>Maya P. Todorova, Technical University – Varna, Computer Sciences Departament, 9010 Varna, Bulgaria, E-mail: mayasvilen@abv.bg

## II. CLASSIFICATION OF ROBOT CONTROL ALGORITHMS

One of the main problems in robotics is the route tracing task. The existing maze solving algorithms can be classified into two basic categories.

The first category – algorithms used when information about the labyrinth is not available;

The second category – algorithms used when an overview of the labyrinth is available;

The algorithms for robot movement in a maze are shown in Fig 2.

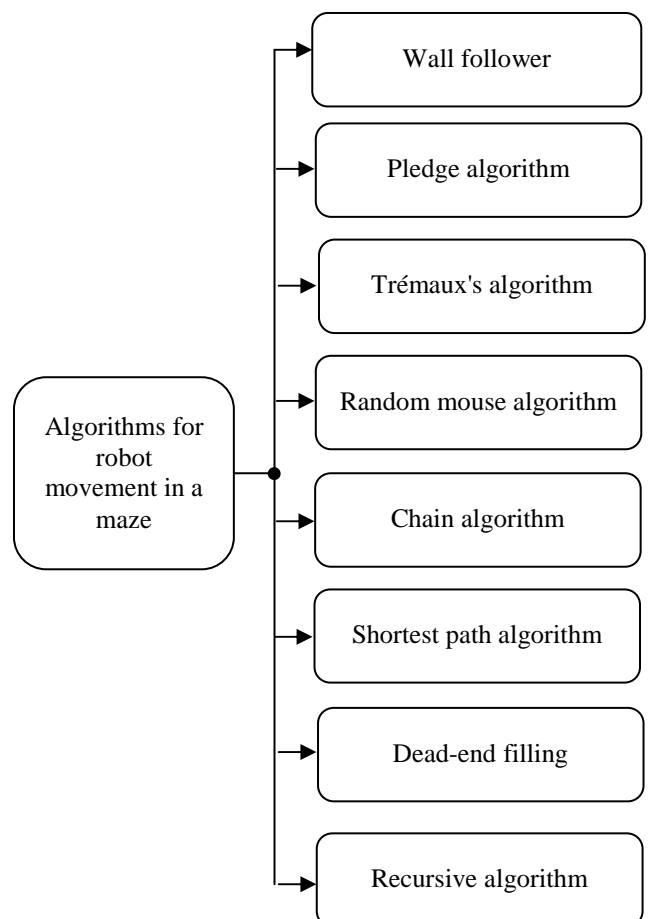


Fig 2. Depending on the means for accomplishing the task

- „Wall follower” – an algorithm also known as the “left or right hand rule”. This algorithm guarantees finding an exit from the maze if such exists. If an exit does not exist a mobile object following the algorithm will get back to

the beginning of the labyrinth. One of the main algorithms used in robotics.

- „Pledge algorithm“ – improved version of the wall follower algorithm. The algorithm solves the maze if it is a two-dimensional (2D) maze and the exits are situated on the external walls and the robot starts moving from any point inside the maze. Using this algorithm the robot does not need to store information about routes. The basic steps for accomplishing the algorithm are two: choosing a direction and following the chosen direction until possible. When a wall is reached it must be followed until the chosen direction becomes possible again. When implementing the algorithm, a count must be kept of the turns made +1 left turn, -1 right turn. When the total count of the turns equals zero the route tracing is aborted. The farthest wall of the current section is searched for and a transition is made to the next section. Thus, the external wall where the exit of the maze lies can be reached. Implementation of the algorithm is presented in Fig 3.

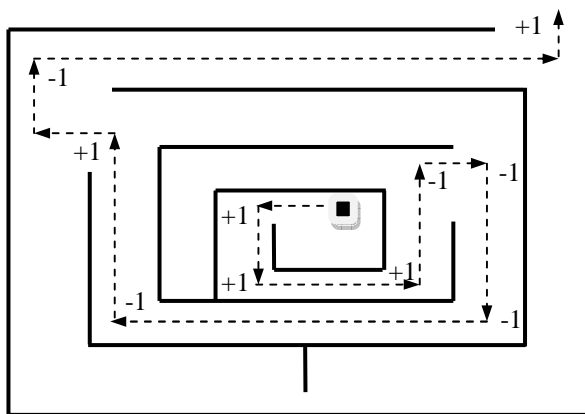


Fig. 3. Movement in a maze

- „Trémaux's algorithm“ – the starting point of the algorithm is inside the maze. When moving down a passage, the path is marked. When a position in which a further movement is not possible the route is traced back following the marked path. When reaching a junction the continuation is chosen randomly. If the passage is marked it is considered a dead end. When following a marked passage an unmarked passage is chosen on the next junction. If all passages at the junction are marked, an old passage is followed and marked once again. Each passage has three possible states: unmarked (unvisited), marked once (visited only once), marked twice. If solution exists, the passages marked once will lead directly from the start to the exit of the maze. If the maze has no exit, all passages will be marked twice.
- „Random mouse algorithm“ – the algorithm includes forward movement until reaching a junction. When a junction is reached, a random direction is chosen. The basic rule of the algorithm is that the U-turns (180 degree turns) are forbidden. They are acceptable only when all other possibilities are exhausted. The algorithm is slow,

ineffective and does not guarantee finding a solution. Tracing the back route from the exit is almost impossible to be implemented. The advantage of the algorithm is that additional memory is not required.

- „Dead end filling“ – the algorithm includes scanning the maze and filling each and every dead end. A dead end is a passage without an exit. The sections constituting parts of dead ends are also filled. The algorithm is characterized by rapidness and does not require additional memory.
- „Chain algorithm“ – the algorithm treats the maze as a number of smaller mazes and solves each of them separately. The algorithm specifies the start and desired end location. The algorithm is similar to the Pledge algorithm. Firstly, a straight line is drawn from the start to the end (even going through walls). Secondly, the line is followed. When a wall is reached the movement goes round the wall. This is achieved by the wall follower algorithm along the reached wall. Upon reaching the guiding line, if the new location is closer to the exit, the line is followed again. If the starting location is reached, the maze does not have a solution.
- „Recursive backtracking“ – the algorithm requires additional memory and is suitable for various types of mazes. When applying this maze solving algorithm the visited cells are marked with a special marker so that repeated entries from other directions are avoided. The algorithm always finds a solution if such exists. The solution found is usually not the shortest one.
- „Shortest path algorithm“ – the algorithm is a quick one. It requires additional memory. It is suitable for various types of mazes [3].

### III. ROBOT MOVEMENT

The robot is a machine that can follow a path or can move in a maze. The path can be invisible or visible. Example for a visible path is black line on a white surface [4]. The tasks related to robot control and robot movement fall into four categories:

- Robot movement along a preset trajectory. In solving this problem no sensors are needed. The main goal is setting the parameters controlling the left, right and U – turns as well as the velocity in line with the clock rate of the processor and the reduction coefficient;
  - Straight line movement;
  - Movement in a maze using one or more distance sensors;
  - Robot movement along a black line using digital sensors;
- A robot movement along a preset trajectories one of the most important tasks.

Having completed it we will have all the necessary values of the parameters controlling the robot. The values of these parameter are used for accomplishing the tasks “Movement in a maze using one or more distance sensors” and “Robot movement along a black line using reflexive sensors”. We have at our disposal two independent motion systems which allow for three different ways of making a turn.

- Firstly – the first wheel is blocked the other wheel moves forward;

- Secondly - the first wheel is blocked the other wheel moves backward;
- Thirdly – simultaneous movement of both wheels in different directions.

When the robot makes a turn using the first or the second method not only its orientation towards its current situation is altered but the situation itself is also changed. When the robot implements the wall follower algorithm the change in the distance from the surrounding walls is a major drawback. That's why the third method has to be applied. Using it, a rotation towards the spatial geometric centre of the mobile object is made.

In order to make a U-turn the function left or right turn has to be carried out twice in a row. For forward movement equal velocities have to be set for both engines. As a result the robot will move forward following a straight line. This is possible only in a perfect environment. In real situation there are various disturbances such as:

- using two different engines reflecting on the seed of the two wheels – major flaw resulting in a robot moving off the straight line;
- the surface is not perfectly smooth – the discrepancy in the resistance leads to diversion from the direction of movement.

These disturbances lead to breaks from the perfect trajectory both in the straight sections and in the turns. This calls for corrective actions in the control algorithm in order the system to achieve a perfect trajectory. The nature of the actions depends on the given task. Deviations from the perfect trajectory are given in Fig.5.

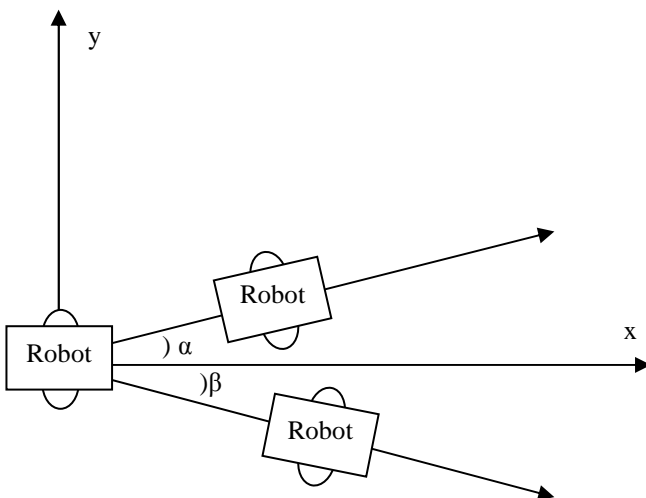


Fig. 5. Types of deviations

#### IV. CONCLUSIONS

The choice of a mobile robot control and movement algorithm depends on the problems to be solved, the hardware of the mobile device, i.e. the type and number of the sensors used for obtaining information about the robot location in the environment, and the disturbances arising from the random characteristics of the incoming influences. In order to avoid disturbances when implementing the algorithm of robot

movement along a preset trajectory, it is necessary to carry out tests on every surface the robot might come along. The values of the coefficients of each wheel are determined thus avoiding diversions from the straight line of movement. Another way of overcoming disturbances is real – time corrections of movement by reading information from the sensors.

#### REFERENCES

- [1]. <http://bg.wikipedia.org/wiki/Алгоритъм>
- [2]. доц. д-р. Димитър Димитров, "Системи с интелигентно поведение - Записки", 2007
- [3]. Дипломна работа, дипломант И. Иванов, научерн ръководител доц. д-р инж. Недялко Николов
- [4]. Priyank Patil, Department of Information Technology, K. J. Somaiya College of Engineering Mumbai, India, "Line following Robot
- [5]. Александров, П. С., „Проблемы Гильберта“, Москва: с.н., 1969..
- [6]. Harris, Tom. "How Robots Work", <http://science.howstuffworks.com/robot.htm>.
- [7]. Юревич И. Е., „Основы робототехники”, Санкт-Петербург, 2010

**This Page Intentionally Left Blank**

# Elaboration of Internet of Things Security Functional Model

Evelina Pencheva<sup>1</sup>

**Abstract –** Security is an important issue in Internet of Things (IoT). Besides device to device communications it concerns service access and discovery. The paper presents analysis on security aspects at IoT service level considering constrained Web Services. Based on the functional model of IoT Reference Architecture, new service security functions are suggested including mutual authentication, service selection and signing of service agreements.

**Keywords –** Internet of Thing, Reference Architectural Model, constrained Web Services, security, privacy.

## I. INTRODUCTION

Internet of Things (IoT) is defined as a network infrastructure, linking physical and virtual objects through the exploitation of data capture and communication capabilities. The infrastructure is based on internet evolution and network developments. It offers specific object identification, sensor and connectivity capabilities as a basis for development of independent federated services and applications. Services are expected to feature a high degree of autonomous data capture, transfer event network connectivity and interoperability [1], [2], [3].

One of the most challenging topics in such an interconnected world of objects including systems, sensors and services are security and privacy aspects. Without confidence that safety of private information is assured and adequate security is provided, users will be unwilling to adopt the IoT technology that invisibly integrates into their environment and life [4], [5].

IoT security features diverse challenges. Heterogeneous interactions in IoT include different communication patterns such as: human-to-human, human-to-thing, thing-to-thing, or thing-to-things. Communication protocols that enable information exchange between devices and users must provide integrity, authenticity, and confidentiality at different layers [6]. While the confidentiality of data captured from the physical world and represented in the digital world may rely on communication infrastructure, sensor privacy mainly targets the physical world [7]. Actuators execute actions in the physical world triggered in the digital world and the integrity, authenticity, and confidentiality of data sent to an actuator mostly depend on communication security, while the privacy on actuators is highly specific to the scenario [8]. Moreover, security mechanisms for storage device must be extended to provide adequate protection of user privacy [9]. Confidentiality and integrity of devices for interaction with humans in the physical world must insure that no third party has access to the device internal data and that device privacy depends on communication privacy [10]. Integrity and

authenticity of processing that provide data mining and service are based on device and communication integrity and on the correct design and implementation of the respective algorithms [11]. Localization and tracking are required to manage the mobility of the physical world. Identities provide unique physical object identification in the digital world. While the authenticity of these functions depends on the communication authenticity and device integrity, the confidentiality in this context features high sensitivity [12].

Services and applications security spans on different perspectives. It covers information, functional, operational and deployment views [13]. Access policies can accompany service description and information about services and software components must be hidden or made anonymous in order to protect the service provider privacy. Security related functions need to be implemented to manage the above mentioned issues. IoT system operation and deployment should follow specific best practices [14], [15].

The aim of the research is to analyze existing solutions for security functions concerning IoT service and application and to suggest some enhancements to the IoT Reference functional model [16].

The paper is structured as follows. In Section II, related works in the area of IoT service security are discussed. Section III presents the new security functions in the IoT Reference functional model that extend the authentication in service discovery and add service selection supplement service agreement. The conclusion summarizes the contribution.

## II. RELATED WORKS

*Things* in Internet of Things may be regarded as interconnected nodes in a Building Automation Control (BAC) system. The nodes vary in functionality and usually are constrained devices demanding low energy consumption.

Multiple control protocols for the IoT are developed. Key roles for BAC systems play the ZigBee standard [17], BACNet [18], or DALI [19]. Due to requirement for Internet Protocol (IP) connectivity the focus is on an all-IP approach for system control. Nowadays, the standardization activities are focused on design of new protocols for resource constrained networks of smart things. The 6LoWPAN standardization work includes definitions of methods and protocols for the efficient transmission and adaptation of IPv6 packets over IEEE 802.15.4 networks [20]. A framework for resource-oriented applications running on constrained IP network is developed in [21]. A lightweight version of the HTTP protocol, the Constrained Application Protocol (CoAP), uses UDP services and enables efficient application-level communication for things [22].

<sup>1</sup>The author is with the Faculty of Telecommunications, Technical University of Sofia, Kl. Ohridski 8, 1000 Sofia, Bulgaria, E-mail: iia@tu-sofia.bg

IPv6 over Low-Power Wireless Personal Area Networks (6LoWPANs) require simple service discovery network protocols to discover, control and maintain services provided by devices [20]. 6LoWPAN applications often require confidentiality and integrity protection. This can be provided at the application, transport, network, and/or at the link layer. Given the constraints, first, a threat model for 6LoWPAN devices needs to be developed in order to weigh any risks against the cost of their mitigations while making meaningful assumptions and simplifications. Some examples for threats that should be considered are man-in-the-middle attacks and denial of service attacks. A separate set of security considerations applies to bootstrapping a 6LoWPAN device into the network (e.g., for initial key establishment). This generally involves application level exchanges or out-of-band techniques for the initial key establishment, and may rely on application-specific trust models. Beyond initial key establishment, different protocols (TLS, IKE/IPsec, etc.) for subsequent key management as well as to secure the data traffic must be evaluated in light of the 6LoWPAN constraints. One argument for using link layer security is that most IEEE 802.15.4 devices already have support for Advanced Encryption Standard (AES) link-layer security. For network layer security, two models are applicable: end-to-end security, e.g., using IPsec transport mode, or security that is limited to the wireless portion of the network, e.g., using a security gateway and IPsec tunnel mode. The disadvantage of the latter is the larger header size, which is significant at the 6LoWPAN frame messages. To simplify 6LoWPAN implementations, it is beneficial to identify the relevant security model, and to identify a preferred set of cipher suites that are appropriate given the constraints.

Constrained RESTful Environments (CoRE) Link Format defines Web Linking using a link format by constrained web servers to describe hosted resources, their attributes, and other relationships between links [21]. The CoRE Link Format can be used by a server to register resources with a resource directory or to allow a resource directory to poll for resources. Based on the HTTP Link Header field, the CoRE Link Format is carried as a payload and is assigned an Internet media type. "RESTful" refers to the Representational State Transfer (REST) architecture. A well-known URI is defined as a default entry point for requesting the links hosted by a server.

The Constrained Application Protocol (CoAP) is a specialized web transfer protocol for use with constrained nodes and constrained networks [22]. The nodes often have 8-bit microcontrollers with small amounts of ROM and RAM, while constrained networks such as 6LoWPAN often have high packet error rates and a typical throughput of tens of kbit/s. The protocol is designed for device-to-device applications and provides a request/response interaction model between application endpoints, supports built-in discovery of services and resources, and includes key concepts of the Web such as URIs and Internet media types. CoAP easily interfaces with HTTP for integration with the Web while meeting specialized requirements such as multicast support, very low overhead and simplicity for constrained environments.

Host Identity Protocol Diet EXchange (HIP DEX) is a variant of the HIP Base EXchange (HIP BEX) specifically designed to use as few crypto primitives as possible yet still delivering the same class of security features as HIP BEX [23]. The design goal of HIP DEX is to be usable by sensor devices that are code and processor constrained. Like HIP BEX it is expected to be used together with another suitable security protocol, such as the Encapsulated Security Payload. HIP DEX can also be used directly as a keying mechanism for a MAC layer security protocol as it is supported by IEEE 802.15.4.

Security features and components are well defined in IoT Reference Architecture [16]. Layering approach is adopted to describe communication security and service security which are foundation for IoT service access and resolution service. Resolution is a service by which a given identification is associated with a set of addresses of information services and interaction services. Information services allow querying, charging and adding information about the thing in question, while interaction service enable direct interaction with the thing by accessing software resources of the associated devices. Resolution is based on a priori knowledge achieved by service discovery. Discovery is a service to find unknown services based on a rough specification of the desired result. It may be utilized by a human or another service. The discovery execution considers credentials for authorization. The security related functional components provide secure discovery of an IoT service and restricted discovery.

Secured discovery of an IoT service restricts the discovery of service to those users or applications that are authorized to know about it, including the creation of a new pseudonym (to ensure privacy of a user). As to [16] secured service discovery includes the following functional components: user authentication and assertion of his identity and discovery of person related IoT services for authorized personnel. The later functional components cover authorization to general access to discovery, service discovery based on service specification, filtering of discovery results, creation and deployment of new pseudonym. Secure direct discovery of IoT service is applied when the related credentials have to be processed prior to the discovery. In this case, first the user is authenticated and a list of credentials is provided based on the user identity. Then the user may communicate directly with an isolated discovery component performing the following actions: credentials presentation, service discovery and restricted access based on credentials.

Both scenarios for IoT service discovery presented in [16] rely on authentication authority and guarantee the user related security aspects. In some case, service authentication is also a matter of concern, for example, how to authenticate requests coming from other Web Services. So, where appropriate, authentication in IoT must be mutual including both user and service authentication. Moreover, for charging purposes, there is a need for the authenticated user to confirm the intention to use the discovered IoT service by signing a service agreement. The signing of service agreement is to ensure non-repudiation, or in other words to prevent the user from denying he or it has used the service. Typical service agreement presentation and signing is done by digital signature.

Section III presents the suggested elaboration of the IoT security model at application level, which faces the above mentioned issues.

### III. ELABORATION OF THE IOT SECURITY MODEL

The suggested use cases related to secure IoT service access are shown in Fig.1. The access to IoT service includes Initial Access, Application level Authentication, Service Discovery and Service Selection use cases.

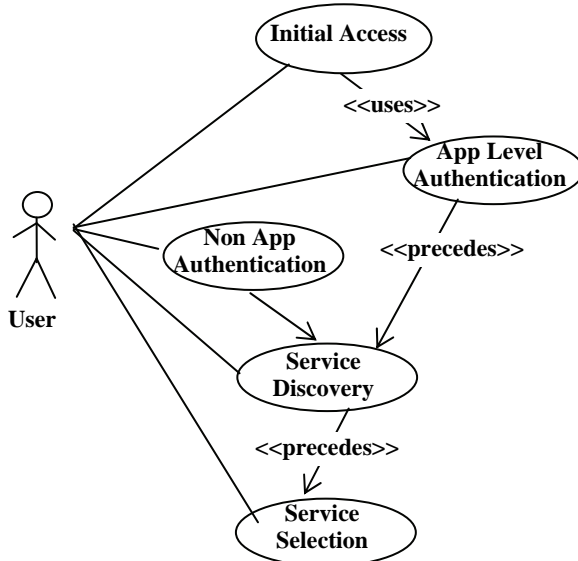


Fig.1 Use cases for secure IoT service access

Before using IoT services, the user and the Service Repository authenticate each other. Authentication prevents from unauthorized access. Once authenticated, the user selects the service interface to be used. To ensure non-repudiation, the Service Repository can request signing of a service agreement before allowing the IoT to be used. Only after the authentication, service selection, and signing of the service agreement have been done the user starts using the actual IoT service. Apart from providing security, the authentication and service selection process also allows IoT service providers to define permission profiles for different users. The amount of privileges can be made to depend on the level of trust awarded to the user.

Fig.2 shows the sequence diagram related to authentication use case. The steps are as follows:

- At initial contact, the User requests authentication by invoking the `initiateAuthentication` operation. The Service Repository replies with an indication of the authentication operation to be used. An agreed authentication method is used. If more than one authentication operations are supported, the `initiateAuthentication` operation serves to tell which operation to use.
- The User requests authentication from the Service Repository by invoking `authenticateServiceRepository` operation. When the Service Repository has successfully

authenticated itself, the User acknowledges this with the `authenticationSucceeded` operation.

- Once the User has authenticated the Service Repository, the Service Repository requests authentication from the User by invoking `authenticateUser` operation. The security mechanisms are symmetric. Not only the Service Repository authenticates the User, but the User authenticates the Service Repository also.

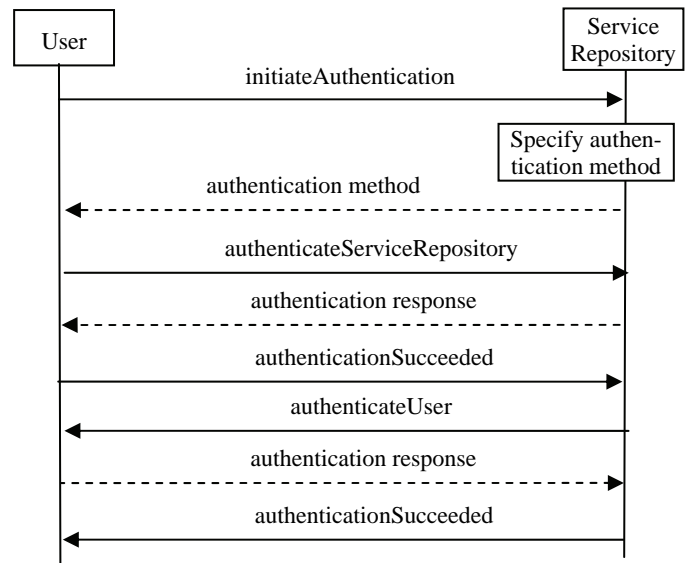


Fig.2 Authentication

Fig.3 shows the service discovery and signing of service agreement. The steps are as follows:

- After the Service Repository and User have successfully authenticated each other, they agree on an algorithm to be used for signed exchanges by invoking `selectSigningAlgorithm` operation.
- The User may not know the services available and may request a list of service types by invoking `listServiceTypes` operation.
- The User may need to examine the leading properties of selected services using `describeServiceTypes` operation.
- The core operation, `discoverServices` informs the Service Repository of the required service using parameters `serviceTypeName` and `servicePropertyList` as well as the maximum number of matches the User wishes to receive. The Service Repository returns a list of IoT services meeting the requirements and their service properties.
- Using the `selectService` operation, the User informs the Service Repository of the `ServiceID` of the IoT service it wishes to select. The Service Repository provides a token that is private to the User.
- The User and Service Repository sign a service agreement electronically by invoking `signServiceAgreement` operation..

Once the service agreement has been successfully signed by both sides, the User can start using the IoT service.

#### IV. CONCLUSION

The paper studies security aspects of IoT services. Based on the analysis on current standards and research work, security issues at the application, transport, network, and/or at the link layer in constrained networks are discussed. Some weaknesses in authentication and authorization of IoT service security are identified. As countermeasures mutual authentication procedure between the user and IoT service, as well as service selection procedure are suggested. In addition to increased security, the suggested authentication and service selection procedures allow differentiation of IoT service users.

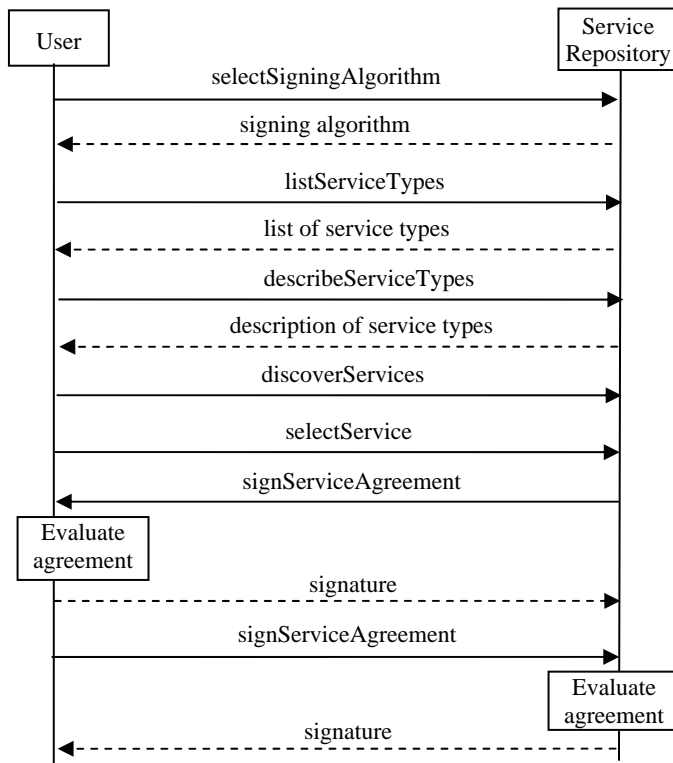


Fig.3 Service discovery, service selection and signing of service agreement

#### ACKNOWLEDGEMENT

The research is in the frame of Project DDBY02/13/17.02.2010 funded by National Science Fund, Bulgarian Ministry of Youth, Education and Science.

#### REFERENCES

- [1] ITU Internet Reports. The Internet of Things (Ed. 2005), 2005.
- [2] INFSO D.4 Networked Enterprise & RFID INFSO G.2 Micro & Nanosystems, in cooperation with the WG on RFID of the ETP EPOSS, "Internet of Things in 2020, Roadmap for the future", vol 1, pp.1-27, 2008.
- [3] A.BekiarSKI, E. Altimirski, S. Pleshkova. "Multimedia Surveillance Station for Audio-Visual Objects Tracking with

Mobile Robot", Proc. Of International Conferences of Systems, Greece, pp.240-247, 2010.

- [4] L. Galluccio, G. Morabito, S. Palazzo. "On the Potentials of Object Group Localization in the Internet of Things", Proc. of IEEE International Symposium on World of Wireless, Mobile and Multimedia Networks WoWMoM'2011, pp.1-9, 2011.
- [5] T. Heer, et al. "Security Challenges in the IP-based Internet of Things", Springer Journal on Wireless Personal Communications, vol.61, issue 3, pp.527-542, 2011.
- [6] S. Pleshkova. "Algorithm of feature estimation for real time objects detection in thermal images", Proc. Of International Conference on Computational Intelligence, Man-Machine Systems and Cybernetics, CIMMACS 2011, Jakarta, Indonesia, 2011, pp.209-215.
- [7] S. Park, et. al. "IPv6 over Low Power WPAN Security Analysis", Internet Draft, 2011.
- [8] R. Weber. "Internet of Things – new security and privacy challenges", Computer low and Security review, vol.26, pp.23-30, 2010.
- [9] T. Li, L. Chen. "Internet of Things: Principle, Framework and Application", Future Wireless Networks and Information Systems, Springer LNEE 144, pp.477-482, 2012.
- [10] A. Serbanati, C. Medaglia, U. Ceipidor. "Building Blocks of the Internet of Things: State of the Art and Beyond", Chapter 20 in edited book "Deploying RFID - Challenges, Solutions, and Open Issues", 2011.
- [11] R. Roman, P. Najera, J. Lopez. "Securing the Internet of Things", IEEE Computer, vol.44, no.9, pp.51-58, 2011.
- [12] C. Mayer. Security and Privacy Challenges in the Internet of Things", Electronic Communications of the EASST, vol.17, pp.1-12, 2009.
- [13] P. Castellani, et. al. "Web Services for the Internet of Things through CoAP and EXI", Proc. of IEEE International Conference on Communications Workshops, pp.1-6, 2011.
- [14] H. Suo, et. al. "Security in the Internet of Things: A Review", Proc. of International Conference on Computer and Electronics Engineering ICCSEE'2012, vol.3, pp.648-651, 2012.
- [15] R. Kranenburg, et. al. "The Internet of Things", Proc. of Berlin Symposium on Internet and Security, 2011.
- [16] FP7 Project Internet of Things – Architecture. "Introduction to the Architectural Reference Model for the Internet of Things", <http://www.iot-a.eu/arm/d1.3>, 2012.
- [17] ZigBee. <http://www.zigbee.org/>.
- [18] S. Ramon. "ZigBee Alliance Completes ZigBee Building Automation Standard, BACnet. <http://www.zigbee.org/Default.aspx?Contenttype=ArticleDet&tabID=332&moduleId=806&Aid=354&PR=PR>", 2011.
- [19] DALI. <http://www.dalibydesign.us/dali.html>.
- [20] N. Kushalnagar, G. Montenegro, C. Schmacher. "IPv6 over Low-Power Wireless Personal Area Networks (6LoWPANs): Overview, Assumptions, Problem Statement, and Goals", RFC 4919, 2007.
- [21] Z. Shelby. Constrained RESTful Environments (CoRE) Link Format, RFC 6690, 2012.
- [22] Z. Shelby et. al. "Constrained Application Protocol (CoAP)", Internet Draft, 2012.
- [23] R. Mozkowitz. "HIP Diet Exchange (DEX)", Internet Draft, 2011.

# Internet of Things in Healthcare Applications

Evelina Pencheva<sup>1</sup>, Ivaylo Atanasov<sup>1</sup>, Raycho Dobrev<sup>1</sup>

**Abstract – Internet of Things (IoT) is a pervasive technology which covers a number of application domains. The paper presents a survey on telemedicine standards and a study on applicability of IoT Reference Domain Model in the area of healthcare. The IoT Reference Domain Model introduces the main concepts of IoT and the relations between these concepts. As far as the abstraction level describes the concepts in a way which is independent of specific application area, it is important to investigate potential application scenarios and use cases. The paper presents the main abstraction and relationships and discusses their implementation analyzing existing solutions in healthcare applications. An enhancement of the IoT Reference Domain Model is suggested.**

**Keywords – Internet of Thing, e-health, architectural domain model, device-to-device communications.**

## I. INTRODUCTION

Development of Internet is a continuous process and one of the next steps is the evolution from network of networks composed of interconnected computers to interconnected objects which result in Internet of Things (IoT) [1], [2]. The objects possess own Internet protocol (IP) addresses. They can be embedded in complicated systems and use sensors to receive information from their environment [3]. The objects recognize each other and become more intelligent exchanging data gathered from other objects. The IoT applications are expected to contribute to solving challenges in aging society, vehicle telematics and transport logistics, agricultural monitoring, environment prevention and so on. [4], [5], [6], [7], [8]. It is envisaged that this interconnection between physical objects will have significant impact in the area of healthcare [9].

There are three main organizations that create standards related to Electronic Health Records- CEN TC 251, HL7 and ASTM E31[10]. An important area of CEN/TC 251 work are standards for the Electronic Healthcare Record [11]. These include a record architecture establishing the principles for representing the information content and record structure, a set of concepts and terms for record components, and rules and mechanisms for sharing and exchanging records. A domain model representing a formal description of the context within which the healthcare records are used, is established to document requirements for these standards. The standards are aimed at the semantic organization of information and knowledge so as to make it of practical use in the domains of health informatics and telematics, and the provision of information and criteria to support harmonization. This encompasses clinical, managerial and operational aspects of the medical record and enabling access to other knowledge. Further the activities are focused at providing a statutory framework to ensure that information systems used in healthcare have appropriate levels of quality, safety and

security.

ASTM (American Society for Testing and Materials) develops standards related to the architecture, content, storage, security, confidentiality, functionality, and communication of information used within healthcare and healthcare decision making, including patient-specific information and knowledge [12].

Health Level Seven (HL7) is involved in producing standards for a particular healthcare domain such as pharmacy, medical devices, imaging or insurance (claims processing) transactions [13]. The name refers to the application level of the Open Systems Interconnection (OSI). Standards address definition of the data to be exchanged, the timing of the interchange, and the communication of certain errors to the application. The seventh level supports such functions as security checks, participant identification, availability checks, exchange mechanism negotiations and, most importantly, data exchange structuring.

Healthcare is an information-intensive and a communication-intensive business. The volume of information exchanged between departments within hospitals and between primary and secondary care providers is large. EDI stands for Electronic Data Interchange. EDI is the interchange of standard formatted data between the computer application systems of trading partners with minimal manual intervention [14], [15]. EDI standard, consists of a grammar (syntax and rules for structuring the data) and a vocabulary (contained in the directories of data elements, composite data elements, segments, and messages).

The IoT Architectural Reference Model provides interoperability solutions at communication and service levels across various platforms [16], [17]. It reflects the requirements of different stakeholders groups and adopts established working solutions of various aspects of the IoT. The foundation of the Reference Architectural Model is the Domain Model that introduces the main concepts of Internet of Things and the relations between these concepts. The abstraction level describes the concepts in a way which is independent of specific application area. The aim of the paper is to outline potential application scenarios of IoT Domain Model and use cases in the area of telemedicine.

The paper is structured as follows. In Section II, the main Domain Model abstractions and relationships are presented and their implementation in healthcare applications is discussed. Section III describes the suggested enhancement of the IoT Reference Domain Model that reflects the device-to-device communications in a network. A new abstract concept and its relationships are added. Section IV illustrates the application of the concept in healthcare area. Finally the conclusion summarizes the contribution.

<sup>1</sup>The authors are with the Faculty of Telecommunications, Technical University of Sofia, KI. Ohridski 8, 1000 Sofia, Bulgaria, E-mails: enp@tu-sofia.bg; iia@tu-sofia.bg; r\_dobrev@tu-sofia.bg

## II. MAPPING OF IOT REFERENCE DOMAIN MODEL ONTO HEALTHCARE APPLICATIONS

The IoT Reference Domain Model provides a description of greater abstraction than that, what is inherent to real systems and applications. It describes concepts belonging to IoT area defining basic attributes of objects, their responsibilities and relationships between objects as shown in Fig.1.

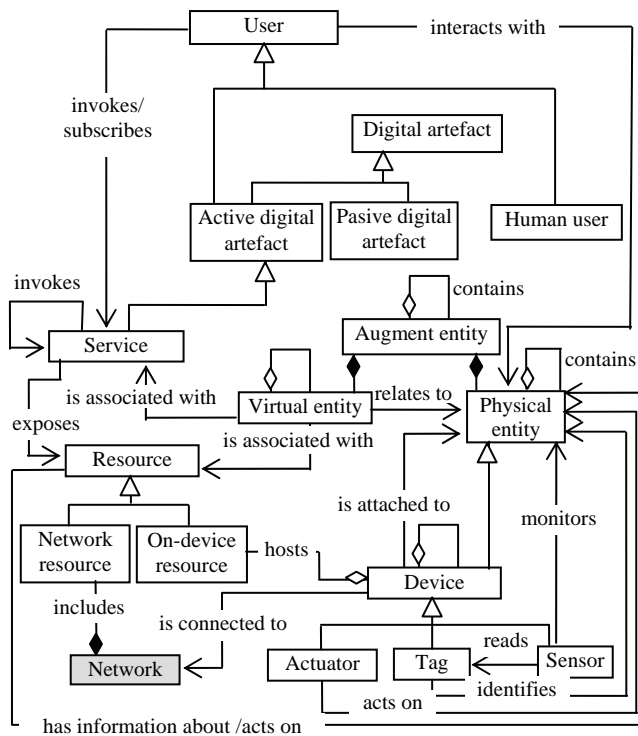


Fig.1 IoT Domain model [16]  
(the suggested enhancement is shown in grey)

The *User* is a human or a software program acting according business logic that is interested in interacting with a particular physical object. *Users* across healthcare spectrum include healthcare professionals (physicians, nurses, dentists), healthcare provider organisations (hospital, clinics, nursing homes, rehabilitation centres), support service providers (pharmacies, diagnostic centres, blood banks, laboratories), individuals, employers, payers (insurance firms, 3<sup>rd</sup> party administrators, brokers) and relevant software applications.

The user interacts with a *Physical Entity*. The *Physical Entity* is any physical object that is relevant from a user or application perspective. In the area of healthcare, *Physical Entity* is the patient.

*Virtual Entity* is the Physical entity's digital representation. Digital representation of a patient can be 3D models, database entries, instances of a class in an object-oriented technology, and a social network account also. *Virtual Entities* are *Digital Artefacts* that can be classified as either active or passive. *Active Digital Artefacts* are running software applications, agents or *Services* that can access other *Services* or *Resources*. For example, an *Active Digital Artefact* can be an application that monitors the blood pressure of the patient and sends a

message to the healthcare professional in case of emergency, or videoconference application enabling doctors to be digitally connected through mobile communications and to develop therapies in cooperation with other doctors and liaise closely with patients. *Passive digital artefacts* are passive software entries such as database entries with vital signs measurements or other digital representations of the *Physical entity*.

Things in the IoT are represented as *Augment entity* which is composed of one *Virtual Entity* and the associated *Physical entity*. The technological interface for interacting with or gaining information about the *Physical entity* is the *Device* or *Devices*. *Devices* are usually embedded into, attached to or placed closed to the *Physical Entity*. A *Device* is a mediator between *Physical* and *Virtual Entities*. Clinical devices are instruments used to assess the human condition and to deliver medical treatment.

Medical technology has benefited greatly by incorporating rapid advances in the science of information technology into many measurements and devices. But often this has been done in an unstructured manner with many devices being developed in an isolated way that makes impossible both communication between them and with hospital data management systems. As the advantages of such communication became more and more obvious, a pressing need for technical standardisation and new protocols resulted in the creation of some standardisation activities. Great efforts were mainly held by the IEEE 1073, VITAL and the Point of Care Connectivity Industry Consortium to enable communication to exist in an easy and open way, with subsequent clinical, administrative and research benefits. Using a complete data-transfer protocols such as RS-232, RS-422, or RS-485, or using wireless protocols such as Bluetooth, new functionality can be built into medical devices. That enables them in many cases to upload some of the manual tasks to the server. Traditional patient charts are replaced by the data delivered to a central processing station. These data are then analyzed and timestamped by a knowledge-based engine and delivered to a nursing station in real time, along with an at-a-glance summary. Such a system eliminates delays between the gathering and the delivery of the information to the clinician. The systems are also designed to prevent manipulation of the database, ensuring the validity of the data. Examples of medical *Devices* include spirometers, capnographs, weight and fat scales, pulse oximeters, clucometers, heart rate monitors, electrocardiograms, holters, echocardiographs, thermometers, multiparameter devices etc. [18]. Specially designed for telemedicine and home care applications, some devices transmit the data wirelessly to a gateway, which then forwards this information via internet to a telemedicine call centre or a secure data repository.

Regarding healthcare area, there exist some assumptions based on the limited capabilities of devices within low power wireless personal networks. While some devices are expected to be extremely limited (reduced function devices), more capable full function devices will also be present, albeit in much smaller numbers. The full function devices typically have more resources and may be mains powered. Accordingly, they aid reduced function devices by providing

functions such as network coordination, packet forwarding, interfacing with other types of networks, etc.

From an IoT point of view the following three types of *Devices* are of interest. *Sensors* provide information about the physical state of the Physical entity. Information from *Sensors* can be recorded for later retrieval. *Sensors* assist patients with home diagnostics for chronic illnesses and help them with prevention or to make lifestyle changes advised by medical professionals. Blood pressure, weight or blood sugar - handy measuring sensors ensure that the most important vital data might be always to hand, even when on the move [19]. *Sensors* transfer the relevant data to the patient's cell phone or smartphone e.g. by Bluetooth. From there it is transferred to his or her personal online diary. The patient can also add information such as medications, mealtimes, sporting activities or visits to the doctor, to this diary via a web portal or while on the move.

*Tags* are used to identify *Physical Entities* to which they are usually attached to. The identification process can be optical (barcodes or QR code) or it can be radio frequency based (RFID) [20], [21].

*Actuators* are special *Devices* that can modify the physical state of one or more *Physical Entities*. An example of *Actuator* is defibrillator which is designed to pass electrical current through a patient's heart and to restore a patient's heart rhythm to normal.

*Resources* are heterogeneous, system specific software components that store or process data or information about one or more *Physical Entities*, or that provide access to measurements and actuations in case of *Sensors* and *Actuators* respectively. Two types of resources can be distinguished. *On Device Resources* are hosted on *Devices* and are regarded as software deployed locally on the *Device*. *Network Resources* are resources available in the network. *Network Resources* run on a dedicated server in the network or in the 'cloud'.

A *Service* provides a well-defined and standardized interface offering all necessary functionalities for interacting with *Physical Entities* and related processes. An important issue related to *Service* is service orchestration both for IoT *Service* and non-IoT *Service* [22]. Service platform independency can be achieved, for example by using Web Services technology [23]. In the area of healthcare, *Services* are aimed at people that require nursing care or incur certain medical risks such as slip and fall accidents and provide location information in case of injury for family members and emergency services.

### III. ENHANCEMENT OF THE IoT DOMAIN MODEL

The concept that is suggested to be included in the IoT Domain reference model is *Network*. Devices can be connected in a low power personal area *Network*. The main requirement to this type of *Network* is to provide IP connectivity. The requirement for IP connectivity is driven by the following: The many connected devices make network auto configuration and statelessness highly desirable and for this, IPv6 has ready solutions; The large number of devices poses the need for a large address space, well met by IPv6; Given the limited packet size, the IPv6 address format allows

subsuming of IEEE 802.15.4 addresses if so desired; Simple interconnectivity to other IP networks including the Internet.

The network must support various topologies including mesh and star. Mesh topologies imply multi-hop routing, to a desired destination. In this case, intermediate devices act as packet forwarders at the link layer (akin to routers at the network layer). Typically these are full function devices that have more capabilities in terms of power, computation, etc. The requirements on the routing protocol are formulated in [24], [25] and include the following:

- The routing protocol must impose low (or no) overhead on data packets independently of the number of hops.
- The routing protocols should have low routing overhead balanced with topology changes and power conservation.
- The computation and memory requirements in the routing protocol should be minimal to satisfy the low cost and low power objectives. Thus, storage and maintenance of large routing tables is detrimental.
- Support for network topologies in which devices may be battery or mains-powered. This implies the appropriate considerations for routing in the presence of sleeping nodes.

As with mesh topologies, star topologies include provisioning a subset of *Devices* with packet forwarding functionality. If, in addition to IEEE 802.15.4, these *Devices* use other kinds of network interfaces such as Ethernet or IEEE 802.11, the goal is to seamlessly integrate the *Networks* built over those different technologies.

### IV. USE CASE

The sketched use case presents healthcare at home by remote assistance. Data is collected on periodic base and upon occurrence of events. In healthcare applications, delays or loss of information may be a matter of life or death, so data transmission must be real time and reliable. The patient's network is of small size with high density of nodes powered by hybrid sources. The devices are always on. They are connected in a patient's body network in star topology and controlled by a local controller dealing with data aggregation and dynamic network attachment when the patient moves around at home. Some devices can be installed with mains powered status. There may be multipath interference due to walls and obstacles. The communication between patient's network nodes is limited to a home environment. The traffic pattern for data collection is point-to-multipoint or multipoint-to-point and for local diagnostics it is point-to-point. An example scenario is shown in Fig.2.

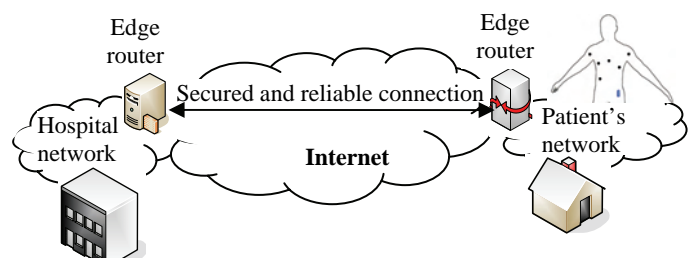


Fig.2 An example healthcare scenario

Being at home or visiting the connected hospital the patient, whose sensed information is of interest, must be identifiable uniquely. When the patient's network is configured to use unique global IPv6 address, then it is possible to identify the patient by the very same address. Unfortunately issues regarding privacy and security must be considered. Moreover, an obligatory identification system featuring string authority and authentication must be deployed at the hospital network where the patient's information is transferred to. The high level of data privacy imposes a reliable and secure connection between the hospital edge router and the patient's edge router. This implies an additional security policy between two networks.

## V. CONCLUSION

The paper studies the applicability of the IoT reference domain model to healthcare applications. The main abstract concepts and their relationships are mapped onto healthcare views and perspectives. An enhancement of the IoT reference domain model is suggested and discussed. The new concept representing the device interworking in an IP based network with its relationships is introduced. A use case scenario with inherent characteristics is investigated.

## ACKNOWLEDGEMENT

The work is conducted under the grant of the Project 122pd0007-07 funded by Research and Development Sector, TU-Sofia, Bulgaria.

## REFERENCES

- [1] ITU Internet Reports. The Internet of Things (Ed. 2005), 2005.
- [2] INFSO D.4 Networked Enterprise & RFID INFSO G.2 Micro & Nanosystems, in cooperation with the WG on RFID of the ETP EPOSS, "Internet of Things in 2020, Roadmap for the future", vol 1, pp.1-27, 2008.
- [3] L. Galluccio, G. Morabito, S. Palazzo. "On the Potentials of Object Group Localization in the Internet of Things", Proc. of IEEE International Symposium on World of Wireless, Mobile and Multimedia Networks WoWMoM'2011, pp.1-9, 2011.
- [4] L. Atrozi, A. iera, G. Morabito. "The Internet of Things: A survey", Computer Networks, vol. 54, pp. 2787-2805, 2010.
- [5] J. Wang, D. Yang, X. Liu, Y. Zeng. "The Key Technologies and Development Research of Chinese Light Industry IOT Application", Advances in Wireless Sensor Networks Communications in Computer and Information Science, vol. 334, pp 438-446, 2013.
- [6] T. Li, L. Chen. "Internet of Things: Principle, Framework and Application", Future Wireless Networks and Information Systems, Springer LNEE 144, pp.477-482, 2012.
- [7] A. Bekiaraki, E. Altimirski, S. Pleshkova. "Multimedia Surveillance Station for Audio-Visual Objects Tracking with Mobile Robot", Proc. Of International Conferences of Systems, Greece, pp.240-247, 2010.
- [8] S. Pleshkova. "Algorithm of feature estimation for real time objects detection in thermal images", Proc. Of International Conference on Computational Intelligence, Man-Machine Systems and Cybernetics, CIMMACS 2011, Jakarta, Indonesia, 2011, pp.209-215.
- [9] Tarouco, et. al. "Internet of Things in healthcare: Interoperability and security issues", Proc. of IEEE International Conference on Communications ICC'2012, pp. 6121-6125.
- [10] A. Anagnostaki, et. al. "Integration of CEN/TC251/PT5-021 "VITAL" preENV standard and of "DICOM supplement 30.0" into a telemedicine system for vital signs monitoring from home", Proc. of IEEE International Conference on Engineering in Medicine and Biology Society, vol. 2, pp. 1368 - 1371 , 2000.
- [11] O. Bott. "The Electronic Health Record: Standardization and Implementation", Proc. of 2nd OpenECG Workshop, 2004, pp. 57-60.
- [12] G. Schaefers. "Testing Mr Safety and Compatibility, An Overview of the Methods and Current Standards", Proc. of IEEE Engineering in Medicine and Biology Magazine, pp. 23-27, 2008.
- [13] P. Schloeffel, et al. "The relationship between CEN13606, HL7, and openEHR", Proc. of HIC Bridging the Digital Divide: Clinician, consumer and computer, 2006, pp. 1-4.
- [14] M. Eichelberg, et al. "A Survey and Analysis of Electronic Healthcare Record Standards", Int. J. ACM Computing Surveys, vol. 37, no 4, 2005, pp. 277-315.
- [15] D. Kalra, "Electronic Health Record Standard" IMIA Yearbook of Medical Informatics, 2006, pp. 136-144.
- [16] A. Serbanati, C. Medaglia, U. Ceipidor. "Building Blocks of the Internet of Things: State of the Art and Beyond", Chapter 20 in edited book "Deploying RFID - Challenges, Solutions, and Open Issues", 2011.
- [17] FP7 Project Internet of Things – Architecture. "Introduction to the Architectural Reference Model for the Internet of Things", <http://www.iot-a.eu/arm/d1.3>, 2012.
- [18] ITU-T, "FSTP-RTM Roadmap for Telemedicine", 2006.
- [19] "Vital Signs and Measurements" in Student textbook "Integrated Clinical Procedures", pp563-598, [http://cengagesites.com/academic/assets/sites/3985\\_lindh\\_ch\\_24.pdf](http://cengagesites.com/academic/assets/sites/3985_lindh_ch_24.pdf).
- [20] E. Welbourne, et. al. "Building the Internet of Things Using RFID The RFID Ecosystem Experience", Proc. of IEEE Internet Computing, pp. 48-55, 2009.
- [21] T. Kriplean, et al., "Physical Access Control for Captured RFID Data", Proc. of IEEE Pervasive Computing, vol. 6, no. 4, 2007, pp. 48-55.
- [22] J. Pascual-Espada, "Service Orchestration on the Internet of Things," International Journal of Interactive Multimedia and Artificial Intelligence, 2012.
- [23] P. Castellani, et. al. "Web Services for the Internet of Things through CoAP and EXI", Proc. of IEEE International Conference on Communications Workshops, pp.1-6, 2011.
- [24] E. Kim, D. Kaspar, JP. Vasseur. "Design and Application Spaces for IPv6 over Low-Power Wireless Personal Area Networks (6LoWPANs)", RFC 6568, 2012.
- [25] N. Kushalnagar, G. Montenegro, C. Schmacher. "IPv6 over Low-Power Wireless Personal Area Networks (6LoWPANs): Overview, Assumptions, Problem Statement, and Goals", RFC 4919, 2007.

# Determining the importance of the usability attributes of Web-based GIS applications

Nebojša D. Djordjević<sup>1</sup>, Dejan D. Rančić<sup>2</sup>

**Abstract –** This study considers the usability of Web-based GIS applications (Web-based GIS) in terms of their quality of use for specific end users seeking to achieve work goals in particular environments. Aim of the paper is to propose a suitable model for quality in use based on a weighting approach to identify those characteristics that are most important and that contribute to the quality in use of the usability factors of WebGIS applications from the perspective of different types of potential users. The objective of this study is to use a weighting approach to determine the relative importance of Analytical Network Process (ANP) which is used to analyse the relative importance of the factors.

**Keywords –** Web-based GIS, usability, quality of use, ANP.

## I. INTRODUCTION

Usability is one relevant factor of the quality of Web applications. Recently, it has been receiving great attention, being recognized as a fundamental property for the success of Web applications. Defining methods for ensuring usability is therefore one of the current goals of the Web engineering research.

The notion of usability is a key theme in the human-computer interaction (HCI) literature. The overarching goal of a majority of the HCI work has been to propose techniques, methods, and guidelines for designing better and more “usable” artifacts. Determining the degree of usability is a process in which systems are evaluated in order to determine product-success using methods available to the evaluator.

GIS is defined as a set of tools used to collect, store, retrieve, transform and display spatial data from the real world as defined previously [1-3]. A web-based GIS application means a browser supporting an application in order to make its information accessible. Web-based GIS applications have client side and server side architecture over network. Client side is capable to edit and improve performance, user access the GIS functions (information) through any internet browser on computer where people interact with GIS interface [4], [5]. Server side is using web remote in application server and address matching, where server is performing storage and process the data from central database to user query [5-7]. Database side is responsible, and consists of many different databases for different functionalities like store and access the

server in order to return the data to the client server. Web browser is used for generating server requests and displays the data results [5].

Today, many various kinds of GIS applications are in everyday use. They significantly vary in available functions. Some of them are commercial solutions; some of them are open source solutions.

The paper deals with a quality evaluation of a Web-based GIS intranet application providing access to spatial information. WebGIS application developed for the Ministry of Defense was selected as the case study for this work.

An Intranet is an internal information system based on Internet technology, web services, TCP/IP and HTTP communication protocols, and HTML publishing [8]. Intranet resources are available for employed of a company only and number of available respondents for evaluation application is limited. For using these technologies by WebGIS applications all necessary standards were adopted several years ago.

Since all of the usability factors do not have the same importance in the overall usability assessment of the WebGIS applications, the proposed factors have been weighted by adopting ANP (Analytic Network Process) approach [9].

Assessing the quality in use will allow WebGIS application owners to estimate how usable a WebGIS application might be and the user's satisfaction.

These studies are certainly important as that would further deepen our understanding on factors that contributes towards the usability of WebGIS applications.

## II. MODEL FOR QUALITY IN USE IN WEBGIS

Usability as a quality characteristics has been defined by different researchers [10-12] and several ISO standards, e.g. ISO/IEC 25010 [13] and ISO/IEC 9241-11 [14].

In order to evaluate the quality of developed systems, a set of quality characteristics and criteria are required as a basis to describe the system quality. This set of characteristics and the relationship between them is called the Quality Model [15].

Many quality models have been proposed to allow software quality evaluation. ISO has recently developed a new more comprehensive definition of quality in use, which has usability, flexibility and safety as subcharacteristics that can be quantified from the perspectives of different stakeholders, including users, managers and maintainers. It describes a practical method for identifying contextual aspects of usability in software systems, and for helping ensure that usability evaluations reflect the context of use and give data with acceptable validity. In fact, each author can propose his own quality model to cover all important issues and to take aim of an evaluation into account [16].

<sup>1</sup>Nebojsa D. Djordjevic is with the Faculty of Electronic Engineering, Aleksandra Medvedeva 14, 18000 Nis, Serbia, E-mail: djnebojsa@open.telekom.rs.

<sup>2</sup>Dejan D. Ranic is with the Faculty of Electronic Engineering, Aleksandra Medvedeva 14, 18000 Nis, Serbia, E-mail: dejan.ranic@elfak.ni.ac.rs.

In this work, ISO/IEC 25010 [13] quality model was selected to identify relevant quality characteristics. Since all of these characteristics affect the use of WebGIS applications by final users, they were adapted to the WebGIS application context.

ISO/IEC 25010 is the new standard of software product quality that is awaiting publication, and is a part of the new series of SQuaRE (Software product Quality Requirements and Evaluation) standards [13]. ISO/IEC 25010 is an evolution of the ISO/IEC 9126 [15] and defines a more complete and detailed quality in use model. According to both standards, the quality of a system can be assessed as the extent to which the system satisfies the stated and implied needs of its various stakeholders.

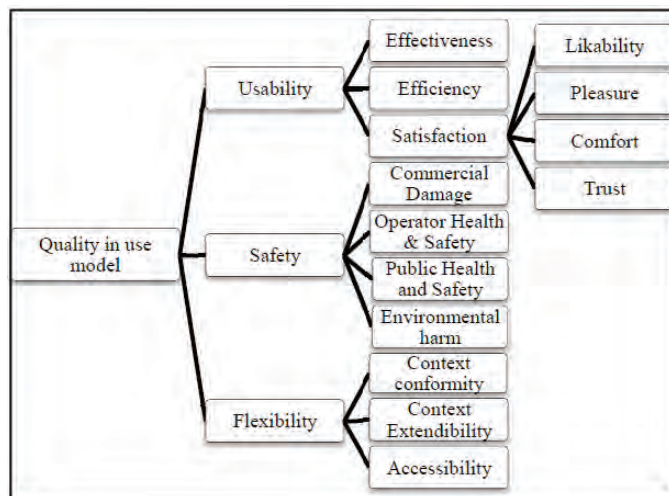


Fig. 1. Model for quality in use in ISO/IEC 25010

The quality in use model defined by ISO/IEC 25010 is shown in Fig. 1, and a complete definition of the quality characteristics and sub-characteristics can be found in [13].

Quality in use is the degree to which a product or system can be used by specific users to meet their needs to achieve specific goals in specific contexts of use. The quality in use of a system characterizes the impact that the product (system or software product) has on stakeholders. It is determined by the quality of the software, hardware and operating environment, and the characteristics of the users, tasks and social environment. All these factors contribute to the quality in use of the system. A quality in use model composed of five characteristics (effectiveness, efficiency, satisfaction, freedom from risk, and context coverage) that relate to the outcome of interaction when a software product is used in a particular context of use. Some of characteristics are further subdivided into sub-characteristics. Each characteristic can be assigned to different activities of stakeholders, for example, the interaction of an operator or the maintenance of a developer.

After extensive research that we conducted to analyze and compare different software quality models, the ISO/IEC 25010 quality model has been adopted as a basis to focus on usability characteristics of WebGIS applications. For customizing these characteristics especially for web applications, a wide range of usability guidelines and

checklists were studied. It is important to emphasize the fact that the analyzed quality characteristics are those concerning the quality in use and those that are of interest to the end users of WebGIS applications.

In order to define a quality in use model for WebGIS applications, ISO/IEC 25010 quality in use model was adapted.

Since all of these characteristics affect the use of WebGIS applications by final users, they were adapted to the WebGIS application context. Some sub-characteristics defined in the standard, were adapted to the contexts of WebGIS applications. However, other sub-characteristics were not included because they could be considered as not being sufficiently relevant for WebGIS application usage.

### III. THE RELATIVE IMPORTANCE OF THE USABILITY ATTRIBUTES

Although the scope of the product quality model is intended to be software and computer systems, many of the characteristics are also relevant to wider systems and services. These models provide a set of quality characteristics relevant to a wide range of stakeholders, such as: software developers, system integrators, acquirers, owners, maintainers, contractors, quality assurance and control professionals, and users.

The full set of quality characteristics across these models might not be relevant to all types of user. Therefore, for each type of user should be considered the relevance of the quality characteristics in each model before finalizing the set of quality characteristics that will be used. The relative importance of quality characteristics will depend on the high-level goals and objectives for the project. Therefore the model should be tailored before use as part of the decomposition of requirements to identify those characteristics and sub-characteristics that are most important, and resources allocated between the different types of measure depending on the stakeholder goals and objectives for the product.

The quality models provide a framework for collecting stakeholder needs [13]. Stakeholders include: **Primary user** (person who interacts with the system to achieve the primary goals), **Secondary user** (person who provide support, e.g. content provider, system manager/administrator, security manager; maintainer, analyzer, porter, and installer), and **Indirect user** (person who receives output, but does not interact with the system). Each of these types of user has needs for quality in use in particular contexts of use [13]. However, before any usability evaluation can begin, it is necessary to understand the Context of use for the product, i.e. the goals of the user community, and the main user, task and environmental characteristics of the situation in which it will be operated.

Attempts to objectively evaluate quality of information systems are old. Many various methods of usability evaluation have been developed. These methods belong to classical experimental methods; there are qualitative and quantitative methods available. A suitable method must be selected for each evaluation.

User characteristics are also important determinants of usability. The term 'context' includes the characteristics of the users and the work goals they are seeking to achieve, as well as the technical, physical and organizational environments in which they work.

In practice, key issues to be decided are the choice of the evaluation tasks, and identifying the profiles of users for the evaluation, taking into account the availability of suitable users within the resources and timescale of the evaluation.

#### IV. ANP

Since all of the usability factors do not have the same significance in the overall usability assessment of the WebGIS applications, the proposed factors have been weighted by adopting ANP (Analytic Network Process) approach [18].

Literature review was performed to determine the usability factors that are important for the software we analyzed. ANP is applicable when it is difficult to formulate criteria evaluations and it allows quantitative evaluation [17]. As seen above, usability of a system, but also some of their other factors are related to each other. Hence, these interactions go to create a complex model composed of dependence and feedback among the factors. In evaluating software, such a model can be treated with the ANP proposed by [17], [18] in order to determine the relative importance of the usability factors.

ANP has three stages: structuring (design), assessment (comparison), and synthesis (computation).

At the structuring stage, pertinent factors and alternatives, if necessary, are determined. Next, associations between pairs of factors are identified by experts. As a result, a network model, which consists of factors and relations among them, is constructed.

At the assessment stage, a nine-point scale suggested by [17] is used by the decision makers to make pairwise comparisons of the factors in the network. Pair-wise comparisons are made by identifying the less dominant of two elements and using it as the unit of measurement. Users can input their preferences regarding the relative importance of each criterion using a set of linguistic terms.

According to this scale, a value of 1 shows that both factors compared have equal influence levels on the affected factor, while a value of 9 shows that one factor has extremely more influence than the other on the affected factor [19].

Then we construct the matrix of pair-wise comparisons where the reciprocal value of the judgment is automatically used for the comparison of the less dominant element with the more dominant one. After we determined the priority weights for each participant, we aggregate the individual judgments using the geometric mean value method. Using these aggregated group judgments, pairwise-comparison matrices are generated.

At the synthesis stage the relative importance of the factors is computed. Importance is viewed as the influence of the factors on a common goal. To synthesize aggregated judgments to compute the relative importance of the factors, the computation of the eigenvector for each pairwise comparison matrix, the generation of a super-matrix and a

weighted super-matrix, and the computation of the convergence of the super-matrix (limit matrix) are required. The relative weights (desired priorities) of the factors in the decision network are the values of the limit matrix.

#### V. EVALUATION OF WEBGIS APPLICATION

Making the right decision has always been a complex task; therefore we used ANP methodology in our questionnaire to help the respondents to find one that best suits their goal and their understanding of the problem.

Based on the above discussion, this study uses ANP approach in order to identify the most important factors influencing the adoption of WebGIS applications based on consumers' preferences as the research objective.

After the determination of usability factors, the group of experts whose working areas are usability engineering filled in a pairwise relationship matrix separately. Once the hierarchy was established, pairwise comparisons were performed by the participants to assign priorities to each node in each level of the hierarchy. For the higher levels (Fig. 3.), they performed pairwise comparisons among the combinations of usability, flexibility and safety (Level 2) on overall quality in use of WebGIS applications (Level 1).

Of the factors given below which one influences "quality of use" more and how much more?

1=Equally 3=Moderately more 5=Strongly more 7=Very strongly more 9=Extremely more

Factors Influencing the Adoption of Web Portals								
Usability	9	8	7	6	5	4	3	2
Usability	9	8	7	6	5	4	3	2
Flexibility	9	8	7	6	5	4	3	2
Flexibility	9	8	7	6	5	4	3	2
Flexibility	9	8	7	6	5	4	3	2
Flexibility	9	8	7	6	5	4	3	2
Flexibility	9	8	7	6	5	4	3	2
Flexibility	9	8	7	6	5	4	3	2

Fig. 2. The relative importance of the quality of use factors for WebGIS applications

For the lower levels, they performed pairwise comparisons among the combinations of effectiveness, efficiency, and satisfaction (Level 3) on usability (Level 2).

In the judgment assessment stage, 30 potential users (22 primary users, 3 person who provide support and 5 indirect users who receives output) filled a pairwise comparison questionnaire. We used paper-and-pencil questionnaire, consisted of series of questions. An example question from the questionnaire can be seen in Fig. 2. The questionnaire was designed through informal interviews with experts on ANP. Then, using the 1-9 scale, the respondent determines how many times more important the dominant member of the pair is. The respondents express their opinion on a numerical scale, where each number can be associated with the importance level of one factor over the other. The data collected from respondents is a list of pair-wise comparisons concerning the relative importance of each criterion. The respondents judged the relative importance of the affecting factors on the affected factor for all possible pairs. Then, the geometric means of all paired comparison judgments for each question were computed for each group (primary users, secondary users and indirect users) in order to arrive at the aggregated group judgments. By using the ANP methodology, we are able to

find the degree of preference of one factor to another with respect to each criterion.

Those respondents who completed the questionnaire were asked for some demographical information for the user statistics. Table II presents a summary of the demographic profiles of the respondents.

TABLE II  
DEMOGRAPHIC PROFILES OF POTENTIAL USERS

Gender (*)	Female: 4 Male: 26
Age	Min: 22 Max: 52 Average: 34
Education level (*)	High school: 20 Undergraduate: 4 MSc: 6
Work experience in full time position (*)	1-2 years: 2 2-5 years: 9 / >5 years: 19
Computer use (year)	Min: 1 Max: 8 Average: 4
Computer use in a week (h)	Min: 12 Max: 60 Average: 45

\* # of respondents

Table III presents a summary of the relative importance of the factor items of the respondents.

The result of the questionnaire interestingly reveals that Usability had the highest weight (0.5166) among the other criteria.

With respect to Usability, Satisfaction is the most popular choice followed by Effectiveness and Efficiency which are less important ones. With respect to Usability, Satisfaction is the most popular choice followed by Effectiveness and Efficiency which are less important ones.

TABLE III  
THE IMPORTANCE OF THE QUALITY IN USE FACTORS FOR WEBGIS APPLICATION

Factor	Weight	Factor Items	Weight	Factor Items	Weight
Usability	0.66	Effectiveness	0.35		
		Efficiency	0.28		
		Satisfaction	0.37	Likability	0.27
				Pleasure	0.34
				Comfort	0.22
				Trust	0.07
Safety	0.18	Commercial damage	0.24		
		Operator Health & Safety	0.26		
		Public Health & Safety	0.22		
		Environmental harm	0.18		
Flexibility	0.16	Context conformity	0.43		
		Context Extendibility	0.23		
		Accessibility	0.34		

## VI. CONCLUSION

Till now WebGIS quality attribute weighting is considered as a completely subjective task in quantitative WebGIS quality evaluation. This is mostly be done by experts with experiences. Usability, Safety and Flexibility were defined as the main factors in our ANP model. We have proposed an Analytical Network Process (ANP) approach for weighting

WebGIS quality attributes in quantitative WebGIS quality evaluation. The present study confirms that an Analytical Network Process (ANP) approach in WebGIS domain can be used to substitute the experts' weights (weights by direct weighting method without prior ranked attributes).

## REFERENCES

- [1] P. A. Burrough, "Principles of Geographical Information Systems for Land Resources Assessment", ISBN-10: 0198545924, Oxford University Press, New York, USA, 1986.
- [2] P. A. Burrough, and R. A. McDonnell, "Principles of Geographical Information Systems", 1998.
- [3] GIS Cloud. (2010, December, 21). [Online] available: <http://www.giscloud.com/>
- [4] G. Luciano, and V. Elisabetta, "Web Usability Today: Theories, Approach and methods", Towards Cyber Psychology: Mind, Cognitions and Society in the Internet Age, Amsterdam, IOS Press, 2003.
- [5] M. Man, and et al, "An architecture for Web-based GIS System for Artified Reefs", Universiti Malaya 50603 Kuala Lumpur, 2009.
- [6] H. Lan, and C.D. Martin, "A Web-based GIS Tool for Managing Urban Geological Hazard Data", Canada, 2009.
- [7] H. Lan, and et al, "A Web-based GIS for managing and assessing landslide of Likert scale and visual analog scale as response options in children questionnaires", Copernicus Publications on behalf of the European Geosciences Union, 2009.
- [8] R. J. Hinrichs, "Intranets: What's The Bottom Line? Mountain View, " Calif., USA: Sun Microsystems Press, 1997.
- [9] T. L. Saaty, "The analytic hierarchy process: planning, priority setting, resource allocation", McGraw-Hill International Book Co., 1980.
- [10] A. Abran, A. Khelifi, W. Suryn, and A. Seffah, "Usability Meanings and Interpretations in ISO Standards," Software Quality Journal, vol. 11, November 2003, pp. 325-338.
- [11] J. Nielsen, R. L. Mack, Usability Inspection Methods. New York: John Wiley & Sons, 1994.
- [12] J. Rubin, and D. Chisnell, Handbook of Usability Testing: How to Plan, Design, and Conduct Effective Tests. 2nd edition. Indiana: Wiley Publishing, Inc., 2008, chap. 1 and 2.
- [13] ISO/IEC CD 25010.3, "Systems and software engineering – Software product Quality Requirements and Evaluation (SQuaRE) – Software product quality and system quality in use models", ISO (2010).
- [14] ISO 9241-11, "International Standard, ISO 9241-11", Ergonomic requirements for office work with visual display terminals (VDTs): Guidance on usability, 1998.
- [15] ISO/IEC 9126-1, "Software engineering – Product quality - Part 1: Quality model", ISO, 2001.
- [16] N. E. Fenton, and S. L. Pfleeger, *Software metrics: A Rigorous and Practical Approach*. 2nd ed. Boston: PWS Publishing Company, 1997, chap. 9.
- [17] T. L. Saaty, "Decision-making with dependence and feedback: The Analytic Network Process", Pittsburg, NJ: RWS Publishing, 1996.
- [18] R. Haas and O. Meixner, "An Illustrated Guide to the Analytic Hierarchy Process", Institute of Marketing and Innovation, University of Natural Resources and Applied Life Sciences. Vienna, Austria, 2009.
- [19] S. Boroushaki and J. Malczewski, , "ParcipatoryGIS.com: A WebGIS-based Collaborative Multicriteria Decision Analysis", Submitted to *URISA Journal*, 2009.

# Implementation of LMS in the Education in the Field of Programming

Niko Naka<sup>1</sup>, Snezana Savoska<sup>2</sup> and Josif Petrovski<sup>3</sup>

**Abstract –** LMS (learning management system) represents a software application for administration, documentation, monitoring, informing and delivery of educational courses or training programs. The implementation of such systems in teaching and in the educational process has many advantages as online courses, accessing materials from any place, interactive teaching, opportunity for testing with these learning systems, higher concentration during the lectures. This whole article is devoted to the needs of the use of these learning systems, our benefits, as well as its use within the educational process, particularly at the faculty of Management and Information Systems.

**Keywords –** LMS, web-based application, courses, education.

## I. INTRODUCTION

LMS is a software application for administration, documentation, monitoring, informing and delivery of educational courses or training programs. The LMS spectrum of systems for managing training and education registers software for distribution of Internet or mixed/hybrid courses on the Internet, with functions for online cooperation. Colleges and universities use LMS to provide online courses. Corporate training departments use LMS to offer online training, as well as to automate the records and staff subscription. Most LMS are web-based in order to make the access to the learning content and the administration easier. LMS is used by the regulated activities to comply the training. They are also used by the educational institutions to improve and support the teaching and to offer courses for wider population of students from all over the world. This software application or web-based technology which is used for planning, implementation and evaluation of specific learning processes, provides instructions in order to create and provide content, to observe the student's participation and to assess the students' performance.

LMS should be able to do the following:

- to centralize and to automate the administration
- to use self-service and self-managing
- quickly gather and deliver learning contents
- consolidate training initiatives on a scalable web-based platforms

<sup>1</sup>Niko Naka – Master student - Faculty of administration and information system management, Bitola 7000, R.of Macedonia, E-mail: naka\_niko@yahoo.com.

<sup>2</sup>Snezana Savoska, Faculty of administration and information system management, University St.Kliment Ohridski, Bitola 7000, R.od Macedonia, E-mail: snezana.savoska@uklo.edu.mk

<sup>3</sup>Petrovski Josif – PhD student - Faculty of administration and information system management, Bitola 7000, R.of Macedonia, E-mail: thejosif@yahoo.com.

- personalization of the content and an opportunity to re-use the knowledge

This powerful software for managing complex databases performs a combination of digital management within the program, training materials and evaluation. Some LMS services include "performance management systems", which include staff views, competency for managing, analysis of the skills, succession planning and assessment. The contemporary techniques now include competency based learning, in order to discover gaps in the educational process and the choice of materials.

## II. LMS AS A FACTOR FOR SUCCESS

If a faculty wants to succeed and to fit in today's rapidly changing and competitive market, it must increase the labor productivity and to optimize the level of organizational talent. With the rapidly changing set of skills and job requirements, this becomes even more difficult challenge for the faculties.

"The best in their class" Learning Management System (LMS) allow universities and the organizations of human resources to create, deliver, assess and evaluate the corporative learning programs to create high-performing labor. It enables:

- Change of the employees efficiency on new levels - it effects dramatically the bottom line of the business
- Linking the learning with various human activities: Engaging the employees with opportunities of development, such as monitoring the performances, career developments and continuous planning.
- Strongly related learning initiatives with key business operations: increase of the incomes, clients satisfaction and overall results.

### Benefits

- Easy adaptation and re-use of materials over time
- Multiple choice for the curriculum creators, such as the delivery method, the material designs and the evaluation techniques
- Creating economies of scales that make it cheaper for organizations to develop and maintain content
- Improvements of professional development and evaluation, allowing companies to get more value from human resources, strengthening people with additional tools for self-improvement

### III. LMS DISTANCE LEARNING SYSTEMS

The distance learning system is becoming a greater need today. This learning system should contain an average computer, with an average Internet connection and above all a great willpower and self-discipline. By subscribing to a particular item it enters the virtual classroom, which is shared with colleagues who may be from another town or from any other country. The professor is available 24 hours. You have the time and place freedom to access the learning materials, but you also have the responsibility to send the professor electronically the tasks that you should do. The technology plays a key role in enabling the functioning of the remote learning system, which is a generator of changes and obstacles in the adoption of this concept. Distance learning is defined as a formal type of education with institutionally oriented character in which, those who attend the course are organized in groups, while the telecommunication systems are used to establish connection between the students, the professors and the learning content.

- Online learning provides immediate information, and allows faster realization of the efficiency and the competence. By online learning you can repeat the learning process as many times as you want.
- It adapts to long-distance and flexible learning
- The online learning is a mechanism for realization of knowledge and solutions that are focused on the student – if required they deliver short control segments, consistent and relevant for the organizational management of knowledge.
- It reduces the costs of the students training, such as travel, accommodation and childcare

The distance LMS crosses all barriers such as geographical barrier, isolation in some mountain areas and unites the students from all over the world in one common group where they use audio and video contacts, they learn and collaborate. There are numerous examples that prove the functionality of the LMS systems.

### VI. LMS TOOLS

It is a system that can make the creation and distribution of a graphic display for managing reports[4]. It can also achieve other benefits:

- Managing, schedule and cost of a school - based training
- Facilitating online booking
- Assigns an industry standard for e-learning including all SCORM 1.2, 2004 and AICC objects
- Submit and share learning content including documents, video and audio
- Getting Accreditation, Certification and Compliance
- Creating job profiles, appointment of plans and objectives of learning
- Managing the Extended Enterprise Ecommerce, Finance and Marketing

- Customization of the interface with branding and language support

### VII. LMS Implementation for the Subjects in the Field of Programming

For the needs of the Faculty of Administration and Management of Information Systems, for the needs of the subject web programming and applications, it is installed Front LMS through which we planned to cover the classes for exercises and to allow the use of the system as a knowledge base [2]. It was found that there is a need for such a system for greater precision when explaining the parts of the code. This system contains a MySQL database which included lectures from each lesson, especially in the form of a power point presentation, where there are examples of exercises with pictures and instructions on how to perform the exercises, and what you will get after the execution of PHP code and steps until it gets to the performance of that code. As a result of the internal instruction, it is set an intranet environment that gives students the opportunity to complete the exercises at a certain period of time to see and download the lectures and to use additional literature in the type of books or pdf formats (Fig. 2). Also, there is a possibility to organize online examination for the course, because the test questions are included and there is an opportunity to define the time frame for each test. The test generates random and is assigned to the user who calls, and the results are recorded in Negoita result – the time passed, the number of points scored.

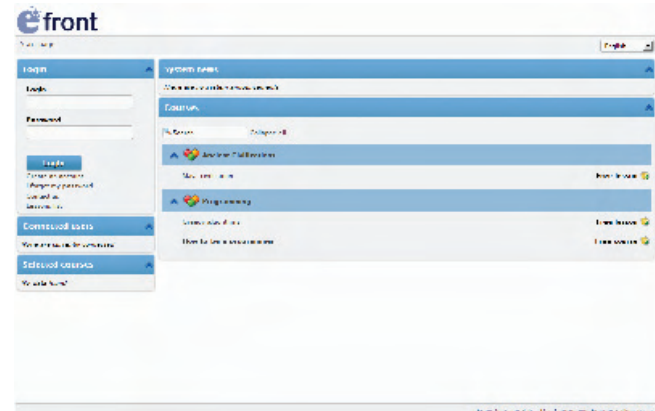


Fig. 1. Screen of the eFront login user

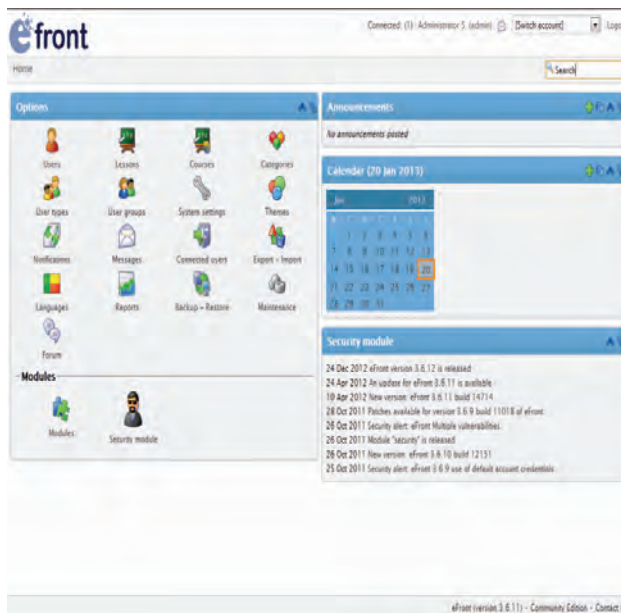


Fig. 2. Screen of the practical implementation of eFront

On the left side is the entry box, shown in Fig. 1, through which the professors can log and post some new classes, and students can log in. It is possible to publish current users, and the most important thing that you can notice immediately, are the courses that are loaded (uploaded) by teachers, which can be attended by students. Another screenshots are shown on the Fig. 2 and 3.

Experience in working with the system showed that students can learn the lessons much easier, use the codes and instructions for programming and efficiently to complete the exercises provided in class. The interest in the subject has increased and with the possibility of using manuals made for this purpose and the students' opportunity to try to fit some of the codes in any of the previously created applications. After that, they can run and see the concrete effects, to find errors in the code and remove them by using the base for most common errors occurring. All this increases the engagement of students in class and their commitment to complete the provided and other exercises.

### VIII. FINAL CONCLUSIONS

LMS system that is used for enrichment of the teaching subjects in the field of programming can promote the learning of the subjects because of the possibility of students to focus on solving the issues and get help from the system and from the professor.



Fig. 3. Screen of the professor dashboard

The system allows the use of a base of knowledge, tutorials and opportunities to help the students on the lessons for exercises as well as the cooperation between students during classes. With this is achieved active participation of students in class, evaluation of the work done by the subject teacher and detecting program errors, which allows students to learn thematic content easier and faster.

As future recommendations on the use of the system that we think are interesting for assessment through the LMS system, creating a database of frequently asked questions from students and learning system, with which can be carried out and evaluation of the hours that each student spend in the system, the tasks they did and can evaluate the level of knowledge of the student.

### REFERENCES

- [1] Kim, S. W., & Lee, M. G. (2008). Validation of an evaluation model for learning management systems. *Journal of Computer Assisted Learning*, 24(4), 284-294. doi:10.1111/j.1365-2729.2007.00260.x
- [2] White, Brandon, and Johann Ari Larusson. "Strategic Directives for LMS Planning" (Research Bulletin 19, 2010). Boulder, CO: EDUCAUSE Center for Applied Research, 2010,
- [3] <http://lms.au.edu/>
- [4] <http://www.efrontlearning.net/>
- [5] [http://en.wikipedia.org/wiki/Learning\\_management\\_system](http://en.wikipedia.org/wiki/Learning_management_system)

**This Page Intentionally Left Blank**

# Adaptive vs. Non-adaptive e-Learning Systems – a Petri Net-based Evaluation Approach

Emilija Spasova Kamceva<sup>1</sup> and Pece Mitrevski<sup>2</sup>

**Abstract** – This paper deals with the principles of specification, modeling and implementation of an educational information system. The behavior in a sample e-learning application is described using a formal model, based on Petri Nets. An adaptive model of student's transitions during the course of an e-learning cycle is proposed and a comparison with non-adaptive systems is made. Depending on the type of student, learning style, level of knowledge and dynamic behavior, a general conclusion is drawn that the students spend more time in non-adaptive vs. adaptive e-learning systems.

**Keywords** – Adaptive E-learning system, Petri Nets, modeling, simulation.

## I. INTRODUCTION

Education theories argue that different students use different strategies in the learning flow and demonstrate different adjustments when using the learning materials. Similarly, results indicate that learning styles can be identified on an individual basis, and the adaptation to build a personal style increases the efficiency of learning in some students [1].

Very often, web based e-learning systems manifest some technical problems, e.g. in case if the corpus of learning materials is too burdened, or some content data are lost, etc. Adaptive e-learning has the purpose to solve the problems of understanding the learning content and disorientation of the students, i.e. to change with some user adaptive methods, which optimize the learning material and decrease the time spent for the learning process [2]. These systems generate intern representation for every student. For example, personal characteristics, purposes and knowledge are taken into account. In the past, with decades, different strategies of how students can adjust to learning were developed, like learning materials modification, adaptation of the learning content, etc.

Chapter 2 introduces math formulas which help to determine the efficient learning time which the students spend in a course, the time passed in a given state, the time that a student spends while searching in some unit, and the time when the student is in answering or testing phase. Later on, in Chapter 3, a Petri Net model of a sample course is presented, which provides a student to decide the style of learning of the course and, based on his/her previous knowledge, to decrease/increase the required time to pass the course.

<sup>1</sup>Emilija Spasova Kamceva is with the Faculty of Informatics, FON University, Bul. Vojvodina bb, 1000 Skopje, Republic of Macedonia, E-mail: emilija.kamceva@fon.edu.mk

<sup>2</sup>Pece Mitrevski is with the Department of Computer Science and Engineering, Faculty of Technical Sciences, St. Clement Ohridski University, Ivo Lola Ribar bb, 7000 Bitola, Republic of Macedonia, E-mail: pece.mitrevski@uklo.edu.mk

## II. THE FOUNDATIONS OF AN ADAPTIVE METHOD

One of the aims of this paper is to identify the states in which an e-student can be found and to estimate the average time that a student spends in a particular state. Initially, we use graph representation to describe the method, following by a Colored Petri Net-based model. The places in the Petri Net are titles, subtitles, exams and examples, while the colored tokens represent students.

In an adaptive method, learning style is checked in every node, and the path is built for each student. The next node is chosen according to the previous level of knowledge and the points obtained (scores). For example, in the Petri Net, tokens with time stamp which is equal to time of response are used. It is necessary to calculate the time of searching which student spends in a unit, the time needed the student to make estimation and the time of remaining in the queue.

The time LT is the time of arrival of the next student and it is calculated by Poisson distribution (Eq. 1):

$$LT = \frac{e^{\lambda t} (\lambda t)^n}{n!} \quad (1)$$

where  $t$  is time of waiting of the student in the queue before the start to use the system,  $\lambda$  is number of arrivals and LT is used to calculate the time when the student will arrive, when  $n=1$ .

The time of searching through a given learning unit is calculated by Normal distribution (Eq. 2):

$$BT = \frac{\frac{-1}{2} \left[ AVG_B - \alpha \right]^2}{e^{\frac{-1}{2} \left[ AVG_B - \alpha \right]^2 / \delta^2}} \quad (2)$$

where  $AVG_B$  refers to the average length of the time in which the student remains in the learning unit (lesson),  $\alpha$  is variation of the spent time among the students and  $\delta$  is the standard deviation of the spent time of learning among the students.

The time when the student is into a state of answering or testing is also calculated by Normal distribution (Eq. 3):

$$BT = \frac{\frac{-1}{2} \left[ AVG_A - \beta \right]^2}{e^{\frac{-1}{2} \left[ AVG_A - \beta \right]^2 / \rho^2}} \quad (3)$$

where  $AVG_A$  is the average time of testing,  $\beta$  is the variation of the spent time in the node of testing among the students,  $\rho$  is the standard deviation of the spent time in node of testing among the students.

The score which the student is obtaining is again calculated by Normal distribution (Eq. 4):

$$Score = \frac{e^{\frac{-1}{2} \left[ \frac{AVG_S - \mu}{\gamma} \right]^2}}{\sqrt{2\pi}\gamma} \quad (4)$$

where  $AVG_S$  is the average score,  $\gamma$  is the standard deviation,  $\mu$  is the variation of the score as a result of learning and testing among the students.

In terms of colors used for representing the user characteristics, we need some additional colors for calculating the time of response [3]. These colors are the following: the time of arrival of the student, the total sojourn time of the student into the system (initialized to zero at the start), the path of the student, and the time which elapses on every unit by the student.

### III. A SAMPLE COURSE AND THE PROPOSED MODEL

The sample course of the subject Calculus 1 will be displayed as a whole (Fig. 1). In this particular course, there are two chapters (content 1, content 2), two sub-contents (content 1.1 and content 1.2), seven examples, introduction and conclusion. The graph of the course of the subject Calculus 1 is represented on Fig. 2.

This graph also can be represented using a Petri Net (Fig. 3). It is necessary to declare three base colors for the CPN tool: 1) for the style of learning, 2) for the level of learning, 3) for the score. Additionally, we need four new colors: 1) for LT – the time of arrival, 2) for the path of traversing of the students, 3) the time of learning of a single unit, 4) the time of the learning process which represents the total time of learning that the student spends in the system. Once we have defined all the characteristics of the student (i.e. “the colors”), we define a student as a mix of colors from all the abovementioned characteristics [4,5]. Also, we are going to define the set of colors called “students” which we will use for managing the FIFO queue when they arrive in the system.

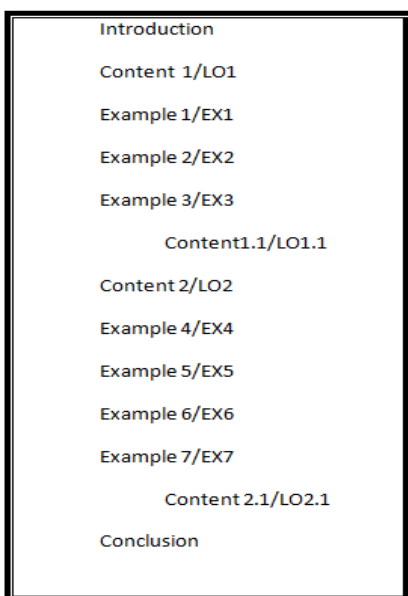


Fig. 1 The structure of a sample course (Calculus 1)

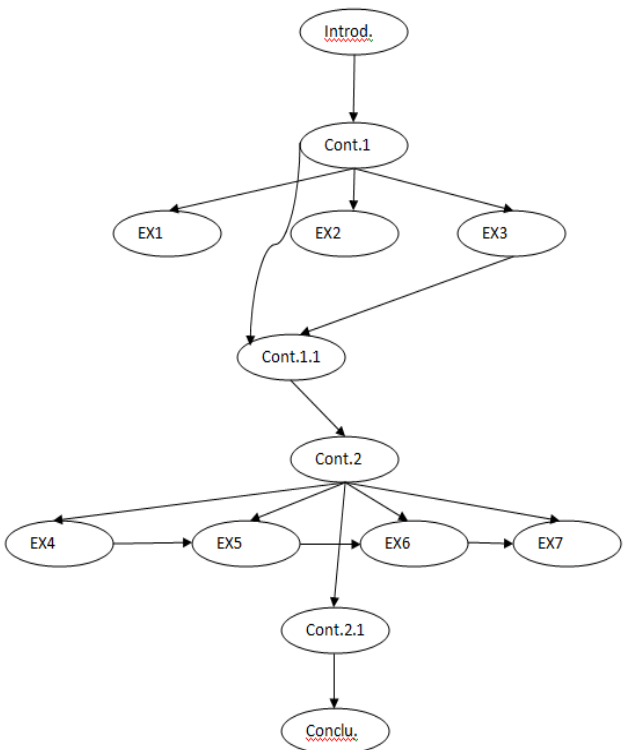


Fig. 2 Graph of the sample course structure (Calculus 1)

As the new students arrive, the *newLearner()* function is used for creating a token representing the new student. When it is called, it returns the set of colors *STUDENT* (Fig. 4). The first component represents the type of the learning style and uses the *Learning\_Style.ran()* function, which is randomly generated. The second component is the level of knowledge and it uses the function *Knowledge\_Level.ran()*. The third and the fourth component are the scores from *content 1* and *content 2* of the book. The fifth component is the time of arrival and the sixth component is the sum of the total time which the student spends in the system. The seventh component is the path of the student, while the eighth component is the time which the student passes in each learning unit (Fig. 5).

All the students should pass the introduction and *content 1*, as a suggestion of the course teacher. Because *content 1* is a chapter with a test, according to the score and the level of knowledge the student can decide from 4 different paths to continue with learning (because in the first process the decision is based solely by the style of learning, now we have two factors which impact the decision, so we have  $2^2$  number of paths). After that, the student is returned to the page with *RWStyle*. In this part (Fig. 6), if the level of knowledge is low and the score is less than 10, the student should pass through *example 1*, *example 2*, *content 1.1 (LO1\_1)*, respectively. As soon as they pass *LO1\_1*, all the students (four in total) should pass through *content 2*. For that purpose, the students go on the next chapter *LO2*. In the subpart of *LO2*, firstly the decision for the next path is made based on the level of knowledge and the score from *LO1* [6].

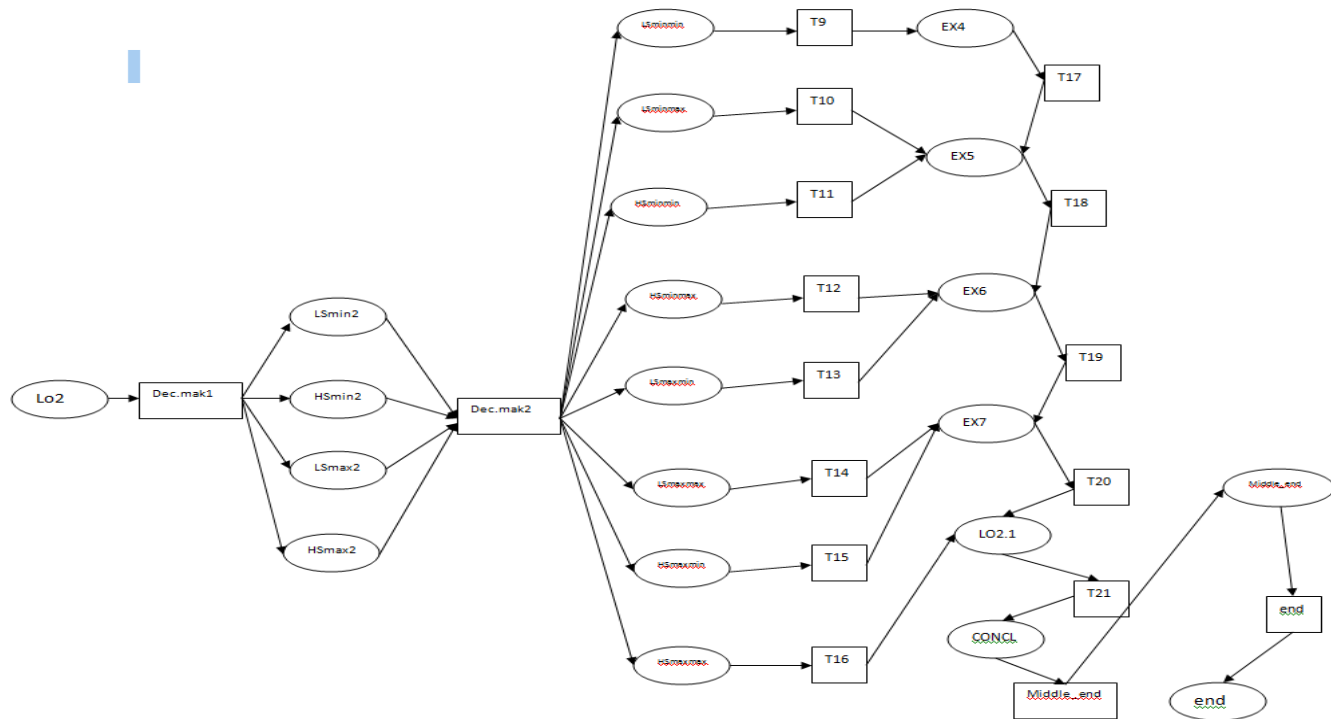


Fig. 3. Petri Net presentation of the sample course structure (Calculus 1)

```

▼ Declarations
▶ Standard priorities
▶ Standard declarations
▶ colsets
▼ colset Score=int with 0..20;
▼ colset Knowledge_Level=with L|H;
▼ colset Learning_Style=with V|RW ;
▼ colset ProcessTime=INT;
▼ colset LT=INT;
▼ colset PATH=string;
▼ colset DetailTime=string;
▼ colset LEARNER=product
  Learning_Style*
  Knowledge_Level*
Score*
Score*
LT*
ProcessTime*
PATH*
DetailTime timed;
▼ colset Learners=list LEARNER;
    
```

Fig. 4. Declaration of the set of colors

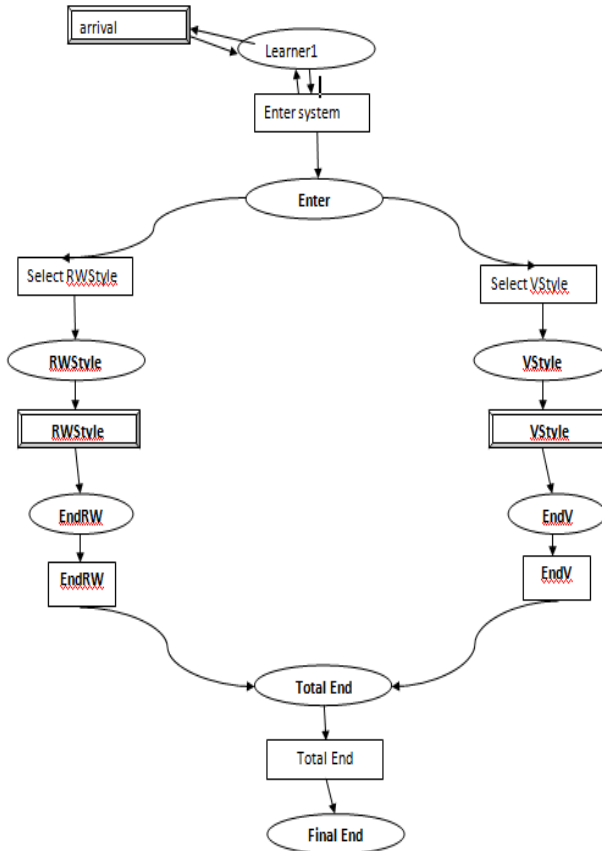


Fig. 5. The graph of the main page of the sample course

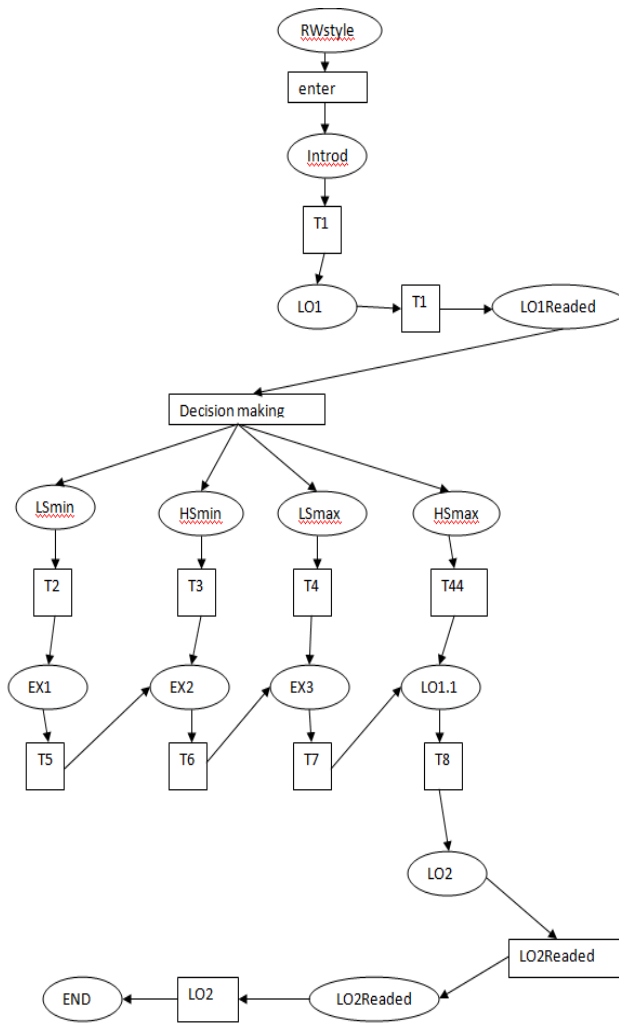


Fig. 6. RWstyle subpages

For the evaluation of the efficiency of the proposed model, we should calculate the time of response for the two types of users and to compare it with the time of response of the students which do not use an adaptive system. We should underline that, in the adaptive system, the students choose the learning units, which is not the case in a non-adaptive system.

We want to illustrate that if the user has a higher level of knowledge, he/she does not need to pass some of the units of the course, and will arrive at the end in shorter time. Otherwise, the user should pass through additional contents, which directly translates in longer sojourn time.

If the user has lower level of knowledge and did not pass the test successfully, then he should pass the course for shorter time, but he/she can also skip some units. For calculating the time of response, the conditions for intercrossing are removed and they allow the student to choose arbitrary paths without restrictions.

If we summarize the results of the two types and the time of the response of both the adaptive and non-adaptive systems, a conclusion could be drawn that the time of response of adaptive systems is shorter than the time of response of non-adaptive systems.

#### IV. CONCLUSION

Nowadays, with the fast development of the technology and the Internet, the traditional way of education is more or less abandoned, giving its way to the e-learning paradigm. An e-learning system is a web based environment where all the individuals have the access, willing to learn and expand their knowledge. In an e-learning system, all the coursework can be accessed in some of the available formats: text, audio, video, photography, presentations, tests, etc. A plenty of e-learning systems exist, based on different technologies, and they use different algorithms for evaluating the efficiency of the system. Among all of them, adaptive and dynamic systems appear to be the best choice. In our current research efforts, we tried to investigate and prove that these systems exhibit the best time of response.

The main characteristics, which were included in the research, are: the learning style, the level of knowledge and the score. These are the main characteristics, based on which the efficiency of a given system is evaluated. As a next research step, we will focus on calculating the transition probabilities, in order to compare the theoretically obtained results and the simulation results obtained by employing the class of Deterministic and Stochastic Petri nets (DSPNs) [7].

#### REFERENCES

- [1] K.L. Rasmussen and G.V. Davidson-Shivers, Hypermedia and learning styles: can performance be influenced?, *Journal of Educational Multimedia and Hypermedia* 7 (4), pp. 291-308, 1998.
- [2] Kamceva, E., Mitrevski, P., "On the General Paradigms for Implementing Adaptive e-Learning Systems", *ICT Innovations 2012*, Web Proceedings, pp. 281-289, Ohrid, Macedonia, 2012.
- [3] Y. C. Chang, Y. C. Huang and C. P. Chu, "B2 Model: A Browsing Behavior Model Based on High-Level Petri Nets to Generate Behavioral Patterns for E-Learning", *Expert Systems with Applications*, Vol. 36, No. 10, pp. 12423-12440, doi:10.1016/j.eswa.2009.04.044, 2009.
- [4] K. Jensen, L. M. Kristensen and L. Wells, "Coloured Petri Nets and CPN Tools for Modelling and Validation of Concurrent Systems," *International Journal on Software Tools for Technology Transfer*, Vol. 9, No. 3-4, pp. 213-254, doi:10.1007/s10009-007-0038-x, 2007.
- [5] A. Ratzer, L. Wells, H. Lassen, M. Laursen, J. Qvortrup, M. Stissing, M. Westergaard, S. Christensen and K. Jensen, "CPN Tools for Editing, Simulating, and Analysing Coloured Petri Nets," *Proceedings of the 24th International Conference on Applications and Theory of Petri Nets*, Eindhoven, pp. 450-462, 2003.
- [6] F. Omrani, A. Harounabadi, V. Rafe, "An Adaptive Method Based on High-Level Petri Nets for E-Learning" –*Journal of Software Engineering and Application (JSEA)*, No. 4, pp. 559-570, 2011.
- [7] H. Choi, V. G. Kulkarni, K. S. Trivedi, "Transient analysis of deterministic and stochastic Petri nets", *Application and Theory of Petri Nets*, Lecture Notes in Computer Science 691, Springer, Berlin, pp. 166–185, 1993.

# Content Management Systems – Unleashed Possibilities

Jove Jankulovski<sup>1</sup>, Mimoza Anastoska-Jankulovska<sup>2</sup> and Pece Mitrevski<sup>3</sup>

**Abstract** – Digital products and services providers need to maintain their attractiveness among Internet users and online clients, end-users of web sites. Content management systems (CMSs) are one of the tools that can respond to these challenges. This paper introduces a new taxonomy of CMSs, based on their security, community platform, support, and feature sets, to assist organizations to identify CMS that will match the expectations and demand from clients and end-users of the organization products and services offered via the CMS.

**Keywords** – Content Management Systems, digital assets, taxonomy.

## I. INTRODUCTION

Rapid development of Internet technologies is providing users with infinite access to information, as well as, vast communication and networking opportunities. Currently, the amount of information that exists, and is increasingly created, is overwhelming. As a consequence, digital products and services providers need to maintain their attractiveness among Internet users and online clients, end-users of web sites. Content management systems (CMSs) are one of the tools that can respond to these challenges. Such a system organizes and provides access to all types of digital content (digital assets) – files containing images, graphics, animation, sound, video or text. It contains information about these files, and may also contain links to the files in order to allow them to be located or accessed individually. CMS can encompass an organization's entire content creation and organization system. At the same time it is a depot where information can be edited and uploaded, independently from the web design or web context.

There are no standards or features that are minimum or a must for CMSs to contain or functions to perform. The most common use of a CMS is to manage web content, starting from content creation / editing and content management, through publishing and concluding with presentation. Still, many of the CMSs have possibilities to provide document management, records management, and digital asset management in an integrated system. Furthermore, CMSs have the potential to dramatically simplify the maintenance of both websites and intranets.

An organization that intents to be present and appealing on Internet, with freshly updated content, close to its community

<sup>1</sup>Jove Jankulovski is with the Faculty of Technical Sciences, St. Kliment Ohridski University, Ivo Lola Ribar bb, 7000 Bitola, Republic of Macedonia, e-mail: jove.jankulovski@yahoo.com.

<sup>2</sup>Mimoza Anastoska-Jankulovska is with the Faculty of Technical Sciences, St. Kliment Ohridski University, Ivo Lola Ribar bb, 7000 Bitola, Republic of Macedonia, e-mail: jankmj2@yahoo.com.

<sup>3</sup>Pece Metrevski is with the Faculty of Technical Sciences, St. Kliment Ohridski University, Ivo Lola Ribar bb, 7000 Bitola, Republic of Macedonia, e-mail: pece.mitrevski@uklo.edu.mk.

of users / clients, and administer internally most probably will look for a CMS that is able to meet all of the above for a concrete constituents. In order to be able to identify the most suitable CMS for organization purposes, features of the CMS need to be examined, to be compared with the short and long term intentions of the organizations and adequate CMS identified. The paper intents to help organizations make the right decision when identifying CMS they will use. It elaborates some of the most relevant features of the CMSs and reasons why some of the CMSs are more suitable for a specific purpose.

## II. WHAT IS A CONTENT MANAGEMENT SYSTEM?

Developments that occurred in recent decades dramatically changed the approach in the information provision. In the period through 1990 a book-centric publishing approach was used. Ever since Internet got operational, Standard Generalized Markup Language, SGML/HTML and XML publishing [3] was applied. Web 2.0 and social Web marked the beginning of the new century (2003+); were followed by XML multi publish format (2004+); from 2006 and on, information provision is specialized and content distribution is on-demand – by adapting publishing solutions for specific areas. For everybody present on-the-net, it was clear that responsiveness to users' demand for current information, technology and design is a must. The Web, that used to be characterized by a highly manual approach to maintenance, had to respond to new expectations / requirements: having regularly added fresh content and up-to-date information.

Therefore, the content management approach was developed as a mechanism to address the need of companies and organizations to maintain and update websites internally, rather than relying on the availability of specialized developers and programmers for routine or regular tasks. It is the strategy and technology of storing and indexing information from and about analogue or digital media. CMSs range from very basic databases, to sophisticated tailor-made applications that enable access to digital assets and to allow regular updating. In all cases, content is either created or acquired by users. It is then automatically converted into a master format (such as XML) and segmented into discrete chunks (content components). Components can be thought of as “containers” that make it easier to organize, store and retrieve content [1]. CMS contributes to the effective management of various kinds of content by combining rules, process and workflows. This way, centralized webmasters and decentralized web authors/editors can create, edit, manage and publish the content of a web page in accordance with a given framework or requirements (i.e. design, branding, media type, etc.) [1]. This allows users to take control of the specific content and contribute to development of a content management product offering target information to specific audiences.

### III. FUNCTIONS OF CONTENT MANAGEMENT SYSTEMS

#### A. Content Creation / Collection (Authoring)

Content can include any type or unit of digital information that is used to populate a web page or updating content. It can be text, images, graphics, video, sound, etc. – anything that could be published via the Internet [2]. On the user side, a CMS is an easy-to-use authoring environment, designed to provide a non-technical way of creating new pages or updating content, without having to know any HTML [2]. CMS provides efficiency and autonomy to website owners, who may want to make changes, add content and maintain websites from within an organization that may lack designers, programmers or technically trained staff. It might be used by staff digitizing images, authors and editors, or those responsible for the management of the content development process. Almost all CMSs now provide a web-based authoring environment, which further simplifies implementation, and allows content updating to be done remotely. The CMS also allows managing the structure of the site.

#### B. Content Management (Storage)

All the content of a CMS product, along with other supporting details is saved into a central repository in the CMS. It provides a range of useful features: keeping track of all the versions of a page, and who changed what and when; ensuring that each user can only change the section of the site they are responsible for; integration with existing information sources and IT systems [2]. The CMS provides a range of workflow capabilities, or categorized content to be handled by multiple people, while CMS is maintaining control over the quality, accuracy and consistency of the information. CMS can assign users permission to add, edit or publish content by site-specific criteria. For instance, after a page is created by an author, it can be sent to content manager for approval. A person dealing with legal issues in giving the final approval before a page is published to the site. At all of the stages of the workflow, CMS handles the status of the page, notifies the people involved, and where required, prompts jobs.

#### C. Publishing

After final version of the content is stored in the repository, it is published to either the website or intranet. CMSs automatically apply the appearance and page layout to a web site, or prompt the same content to be published to multiple sites. This CMS function allows the authors to concentrate on writing the content, and the appearance of the site entirely to the CMS, or designers and web developers.

#### D. Presentation

One of the strengths of the CMS is that it can offer features to enhance the quality and effectiveness of the site itself. For instance, building the site navigation; support multiple

browsers; or users with accessibility issues. The CMS can be used to make a site dynamic and interactive, thereby enhancing the site's impact [2].

### IV. SOME IMPORTANT FEATURES OF CONTENT MANAGEMENT SYSTEMS

#### A. Easy to Understand and Use

A CMS has to be easy on the eyes, meaning that it should have a user friendly GUI (Graphical User Interface); with not very complicated options, and to offer simplicity in its administration interface. Creating and managing content should be quicker, saving time, or increasing productivity. In principle, CMS is intended for end users who are not "technology-savvy". If CMS solution requires highly skillful IT user, than end users will unlikely be using such a CMS, which is diminishing the primary purpose of CMS – to empower users to do content authoring in the frame of CMS [6].

#### B. Content Administration

In principle, Web sites are developed after substantial planning, development, testing, and publishing. Yet, sometimes, there is a need for updating web site structure, text and images. If CMS was used for web site development it should offer simple figures like: adding a new page, or section; add an image or a link to a document; quickly find and quickly edit pages; paste text from Microsoft Word.

#### C. Site development

For building a relatively not so complicated site, without a lot of extra features, it is important to use a system that makes it easy to set up pages, and provides everything needed to allow non-technical staff members to do authoring. If the intention is to develop more complex web site, than time should be allocated to: understand the administration tools, develop custom graphic themes, master more advanced features and understand the tools available to build a navigation structure. Also, it is important to learn how easy it is to find out what is available: resources for help/assistance, add-on modules, support on the CMS web site.

#### D. Customization / Flexibility and Navigation

If CMS is having only fixed and not changeable design themes (templates), than there is a probability that web site will look like other web sites which might not be appealing to the users / clients. Therefore, it is better to look for CMS that allows customization of own design without major restrictions. A theme is a graphic design layer that controls graphic elements, font styles, navigation styles, and page layouts. "Themes" that can be easily installed can help in building a Web site quickly. Along with solid themes, systems that easily set up pages and a simple navigation scheme are important too. If there is a need site to include an events

calendar or list of news stories, it would be good such features to be included with the basic CMS. Otherwise, they will need to be installed separately which sometimes might not be easy. If navigation and theme setup in a particular CMS is complicated, or requires knowledge of HTML programming, it might be wise to install WYSIWYG (What-You-See-Is-What-You-Get) editor as an add-on module for personnel to edit text or images on the site.

#### E. Structural Flexibility

Systems that offer the ability to display some information, like news of some kind, or a description of an upcoming event, in different ways in various lists on the site are considered to have structural flexibility. For instance, the titles of next two upcoming events are shown on the homepage, and a full list with descriptions for the next two months is shown on the events page.

#### F. Extending Default CMS Configuration

If an organization wants to enhance its site's ability to provide site users with useful options for interfacing with the site, than extensibility of the default configuration with plugins/extensions/modules should be possible. In fact, the more plugins there are in the CMS, out-of-the-box, the better it is [4]. It might be that not all of them will be promptly needed, but most probably some of them will be needed on a later stage. Numerous organizations might want to integrate their CMS with other organizational systems, i.e. user databases, accounting systems, or broadcast email packages.

#### G. Interaction with constituents

Interaction with constituents is of paramount importance to organizations. CMS product that allows visitors to comment on site content; publish blogs; can subscribe to site content through RSS feeds; create their own profiles and link it to other people or groups; accept and post content, are very much welcome. Also, a good Spam filter is important too. So, such a CMS product takes users 'on-board' the system – active users and proud community members, and is assuring own further development and sustainability.

#### H. Roles and workflow

If a web site should have categorized content that is handled by multiple people, than adequate to use is a CMS that can assign users permission to add, edit or publish content by site-specific criteria. For example, a number of people can edit the pages in their own sections, but a central person must approve everything before it can be published. It also helpful to be able to: easily see what needs to be done by whom and when (get notifications from the system when something needs to be checked / reviewed); control who can view what on the site; go back to a previous version of a page; or create a to-do list.

#### I. Security

Security of the CMS content is another very important feature. CMS that has fewest identified and fastest resolved vulnerabilities would be the most adequate choice. Fixing vulnerabilities immediately is a must for a CMS that tends to offer reasonable security. Therefore, CMS that allows installation of specific plugins to protect the integrity of the content and editing of files/permissions to increase security levels should be an option.

#### J. Backup and Update

As all digital products / systems, CMS must be backed up regularly, just in case there is a need to go back to an older version. Another aspect is to look for CMS with an easy system update (address security issues and fix bugs). Systems that continue to support old versions of the system with security updates are welcome.

#### K. Speed

The faster pages load on the browser, and the faster site is connecting to a server, the better web site is. Simply, visitors do not want to spend their time on sites that are not alive and up-to-date. Therefore, CMSs that offer adding plugins and caching of objects is important for making good choice. Also, by choosing a good host the load time of the site will be decreased.

### V. A NEW TAXONOMY OF CONTENT MANAGEMENT SYSTEMS

Identifying CMS is not an easy thing to do since there are many CMS functionality aspects that need to be identified and determined well before actually purchasing proprietary CMS, or hosting / installing open source CMS.

In cases where investment of large amount on Web site design and implementation is possible, or substantial customization is anticipated, CMSs that provide compelling and useful feature sets can be the right choice [5]. Investing in CMS that could work well for some sophisticated needs only, unfortunately, can lead to a situation where, after a period of time, demand towards the CMS is exceeding the feature sets that the CMS can offer. If complex workflows are needed, or integration into standard business systems, systems that can provide complete solution to the specific and complex need are necessary. Sometime this can be too demanding towards some of the open source CMSs.

Some organizations prefer their Web sites to have tools to handle constituent and donor tracking, emailing and online payments. While many of the open source CMSs (e.g. WordPress, Joomla, Drupal, Plone) can provide options for these features, there are a number of other integrated platforms that might be compelling for such needs. CMS community and its strength is one of the important factors for choosing a particular CMS. WordPress has many blogging and comment features, but not robust support for more

advanced functionality in this area. Drupal was designed to be a community platform and offers profiles, blogs and comments out of the box, with enhancements available through add-on modules. Therefore, is one of the most preferred and logical solutions for such a target.

Security was, is and will be one of the most important categories according which any software, including CMSs is judged. Concretely speaking, some of the most common types of attacks on CMS products are: capturing sensitive data (usernames and password); inserting links (usually invisible) to Spam and/or pornographic sites; preventing visitors from viewing digital content; defacing of site content through various means by hackers. Plone is among the most secure CMS since it has very few reported security vulnerabilities, and is immune to capturing sensitive data attacks. WordPress is among the most used and the most wide-spread CMSs, so most likely it will be targeted. Hence, it is critical to keep up

with its security updates. WordPress and Drupal issue bug fixes and security releases relatively frequently.

Possibility for updating / upgrading of the CMS product is assumed, yet sometimes it can be painful process, because major updates can break existing themes and add-ons. Therefore, organization should look for systems with only few changes to their common overarching features. Needless to say, yet, systems that continue to support features of the old major versions are welcome too. WordPress recently introduced easy automatic upgrades, while DotNetNuke, WordPress and Drupal provide support to old versions and issue feature upgrades relatively frequently. On contrary, Joomla had only one more significant upgrade in the recent period.

Having in mind all of the above, we are proposing the below taxonomy for CMSs (Fig. 1) in order to help future users identify suitable CMS for their short-term and long-term purposes.

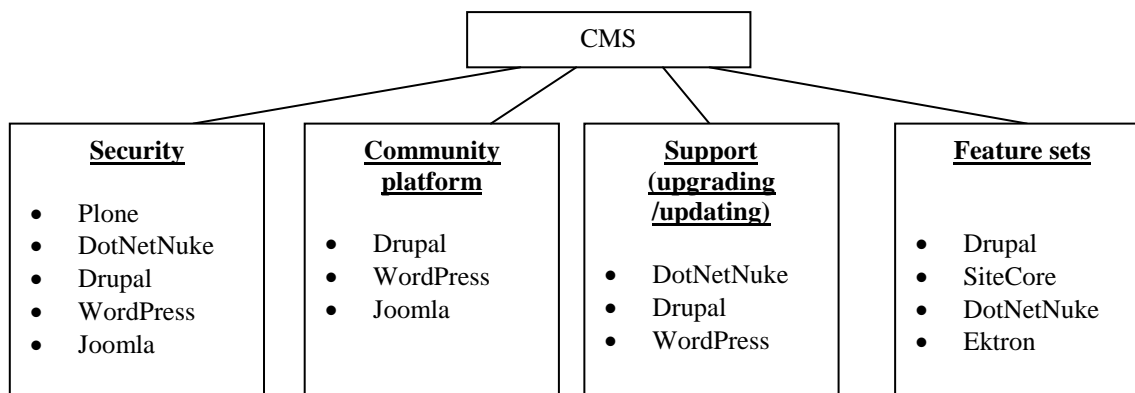


Fig. 1. Taxonomy of content management systems

## VI. CONCLUSION

A CMS allows and helps to easily conceive, organize and automate the collection, management, publishing, and presentation of content. Identification of CMS suitable for the organization purposes is of paramount importance to organizations. It is complicated task because there is a great variety of proprietary and open source CMS that have their own weaknesses and strengths. Hence, solid analysis needs to be completed in order to identify CMS that is fit-for-purpose in order to appropriately meet organization and user expectations from its products at the same time. There are no universally accepted standards or features for what CMSs should contain or how should function. Logically, unleashed possibilities of CMSs on the market offer diverse features, variety of purposes, a range of plugins/modules from-the-box, and are specific in many ways.

Therefore, in this paper we introduced a new taxonomy of CMSs, based on their security, community platform, support, and feature sets, to assist organizations to identify CMS that will match the expectations and demand from

clients and end-users of the organization products and services offered via the CMS. We clustered selected CMSs according to important aspect of their functionality that should be considered in making optimal decision when selecting CMS adequate for organization, its clients and end-users.

## REFERENCES

- [1] Halperin Creative Content Management System, White Paper, Halperin Creative, USA, 2012.
- [2] Step Two Designs: So, what is a content management system?, Step Two Designs, Australia, 2003.
- [3] Tran T. et al.: Document Builder, San Jose State University, USA, 2010.
- [4] Comentum, Drupal vs Joomla vs WordPress, Open Source CMS Comparison; April 2013; <http://www.comentum.com/drupal-vs-joomla-cms-comparison.html>
- [5] CMS comparison; April 2013; <http://www.r2integrated.com/dnn/services/cms-comparison.aspx>
- [6] Reyes J.: How to Evaluate What CMS to Use; April 2013; <http://sixrevisions.com/web-development/how-to-evaluate-what-cms-to-use/>

# Appropriate Learning Tools and Approaches According to the Different Learning Styles and Collaboration Skills of the Students

Donika Valcheva<sup>1</sup> and Margarita Todorova<sup>2</sup>

**Abstract –** In this report the authors made an attempt to categorize and defined the most appropriate teaching tools and approaches for students with different learning styles and collaboration skills by using two classifications – learning styles according the human perceptual modalities and learning types depending on the student's collaboration skills.

**Keywords –** E-learning, Learning modalities, Collaboration skills, Learning Tools and approaches

## I. INTRODUCTION

In the traditional classroom form of studying, the teaching is realized in front of a group of students with different learning styles and skills for collaboration. In most of the cases, although the professionalism and the wish of the teachers to work individually with each student separately, the personalization is very low.

The main goal of e-learning nowadays is to personalize the learning process according to the individual skills and learning style of each student. The modern technologies offer great range of tools and approaches for realizing effective learning process for students with different learning styles and needs.

There are many theories [[1],[13]], which define student learning styles according to different criteria. A lot of research is made in this direction [[1],[2],[3],[4],[6],[7],[8],[9],[9],[11],[12]].

It is obvious that the more theories are taken in consideration when designing a given learning tool the more effective and personalized will be the teaching process.

In this report we made an attempt to categorize and defined the most appropriate teaching tools and approaches for students with different learning styles and needs by using two classifications – learning styles according the human perceptual modalities and learning types depending on the student's collaboration skills.

## II. DESCRIPTION OF THE LEARNING MODALITIES

People tend to have a preferred learning, so will learn more effectively if they have access to learning resources that utilize their preferred way of learning. In this report we use three basic modalities to process information to memory: visual (learning by seeing), auditory (learning by hearing), and kinesthetic (learning by doing). Many students are not aware of their preference, which takes them difficult to approach their own learning [[1],[13]].

In tab.1 are discussed some of the main personality characteristics of the learning modalities, according to which the students could be differentiated.

TABLE I  
PERSONALITY CHARACTERISTICS OF THE LEARNING MODALITIES

Visual	Auditory	Kinesthetic
<ul style="list-style-type: none"> <li>- Mind wanders during verbal activities;</li> <li>- Has trouble following or remembering verbal instructions;</li> <li>- Prefers to observe rather than actively participate in group activities;</li> <li>- Likes to read silently;</li> <li>- Is neat and organized;</li> <li>- Pays attention to detail;</li> <li>- Has neat handwriting and is a good speller;</li> <li>- Easily memorizes by seeing pictures and diagrams;</li> <li>- May have a „photographic memory”;</li> <li>- Use highlighters, circle words, underline.</li> </ul>	<ul style="list-style-type: none"> <li>- Is easily distracted;</li> <li>- Quickly loses interest in visual demonstrations;</li> <li>- Enjoys listening activities;</li> <li>- Is active in group activities and discussions;</li> <li>- Prefers reading aloud to silent reading;</li> <li>- Listens to music while studying or doing homework;</li> <li>- Has sloppy handwriting;</li> <li>- Often read to themselves as they study;</li> <li>- Are not afraid to speak in class.</li> </ul>	<ul style="list-style-type: none"> <li>- Taps pencil or foot while thinking, studying, or writing tests;</li> <li>- Enjoys doing experiments;</li> <li>- Uses excessive hand gestures and body language;</li> <li>- Tends not to enjoy reading;</li> <li>- Enjoys hands-on activities;</li> <li>- Enjoys problem-solving;</li> <li>- Is a poor speller;</li> <li>- May have trouble memorizing lists, numbers, etc.;</li> <li>- Easily expresses emotions.</li> </ul>

<sup>1</sup> Assistant Prof. PhD Donika Valcheva, Faculty of Mathematics and Informatics, St. Cyril and St. Methodius University, Veliko Tarnovo, Bulgaria, e-mail: donika\_valcheva@abv.bg

<sup>2</sup> Prof. Margarita Todorova, Faculty of Mathematics and Informatics, St. Cyril and St. Methodius University, Veliko Tarnovo, Bulgaria, e-mail: marga\_get@abv.bg

Depending on their preferred learning modality, different teaching techniques have different levels of effectiveness. Effective teaching requires a variety of teaching methods which cover all three learning modalities (tab.2). No matter

what their preference, students should have equal opportunities to learn in a way that is effective for them.

TABLE II  
SOME APPROPRIATE TEACHING TECHNIQUES

Visual	Auditory	Kinesthetic
-visual demonstrations, - video lessons, - presentations, - animation, -3Dgraphic applications, - maps, - charts, -graphics, photos, etc.	- audio lessons, - video lessons, - animation with voice instructions, -discussion forums and social networks.	-interactive learning content, - simulations and games, - problem-solving tasks, - experiments.

### III. CLASSIFICATION DEPENDING ON THE STUDENT'S COLLABORATION SKILLS

According this classification the learning types (styles) could be defined as cooperative, competitive and individualized learning types [[5]].

An **individualized learning type** indicates a preference for achieving individual goals having no involvement with peers.

The **cooperative learning type** indicates a preference for achieving individual goals while working conjointly with peers.

The **competitive learning type** indicates a preference for learning in competition with others, often achieving individual goals when others fail to achieve their goals.

### IV. APPROPRIATE LEARNING APPROACHES AND TOOLS ACCORDING TO THE DIFFERENT LEARNING STYLES AND COLLABORATION SKILLS

In the following table is shown an attempt to summarize and to define the most appropriate learning approaches and tools for the students with different learning modalities and collaboration skills. Combining these two criteria we commonly may categorize these students into the following:

- Individualists with dominating learning by seeing modality;
- Cooperative students with dominating learning by seeing modality;
- Competitive students with dominating learning by seeing modality;
- Individualists with dominating learning by hearing modality;

- Cooperative students with dominating learning by hearing modality;
- Competitive students with dominating learning by hearing modality;
- Individualists with dominating learning by doing modality;
- Cooperative students with dominating learning by doing modality;
- Competitive students with dominating learning by doing modality.

In tab.3 we suggest appropriate tools and approaches for students with different learning modalities and collaboration skills. This is an attempt to summarize and arrange some of the most used tools that offer the modern ICT and to define some good approaches for presenting and offering effective e-learning. The table is not full. It could be improved and more tools and approaches could be added. Also other criteria for defining personal individuality and learning styles could be taken into consideration.

TABLE III  
APPROPRIATE TOOLS AND APPROACHES FOR STUDENTS WITH DIFFERENT LEARNING MODALITIES AND COLLABORATION SKILLS.

Modality/ Collabora- tion Skills	Individualists	Cooperative students	Competitive students
<b>ICT tools and teaching approaches</b>			
Visual (learning by seeing)	-visual demonstration video lesson; -presentations, animation, 3d graphic applications, maps, charts, graphics, photos, etc. for individual work.	-real time visual demonstration + use of video conversation (or other synchronous communication tool) between the students and the teacher; - presentation s, animation, 3d graphic applications, maps, charts, graphics, photos, etc. used as helping tool for virtual discussions and studying together in a team.	-real time visual demonstration + online time testing after the demonstration for obtaining immediate feedback for the rate of absorbing the information by the students; -presentations, animation, 3d graphic applications, maps, charts, graphics, photos, etc. used for virtual brain storming and problem solving.

<b>Audio (learning by hearing)</b>	Audio lessons, video lessons, animation with voice instructions, stored in memory device.	Audio lessons, video lessons, animation with voice instructions, combined with discussion forums and social networks for cooperative work and study.	Audio lessons, video lessons, animation with voice instructions, combined with discussion forums and social networks for providing dispute and nominating the best student in it.
<b>Kinesthetic (learning by doing)</b>	-use of simulators; -playing individual practical games; -doing individual project with real problem-solving tasks.	-real time simulation + use of video conversation (or other synchronous communication tool) between the students and the teacher; -playing practical games + use of video conversation (or other synchronous communication tool) between the students and the teacher; -doing a real project with problem-solving tasks in a team + use of video conversation (or other synchronous communication tool) between the students and the teacher.	-real time simulation with competitive character (with assessment of the results); - competitive virtual practical games; - doing a real project with problem-solving tasks by dividing the students into teams after finishing the project + presentation of the results by use of video conversation (or other synchronous communication tool) between the students and the teacher. At the end assessment of the results.

## V. CONCLUSION

One of the reasons that make authors think that this investigation is useful is that one of the most serious problems

nowadays in e-learning is the lack of personalization of the teaching and learning process. In the Internet space can be found countless courses in one and the same theme, presented in different way, with different level of usage of multimedia elements, directed to different learning styles, with different duration and complexity. The user has the very difficult task – to find in the ocean of e-learning courses, the most appropriate for his learning style, basic knowledge and skills. This is not always possible, and even when the choice of an appropriate course is a fact, the chance the initial goal (gaining knowledge and skills in a given field) to be reached for a short time is not high.

It is necessary to be investigated the concept about increasing the personalization of the e-learning environment according to the individuality of each student and his expectations about the final results.

The personalization in the e-learning may be defined as a composition of procedures, approaches and techniques for giving the students the tools for learning, which will give them the opportunity to study according to their own capabilities, learning style, knowledge and skills for collaboration.

In future we planed to improve this attempt to categorize and arrange the countless ICT tools according to the defined students learning profiles and also to add new criteria for increasing the personalization in the e-learning process.

## REFERENCES

- [1]. Иванов И. (2003) Стилове на учене. Втора национална научнопрактическа конференция “сихолого-педагогическа характеристика на детството”, опово’, Университетско издателство “Св. Кл. хридски”, 29-39.
- [2]. Alfano M., Biagio Lenzitti. A Web Search Methodology for Different User Typologies. CompSysTech'09, Ruse, Bulgaria, 18-19 June, IV.6.
- [3]. Dureva Daniela, Georgi Totkov. Learning Styles Testing in Moodle. CompSysTech'08, Gabrovo, Bulgaria, 12-13 June, IV-11-1.
- [4]. Jones K., Juliet M.,V. Reid. Modifying Teaching to Address Thinking Styles. CompSysTech'07, Rousse, Bulgaria, 14-15 June, IV-10.
- [5]. Margarita Todorova, T. Kalushkov, Donika Valcheva, APPROPRIATE E-LEARNING ENVIRONMENT, ACCORDING TO STUDENTS LEARNING TYPE, International Conference on Information Technologies (InfoTech-2008) 19th – 20th September 2008, Bulgaria
- [6]. Paiva A. (1997). LEARNER MODELLING FOR COLLABORATIVE LEARNING ENVIRONMENTS. *In Proceedings of AIED'97, Kobe, Japan*, IOS Press, 215-222.
- [7]. Rong Wen Jia, Yang Szu Min. The Effects of Learning Style and Flow Experience on the Effectiveness of ELearning. *Proceedings of the Fifth IEEE International Conference on Advanced*

Learning Technologies (ICALT'05) 0-7695-2338-2/05 \$20.00 © 2005 IEEE.

- [8]. Sonnenwald, Diane H. and Kim, Seung-Lye (2002) INVESTIGATING THE RELATIONSHIP BETWEEN LEARNING STYLE PREFERENCES AND TEACHING COLLABORATION SKILLS AND TECHNOLOGY: *An Exploratory Study*. In Toms, E., Eds. *Proceedings American Society for Information Science and Technology*, pages pp. 64-73.
- [9]. Valcheva D., Todorova M., Asenov O. (2010b). One Approach for personalization of e-learning. International Conference on e-Learning and the Knowledge Society –e-Learning'10, Riga, Latvia.
- [10]. Valcheva, D., M.Todorova, T. Kalushkov. Structuring Multimedia Scenarios According to the Different Learning Modalities. EATIS 2009, Prague, Czech Republic, ISBN #978-1-60558-398-3.
- [11]. Wen Jia Rong; Yang Szu Min. The effects of learning style and flow experience on the effectiveness of e-learning. Advanced Learning Technologies, 2005. ICALT 2005. Fifth IEEE International Conference page. 802- 805, <http://www.ieeexplore.ieee.org/stamp/stamp.jsp?tp=&arnumber=1508821&isnumber=32317>
- [12]. Zhuhadar L. Romero E. Wyatt R. The Effectiveness of Personalization in Delivering E-learning Classes. Advances in Computer-Human Interactions, 2009, ACHI '09, Second International Conferences page 130-135, 1-7 Feb. 2009,
- [13]. [http://library.thinkquest.org/C005704/content\\_hw1\\_learningmodalities.php3](http://library.thinkquest.org/C005704/content_hw1_learningmodalities.php3).

# Optimal Design of Elements in Confirmation of Panel Buildings

Vassil Guliashki<sup>1</sup>, Chavdar Korsemov<sup>2</sup>, Hristo Toshev<sup>3</sup>, Leoneed Kirilov<sup>4</sup> and Krassimira Genova<sup>5</sup>

**Abstract:** – The paper presents the possibilities for optimal design of elements in confirmation (joinery work) of multifunctional panel apartment buildings. The basic structure of the program system for optimal design of the profiles and glass plates of the joinery work is proposed. The usage of a basic structure of the system for optimal design of the profiles and glass plates of the joinery work is proposed. The usage of the described system will contribute to decreasing of the price, materials and time for design of joinery work.

**Keywords:** – Optimal design, joinery work, linear integer programming

## I. INTRODUCTION

The paper concerns the possibilities for optimal design of elements in confirmation (joinery work) for multifunctional panel apartment buildings. The research is motivated by the program “Support of the Energy Efficiency of Multifamily Buildings” Bulgaria. The object of this program is a set of 700 000 apartments in panel buildings with more than 2 million and 700 000 inhabitants. According to Regulation 7 for energy efficiency and energy saving, the main renovation and reconstruction of buildings requires the use of modern joinery work with certain qualities. The replacement of the old woodwork by joinery work made of modern materials (plastic or aluminum), is a basic stage in the process of panel buildings renovation. The result of the research is the study of a unified program system for joinery work for the purposes of renovation. The possibilities will be investigated for determination of the size of the modular joinery constructions that will decrease the material costs and the price of the joinery work, as well as lessening the time for modules design. The approaches for optimization of the size of the profiles and the glass, necessary for the production of different modules will be analyzed, with the purpose to decrease the wastage, as well as to optimize the additional accessories of the joinery work (distanioners, persiennes, etc.). As a result, a modular system architecture will be proposed for optimal joinery design and construction of groups of panel buildings. Having in mind the national program of the MRDPW for renovation of these buildings, the economic

<sup>1</sup> Vassil Guliashki, <sup>2</sup> Chavdar Korsemov, <sup>3</sup> Hristo Toshev, <sup>4</sup> Leoneed Kirilov and <sup>5</sup> Krassimira Genova are with the Institute of Information and Communication Technologies, Bulgarian Academy of Sciences, Acad. G. Bonchev str., bl. 2, 1113 Sofia, Bulgaria, E-mail: [vggul@yahoo.com](mailto:vggul@yahoo.com), [chkorsemov@iinf.bas.bg](mailto:chkorsemov@iinf.bas.bg), [hr\\_toshev@mail.bg](mailto:hr_toshev@mail.bg), [leomk@abv.bg](mailto:leomk@abv.bg), [kgenova@iinf.bas.bg](mailto:kgenova@iinf.bas.bg)

effect from the realization of such a project will be found in decreasing of the time for contemporary joinery work design,

decreasing in the resources of materials, labor and price of the joinery, increasing of the buildings energy efficiency (decrease of the heating expenses up to 40 %) and last, but not least – improvement of the living conditions.

## II. ANALYSIS OF DIFFERENT METHODS FOR OPTIMAL DESIGN OF PROFILES AND GLASS FOR JOINERY WORK

Cutting stock problems are encountered at the production stage of profiles and glass for joinery work. Cutting stock problems consist in cutting large pieces (objects), available in a stock, into a set of smaller pieces (items) in order to fulfil their requirements, optimizing a certain objective function, for instance, minimizing the total number of objects cut, minimizing the waste, minimizing the cost of the objects cut, etc. These problems are relevant in the production planning of many industries, such as paper, glass, furniture, metallurgy, plastics and textile industries. In the last four decades cutting stock problems have been studied by an increasing number of researchers [1-10]. The interest in these problems can be explained by their practical application and the challenge they offer to researchers. For despite their apparent simplicity, they are, in general, computationally difficult to solve. The continuous growth of the prices of the materials and of the energy requires minimization of the production expenses for every element. The coefficient of usage  $K_u$  [10, 11] is used as a criterion of efficiency. In order to solve similar problems, a set of mathematical methods are proposed. The cutting stock problem is an optimization problem, or more precisely an integer linear programming problem that minimizes the total waste while satisfying the given demand [12].

$$\min \rightarrow \sum_{j=1}^n \sum_{i=1}^p c_{ji} x_{ji} \quad (1)$$

$$\sum_{j=1}^n \sum_{i=1}^p a_{jik} x_{ji} = b_k, \quad k = 1, \dots, q \quad (2)$$

$$x_{ji} \geq 0, \quad j = 1, \dots, n; \quad i = 1, \dots, p \quad (3)$$

where (1) is the objective function, (2) are constraints determining the number of pieces needed to complete the order and (3) are conditions of non-negativity of the variables.

One of the cutting stock problems is cutting out glass surfaces and profiles in the production of glass packets for windows, shop windows, doors, roofs and other for joinery work. The dimensions of the glass are different depending on the case considered. Depending on the type of the orders/requests, rod sheets which differ in size, width and

brands, are used for cutting out. That is why the portfolio of the orders is divided into groups, depending on the characteristics of the initial parameters [9, 10]. The cutting problem can be formulated in the following way: a number of items (glass for doors, windows, etc.) must be selected from the requests portfolio and depending on the size and type of the primary material, optimal cutting out must be done, with minimal loss of the material used. Since these losses have to be minimal, it is necessary to maximize  $K_u$  according to the formula [9-11]:

$$K_u = \frac{\sum_{r=1}^n S_r}{S_{eb}} \quad (4)$$

where the numerator is the sum of the areas in the requests portfolio and  $S_{eb}$  is the area or length of the source material. The maximal value of  $K_u = 1$ , but in real life it is hardly reached. Knowing the value obtained for  $K_u$  and comparing it with  $K_u = 1$ , we could make a conclusion about the optimality of the cutting. The scientific area, connected with the present study, is operational research. It includes a scientific approach for making an optimal decision under conditions of technical, economic and other constraints, connected with the definition of adequate mathematical models and the formulation and solution of the corresponding optimization problems.

Within the frame of the present study, a brief comparison of available methods for optimal design of the profiles and glass for joinery work, used in practice by Bulgarian companies, is proposed:

- Software program PVC 3.2.2 – gives the possibility to solve the problem for optimal design of different profiles of PVC joinery.
- Software for optimal cutting out of glass packets – GlassOptimizer is a program for glass sheets cutting with optimization of the remainders and additional computations for glass packets.
- Software for ALU joinery work design – AluDesign is automated software for the design and production of aluminum joinery elements. It aids the design of windows, doors, terraces, etc.
- Software for PVC joinery work – PVCDesign is automated software for the design and production of PVC joinery work.

Since, there is no unified system for optimal design of joinery work the authors propose a basic components of such structure.

### **III. BASIC STRUCTURE OF THE PROGRAM SYSTEM FOR OPTIMAL DESIGN**

After acquisition of sufficient data about the size of different elements (doors and windows) in the different types of the panel buildings apartments (bachelor's apartment, one-room apartment, two-rooms apartment, three-rooms apartment and four-rooms apartment) and the detailed analysis of the data collected, it was established that the dimensions of certain elements in different apartments are quite close. This

gives the possibility to unify them, since the differences within the range of  $\pm 20$  mm are acceptable.

Following the above conclusions, the large number of elements in the panel apartments (about 28 in number) may be reduced to the following unified modules:

- Module 1 – a door with dimensions 2200/730
- Module 2 – two-wings window with dimensions 1700/2100
- Module 3 – one-wing window with dimensions 1400/1400
- Module 4 – two-wings window with dimensions 2050/1370
- Module 5 – two-wings window with dimensions 2800/1700 (Fig. 8e), for elements T6, F4.
- Module 6 – a door 650/2000
- Module 7 – a front entrance door with dimensions 2200/3200
- Module 8 – a rear entrance door with dimensions 2400/2500

The analysis of the realized study and the acquired database for dimensions of the elements in the windows and doors in different buildings and apartments in panel buildings show that all modules can be reduced to several unified modules. This leads to the conclusion that a project for optimal technology in the design of joinery work in panel buildings could be accomplished by the following steps:

- definition of the unified modules of joinery in panel apartment buildings;
- determining the size of the joinery work on the basis of the optimization problems solved;
- formulation of the requests towards the profiles manufacturers with respect to optimal dimensions of the initial materials.

All these steps will decrease the joinery price by decreasing the loss of the material, or the so called wastage. Furthermore, the time for realization of a large request by the use of unified modules will be decreased too. Up to the present moment there is no data about the application of a similar approach towards the problem of optimal joinery design. The existing approaches towards the design of joinery work, used in competitor companies, are reduced to automation of the offers for joinery production and optimal cutting of the corresponding glass packets for separate requests. The innovative technology developed can be suggested on the market after modification with respect to the specifics of the construction types and joinery dimensions.

The basic structure of the system for optimal design of the joinery work in panel buildings renovation is shown in Fig. 1. The brief description of the proposed structure is summarized as follows:

- entry of the request and different computations – the order parameters are given – number of the apartment buildings, number of the floors, number of the different types of apartments; and computation of the total number of the types of

apartments, elements, staircase windows and entrance doors;

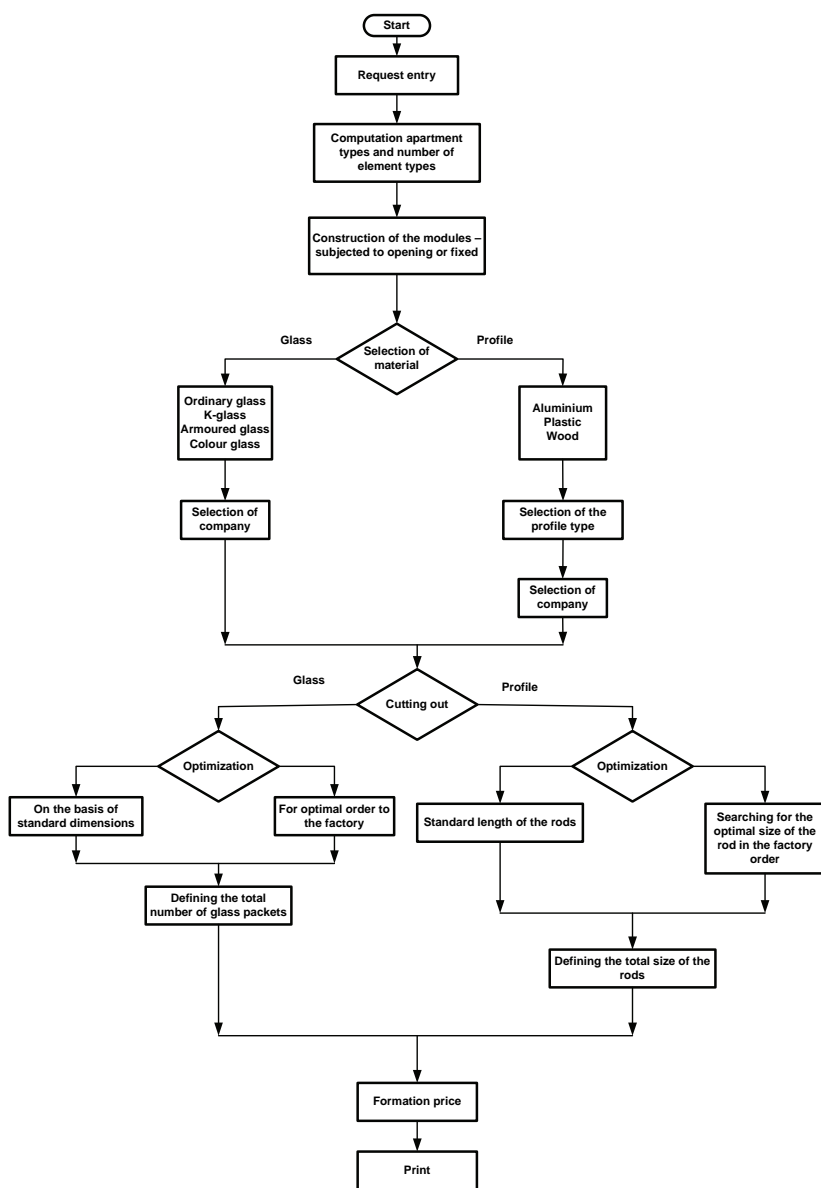


Fig. 1

- analysis and determination of the unified modules and defining the type of the unified modules – subjected to opening or fixed;
- type of the modules – subjected to opening or fixed – depending on the requests each module is divided into two parts – subjected to opening and fixed, and their number is computed;
- selection of the material – the algorithm divides here into two branches;
- profile – selection of Al, PVC, wood, type of the profile and manufacturing plant;
- glass – type of the glass – ordinary glass, K-glass, armoured glass, colour glass and producing company;

- cutting out – this is a very important element in joinery production. In the modular system proposed two elements of cutting are pointed out: glass and profiles, but enhancing the system possibilities, some other elements of production could be additionally cut out such as distancioners, persiennes, etc.

As a result of the system execution an optimal design of joinery work made of contemporary materials (plastic, Al) is available. The technology is based on the formulation of models [6, 11] and the mathematic optimization problems [7-10], and contributes to the optimal design of unified modules of joinery work for panel apartment buildings.

Optimizing the joinery cutting out requires the development of new mathematic models and methods implemented in a software system. It could be combined with the software products already available on the market, or be used as a new integrated library. Two approaches for optimization of the glass cutting out are proposed:

- on the basis of the standard dimensions – considering the available different types of glass sheets to do optimal cutting with respect to minimal quantity of the wastage;

- for optimal order/request towards the manufacturing plant – the optimization problem here is the inverse – on the basis of the given request (that has to be quite large), an optimal variant for the production of a glass sheet is searched for, that will ensure minimal wastage.

The optimization in profiles cutting out is accomplished in a similar way:

- with respect to the standard length of the rods – having in mind several standard lengths of the rods, made of Al and PVC, offered by the producing factories, for smaller in volume requests, the optimal cutting out of the suggested length is realized with respect to the criterion for minimal waste.

- searching for optimal dimensions of non-standard rods in the special requests towards the manufacturing plant, when the order is large (over 50 apartment buildings).

At the end, the total number of the modules and glass packets is determined, their price is computed and the module types with their dimensions are printed.

#### IV. CONCLUSIONS

EC policy connected with energy consumption in buildings, as well as the Bulgarian law for energy efficiency and the regulations referred to it, require the application of some actions, when repairing buildings, that lead to increase in their energy efficiency. These actions lead to decrease in the expenses of fuel and electrical energy, raising the comfort in such buildings, lengthening their exploitation period and increasing their price. The buildings with low energy consumption have easy support and maintenance, which guarantees low expenses and at the same time smaller ecological influence. The closest alternative of the modular system offered for optimal design of joinery work for panel apartment buildings is the replacement of the existing woodwork by qualitative aluminum or plastic joinery elements. This development will aid the renovation of the widely spread in Bulgaria panel buildings in accordance with the European standards. In some East European countries (for example East Germany), such renovation has been completed, but there is no data about the use of mathematic optimization models and methods for joinery design. Having in mind that the renovation process will cover a large volume and the requests will include large groups of apartment buildings, neighborhoods and cities, the advantages of the current proposal may be resumed as follows:

- decrease in the expenses for joinery work manufacturing (up to 25 %), thanks to the optimized dimensions of the modules;
- decrease of the time for joinery design, as a result of the use of optimal unified modules;
- decrease of the heating expenses (up to 40 %), as a result of the use of contemporary joinery, that will contribute to the decrease of the noxious gas, emitted in atmosphere by the sources of heat energy, i.e. smaller ecological influence;
- improvement of the quality of life of the inhabitants in the renovated flats.

The expected time of investment return, connected with the development of the innovative service proposed, will depend on the time for replacement of the joinery work in more than 50 multistory apartment buildings. Taking into account that above 700 thousand buildings are to be renovated, the turnover expected is of the order of millions BGL. The rate of profit is comparable to the expected effect of materials saving when renovating groups of apartment buildings, namely up to 20%. This rate does not include the time saving in design and the decrease of the heating funds in the renovated apartment buildings (up to 40 %).

#### REFERENCES

- [1] A. Mobasher and A. Ekici, Solution approaches for the cutting stock problem with setup cost. *Computers & Operations Research*, Vol. 40, 2013, pp. 225-235, 2013.
- [2] A. C. Dikili, E. Sarıoz and N. A. Peck, A successive elimination method for one-dimensional stock cutting problems in ship production. *Ocean Engineering*, Vol. 34, 2007, pp. 1841-1849, 2007.
- [3] Y. Cui and Y. Lu Heuristic algorithm for a cutting stock problem in the steel bridge construction. *Computers & Operations Research*, Vol. 36, 2009, pp. 612-622, 2009.
- [4] C. Cherri, M. N. Arenales and H. H. Yanasse, The one-dimensional cutting stock problem with usable leftover – A heuristic approach. *European Journal of Operational Research*, Vol. 196(3), 2009, pp. 897-908, 2009.
- [5] P. C. Gilmore and R. E. Gomory, A linear programming approach to the cutting stock problem, Part 2, 1963, pp. 863-887, 1963.
- [6] Y. Pochet and L. A. Wolsey, Lotsizing models with backlogging: strong formulations and cutting planes, *Mathematical Programming*, Vol. 40, 1988, pp. 862-872, 1988.
- [7] P. H. Vance, C. Banhart, E. J. Jonson and G. L. nemhauser, Solving binary cutting stock problems by columngeneration and branch- and bound, *Computational Optimization and Applications*, 1994, pp. 111-130, 1994.
- [8] P. V. Afonin, System for rational cutting out of materials applying genetic optimization algorithms, In: Proc. of 4<sup>th</sup> International Summer Workshop in Artificial Intelligence for Students and Ph.D. Students, Minsk, 2000, pp. 125-128 (in Russian), 2000.
- [9] V. V. E;lyanov, V. M. Kureychik and V. V. Kureichik, *Theory and Practice of Evolutionary Modelling*, Moscow. 2003 (in Russian), 2003.
- [10] H. I. Toshev, S. L. Koynov and Ch. D. Korsemov, Genetic algorithms for optimal cutting panes of glass. In: Proc. of the IV International Bulgarian-Greek Scientific Conference on Computer Science 2008, (Ed. Borovska, Pl.), Kavala, Greece, Part II, Kavala, Greece, pp. 657-662, 2008.
- [11] H. I. Toshev, S. L. Koynov and Ch. D. Korsemov, Evolutionary approaches to cut wooden sheets in the furniture production, In: Proc. of the XLIV International Scientific Conference on Information, Communication and Energy Systems and Technologies ICEST 2009, (Ed. Arnaudov, R.), Veliko Tarnovo, Bulgaria, Vol. 2, pp. 467-470, 2009.
- [12] S . M . S u l i m a n , A Pattern generating procedure for the cutting stock problem. *Int. J. Production Economics*, Vol. 74, 2001, pp. 293-301, 2001.

#### ACKNOWLEDGMENT

The authors gratefully acknowledge the support of Bulgarian National Science Fund, Grant No DTK02/71 “Web-Based Interactive System, Supporting the Building Models and Solving Optimization and Decision Making Problems”.

# Modification of Algorithms to Control of Mobile Object

M. Todorova<sup>1</sup>

**Abstract** – The paper presents an algorithm for following the line of the mobile object. The results are analyzed. The paper suggests improvements in the algorithm. Several sensors are used to solve this task. The type and accuracy of the sensors are allowed to obtain the information which is transformed of kind that helps to manage and control the process of movement. The sensors that used are analogue and digital type. The robot is discussed as a complex technical system.

**Keywords** – robot, robot control algorithms, sensor, mechanical system, working process.

## I. INTRODUCTION

Robot as a mobile object can be seen as a complex technical system which consolidated several subsystems. Its management is possible as the fundamental characteristics are taken from different measurement devices. Different types and numbers of sensors are used. A information that coming from the sensors determine the color of the surface on which the robot moves. The sensor determining the color of surface is shown in Fig.1.



Fig 1. Surface color sensor

Using of optical reflective sensors such as RPR220 register reflected light from the surface to a distance of 8 mm. These sensors are used for the registration of black and white stripes.

## II. FUNCTIONAL STRUCTURE OF MOBILE OBJECT

The process that is operated as well as the structure of the robot depends on the type and number of used motors. The created model is based on two reversible dc motors. It can be classified as multi-engine machine. Functional structure of the robot is shown in Fig. 2.

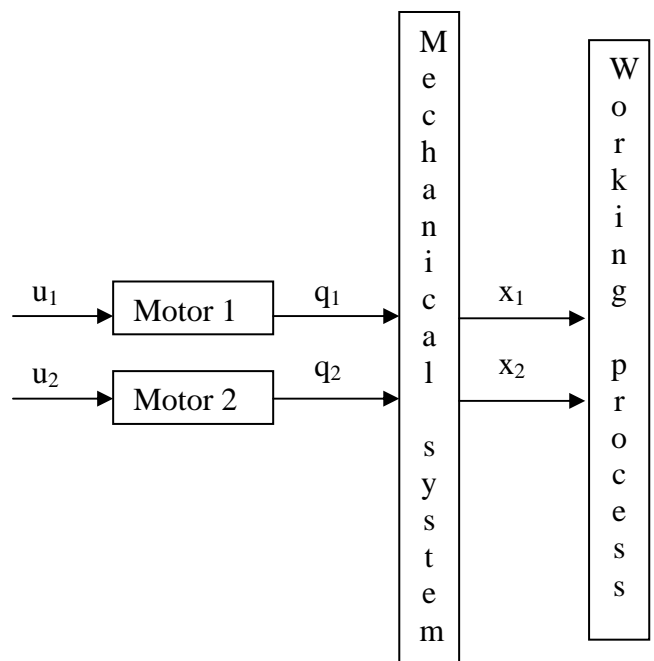


Fig 2. Functional structure

The input parameters are  $u_1$  and  $u_2$ . The coordinates that put in motion one mechanical system are  $q_1$  and  $q_2$ . The coordinates of the operating conditions of the robot are  $x_1$  and  $x_2$ . Both motors are set in motion independently. Dynamic relation between them is realized when the system is brought from a state of rest in motion. The input parameters  $u_1$  and  $u_2$  manage the transformation of energy into the motors. Used motors are direct current. For them  $u_1$  and  $u_2$  are applied to the input voltage. Mechanical system is a multitude of mechanisms subordinate to general objective laws. [1]

## III. ALGORITHM FOR FOLLOWING THE LINE

For realization of this algorithm can be use one, two, three or more sensors. The sensor reads 1 when it is on a light surface and 0 when it is on a dark surface. The number of

<sup>1</sup>Maya P. Todorova, Technical University – Varna, Computer Sciences Department, 9010 Varna, Bulgaria, E-mail: mayasvilen@abv.bg

used sensors is of great importance for obtaining more accurate results. The results are presented and analyzed. The advantages are indicated by using more number of sensors compared to use of smaller number. The basic disadvantages are pointed.

#### A. Resolve the task by using one sensor

The basic disadvantages in solving the task by using one sensor are:

- Very slow speed - The movement of robot which is realized is represented in Fig. 3.

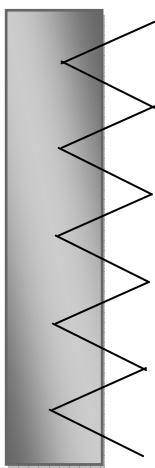


Fig. 3. Crablike movement of a robot with one sensor

- The robot can be in only two position. The two states of the sensor 0 and 1 are the reason of that.
- In case of loss of the line is impossible the robot to position on the line again.

#### B. Resolve the task by using two sensors

The combinations of states of both sensors are four:

00 - range between the ends of the line

11 - outside of line

10 - right side of the line

01 - left side of the line

Right side of the line and left side of the line are presented in Fig. 4

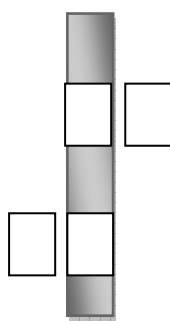


Fig. 4. Position on two sensors

Advantages:

- The information that incoming from sensor 1 leads to control the motor 1. The information that incoming from sensor 2 control the motor 2.
- When the sensors are located at a small distance, the robot tends to follow a line. When distance is greater are reported variations in the behavior of the robot.

Disadvantages:

- Low speed of movement.
- In case of loss of the line is impossible the robot to position on the line again.

#### C. Resolve the task by using three sensors

Combinations of states of three sensors are 000,010,001,100,011,100,101,110,111. In Fig 5 are shown the following combinations:

011 - the line is in leftmost position;

101 - central position;

110 - the line is in rightmost position;

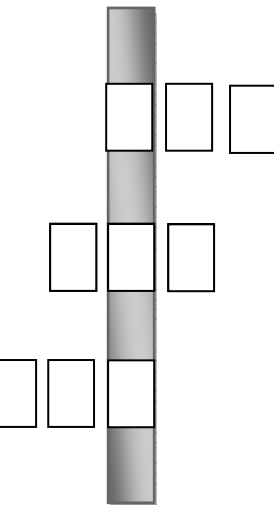


Fig. 5. Position on three sensors

Advantages:

- The border on the line can be determined by the robot.
- In case of loss of the line, it can be detected from the robot.
- Higher speed to movement of robot;
- More precise is made a turn.

Disadvantages:

- Low speed when make the turns [2].

The algorithm is related with the positioning of the robot on the line. Robot is driven when is supplied voltage to both motors. The data that come from the sensors is processed and verified. If the received data are with value 101, the robot continues to move forward, because it is on the line. If the mobile object is located at the leftmost or rightmost position of the line then have to be maneuvered with a sharp turn to the left or right, because the robot can lose the line. The maneuvers are carried out by controlling the voltage of both the engines. A part of the algorithm is shown in Fig. 6.

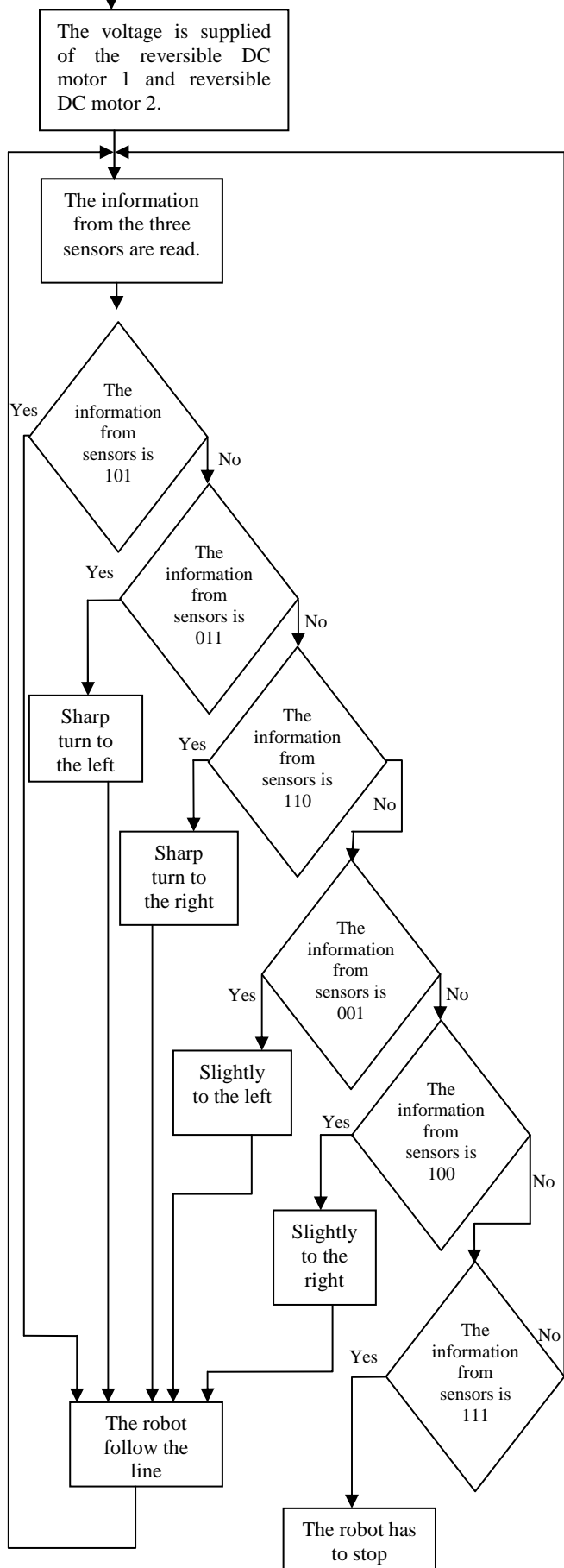


Fig. 6. Block diagram of algorithm for following the line.

### C. Resolve the task by using five sensors

Combinations of states of five sensors are thirty-two ( $2^5$ ) - (00000, 01111, 11110, 11111, 11011...) [3]

Advantages:

- The precise motion control the robot following the line.
- When changing the combination of the signals can be easily programmed logical decisions which to be taken by the robot to correctly move.

## IV. CONCLUSIONS

The task for following the line can be resolve with using three sensors. For more precise control of the robot must be used five sensors. The presented algorithm describes the process of movement of the robot in a line. Effectiveness and accuracy of the algorithm depends on:

- The type and number of sensors;
- The type of engines;
- The information that coming from sensors. It has to be correctly processed.
- The maneuvers such as turn left and right have to be tested.

## REFERENCES

- [1]. доц. д-р инж. Стефан Русев Генчев, Лекции, Тема - Функционална структура на машините и уредите
- [2]. <http://ironfelix.ru/modules.php?name=Pages&pa=showpage&pid=113>
- [3]. Дипломна работа, дипломант И. Иванов, научерн ръководител доц. д-р инж. Недялко Николов
- [4]. Priyank Patil, Department of Information Technology, K. J. Somaiya College of Engineering Mumbai, India, "Line following Robot"
- [5]. Harris, Tom. "How Robots Work", <http://science.howstuffworks.com/robot.htm>.
- [6]. [www.pololu.com](http://www.pololu.com).
- [7]. [www.microchip.com](http://www.microchip.com) – PIC18F6585 Data Sheet – 68 pin High performance 64 KB Enhanced Flash Microcontroller with ECAN module – 2004

**This Page Intentionally Left Blank**

# Creating a virtual reality application from Memorial Museum “11<sup>th</sup> October” - Prilep

Boban Mircheski<sup>1</sup>, Igor Nedelkovski<sup>2</sup>, Aleksandra Lozanovska<sup>3</sup> and Jove Pargovski<sup>4</sup>

**Abstract – In this paper is presented complete process of creating a virtual reality application. It's about creating a virtual tour of the Memorial Museum “11<sup>th</sup> October” – Prilep. The creation starts with collecting information about the object, appropriate modeling software for 3D modeling and creation of the final application (virtual tour) in EON Studio.**

**Keywords – Virtual reality, Museum, EON Studio, Model, Application.**

## I. INTRODUCTION

In the last few years, technology associated with virtual reality has yet to prove its usefulness for computer users. Until now, virtual environments require a computer with high quality graphics with specialized hardware and research software. This picture is changing quite quickly and VR applications from expensive, single-user applications have changed to very acceptable configurations with joint virtual worlds.

This development of technology contributing designers to add new ways of communication with what we see. One of those ways is a virtual communication with a particular subject, object or model. Thus the user has better perception in terms of what he sees and can see the model in three dimensions. This technology is used in this paper in which it's created virtual tour thus really existing objects.

Created application can be used as a stand-alone application or be attached to the internet and be accessible to all users who are interested in interacting with it.

## II. MEMORIAL MUSEUM “11<sup>th</sup> OCTOBER” - PRILEP

The Memorial Museum “11<sup>th</sup> October 1941” is located in the center of Prilep. The building in which the museum is hosted was built at the beginning of XX century. May 1, 1952 in this building was opened for the first time Museum of

<sup>1</sup>Boban Mircheski is with Faculty of Technical sciences at University "St. Kliment Ohridski" - Bitola, Ivo Lola Ribar bb, Bitola 7000 Macedonia, E-mail: boban.mircheski@tfb.uklo.edu.mk.

<sup>2</sup>Igor Nedelkovski is professor at Faculty of Technical Sciences, University "St. Kliment Ohridski" - Bitola, Ivo Lola Ribar bb, Bitola 7000 Macedonia, E-mail: igor.nedelkovski@tfb.uklo.edu.mk.

<sup>3</sup>Aleksandra Lozanovska with Faculty of Technical sciences at University "St. Kliment Ohridski" - Bitola, Ivo Lola Ribar bb, Bitola 7000 Macedonia, E-mail: aleksandra.lozanovska@gmail.com.

<sup>4</sup>Jove Pargovski is with the Cultural Heritage Protection Office of Republic of Macedonia, Gjuro Gjakovic No 61, Skopje 1000, Macedonia, E-mail: j.pargovski@uzkn.gov.mk.

NLW (National Liberation War) in Prilep, and on the occasion of 20<sup>th</sup> anniversary of NLW on October 11 1961 it's opened permanent museum exhibition.

For cultural monument Memorial Museum “11 October 1941” was proclaimed in 2003. Museum exhibition, which consists of photographs, documents, maps, drawings, objects and partisan equipment is located in an area of about 236 m<sup>2</sup>, on the ground floor in Hall 1, and the floor in Hall 2 and Hall3 shown in Fig.1.



Fig.1.Memorial museum “11<sup>th</sup> October” - Prilep.

## III. CREATING 3D MODEL FROM MUSEUM

The principle of creating such an application starts with collecting information from the Memorial Museum. Information are the actual dimensions of the museum, the size of rooms, taking pictures from the exterior and the interior of the building and photographing all panels in the museum. These pictures later are used to create the needed textures for the 3D model.

When is finished with collection of information, is accessed to modeling process, i.e. creating a 3D model from the real model. Modeling is performed inside and outside the museum and attaches the texture of the object. In our case, modeling is done with animation and modeling software, Autodesk Maya.

For the external environment (square) it is used a primitive plane without any special modifications, only increased dimension and position of that plane. In the middle is deducted the surface of the object using a Boolean operation – Difference, presented on Fig. 2.

Next you have to do is start with the modeling of the external walls of the object. Modeling of the walls is made with primitive cube on which are given the actual dimensions of the object scale. Modeling of the windows and the entrance of the building was done using the Boolean operation – difference (Fig. 2), which is modeled new facility with the

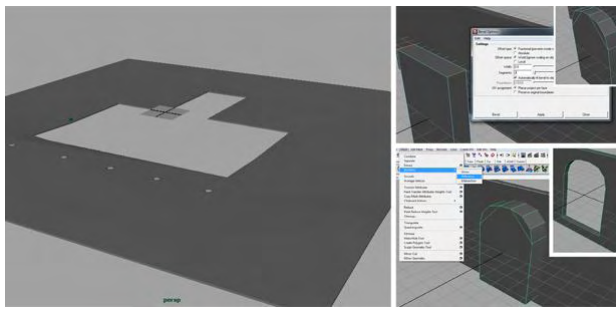


Fig.2. Creating external environment (square) of the museum, bevel option and design of the windows.

look of the window and that object is taken from the wall, than gets the final appearance of the wall shown on Fig. 3. On the same principle are constructed the walls in the interior of the object, i.e. is created the base of the wall and from that base are deducted models in form of windows.

After is finished with modeling of the walls, are modeled the windows and the other objects which are on the facade of our facility. Rounding the objects and windows is made using the tool Edit Mesh -> Bevel and is entered the radius of the rounding and number of polygons (smoothness) of rounding (Fig. 2). Is needed smaller number of polygons to obtain the desired shape, because of the bigger number of polygons means more triangulation and rendering problems.



Fig.3.Final look at the entrance and one of the windows and a complete view of the model without texture.

Objects (panels) in the building are created using primitives (cubes). Create as many primitives as there are panels and then are changing the dimensions accordingly. When modeling of other object, are used primitives such as cylinder, spheres as well as their combination. Also in this model are used some readymade objects (guns, etc.), which have a proper look at our requirements. This gives the final layout of the ground floor of the model shown in Fig. 4.

In a similar principle is created the first floor of the building, first by creating the exterior walls, then with modeling of the premises and objects in the premises. Used are the same tools for creating the windows and primitives for adding the final layout of the building shown in Fig. 4. We are completing with raising the roof of the building and after that starts with phase of texturing scenes.

After modeling of the museum, acceding to the insertion the texture and materials. The quality of the layout depends on the type of material that is used by its visual components, such as the color, brightness, transparency and the surface on which is applied. Textures are used to provide material variation and greater realism, thus simulating different types of material using image file texture or computer generated procedural maps.



Fig.4. A complete view of model with texture

Working with textures significantly slows performance and rendering the application in EON, so it's recommended not to use high-resolution textures and how much it is possible to use a smaller number of textures. The maximum resolution is 1024x1024 and can be inserted .jpeg, .png and .ppm textures. Textures can be imported along with the model or to create separately in EON Studio. In Fig. 4 is shown the complete layout of the model and its interior along with textures and created materials.

#### IV. CREATING VR APPLICATION

Once we are finished with the process of modeling the object in Maya, we approach to his preparation for input in to EON Studio, i.e. preparing of the object and textures. Before entering of the object, it's necessary to make a triangulation of the object. Triangulation represents a process of dividing the polygons which are defined by four or more points, to polygons defined by three points, shown on Fig. 5.

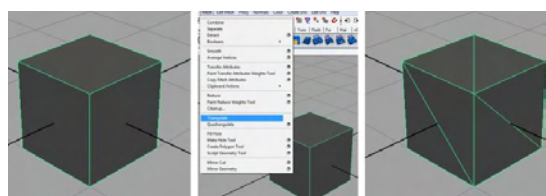


Fig.5. Triangulation.

This process of triangulation can be performed in two ways: the first one – on the side of the software the object is created (in our case Maya), and the second way – on the side of the software the object is inputted (EON Studio). Because of the size and complexity of the object, triangulation is performed

in Maya, not in EON Studio because of greater stability of the software. If triangulation is not performed on the side of the software the object is created, input in EON Studio automatically run, but in our case it was not possible because of the number of polygons of the object, EON Studio was unable to process by which the program blocks.

Once it is completed the process of triangulation, it is necessary to export the object into a format that can be inputted in EON Studio. The basic format in which files are recorded from Maya (.ma and .mb), EON Studio does not recognize, so this object will be exported in .obj format which is readable into EON. In addition, our object is ready for input into EON Studio.

From the File menu of EON Studio chose Import, from the given options we choose to enter Wave front (+Rhino) .obj. Than a dialog window shows, where can choose which model we want to import, and select the options we want to have this object Fig. 6.

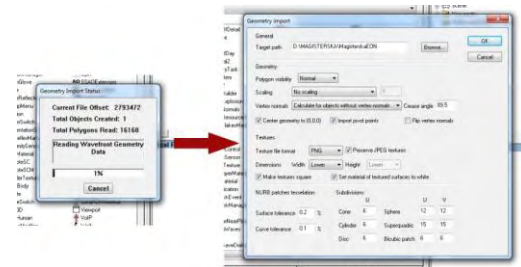


Fig.6. Importing a model in EON Studio.

Then it is necessary to create interactivity of the object and the user. For this purpose the tree of simulation in terms of camera, we erase the node Walk and add the node Walk About. With the first node we were limited with the movements of the mouse; while with the second node (Walk About) movement of the camera around the object is executed using the keyboard. Also in the tree of simulation Fig. 7, we can notice our facility which was entered into EON Studio.



Fig.7. Deleting Walk node, import WalkAbout, ClickSensor and DirectSound node and display our model in the scene.

Next interaction that we create is displaying text and sound with a click on some of the panels. For that purpose, firstly in the node of our object (Master EON) we entered the sound node (Direct Sound) shown on Fig. 8, which should display when click on some of the panels. Once is inserted the sound field, it is necessary to select the sound file that will be emitted when click on that panel sound in .wav format (Proba.wav).

To display the text, it is necessary in Camera node to insert node for showing text (2D Text), Fig. 8. The characteristics of this node in the Text field we write the text we want to be shown on the screen when clicking on some of the panels.

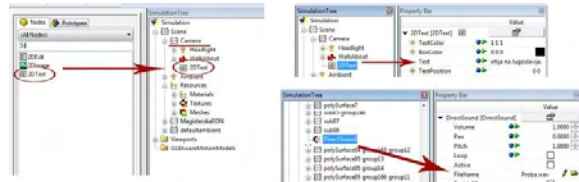


Fig.8. Left: Importing node to display text (2D Text); Right up: Text input field for entering the text you want to display; Right below: Input sound file that will be broadcast;.

Our model is composed of several panels, walls and objects, so we need to find the panel through which we want to play sound and text. In our case it is the frame (node) group 17 group 31 pCube496 and in that section enter Click Sensor node, Fig. 7. With this node we say that when click the panel should show some events, in our case should play the sound and show the text.

The last thing to do is to create a simulation, i.e. to create events that will occur in the simulation. The first event is: to show text when clicking on the panel; Second event is: to play sound on click on the panel, and the last event is to close the text field when click on already displayed text. These events are created in the section Routes: Simulations shown in Table I and Fig. 9.

TABLE I  
LINKS FOR CREATING INTERACTION

Node	Output event	Node	Input event
Click Sensor	On Button Down True	DirectSound	SetRun
Click Sensor	On Button Down True	2D Text	SetRun
2D Text	On Click	2D Text	SetRun_



Fig.9. Entering nodes and creating links, and launch the simulation.

With that ends the creation of the simulation and events that will contain the simulation, so we can start it. When we click on the panel marked on the picture, in the left part of the simulation shows the text, and in background play the sound which refers to this panel, shown in Fig. 9. When clicking on the text, it closes.

## V. CONCLUSION

The technology of virtual reality is a complex area. Characteristic of VR technology over other multi-media systems is behavior in real time. Here is presented step by step, process of creating such applications and at the end will mention some of the problems faced when creating this virtual tour. In Fig. 10 can be noted that the model largely correspond with the real object, which means that the process of modeling and texturing is successful.



Fig.10. Comparison of the outside of the actual object and the model.

In addition there is a comparison between the model in Autodesk Maya and model in EON Studio shown in Fig. 12. From the comparison can be seen that the model in EON Studio looks a bit unreal because we have a great reflection and clarity of the image, so that can be specified as a small disadvantage. However, it may be noted that to some extent, correspond to the model in Maya, and to the real object.



Fig.11. Top - Picture of the rooms, obtained by rendering the model in Maya; Below - picture of the rooms received the application in EON Studio.

It is important to note that when insertion of the model in EON Studio, was required to do triangulation. But in process of triangulation, all models made by NURBS are excluded from the model after triangulation as can be seen in Fig. 12. It is recommended during the modeling to use exclusively polygonal objects, because none software can perform triangulation of many irregular shapes created by NURBS.

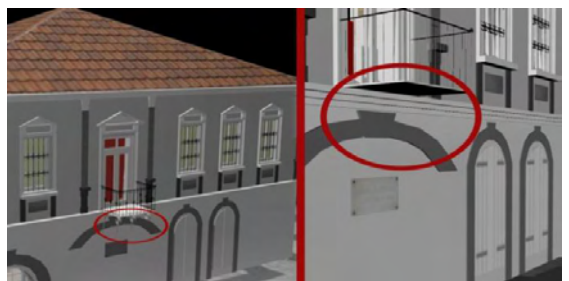


Fig. 12 Loss of NURBS objects in triangulation.

Last dependence which will be mentioned is the reliability of the model in EON from configuration the application is launched. Fig. 13 shows a graphical application started on weaker graphic configuration, so it can be notice that the model has high losses which means that these VR applications greatly depends on the configuration of the computer, especially from graphic cards.



Fig.13. Configuration: Laptop computer; CPU - Intel Core i7 - 2630QM 2.0 GHz; RAM - 6 GB; Video adapter - Intel Graphics 3000

With this it is completed the process of creating VR application and we saw all the advantages and disadvantages of creating such application.

## REFERENCES

- [1] D. Blythe, "Advanced graphics Programming Techniques Using OpenGL", Siggraph, 1999.
- [2] G. Burdea, P. Coiffet, J. Wiley, "Virtual reality technology 2nd edition", 2003.
- [3] J. Foley, A. Van Dam, S. Feiner, J. Hughes, "Computer Graphics: Principles and Practice", Addison-Wesley, 1995.
- [4] L. Graft, B. Dwelly, D. Riesberg, C. Mogk, 2002, "Learning Maya: Character rigging and animation", ISBN: 0-9730052-3-8.
- [5] M. Gutierrez, F. Vexo, D. Thalmann, "Stepping into Virtual Reality", 2008.
- [6] J. Justice, M. Bergerud, J. Garrison, D. Cafiero, L. Churches, "Interactive 3D application development: Using EON professional for creating 3D visualizations", 2009.
- [7] I. Nedelkovski, "Computer Graphics (3D modeling and animation)", 2008.
- [8] An EON Reality whitepaper, "EON – Creating applications applying interactive visual simulation technology for the PC", 1999.

# Improved Data Transfer for Wireless Meteorological Stations

Orlin Plamenov Stanchev<sup>1</sup>, Emilian Boyanov Bekov<sup>2</sup> and Vencislav Cekov Valchev<sup>3</sup>

**Abstract –** In this paper the preferred wireless data transfer technologies are described and analysed. A meteorological data organization and management is proposed. An improved data processing algorithm is given. An implementation in microprocessor system is proposed and experiment with GPRS data transfer and FTP protocol is accomplished.

**Keywords –** Meteorological Station, Wireless Data Transfer, GPRS.

## I. INTRODUCTION

The modern technologies represent variety of possibilities for research in the area of communications. This progress also affects the technical resources for handling meteorological data. A major problem for transferring such a data is the available communication options, especially for more distant and inaccessible meteorological stations. Therefore the wireless data transfer methods are preferred as they are offer a number of advantages when used in a meteorological data acquisition system. But these methods have their own specifics and factors that have to be taken in account when choosing the most appropriate one. These problems and their improved solutions are introduced and analyzed in this paper. The main focus is on the computer based data processing and the network based communication methods that are convenient for post processing and complicated meteorological analysis. The meteorological system could be organized in different way when the information is used for synoptic meteorology, warnings for dangerous weather conditions, climatology, past analysis etc. [1].

## II. PREFERRED WIRELESS DATA TRANSFER TECHNOLOGIES

### A. Requirements and Criteria

The preferred wireless data transfer technologies have to fulfill several requirements and criteria which matter is determined by the exact application of the meteorological station and the organization of the whole data acquisition

<sup>1</sup>Orlin Plamenov Stanchev is with the Faculty of Electronics at Technical University of Varna, 1 Studentska Str., Varna 9000, Bulgaria, E-mail: or.stanchev@gmail.com.

<sup>2</sup>Emilian Boyanov Bekov is with the Faculty of Electronics at Technical University of Varna, 1 Studentska Str., Varna 9000, Bulgaria, E-mail: vencivalchev@hotmail.com.

<sup>3</sup>Vencislav Cekov Valchev is with the Faculty of Electronics at Technical University of Varna, 1 Studentska Str., Varna 9000, Bulgaria, E-mail: emo\_bekov@hotmail.com.

system [2].

The first criterion is the *data transmission interval*. It depends on the purpose of the measurement data. If a real time monitoring is accomplished, the data transmission should be initialized on relatively small intervals of time, depending on the speed of change of the measurement values. On other hand the station could be used for data logging for the purpose of climatological researches and in that case a data transmission on relatively long interval of time i.e. one or few days with proper processing and compression, is enough. An emergency situation could occur when a rapid change of measurement value occurs or a predefined limit is approached and this situation could be reported with immediate unplanned transmission session.

The second criterion combines *speed and reliability of transmission*. In real time monitoring the measurement data has to be transferred with proper speed that can be achieved with the wireless technology. The transfer has to be reliable enough so that the measurement data stays unchanged. This is provided by the high and low level protocols.

Another criterion is the *price*. The price of the communication could be a crucial factor and it has two main aspects. The first one is the initial price of the communication equipment and the second aspect is the data transfer price. A meteorological measurement system that comprises of more than few stations, working with several sensors at short sampling period generates lots of traffic that could be very expensive if improper wireless technology is chosen.

The last reviewed determining criterion is the *accessibility*. The wireless technology has to be accessible to all meteorological stations during the scheduled and possible unscheduled transmission sessions. This is more difficult to implement when measurement stations are situated on a wide area and/or are significant number.

The preferred wireless technologies are introduced in the following sections.

### B. UHF Radio Technology

The Ultra-High Frequency (UHF) radio technology works in the frequency range between 300 MHz and 3 GHz. The exact communication frequency has to be selected according to the free and allowed by laws range which is specific for most of the countries. The UHF Radio Technology gives lots of freedom of design due to the specifics of the measurement systems, although it requires more time and expenses for design. A factory radio transmitter or transceiver modules are more appropriate to be used, giving a physical range up to few hundred meters, which could be easily embedded into the meteorological station hardware. Also a custom transmission protocols have to be designed and special care has to be taken for low-power consumption. The physical range could be

expanded on relatively short distances, using retranslators or on unlimited distances, changing the communication media i.e. using Internet. Major disadvantages of these approaches are the additional complexity and the additional expenses of the measurement system.

The custom UHF radio technology in the common case is suitable for data acquisition systems with more than few meteorological stations that are situated on limited area.

#### *C. ZigBee Technology*

The ZigBee technology is a suite of high level communication protocols that use low-power digital radios, all unified into single housing. It is based on the UHF standard and normally uses the legalized 2.4 GHz transmission frequency [4]. ZigBee technology has a low data rate but low-power consumption and secure networking. The physical range is up to 1000 m. The ZigBee modules are capable of rerouting signal from other devices and expand the physical range. They could be used for building wireless personal area networks (WPAN) for the needs of meteorological data acquisition systems and give flexibility.

The ZigBee technology is cost effective solution which is appropriate for meteorological system with one or more meteorological stations, situated on limited area.

#### *D. GSM Technology*

The Global System for Mobile communications (GSM) is widely used, constantly developed and adapted for the needs of small size, low-consumption mobile devices such as mobile phones. There are factory application specific transceiver radio modules with different characteristics, working with the GSM standard.

The coverage and the service itself are provided by GSM operators. In Bulgaria they are available in the inhabited territories and in most of the agricultural and forest territories. The same situation exists in most of the European countries. This is major advantage for big meteorological data acquisition systems, situated on large territory i.e. for creating wind solar map or researching agricultural conditions.

The GSM technology includes several communication services that differ from audio (voice) transfer.

The Short Message Service (SMS) transfers digital messages with fixed size of 1120 bits. They are sent to SMS center which provides store and forward mechanism. The time of delivery and the delivery itself are not guaranteed, but in the common case it is almost immediate. SMS are charged per unit and are not cost effective for transfer of meteorological data. In meteorological stations they could be used for activating the other GSM services when they are switched off or in some kind of emergency situations i.e. system fault.

The unlimited communication service that is the most suitable for meteorological stations is the General Packet Radio Service (GPRS). It communicates through Internet and the GPRS device has unique Internet Protocol (IP) address. It is extremely flexible and cost effective as only the used traffic is charged and it is not affected by the destination or the active connection time. GSM GPRS communication is suitable for

all kinds of meteorological stations that could be easily centralized through Internet into single database server and/or mobile devices.

### III. METEOROLOGICAL DATA ORGANIZATION

The meteorological data acquisition system consists of single or numerous measurement stations that constantly send data. The data has to be properly managed so that it is properly stored and could be rapidly accessible and used. The best approach to satisfy these conditions is to use a centralized server (a dedicated computer, a web based application or a portable device) where the meteorological station/s periodically synchronize data (not only send meteorological data but also receive new settings and necessary operational information). The server provides long-term data storing into database that supports the necessary queries. The server also has to be on-line for scheduled synchronizations and be able to communicate with multiple stations at the same time.

A sample meteorological data organization is given on Figure 1.

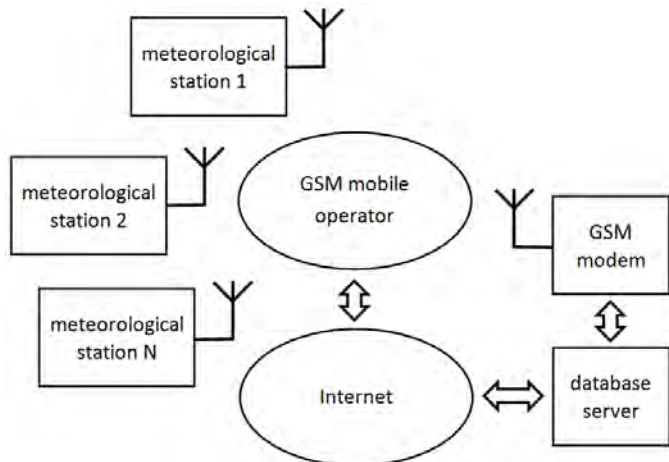


Fig. 1. Meteorological data organization using GSM technology

A major advantage of such a system is the usage of an improved data processing algorithm that obtains processes data in advance so that the communication line is unloaded and server storage place is reduced.

### IV. IMPROVED DATA PROCESSING ALGORITHM

The data processing algorithm manages the data from the digital sensors outputs to the report file that is ready to be sent by the preferred wireless data transfer technology. It consists of two major stages. The first stage is adapted due to measurement value specifics of each sensor. It implements digital filtering and decimation of the sensor output [7]. The digital filter is low pass filter with finite impulse response (FIR) which band stop frequency depends on the typical signal frequency range. Decimation is accomplished, gaining efficiency to the digital filter. It is combined with averaging so that samples are reduced with interval of seconds or minutes, depending on the needed meteorological value minimal

resolution that is determined due to speed of change of the measured value i.e. samples reduction for wind velocity is completely different, compared to ambient temperature.

The FIR filter performs the following convolution equation:

$$y_n = h(k) * x(n) = \sum_{k=0}^{N-1} h(k) \cdot x(n-k) \quad (1)$$

The second data processing algorithm stage implements different kind of data sample reduction. It is similar to data compression as the total data size is reduced. Its purpose is to decrease sampling rate in the signal sections where the signal speed of change is lower and to keep the sampling rate high or unchanged where the signal speed of change is high so that the substantial information of the signal remains, local and global maximal, and minimal values are available. It is one directional data signal compression with quality reduction in the less important sections of the signal. This approach is appropriate for meteorological data management as the necessary information for analysis can be obtained from the compressed signal and the data size and server storage place are optimized without using decompression when the signal is analysed. A sample wind velocity data is given on Figure 2. The data are taken from DAVIS weather station Vantage Pro2 installed on the territory of Technical University of Varna.

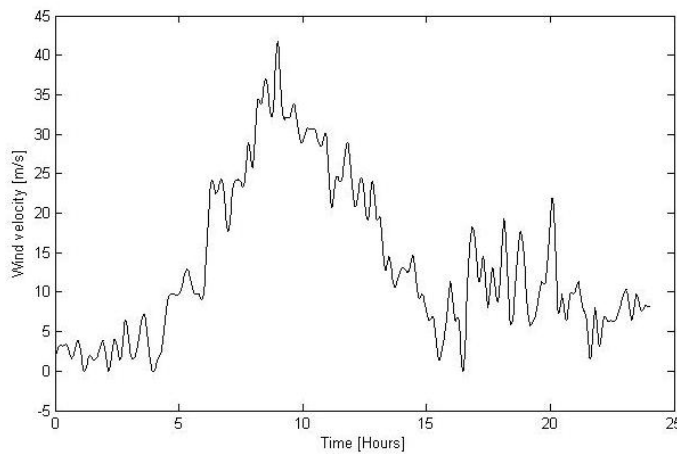


Fig. 2. Wind velocity data per day

The proposed approach for implementing the second part of the data processing algorithm is wavelet transformations [8]. The wavelet transformations provide information for the signal in both frequency and time domain so that rapid changes in the signal could be localized in time. Higher the resolution in time, lower the resolution in frequency so a proper balance has to be maintained.

So the second part of the improved data processing algorithm implements a wavelet analysis of a time window of the signal from a sensor that is already decimated and averaged. Afterwards the signal is variably compressed due to wavelet analysis results.

## V. IMPLEMENTATION IN MICROPROCESSOR SYSTEM

The proposed data processing algorithm is designed to be implemented into a microprocessor system that will satisfy application specific requirements. The microprocessor has to be capable of performing the algorithm calculations in parallel while reading the sensors and managing the station periphery, combined with low-power consumption as distant meteorological stations run on limited power supplies. The 32bit ARM Reduced Instruction Set Computer (RISC) microprocessor fulfills the requirements and it is widely used in high performance portable devices [5].

Experiments are accomplished using the combined communication module GE863-PRO<sup>3</sup> of Telit Wireless Solutions [6]. It combines an independent ARM9 microprocessor, driving a four band GSM/GPRS modem, memory and periphery, giving a major part of the necessary hardware for an embedded microprocessor communication system. The module has major advantages that make it very suitable for these experiments. The ARM core has operating frequency of 180 MHz, enough for algorithm calculations. The module has built in TCP/IP protocol stack, FTP and SMTP protocols. It operates in wide temperature range from -30 °C to +80 °C so it can withstand real operating conditions of a meteorological station.

The GE863-PRO<sup>3</sup> combined module is embedded into a development kit so that all resources are easily accessible. The kit provides fours standard COM ports and USB port for direct connection with personal computer and monitoring the inner state. The ARM core is programmed via JTAG interface and the GSM/GPRS modem is controlled by AT commands through a serial interface [4]. The sensors board is plugged in the connector, placed on the top side of the board that provides direct access to the ports of the ARM microprocessor.

The development board is given in Figure 3.

The communication experiment is accomplished with the GSM/GPRS part of the combined module. The GPRS service

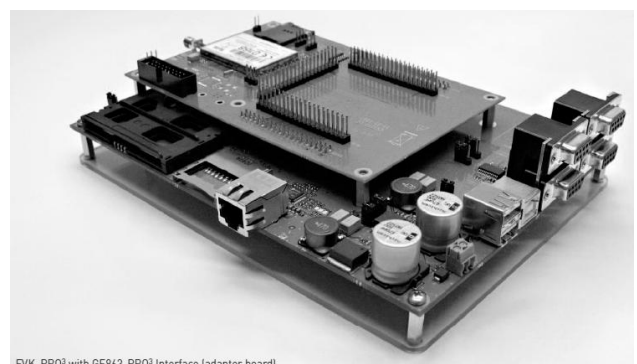


Fig. 3. EVK-PRO<sup>3</sup> Development board

is activated using a SIM card with mobile internet, provided by a mobile operator. A measurement data file is sent to a specially configured ftp server that is connected to the Internet.

The AT command sequence is given in Table I.

**TABLE I**  
AT COMMANDS SEQUENCE FOR GPRS COMMUNICATION

Terminal window	Comment
AT OK	Available communication with GSM/GPRS module
AT#QSS=1 OK	SIM card is available
AT+CPIN? +CPIN: READY OK	PIN code check
AT#MONI #MONI: GLOBUL BSIC:66 RxQual:0 LAC:1392 Id:9C6A ARFCN:91 PWR:-60dbm TA:0 OK	Mobile operator cell is available with the stated signal power
AT+CGDCONT=1,IP,globul OK	Defining Packet Data Protocol (PDP) - Access Point (AP) "globul", data protocol is Internet Protocol (IP)
AT#GPRS=1 +IP: 10.8.215.135 OK	The GPRS service is activated and an IP address is assigned
AT#FTPOPEN=87.126.32.18:21, AMStation, 123456,0 OK	Opening a FTP connection to server with username and password
AT#FTPPWD #FTPPWD: 257 "/" is current directory. OK	Checking the working directory
AT#FTPCWD=station_1000023 OK	The working directory is changed
AT#FTPPWD #FTPPWD: 257 "/station_1000023" is current directory. OK	Checking the working directory
AT#FTPPUT=20121103_183045.XML CONNECT	Opening a data transmission line and transferring data into a specific file
AT#FTPCLOSE OK	Closing the FTP connection

## VI. CONCLUSION

In this paper the different wireless data transfer technologies are given and analyzed. It is proposed which method for what type of meteorological station and for what distances is more appropriate.

A methodology for data processing in advance is proposed. The measured signal is processed with digital filter and wavelet transformations. As a result the significant meteorological information from the meteorological sensor signal is retained and the total data size is reduced.

An implementation in ARM based microprocessor system and experiential communication module are proposed.

An experimental data transmission is accomplished over Internet using the GPRS service of GSM communication technology and the embedded FTP client protocols.

## ACKNOWLEDGEMENT

The carried out research is realized in the frames of the project BG051PO001-3.06-0005, Program 'Human Resources Development', Ministry of education, youth and science, Bulgaria.

## REFERENCES

- [1] Koninklijk Nederlands Meteorologisch Instituut, "Handbook for the Meteorological Observation" September 2000.
- [2] Lewis. F. L. "Wireless Sensor Networks", Smart Environments: Technologies, Protocols and Applications, New York, 2004
- [3] Bekov E., Kiryakov J., "Resources for Wireless Transfer of Meteorological Data", Computer Science and Technologies
- [4] ZigBee Aliance, www.zigbee.org, 2013
- [5] ARM Ltd. arm.org, 2013
- [6] Telit Wireless Solutions, www.telit.com, 2013
- [7] Kester W., "Mixed-Signal and DSP Design Techniques", Analog Devices, 2000
- [8] C. S. Burrus, R. A. Gopinath, "Introduction to Wavelets and Wavelet Transforms", Prentice Hall, 1997.

# Interoperability of Cloud and Mobile Services

Aleksandar Bahtovski<sup>1</sup> and Marjan Gusev<sup>2</sup>

**Abstract –** Cloud Computing picks up speed in the last few years as a result of the well-known key characteristics, such as Virtualization and pay-by-use, which together form an innovative concept. The main purpose of this article is to explain why *interoperability* is a huge challenge in cloud computing. We define and explain some of the cloud computing *interoperability* standards and reasons why they should be used. *Interoperability* of Mobile Services is within the focus of this work. Three different types of models are explained.

**Keywords –** Cloud Computing, SaaS, PaaS, IaaS, Interoperability, Mobile Services.

## I. INTRODUCTION

Cloud computing is an entirely new technology based on the development of parallel computing, distributed computing, grid computing and virtualization technologies, thus defining the shape of a new era [1]. It has emerged as a result of the evolution of Virtualization, Utility computing, Software-as-a-Service (SaaS), Infrastructure-as-a-Service (IaaS) and Platform-as-a-Service (PaaS). Cloud computing can be defined as accessing third party on-demand software and services[2]. It allows scalability and virtualized resources over the Internet as a service, providing a cost effective and scalable solution to the customers. Cloud computing rapidly evolved as a technology especially in the last 3-4 years with the presence of many vendors in the cloud computing market.

The presence of numerous vendors in the cloud requires a need of *interoperability*. With *interoperability* consumers can share applications, services, data on different machines from different vendors. This means that application and services that are used by an enterprise can be placed on different platforms hosted by different vendors. *Interoperability* means a possibility for two or more networks, systems, applications, or devices to externally exchange and readily use information, in a secure and effective manner, as presented on Figure 1.

As the hype over cloud computing evolves into a more substantive discussion, one thing has become clear – customers do not want to be locked into a single cloud provider[3]. They like to move among the clouds, from private to public and back again. This would give customers the freedom to switch between providers according to their needs and also the ability to move applications around as their business requirements change. True cloud *interoperability* will not occur for some time. Standards are nascent and will take years to fully develop.

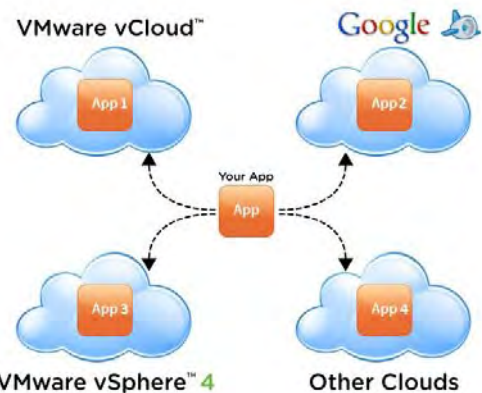


Fig. 1. Interoperability in Cloud Computing

The rest of the paper is organized as follows: In Section II we define *interoperability* in cloud computing, definition of *interoperability*, requirements, as well as two dimensions of *interoperability*, Vertical and Horizontal. Then in Section III we define *Interoperability Issues* in cloud computing. Correlation to Mobile technologies is explained in Section IV. Finally, the related work and conclusion are presented in Sections 5 and 6 respectively.

## II. INTEROPERABILITY IN CLOUD COMPUTING

This section explains the definition of *interoperability*, as well as the requirements that each of three service models (IAAS, PAAS, SAAS) have. Also this section covers two dimensions of cloud computing, Vertical and Horizontal.

### A. Definitions of Interoperability

In the IEEE glossary [4], *interoperability* is defined as the ability of two or more systems or components to exchange information and to use the information that has been exchanged. According to Petcu[5], there can be several definitions of cloud *interoperability* in the literature. For example, *interoperability* has been defined as the possibility to abstract programmable differences from one cloud to another, the possibility to translate between the abstraction supported from different clouds, to flexibly run application, locally, in the cloud or in a combination, or to use the same management tools, server images, software in multiple clouds.

### B. SAAS Interoperability

*Interoperability* in SAAS enables different applications to exchange information between themselves. Enterprises store and maintain their data in an existing enterprise application, on premise, or somewhere in the cloud. Therefore they need

<sup>1</sup>Aleksandar Bahtovski is with the Faculty of Information Sciences and Computer Engineering Skopje, Macedonia,  
E-mail: abahтовски@gmail.com.

<sup>2</sup>Marjan Gusev is with the Faculty of Information Sciences and Computer Engineering Skopje, Macedonia,  
E-mail: marjangusev@gmail.com.

to be sure that every SaaS application which is a part of their global strategy will be interoperable. This means that every SaaS vendors must provide the exchange of data interfaces in order to keep applications synchronized. Nevertheless, heterogeneous, common data must be able to flow between applications. Also, data modification, in master enterprise application should be synchronized with other SaaS applications, in a seamless manner.

#### C. PAAS Interoperability

During the deployment of the applications in PaaS, developers are able to use tools, libraries or APIs from different PaaS providers. PaaS providers make efforts to achieve better *interoperability* between cloud providers. One of the main elements of PaaS is the existence of APIs. Although having an API doesn't make a certain system a platform, APIs are the key of the great success of PaaS. APIs facilitate the work of the developers and allow them easier access to the platform functionalities. Instead, they use the API from the very beginning and have easy access to the functionality. *Interoperability* of the applications deployed on PaaS is limited because every application is developed using a different programming language, .NET, Java, PHP, Python, Ruby. This enables dealing with different data models and proprietary runtime frameworks that each application requires and each provider enables quite challenging. At the moment, there are no developed standards for *interoperability*, but there are several initiatives by nonprofit groups and some providers [7].

#### D. IAAS Interoperability

*Interoperability* in IAAS refers to the ability of the client to use infrastructure resources from different vendors through a common management API. VMs comprise the fundamental working structure for an IaaS platform. The number of consumers that want to have mixed virtual environment in theirs enterprises and to be able to move VMs between providers is growing. For instance, every customer should be able to do the same set of operations on VMs from different providers without creating clients for them[6].

#### E. Two Dimension of Cloud Computing Interoperability

There are two main dimensions of cloud computing *interoperability*: Vertical and Horizontal. Vertical dimension defines how cloud computing facilitates *interoperability* in one enterprise cloud platform, but between different devices and applications which are used by the end users to access the information stored by the cloud provider. The vertical dimension defines *interoperability* in terms of the cloud computing affordances of a single provider, generally from an end-user or a consumer perspective[8]. Assessing the vertical dimension implies asking such questions as *Does cloud based software works on most Internet connected devices?* or *Can cloud based software allow using of other applications or data available from users' device?*

The vertical dimension simplifies two interrelated elements, device independence and location independence. When a customer accesses their data or services on the cloud, they are not limited to use the device on which the data and applications are stored. Instead they can use any Internet-connected device to do this. The possibility to store and use the applications on the cloud allows the user to access the information and applications from devices with lower performances. The customer becomes less dependent from devices performance and also may benefit in both convenience and cost savings.

On the other hand, horizontal dimension defines *interoperability* between different platforms. This dimension implies how an enterprise which hosts its service on a cloud can easily switch it to a competing provider which offers favorable rates and reliable service. It also addresses whether there are consistent ways to coordinate among distinct cloud products, such as standardized contractual arrangements, security features, data privacy terms of service, or identity management capabilities. These multifaceted dimensions of horizontal *interoperability* might be salient for end-users as well as for companies that purchase cloud products[8].

### III. INTEROPERABILITY ISSUES

Initiatives like OGFs Open Cloud Computing Interface (OCCI, 2010), are trying to bring APIs specification for development and monitoring in a short period of time. It takes time for standards to mature and for reference implementations to become available. Until then, the users will use APIs from cloud computing vendors, which they think are most suitable for their requirements. When standards emerge and vendors want to use services from other vendors then brokers/adapters need to be used for *interoperability*. However new users will be able to use the new standard APIs. With some of the major vendors like Microsoft and Amazon rejecting CCIF agenda and using their own *interoperability* agenda, standardization becomes more difficult to achieve. This could lead to a scenario in the long run where multiple standards co-exist and customers would use brokers/adapters for *interoperability* for using services from multiple cloud service providers[9].

#### A. Towards a solution

Stepping towards a commonly and widely adapted solution means that there is a considerable amount of work and research to be performed. However, initially there are key observations collected, which cannot be ignored simply by an approach for developing a new *interoperability* standard[10]. Amazon, GoGrid, SalesForce, Google, AT&T, and other cloud providers, probably will not accept the standardization for export/import of cloud configurations. They are not interested in giving total freedom to their clients in changing providers and they don't want to compete with other companies. Each of the cloud providers offers different services and wants to have unique services to attract more customers.

### B. Upcoming cloud standards

In order to regulate cloud computing, a standard similar to the popular TCP/IP for networking is required. Most likely it would be an API that will be implemented in all cloud products and services and would promote transparent *interoperability*. But such implementation is way out in the future. It is more straightforward to come up with standards to the low-level cloud concept (IaaS), than PaaS (Platform as a Service) or SaaS. In this way, efforts have to be undertaken to distinguish which features or common characteristics should be interesting to standardize in each level[10]. Some of the vendors are pushing their own standard. VMware has submitted its vCloud API to the Distributed Management Task Force (DMTF) for ratification as an open standard, and Red Hat has submitted its Delta cloud platform to the DMTF as well. VMware's vCloud is being used in VMware-based private clouds and in its partners' vCloud Express public clouds, providing users with some cloud *interoperability*, but at the expense of almost total lock-in. The only real cloud standard to date is OVF (Open Virtualization Format). However, it only relates to the packaging of virtual machines for facilitating their mobility [3].

## IV. RELATED WORK

Recently, some of the CC concerns are about the *interoperability* between different providers (Parameswaran and Chaddha,2009), (Dikaiakos et al., 2009). It should be possible for developers to swap enablers between platforms whenever they need to (performance issues, actual costs, etc.) without re-architecting the solutions. This can be very challenging with different data models and runtime frameworks that each application required and each provider enables. Currently there are no standards for *interoperability*, but there are initiatives from non-profit groups with the collaboration of researchers and some Cloud service providers.

The Open Cloud Manifesto (OCM, 2010) is an initiative supported by various vendors with the vision to standardize Cloud Computing (interoperability, portability, security, governance and management, etc.). The goals of open cloud such as flexibility, speed and agility are outlined to lead a discussion for the new cloud computing paradigms and impacts.

Another group, the Cloud Computing Interoperability Forum (CCIF, 2009), proposes to unify Cloud APIs with a standardized semantic interface (Unified Cloud Interface) (UCI, 2009) and abstraction layers from the underlying infrastructure. The orchestration layer and the federation of clouds are the characteristics of the CCIF presented architecture.

## V. CORRELATION TO MOBILE TECHNOLOGIES

Mobile and Cloud Computing are the two dominant transformations driving the IT industry in the recent and moreover, upcoming years. The mobile devices (smartphones,

computers, etc.) are increasingly becoming an important part of the human life as most efficient and most proper communication tools. The mobile device users accumulate wide experience of different services from mobile applications (iPhone Applications, Google Applications etc.) which work on devices and/or on remote servers through wireless networks. Mobile devices that access the Internet perform mobile cloud computing: handsets need to borrow storage and computing power from the cloud because of their limited resources or because it makes more sense. Accessing data in the cloud from mobile devices is becoming a basic need.

### A. SAAS interoperability vs. Mobile Technology

Mobile cloud services are largely dominated by the vendors. Installing new software on phones was not an option for the mass market until recently. Vendors like Apple and Google that host applications and services used by the mobile devices are "closed" for using *interoperability* (Figure 2). That is the reason why *interoperability* is facing a lot of problems. Users of one handset may want to get their email from a provider but sync pictures with another. Or if they buy music from a digital store from the desktop computer, they want to sync their playlists with any phone. Consider these recent cases that demonstrate that users of mobile cloud services are exposed to serious problems. For example, users cannot access the music that they bought and stored in Apple's iTunes: Apple still wants to own the music they sold to its users and keep their data hostage. Similar risks are run by owners of Amazon Kindle, who had their purchased books deleted too easily by Amazon from the devices. Also most of the providers like RIM, Apple, prevent user to run applications which are not digitally signed. With mobile cloud it is more important than ever that people have the full ability to access and preserve their data, which means using the open mobile cloud. These are just visible signals of proprietary services battling to own user data. If iTunes and Amazon used interoperable and open standards, which could be safely implemented in free open source software, their users would not face these problems. Due to the fact that there are nearly 6 billion mobile devices, the use of *interoperability* is more than necessary in MCC, but it is still not deployable enough in CC.

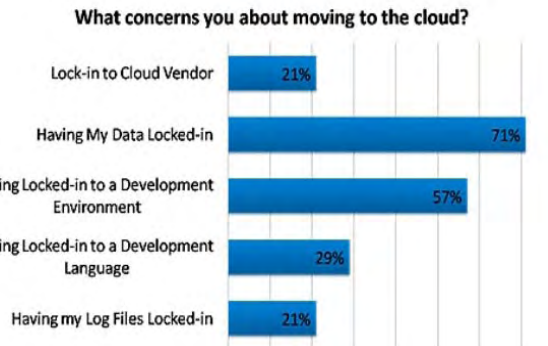


Fig. 2. Interoperability Lock-In

### B. PAAS interoperability vs. Mobile Technology

Developing an application which can be used on various mobile platforms is very difficult. All of them (Android, iOS, BlackBerry, Symbian, Windows Phone, etc.) are using different SDK (Software Development Kits), different libraries and different ways of design user interfaces. Programming languages are also different for each platform. Developer should know these languages in order to deploy an application. Also, developer should be familiar with platform standards, SDKs, etc. In addition, developers need to know devices available for each platform. For instance, Android has many different devices available, like smart phones, tablets. iOS, has only iPhone and iPad. These devices have different screen resolution, different aspect ratio, which makes difficult for developer to make user interface well scalable. The solution to this is using multiplatform Frameworks like JQuery Mobile, PhoneGap and Titanium Mobile. These multiplatform frameworks come in many variations. Some of them only change the visual appearance of web apps while others offer whole software development kits on their own, which can build the developed apps to multiple target platforms as native apps. These frameworks are growing rapidly and new features are being added. So when developers want to use some of the frameworks, they first should check several platforms features before starting multi-platform development.

### C. IAAS interoperability vs. Mobile Technology

As stated before IAAS refers to the ability of the providers to use infrastructure resources from different vendors. In Mobile IAAS, *Interoperability* means the use of infrastructure and standards from different mobile providers. A pure example for IAAS *Interoperability* is Roaming. Roaming refers to the extension of connectivity service in the locations different from home location. Roaming enables customers to use services provided by his home provider while travelling outside the coverage area of the home network. There are a couple of roaming types:

Regional Roaming enables customer to move between different regions inside the national coverage of the mobile operator and to use the services provided in that region by the operator.

National Roaming allows customers to move from one operator to another in the same country. This usually happens when a mobile provider gets a license and starts trying to be competitive but doesn't have coverage in all areas. This kind of operator requires the existing operators to allow roaming for the customers while he has time to build his own network.

International Roaming means moving to foreign service providers networks. The easiest way is by using the GSM standard, used by approximately 80% of the providers worldwide. But still there may be a problem, because countries using different frequency band. Most of the world operators are using GSM 900/1800MHz frequencies, but United States and most of the countries in the East are using 850/1900MHz.

The solution is in Inter-Standard Roaming. Customers want to use their phones in areas where there is no standard used in their home network or there is no Roaming agreement with the country they originate from. So with Inter-Standard Roaming customers arriving in Europe from USA or East can register on available GSM network.

## VI. CONCLUSION

*Interoperability* between cloud providers is the only way to avoid vendor lock-in and open the way towards a more competitive market for cloud providers and customers. Hence, addressing the issue of *interoperability* and *portability* is both timely and necessary. In this article we explained two dimensions of cloud computing *interoperability* and their advantages, why they are so important and where they can be used. The only way to achieve *interoperability* is by introducing cloud standards accepted by all big cloud vendors. Until now most of them are not interested to give total freedom of their clients. Each of them offers different services and wants to have unique services to attract the customers. That's why *interoperability* standards are far from adoption and there is a long way to go in order to achieve *interoperability*. True cloud *interoperability* will not occur for some time. Standards are nascent and will take years to fully develop.

## REFERENCES

- [1] G. Fotis, I. Paraskakis, and D. Kourtesis, "Addressing the challenge of application portability in cloud platforms," in 7th SEE Doctoral Student Conference, 2012, p. 565576.
- [2] C. Ashesh and A. V. Parameswaran, "Cloud interoperability and standardization," Journal of Networks, vol. 7, no. 7, 2009.
- [3] Claybrook Bill. (2013, April) computerworld. [Online].Available:  
<http://www.computerworld.com/s/article/9217158/Cloud>  
interoperability Problems and best practices
- [4] IEEE. (2012, Mar.) Ieee standard glossary. [Online]. Available:  
[http://www.ieee.org/education\\_careers/education/standards/standards\\_glossary.html](http://www.ieee.org/education_careers/education/standards/standards_glossary.html)
- [5] P. Dana, "Portability and interoperability between clouds: challenges and case study," Proc. of the 4th European conf. on towards a service-based internet, Poznan, pp. 62–74, 2011.
- [6] D. Cunha, P. Neves, and P. Sousa, "Interoperability and portability of cloud service enablers in a paas environment," in CLOSER'12, 2012, pp. 432–437.
- [7] H. Piyush, F. Dudouet, R. G. Casella, Y. Jegou, and C. M. I. Rennes, "Using open standards for interoperability issues, solutions, and challenges facing cloud computing," 6th International DMTF Academic Alliance Workshop on Systems and Virtualization Management: Standards and the Cloud, 2012.
- [8] B. Matthew, "Interoperability case study: Cloud computing," Berkman Center for Internet and Society, Harvard University, 2012.
- [9] V. P. Chaddha Asheesh, "Cloud interoperability and standardization," SETLabs Briefings, vol. 7, no. 7, pp. 19–26, 2009.
- [10] S. Guilherme Sperb Machado, David Hausheer, "Considerations on the interoperability of and between cloud computing standards."

---

---

## Poster 5 - Digital Image Processing

---

---



# Adaptive Vision System

Rosen Spirov<sup>1</sup> and Neli Grancharova<sup>2</sup>

**Abstract –** This paper presents the object detection algorithm implemented in FPGA was based on feature detection and image filtering. Object detection and tracking is the process of determining presentation it in an image. A software-based algorithm was independently developed and examined in MATLAB to evaluate its performance and verify its effectiveness.

**Keywords –** Image Processing, Filters, FPGA, Video.

## I. INTRODUCTION

The goal of this project was to create an FPGA system to detect and track an object in real time. The overall setup included the Verilog program, an Altera DE2 board, a camera, and a VGA monitor. The object detection algorithm implemented here was based on feature detection and image filtering. After the object region was detected, its location was determined by calculating the centroid of neighboring feature pixels [1].

A software-based algorithm was independently developed and examined in MATLAB to evaluate its performance and verify its effectiveness. However, it was infeasible to implement the same algorithm in Verilog due to the limitations of the language. Hence, several stages of the algorithm were modified.

Experimental results proved the accuracy and effectiveness of the hardware realtime implementation as the algorithm was able to handle varying types of input video frame. All calculation was performed in real time. Although the system can be furthered improved to obtain better results, overall the project was a success as it enabled any inputted face to be accurately detected and tracked.

## II. DESIGN AND THE SOFTWARE ALGORITHM

Different approaches to detect and track dynamic objects, including feature-based, appearance-based, and color-based have been actively researched and published in literature. The feature-based approach detects a dynamic's objct based on dynamic object features, such as human eyes and nose. Because of its complexity, this method requires lots of computing and memory resources. Although compared to other methods this one gives higher accuracy rate, it is not suitable for power-limited devices.

<sup>1</sup>Rosen Spirov is with the Faculty of Electronics at Technical University of Varna, 1 Studentska Str, Varna 9010, Bulgaria, E-mail: rosexel@abv.bg.

<sup>2</sup>Neli Grancharova is with the Faculty of Telecommunications at Technical University of Varna, 1 Studentska Str, Varna 9010, Bulgaria

Hence, a color-based algorithm is more reasonable for applications that require low computational effort. In general, each method has its own advantages and disadvantages. More complex algorithm typically gives very high accuracy rate but also requires lots of computing resources. General design stages are illustrated in next steps.

- ❖ First, the original image was converted to a different color space, namely modified YUV. Then the skin pixels were segmented based on the appropriate U range.

- ❖ Morphological filtering was applied to reduce false positives. Then each connected region of detected pixels in the image was labeled.

- ❖ The area of each labeled region was computed and an area-based filtering was applied.

- ❖ Only regions with large area were considered face regions.

- ❖ The centroid of each face region was also computed to show its location.

Converting the object pixel information to the modified YUV color space. The conversion equations are shown as follows:

$$Y = (R+2G+B)/4; U=R-G; V=B-G \quad (1)$$

These equations allowed *thresholding* to work independently of object color intensity.

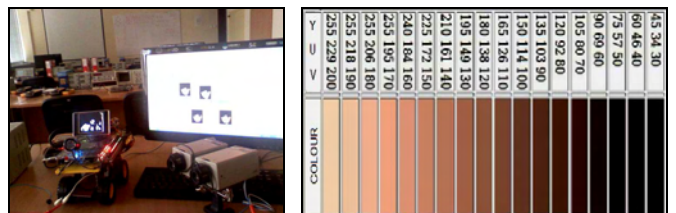


Figure 1 Experimental kit and different tone samples

After object pixels were converted to the modified YUV space, the pixels can be segmented based on the following experimented threshold  $10 < U < 74$  and  $-40 < V < 11$ .



Figure 2 The MATLAB results

As seen in figure2, the blue channel had the least contribution to human skin color. Additionally, leaving out the blue channel would have little impact on thresholding and

skin filtering. This also implies the insignificance of the V component in the YUV format. Therefore, the object detection algorithm using here was based on the U component only. Applying the suggested threshold for the U component would produce a binary image with raw segmentation result.

*Applying morphological filtering including erosion and hole filling would, firstly, reduce the background noise and, secondly, fill in missing pixels of the detected face regions [2]. The MATLAB provided built-in functions—*imerode* and *imfill* for these two operations as:*

- `outp = imerode(inp, strel('square', 5));`

The command *imerode* erodes the input image *inp* using a square of size 5 as a structuring element and returns the eroded image *outp*. This operation removed any group of pixels that had size smaller than the structuring element's.

- `outp = imfill(inp, 'holes');`

The command *imfill* fills holes in the binary input image *inp* and produces the output image *outp*. Applying this operation allowed the missing pixels of the detected face regions to be filled in. Thus, it made each face region appear as one connected region.

*After each group of detected pixels became one connected region, connected component labeling algorithm was applied.* This process labeled each connected region with a number, allowing us to distinguish between different detected regions. The built-in function *bwlabel* for this operation was available in MATLAB. In general, there are two main methods to label connected regions in a binary image, known as recursive and sequential algorithms. The command *regionprops* can be used to extract different properties, including area and centroid, of each labeled region in the label matrix obtained from *bwlabel*.

*Filtering detected regions based on their areas would successfully remove all background noise and any skin region that was not likely to be a object.* To be considered a object region, a connected group of skin pixels need to have an area of at least 26% of the largest area. This number was obtained from experiments on training images. Therefore, many regions of false positives could be removed in this stage, as depicted in:

```
> object_idx = find(object_area > (.26)*max(object_area));
> object_shown = ismember(L, object_idx);
```

These two commands performed the following tasks:

- o look for the connected regions whose areas were of 26% of the largest area and store their corresponding indices in *face\_idx*;
- o output the image *face\_shown* that contained the connected regions found.

The final stage was to determine object location.

*The centroid of each connected labeled object region can be calculated by averaging the sum of X coordinates and Y coordinates separately.* The centroid of each object region is denoted by the blue asterisk. Here the centroid of each connected region was extracted using *regionprops*

### III. DESIGN AND IMPLEMENTATION

Each current video frame was captured by the camera and sent to the FPGA's decoder chip via a composite video cable [3]. After the video signal was processed in different modules

in Verilog, the final output passed through the VGA driver to be displayed on the VGA monitor. The hardware algorithm is shown in Figure 3.

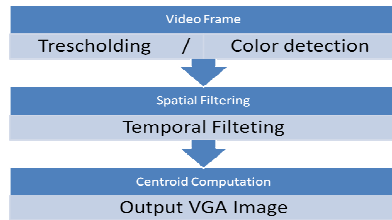


Figure 3 - Hardware Algorithm

❖ Thresholding is in this step, each input video frame was converted to a “binary image” showing the segmented raw result. Since 10-bit color was used in Verilog, adjusting the aforementioned U range yields  $40 < U < 296$ .

❖ Spatial Filtering is in this step was similar to the erosion operation used in the software algorithm. However, the structuring element used here did not have any particular shape. Instead, for every pixel  $p$ , its neighboring pixels in a  $9 \times 9$  neighborhood were checked. If more than 75% of its neighbors were skin pixels,  $p$  was also a skin pixel. Otherwise  $p$  was a non-skin pixel. This allowed most background noise to be removed because usually noise scattered randomly through space.

To examine the neighbors around a pixel, their values needed to be stored. Therefore, ten shift registers were created to buffer the values of ten consecutive rows in each frame. As seen in Figure 4, each register was 640-bit long to hold the binary values of 640 pixels in a row.

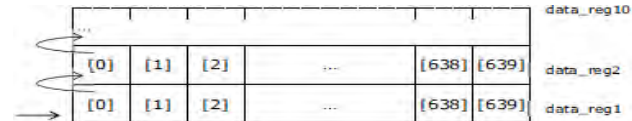


Figure 4 - Ten shift registers for ten consecutive rows

Each bit in *data\_reg1* was updated according to the X coordinate. For instance, when the X coordinate was 2, *data\_reg1[2]* was updated according to the result of thresholding from the previous stage. Thus, *data\_reg1* was updated every clock cycle. After all the bits of *data\_reg1* were updated, its entire value was shifted to *data\_reg2*. Thus, other registers (from *data\_reg2* to *data\_reg10*) were only updated when the X coordinate was 0. Values of *data\_reg2* to *data\_reg10* were used to examine a pixel's neighborhood.

There was a trade-off between the number of shift registers being used (i.e. the size of the neighborhood) and the performance of the spatial filter. A larger neighborhood required more registers to be used but, at the same time, allowed more noise to be removed.

❖ Applying temporal filtering allowed flickering to be reduced significantly. The idea of designing such a filter was borrowed from the project “Real-Time Cartoonifier” [4]. Even small changes in lighting could cause flickering and made the result displayed on the VGA screen less stable. The temporal filter was based on the following Verilog fragment:

```
// *** TEMPORAL FILTERING ****
IF ((VGA_XI < AVGX_LPF + 10'D5) && (VGA_XI > AVGX_LPF - 10'D5) &&
```

```

(VGA_YI < AVGY_LPF - 10'D5) && (VGA_YI > 10'D5))
BEGIN      FLTR_REG <= FLTR_REG + FLTR3[0];
END
ELSE IF ((VGA_XI == 10'D600) && (VGA_YI == 10'D400))
BEGIN      FLTR_REG <= 16'D0;
END      IF (FLTR_REG > 16'D50) BEGIN
IF (AVG2 > 10'B11011111)
BEGIN // CAN ALSO TRY B1110110111
FLTR3 <= 10'H3FF;
FLTR3_R <= 10'H3FF;
FLTR3_G <= 10'H3FF;
FLTR3_B <= 10'H3FF
// DRAW CENTROID
IF (CNTR > 19'D500) BEGIN // THRESHOLD WHEN #PIXELS IS TOO SMALL, NOTHING WILL BE
DETECTED
IF ((VGA_XI < AVGX_R2 + 10'D10) && (VGA_XI > AVGX_R2 - 10'D10)) &&
(VGA_YI < AVGY_R2 + 10'D10) && (VGA_YI > AVGY_R2 - 10'D10)) ||
((VGA_XI < AVGX_L2 + 10'D10) && (VGA_XI > AVGX_L2 - 10'D10)) &&
(VGA_YI < AVGY_L2 + 10'D10) && (VGA_YI > AVGY_L2 - 10'D10)) ) BEGIN
FLTR3_R <= 10'HO;
FLTR3_G <= 10'HO;
FLTR3_B <= 10'H3FF;
-----
END
ELSE BEGIN
FLTR3 <= 10'HO;
FLTR3_R <= 10'HO;
FLTR3_G <= 10'HO;
FLTR3_B <= 10'HO;
IF (CNTR > 19'D500) BEGIN
IF ((VGA_XI < AVGX_R2 + 10'D10) && (VGA_XI > AVGX_R2 - 10'D10)) &&
(VGA_YI < AVGY_R2 + 10'D10) && (VGA_YI > AVGY_R2 - 10'D10)) ||
((VGA_XI < AVGX_L2 + 10'D10) && (VGA_XI > AVGX_L2 - 10'D10)) &&
(VGA_YI < AVGY_L2 + 10'D10) && (VGA_YI > AVGY_L2 - 10'D10)) ) BEGIN
FLTR3_R <= 10'HO;
FLTR3_G <= 10'HO;
FLTR3_B <= 10'H3FF;
-----
END

```

The filtered result of a pixel in this stage was determined based on its average value  $avg\_out$ . If its average value was greater than 0.06 , because the number obtained from experiments, the pixel was considered skin. Otherwise, the pixel was non-skin. Experiments of temporal filtering for a two pixels is shown in Figure 5 and Figure 6, / blue is 1,orange is 0.

Figure 5 Example of temporal filtering for a pixel p1

Figure 5 Example of temporal filtering for a pixel p2

❖ Centroid Computation, was computed to locate the face region. Because connected component labeling was not implemented as initially planned, it was infeasible to calculate the centroid for each face region separately. This limited the number of faces to be detected to two as maximum. First assume that only one face was present. Therefore, its centroid would just be the centroid of all detected pixels, as shown in figure7. Note that this calculation would only be correct if one face was present. Although the pixels of one face region might not be connected and labeled as originally planned, simply calculating the centroid of all detected pixels still gave a good estimate for the face location. However, even if the hands were present, calculating the centroid of all detected pixels still allowed us to locate the face region. This was a reasonable estimate because, compared to the face area, the area of the hand/hands was much smaller. However, when there were two faces present, calculating the centroid of all detected pixels would only track the location between two faces, rather than track each face separately. To separately track each face in a two-person frame, additional steps were required.



Figure 7 The FPGA results, when there was a moved man

First the neighboring pixels around the centroid were checked to see if they were skin pixels. If they were, it meant the centroid accurately located the face region. However, if the neighboring pixels of the centroid were not skin pixels, it meant the centroid was somewhere in the background located between two detected face regions. The Verilog fragment is:

```

//*** COMPUTING CENTROID FOR ALL DETECTED PIXELS ***// 
IF((VGA_XI > 10'd20) && (VGA_XI < 10'd620) &&
(VGA_YI > 10'd20) && (VGA_YI < 10'd460)) BEGIN
IF (FLTR3 == 10'h3FF) BEGIN
SUMX <= SUMX + VGA_XI;
SUMY <= SUMY + VGA_YI;
CNTR <= CNTR + 19'BI;
END
END
IF ((VGA_XI == 10'd2) && (VGA_YI == 10'd478)) BEGIN
AVGX <= SUMX / CNTR;
AVGY <= SUMY / CNTR;
AVGX_LPF <= AVGX_LPF - (AVGX_LPF >> 'D2) + (AVGX >> 'D2);
AVGY_LPF <= AVGY_LPF - (AVGY_LPF >> 'D2) + (AVGY >> 'D2);
SUMX <= 30'BO;
SUMY <= 30'BO;
CNTR <= 19'BO;
END
//***COMPUTING CENTROID FOR LEFT HALVED FRAME *****//
IF ((VGA_XI > 10'd20) && (VGA_XI < AVGX_LPF - 10'd10) &&
(VGA_YI > 10'd20) && (VGA_YI < 10'd460)) BEGIN
IF (FLTR3 == 10'h3FF) BEGIN
SUMX_L <= SUMX_L + VGA_XI;
SUMY_L <= SUMY_L + VGA_YI;
CNTR_L <= CNTR_L + 19'BI;
END
END
IF ((VGA_XI == 10'd20) && (VGA_YI == 10'd478)) BEGIN
AVGX_L <= SUMX_L / CNTR_L;
AVGY_L <= SUMY_L / CNTR_L;
AVGX_L2 <= AVGX_L2 - (AVGX_L2 >> 'D2) + (AVGX_L >> 'D2);
AVGY_L2 <= AVGY_L2 - (AVGY_L2 >> 'D2) + (AVGY_L >> 'D2);
SUMX_L <= 30'BO;
SUMY_L <= 30'BO;
CNTR_L <= 19'BO;
END
//*** COMPUTING CENTROID FOR RIGHT HALVED FRAME ***// 
IF ((VGA_XI > AVGX_LPF + 10'd10) && (VGA_XI < 10'd620) &&
(VGA_YI > 10'd20) && (VGA_YI < 10'd460)) BEGIN
IF (FLTR3 == 10'h3FF) BEGIN
SUMX_R <= SUMX_R + VGA_XI;
SUMY_R <= SUMY_R + VGA_YI;
CNTR_R <= CNTR_R + 19'BI;
END
END
IF ((VGA_XI == 10'd621) && (VGA_YI == 10'd478)) BEGIN
AVGX_R <= SUMX_R / CNTR_R;
AVGY_R <= SUMY_R / CNTR_R;
AVGX_R2 <= AVGX_R2 - (AVGX_R2 >> 'D2) + (AVGX_R >> 'D2);
AVGY_R2 <= AVGY_R2 - (AVGY_R2 >> 'D2) + (AVGY_R >> 'D2);
SUMX_R <= 30'BO;
SUMY_R <= 30'BO;
CNTR_R <= 19'BO;
END

```

Since area-based filtering was also not applied, other skin regions—mostly the hands were not entirely removed. However, even if the hands were present, calculating the centroid of all detected pixels still allowed us to locate the face region. This was a reasonable estimate because, compared to the face area, the area of the hand/hands was much smaller.

However, when there were two objects present, calculating the centroid of all detected pixels would only track the location between two objects, rather than track each object separately. To separately track each object in a two-object frame, additional steps were required. First the neighboring pixels around the centroid were checked to see if they were colour object pixels. If they were, it meant the centroid accurately located the object region. However, if the neighboring pixels of the centroid were not object pixels, it meant the centroid was somewhere in the background located between two detected object regions. To solve this problem, the video frame was split into two according to where the centroid.



Figure 8 The FPGA results, when there was light effects

To show how an object was tracked, a small box was drawn around the centroid. The box moved according to the movement of the object. However, if the object moved too fast, the movement of the box might become less stable. Applying temporal filtering here allowed the box to move smoothly. The implementation of the temporal filter here was slightly different from the one shown previously.



Figure 9 The object tracking

The input  $X_n$  here was the location of the centroid before filtering. What this equation meant was, with  $\alpha$  being close to 1, current output  $Y_n$  would be more dependent on previous output  $Y_{n-1}$  than on current input. This prevented the centroid box from moving too fast when there was an abrupt change in the movement of an object, as:  $Y_n = (1 - \alpha)X_n + \alpha Y_{n-1}$

A clock of 27 MHz was used for the face detection and tracking algorithm. Since the timing was synchronized with the VGA clock, the VGA display was able to update within the time gap between drawing two consecutive frames [5]. The camera was able to detect and track objects in real time. Error seemed to occur only when there was a transition from one person to two people or vice versa in the video frame. The figure 10 shown blocks and the working hardware system.

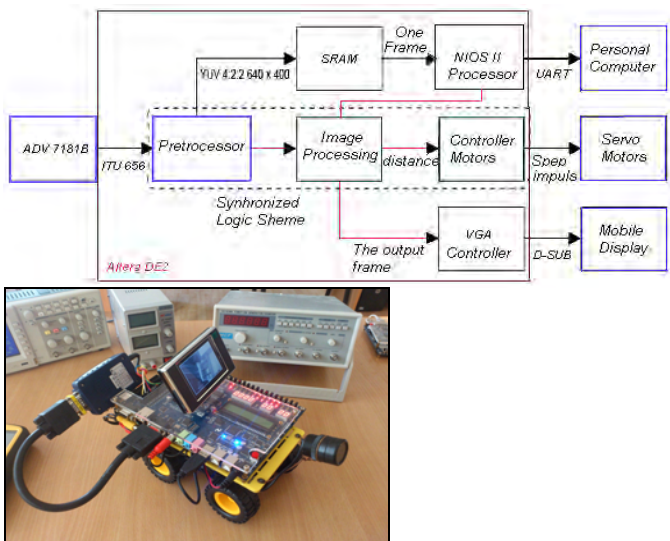


Figure 10 The blocks and the hardware system

Within the lab setting, noise was very minimal and did not alter the results. As long as a person was in the camera's view, his face would be accurately detected and tracked. His distance relative to the camera did not affect the result. In the presence of three or more people, the system could only detect the faces but failed at tracking them.

### III. CONCLUSION

The Image Processing Toolbox provided in MATLAB allowed the process of developing and testing the algorithm to be more efficient. Furthermore, verifying the accuracy of the detection algorithm on still pictures provided fair results. Object detection and tracking is the process of determining whether or not present it in an image. Unlike face recognition, which distinguishes different human faces, face detection only indicates whether or not an object is present in an image. Object detection and tracking has been an active research area for a long time because it is the initial important step in many different applications, such as video surveillance, face recognition, image enhancement, video coding, and energy conservation.

### REFERENCES

- [1] Furi A., Hang H.M., An efficient block-matching algorithm for motion compensated coding, Proc. JSASSP, pp.1063-1066, 2007.
- [2] Хуанга М. Обработка изображений и цифровая фильтрация, Под ред. Т:Мир 2009.
- [3] Diaz J., E. Ros, F. Pelayo, "Fpga-based real-time optical-flow system," Circuits and Systems for Video Technology, IEEE Transactions on, vol. 16, Feb. 2006
- [4] Advanced Microcontroller Final Projects, or online at: <http://people.ece.cornell.edu/land/courses/ece5760/FinalProjects>
- [5] Jentz B, J. Rotem, Leveraging FPGA coprocessors to optimize high-performance digital video surveillance systems. [www.dsp-fpga.com/articles/jentz\\_and\\_rotem](http://www.dsp-fpga.com/articles/jentz_and_rotem)

# An Approach for Position Detection of Industrial Objects

Veska Georgieva<sup>1</sup> and Plamen Petrov<sup>2</sup>

**Abstract –** In this paper, an approach for position detection of industrial objects by using a monocular camera mounted on a pick-and-place manipulator is presented. The proposed algorithm is based on Circular Hough transform. The camera-manipulator configuration is described in order to obtain information for the relative position of an object with respect to the end-effector.

**Keywords –** Monocular camera, Edge detection, Circular Hough transform, Position camera-manipulator model.

## I. INTRODUCTION

During the last decades, the computer vision has been used to locate objects in an industrial environment [1, 2]. By using a fixed or moving camera, the manipulator can obtain information for the relative position of an object with respect to the end-effector.

In this paper, an approach for position detection of industrial objects by using a camera mounted on a pick-and-place manipulator is presented. The proposed algorithm is based on Circular Hough transform. The camera-manipulator configuration is described in order to obtain information for the relative position of an object with respect to the end-effector.

The highly-reflective nature of the metal object surface may cause unwanted side effects such as glare that can make problems in precisely identifying position of the industrial objects. In addition the illumination in the room may cause low contrast and shadows by obtained images with the camera. These problems can be dealt with in post-processing.

The rest of the paper is organized as follows: In Section 2, the basic stages in the proposed algorithm for image processing is presented. The camera-manipulator configuration is described in Section III. Some experimental results are given in Section IV. Section V concludes the paper.

## II. BASIC STAGES IN ALGORITHM FOR IMAGE PROCESSING

In the paper is proposed an effective pre-processing algorithm to position detection of the industrial objects. It consists of:

- Image Enhancement
- Edge Detection via the Sobel Operator
- Circle Detection via the Circular Hough Transform

<sup>1</sup>Veska Georgieva is with the Faculty of Telecommunications at Technical University of Sofia, 8 Kl. Ohridski Blvd, Sofia 1000, Bulgaria, E-mail: [vesg@tu-sofia.bg](mailto:vesg@tu-sofia.bg)

<sup>2</sup>Plamen Petrov is with the Faculty of Mechanical Engineering at Technical University of Sofia, 8 Kl. Ohridski Blvd, Sofia 1000, Bulgaria, E-mail: [ppetrov@tu-sofia.bg](mailto:ppetrov@tu-sofia.bg)

The first step in pre-processing is image enhancement. It includes noise reduction and contrast enhancement. As first is proposed to use a median filter in order to reduce some kind of noise, introduced by the creating of digital images. The median filtering is a specific case of order-statistic filtering, in that the value of an output pixel is determined by the median of the neighbourhood pixels. The median is much less sensitive than the mean to extreme values (outliers). Median filter is therefore better able to remove the outliers without reducing the sharpness of the image and with less blurring of edges [3].

The intensity of the image can be adjusted as next. So can be increased the contrast in image in order to obtain better visualization on the boundaries of the object, which are obscured by the shadow. It is made on the base of calculation the histogram of the image and determination the adjustment limits [4].

As next step in detecting the position of the disk on the cube is proposed to perform edge detection via the Sobel Operator, applied in both the horizontal and vertical axes [5]. It is necessary to detect circular edges and reject some of more linear edges. A threshold is applied to thin the edges as well as avoid detection of non-circular shapes.

Although edge detection can successfully extract most of the circle from the image, we must now focus on extracting the circular shapes and their position on the disk. The proposed method for this is the Circular Hough Transform [6].

The Circular Hough Transform is useful for detecting circles of known radius as well to detect circles of various radii. This method is based on creating an accumulator matrix of size of the original image to be processed and is illustrated in Fig.1, [7].

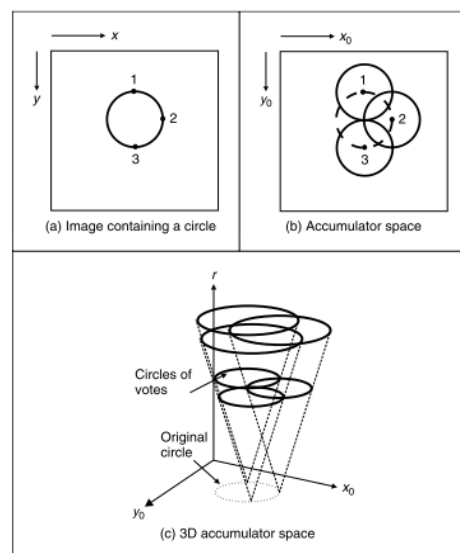


Fig. 1. Principle of Circular Hough Transform

An accumulator is an array used to detect the existence of the circle in the Circular Hough Transform. The local maxima in accumulator space are obtained by voting procedure. Parameter space is defined by the parametric representation used to describe circles in the picture plane, which is given by Eq.1[8]:

$$r^2 = (x - x_0)^2 + (y - y_0)^2 \quad (1)$$

It implies that the accumulator space is three-dimensional (for three unknown parameters  $x_0$ ,  $y_0$  and  $r$ ) and defines a locus of points  $(x, y)$  centered on an origin  $(x_0, y_0)$  with radius  $r$ . Points corresponding to  $x_0$ ,  $y_0$  and  $r$ , which has more votes, are considered to be a circle with center  $(x_0, y_0)$  and radius  $r$ .

### III. CAMERA-MANIPULATOR CONFIGURATION

The camera-manipulator configuration considered in this paper is shown in Fig. 2. The kinematic scheme of the pick-and-place robot consists of three links connected by prismatic joints, and a gripper connected by a revolute joint. The robot has four degree-of-freedom. Complete derivation of the manipulator position and orientation kinematics is given in [9]



Fig. 2. Experimental platform: 4-DOF manipulator with a moving camera

The camera is fixed to the third link of the manipulator, as shown in Fig. 3.

An auxiliary coordinate frame  $Dx_Dy_Dz_D$  is introduced which is fixed with respect to  $O_4x_4y_4z_4$  coordinate frame and has his center  $D$  on  $O_4y_4$  axis at distance  $d_{y4}$  from  $O_4$ . The axes of  $Dx_Dy_Dz_D$  are parallel to those of  $O_4x_4y_4z_4$ . The origin of the camera frame  $Cx_Cy_Cz_C$  coincides with the center of the coordinate system  $Dx_Dy_Dz_D$  but rotated at angle  $\beta$  about the  $x_D$  axis.

Let us denote the position of a feature point  $G$  with respect to the camera frame by

$${}^C p_G = \begin{bmatrix} {}^C x_G \\ {}^C y_G \\ {}^C z_G \end{bmatrix} \in \Re^3. \quad (2)$$

The corresponding pixel coordinates in the image plane are obtained as follows given in Eq.3:

$${}^I p_G = \begin{bmatrix} u_G \\ v_G \\ 1 \end{bmatrix} = \frac{1}{{}^C z_G} T_C {}^C p_G \quad (3)$$

where the  $3 \times 3$  invertible matrix  $T_C$  (Eq.4)

$$T_C = \begin{bmatrix} fw_u & 0 & u_0 \\ 0 & fw_v & v_0 \\ 0 & 0 & 1 \end{bmatrix} \quad (4)$$

is the so-called intrinsic camera calibration matrix [10], ( $w_u$ ,  $w_v$ ) are the camera scaling factors, and  $f$  is the focal length.

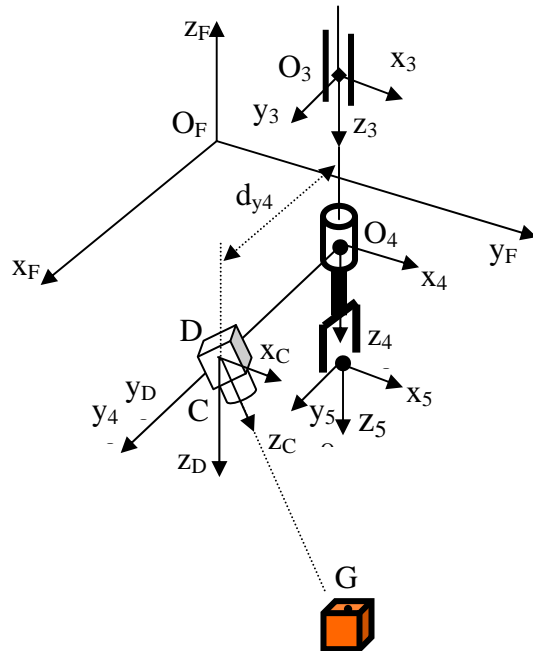


Fig. 3. Schematic of the camera-manipulator configuration

Using Eqs. (2), (3) and (4), the coordinates of point  $G$  in  $Dx_Dy_Dz_D$  are obtained as follows

$${}^D p_G = \begin{bmatrix} {}^D x_B \\ {}^D y_B \\ {}^D z_B \end{bmatrix} = {}^C z_G R_{x,\beta} T_C^{-1} {}^I p_G \quad (5)$$

where  $R_{x,\beta} \in SO(3)$  is a rotation matrix about the  $x_D$  axis by angle  $\beta$ . Finally, the coordinates of point  $G$  in  $O_4x_4y_4z_4$  are obtained as follows

$${}^o_4 p_G = {}^D p_G + {}^o_4 d_D \quad (6)$$

where  ${}^o_4 d_D = [0 \quad d_{y4} \quad 0]^T$ . It should be noticed that the axes  $O_4 z_4$  and  $O_5 z_5$  point out at the same point. In this way, by using the coordinates of a detected feature point G in  $O_4 x_4 y_4 z_4$ , we obtain information for the relative position of an object with respect to the end-effector. The manipulator is moving from one position to another over different objects placed in the operational space in order to detect an object with a specific feature (a circular element in our experiment).

#### IV. EXPERIMENTAL RESULTS

The experiments are made in MATLAB 7.14 environment by using IMAGE PROCESSING TOOLBOX. Some results, which illustrate the working of the proposed algorithm, are presented in the next figures below.

In Fig. 4 is presented the original image of size 640x480 pixels obtained by the camera and in Fig. 5 is shown its enhancement modification.



Fig. 4. Original Image



Fig. 5. Enhancement Image

The computed histograms of these images are given in Fig. 6. The increased contrast in the processed image represents that the histogram now fills more room in the dynamic range.

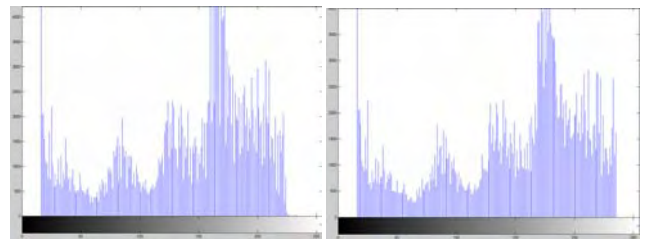


Fig. 6. Calculated histograms of the original and enhancement images

For edge detection was used a threshold value of 0.08, which provided good performance to thin the edges as well as avoid detection of non-circular shapes [7]. Fig.7 presents an edgemap image obtained via Sobel Operator.



Fig. 7. Edgemap image obtained via Sobel Operator.

The obtained result of the Circular Hough Transform is finding the coordinates of the center of the disk and its radius.

After the proposed image processing techniques is applied, we can identify the location of the disk in the original image, as shown in Fig.8.

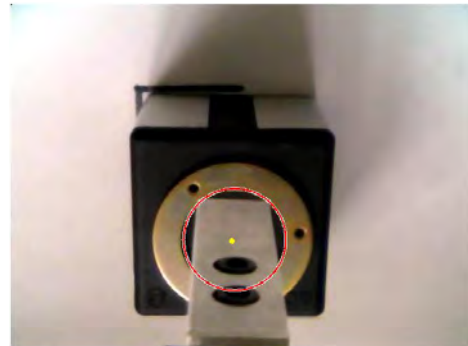


Fig. 8. Processed Image with detected position of the object

Sensitivity factor is an important parameter and specifies the sensitivity for the Circular Hough transform accumulator array [4]. Its value is in the range [0, 1]. By increasing of the sensitivity factor, can be detected more circular objects, including weak and partially obscured circles. Higher sensitivity values also increase the risk of false detection. It was used a sensitivity factor value of 0.92.

The obtained results for the computed coordinates of center of the circular object and its radius are more precise than the results obtained on the base of weighed centroids.

## V. CONCLUSION

In this paper, an approach for position detection of industrial objects by using a camera mounted on a pick-and-place manipulator has been presented. The proposed algorithm is based on Circular Hough transform. The camera-manipulator configuration is described in order to obtain information for the relative position of an object with respect to the end-effector. Based on the proposed algorithm, when the manipulator is moving consecutively from one position to another over the different objects placed in the operational space, it is possible to detect an object with a specific feature (a circular element in our experiment), and to take it with the gripper. Future work will include the design of visual servoing of the pick-and-place manipulator.

## REFERENCES

- [1] I. Shin, 3, S-H. Nam, H. Yu, R. Roberts, S. Moon, Conveyor Visual Tracking using Robot Vision, 2006 Florida Conf. Recent Adv. in Robotics (FCRAR 2006), pp. 1-5.
- [2] A. Denker, T. Adiguzel, Visual object tracking and interception in industrial settings, Eng. and Technology, No9, 2005, pp. 86-90.
- [3] W. Pratt, Digital Image Processing, John Wiley & Sons Inc., 2001.
- [4] MATLAB User's Guide. Accessed at: [www.mathwork.com](http://www.mathwork.com)
- [5] R. Gonzales and R. Woods, Digital Image Processing, Addison Wesley, 1992.
- [6] Simon Just Kjeldgaard Pedersen, Circular Hough Transform, Aalborg University, Vision, Graphics and Interactive Systems, 2007.
- [7] M. Johnson, Object Position and Orientation Detection for Mars Science Laboratory Helicopter Test Imagery, Project EE368, Stanford University, June 2012.
- [8] Soo-Chang Pei, Ji-Hwei Horng, Circular detection based on Hough transform, Pattern Recognition Letters (16), pp. 615-625, 1995.
- [9] P. Petrov, L. Dimitrov, Position kinematic modelling of a 4-DOF pick-and-place manipulator, Accepted for publication in XXII MHTK "АДП-2013", 2013.
- [10] E. Malis, Ф. Chaumette, 2,5 visual servoing with respect to unknown objects trough a new estimation scheme of camera displacement, *Int. J. Comp. Vision*, no.1, pp.79-97, 2000.

# Approaches for Texture Image Creation

Daniela Ilieva<sup>1</sup>

**Abstract** –This article discusses two ways to create texture images - procedural (texture generation) and texture synthesis. The procedural approach is used to create images of natural phenomena such as terrain, fire, clouds, water, fog, vegetation for the purposes of computer graphics. Texture synthesis is applied when analyzing a small digital image we receive a larger one without visible repetitions and boundaries. The results of the generation and synthesis of the textures are applied.

**Keywords** – Texture image, Texture generation, Texture synthesis

## I. INTRODUCTION

An image texture is a set of metrics calculated in image processing designed to quantify the perceived texture of an image. Image texture gives us information about the spatial arrangement of color or intensities in an image or selected region of an image.

In 3D computer graphics, a texture is a digital image applied to the surface of a three-dimensional model by texture mapping to give the model a more realistic appearance.

In image processing, every digital image composed of repeated elements is called a "texture".

Texture can be arranged along a spectrum going from stochastic to regular.

Image textures can be artificially created or found in natural scenes captured in an image. Image textures are one way that can be used to help in segmentation or classification of images. To analyze an image texture in computer graphics, there are two ways to approach the issue: Structured Approach and Statistical Approach.

The image texture can be a photograph of a "real" texture or can be created by a procedural order.

## II. PROCEDURAL TEXTURE GENERATION

Procedural techniques [1], [2] are code segments or algorithms that specify some characteristic of a computer-generated model or effect. Procedural texture does not use a scanned-in image to define the color values. Instead, it uses algorithms and mathematical functions to determine the color.

One of the most important features of procedural techniques is abstraction. In a procedural approach, rather than explicitly specifying and storing all the complex details of a scene or sequence, we abstract them into a procedure and evaluate that procedure when and where needed. This allows

<sup>1</sup>Daniela Ilieva is with the Department of Computer Science & Engineering at Technical University of Varna, 1 Studentska str., Varna 9009, Bulgaria, E-mail: ilievadaniela@mail.bg.

us to create inherent multiresolution models and textures that we can evaluate to the resolution needed.

We also gain the power of parametric control, allowing us to assign to a parameter a meaningful concept (e.g., a number that makes mountains rougher or smoother). This parametric control unburdens the user from the lowlevel control and specification of detail.

Procedural models also offer flexibility. Procedural techniques allow the inclusion in the model of any desired amount of physical accuracy. The designer may produce a wide range of effects, from accurately simulating natural laws to purely artistic effects.

One major defining characteristic of a procedural texture is that it is synthetic - generated from a program or model rather than just a digitized or painted image.

The advantages of a procedural texture over an image texture are as follows:

- A procedural representation is extremely compact. The size of a procedural texture is usually measured in kilobytes, while the size of a texture image is usually measured in megabytes. This is especially true for solid textures, since 3D texture images are extremely large. Nonetheless, some people have used tomographic X-ray scanners to obtain digitized volume images for use as solid textures.

- A procedural representation has no fixed resolution. In most cases it can provide a fully detailed texture no matter how closely you look at it (no matter how high the resolution).

- A procedural representation covers no fixed area. In other words, it is unlimited in extent and can cover an arbitrarily large area without seams and without unwanted repetition of the texture pattern.

- A procedural texture can be parameterized, so it can generate a class of related textures rather than being limited to one fixed texture image.

The disadvantages of a procedural texture as compared to an image texture are as follows:

- A procedural texture can be difficult to build and debug. Programming is often hard, and programming an implicit pattern description is especially hard in nontrivial cases.

- Evaluating a procedural texture can be slower than accessing a stored texture image. This is the classic time versus space trade-off.

- Aliasing can be a problem in procedural textures. Antialiasing can be tricky and is less likely to be taken care of automatically than it is in image-based texturing.

To generate irregular procedural textures, we need an irregular primitive function, usually called noise. This is a function that is apparently stochastic and will break up the monotony of patterns that would otherwise be too regular.

The obvious stochastic texture primitive is white noise, a source of random numbers, uniformly distributed with no correlation whatsoever between successive numbers.

Procedural texturing uses fractal noise extensively. The noise function simply computes a single value for every

location in space. We can then use that value in literally thousands of interesting ways, such as perturbing an existing pattern spatially, mapping directly to a density or color, taking its derivative for bump mapping, or adding multiple scales of noise to make a fractal version. While there are infinitely many functions that can be computed from an input location, noise's random (but controlled) behavior gives a much more interesting appearance than simple gradients or mixtures of sines.

Below are shown the images (fig.1) procedurally generated with midpoint displacement procedure that can be used in terrain scenes, scenes with landscapes, clouds and meadows. The images (a) are created by a procedure and then the intensity of each point is used as a height for receiving 3D terrain (b). The images (c) are created with different color scheme and control parameter.

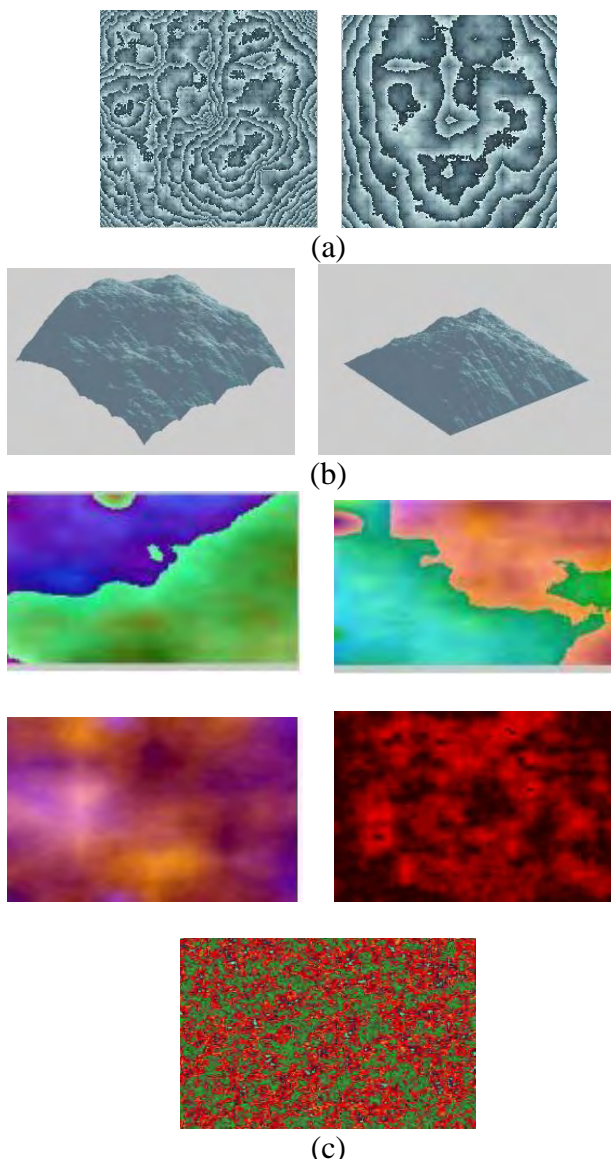


Fig.(1). Generated texture images by generalized stochastic subdivision (midpoint displacement procedure)

### III.TEXTURE SYNTHESIS

The texture synthesis problem may be stated as follows: Given an input sample texture, synthesize a texture that is sufficiently different from the given sample texture, yet appears perceptually to be generated by the same underlying stochastic process.

Texture synthesis algorithms are intended to create an output image that meets the following requirements:

- The output should have the size given by the user.
- The output should be as similar as possible to the sample.
- The output should not have visible artifacts such as seams, blocks and misfitting edges.
- The output should not repeat, i. e. the same structures in the output image should not appear multiple places.

Like the most algorithms, texture synthesis should be efficient in computation time and in memory use.

#### Pyramid-Based Texture Synthesis

Pyramid-based texture synthesis [Heeger and Bergen] [3] is a very first 'fast' algorithm that generates a new texture by matching certain statistics with the training sample. In the method, a texture is decomposed into pyramid-based representations, i.e. an analysis and a synthesis pyramids are constructed from the training and the output textures respectively.

#### Multi-resolution Sampling

Multi-resolution sampling [4], proposed by DeBonet, also constructs an analysis and a synthesis Gaussian/Laplacian pyramids in texture synthesis. But it has two major improvements over the previous method. First, multi-resolution sampling extracts a set of more detailed and sophisticated image features by applying a filter bank onto each pyramid level. Second, multi-resolution sampling explicitly takes the joint occurrence of texture features across multiple pyramid levels into account, while the previous method processes each pyramid level separately.

#### Pixel-based Non-parametric Sampling

Pixel-based non-parametric sampling [5], [6], [7], constrains pixel sampling using a similarity metric defined with respect to a local neighbourhood system in an MRF (fig.2).

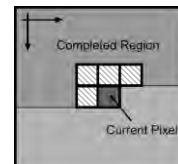


Fig.2. The 'L'-shaped neighbourhood in a pixel-based non-parametric sampling (a 3X3 neighbourhood window in this case). Each square represents a pixel and the arrows indicate

the synthesis is performed in a raster scanline order.

The method assumes an MGRF model of textures so that a pixel  $i \in g$  only depends on the pixels in a local

neighbourhood  $N_i \in g$ . The distance between neighbourhoods  $N_i$  and  $N_j$ , e.g., the sum-of-square-difference (SSD), provides a metric of pixel similarity between  $i$  and  $j$ . To synthesise a pixel  $i$ , the algorithm searches for a pixel  $j$  from the training texture that minimises the distance between  $N_i$  and  $N_j$ , and then uses the value of pixel  $j$  for pixel  $i$ .

### Block Sampling

Block sampling [8] is a natural extension to the previous pixel-based methods, which improves time efficiency of the synthesis by using image blocks as basic synthesis units. So, instead of pixel by pixel, block sampling synthesises a texture on a block by block basis (fig.3).

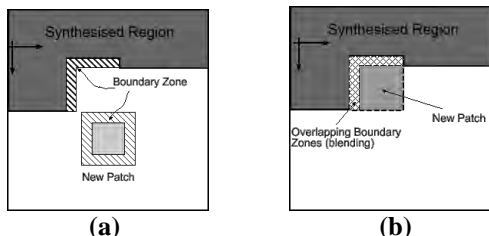


**Fig. 3:** Patch-based non-parametric sampling: (a) The boundary zones in a new and already synthesised patches. (b) The overlapping boundary zones after a new patch is placed into the output texture. The arrows indicate the synthesis is performed in a scanline order.

### Image Quilting

Image quilting [9,10] improves the patch-based non-parametric sampling by developing a more sophisticated technique to handle the boundary conditions between overlapped image patches. Instead of using the oversimplified blending technique, image quilting exploits a *minimum error boundary cut* to find an optimal boundary between two patches. An optimal cut defines an irregular path separating overlapping patches, so that each patch provides the synthetic texture only image signals on its side of the path.

Results of our algorithm based on block sampling procedure with image quilting (Fig. 4):



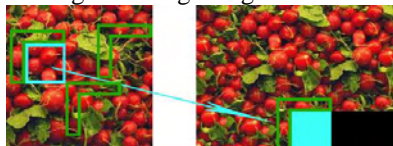
Step 1. Define patch that will be filled from the input image. It will be synthesized in step M



Step 2. Create a "neighbor" - an image formed around a patch.



Step 3. Detecting matching "neighbors"



Step 4. Selecting the best of all "neighbors"



Step 5. Copy selected "neighbor" and patch of the original image.



Step 6. Implement a strategy to remove the gap



Step 7. Forming of the patch from step N



Step M. Synthesis the whole texture image  
Fig.4. Algorithm for texture image synthesis

Finding an optimal neighbor.

Algorithm to search for optimal "patch" is based on the following steps:

- Forming of piece with all-black color (Fig.5)
- Forming of mask image  $J_i$



Fig.5. Algorithm to search optimal "patch"

- Calculate (Eq.1) the error  $E_i(x_0)$  between  $I_i$  and  $T$  (boot image) for each displacement  $x_0 = (\Delta x, \Delta y)$  of the input texture  $T$  (Fig.6)

$$E_i(\mathbf{x}_0) = \frac{1}{\kappa_i} \sum_{\mathbf{x}} \sum_c J_i(\mathbf{x}) w_c (I_{i,c}(\mathbf{x}) - T_{i,c}(\mathbf{x} + \mathbf{x}_0))^2 \quad (1)$$



Fig.6. Determination of the error image

- Determination of error overlap of  $S_i$  mask image  $I_i$  (Eq.2) and  $P_i$  selected piece (Fig.7).

$$S_i(\mathbf{x}) = \sum_c J_i(\mathbf{x}) w_c (I_{i,c}(\mathbf{x}) - P_{i,c}(\mathbf{x}))^2 \quad (2)$$

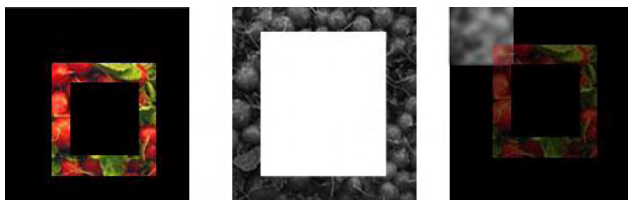


Fig.7. Determination of error overlap  $S_i$

- When found the patch with a  $S_i = \min$  to copy selected patch in the  $i$ -th image area.

The algorithm is repeated until all texture image is created.

Developed application is shown in Fig. 8.

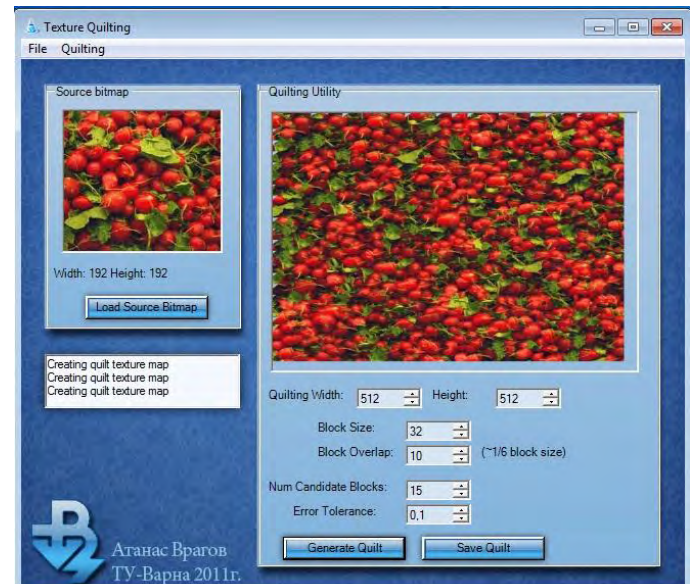


Fig.8. Texture synthesis application

## I. IV. CONCLUSION

The results obtained are with satisfactory appearance and speed of preparation and can be used for computer graphics and visualization.

## REFERENCES

- [1] D. Ebert, K. Musgrave, D. Peachey, K. Perlin, S. Worley "Texturing and modeling. A procedural approach. Third edition. Morgan Kaufman Publishers. 2003. ISBN: 1-55860-848-6
- [2] P. Schneider, D. Eberly "Geometric Tools for Computer Graphics". Third edition. Morgan Kaufman Publishers. 2002.
- [3] D. J. Heeger and J.R. Bergen. Pyramid-based texture analysis/synthesis. In *SIGGRAPH*, pages 229-238, 1995.
- [4] J. S. DeBonet. Multiresolution sampling procedure for analysis and synthesis of texture images. *Computer Graphics*, 31(Annual Conference Series):361-368, 1997.
- [5] A. A. Efros and T. K. Leung. Texture synthesis by nonparametric sampling. In *ICCV*(2), pages 1033-1038, 1999.
- [6] L. Wei and M. Levoy. Fast texture synthesis using tree-structured vector quantization. In K. Akeley, editor, *Siggraph 2000, Computer Graphics Proceedings*, pages 479-488. ACM Press / ACM SIGGRAPH / Addison Wesley Longman, 2000.
- [7] M. Ashikhmin. Synthesizing natural textures. In *The proceedings of 2001 ACM Symposium on Interactive 3D Graphics*, pages 217-226, 2001.
- [8] L. Liang, C. Liu, and H. Y. Shum. Real-time texture synthesis by patch-based sampling. *Technical Report MSR-TR-2001-40, Microsoft Research*, 2001.
- [9] A. A. Efros and W. T. Freeman. Image quilting for texture synthesis and transfer. In Eugene Fiume, editor, *SIGGRAPH 2001, Computer Graphics Proceedings*, pages 341-346. ACM Press / ACM SIGGRAPH, 2001.
- [10] D. Zhou and G. L. Gimel'farb. Texel-based texture analysis and synthesis. In *Proc. Image and Vision Computing New Zealand (IVCNZ 2004), Akaroa, New Zealand*, pages 215-220, November 2004.

# Coding of a Video with the Inserted Watermark using H.264/AVC Coder

Zoran Veličković<sup>1</sup> and Zoran Milivojević<sup>2</sup>

**Abstract** –This paper presents the analysis of performances of SVD algorithm for inserting the watermark that influence on the quality of the video coded by H.264/AVC coder. The influence of the imprinting factors on the quality of the separated watermark in the uncompressed, i.e. compressed video is analysed. The quality of the separated watermark for the standard parameters of a protected video coding was analyzed on the base of the mean squared error.

**Keywords** – Singular value decomposition, Digital watermark, H.264/AVC codec, Multimedia.

## I. INTRODUCTION

Development of the modern digital telecommunications and especially the universal mobile telecommunication systems UMTS (Universal Mobile Telecommunication System) 3G/4G has contributed to introduction of new mobile telecommunication services. A considerable increase of the number of users of UMTS and terminal devices supported by multimedia contents resulted in an enormous increase of the multimedia and especially video communication on the Internet. Although the Internet was designed to offer through applications the best possible communication services in every moment, it is usually not enough for realization of contemporary multimedia services [1]. The reason for this lies in the fact that the video is most demanding regarding the net resources it engages, so that it is necessary to develop effective optimization (compression) algorithms for its application [2], [3].

In this paper H.264/AVC standard for compressing the video contents was taken into consideration; it has considerable advantages in regard to the previous ones [4], [5]. This standard was developed by the organizations ITU-T VCEG and ISO/IEC MPEG and it is believed that it will conquer a considerable part of the video market. Possibility of protection of video contents from illegal copying and distribution with H.264 codec was especially taken into consideration in this paper. This problem becomes more and more important having in view the enormous increase of the video communication in the Internet. Illegal copying and distribution of the electronic contents are present in many areas of acting, yet the software, music and film industries are especially affected. The illegal film market takes ca. 35% of the total pirated contents. Although protection from copying

can be realized by using hardware or software techniques, none of them proved to be totally reliable. The shortcoming of these techniques is that they prevent making the spare copies for the case where the original medium might be damaged. Another extreme in solving this problem is that the multimedia companies may abandon any kind of technical protection. The concept of the copyrights protection lean only on the law regulations in the battle against the piracy. The basic problem to be solved with this concept is how to prove the copyright of a video content.

In order to protect copyrights many sofisticated digital technologies have been developed which are based on the digital processing of the video signal. One of often used technologies for proving the copyright is watermarking into the original multimedia contents [6]. The watermark should with its contents in a unique way identify the owner of the multimedia contents and it should be therein as long as they last. The watermark technique is realized by inserting of small secret copyright information (watermark) into the digital contents so that it is indiscernible, yet at the same time robust to a try of degrading or removing from the multimedia contents. In real-time video applications it is exceptionally important for the watermark to be robust to compressing and transcoding the video contents by various bit rates. Basically, there are two big classes of algorithms for watermarking. The first class of algorithms is based on watermarking in the spatial domain. In these algorithms the watermark is hidden in values of the luminance or chrominance component of spatially arranged pixels. The algorithms which belong to this class are realized relatively simply, yet they are not robust enough in the processing of the video signal and especially in realization of the video compression. The second class of algorithms is based on inserting the copyright information into the transformation domain. The transformation domain can be realized by using DCT (Discrete cosine Transform), FFT (Fast Fourier Transform) or SVD (Singular Value Decomposition) transformation to the video contents and then the obtained transformation coefficients are modified suitably to inserted picture. By the inverse procedure the inserted information can be taken out of the protected video in order to prove the copyright [6], [7], [8], [9], [10]. The algorithms of this class have better performances of robustness in relation to the watermark inserted in the spatial domain.

The algorithms for watermarking of a video coded by H.264 codec can be divided according to the place where inserting is done in the process of coding. Thus inserting the watermark can be done before the video compression, before or after quantization and during the process of coding. Having in view that the standard H.264/AVC belongs to a group of compression techniques with losses, it is very important to analyze the endurance of the watermark in a video when its removal is attempted. This paper presents the analysis of

<sup>1</sup>Zoran Veličković is with the High Technical School, Niš, A. Medvedeva 20, 18000 Niš, Serbia, E-mail: zoran.velickovic@vtsnis.edu.rs

<sup>2</sup>Zoran Milivojević is with High Technical School, Niš, A. Medvedeva 20, 18000 Niš, Serbia, E-mail: zoran.milivojevic@vtsnis.edu.rs

performances of an algorithm for watermarking based on SVD decomposition proposed in [9]. This class of algorithms is successfully applied for protection of pictures. Problems in application of this algorithm to a video are analyzed and the key parameters are also identified.

The structure of the paper is the following. In the second section the applied SVD algorithm for watermarking is presented, while peculiarities of H.264 codec are given in the third section. The effect of the rounding during the insertion of the watermark and its influence on the quality of the watermark, i.e. of a video, were separately analyzed.

## II. THE SVD WATERMARKING ALGORITHM

For inserting the watermark into a video an algorithm based on SVD decomposition was applied, suggested also in [9]. This algorithm results from the idea presented in [8]. In spite of a good concept suggested in [9], a problem of false detection of the watermark was identified. This imperfection was eliminated by an algorithm from [9]. Inserting the watermark into a picture is can be done by the algorithm realized in the following steps:

*Input:* the matrix of the picture  $A_{m \times n}$  Watermark  $W_{m \times n}$ .  
*Output:* the picture with the watermark  $A_w$ .

*Step 1:* Decomposition of the matrix of the picture:

$$A = USV^T, \quad (1)$$

where  $A$  is the original picture,  $U$  and  $V$  the orthogonal matrices whose dimensions are  $m \times m$  and  $n \times n$ , respectively,  $S$  the diagonal matrix whose dimensions are  $m \times n$  with the elements that represent singular values. The columns of the matrix  $U$  are left singular vectors, while the columns of the matrix  $V$  are the right singular vectors of  $A$ . The pair singular vectors specify the geometry of the picture, while the singular values specify the luminance of the picture.

*Step 2:* SVD decomposition of the watermark:

$$W = U_w S_w V_w^T = A_{wa} V_w^T. \quad (2)$$

*Step 3:* Inserting  $A_{wa}$  into the diagonal matrix  $S$ :

$$S_1 = S + \alpha A_{wa}. \quad (3)$$

*Step 4:* Forming the picture with a watermark:

$$A_w = U S_1 V^T. \quad (4)$$

Extraction of the watermark out of the picture  $A_w^*$  that is potentially different from  $A_w$  because of superimposed noises, is realized by the algorithm that consists of the following steps:

*Input:* The picture with the watermark  $A_w^*$ .

*Output:* watermark  $W^*$ .

*Step 1:* Forming the difference between the original  $A$  and the picture with the watermark  $A_w^*$ :

$$(A_w^* - A) = A_I. \quad (5)$$

*Step 2:* Counting of the watermark  $W^*$ :

$$W^* = \frac{\left( U^{-1} A_I (V^T)^{-1} \right)}{\alpha} V_w^T. \quad (6)$$

In Fig. 1 there is an example for the black and white watermark imprinted into a video.

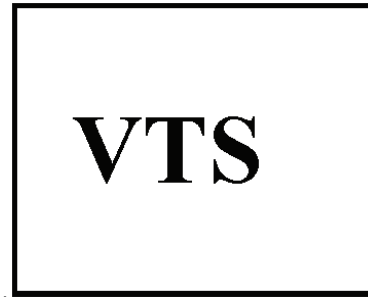


Fig. 1. The original watermark used in this paper.

## III. H.264/AVC VIDEO CODEK

The new standard for compression of the video, known under the designation H.264/AVC, includes the widest spectrum of video formats. This standard ranges from the modest video applications on the Internet to the high definition video applications. This paper is considering CIF video format whose resolution is 352x288 pixels and it is often applied on the Internet. For coding of one frame of the uncompressed CIF video format it is necessary to have 1216512 b/frames. If the resolution of the video formats (SD format, HD 720p and HD 1080p formats) increases, the number of bit/frame increases enormously. This is the reason, among other things, why the video applications belong into the most demanding multimedial applications. Obviously, a kind of compression technique over the multimedial contents is necessary. The standard compression techniques without losses are not applicable to the multimedial contents because they do not have the necessary compression performances. However, compression techniques with losses can reach desired performances with an acceptable level of degradation of the multimedial contents. H.264 is a compression standard that offers excellent compression solutions in relation to the previous ones. In comparison to other codec, H.264/AVC realizes the higher degree of compression for the same quality of the picture. In order to make H.264 standard applicable for the widest possible group of devices, various profiles are defined that determine a group of tools for generating the comprised video stream. Every profile is predetermined for a defined class of application. H.264 defines the following profiles: Baseline, Constrained Baseline, Extended, Main and several classes of High profile. The Baseline profile is convenient for video applications with small delaying (e.g. videoconferences) with not so demanding hardware resources on reception, while High 10 and High444Pred profiles are

meant for the professional usage. Imposing restrictions for the size of syntactic elements in H.264 stream defined the levels that determine the necessary computer power and memory demands for realization of H.264 decoders. H.264 compression algorithms are based on removing the redundant information out of video (temporal and spatial prediction). The frame prediction is done on the base of one or more previous or future frames called referent frames. Prediction reliability is attained by compensation of the movements between the referent and the current frames. Macroblock MB is a region in the picture determined by 16x16 pixels and represents the fundamental unit the movement is compensated over. So we differ frames of type I (intra), P (inter) and B (bidirectional) that uses one or more (previous or future) referent frames. A powerful mechanism for investigating the similarities in the current picture or pictures that precede, i.e follow, represents the base for the prediction models of H.264 coder. By predicting the contents of certain parts of the picture on the base of noticed similarities it is possible to form a "residual" frame with considerably less data. The result of this access can be neglecting the fine details in the frame which will have a negative effect on the inserted watermark. The result of this access is also the variable quality of the video and the separated watermark especially with lower bit rates.

#### IV. EXPERIMENTAL RESULTS AND DISCUSSIONS

##### A. Experimental setup

The experimental results obtained by inserting/separating the watermark out of the uncompressed video by the proposed SVD algorithm were presented in the first part of this section. The second part of this section brings the results of separating the watermark out of the protected compressed video coded by H.264 coder. The watermark from Fig. 1 is inserted into the uncompressed video sequence *Foreman\_cif.yuv* of resolution 352x288. The watermark is inserted into every frame of the uncompressed sequence with the constant value of the imprinting factor  $\alpha$ . The quality of the watermark separated out of the uncompressed video was especially analyzed in the function of the inserting factor  $\alpha$  and of the available number of bits for coding the video source. Since the video was coded with 8 bits and in the process of inserting the watermark it comes to rounding (cutting) not-integer-values of samples, the separation of the video watermark itself is made difficult. In order to explore dependence of the quality of the inserted watermark on the number of bits for coding the wholes series of simulations was performed.

##### B. Experimental results

In the simulation tests it was noticed that the quality of the separated watermark depends on the number of bits available for placing the sequence whit an inserted watermark. This is the reason why we do in this paper first analyze the influence of the number of bits for coding the video source to the quality of the separated watermark. Fig. 2 presents the watermarks separated out of the uncompressed sequence for

and a) 8 bits b) 9 bits c) 10 bits and d) 11 bits available for coding the samples. In Fig. 2 it can be noted that for the same value of the inserting factor  $\alpha$  the subjective quality of the separated watermark increases with the increase of the number of coding bits. The objective estimation of the quality of the separated watermark is presented in Fig. 3 in the function of the mean square error MSE:

$$MSE = \frac{1}{N_x \cdot N_y} \sum_{x=0}^{N_x-1} \sum_{y=0}^{N_y-1} [W(x, y) - W'(x, y)]^2 \quad (7)$$

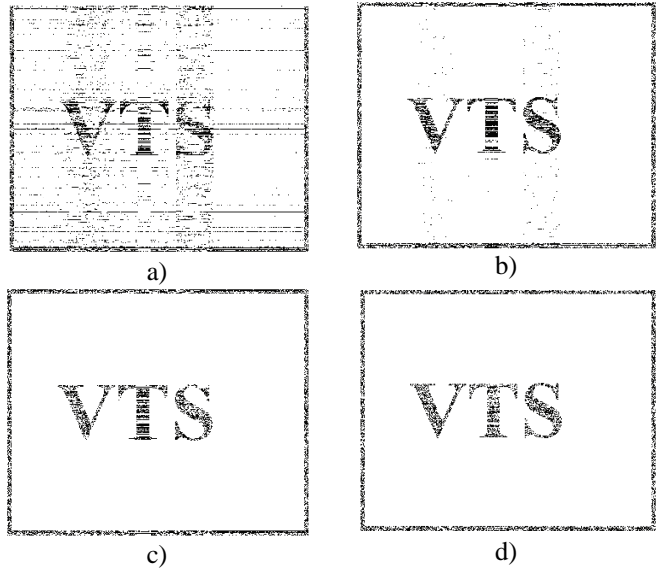


Fig. 2. The watermark separated out of the first frame of the uncompressed video when coding is realized with a) 8 bits b) 9 bits  
c) 10 bits d) 11 bits and for  $\alpha=0.002$ .

The analysis was done on the base of value of the mean square error of a separated watermark. The obtained results are presented in Fig. 3. With the increase of the number of bits for coding the source, the mean square error of the separated watermark in the uncompressed video considerably decreases, i.e. the quality of the watermark increases, which was the expected result. In the second part of the experiment the obtained protected video is coded by H.264/AVC coder.

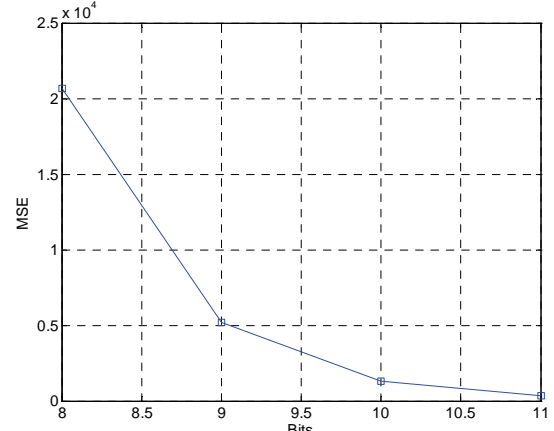


Fig. 3. MSE of the separated watermark in the function of the number of bits for coding the video source for  $\alpha=0.002$ .

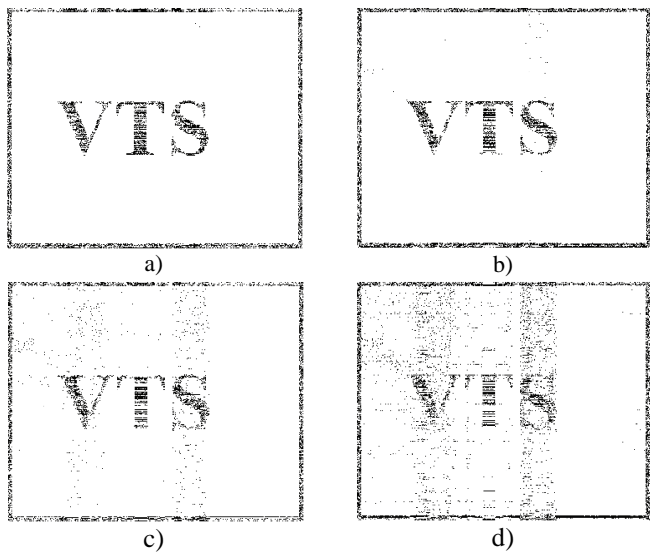


Fig. 4. The watermark separated out of the compressed video by H.264 coder from a) the first, b) second, c) third, and d) forth frame when the coding of the watermark is realized with 8 bits and  $\alpha=0.002$ .

JM referent software was used for coding and decoding the video sequences. It represents an official version of ITU in the version 14.2 FRExt [11], [12]. Coding of the protected video was done for a group of code parameters that define the code profile. The chosen parameters of H.264 coder in relation to [11] had the following values: *IntraPeriod*=12, *NumberReferenceFrames*=5, and *RateControlEnable*=0, *InitialQP*=28. The value of the code parameter QP is in this case adapted to the demanded bit rate and the maximally attainable quality of the video. The starting value of the code parameter in the beginning of GOP is QP=32. The analysis of the influence of the prediction schemes and the demanded bit rate on duration of the watermark after coding will be presented in the following papers.

### C. Analysis of the results

The watermarks separated out of the protected and compressed video sequence are presented in Fig. 4. Fig. 4 presents the watermarks separated out of a) the first, b) second, c) third, and d) forth frame where the coding of the watermark was realized with 8 bits and factors of inserting  $\alpha=0.002$ . Because the coding of the video source with more than 8 bits is not a standard procedure, here we have a presentation of a coded video by H.264 codec with 8 bits, yet with the variation of the imprinting factor  $\alpha$ . Newer versions of the video coder will have the possibility of coding the video source by the greater number of bits. Therefore, the developing version of JM software 18.6 offers the possibility of video coding in resolution from 8 to 16 bits. In addition to the quality of the separated watermark, its invisibility is one of the most important demands. The illustration of degradation of the video contents in the function of the imprinting factor  $\alpha$  is presented in Fig. 5. The first frames of the coded video with the watermark are presented. The simulation was performed for the following values of the parameter  $\alpha=[0.005\ 0.01\ 0.05]$ .



Fig. 5. The first frame of the video coded by H.264 codec where the watermark with a)  $\alpha=0.005$  b)  $=0.01$  c)  $\alpha=0.05$  was inserted.

## V. CONCLUSION

In this paper the performances of the algorithm for insertion/extraction of the watermark from the coded video with H.264/AVC coder are analyzed. The effects of rounding in the process of the watermarking are identified and confirmed through simulation. The quality of the separated watermark for the standard parameters of a protected video coding was analyzed on the base of the mean squared error. Values of the optimal parameters of imprinting and coding should be found in a compromise between the quality of the video and the quality of the separated watermark. The following works will be tested the robustness of the proposed solutions to various types of attacks. There will also be tested video encoding with more bits than the Internet standard.

## REFERENCES

- [1] M. van der Schaar, P. Chou, editors, "Multimedia over IP and Wireless Networks: Compression, Networking, and Systems," Academic Press, 2007.
- [2] M. Jevtović, Z. Veličković, "Protokoli preletenih slojeva", Akadembska misao, Beograd, 2013.
- [3] Z. Veličković, M. Jevtović, „Adaptive Cross-layer Optimization Based on Markov Decision Process”, International Journal Elektronika Ir Electrotehnika, pp. 39-42, 2011.
- [4] ITU-T, Recommendation H.264, Advanced Video Coding for Generic Audiovisual Services. Technical report, ITU-T, 2011.
- [5] I. E. Richardson, *The H.264 advanced video compression standard*, 2nd ed., John Wiley & Sons, Ltd, 2010.
- [6] X. Zhang, K. Li, Comments on "An SVD-Based Watermarking Scheme for Protecting Rightful Ownership", IEEE Transactions on Multimedia, vol. 7, no. 2, April 2005.
- [7] J. Cox, J. Kilian, T. Leighton, T. Shamoon, "Secure Spread Spectrum Watermarking for Multimedia", *IEEE Transaction on Image Processing*, Vol. 6, no. 12, pp. 1673-1687, 1997.
- [8] R. Liu, T. Tan, "An SVD-Based Watermarking Scheme for Protecting Rightful Ownership", *IEEE Transactions on Multimedia*, vol. 4, no. 1, pp. 121-128, March 2002.
- [9] C. Jain, S. Arora, P. Panigrahi, "A Reliable AVD based Watermarking Scheme", *Journal CoRR*, vol. abs/0808.0309, 2008, <http://dbpl.uni-trier.de>.
- [10] A. Rajwade, A. Rangarajan, A. Banerjee, "Image Denoising Using the Higher Order Singular Value Decomposition", *IEEE Transactions on Pattern Analysis and Machine Intelligence*, vol. 35, no. 4, april 2013.
- [11] A. M. Tourapis, A. Leontaris, K. Suehring, G. Sullivan, "H.264/MPEG-4AVC Reference Software Manual", Joint Video Team Document JVT-AD010, January 2009.
- [12] JM reference software version 16.0, <http://iphome.hhi.de/suehring/tml/>, July 2009.

# 3D Modelling from video

Svetlana Mijakovska<sup>1</sup>, Igor Nedelkovski<sup>2</sup>

**Abstract – In this paper the research on the 3D modelling from video is presented. We give overview of 3D modeling from video, especially the second step (structure and motion recovery) and the goal is to find the best algorithm for finding and fitting features to create a 3D model from multiple view of images.**

**Will be considered suitable algorithms to describe the facilities, whether used triangular polygonal mesh etc. cloud of points to describe the exterior of the building.**

**Keywords – 3D Modelling, 3D Model, Video, Epipolar geometry, Structure from Motion (SfM), RANSAC, MLESAC, MSAC, Least Square.**

## I. INTRODUCTION

The rapid increase in recent years of the graphics processing capabilities of even relatively modestly priced personal computers has lead to the widespread use of 3D graphics. Complex and large-scale 3D models are commonly used in areas such as animation, computer games and virtual reality. Currently most 3D models are created manually by graphic artists making it a time-consuming, and therefore expensive, process. If the model to be created has no real-world counterpart then there is little choice but to design it by hand. However, in many cases the aim is to create a model of an actual scene or object and, in this case, it is obviously highly desirable to create a process whereby the model may be automatically acquired. The increase in availability of high quality, consumer-level, digital video and still cameras means that the capability to capture high-resolution digital images and subsequently perform processing on them is now within the reach of most people.

The automatic recovery of three dimensional structure from video footage of scenes has been a long-standing area of research in computer vision. This problem, known as Structure from Motion (SfM), involves trying to recover, solely from the sequence of images, the 3D structure of a scene and the position and orientation (pose) of the camera at the moment each image was captured.

Applications for SfM can be broadly split into two

categories, those that require geometric accuracy and those that require photorealism:

**Geometric accuracy:** These types of application are generally less concerned with the visual appearance of the model but require the scene structure and camera motion to be reconstructed with a high degree of accuracy. Robot navigation, for instance, requires high-accuracy models, but the visual appearance of the model is unimportant. The reverse engineering of existing objects for use in CAD requires the structure of the object to be recovered with a high degree of accuracy. Film special effects that place computer-generated objects into the film and other ‘augmented reality’ applications require the camera motion to be very accurately reconstructed but the appearance of the structure is irrelevant as it is never seen in the finished product.

**Photorealism:** In contrast, there are a growing number of situations geometric accuracy of the underlying reconstruction is less important as long, as, for the purposes of the application the model visually resembles the real scene. This is the case for applications such as virtual reality, simulators, computer games and special effects that require a virtual set based on a real scene [1].

In computer vision, several systems have been developed to automatically recover a cloud of 3D scene points from a video sequence (e.g. [Pollefeys et al. 2004]). However these are vulnerable to ambiguities in the image data, degeneracies in camera motion, and a lack of discernible features on the model surface. These difficulties can be overcome by manual intervention in the modelling process. In the extreme case, a modelling package such as Blender3D can be used to build a model manually, but it is difficult and time consuming to create a photorealistic result by this process. A more appealing option is to use all of the information that can be derived from the video using computer vision techniques to inform and accelerate an interactive modelling process [2].

## II. OVERVIEW OF 3D RECONSTRUCTION FROM VIDEO SEQUENCES

Main tasks of 3D reconstruction are:

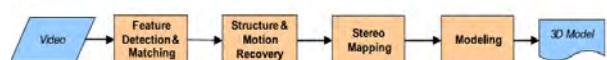


Figure 1: Main tasks of 3D reconstruction

The 3D reconstruction can be divided into 4 main tasks (Figure 1), which are discussed in the following sections:

1. Feature detection and matching: The objective of this step is to find out the same features in different images and match them.

<sup>1</sup>Svetlana Mijakovska is with the Technical Faculty of Bitola, address: ul. Ivo Ribar Lola bb, 7000 Bitola, Macedonia, e-mail: [svetlanamijakovska@gmail.com](mailto:svetlanamijakovska@gmail.com)

<sup>2</sup>Igor Nedelkovski is with the Technical Faculty of Bitola, address: ul. Ivo Ribar Lola, 7000 Bitola, Macedonia, e-mail: [igor.nedelkovski@uklo.edu.mk](mailto:igor.nedelkovski@uklo.edu.mk).

2. Structure and Motion Recovery: This step recovers the structure and motion of the scene (i.e. 3D coordinates of detected features; position, orientation and parameters of the camera at capturing positions).

3. Stereo Mapping: This step creates a dense matching map. In conjunction with the structure recovered in the previous step, this enables us to build a dense depth map.

4. Modeling: This step includes procedures needed to make a realistic model of the scene (e.g. building mesh models, mapping textures).

Feature detection and matching (Fig.3) is process that detects and match features in different images. Video sequence is created of more images so in this step we must find interested points (point feature), i.e. detectors and descriptors.

The most important information a detector gives is the location of features, but other characteristics such as the scale can also be detected. Two characteristics that a good detector needs are repeatability and reliability. Repeatability means that the same feature can be detected in different images. Reliability means that the detected point should be distinctive enough so that the number of its matching candidates is small.

A descriptor is a process that takes information of features and image to produce descriptive information i.e. features description which are usually presented in form of features vectors. The descriptions then are used to match a feature to one in another image. A descriptor should be invariant to rotation, scaling, and affine transformation so the same feature on different images will be characterized by almost the same value and distinctive to reduce number of possible matches.

The second task Structure and motion recovery recovers the structure of the scene and the motion information of the camera. The motion information is the position, orientation, and intrinsic parameters of the camera at the captured views. The structure information is captured by the 3D coordinates of features. Because the fact that video sequence is created of more images, for this step we must research 3D reconstruction from multiple views i.e. multiple view geometry.

For the calibrated case, the essential matrix  $E$  [3] is used to represent the constraints between two normalized views. Given the calibration matrix  $K$  (a  $3 \times 3$  matrix that includes the information of focal length, ratio, and skew of the camera), the view is normalized by transforming all points by the inverse of  $K$ :  $\hat{x} = K^{-1}x$ , in which  $x$  is the 2D coordinate of a point in the image. The new calibration matrix of the view is now the identity. Then with a corresponding pair of points  $(x, x')$  in homogeneous coordinates,  $E$  is defined by a simple equation:  $\hat{x}^T E \hat{x} = 0$ .

The research has later been extended to the uncalibrated case. During the 1990s, the concept of fundamental matrix  $F$  was introduced and well-studied by Faugeras [4] and Hartley [5]. The  $F$  matrix is the generalization of  $E$  and the defining equation is very similar:  $x^T F x = 0$ .

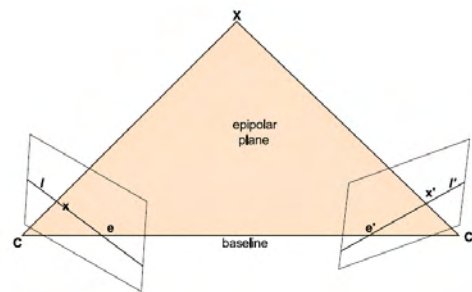


Fig.1 Two-view geometry

Three-view geometry is also developed during the 1990s. The geometry constraints are presented by trifocal tensors that capture relation among projections of a line on three views. The trifocal tensor defines a richer set of constraints over images (Fig.2). Apart of a line-line-line correspondence, it also defines point-line-line, point-line-point, point-point-line, and point-point-point constraints. Furthermore, it introduces the homography to transfer points between two views.

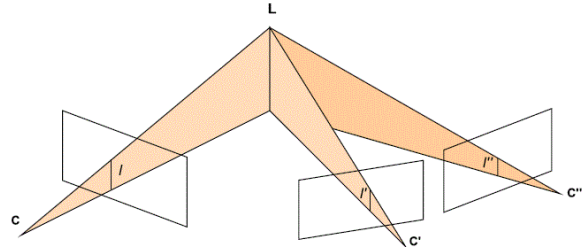


Fig.2 Line correspondence among three view - basis to define trifocal tensors

Reconstruction with only knowledge of feature correspondences is only possible up to a projective reconstruction and there are many ways to obtain projection matrices from a geometry constraint, i.e. a fundamental matrix or a focal tensor. Hence projective reconstruction is mainly the recovery of fundamental matrices or focal tensors. Methods, implementation hints, and evaluations are well discussed by Hartley and Zisserman in [6]. If the input, i.e. feature correspondences, includes outliers, robust methods such as RANSAC, LMS can be employed to reject them.

Stereo mapping task can be divided into two sub tasks: rectification and dense stereo mapping. The first one exploits the epipolar constraint to prepare the data for the second one by aligning a corresponding pair of epipolar lines along the same scan line of images thus all corresponding points will have the same y-coordinate in two images. This makes the second task, roughly search and match over the whole image, faster.

The final step is to map texture on the model. Triangulation is quite a simple task. Points of each stereo map are triangulated to generate depth maps. Those maps are used to construct the mesh of the scene and finally, with texture extracted from frames, the complete textured model can be built.

### III. STRUCTURE AND MOTION RECOVERY

This step is actually the main step in 3D modeling from video, because in this step we must choose which algorithm to be used for find corresponding points of two images or more images with moving cameras at different points in time, with moving objects using different methods such as feature matching and block matching. We are research RANSAC, Least Squares, MSAC and MLESAC.

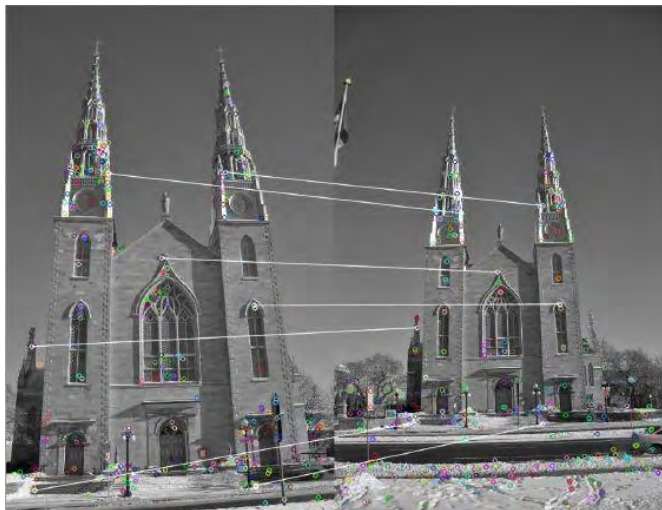


Fig.3 Feature matching

RANdom SAmple Consensus algorithm is:

- ❖ introduced Fischler and Bolles in 1981
- ❖ iterative method
- ❖ non deterministic

1. randomly select smallest possible subset of data (hypothetical inliners) an create model
2. test data against model, expand hypothetical inliners with all points inside a threshold
3. reestimate model with all points supporting the model
4. repeat and keep models with most support

RANSAC algorithm is method to estimate the parameters of a certain model starting from a set of data contaminated by large amounts of outliers of a model using datasets containing more than 50% of outliers. A datum is considered to be an outlier if it will not fit the “true” model instantiated by the “true” set of parameters within some error threshold that defines the maximum deviation attributable to the effect of noise. [7]

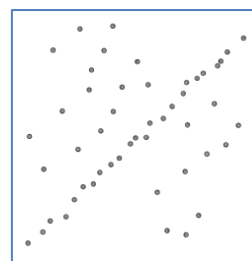
Despite many modifications, the RANSAC algorithm is essentially composed of two steps that are repeated in an iterative fashion (hypothesize and test framework):

- **Hypothesize.** First minimal sample sets (MSSs) are randomly selected from the input dataset and the model parameters are computed using only the elements of the MSS. The cardinality of the MSS is the smallest sufficient to determine the model parameters (as opposed to other approaches, such as least squares, where the parameters are

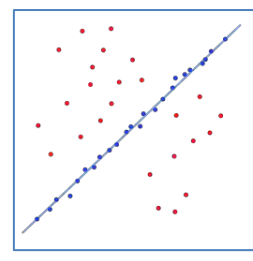
estimated using all the data available, possibly with appropriate weights).

- **Test.** In the second step RANSAC checks which elements of the entire dataset are consistent with the model instantiated with the parameters estimated in the first step. The set of such elements is called consensus set (CS).

RANSAC terminates when the probability of finding a better ranked CS drops below a certain threshold. In the original formulation the ranking of the CS was its cardinality ( i.e. CSs that contain more elements are ranked better than CSs that contain fewer elements).



Data with outliers



Line obtained with RANSAC, no influence of the outliers.

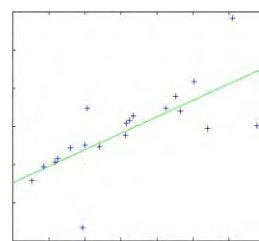
Fig.4 Example of line obtained with RANSAC algorithm without influence of outliers.

The benefits of RANSAC are:

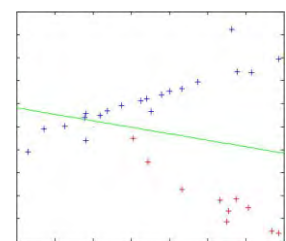
- ❖ only takes into account the number of inliers
- ❖ RANSAC minimizes cost.

### Least Squares

- ❖ Calculate parameters of model function
- ❖ Overdetermined data set
- ❖ Minimize sum of squared residuals



Least squares without outliers



Least squares with outliers.

Fig.5 Example of line obtained with Least Squares

MSAC - M-estimator SAmpling Consensus use score for inliners.

## MLESAC - Maximum Likelihood Estimation SAmple Consensus

The MLESAC algorithm is an example of RANSAC that uses different cost function than the cardinality of the support. The algorithm was introduced by Torr and Zisserman [8] and further improvements were made by Tordoff and Murray [9]. Instead of maximizing the support of the model, the likelihood of the model is maximized. The error distribution is represented as a mixture of inlier and outlier distributions.

## IV. CONCLUSION

The process of 3D modeling over the four main steps: feature extraction and matching, structure and motion recovery, stereo mapping, and modeling. Each step or even sub-step is already a field of research. The goal of this paper is to give overview of 3D modeling from video, especially the second step (structure and motion recovery) and to find the best algorithm for finding and fitting features to create a 3D model from multiple view of images. Of the process of choose the algorithm and its testing, we can define as:

- ❖ correspondence problems provide environments with high number of outliers
- ❖ least squares fails in these environments
- ❖ RANSAC provides significant improvement in presence of high numbers of outliers
- ❖ Performance can be additionally improved by using more complex error models
  - \_ Counting (RANSAC)
  - \_ Square distance (MSAC)
  - \_ Negative log likelihood (MLESAC).

- [7] Overview of the RANSAC Algorithm, Konstantinos G. Derpanis, Version 1.2, May 13, 2010.
- [8] P. H. S. Torr and A. Zisserman. MLESAC: A new robust estimator with application to estimating image geometry. CVIU, 78:138–156, 2000.
- [9] B. Tordoff and D.W. Murray. Guided sampling and consensus for motion estimation. In Proc. 7th ECCV, volume 1, pages 82–96. Springer-Verlag, 2002.
- [10] M.A. Fischler and R.C. Bolles. Random sample consensus: A paradigm for model fitting with applications to image analysis and automated cartography. Communications of the ACM, 24(6):381–395, 1981.
- [11] R. Hartley and A. Zisserman. Multiple View Geometry in Computer Vision. University Press, Cambridge, 2001.
- [12] P. Torr and C. Davidson. IMPSAC: A synthesis of importance sampling and random sample consensus to effect multi-scale image matching for small and wide baselines. In European Conference on Computer Vision, pages 819–833, 2000.
- [13] P. Torr and A. Zisserman. MLESAC: A new robust estimator with application to estimating image geometry. Computer Vision and Image Understanding, 78(1):138–156, 2000.

## REFERENCES

- [1] Cooper, O., Campbell, N., Gibson, D. 2003. Automated meshing of Sparse 3D Point Clouds. In Proceedings of the SIGGRAPH 2003 conference on Sketches and Applications, San Diego.
- [2] Gibson, S., Hubbold, R., Cook, J., and Howard, T. 2003. Interactive reconstruction of virtual environments from video sequences, Computers & Graphics 27, 2 (April), 293–301.
- [3] H.C. Longuet Higgins. A computer algorithm for reconstructing a scene from two projection. Nature, 1981.
- [4] S. Maybank O.D. Faugeras, Q. Luong. Camera self-calibration: Theory and experiment. European Conference on Computer Vision, 1992.
- [5] R.I. Hartley. Estimation of relative camera positions for uncalibrated cameras, Lecture Notes In Computer Science, 588, 1992.
- [6] R. Hartley and A. Zisserman. Multiple view geometry in computer vision 2<sup>nd</sup> edition. Cambridge University Press, 2004.

# Automated Vegetation Classification for LANDSAT 7 Multispectral Images

Dragan Stevic<sup>1</sup>, Igor Hut<sup>2</sup>, Nikola Dojčinović<sup>3</sup> and Jugoslav Joković<sup>4</sup>

**Abstract** –In this paper, one possible neural network based approach for vegetation classification for LANDSAT 7 multispectral image set is presented. Different training models are presented and results are discussed in terms of accuracy, alongside with framework for further research.

**Keywords** –Remote sensing, Neural networks, Multispectral images.

## I. INTRODUCTION

Vegetation classification is an important component in the management and planning of natural resources [1]. Recently, there were efforts to characterize vegetation culture by its reflectance [2,3]. It is shown that vegetation cultures can be distinguished by their reflectance. Remote sensing with multispectral or/and hyperspectral data derived from various satellites in combination with topographic variables is valuable tool in vegetation classification. Based on this requirement, we propose method for automatic vegetation culture recognition based on its reflectance data from multispectral Landsat 7 satellite image sets, using neural networks.

Landsat 7 satellite is equipped with Enhanced Thematic Mapper Plus (ETM+) imaging system. In addition to Thematic Mapper, system that operates on Landsat 4 and Landsat 5, ETM+ is capable of acquiring panchromatic band with 15m spatial resolutions, enhanced radiometric calibration and a thermal IR channel with 60m spatial resolution. Altogether, ETM+ acquires images of 7 wavelength bands, plus panchromatic channel[4, 5], as is presented in Table I.

Each channel is represented with corresponding image and it covers 185km width and length of a land surface. Therefore, maximal resolution of usable rectified image area is (12333×12333)pixels for panchromatic, or (6166×6166)pixels for channels 1, 2, 3, 4, 5 and 7. The IR channel 6 usable area resolution is (3083×3083)pixels. Each pixel is represented with 8 bit values, ranging from 0 to 255. Channel images are stored in uncompressed image formats.

TABLE I  
LANDSAT 7 CHANNELS PROPERTIES

Band Number	Spectral range (nm)	Ground resolution
1	450 - 515	30
2	525 - 605	30
3	630 - 690	30
4	750 – 900	30
5	1550 - 1750	30
6	10400 - 12500	60
7	2090 - 2350	30
Pan	520 - 900	15

## II. METHODOLOGY

In order to characterize reflectance of vegetation culture represented on an image, construction of a multi-spectral descriptor is proposed. The descriptor is constructed as vector of acquired reflectance values by wavelength bands. Due unavailability of 6<sup>th</sup> band for civil use, descriptor consists of values of averaged reflected light intensity in period of acquisition for bands 1, 2, 3, 4, 5 and 7. This approach to the descriptor construction quantifies reflected light intensities, quantizing it to non-overlapping and non-continuous bands, yielding vector of six elements with values ranging from 0 to 255.

However, due to information loss caused by the quantization, no information between bands boundaries and averaging within bands, mapping from reflectance to descriptor is not injective, and therefore not invertible. Let's denote mapping  $f$  from continuous reflectance value  $R_\lambda$  to discrete descriptor  $D_A$  as:

$$f : R_\lambda \rightarrow D_A, \quad f(r_\lambda) = d_\lambda$$

where  $r_\lambda \in R_\lambda$  and  $d_\lambda \in D_A$ . Due non-invertibility of mapping  $f$ , it is not possible to define analytical inverse mapping  $f^{-1}$  from  $f$ . Therefore, mapping  $g$  is defined as inverse mapping:

$$g : D_A \rightarrow R_\lambda, \quad g(d_\lambda) = r'_\lambda$$

where  $r'_\lambda \in R_\lambda$ , satisfying condition

$$|r'_\lambda - r_\lambda| = 0(1)$$

In order to compensate nonlinearities and unknown complexity of inverse mapping function, our method employs artificial neural network (ANN) to estimate inverse mapping  $g$  in order to minimize the difference in (1).

<sup>1</sup>Dragan Stević is with Faculty of Technical Science, University of Pristina, Kneza Miloša 7, 38220 Kosovska Mitrovica, Serbia

<sup>2</sup>Igor Hut is with the Faculty of Mechanical Engineering, University of Belgrade, Kraljice Marije 16, 11120 Belgrade, Serbia, E-mail: ihut@mas.bg.ac.rs.

<sup>3</sup>Nikola Dojčinović is with MySkin, Inc, Kosovska 17, 11000 Belgrade, Serbia, E-mail: nikoladojcinovic@gmail.com

<sup>4</sup>Jugoslav Joković is with Faculty of Electronic Engineering, University of Nis, Aleksandra Medvedeva 14, 18000 Niš, Serbia, E-mail: jugoslav.jokovic@elfak.ni.ac.rs

The additional simplification can be achieved with discretization of vegetation cultures to classes. Using finite number of classes,  $N_{out}$ , a recognition problem is reduced to a classification problem. A number of classes yields number of neurons in output layer to be equal as a number of vegetation classes. The input layer of the neural network is defined with the descriptor vector length. In order to compensate nonlinearities, the network in the proposed solution has one hidden layer with 3 times more neurons than in the input layer. All neurons are activated with the sigmoid function. If network weights are denoted with  $\Theta$ , than corresponding cost function of network can be presented as:

$$J(\Theta) = -\frac{1}{m} \left[ \sum_{i=1}^m \sum_{k=1}^{10} y_k^{(i)} \log(h_\Theta(x^{(i)})) + (1 - y_k^{(i)}) \log(1 - h_\Theta(x^{(i)})) \right] + \frac{\lambda}{2m} \sum_{l=1}^3 \sum_{i=1}^{s_l} \sum_{j=1}^{s_{l+1}} (\Theta_{ij}^{(l)})^2 \quad (2)$$

where  $m$  is dimension of training set,  $h_\Theta$  is hypothesis calculated of  $x(i)$ , input value of  $i$ -th training sample, and  $y_k$  is correct response on  $k$ -th output, for  $i$ -th training sample, and  $s_l$  number of neurons in  $l$ -th layer. Neural network is trained to minimize the cost function  $J(\Theta)$  on training set.

It is assumed that each pixel corresponds to a single class. A pixel purity problem is not treated. A classification of such pixels requires additional physical information. The availability of data representing reliable ground truth is often a problem in a remote sensing pattern classification and the problem would be further complicated with mixed pixels. Therefore, special attention was paid to proper training set forming, omitting location positioned on boundaries between classes.

Training set consists of the descriptor vector for a particular pixel as input data and matching vegetation culture for that geographic position, as desired response. The vegetation data was organized in geo-referent map covering same area as Landsat 7 image set. For easier visualization hybrid image was created by placing of translucent geo-referent vegetation map over geo-referenced Landsat 7 image set image of one of channels.

Process of training set formation was semi-automatized with software written for this purpose, presented in Fig. 1. It allows observer/network\_trainer to navigate through hybrid image in search for desired vegetation class for training set labeling. Once suitable class is found, observer chooses one location in particular class region. Selecting location by clicking mouse positioned over desired location dialog window pops-up, allowing observer to specify vegetation class present in that particular position. As temporary data pair of an image location and corresponding class are stored in memory. After process of labeling is finished, training set is exported by creating training pair that consists of the descriptor created for location stored in temporary data set, and corresponding vegetation class.

Four descriptor models were used for training. The first model takes into account only descriptor of selected position, while other three models takes into account local neighborhood of dimensions 1 pixel ( $3 \times 3$ window), 2 pixels ( $5 \times 5$ window) and 3 pixels ( $7 \times 7$ window). The descriptor is

than formed by sequencing single pixel descriptor from upper left corner of local window, row by row. Therefore, descriptors for models with 0, 1, 2 and 3 neighborhood consists of 6, 54, 150 and 294 features, respectively.

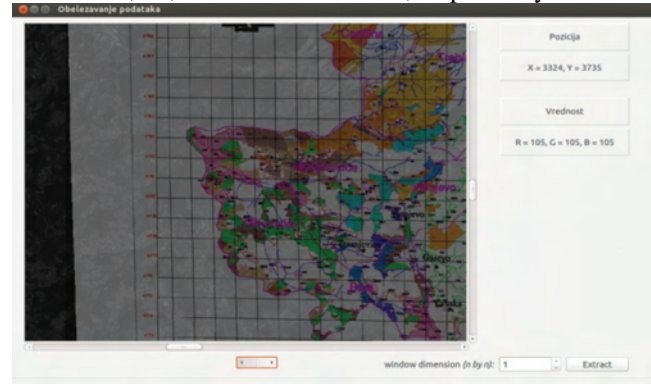


Fig 1: Software for semi-automatic data labelling

### III. RESULTS AND DISCUSSION

We tracked the change of training set error and test set error with the respect to four different models and 6 chosen values for the regularization parameter  $\lambda$ . The training error is likely to be lower than the actual generalization error, which is the case for our models as well. Fig. 2. and Table II present comparison of accuracy for the training set and the test set, in the cases of descriptors for models with one pixel and 1-, 2- and 3- neighborhood, respectively.

As can be seen from the data presented Table II as well as charts in Fig. 2, performance, in the terms of accuracy, of all four neural networks varies significantly for the data regarding training set. The accuracy in this case is defined as a relative number of accurate predictions ((#accurate predictions)/(#all predictions)\*100%), that neural network outputs for the training set or the test set as an input. As one would expect, the model with the largest number of features (3-neighbourhood, 294 input neurons) displays the best performance in fitting the training data set (97.5% for  $\lambda=3$ ), whilst the simplest, one-pixel, model has the lowest accuracy in fitting the training set (68.25% for  $\lambda=1$ ). Situation is rather different if accuracy of our models for fitting the test data set is compared. For the test set, accuracy of all four models is between 48.5 and 60%. Taking into account that with every added feature computing cost for neural network training progressively increases, choosing “one pixel” model over the remaining three would be adequate. A relatively low accuracy is, probably, primarily due to low separability of chosen classes. Precision of terrain map is questionable, spatial resolution in visible bands is 30m, therefore one pixel can encompass area with mixed vegetation [6].

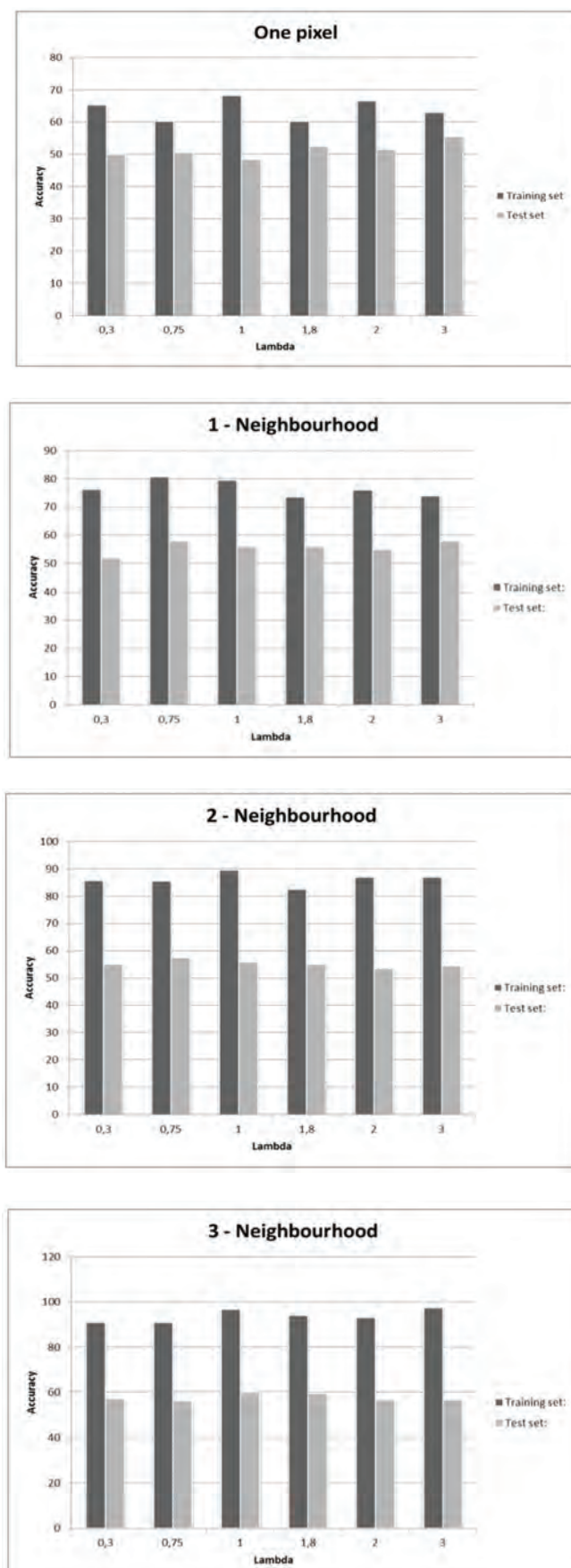


Fig. 2. Comparison of model accuracy for the training set and the test set, as a function of regularization parameter  $\lambda$

**TABLE II**  
COMPARISON OF MODEL ACCURACY FOR THE TRAINING SET AND THE TEST SET, AS A FUNCTION OF REGULARIZATION PARAMETER  $\lambda$ :  
"ONE PIXEL", "1-", "2-" AND "3-NEIGHBOURHOOD"

1 x 1		Lambda					
		0,3	0,75	1	1,8	2	3
<b>Training set:</b>		65,25	60,25	68,25	60,25	66,5	63
<b>Test set:</b>		50	50,5	48,5	52,5	51,5	55,5
3 x 3		Lambda					
		0,3	0,75	1	1,8	2	3
<b>Training set:</b>		76,25	80,75	79,5	73,5	76	74
<b>Test set:</b>		52	58	56	56	55	58
5 x 5		Lambda					
		0,3	0,75	1	1,8	2	3
<b>Training set:</b>		85,75	85,5	89,5	82,5	87	87
<b>Test set:</b>		55	57,5	56	55	53,5	54,5
7 x 7		Lambda					
		0,3	0,75	1	1,8	2	3
<b>Training set:</b>		91	91	96,75	94	93,25	97,5
<b>Test set:</b>		57,5	56,5	60	59,5	57	57

#### IV. CONCLUSION

In this paper one possible approach for automated vegetation classification for Landsat 7 multispectral images is proposed and early stage research results are presented. Generally, automated vegetation classification based on Landsat 7 multispectral images can be helpful for human interpretation of remote sensing images as the classification results could be used along with the original image data. In order to clearly identify types of vegetation on land surface and achieve an accurate classification based on satellite imagery, it is of crucial importance to determine the number of discrete vegetation categories (number of classes) and to choose distinctive characteristics (based on reflectance power distribution spectra) of these that are considered most suitable for the vegetation type categorization of the study area. More specifically, the first step of the classification procedure is the careful selection of the number of classes that represent sufficiently every discrete vegetation type. The good knowledge of the study area should help us to choose more representative classes depicted at the satellite images. Further, larger training and test set has to be made based on carefully collected pixels for every class from the study area. Recently, Support-Vector Machines (SVM) with kernels has been used very successfully for classification in remote sensing applications[7], so it is possible to compare behavior of ANN and SVM for this concrete application.

## REFERENCES

- [1] C. Walthall, "A comparison of empirical and neural network approaches for estimating corn and soybean leaf area index from Landsat ETM+ imagery\*1," *Remote Sensing of Environment*, vol. 92, no. 4, pp. 465–474, Sep. 2004.
- [2] M. Govender, K. Chetty, and H. Bulcock, "A review of hyperspectral remote sensing and its application in vegetation and water resource studies," vol. 33, no. 2, pp. 145–152, 2007.
- [3] M. A. Cochrane, "Using vegetation reflectance variability for species level classification of hyperspectral data," vol. 21, no. 10, pp. 2075–2087, 2000.
- [4] "No Title." [Online]. Available: <http://geo.arc.nasa.gov/sge/landsat/l7.html>.
- [5] N. Aeronautics, "Landsat 7 Science Data Users Handbook Landsat 7 Science Data Users Handbook," 1972.
- [6] C. H. Chen and P.-G. Peter Ho, "Statistical pattern recognition in remote sensing," *Pattern Recognition*, vol. 41, no. 9, pp. 2731–2741, Sep. 2008.
- [7] S. Kolios and C. D. Stylios, "Identification of land cover/land use changes in the greater area of the Preveza peninsula in Greece using Landsat satellite data," *Applied Geography*, vol. 40, pp. 150–160, Jun. 2013.  
f

---

---

## Poster 6 - Informatics and Computer Science

---

---



# Numerical Experiments for the Study of the Influence of Wavelength in Laser Impact onto Metals and Alloys

Nikolay Angelov<sup>1</sup>

**Abstract –** The program TEMPERATURFELD3D, working in MATLAB, has been used to conduct numerical experiments. The study of the influence of the wavelength of the laser, is pertained to CuBr laser ( $\lambda_1 = 511$  nm), ruby laser ( $\lambda_2 = 690$  nm), diode laser ( $\lambda_3 = 940$  nm), fiber laser ( $\lambda_4 = 1,06 \mu\text{m}$ ) and CO<sub>2</sub>-laser ( $\lambda_5 = 10,6 \mu\text{m}$ ). Numerical experiments with different types of lasers are for the same power density and speed. A Graph of the dependence of the maximum temperature of the heating on the surface of the product from the wavelength is built. The obtained results are analyzed.

**Keywords** – Numerical experiments, Software TEMPERATURFELD3D, Laser, Wavelength.

## I. INTRODUCTION

Factors that influence the contrast on the laser marking, and hence on the optimization of the process, in general, can be summarized into three groups [1, 2] (see Fig. 1) associated with:

- material properties - optical characteristics (reflectance, absorptivity, depth of penetration) and thermo-physical characteristics(thermal conductivity, thermal diffusivity, specific heat capacity);
- laser source - power density, pulse energy, pulse power, frequency, pulse duration;
- technological process – speed, defocusing, step, number of repetitions.

To these must be added the following factors – the coefficient of overlapping (related to those of the laser source and technological process) and the volume density of the absorbed energy (related to the factors of the three groups).

These basic factors are in certain physical relationships to each other. Relationships and dependencies between them are important for understanding the physical nature of the process and for building its model.

The wavelength is a factor that indirectly influences the research process. Absorptivity (reflection coefficient, respectively) strongly depends on the wavelength of the laser radiation. [3].

On Fig. 1 is represented the dependence  $A = A(\lambda)$  for various metals and steel. A trend was observed - the significantly lower absorptivity of the radiation in the far infrared area compared to that of the radiation in the ultraviolet and visible area.

Many authors have studied the dependence of the

absorptivity  $A$  on the wavelength  $\lambda$  of the laser radiation for Fe [4-8]. On Fig. 2 is presented a summary of the experimental dependence  $A = A(\lambda)$ . With increasing wavelength  $\lambda$  absorptivity decreases and almost linearly throughout the studied interval. For radiation in the infrared region experimental results are consistent with the formula of Hagen-Rubens [9]

$$A = \left( \frac{4c}{\lambda \sigma} \right)^{\frac{1}{2}} \quad (1)$$

where  $c$  is the speed of light in vacuum,  $\sigma$  - electrical conductance in system CGS.

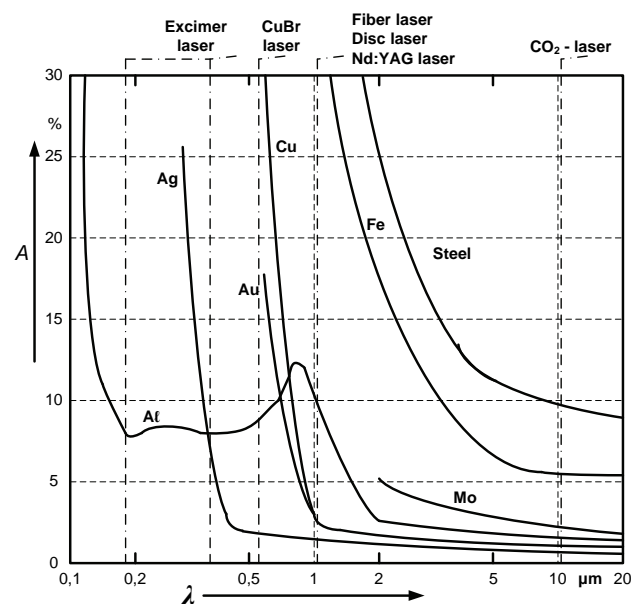


Fig. 1. Dependence of the absorptivity  $A$  on the wavelength  $\lambda$  of the laser beam for certain metals and steel

<sup>1</sup>Nikolay Angelov is with the Department of Physics, Chemical and Ecology at Technical University of Gabrovo, 4 Hadzhy Dimitar str., Gabrovo 5300, Bulgaria, E-mail: [angelov\\_np@abv.bg](mailto:angelov_np@abv.bg).

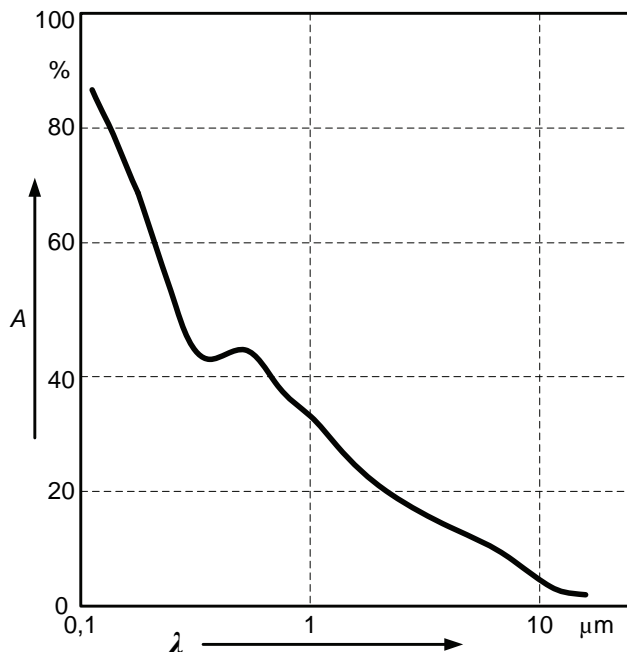


Fig. 2. Experimental dependence of absorptivity  $A$  on the wavelength  $\lambda$  of the laser radiation for Fe

## II. PRESENTATION

The objective of this report was to investigate the influence of the wavelength on the process of laser marking of articles made of metals and alloys. Lasers operating in the visible, near and far infrared areas are used.

### A. Numerical experiments

There have been a series of numerical experiments for calculation of the temperature field in the zone of impact on laser marking by melting on metals and alloys. In Table. 1 are given the used lasers and their wavelengths.

Calculations refer to stainless steel, copper and aluminum. Their main parameters are presented in Table 2 [10, 11].

TABLE 1  
USED LASERS AND THEIR WAVELENGTH

Laser	Wavelength $\lambda$ , nm	$\log [\lambda]$
CuBr laser	511	2,708
Ruby laser	694,3	2,842
Diode laser	940	2,973
Fiber laser	1060	3,025
CO <sub>2</sub> -laser	10600	4,025

TABLE 2  
BASIC PARAMETERS OF THE STUDY MATERIALS

Material Magnitude	Steel 12X17	Cu	Al
Thermal conductivity $k$ , W/(kg.K)	24	401	236
Density $\rho$ , kg/m <sup>3</sup>	7720	8920	2700
Specific heat capacity $c$ , J/(kg.K)	462	380	830
Thermal diffusivity $a$ , m <sup>2</sup> /s	7,01.10 <sup>-6</sup>	1,18.10 <sup>-4</sup>	1,15.10 <sup>-4</sup>
Temperature of melting $T_m$ , K	1750	1357,6	933,47

The numerical experiments were performed with the program TEMPERATURFELD3D [12], specialized in studying of the temperature fields by laser impact. It requires four types of input parameters:

- program;
- geometric;
- of the laser;
- of the material.

At the end are realised the following options:

- 3D and 2D profile of the maximum temperature on the surface of the sample.
- 3D and 2D temperature profile of the sample in depth (layer by layer).
- Dependence of the temperature on the depth in various time points.
- Determination of the speed of heating and cooling in different parts of the product when there is laser impact.
- Animation of the process.

Constant technological parameters in the calculations are given in Table. 3. The speed is typical for an industrial laser marking on products from the studied materials.

TABLE 3  
CONSTANT TECHNOLOGICAL PARAMETERS DURING THE CALCULATIONS

Parameter	Value
Power density $q_s$ , W/m <sup>2</sup>	
Speed $v$ , mm/s	
Number of repetition $N$	1
Defocusing	0

The samples are in the shape of a rectangular plate with a thickness  $h = 500 \mu\text{m}$ . Its upper surface lies in the plane OXY. The movement of the laser beam is in a direction parallel to the OY axis and starting from a point with coordinates  $(8,0.10^5; 0)$  m.

## B. Results

In fig. 3, 4 and 5 are presented 3D temperature fields in the area of the laser impact for stainless steel 12X17. At impact with the given in Table. 3 parameters, the maximum surface temperature of the specimen is  $T_1 = 2250$  K for laser CuBr (fig. 3),  $T_2 = 1790$  K for fiber laser (fig. 4) and  $T_3 = 555$  K for CO<sub>2</sub>-laser (fig. 5).

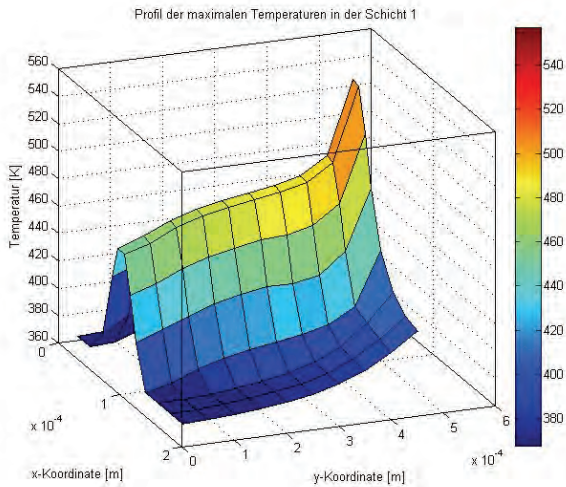


Fig. 3. Temperature profile of the surface of a sample of stainless steel 12X17 when there is an impact with a CuBr laser

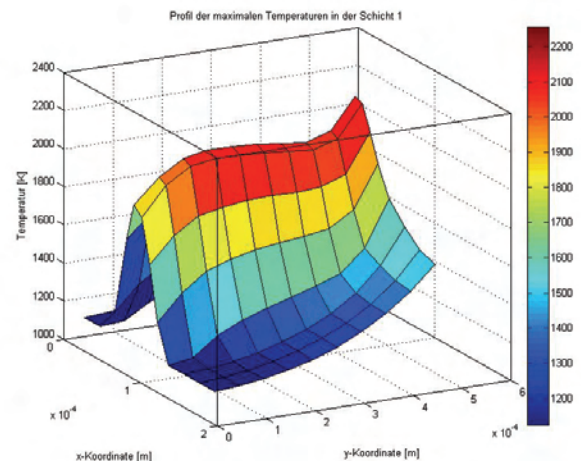


Fig. 5. Temperature profile of the surface of a sample of stainless steel 12X17 when there is an impact with a CO<sub>2</sub> laser

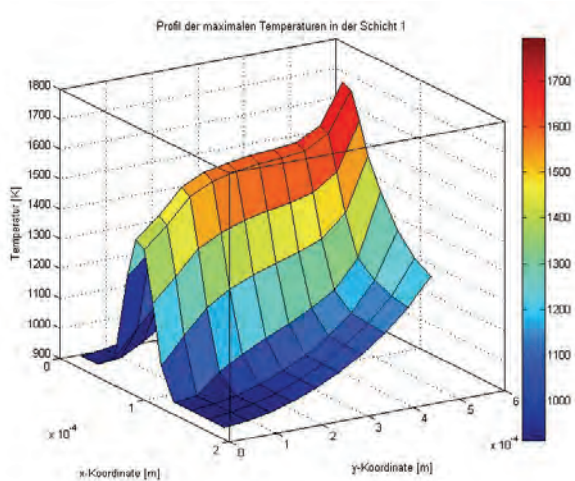


Fig. 4. Temperature profile of the surface of a sample of stainless steel 12X17 when there is an impact with a fiber laser

In fig. 6, 7 and 8 are presented graphs of the dependence  $T = T(\log [\lambda])$  for samples of steel 12X17, copper and aluminium. From their analysis can be made the following conclusions:

For samples of steel 12X17

- With the increase of the wavelength decreases the temperature of the heating on the surface of the sample in the zone of impact.
- In the studied parameters the temperature is above the melting temperature when there is an impact with the lasers in the visible and near infrared area. With a laser in the far infrared area it is 550 K, i.e. considerably lower than the melting temperature.
- For laser marking of samples are suitable lasers, working in the visible and near infrared areas.

For samples of copper

- With the increase of the wavelength sharply reduces the heating temperature on the surface of the sample in the area of impact.
- In the studied parameters the temperature is above the melting temperature when there is an impact with a CuBr laser and with lasers in the near and far infrared areas in the interval  $T \in [450, 700]$  K. This is explained with the significantly lower absorbency of radiation with wavelengths in the near and far infrared areas as compared to that of the visible region.

For samples of aluminium

- The radiation is absorbed best in the near infrared region and in the upper part of the visible region.
- The radiation in the far infrared area is slightly absorbed by the samples and it slightly increases the temperature on the surface within the area of impact. It is not suitable for laser marking by melting.

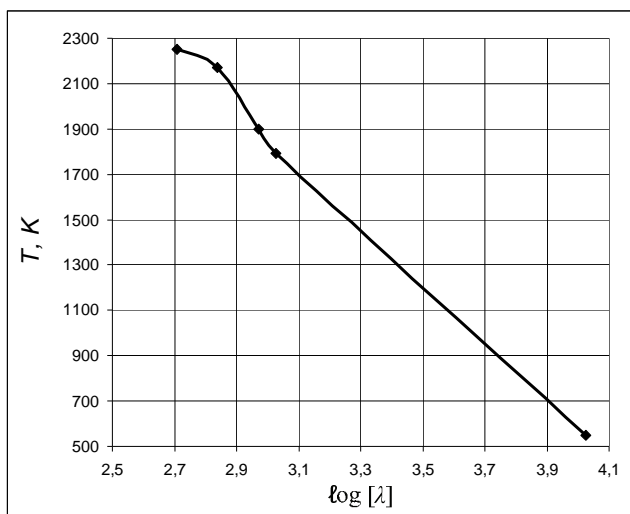


Fig. 6. Graphs on the experimental dependence of the temperature on  $\log [\lambda]$  for a sample of steel 12X17

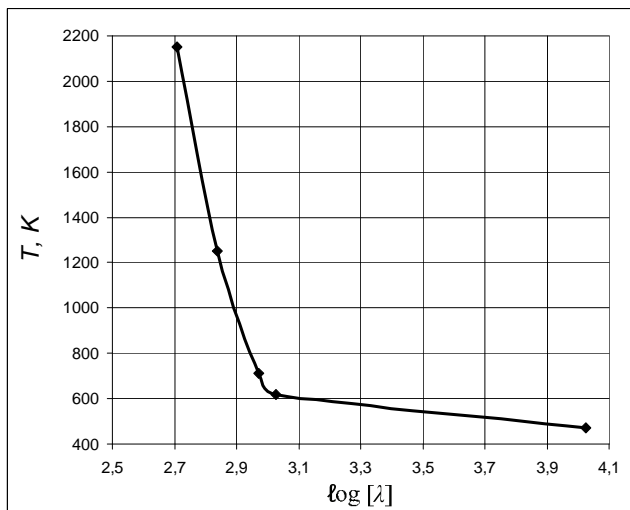


Fig. 7. Graphs on the experimental dependence on the temperature on  $\log [\lambda]$  for a sample of copper

According to the experimental studies can be summarized that the radiation wavelength  $\lambda = 10,6 \mu\text{m}$  is not suitable for marking of steel and metals. From an energetic point of view, the radiation in the visible range is the most suitable for the studied process. For lasers in the near infrared area the absorptivity is relatively good. They possess a very good quality of radiation and a high efficiency coefficient. They are also suitable for marking these materials.

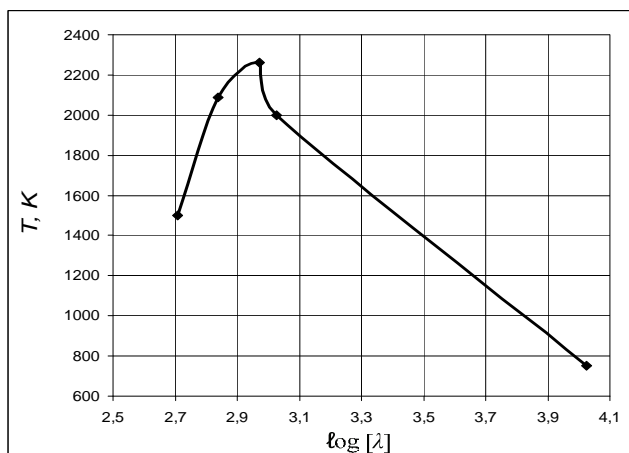


Fig. 8. Graphs on the experimental dependence on the temperature on  $\log [\lambda]$  for a sample of aluminium

### III. CONCLUSION

In the study of the laser marking of metals and alloys should be determined the importance of the various factors affecting the process. The application of numerical experiments leads to faster attainment of optimum results. Thus, it speeds up the attainment of greater efficiency in production and the better quality of the marking.

### REFERENCES

- [1] Lazov L., N. Angelov, Osnovni faktori, opredelyashti kachestvoto na lazernata markirovka na metali i splavi, mejdunarodna nauchna konferenciya AMTECH '07, Gabrovo, 23-24 noemvri 2007, tom I
- [2] Angelov N., Optimizaciya na procesa markirane s lazerno lachenie na obrazci ot instrumentalna stomana, Disertacionen trud za pridobivane na stepen doctor, Tehnicheski universitet – Gabrovo, 2011
- [3] Stern, G.: Absorptivity of cw CO<sub>2</sub>, CO and YAG-laser beams by different metallic alloys, 3rd European Conference on Laser Treatment of Materials (ECLAT) ; 17.-19.09.1990, Erlangen
- [4] Roberts S. Interpretation of the optical properties of metal surface, Physics Revue, 100, 1955
- [5] Weaver J., C. Kafka, D. Lynch, E. Koch Optical Properties of Metals, Fachinformationszentrum Energie, Physik, Matematik, Karlsruhe, 1981
- [6] Schuöcker D. Handbook of the Eurolaser Academy, CHAPMAN&HALL, London, 1998
- [7] Georgiev D., I. Chomakov, B. Bogdanov, Viscosity Behaviour of Cristalizing Glass-Forming Melts, Comptes rendus de l'Academie bulgare des Sciences, Vol. 57, N 12, 2004, 55-60.
- [8] Miller J. Optical properties of liquid metals at high temperatures, Phil. Magazine, 20, 1969
- [9] Hagen E., H. Rubens Über Beziehungen des Reflexions- und Emissionsvermögens der Metalle zu ihrem elektrischen Leitvermögen
- [10] Dinev S., Lazerite v modernite tehnologii, izd. Alfa, Sofia, 1993
- [11] [www.splav.kharkov.com/main.php](http://www.splav.kharkov.com/main.php)
- [12] Belev I., Sreda za presmyatane na lazerno inducirani temperaturni poleta, Diplomna rabota, Tehnicheski universitet, Gabrovo, 2009

# Similarity search in text data for Serbian language

Ulfeta Marovac<sup>1</sup>, Adela Crnisanin<sup>2</sup>, Aldina Pljaskovic<sup>3</sup>, Ejub Kajan<sup>4</sup>

**Abstract – Daily increase in the number of documents on Serbian language in digital form has led to the need for their search. In order to reduce the time required for searching in document, it is necessary to prepare the documents and to group them. This paper presents a method that makes analysis of documents easier, using a small number of lexical resources.**

**Keywords – search engine, indexing, keywords, clustering, Serbian language.**

## I. INTRODUCTION

In order to speed up the process of searching for documents with relevant content in a large data set, the documents must be grouped on the basis of their content. Complex grammar of Serbian language and use of two official alphabets made the searching of documents in Serbian language real challenge. Ambiguity of words and sentence structures aggravate the problem of analyzing the contents of documents. For analysis, there is the need for different lexical resources: corpus of Serbian language, morphological dictionary, stop-words, dictionary of abbreviations, dictionary of proper names and so on. Difficulties in finding appropriate resources are large and depend on the type of document that is being examined. Meaning of the words in legal documents and the words in documents that describe the natural wealth of a country are not the same. Additional problems associated with the analysis of text documents in Serbian are: the lack of adequate resources, constant changes in natural languages (e.g. introduction of new terms) and a great time for processing text when large resources are used.

The search engine for documents in Serbian language described in this paper consists of the following layers: a document preparation, the normalization layer, layer for extracting keywords, clustering layer, and indexing layer within a single cluster. Documents, that represent repository to search, should be prepared, before being inserted into the database, in form that makes it easier to search. Preparation of the document is executed when a new document is inserted into the system. Before inserting into the database, document need to be normalized. Preparation of documents includes: documentation intended change of format, removing redundant and informal character and

structure of the document according to the rules corresponding to the next step, normalization. Preparation of documents in this case includes the following steps:

- Processing of documents in Cyrillic and Latin script
- Processing documents in HTML format
- Removing unnecessary characters (emoticons, slang,...)
- Removing stop words
- Switching between ASCII, UTF8 and Latin letters for the preparations

Finally, after normalization the document should be in Latin script in UTF8 format.

The normalization of the text involves the transformation of the text in some other form that is suitable for any type of computer processing. In our case it is searching. The purpose of the normalization of the word is the releasing of excessive modification of words that do not make changes in meaning, and the reduction of these modifications on the common, basic form. Normalization can be done by: lemmatization word-elimination format for extensions and extensions of the constituent words and the reduction of the lemma, ripping the longest found suffix for the appropriate type of words, allocating to the first  $k$  letter of the word, n-gram analysis of words.

Each of the normalization described above has its advantages and disadvantages. For some required large and specific lexical resources (morphological dictionary, extensions to form words [1], which can make processing more complex, the other does not solve complex derivative words, prefixes and other grammatical peculiarities.

This paper presents a method that makes analysis of documents easier using a small number of lexical resources, using clustering based on keywords, and indexing within the cluster. The rest of the paper is organized as follows. The second chapter describes existing methods for grouping and searching documents, which are applied on other languages. The third chapter contains description of way for grouping documents in Serbian language that is used in our searching system. The fourth section demonstrates similarity searching using indexing. In the end, the significance of the obtained results and directions for further research are given.

## II. RELATED WORK

<sup>1</sup>Ulfeta Marovac is with the State University of Novi Pazar, 36300 Novi Pazar, Vuka Karadzica bb, Serbia, e-mail: umarovac@np.ac.rs

<sup>2</sup>Adela Crnisanin is with the State University of Novi Pazar, 36300 Novi Pazar, Vuka Karadzica bb, Serbia, e-mail: acrnisanin@np.ac.rs

<sup>3</sup>Aldina Pljaskovic is with the State University of Novi Pazar, 36300 Novi Pazar, Vuka Karadzica bb, Serbia, e-mail: apljaskovic@np.ac.rs

<sup>4</sup>Ejub Kajan is with the State University of Novi Pazar, 36300 Novi Pazar, Vuka Karadzica bb, Serbia, e-mail: ekajan@ieee.org

In widespread languages, such as English, there are number of specific techniques and algorithms for the solution of this problem. These existing techniques can not be a solution for searching documents in Serbian, but the basis for a solution to the problem, which can be extended for specific rules regarding Serbian language.

Primary indexes are used for short queries in search engine where keywords are specified by user. Documents searched using these techniques need to be in a form that provides

metadata about where particular words from a document are placed in the database [2].

Latent Semantic Indexing is a method that improves the quality of search by similarity making transform data in the form where there are no synonymy and polysemy problems [3, 4, 5, 6].

Document indexing can be performed using methods dependent on the language, like the dictionary based approach and machine learning. The dictionary based approach uses a set of possible words in a dictionary for morphological matching and segmenting an input text document into words. The machine learning based approach uses some learning algorithms to learn from text corpuses using collection [7].

But there are methods that do not require additional resources and rules of language. N-gram analysis is language-independent as it does not require linguistic knowledge of the language, or the use of a dictionary or a corpus. This approach is not concerned with the meaning of indexing terms. This approach is described for languages with a number of specific characteristics [7, 8].

The suffix array approach identifies substring indexing based on suffixes, which does not require pre-processing text and query processing. This technique is used to construct a substring index, in order to allow for finding the relevant documents containing the user's query [9, 10]

### III. GROUPING DOCUMENTS

Grouping of documents is based on similarities of their content. There are many classes of clustering algorithms such as  $k$ -means algorithm or hierarchical algorithms, which are general-purpose methods and can be extended to any kind of data, including text data. Document clustering is an aggregation of documents by discriminating the relevant documents from the irrelevant documents. The relevance determination criteria of any two documents is a similarity measure and the representatives of the documents. There are some similarity measures such as Euclidian distance, Jaccard's coefficient, and cosine measure. The number of words in the different documents may vary widely. Therefore, it is important to normalize the document representations appropriately during the clustering task. Document vectors are simply constructed from the term frequency (TF) and the inverted document frequency (IDF). [11-13].

The most critical problem for document clustering is the high dimensionality of the natural language text. To reduce the dimension of the vector each document has been represented by the keywords. Keyword in a document is the most frequent word, and not in just one form but in all forms for its semantic meaning. Clustering is performed by using  $k$ -mean algorithm based on keywords. Euclidian distance had been used as distance measures between cluster centre and concrete data point.

Automated keywords extraction is a way to find a small set of words and phrases that describe the content of the document. In the absence of corpus, keywords can be extracted by number of occurrences of concrete terms in the given document. In order to single out the key words, the text must be normalized; in this case, normalization with n-gram

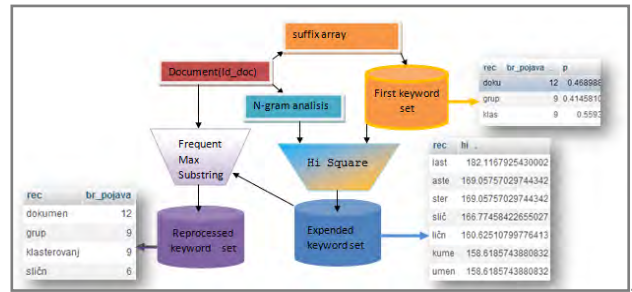


Fig. 1. Keyword extraction

has been used. Most of the word segmentation techniques are language-dependent. They usually rely on language analysis or on the use of dictionary. The preparation of such method is very time consuming. This makes n-gram technique more popular technique. Apart from the n-gram technique, the frequent max substring technique is another technique, which has been proposed to extract index-terms from non-segmented texts. The main strength of this technique is that it was proposed as a language-independent technique, which does not rely on the use of language analysis.

As previously noted, the text is cleared of stop words and all no-letter marks, and divided into sentences. The most frequent terms using suffix array approach are stored in a set of basic keywords. (Fig. 1). As an example, abstract from similar paper to this is used to present this. Top three frequent 4-gram in abstract are : "doku" "klas", "grup ". The document consists of sentences and the frequency of the term is calculated at the sentence level. Extracted keywords are the basis for further searching for keywords and phrases. If a term occurs more frequently in sentences together with certain key words, then it closely define that keywords and is also a candidate for a keyword.[14].

To extract these terms, co-occurrence matrix has been calculated. Matrix contains the number of sentences in which some of the key words ( $q$ ) and other terms( $w$ ) occur together. If a term occurs selectively with only some keywords, that is an indication that term has greater significance. Calculating the deviation from the expected values was performed by h-square test. The expected value is calculated as the product of  $n_w$ , the total number of terms in sentences in which the observed term( $w$ ) appears, and  $p_q$ , as (the sum of the total number of terms in sentences where keyword  $g$  appears) divided by (the total number of terms the document) (Formula 1) [15].

$$\chi^2(w) = \sum_{g \in G} \frac{(freq(w,q) - n_w * p_q)^2}{n_w * p_q} \quad (1)$$

If there are groups of words that are often used together, their n-grams will be singled out. N-grams with the largest h-square test are additional keywords candidate. By allocating only the first n-grams, we ignore the rest of the word, and it may be that some of the words that appear frequently could be overlooked due to different prefixes. On the other hand, the meaning of different words can have the same prefix, so it will be included in the n-gram keywords. For detecting these characteristics, the n-gram analyses of words are made. For the first set of key n-grams, only the initial n-grams, are taken,

but the number of their appearance is calculated independently of their position in the text. Therefore, if the word longer than four letters is significant, it will be identified by extracting all the n-grams that appear in it, because they will show up a greater number of times in

sentences in which the first n-gram of the word appears. In paper [1], the results of applying different normalization for extracting key words have been presented. In our example keyword set had been expended with next 4-grams: "last", "aste", "ster", "slič", "ličn", "kume", "umen", ... (Fig. 2.)

This n-grams are part of word "dokumenat", "klasterovanje" i "sličnost". N-grams part of word "sličnost" are extracted as a part of phrase "sličnost dokumenta". Else showed n-gram are addition the already extracted the key words. To reduce number of keyword frequent max substring technique has been used.[16]

For each extracted keyword had been searched all n-grams ( $n=5,6,\dots$ ) in document with it as suffix. If exist substring of new n-gram in keyword set with same frequency it would be deleted and new n-gram would be add to keyword set. Example: Keyword set {"klas"(frequency  $f=9$ ), "last"( $f=7$ ), "aste" ( $f=7$ ), "ster" ( $f=7$ ), "ovnj" ( $f=5$ ), "rovn" ( $f=5$  )}. N-gram "last" would be replaced with with "klast", then "klast", "aste" would be replaced with "klaste", ... (Fig. 2) Final keyword set {"klas"(frequency  $f=9$ ), "klaster"( $f=7$ ), "klasterovanj"( $f=5$  )}

This step deleted n-gram from a set of keywords which are substring of longer key n-gram and replace them with the longest of that n-gram . For example: "klas" may participate in the formation of the word "klasa" and "klaster" but will n-gram "last", "aste", "ster" to be replaced with a "klaster".

#### IV. INDEXING

Similarity search in text has proven to be an interesting problem from the qualitative perspective because of inherent redundancies and ambiguities in textual descriptions. The method used in search engines in order to retrieve documents most similar to user-defined sets of keywords are mostly presented with the inverted representation, which is the dominant method for indexing text for short user-queries. [17]

In this paper, system needs to be able to retrieve documents containing keywords similar or same to user defined query. Proposed system is possible to search documents by keywords. Data flow diagram of described search engine is depicted. (Fig.3.)

Indexing mechanisms are used to optimize certain accesses to data (records) managed in files. Search key is attribute or combination of attributes used to look up records in a file. An index file consists of records (called index entries) in the form <search key value, pointer to block in data>.

There are two basic types of indexes:

- Ordered indexes: Search keys are stored in a sorted order (type used in this paper).
- Hash indexes: Search keys are distributed uniformly across "buckets" using a hash function

Indexing techniques are evaluated on the basis of:

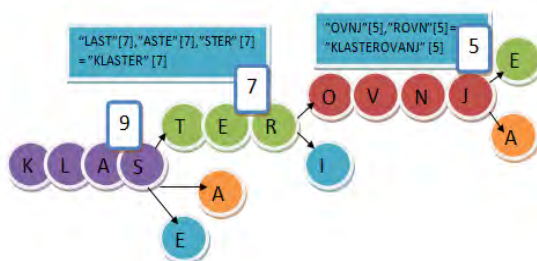


Fig. 2. Max substring technique

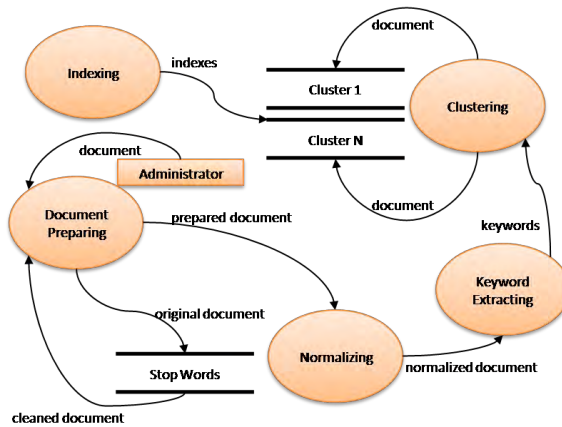


Fig. 3. Data flow diagram of described search engine

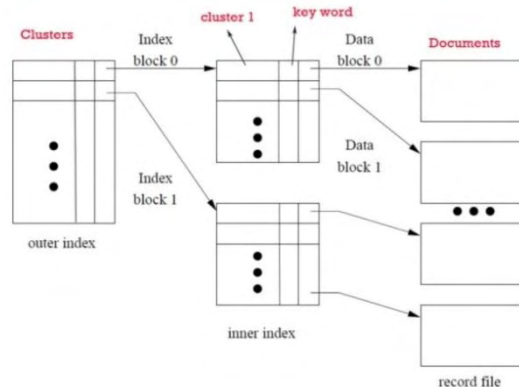


Fig. 4. Multilevel index structure for indexing inside cluster

- Access types that are efficiently supported
- Access time (index entry to record)
- Insertion time (record to index entry)
- Deletion time (record to index entry)
- Space and time overhead (for maintaining index)

Multilevel indexing has been used as the most suitable for this type of search. In query, all words not belonging to one of keywords n-grams have been omitted. In order to speed up searching process, documents are clustered (as previously described). As documents are clustered by keywords, all keywords belonging to one cluster are in one group. Additionally, primary index (ordered cluster index) was created on attributes <id\_cluster, keyword>, which means all keywords belonging to one cluster are searchable in alphabetic order.

In order to speed up searching process, documents are clustered (as previously described). As documents are clustered by keywords, all keywords belonging to one cluster are in one group. Additionally, primary index (ordered cluster index) was created on attributes <id\_cluster, keyword>. This is first-level index. Second-level index is index created to the first level index. Second-level index is also called outer index. Schema and indexed attributes are presented in figure (Fig. 4).

Query (question) consists of small number of words. When user insert query, it has been normalized to n-grams. n-grams made are for keywords already existing (in documents). As documents are already clustered, keywords belonging to particular cluster are defined and centroid for every cluster calculated. Distance for query n-grams and centroids have been calculated and determined to which cluster query n-grams belongs to. After that, searching for documents have been performed just in one cluster (whit the smallest distance do n-grams made of words in query).

## V. CONCLUSION

Solution presented in this paper reduces the problems of large amount of data in text documents in natural languages and also reduce the need for lexical resources to minimum. Further research will improve algorithms for extracting keywords, clustering and indexing documents. Searching will be enhanced using inverted index structure for indexing word in documents.

## ACKNOWLEDGEMENT

This research was partially supported by Ministry of Education, Science and Technological Development of Serbia, under the grants III44007.

## REFERENCES

- [1] U. Marovac, A. Pljasković, A. Crnišanin, E. Kajan, " N-gram analiza tekstualnih dokumenata na srpskom jeziku", Proceedings of TELFOR 2012, Belgrade, Serbia, 2012.
- [2] G. Salton, M. J. McGill. *Introduction to Modern Information Retrieval*. Mc Graw Hill, New York, 1983.
- [3] C. C. Aggarwal. "On the Effects of Dimensionality Reduction on High Dimensional Similarity Search" ACM PODS Conference, 2001.

- [4] C. C. Aggarwal, S. Parthasarathy. Mining Massively Incomplete Data Sets by Conceptual Reconstruction. ACM KDD Conference, 2001.
- [5] Dumais S., Furnas G., Landauer T. Deerwester S., "Using Latent Semantic Indexing to improve information retrieval" ACM SIGCHI Conference, 1988.
- [6] J. Kleinberg, A. Tomkins. "Applications of Linear Algebra in Information Retrieval and Hypertext Analysis" ACM PODS Conference, 1999.
- [7] T. Chumwatana, A Frequent Max Substring Technique for Thai Text Indexing, this thesis is presented for the Degree of Doctor of Philosophy of Murdoch University, 2011.
- [8] M. Mansur, N. UzZaman, M. Khan "Analysis of n-gram based text categorization for Bangla in a newspaper corpus" , ICCIT 2006, Dhaka, Bangladesh, 2006.
- [9] E. Kajan, A. Pljasković, A. Crnišanin „Normalization of text documents in serbian language for eficient searching in e-government systems“,ETRAN 2012, Zlatibor, Serbia, 2012.
- [10] A. Crnišanin, A. Pljasković, U. Marovac, E. Kajan "One solution of searching text documents in Serbian language", ICIST, Kopaonik, Serbia, 2013.
- [11] C. C. Aggarwal, C. X. Zhai, "A Survey Of Text Clustering Algorithms", Mining Text Data, 2012
- [12] K.Subhadra, M.Shashi , "Hybrid Distance Based Document Clustering with Keyword and Phrase Indexing" , IJCSI International Journal of Computer Science Issues, Vol. 9, Issue 2, No 1, March 2012
- [13] S. Kang, "Keyword-based document clustering", Proceeding AsianIR '03 Proceedings of the sixth international workshop on Information retrieval with Asian languages – vol. 11 pp. 132-137, 2003.
- [14] U. Marovac, E. Kajan, G. Šimić," A solution of semantic clustering of text documents ",CPPMI 2012, Novi Pazar, Serbia, 2012.
- [15] Y. Matsuo, M. Ishizika "Keyword Extraction from a Single Document using Word Co-occurrence Statistical Information" International Journal on Artificial Intelligence Tools. Vol. 13, No 1, pp. 157-169, 2004.
- [16] T. Chumwatana, K. W. Wong and H. Xie, "Using Frequent Max Substring Technique for Thai Text Indexing", accepted for publication in the Australian Journal of Intelligent Information Processing Systems (AJIIPS)
- [17] G. Salton and M.J. McGill. Introduction to Modern Information Retrieval. McGraw-Hill, New York, 1983.
- [18] J. Zobel, A. Moffat , R. Sacks-Davis, "An efficient indexing technique for full-text database systems", In Proceedings of 18th International Conference on Very Large Databases, 1992.
- [19] C. C. Aggarwal, P. S. Yu, "On Effective Conceptual Indexing and Similarity Search in Text Data", Proceedings 2001 IEEE International Conference on Data Mining

# Optimization of Vehicle Maintenance Concept Using Simulation

Ivan Djokic<sup>1</sup>, Ljubomir Lazic<sup>2</sup>, Aldina Pljaskovic<sup>3</sup>, Aleksandra Pavlovic<sup>4</sup>

**Abstract –** This paper addresses a discrete-event simulation model, which estimates the operational availability and maintenance cost of a vehicle fleet throughout complete life cycle, under a variety of acquisition requirements, operational tempos, and maintenance scenarios. Based on simulation results one can make cost-effective decision relative to buying adequate vehicles and organizing proper fleet maintenance. In this work we have analyzed application of our model on an example - finding potential vehicles, capable of fulfilling requirements, under different maintenance conditions and working within a set of operational tempos.

**Keywords –** Vehicle, simulation, life-cycle, maintenance, availability, cost.

## I. INTRODUCTION

The technical performance of vehicles (such as speed, range, stability, payload, power generation) has been studied and improved significantly over the last several decades. On the other hand, suitability parameters (such as reliability, availability, and maintainability) have not been analyzed and improved. Suitability determinants are generally not addressed early enough during program development and are not prioritized with the same seriousness and discipline as performance parameters. The cost of operating and maintaining a vehicle fleet is a large expense for the owner, and suitability performance is a major factor affecting these costs. Most maintenance strategy optimization techniques are designed to increase system availability, without accounting for customer need as minimal service level or cost-effectiveness of the whole life cycle. Very often logistics and maintenance objectives are separately optimized and optimization results are moderate. The development of life-cycle models is necessary to identify key factors that affect operational readiness and cost of required readiness. Modeling needs complex and time consuming research to examine many input parameters and possible scenarios, and models usually cover specific system or only a part of a life-cycle.

This work is aimed at developing simulation tool for revealing the mutual impact of acquisition, operational

tempo and maintenance, proving evidence for benefit of a joint optimization, incorporating availability, logistics, and financial aspects. In this paper we suggest a simulation model, based on General Purpose Simulation System (GPSS) [1], which allows integrated analysis of complete transportation fleet life cycle, from acquisition to retirement. Simulation results show fleet availability for different acquisition alternatives, different maintenance strategies and different operational tempos. Simulation results are sufficient to estimate fleet life cycle ownership cost (fleet acquisition, scheduled preventive maintenance cost, and corrective maintenance cost).

## II. RELATED WORK

The development of life-cycle models is necessary to identify key factors that affect operational readiness and cost of required readiness. Transportation systems, with different levels of importance, are analyzed via simulation, covering specific aspect and using specific simulation technique.

One model utilizes expert knowledge to predict the operational requirements of a spacecraft concept, including the ground activities, flows, resources, and costs; all the components of the transportation system. The model incorporates simulation in order to include spaceport characteristics as alternative flows, processing variability, and other random events [2]. A method of reliability and functional analysis related to discrete transport systems is based on modeling and simulating of the system behavior. Monte Carlo simulation is used for proper reliability and functional parameters calculation. The simulator is built using Scalable Simulation Framework (SSF) [3], [4]. Simulation is also used to examine the dependency between safety factor and system availability. In addition to the classic optimization criteria, as minimizing costs and maximizing system availability, the overall cash flow and the discounted cash flow of the production system were taken as supplementary objective functions [5]. A simulation method of repairable one-unit system's reliability and spare requirement under preventive maintenance especially preventive maintenance with periodic testing is used. Simulating model is developed to solve the multi-objective constrained optimization problem of maximizing system availability and minimizing maintenance cost under constraints of repair time, test interval, spare number [6]. A specific case is the decision support system using simulation in the dynamic environment of vehicles repair and maintenance. Simulation results as decision support system and analysis have given a valuable insight of the systems involved [7]. To understand the bottleneck operations and to improve the service rate of the four wheeler service sector, a discrete event simulation model has been developed [8]. Modern logistics systems are much

<sup>1</sup>Ivan Djokic is with the State University of Novi Pazar, 36300 Novi Pazar, Vuka Karadzica bb, Serbia, e-mail: idjokic@np.ac.rs

<sup>2</sup>Ljubomir Lazic is with the State University of Novi Pazar, 36300 Novi Pazar, Vuka Karadzica bb, Serbia, e-mail: llazic@np.ac.rs

<sup>3</sup>Aldina Pljaskovic is with the State University of Novi Pazar, 36300 Novi Pazar, Vuka Karadzica bb, Serbia, e-mail: apljaskovic@np.ac.rs

<sup>4</sup>Aleksandra Pavlovic is with the State University of Novi Pazar, 36300 Novi Pazar, Vuka Karadzica bb, Serbia, e-mail: apavlovic@np.ac.rs

more than simply networks of material flow. For a sustainable practice of simulation in logistics a model-based approach which begins with a formal language is developed [9].

### III. SIMULATION CONCEPT

The simulation model, used in this work, was built using GPSS in such a way that software not only provides tools for modeling and simulation of a wide variety to acquisition policies, operational plans and maintenance services, but also has possibility to shape input data and carry out output statistics. The vehicle life-cycle simulation concept is shown on Fig. 1. The proposed model is subdivided into three parts, acquisition module, operational tempo module, and maintenance and failure module. This subdivision provides easy maintainability and simple extendibility of the model. Within those modules, all cost-effective processes are modeled.

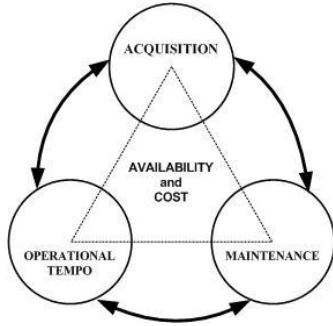


Fig. 1. Vehicle life-cycle simulation concept

**Acquisition module** defines number of vehicles (operational and reserve), vehicle delivery dynamics, vehicle serial numbers, vehicle reliability (probability to fulfill a daily mission without a failure), failure distribution between minor and serious failures, maximal path between preventive maintenance actions, vehicle acquisition price, etc.

**Operational tempo.** Operational tempo is a measure of the dynamics of an operation in terms of equipment usage. In this model operational tempo is defined by daily driving hours (5 days per week) and speed distribution, which gives average vehicle's path per year. Operational tempo can be changed by increasing/decreasing number of driving hours. The driving speed depends on operational environment. Higher than expected utilization rates and fatigue caused by operating environment are resulting in reduced service life. Statistical data show that higher operational tempo have resulted in increased requirements for maintenance, and this maintenance is targeted at restoring the vehicles back to operational and mission-readiness standards through the replacement of consumable and repairable parts (e.g., tires, engines, transmissions, shocks, etc.).

**Maintenance.** Maintenance depicts the entity of all technical, technological, organizational, and economic actions to delay wearout and/or recovery of functional capability, including technical safety, of a technical system. A maintenance strategy defines type, content and temporal sequence of maintenance tasks for a technical system.

Elaboration of a maintenance strategy optimization is a non-trivial issue since many different and partially contradictory requirements have to be incorporated. Different maintenance strategies are shown in Fig. 2, all of them are with regular scheduled maintenance actions for restoring the lost capability of subsystem impairments (restores assets to operational standards by replacing and/or repairing impaired consumables), and these maintenance actions allow the vehicles to meet operational standards and requirements. That means - vehicle failure intensity can be considered constant throughout complete service life. In the case of extreme operational tempo maintenance done to counter the effects of it, to some degree, but regardless of the maintenance or "reset" completed, it does not bring the vehicle to a true "zero-km" condition.

MAINTENANCE ACTIVITY	MILITARY IV-LEVEL MAINTENANCE CONCEPT	MILITARY II-LEVEL MAINTENANCE CONCEPT	TYPICAL VEHICLE MAINTENANCE WORKSHOP
Preventive maintenance, Inspections, Minor adjustments	UNIT Maintenance Level	FIELD Maintenance Level	Minor Repair Bay
Fault detection, Equipment/Part repair, Calibration, Adjustment	DIRECT SUPPORT Maintenance Level	GENERAL SUPPORT Maintenance Level	Major Repair Bay
Diagnose faults, Isolate faults, Repair, Minor modifications		SUSTAINMENT Maintenance Level	
Overhaul, Modifications, Manufacture of parts	DEPOT Maintenance Level		Body Work Bay

Fig. 2. Vehicle maintenance levels

*Output parameters* in our model are: fleet availability, vehicle availability, vehicle usage histogram, number of preventive maintenance actions, vehicle preventive maintenance histogram, number of minor corrective actions, number of serious corrective actions, field maintenance station utilization, field stations queue, depot utilization, depot queue, total preventive maintenance working hours, total field level corrective maintenance working hours, total depot level corrective maintenance working hours, vehicle failure histogram, vehicle daily path, vehicle total path, vehicle maintenance cost.

Operational Availability is a measure of the percentage of the total inventory of a system operationally capable (ready for tasking) of performing an assigned mission at a given time, based on materiel condition. This can be expressed mathematically (as the number of operational items divided by the total population). Operational Availability also indicates the percentage of time that a system is operationally capable of performing an assigned mission and can be expressed as uptime divided by uptime plus downtime:

$$A_O = \frac{t_{uptime}}{t_{uptime} + t_{downtime}} \quad (1)$$

Where  $t_{uptime}$  is the time when a system is ready for operation, and  $t_{downtime}$  is the maintenance down time, which includes repair time, administrative and logistics delay times. Determining the optimum value for Operational Availability requires comprehensive analysis of the system and its planned use, including the planned operating environment, operating tempo, reliability alternatives, maintenance approaches, and

supply chain solutions. In this model Operational Availability is calculated for every vehicle and complete fleet using Eq. (1). Clearly, Operational Availability can be improved by increasing reliability and/or decreasing repair or cycle-time. Thus, the two key issues to improve systems readiness are reliability improvement and cycle-time reduction.

The costs of owning and operating a vehicle fleet can be defined in many different ways: capital and operating costs; fixed and variable costs; direct and indirect costs; avoidable and unavoidable costs; average and marginal costs; current and future costs; fiscal and economic costs. The distinctions between these terms are not merely semantic, and decisions regarding the management of these costs can have a profound impact on a fleet organization. The goal of our simulation model is to predict the availability of a transportation fleet and to estimate vehicle total cost, consisting of ownership cost (fixed) and vehicle maintenance cost (variable). The maintenance cost is defined by Eq. (2), and consists of two components, cost of preventive and corrective maintenance activities.

$$MC_{\text{total}} = MC_{\text{prev}} + MC_{\text{corr}} \quad (2)$$

Fig. 3 shows simplified, easy understandable simulation algorithm, where all parts defined in simulation concept and their relationships are visible. Model has 1289 lines of GPSS code.

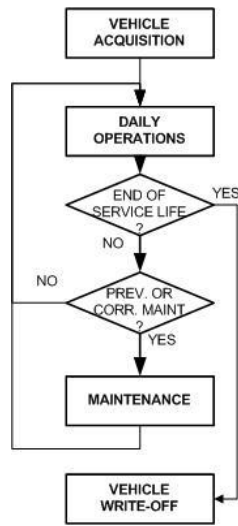


Fig. 3. Simplified simulation algorithm

The simulation model is a very flexible one, and gives the opportunity to change a variety of parameters: fleet size, vehicle reliability, operational tempo, work allocation between several maintenance levels, time-to-repair distribution, maintenance cost – vehicle age correlation, preventive maintenance strategy, etc. The simulation results give a detailed insight into fleet life cycle: obtained availability of the fleet and every vehicle, every vehicle and fleet daily and total path, maintenance facilities utilization, queues, logistics administrative time, maintenance labor, maintenance cost (minimal, maximal, mean, standard

deviation). The simulation model applied on procurement (or development) and maintenance alternatives, supports decision makers in finding the optimal solutions at an early phase of a project.

#### IV. THE EXAMPLE

Importance of simulation and its use in optimization lies in the fact that many problems are too complex to be described in mathematical formulations. Nonlinearities, combinatorial relationships or uncertainties often give rise to simulation as the only possible approach to solution. Our simulation model is tested through relatively complex example: find the acceptable vehicle reliability for defined acquisition policy and set of two-level maintenance concepts (one depot and a number of mobile maintenance teams), and determine life-cycle maintenance cost. The vehicle fleet consists of 220 light tactical vehicles with required availability 0.89. The optimization process consists of six steps: (1) Requirements establishment, (2) Definition of vehicle procurement or development policy, (3) Definition of maintenance alternatives, (4) Fleet life cycle simulation for different vehicle reliability-operational tempo-maintenance concept combination, (5) Cost estimation for every simulation scenario, and (6) Selection of cost-effective fleet solution acceptable vehicle and efficient maintenance concept).

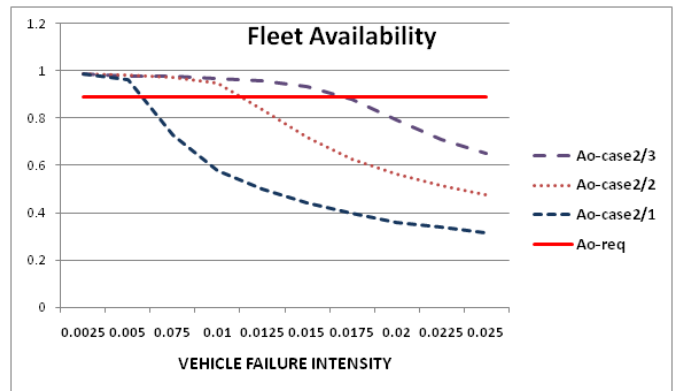


Fig. 4. Fleet availability as a function of vehicle failure intensity

The objective in our example was the satisfaction of availability requirement (0.89) with a modern two-level maintenance system. Optimization process consists of repetitive simulation runs with different values of the influence variables. Those variables are varied from simulation to simulation to find optimal combination of parameter values to solve the problem with respect to the objective function and constraints. Influence variables are vehicle failure intensity and maintenance alternatives. The total number of runs was 90 (10 vehicle failure intensities x 9 maintenance alternatives). Fig. 4 shows fleet availability as a function of vehicle failure intensity, for three maintenance alternatives (case2/3 = 1 depot + 3 mobile stations, case2/2 = 1 depot + 2 mobile stations, and case2/1 = 1 depot + 1 mobile station). The results clearly indicate that maximum acceptable

vehicle failure rate for case2/3 is 0.016, for case2/2 is 0.0112, and for case2/1 is 0.006. Total vehicle maintenance cost, for the vehicle life-cycle of 22 years, was also analyzed for every maintenance case. Fig. 5 shows, as an example, the maintenance cost for case2/2.

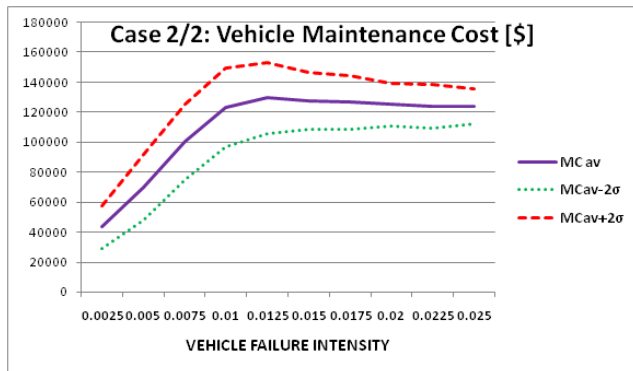


Fig. 5. Vehicle life-cycle maintenance cost as a function of vehicle failure intensity

Buying the vehicle with failure intensity of 0.0075 and applying maintenance case2/2, a buyer can expect 0.972 fleet availability and 100000\$ mean life-cycle maintenance cost (per vehicle).

## V. CONCLUSION

Many simulation runs confirmed the assumption that system availability alone is an insufficient objective function for determine and optimize a vehicle maintenance strategy. Availability considerations have to be merged with financial aspects to achieve optimal maintenance strategy that satisfies both, the required availability and lowest possible total life cycle costs. Our simulation model is flexible enough to cover variety of scenarios: different acquisition requirements, different operational tempos, and different maintenance strategies. The model functionality was demonstrated through an illustrative example – finding potential vehicles, capable of fulfilling requirements, under a set of maintenance conditions and variety of operational tempos.

Further work would include new preventive maintenance concepts and different failure rate shapes.

## ACKNOWLEDGEMENT

This research was partially supported by Ministry of Education, Science and Technological Development of Serbia, under the grants TR32023 and TR35026.

## REFERENCES

- [1] T. J. Schriber, *Simulation Using GPSS*, John Wiley & Sons, 1974.
- [2] A. J. Ruiz-Torres, E. Zapata, „Simulation Based Operational Analysis of Future Transportation Systems“, Proceedings of the Winter Simulation Conference, pp. 1123-1131, Orlando, USA, 2000.
- [3] T. Walkowiak, J. Mazurkiewicz, “Discrete transport system simulated by SSF for reliability and functional analysis”, Proceedings of the 2nd International Conference on Dependability of Computer Systems (DepCoS-RELCOMEX'07), pp. 352-359, Szklarska Poreba, Poland, 2007.
- [4] T. Walkowiak, J. Mazurkiewicz, “Availability of Discrete Transport System Simulated by SSF Tool”, Proceedings of Third International Conference on Dependability of Computer Systems DepCoS-RELCOMEX 2008, pp. 430-437, Szklarska Poreba, Poland, 2008.
- [5] D. Achermann, *Modelling, Simulation and Optimization of MaintenanceStrategies under Consideration of Logistic Processes*, A dissertation submitted to the SWISS Federal Institute of Technology Zurich for the degree of Doctor of Technical Sciences, 2008.
- [6] H. Ying, C. Jian, Y. Rong, X. Shulin, “Reliability and spare parts requirement prediction of repairable one-unit system under periodic testing and preventive maintenance”, Second International Conference on Intelligent Computation Technology and Automation, pp. 590-593, Changsha, Hunan, China, 2009.
- [7] A. Mehmood, M. Jahanzaib, “Simulation Based Decision Support System (SBDSS) for the Vehicles Repair and Maintenance in Dynamic Business Environment”, Proceedings of the 2010 International Conference on Industrial Engineering and Operations Management, pp. 452-459, Dhaka, Bangladesh, 2010.
- [8] Ch. Venkatadri Naidu, P. Madar Valli, A. V. Sita Rama Raju, „Application of Simulation for the Improvement of Four Wheeler Service Sector”, International Journal of Engineering and Technology vol.2, no.1, pp. 16-23, 2010.
- [9] G. Thiers, L. McGinnis, “Logistics Systems Modeling and Simulation”, Proceedings of the Winter Simulation Conference, pp. 1536-1546, Arizona, USA, 2011.

# Use of genetic algorithms for optimal design of electrical resistive furnaces insulation

Hristo Nenov<sup>1</sup> and Borislav Dimitrov<sup>2</sup>

**Abstract –** The using of genetic algorithms approach for design of chamber resistive furnaces (CRF) insulation is presented in this paper. The solution of the specified optimization problem and finding the optimal parameters are the basic precondition for increasing the efficiency of resistance furnaces.

**Keywords –** genetic algorithms, optimization, electrical resistive furnaces.

## I. INTRODUCTION

Electric resistance furnace chambers (EFC) are designed for heat treatment of steel parts - annealing, normalization and more. They are powerful consumers of electricity, which is why the problems related to improving the energy effectiveness are particularly relevant. The analysis of the processes run in the chamber resistance furnaces using model and numerical methods gives significant opportunities for optimization when setting different target functions. Proper results are achieved by working with detailed models, whose parameters correspond to maximum facility.

## II. ANALYSIS

### A. Genetic algorithm

The genetic algorithm is a method for solving both constrained and unconstrained optimization problems that is based on natural selection, the process that drives biological evolution. The genetic algorithm repeatedly modifies a population of individual solutions. At each step, the genetic algorithm selects individuals at random from the current population to be parents and uses them to produce the children for the next generation. Over successive generations, the population "evolves" toward an optimal solution. You can apply the genetic algorithm to solve a variety of optimization problems that are not well suited for standard optimization algorithms, including problems in which the objective function is discontinuous, nondifferentiable, stochastic, or highly nonlinear. The genetic algorithm can address problems of mixed integer programming, where some components are restricted to be integer-valued.

The genetic algorithm uses three main types of rules at each step to create the next generation from the current population:

- Selection rules select the individuals, called parents that contribute to the population at the next generation.
- Crossover rules combine two parents to form children for the next generation.
- Mutation rules apply random changes to individual parents to form children.

The genetic algorithm differs from a classical, derivative-based, optimization algorithm in two main ways, as summarized in the following table.( Table 1).

TABLE I  
ALGORITHM COMPARE

Classical Algorithm	Genetic Algorithm
Generates a single point at each iteration. The sequence of points approaches an optimal solution.	Generates a population of points at each iteration. The best point in the population approaches an optimal solution.
Selects the next point in the sequence by a deterministic computation.	Selects the next population by computation which uses random number generators.

### B. Genetic Algorithm Terminology

#### Fitness Functions

The fitness function is the function you want to optimize. For standard optimization algorithms, this is known as the objective function. The toolbox software tries to find the minimum of the fitness function.

Write the fitness function as a file or anonymous function, and pass it as a function handle input argument to the main genetic algorithm function.

#### Individuals

An individual is any point to which you can apply the fitness function. The value of the fitness function for an individual is its score.

#### Populations and Generations

A population is an array of individuals. For example, if the size of the population is 100 and the number of variables in

<sup>1</sup>eng. Hristo Nenov, Ph.D– Technical University of Varna, Bulgaria, assistant professor. E-mail – [ico762001@gmail.com](mailto:ico762001@gmail.com)

<sup>2</sup>eng. Borislav Dimitrov, Ph.D– Technical University of Varna, Bulgaria, associated professor.  
E-mail – [bdimitrov@processmodeling.org](mailto:bdimitrov@processmodeling.org).

the fitness function is 3, the population is represented by a 100-by-3 matrix. The same individual can appear more than once in the population. For example, the individual (2, -3, 1) can appear in more than one row of the array.

At each iteration, the genetic algorithm performs a series of computations on the current population to produce a new population. Each successive population is called a new generation.

### Diversity

Diversity refers to the average distance between individuals in a population. A population has high diversity if the average distance is large; otherwise it has low diversity. In the following figure, the population on the left has high diversity, while the population on the right has low diversity.

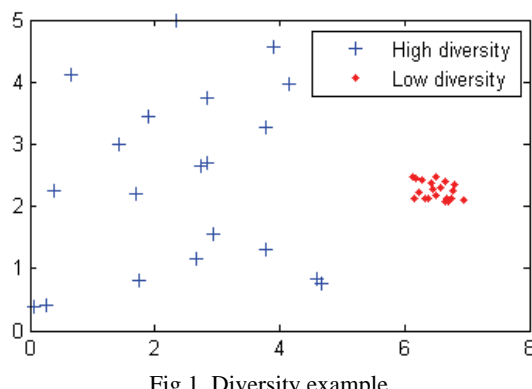


Fig.1. Diversity example

Diversity is essential to the genetic algorithm because it enables the algorithm to search a larger region of the space.

### Fitness Values and Best Fitness Values

The fitness value of an individual is the value of the fitness function for that individual. Because the toolbox software finds the minimum of the fitness function, the best fitness value for a population is the smallest fitness value for any individual in the population.

### Parents and Children

To create the next generation, the genetic algorithm selects certain individuals in the current population, called parents, and uses them to create individuals in the next generation, called children. Typically, the algorithm is more likely to select parents that have better fitness values.

### C. How it works

1. The algorithm begins by creating a random initial population.
2. The algorithm then creates a sequence of new populations. At each step, the algorithm uses the individuals in the current generation to create the next population. To create the new population, the algorithm performs the following steps:

- a. Scores each member of the current population by computing its fitness value.
- b. Scales the raw fitness scores to convert them into a more usable range of values.
- c. Selects members, called parents, based on their fitness.
- d. Some of the individuals in the current population that have lower fitness are chosen as elite. These elite individuals are passed to the next population.
- e. Produces children from the parents. Children are produced either by making random changes to a single parent—mutation—or by combining the vector entries of a pair of parents—crossover.

### 3. Replaces the current population with the children to form the next generation.

#### Creating the Next Generation

At each step, the genetic algorithm uses the current population to create the children that make up the next generation. The algorithm selects a group of individuals in the current population, called parents, who contribute their genes—the entries of their vectors—to their children. The algorithm usually selects individuals that have better fitness values as parents. You can specify the function that the algorithm uses to select the parents in the Selection function field in the Selection options.

The genetic algorithm creates three types of children for the next generation:

Elite children are the individuals in the current generation with the best fitness values. These individuals automatically survive to the next generation.

Crossover children are created by combining the vectors of a pair of parents.

Mutation children are created by introducing random changes, or mutations, to a single parent.

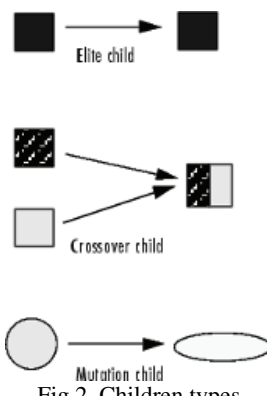


Fig.2. Children types

The algorithm stops when one of the stopping criteria is met.

### Crossover Children

The algorithm creates crossover children by combining pairs of parents in the current population. At each coordinate of the child vector, the default crossover function randomly selects an entry, or gene, at the same coordinate from one of the two parents and assigns it to the child. For problems with linear constraints, the default crossover function creates the child as a random weighted average of the parents.

### Mutation Children

The algorithm creates mutation children by randomly changing the genes of individual parents. By default, for unconstrained problems the algorithm adds a random vector from a Gaussian distribution to the parent. For bounded or linearly constrained problems, the child remains feasible.

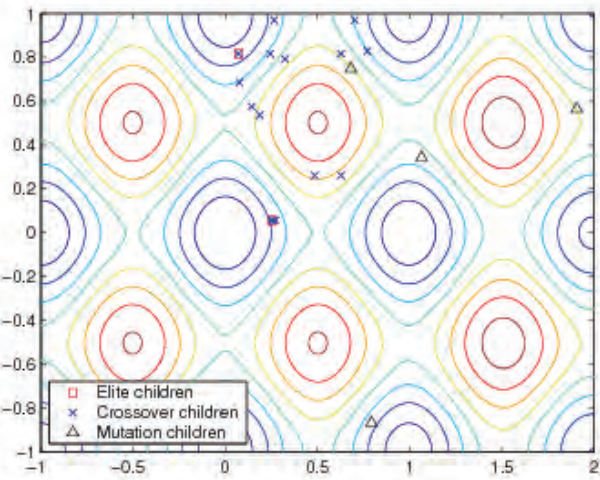


Fig.3. Children types

### Stopping Conditions for the Algorithm

The genetic algorithm uses the following conditions to determine when to stop:

- Generations — the algorithm stops when the number of generations reaches the value of Generations.
- Time limit — the algorithm stops after running for an amount of time in seconds equal to Time limit.
- Fitness limit — the algorithm stops when the value of the fitness function for the best point in the current population is less than or equal to Fitness limit.
- Stall generations — the algorithm stops when the weighted average change in the fitness function value over Stall generations is less than Function tolerance.
- Stall time limit — the algorithm stops if there is no improvement in the objective function during an interval of time in seconds equal to Stall time limit.
- Function Tolerance — the algorithm runs until the weighted average relative change in the fitness function value over Stall generations is less than Function tolerance. The weighting function is

$1/2n$ , where  $n$  is the number of generations prior to the current.

- Nonlinear constraint tolerance — The Nonlinear constraint tolerance is not used as stopping criterion. It is used to determine the feasibility with respect to nonlinear constraints. Also, a point is feasible with respect to linear constraints when the constraint violation is below the square root of Nonlinear constraint tolerance.

### Reproduction Options

Reproduction options control how the genetic algorithm creates the next generation. The options are

**Elite count** — the number of individuals with the best fitness values in the current generation that are guaranteed to survive to the next generation. These individuals are called elite children. The default value of Elite count is 2.

When Elite count is at least 1, the best fitness value can only decrease from one generation to the next. This is what you want to happen, since the genetic algorithm minimizes the fitness function. Setting Elite count to a high value causes the fittest individuals to dominate the population, which can make the search less effective.

**Crossover fraction** — the fraction of individuals in the next generation, other than elite children, that are created by crossover. Setting the Crossover Fraction describes how the value of Crossover fraction affects the performance of the genetic algorithm.

### Mutation and Crossover

The genetic algorithm uses the individuals in the current generation to create the children that make up the next generation. Besides elite children, which correspond to the individuals in the current generation with the best fitness values, the algorithm creates

Crossover children by selecting vector entries, or genes, from a pair of individuals in the current generation and combine them to form a child

Mutation children by applying random changes to a single individual in the current generation to create a child

Both processes are essential to the genetic algorithm. Crossover enables the algorithm to extract the best genes from different individuals and recombine them into potentially superior children. Mutation adds to the diversity of a population and thereby increases the likelihood that the algorithm will generate individuals with better fitness values.

Some of the advantages of a GA include that it

- Optimizes with continuous or discrete variables;
- Doesn't require derivative information;
- Simultaneously searches from a wide sampling of the cost surface;
- Deals with a large number of variables;
- Is well suited for parallel computers;
- Optimizes variables with extremely complex cost surfaces (they can jump out of a local minimum);
- Provides a list of optimum variables, not just a single solution;

- May encode the variables so that the optimization is done with the encoded variables, and
- Works with numerically generated data, experimental data, or analytical functions.

These advantages are intriguing and produce stunning results when traditional optimization approaches fail miserably.

#### D. Optimisation of chamber resistive furnaces (CRF) insulation

The main factor determining the energy performance of CRF is the loss. The realization of the assigned tasks is reduced to: define minimum losses - for stationary furnaces operating in continuous mode (industrial, large-sized furnace, etc.); define minimum size and weight - use the CRF if necessary with incidentals – furnace that are non-essential facilities and are required to take minimum space, mobile furnace mounted on a platform, laboratory ones, etc.

The object of research is a CRF. As a target function to solve the optimization problem is set minimization of heat losses.

The parameters involved in the mathematical model that describes the heat losses of the furnace are:

- number of layers
  - ✓ fire resistant layer size/weight
  - ✓ insulation layer size/weight
  - ✓ thickness of the layers
- rated temperature
- productivity
- voltage
- specific heat capacity
- thermal conductivity
- density
- degree of blackness
- size of the walls.

As restrictive conditions are determined the range of variation of the material specific heat, size of the walls and thickness of the insulating layers.

On the fig.4 is shown the situation before the process of optimization

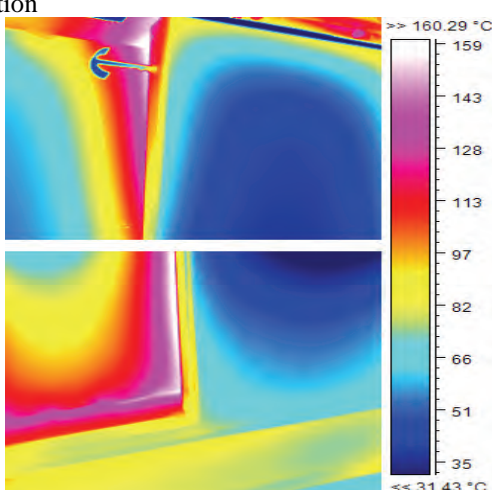


Fig.4. infra-red thermo picture of CRF before optimization (manhole chamber)

The figure clearly shows that the resulting temperature of the outer shell ( $\approx 160$  C°) of the furnace is unacceptable to the conditions of work of this type of facility.

The optimization process, correct the values of the different parameters of the CRF, and after changes to the technical characteristics of the furnace, the following results were achieved (Fig.5).

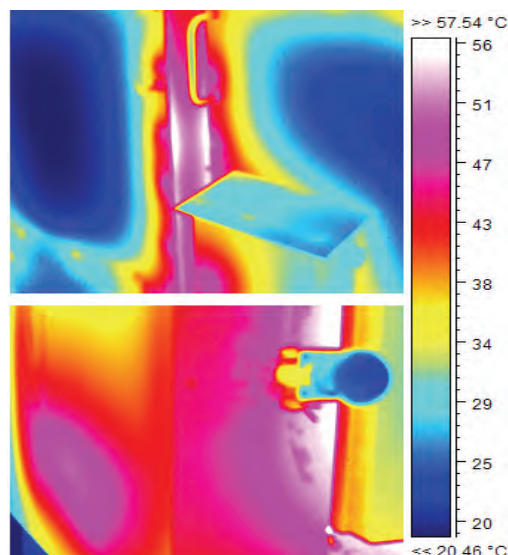


Fig.4. infra-red thermo picture of CRF after optimization (manhole chamber)

It is clear from the figure that after optimization, the maximum temperature which is obtained in the furnace housing is now only 57 C°.

### III. CONCLUSION

Genetic algorithms are a powerful tool for solving optimization problems with many variables and complex calculations. In some cases, they have an advantage over traditional (calculus-based) optimization methods. Their uses help the improvement of mathematical models describing the various furnaces and solve some specific problems in the operation of this type of systems.

### ACKNOWLEDGEMENT

This paper is developed in the frames of project "Improving energy efficiency and optimization of electro technological processes and devices", № MY03/163 financed by the National Science Fund.

### REFERENCES

- [1] P. Watson, K. C. Gupta, "EM-ANN Models for Microstrip Vias and Interconnects", IEEE Trans., Microwave Theory Tech., vol. 44, no. 12, pp. 2395-2503, 1996.
- [2] B. Milovanovic, Z. Stankovic, S. Ivkovic and V. Stankovic, "Loaded Cylindrical Metallic Cavities Modeling using Neural Networks", TELSIKS'99, Conference Proceedings, pp.214-217, Nis, Yugoslavia, 1999.
- [3] S. Haykin, *Neural Networks*, New York, IEEE Press, 1994.

# Communications in Realized Industrial Computer Networks

Viša Tasić<sup>1</sup>, Dragan R.Milivojević<sup>2</sup>, Vladimir Despotović<sup>3</sup>, Darko Brodić<sup>4</sup>,  
 Marijana Pavlov<sup>5</sup>, Ivana Stojković<sup>6</sup>

**Abstract** – This article describes different ways of communication between nodes in realized industrial computer networks in the Copper Mining and Smelting Complex Bor. Industrial computer networks were realized to enable monitoring and control of the copper production process. Data acquisition and control was performed with the use of Programmable Logic Controller (PLC). The simplest control network consists of two nodes: one PLC and one workstation, used for visualization and interaction with the process. Solutions developed for networking purposes, as well as configuration and topology of industrial networks are emphasized in the article.

**Keywords** – communications, control system, industrial network, monitoring

## I. INTRODUCTION

Three generations of computer control and monitoring systems, from mainframes to PC-based computer systems were implemented and developed in the Copper Mining and Smelting Complex Bor (RTB Bor) [1] during the last 20 years. Starting as a simple monitoring system in one of the company's factories, it grew to a complex industrial network that is covering local and geographically distributed plants.

The monitoring and control systems were constantly upgraded and improved until nowadays, both in terms of hardware devices and software support. Specific hardware solutions required the development of specialized

communication protocols. This paper gives a brief overview of communications between nodes in the realized industrial networks throughout the years.

## II. SYNCHRONOUS COMMUNICATIONS

The existence of the central host computer system (ICL 2958D) in RTB Bor at the beginning of 1990s [2] dictated the development of the specific communication solutions based on synchronous communications in the first generation of the monitoring and control systems. The implemented system had the following structure (as shown in Fig. 1):

- Distributed measuring stations (MS) installed at each transformer station,
- Data concentrators and remote workstations (RWS) installed at Control Centers,
- Host computers installed at Computer Centers in Bor (ICL 2958D) and Majdanpek (ICL ME29).

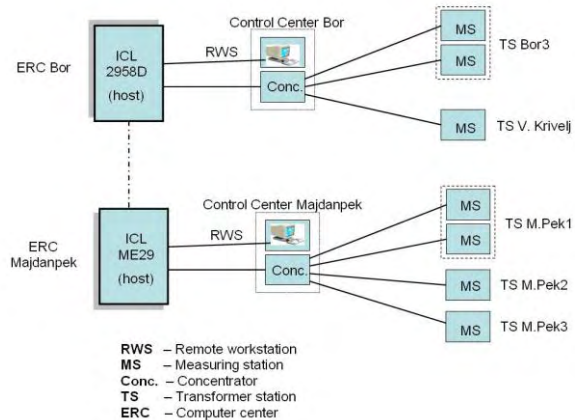


Fig. 1. The configuration diagram of monitoring system [3]

The integral monitoring system was organized as a three-level MAN network. Data concentrator (master node) was connected via base-band modems and leased lines with the measuring stations (slaves) at one, and host computer, at the other side. Communication protocol, BSCP (Binary Synchronous Communication Protocol) [4] was specially designed and applied in order to support real-time data transfer between all network nodes.

BSCP was designed for master-slave type of communications. Hence, one can differentiate two basic types of messages, *Request Message* and *Reply Message*. One communication cycle consists of a successful exchange of

<sup>1</sup> Viša Tasić is with the Institute of Mining and Metallurgy, Department of Industrial Informatics, Zeleni bulevar 35, 19210 Bor, Serbia, e-mail: [visa.tasic@irmbor.co.rs](mailto:visa.tasic@irmbor.co.rs),

<sup>2</sup> Dragan R. Milivojević is with the Institute of Mining and Metallurgy, Department of Industrial Informatics, Zeleni bulevar 35, 19210 Bor, Serbia, e-mail: [dragan.milivojevic@irmbor.co.rs](mailto:dragan.milivojevic@irmbor.co.rs).

<sup>3</sup> Vladimir Despotović is with the University of Belgrade, Technical Faculty in Bor, Vojske Jugoslavije 12, 19210 Bor, Serbia, e-mail: [ydespotovic@tf.bor.ac.rs](mailto:ydespotovic@tf.bor.ac.rs).

<sup>4</sup> Darko Brodić is with the University of Belgrade, Technical Faculty in Bor, Vojske Jugoslavije 12, 19210 Bor, Serbia, e-mail: [dbrodi@tf.bor.ac.rs](mailto:dbrodi@tf.bor.ac.rs).

<sup>5</sup> Marijana Pavlov is with the Institute of Mining and Metallurgy, Department of Industrial Informatics, Zeleni bulevar 35, 19210 Bor, Serbia, e-mail: [marijana.pavlov@irmbor.co.rs](mailto:marijana.pavlov@irmbor.co.rs)

<sup>6</sup> Ivana Stojković is with the University of Niš, Faculty of Electronic Engineering, Aleksandra Medvedeva 14, 18000 Niš, Serbia, e-mail: [ivana.stojkovic@elfak.ni.ac.rs](mailto:ivana.stojkovic@elfak.ni.ac.rs)

messages between two network nodes (master and slave) in both directions. Request message sent by the master node (data concentrator) initiates the data transfer, whereas reply message sent by the slave node ends the data transfer (one communication cycle). The format of the message is shown in Table 1.

TABLE I  
FORMAT OF THE MESSAGE IN BSCP

Syn	SoB	Addr	ComS	Cat	State	Text	Etx	Bcc
-----	-----	------	------	-----	-------	------	-----	-----

- *Syn* – Synchronization character
- *SoB* – Start of Block
- *Addr* – Destination address
- *ComS* – Communication Status
- *Cat* – Category (type) of message
- *State* – Transmitter state
- *Text* – Useful information
- *Etx* – End of Text
- *Bcc* – Block Check Character

According to its characteristics BSCP was not inferior to standard communication protocols of the same class (e.g. Modbus protocol). Compared to similar protocols one could note smaller header, while special “data packetization” increased its efficiency. Since it was based on synchronous communications it required specific hardware solutions in order to be used with personal computers. Hence, a communication module had to be developed for this purpose. A configuration diagram for one part of the control system is shown in Fig. 2.

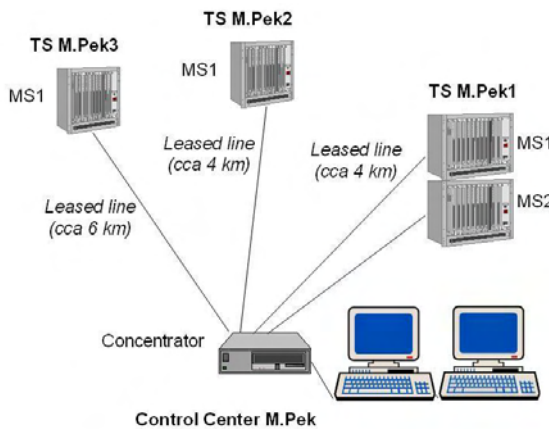


Fig. 2. Example of the electrical energy consumption control system configuration diagram

### III. ASYNCHRONOUS COMMUNICATIONS

The next step in development of the communications between nodes, in the realized industrial networks in RTB Bor, was the transition from synchronous toward asynchronous communications [5]. The new generation of Monitoring Measuring Station (MMS), fully designed and

developed at the Department of Industrial Informatics of the Mining and Metallurgy Institute, was used as a Programmable Logic Controller (PLC), which was a slave node in a realized network. The master PC was added as an interactive workstation, forming an entity which was a core of the complex distributed control and monitoring system, as shown in Fig. 3.

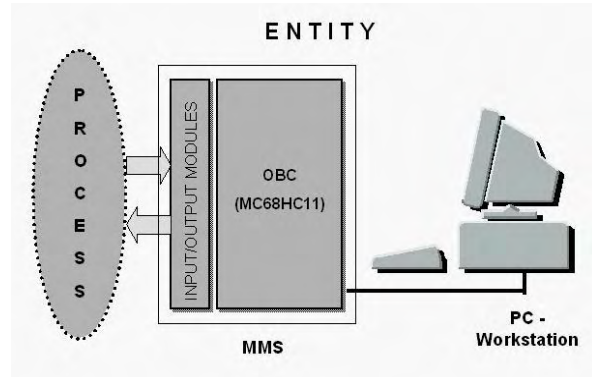


Fig. 3. Simple control system - entity (MMS and PC)

In a hardware point of view, MMS contains the serial communication interface with direct back-to-back connection to standard PC RS232 serial port. The connection between PC and MMS is permanent. The two-node network runs according to the master-slave principle. The PC as a master node starts the session, maintaining the data transfer and regular end of the session. The MMS has to respond to every PC demand.

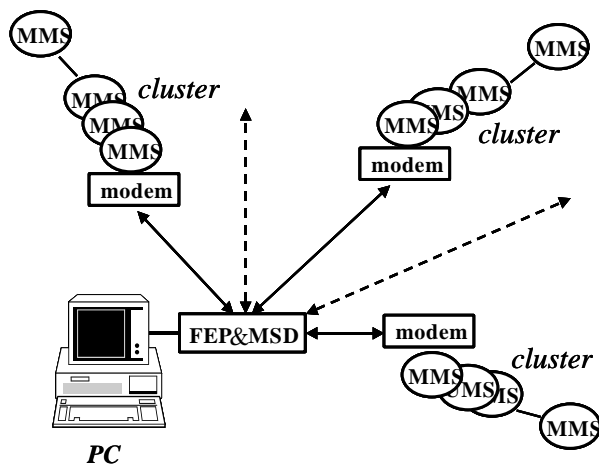


Fig. 4. Control system configuration diagram [5]

Independently from the fact whether the local control is in use or not, data about the status of the process are transferred from MMS to PC. These data are processed on PC and results are presented in corresponding form on the screen and stored in external memory using the specially designed software. If the system performs remote control function, depending on the status of the process, commands are sent from PC to

MMS, which initiates adequate actions and affects the process flow.

Designed and implemented network must satisfy several basic requirements:

- to provide correct and efficient data transfer to PLC in the shortest possible time from the time of their origination,
- to solve uniformly transfer of command to PLC while the command is active and actual
- to provide successive transfer of data from PLC to PC for the case that there are any faults in normal transfer.

FEP&MSD (Front End Processor and Modem Sharing Device) is a microprocessor device whose function is to ensure solid communication link with belonging PC, and to establish, maintain and control network operation of local and remote groups of PLCs (clusters shown in Fig. 4). It is a central node in the network located next to PC and it is directly connected to one of its communication ports.

Physical connection between nodes is realized with two-wire leased line. For conditioning of transfer signal simple assemblies are used as line amplifiers. Only the first one in the cluster is slightly more complex and is directly connected to the modem. Physical connection between nodes within the cluster is realized with two lines in multipoint. The distance from the first to the last MMS in the cluster may extend up to 2.5 km. One cluster, in theory, contains up to 128 nodes (MMS) but in practice only 16 has been used. Applied FEP&MSD devices may support up to 16 clusters.

TABLE II  
FORMAT OF THE MESSAGE IN ASP [5]

DAd	SAd	EAd	Code	CSt	Text	EoM	Bcc
-----	-----	-----	------	-----	------	-----	-----

- *DAd* – Destination Address
- *SAd* – Source Address (Message originator)
- *EAd* – End Address
- *Code* – Status or Command
- *CSt* – Communication Status
- *Text* – Useful information
- *EoM* – End of Message
- *Bcc* – Block Check Character

In order to support the data transfer in a realized network a complex communication subsystem is developed. It is based on the serial communication PC port (RS 232 C, Recommendation V24) and capabilities of the serial communications of the microcontroller MC68HC1, which is the basis of the MMS. Serial communication interface of the microcontroller is a full duplex asynchronous system that uses NRZ (Non Return to Zero) format with one START bit, 8-bit or 9-bit character and one STOP bit. Bitrates can be chosen between 600 and 78000 bps. 19200 bps are used in practice.

To be able to establish connections between network nodes and to achieve optimal speed and reliability of transfer a communication protocol named Asynchronous Serial Protocol (ASP) is designed [5]. There are two basic classes of

messages in the ASP: Master message sent by the primary network node and Slave message sent by the secondary network node. Connection establishment and transfer control are initiated by the primary node (master). Prior to sending the master message a secondary network node (slave) has to be selected. The standard message format is shown in Table 2.

#### IV. CONCLUSION

BSCP protocol is not inferior, according to its performances, to the protocols of the same class. Its main drawback is the fact that it is a synchronous communication protocol, hence it requires specific hardware, as well as the PC extending communication module. Thanks to the precise definition of the time duration of transmission, this protocol is a very good choice for hard synchronization between network nodes. There are several industrial MAN networks in operation that use BSCP protocol. Data transfer efficiency between nodes has shown to be satisfactory for the applications they serve.

ASP requires no additional hardware on MMS or at PC, which is its main advantage compared to the BSCP. Software support is written in VC++ and Delphi. Both protocols showed high stability in operation, almost without lost messages.

First impression is that realized networks, by its characteristics, do not belong to the group of high performance solutions. For standard networks megabit transfer rates are present nowadays. However, for the purpose they are designed they have shown to be a very rational solution. Processes and events, which are monitored and controlled by such systems, are relatively slow (central heating system, water supply network, electrolytic copper refinery plant, etc.). Actual information about the state of these processes is generated at minute intervals or even more rarely, so that efficiency of communication system can not be questioned. Apart from favorable price/performance ratio, functioning of realized network has shown to be very efficient and reliable and especially resistant to poor communication conditions, thanks to solid transfer quality control and possibility of dynamic network reconfiguration.

#### ACKNOWLEDGEMENT

This work was partly funded by the Grant of the Ministry of Education, Science and Technological Development of Republic of Serbia, as a part of Project No. TR33037 "Development and Application of Distributed System for Monitoring and Control of Electrical Energy Consumption for Large Consumers."

#### REFERENCES

- [1] V.Tasić, N. Milošević, R. Kovačević, N.Petrović, "The analysis of air pollution caused by particle matter emission from the copper smelter complex Bor (Serbia)," Chemical Industry & Chemical Engineering Quarterly, vol. 16, no. 3, pp. 219-228, 2010.

- [2] M. Radojković, D. Milivojević, G. Jojić-Blagojević and M. Cajić, "System for Monitoring and Control of Electrical Energy Consumption in RTB Bor," Proceedings of VII Scientific Convention on Microcomputers in Process Control Systems, MIPRO'88, pp. 5-31 – 5-35, Rijeka, Croatia, 18-20.05.1988.
- [3] V.Tasić V.Despotović, D.Brodić, M.Pavlov and D.Milivojević "Twenty years of monitoring and control of electricity consumption in RTB Bor, Serbia," accepted for presentation on MIPRO 2013 - 36th International Convention, Opatia, Croatia
- [4] D. Milivojevic, M. Radojkovic, G. Jojic Blagojevic, Dj. Simon, S. Lalovic, "Communication Subsystem of DSKP Systems," Proceedings of XIV International Conference of Information Technology, Book 1, pp. 173.1-173.5, Sarajevo-Jahorina, BiH, 1990
- [5] D.R.Milivojevic, V.Tasic, "MMS in Real Industrial Network," Information Technology and control, vol. 36, no. 3, pp. 318-322, 2007.

# Information technology to calculate energy savings using solar panels and home appliances

Nanko Bozukov<sup>1</sup>, Tanya Titova<sup>2</sup> and Veselin Nachev<sup>3</sup>

**Abstract –** In this paper describes the algorithm of the program that was developed to determine the assessment of energy savings using solar panels and home appliances. Amount of energy saved in one year is calculated by a formula specified in methodology. The evaluation of the energy savings is done by measuring and/or estimating consumption before and after the implementation of the energy efficiency measure.

**Keywords –** energy savings, program algorithm

## I. INTRODUCTION

To achieve energy efficiency in the installation of solar collectors for domestic hot water and replace existing or purchase new appliances in residential and public buildings are required to select optimal process a certain quality at minimum energy consumption.

Reducing the energy consumption can be achieved by using new technologies. Energy efficiency may be achieved by applying intelligent management systems and the use of renewable energy sources.

## II. ASPECTS IN THE EVALUATION OF ENERGY SAVINGS

The data availability and the ability of recovery is essential for precise and accurate assessment of energy savings in methodologies for energy efficiency. It is important to be provided most accurate information and a set of necessary data before any assessment. It should be borne in mind that the evaluation of energy service or measure energy efficiency is usually not possible to rely on specific measurements.

It is necessary to distinguish between methods for measuring energy savings and methods estimating energy savings, the latter are more common and are associated with much lower costs.

Energy audit is to determine the level of energy consumption to identify opportunities to reduce it and to recommend measures to improve energy efficiency.

Methods have developed that aim to demonstrate the implementation of individual measures or groups of measures

<sup>1</sup>Nanko Bozukov, Department "Informatics and Statistics" at University of Food Technologies - Plovdiv, 26 Maritsa Blvd, Plovdiv 4002, Bulgaria, e-mail: bozukovnanko@abv.bg.

<sup>2</sup>Tanya Titova, Department Automation and Control Systems University of Food Technologies, 26 Maritsa Blvd, Plovdiv, 4002 Bulgaria, e-mail: t\_titova@abv.bg

<sup>3</sup>Veselin Nachev, Department Automation and Control Systems University of Food Technologies, 26 Maritsa Blvd, Plovdiv, 4002 Bulgaria, e-mail: v\_nachevbg@yahoo.com

to improve energy efficiency in various sectors of economic and social life [4, 6].

Energy savings are determined by measuring and / or estimating consumption before and after the implementation of the energy efficiency measure. The amount of the saved energy is equal to the difference between the energy used before the introduction of the measure or program to improve energy efficiency and use of energy, measured after administration.

The developed methods include the following directions [3, 6]:

- Replacement of equipment with energy efficient one. In this direction the baseline is the specific energy consumption of existing equipment before replacement, if there is evidence of this. In the event of no evidence that consumption as a baseline can be used for data average specific energy consumption of similar existing equipment.

- Updating equipment or building. The baseline in this direction is the specific energy consumption before the modernization of equipment or building. If there are no specific data on the consumption of the equipment average consumption of such existing equipment can be used for data. In the absence of specific energy consumption of the building prior to the implementation of energy saving measures the baseline can be used for specific consumption of buildings built according to the design standards for the year of construction of the building.

- Acquisition of energy-efficient equipment or building. In this direction the baseline is the specific energy consumption of older equipment before replacement. In the absence of baseline data average specific energy consumption of new equipment sold in the country as the base year, or the rules for the energy performance of buildings existing in the base year are considered.

## III. ADVANTAGES AND DISADVANTAGES OF THE ALGORITHM

Information technology assessment of energy savings and its algorithm have advantages and disadvantages. Some of the advantages are:

- in the accumulation of sufficient data base the real impact of energy savings in the industry can be assessed very accurately;

- using the database a complete analysis can be made and the planned project and the achieved energy performance in the real operation can be compared

- certificate issued within the period provided by law for energy efficiency would have a solid justification of factual data.

- it is easy to handle and calculate the data required for the application of the methodology, which aims to demonstrate the implementation of individual measures or groups of measures to improve energy savings in the industry with information technology.

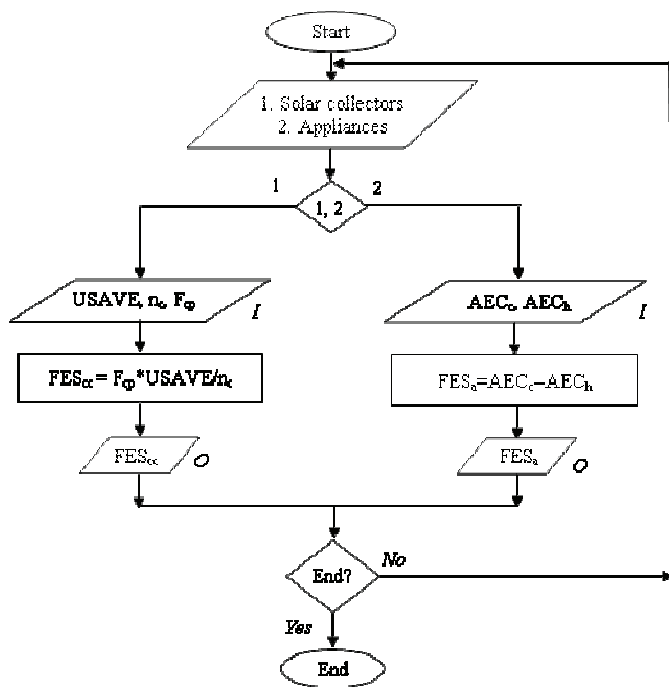


Fig. 1. Block - diagram of the algorithm

#### IV. DESCRIPTION AND IMPLEMENTATION OF ALGORITHM FOR ENERGY SAVINGS

Developed a computer program to calculate energy savings using solar collectors for domestic hot water and replace existing or purchase new appliances in residential and public buildings, whose algorithm is described with a block - diagram (fig. 1).

The program is implemented in two versions. The first option is a programming language MatLab [1, 2, 7]. The second option is to use the spreadsheet capabilities of MS Excel. After starting the program chooses one of two options:

1. Calculation of energy savings using solar collectors for domestic hot water in residential and public buildings.

2. Calculation of energy savings when replacing existing or purchase new appliances (refrigerators, washing machines, televisions, etc.) in buildings.

To calculate energy savings using solar collectors for domestic hot water in residential and public buildings to input data:

1. USAVE - average annual saving specific heat of 1 m<sup>2</sup> solar collector [kWh/m<sup>2</sup>];

n<sub>c</sub> - efficiency replace existing hot water installation (for new plant is assumed to average performance ratio of marketable plants in 2007);

F<sub>cp</sub> - collector area [m<sup>2</sup>].

2. Calculate:

FES<sub>a</sub> - saved energy by installing solar panels for hot water for one year [kWh / year].

3. Display: FES<sub>cc</sub>.

To calculate energy savings when replacing existing or buying new appliances (refrigerators, washing machines, televisions, etc.) in buildings input:

1. AEC<sub>c</sub> - the replacement of an existing device - an average annual energy consumption of the old appliance or average consumption of commercially available devices in 2007 [kWh/year];

AEC<sub>h</sub> - when buying a new appliance, the average energy consumption of new equipment [kWh / year].

2. Calculate:

FES<sub>a</sub> - Save energy by replacing an old or buy a new household appliance [kWh / year].

3. Display: FES<sub>a</sub>.

All information on working with the program and all variables are stored in a file. The file can be opened, viewed and printed.

The program for energy saving is a modern tool for data processing, calculation of results, control and objective analysis of the impact of implementation of energy efficiency measures.

#### V. CONCLUSION

Information technology assessment of energy savings and its algorithm have advantages and disadvantages.

Information technology, data processing, evaluation and calculation of energy savings is a good and convenient way to control and give objective analysis of the impact of the application of energy efficiency measures in industry. In applying such information technology for calculating the energy savings in the industry high reliability, easy transfer and data processing can be achieved.

The availability of data and the possibility of collecting and processing them is essential for accurate and fair assessment of the energy savings in the developed methodologies. It is important to have most accurate information and data before any assessment.

Information technology should be used in each of the methodologies for energy savings. Energy saving systems are focused on efficient energy use through innovative technologies. Due to modern industry it combines flexibility, functionality, aesthetics, environmental and energy efficiency.

#### REFERENCES

- [1] Chen C., P Dzhibling A., Irving, Mathematical Explorations with MATLAB, Cambridge University Press, 1999.
- [2] Moore H. MATLAB for Engineers, Pearson Education, 2012
- [3] [http://www1.bpo.bg/images/stories/buletini/\\_binder-2012-09.pdf](http://www1.bpo.bg/images/stories/buletini/_binder-2012-09.pdf)
- [4] <http://www.eulaw.egov.bg/DocumentDisplay.aspx?ID=382929>
- [5] <http://www.climamarket.bg/>
- [6] [http://www.mi.govtment.bg/files/useruploads/files/microsoft\\_word-metodiki.pdf](http://www.mi.govtment.bg/files/useruploads/files/microsoft_word-metodiki.pdf)
- [7] [www.mathworks.com](http://www.mathworks.com)

# Using Dashboards as tools to improve the process of decision making in healthcare

Jasmina Nedelkoska<sup>1</sup>, Snezana Savoska<sup>2</sup> and Emilija Taleska<sup>3</sup>

**Abstract** – Dashboards today are the preferred tool for managers in the process of management of companies. They use comparative tables to improve the process of decision making. The graphical presentation and visualization of data allows quick and efficient viewing of changes, recognition of important information and sometimes viewing the „invisible“ in the data.

The aim of this paper is to examine the need for using visual systems in the management process, which will lead to better decision making in Public Healthcare Institutions in the Republic of Macedonia. The aim is to achieve critical decisions to be supported by information received from a dashboard-the visual systems that follows the plan and its execution.

**Key words** - Dashboards, Health institutions, Decision making

## I. INTRODUCTION

Many years ago people were aware that “a picture is worth a thousand words”. Therefore efforts were made to apply visualization wherever it is possible. Visualization is an area rapidly developed in recent decades. It is a method that allows the data viewing and with its help the discovery of connections and dependencies between data, i.e. “penetrating” into the data. Visualization can be applied to data from all areas, which confirms its great applicability. With its help, it can be said that the thinking of people has changed and visualization has become a preferred form of getting information.

In order to have a good and efficient data visualization, data should be well prepared. That process includes the selection of the data that will be subject of visualization and their form of visualization, i.e. their representation.

The use of the graphical visualization involves a number of advantages for usage in almost all branches of science and business, such as reducing the need for time spent for analyzing data and time for decision making, but also reducing the number of required analysts. Visual tools have an impact on everyday life through their use in many areas such as art and film animation. It also occurs in all scientific research and scientific hypotheses, which is called scientific visualization. [1]

Visualization can have different purposes depending on what needs to be visualized. The most important goal is

<sup>1</sup>Jasmina Nedelkoska is with Faculty of Administration and Management of Information Systems, Bitola, Macedonia

<sup>2</sup>Snezana Savoska is with Faculty of Administration and Management of Information Systems, Bitola, Macedonia

<sup>3</sup>Emilija Taleska is with Faculty of Administration and Management of Information Systems, Bitola, Macedonia

making the “invisible visible”, i.e. obtaining new understandings, effective presentations of the significant features, more research and use of the data and information.

## II. DASHBOARDS THAT ASSIST MANAGERIAL DECISION MAKING

Visual tools that are used today can usually be part of the systems of business intelligence.

Business intelligence is the ability of an organization to collect, maintain and organize data in an appropriate manner in order to obtain information for the management of all levels. This produces a range of information to assist in the building of new opportunities. By identifying these opportunities and implementing an effective strategy, a company can gain a competitive advantage in the market and long-term stability [2].

Today's visual tools are the most desirable tool for managers and analysts of data and information, so with their help the decision-making process is more effective and efficient. These systems with visual tools allow:

“Access easy to read, usually one page, real-time user interface, shows graphical representation of the current status and the historical trends of organizational key performance indicators to provide support for quick decisions that are made according to the view”. [3]

## III. VISUAL SYSTEM TO SUPPORT DECISION MAKING

The lack of clarity of the reports that managers, for various application areas, receive, such as comparisons of the planned budget and performing an analysis of drug use by departments and others, led to the detection of the need to create a system of visual support that will be suitable in making decisions.

A visual system is designed to assist managers in decisions making. The visual system administrators will be able to better see the changes, in their part, of the operation and to faster react to those changes. Administrators can select the parameters they need to follow, and it is this dynamic damping system that is desired and used by managers.

In the opinion of the managers of the hospitals, the information obtained from the panels will be useful with the operational control as an opportunity for managers to timely respond to deviations that may occur and contribute to a better and timely decisions in all segments to which the boards operations apply.

#### IV. RESEARCH

This research that we have done for this purpose should perceive the need to use flash reports, accurate and timely help in decision-making. Here we must emphasize the need to achieve a good and understandable reports by the institution to operate successfully and achieve positive results. We explored whether and how managers are familiar with the visual systems support the is used and whether such visual systems are used in health care today. Also a prototype software solution is build that is used to improve the decision making process.

The need for which this research is made is the lack of clarity of the reports that healthcare managers receive for various application areas, such as comparisons of budget planned and performed, the analysis of drug use and other departments. As under investigation, dashboard applications improve the decision-making of health managers. The purpose of this paper is to highlight the need for a visual system to support decision-making, and the construction of a visual and practical system to show its benefits for the health organization.

The case study is performed in a public hospital in the Republic of Macedonia. The information system that is used is installed in most public healthcare institutions in Macedonia. The information system is actually a set of different systems that use different databases that are placed on different platforms (Microsoft, Linux). Some of the systems used are unrelated. Because each system separately receives reports. The reports are printed tables that are bulky and difficult to read. From them we can't quickly recognize information even though they contain a lot of information. The questionnaire was completed by administrators – managers in several public healthcare institutions in Macedonia (in order to obtain reliable information about their preferences and information needs) a framework for research is defined.

#### V. ANALYSIS OF THE RESULTS

In the survey 76.2% of respondents answered that they always need to get quick, accurate and timely reports that help in the decision making, 19% said that they usually require obtaining fast, accurate and timely reports and 4.8% said they sometimes require getting fast, accurate and timely reports. None of the respondents answered that he needed very little or never to obtain reports. (Fig.1)

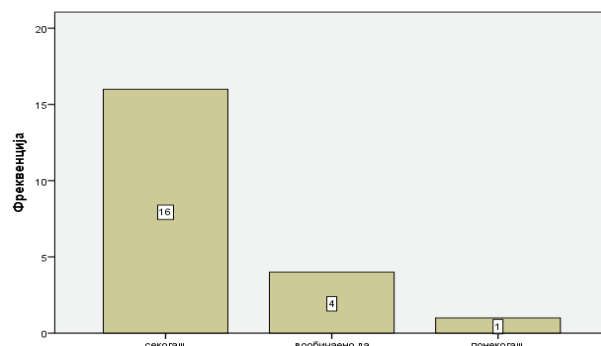


Fig.1. Division answers for the need for fast, accurate and timely reports that help in decision making

For the question “how often do you usually receive reports?”, 61.90% of respondents said that they received reports daily, 28.57% answered that receive reports weekly, while 9.52% said that they receive reports monthly. None of the respondents answered that receive reports quarterly or annually. (Fig 2)

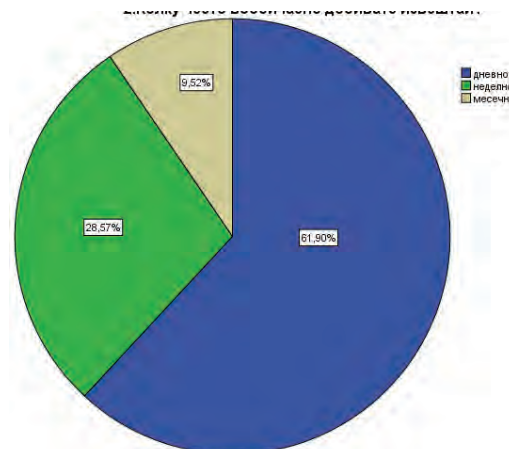


Fig. 2. Division answers of how often managers receive reports

According to the answers, 42.86% of the respondents said that the received reports always help in the decision making process and meet their requests for information, 52.38% said that the received reports usually help in the decision making process and meet their requirements information, while 4.76% said that the received reports sometimes help in the decision making process and meet their requests for information. None of the respondents replied that the received reports help very little or never. (Fig. 3)

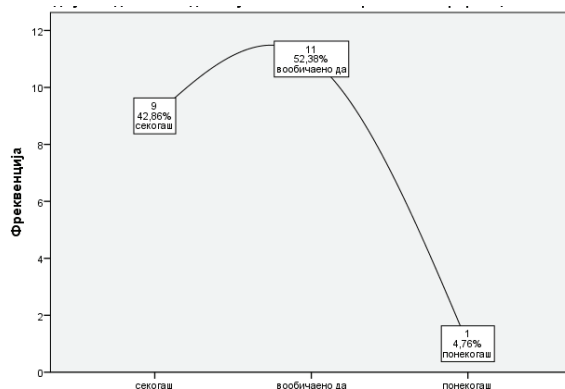


Fig. 3. Division answers about whether received reports help in the decision making process and satisfy the information requirements

Of the respondents, 66.7% said that getting good and understandable reports that help in the decision-making process is always necessary for the institution to work successfully and to realize positive results, 33.3% said that getting good and understandable reports that help in the decision-making process is usually necessary for the institution to work successfully and to realize positive results. Nobody responded that obtaining good and understandable reports that help in the decision-making process sometimes are very little or never necessary for the institution to work successfully and to create positive results. (Fig 4)

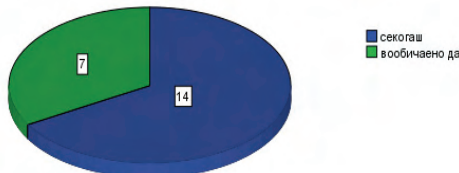


Fig. 4. Division answers about whether understandable reports are necessary for positive results and success of the company

According to the survey, 52.4% of the respondents said they think they know what are visual systems for supporting decision-making, 23.8% said that they know well what visual systems for supporting decision-making are, 14.3% said they knew little, 9.5% said they heard about the visual systems for supporting decision-making and no one answered that they had not heard about them. (Fig 5)

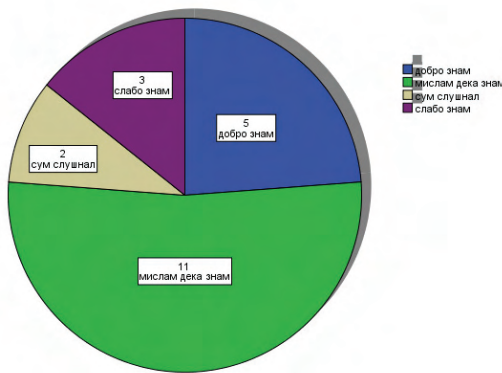


Fig. 5. Division answers for whether managers are familiar with the visual systems to support decision-making

From the obtained answers, 42.9% of respondents believe that the use of visual systems for supporting decision-making will certainly advance the overall operation of the institution, 47.6% believe that the use of visual systems for supporting decision-making can improve the overall operation of the institution, 9.5% do not know whether the use of visual systems will improve the operations of the institution. Nobody believes that the use of visual decision support systems will help to advance the overall operation of the institution. (Fig 6)

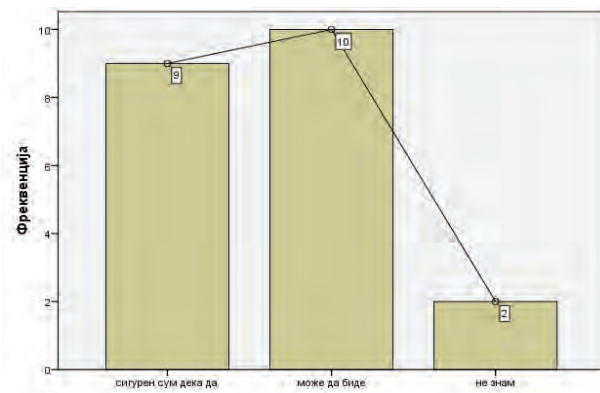


Fig. 6. Division answers for whether the use of visual systems can afford to improve the operation of the institution

Of respondents, 57.1% think they will accept to implement and use visual systems for supporting decision-making, 19% will certainly accept the implementation and use of visual systems, 14.3% would try to accept the implementation and the use of visual systems, 9.5% do not know whether to accept the implementation and use of visual systems. (Fig 7)

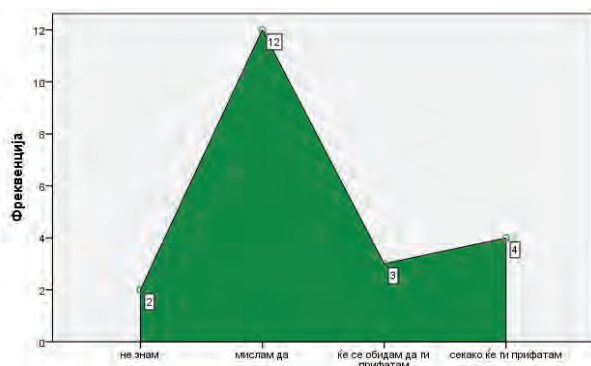


Fig. 7. Division answers for whether managers will accept to implement and use visual systems for support decision-making

All respondents said they do not use the visual system for supporting decision-making in their work.

## VI. CONCLUSION

Fact-based research to conclude that managers have a continuing need for fast and accurate reports, and visually see the changes and make better decisions. Reports now are not sufficient for the timely detection of changes and improving decision making.

Managers, according to research, are not sufficiently familiar with the visual systems for supporting decision-making. The concept of these visual systems should be broader, managers need to learn about this concept and understand the need for its use.

The future of improving the decision-making process is in the use of such visual systems. It will improve the functioning of healthcare institutions that will lead to improvement of services and institutions with increased health benefits. If they react quickly to changes, the health institutions will only progress.

The implementation of visual systems in all public healthcare institutions in Macedonia requires time and expertise of the employees in the information area. First they need to create dashboards that will be useful for all administrators and will be created for each part of the operations of the institution. Because the health care facilities have a variety of data to all parts of the operation, creating a system will be a laborious process. But when once established, it can be used in all public healthcare facilities. The benefits that the visual system will bring are much greater than the time and cost of creating such a system.

Once the visual system is developed and implemented, it is necessary to train managers to use. If previously managers understand the need and usefulness of the system, they will be motivated enough to use that system. Using the system is simple. Administrators simply choose which control tables to view data from and visual system displays them. With this change in the operation of the healthcare institution is detected early, and appropriate actions are taken promptly.

As a recommendation for further research I think the concept should be extended to all public healthcare

institutions in the Republic of Macedonia to get the data that managers want to see in these control panels and part of the operation of a visual system need. Once you collect and process the data, you need to create a system that meets the needs of all managers and the same visual system needs to be implemented in all public healthcare institutions in Macedonia.

## REFERENCES

- [1] M. Kaufman, *Information visualization – Perception for design*, 2005
- [2] Rud, Olivia, *Business Intelligence Success Factors: Tools for Aligning Your Business in the Global Economy*. Hoboken, NJ: Wiley & Sons, 2009
- [3] Peter McFadden CEO of ExcelDashboardWidgets, *What is Dashboard Reporting*. Retrieved: 2012
- [4] E. Turban, Volonino L., *Information technology*, Wiley, 2011
- [5] Albright Winston, *Data Analysis & Decision making*, Thompson, 2009
- [6] K.C. Laudon, and J.P. Laudon, *Management Information Systems – Managing the Digital Firm*, New Jersey, Prentice-Hall, 2012
- [7] A. Gunasekaran, *Handbook On Business Information Systems*, Word Scietific Publishing Co.Pte.Ltd, 2010
- [8] Maria Antonina Mach, Abdel-Badeeh M. Salem, *Intelligent Techniques for Bisiness Intelligence in Healthcare*, 10<sup>th</sup> International Conference on Intelligent Systems Design and Applications, 2010
- [9] Matteo Gofarelli, Federica Mandreoli, Wilma Penzo, Stefano Rizzi, Elisa Yuricchia, *Business Intelligence Networks*, IGI Global, 2011
- [10] Adam Funk, Yaoyong Li, Horacio Saggion, Kalina Bontcheva, Christian Leibold, *Opinion Analysis for Business Intelligence Applications*, OBI (Germany), 2008

# Preparation of data for visualization using SQL Server 2008

Emilija Taleska<sup>1</sup>, Snezana Savoska<sup>2</sup>, Jasmina Nedelkoska<sup>3</sup>

**Abstract** - Analysis of a huge amounts of data that flow into databases, successfully dealt with methods of data visualization that graphical representations of data and information provide better awareness of the management and making better decisions. Information describes things that are sometimes abstracting in schematic format that includes analysis of attributes and variables such units of information.

The purpose of this paper is to study the practical concepts and algorithms for preparing the data for visualization and creating visual representations of large amounts of data. In this paper will be given attention to the way in which data is transformed from the original format into a format suitable for their further processing using algorithms.

**Key words** – Data visualization, database, algorithms, preparation for visualization

## I. INTRODUCTION

The data are required and important component in daily life, business, medicine, administration, science, etc. However, management and access to data is not always easy. Daily data are stored in different formats, relational tables and databases. To be able to analyze them it is necessary to use appropriate methods for data visualization, which facilitates the presentation and understanding of data and information. This enables increasing efficiency in the work of analysts and managers.

The design of the database is the process of producing a detailed data model for the database. It can be conceptual, logical and physical. The model contains all the needed logical and physical design choices and physical storage of all parameters needed to generate a design in a Data Definition Language, which can then be used to create a database. The full data model contains detailed attributes for each entity within the database management system (DBMS).

## II. PARADIGMS ASSOCIATED WITH DATABASE MANAGEMENT SYSTEMS

“The main purpose of a database management system (DBMS) is to bridge the gap between information and data - the data stored in memory or on disk must be converted to usable information.

The basic processes that are supported by a DBMS are:

- Specification of data types, structures and constraints to be considered in an application.
- Storing the data itself into persistent storage.
- Manipulation of the database.
- Querying the database to retrieve desired data
- Updating the content of the database

A database is a model of a real world system. The contents (sometimes called the extension) of a database represent the state of what is being modeled. Changes in the database represent events occurring in the environment that change the state of what is being modeled. It is appropriate to structure a database to mirror what it is intended to model.”[1]

Databases can be analyzed at different levels:

- Conceptual Modeling. These concepts allow application modeling the world in terms that are independent of the particular data (logical) model. Conceptual models provide a framework for the development of a database schema from the top to the bottom in the process of database design. This model examines the entity-relationship and object-oriented model to represent conceptual modeling. The entity-relationship model is widely used and the object-oriented model is gaining more acceptances of non-traditional databases.
- Logical Modeling. At the logical level, the conceptual schema is translated into the data model of a particular DBMS. A logical model is described as a set of relatively simple structures. In addition to the data representation, a DBMS needs to specify the handling of data, which is done through queries and other operations in a data manipulation language.
- Physical Modeling. At the physical level, a DBMS is responsible for:
  - Storage. The representation of the efficient organization of data into a persistent secondary drive.

<sup>1</sup> Emilija Taleska is with Faculty of Administration and management of Information Systems, Bitola, Macedonia

<sup>2</sup> Snezana Savoska is with Faculty of Administration and management of Information Systems, Bitola, Macedonia

<sup>3</sup> Jasmina Nedelkoska is with Faculty of Administration and management of Information Systems, Bitola, Macedonia

- Access Methods. Organization of data to accelerate data recovery through defining data structures or index.
- Processing queries. The set of operations for responding to a query. Those transactions define algorithms that make use of access methods.
- Query Optimization. Evaluation strategy for query processing.
- Concurrency and recovery. Strategy for managing concurrent access to data and resources from multiple users and recovering the database after a system failure.

Data visualization is the graphical representation of abstract information for two purposes: the sense-making (also called data analysis) and communication. Important stories live on our data and data visualization is a powerful means to discover and understand these stories, and then present them to others. The information is summarized in describing things that are not physical. Statistical information is abstract. Whether the case of sales, the incidence of the disease, athletic performance, or anything else, although not in the physical world, you can still show visually, but for this we have to find a way of shaping it has none. [2]

In the modern operating environment, any serious application must simultaneously confront for at least four paradigms:

- Paradigms associated with data or data paradigms, which means that data is used by a single application.
- Resources paradigm that involves everything about resources that may be required of the application in data processing (type of resources and the manner of their usage).
- Communication paradigms, which can be divided into three subsets: communication with the database, communication and coordination of components (object modules) that make up the application, and finally, communication with other utilities (services). These are paradigms that provide data access only by authorized person and no one else.
- Security paradigms. Security paradigms involve collection of measures and procedures that must be completely observed, so that an individual can work with data.

### III. THE NEED FOR PREPARING DATA FOR VISUALIZATION

The data stored in a data warehouse is usually hard and is not suitable for data visualization. Therefore, to obtain visual representations the data need to be prepared. Sometimes it is

important to extract the necessary data and put the data into separate repositories, even recode them and normalizing their values. But when it comes to large amounts of data, it is still necessary to aggregate forms or views (Views) to accelerate the visual representation. During the preparation of data, it is important to know the amount of data which is represented, its dimensions and data interaction. Because of all these factors, it can be said that the preparation of data for visualization is not at all an easy process. [3]

When it comes to data used in the health care and preparation for display, we can say that this is a complex process that requires a detailed knowledge of data (bottom-up analysis) and detailed knowledge of the administrators that need visual reports, because it is necessary to know the transaction information systems and to make them appropriate repositories of data that are required to manage.

In Macedonia transactional information systems are placed on multiple platforms, databases and applications. Its integration inevitably requires a uniform deposit of data that will be the basis for the visualization. Some of the data is encoded differently in different transactional systems and needed to be stored in recoded parallel codes. After defining the logical and physical model of the repository that will be used for data visualization, it is necessary to create views that will contribute to get an efficient and effective data visualization.

### IV. PROCEDURES FOR PREPARING DATA FOR VISUALIZATION

For the research that we made and received information about the needs of managers in health institutions in Macedonia, was required to obtain certain information to be presented visually through dashboards. For this purpose, have been defined procedures for the preparation of the data.

The software that is used is conceptualized in classic reports in Excel or pivot tables. The reports include analytical data. Managers and analysts themselves can choose which data they want to see in the reports. But this method of selection is used often by our site managers from our side analysts. The data which were stored data on drugs and their consumption by departments, the financial plan for the budget accounts and subaccounts, the realization of the budget accounts for certain quarters, codes for performed services, diagnoses and other statistics.

Results		Messages					
SmetkaID	KvartalID	KontoID	Planirani	Fakturirani	Plateni	Ostatok	Procent
1	73729	1	401	36645819	0	36645819	0
2	73729	1	401130	0	0	33596562	-33596562
3	73729	1	401310	0	0	2504124	-2504124
4	73729	1	401320	0	0	0	0
5	73729	1	402	13554123	0	0	13554123
6	73729	1	402110	0	0	8902970	-8902970
7	73729	1	402210	0	0	3610661	-3610661
8	73729	1	402220	0	0	247292	-247292

Godina	Prindi	Suma	log	In
1	2009	Камати и депозити	6959	3.84254683649502
2	2009	Приходи од продажба на лекови	1013431	6.0057941848595
3	2009	Приходи од специјални здравствени услуги	402637	5.60491368152504
4	2009	Приходи од здравствени услуги	6008879	6.77879345877087
5	2009	Закупнина на деловен простор	854452	5.9316876706044
6	2009	Приходи од министри години и тенденции	154000	5.18752072083646
7	2009	Донации	NULL	NULL
8	2009	Други вонредни приходи	3767721	6.57607873577514

Godina	Trosoci	Suma	log	In
1	2009	Исплатено бруто плани	227278461	8.35655827993051
2	2009	Трошоци за превоз	187650	5.2733485687491
3	2009	Трошоци за хранарина	2334922	6.36827237717819
4	2009	Надомест за односни ...	888135	5.94847898525929
5	2009	Отпремнина за пенсии...	563730	5.75107114726967

Fig. 1. Display of data that are briefly generated reports

The next step is to create a repository in parallel codes that are created. But in the system as a problem arises in aligning the codes of different drugs were enrolled in the Fund for Health Insurance and pharmacies. The beginning of this year it has been overcome and the system started working properly.

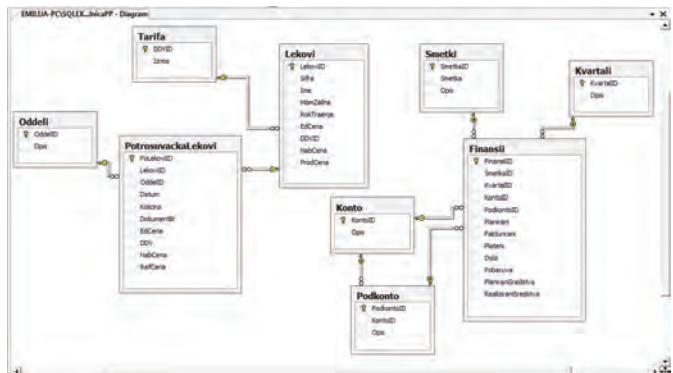


Fig. 2. Database diagram represented by the star schema

In the design of relational databases (RDBMS), normalization of databases is the process of organizing data to reduce the burden. The purpose of normalizing the database is to break the anomalies to make a smaller, well structured relationship between data. Normalization usually involves dividing large tables into small tables and define relationships between them. The task is to isolate data for gathering, deletions and changes in the field can be done at one table and, as such, to operate across the entire database, defined by relationships.

The next step in data preparation for visualization is process of creating views. By considering the original data, views depend on the visual representation and the whole process of preparation of the data is shown in Figure 3.

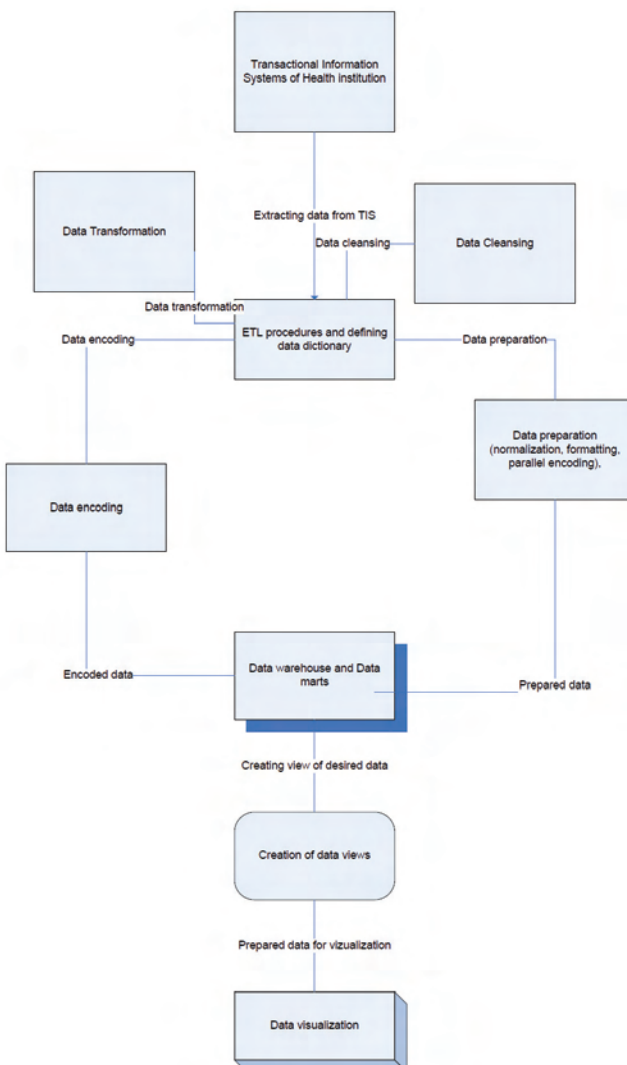


Fig. 3. The process of preparation of the data for visual representation

## V. CONCLUDING OBSERVATIONS

All these requires accessibility to databases as in Republic of Macedonia is a problem considering to outsourcing the software that is used and the lack of staff in some health institutions responsible for database administration. There are problems with inconsistency in transaction systems, with different ways of coding the entities and their attributes, and sometimes with the relations between them. In fact, have not yet been made appropriate integration of the health system and therefore it is difficult to get to the data.

This way of presenting the data is preferred by managers of health institutions, but it needs a serious approach and responsible people who will administer data warehouse and will take care of proper preparation and implementation of procedures, their automation and continuous work.

## REFERENCES

- [1] Andrea Rodriguez, "Brief Introduction to Database Concepts", Department of Computer Science, 2004
- [2] M. Kaufman, "Information visualization – Perception for design, 2005
- [3] E. Turban, Volonino L., Information technology, Wiley, 2011
- [4] A. Gunasekaran, Handbook On Business Information Systems, Word Scietific Publishing.Co.Pte.Ltd, 2010
- [5] [http://www.interaction-design.org/encyclopedia/data\\_visualization\\_for\\_human\\_perception.html](http://www.interaction-design.org/encyclopedia/data_visualization_for_human_perception.html)

# Statistical parameters of the first order for Rayleigh Fading with EGC Diversity combiner using MATLAB

Borivoje Milosevic<sup>1</sup> and Mihajlo Stefanovic<sup>2</sup>

Slobodan Obradovic<sup>3</sup> and Srdjan Jovković<sup>4</sup>

**Abstract –** This paper discusses the application of MATLAB tools for the realization of Rayleigh Fading using EGC diversity combiner. In this paper the dual EGC ( Equal Gain Combiner ) Diversity system is considered. The uncorrelated Rayleigh fading is presented. The cummulative density function - CDF of the dual EGC output signals and the joint of output signal and its first time derivative are determined. The probability density function -PDF of the dual EGC output signals and the joint of output signal and its first time derivative are determined.

**Keywords –** EGC, PDF, CDF, Fading, Rayleigh, Combiner.

## I. INTRODUCTION

Problems that occur during the implementation of applications for statistical analysis of signal in the presence of fading are mainly related to difficulties in editing formulas and expressions, their computation (Mathematica), drawing graphics (Origin), etc. This paper provides a simpler approach to solving this problem, of course, using an excellent tool: MATLAB.

Some of the most well-known diversity techniques are MRC ( Maximum Ratio Combining ), EGC (Eqal Gain Combining ) and SC ( Selection Combining ) [1]. Around them, EGC presents significant practical interest, because it provides performance comparable to MRC but with simpler implementation complexity. In EGC, the desired signals of the output of the two antennas are caphased, equally weighted and then summed to give the desired resultant signal.

Diversity combining is one of the most practical, effective and widely employed techniques in digital communication receivers for mitigating the effect of multipath fading and improving the overall wirless systems performance.

The performance of EGC, assuming independet channel fading, has been studied extensively in the literature, although there are less published results concerning EGC receiver, compared with those of other the diversity methods, such are MRC and SC. This lack is mainly due to the difficulty of finding the probability density function ( PDF ) and cummulative distributions function ( CDF ) of the EGC output

<sup>1</sup>Borivoje Milosevic is with the Technical College University of Nis, A. Medvedeva 20, Nis 18000, Serbia, E-mail: borivojemilosevic@yahoo.com.

<sup>2</sup>Mihajlo Stefanovic is with the Faculty of Electronic Engineering, University of Niš, A. Medvedeva 14, Nis 18000, Serbia,

<sup>3</sup>Slobodan Obradovic is with the SANU, Beograd, Serbia

<sup>4</sup>Srdjan Jovkovic is with the Technical College University of Nis, A. Medvedeva 20, Nis 18000, Serbia

signal to noise ratio (SNV) [3]. However, independent fading is not always realised in practice due to insufficient antena spacing. Therefore, it is important to understand how the correlation between received signals effect the offered diversity gain. Reviewing the literature, it can be seen that there are few approaches for the performance evaluation of predetection EGC over correlated fading channels.

## II. EXPOSITION

### A. Choice of mathematical methods and mathematical modeling problems

When analyzing the process of propagation of digital communication systems, methods and models of statistical theory of telecommunications are to be used. The accuracy of proposed model will be checked by deductive methods and simulation systems for known cases. In doing so, it is very important to set the criteria for selection of models, each of which has its advantages and disadvantages, which must be viewed through the purpose of a certain type of software.

When choosing to be analyzed:

- Why it is purchased
- Who will use it
- What is the expected benefit

Analysis of the previous factors significantly narrows the circle of appropriate tools. Within such a selection, the remaining tools need to be paid attention to the following factors:

- Flexibility of use
- Whether the tool is known by a customer
- Purchase price and maintenance tools
- Tools mobility

For design software package, the most modern will be used methods, techniques and principles of agile, modular, procedural and object-oriented programming. They will be used to generate a regular expression applied methods of symbolic data processing.

In addition, several mathematical models and methods have been developed for solving the problem of fading phenomenon and improve the quality of digital telecommunications data transmission. Examples of these models are described by Rice, Rayleigh, Nakagami, Veibull and Log-normal fading distribution. Since there are no

specific requirements for performing mathematical calculations and simulation, implementation and calculating complex mathematical functions and expressions, visualizing the results and creating dynamic GUI\_a, the main problem we had to solve was the application of an appropriate application program that could meet all the listed requirements, but at the same time be flexible to use, be a tool known to the user, be unrestricted portability tool, that is stable and fast (because some processes of calculation in the loop require a large number of iterations to meet the convergence conditions, and therefore spend a lot of processor time). All my thoughts regarding this issue boiled down mainly to the selection and application of extraordinary application program: MATLAB.

The work is part of a " Software Package to Determining the Performance of Digital Telecommunications Systems in The Presence of Fading ".

#### B. Calculation and plotting PDF

The application allows the user to start, a simple click of the mouse, calculate and draw the basic elements of the statistical theory of telecommunication channels, statistical parameters of the first order system in the channel with the Rayleigh fading by two functions: the probability density and cummulative probability density.

One of the most common methods for characterizing a fading channel is the use of a probability density function (PDF), which represents the probability density of the received signal strength. The shape of a PDF determines the performance of a wireless receiver in the presence of noise and interference. Figure 1 shows probability density function EGC Diversity receivers with two branches and Rayleigh fading.

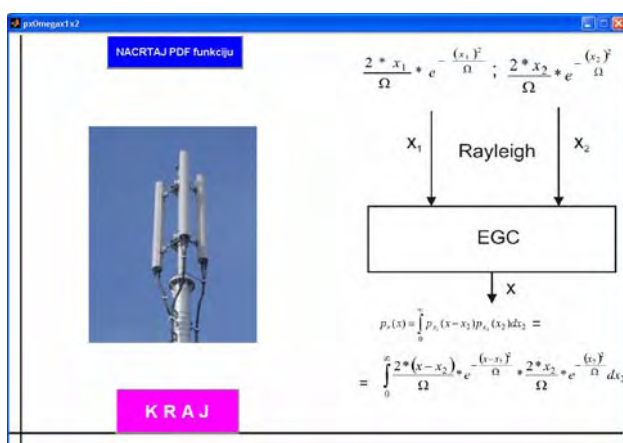


Fig. 1. Probability density function EGC Diversity receivers with two branches and Rayleigh fading

% The expression for the probability density function of %EGC Diversity receivers with two branches and Rayleigh %fading with MATLAB solutions\*\*\*\*\*

.....  
for x=0:0.05:6;  
Omega=0.4;

```

PP=@(x2) (2.*(x - x2))./(Omega).*exp(-((x - x2).^2/(Omega))).*(2.*x2)./(Omega).* exp (-((x2).^2./Omega));
P=quad(PP,0,x);
Omega=0.5;
PP1=@(x2) (2.*(x - x2))./(Omega).*exp(-((x - x2).^2/(Omega))).*(2.*x2)./(Omega).* exp (-((x2).^2./Omega));
P1=quad(PP1,0,x);
Omega=0.7;
PP2=@(x2) (2.*(x - x2))./(Omega).*exp(-((x - x2).^2/(Omega))).*(2.*x2)./(Omega).* exp (-((x2).^2./Omega));
P2=quad(PP2,0,x);
Omega=0.8;
PP3=@(x2) (2.*(x - x2))./(Omega).*exp(-((x - x2).^2/(Omega))).*(2.*x2)./(Omega).* exp (-((x2).^2./Omega));
P3=quad(PP3,0,x);

```

```

% Create plot in proper axes
plot (x,P,'bx-','LineWidth',2);
hold on
plot (x,P1,'rd-','LineWidth',2);
plot (x,P2,'mp-','LineWidth',2);
plot (x,P3,'ko-','LineWidth',2);
axis([0 6 0 1])
grid on
legend('Omega=0.4','Omega=0.5','Omega=0.7','Omega=0.8');
xlabel('x-->');
ylabel('PDF');
title('PDF za SC diverziti sa dva ulaza i Rejlijevim kanalima');
end

```

Figure 2 shows probability density graph of the EGC Diversity receivers with two branches and Rayleigh fading.

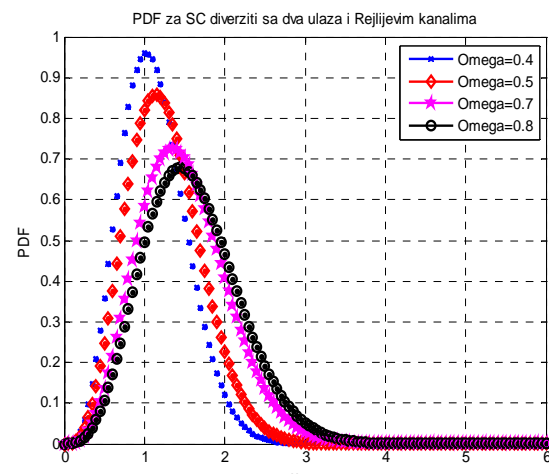


Fig. 2. Probability density graf EGC Diversity receivers with two branches and Rayleigh fading vs. Omega

### C. Calculation and plotting CDF

Using cummulative probability, the probability of the system signal is determined. Probability of the system is defined, as the signal has less than some allowable value. Using probability density signal, the capacity of the channel is determined. Channel capacity is obtained by averaging the Shannon's terms of channel capacity. Using the moment of the signal at the output of macro diversity systems we can calculate the amount of fading. Using the joint probability density signals and extracting the signal at the output of the micro-diversity systems in operation is determined by the joint probability density signal and performs the signal at the output of macro diversity systems.

Using the bit error probability and failure probabilities we can determine the signal strength and distance connections, depending on the parameters of fading and interference. On the basis of these elements it is proved that the application of these techniques can be used by transmitters with less power at greater distances. Using the joint probability density of signal and derivative of the signal we can determine the level crossing rate of signals. Average number of signal level crossing rate is equal to the average of the first derivative of the signal. Using the signal level crossing rate we can determine the duration of the signal. Mean value of the duration of the signal is equal to the error probability quotient failure and the mean number of signal level crossing rate.

Figure 3 shows cummulative probability density function CDF Diversity receivers with two branches and Rayleigh fading.

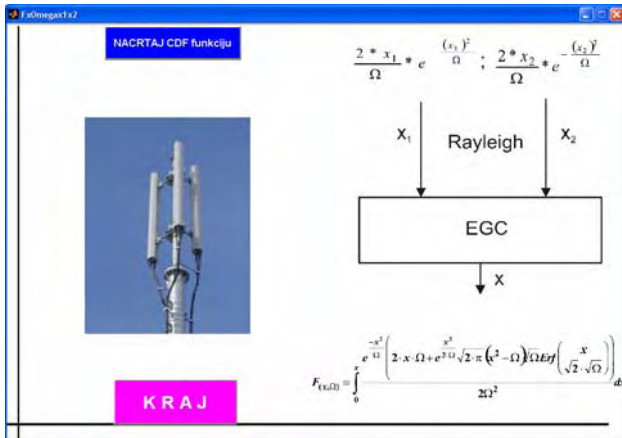


Fig. 3. cummulative probability density function CDF Diversity receivers with two branches and Rayleigh fading.

Next calculation model is based on the same receiver, only the case is calculating the cummulative probability density function of the signal at the output of the EGC combiner. Receiver has two independent branches with Rayleigh fading.

% The expression for the cummulative probability density function CDF of diversity receivers with two branches and Rayleigh fading with MATLAB solutions\*\*\*\*\*

.....  
for x=0:0.05:3.5;  
Omega=0.4;

```

PP1=@(x)(exp((-x.^2)./(Omega)).*(2.*x.*Omega+exp((x.^2)./(2.*Omega)).*sqrt(2.*pi).*x.^2-Omega).*sqrt(Omega).*erf(x./sqrt(2.*Omega)))./(2.*Omega.^2);
P1=quad(PP1,0,x);
Omega=0.5;
PP2=@(x) (exp((-x.^2)./(Omega)).*(2.*x.*Omega+exp((x.^2)./(2.*Omega)).*sqrt(2.*pi).*x.^2-Omega).*sqrt(Omega).*erf(x./sqrt(2.*Omega)))./(2.*Omega.^2);
P2=quad(PP2,0,x);
Omega=0.7;
PP3=@(x)(exp((-x.^2)./(Omega)).*(2.*x.*Omega+exp((x.^2)./(2.*Omega)).*sqrt(2.*pi).*x.^2-Omega).*sqrt(Omega).*erf(x./sqrt(2.*Omega)))./(2.*Omega.^2);
P3=quad(PP3,0,x);
Omega=0.8;
PP4=@(x)(exp((-x.^2)./(Omega)).*(2.*x.*Omega+exp((x.^2)./(2.*Omega)).*sqrt(2.*pi).*x.^2-Omega).*sqrt(Omega).*erf(x./sqrt(2.*Omega)))./(2.*Omega.^2);
P4=quad(PP4,0,x);
% Create plot in proper axes
plot (x,P1,'bx-','LineWidth',2);
hold on
plot (x,P2,'rd-','LineWidth',2);
plot (x,P3,'mp-','LineWidth',2);
plot (x,P4,'ko-','LineWidth',2);
axis([0 4 0 1])
grid on
legend('Omega=0.4','Omega=0.5','Omega=0.7','Omega=0.8');
xlabel('x-->');
ylabel('CDF');
title('CDF za EGC diverziti sa dva ulaza i Rejlijevim kanalima');
end

```

Figure 4 shows cummulative probability density graph of the CDF Diversity receivers with two branches and Rayleigh fading.

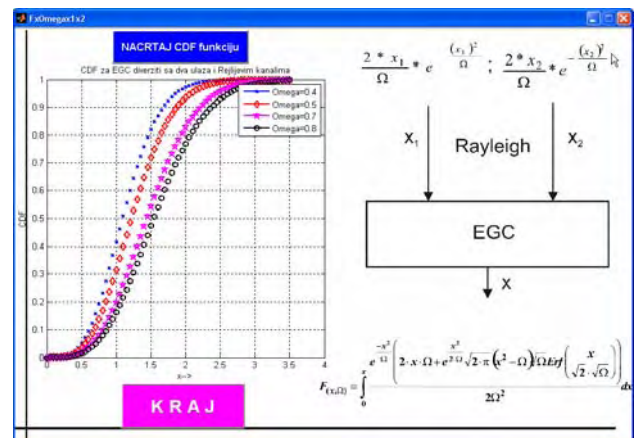


Fig. 4. Cummulative probability density graph of the CDF Diversity receivers with two branches and Rayleigh fading vs. Omega

### III. CONCLUSION

In this paper statistical probability of the signals gain of combining output signals in the presence of Rayleigh fading is determined using MATLAB application. The probability density function of the output signal in the presence of Rayleigh fading channel is obtained. Input EGC combiner works by the summed input symbols and on the basis of the sum the decisions are made. In EGC (Equal Gain Combining) ways of combining the signal at the output are equal to the sum of the signal from its input. This way of combining shows slightly lower scores than the MRC combining, but is more suitable for implementation because it takes the signal input lead in phase and it makes it not necessary to estimate the parameters of the channel. Numerically evaluated results were presented, showing the effects of fading severity on the system's performance.

### ACKNOWLEDGEMENT

This work was carried out in the framework of the project III 44006 Ministry of Education, Science and Technological Development of the Republic of Serbia.

### REFERENCES

- [1] Borivoje Milošević, Slobodan Obradović, Programska paket za određivanje performansi digitalnih telekomunikacionih sistema – FEDING, 18th TELECOMMUNICATIONS FORUM - TELFOR 2010, Beograd
- [2] Borivoje Milošević, Slobodan Obradović, GREŠKA PO BITU U L-GRANSKOM MRC DIVERZITIJI SA BPSK MODULACIJOM, YUInfo 2011, Копаоник, Србија.
- [3] Borivoje Milosevic, Mihajlo Stefanovic, Mile Petrovic, Zorica Nikolic, "PERFORMANCE OF EGC DIVERSITY SYSTEMS IN THE PRESENCE OF CORRELATED RAYLEIGH FADING", International Scientific Conference 21 – 22 November 2008, GABROVO
- [4] Borivoje Milošević, Slobodan Obradović, Mihajlo Stefanović, PROGRAMMING PACKET FADING, UNITECH 2012, International Scientific conference, november 2012, Bulgaria.
- [5] A. Annamalai, C. Tellambura, and Vijay K. Bhargava, "Equal gain diversity receiver performance in wireless channels", IEEE Trans. Communic. vol 48, Oct 2000.
- [6] G. M. Vitetta, U. Mengali, and D. P. Taylor, "An error probability formula for noncoherent orthogonal binary FSK with dual diversity on correlated Rician channels", IEEE Trans. Commun., Lett.Feb. 1999.
- [7] Borivoje Milošević, Slobodan Obradović, Mihajlo Stefanović, Radoslav Bogdanović, POSTDETECTION macro SC diversity system with two micro diversity systems for FSK demodulation, UNITECH 2010, International Scientific conference, november 2010, Bulgaria.
- [8] Borivoje Milošević, Slobodan Obradović, Zoran Mijović, MATLAB SOLUTIONS FOR MaxFLOW/MINCUT AND Ford fulkerston algoritM, UNITECH 2011, International Scientific conference, november 2011, Bulgaria.
- [9] L. Fang, G. Biand A.C.Kot, "New method of performance analysis for diversity reception with correlated Rayleigh fading signals", IEEE Trans.Veh.Technol.vol 49, Sept. 2000.
- [10] Milosevic Borivoje, Jovkovic Srdjan, Todosijevic Vasko, " DIVERSITY BFSK SYSTEM WITH L BRANCHES ", UNITECH 2007, Gabrovo, Bulgaria.
- [11] Milosevic Borivoje, Jovkovic Srdjan, Mile Petrovic, " CATEGORIES OF FADING EFFECTS AND DIVERSITY SOLUTIONS ", UNITECH 2007, Gabrovo, Bulgaria.
- [12] Marvin K.Simon, Mohamed-Slim Alouani, Digital Communication over Fading Channels, Second Edition, Wiley Interscience, New Jersey , 2005, str. 586.
- [13] A.Goldsmith: "Wireless Communications", CAMBRIDGE UNIVERSITY PRESS, 2005
- [14] E. BIGLIERI, "Coding for Wireless Channels", New York: Springer, 2005
- [15] N. Morinaga, R. Kohno, S.Sampei, "Wireless communications technologies: new multimedia systems", Kluwer Academic publishers, 2002
- [16] Mihajlo C. Stefanovic, Dragana S. Krstic, Borivoje M. Milosevic, Jelena A. Anastasov, Stefan R. Panic, Channel Capacity of Maximal-Ratio Combining over Correlated Nakagami-m Fading Channels, TELSIKS 2009, EF NIŠ.
- [17] THE CO-CHANNEL INTERFERENCE EFFECT ON AVERAGE ERROR RATES IN NAKAGAMI-Q (HOYT) FADING CHANNELS, Petar Spalević, Mihajlo Stefanović, Stefan R. Panić, Borivoje Milošević, Zoran Trajčevski, Revue roumaine des sciences techniques, Year 2011, Issue 3, <http://www.revue.elth.pub.ro/viewpdf.php?id=301>
- [18] Selection combining system over correlated Generalized-K (KG) fading channels in the presence of co-channel interference, Bojana Nikolic, Mihajlo Stefanovic, Stefan Panic, Jelena Anastasov, Borivoje Milosevic, ETRI Journal, 2010, Paper No. : RP1005-0311, 138 Gajeongno, Yuseong-gu, Daejeon, 305-700, Rep. of Korea
- [19] STATISTIKA SLOŽENOG EGC MAKRO-DIVERZITI SISTEMA, Milošević Borivoje Srđan Jovković, Danijela Manić, INFOTEH 2010, March 2010, Jahorina, Vol. 9, Ref. B-I-1, p. 128-130, Republika Srpska.
- [20] Borivoje Milošević, Petar Spalević, Mile Petrović, Darko Vučković, Srđan Milosavljević, Statistics of macro SC diversity system with two micro EGC diversity systems and fast fading, ELECTRONICS AND ELECTRICAL ENGINEERING JOURNAL. – Kaunas: ELEKTRONIKA T170, – No. 8(96).2009, Litvanija.

# Expert systems for managing asbestos in premises

Igor Nedelkovski<sup>1</sup>, Boban Mircheski<sup>2</sup> and Aleksandra Lozanovska<sup>3</sup>

**Abstract – In this paper is presented an Expert System for Managing Asbestos in Premises.** Asbestos is one of the most dangerous materials on human health that causes cancer. The Expert System is created on the basis of production rules (IF...Then) and quantified facts about asbestos harmful presence. The process of creating the expert system as well as its application are also explained in the paper.

**Keywords – Expert system, asbestos, managing.**

## I. INTRODUCTION

Expert systems are used to advise, diagnose, or troubleshoot problems that were once only performed by humans. A knowledge automation expert system contains practical knowledge culled from a human expert. Expert systems bring specialized knowledge directly to the fingertips of a novice. This enables people with little or no training to perform far more complex tasks than were previously possible.

Knowledge automation expert systems are expanding the scope of information systems. They allow conceptually new types of applications to be created and existing applications to be expanded and leveraged. The goal of expert systems is to deliver answers and knowledge, not merely to provide information for a person to think about.

Such systems have great importance and huge application in environmental and health protection. A diagnostic expert system is given identifiable information through the user's observation or experience. Built into the system's knowledge base is a list of all identifiable symptoms of specific causal factors.

For a medical diagnostic system, the goal is to identify the patient's illness. It starts by assuming that the patient has a particular illness. It proceeds by reviewing the rules and their actions and asks the patient for additional information about unique symptoms in order to create a description of the illness. If it cannot prove an illness exists on the basis of the symptoms, the system takes up another possible illness as the assumed illness and proceeds in the same fashion. All previous responses by the patient are retained in working memory so that repetitive questioning of the patient is avoided.

An efficient environmental management system has to include software tools for air, water and soil pollution diagnosis.

<sup>1</sup>Igor Nedelkovski is professor at Faculty of Technical Sciences, University "St. Kliment Ohridski" - Bitola, Ivo Lola Ribar bb, Bitola 7000 Macedonia, E-mail: igor.nedelkovski@tfb.uklo.edu.mk.

<sup>2</sup>Boban Mircheski is with Faculty of Technical Sciences, University "St. Kliment Ohridski" - Bitola, Ivo Lola Ribar bb, Bitola 7000 Macedonia, E-mail: boban.mircheski@tfb.uklo.edu.mk.

<sup>3</sup>Aleksandra Lozanovska is director at Gauss Institute – Bitola, Republic of Macedonia, Pitu Guli 27, Bitola 7000 Macedonia, E-mail: director@gaussinstitute.org.

This group includes systems that we will consider in this paper, expert systems for managing asbestos. This expert system performs diagnostic and interpretive chores in a time-sensitive environment such as old buildings. If the findings differ from the standard, the system alerts the human technician and suggests an action. Final decisions are left to the human in charge.

## II. ABOUT ASBESTOS

Asbestos is a group of fibrous silicate minerals that naturally produced in the environment. Asbestos in Europe was very used in industry, manufacturing and construction between 1940 and 1990, but there are examples and for his later use. More than 3000 products are used in production due to their durability, resistance to fire and excellent insulating properties. There are three main types of asbestos:

- [1] Chrysotile (white asbestos)
- [2] Crocidolite (blue asbestos)
- [3] Amosite (brown asbestos)

Other rare forms of asbestos include actinolite, anthophyllite and tremolite.

Legally, asbestos is defined as a material or object, whether natural or manufactured, which contains one or more mineral silicates listed above.

When asbestos is affected by heat or chemicals or combined with other substances, its color and texture may be changed. There is no simple test to identify the presence of asbestos-accredited laboratory analysis is the only reliable method.

All types of asbestos can be harmful to health. Generally, the presence of asbestos is not a health risk, unless due to damage, poor condition or inquiry during operations, produce dust containing asbestos fibers.

Inhaling asbestos fibers pose a serious health risk and can lead to diseases such as mesothelioma, lung cancer and asbestososis.

Expert system has been developed which helps when dealing with asbestos containing materials. The System uses a two-part numerical algorithm. The first algorithm is to estimate the material, and the second algorithm is to assess the priorities for action. The end result of dealing with the material is a combination of these two algorithms.

## III. CREATING EXPERT SYSTEMS FOR MANAGING ASBESTOS IN PREMISES

The system of risk assessment, which has been adopted here, is based on the current guidance and recommendations

as set out by the HSE. The System uses a two-part numerical algorithm.

The algorithm sets out the factors, which are most relevant in assessment of the potential release of fibers from a suspect material. These factors have been assigned quantifiable numerical values. The algorithm produces a single numerical value for each asbestos item, which may then be used as a priority rating for remedial work.

Both the material and priority assessments have been undertaken with regard to the parameters as set out in the following Tables I and II:

**TABLE I**  
**MATERIAL ASSESSMENT ALGORITHM**

Sample Variable	Score	Examples
Product type (or debris from product)	1	Asbestos reinforced composites
	2	Asbestos insulating board, mill board
	3	Thermal insulating, sprayed asbestos...
Extent of damage/deterioration	0	Good conditions
	1	Low damage
	2	Medium damage
	3	High damage
Surface treatment	0	Composite materials containing asbestos
	1	Enclosed sprays and lagging
	2	Unsealed AIB
	3	Unsealed lagging and sprays
Asbestos type	1	Chrysotile
	2	Amphibole asbestos excluding crocidolite
	3	Crocidolite
<b>TOTAL</b>	<b>2 - 12</b>	

**TABLE II**  
**RISK ASSESSMENT ALGORITHM**

Assessment parameter	Score	Example
<b>Normal occupant activity:</b>		
Main type of activity in area	0	Rare disturbance activity
	1	Low disturbance activities
	2	Periodic disturbance
	3	High levels of disturbance
<b>Likelihood of disturbance:</b>		
Location	0	Outdoors
	1	Large rooms or well-ventilated areas
	2	Rooms up to 100 m <sup>2</sup>
	3	Confined spaces
Accessibility	0	Usually inaccessible or unlikely to be disturbed
	1	Occasionally likely to be disturbed

	2	Easily disturbed
	3	Routinely disturbed
Extent/amount	0	Small amounts or items
	1	>10 m <sup>2</sup> or 10 m pipe run
	2	>10 < 50 m <sup>2</sup> or >10 < 50 m pipe run
	3	>50 m <sup>2</sup> or >50 m pipe run
<b>Human exposure potential:</b>		
Number of occupants	0	None
	1	1 - 3
	2	4 - 10
	3	> 10
Frequency of use of area	0	Infrequent
	1	Monthly
	2	Weekly
	3	Daily
Average time area is in use	0	<1 hour
	1	>1 - < 3 hours
	2	>3 - < 6 hours
	3	>6 hours
<b>Maintenance activity:</b>		
Type of maintenance activity	0	Minor disturbance
	1	Low disturbance
	2	Medium disturbance
	3	High levels of disturbance
Frequency of maintenance activity	0	ACM unlikely to be disturbed for maintenance
	1	≤1 per year
	2	>1 per year
	3	>1 per month

The algorithm value has been considered in providing a basis in determining a recommendation for management and/or remedial works. It must always be remembered that asbestos is only harmful if fibers are released into an area where they can be inhaled. The potential for fiber release can be determined by four factors:

- [1] The type of material and its properties e.g. friability
- [2] The type of asbestos used
- [3] The condition of the material and any sealant or enclosure
- [4] The location of the material

The first three factors listed fall within the category of 'Material Assessment' whilst the fourth can be used to decide a priority and is covered in the Risk Assessment. For the material assessment a score for each part of the algorithm is assigned and they are totaled to give a final score between 2 and 12. (Presumed or strongly presumed ACMs are always scored as crocidolite (blue asbestos) unless there is strong evidence to the contrary).

This material assessment identifies the high hazard materials, that is those that will most likely release air bone fibers if disturbed (Fig. 1). It does not automatically follow that those materials assigned the highest score in the material

assessment will be the materials that should be given the priority for the remedial action.

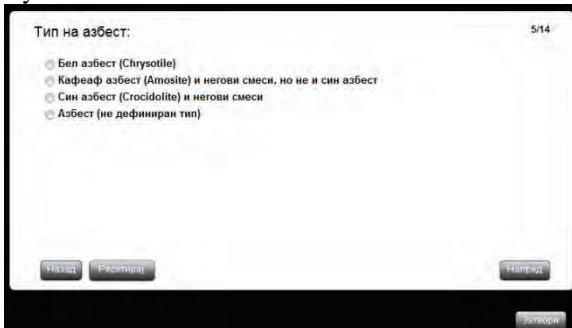


Fig. 1 Part of the expert system for selecting the type of asbestos (Material Assessment)

This information can then be used to form part of a risk assessment. Materials with assessment scores of 10 or more are regarded as having a high potential to release fibres, if disturbed. Scores of between 7 to 9 are regarded as having a medium potential and between 5 to 6 a low potential. Scores of 4 or less have a very low potential to release fibres.

The material assessment gives a figure relating to the likelihood of an ACM to release fibres. As mentioned earlier, a high figure does not necessarily mean that that ACM has to be dealt first. The figure gives an estimate of likely bold. In order to determine the bold other factors have to be considered. The guidance to be produced by HSE suggests the following:

[1] Occupant activity – compare a little used storage room to a frequently used fire door made from AIB.

[2] Likelihood of disturbance – 3 parameters are considered here; location of ACM, accessibility and the amount or extent of the ACM.

[3] Human exposure potential – again 3 different parameters are noted; number of occupants, frequency of use of the area and average time or use of the area.

[4] Maintenance activity – is scored for type and also frequency.

Algorithm is used as follows:

Each of the factors listed above should be scored using the attached table. The score for each factor is the sum of the scores for the parameters divided by the number of parameters; e.g. Factor = maintenance activity. If the score is a 2 for type and a 1 for frequency then the score would be 3 (sum of scores) divided by 2 (number of parameters) = 1.5. Figures should be rounded up but as this is not a precise science, some practical consideration of the area will be needed.

The resultant figures are then summed together and added to the material assessment figure.

If this process is repeated for a number of ACMs, a comparative list for action may be drawn up.

Algorithm is a tool. Further discussion/ interpretation may be required. The recommended actions stated in this report represent our considered opinion as to the appropriate course of action for each material.

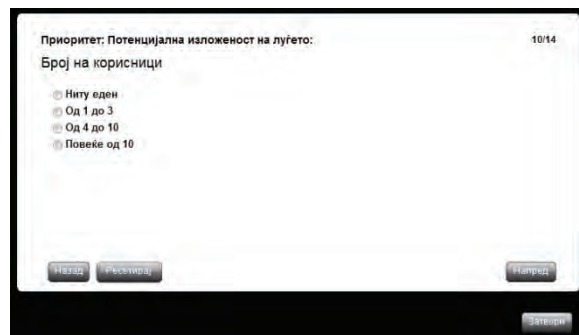


Fig. 2 Part of the expert system for selecting number of occupants, parameter of Human exposure potential

The risk assessment (Fig. 2) should produce a ranking of materials which reflects the risk they present to people working on or near them. This will also form part of the final management plan and can be used to prioritise any work needed. It is important to understand that if the use of the space changes, in which the asbestos containing materials are present, this may alter the risk associated with that material. The condition of the material will also deteriorate over time and therefore risk assessments should be carried out on a regular basis.

For each sample/inspection a priority risk assessment is compiled using an algorithm. A point score (weighting) is allocated on the basis of the examination of a number of parameters. The value assigned to each of these parameters is added together to give a total score, the higher scores indicating high priority risk. These scores are added to the material assessment scores to give an overall score, from this final score an accurate management plan can be put in place, and depending on the score depends on the recommendation shown on Fig. 3.

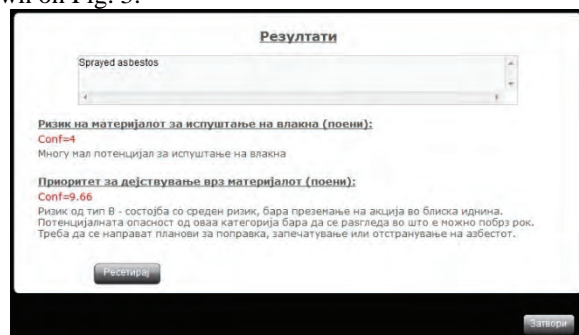


Fig. 3 Results of the expert system by selecting arbitrary parameters

The following describes the different risk bands and associated appropriate actions. These are only guidelines and should still be reviewed for suitability in each circumstance.

[1] Risk Band A (15 Points or more) – High risk situation requiring immediate action. The potential hazard arising from this category warrants urgent attention. Immediate plans should be made for the room/area to be isolated and signage positioned highlighting the immediate danger. Immediate plans should be made for the removal or permanent enclosure of the ACM.

[2] Risk Band B (10 – 14 Points) – Medium risk situation requiring near term action. The potential hazard arising from this category warrants near term attention. Immediate plans

should be made for the repair/encapsulation/enclosure or removal of the ACM.

[3] Risk Band C (7 – 9 Points) – Low risk situation requiring minor remedial works. The potential hazard arising from this category warrants minor remedial works. Immediate plans should be made for the repair/encapsulation/enclosure of the ACM.

[4] Risk Band D (6 Points or less) – Minor risk situation requiring annual inspection. The potential hazard arising from this category warrants an annual visual inspection in order to ascertain any change to the ACM and priority risk.

[5] Risk Band E (0 Points) – No asbestos detected in sample. No action necessary.

Expert systems are developed, for individual materials such as: sprayed asbestos, lagging (pipes, boilers), asbestos insulating boards, asbestos cement, etc. In addition, on Fig. 4 we presented scheme under which manages expert system for asbestos cement.

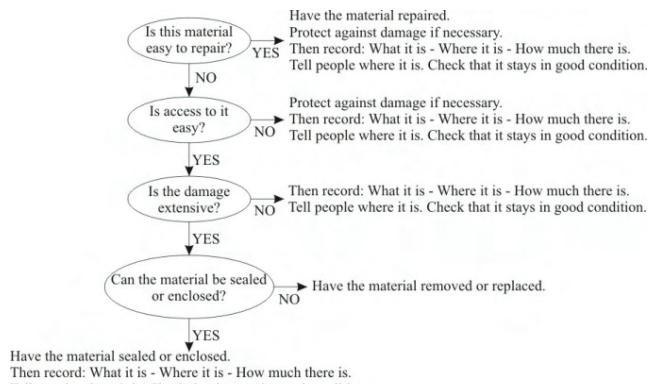


Fig. 4 Scheme for expert system for asbestos cement

The following on Figs. 5 and 6 are shown pictures of the expert system for asbestos cement.

Дали пристапот до материјалот е лесен?

да  
 не

Назад Реконструкција Напред Затвори

Fig. 5 Part of expert system for asbestos cement (Question: Is access to it easy?)

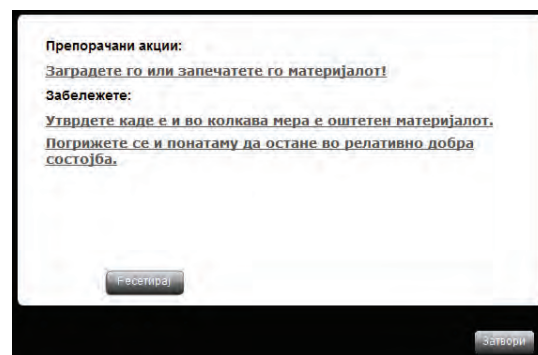


Fig. 6 Results from expert system for asbestos cement with arbitrary parameters

Similar expert systems are made and for other materials, that help us to deal with these materials.

#### IV. CONCLUSION

Asbestos is the one of the most dangerous materials on human health that causes cancer. Expert systems are a great tool to make an assessment of the material and the risk of release of asbestos fibres. Once you are done assessing the presence and type of the asbestos containing material, the expert system offers recommendations on how to proceed with such material.

#### REFERENCES

- [1] Bransford J. D., Brown A. L., Cocking R. R., *How people learn: Brain, mind, experience, and school*, Washington DC: National Academy Press, 2000.
- [2] Chad Lane H., *Intelligent Tutoring Systems: Prospects for Guided Practice and Efficient Learning*, Institute for Creative Technologies University of Southern California, 2006.
- [3] Elias M. Awad, *Building Knowledge Automation Expert Systems: With Exsys CORVID*, 2<sup>nd</sup> ed, ISBN:0-9741390-0-9.
- [4] Eurosafe UK, *Legislative guidance notes – management survey*, QM77.
- [5] Hsieh T. Sheng-Jen, Hsieh Y. Patricia, *Intelligent Tutoring System: Authoring Tool for Manufacturing Engineering Education*, 2001.
- [6] McKendree J., *Human Computer Interaction*, 1990.
- [7] Nedelkovski I., *Engineering Expert Systems*, 2009.
- [8] Riccucci S., *Knowledge Management in Intelligent Tutoring Systems*.
- [9] <http://clipsrules.sourceforge.net/>
- [10] <http://www.einstein-energy.net/>
- [11] <http://www.hse.gov.uk/>
- [12] <http://www.wtec.org/>
- [13] <http://www.xpertrue.com/>
- [14] <https://engineering.purdue.edu/>

# Ontology-based Personalization and Recommender System in Digital Libraries

Daniela Kjurchievska<sup>1</sup>

**Abstract –** The widespread use of the internet has resulted in Digital Libraries (DL) that are increasingly used by diverse communities of users for diverse purposes, and in which sharing and collaboration have become important social elements. In that sense, Academic Digital Libraries (ADL) have emerged as a result of current technology in learning and researching environment, which offers myriad of advantages especially to students and academicians from one side, and advances in computing and information system technologies from other side; thus had been introduced in universities and to the public. This is due to dramatic change in learning environment through the use of Digital Library System (DLS) which impacts on these societies' way of performing their study/research. A simple search function increasingly leads to user dissatisfaction as user's needs become more complex and as the volume of managed information increases. Proactive DL, where the library evolves from being passive and untailored, are seen to offer a great potential to overcome those issues and include techniques such as personalization and recommender systems. Personalization is viewed as an application of data mining and machine learning techniques to build models of user behavior that can be applied to the task of predicting user needs and adapting future interaction with the ultimate goal of improved user satisfaction.

**Keywords –** Personalization and Recommendation Systems, Digital Library, Ontology, Ontology-Based Personalization System.

## I. INTRODUCTION

The emerging generation of DL is more heterogeneous along several dimensions. The collections themselves are become more heterogeneous in terms of their creators, content, media, and communities served. The range of library types is expanding to include long-term personal digital libraries, as well as DLs that serve specific organizations, educational needs, and cultural heritage and they vary in their reliability, authority, and quality. The user communities have become heterogeneous in term of their interests, background, skill levels, ranging from novices to experts in a specific subject area. The growing diversity of DLs, the communities accessing them, and how the information is used requires that the next generation of DLs be more effective at providing information that is tailored to a person's background knowledge, skills, tasks, and intended use of the information.

Information retrieval technologies have matured in the last

decade and search engines do a good job of indexing contents available on the Internet and making it available to users, even the user knows exactly what he is looking for but often, search engines themselves can return more information than the user could possibly process. Also, most widely used search engines use only the content of DL documents and their link structures to access the relevance of the document to the user's query.

Hence, no matter who the user of a search engine is, if the same query is provided as input to the search engine, the results returned will be exactly the same.

The need to provide users with information tailored to their needs led to the development of various information filtering techniques that build profiles of users and attempt to filter large data stream, presenting the user only those items that it believes to be of interest.

The goal of personalization is to provide users with what they want or need without requiring them to ask for it explicitly. This doesn't in any way imply a fully automated process, instead it encompasses scenarios where the user is not able to fully express exactly what they are looking for, but the interaction with an intelligent system can lead them to items of interest.

Intelligent Techniques for Personalization is about leveling all available information about users of the DL to deliver a personal experience. The "intelligence" of these techniques is at various levels ranging from the generation of useful, actionable knowledge through to the inferences made using this knowledge and available domain knowledge at the time of generating the personalized experience for the user. As such, this process of personalization can be viewed as an application of data mining and hence requiring support for all the phases of a typical data mining cycle including data collection, pre-processing, pattern discovery and evaluation, in off-line mode, and finally the deployment of the knowledge in real-time to mediate between the user and the DL.

## II. THE PERSONALIZATION PROCESS

Personalization can be defined as the way in which information and services can be tailored in a specific way to match the unique and specific needs of the individual user or community of users. This is achieved by adapting the presentation and/or the services presented to the user by taking into account the user's tasks, background, history, device, information needs, location, etc., essentially the user's context. Personalization can be user-driven which involves a user directly invoking and supporting the personalization process by providing explicit input, i.e., the user explicitly initiates actions and provides example information in order to control the personalization. On the other hand, personalization

<sup>1</sup>Daniela Kjurchievska, Technical Faculty at University "St. Kliment Ohridski" - Bitola, Republic of Macedonia, E-mail: daniela.curievska@uklo.edu.mk

can be completely automatic, where the system observes some user activity and identifies the input used to tailor some aspects of the system in personalized way. These two examples of user-driven and automatic personalization are the extreme ends of the spectrum and many personalization tools will have elements of both approaches.

### III. CLASSIFICATION OF APPROACHES TO PERSONALIZATION

In this section we discuss various dimensions along which personalization systems can be classified based on the data they utilize, the learning paradigm used, the location of the personalization and the process that the interaction takes with the user.

#### A. Individual Vs Collaborative

The term personalization impresses upon the individuality of users and the need for systems to adopt their interfaces to the needs of the user. This requires data collected on interactions of users within the system to be modeled in user-centric fashion.

A personalization system may choose to build an individual user model, which is a data structure that represents user interests, goals and behaviors. The more information a user model has, the better content and presentation will be tailored for each individual user. The user model is created through a user modeling process in which unobservable information about a user is inferred from observable information from that user, for example, using interactions with system. User model can be created using a user-guided approach, in which the models are directly created using the information provided by each user, or an automatic approach, in which the process of creating a user model is hidden from the user. This approach commonly requires content descriptions of items to be available and is often referred to as content-based filtering systems.

An alternative approach to recommendation is not only the profile for active user but also other users with similar preferences, referred to as the active user's neighborhood, when recommending items. In that sense, the DLs may be viewed as common working place where users may become aware of each other, open communication channels, and exchange information and knowledge with each other or with experts. This means that it is quite possible that users may have overlapping interests if the information in a DL matches their expectations, backgrounds, or motivations. Such users might well profit from each other's knowledge by sharing opinions or experiences or offering advice. This approach is referred to as social or collaborative filtering.

A major disadvantages of approaches based on an individual profile include the lack of serendipity as recommendation are focused on the users previous interests. Also, the system depends on the availability of content descriptions of the items being recommended. On the other hand the advantage of this approach is that it can be implemented on the client side, resulting in reduced worries

for the user regarding privacy and improved data collection for implicit user preference elicitation.

The collaborative approach also suffers from a number of disadvantages, not least the reliance on the availability of rating for any item prior to it being recommendable, often referred to as the new item rating problem. Also, a new user needs to rate a number of item before he can start to obtain useful recommendations from the system, referred to as the new user problem.

#### B. Reactive Vs Proactive

Reactive approaches view personalization as a conversational process that requires explicit interaction with the users either in the form of queries or feedback that is incorporated into the recommendation process, refining the search for the item of interest to the user.

Proactive approaches, on the other hand, learn user preferences and provide recommendations based on the learned information, not necessarily requiring the user to provide explicit feedback to the system to drive the current recommendation process. Proactive systems provide users with recommendations, which the user may choose to select or ignore.

#### C. User Vs Item Information

Personalization systems vary in the information they use to generate recommendations. Typically, the information utilized by these systems includes:

- Item Related Information: This includes content descriptions of the items being recommended and a product/domain ontology
- User Related Information: This includes past preference rating and behavior of user, and user demographics

Most systems that use user related information, tend to be based on past user behavior such as the items they have bought or rated in the past.

In addition to the system that depend solely on item related or user related information, a number of hybrid systems have been developed that use both types of information.

#### D. Memory Vs Model Based

As mentioned before the process of personalization consists of an off-line and online stage. In the off-line stage the key tasks are the collection and processing of data pertaining to user interests and the learning of a user profile from the data collected. Learning from data can be classified into memory based learning (also known as lazy learning) and model based learning (or eager learning) based on whether it generalizes beyond the training data when presented with a query instance (online) or prior to that (off-line).

Traditional Collaborative filtering and content-based filtering based systems that use lazy learning algorithms, are examples of memory-based approach to personalization, while

item-based and others collaborative filtering approach that learn models prior to deployment are examples of model-based personalization systems.

#### E. Client Vs Server Side

Approaches to personalization can be classified based on whether they have been developed to run on a client side or on the server side. The key distinction between these personalization approaches is the breadth of data which is available to the personalization system. On the client side, data is only available about the individual user and hence the only approach possible on the client side is Individual.

On the server side, the system has the ability to collect data on all its visitors and hence both Individual and Collaborative approaches can be applied.

### IV. PERSONALIZATION TECHNIQUES

The traditional systems for personalization of DL, based on the previously described approaches are:

- Content-Based Filtering
- Traditional Collaborative Filtering
- Model-Based Technique
  - Item-Based Collaborative Filtering
  - Clustering-Based Approach

Beside these traditional personalization systems, a number of hybrid approaches to personalization have been proposed. These hybrid recommenders have been motivated by the observation that each of the recommendation technologies in the past has certain deficiencies that are difficult to overcome within the confines of a single recommendation approach.

One form of hybrid recommender that has recently been gaining a lot of attention is that which is based on the use of ontologies to describe the relationship between all the elements which take part in a DL scenario of use.

### V. ONTOLOGY-BASED PERSONALIZATION SYSTEM FOR DL

Every day a huge amount of newly created information is electronically published in DL, whose aim is to satisfy users' information needs. Both, the collectors and the user communities become more heterogeneous and this growing diversity has changed the initial focus of providing access to digital content and transforming the traditional services into digital ones to a new handicap where the next generation of libraries should be more proactive offering personalized information to their users taking in consideration each person individually.

In order to build such personalization system, several multidisciplinary aspects must be addressed: first, there are cognitive and behavioral aspects that determine the way users perform search and examine the obtained results. Second, personalization issues must be addressed from a user-centered point of view, under the approach of human computer interaction and third, there are technological and knowledge

engineering aspects related to the way all this information is structured for both updating and querying purposes. In this point, Ferran et al. purposed the set of desired functionalities and requirement of an ideal scenario for DL which include personalization capabilities by means of ontologies. The use of ontologies for describing the possible scenarios of use in a DL brings the possibility of predicting user requirement in advance and to offer personalized services ahead of expressed need. They suggest building ontologies by using other sub-ontologies which describe the basic element of the personalization system: users, digital resources, action, navigational profiles, etc.

In this system, collaborative filtering approaches are used for guidance and providing recommendation to the user. That means that the system automatically collects information about the user's action and determines the relative importance of each content by weighting all the collected information among the large amount of users. In this DL scenario of use both navigation techniques are also valid, simple searches starting from a single search term or advanced search using multiple criteria. The basic idea of this approach is the efforts for finding a useful piece of information in DL carried out by an individual, and which can be stored in structured way and then shared for future users with similar necessities.

Two elements determine the functionalities of the desired PS, the user's profile which include navigational history and user preferences, and the information collected from navigational behavior of the DL users. User profile should include all the information relevant to the user: personal information, which can be publicly made available by each user in order to facilitate the discovery of similar interest and navigational history and behavior records, which will be used altogether with the personal information by PS to build the set of recommendations that will help each user in browsing and searching the DL.

Depending to the users' navigation, two different behaviors can be identified, exploratory and goal-oriented navigation. The exploratory navigation can be mainly oriented to obtain a general vision of the available resources in the library. Depending on user profile, this navigation would have different implicit intentions. In the case of goal-oriented navigation, it is usually considered that the user is looking for a resource. Both searches can be classified in different use cases. For example, in case of searching for an author, if the user is a student, the recommendations associated to search results should be oriented to the area of the course subject, taking into account the navigation of other students and also the teacher's recommendations. If the user is a researcher, recommendation should be oriented by different criteria dependent on the searches that have been carried out by other investigators, or to magazines, books and conferences where searched author had published. Recommendation are generated by using the knowledge extracted from the searching and browsing profiles of users with similar interests and knowledge integrated in the ontology, or by following citation of similar documents.

The use of ontology could be also interesting when it comes to incorporating new functionalities into existing DL, by describing the relationships between elements. For instance, if

a teacher defines one or more books as recommended bibliography for given subject, students enrolled in such subject should be aware of those books when performing searches related to the subject.

It is important to clarify that ontologies are not built for describing the contents of a DL, but for describing the way users browse and search contents, with the aim of building a PS based on accurate recommendations. The ontology itself is composed of sub-ontologies which describe all the interesting relationships between the elements of the small micro-scenarios that emerged in using of DL system. Into the DL, the creation of ontology will help library managers to construct tailored libraries for each subject. Every library is built on the explicit recommendation from a teacher. With ontology, those specialized libraries could be built from the use that previous student gave to the resources and new information could be added from use of the library by experts.

It is remarkable that the use of ontologies can be also extended to implement and transfer the concept of user profiles and user navigational behavior to other DLs and databases, so when a user leaves one service to connect into another one, the user profiles can be transferred from one database to another through the appropriate semantic web services.

## VI. CONCLUSION

The need to provide users with information tailored to their needs led to the development of various information filtering techniques that build profiles of users and attempt to filter large data stream, presenting the user only those items that it believes to be of interest.

Beside the traditional approaches for personalization systems, ontologies are powerful tool for describing complex scenarios of use such as in DLS. The use of ontologies promotes the integration of new scenarios into existing ones. New system functionality and requirement can be added by including the appropriate description into the ontology framework that defines the DL scenario of use.

## REFERENCES

- [1] B. Mobasher and S.S. Anand , "Intelligent Techniques for WEB Personalazation", pp. 1–36, Springer-Verlag Berlin Heidelberg 2005
- [2] N. Ferran, E. Mor, J. Mingüllón, "Towards personalization in digital libraries through ontologies", Library Management, Vol. 26 Iss: 4/5, pp.206 – 217, 2005
- [3] M. Lytras, M. Sicilia, J. Davies, V. Kashyap, "Digital libraries in the knowledge era: Knowledge management and Semantic Web technologies", Library Management, Vol. 26 Iss: 4/5, pp.170 – 175, 2005
- [4] M.E. Renda, U. Straccia , "A personalized collaborative Digital Library environment: a model and an application ", Original Research Article Information Processing &Manag., Volume 41, Issue 1, Pages 5-21, January 2005
- [5] S. Grigoriadou, A. Kipourou, E. Mouratidis , M. Theodoridou , "Digital Academic Libraries: an important tool in engineering education", 7th Baltic Region Seminar on Engineering Education, St Petersburg, Russia, 4-6 September, 2003

- [6] A. F. Smeaton, J. Callan, "Personalization and recommender systems in digital libraries", International Journal on Digital Libraries, Volume 5, Issue 4, pp 299-308, 2005
- [7] E. Frias-Martinez, G. Magoulas, S. Chen, R. Macredie, "Automated user modeling for personalized digital libraries", International Journal of Information Management, Volume 26, Issue 3, Pages 234–248, 2006
- [8] M. Kumar,"Academic Libraries in Electronic Environment: Paradigm Shift", International Conference on Academic Libraries (ICAL), New Delhi, 2009
- [9] M. Nisheva-Pavlova, P. Pavlov, "Search Engine in a Class of Academic Digital Libraries" In: T. Hedlund, Y. Tonta (Eds.), "Publishing in the Networked World: Transforming the Nature of Communication. 14th International Conference on Electronic Publishing, 16-18 June 2010, Helsinki, Finland", Edita Prima Ltd, Helsinki, 2010, ISBN 978-952-232-085-8, pp. 45-56. (2010)
- [10] M. Nisheva-Pavlova, "Providing and Maintaining Interoperability in Digital Library Systems', Proceedings of the Fourth International Conference on Information Systems and Grid Technologies (Sofia, May 28-29, 2010), St. Kliment Ohridski University Press, 2010, ISBN 978-954-07-3168-1, pp. 200-208. (2010)
- [11] R.A. Razilan, W. Dollah, F.A.Saad, S. Diljit, "Academic Digital Library's Evaluation Criteria: User-Centered Approach", International Journal of Social and Human Sciences, 2009

---

---

## Poster 7 - Electronics

---

---



# Autonomous Inverters With Energy Dosing For Ultrasonic Applications

Nikolay Dimitrov Madzharov<sup>1</sup>

**ABSTRACT.** An resonant inverter with energy dosing (RI with ED) for ultrasonic application have been developed. An original method of energy dosage has been used in these power supplies for an improved output power control. These power supplies are especially attractive for different ultrasonic applications where the compact transducer (CT) impedance could be change strongly in the technological process. A computer simulation and experimental study allowed to define the ranges of the parameters variation for typical current frequencies and to investigate their performance. The test have shown an enhancement in loads matching and process control in a wide range of loads impedances without or with a small variation in frequency. The proposed principle of energy control provides a high reliability and flexibility of ultrasonic installations even with a simplified system of automatic control and fault protection. The results of study, power sources development and test are given in this report.

**Keywords**—inverter, energy dosing, ultrasonic, compact transducer.

## I. INTRODUCTION

It is well known that one of the major requirements to power sources is that they provide the necessary voltage for the CT, as a guarantee for obtaining the specified power and for meeting all requirements to the technological process. Owing to the variety in geometrical dimensions, configuration, different CTs should be supplied with different voltage and respectively frequency [1,5,6,7,8,9,10].

Not with standing the progress made, the methods used to regulate the output voltage of power sources, are not sufficiently smooth and envisage the use of relatively complex matching transformers. A solution to this problem has been used, based on autonomous invertors with energy dosing, which, in their method of operation, generate, with a specified power, an output voltage corresponding to the particular parameters of the load [3,4,9].

## II. RESONANCE INVERTERS WITH ENERGY DOSING

The block diagram of the inverter with energy dosing is presented in the Figure 1. It is shown schematically that between the source of constant voltage (the rectifier) and the autonomous inverter another block is connected - a doser. By means of this block the energy is transmitted to the load in definite portions (doses). It is from the term dose that the name converter with energy dosing derives.

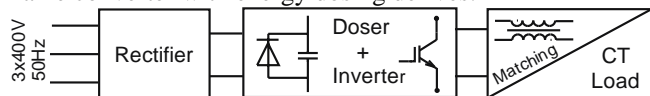


Figure 1. Inverter with energy dosing - block diagram

Figure 2 presents a half-bridge resonant inverters with

energy dosing. The number of additional elements here is minimum - two diodes in the half-bridge circuit ( $VD_3$  and  $VD_4$ ). The time charts in Figures 3 illustrate the method of operation and the order in which the switching devices (the transistors) and the diodes. It can be seen that in the course of one half-period the capacitor  $C_K$  in the circuit in Figure 4, which is charged in a stationary mode up to voltage  $E$ , is discharged completely, a dose of energy  $W$  and power  $P$  being formed at that, equal to  $W = E^2 C_K$ ,  $P = E^2 C_K f$ .

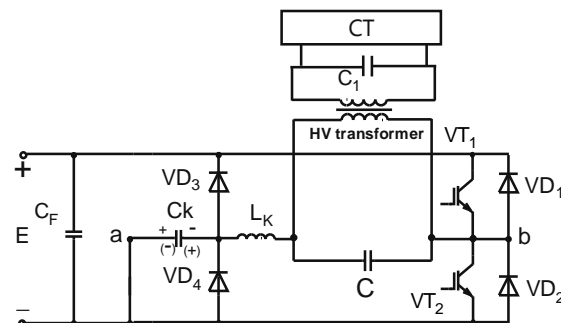


Figure 2. Half-bridge RI with ED

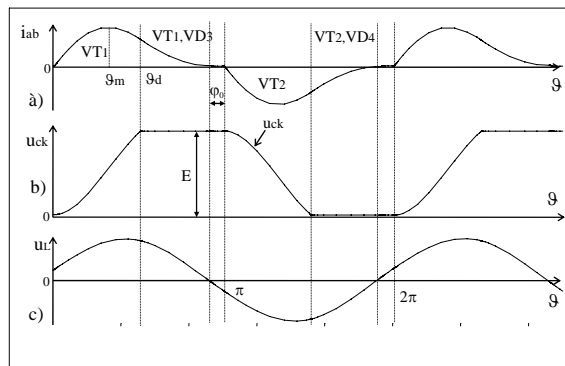


Figure 3. Time charts of RI with ED

It must be noted that in the two inverters the transistors operate with a zero current of switching on and off. The dose of energy  $W$  and the power  $P$  in the inductor equal, respectively

$$W = kE^2 C_K \quad (1)$$

$$P = kE^2 C_K f = \frac{U_L^2 \cos^2 \varphi_L}{R_L} \quad , \quad (2)$$

where  $C_K$  is the capacitance of the dosing capacitor;  $f$  - the frequency of switching (operating frequency) of the inverter;  $k$  - a coefficient dependent on the circuit of the doser and the inverter, e.g.  $k=1,2,4$ ;  $U_L$  - effective value of the variable

<sup>1</sup> Technical University of Gabrovo  
H.Dimitar str. 4, 5300 Gabrovo, Bulgaria

voltage,  $\cos\varphi_L$  and  $R_L$  - power factor and ohmic resistance of the CT, respectively. According to (2) when the values of  $E$ ,  $C_d$  and  $f$  do not vary, the power  $P$  is a constant value independent of the load parameters and the changes in them, regardless of the reason which caused them. In practically, this means that the output voltage of the converter with energy dosing (voltage  $U_L$ ) changes in strict accordance with the concrete load parameters, i.e. self-harmonization is performed without the necessity of influence by the control system. It is exactly this fact that is new and of major importance, the fact that enables the principle of energy dosing in power supply sources for ultrasonic applications. But it is not the only new thing. Another equally important advantage of the converter with energy dosing is the fact that the extreme operation modes - idle running and short circuit are safe, since they do not cause overvoltages and overcurrents.

By changing the values  $E$ ,  $C_d$  and  $f$  it is possible to regulate the output voltage and output power or to fix an assigned level for them.

$$U_L = \left[ \frac{E}{\cos\varphi_L} \sqrt{kC_k R_L} \right] \sqrt{f} \quad (3)$$

The equation (3) suggest that the output voltage can be maintained constant if the switching frequency is varied when the load and input voltage are modified [3,4].

### III. PRACTICAL REALIZATIONS AND COMMERCIAL INTRODUCTIONS

Autonomous inverters with energy dosing for ultrasonic application have been studied well both theoretically and in practice. Mechanical phenomena in the CT circuit may be reflected into an electrical circuit (Figure 4) with the following elements:

- $C_0$  - transducer capacitance (static capacitance);
- $C$  - capacitance due to mechanical elasticity of CT;
- $L$  - inductance describing CT mass;
- $R$  - electrical resistance reflecting mechanical power dissipation in the CT and in treated material.

While capacitance  $C_0$  is almost constant at different loading conditions, values of  $C$ ,  $L$  and especially of  $R$  vary with loading. The CT capacitance must be compensated with an inductance, which is usually located inside of the generator. There are two possibilities for compensation – by series or by parallel choke. Also, there are two resonances of CT in the operation frequency range – one series with small equivalent resistance of the device, close to  $R$ , and one parallel with high value of  $R$  equivalent. Resonance curve of a circuit  $C - L$  is very steep (narrow) due to high quality factor. If  $C_0$  is compensated by  $L_0$  at the resonant frequency of  $C - L$ , CT is in conditions of series resonance. Parallel resonance takes place at higher frequency than series resonance. In this case circuit  $C - L$  has inductive reactive power, which is compensated by additional capacitive power of capacitor  $C_0$ . Value of  $R_{res}$  for parallel resonance is much higher than for series one. Real operating frequency must be selected by the generator control system in the process of matching. If we vary the load, i.e. applied pressure on the CT,

the current through  $R$  will change. By shifting the frequency we are able to keep this current constant.

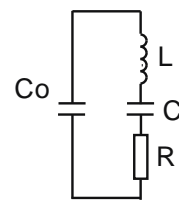


Figure 4. Basic scheme of piezoelectric CT

In the case of the ultrasonic application of the resonant inverter with energy dosing the output power remains constant and equal to the assigned one during the whole process. The converter is absolutely safe when operating with an unloaded CT, as well as with partial or full short-circuit of the load. In accordance with (2) the power level is regulated by changing one of the three quantities -  $E$ ,  $C_k$  or  $f$ .

It must be noted that the self-sustaining of the power, retaining zero current of switching on and switching off of the transistors, is best realized in the case of an active load, or tank circuit adjusted to a resonance. Therefore a *PLL* control system is envisaged in the converters, by means of which the state of the tank circuit is monitored and if necessary the operation frequency is changed. If the requirement for zero current of switching off is overlooked, which is absolutely permissible, the *PLL* system is not necessary. In this case the power remains constant, at a constant frequency [5,8].

The goal of experiments was to determine the working characteristics of inverter with energy dosing, the best matching, efficiency and amplitude of CT vibration. The amplitude of CT was measured by Dynamic Vibration Sensor.

The CT parameters:

- $C_0$  as measured at 1 kHz, is  $20 \pm 1$  nF. This value increases with temperature and aging. In service conditions at 28 kHz the capacitance is about 20 % higher, but it was not possible to measure it directly.
- $C$  and  $L$  with a 200 Hz gap between serial and parallel resonance are 274 pF and 116 mH.
- $R$  varies in a wide range between 5 Ohm in free air and ~250 Ohm under load, depending upon paper and pressure.

Analyzing the "II" equivalent parameters (Figure 5) it was found that the value of  $L_2$  ( $Z_2$ ) was small. Hence, the capacitor  $C_2$  must be big and does not influence matching essentially.

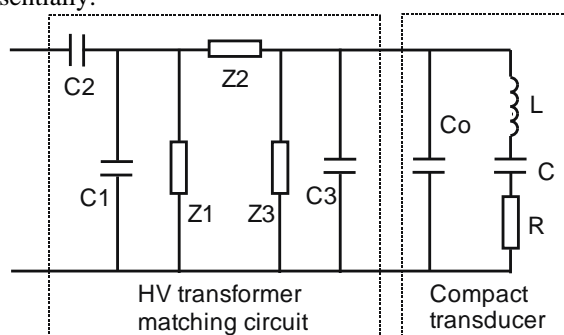


Figure 5. HV transformer, matching capacitors and CT equivalent circuit

Tables 1 and 2 show the CT amplitude and RI with ED power vs C1 value.

Table 1. Amplitudes for idle and loaded CT vs C1 value

Force 4000 N on the CT			
C1, nF	Amplitude idle, mV	Amplitude load, mV	Power RI with ED, W
2,95	1943	1941	2583
3,9	1948	1918	2482
4,9	1942	1872	2405
6,1	1945	1877	2380

Table 2. Amplitude measurement for C1=7.8nF

C1 = 7,8 nF					
Force N	Amplitude idle, mV	Amplitude load, mV	Gen.Power W	Power load W	Efficiency %
4000	1939	2017	2498	2389	95,6
5500	1933	1977	3663	3466	94,6

Along with the experimental study of the ultrasonic system, computer simulation of its operation was done using PSPICE. For that purpose, a PSPICE – model was developed on the basis of the Figure 5. The values of the elements corresponded to the measurements of the OS and SC tests and to the calculations of the “ $\Pi$ ” equivalent circuit are shown in table 3.

Table 3. “ $\Pi$ ” parameters of the HV transformer, CT and compensating capacitors vs. force on the CT.

Force %	Z1, Ohm	L1, mH	C1, nF	Z2, Ohm	L2, mH	C2, nF	Z3, Ohm	L3, mH	C3, nF
120	1730	9,8	3,2	152,6	0,86	37,3	326	1,86	17,4 92%
110	1734	9,86	3,3	152,5	0,867	37,3	316	1,8	18,0 95%
100	1802	10,25	3,16	152	0,864	37,4	301	1,71	18,9 100%
90	1835	10,4	3,09	150,38	0,855	37,8	288,87	1,64	19,7 104%
80	1857	10,56	3,06	150,2	0,854	37,8	280,17	1,59	20,3 107%
70	1865	10,6	3,05	150	0,854	37,8	269,9	1,53	21,0 1 11%

Figures 6,7 and 8 show the waveforms of the RE with ED (Ugen and I gen) and CT voltage, current and phase shift vs frequency.

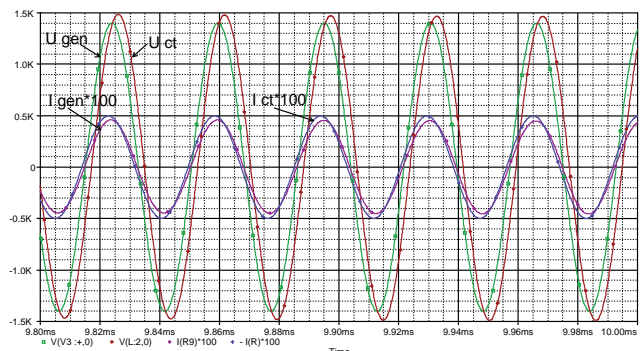


Figure 6. Waveforms of the voltages Ugen, Uct and currents Igen, Ict

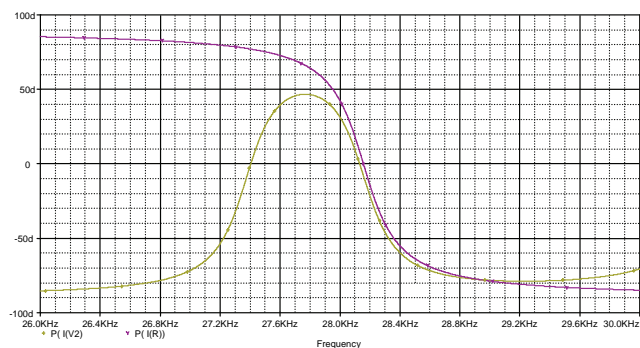


Figure 7. Phase-frequency characteristics of the generator P(I(V2)) and CT currents P(I(R))

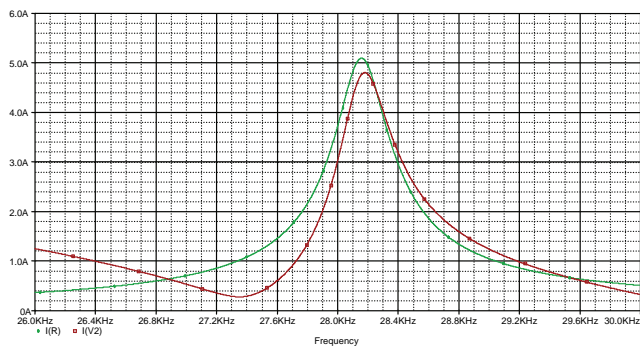


Figure 8. Amplitude-frequency characteristics of the generator I(V2) and CT currents I(R).

Methodology has been worked out for CT matching and optimization, taking into consideration the non-sinusoidal character of the electrical quantities, and it has been verified computer simulations and by experimental investigations. The investigations have been performed with the different loads for ultrasonik applications. When the load has the form of a high-resonant CT the operation of the inverter with energy dosing is analogous - the power is the same in the case of an low-resonat CT. This result, as well as the adaptive properties in other loads, and the safe operation of the inverter in extreme modes, are unique.

Two investigations were conducted: the first one with the automatic control system being switched off (Figure 10), and the second one - with the system being switched on (Figure 9). Figure 9 and figure 10 presents a characteristics, taken

experimentally of the converter described, as well as of any other converters constructed using the principle of energy dosing. The characteristic manifests the dependence of the output voltage and the power on the load resistance i.e. force on the CT. It can be seen that when the force on the CT increases, the voltage decreases, and what is more, it decrease sufficiently to keep the power constant.

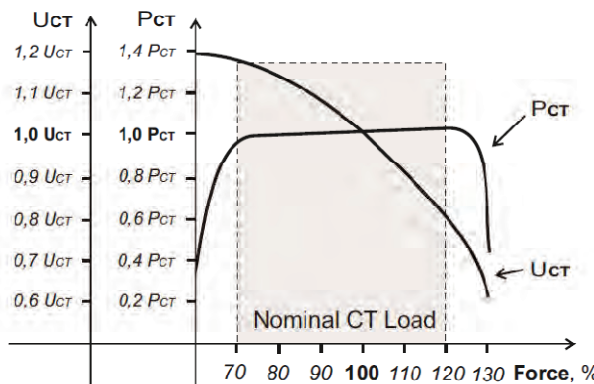


Figure 9. Load characteristics with the control system being switched on.

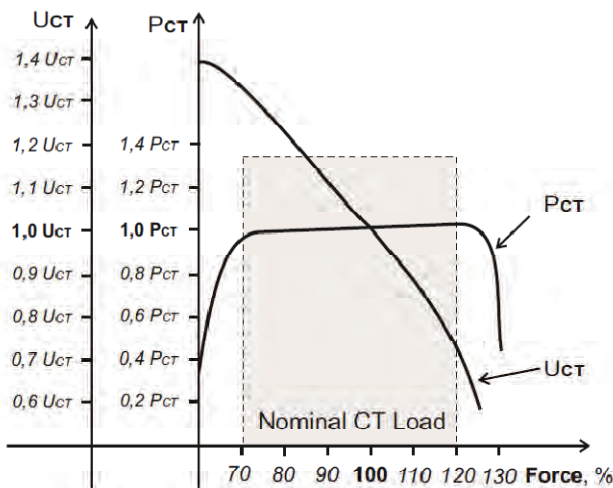


Figure 10. Load characteristics with the control system being switched off.

When the load is in a state close to short circuit (force more than 120% of the nominal one) and idle running (force less than 70% of the nominal one) the power naturally drops. The voltage in the case of short circuit also decreases, and in idle running it increases but not as much as with the conventional circuits of autonomous inverters used in installations for ultrasonic applications.

#### IV. CONCLUSIONS

The investigation has been done on a resonant inverter with energy dosing potentially suitable for use in ultrasonic systems. The experimental tests and measurements of the ultrasonic mock-ups were made including design and construction of the supporting circuitry-matching capacitors and HV transformer. The information up to here although incomplete, allows us to draw the following conclusions:

1.A half-bridge circuit of a resonance inverter with energy

dosing has been analysed.

2. It has been found that the autonomous inverter must operate with a load circuit tuned in resonance on the first harmonic of the alternating current. This is in practice the condition for commutation of switching devices in the mode ZCS.
3. The non-sinusoid character of the alternating current has been taken into account and in accordance with this a methodology for design has been created.
4. Computer modelling with PSPICE program and experimental study with real CT have been made. The values of the elements were set correspondingly to the measurements of the OS and SC tests and to the calculations of the "T" and "Π" parameters.
5. The ability of resonance inverters with energy dosing to maintain constant power in the load has been confirmed, for different combinations of the load parameters, when the ZCS of the switching device is maintained.

#### REFERENCES

- [1] Lin L., F. Lee. Novel zero-current switching and zero-voltage switching Converters. IEEE 5/1996.
- [2] Thornton C. Simplified simultaneous power supply voltage sequencing. Power electronics, 4/2003.
- [3] Madzharov N.D., A DC/DC converter with energy dosing , Proceeding PCIM'04, PC, Nurnberg, Germany, 2004.
- [4] Madzharov N.D., Resonant Power Supplies with Energy Dosing and PLL Control System, Proceeding PCIM'08, Power Conversion, Nurnberg, Germany, 2008.
- [5] 1. Kraev G., N. Hinov, L. Okoliyski, "Analysis and Design of Serial ZVS Resonant Inverter", Annual Journal of Electronics, Volume 5, BOOK 1, Technical University of Sofia, Faculty of Electronic Engineering and Technologies, ISSN 1313-1842, pp.169-172, 2011.
- [6] Kraev G., N. Hinov, D. Arnaudov, N. Rangelov and N. Gradinarov, „Multiphase DC-DC Converter with Improved Characteristics for Charging Supercapacitors and Capacitors with Large Capacitance”, Annual Journal of Electronics, Vol. 6, BOOK 1, TU Sofia, Faculty of Electronic Engineering and Technologies, ISSN 1314-0078, pp.128-131, 2012.
- [7] Bankov, N., Tsv. Grigorova. "Series Resonant DC/AC Converters Methods of control – Investigation, Modelling and Applications" – Chapter 4 in book "Advanced Technologies: Research-Development-Applications" / Edited by Bojan Lalic. ISBN 3-86611-197-5, plV pro literature Verlag Robert Mayer-Scholz, Mammendorf, Germany, 2006, pp. 57-76.
- [8] Bankov, N., Al. Vuchev, G. Terziyski. „Study of LCC Resonant Transistor DC/DC Converter with Capacitive Output Filter” – Chapter 4 in book “Power Quality Harmonics Analysis and Real Measurements Data”, Edited by Gregorio Romero Rey and Luisa Martinez Muneta, ISBN 978-953-307-335-4, INTECH, November 2011, pp. 111-130.
- [9] Nedelchev I., I. Nemigenchev. Analysis of the Class E Amplifier with Load Variation. International Scientific Conference on Information, Communication and Energy Systems and Technologies, iCEST, IEEE, Ohrid, Macedonia, vol. 1, pp. 313-316, 24-27 June, 2007.
- [10] Nedelchev, I. Power RF Amplifier Class E Using Impedance Matching Transformer. International Scientific Conference, UNITECH'11 Gabrovo,pp.I-331-I-336,18-19 November 2011.

# Virtual System for Magnetic Field Measurement

Nikola Draganov<sup>1</sup> Totka Draganova<sup>2</sup> Anatolii Aleksandrov<sup>3</sup>

**Abstract – Progress of electronics and automation have increased the accuracy and reliability of the measurement processes, and with it the creation of new sensors and measurement systems.**

The magnetic field is one of the most commonly measured variables, but the accuracy depends on the system for processing measurement signals. Suitable for use in measuring and automatic techniques are computer-based systems for collecting and processing information.

The article presents an example computer-based system for measuring of magnetic field developed based magnetic field sensitive IC manufactured by Melexis, DAQ-module for data acquisition and LabView software environment of the company National Instruments®.

**Keywords – Hall sensors, measuring of magnetic field, DAQ-systems, virtual instruments.**

## I. INTRODUCTION

Different types of sensors for measurement and detecting of magnetic field like as Hall elements, magnetoresistors, magnetotransistors,, magnetodiodes, magnetothyristors, magnetosensitive integrated circuits are known. Hall elements are among the widely used galvanomagnetic elements. Their planar structure [4] is absolutely compatible with modern integral technologies and is conducive to magnetosensitive integrated circuits making. They have good magnetic sensitivity, a wide change range of measured magnetic field and high reliability of output signal [1-4].

In much areas of automatics, instrumentation, electronics, machine building, chemical industry and etc is necessary to fulfill precise automatized measurements checking and observation of different processes and quantities. A creating of a such kind apparatuses is possible but their bulk, reliability and operational period do not justify the experiments. In the modern electronic system it is made by fulfilling of virtual devices which enable information signals collection and their treatment, visualization, storage and decision taking for processes control.

The purpose of the present working is to create and investigate an automatized virtual system for measurement of magnetic field on a basis of magnetosensitive integrated circuit MLX242 manufactured by Melexis and DAQ-module

<sup>1</sup>Nikola Draganov is with the Faculty of Electrical Engineering and Electronics at Technical University of Gabrovo, 4 Hadgi Dimitar, Gabrovo 5300, Bulgaria, E-mail: [ndrag@abv.bg](mailto:ndrag@abv.bg).

<sup>2</sup>Totka Draganova is with the Faculty of Electrical Engineering and Electronics at Technical University of Gabrovo, 4 Hadgi Dimitar,Gabrovo 5300, Bulgaria, E-mail: [totka\\_draganova@mail.bg](mailto:totka_draganova@mail.bg).

<sup>3</sup>Anatolii Aleksandrov is with the Faculty of Electrical Engineering and Electronics at Technical University of Gabrovo, 4 Hadgi Dimitar, Gabrovo 5300, Bulgaria, E-mail: [alex@tugab.bg](mailto:alex@tugab.bg).

USB6009 manufactured by National Instruments for data acquisition [5, 6].

## II. RESENTATION

Block diagram of a realized virtual system is shown in a Fig.2. It is composed of magnetosensitive integrated circuit (IC) of the type MLX242. Its power supply leads U<sub>CC</sub>, GND and the output lead U<sub>O</sub> are connected to DAQ-module for data acquisition and processing of the type USB6009 which is connected by USB interface to personal computer [6].

The chosen magnetosensitive IC is linear transducer of magnetic field to electrical voltage. Its conversion characteristic U<sub>O</sub>=f(B) at U<sub>CC</sub>=const is investigated and depicted in Fig.1. It is disposed in the first and fourth quadrants and shows a good linearity. The investigation is fulfilled for magnetic field B=(-50÷50)mT and supply U<sub>CC</sub>=5V. For this type sensor is typical that in magnetic field absence the output voltage is U<sub>O</sub> = 2,5V at U<sub>CC</sub>=5V. This chosen voltage enables to use the build in DAQ-module stabilized supply (5V).

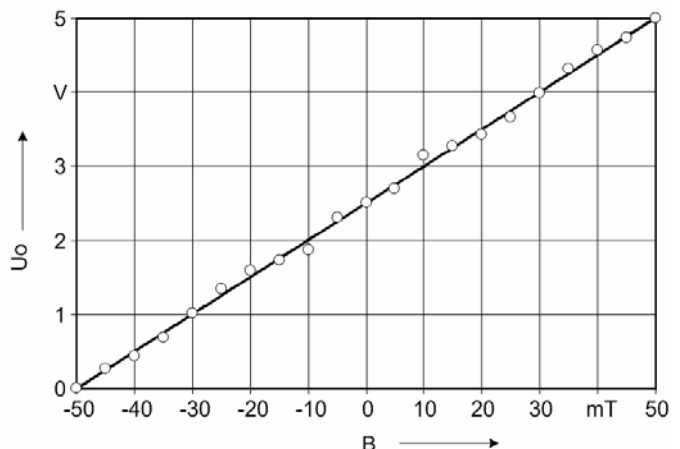


Fig.1. Conversion characteristic U<sub>O</sub>=f(B), U<sub>CC</sub>=5V of magnetic field linear transducer MLX242

The module USB-6009 collects and treats an information. It has 14bits analog-to-digital converter with a system of 10 channels. A signal from an investigated galvanomagnetic sensor is handed to one of all converter input.

The software environment is provided by LabView v.8.5 program package manufactured by National Instruments. The created virtual device consists of two modules: instrumental in which are placed measuring instruments and program where is introduced a virtual system real software. They are depicted respectively in Fig.3 and Fig.4.

On the instrumental panel (Fig.3) are placed two identical measuring instruments for measurement of output voltage U<sub>O</sub> from magnetosensitive IC an of applied magnetic field inductance B.

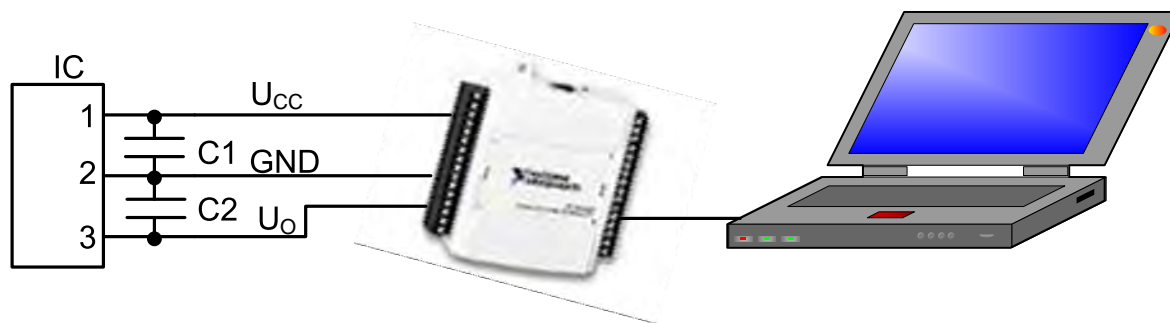


Fig.2. Block diagram of a system for magnetic field measurement

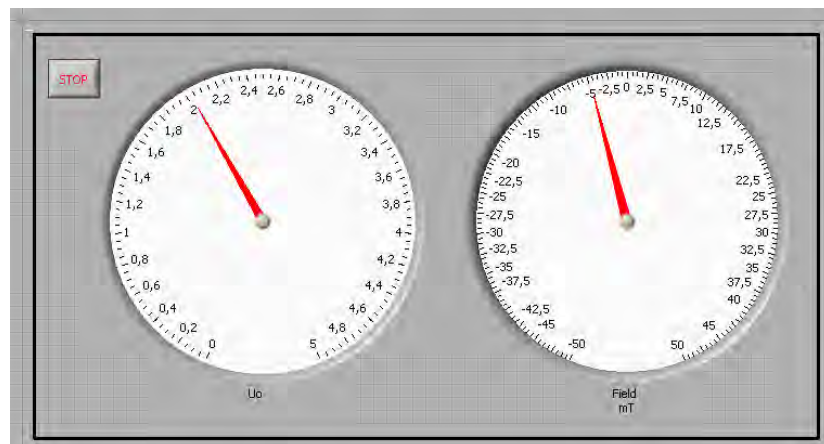


Fig.3 Instruments panel

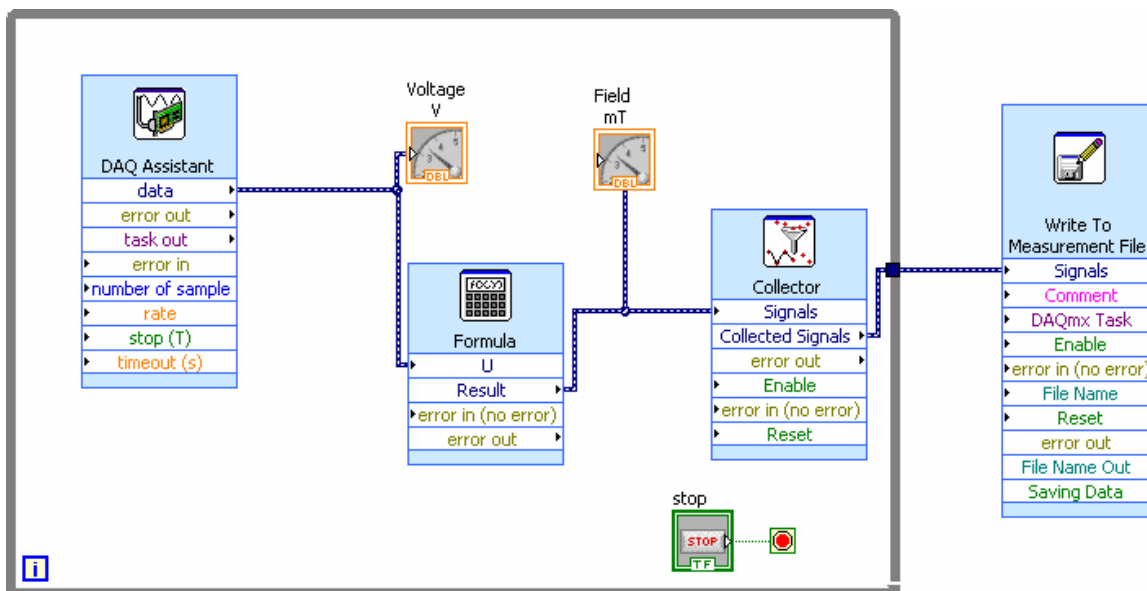


Fig.4 Software block schematic diagram

By means of depicted in Fig.2 experimental obtained conversion characteristic the output signal from magnetosensitive IC is transformed in magnetic field. By

means of the lesser squares method is obtained a describing the conversion characteristic mathematical equation:

$$U_O = 0,0501B + 2,5001 \quad (1)$$

For a magnetic field is necessary the obtained equation to be introduced in block Formula (Fig.4). To input U on the block diagram is handed the measured by DAQ Assistant signal which represents the magnetosensitive IC output voltage. The magnetic field measured magnitudes are obtained on output Result.

The results are stored in generated by a program package file. For this purpose in block diagram (Fig. 4) blocks Collector and Write To Measurement File are introduced. The first gives for the recording of measurements necessary number. The second shows an address and a file type with data.

### III. CONCLUSION

Virtual system for measurement of magnetic field on a basis of magnetosensitive integrated circuit MLX242 manufactured by Melexis and measuring system DAQ-6009 manufactured by National Instruments has been created. The magnetosensitive integrated circuit is investigated. Its conversion characteristic is obtained. A mathematical equation describing this characteristic is drawn.

By means of a virtual system instruments panel is possible to measure as applied to sensor magnetic field so a generated by him output voltage.

It is foreseen to keep results of measurements in generated by programm product LabView special file.

A created virtual system for magnetic field measurement can find a wide application in electronics, instrumentation and automatics. Its possibility to collect and treat measuring information makes it accessible for anyone research laboratory. Thanks to the small gauges of used components (sensor and DAQ-module) and their operation without external power supply a function of measuring system is increased. This system can be used out of laboratories in field conditions.

### REFERENCES

- [1] Aleksandrov, A., N. Draganov. Galvanomagnetic regulator of induction motor rotation frequency, Proceedings of papers – ICEST, Niš, Serbia, 29 June -1 July 2005, p. 66-69.
- [2] Aleksandrov, A., N. Draganov. Study of a galvanomagnetic digital-to-analogue converter, Proceedings of papers – ICEST, Niš, Serbia, 29 June -1 July 2005, p. 60-65.
- [3] Draganov, N., A. Aleksandrov. Galvanomagnetic antilock braking system. Proceedings of papers – ELMA, Sofia, 15-16 Sept. 2005, p.134-136.
- [4] Draganov, N. Investigation of three wire connection of Hall element with orthogonal magnetic sensitivity. Proceedings of papers – UNITECH-08, Gabrovo, Bulgaria, 21-22 Nov. 2008. Vol.1, p.138-141.
- [5] Melexis, product technical data rev. 12.2011
- [6] National Instruments, Lab View – user guide.

**This Page Intentionally Left Blank**

# Based on AMR Sensor Device for Contactless Measurement of AC Current

Nikola Draganov

**Abstract –** There are diverse electrical quantities. One of them is an electrical current. A lot of indirect and direct methods for its measurement are known. Very spread is indirect contactless method by a measurement of a magnetic field created by a flowing through a conductor electrical current. Connected in parallel bridge anisotropic magnetoresistors (AMR) are widely applied to contactless measurement of an alternating current in the modern installation. They have high sensitivity, wide frequency band, good linear characteristics and high reliability.

**Keywords –** AMR sensors, magnetoresistors, contactless measuring, magnetic field measuring, sensors of magnetic field.

## I. INTRODUCTION

There are different electrical quantities. For their reading and treatment definite approaches are necessary. The electric current is one of the most often measured quantity in a techniques.

Classical sensors like as shunting resistors, current transformers and magnetic amplifiers are still used for electrical current measurement. Anyone of these sensors groups has their priorities but and much disadvantages as a big bulk, high price, measurement only constant or alternating values and etc. All of these disadvantages are eliminated in new generation sensors for contactless measurement of current and voltage [1, 2, 4].

The purpose of the present elaboration is to create and investigate on the basis of anisotropic magnetoresistors (AMR) a device for contactless alternating current measurement which can find a wide practical application.

## II. PRESENTATION

The electric current flow across a conductor is connected with a magnetic field generation around it (fig.1). Its value is proportional to electric current magnitude. The modern galvanomagnetic sensors are microelectronic circuits. Its operation principle is established on a measurement of a magnetic inductance created by flowing through a conductor electrical current.

Different kinds of galvanomagnetic transducers as Hall elements, magnetodiodes, magnetoresistors, magnetotransistors and etc are used as transducers which transform a magnetic field to an electrical signal. The magnetoresistors and especially anisotropic magnetoresistors (AMR) are the most

used as sensors for small currents up to 500mA. Hall elements operate as sensors for current measurement up to 1000A. Both galvanomagnetic transducers do not take part as discrete elements. They are constituent part of high technological magnetosensitive integrated circuits.

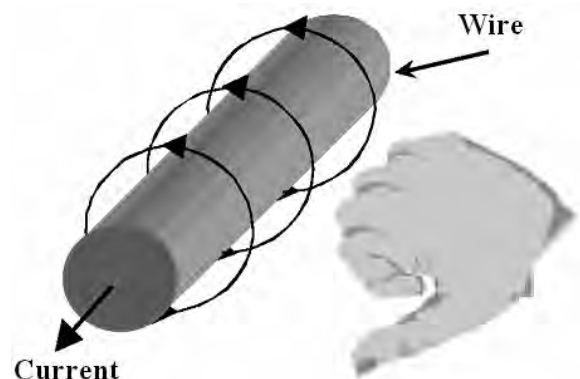


Fig.1. Magnetic field direction around conductor with electrical current

There are two methods for obtaining of dependent on a measured current sensor value (magnetic field). The first way is by means of direct effect of generated around a conductor magnetic field. The second way is to use a magnetic amplifier (concentrator) [3, 4]. Fig. 2 shows how the generated around a conductor alternating or constant magnetic field brings influence on magneto-sensitive integrated circuit.

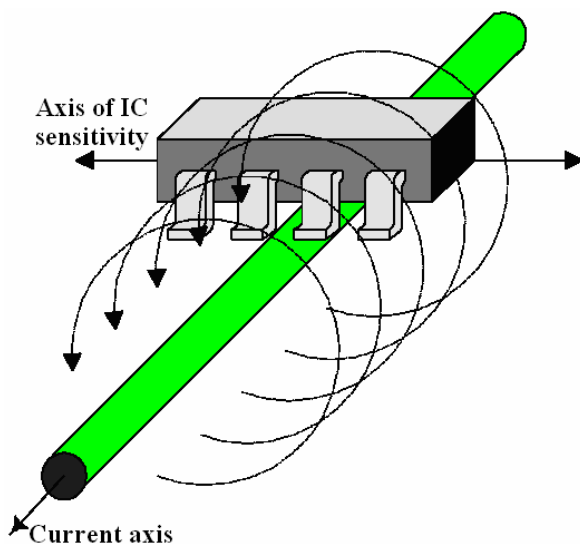


Fig.2 Magneto-sensitive integrated circuit current measurement by magnetic field direct action

<sup>1</sup>Nikola Draganov is with the Faculty of Electronics at Technical University of Gabrovo, 4 Hadji Dimitar str., Gabrovo 5300, Bulgaria, E-mail: ndrag@abv.bg.

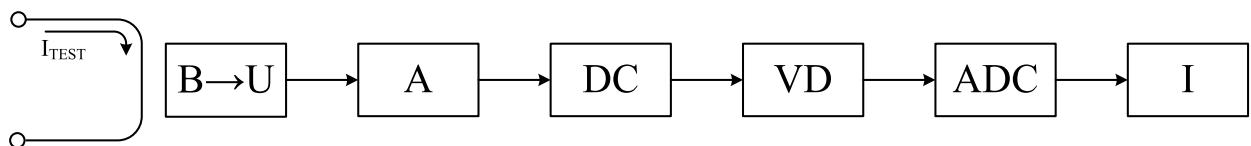


Fig.3. Block schematic diagram of device for contactless measurement of alternating electrical current

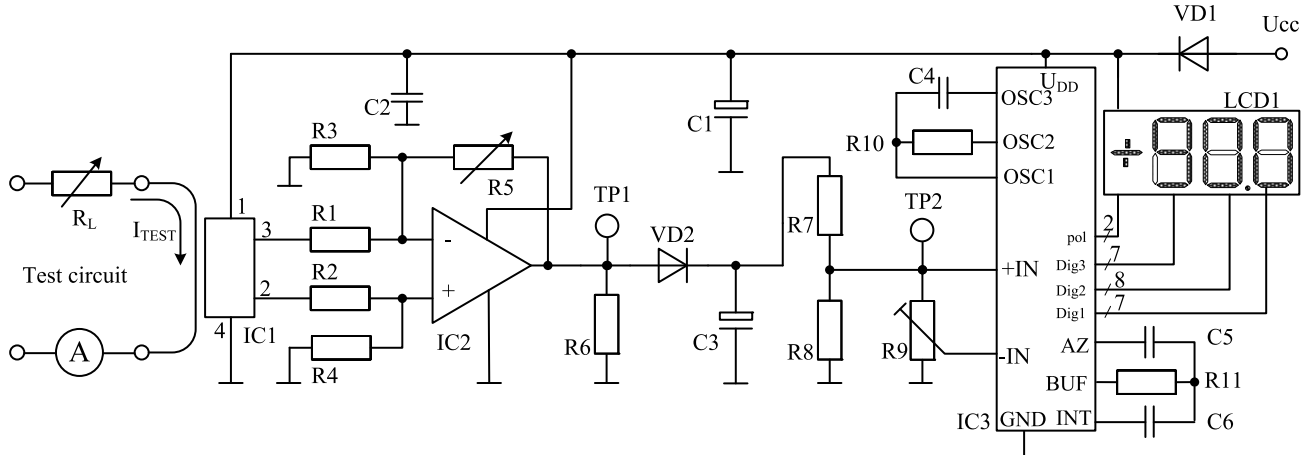


Fig.4. Simplified schematic circuit diagram of a device for contactless alternating current measurement

Block schematic diagram of device for contactless measurement of constant and alternating current is depicted in Fig.3. It is consisted of converter of magnetic field to electrical voltage (B-U). It transforms the generated by electrical current magnetic field. The output converter voltage is proportionately to the measured current value  $I_{TEST}$ . After its amplification by amplifier (A) this voltage is transformed by means of detector circuit (DC) to constant current level. The obtained constant voltage is regulated by a voltage divider (VD) to a suitable for ADC input level after that its magnitude is measured by ADC. A indicator device (I) shows results in amperes.

The schematic circuit diagram of a device for contactless alternating current measurement is depicted in Fig.4.

The transducer IC1 is a magnetosensitive integrated circuit of the type ZMC20M manufactured by Zetex [4] which represent a connected in a parallel bridge four anisotropic magnetoresistors circuit. The amplifier IC2 is constructed on a basis of an operating amplifier connected as a differential amplifier. Its operation modes are tuned by resistors R1-R5. The detector circuit as realized by elements R6, C3 and VD2. Resistors R7 and R8 are used as a voltage divider. The ADC is tuned by alternating resistor R9 and the results are indicated in amperes. ADC is built of a basis of MC7106R (IC3) used in many modern electronic multimeters.

A device printed board is projected so that on one side are placed strong current power and measuring wires while the small current wires are placed on another side.

The measured current conductor must be placed exact under a magnetosensitivi integrated circuit (Fig. 5). So it is guaranted a maximum influence of a generated around a conductor magnetic field to semiconductor chip. The

measuring conductor and sensor arrangement is depicted in Fig.5. The measuring conductor is arranged on another layer towards to the sensor.

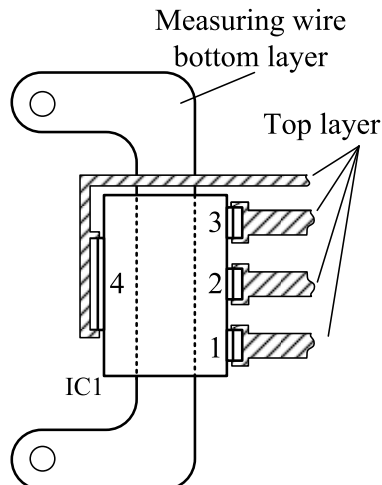


Fig.5. AMR sensor assembling draft

### III. EXPERIMENTS

Experiments are fulfilled. The voltages in special control points TP1 and TP2 are measured. Analog-to-digital converter

reading at a change of a current  $I_{TEST}$  through measuring circuit is registered.

At an experiment accomplishment a water rheostat as a load is used. So a fluent resistance adjustment respectively a current through it is possible.

In Table I are shown a received value of the experimental transducers characteristic. The graphic result of experiments ( $U_{TP1}=f(I_{TEST})$  and  $U_{TP2}=f(I_{TEST})$ ) are depicted in Fig.6. They represent the changes of a voltage at an amplifying block (TP1) output and of a voltage at an ADC input (TP2) as a result of double conversion of measuring current  $I_{TEST}$ .

TABLE I  
EXPERIMENTAL RESULTS

$I_{TEST}, A$	0,248	0,3	0,35	0,4	0,45	0,5
$U_{TP1}, V$	0,0555	0,0674	0,0778	0,0878	0,0959	0,107
$I_{TEST}, A$	0,55	0,6	0,65	0,7	0,75	0,8
$U_{TP1}, V$	0,118	0,128	0,139	0,149	0,157	0,168
$I_{TEST}, A$	0,85	0,9	0,95	1	1,1	1,2
$U_{TP1}, V$	0,178	0,19	0,2	0,21	0,228	0,248
$I_{TEST}, A$	1,3	1,4	1,5	1,6	1,7	1,8
$U_{TP1}, V$	0,269	0,291	0,31	0,33	0,35	0,369
$I_{TEST}, A$	1,9	2	2,5	3	3,5	4
$U_{TP1}, V$	0,389	0,408	0,53	0,632	0,694	0,793
$I_{TEST}, A$	4,5	5	5,5	6	6,5	7
$U_{TP1}, V$	0,888	0,963	1,07	1,16	1,26	1,35
$I_{TEST}, A$	7,5	8	8,5	9	9,5	10
$U_{TP1}, V$	1,42	1,53	1,61	1,71	1,79	1,89
$I_{TEST}, A$	11	12	13	14	15	16
$U_{TP1}, V$	2,05	2,25	2,35	2,49	2,6	2,73
$I_{TEST}, A$	17	18	19	20		
$U_{TP1}, V$	2,81	2,91	2,99	3,14		

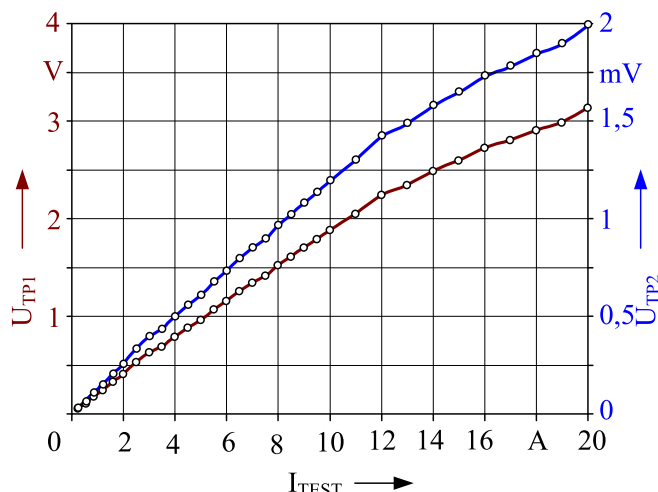


Fig.6. Experimental characteristics  $U_{TP1}=f(I_{TEST})$  and  $U_{TP2}=f(I_{TEST})$

It may be remarked that the both dependences have an similar character, but the voltages have a different change range in relation to the measuring value (from 0,05V to 3,14V for TP1 and from 0,025V to 2V for TP2) at  $I_{TEST} =$

(0,15÷20)A. This difference is artificially made, because of the ADC high input resistance and the possibility to use the whole range of input voltage ( $U_{IFNS} = 0,2 \div 2V$ ).

The characteristic  $I_M = f(I_{TEST})$  is depicted in Fig.7.

The quantity  $I_M$  represents the registered on a created device display testimony of a ADC. The measured current value  $I_{TEST}$  is determined by water rheostat and is obtained by current pliers with inexactness of 2%.

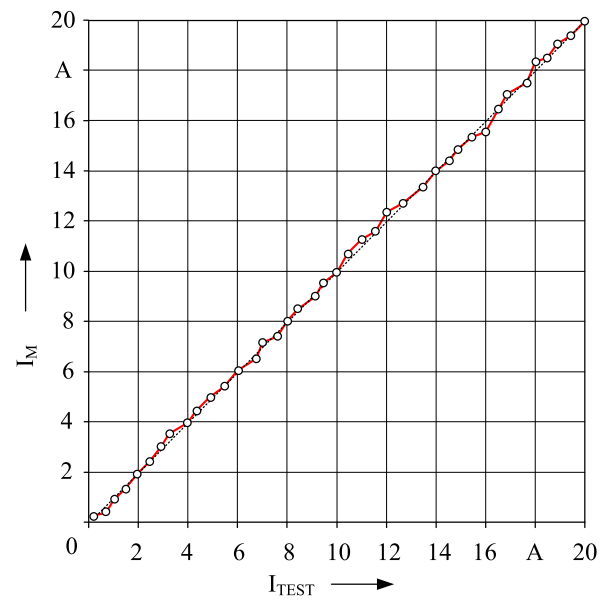


Fig.7. Experimental characteristic  $I_M=f(I_{TEST})$

#### IV. ANALYSES

The obtained results analysis shows that at a measured current  $I_{TEST}$  change in interval from 0,15mA to 20A the reading  $I_M$  of a created device for contactless current measurement is changed linear with minimum deviation towards to the straight line (Fig.7). Maximum deviations are obtained at measured currents 12A, 14A, 18A. They are respectively +250mA at 12A and 18A and -250mA at 14A, which be due to perturb of surroundings.

#### V. CONCLUSION

A device for contactless alternating electrical current measurement on the basis of bridge AMR sensor of type ZMC20M produced by Zetex [4] and of integrated 10 bits analog-to-digital converter of type MC7106R has been created.

The elaborated device operates on the basis of energy double conversions from electrical current into magnetic field and back into electrical voltage.

The device for contactless alternating electrical current measurement is widely applied in industry, instrumentation, motorcar electronics and etc. It can be a useful instrument at high frequency currents measurements in power electronics. By means of minimum changes it can operate as with battery supply and so with local power supply. So it is very suitable

for an assembling in motorcars or for application in a portable measuring instruments.

## REFERENCES

- [1] Draganov, N., T. Draganova. Based of AMR Sensors Device for Multicannal Contactless Measurement of AC Current. Journal of the Technical University of Gabrovo, Vol. 41, Gabrovo, 2011, p. 84-87.
- [2] Karadzhov, Ts., I. Balabanova. Illuminance to Frequency Converter also Used for Conversion of the Ratio between Two Illuminances into a Number of Pulses. Proceedings of papers ICEST-11, Vol. 3, Niš, Serbia, June 29 – July 1, 2011, pp. 903-905.
- [3] Spirov, D. Sensorless Speed and Energy Characteristics Identification of the Induction Machine. Proceedings of papers UNITECH-09, Vol.1, Bulgaria, Gabrovo, 20-21. Nov. 2009
- [4] Zetex application data, [www.zetex.com](http://www.zetex.com), last updated: Dec. 2011

# Design and Signal Processing Techniques on 0.18 $\mu$ m CMOS Hall Microsensors

Tihomir Takov<sup>1</sup>, Ivelina Cholakova<sup>1</sup> and Yavor Georgiev<sup>1</sup>

**Abstract –** This paper presents the design of 0.18 $\mu$ m CMOS Hall plates, characterized with high sensitivity and very low offset and the further signal processing block comprised of main second order switched capacitor filter and anti-aliasing filter. As a result, we developed a method for signal processing, which presents minimal 1/f noise values.

**Keywords –** Hall microsensor, 0.18 $\mu$ m CMOS technology, offset, sensitivity, signal processing, switched capacitor filter.

## I. INTRODUCTION

Most of the magnetic sensors nowadays are used as integrated circuits, because of the opportunity the sensor and the electronic circuit which amplifies the signals to be integrated in one chip.

Hall effect switch sensors have been well established for their great application in many fields. Due to the development of the CMOS techniques and its advantageous characteristics related to cost, high-gain of amplifier and chip size, Hall sensors using CMOS technology has been proposed [1].

Unfortunately, CMOS integrated Hall sensors have suffered from a lot of non-idealities, such as large offset, temperature drifts, low sensitivity, non-linearity and packaging stress influence etc., which severely deteriorates their performance.

The reasons for these drawbacks are geometrical errors in mask alignment, mechanical strain, crystal damage and stress, non-uniform temperature distribution and heat dissipation in the substrate, thermoelectric voltage across Hall leads, non-homogeneities, etc. The problems with offset may come from process variation over the device, temperature gradients across the device in operation, mechanical stress imposed by packaging, etc. Different methods for offset compensation are known, as improvement of the manufacturing technologies, device symmetry, calibration, mutual compensation, trimming, spinning current offset reduction, etc [1] and [2].

Continuous time sensors are the most basic of the Hall effect sensors. Their architecture contains just a voltage regulator, the Hall transducer, an amplifier and a comparator with an output stage [3]. One of its major disadvantages is the big input offset voltage of the amplifier which in CMOS fabrication processes may have typical values of 1mV to 20mV multiple times larger than signal generated by the Hall transducer for usual magnetic fields values (1...20mT) which is smaller than 1mV. Common technique to reduce this offset voltage is to use a chopper stabilized amplifier which may

<sup>1</sup>Tihomir Takov, Ivelina Cholakova and Yavor Georgiev are with the Faculty of Electronic Engineering and Technologies at Technical University of Sofia, 8 Kl. Ohridski Blvd, Sofia 1000, Bulgaria, E-mail: inch@ecad.tu-sofia.bg.

have input offset voltages in the field of 100 $\mu$ V and less. In this technique the amplifier modulates the input offset at a high frequency and then it has been removed using a low-pass filter. Another benefit is that when modulating the Hall transducer signal into the high frequencies, we are minimizing the noise. Chopper stabilization and the design of chopper stabilized switched capacitor amplifiers are presented in detail in [3] and [4].

In this paper we focus on the design of the subsequent filter stage and the necessary supplementary circuit blocks – switch control generation circuitry and anti-aliasing filter on a modern 0.18 $\mu$ m CMOS fabrication process.

## II. SENSOR LAYOUT AND OFFSET COMPENSATION METHOD

The investigated Hall sensors were designed on 0.18 $\mu$ m CMOS technology. The designed sample is a thin plate of conducting material (pSi) with four electrical contacts at its periphery. A bias current (or voltage) is applied to the device through two of the contacts, called the current contacts (C<sub>1</sub> and C<sub>2</sub>). The other two contacts are placed at two equipotential points at the plate boundary and are called the voltage contacts or the sense contacts. If a magnetic field is applied to the device, a voltage appears between the sense contacts, called the Hall voltage.

The Hall device is with the form of a square plate and is with microscopic dimensions (40x40 $\mu$ m). A bias voltage V<sub>DD</sub> is applied to the plate through the two current contacts C<sub>1</sub> and C<sub>2</sub>. The bias voltage creates an electric field E and forces a current I. If the plate is exposed to a perpendicular magnetic induction  $\mathbf{B}$ , the Hall electric field E<sub>H</sub> occurs in the plate. The Hall electric field gives rise to the appearance of the Hall voltage V<sub>H</sub> between the two sense contacts H<sub>1</sub> and H<sub>2</sub>. The designed and investigated sensor's layout is illustrated on Fig. 1.

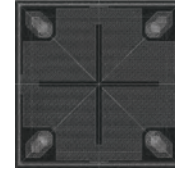


Fig. 1. Hall Plate Layout

The Hall microsensors were manufactured in a standard planar technology on p-Si wafers, with substrate resistivity 0,01  $\Omega$ cm and crystallographic direction (100). The heavy doped n+ and p+ regions are with depth of 35nm and STI (shallow trench isolation, which is used) depth is 400nm. The microdevices are confined in N-well, which serves as an active sensor zone with depth of 1.5 $\mu$ m.

In order the offset to be compensated, a four-phase spinning method was used which involves a combination of reversing source voltage polarity and the input and output terminals, which is explained in details in [5]. Due to the fact that the Hall structure is symmetric with rotation, this technique leaves the output Hall voltage  $V_H$  unchanged in value and sign. During the terminals' rotation, this results in polarity reversion of the offset voltage.

### III. SIGNAL PROCESSING

In accordance with the amplifier and subsequent comparator which both are often realized in switched capacitor manner, our filter will be also realized using switched capacitor design techniques. We have chosen elliptic approximation because of its optimally fast pass band to stop band transitions for a given maximum attenuation variation (ripple) and optimal group delay.

The filter specification is given in Table 1.

TABLE I  
FILTER SPECIFICATION

Cut-off frequency: fc	$15\text{kHz} \geq 6 \text{ dB/oct}$
Transition band slope: fs	$166.7 \text{ kHz}$
Stopband attenuation: As	$\geq 20 \text{ dB}$
Attenuation on the odd harmonics of fs	$\geq 40 \text{ dB}$
Maximum ripple - $\epsilon$	$\leq 0.5 \text{ dB}$
Step response overshoot	$\leq 5\%$
Group delay	$\leq 12 \mu\text{s typ.}$
Sampling frequency - fCLK	$1.33 \text{ MHz}$
Gain	5
Supply voltage range	$3\text{V} \pm 10\%$
Temperature range	$-40^\circ\text{C} \div 135^\circ\text{C}$

The stop band frequency is the same as the frequency of the modulated input signal. Step response overshoot should be less than 5% of the median value because of the subsequent comparator circuit. The sampling frequency was chosen 8 times the stop band frequency.

Our design is second order low pass elliptic switched capacitor filter, where the switches have the configuration from Fig.2.

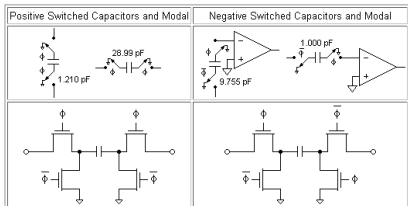


Fig. 2. Switch configurations

Its transfer function in the s-plane is:

$$H(s) = \frac{R_{1,4}C_{1,2}R_{1,7}C_{1,3}R_{1,1}R_{1,6}s^2 - R_{1,4}R_{1,7}}{-R_{1,4}R_{1,7}C_{1,3}R_{1,1}R_{1,6}C_{1,5}s^2 - R_{1,7}C_{1,3}R_{1,1}R_{1,6}s + R_{1,4}R_{1,1}} \quad (1)$$

$$\text{where } R_{1,i} = \frac{1}{C_{1,i}f_{CLK}} \quad (2)$$

The next step in the design of switched capacitor circuits is to choose switch topology and to verify its parameters. For this design we used 3.3V low power NMOS and PMOS devices available as part of the 0.18μm CMOS fabrication process. In order to minimize charge injection and complexity we have chosen the transmission gate as switch topology.

The other vital size dependable parameters of the switches are the charge clock feed through, which increases with W/L ratio, the on resistance which decreases with W/L ratio, the thermal noise which increases with the increase of the on resistance.

In order to obtain good balance between all these parameters and acceptable topological area, in the sizing process, the transmission gate was verified across supply voltage margins (2.7, 3.0, 3.3V), temperature margins (-40°C, 27°C, 125°C). Based on the worst case scenario, where  $R_{ON}$  of the switch should not exceed 5% of the minimal switched capacitor equivalent resistance in the design (because in "on state" it is in series with the equivalent resistance) and its calculated value, using (2) is  $1.5\text{M}\Omega$ .

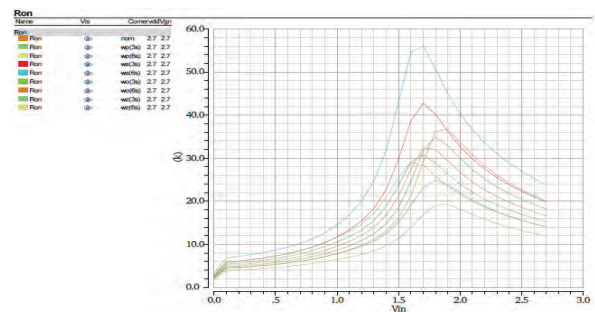


Fig. 3. Corner analyses of the transmission gate

$$\text{We have chosen } \frac{w_N}{w_P} = \frac{w_P}{L_P} = \frac{0.4}{0.35} \mu\text{m}.$$

As operational amplifier in the design of the filter, we used single stage amplifier with gain boosting stages and switched capacitor common-mode feedback, provided in the design kit for the given technology process. It is characterized by DC gain of 100 dB and gain bandwidth of 30MHz which were sufficient according to the rule of the thumb that the GBW should be 5 to 10 times the sampling frequency  $f_{CLK}$ .

In order to eliminate first order mismatch effects the capacitors were formed so that the ratio between their area and perimeter is kept constant. Capacitor dimensions and predicted mismatch are given in Table 2.

TABLE II  
CAPACITOR DIMENSIONS AND MISMATCH

Label	Value [fF]	Area [ $\mu\text{m}^2$ ]	Perimeter [ $\mu\text{m}$ ]	Mismatch [%]
C1.1	500	588.24p	130	0.056
C1.2	108.32	127.44p	28.16	0.12
C1.3	787.59	926.58p	204.78	0.044

C1.4	178.88	210.44p	46.51	0.093
C1.5	787.59	926.58p	204.78	0.044
C1.6	100	117.65p	26	0.125
C1.7	100	117.65p	26	0.125

The mismatch values were calculated based on the process specification according to (4).

$$\sigma(\frac{\Delta C}{C}) = \frac{X}{\sqrt{A}} [\%] \quad (3)$$

where  $X \approx 1.30 \text{ \%}/\mu\text{m}$ .

The filter schematic (Fig. 4) was verified with periodic analyses available in Cadence® Virtuoso® Spectre® circuit simulator – Periodic Steady State (PSS), Periodic AC (PAC) and transient analysis.

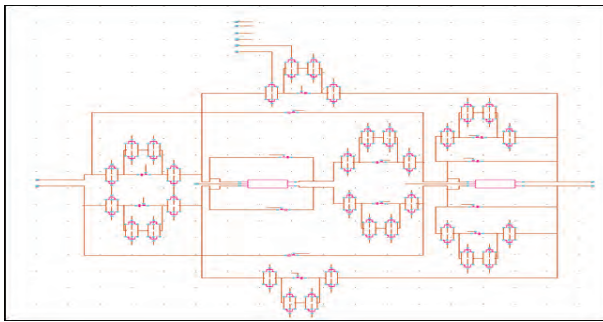


Fig. 4. Filter schematic in Cadence® Virtuoso®

As required by the Nyquist–Shannon sampling theorem we need one additional low-pass filter before the main switched capacitor filter to reduce the signal aliasing to minimum. According to the theorem the cut-off frequency of this filter should be calculated using (4).

$$f_{-3dB} = \frac{f_{CLK}}{2} \quad (4)$$

But the optimum solution for our design (Attenuation on 1.33 MHz = -20 dB and group delay  $\tau \leq 1\mu\text{s}$ ) is shown in (5).

$$f_{-3dB} = \frac{f_{CLK}}{10} = 133\text{kHz} \quad (5)$$

The filter topology of choice will be first order passive low-pass filter with the well known transfer function, shown in (6).

$$f_c = \frac{1}{2\pi RC} \quad (6)$$

And group delay is equal to (7).

$$\tau(f_c) = \frac{1}{2\pi f C} = RC \quad (7)$$

The 133 kHz cut-off frequency is possible with  $R = 1\text{M}\Omega$  и  $C = 1.2 \text{ pF}$  but when taking into account the fully differential nature of our design we can halve the value of one of the elements. Because the resistors are two and their area is technologically larger than the capacitor area it is logical to choose to use  $R = 500\text{k}\Omega$ .

When taking into consideration the load of the filter which is actually the input impedance of the main switched capacitor filter –  $R1.E = 1.5\text{M}\Omega$  and  $C1.2 = 100\text{fF}$  connected to the virtual grounds of the amplifiers, we have that in order to meet our specification for  $f_{-3dB}$  we need to use  $R = 330\text{k}\Omega$ .

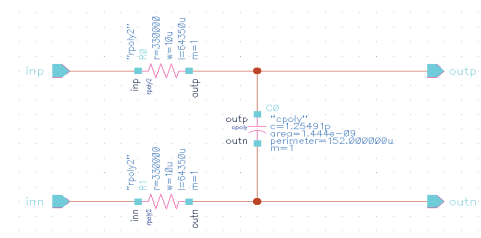


Fig. 5. Anti-aliasing filter schematic in Cadence® Virtuoso®

After optimization and for smaller process variations the capacitor was chosen with area of  $38\mu\text{m}$  by  $38\mu\text{m}$  and capacitance  $C = 1.25 \text{ pF}$ .

#### IV. EXPERIMENTAL RESULTS

The structure from Fig. 1 was tested at six supply voltages (0.5, 1.0, 1.5, 2.0, 2.5, 3.0V) and three constant currents (100, 200 and 300 $\mu\text{A}$ ). Also the magnetic measurements involve generation of a perpendicular magnetic field which value is  $\pm 8\text{mT}$ . All measurements were taken at room temperature (25°C).

The first experimental results for the residual offset are shown in Fig. 6a) at  $V_{DD}$  and in Fig. 6b) at  $I_{DD}$ .

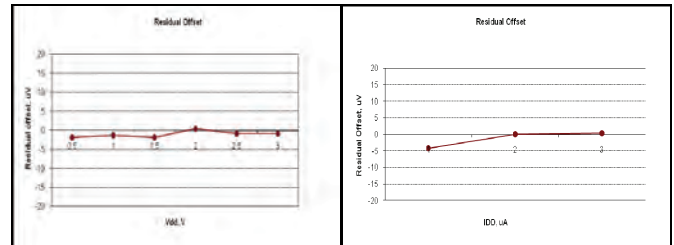


Fig. 6. Residual Offset as a Function of  $V_{DD}$  (a)) and as a function of  $I_{DD}$  (b))

At supply voltage the highest offset value is  $1.42\mu\text{V}$  and at constant current supply is  $2.41\mu\text{V}$  which are excellent results for such type magnetic sensors at this technology. They are specified to be under  $10\mu\text{V}$  and they are much smaller than this value taking into consideration that the output signal is about mV. There is no need to use compensation offset circuits which complicate the design.

Next, the voltage and current related sensitivities were investigated. The maximum achieved voltage related sensitivity is  $0.1\text{T}^{-1}$ , and the current related sensitivity is  $170\text{V/AT}$ . For example, typical value for the voltage related sensitivity is 0.5 to  $0.8\text{T}^{-1}$ . We achieved really high sensitivity in this technology which is a great advantage for our sensor. Typical value for  $S_I$  is from 85 to  $250\text{V/AT}$ , but it depends on the size of the sensor and the supply constant current.

Next, the simulations were made in order to prove the performance of the designed filters, which will be part of the sensor integrated circuit. First frequency response, step and transient response of the second order low pass elliptic switched capacitor filter were given in Fig. 7, Fig. 8 and Fig. 9 respectively.

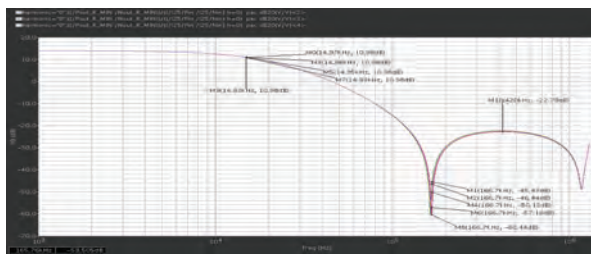


Fig. 7 Frequency response of the filter – PAC corner analyses

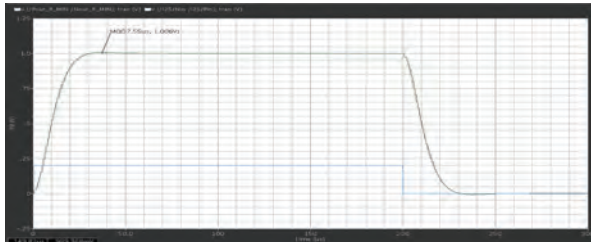


Fig. 8 Step response of the filter

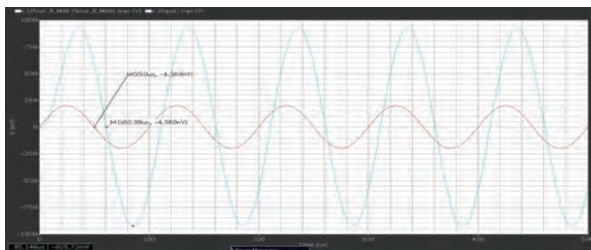


Fig. 9 Transient response of the filter for group delay verification typical conditions (27°C, VDD = 3V)

The switch control clock generation circuit have been developed prior the design of the main switched capacitor filter so that the later be verified with real control signals for the switches.

Next the anti-aliasing filter was simulated to see the frequency response for verification of the cut-off frequency (Fig. 10).

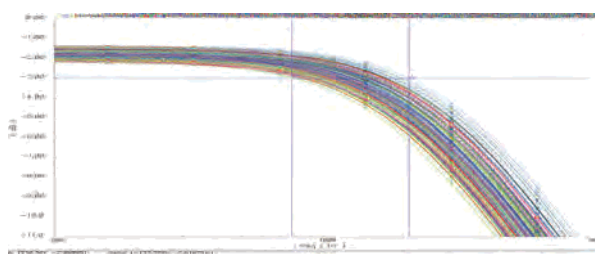


Fig. 10 Frequency response of the AA filter for verification of the cut-off frequency

As seen from the above figure process and temperature variations have significant impact on the value of the cut-off frequency:

$$f_{C\text{ideal}} = 133.333 \text{ kHz}$$

$f_{C\text{min}} = 77.001 \text{ kHz} \approx -42\% \text{ of the ideal value}$

$f_{C\text{max}} = 210.360 \text{ kHz} \approx +58\% \text{ of the ideal value}$

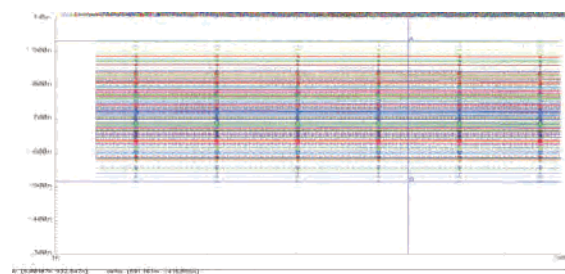


Fig. 11 Transient response of the AA filter for verification of the group delay

$$\tau_{\text{ideal}} \approx 705 \text{ ns}$$

$$\tau_{\text{min}} \approx 516 \text{ ns} \approx -27\% \text{ of the ideal value}$$

$$\tau_{\text{max}} \approx 933 \text{ ns} \approx +33\% \text{ of the ideal value}$$

The impact of the temperature and process variations is clearly seen in the group delay values as well but nevertheless the obtained values are well tolerable for the design margins.

## V. CONCLUSION

In this paper microscopic Hall structure was designed and characterized, achieving highly sensitive sensor which have wide range of practical applications. We presented a method for signal processing in integrated CMOS Hall effect sensors, which greatly diminished sources of errors like amplifiers input offset voltage and the low frequency 1/f noise.

We have shown the design of several practical signal processing blocks: main low pass switched capacitor filter and anti-aliasing filter. Furthermore all of these blocks were designed and verified for 0.18 μm CMOS fabrication process, so in effect this paper also shows the main characteristics and possibilities offered by this process for integrated Hall effect sensors.

## ACKNOWLEDGEMENT

This work is funded with support from the Contract no. 122PD0060-03.

## REFERENCES

- [1] S. Lozanova, Ch. Roumenin, "A novel parallel-field double – Hall microsensor with self-reduced offset and temperature drift", Science Direct, Procedia Engineering 5, 2012, pp. 617-620.
- [2] Ed Ramsden, Hall Effect Sensors Theory & Application, Advanstar Communications Inc, 2001.
- [3] Ionescu M., Bogdan D., Danchiv A., Bodea M., "Signal processing for integrated Hall effect sensors using switched capacitor circuits", Sci. Bull., Ser. C, Vol. 73, Iss. 4, 2011.
- [4] Enz, C. and Temes G., "Circuit Techniques for Reducing the Effects of OP-Amp Imperfections: Autozeroing, Correlated Double Sampling, and Chopper Stabilization", IEEE 1996
- [5] Cholakova I., Takov T., Tsankov R., Simonne N., "Temperature Influence on Hall Effect Sensors Characteristics", IEEE 20<sup>th</sup> TELFOR 2012, Republic of Serbia, Belgrade, pp. 967-970.

# Investigation of the Defects Formation in Flexible Organic Light Emitting Devices by Thermal Activated Currents

Mariya Aleksandrova<sup>1</sup>

**Abstract** – Electrical behaviour of flexible light emitting devices at different temperatures was investigated. Organic electroluminescent layers were produced by different deposition methods – thermal evaporation in vacuum and spray coating. Thermally activated currents of the structures were measured in the range from 0 to 70 °C and the defect's origin, and activation energy were determined and compared for both cases. It was established that the thermal activated current for thermal evaporated films was higher (~900 nA) than for spray deposited (~430 nA) and consists of several distinctive peaks. Therefore higher defect density, embracing broad energy spectrum are typically revealed for the evaporation process and can be ascribed to structural films deformations. Just the opposite for the pulverization process there is only slight change in the current-temperature characteristic (~1nA/°C), which is evidence for lack of structural deep traps and presence of impurity defects or shallow traps.

**Keywords** – Organic light emitting devices, Thin films, Defects investigation, Thermal activated current.

## I. INTRODUCTION

Organic materials used in light emitting devices serve as electroluminescent, hole transport or electron transport layers (HTL or ETL) [1,2]. These materials are either low molecular weight (small crystalline) or high molecular weight (polymeric) compounds [3]. Normally the first type is more widely spread, because of their higher quantum efficiency and they are deposited as thin films by thermal evaporation in vacuum [4]. For the needs of flexible organic light emitting displays (OLED), the high temperature deposition process must be replaced by lower temperature coating, like spin coating or spray deposition for example [5]. However, problems with the solubility in this class of organic semiconductors still exist, so mixture of different solvents have to be used for obtaining of homogenous solution and high quality films. Independently of the deposition method different varieties of defects are induced in the layers, like lattice imperfections, impurities or irregularities [6]. They affect on the charge carriers motion and prevent some of the main processes in the device like conduction and radiative recombination, therefore on the quantum efficiency. Defects concentration and energy distribution can be influenced and minimized by precise tuning of the deposition process and modes.

<sup>1</sup>Mariya Aleksandrova is with the Faculty of Electronic Engineering and Technologies, Department of Microelectronics at Technical University of Sofia, 8 Kl. Ohridski Blvd, Sofia 1000, Bulgaria, E-mail: m\_aleksandrova@tu-sofia.bg.

Several techniques for defects parameters determinations are developed. Some of the more popular are thermally stimulated luminescence (TSL)[7], photo induced absorption (PIA) [8], etc. TSL is popular and usually applied method for luminescent materials, working on the emissive recombination principle, but in one OLED, there are HTL and ETL too. Another disadvantage is the difficulty in differentiation of electron traps and hole traps. This is the reason another quantitative measure to be chosen, like thermally activated current. Linear temperature activation (LTA) would cause simultaneously escaping of the whole entrapped charges without distinguishing of the specific energetic levels of the traps, releasing this charge. However, filling the traps at temperatures lower than the room temperature, followed by their controllable releasing with cycles of step increase of the applied thermal energy will lead to precise determination of the traps parameters.

In this paper modification of the method with thermally activation of charges (TAC) is developed and applied for investigation of defects in layers for flexible OLEDs. Low molecular weight compounds are deposited as thin films by vacuum thermal evaporation and spray deposition, and both layers are investigated for traps formation, defect density and energy distribution. It is proven that the spray deposited layers show lower thermally activated current and narrow spectrum of traps energies, which means that the pulverized structure is defect less and more favorable for high efficiently luminescent devices. By the author's knowledge this approach is still not applied for traps investigation in flexible OLED structures with sprayed layers.

## II. METHODS AND MATERIALS

### A. Theoretical Background of TAC Principle

By cooling the organic material to temperatures  $T_0$  lower than the room temperature  $T_r$ , the charge carriers in the small molecules take place on the lowest unoccupied energy levels, which are their initial, stable states and there are no free charges in the gap even at supplied electrical field equal to the turn on voltage. At elevation of the temperature with a certain step of increasing charge carriers hop to the next unoccupied level and this moving can be detected by measuring of like very small current in the nano-ampere range. The current-temperature curve contains peaks, which mean activation and escape of charges at many different energy levels situated between the occupied and the unoccupied molecular levels of the organic molecules. These levels are traps for the useful charges and they are caused by structural defects formation or

introduction of impurities. They are energetically favorable states, so if the temperature is not further elevated the supplied electrical field would be not enough to cause charge releasing, so the conductivity in the device would be lower than the expected. If we can provide information about the density of states in the film and about their energy of activation we can optimize the deposition conditions in a way to minimize traps present. However, it must be taken into account that after heating of the material the relaxation time as a function of the temperature decreases and thermal motion of polarons is induced. It is responsible for the continuity of the current curves instead consisting of only discrete levels, corresponding to the traps activation energies. Fig. 1 illustrates the principle of thermally activated current measurement and its connection with the electrophysical properties of the organic layer.

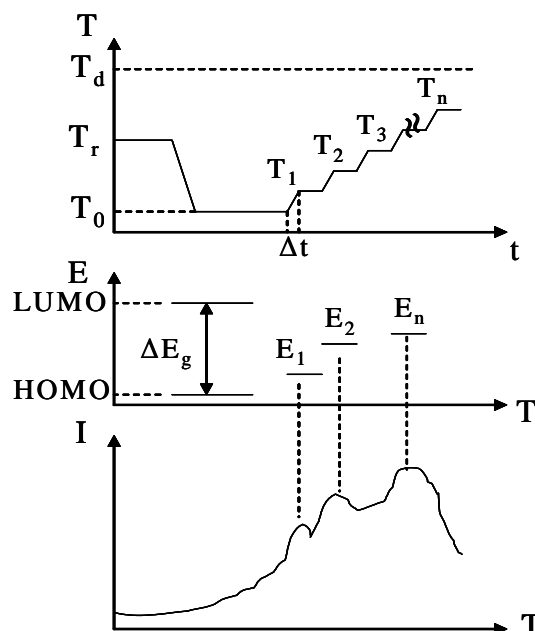


Fig. 1. Principle of thermally activated current measurement:  $T_d$  – temperature of organic material degradation or maximal temperature;  $T_1, \dots, T_n$  – temperatures, scanning the band gap for traps activation; HOMO – highest occupied molecular orbital; LUMO – lowest unoccupied molecular orbital;  $\Delta t$  – rate of temperature increase;  $\Delta E_g$  – energy band gap of the organic semiconductor;  $E_1, \dots, E_n$  – energies of the induced traps, activated at temperatures from the range  $T_1, \dots, T_n$ .

Eq. (1) shows in general form the connection between the current, formed by thermally activation of the charge carriers, energy of activation of the traps and the applied temperature [9].

$$I(T) \approx \exp\left(-\frac{E}{kT}\right) \exp\left(-\frac{B}{\beta} \int_{T_0}^{T_d} \exp\left[-\frac{E}{kT}\right] dT\right) \quad (1)$$

where  $E$  is activation energy;  $T$  – temperature,  $k$  - Boltzman's constant;  $B$  – heat capacity of the material;  $\beta$  – heating rate that the equipment can ensure;  $T_0$  – initial low temperature. According to the initial rise method [10] the integral term in Eq. (1) is low for  $T < T_{max}$  so the first exponent is predominant for the initial part of the TAC curve, where  $T_{max}$  is the

temperature where the current peak is situated. Then the current can be expressed only by the Arrhenius like equation. Activation energy can be determined by the rising slope of the current peaks (Eq.(2)).

$$E = \frac{kT_{max}}{\beta \Delta t} \quad (2)$$

### B. Samples Preparation

On PET substrate, ITO film with thickness of 148 nm was deposited by low-temperature reactive RF sputtering. The deposition conditions are oxygen partial pressure  $2.10^{-4}$  Torr, total gas pressure in the vacuum chamber after sputtering gas (argon) bleeding is  $2.5.10^{-2}$  Torr, sputtering power varies between 75 W and 105 W with rate 0.5 W/s during deposition of the initial ITO monolayer. Sheet resistance reaches 19.2  $\Omega/\text{sq}$ . after 10 minutes of ITO treatment with UV light (UV 365 nm, source power 250 W). The basic structure of the OLED devices is single layer, containing light emitting layer of tris(8-hydroxyquinolinato)aluminium (Alq3; Sigma-Aldrich). It was situated between transparent ITO anode and nickel vacuum sputtered cathode. The organic dust was dissolved in solvent mixture from chloroform and methylethylketon heated to 40°C. Solution was stirred for several hours until fully dissolving was observed. For good adhesion of the Alq3 layer to the smooth surface of PET/ITO, additionally polymer polystyrene was added. For spraying, atomizer with nozzle having regulating orifice up to 200  $\mu\text{m}$  was used. The established optimal deposition conditions regarding layer uniformity was as follows: substrate temperature 70°C; distance nozzle-substrate 15 cm; pulverizing pressure 4 bars; solution concentration 5 mg/ml. Alternative structure with thermal evaporated Alq3. The thickness of the organic layer in both types of OLED structures is the same – 139 nm. The current was measured by a Keithley 6485 picoammeter with resolution 1 fA at special conditions, concerning electromagnetic guards and shields of the measurement circuit and thermal insulation of the chamber, where the Peltier element and the sample are situated. The temperature was measured by a temperature sensor with accuracy of 0.01°C.

## III. RESULTS AND DISCUSSION

### A. Technical Realization of the TAC Method

In A Peltier thermoelectric device is the main element in the specially designed apparatus for investigation of traps activation. This element works as cooler and heater, and switches over the two modes to reach temperatures in the interval 0–70°C. A block diagram of the setup is presented in Fig. 2. The heat is generated from pulse voltage, and it is transferred in portions to the sample with a narrow steps. The traps were filled after cooling the sample by applying forward turn-on voltage to the leads. The cooling cycle was followed by heating, and the shallowest filled traps determine the initial rise of the formed current flow. However, if the previous

heating to specific temperature has already released these shallow states, the initial rise in the next temperature interval will be conditioned by the traps from the next, deeper energy levels. The current value for each cooling-heating step was measured from the released charge carriers and consequently used for the trap concentration at certain energy. Peltier element PE-127-10-25 with maximum current 2 A was situated between two heat comb sinks for higher thermoconductivity. Additionally, the contacted surfaces were smeared with thermocontact paste to decrease thermal resistance. The heat sinks were enveloped with a thermoinsulating chamber, which closes a small bulk of air above the sample and thus eliminates heat (or cold)

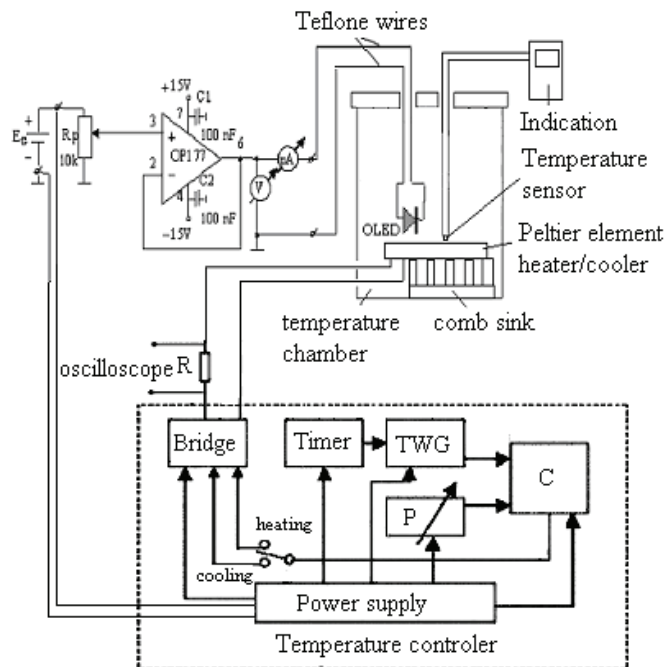


Fig. 2. Block diagram of the test circuit for thermally activated current measurement; TWG - triangle wave generator; P - potentiometer; C - comparator

dissipation into the surroundings.

The driving voltage was impulse and the rate of temperature change depends on its duty cycle, which is determined by a multi-turn potentiometer. The accuracy of establishment of the temperatures was  $0.03^{\circ}\text{C}$ , which allows scanning of energies in the band gap with resolution of  $\mu\text{eV}$ . Thus, precisely distinguishing even traps with close energy levels was possible. The rate of the temperature change was  $2^{\circ}\text{C}/\text{min}$ , providing abrupt heating/cooling and short time of the transient process.

Technically it is possible to be realized lower temperatures and steeper temperature fronts but it will cause condense from the big temperature difference and thermal stress. Besides, even at positive temperatures the conductivity abruptly decreases, because the organic materials are wideband gap semiconductors. It is not necessary faster temperature change, because the time for settle of the new state for the organic molecules is approximately comparable with the provided from this equipment.

#### B. Measured TAC for Thermal Evaporated and Spray Deposited Flexible OLED Structures

The samples, consisting of sprayed and thermal evaporated organic layers exhibit different thermal behavior, which can be detected by the TAC curves (Fig. 3).

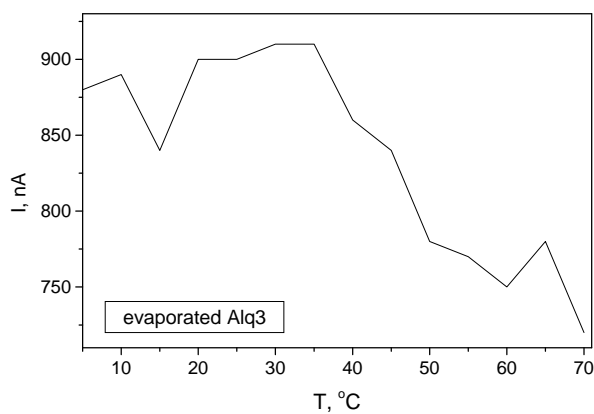
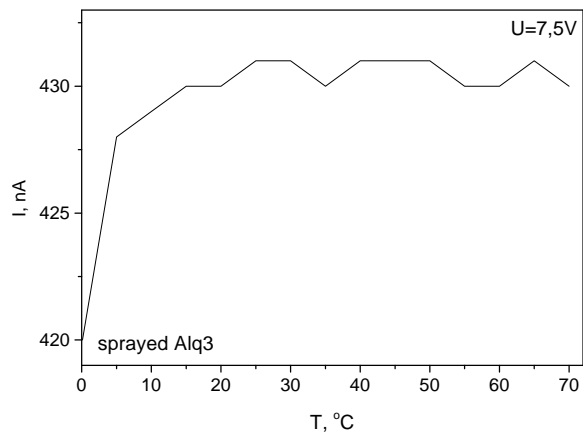


Fig. 3. TAC curves as a function of the applied temperature for spray deposited (up) and thermal evaporated (down) flexible OLED samples

For the thermal evaporated samples, the TAC is higher ( $\sim 900 \text{ nA}$ ), which is indication for higher defect density, releasing bigger amount of charge carriers in the structure. The great numbers of abrupt peaks, closely situated in the curve are evidence for presence of defects having wide spread energies of activation. Their occurrence in the high temperature supplied range (above  $42^{\circ}\text{C}$ ) shows “deep” traps formation lying close to the higher occupied molecular orbital or structural defects (not impurities). Based on previous observations [11] there is a reason to accept that the structural defects are caused by partially thermal degradation of the chemical bonds during thermal evaporation. The activation energies in this case are: 4.3 meV ( $10^{\circ}\text{C}$ ); 7.74 meV ( $18^{\circ}\text{C}$ ); 12.04 ( $28^{\circ}\text{C}$ ); 15.48 ( $36^{\circ}\text{C}$ ); 18.92 ( $44^{\circ}\text{C}$ ); 37.95 ( $65^{\circ}\text{C}$ ).

The relatively small TAC current for the pulverized layers ( $430 \text{ nA}$ ) is evidence for the low defect concentration and its almost permanent value at different temperature – for narrow

traps energy spectrum or four single (discrete) defect states. In this case, the origin of the defects can be ascribed as individual impurities incorporated in the layer, probably due to the lack of vacuum environment during pulverization. They cause “shallow traps” formation lying close to the lower unoccupied molecular orbital and easy activated even around room temperature (like for example at 16 °C and 27 °C). The activation energies of these discrete levels calculated according to the Eq. (2) are as follows: 6.88 meV (16°C); 10.32 meV (24°C); 17.63 meV (41°C); 27.95 meV (65 °C). The dependences of the activation energy on the temperature for both technologies of organic films deposition are shown on fig. 4.

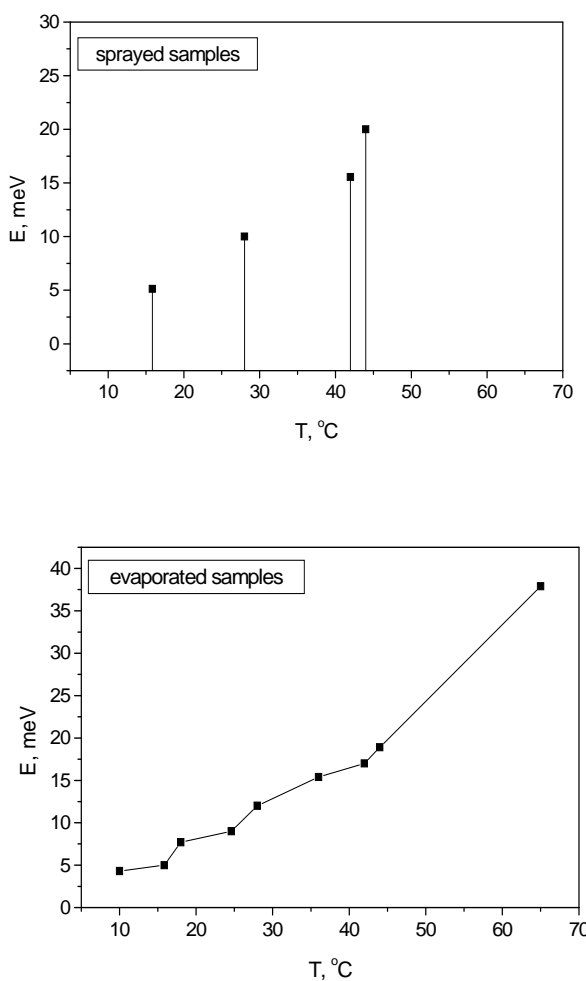


Fig. 4. Activation energy of the traps as a function of the applied temperature for spray deposited (up) and thermal evaporated (down) flexible OLED samples

#### IV. CONCLUSIONS

TAC is a very sensitive probe for internal organic structure investigation. Especially designed for the experiment home made equipment for supplying of heating and cooling in wide temperature range, allows scanning of the energy levels in the

organic semiconductor with μeV resolution. The current data illustrate that the spray technology is more suitable for deposition of organic layers in flexible OLED fabrication, because it is able to produce almost defect less structures. This leads to less captured charges, which can fluently contribute to the conduction process and light emission generation.

#### ACKNOWLEDGEMENT

The work is financial supported by grant DMY 03/5 – 2011 of Fund “Scientific Research”, Bulgarian Ministry of Education, Youth and Science. The author is thankful to Assoc. Prof. Nikola Nikolov and Assoc. Prof. Ivaylo Pandiev for the help during measurement equipment’s design and set.

#### REFERENCES

- [1] S. H. Hwang, Y. K. Kim, Y. Kwak, Ch. Lee, J. Lee and S. Kim, “Improved performance of organic light-emitting diodes using advanced hole-transporting materials”, *Synth. Met.*, vol. 159, no. 23–24, pp. 2578-2583, 2009.
- [2] J.H. Lee, P. Wang, H. D. Park, C. Wu and J. J. Kim, “A high performance inverted organic light emitting diode using an electron transporting material with low energy barrier for electron injection”, *Org. Electron.*, vol. 12, no. 11, pp. 1763-1767, 2011.
- [3] W. Junfeng, J. Yadong, Y. Yajie, Y. Junsheng and X. Jianhua, “Self-Assembled of Conducting Polymeric Nanoparticles and its Application for OLED Hole Injection Layer”, *Energy Procedia*, vol 12, pp. 609-614, 2011.
- [4] M.M. El-Nahass, A.M. Farid and A.A. Atta, “Structural and optical properties of Tris(8-hydroxyquinoline) aluminum (III) (Alq3) thermal evaporated thin films”, *J. Alloy Compd.*, vol. 507, no. 1, pp. 112-119, 2010.
- [5] J. Lin, L. Qian and H. Xiong, “Relationship between deposition properties and operating parameters for droplet onto surface in the atomization impinging spray”, *Powder Technol.*, vol. 191, no. 3, pp. 340-348, 2009.
- [6] P. E. Burrows, V. Bulovic, S. R. Forrest, L.S. Sapochak, D. M. McCarty and M. E. Thompson, “Reliability and degradation of organic light emitting devices”, *Appl. Phys. Lett.*, vol. 65, no. 23, pp. 2922-2924, 1994.
- [7] M. Martini and F. Meinardi, “Thermally stimulated luminescence: New perspectives in the study of defects in solids”, *Riv Nuovo Cimento*, vol. 20, no. 8, pp 1-71, 1997.
- [8] R. A. J. Janssen, N. S. Sariciftci and A. J. Heeger, “Photoinduced absorption of conjugated polymer/C60 solutions: Evidence of triplet-state photoexcitations and triplet-energy transfer in poly(3-alkylthiophene)”, *J. Chem. Phys.*, vol. 100 no. 12, pp. 8641-8645, 1994.
- [9] E. R. Neagu, J. N. Marat-Mendes, D. K. Das-Gupta, R. M. Neagu and R. Igreja, “Analysis of the thermally stimulated discharge current around glass-rubber transition temperature in PET”, *J. Appl. Phys.*, vol. 82, no. 5, pp. 2488–2496, 1997.
- [10] T. S. C. Singh, P. S. Mazumdar and R. K. Gartia, “On the determination of activation energy in thermoluminescence by the initial rise method”, *J. Phys. D: Appl. Phys.*, vol. 21, 1312, 1988.
- [11] M. Aleksandrova, “Influence of the Operating Temperature on the Organic Flexible Display’s Performance for Mobile Applications”, *TELFOR’12*, Conference Proceedings, pp. 20-22, Belgrade, Serbia, 2012.

# Incremental Encoder Macromodel for Educational Purpose

Marieta Kovacheva<sup>1</sup> and Peter Yakimov<sup>2</sup>

**Abstract –** In this paper a macromodel of incremental rotary encoder is described. The basic characteristics and the behaviour of the encoders are studied. A digital electronic circuit generating the output signals of the incremental encoder and simulating its operation is designed. Results of the macromodel simulations are given.

**Keywords –** Rotary incremental encoder, Macromodelling, Digital circuits design, Simulation.

## I. INTRODUCTION

In the past decade, the simulation has taken on an increasingly important role within electronic circuit design. The most popular simulation tool for this is PSpice A/D, which is available in multiple forms for various computer platforms. However, to achieve meaningful simulation results, designers need accurate models of many system components.

Simulation and modelling are investigations approaches which take place in different fields of scientific and applications developments [4, 5]. First the behaviour of a circuit or module is simulated and the parameters are adjusted and then they are verified by investigation over real object.

Harsh industrial applications often expose plant equipment to caustic chemical materials, resulting in premature deterioration and failure. Complex systems control requires complete cover of the behaviour of every industrial object and process in all working regimes. This could be achieved using the possibilities of the simulation and modelling. These methods have wide application in industry areas like electric power production, chemical manufacture, machine building and etc. where interruption and accident regimes creation in order to adjust the control equipment are impermissible.

The use of motion transducers has become commonplace and increasingly important to motion control systems designers in all sectors of manufacturing industries. As rapid advances in size, accuracy, resolution, and application sensitive mechanical packaging develops, close loop systems become more attractive to design engineers. The broad range of devices that are currently available can offer design engineers multiple solutions to their motion control needs.

Encoders enable design engineers to control motion by providing reliable feedback within the process loop. Optical rotary encoders are the most widely used method of

transforming mechanical rotary motion into electrical output.

Compact macromodels of different devices and in particular, incremental encoders are desired to speedup the simulation without sacrificing any of the required accuracy. One method to decrease simulation time and improve the convergence, without a significant loss of information, is by using behavioural macromodelling technique. Macromodelling is a way of providing macroscopic models of the corresponding devices.

Simulation investigations are of great importance for systems intended for applications in gas and oil production, chemical processing, grain and coal dust, and other hazardous environments.

Macromodels are very useful in education, where the students can investigate and study the basic characteristics of the encoders and the circuits processing their output signals.

Without any doubt macromodels of incremental encoders are necessary for simulating controllable motion systems. However, powerful simulation macromodels have not been available yet.

## II. ENCODERS PRINCIPLES

### A. Classification

Encoders are mechanical to electrical transducers whose output is derived by “reading” a coded pattern on a rotating disk or a moving scale. Encoders are classified by the:

- method used to read the coded element - contact or non-contact;
- type of output - absolute digital word or series of incremental pulses;
- physical phenomenon employed to produce the output - electrical conduction, magnetic, optical, capacitive.

In comparison to the absolute encoders the incremental ones have some advantages. Generally, incremental encoders provide more resolution at a lower cost than their absolute encoder analogs. They also have a simpler interface because they have fewer output lines. In a simple form, an incremental encoder would have 4 lines: 2 quadrature (A & B) signals, and power and ground lines. A 12 bit absolute encoder, by contrast, would use 12 output wires plus a power and ground line.

### B. Theory of operation

The principle of incremental encoder operation is generation of a symmetric, repeating waveform that can be used to monitor the input motion. The basic components of all optical incremental encoders are the light source, light shutter system, light sensor, and signal conditioning electronics.

<sup>1</sup>Marieta Kovacheva is with the Faculty of Electronic Engineering and Technologies at Technical University of Sofia, 8 Kl. Ohridski Blvd, Sofia 1000, Bulgaria, E-mail: m\_kovacheva@tu-sofia.bg.

<sup>2</sup>Peter Yakimov is with the Faculty of Electronic Engineering and Technologies at Technical University of Sofia, 8 Kl. Ohridski Blvd, Sofia 1000, Bulgaria, E-mail: pij@tu-sofia.bg.

These components will be housed and assembled to various mechanical assemblies, either rotary or linear in design depending on how motion will be monitored. The encoder mechanical input operates the light shutter which modulates the intensity of the light at the sensor. The sensors electrical output is a function of the incident light. The encoders electrical output is produced from the sensor output by the signal conditioning electronics and can be either:

- a sine-wave;
- a shaped, square-wave;
- a series of equally spaced pulses produced at regular points on the waveform.

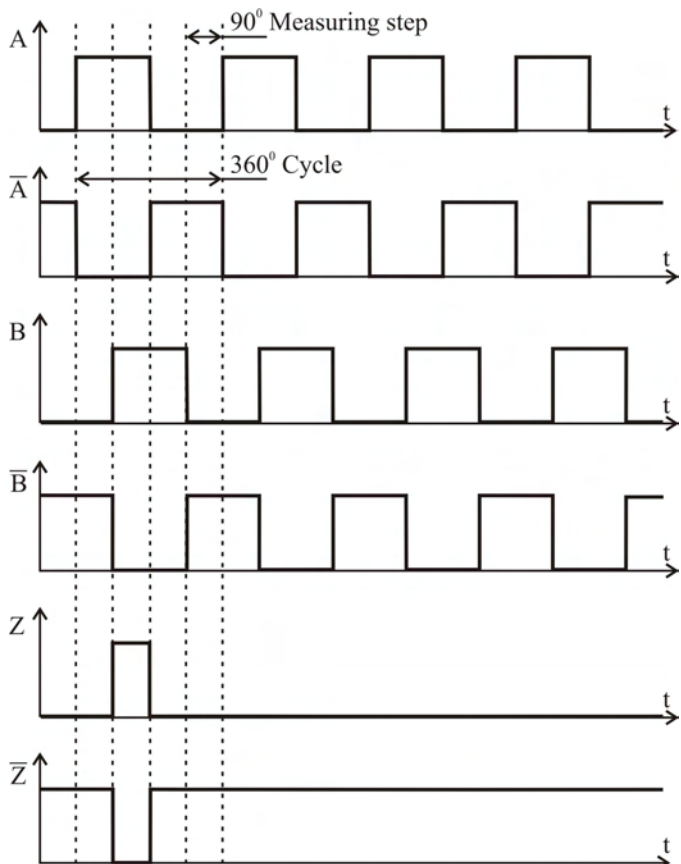


Fig. 1. Output signals in CCW rotation

An incremental encoder produces a series of square waves as it rotates. The number of square wave cycles produced per one turn of the shaft is called the encoder resolution. Incremental encoders work by rotating a code disc in the path of a light source. The code disc acts like a shutter to alternately shut off or transmit the light to a photodetector. The pulse range of an encoder is dictated by the number of tracks of clear and opaque lines located on the disc. Thus, the resolution of the encoder is the same as the number of lines on the code disc. A resolution of 360 means that the encoder code disc will have 360 lines on it and one turn of the encoder shaft will produce 360 complete square wave cycles, each cycle indicating one degree of shaft rotation. Since the resolution is "hard coded" on the code disc, optical encoders are inherently very repeatable and, when well constructed,

very accurate. The square wave output is inherently easy for digital signal processing techniques to handle.

Incremental encoders are usually supplied with two channels (A & B) that are offset from one another by 1/4 of a cycle (90 electrical degrees). This signal pattern is referred to as quadrature and allows the user to determine not only the speed of rotation but its direction as well. By examining the phase relationship between the A and B channels can be determined that A leads B for counterclockwise (CCW) rotation of the input shaft as it is shown on Fig. 1.

Generally in addition to the signals A and B, their inverse forms are also available. The complete signals set includes also a "zero" pulse – Z and its inverse form. This signal is generated using another track on the disc that has only one opaque line. Signal Z rises high once per one turn of the shaft.

The relationship of the encoder output signals for turning clockwise (B leads A) is shown on Fig. 2.

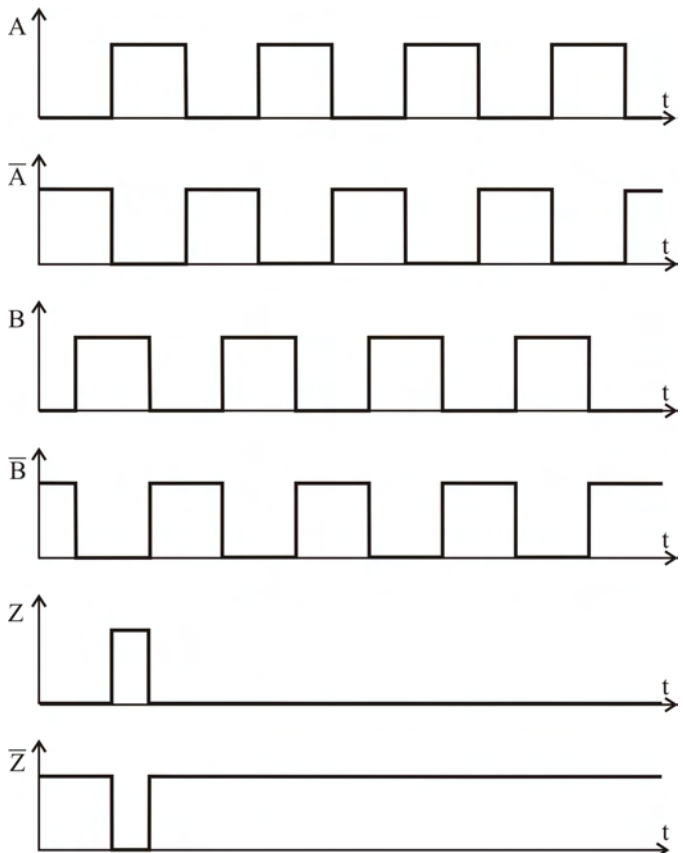


Fig. 2. Output signals in CW rotation

Except for discrimination between direction of movement (CW versus CCW), the quadrature relation allows for error detection in high vibration environments and higher resolution by using edge detection. With quadrature detection the controller can derive 1X, 2X or 4X the basic code disc resolution. 10,000 counts per turn can be generated from a 2500 cycle, two-channel encoder by detecting the Up and Down transitions on both the A and B channels as it is shown on Fig.1. In this case the measuring step is 90 electrical degrees. With a quality disc and properly phased encoder, this 4X signal will be accurate to better than 1/2 count.

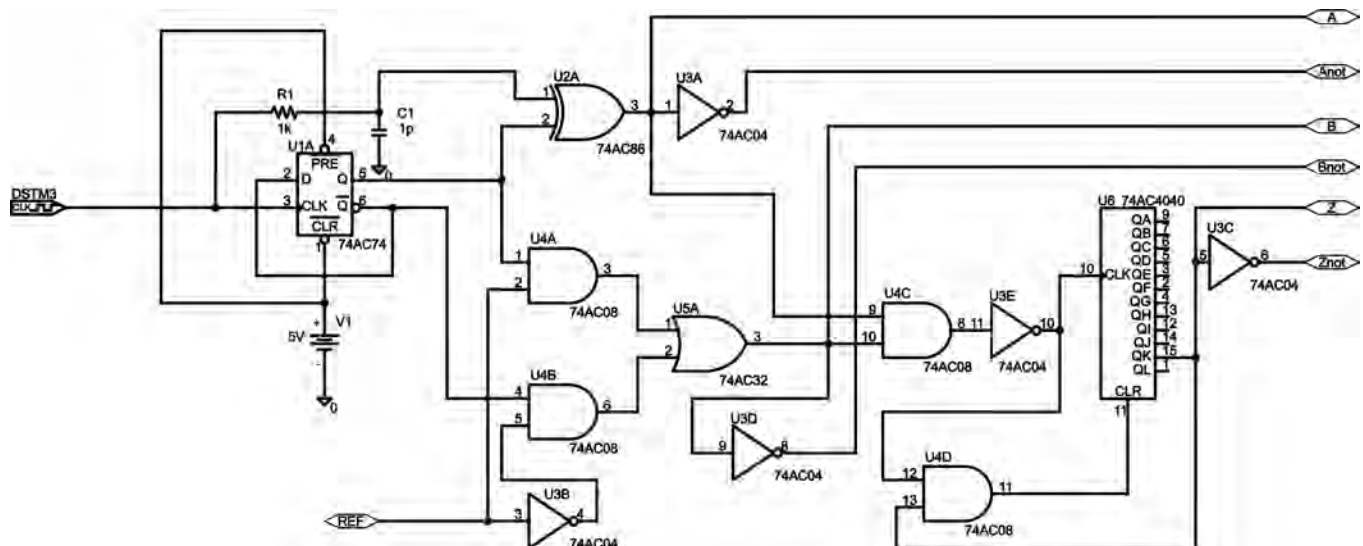


Fig. 3. Macromodel electric circuit

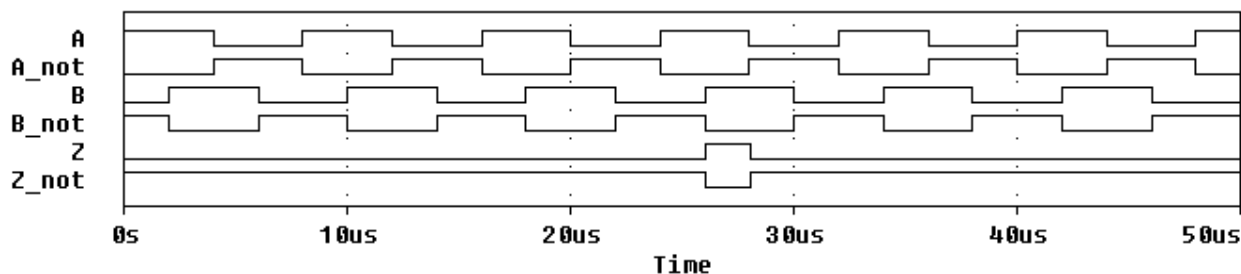


Fig. 4. Simulation results in CCW rotation

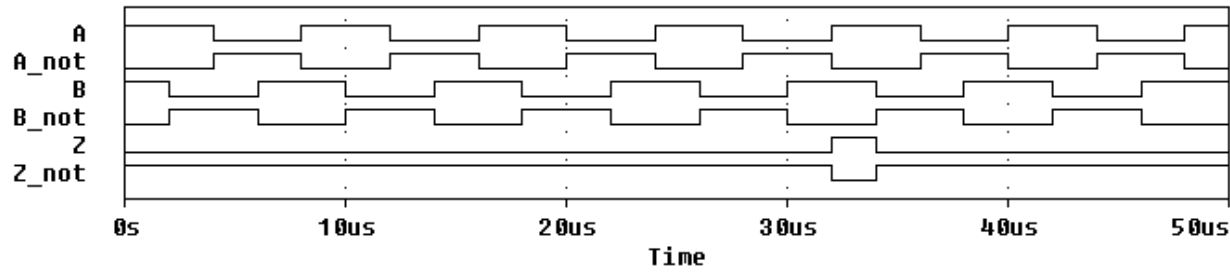


Fig. 5. Simulation results in CW rotation

### III. MACROMODEL DEVELOPMENT

The macromodel electric circuit is designed using standard advanced CMOS combinational and sequential logic circuits and is shown on Fig. 3. It simulates the action of a rotary encoder. The frequency of the output signals A and B is set by the digital stimulus DSTM3 and can be adjusted editing its model parameters. This is important for the flexibility of the macromodel because this is the possibility to set the value of the speed of the movement. The main part of the circuit is the generation of the signals with quadrature relation. This is obtained using the D flip-flop (U1A) acting as a frequency

divider and the XOR logic gate (U2A). To the inputs of the same gate are applied the signal with the clock frequency and the one with its half value. In this way the signal produced by the XOR gate and the signal produced by the normal output of the flip-flop are with 90 electrical degrees phase shift. If the initial state of the flip-flop is high then the signal from its normal output will lead the signal produced by the XOR gate. In the same time the signal obtained from the inverted output of the flip-flop will lag the output signal of the XOR gate. If it is accepted that the output of the XOR gate produces the signal A, then there must be a part of the circuit that will simulate the signal B and the change of the direction of the rotation. Thus there is a two-input multiplexer realized with the AND gates U4A and U4B, the inverter U3B and the OR

gate U5A. The signal B is obtained from the output of the multiplexer. An external logic signal applied to the input REF determines the relation between the signals A and B. When this input is tied low signal B will be produced by the inverted output of the flip-flop and then A will lead B as it is shown on Fig. 4. In contrary when a high level is applied to the REF input the signal B will lead the signal A as it is depicted in Fig. 5. Thus the change of the logic level applied to the REF input simulates the change of the direction of the rotation. In order to have the inverted forms of the signals A and B, two inverters are added. The logic gate U3A produces the inverted form A<sub>not</sub> and the logic gate U3D – the inverted form B<sub>not</sub>. The complete set of signals of the rotary encoder includes the “index” signal Z. There is another part of the circuit that generates it. The circuit consists of the 12-stage binary ripple counter 74AC4040 (U6) and the logic gates U4C, U4D, U3E and U3C. This circuit must produce a pulse on every previously defined number of pulses on outputs A and B. So this pulse is generated once per one turn of the shaft of the encoder. Because the counter advances on the high-to-low transition of CP input and to simulate correctly the operation of the rotary encoder the clock pulses for the counter are produced by AND function of the signals A and B followed by inversion. The number of cycles of A and B signals per one turn of the encoder shaft is simulated by choosing the output of the counter from which the Z signal will be derived. In the shown example the Z signal is derived from the output QK which means that there will be 1024 cycles per one turn. The biggest number of cycles that can be simulated using this macromodel is 2048 if the signal Z is derived from the output QL. Any less number equal to a power of two can be obtained. In this way the resolution of the encoder is simulated. To shape the Z pulse an additional logic for resetting the counter is used. The width of this pulse must be equal to one quarter of the cycle. To achieve it the AND gate U4D produces the active high level for the master reset input of the counter. Since the chosen output has risen after the falling edge of the clock signal one of the inputs of the AND gate receives logic one. The output of the counter will hold its high level till the clock pulse raises its state. This time interval will continue one quarter of the cycle and after low-to-high transition of the clock pulse logic “1” will be applied to the other input of U4D. At that moment MR input of the counter will receive its active level and all outputs will be cleared. The inverter U3C produces the inverted form of the signal Z<sub>not</sub>. So all output signals of the incremental encoder are generated and the simulated timing diagrams are shown on Figs. 4 and 5.

#### IV. CONCLUSION

In this paper an incremental rotary encoder macromodel is presented. It simulates the operation of the encoder in both directions of rotation. The full set of output signals is generated. The simulated timing diagrams of the signals correspond to the real ones. This macromodel has been used in the laboratory work of the students at the Technical university of Sofia. The macromodel can be used in design

and studying electronic circuits for processing incremental rotary encoder signals.

#### REFERENCES

- [1] PSpice models, Cadence Design Systems, 2008.
- [2] Spice models, Texas Instruments, 2008.
- [3] MicroSim PSpice A/D Reference manual. Micro-Sim Corp. Version 8, 1996.
- [4] Robinson, S. Conceptual Modeling for Simulation: Issues and Research Requirements, Proceedings of the 2006 Winter Simulation Conference, 2006, pp. 792-799.
- [5] Pandiev, I., P. Yakimov, D. Doychev, T. Todorov, V. Stanchev. A practical approach to design and modeling digitally programmable analog circuits. Proceedings of the Seventeenth International Scientific and Applied Science Conference Electronics-ET2008, September 24 - 26, 2008, Sozopol, Bulgaria, b.3, pp. 118-124, ISSN 1313-1842.
- [6] [www.heidenhain.de](http://www.heidenhain.de)
- [7] [www.sick.com](http://www.sick.com)
- [8] [www.baumer.com/motion](http://www.baumer.com/motion)
- [9] <http://www.ia.omron.com/>
- [10] [www.beiied.com](http://www.beiied.com)

# Electrical Properties of Poly(Vinylidene Fluoride-CO-Hexafluoropropylene) Nanocomposites with Nanoclays

Pavlik Rahnev<sup>1</sup>, Dimitrina Kiryakova<sup>1</sup>, Lyudmila Borisova<sup>1</sup> and Atanas Atanassov<sup>1</sup>

**Abstract –** Polymer nanocomposite materials based on PVDF with 15 mol% content of hexafluoropropylene and Cloisite® 15A and Cloisite® 30B were prepared by melt-mixing at 200°C. In pure copolymer, the crystalline phase is the  $\alpha$ - phase. Materials consisting organoclays Cloisite show significant increasing of  $\beta$ -phase from 30% to 55-60%. It is expected these materials to have piezoeffect but primarily they are dielectrics. In this work the main parameters as dielectric constant  $\epsilon_r$  and critical electric field  $E$  are investigated.

**Key words** - nanoclays, nanocomposites, poly(vinylidene fluoride-co-hexafluoropropylene),  $\beta$ - phase, electrical properties, piezoeffect, polymer piezo materials.

## INTRODUCTION.

Poly(vinylidene fluoride) (PVDF) and copolymers on its basis have been some of the most researched polymers, due to their ferroelectric properties. These polymers have different unit cells of varying polarity, because of its different crystal modifications. They are known at least four different crystal modifications of PVDF with different molecular conformations and lattice parameters [1–3]. The most common, easily obtainable and thermodynamically stable phase is the  $\alpha$ -phase. It does not show a net lattice polarization due to its ant parallel chain arrangement (a trans-gauche conformation). In  $\beta$ -phase the molecules are configured in all-trans conformation. This gives the  $\beta$ -phase crystals a spontaneous lattice polarization, which is necessary to observe ferroelectricity in PVDF. The  $\gamma$ -phase is combination of alternating conformational units from the  $\alpha$ - and  $\beta$ -phases, a  $\delta$ -phase is a polar version of the  $\alpha$ -phase. The crystal forms of PVDF homopolymer is retained in many copolymers of VDF containing small amounts of comonomer [4]. The fluorine atoms in the copolymers produce steric hindrance that prevents the molecular chains from assuming conformations similar to non-electroactive  $\alpha$ -phase of PVDF.

<sup>1</sup>Pavlik Rahnev – Technical College, Assen Zlatarov University, Y. Yakimov Str. 1, Burgas 8010, Bulgaria, E-mail: [pavlikrahnev@abv.bg](mailto:pavlikrahnev@abv.bg)

<sup>1</sup>Dimitrina Kiryakova – Department of Materials Science, Assen Zlatarov University, Y. Yakimov Str. 1, Burgas 8010, Bulgaria, E-mail: [dskiryakova@abv.bg](mailto:dskiryakova@abv.bg)

<sup>1</sup>Lyudmila Borisova – Department of Materials Science, Assen Zlatarov University, Y. Yakimov Str. 1, Burgas 8010, Bulgaria, E-mail: [invitations@linkedin.com](mailto:invitations@linkedin.com)

<sup>1</sup>Atanas Atanassov – Department of Materials Science, Assen Zlatarov University, Y. Yakimov Str. 1, Burgas 8010, Bulgaria, E-mail: [aatanasov@btu.bg](mailto:aatanasov@btu.bg)

Many of the copolymers directly crystallize into the polar electroactive  $\beta$ -phase [3], which give the ferro-, pyro-, and piezoelectric behavior in PVDF and its copolymers [3, 5].

It is known, that films of poly (vinylidene fluoride hexafluoropropylene) copolymer (VDF-HFP) with different contents of HFP indicates prominent piezo-, pyro-, and ferroelectricity, comparable to that in PVDF [6–13].

It is established that these properties were highly dependent on the crystal structure and polymer chain orientation of the VDF-HFP copolymer [14].

Very high electrostrictive response was reported for VDF-HFP copolymer with content of 5 and 15 mol% HFP – 1700 pm/V and 1200 pm, respectively.

The remnant polarization of copolymer films with the same content of HFP was 60 mC/m<sup>2</sup> and 48 mC/m<sup>2</sup> [6, 8]. In the solution-cast sample the remnant polarization was found to be 80 and 50 mC/m<sup>2</sup> for VDF-HFP copolymer films with 5 and 15 mol% HFP content, respectively [8].

Casting from dimethylformamide solution [11, 12] or stretching PVDF-HFP films [10] leads to chain conformations that are similar to those of polar  $\beta$ -PVDF.

Over the past decade, many researchers have reported a possibility to stabilize  $\beta$ -phase in PVDF and copolymers with HFP in the presence of layered silicates well scattered within the polymer matrix.

The addition of 1 – 6 mass% nanoclays is a prerequisite for the improvement of the mechanical, barrier, piezo-, pyro- and ferroelectric properties [15–17].

In the work [16] is reported that the addition of organically modified nanoclays to the VDF-HFP copolymer facilitated the transformation of the polymer crystals from  $\alpha$ - to  $\beta$ -phase.

The nanocomposite materials obtained showed increased values of elongation at break compared to the initial copolymer, as well as high dielectric permeability in wide temperature interval.

The piezoelectric  $\beta$ -phase in PVDF-HFP nanocomposites with layered silicate was retained after swift heavy ion irradiation, indicating that the nanocomposites can be used as radiation-resistant materials at high temperature [17].

The aim of the present work is to obtain nanocomposite materials on the basis of poly (vinylidene fluoride-co-hexafluoropropylene) with organically modified montmorillonite nanoclays Cloisite®15A and Cloisite®30B and study the content of  $\beta$ -phase, dielectric and piezoelectric properties of PVDF-HFP modified copolymers.

The piezoeffect of these materials could be used for many applications very attractive in this way for transforming noise energy into electrical.

## II. EXPERIMENTS

### Materials preparation

Poly(vinylidene fluoride-*co*-hexafluoropropylene) referred as PVDF-HFP is a copolymer (15 mol% HFP comonomer) with melting temperature 117°C and melt index 6.52 g/10 min (220°C, load 98 N) as powder was kindly supplied from Arkema, France.

Two organically modified montmorillonite nanoclays (Cloisite®15A and Cloisite®30B) from Southern Clay Products Inc. were used. Cloisite®15A was dimethyl, dehydrogenated tallow ammonium - exchanged montmorillonite. Cloisite®30B was bis (hydroethyl) methyl tallow ammonium-exchanged montmorillonite.

### Sample Preparation

The compositions of these nanoclays were mixed with PVDF-HFP and homogenized as powder by stirring at 50 – 60°C for 10 min, and then twice in a “Brabender” at 200°C. They were pressed on a laboratory press PHI (England) between aluminium foils under the following conditions: samples thickness about 1 mm, temperature 200°C, melting period at 200°C – 3 min, pressing pressure – 12 MPa; cooling rate – 40°C/min.

### X-ray Structure Analysis

The X-ray diffraction patterns were taken by X-ray diffractometer with generator Iris-M (Russia) and goniometer URD-6 (20) (Germany) at atmospheric pressure, room temperature, Ni-filtered Cu target  $K_{\alpha}$  radiation in the interval  $2\theta = 4 \div 50^\circ$ .

### Fourier Transform Infrared Spectroscopy (FT-IR)

Samples prepared as films were analyzed using spectrophotometer produced by “Bruker” (Germany) in the interval 4000–400  $\text{cm}^{-1}$  with Tensor 27. To determine the relative quantity of the  $\beta$ - phase, the heights of the series of peaks were determined by simulation of the spectrum observed.

This was done using OPUS – 65 software which automatically corrects the baseline. For each sample, the fraction of the  $\beta$ -crystalline phase ( $F_{\beta}^{IR}$ ) was calculated by the formula:

$$F_{\beta}^{IR} = A_{\beta} / (1.26 A_{\alpha} + A_{\beta}) \quad (1)$$

where:  $A_{\alpha}$  и  $A_{\beta}$  – are the heights of the peaks at 764 and 840  $\text{cm}^{-1}$ , respectively while the coefficient 1.26 represents the ratio of the absorption coefficients at 764 and 840  $\text{cm}^{-1}$  [18].

### Electrical measurement

As expected these materials initially must act as dielectrics. For these measurements universal digital multimeter is used with capacitance range ( $C_{\min} > 1 \mu\text{F}$ ) and resistors ( $R_{\max} < 200 \text{ M}\Omega$ ).

The sample for easy measurements are prepared as capacitors (single layer) with two silver electrodes – Fig. 1.

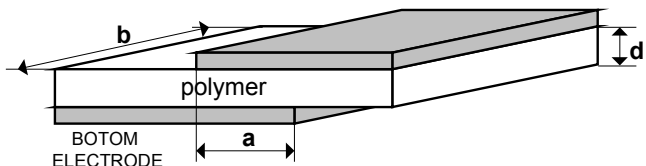
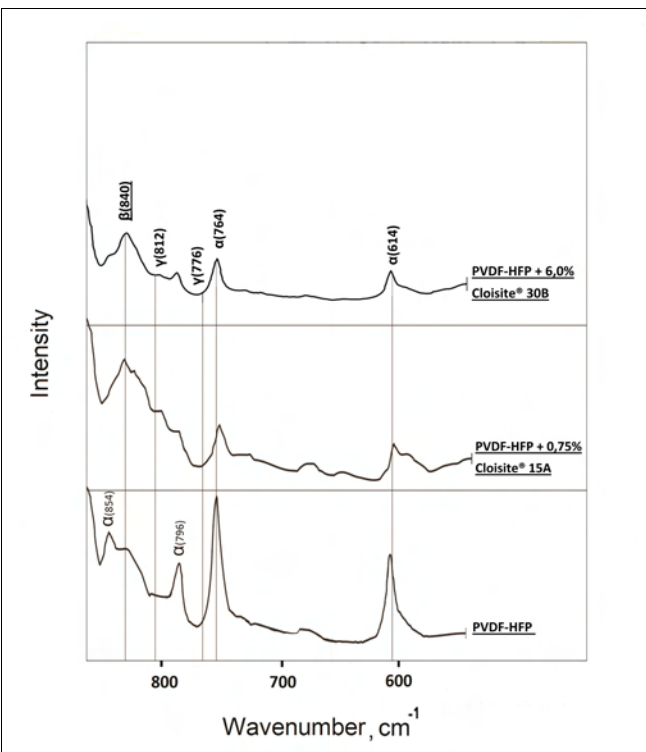


Fig. 1. The shape and dimension of samples.  
 $S=a \times b$  – common surface between upper and bottom electrodes (Ag);  $d$  – thickness of samples.

## III. RESULTS AND DISCUSSION

The XRD diffractograms of VDF-HFP copolymer were analyzed in reference to the standard XRD patterns for PVDF [19], in this way small quantity of HFP (15 mol %) in VDF-HFP copolymer does not change significantly the lattice symmetry of PVDF [20]. Fig. 1 shows the XRD patterns of the PVDF-HFP, organoclays Cloisite® 15 A and Cloisite® 30 B and nanomaterials on their basis.

Fig. 2. X-ray diffraction patterns of the initial PVDF-HFP and



nanocomposite materials containing Cloisite®15A and Cloisite®30B.

The peaks at  $2\theta = 17.7, 18.4, 19.9$  and  $26.6^\circ$  correspond to 100, 020, 110 and 021 diffractions of the PVDF  $\alpha$ - phase while the peaks at  $2\theta = 20.2, 20.6, 20.7$  and  $20.8^\circ$  – to 110 and 200  $\beta$ - phase diffractions [21].

The change in the diffractograms and the appearance of a basic peak above  $20^\circ$  together with a smaller one at  $2\theta = 18 - 19^\circ$  directly proved the formation of a pure and prevalently oriented  $\beta$ -phase in the obtained nanocomposite materials (Fig. 2). In the initial VDF-HFP copolymer, the crystalline phase is predominantly the non-polar  $\alpha$ - phase. Since the

peaks characteristic for the  $\alpha$ - and  $\beta$ -phases are somewhat overlapped in the X-ray diffractogram, the XRD- analysis of PVDF-HFP and its nanocomposites was supplemented by Fourier transform infrared spectroscopy (FT-IR).

The values calculated for  $F_{\beta}^{IR}$  by the FT-IR method for VDF-HFP copolymer and its nanocomposites with Cloisite<sup>®</sup> 15 A and Cloisite<sup>®</sup> 30 B showed that the increase of nanoclay content gave increased  $\beta$ - phase content from about 30 % in the initial PVDF-HFP to 55÷60 % in the composite materials containing organoclays Cloisite<sup>®</sup>15A and Cloisite<sup>®</sup>30B.

Before electrical testing of samples they are numbered as follows (type of material and sizes see Fig. 1):

1. PVDF-HFP, pure S=16×15 mm, d=81  $\mu$ m;
2. PVDF-HFP+0.5%, Cloisite<sup>®</sup>15A, S=15×12 mm, d=98  $\mu$ m;
3. PVDF-HFP+0.75%, Cloisite<sup>®</sup>15A, S=11×13 mm, d=250  $\mu$ m;
4. PVDF-HFP+6%, Cloisite<sup>®</sup>30B, S=12×20 mm, d=207  $\mu$ m;

The first measurement are for estimation of dielectric constant  $\epsilon_r$ [22] - Table I.

TABLE I  
DIELECTRIC CONSTANTS OF SAMPLE

PARAMETER	NUMBER OF SAMPLES			
	1	2	3	4
C(pF)	212	135	60	180
$\epsilon_r$	9	8.5	12	20

TABLE II  
CRITICAL ELECTRICAL FIELD OF THE SAMPLES

PARAMETER	NUMBER OF SAMPLES			
	1	2	3	4
$U_{BR}(\text{kV})$	5.1	5.35	6.3	5.8
E(V/m)	$6.00 \times 10^7$	$5.30 \times 10^7$	$>2.10 \times 10^7$	$3.00 \times 10^7$

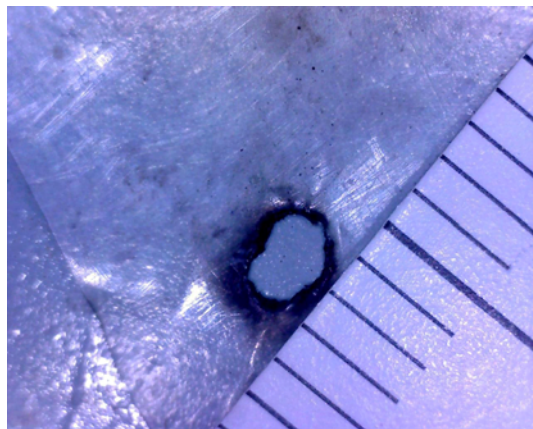


Fig. 3. Destruction pictures of samples (a).

Investigation of breakdown voltage and type of destruction are shown in Table II and Fig.3,a,b



Fig. 3. Destruction pictures of samples ( b).

The presence of piezoeffect is detected only as a phenomena. Bending and pressing the samples the voltages about 8÷20 mV appear between two electrodes.

The interest are the results from temperature dependence of the isolation resistivity  $R_{sample}$  – table III. It could be seen significant drop after 50°C.

TABLE III  
TEMPERATURE CHANGES OF THE SAMPLES

T(°C)	NUMBER OF SAMPLES			
	1	2	3	4
R(MΩ)				
40	200	198	-	-
45	176	153	-	>200
50	88	87	-	170
55	50	49	-	85
60	24	25	200	60
65	13	17	150	40
70	9	12	62	30
75	-	-	43	21
80	-	-	30	-

## CONCLUSION

Nanocomposite materials on the basis of poly (vinylidene fluoride-co-hexafluoropropylene) with Cloisite<sup>®</sup>15A and Cloisite<sup>®</sup>30B were obtained.

The materials obtained were analyzed by X-ray diffraction, FT-IR analyses and electrical measurements.

The addition of organically modified nanoclays changes the structure of the crystalline phase and facilitate the transformation of the polymer crystals from  $\alpha$ - phase to more polar  $\beta$ -phase.

Analyzing electrical parameters several conclusion could be made:

❖ These materials have more semiconductor for behavior then dielectric. The drop of resistant in heating in heating is a result of thermo generation of electrical carriers]

❖ The changes of  $\epsilon_r$  are significant with the additives in polymers;

❖ The shape of destroyed area is approximately 1×1, 2×2 mm. That leas to the conclusion the breakdown mechanism is not very sharp and has slow increased current.

Dielectric semiconductor behavior, piezoeffect, probably photo effect could be used for different sensors and new energy sources.

## REFERENCES

- [1] J. S. Humphrey and R. Amin-Sanaye, *Encyclopedia of polymer science and technology*, New York, Wiley, Vol. 4, 2006.
- [2] A. J. Lovinger, *Developments in crystalline polymers*, Englewood (New Jersey), Applied Science Publishers Ltd, Vol. 1, 1982.
- [3] H. S. Nalwa (Ed.), *Ferroelectric Polymers: Chemistry, Physics, and Applications*, New York, Marcel Dekker Inc., 1995.
- [4] Yu. A. Panshin, S. G. Malkevich and Z. S. Dunaevskaya, *Ftoroplasty*, Leningrad, Khimiya, 1978.
- [5] H. Lefebvre, F. Bauer and L. Eyraud, "Optimization and characterization of piezoelectric and electroacoustic properties of PVDF- $\beta$  induced by high pressure and high temperature crystallization", *Ferroelectrics*, vol. 171, pp. 259-269, 1995.
- [6] X. Lu, A. Schirokauer and J. Scheinbeim, "Giant electrostrictive response in poly(vinylidene fluoride-hexafluoropropylene) copolymers", *IEEE Trans. Ultrason. Ferroelectr. Freq. Contr.*, vol. 47, pp. 1291-1295, 2000.
- [7] W. Künstler, M. Wegener, M. Seiß and R. Gerhard-Multhaupt, "Preparation and assessment of piezo- and pyroelectric poly(vinylidene fluoride-hexafluoropropylene) copolymer films", *Appl. Phys. A*, vol. 73, pp. 641-645, 2001.
- [8] A. C. Jayasuriya, A. Schirokauer and J. I. Scheinbeim, "Crystal-structure dependence of electroactive properties in differently prepared poly(vinylidene fluoride/hexafluoropropylene) copolymer films", *J. Pol. Sci. B: Polym. Phys.*, vol. 39, pp. 2793-2799, 2001.
- [9] M. Wegener, W. Künstler, K. Richter and R. Gerhard-Multhaupt, "Ferroelectric polarization in stretched piezo- and pyroelectric poly(vinylidene fluoride-hexafluoropropylene) copolymer films", *J. Appl. Phys.*, vol. 92, pp. 7442-7447, 2002.
- [10] F. Wang, Z. Xia, X. Qiu, J. Shen, X. Zhang and Z. An, "Piezoelectric properties and charge dynamics in poly(vinylidene fluoride hexafluoropropylene) copolymer films with different content of HFP", *IEEE Trans. Dielectr. Electr. Insul.*, Vol. 13, pp.1132-1139, 2006.
- [11] A. C. Jayasuriya and J. I. Scheinbeim, "Ferroelectric behavior in solvent cast poly(vinylidene fluoride/hexafluoropropylene) copolymer films", *Appl. Surf. Sci.*, vol. 175, pp. 386-390, 2001.
- [12] M. Wegener, W. Künstler and R. Gerhard-Multhaupt, "Piezo-, pyro- and ferroelectricity in poly(vinylidene fluoridehexafluoropropylene) copolymer films", *Integr. Ferroelectr.*, vol. 60, pp. 111-116, 2004.
- [13] F. Wang, P. Frübing, W. Wirges, R. Gerhard and M. Wegener, „Enhanced Polarization in Melt-quenched and Stretched Poly(vinylidene Fluoride-Hexafluoropropylene) Films”, *IEEE Trans. Dielectr. Electr. Insul.*, vol. 17, no. 4, pp. 1088-1095, 2010.
- [14] X. He, K. Yao and B. K. Gan, "Phase transition and properties of a ferroelectric polyvinylidene fluoride-hexafluoropropylene Copolymer", *J. Appl. Phys.*, vol. 97, pp. 084101-084101-5, 2005.
- [15] L. Priya and J. P. Jog, "Intercalated poly(vinylidene fluoride)/clay nanocomposites: structure and properties", *J. Polym. Sci. B Polym. Phys.*, vol. 41, pp. 31-38, 2003.
- [16] A. Kelarakis, S. Hayrapetyan, S. Ansari, J. Fang, L. Estevez and E. P. Giannelis, "Clay nanocomposites based on poly(vinylidene fluoride-co-hexafluoropropylene): Structure and properties", *Polymer*, vol. 51, pp. 469-474, 2010.
- [17] Vimal K. Tiwari, Pawan K. Kulriya, Devesh K. Avasthi and Pralay Maiti, "Poly(Vinylidene fluoride-co-hexafluoro propylene)/Layered Silicate Nanocomposites: The Effect of Swif Heavy Ion", *J. Phys. Chem. B*, vol. 113, no. 34, pp. 11632-11641, 2009.
- [18] A. Salimi and A. A. Yousefi, "Analysis method - FTIR studies of  $\beta$ -phase crystal formation in stretched PVDF films", *Polym. Test.*, vol. 22, pp. 699-704, 2003.
- [19] R. Gregorio, "Determination of the  $\alpha$ ,  $\beta$ , and  $\gamma$  crystalline phases of poly(vinylidene fluoride) films prepared at different conditions", *J. Appl. Polym. Sci.*, vol. 100, pp. 3272-3279, 2006.
- [20] O. F. Guan, J. Pan, J. Wang, Q. Wang and L. Zhu, "Crystal orientation effect on electric energy storage in poly(vinylidene fluoride-co-hexafluoropropylene) copolymers", *Macromolecules*, vol. 43, pp. 384-392, 2009.
- [21] S. Satapathy, P. K. Gupta, S. Pawar and K. B. R. Varma, "Crystallization of  $\beta$ -phase poly (vinylidene fluoride) films using dimethyl sulfoxide (DMSO) solvent and at suitable annealing condition", *Mater. Sci.*, arXiv: 0808.0419, 2008.
- [22] S. Letskovska, P. Rahnev, Material science for electronics, Burgas Free University - Bulgaria, Informa print, ISBN-978-954-8468-04-6, 2008.

# Metal – Polymer Based Power Bulk Resistors

Pavlik Rahnev<sup>1</sup> and Silvija Letskovska<sup>2</sup>

**Abstract** – The goal of this work is the process for producing single end small series power resistors for laboratory application. The production steps include mixing conductive powder with polymere pressing and thermal treatment of the composition. The attention is paid for resistors shape and the possibility of trimming.

**Key words** – power resistors, bulk resistors, polymer resistors.

## I. INTRODUCTION.

Power resistors are commonly used in electrical circuit such as electrical motor control, power supply, grounding etc.

The rang of electrical parameters and sizes is very wide [1÷5].

For example power dissipation ( $P_{max}$ ) varies from 1 W to 1200 W; length (L) from 53 mm to 615 mm; accuracy ( $\Delta R$ ) - 5 to 20%.

There are several types of power resistors:

- ❖ Wire wounded;
- ❖ Film (thin or thick);
- ❖ Bulk (cermets, conductive polymers).

The disadvantage of some of them are: high parasitic inductance (wire – wounded), high capacitance (film resistors).

The best solution for power resistors working at high frequencies are bulk components with their representees:

- ❖ Sintered materials (high temperature, high pressure process);
- ❖ Composition based on polymers.

The first ones have very good stability but heavy technology.

For example, the resistors from boron carbide are sintered at the temperature between 1800 ÷ 2200 °C and they are very hard (black diamond).

For experimental uses the polymers based resistors are easy to be produced, trimmed and tested.

The aim of this paper are the results using compositions polymer (epoxy or silicon) and conductive phase (metals, alloys, semiconductors).

<sup>1</sup>Pavlik Rahnev – Technical College, Assen Zlatarov University, Y. Yakimov Str. 1, Burgas 8010, Bulgaria, E-mail: pavlikrahnev@abv.bg

<sup>2</sup>Silvija Letskovska - Burgas Free University, San Stefano 62, 8000 Burgas, Bulgaria, E-mail: silvia@bfu.bg

## II. PREPARATION OF THE EXPERIMENTAL SAMPLES

### 2.1 Technology and the choice of materials.

There are lots of combinations between organic materials (high temperature silicon and epoxy), conductive powder (Ag, Cu, Ni, est.), the ratio between them and technology parameters. For this reason the experiments are provided using only several combinations:

- ❖ Epoxy (two components 1:1). Hisol; high temperature silicon [7] with the parameters;
  - Adhesion - 35÷45 kg/cm<sup>2</sup>;
  - Working temperature – (-60° C ÷ +600° C);
  - Specific resistivity – 10<sup>12</sup> g.cm;
  - Dielectric strength – 5 kV/mm.
- ❖ Conductor – mainly carbon (C) with small additions of Ag, Cu, Ni;
- ❖ The ratio between organic and conductive phases is 5÷10% to 95÷90%.

In Table 1 the electrical properties of the used materials are given. It is clear that carbon has very wide range of resistance and strongly negative TCR.

To correct this, small additives (metal powder) will drift the specific resistance and TCR to desirable values.

TABLE I  
DEPENDENCE BETWEEN CONDUCTIVE PHASE AND ELECTRICAL PROPERTIES

Conductive phase	Ag	Cu	Al	Ni	C
$\rho$ (μΩ.cm)	0.66	1.78	2.9	8.2	708
$T\Delta\rho$ ( $\times 10^4$ K <sup>-1</sup> )	+0.40	+0.35	+0.41	+0.42	-70 ÷ -10

The technology includes next important steps:

- ❖ Mixing the components with laboratory mixer for 30 min and frequency about 100 t/min;
- ❖ Forming and hardening the compound at 120 °C for 2-3 hours;
- ❖ Measuring, trimming and making protective film.

2.2. Construction and particularities of the samples.  
For the experiments the simple rectangular shape is used (Fig. 1).

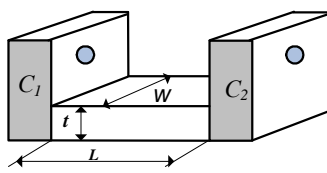


Fig. 1. Rectangular resistor shape.

$C_1, C_2$  - external copper metal contacts with Ni-Ag protection.

The sizes of the test resistor are chosen for easy preparation, testing and trimming:  $L=10$  cm,  $W=1$  cm;  $d=1$  cm. It means if the nominal values must be about  $100 \Omega$  with these dimensions the specific resistance would be approximately  $1 \Omega \cdot \text{cm}$ . The special attention is paid to the external contacts (Fig. 2).

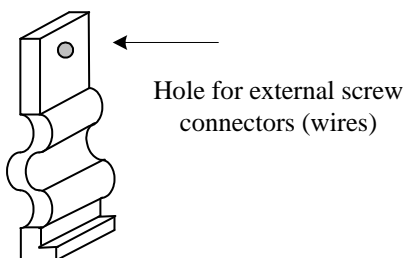


Fig. 2. Shape of the contacts.

The power resistors are usually low ohm that is why the contact resistance is very important. For the experiments the contacts are made using bended  $\text{Cu}$  (covered with parasitic resistance and to increase mechanical strength).

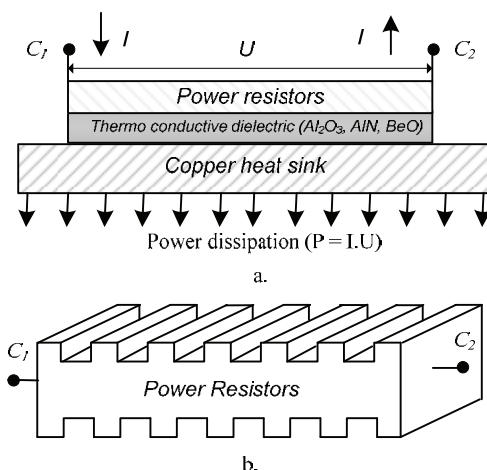


Fig. 3. Resistors for high power application.

The resistors for high and very high power dissipation are designed – Fig. 3,a, b.

### III. RESULT AND TRIMMING

The results after the preparation of samples show that best results are obtained with the composition "epoxy - carbon - silver - nickel" (Table 2). This mixture has sufficient parameters with low price.

TABLE II  
DEPENDENCE  $\rho$ ,  $S$  AND TCR - CONDUCTIVE PHASE PHASE

Composition	C+Ag	C+Cu	C+Ni	C+Ag+Ni
$\rho (\Omega \cdot \text{cm})$	0.35	2÷3	1.2÷2	1.2÷1.8
TCR ( $\text{ppm} \cdot \text{K}^{-1}$ )	$\geq 10^3$	$> 10^2 \div 10^3$	$> 10^2 \div 10^4$	$> 10^2 \div 10^3$

It is interesting to trim the resistors to nominal value. It is easy done removing part of the resistors surface layer. That means decreasing the cross section  $S$  and increasing the value of the resistors to the desirable ones (Fig. 4).

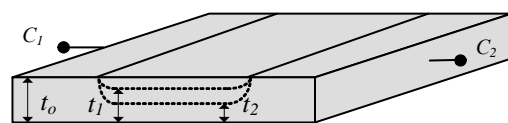


Fig. 4.  $t_0 > t_1 > t_2$ ;  $S_0 > S_1 > S_2$ ;  $R_0 > R_1 > R_2$ .

The best way to adjust the resistors is shown on Fig. 5. Making channels with regulated parameters such as " $t$ ", " $x$ " and " $a$ " it is not only possible to trim the resistors and to increase the surface for power dissipation.

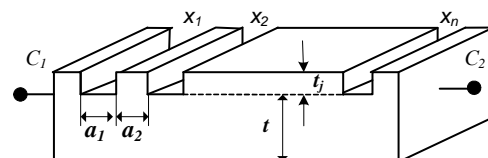


Fig. 5.  $x_n$  - number of the channels;  $d$  - depth of channels,  $t$  - width of channels;  $a$  - step between channels.

### CONCLUSION

As a final conclusion this paper shortly describes simple, easy and cheap power resistors production, laboratory made for own use. This gives flexibility in experimental work with high power devices.

### REFERENCES

- [1] [www.str-restech.de](http://www.str-restech.de)
- [2] [www.tepro-vamistor.com](http://www.tepro-vamistor.com)
- [3] [www.avtron.com](http://www.avtron.com)
- [4] [www.powerohm.com](http://www.powerohm.com)
- [5] [www.caddoc.com](http://www.caddoc.com)
- [6] Haritonov N. P., Krotikov B. A, Ostrovskij B. B., organosilikatnie komposizioni, Leningrad, nauka, 1980
- [7] P. Rachnev, N. Simeonova, S. Letskovska, Non inductive Polymer Based Power Resistors Polymer Based Power Resistors, TECHNOMER 2005-Germany.

# Modeling of high voltage periodically attenuating discharge in liquid with controllable high voltage switch thyatron

Milena Ivanova<sup>1</sup> and Stefan Barudov<sup>2</sup>

**Abstract** The usage of high voltage discharge in liquid finds many technological applications. Control of the moment when the discharge occurs in systems with capacitive energy storage, suggests the usage of a high voltage controllable switch, most often trigatron or thyatron, i.e. gas discharge occurs. The present work is dedicated to modeling of the discharge processes, arising in liquid medium and control by a high-voltage controllable switch-thyatron.

**Keywords** – capacitive energy storage, high voltage discharge in liquid, thyatron

## I. INTRODUCTION

High voltage discharge in liquid is used for water treatment with different purposes, destructions of deposits and incrustations in pipes and other applications [1,2,3]. Some research on power supply for high voltage application is also studied [4].

The experimental prototype for formation of high voltage periodically attenuating discharge in liquid medium with capacitive energy storage is shown in Fig.1. [5].

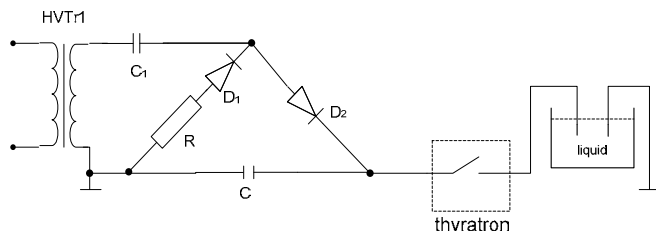


Fig.1 Circuit schematic for formation of high voltage discharge in liquid medium

In Fig.1 C is the capacitance of the capacitor battery, HVTr is a high voltage transformer. As a high voltage controllable switch (HVCS) can be used thyatrons as they can commutate high voltage up to 200kV, current with amplitude up to 100kA, allow pulse width from tens of nanoseconds to hundreds of microseconds and pulse repetitiveness up to 70kHz. In the current experiment is used a hydrogen thyatron

<sup>1</sup>Milena Ivanova is with the Faculty of Electrical Engineering at Technical University of Varna, 1 Studentska Str., Varna, 9010, Bulgaria, E-mail: m.dicheva@tu-varna.bg.

<sup>2</sup>Stefan Barudov is with the Department of Electrical Engineering at Naval Academy "N.Y.Vaptsarov", 73 Vasil Drumev str., Varna 9026, Bulgaria e-mail: sbarudov@abv.bg.

TГИ1-1000/25 – Fig.2. The control circuit of such HVCS is described in the literature [6].

Similar system for realization of high voltage discharge, but with another type HVCS – a trigatron is analyzed in the literature [7], but the described model includes only the discharge current and voltage.



Fig.2. Thyatron ТГИ1-1000/25

The discharge current can be defined by Eq.1:

$$\frac{di}{dt} + 2\delta \frac{di}{dt} + \omega_0^2 i = 0 \quad (1)$$

where:

-  $i(t_0)=0$  – initial condition

-  $\delta$  = damping ratio

The discharge circuit resistance is  $R = R_{HVS} + I$ , where  $R_{HVS} = R_{HVS}$  is the resistance of the HVCS (thyatron) and  $R_W = R_W$  – resistance of the liquid (water).

-  $\omega_0$  = – resonant frequency of the circuit.

The indicated resonant frequency refers to the case of a resonant circuit without losses. Considering that

$R = R_{HVS} + I$ , the resonant frequency is  $\omega_0$ . The adopted relative mistake can be defined by Eq.2:

$$\frac{\omega_0 - \omega_0}{\omega_0} = -\frac{1}{\delta}, \quad (2)$$

where  $\rho =$  is the characteristic resistance and  $R \ll \rho$  is considered.

In the cases when  $\delta < \omega_0$ , the process is periodically attenuating – Fig.3.

At resonant circuit resistance  $R=\text{const}$  is valid Eq.3:

$$\frac{A_1}{A_2} = \frac{A_2}{A_3} = \frac{A_3}{A_4} = \dots = \frac{A_{n-1}}{A_n} = e^{-\delta T} = \text{const} = \dots \quad (3)$$

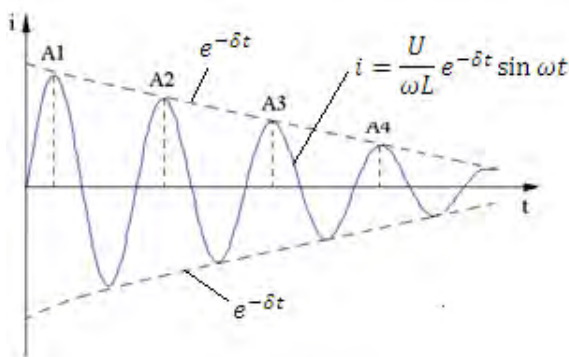


Fig.3 Periodically attenuating oscillation

If we consider that  $R_{HVS} = R_{HVS(t)}$  and  $R_W = R_W$  and accept that within one period  $R_{HVS} = \text{const}$  and  $R_W = \text{const}$ , then is valid Eq.4:

$$B_1^* = \ln B_1 = \delta T = \frac{\pi R}{\mu} \frac{1}{L} \quad (4)$$

If  $T$  is the period of the resonant circuit with losses  $R$ , considering that  $\omega_0^2 = \omega_0^2 (1 - (\frac{R}{L})^2)$ , then Eq.5 is in force:

$$T = \frac{1}{f} = \frac{2\pi}{\omega_0} = \frac{2\pi}{\sqrt{L + R}} \quad (5)$$

After transformation of Eq.4 and Eq.5, Eq.6 is obtained:

$$R = \frac{2\pi E}{\sqrt{L + R}} \quad (6)$$

$$\frac{R}{T} = \sqrt{\frac{1}{L + R}}$$

From Eq.6 can be defined  $R = R(\dots)$  and  $L = L(\dots)$  – Eq.7.

$$L = \frac{T^2}{(2\pi)^2 + R} \quad (7)$$

$$R = \frac{2\pi^2 T}{(2\pi)^2 + R}$$

*Note:* After modeling of the discharge process, it can be accepted that for the time of one period  $T$  ( $B_1^* = \text{const}$ ),  $R$  and  $L$  also don't change.

After experimental obtaining of  $i = i(t)$  – Fig.3-oscilogram, referring the current through  $R$  – Fig.1,  $\dots$  is received for the separate periods, from where  $R$  and  $L$  can be defined.

The purpose of the present work is experimental study by the usage of a thyratron of:

- Resistance of HVCS – thyratron at discharge  $R_{HVS} = R_{HVS(t)}$ ;
- Resistance of the discharge circuit  $R = R_{HVS} + R_W = R(t)$  at two discharge gaps (thyatron and discharge gap in water);

At parameters capacitance of the capacitor battery  $C$  – Fig.1 and voltage  $U_c$ , to which it is charged. On the basis of the experimental study is created a model, which includes the influence of the parameters  $C$  и  $U_c$ .

## II. EXPERIMENT

Two experiments are conducted:

- Measuring the discharge current  $I_{D1}$ , when the capacitor battery discharges only through the thyatron and defining  $R_{HVS} = R_{HVS(t)}$  according to the described method;
- Measuring the discharge current  $I_{D2}$  when the capacitor battery discharges through the HVCS-thyratron and a discharge gap in liquid and defining  $R = R_{HVS} + R_W = R(t)$ .

The experimental data are taken at parameters capacitance of the capacitor battery  $C=0.5\mu F, 1\mu F, 1.5\mu F, 2\mu F$  and voltage  $U_c=9.5, 10, 10.5, 11, 11.5 kV$ .

For the case of one discharge gap in the circuit (thyatron) at  $C=1.5\mu F$  and  $U_c=11kV$  the results for  $\dots$  and calculated  $R$  and  $L$  are presented in Table 1. The same data for the case with two discharge gaps (thyatron and gap in water) connected in series at the same parameters are shown in Tabl.2.

TABLE 1 EXPERIMENTAL RESULTS FOR A THYRATRON AT PARAMETERS  $C=1.5\mu F$  И  $U_c=11kV$

	$A_1/A_2$	$A_2/A_3$	$A_3/A_4$	$A_4/A_5$
$B_1^*$	0.623	0.516	0.462	0.439
$R_{HVS}, \Omega$	0.582	0.402	0.320	0.289
$L, \mu H$	33.32	33.41	33.46	33.47

TABLE 2 EXPERIMENTAL RESULTS FOR TWO DISCHARGE GAPS AT PARAMETERS  $C=1.5\mu F$  И  $U_c=11kV$

	$A_1/A_2$	$A_2/A_3$	$A_3/A_4$	$A_4/A_5$
$B_1^*$	1.50	1.18	1.04	0.940
$R, \Omega$	3.47	2.20	1.70	1.40
$L, \mu H$	36.24	36.99	37.29	37.46

TABLE 3 COEFFICIENTS OF APPROXIMATION a AND b FOR THE CASE WITH ONE DISCHARGE GAP - THYRATRON

U <sub>c</sub> , kV	9.5		10		10.5		11		11.5		
	C, $\mu$ F	a	b	a	b	a	b	a	b	a	b
0.5		1.09E-05	0.0278	1.06E-05	0.0600	1.02E-05	0.0910	9.09E-06	0.144	9.4E-06	0.162
1		1.36E-05	0.0999	1.44E-05	0.109	1.41E-05	0.135	1.39E-05	0.161	1.47E-05	0.178
1.5		1.81E-05	0.119	1.72E-05	0.154	1.74E-05	0.172	1.74E-05	0.1943	1.81E-05	0.206
2		1.99E-05	0.154	2.04E-05	0.176	2.15E-05	0.19	2.16E-05	0.2167	2.2E-05	0.224

TABLE 4 COEFFICIENT OF APPROXIMATION a AND b FOR THE CASE WITH TWO DISCHARGE GAPS –THYRATRON AND GAP IN WATER

U <sub>c</sub> , kV	9.5		10		10.5		11		11.5		
	C, $\mu$ F	a	b	a	b	a	b	a	b	a	b
0.5		6.52E-05	-0.0155	6.518E-05	0.158	6.82E-05	0.243	6.36E-05	0.506	6.92E-05	0.578
1		8.82E-05	0.264	9.55E-05	0.293	9.9E-05	0.408	9.95E-05	0.577	10.6E-05	0.690
1.5		12.2E-05	0.343	12.01E-05	0.531	12.4E-05	0.663	12.9E-05	0.775	13.6E-05	0.868
2		13.3E-05	0.551	14.2E-05	0.664	15.2E-05	0.755	16.2E-05	0.877	17E-05	0.910

At repeating experiments includes aggregation of points, which consider the character and the dynamic of the discharge process development.

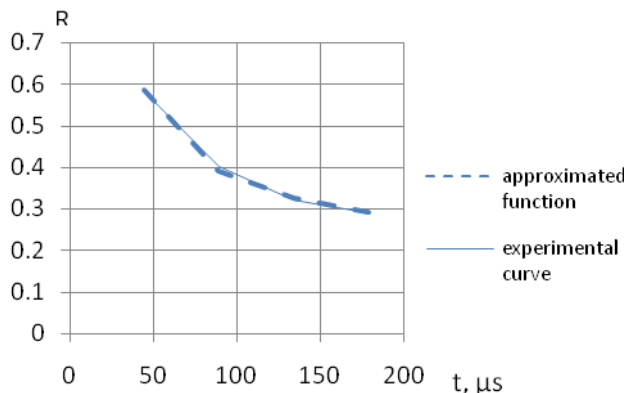
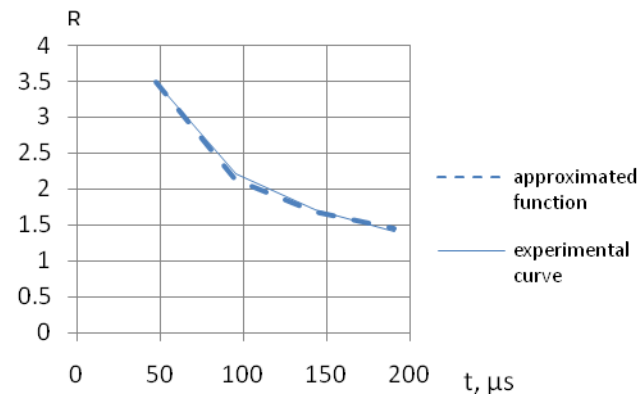
### III. ANALYSIS

The obtained results allow approximation of the curves  $R_{HVS} = R_{HVS}(t)$  и  $R = R_{HVS} + R_W = R(t)$  with a hyperbola –Eq.8:

$$R = \frac{b}{t} + b \quad (8)$$

The coefficients a and b are defined by the least square method as the received results are presented in Table 3 (for a thyatron/ and Table 4 /two discharge gaps/).

In Fig.4 and Fig.5 is shown the change of the resistance  $R_{HVS}(t)$  and  $R(t)$  on the basis of the numeric characteristics in Table 1 and 2 and the curves after approximation for 10 repeated experiments.


 Fig.4 Dependency  $R_{HVS}(t)$ 

 Fig.5 Dependency  $R(t)$ 

The relative error of the model, defined by Eq.9 is shown in Table 5 and Table 6 for the two cases – with one and two discharge gaps.

$$\Delta = \frac{(R_{exp} - R_{model})}{R_{exp}} \cdot 100\% \quad (9)$$

The match between the experimental and analytical results is good enough so that the suggested method could be used as a model for analysis of the electrical processes in the discharge circuit.

For the accepted way of modeling, the coefficients a and b depend on the capacitance of the capacitor battery C, the voltage, to which it is charged  $U_c$  and the number of experiments. After conducting experimental analysis these dependencies could be analytically modeled.

TABLE 5. RELATIVE ERROR OF THE MODEL FOR  $R_{HVS}(t)$ 

$\Delta, \%$	$U_c, \text{kV}$	<b>9.5</b>	<b>10</b>	<b>10.5</b>	<b>11</b>	<b>11.5</b>
<b>C=0,5μF</b>	$A_1/A_2$	2.56	3.28	2.55	2.46	2.14
	$A_2/A_3$	13.4	15.3	11.6	10.3	8.48
	$A_3/A_4$	6.87	4.75	2.17	1.16	1.39
	$A_4/A_5$	12.7	17.3	12.5	10.5	10.9
<b>C=1μF</b>	$A_1/A_2$	0.358	0.905	0.619	0.569	0.447
	$A_2/A_3$	3.07	5.59	4.51	3.56	2.51
	$A_3/A_4$	5.65	6.02	7.14	4.07	1.91
	$A_4/A_5$	2.33	0	2.22	0.513	0.476
<b>C=1,5 μF</b>	$A_1/A_2$	0.885	0.817	0.508	0.509	0.395
	$A_2/A_3$	5.35	4.75	3.003	2.60	2.61
	$A_3/A_4$	5.48	4.63	2.90	1.40	3.40
	$A_4/A_5$	0.182	0.160	0	1.02	0.860
<b>C=2 μF</b>	$A_1/A_2$	1.18	0.882	0.471	0.719	1.20
	$A_2/A_3$	6.45	5.48	4.48	4.84	6.93
	$A_3/A_4$	5.66	6.95	10.2	7.29	8.24
	$A_4/A_5$	1.01	1.19	4.73	2.14	0.915

TABLE 6. RELATIVE ERROR OF THE MODEL FOR  $R(t)$ 

$\Delta, \%$	$U_c, \text{kV}$	<b>9.5</b>	<b>10</b>	<b>10.5</b>	<b>11</b>	<b>11.5</b>
<b>C=0,5μF</b>	$A_1/A_2$	3.11	3.76	2.88	3.07	2.69
	$A_2/A_3$	16.8	17.9	14.1	13.6	11.7
	$A_3/A_4$	9.68	5.77	4.28	2.43	0.0459
	$A_4/A_5$	20.1	24.7	16.6	15.8	15.5
<b>C=1μF</b>	$A_1/A_2$	1.30	0.902	0.984	0.811	0.725
	$A_2/A_3$	7.58	5.61	6.10	4.34	3.12
	$A_3/A_4$	5.25	4.63	5.70	1.77	1.48
	$A_4/A_5$	3.94	1.87	1.23	2.90	5.04
<b>C=1,5 μF</b>	$A_1/A_2$	1.64	1.43	0.765	0.67	0.558
	$A_2/A_3$	8.73	7.41	3.70	2.99	2.49
	$A_3/A_4$	3.80	3.18	0.230	0.773	0.529
	$A_4/A_5$	7.03	5.26	3.73	3.96	3.11
<b>C=2 μF</b>	$A_1/A_2$	1.93	1.64	0.899	0.647	0.948
	$A_2/A_3$	8.61	8.07	5.41	3.74	5.24
	$A_3/A_4$	0.753	2.68	5.22	2.86	3.61
	$A_4/A_5$	11.6	6.49	0.548	0.957	1.87

#### IV.

#### CONCLUSION

Mixed approach is used for the analysis – analytical and identification – for modeling of the discharge processes in a discharge circuit with one and two discharge gaps. The obtained results give possibility to describe the character of the generated high voltage discharge pulse in liquid (water) at the usage of a thyratron as a high voltage controllable switch.

At comparative evaluation of the experimentally and analytically received results for the discharge current amplitudes, the matching is sufficiently good. The assumption that the dependency  $R=R(t)$  can be presented with a hyperbola brings to increasing of the differences between the experimental results and analytical ones in the next periods of the periodically attenuating oscillation.

#### ACKNOWLEDGEMENT

The presented results in the current paper are obtained under working at project Д002-18/23.02.2009, financed by the Scientific Research Fund at the Ministry of Education, Youth and Science of Republic of Bulgaria.

#### REFERENCE

- [1] Yavorovsky, N.A., S.S. Peltsman, J.I.Komev, Yu.V Volkov, Technology of water treatment using pulsed electric discharges,. The 4th Korea-Russia International Symposium on Science and Technology, KORUS 2000. Proceedings, Vol. 3, pp. 422 – 427.
- [2] Lee H Y., H. S. Uhm, H. N. Choi, Y. J. Jung Bang K. Kang Hee C. Yoo, Underwater Discharge and Cell Destruction by Shockwaves, Journal of the Korean Physical Society, Vol. 42, February 2003, pp. S880\_S884.
- [3] Miyazaki Y., K. Satoh, H. Itoh, Pulsed Discharge Purification of Water Containing Nondegradable Hazardous Substances, Electrical Engineering in Japan, Volume 174, Issue 2, pages 1–8, 30 January 2011.
- [4] Martin-Ramos J. A., A. M. Pernía, J. D. F. Nuño, J. A. Martínez, Power Supply for a High-Voltage Application, IEEE Transactions on power electronics, Vol. 23, № 4, July 2008, pages 1608-1619.
- [5] Dillard William C. 21 - Power Electronics in Capacitor Charging Applications. Power Electronics Handbook (Third Edition), 2011, Pages 567-572.
- [6] Ivanova M., Comparative experimental study of the influence of different controllable high-voltage switches over the formation of discharge in liquid medium, Journal of International Scientific Publication: Materials, Methods & Technologies, 2012, Vol. 4, Part 1, pp.60-75, ISSN 1313-2539
- [7] Barudov S., M.Dicheva, Modeling of a discharge pulse in a circuit with two discharge gaps, iCEST 2010, 23-26 June, 2010, Ohrid, Macedonia, vol.2, ISBN: 978-9989-786-58-7, pp. 823-827.

# Analysis and Design of Instrumentation Amplifiers

Ivailo Pandiev<sup>1</sup>

**Abstract –** The paper presents the structure and the principle of operation of the basic instrumentation amplifier (in-amp) circuit employing three voltage-feedback operational amplifiers (VFOAs). Based on the analysis of the principle of operation are obtained equations for the transfer functions and formulas for the most important static and dynamic parameters. Moreover, using the obtained formulas is developed a design procedure and recommendations for simulation modeling, using standard and statistical analyses. The effectiveness of the proposed procedure is shown by simulation modeling of sample circuits of in-amps.

**Keywords –** Analogue circuits, In-Amps, Programmable gain in-amp, VFOA, Design procedure, Analogue simulation.

## I. INTRODUCTION

The instrumentation amplifiers (in-amps) are essential building blocks of data acquisition systems and are used to extract a weak signal from a noisy environment [1-3]. In the last ten years have been created many monolithic two- op amps and three- op amps in-amps [4-6]. Since for the monolithic in-amps the active and the passive components are implemented within the same semiconductor substrate, they can be closely matched. This will ensure that the amplifiers provide a high *CMRR*. In addition, these components will stay matched over temperature, ensuring good performance over a wide temperature range. In comparison with the monolithic in-amps, offered by the manufacturers of analogue ICs, the in-amps with discrete passive components propose design flexibility at low cost and can sometimes provide performance unattainable with monolithic amplifiers, such as high bandwidth.

The analysis of existing literature showed a wide variety of books and technical documents [1, 7-13], which discuss various aspects of the analysis and design of the in-amps. In [1] and [8-13] the attention of the authors is focused primarily on the principles of operation of the basic circuits of in-amps, as well as some recommendations for selecting the values of the feedback resistors are given. In [7] the authors presented a procedure for designing in-amps realized on the basis of the classic three- op amp circuit. Moreover, the procedure does not include recommendations for calculating the output offset voltage, as well as its temperature drift, frequency bandwidth and equivalent output noise voltage. Also in [7] are not defined recommendations for getting values of the feedback resistors to obtain an optimum value of the *CMRR*.

In this paper on the basis of theoretical analysis of the three- op amps in-amps with discrete passive components a new systematic design procedure is proposed.

<sup>1</sup>Ivailo Pandiev is with the Faculty of Electronics at Technical University of Sofia, 8 Kl. Ohridski Blvd, Sofia 1000, Bulgaria, E-mail: ipandiev@tu-sofia.bg.

## II. THEORETICAL ANALYSIS OF THE THREE- OP AMPS IN-AMPS

An object of study is the circuit of the three- op amp in-amp, given on Fig. 1. The input section consists of two op amps with negative feedback through the resistors  $R_2$ ,  $R_3$  and  $R_{GAIN}$ . It has a symmetrical input and output. The output section of the circuit is a differential amplifier with a differential input  $U_{AD}$  and a single-ended output  $U_o$  with respect to a reference terminal *REF*.

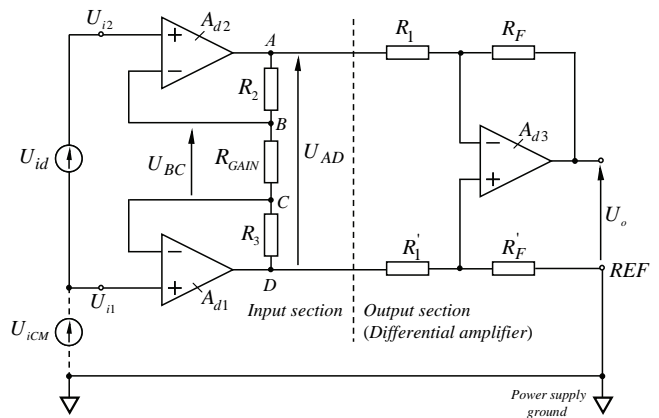


Fig. 1. A structure of the three- op amp circuit

At condition, that the op amps are ideal active elements and  $\frac{R_F}{R_1} = \frac{R'_F}{R'_1}$  for the differential voltage gain is obtained

$$A_U = \frac{U_o}{U_{id}} = A_{U1} A_{U2} = \left( 1 + \frac{R_2 + R_3}{R_{GAIN}} \right) \frac{R_F}{R_1}, \quad (1)$$

where  $A_{U1} = \frac{U_{AD}}{U_{id}} = 1 + \frac{R_2 + R_3}{R_{GAIN}}$  is the differential gain of the input section and  $A_{U2} = \frac{U_o}{U_{AD}} = \frac{R_F}{R_1}$  is the differential gain of the output section.

From equation (1) it can be seen, that the necessary voltage gain for differential signals can be varied by changing the value of the resistor  $R_{GAIN}$ , without affecting the symmetry of the circuit. If  $R_{GAIN} = \infty$  the input section operates as a voltage follower and the differential voltage gain of the circuit is determined only by the gain of the output section.

At condition, that the op amps are real active elements ( $A_d \neq \infty$ ) at high frequencies the open-loop voltage gain is a complex quantity, which in the most cases can be approximated with a first-order transfer function, according to the following equation

$$\dot{A}_d = \frac{A_{d0}}{1 + j(f/f_p)}, \quad (2)$$

where  $A_{d0}$  is the low-frequency open-loop voltage gain and  $f_p$  is the dominant pole of the op amps.

Then the total complex voltage gain of the in-amp is obtained as a second-order transfer function, containing two real poles. Thus the pole frequencies at  $R_2=R_3=R$  are

$$f'_{p1} = f_{p1(2)}(1 + \beta_1 A_{d0,1(2)}) \text{ and} \quad (3a)$$

$$f'_{p2} = f_{p3}(1 + \beta_2 A_{d0,3}), \quad (3b)$$

where  $A_{d0,1(2)}$  and  $A_{d0,3}$  are the low-frequency open-loop gains of the input and output sections,  $f_{p1(2)}$  and  $f_{p3}$  are the dominant pole frequencies of the op amps and  $\beta_1 = \frac{R_{GAIN}/2}{R + R_{GAIN}/2}$  and  $\beta_2 = R_l/(R_l + R_F)$  are the feedback coefficients of the input and output section, respectively.

In the cases when  $A_{U1} > A_{U2}$  the pole frequency of the input section determines the cutoff frequency of the in-amp at high frequencies, i.e. the cutoff frequency  $f_h$  corresponds to value of the pole frequency  $f'_{p1}$ .

Since each part of the input section on Fig. 1 is a non-inverting amplifier, the input resistance of the in-amp is high and is equal to

$$R_{IA} = 2\{2r_{iCM} \parallel [r_{id}(1 + \beta_1 A_{d0})]\}, \quad (4a)$$

where  $r_{iCM}$  is the common-mode input resistance,  $r_{id}$  is the differential-mode input resistance and  $A_{d0}$  is the open-loop voltage gain of the input op amps.

The output resistance is small and is determined by

$$R_{oA} \approx \frac{r_o}{A_{d0,3}} \left(1 + \frac{R_F}{R_N}\right), \quad (4b)$$

where  $r_o$  is the output resistance of the output op amp.

If to the both inputs of the in-amp common-mode voltage ( $U_{i1}=U_{i2}=U_{iCM}$ ) is applied, then  $U_B=U_C=U_{iCM}$  and  $U_A=U_D=U_{iCM}$ . Therefore, the common-mode gain of the input section is equal to one.

Then mathematically, the total common-mode rejection of the in-amp is

$$CMRR = A_{U1} CMRR_3, \quad (5)$$

where  $CMRR_3 = CMRR_{\delta_R} \parallel CMRR_{A_3}$ ,  $CMRR_{A_3}$  is the common-mode rejection of the output amp and  $CMRR_{\delta_R} = (1 + R_F/R_1)/4\delta_R$  ( $\delta_R$  is the tolerance of the resistors  $R_1$ ,  $R_F$ ,  $R'_1$  and  $R'_F$ ).

The total output offset voltage of the in-amp on Fig. 1, caused by the simultaneous action of the input offset voltages  $U_{io1(2)}$  and currents  $I_{io1(2)}$  of the op amps is

$$U_{o,err} = (U_{io1} - U_{io2}) \left(1 + \frac{R_2 + R_3}{R_{GAIN}}\right) \frac{R_F}{R_1} + U_{io3} \left(1 + \frac{R_F}{R_1}\right) - I_{io3} R_F$$

In the worst case  $U_{io1} = -U_{io2}$ , then the value of the output offset voltage is

$$U_{o,err(\max)} = 2U_{io1} \left(1 + \frac{R_2 + R_3}{R_{GAIN}}\right) \frac{R_F}{R_1} + U_{io3} \left(1 + \frac{R_F}{R_1}\right) - I_{io3} R_F. \quad (6)$$

During the implementation of the input section with dual op amp it is possible the output offset, determined by the input offset voltages, to be compensated. The monolithic dual op amp has the advantage, that its components are implemented with the same microelectronic technology and have equal temperature drifts. However, obtaining the same electrical parameters of the two amplifiers is largely accidental. For the worst case the output offset voltage  $\Delta U_{o,err}$ , produced by the temperature drift of the  $U_{io1(2)}$  and  $I_{io1(2)}$ , is

$$\Delta U_{o,err} = 2\Delta U_{io1} \left(1 + \frac{R_2 + R_3}{R_{GAIN}}\right) \frac{R_F}{R_1} + \Delta U_{io3} \left(1 + \frac{R_F}{R_1}\right) - \Delta I_{io3} R_F, \quad (7)$$

where  $\Delta U_{io} = \alpha_{U_{io}} \Delta T$  and  $\Delta I_{io} = \alpha_{I_{io}} \Delta T$  ( $\alpha_{U_{io}}$  and  $\alpha_{I_{io}}$  are the average temperature coefficients of the input offset voltage and current, respectively).

### III. DESIGN PROCEDURE

The above analytical formulas, as a result of the theoretical analysis, are the base of the design procedure for the three-op amp in-amps. The schematic design for the circuit on Fig. 1 is based on the following sequence:

1. *Technical specification.* The circuit elements are calculated using pre-defined: amplitude of the differential-mode input voltage  $U_{id}$  or amplitude of the input differential voltage source  $e_G$  with internal resistance  $R_G$ ; amplitude of the input common-mode voltage  $U_{iCM}$ ; input resistance  $R_{IA}$ ; amplitude of the output voltage  $U_{RL}$  and load resistance  $R_L$ ; output resistance  $R_{oA}$ ; cutoff frequency  $f_h$  at maximum acceptable attenuation coefficient  $M_h$ ; relative error  $\varepsilon_{io}$  [%] defined by the input offset current and voltage, as well as their

temperature drift  $\varepsilon_{\Delta io}$  [%] within temperature range  $\Delta T$ ; minimum value of a signal-to-noise ratio  $SN$  [dB].

*2. An electronic circuit is selected.* An object of an analysis and design is the in-amp circuit shown on Fig. 1. If assume that  $R_2 = R_3 = R$  and  $R_1 = R'_1 = R_F = R'_F$ , then  $A_{U2} = 1$  and  $A_U = A_{U1}$ . Based on the formulas (1) and (5) for the differential gain and common-mode rejection are received

$$A_U = \frac{U_{om}}{U_{id}} = 1 + \frac{2R}{R_{GAIN}} \quad \text{and} \quad CMRR = \left( 1 + \frac{2R}{R_{GAIN}} \right) \frac{1}{2\delta_R}.$$

The typical values for the differential gain  $A_U$  are in the range  $1 \dots 10^3$ . In the case that with the selected op amp can not be achieved the desired differential gain  $A_U$ , but it gets the desired value of the CMRR for the designed in-amp consequently an inverting or a non-inverting amplifier circuit, employing VFOA has to be connected [2].

*3. The op amps are selected.* For the implementation of the input section usually is selected dual precision op amp (for example OP2177 or AD8698) with high common-mode rejection ( $\geq 100dB$ ), small input bias currents ( $< 1nA$ ), and small input offset voltage ( $< 1mV$ ). The output op amp is a single precision amplifier (for example OP1177 or OP177), that provides the maximum output voltage at a given load. Usually for the precision op amps the maximum output current does not exceed several  $mA$  and they no have short-circuit current protection. In addition to the pin marked with  $REF$ , can be applied an external voltage  $V_{REF}$  from a reference voltage source. The  $V_{REF}$  define the signal ground of the in-amp at single power supply. The op amps of the circuit are selected according to the following conditions:

- Common-mode rejection:  $CMRR_{A_{1(2,3)}} \geq 10 \times CMRR$ ;
- Maximum output voltage for the op amps of the input section:  $U_{om,A_{1(2)}} \geq U_{om} + U_{iCM}$  ( $U_{om,A_{1(2)}}$  is the maximum output voltage of the input op amps);
- Maximum output voltage of the output op amp:  $U_{om,A_3} \geq U_{om} + V_{REF}$  for  $V_{REF} \neq 0$  ( $U_{om,A_3}$  is the maximum output voltage of the output op amp);
- The power supply voltage  $\pm V_{CC}$  is selected higher than maximum output voltages  $U_{om,A_{1(2)}}$  and  $U_{om,A_3}$ , as saving the condition  $V_{CC\min} < V_{CC} < V_{CC\max}$ ;
- Maximum output current  $I_{o\max,A_3} > I_{om}$ , where

$$I_{om} = U_{om} / R_L \quad (\text{for } V_{REF} \neq 0 \text{ is found}$$

$$I_{om} = (U_{om} + V_{REF}) / R_L;$$

- Small-signal bandwidth of the input op amps:  $f'_{pA_{U01(2)}} \geq f'_h$ , where  $f'_h = f_h / \sqrt{M_h^2 - 1}$  and  $f'_{pA_{U01(2)}}$  is a cut-off frequency of the closed-loop gain  $|A_U| = A_U(f)$ ;
- Small-signal bandwidth of the output op amp:  $B_{1,A_3} \geq f'_h$ , where  $f'_h = f_h / \sqrt{M_h^2 - 1}$  and  $B_{1,A_3}$  is the unity gain bandwidth;

– Slew rate is selected  $SR_{A_{1(2,3)}} > 2\pi f_h U_{om}$ .

*4. The values of the feedback resistors  $R_2$  and  $R_3$  are selected:* Select  $R_2 = R_3 = R$ . These resistors should be larger than the minimum value  $R_{2\min} = U_{om,A_{1(2)}} / I_{o\max,A_{1(2)}}$ . Otherwise, it can be overload the output stages of the input op amps. On the other hand, the resistance  $R_2$  have not be greater than the maximum value  $R_{2\max}$ , for precision op amps the resistance have not be higher than  $1 \dots 2M\Omega$ . For larger values of  $R_2$  it increases the influence of the  $U_{io}$ ,  $I_{io}$  and noise.

*5. The value of the gain resistor  $R_{GAIN}$  is calculated:*

$$R_{GAIN} = 2R / (A_U - 1).$$

For the resistors  $R_2$ ,  $R_3$  и  $R_{GAIN}$  are selected standard values, usually with a tolerance of  $\pm 1\%$  or less.

*6. The values of the feedback resistors  $R_1$ ,  $R'_1$ ,  $R_F$  and  $R'_F$  are selected:* Select  $R_1 = R'_1 = R_F = R'_F$  ( $A_{U2} = 1$ ). These resistors should be larger than the minimum value  $R_{F\min} = U_{om,A_3} / I_{o\max,A_3}$ . Otherwise, it can be overloaded the output stage of the output op amp. On the other hand, the resistances have not be greater than  $1 \dots 2M\Omega$ .

*7. The necessary value of the tolerance  $\delta_R$  of the resistors  $R_1$ ,  $R'_1$ ,  $R_F$  and  $R'_F$  are calculated:*

$$\delta_R \leq \frac{A_U}{2 \times CMRR} \cdot 100\%.$$

*8. The input and output resistance is calculated using Eq. (4a) and (4b), respectively.* The obtained values for the input and output resistance is compared with the values given in step 1 of the procedure.

*9. The output offset voltage of the circuit is calculated.* First the output offset voltage for room temperature (usually in data-sheets the input offset voltage and current of the op amp is defined at  $25^\circ C$ ) is calculated according to Eq. (6). Then the relative error  $\varepsilon_{io} = (U_{o,err} / U_{R_L}) 100\%$  is compared with the value given in step 1.

*10. The output offset voltage drift is calculated.* First the output offset voltage drift is calculated by Eq. (7) for the given temperature range  $\Delta T$ . Then the relative error  $\varepsilon_{\Delta io} = (\Delta U_{o,err} / U_{R_L}) 100\%$ , is compared with value the given in step 1. If the results for  $\varepsilon_{io}$  and  $\varepsilon_{\Delta io}$  do not satisfy the specification it can be chosen more precision op amps or to make new calculations for the resistances with lower values.

*11. The signal-to-noise ratio (SN) is calculated.* First the resulting noise density at the amplifier's output is calculated:

$$\bar{S}_{U,out} = \sqrt{\sum_i S_{U_i}^2} \quad \text{for } i = 1, 2, \dots,$$

where  $S_{U_i}$  is the individual noise components.

$$\text{Then } SN = \frac{U_{o,eff}}{U_{oN}} = \frac{U_{o,eff}}{\bar{S}_{U,out} \sqrt{B_{eq}}} , \text{ where } B_{eq} = 1,57 f'_h \text{ is}$$

the bandwidth of the circuit multiplied by the correction factor of  $\pi/2 \approx 1,57$  and  $U_{o,eff}$  is the output effective value.

#### 12. Verification check of the designed in-amp in DC and AC domain by using Cadence OrCAD®.

#### IV. SIMULATION TESTING AND ANALYSES

To verify the theoretical analysis and the proposed procedure a digitally programmable gain in-amp (PGiA) (Fig. 2) was implemented with the following pre-defined parameters:  $U_{id} = 0... \pm 10mV$ ,  $\pm 20mV$ ,  $\pm 40mV$  and  $\pm 80mV$  at  $R_G = 5k\Omega$ ;  $R_{IA} \geq 10M\Omega$ ;  $A_U = 250$ , 125, 62,5 and 31,25 at  $R_L = 2k\Omega$ ;  $CMRR \geq 90dB$ ;  $R_{oA} \leq 1\Omega$ ;  $f_h = 100Hz$  at  $M_h = 3dB$ ;  $\varepsilon_{io} < 0,5\%$ ,  $\varepsilon_{\Delta io} < 0,2\%$  (within temperature range  $\Delta T = 40^{\circ}C$ );  $SN_{min} > 80dB$ .

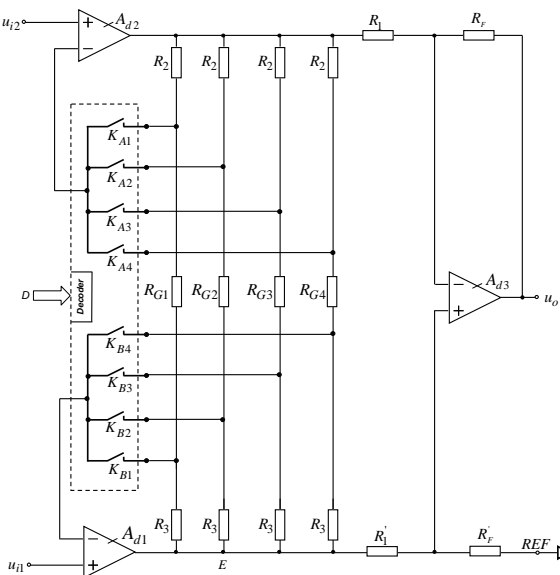


Fig. 2. A structure of the designed PGiA circuit

The circuit is designed using VFOA OP1177 and OP2177 (from Analog Dev.), biased with  $\pm 5V$  supplies. The verification check of the circuit was performed within OrCAD PSpice, using corresponding PSpice-based macro-models. The models reflect typical values of the datasheet parameters for power supply voltages  $\pm 15V$  and not capable of simulating some of the input parameters and the temperature effects.

The values of the calculated passive in-amp components are:  $R_2 = R_3 = 10k\Omega \pm 1\%$ ,  $R_{G1} = 80,6\Omega \pm 1\%$  (at  $A_{U1} = 250$ ),  $R_{G2} = 162\Omega \pm 1\%$  (at  $A_{U2} = 125$ ),  $R_{G3} = 324\Omega \pm 1\%$  (at  $A_{U3} = 62,5$ ),  $R_{G4} = 665\Omega \pm 1\%$  (at  $A_{U4} = 31,25$ ) and  $R_1 = R_1' = R_F = 10k\Omega$  with tolerances  $\pm 0,1\%$ . The controlling digital word  $D$  for the in-amp will provide gains of 31,25, 62,5, 125 and 250, through synchronous switching of the two groups of switches ( $K_{A1}-K_{A4}$ ) and ( $K_{B1}-K_{B4}$ ) with the decoder.

In Table 1 are presented the calculated parameters and the simulation results for the designed in-amp. The maximum

error between calculated values of the electrical parameters and the simulation results is not higher than 5%. Moreover, an error of 5% is quite acceptable considering the tolerances of the technological parameters.

TABLE I  
COMPARISON BETWEEN CALCULATED PARAMETERS AND SIMULATION RESULTS FOR THE DESIGNED IN-AMP.

Parameter	Cal. results	Sim. results
$U_{o,err}$	from 0,03mV to 1...7,5mV	from 0,032mV to 0,95...7,56mV
$\varepsilon_{io}$	from 0,001% to 0,04...0,3%	from 0,0012% to 0,038...0,3%
$\Delta U_{o,err}$	from 0,014mV to 0,5...4mV	n/a
$\varepsilon_{\Delta io}$	from 0,0005% to 0,02...0,16%	n/a
$U_{om}$	2,5V	2,5V
$f'_h$ at $A_U = 250, 125, 62,5$ and $31,25$	5,68kHz, 11,4kHz, 22,7kHz, 45,5kHz	5,75kHz, 11,5kHz, 22,3kHz, 45,6kHz
$R_{IA} / R_{oA}$	$2 \cdot 10^{12}\Omega / 0,03m\Omega$	$1,93 \cdot 10^{12}\Omega / 0,03m\Omega$
$CMRR$	90dB	96,38 <sub>min</sub> ... 98,26dB <sub>max</sub>
$\bar{S}_{U,out}$ at $R_{GI}=80,6\Omega$	$2,85\mu V/Hz^{1/2}$	$2,91\mu V/Hz^{1/2}$
$SN$	93,9dB	93,7dB

#### V. CONCLUSION

A design procedure of three- op amp in-amp circuits has been presented. The efficiency of the procedure is demonstrated by design and verification of concrete electronic circuits using precision VFOAs OP1177 and OP2177. The created approach can be useful for design of various electronic devices, such as precision amps, PGiAs and high-speed video amps.

#### REFERENCES

- [1] Kitchin, C., L. Counts. *A Designer's Guide to Instrumentation Amplifiers*, 3rd Addition, Analog Dev., 2006.
- [2] W. Jung, *Op Amp Applications Handbook*, Newnes, 2005.
- [3] V. Tietze, Ch. Schenk. *Electronic circuits*. 2nd Edition. New York. Springer-Verlag, 2008.
- [4] Instrumentation Amplifiers, Analog Dev., <http://www.analog.com>, last accessed February 20, 2013.
- [5] Instrumentation Amplifiers, Texas I., <http://www.ti.com>, last accessed February 20, 2013.
- [6] Instrumentation Amplifiers, Linear Tech., <http://www.linear.com>, last accessed February 20, 2013.
- [7] V. Zlatarov et al. *The designer's guide to analog circuits and systems*. Tehnika, Sofia, 1993 (in Bulgarian).
- [8] R. Mancini, *Op Amps for Everyone Design Guide* (Rev. B), Texas I., 2002.
- [9] M. Seifart, *Analoge Schaltungen*. 6 Auflage. Verlag Technik Berlin, 2003 (in German).
- [10] T. Kugelstadt, Getting the most out of your instrumentation amplifier design. Texas I., Analog Applications Journal, 2005.
- [11] Instrumentation Amplifier. AN1298.2, Intersil, 2009.
- [12] N. Albaugh, *The instrumentation amplifier handbook*, Cypress Semiconductor, 2012.
- [13] J. Li, S. Pun, M. Vai, P. Mak, P. Mak, F. Wan. "Design of Current Mode Instrumentation Amplifier for Portable Biosignal Acquisition", BioCAS 2009, pp. 9-12, Beijing, 2009.

# Pspice Simulation of Optoelectronic Circuits of Detectors

Hristo Sabev<sup>1</sup> and Tsanko Karadzhov<sup>2</sup>

**Abstract –** The operation of circuits of ionizing radiation detectors, implemented by means of PIN photodiodes, is simulated. Semiconductor optoelectronic detectors of ionizing radiation- silicon and germanium are examined. Two electric circuits for temperature compensation in the performance of optoelectronic detectors of ionizing radiation at low energy levels of ionizing particles in fast and slow changes in temperature are proposed. Simulation of the output voltage of the optoelectronic detectors is implemented.

**Keywords –** Ionizing radiations, PIN photodiodes, PSPICE simulations.

## I. INTRODUCTION

Standards for optoelectronic detectors of ionizing radiations are given in [1, 2, 3]. The optoelectronic detectors of ionizing radiations, including PIN photodiodes, are viewed in [4, 5, 6, 7, 8, 10, 11]. The operation of three circuits of ionizing radiation detectors, realized by means of PIN photodiodes, are simulated. They are considered in [9].

## II. OPTOELECTRONIC CIRCUITS OF DETECTORS

Figure 1 shows a circuit where the PIN photodiode is connected to an AC current circuit. The circuit is used for registering ionizing radiations. The photodiode operates under inverse voltage in photodiode mode. The amplifier DA1 has a high input resistance. A silicon PIN photodiode SFH 520 of large area is used [11].

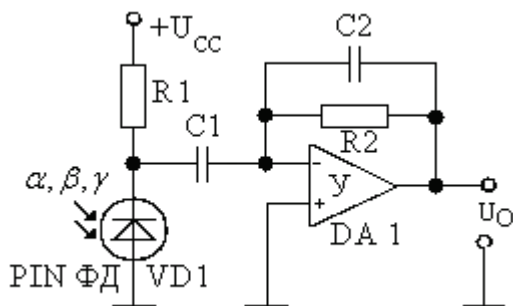


Fig. 1. Circuit where the PIN photodiode is connected

Within the next circuits an operating photodiode (VD1) and

<sup>1</sup>Hristo Sabev is with the Faculty of Electrical Engineering and Electronics at Technical University of Gabrovo, 4 H. Dimitar, Gabrovo 5300, Bulgaria.

<sup>2</sup>Tsanko Karadzhov is with the Faculty of Mechanical and Precision Engineering at Technical University of Gabrovo, 4 H. Dimitar, Gabrovo 5300, Bulgaria.

a compensating photodiode (VD2) are used.

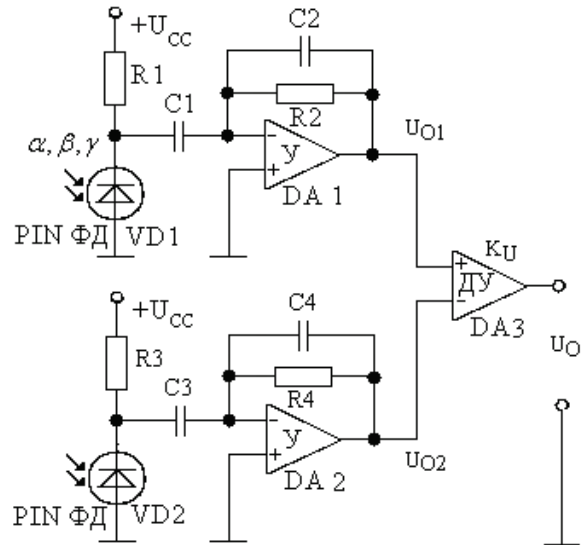


Fig. 2. A detector circuit with compensation of fast temperature changes

The output circuit voltage is:

$$U_o = K_U \cdot I_{ph1} \cdot R_2 \quad (1)$$

$$U_o = K_U \cdot (U_{o1} - U_{o2}) = K_U \cdot [(I_{ph1} + I_{D1}) \cdot R_2 - I_{D2} \cdot R_2] = K_U \cdot I_{ph1} \cdot R_2 \quad (2)$$

When the photodiodes are identical, the two dark currents are equal  $I_{D1} = I_{D2}$

where  $K_U$  - coefficient of amplification according to the voltage of the differential amplifier DA3,  $I_{ph1}$  - photocurrent of the PIN photodiode 1,  $I_{D1}$ ,  $I_{D2}$  - dark currents of the PIN photodiodes 1 and 2. The following conditions must be satisfied:

$$R1 = R3; R2 = R4; C1 = C3; C2 = C4; I_{ph2} = 0 \quad (3)$$

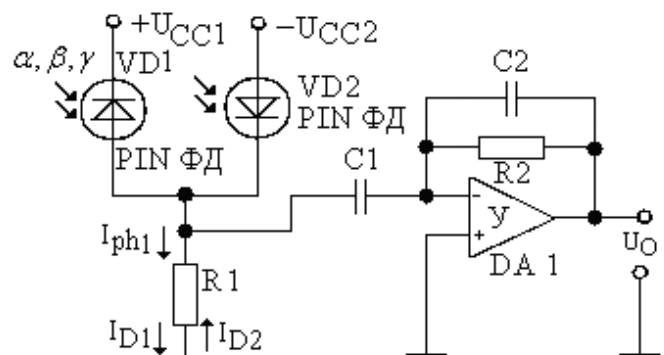


Fig. 3. A detector circuit with compensation of slow temperature changes

The supply voltages of the circuit are equal  $U_{CC1} = U_{CC2}$

The voltage on the resistor R1 is:

$$U_{R1} = [I_{ph1} + (I_{D1} - I_{D2})] \cdot R_1 = I_{ph1} \cdot R_1$$

$$I_{D1} = I_{D2}; I_{ph2} = 0 \quad (4)$$

For the circuits in fig. 2 and fig. 3 differential detectors or coordinate (position)-sensitive detectors (PSD) should be used.

For an operation in a wide temperature range the photodiodes of ORTEC company should be used [10]. ORTEC produces photon detectors made of high purity germanium (Ge), of a P or N type with a cryostat.

The circuits in fig. 1, 2 and 3 possess a common basic circuit shown in fig. 4.

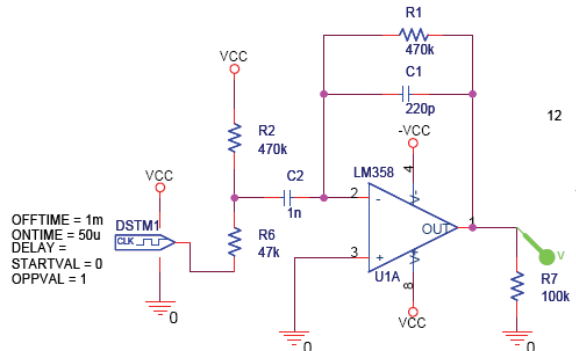


Fig. 4. Basic circuit for PSPICE simulations of optoelectronic detectors

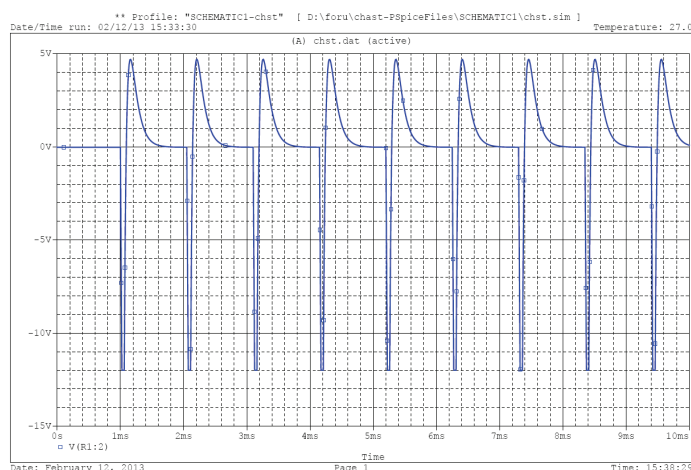


Fig. 4.a. Output voltage of the circuit in fig. 4.

### III. CONCLUSION

Circuits of optoelectronic detectors of ionizing radiation, implemented by means of PIN photodiodes, are simulated. The results from the simulations are compared with those obtained from the calculations and measurements done.

### REFERENCES

- [1] БДС 10165:1972. Ядрено уредостроене. Детектори на ионизиращи излъчвания полупроводникови с електронно-

дупчест преход, силициеви спектрометрични. Технически изисквания.

- [2] ГОСТ 26222-86. Детекторы ионизирующих излучений полупроводниковые. Методы измерения параметров.
- [3] ГОСТ 20766-75. Детекторы ионизирующих излучений полупроводниковые спектрометрические. Типы и основные параметры.
- [4] Колев, И. С. и Е. Н. Колева. Инфрачервена оптоелектроника. (Второ преработено и допълнено издание). Габрово, Унив. изд. "В.Априлов", 2008, ISBN 978-954-683-402-7.
- [5] Колев, И. С. и Е. Н. Колева. Кохерентна оптоелектроника. Пловдив, Автоспектър, 2008, ISBN 978-954-8932-46-2.
- [6] Колев, И. С. и Е. Н. Колева. Некохерентна оптоелектроника. Габрово, Унив. изд. "В. Априлов", 2007, ISBN 978-954-683-373-0.
- [7] Колев, И. С . и Е . Н . Колева. Оптоелектроника. Прибори. Елементи. Приложения. София, Техника, 2007, ISBN 978-954-03-0670-4.
- [8] Колев, И. С. и Е. Н. Колева, Оптоелектронни сензори и оптоелектронни охранителни системи. Габрово, Унив. изд. "В. Априлов", 2009, ISBN 978 – 954 – 683 – 420 – 1.
- [9] И. С. Колев, Е. Н. Колева и Х. П. Събев. Оптоелектронни детектори на ионизиращи лъчения . Optoelectronic Detectors for Ionizing Radiations. International Scientific Conference, UNITECH, 2012, Gabrovo, 16-17.XI.2012, Proceedings, vol. 1, I-209, I- 214.
- [10] ORTEC. Semiconductor Photon Detectors, 2012.
- [11] Siemens Semiconductor Group. SFH520 -  $\alpha$ - $\beta$ - $\gamma$ -Strahlungsdetektoren.  $\alpha$ - $\beta$ - $\gamma$ - Radiation Detectors, 2000.
- [12] Александров Б., "Развитие на методите за защитно кодиране при съхранение и обмен на информация в компютърните системи", дисертационен труд: 2001г., 152 стр.
- [13] B. Aleksandrov, N. Siniagina, P. Kochevski; "Secret Sharing Based on the Residue Theorem"; Jurnal og Communication and Computer; David Publishing Company, US, vol. 9, number 2, 2012; pp.148÷154; ([www.davidpublishing.com/journals](http://www.davidpublishing.com/journals))

# Subtraction Procedure for Removing the Baseline Drift from ECG Signals: Adaptation For Real Time Operation With Programmable Devices

Tsvetan Shoshkov<sup>1</sup> and Georgy Mihov<sup>2</sup>

**Abstract** – The present work is focused on developing a generalized subtraction procedure for suppressing baseline drift from electrocardiogram (ECG) signals, operating in real time and adapting it for programmable logic (FPGA) operation. The development of the algorithm is done in Matlab environment and is tested for many practical scenarios. The prototype version of the subtraction procedure is implemented for programmable logic using VHDL. Here is presented the generated programmable logic structure in FPGA. Converting the theoretical algorithm to real time execution determines the use in calculations of single signal values in their natural sequence. The execution results show that the developed real time algorithm successfully eliminates the baseline drift in one ingoing ECG sample, concluded before the appearance of the next one. This research represents a suitable platform for future investigations and development of the subtraction procedure and also for particular practical applications.

**Keywords** – ECG, drift, drift removing, subtraction procedure.

## I. INTRODUCTION

The electrocardiogram (ECG) is often affected by drift, due to complex mechanical and electro-chemical electrode-to-skin processes. The subtraction procedure shows good results in removing baseline drift from ECG signals. The process flow is shown on fig. 1. Its structure contains three main stages:

– *Detecting linear segments*. Each ECG sample is checked if it belongs to a linear segment by using appropriate linearity criterion. The linearity is defined by comparing the criterion with a predefined threshold  $M$ .

$$Cr \leq M . \quad (1)$$

– *Baseline drift calculation*. If it is detected a linear segment the baseline drift is calculated using a digital filter and it is stored in a temporal FIFO buffer. In the same time the baseline drift is subtracted from the linear segment;

– *Baseline drift extrapolation*. If the current sample belongs to a nonlinear segment the value of the drift is calculated using the data stored in the temporal buffer and it is subtracted from the signal in a nonlinear segment.

The present work describes the organization of the subtraction procedure for ECG drift removing in real time and its adaptation with programmable logic FPGA.

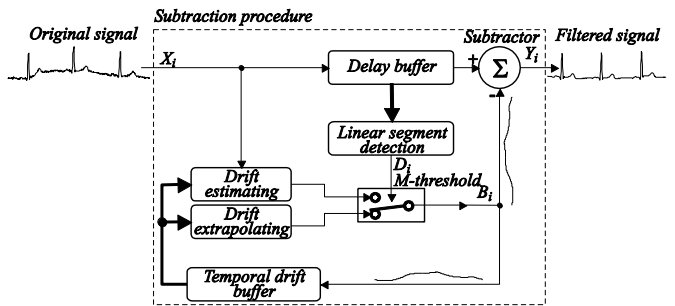


Fig. 1. Basic Structure of the Subtraction Procedure for Baseline Drift Removing.

## II. ADAPTING THE SUBTRACTION PROCEDURE FOR REAL TIME DRIFT REMOVING

The prototype of the drift removing algorithm using the subtraction procedure is developed on the basis of the latest investigations of the subtraction procedure [1, 2]. The baseline drift filtering algorithm in [1] is a procedure that is not working in real time and is processing a buffer with samples of the input signal.

An important point that distinguishes the real time subtraction procedure algorithm is the processing of the signal samples in their natural sequence. Thus the digital filter needs access to several of the previous and next samples. The input signal is being stored in a delay buffer where a sequence of samples that surround the current one can be accessed.

The delay buffer length is defined by the length of the longest epoch that is processed in one stage of the procedure. In this case this is the linearity detection procedure. The linearity criterion is applied over  $k$  periods of the power line frequency, that is  $N = k.n + 1$ . The  $n = \Phi/F$  ratio represents the multiplicity of the sampling frequency  $\Phi$  and the power line frequency  $F$ . It is rarely an integer and in the calculations it is used the rounded value  $n = \text{round}(\Phi/F)$ . Due to some considerations it is selected  $k = 6$ . The length of the delay buffer is  $N = 6.n+1$  samples, its organization is shown on fig. 3. The input sample  $X_i$  is stored in the temporal buffer  $X_i \rightarrow X_{B0}$  and all other values are shifted in one step forward.

The used linearity criterion is

$$Cr = |D| . \quad (1)$$

The value of  $D$  represents the signal acceleration that is calculated using its second derivative. This corresponds to the second difference in digital signal processing. It is calculated

<sup>1</sup>Tsvetan Shoshkov is with the Faculty of Electronic Engineering and Technologies at Technical University of Sofia, 8, St. Kl. Ohridsky Blvd, 1000 Sofia, Bulgaria, E-mail: tsh@tu-sofia.bg.

<sup>2</sup>Georgy Mihov is with the Faculty of Electronic Engineering and Technologies at Technical University of Sofia, 8, St. Kl. Ohridsky Blvd, 1000 Sofia, Bulgaria, E-mail: gsm@tu-sofia.bg.

```

for i=1+N: 1: length(X); % Start of Subtraction procedure
    for j=N: -1: 2; XB(j)=XB(j-1); end % Delay buffer shifting
    XB(1) = X(i); % Storing ongoing sample into Delay buffer
    if Max<XB(1+(N-1)/2);Max=XB(1+(N-1)/2);
    else Max=Max- (Max-Min)/N/20; end;
    if Min>XB(1+(N-1)/2); Min=XB(1+(N-1)/2);
    else Min=Min+ (Max-Min)/N/20; end;
    Mpp= Max-Min;
    if Mmu>Mpp; Mmu=Mpp;
    else Mmu=Mmu+Mpp/N/20; end
    Md = Mpp*mu; % Dynamic threshold
    D = ((XB(1)-2*XB(1+(N-1)/2)+XB(N))/4; % Normalised second difference
    FD = ((XB(1)-XB(N))/2; % Normalised first difference
    Cr = abs(D); % Linearity criterion
    FCr = abs(FD)/5; % Second criterion
    if Cr > Md; % Non-linear segment
        B=DB(1)+(DB(1)-DB(N))/(N-1)/2; % Drift calculating
    else % Linear segment
        if FCr > Md; % Second criterion threshold
            B=DB(1)+(XB(1)-DB(1))/(N-1)/1; % Drift calculating
        else
            B=DB(1)+(XB(1)-DB(1))/(N-1)/2; % Drift calculating
        end
    end
    for j=N: -1: 2; DB(j)=DB(j-1); end % Drift buffer shifting
    DB(1)=B; % Storing Drift into Drift buffer
    Y(i-(N-1)/2)=X(i-(N-1)/2)-DB(1); % Ongoing output sample
end % End of Subtraction procedure

```

Fig.2. Fragment of the Program in the Matlab Environment for Baseline Drift Removing Using the Subtraction Procedure.

by subtracting the first two differences  $FD$  of the signal. Each of the first differences is obtained using the amplitude of two samples that are separated by  $k.n/2$  periods of the power line frequency. The equation of the linearity detecting filter is

$$D_i = (X_{Bi+(N-1)/2} - 2.X_{Bi} + X_{Bi-(N-1)/2})/4. \quad (3)$$

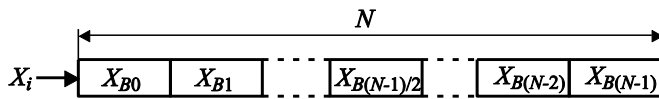


Fig. 3. Organization of the Delay Buffer.

The variety of ECG signals and the difference of their amplitudes demands dynamical defining of the linearity threshold  $M$ . In order to do so there are used two maximum value detectors  $M_{max}$  and  $M_{min}$ , each of them with an appropriate decreasing coefficient. If  $M_{max}$  is lower than the current value of  $X_{Bi}$ , then  $M_{max} = X_{Bi}$ . In the other case  $M_{max}$  is subtracted with  $(M_{max} - X_{Bi})/(16.N)$ . If  $M_{min}$  is larger than the current value of  $X_{Bi}$ , then  $M_{min} = X_{Bi}$ . In the other case  $M_{min}$  is decreased with  $(X_{Bi} - M_{min})/(16.N)$ . The difference  $M_{pp} = M_{max} - M_{min}$  represents the coefficient that is used to determine the dynamical threshold

$$M = M_{pp}.\mu. \quad (4)$$

In this equation  $\mu$  is selected experimentally for ECG signals in the range of 1 mV.

The *baseline drift extrapolation* stage is used in nonlinear segment. The easiest approach for extrapolation is the linear one. It requires two samples of the temporal buffer. The value of the drift in the nonlinear segments is

$$B_{Bi} = B_{Bi-1} + (B_{Bi-1} - B_{Bi-N})/(N-1). \quad (5)$$

A decreased second term of the equation in (5) is used to prevent drift overcompensating.

The temporal buffer contains  $N$  drift samples. Its organization is shown on fig. 4. The calculated drift is stored in the drift buffer  $B_i \rightarrow B_1$  and all other values are shifted forward.

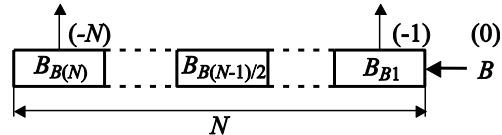


Fig. 4. Temporal Buffer for Drift Storing.

The *baseline drift calculation* stage is used when the linearity criterion detects a linear segment. Here are used two variants of calculation, one described in (6) and another one with decreased second term in (7).

$$B_{Bi} = B_{Bi-1} + \frac{B_{Bi-1} - B_{Bi-N}}{N-1}. \quad (6)$$

$$B_{Bi} = B_{Bi-1} + \frac{B_{Bi-1} - B_{Bi-N}}{2(N-1)}. \quad (7)$$

The periods in which the two methods are used are defined by a second criterion. It is calculated by using the first difference of the signal and defines its slope.

$$FD_i = (X_{Bi+(N-1)/2} - X_{Bi-(N-1)/2})/10. \quad (8)$$

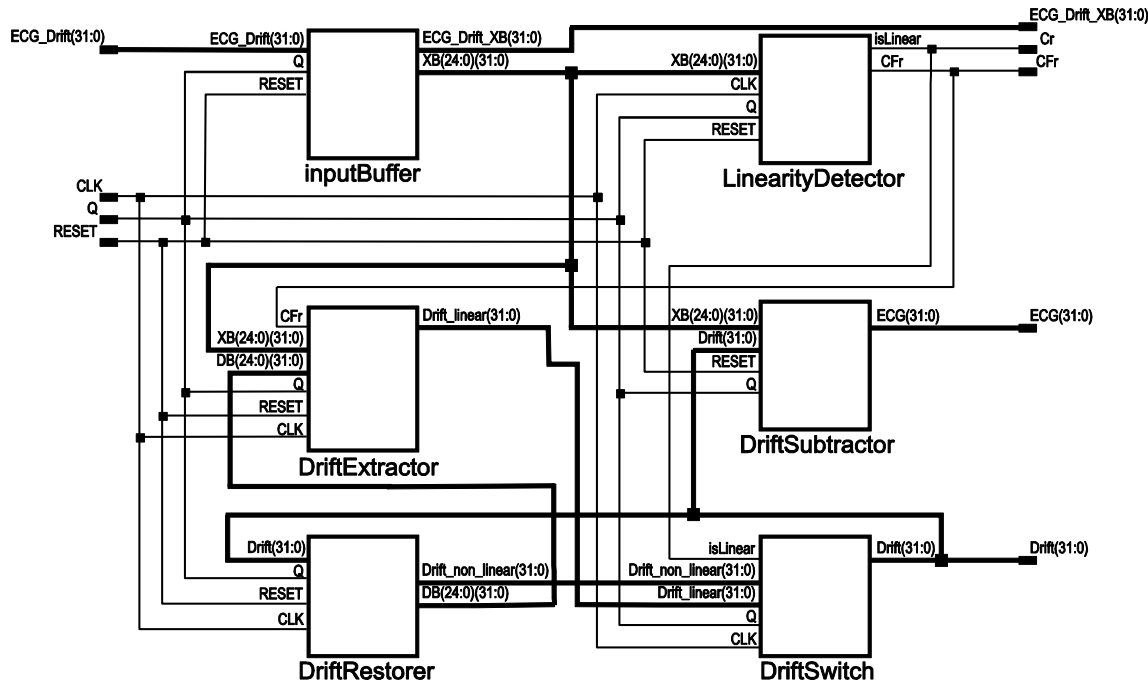


Fig.5. Structure of the Subtraction Procedure Realized For Programmable Logic.

The absolute value of the calculated criterion is compared with the dynamic threshold  $M$ .

$$FCr = |FD_i|. \quad (9)$$

$$FCr < M. \quad (10)$$

Depending on the result of the comparison one of the described equations for drift calculation is used. If (10) is true the equation that is used is (6), otherwise (7) is used.

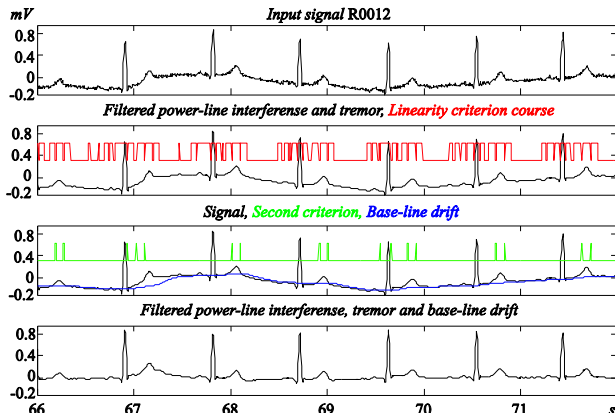


Fig. 6. Experiment in the Environment of Matlab.

Fig. 6 shows an experiment that is processed in the environment of Matlab with a six second long ECG signal that is sampled by 200 Hz signal and with 50 Hz frequency of the power line signal. The experiment shows that the baseline drift is successfully removed using the modeled subtraction procedure in Matlab. On the figure are also shown the graphics of the calculated linearity criterion and the extracted baseline drift.

### III. ADAPTATION FOR REAL TIME OPERATION WITH PROGRAMMABLE LOGIC FPGA

After verifying the efficiency of the subtraction method for drift removing in Matlab, it is developed a hardware realization for real time operation. Programmable logic FPGA and VHDL programming language are used.

The description of the architecture of the device is shown on fig. 5 and it has the same structure of the procedure that is shown on fig. 1. The highest level of the description is structural where are declared and connected the main functional blocks. The descriptions of the blocks are functional and they are located in lower layers of the project. The basic functions of the algorithm are realized by:

- *shift register* is used to store a sequence of input signal samples (InputBuffer);
- *arithmetic logic block* to process input signal drift calculation (DriftExtractor);
- *shift register* stores a sequence of extracted drift samples and an *arithmetic logic block* restores the drift in the nonlinear segments (DriftRestorer);
- *arithmetic logic block* to calculate the linearity criterion (LinearityDetector);
- *signal switching block* that is controlled by the linearity criterion (DriftSwitch);
- *subtraction block* to calculate the output filtered signal using the difference of the input signal and the drift (DriftSubtractor).

There are several approaches used in calculations to simplify the hardware realization. All the calculations are processed using floating point values. The values of the signals used to process the data are 32-bits wide, the higher 16

bits contain the integer part and the lower 16 bits contains the fractional part. In order to avoid calculation mistakes from losing accuracy some of the VHDL signals are 64-bits wide. Fig. 7 shows VHDL code of the DriftSwitch block.

```

entity Drift_Switch is
  Port ( isLinear : in STD_LOGIC;
         Drift_linear : in STD_LOGIC_VECTOR (31 downto 0);
         Drift_non_linear : in STD_LOGIC_VECTOR (31 downto 0);
         Drift : out STD_LOGIC_VECTOR (31 downto 0);
         Q : in STD_LOGIC;
         CLK : in STD_LOGIC );
end Drift_Switch;
architecture Behavioral of Drift_Switch is
begin
  process (CLK) begin
    if (CLK'event and CLK = '1') then
      if Q = '0' then
        if isLinear = '0' then
          Drift <= Drift_linear;
        else
          Drift <= Drift_non_linear;
        end if;
      end if;
    end process;
  end Behavioral;

```

Fig.7. Fragment of the VHDL Code in Xilinx ISE

Two clock signals CLK and Q are used. The results of the calculations are processed for several periods of the CLK signal. The signal Q has frequency that is equal to the sampling frequency (in this case  $\Phi = 200$  Hz), it controls the input of the ECG signal (ECG\_Drift), outputting the values of the filtered signal (ECG), subtracting the (Drift), linearity criterions ( $Cr$  and  $FCr$ ). The second clock (CLK) must have frequency that is 32 times higher than the frequency of Q, a value that is defined by the digits of the numbers, so the required calculations can be processed. The speed of the present FPGA chips allows using clock signals with frequencies up to ten and hundreds MHz, so the frequencies of the CLK and Q signals can be realized. In real time processing of the data the output signal is delayed in comparison to the input ECG signal. This is the time delay needed to fill the input buffer. For more convenient observation of the results, in the output graphics it is used a delayed version of the input signal that is taken from the middle of the input buffer.

#### IV. TESTING THE HARDWARE REALIZATION

The hardware description of the subtraction method for drift removing from ECG signals in real time is realized using the integrated development environment Project Navigator that is included in Xilinx ISE Design Suite 13.1.

To make simulations and test the described digital device, it is created a file with input signals (stimulus) that defines the behavior of the input signals of the device [5]. The input signals data is read from external files and output signals data is stored in external text files. The simulations are processed using the Xilinx ISim simulator and the results are displayed using Matlab. Observation and setting the work of the hardware realization is done with real ECG data.

The input and output signals of the processed simulation are shown on fig. 8. It is shown a processed signal from recording MO1\_012.DCD (the same one is used in the experiment in Matlab on fig. 4).

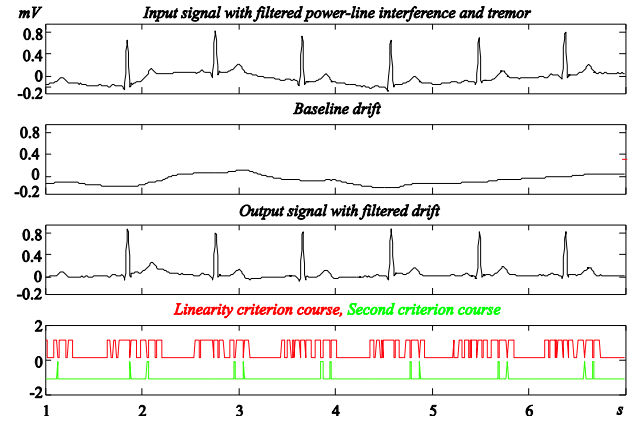


Fig. 8. Test with MO1\_012.DCD.

The achieved accuracy of the hardware realization is remarkable and fully matches the theoretical model that is explored using Matlab. Using 32 bits signals leads to high accuracy and keeps the error of the filtration in the lower 1-2 bits.

#### V. CONCLUSION

The present work describes a practical realization of a very promising method for real time baseline drift removing from ECG signals. The theoretical basics of the method are realized and validated in Matlab. The developed theoretical model is realized in hardware using FPGA. In the process of creating the hardware description of the procedure there are made certain improvements in the calculation procedures. The simulations that are processed and the obtained results show high accuracy and reliability of the device that match the theoretical method.

#### REFERENCES

- [1] G. Mihov, I. Dotsinsky. "Subtraction Procedure For Removing The Baseline Drift From ECG Signals", Annual Journal of Electronics, pp. 118-122, 2010.
- [2] G. Mihov, I. Dotsinsky, C. Levkov, R. Ivanov, "Generalised Equations and Algorithm of the Subtraction Procedure for Removing Power-line Interference from ECG", Proceedings of the Technical University of Sofia, Vol. 58, b. 2, Sofia, pp. 31-38, 2008.
- [3] G. Mihov, I. Dotsinsky, T. Georgieva, "Subtraction Procedure for Powerline Interference Removing from ECG: Improvement for Non-Multiple Sampling", Journal of Med. Engineering & Technology, 29, No 5, pp. 238-243, 2005.
- [4] Ch. Levkov, G. Mihov, R. Ivanov, Ivan K. Daskalov, I. Christov, I. Dotsinsky, "Removal of power-line interference from the ECG: a review of the subtraction procedure", BioMedical Engineering OnLine, 4:50, 2005.
- [5] S. Mihov, R. Ivanov, A. Popov, "Real-Time Subtraction Procedure for Eliminating Power-Line Interference from ECG", ET2008, b. 1, Sozopol, pp. 55-60, 2008.

# Investigation of Thin PZT and ZnO Piezoelectric Layers in Dynamic Mode for Application in MEMS

Georgi Kolev<sup>1</sup>, Krassimir Denishev<sup>1</sup>, Mariya Aleksandrova<sup>1</sup> and Yordanka Dutsolova<sup>1</sup>

**Abstract –** In this paper, some of the results from the investigations of thin piezoelectric layers, created by using of lead zirconate titanate (PZT) and zinc oxide (ZnO) are presented. Both materials are investigated by surface acoustic waves (SAW) method for registration of forward and reverse piezoelectric effect. The MEMS micro generator is prepared by using of PZT layer and investigated in dynamic mode. The dependence between the generated piezoelectric voltage and the frequency of mechanical vibration, applied to the structure, is presented.

**Keywords –** MEMS, EHD, piezoelectric effect, PZT, ZnO, microgenerator.

## I. INTRODUCTION

Nowadays, it has been paid serious attention on developing of systems, using the resources, taken from renewable energy sources, such as sun, wind, vibrations, temperature differences etc [1]. Such primary resource can be stress/pressure, vibration or more generally called mechanical stress [2, 3]. By the choice of appropriated material, which has piezoelectric properties, that mechanical stress can be used for generating of electrical energy [4]. It is possible because of the properties of piezoelectric materials in which a piezoelectric effect is observed. In some materials this effect is so called “forward piezoeffect” - generating electric energy by the applied mechanical pressure, or the “reverse piezoeffect” – when applying voltage to them, they are mechanically deformed. These properties of piezoelectric materials are used generally in system as small-output supply sources.

Nowadays, some of the most frequently investigated energy harvesting devices (EHD) are the piezoelectric microgenerators. Values of 244  $\mu\text{W}$  for the output power have been reported [5]. The piezoelectric microgenerators usually work in so called dynamic mode - periodical mechanical load with different frequency and amplitude and they generate AC piezovoltage. Therefore, this is the reason to make investigations of the layers in dynamic mode by taking into account the dependence of output voltage, according to the frequency of mechanical vibrations.

Lead zirconate titanate (PZT) and zinc oxide (ZnO) films are the most frequently used materials for implementation in such types of devices, because of their relatively high piezoelectric coefficients. There are many reports, concerning different approaches for deposition of such layers [6, 7, 8]. It seems that the sputtering technique is the most favorable,

regarding crystalline structure, chemical composition and thickness control.

In this paper, two of the most widely used piezoelectric materials, PZT and ZnO, are investigated. At the MEMS piezoelectric microgenerators, these materials have to be in form of thin films, with thickness about several hundreds of nanometers. For the investigation of the films a Surface Acoustic Wave (SAW) structure is used, by using of which, the piezoelectric effects, both in the two materials, can be easily registered.

## II. EXPERIMENTAL SECTION

For the experiment, thin PZT and ZnO layers were deposited, with thickness of around  $\sim 100$  nm. A sputtering target ( $\text{Pb}(\text{Zr}_{0.52}\text{Ti}_{0.48})\text{O}_3$ ), purchased from “Semiconductor Wafer, Inc.” and “Goodfellow”, with 75 mm in diameter, and thickness of 3 mm was used. The layers deposition was done in vacuum chamber A400 VL at the following parameters: working vacuum level of  $10^{-5}$  Torr, sputtering inert gas – Ar<sub>2</sub> with partial pressure of  $2.10^{-2}$  Torr, plasma voltage and current, respectively  $U_{\text{plsm}} = 0.75$  kV and  $I_{\text{plsm}} = 150$  mA, plasma power  $P_{\text{plsm}} = 112$  W, deposition time of 1 hour.

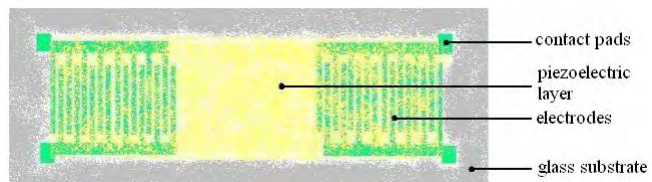


Fig.1. Top view of SAW structure

The structure includes two pairs comb electrodes, which are input and output transducers respectively. They are prepared by chrome layer, deposited on glass substrate and patterned by photolithography. The dimensions are shown in fig 2. The both samples (PZT and ZnO) are with the same construction and dimensions.

For better elasticity, a flexible organic substrate of polyethyleneterephthalate (PET) is used, by which the maximal allowable temperature of the technological processes must not exceed 70°C, to avoid thermal deformation. In fig. 2, a simplified technological sequence and the cross-section view of the microgenerator is shown. For the top and bottom electrodes Al layers, with thickness of 200 nm, are used, deposited by thermal evaporation in vacuum.

The bottom electrode is deposited on the whole surface of the substrate, and the top electrode is evaporated through shadow mask, by using of lift-off process. In this way, the

<sup>1</sup>Georgi Kolev, Krassimir Denishev, Mariya Aleksandrova and Yordanka Dutsolova are with the Faculty of Electronic Engineering and Technologies at Technical University of Sofia, 8 Kl. Ohridski Blvd, Sofia 1000, Bulgaria, E-mail: georgi\_kolev1@abv.

photolithography process is avoided for the top layer. In fig. 3, the dimensions of the structure are shown. To investigate the influence of the electrodes areas on the output voltage, five top electrodes are deposited at the same conditions, having the same dimensions and at a distance of 3 mm from each other. In this way, the area of the electrodes is increased from  $18 \text{ mm}^2$  (1 electrode) to  $90 \text{ mm}^2$  (5 electrodes), one by one.

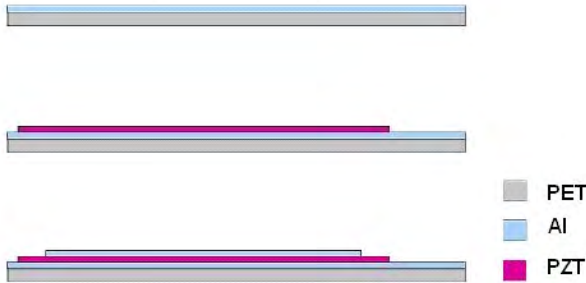


Fig. 2. Technological sequence of microgenerator

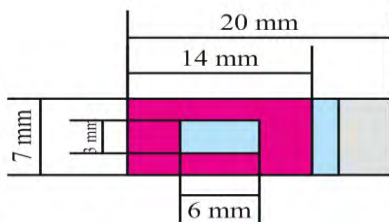


Fig. 3. Topology's dimension

In the construction proposed, a piezoelectric material PZT, with a thickness of about  $\sim 150 \text{ nm}$  and piezoelectric coefficient  $d_{33}=360 \text{ pC/N}$  is used, deposited for 1 hour at the same parameters of the process. By this approach, a bigger amplitude of the output voltage, in dynamic mode, in comparison with the ZnO ( $d_{33}=12.4 \text{ pC/N}$ ), is provided. The electrical connections, between the contact pads and the testing equipment, are wire bonded by using of silver paste.

### III. MEASUREMENTS AND RESULTS

For detection of the forward and reverse piezoelectric effect from one structure, the method of SAW is used [9]. The test of the piezomaterials is performed by using of the following experimental disposition, shown in fig. 4, which consists of two groups of comb electrodes - for input and output transducers, and layer of piezoelectric material, deposited on them.

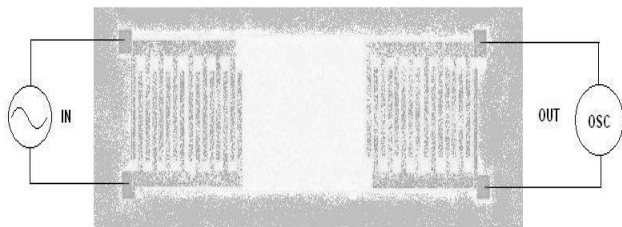


Fig. 4. Schematic of the setup for SAW test.

The aim is, by making of the input transducer to vibrate, a mechanical wave in the piezomaterial to be generated. The vibration is excited by sinusoidal signal, obtained from functional generator (MPF3060, 60MHz) at certain frequencies. When a mechanical wave is generated, it is spread into the whole piezoelectric layer, deposited on the electrodes and the area between them. The wave induces a voltage between the electrodes, when it reaches the output transducer. In fig. 5, the curves of ZnO and PZT reactions are shown.

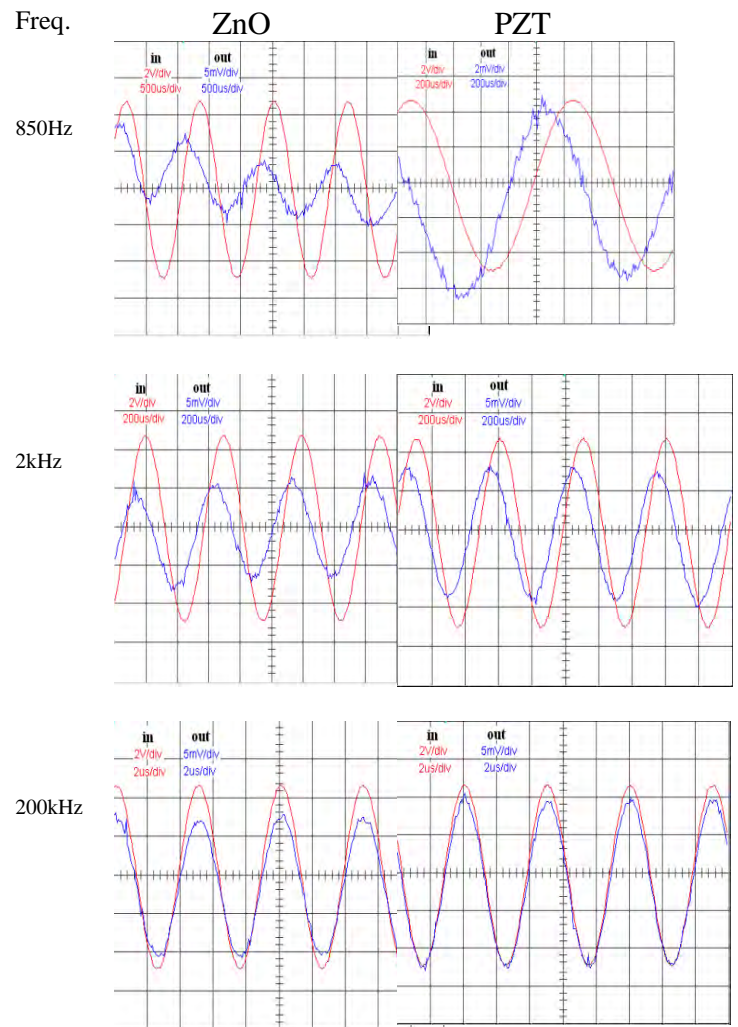


Fig. 5. Measured results from the SAW test.

By dual channel oscilloscope (DQ2041CN, 40MHz), the signals of the structure's input and output are observed simultaneously.

Because of the low elasticity of the glass substrate we cannot estimate the electromechanical coupling coefficients in this way. This is the reason, the mechanical waves, induced by the input transducer to be restricted in their magnitude. As a consequence, the amplitude of the output voltage is also limited.

For testing of the piezoelectric microgenerator in dynamic mode, the setup, presented in fig. 6, was used. As a mechanical wave source an electromagnetic shaker was used. It contains a coil with anchor, at the end of which the sample is clipped. The coil was supplied by sinusoidal voltage with defined frequency, coming from low frequency signal generator G3-109. This cause a vibration of the anchor with the same frequency. During the mechanical vibration of the structure, a voltage with almost the same sinusoidal shape is generated. The measurement is performed again by using of a digital oscilloscope, connecting its two channels, respectively to the sample and the coil. Fig. 7 represents the dependence of the generated voltage (peak-to-peak value) on the electrode's area, respectively for 100Hz and 200Hz.

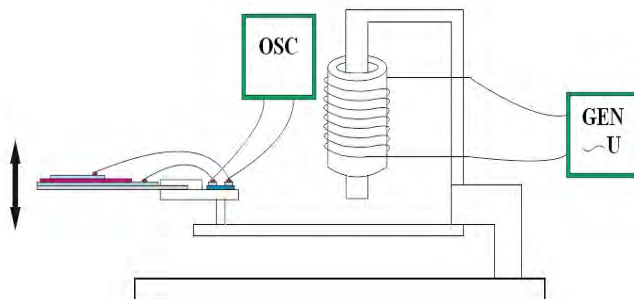


Fig. 6. Measurement setup for dynamic mode testing.

It is obtained as a result of the mechanical transformations and the time delays, which happen during vibrations propagation, from anchor to the sample.

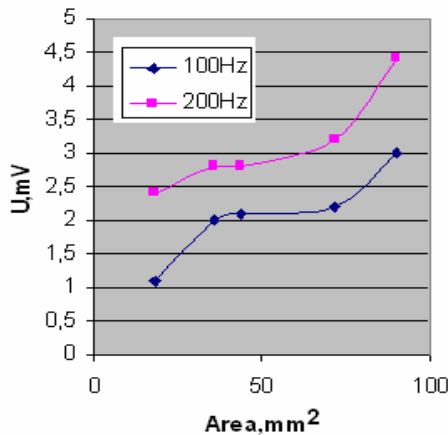


Fig. 7. Dependence of the generated voltage (peak-to-peak value) versus the electrode's area

During the measurement, some shift in the phase of generated voltage, in relation to input voltage, feeded to the coil was observed.

The generated voltage has nearly sinusoidal shape. With the enlarging the area of the electrodes, an increasing of its amplitude occurs. This is as a result of transferring of bigger quantity of charges to the electrodes. The measurements show that, in case of increasing the frequency of the vibrations, the output voltage is also increased, keeping the same amplitude of the sinusoidal signal of the generator. This effect could be explained by the fact that, for shorter time more current carriers to the electrodes are generated.

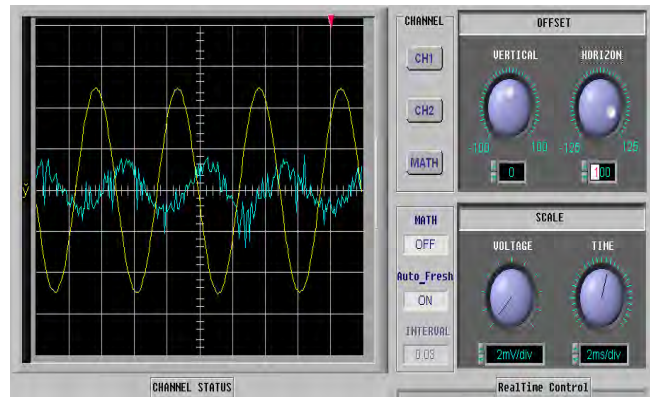


Fig. 8. Waveform of the signals

During the design of the microgenerator, it have to bear in mind that the thickness of PZT should be more than 150 nm, because, in the case of thinner layer, several metal microbridges occur, which lead to creation of short connections through the layers.

#### IV. CONCLUSION

During the design of piezoelectric microgenerators, we have to bear in mind the needed output power and also the frequency range of the vibrations, which would be transformed in voltage.

The voltage, generated in this way, is with alternative current (AC) character. For its rectifying, electron rectifiers are necessary.

The application and using of flexible substrate provides higher elasticity of the whole structure, which fact ensure the corresponding voltage generation, by using of lower mechanical loading.

The increasing of the electrodes area and the vibration frequency, increase the output power of the generator.

#### REFERENCES

- [1] Dobrucky, B, Drodzy, S.; Frivaldsky, M.; Spanik, P., "Interaction of Renewable Energy Source and Power Supply Network in Transient State", International Conference on Clean Electrical Power, pp.563 – 566, 2007.

- [2] Kyung Ho Cho, Chang Eui Seo, Yoon Soo Choi, Young Ho Ko, Kwang Joo Kim, "Effect of pressure on electric generation of PZT(30/70) and PZT(52/48) ceramics near phase transition pressure", Journal of the European Ceramic Society, Volume 32, Issue 2, February 2012, pp.457-463.
- [3] Daisuke Koyama, Kentaro Nakamura, "Electric power generation using vibration of a polyurea piezoelectric thin film", Applied Acoustics, Volume 71, Issue 5, May 2010, pp.439-445.
- [4] Brown, C.S.; Kell, R.C. ; Taylor, R. ; Thomas, L.A., Piezoelectric Materials, A Review of Progress, IRE Transactions on Component Parts, Volume: 9 , Issue: 4, 1962, pp. 193 – 211.
- [5] Keiji Morimoto, Isaku Kanno, Kiyotaka Wasa, Hidetoshi Kotera. "High-efficiency piezoelectric energy harvesters of c-axis-oriented epitaxial PZT films transferred onto stainless steel cantilevers", Sensors and Actuators A: Physical, Volume 163, Issue 1, September 2010, pp.428-432.
- [6] Shun Fa Hwang, Wen Bin Li, "PZT Thin Films Deposited by RF Magnetron Sputtering", Applied Mechanics and Materials (Volume 302), pp.8-13, 2013.
- [7] J. S. Horwitz, K. S. Grabowski, D. B. Chrisey, and R. E. Leuchtmeyer, "In situ deposition of epitaxial PbZrxTi(1-x)O3 thin films by pulsed laser deposition", Applied Physics Letters, Volume: 59 , Issue: 13, pp.1565 – 1567, 1991.
- [8] Jae Bin Lee, Hyeong Joon Kim, Soo Gil Kim, Cheol Seong Hwang, Seong-Hyeon Hong, Young Hwa Shin, Neung Hun Lee, "Deposition of ZnO thin films by magnetron sputtering for a film bulk acoustic resonator", Thin Solid Films 435, pp.179–185. 2003.
- [9] Georgi Kolev, "Investigation of piezoelectric effect in thin layers, for application in harvesting devices and MEMS sensors", Annual Journal of ELECTRONICS, ISSN 1314-0078, 2012.

# Sputtering of Thin Films on Flexible Substrates

Pavlik Rahnev<sup>1</sup>, Silvija Letskovska<sup>2</sup>, Dimitar Parachkevov<sup>1</sup> and Kamen Seimenliyski<sup>2</sup>

**Abstract –** The aim of this work is to investigate the properties of thin film deposited on flexible substrates. The main instrument for experiment is high rate magnetron sputtering. For this purpose high vacuum modified installation B55 (Hoch Vacuum Dresden) is used. As substrates different kind of no organic (metal foil) and organic materials are used. The main parameters of films (resistive, semiconductor, dielectric) are described as deposited and after thermal treatment. The comparison between electrical parameters and composition, structure is done. The main applications of such thin films are in photo voltaic and thin film displays.

**Key words –** thin films, sputtering, flexible substrates, organic substrates.

## I. INTRODUCTION

In the last years there is an increasing interest of using flexible substrates in electronics. Usually the investigations are provided mainly in three directions:

- Materials for substrates [1];
- Technology for deposition of different films [2];
- Circuit application [3] ;
- Problems appearing in the time of technology processes [4].

The application of flexible substrates is usually in organic light – emitting displays [5, 6], thin film transistors [7-9], sensors [10, 11] and microelectronic modules [12, 13]. The advantages of polymers substrates are mainly in there multiple elastic deformation, easy mechanical shaping, wide range of polymer materials, low cost and est.

The use of polymer materials in integrated circuits is difficult because organic can not be included into the microelectronic processes. Polymers have low temperature stability and low resistance against concentrated chemicals which limited their application in integrated circuits.

It is clear that the choice of polymer substrate is very wide, the combination substrate and deposited films depends on the specific technology - method of deposition, equipment, parameters of the processes.

<sup>1</sup>Pavlik Rahnev – Technical College, Assen Zlatarov University, Y. Yakimov Str. 1, Burgas 8010, Bulgaria, E-mail: pavlikrahnev@abv.bg

<sup>2</sup>Silvija Letskovska - Burgas Free University, San Stefano 62, 8000 Burgas, Bulgaria, E-mail: silvia@bfu.bg

<sup>1</sup>Dimitar Parachkevov – Assen Zlatarov University, Y. Yakimov Str. 1, Burgas 8010, Bulgaria, E-mail: parashkevov@abv.bg

<sup>2</sup>Kamen Seimenliyski –Burgas Free University, San Stefano 62, 8000 Burgas, Bulgaria, E-mail: silvia@bfu.bg

The question in front of this work is to check the combination of different flexible substrates and different thin films deposited in one and same technological cycle as well as the electrical parameters of the films compared with common used quartz substrates.

## II. CHOICE OF MATERIALS

### 2.1. Flexible substrates.

As it was described above there is a wide choice of materials used in the technology – stainless steel (metal), polymers (polyimide, polyester, Teflon, polystyrol) and flexible special glass based materials.

The main parameters of the substrates are directly connected with properties of the deposited films and prepared circuits:

- Structure of the films;
- Parasitic capacitance;
- Power dissipation.

TABLE I  
SUBSTRATE MATERIAL

Parameter	Stainless steel	Teflon (Du Pont Trade Mark)	Polyimide	Polyester	Sital (CT-50-1)
$R_{iz}$ (ohm)	-	$>10^{10}$	$>10_{10}$	$>10_9$	$>10_9$
$\epsilon$ (-)	-	2-3	2-3	2-3	5
$\lambda$ (W/mK)	30	1.2	1.5	1.5	6
$T_{max}$ ( $^{\circ}$ C)	$>1000$	150	150	150	400

From Table I is seem that polymer materials are good insulators, but with low thermo conductivity.

This will cause problems in device and circuit with high power dissipation.

The sizes of the experimental substrates are as follows;

- Thickness – 0.2÷0.5 mm;
- Linear dimensions – 60x48 mm (2"x2") as a standard for glass and ceramic substrates.

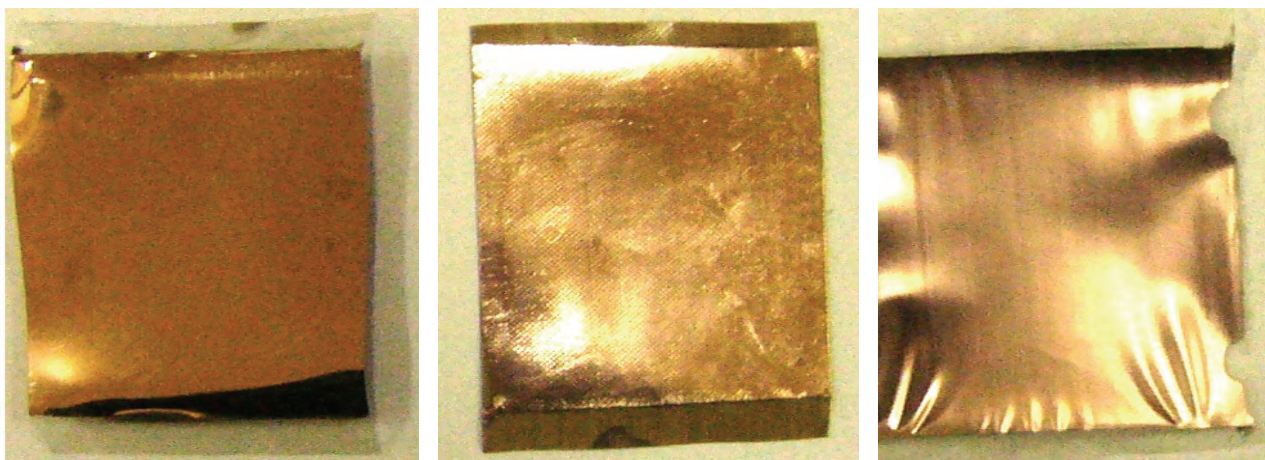


Fig. 1. Organic substrates after thermal evaporation.

### 2.2. Materials for deposition.

For experimental work four different materials are chosen:

- Cu - as a good conductor;
- NiCr – typical resistive film;
- Si – typical semiconductor;
- $\text{SiO}_2$  – usual dielectric in MOS integrated circuits.

To estimate the parameters of the deposited film sheet resistance ( $R_s$ ) is used.

## III. METHOD OF VACUUM DEPOSITION AND MATERIALS

### 2.1. Thermal evaporation.

The evaporation in high vacuum is commonly used technology for thin films because it has simplicity and it is well known in practice. In the same time thermal evaporation has several disadvantages and difficultness such as:

- Evaporation of W, Pt, ta, Mo;
- Evaporation of alloys;
- Evaporation of compands;
- Deposition on unstable thermally organic substrates (Fig. 1).

From Fig. 1 is clear that some of the polymer materials lose their form, flatness, that is why evaporation is not suitable some organic materials.

### 3.2. Sputtering of thin films.

As it is clear from above the only universal method of deposition is sputtering technique.

For the provided experiments the modified high vacuum installation B55 (Hoch Vacuum Dresden) is used (Fig. 2).

The advantages of this machine are:

- Four sputtering targets;
- Rotation of substrates holders;
- Possibility of heating or cooling of substrates.

The main technology parameters are:

- Final vacuum  $p < 0.5 \times 10^{-2}$  Pa;
- Argon pressure  $p_{\text{Ar}} \approx 10 \div 40$  Pa;
- Sputtering voltage  $300 \div 700$  V and Power  $\approx 100$  W.

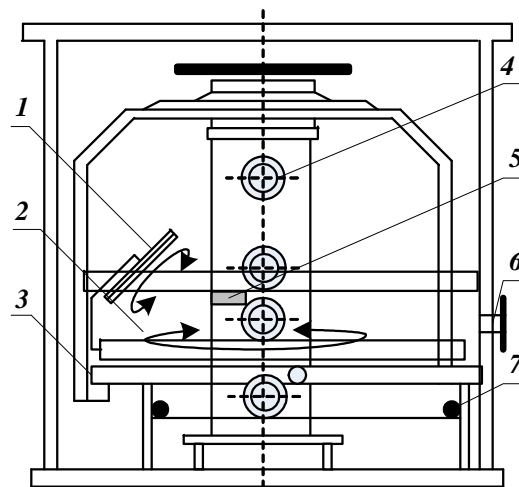


Fig. 2. Vacuum installation B55 with magnetrons.

- 1 - Substrate holder; 2 - Chamber heating/cooling;
- 3 - Rotating table; 4 – Sputtering target;
- 5 – Sensor for  $R_s$ ; 6 – Vacuum meter;
- 7 – Infrared heaters.

## IV. PREPARATION OF SIMPLE AND RESULTS.

The deposited materials used for the experiments have very wide range of specific resistance.

That is why for estimation sheet resistance  $R_s = \rho/d$  is better to be used.

The ratio  $n=L/w$  can change from  $n=100$  for good conductor (Cu),  $n=1$  for NiCr and  $n=0.1$  for semiconductor (Si).

The final step in sample preparation is forming of the resistor patterns. For this conventional wet etching or through mask deposition are used.

Finally, the samples have topology and sections are given in Fig.3.

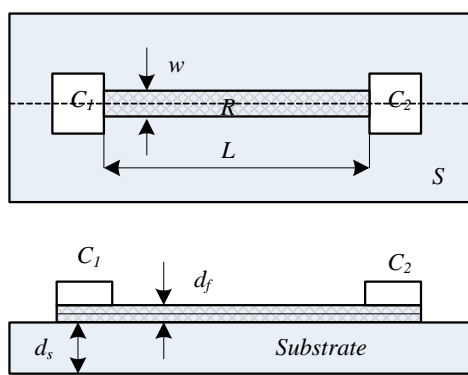


Fig. 3. Topology and cross section of samples.

The results for  $R_s$  are shown in Table II. The  $R_s$  for different materials are compared with  $R_s$  on glass substrates.

TABLE II  
COMPARISON OF  $R_s$  ON GLASS AND POLYMER SUBSTRATE

Substrate	$R_s$ (omh/sq)		
	Cu	NiCr	Si
Glass	0.10	150	2000
Polymer	0,12	170	3000

It is clear from Table II that sheet resistance on polymers is higher compared with glass substrate. It could be a result of structure changes (defects) and some implantation into the soft organic surface.

## REFERENCES

- [1] Flexible Circuit Technology" 3rd Edition by Joseph Fjelstad, BNR Publishing, Seaside OR 2006.
- [2] "Flexible Printed Circuitry" by Thomas Stearns, McGraw-Hill, NY, NY 1995.
- [3] "Handbook of Flexible Circuits" by Ken Gilleo, Van Nostrand Reinhold, NY, NY 1992.
- [4] Pavlik Rahnev, Silvija Letskovska, Dimitar Parachkevov, Problem in using polymer substrates for solar cells, SIELA, 2009.
- [5] J.-W. Kang, W.-I. Jeong, J.-J. Kim, H.-K. Kim, D.-G. Kim, G.-H. Lee, Electrochim. Solid-State Lett. 2007, 10, 75.
- [6] L. Hou, Q. Hou, Y. Mo, J. Peng, Y. Cao, Appl. Phys. Lett. 2005, 87, 243504.
- [7] S. H. Ko, H. Pan, C. P. Grigoropoulos, C. K. Luscombe, J. M. J. Fréchet, D. Poulikakos, Nanotechnology 2007, 18, 345202.
- [8] U. Haas, H. Gold, A. Haase, G. Jakopic, B. Stadlober, Appl. Phys.Lett. 2007, 91, 043511.
- [9] A. L. Briseno, S. C. B. Mannsfeld, M. M. Ling, S. Liu, R. J. Tseng, C. Reese, M. E. Roberts, Y. Yang, F. Wudl, Z. Bao, Nature 2006, 444, 913.
- [10] V. Shamanna, S. Das, Z. Celik-Butler, K. L. Lawrence, J. Micromech. Microeng. 2006, 16, 1984.
- [11] F. Jiang, G.-B. Lee, Y.-C. Tai, C.-M. Ho, Sens. Actuators A 2000, 79, 194.
- [12] S. A. Dayeh, D. P. Butler, Z. Celik-Butler, Sens. Actuators A 2004, 118, 49.
- [13] S. Tung, S. R. Witherspoon, L. A. Roe, A. Silano, D. P. Maynard, N. Ferraro, Smart Mater. Struct. 2001, 10, 1230.

**This Page Intentionally Left Blank**

# Design and Realization of a small 10 Watt Forward Converter

Zoran Zivanovic<sup>1</sup> and Vladimir Smiljakovic<sup>2</sup>

**Abstract –** In this paper the straightforward design of a small forward converter is presented. The converter was built and tested through lab measurements. Design steps are described and well documented with measurement results.

**Keywords –** DC/DC converter, forward, efficiency

## I. INTRODUCTION

The most frequently used DC/DC converter is a single switch forward converter, especially for telecom use with input voltage range from 18 to 36 or 36 to 72V. It is used in Digital Radio Relay Systems and Radio Base Stations. From few watts to a couple hundred watts, with one or multiple outputs, they need to have high efficiency and high density. Unlike the flyback converter they have two magnetic components: the transformer and the output inductor.

## II. PRINCIPLE OF FORWARD CONVERTER

The basic forward converter circuit is shown in Fig. 1. During the time when the primary power switch (MOSFET Q) is on, the energy is transferred to the secondary. Diode D1 is forward biased and the current flows through inductor L to the capacitor C and the load. When the power switch turns off, diode D1 is reverse biased and forward biased diode D2 provides freewheeling path for inductor current from input and stored in the transformer. Capacitor C acts as a reservoir and holds the output voltage nearly constant.

## III. DESIGN AND ANALYSIS

The task is to design a 10W forward converter using current mode control IC with careful choice of operating parameters and components. Achieving the efficiency as much as possible near 85% is the primary objective. The footprint size must be smaller than 50x25mm.

First we choose the switching frequency to be around 340 kHz, which is a compromise between the efficiency and size. Knowing that, a good choice of core for the transformer and the inductor is RM4, N49 material from TDK-EPCOS.

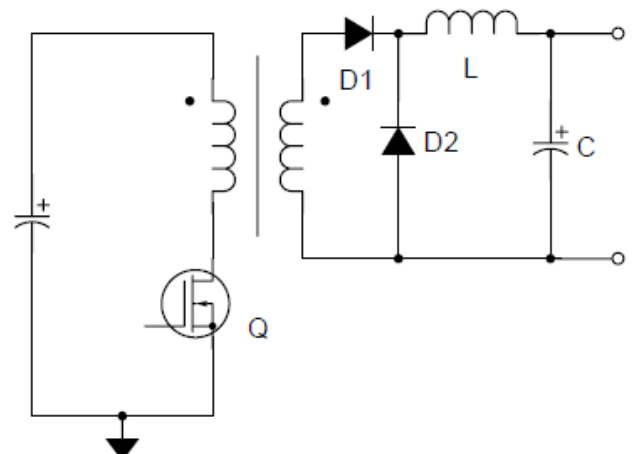


Fig.1. Forward converter

Design specifications are given in Table I.

TABLE I  
DESIGN SPECIFICATIONS

		Min	Typ	Max	
Input voltage	$V_{IN}$	18	24	36	V
Output voltage	$V_O$		5		V
Output current	$I_O$	0.1	2		A
Output current limit	$I_{OCL}$		2.4		A
Full load efficiency	$\eta$		85		%
Switching frequency	$f_{SW}$		340		kHz

The main contributors to power losses are transformer, output inductor, power switch, current sensing and secondary rectifiers.

Starting from design specifications we will now calculate basic parameters for the transformer and output inductor (Table II).

TABLE II  
BASIC PARAMETERS

		Max	Typ	Min	
Duty cycle	D	0.43	0.32	0.21	
Number of primary turns	$N_P$		12		
Number of secondary turns	$N_S$		8		
Primary RMS current	$I_{PRMS}$	1.00	0.86	0.70	A
Secondary RMS current	$I_{SRMS}$	1.31	1.13	0.92	A
Output inductance	L		21		$\mu$ H
Number of induct. turns	N		14		

<sup>1</sup>Zoran Zivanovic is with the IMTEL KOMUNIKACIJE AD, Bul. Mihajla Pupina 165b, 11070 Belgrade, Serbia, E-mail: zoki@imtelkom.ac.rs.

<sup>2</sup>Vladimir Smiljakovic is with the IMTEL KOMUNIKACIJE AD, Bul. Mihajla Pupina 165b, 11070 Belgrade, Serbia, E-mail: smiljac@imtelkom.ac.rs.

Now it is time to wind the transformer and output inductor. We will use 2 parallel strands of 0.3mm copper wire for the primary and the secondary, in order to minimize copper losses. For the output inductor we will use 3 parallel strands of 0.3mm copper wire.

Knowing specific core losses we can now calculate the losses in both magnetic components (Table III). Total transformer power loss at 24V input voltage is 188mW. This results in approximately 24 °C rise above ambient temperature. The temperature rise on the inductor is 19 °C. Satisfied with results, we will keep the chosen core geometry.

TABLE III  
TRANSFORMER AND INDUCTOR LOSSES

		Max	Typ	Min	
Core effect. volume	V <sub>E</sub>		0.29		cm <sup>3</sup>
Specific core losses	P <sub>V</sub>		0.32		W/cm <sup>3</sup>
Primary resistance	R <sub>P</sub>		66		mΩ
Secondary resistance	R <sub>S</sub>		45		mΩ
Core loss	P <sub>CORE</sub>		93		mW
Primary loss	P <sub>PRI</sub>	66	49	33	mW
Secondary loss	P <sub>SEC</sub>	77	57	38	mW
Inductor loss	P <sub>IND</sub>		157		mW

As the next step we will compute the power losses for power switch IRFR3410 (Table IV).

TABLE IV  
IRFR3410 POWER LOSSES

IRFR3410			Typ		
ON resistance	R <sub>DS</sub>		39		mΩ
Reverse transfer capac.	C <sub>RSS</sub>		250		pF
Conduction loss	P <sub>CON</sub>	59	43	29	mW
Switching loss	P <sub>SW</sub>	78	138	300	mW
Total loss	P <sub>TOT</sub>	137	181	329	mW

Obviously MOSFET IRFR3410 is a good choice because of the low power losses.

For current sensing we can use a current sense resistor or a current transformer. For simplicity and smaller losses we will use current sense resistor. Power dissipated in current sense resistor is given in Table V.

TABLE V  
CURRENT SENSE RESISTOR POWER LOSSES

		Max	Typ	Min	
Current sense resistance	R <sub>CS</sub>		0.5		Ω
CS resistance loss	P <sub>CS</sub>	500	370	245	mW

Dissipation of 500mW at low line will reduce efficiency about 4%. For higher efficiency the circuit shown in Fig. 2 will be used. Resistors R<sub>2</sub> and R<sub>3</sub> bias the current sense resistor R<sub>1</sub> reducing a current sense amplitude, so the sense resistor can be three times smaller. As a result we have smaller power loss. The new calculation results are given in Table VI.

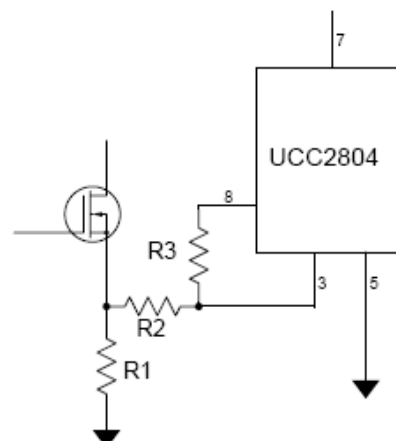


Fig.2. Current sense circuit with bias

TABLE VI  
BIASED CURRENT SENSE RESISTOR POWER LOSSES

		Max	Typ	Min	
Current sense resistance	R <sub>CS</sub>		165		mΩ
CS resistance loss	P <sub>CS</sub>	165	122	81	mW

With this simple circuit the dissipation is reduced significantly (from 500 to 165mW at low line).

At the end we will calculate the power losses for secondary rectifier – Schottky diode MBRD660CTG (Table VII).

TABLE VII  
RECTIFIERS POWER LOSSES

MBRD660CTG		Min	Typ	Max	
Conduction loss	P <sub>CON</sub>		0.8		W
Switching loss	P <sub>SW</sub>		0.4		W

Comparing to the other losses it is obvious that the choice of secondary rectifier is critical for the converter efficiency.

#### IV. REALISATION

DC/DC converter was built on FR-4 substrate with 35μm copper with footprint 50x25mm. The transformer and the output inductor are wounded on through hole coil formers according to calculations. Current sense resistor (with bias) is adopted for primary current sensing.

Using lab power supply 0-60V/3A and resistive load we have measured full load efficiency at various input voltages. The results are given in Table VIII. The efficiency is around 83%, which is not so bad. Simultaneously with efficiency measurements we have recorded the waveforms at the point of interest.

**TABLE VIII**  
**EFFICIENCY**

		Typ		
Input voltage	$V_{IN}$	18	24	36
Input current	$I_{IN}$	0.679	0.50	0.340
Input power	$P_{IN}$	12.22	12.00	12.24
Efficiency	$\eta$	81.82	83.33	81.70
		%		

The drain waveforms of primary power switch at full load and input voltages of 18, 24 and 36V are given in Figs. 3, 4 and 5 respectively. Drain current waveforms can be seen in Figs. 6 and 7.

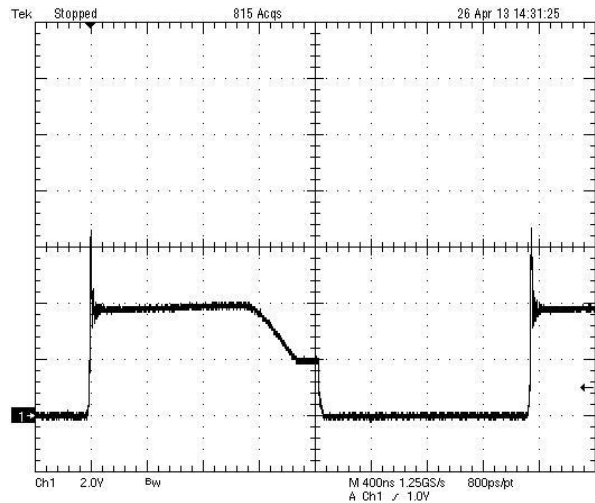
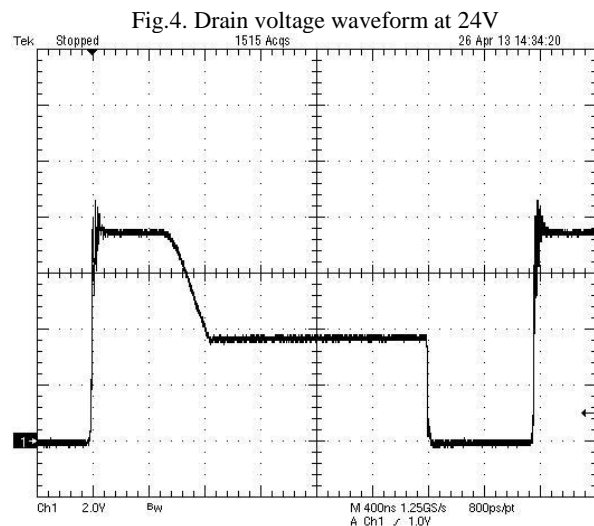
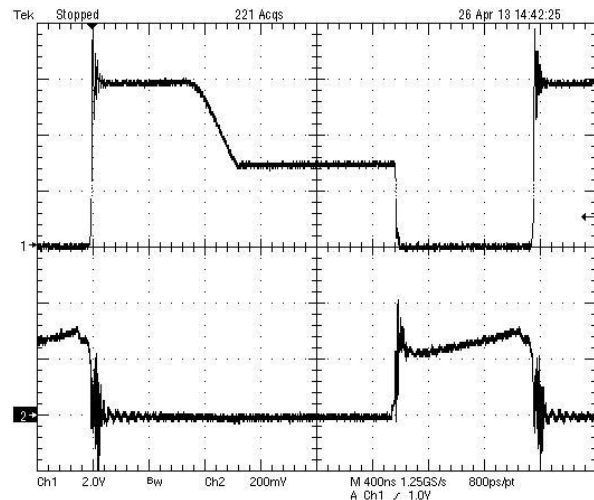
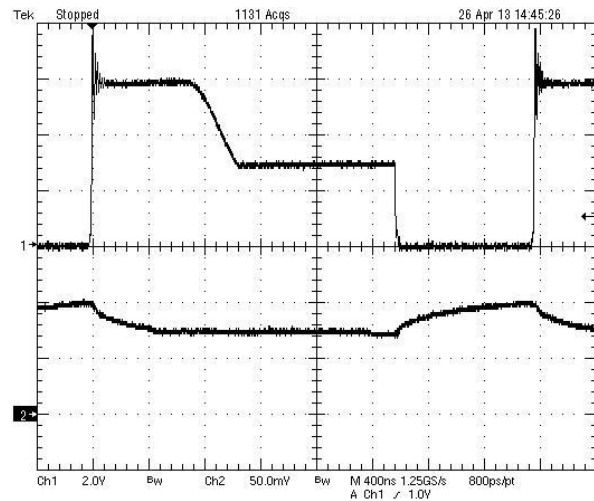
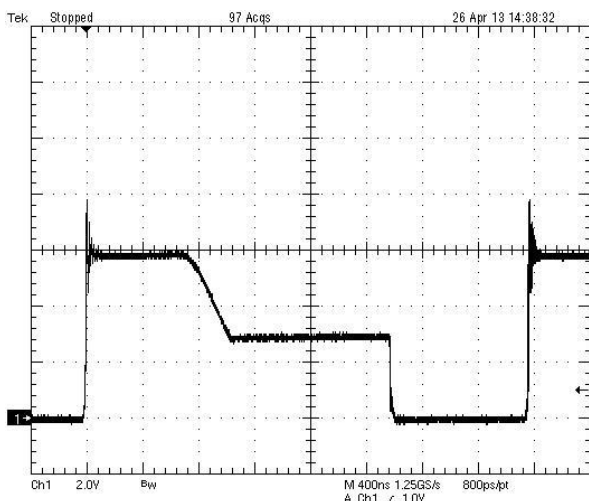

**Fig.3. Drain voltage waveform at 18V**

**Fig.4. Drain voltage waveform at 24V**

**Fig.5. Drain voltage waveform at 36V**


Fig.7. Drain voltage and current waveform (offset) at 24V

At full load, input voltage of 24V and convection cooling we have measured the temperatures of critical components using thermocouple. The results are given in Table IX.

TABLE IX  
TEMPERATURE OF CRITICAL COMPONENTS

Temperature (°C)	
Ambient	31
MOSFET	55
Diode	81
Transformer	58
Inductor	57

MOSFET and diode junction temperature can be done more precisely using DMM and stopwatch. DMM must have diode threshold measurement option. First with power off and no load we will measure the forward voltages of FET and diode and ambient temperature.

When the converter reach the steady-state condition, we will turn the power off and remove the load simultaneously starting the stopwatch. At every 20 seconds the forward voltage needs to be measured. The procedure was done for FET and output diode. The results are given in Tables X and XI.

TABLE X  
MOSFET VSD

t(s)	20	40	60	80	100	120
V <sub>sd</sub> (mV)	463	472	480	486	491	495

TABLE XI  
DIODE VF

t(s)	20	40	60	80	100	120
V <sub>f</sub> (mV)	103	130	142	150	155	158

Using curve-fitting software we can find that at t=0 MOSFET diode voltage is  $V_{sd\ HOT} = 452\text{mV}$  and output diode voltage  $V_{f\ HOT} = 79\text{mV}$ . In a cold state we have measured  $V_{sd\ COLD} = 512\text{mV}$  and  $V_{f\ COLD} = 184\text{mV}$ . Knowing temperature coefficients for MOSFET diode  $k_1 = -2.2\text{ mV/}^{\circ}\text{C}$  and for output diode  $k_2 = -1.8\text{ mV/}^{\circ}\text{C}$  we can calculate junction temperature for MOSFET using equation

$$T_{JMOSFET} = T_{amb} + \frac{(V_{sdHOT} - V_{sdCOLD})}{k_1} = 58^{\circ}\text{C}$$

Similarly for output diode we have

$$T_{JDIODE} = T_{amb} + \frac{(V_{fHOT} - V_{fCOLD})}{k_2} = 89^{\circ}\text{C}$$

The results are showing sufficient thermal margin for all components. At the maximum ambient temperature of 55°C the output diode junction temperature will be 113°C which is

OK, but we can consider changeover to FR-4 substrate with 70μm copper and bigger heatsink surface.

The picture of converter prototype is given in Fig.8.

## V. CONCLUSION

In this paper the design and analysis of 10W forward converter are presented.

The prototype was built and tested. The results verified that the full load efficiency is about 83%.

Further improvements are possible thorough Active Clamp Reset with controller change and Synchronous Rectifier in the secondary. The efficiency will go over 90%.

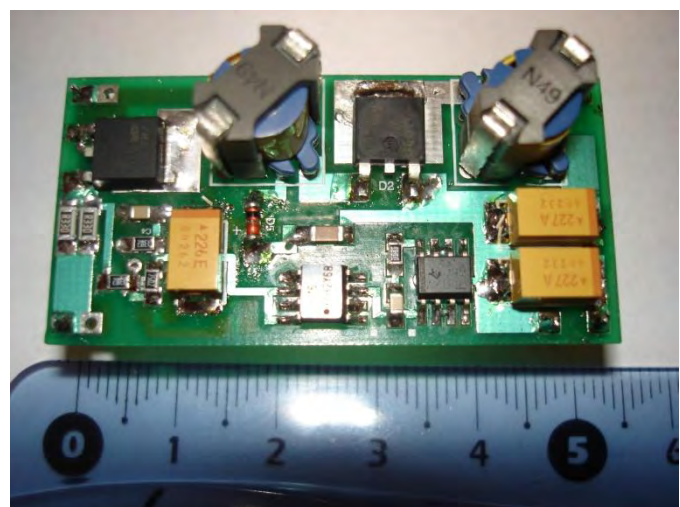


Fig.8. Converter prototype

## ACKNOWLEDGEMENT

The work is partially supported by the Serbian Ministry of Education and Science (Project III-44009).

## REFERENCES

- [1] Texas Instruments, "Low Power BiCMOS Current Mode PWM", SLUS270d Data Sheet, [www.ti.com](http://www.ti.com)
- [2] Robert W. Erickson, Dragan Maksimović, Fundamentals of Power Electronics, Second Edition, Colorado, Kluwer Academic Publishers 2004.
- [3] TDK-EPCOS, "Ferrites and accessories RM4", Data Sheet, [www.epcos.com](http://www.epcos.com)
- [4] Texas Instruments, Power Transformer Design, Application Note SLUP126, [www.ti.com](http://www.ti.com)
- [5] David Magliocco, "Semiconductor Temperature Measurement in a Flyback Power Supply", Switching Power Magazine, 2005.

---

---

## Poster 8 - Measurement Science and Technology

---

---



# Vibration Measurement with Piezoelectric Transducer

Bozhidar Dzhudzhev<sup>1</sup>, Veselka Ivanceva<sup>2</sup>, Silviya Kachulkova<sup>3</sup> and Ekaterina Gospodinova<sup>4</sup>

**Abstract –** This article discusses piezoelectric transducers and their application for vibration measurement. The functions of conversion are experimentally defined and investigated.

**Keywords –** Vibrations, no electrical measurement, piezoelectric transducer, amplitude, frequency.

## I. VIBRATION – BASICS

### A. Definition

Vibration is the motion of a particle or a device or system of connected devices scattered around the balanced position. Most vibrations are undesirable in machines and equipment because they lead to increased loads, fatigue and energy loss, increased bearing loads, creating discomfort for passengers in vehicles and absorbing energy from the system. The rotating parts in machines must be carefully balanced to prevent vibration damage. [1]

Vibrations can be obtained from natural forces, such as earthquake [2]. There are vibrations created by the people who influence the environment. Such vibrations can be caused by industry, transport [3], construction [2] and other activities.

Vibration is a response of the system to internal or external impact, which causes it to fluctuate or pulsate.

Although it is commonly believed that vibrations do damage to the equipment and the machinery, they do not. Instead, the damage is done by dynamic loads, which lead to fatigue and dynamic loads are caused by vibration. [4]

If a vibrating object can be seen in slow motion, it will be found running in different directions. Each vibration has two measurable variables that help to determine the vibration characteristics, how far (magnitude or intensity) and how fast (frequency) the subject is moving. The parameters used to describe this movement are displacement, frequency, amplitude and acceleration. (Figure 1)

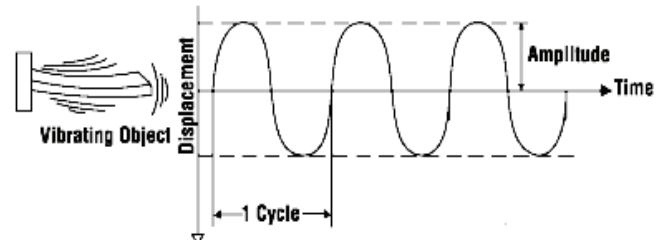


Fig.1 Parameters of vibration

### B. Amplitude

The generally accepted term for this how big is the vibration is amplitude, A. The definition of amplitude depends on the systems. One can work in units of distance from the vibrating subject from extreme left to extreme right (double amplitude) but in physics more often is used the distance from the center to one of the extremes.

### C. Frequency

Frequency f is the number of cycles that occur per unit of time. [4]. Unit rate is usually 1 cycle/second, which is defined as a special unit 1 Hertz (1Hz). The term frequency is common in determining the vibration.

If one cycle takes time T, then the number of cycles that occur per unit time is:

$$f = \frac{1 \text{ cycle}}{T} \quad (1)$$

### D. Units for vibration measurement

#### Vibration displacement " s "

This is a deviation of the measured point from the equilibrium position. The unit is usually  $\mu\text{m}$ . [5]

#### Vibration velocity " v "

This is the rate at which the measured point moves around its equilibrium position. The unit is  $\text{mm}/\text{s}$ . [5]

#### Vibration acceleration " a "

This is the acceleration with which the measured point moves about the equilibrium position. The unit is either  $\text{m}/\text{s}^2$  or g ( $1g = 9,81\text{m}/\text{s}^2$ ). [5]

<sup>1</sup> Bozhidar Dzhudzhev is with the Faculty of Automatics at Technical University of Sofia, 8 Kl. Ohridski Blvd, Sofia 1000, Bulgaria, E-mail: bojidar.djudjev@abv.bg

<sup>2</sup>Veselka Ivanceva is with the Faculty of Automatics at Technical University of Sofia, 8 Kl. Ohridski Blvd, Sofia 1000, Bulgaria.

<sup>3</sup>Silviya Kachulkova is with the Faculty of Automatics of Sofia, 8 Kl. Ohridski Blvd, Sofia 1000, Bulgaria.

<sup>4</sup>Ekaterina Gospodinova is with the Faculty of Automatics at Technical University of Sofia, 8 Kl. Ohridski Blvd, Sofia 1000, Bulgaria.

## II. PIEZOELECTRIC TRANSDUCER

Piezoelectric effect occurs in some crystalline substances - natural quartz, Rochelle salt, lithium sulphate, some ceramics and more. When such a crystal is placed in an electric field it changes its size synchronously with the changes of the field – opposite Piezoelectric effect (used to generate audible and ultrasonic signals). When the crystal is deformed in an appropriate direction an electric charge is generated (straight Piezoelectric effect). [6]

One of the commonly used structures for vibration measurement while controlling the state of the machine is shown in Figure 2. The Piezoelectric transducer is glued strong at the one end of the bending under the forces of inertia plate and the free end is soldered seismic mass. Attenuation is achieved through the oil drops placed in the gap between the seismic mass and the attenuator. When the base is moving downside-up the inertia opposes and deforms the Piezoelectric transducer. This generates an electrical charge that is proportional to the acceleration. Typical values of the sensitivity of these sensors are 0,5-50 mVs<sup>2</sup>/m in the frequency range 0,1 Hz to 200 kHz.

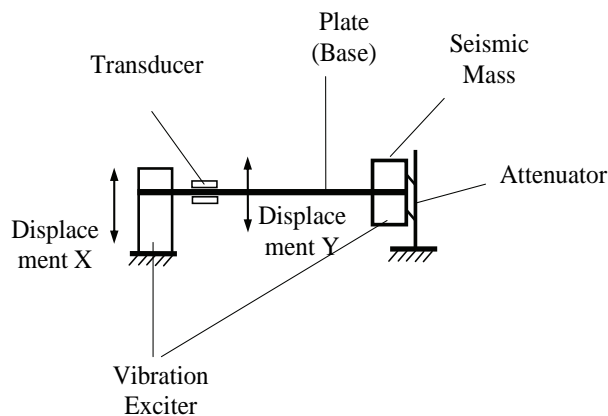


Fig.2 Stand for vibration measurements

Between the vibrational displacement  $x$ , absolute displacement of the seismic mass  $y$  and its relative movement  $z$  exist dependence ( $z = x - y$ ).

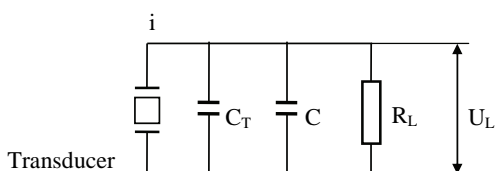


Fig.3 Equivalent replacement scheme

Piezoelectric vibration transducer generates an electrical charge that is proportional to the deflection of the piezoelectric transducer.

$$q = S_q z \quad (1)$$

where  $S_q$  the sensitivity of Piezoelectric vibration transducer for amount of electricity.

The equivalent replacement scheme of the structure from Fig. 2 is shown in Fig. 3, in which with  $C_T$  is marked the capacity of the converter with  $C$  - the additional capacity with  $R_L$  - the output load resistance of Piezoelectric vibration transducer. The current is  $i = \frac{d\alpha}{dt}$ . The output voltage of the vibration transducer in harmonic mode is:

$$\dot{U}_n = \frac{j\omega S_q \dot{z}}{j\omega C_\Sigma + \frac{1}{R_L}} \approx \frac{S_q}{C_\Sigma} \dot{z} \quad (2)$$

Here  $C_\Sigma = C_T + C$

The approximate equation is valid when  $R_L \gg \frac{1}{\omega C_\Sigma}$ .

Sometimes this condition is achieved with the given shunt of the transducer with additional capacitor with significant capacity. This, however, reduces the voltage sensitivity of the scheme:

$$\dot{U}_n \approx \frac{S_q}{C_T + C} \dot{z} = S_U \dot{z} \quad (3)$$

Construction of the piezoelectric transducer is such that any additional resonant frequencies are much higher than the primary. It is assumed that there is only the main resonance. It is determined by the equivalent vibrating mass  $m$ , the equivalent elastic counteraction with constant  $W$  and without hysteresis friction with constant  $P$ . The parameters own frequency of oscillation  $f_0 = \frac{\omega_0}{2\pi} = \frac{1}{2\pi} \sqrt{\frac{W}{m}}$ , decay

$\beta = \frac{P}{2\sqrt{mW}}$  and relative frequency  $v = f/f_0$  are obtained.

The condition for the use of piezoelectric transducer as a vibrator for measuring the amplitude of the vibration is given by:

$$\dot{U}_n \approx \frac{S_q}{C_\Sigma} \dot{x} \frac{v^2}{(1-v^2) + j2\beta v} \quad (4)$$

To one of the two working ends of the vibrator is attached piezoelectric transducer (Fig. 2).

When  $v \gg 1$ , amplitude-frequency response and phase-frequency response of the piezoelectric transducer tend to:

$$(U_n)_{v \gg 1} = \frac{S_q}{C_\Sigma} x \quad (5)$$

$$(\varphi)_{v \gg 1} = \arg \frac{\dot{U}_n}{\dot{x}} = \arctg \frac{2\beta}{v} \rightarrow 0 \quad (6)$$

Therefore in the above resonant area it is received a signal for the amplitude of the vibration.

If  $\dot{X}$  in Eq. (1) is replaced by  $\frac{1}{\omega^2} \frac{d^2}{dt^2}(\dot{x})$  it is obtained:

$$\dot{U}_n = \frac{1}{4\pi^2 f_0^2} \frac{S_q}{C_\Sigma} (\dot{x}) \frac{1}{(1-v^2) + j2\beta v} \quad (7)$$

For  $v \ll 1$ , amplitude-frequency response and phase-frequency response tend to:

and the frequency response FCHH tend to express:

$$(\dot{U}_n)_{v \ll 1} \rightarrow \frac{S_q}{C_\Sigma} x'' \quad (8)$$

$$(\varphi)_{v \ll 1} = \arg \frac{\dot{U}_n}{x''} \rightarrow 0 \quad (9)$$

Therefore in the under resonant area it is received a signal for the amplitude of the vibration acceleration.

### III. DESCRIPTION OF THE EXPERIMENTAL SETUP

The setup for vibration measurement and processing of results is shown in Figure 4. It includes the following blocks:

- Frequency Generator - Philips GM 2315. Frequency range of 20Hz to 20kHz. Range from 0 to 10V.
- Digital Multimeter - Fluke 83 Multimeter
- Amplifier - Brüel & Kjaer power amplifier type 2712
- Vibration exciter - Brüel & Kjaer, permanent magnetic vibration exciter type 4808. Maximum acceleration 71g.
- Sensors for measuring vibration acceleration - Piezoelectric - Kistler K-Shear accelerometer Type 8704B500M1. Frequency range of 1Hz to 10kHz. Measuring range  $\pm 500g$ .
- Power supply for the piezoelectric sensor - Kistler power supply/coupler, type 5134.
- Amplifier - Hottinger Baldwin messtechnic, type spider 8
- Computer
- Software - Catman Professional 5.0

From the frequency generator we are setting the frequency and the amplitude of the signal. We are monitoring these values with a multimeter. The signal from the generator passes through the amplifier 2712 and is supplied to the vibration exciter. It produces in turn a vibration that is measured by the transducer. The piezoelectric transducer is

powered externally. It produces a signal proportional to ground acceleration g. The signal from the transducer passes through the amplifier - Hottinger Baldwin messtechnic Type spider 8, where it is transformed in appropriate form and is fed to the computer. The results are displayed using the program Catman Professional. The program is dedicated measurement software that provides great opportunities for visualization and analysis of signals. The program allows to measure frequencies and amplitudes.

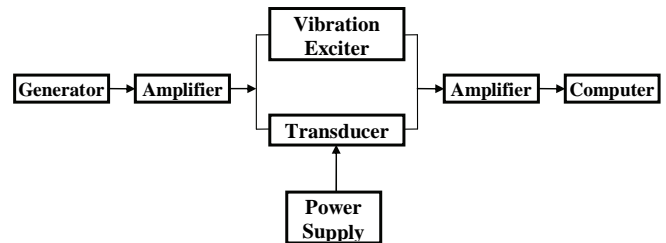


Fig.4 Block diagram of the stand for measuring vibration

### IV. RESULTS FROM THE MEASUREMENT

1. Testing the transducer on measuring frequency. The amplitude of the signal coming from the piezoelectric transducer is maintained constant with the amplifier - Brüel & Kjaer power amplifier Type 2712 with values - 5g and 10g. The results are presented in Table I. There are very small differences (from 0 to 1.2%) between the one from the generator and the measured from the transducer.

TABLE I  
DEPENDING ON THE FREQUENCY OF THE PIEZO TRANSDUCER FROM FREQUENCY GENERATOR

Frequency from the generator, Hz	Frequency from the piezoelectric transducer, Hz
20	20
30	30,303
40	40
50	50
60	60,606
70	71,428
80	80
90	90,909
100	100

2. Study on the dependence of the amplitude of the vibration frequency against the frequency signal from the generator,  $A = f(f)$ . The measurements were made at frequencies from 20 Hz to 500 Hz over 10 Hz (Table II). The

measurement was conducted in the same gain.

The change of amplitude against frequency is shown in Fig. 5. The figure shows that the vibration exciter has resonance at 100 Hz.

**TABLE II**  
AMPLITUDE OF THE TRANSDUCER AS A FUNCTION OF FREQUENCY

Frequency from the generator, Hz	Amplitude from the transducer, g	Frequency from the generator, Hz	Amplitude from the transducer, g
20	3,5		
30	4,4	270	3,2
40	6,0	280	2,85
50	7,3	290	2,85
60	8,5	300	2,45
70	9,0	310	2,45
80	9,75	320	2,05
90	9,75	330	2,05
100	9,75	340	1,6
110	9,2	350	1,6
120	8,9	360	1,6
130	8,5	370	1,2
140	8,0	380	1,2
150	7,7	390	1,2
160	7,3	400	1,0
170	6,9	410	1,0
180	6,5	420	0,8
190	6,5	430	0,8
200	6,0	440	0,8
210	5,6	450	0,8
220	5,2	460	0,8
230	4,8	470	0,4
240	4,4	480	0,4
250	4,0	490	0,4
260	3,6	500	0,4

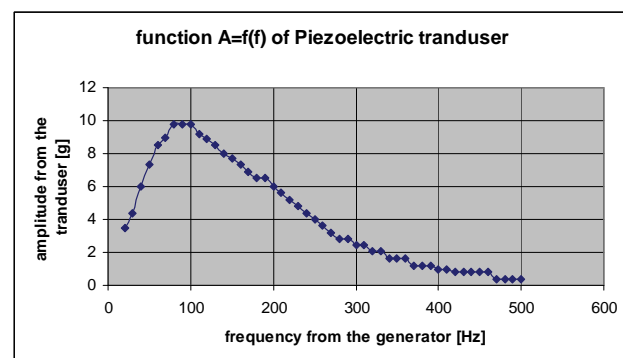


Fig.5 Function of the converting of the piezoelectric transducer from frequency of the generator

## V. CONCLUSIONS

The piezoelectric transducer measures frequency very accurate. There are differences in some of the results between the transducer and the report of the assigned frequency of the generator, the biggest difference is 1,4 Hz. This difference is caused by the rounding made when reporting the actual data from the transducer. The transducer has a large frequency range.

Piezoelectric transducer measures better signals with larger amplitudes and around the resonant area. For signals with very small amplitudes, the sensor may not report them.

## ACKNOWLEDGEMENTS

The researches, the results of which are presented in this publication are funded by internal competition TU-2012 contract to support PhD student № 122 RP 0074-08 "Study and optimization of processes for measuring vibration".

## REFERENCES

- [1] <http://www.newagepublishers.com/samplechapter/001413.pdf>
- [2] <http://www.acousticassociates.co.uk/environmental-vibration.htm>
- [3] Department of Environment and Conservation, "Assessing Vibration: a technical guideline", 2006
- [4] Torex sensors, "Vibration"
- [5] Brüel & Kjær Vibro "Basic Vibration – Measurement & Assessment"
- [6] James Kark, "Signal Conditioning Piezoelectric Sensors", 2003

# Examination of capacitive transducers and their use for measurement of small linear displacements

Veselka Ivancheva<sup>1</sup>, Silvia Kachulkova<sup>2</sup>, Bozhidar Dzhudzhev<sup>3</sup> and Vladislav Slavov<sup>4</sup>

**Abstract –** This article discusses capacitive transducers and their application for measurement of small linear displacements. Experimentally defined and analyzed are the functions of transformation of capacitive transducers with change of the distance between electrodes and the overlapping area between the electrodes.

**Keywords –** small linear displacement, capacitive transducer, Wheatstone bridge, resonant circuit, oscillator.

## I. CAPACITIVE TRANSDUCERS FOR MEASUREMENT OF SMALL LINEAR DISPLACEMENT

### A. Capacitive transducers

Capacitive transducers are capacitors that change their capacity under the influence of the input magnitude, which can be linear or angular movement.

The capacity of a flat capacitor, composed of two electrodes with sizes  $a \times b$ , with area of overlapping  $s$ , located at a distance  $\delta$  from each other (in  $\delta \ll a/10$  and  $\delta \ll b/10$ ) is defined by the formula [4],[7]:

$$C = \frac{\epsilon_0 \epsilon \cdot s}{\delta} \quad (1)$$

where:  $\epsilon_0 = 8,854 \cdot 10^{-12}$  F/m is the dielectric permittivity of vacuum;

$\epsilon$  - permittivity of the area between the electrodes (for air  $\epsilon = 1,0005$ );

$s=a \cdot b$  – overlapping cross-sectional area of the electrodes.

The capacity can be influenced by changing the air gap  $\delta$ , the active area of overlapping of the electrodes  $s$  and the dielectric properties of the environment  $\epsilon$ . Used in single (Fig.1) or differential performance (Fig.2) [1].

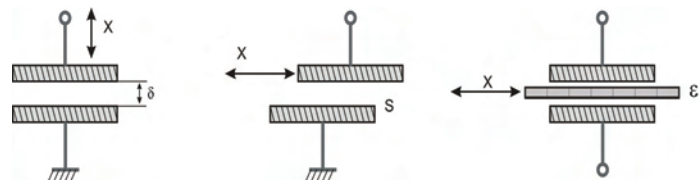


Fig. 1. Single capacitive transducers

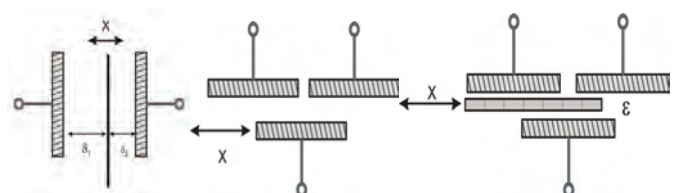


Fig. 2. Differential capacitive transducers

### B. Application of capacitive transducers

Capacitive sensors have found wide application in automated systems that require precise determination of the placement of the objects, processes in microelectronics, assembly of precise equipment associated with precise positioning, accurate measurements of shafts, axes of disk devices, spindles for high speed drilling machines, ultrasonic welding machines and in equipment for vibration measurement. They can be used not only to measure displacements (large and small), but also the level of fluids, fuel bulk materials, humidity environment, concentration of substances and others [6].

Capacitive sensors are often used for non-contact measurement of the thickness of various materials, such as silicon wafers, brake discs and plates of hard discs. Among the possibilities of the capacitive sensors is the measurement of density, thickness and location of dielectrics.

When used to measure linear or angular displacement, they are composed from movable and fixed electrodes. The movable is attached to the object, whose parameters of the movement are being measured. When moving the capacity of the transducer is changing and because of it there is a change in the output information.

### C. Measuring circuits

The most preferred for measurement of physical quantities with transducers are bridge circuits, they are characterized by high accuracy measurement in the equilibrium mode. In this mode, the display is independent of the calibration uncertainty

<sup>1</sup> Veselka Ivancheva is with the Faculty of Automatics at Technical University of Sofia, 8 Kl. Ohridski Blvd, Sofia 1000, Bulgaria, e-mail:&vivancheva@yahoo.com

<sup>2</sup> Silvia Kachulkova is with the Faculty of Automatics of Sofia, 8 Kl. Ohridski Blvd, Sofia 1000, Bulgaria.

<sup>3</sup> Bozhidar Dzhudzhev is with the Faculty of Automatics at Technical University of Sofia, 8 Kl. Ohridski Blvd, Sofia 1000, Bulgaria=

<sup>4</sup>Vladislav Slavov is with the Faculty of Automatics at Technical University of Sofia, 8 Kl. Ohridski Blvd, Sofia 1000, Bulgaria.

of the indicator. In the arms of the bridge there can be one, two or four transducers.

Very often, the measuring methods using bridge circuits are inappropriate because of the specific characteristics of the transducers, that is why other methods are used.

In the upper quoted applications is important to know not the exact capacity change of the condenser, but the relationship between the measured value and the output.

Perhaps one of the most commonly used measurement schemes in this context is the so-called resonant oscillating circuit. It contains inductance and capacitance, operating at resonance (Fig. 3) [5]. The principle of this scheme lies in the well-known formula of the resonant circuit:

$$f_r = \frac{1}{2\pi\sqrt{RC}} \quad (2)$$

where it is obvious that when there is a change in C or L the resonant frequency  $f_r$  will change too.

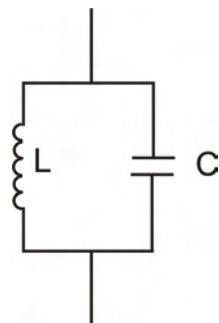


Fig. 3. L-C oscillating circuit

The resonant circuit can be used together with an amplifier circuit, thereby forming a scheme known as oscillator. The oscillator generates a sinusoidal AC output signal with a frequency equal to the resonant frequency of the LC circuit. Therefore, if the resonant frequency of the oscillating circuit is changed by modifying the capacity C, the variable frequency signal to the oscillator output will also change.

## II. SCHEMES FOR TESTING OF CAPACITIVE TRANSDUCERS FOR MEASURING SMALL LINEAR DISPLACEMENT

The block diagram for the examination of capacitive transducers measuring small linear displacement is shown in Fig. 4.

In it the oscillating circuit is realized by the coil L, a capacitor with a capacitance 290 pF and parallel the examined capacitive transducer  $C_x$  (Fig. 5). Using a variable capacitor it is possible a change in the capacity of C, hence the frequency of the oscillating circuit and hence the frequency of the oscillator.

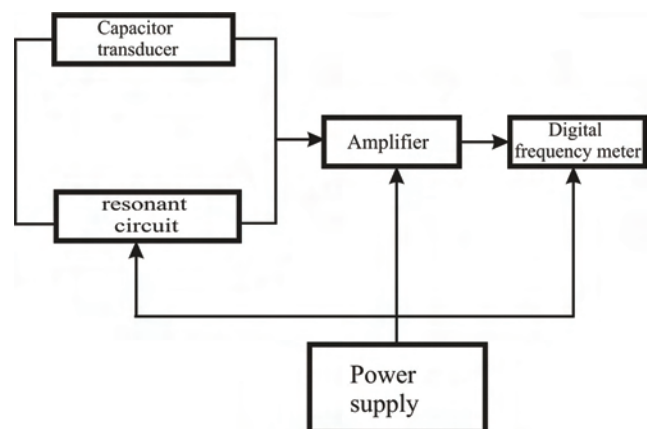


Fig. 4. Block diagram for the examination of capacitive transducers

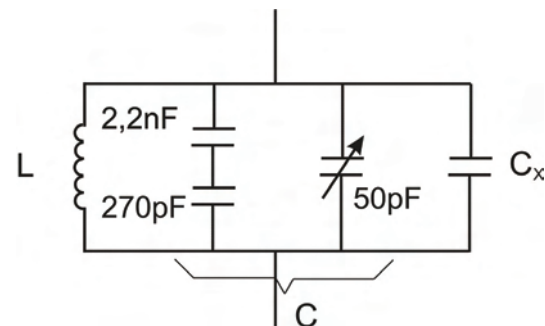
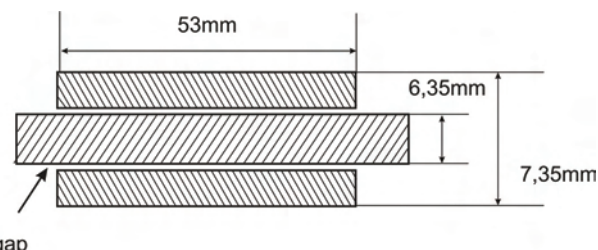


Fig. 5. Scheme of resonant circuit

For the tests two types of capacitive transducers are used:

- cylindrical (coaxial) transducer with a change of the active area of the electrodes overlap "s" - (Fig.6.) This transducer has internal movable electrode. The capacity of this capacitor, calculated by formula 2 is 20,2 pF;

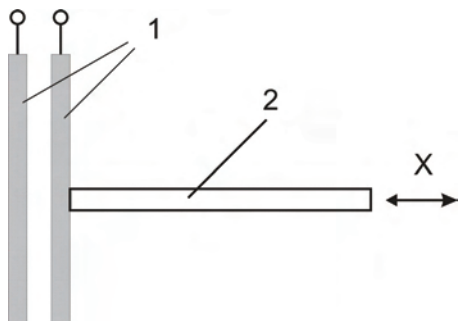


Air gap



Fig.6. Capacitive transducer with a change of the active area of overlap

- capacitive transducer with a change of the distance "d" between its flat electrodes (Fig. 7).



1 - plates of the capacitive transducer;  
2 - micrometer screw;  
X- linear moving.



Fig. 7. Capacitive transducer with change of the distance between the plates

The principal electrical circuit for examining the transformation functions of the capacitive transducers is shown in fig. 8.

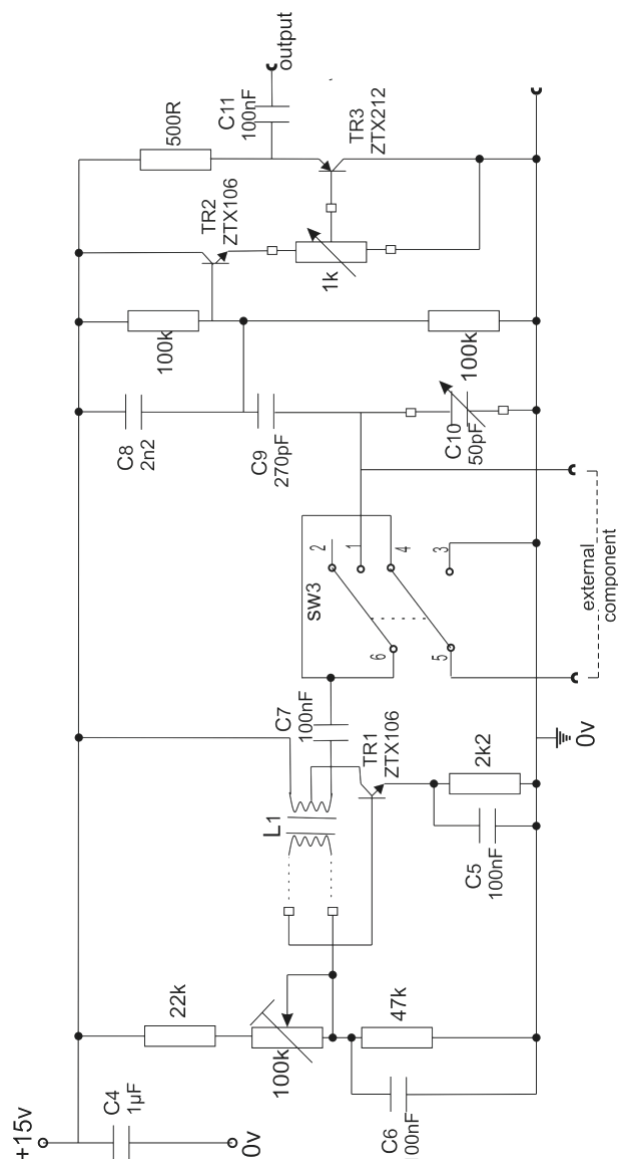


Fig. 8. Oscillator circuit

### III. MEASUREMENT RESULTS

#### 3.1. Examination of capacitive cylindrical transducer's transfer functions with variable overlapping area.

There is full overlapping of the active electrodes' area in position of 20 mm of the micrometric screw. The transducer is studied when changing the position of the slider micrometer screw between 20 and 65, which corresponds to a linear shift from 0 to 45 mm and three values of the capacity of the included vibrating capacitor circuit (30 pF, 40 pF and 50 pF). The results are given in the table (Table I) and graphically (fig. 9). Figure 9 shows that almost linear function of conversion for linear displacement of 45 mm can be achieved.

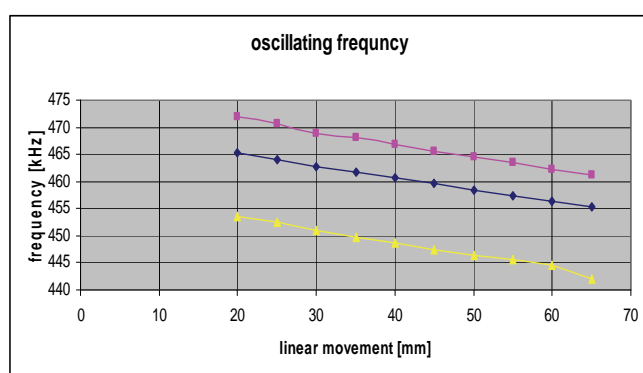


Fig. 9. Cylindrical capacitive transducer's transfer function

TABLE.I  
INVESTIGATION OF CYLINDRICAL CAPACITIVE TRANSDUCER

Slider position [mm]	Frequency [kHz] with $C_{var}=30$ pF	Frequency [kHz] with $C_{var}=40$ pF	Frequency [kHz] with $C_{var}=50$ pF
20	465,3	471,97	453,65
25	463,96	470,60	452,40
30	462,76	468,84	451,09
35	461,7	468,01	449,68
40	460,59	466,89	448,60
45	459,61	465,67	447,50
50	458,47	464,53	446,46
55	457,33	463,39	445,54
60	456,27	462,27	444,49
65	455,43	461,32	442,15

3.2 Examination of the transfer function of a capacitive transducer with a variable distance between the plates of a flat capacitive transducer.

The transducer is studied when changing the position of the slider micrometer screw between position 10 and 15, which corresponds to a linear shift from 0 to 5 mm. The results are given in the table (Table II) and graphically (figure 10). Figure 10 shows that linear function of conversion for linear displacements of about 5 mm cannot be achieved, but this type of very successful transducers can be used to measure displacements of the order of  $\mu m$ .

TABLE.II  
INVESTIGATION OF FLAT CAPACITIVE TRANSDUCER

Slider position [mm]	Oscillating frequency [kHz]
10,0	466,7
10,5	466,17
11,0	465,43
11,5	464,53
12,0	463,39
12,5	461,91
13,0	459,9
13,5	457,0
14,0	445,16
14,5	435,12
15,0	425,0

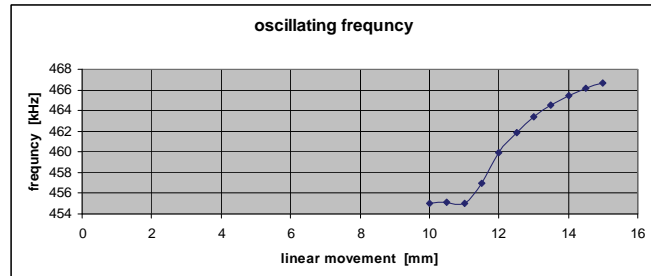


Fig.10.Transfer function of a capacitive transducer with a variable distance between the flat plates

#### IV. CONCLUSIONS

The article is dedicated to the capacitive transducers and their applications for measurement of small linear displacements in the order of mm. Experimentally were defined and investigated the transfer functions of two capacitive transducers: with a variable overlapping area of the plates and variable distance between the plates. Transducers are included in the resonant circuit and the received signals are amplified. They can very well be used where a precise determination of the location of objects in the order of  $\mu m$  and mm.

#### ACKNOWLEDGEMENTS

The researches, the results of which are presented in this publication are funded by internal competition TU-2012 contract to support PhD student № 122 RP 0074-08 "Study and optimization of processes for measuring vibration".

#### REFERENCES

- [1] www.AutoMatic-Project.eu
- [2] www.mgu.bg/drugi/ebooks/tokmak/2\_1.pdf
- [3] http://dtnpe.tu-sofia.bg/uploads/materials/ITHMV.pdf
- [4] Metrology and Measuring Equipment, Volume 2 - edited by Prof. Hristo Radev, Sofia, Softrade, 2010.
- [5] Feedback Instruments Ltd - Manuals 2942, 342A/B, EEC 470/1/2/3/4/7, UK, 1996.
- [6] Measurement Systems: Application and Design – 5-th ed. (McGraw-Hill Series in Mechanical and Industrial Engineering), Author: Ernest O. Doebelin, 2004.
- [7] The Measurement, Instrumentation and Sensor, John G. Webster, 1999 by CRL Press LLC.

# RADFET as a sensor and dosimeter of gamma-ray irradiation

Milić M. Pejović<sup>1</sup>, Momčilo M. Pejović<sup>1</sup> and Nikola T. Nešić<sup>1</sup>

**Abstract – Gamma-ray irradiation and post irradiation response at room and elevated temperature have been studied for RADFETs with gate oxide thickness of 100 nm with gate polarization during irradiation of 5 V as well as for RADFETs with gate oxide thickness of 400 nm with gate polarization of 0, 2.5 and 5 V. The response was observed on the basis of threshold voltage shift,  $\Delta V_T$ . Approximately linear dependence between  $\Delta V_T$  and absorbed dose was established. During the annealing at room temperature the RADFETs with the gate thickness of 400 nm and the gate polarization during irradiation of 2.5 V and 5 V shows the tendency in  $\Delta V_T$  decrease, while for 400 nm RADFETs with the zero gate polarization during irradiation and 100 nm RADFETs  $\Delta V_T$  remains approximately. Continued annealing at 120 °C leads to the decrease of  $\Delta V_T$ . For 100 nm RADFETs,  $\Delta V_T$  decreases to zero while for 400 nm RADFETs such decrease is considerably smaller.**

## I. INTRODUCTION

Radiation sensitive Al-gate p-channel MOSFETs (also known as RADFETs, or pMOS dosimeters) have been developed for applications such as space, nuclear industry and radio therapy [1-3]. The basic concept of RADFET is to convert the threshold voltage shift,  $\Delta V_T$ , induced by gamma-ray irradiation into absorbed dose  $D$ . This dependence can be expressed in the form [4]

$$\Delta V_T = AD^n, \quad (1)$$

where  $A$  is the constant and  $n$  is the degree of linearity which depends from electric field, oxide thickness and absorbed radiation dose. Ideally, the dependence should be linear, i.e.  $n=1$  and in that case  $A$  represents sensitivity,  $S$  of RADFETs:

$$S = \frac{\Delta V_T}{D}. \quad (2)$$

Irradiation leads to the creation of positive gate oxide charge and interface traps at Si/SiO<sub>2</sub> interface. Both the positive gate oxide charge and interface traps in p-channel MOSFETs contribute to the  $\Delta V_T$  in same direction and this fact is one of the main reasons for transistor application as a detector of absorbed dose of gamma irradiation. The RADFETs must satisfy two fundamental demands: a good compromise between sensitivity to irradiation and insignificant recovery at room temperature after irradiation, i.e. the information about radiation dose must be preserved over time.

<sup>1</sup> University of Nis, Faculty of Electronic Engineering, Aleksandra Medvedeva 14, 18000 Nis, Serbia-milic.pejovic@elfak.ni.ac.rs

## II. EXPERIMENT

The experimental samples were RADFETs manufactured by Tyndall National Institute, Cork, Ireland [5]. Oxide thickness was 100 and 400 nm, and they were grown at 1000 °C in dry oxygen and annealed for 15 minutes in nitrogen. The post-metallization anneal was performed at 440 °C in forming gas for 60 minutes.

Irradiation was performed in the Metrology Laboratory of the Vinca Institute of Nuclear Science, Belgrade. The RADFETs were irradiated at room temperature using <sup>60</sup>Co source up to absorbed dose of 35 Gy(Si) at absorbed dose rate of 0.002 Gy(Si)s<sup>-1</sup>. The gate polarization,  $V_{irr}$ , during irradiation of RADFETs with the gate oxide thickness of 400 nm was 0, 2.5 or 5 V, while for the samples with oxide thickness of 100 nm polarization was 5 V (all other pins were grounded). After irradiation the samples were annealed at room temperature for 218 days without polarization (all pins were grounded). After that, the annealing was continued at elevated temperature of 120 °C also without gate polarization for 15 days.

The change in threshold voltage shift  $\Delta V_T$  due to gamma-ray irradiation and annealing can be expressed as [6]

$$\Delta V_T = \Delta V_{ot} + \Delta V_{it}, \quad (3)$$

where  $\Delta V_{ot}$  and  $\Delta V_{it}$  are contributions to the change in threshold voltage due to the positive oxide charge and interface traps, respectively.  $\Delta V_{ot}$  and  $\Delta V_{it}$  can be expressed as a function of areal density of positive gate oxide charge  $\Delta N_{ot}$  and areal density of interface traps  $\Delta N_{it}$  [7]

$$\Delta V_{ot} = \pm \frac{q}{C_{ox}} \Delta N_{ot}, \Delta V_{it} = \frac{q}{C_{ox}} \Delta N_{it}. \quad (4)$$

In the above expression, the upper sign refers to n-channel MOSFETs and the lower sign refers to p-channel MOSFETs (the absolute value of p-channel MOSFETs threshold voltage is given throughout the paper),  $C_{ox}$  is the gate capacitance per unit area and  $q$  is absolute value of electron charge.

In order to detect the radiation and post irradiation response, the RADFETs transfer characteristics were measured, and the threshold voltage was determined as the intersection between  $V_G$  axis and extrapolated linear region of  $(I_D)^{1/2} - V_G$  curve. The sub threshold charge separate technique [7] was used to determine the contributions of  $\Delta V_{ot}$  and  $\Delta V_{it}$  to the threshold voltage shift  $\Delta V_T$ .

The I-V characterization was performed by Keithley 4200 SCS (Semiconductor Characterization System). The system is equipped with three medium power source measuring units (4200 SMU) for I-V characterization. The source measuring units have four voltage ranges: 200 mV, 2V, 20 V and 200 V, while the current ranges are 100  $\mu$ A, 1 mA, 100 mA and 1A. One of the source-measuring units is equipped with a preamplifier which provides the measurements of very small currents (in the order of 1 pA).

To illustrate the influence of irradiation on RADFETs behavior in Figure 1 we have plotted transfer characteristics in saturation before irradiation (curve (0)) and after irradiation for absorbed dose of 35 Gy(Si). The threshold voltage shift  $\Delta V_T$  can be expressed as  $\Delta V_T = V_T - V_{T0}$ , where  $V_{T0}$  is the threshold voltage before irradiation and  $V_T$  is the threshold voltage after irradiation (in Figure 1  $V_T$  is the threshold voltage after absorbed dose of 35 Gy). During annealing  $V_T$  represents the threshold voltage after determined time of annealing at room or elevated temperature.

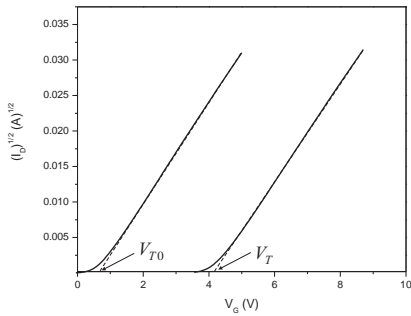
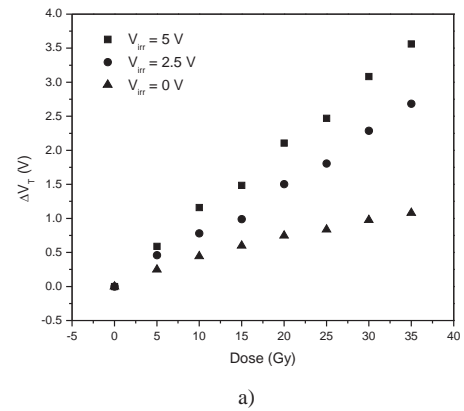


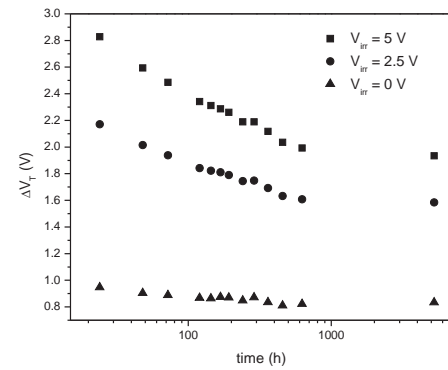
Figure 1. Transfer characteristics and values of threshold voltage shift before irradiation ( $V_{T0}$ ) and after irradiation of 35 Gy and  $V_{irr} = 5$  V ( $V_T$ ) for RADFET with 400 nm gate oxide thickness.

### III. RESULTS AND DISCUSSION

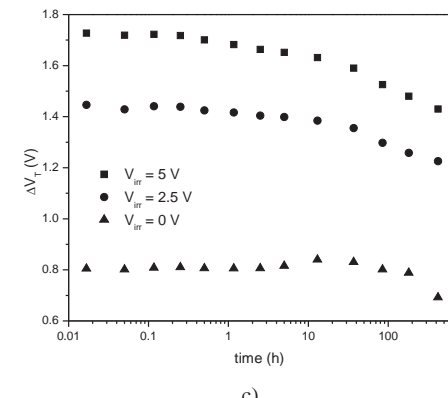
Figure 2a gives  $\Delta V_T = f(D)$  dependence of RADFETs with gate thickness of 400 nm for  $V_{irr}$  0, 2.5 and 5 V. It can be seen that  $\Delta V_T$  strongly depends on  $V_{irr}$  values during irradiation. For example, for the dose of 35 Gy the ratio of  $\Delta V_T$  for  $V_{irr} = 2.5$  V and  $V_{irr} = 0$  V is about 2.7 V, while for  $V_{irr} = 5$  V and  $V_{irr} = 0$  V the ratio is about 4.2. It can be concluded that the polarization on the gate can cause significant influence on the range of measured gamma-ray dose. Namely, with the increase of gate polarization the threshold voltage shift is higher for the same irradiation dose, what can drive the RADFET away from the area of linear dependence between threshold voltage shift and irradiation dose and also transistor is much more likely to fail. Doses used in our experiments are relatively small so they don't lead to significant degradation of RADFETs, i.e. there is approximately linear dependence between  $\Delta V_T$  and  $D$ .



a)



b)



c)

Figure 2. Threshold voltage shift  $\Delta V_T$  during a) irradiation, b) spontaneous annealing and c) annealing at 120 °C for RADFETs with 400 nm gate oxide thickness and gate polarization of 0, 2.5 and 5 V.

Figure 3a presents  $\Delta V_T = f(D)$  dependence for RADFETs with 100 and 400 nm thick oxide, respectively with the gate polarization of  $V_{irr} = 5$  V. It can be seen that there is also approximately linear dependence between  $\Delta V_T$  and  $D$  for RADFETs with the 100 nm oxide thicknesses, but these values are smaller than for RADFETs with the 400 nm oxide thicknesses. This shows that the sensitivity to gamma irradiation is bigger for RADFETs with thicker gate oxide due to larger density of positive oxide charge and interface traps for the same value of absorbed dose.

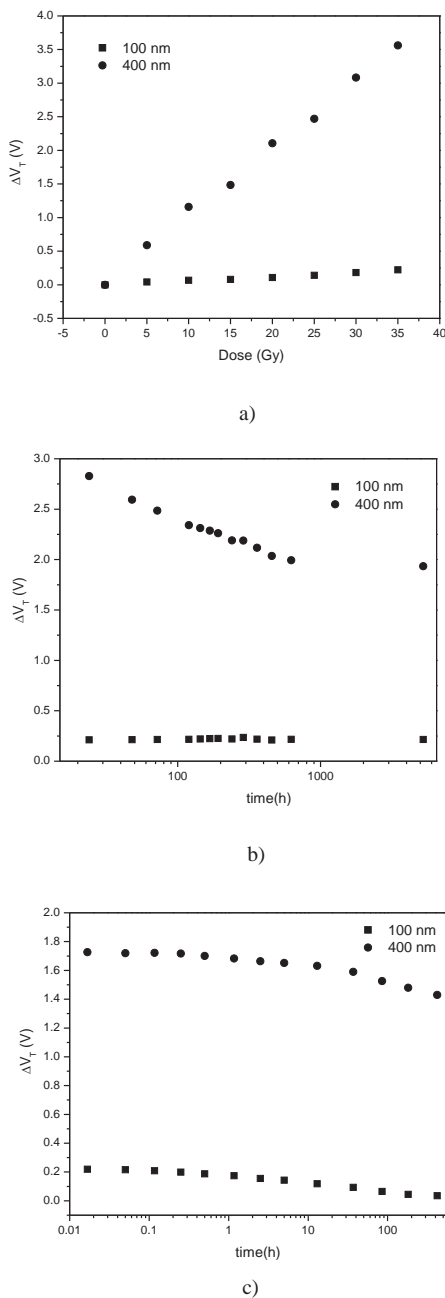


Figure 3. Threshold voltage shift  $\Delta V_T$  during a) irradiation, b) spontaneous annealing and c) annealing at 120 °C for RADFETs with 100 and 400 nm gate oxide thickness and gate polarization  $V_{irr} = 5$  V .

Figure 2b presents  $\Delta V_T$  evaluation during annealing at room temperature (spontaneous recovery) of irradiated RADFETs with the gate thicknesses of 400 nm for the duration of 218 days. It can be seen that the rate of dosimetric information loss (fading), i.e. the rate of  $\Delta V_T$  decrease in the early phase of spontaneous recovery depends on  $V_{irr}$  values during irradiation. For bigger  $V_{irr}$  values the rate of  $\Delta V_T$  decrease during annealing is higher. For RADFETs with  $V_{irr} = 0$  V during irradiation,  $\Delta V_T$  remains

approximately constant, while for RADFETs with  $V_{irr} = 2.5$  V and  $V_{irr} = 5$  V ,  $\Delta V_T$  decreases during spontaneous recovery during 1000 h, and after that period of time it remains approximately constant.

Figure 3b presents  $\Delta V_T$  evolution during spontaneous recovery for RADFETs with gate oxide thickness of 100 and 400 nm which were irradiated with gamma ray radiation up to 35 Gy and with  $V_{irr} = 5$  V gate polarization. It can be seen that  $\Delta V_T$  insignificantly changes during spontaneous recovery for RADFETs with 100 nm gate thickness, i.e. the dosimetric information is saved over time.

In order to determine whether the process of dosimetric information loss is finished after spontaneous annealing, the annealing is continued at the temperature of 120 °C for the 15 days. The threshold voltage shift,  $\Delta V_T$  , during such annealing for RADFETs with gate oxide thickness of 400 nm and gate polarization of 0, 2.5 and 5 V, is presented in figure 2c. It can be seen that the changes in  $\Delta V_T$  for RADFETs with gate polarization of 2.5 and 5 V are much smaller than the changes in the beginning of spontaneous annealing.

The continuation of annealing at 120 °C for RADFETs with 100 and 400 nm oxide thickness and gate polarization of  $V_{irr} = 5$  V is presented in figure 3c. It can be seen that 100 nm RADFETs show rapid  $\Delta V_T$  loss during annealing. For the time of 15 days RAFETs with 100 nm gate thickness loses all of the dosimetric information. For RADFETs with 400 nm gate thickness loss of dosimetric information is very small. It should be pointed out that mechanisms responsible for threshold voltage shift during irradiation and later annealing at room and elevated temperature are discussed in detail in the papers [8, 9].

#### IV. CONCLUSION

On the basis of above consideration, the following conclusion can be derived. In the range of absorbed dose of gamma radiation from 5 to 35 Gy there is approximately linear dependence between threshold voltage shift  $\Delta V_T$  and absorbed dose  $D$  and the degree of linearity rises with the increase of gate polarization during irradiation. Also, the sensitivity of RADFETs to gamma radiation increases with the increase of gate oxide thickness and gate polarization during irradiation. During spontaneous recovery for RADFETs with the gate oxide thickness of 100 nm and with gate polarization of 5 V as well as for RADFETs with gate oxide thickness of 400 nm and with no polarization on the gate,  $\Delta V_T$  remains approximately constant, i.e. dosimetric information is very well preserved. The continuation of annealing at 120 °C leads to complete loss of dosimetric information for RADFETs with gate oxide thickness of 100 nm and to partial loss of dosimetric information for RADFETs with gate oxide thickness of 400 nm.

#### ACKNOWLEDGMENT

Presented work was funded by Ministry of Science of Republic of Serbia under contract 177007.

## REFERENCES

- [1] A. Holmes-Siedle and L. Adams, "RADFET: A review of the use of metal-oxide-semiconductor devices as integrating dosimeters," *Radiat. Phys. Chem.*, vol. 28, pp. 235–244, 1986.
- [2] A. Kelleher, N. McDonnell, B. O'Neal, L. Adams and W. Lane, "The effects of gate oxide process variations on the long-term fading of pMOS dosimeters," *Sensor Actuators A*, vol. 37–38, pp. 370–374, 1993.
- [3] D. Gladstone, X. Q. Lu, J. L. Humm, H. F. Bowman and L. M. Chin, "Miniature MOSFET radiation dosimeter probe," *Med. Phys.*, vol. 21, pp. 1721–1728, 1994.
- [4] G. Ristic, S. Golubovic and M. Pejovic, "Sensitivity and fading of pMOS dosimeters with thick gate oxide," *Sensors and Actuators A*, vol. 51, pp. 153–158, 1996.
- [5] M. M. Pejovic, M. M. Pejovic and A. B. Jaksic, "Radiation-sensitive field effect transistor response to gamma-ray irradiation," [6] Nuclear Technology and Radiation Protection, vol. 26, pp. 25–31, 2011.
- [7] N. Stojadinovic, S. Golubovic, S. Djoric and S. Dimitrijev, "Modeling radiation-induced mobility degradation in MOSFETs," *Phys. Stat. Sol. (a)*, vol. 169, pp. 63–66, 1998.
- [8] J. P. McWhorter and P. S. Winokur, "Simple technique for separating the effects of interface traps and trapped-oxide charge in metal-oxide semiconductor transistor," *Appl. Phys. Lett.*, vol. 48, pp. 133–135, 1986.
- [9] A. Jaksic, G. Ristic, M. Pejovic, A. Mohammadzadeh, S. Sudre and W. Lane, "Gamma-ray irradiation and post-irradiation response of high dose RADFETs," *IEEE Trans. Nucl. Sci.*, vol. 49, pp. 1356–1363, 2002.
- M. M. Pejovic, M. M. Pejovic and A. B. Jaksic, "Contribution of fixed oxide traps to sensitivity of pMOS dosimeters during gamma ray irradiation and annealing at room and elevated temperature," *Sensors and Actuators A: Physical*, vol. 174, pp. 85–90, 2012.

# New approach for designing high-performance controllers in electrical drives systems using Programmable Logic Devices

Vladimir Karailiev<sup>1</sup> and Valentina Rankovska<sup>2</sup>

**Abstract –** A general architecture of an electromechanical system is suggested. Basic and auxiliary functions of its control device are described. Suitable components for high-efficiency control devices design are selected. A new approach for designing high-efficiency control devices in the electromechanical system is suggested, based on programmable logic devices (PLD). Basic information is given for the development flow hardware and software.

**Keywords –** Electromechanical System (EMS), Electrical drives, Field-Programmable Gate Arrays (FPGA), Design, Simulation.

## I. INTRODUCTION

More than 90% of the electrical drives in the world include induction motors. But the necessity of a fluent velocity adjustment in a wide range and the requirements for a high starting torque and high energy indices have been an introduce holdback of the induction motors in the automotive and electrical transport. Only the recent twenty years thanks to the development of the power electronics and the microprocessor circuits the inductive electrical drives have become competitive to the asynchronous ones. A variant of a new approach for designing high efficiency control devices in the electrical drive systems is presented in the paper.

## II. GENERAL BLOCK DIAGRAM OF ELECTROMECHANICAL SYSTEM

The examined Electromechanical Systems (EMS) are various kinds of electric drive systems, which convert the electrical energy into mechanical or vice versa. Generally these systems can be depicted by a simple block diagram, shown in Fig. 1, where: IN is an Interface node; CD – Control Device; PC – Power Converter; M – Motor; MN – Mechanical Node; ON – Operating Node; S1, S2, ..., Sn – sensors for the adjustable coordinates; PS – Power Supply; PG – Power Group of the EMS; ICG – Information Control Group.

<sup>1</sup>Vladimir Karailiev is with the Faculty of Electrical Engineering at Technical University of Sofia, 8 Kl. Ohridski Blvd, Sofia 1000, Bulgaria, E-mail: vkarailiev@gmail.com.

<sup>2</sup>Valentina Rankovska is with the Faculty of Electrical Engineering and Electronics at Technical University of Gabrovo, 4 H. Dimitar str., Gabrovo 5300, Bulgaria, E-mail: rankovska@tugab.bg.

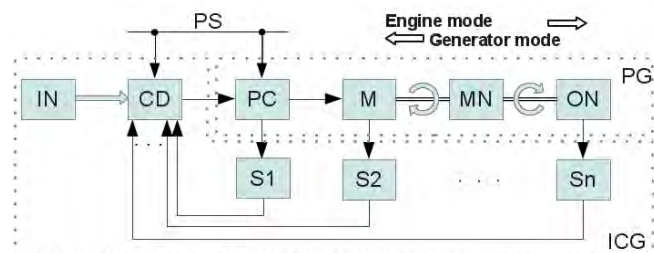


Fig. 1. Block diagram of electromechanical system

## III. BASIC AND AUXILIARY FUNCTIONS

IMPLEMENTED BY THE EMS CONTROL AND A CHOICE OF SUITABLE COMPONENTS FOR HIGH EFFICIENCY CONTROL DEVICES

**Functions, performed by the EMS control with a closed operational loop**

A control of the considered EMS means a process organization of the power conversion, supplying the necessary operation modes of the mechanical nodes. The control is automated, where the corresponding control signals could come from higher hierarchical level via wire or wireless interface (IN).

*The main functions executed by the EMS control are the following:*

- Starting, stopping and reversing the rotation direction;
- Keeping the defined coordinates values;
- Defined operation mode implementation by a control program;
- Watching arbitrary changing signals coming from the sensors.

*Auxiliary functions, performed at the monitoring, the control and the protection of EMS*

Except the main control functions some auxiliary functions can be performed such as:

- Protection of the electric motors, converters and mechanical nodes against various overloads;
- Locks preventing from failures and abnormal modes;
- Diagnostics and signaling for the system blocks states and for the progress of the technological process, etc.

**Selecting suitable components for the high efficiency control devices design**

The last tendencies in the high efficiency control systems in the electrical drive systems, based on control methods like: Magnetic field orientation; Vector control; Neural networks;

Searching based on fuzzy logic, use microcontrollers and DSP. However they have got many disadvantages, which do not allow them to achieve best results.

*Drawbacks of the traditional and DSP microcontrollers [1], [7]:*

- The lack of options for parallel data processing;
- Difficult interrupt request handling in complex system working in real time;
- Limited resources which make difficult the complex systems implementations;
- Lack of differential signaling inputs and outputs leading to low noise resistance;
- More difficult implementation of bit operations made entirely by software;

*Advantages of the programmable logic devices:*

The FPGA and CPLD production and applying is one of the fastest growing areas in electronics, because of the number of their advantages, like: ([3], [6], [7])

- Possibilities for synthesizing hardware by software means;
- Possibilities for integrating various functions and several microcontrollers in one chip;
- Implementing complex algorithms for parallel processing;
- Possibilities for using various embedded features;
- Higher information power at data processing;
- Software tools with many features for synthesis, simulation and verification of the designs;
- Easy implementation of bit operations, which leads to increased effectiveness of the processed information.

#### IV. A NEW APPROACH IN DESIGNING HIGH EFFICIENCY CONTROL DEVICES IN THE ELECTRICAL DRIVE SYSTEMS BASED ON FPGA

The appearance of the programmable logic devices (PLD) is a new era in the digital devices and systems design flow development. The configurable and reconfigurable logic devices are highly integrated flexible universal circuits, including power logic, memory and allowing In-system Programming (ISP).

**Main features, special purpose blocks and PLD selection criteria**

**FPGA main features** [8]

The system operation of FPGAs is defined by their features; their parameters are like of the other integrated circuits. An idea of the complexity of the FPGAs is derived from the number of the equivalent logic elements (LE), usually called System Gates (SG), and together with them the number of the Logic Cells (LC) is usually given in the technical data.

The ability of the FPGAs to communicate with other devices can be appreciated by the number of the parallel inputs and outputs and the highest possible speed. Other features are the number of embedded interface modules, the type of embedded memories and their volume. The memory organization is not fixed and can be configured during programming. The same is referred to the embedded FIFO memory blocks in some FPGAs often used as buffers. The

main features of the DSPs, which are optional blocks too, are the length of the multiplied numbers and the maximum operating frequency.

**Special purpose peripheral blocks in FPGAs**

- **Phased-Lock Loop (PLL) blocks**

Cyclone FPGAs include PLL blocks and a global clock network. The PLL allow:

- Clock multiplication and division;
- Phase shift;
- Programmable duty cycle;
- External clock outputs.

All the features allow the clock signals and edge delays control at system level.

- **Embedded hardware multipliers**

Most of the FPGAs of Xilinx and Altera include hardware multipliers. They could be used for digital signal processing, where many multiplications are implied, such as Finite Impulse Response (FIR) filters, quick Furrier transform, discrete cosine transform, etc.

- **Digital Signal Processors (DSP)**

Traditionally Digital Signal Processing/ Processors (DSPs) are used to process digital signals. They have a standard architecture, which advantage is that they are flexible and can be used for filtering and modulations. Only the software is changed for that purpose. On the other hand their flexibility limits their efficiency. Initially the DSPs include only one multiplier but the recent ones have to 8 multipliers. Iteration calculations consisting of 2 - 8 multiplications for the corresponding system clocks are usually used to calculate the result. That is why the DSPs are more suitable for signal processing in systems of medium to low productivity.

**Programmable logic selection criteria**

The FPGAs selection criteria depend on the application of the designed system. They can be as follows:

- An availability of embedded resources according to the application;
- Enough logic capacity, for the monitoring and control algorithms implementation;
- The features and the cost of the hardware and software development tools and configuration memories;
- The cost of the programmable logic devices;
- Availability of development tools, methodological and technical supplement, etc.

**Design flow for high efficiency electrical drive control devices**

There are two separate design stages which are carried out in parallel in time in order FPGA system to reach the market: design stage and debug and verification stage (Fig. 2). The detailed system design flow is presented in [2], [4], [5] and [8].

- **System design stage**

The main design stages are input, simulation, implementation and programming in FPGA. At this stage the debug also begins using simulation tools.

- **Debug and verification stage**

The severe problems not seen at the simulation process should be found out at the debug stage.

**Integrated development environment for system design**

The modern integrated development environments include program modules with wide range of features. They include:

- Tools used to input/ edit, compile, simulate, program the project;
- IP (Intellectual Property) cores, ready to use, implementing various functions – general purpose processor and DSP, components implementing various interfaces and communication protocols, modulators and demodulators, coders, memories, etc.;
- Software tools allowing creating projects including DSP modules; various tools for functional or timing design simulation;
- Various design and test modules for complex systems at block level;
- Software tools for design and simulation of applications based on 16- or 32-bit software CPU core including peripheral blocks, etc.

#### **Design approaches and stages**

There are two design approaches: Bottom-Up and Top-Down [4]. At the Top-Down approach a leading designer creates and optimizes the top level of the project on the whole. The Bottom-Up approach allows creating the project top level, which includes any number of projects from a lower level as partitions of it. Therefore the designer (or the designers in the team) can design and optimize every partition as a separate project.

The FPGA based devices and systems design consequence is nearly identical for the various producers and consists of the following stages, shown in Fig. 2.

a) It is possible to input a device or a system design as a behavior or structure model with various design automation software tools in the following ways:

- By a program written on some of the following hardware description languages - AHDL, VHDL, Verilog, etc.
- Usage of ready library components;
- Creation of a memory initialization file using a special memory editor;
- As a block diagram using a block editor;
- A combination of the above approaches.

#### **6) Defining project assignments and integrated environment settings**

The preliminary assignments of various requirements to the project and software environments settings allow controlling their features and options in order to increase its effectiveness. Conditions for project optimization can be also defined.

##### **e) Project compilation**

Two main approaches for design compilation exist – flat and incremental compilation. In the flat compilation the compiler uses several modules to manage the project, creating one or more files for programming.

In the incremental compilation it is possible to compile project partitions independently. It reduces the necessary memory and time for the compilation process, allowing recompiling only the modified parts of the design. The incremental compilation is used with large designs and when changes have to be made only in some parts.

The compilation stage consists of several sub-stages: *Analysis & Synthesis, Place & Route, Assembling and Timing Analysis*.

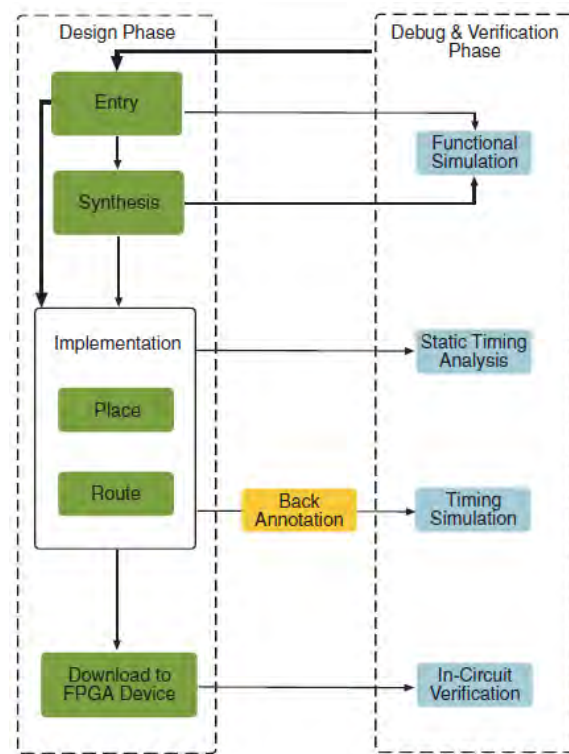


Fig. 2. Design flow for FPGA based systems

The design database is created at the *Analysis & Synthesis* process. A logical synthesis is made with minimizing the logic used and verifying the logical completeness and for syntax errors. An optimization is made considering the volume of the resources used.

*Fitting* (place and route) the design logic blocks is performed after that according to the available chip capacity. At the same time the defined logical and timing requirements for the project are checked.

During *the assembly* the design processing is finished by creating device programming files and data for the consumed power.

*The time analysis* is a method for analyzing, debugging and verification the correct operation of the project. The all signal path times in the project are measured and the project operation and efficiency is verified.

##### **Design simulation**

The integrated environment simulator is a tool used to test and debug the design logical operation and the internal timings. It allows the verification of the design before its hardware implementation. The simulator can reduce considerably the time for initial design transmutation into a working circuit.

According to the type of the necessary information, functional or timing simulation could be carried out, to test the design logical operation.

##### **a) Simulator settings**

A vector waveform file consisting of the input vectors has to be created before simulation. The simulator uses it to simulate the input signals which the programmed circuit

would generate at the same conditions. Break points could be also added at which the simulation will stop allowing to the designer to correct the errors.

Other user settings could be also defined, such as simulation period, setting time and delay errors, detecting glitches in the transients, etc.

#### b) Options of the Vector Waveform Editor

The Vector Waveform Editor allows inputting simulation vectors and examining the simulation results in a graphical form. It can be used to create Vector Waveform Files (.vwf) or Compressed Vector Waveform Files (.cvwf), which contain the input simulation vectors. The waveform file can be created by defining the input logical levels as a graphical time diagrams.

#### c) Creating a Waveform file for design simulation

The waveform file is an ASCII file depicting the simulating input and output vectors in a graphical form. It is possible to input and edit the file, to add new nodes, to delete nodes, to change their order, to define the numbering system radix, to rename nodes and to change their type. An existing file also could be used. If the vector waveform file is used, it defines the following:

- Input logic levels, which control the pins and define the internal logic levels of the design.
- The nodes we want to watch at the times when the applied vectors start, stop and their duration.
- The nodes, which have to be grouped in the simulation process.
- The numbering system radix used at the interpretation of the logic levels.
- Bidirectional line simulation. They are represented in the .vWF or .cvwf file by two ports: one input and one output.

#### d) Design simulation and results report

The simulation process is carried out until its completion, till break point reached, till stopping or cancelling. The eventual errors and warnings could be examined in the Messages window.

### Hardware tools for FPGA and CPLD based system design

Altera produces several types of development tools according to the FPGA family an application area of the selected circuit [8]:

- For digital signal processing – variants of DSP Development Kits for various FPGA families;
- High-Speed Development Kits including various high speed interfaces;
- PCI/PCI-X - PCI Development Kits and PCI High-Speed Development Kits – including various type and quantity of memory, interfaces on a standard PCI card.

- Nios II Development Kits, including the software processor Nios II, the necessary software and an access to many Intellectual Property (IP) cores and example projects.
- General purpose design tools. All they use in-circuit serial programming.
- Autonomous Programming Units (APU) (with USB interface) including hardware and software for programming all the FPGA families of Altera.

## V. CONCLUSION

A new design approach for high efficiency control devices in the electrical drive systems is suggested in the paper. The main design and verification stages and hardware and software tools are examined. The approach allows reducing the design time and money for electrical drive systems operating at many times higher frequencies and applying new control methods with higher efficiency and better reliability.

## ACKNOWLEDGEMENT

The present work is partially supported by the Science Research Fund at the Ministry of Education, Youth and Science under contract № E1301/2013.

## REFERENCES

- [1] A. Bazzi, P. Krein. A Complete Implementation Procedure for State Estimation in Induction Machines on the eZdsp F2812, University of Illinois at Urbana-Champaign, 2010.
- [2] V. Rankovska, H. Karailiev. Digital Devices and Systems Design using Field-Programmable Gate Arrays, «E+E», no.1-2, pp. 8-15, 2011. (in Bulgarian)
- [3] Roger Woods et al. *FPGA-based Implementation of Signal Processing Systems*. John Wiley&Sons, New York, 2008.
- [4] *Quartus II Version 12.1 Handbook*. Vol. 1: Design & Synthesis, Altera Corp., 2012.
- [5] R. C. Coferand and Ben Harding. *Rapid System Prototyping with FPGAs: Accelerating the design process*. Oxford, Elsevier, 2006
- [6] Steve Kilts. *Advanced FPGA Design: Architecture, Implementation, and Optimization*. New York, John Wiley&Sons, 2007.
- [7] Implementation of a Speed Field Orientated Control of Three Phase AC Induction Motor using TMS320F240, Texas Instruments, 1998.
- [8] [www.altera.com](http://www.altera.com)

---

---

## Poster 9 - Energy Systems and Efficiency

---

---



# Analysis of the Mesh Voltage Calculation Method in the Presence of a Two-Layer Soil

Marinela Yordanova<sup>1</sup> Margreta Vasileva<sup>2</sup> Rositsa Dimitrova<sup>3</sup>

**Abstract –** This paper proposes a simplified method of accounting for a two-layer soil structure based on the value of the mesh voltage  $E_m$  in applying the computational procedure of the standard IEEE Std 80-2000. The approximation of the horizontally stratified medium with homogeneous earth is accomplished using a formula for equivalent resistivity.  $E_m$  has been determined for grounding grids with a square or rectangular shape.

**Keywords –** Grounding, Ground grid, Mesh voltage, Two-layer soil.

## I. INTRODUCTION

Standard IEEE Std 80-2000 [1], being a guide for the design of grounding system of electrical substations, uses the tolerable step and touch voltage depending on the duration of shock current as a criterion for assessment of the efficiency of safe grounding. In the standard, “Mesh voltage  $E_m$ ” is the maximum touch voltage within a mesh of a ground grid. That voltage  $E_m$  must be less than the tolerable touch voltage  $E_{touch}$ , defined according to [1].

The standard introduces a coefficient  $K$  that takes into account the two-layer structure of the soil:

$$K = \frac{\rho_2 - \rho_1}{\rho_2 + \rho_1} \quad (1)$$

$\rho_1, \rho_2$  - soil resistivity of the upper and the lower layer.

The annex F of [1] gives a brief discussion of how the different parameters affect the behavior of grounding systems for uniform soil resistivity and for a two-layer soil resistivity.

The thickness of the upper layer ( $h_1$ ) and  $K$  can have considerable influence on the performance of the ground system [1], i.e. the calculated ground grid resistance may be higher or lower than the same grid in a uniform soil.

The paper [5] shows the potential around the single end group grounding system for a two-layer soil, but there is no formula to calculate the influence of the kind of soil over the resistance of grounding system. There are no results for grid grounding system, either.

The paper [2] extends an electromagnetic model for a time-harmonic analysis of a grounding system to a horizontally stratified multilayer medium which consists of air and arbitrary number of soil layers. The model is based on

<sup>1</sup>Marinela Yordanova is with the Electrical Engineering Faculty of the Technical University of Varna, 1 Studentska St, Varna 9010, Bulgaria, E-mail: mary\_2000@abv.bg.

<sup>2</sup>Margreta Vasileva is with the Electrical Engineering Faculty of the Technical University of Varna, 1 Studentska St, Varna 9010, Bulgaria, E-mail: greta\_w@mail.bg.

<sup>3</sup>Rositsa Dimitrova is with the Electrical Engineering Faculty of the Technical University of Varna, 1 Studentska St, Varna 9010, Bulgaria, E-mail: r.dimitrova@tu-varna.bg.

applying the finite element approach to an integral equation formulation.

Expressions for the mesh voltages [3] caused by earth fault currents leaking from earthing grids buried in uniform, two- and three-layer soils are proposed based upon the examination of a large set of grids and soil structures using the finite element approach. Simple empirical correction factors are developed to modify the mesh voltage formulae for uniform soils so as to account for multi-layer soil structures. The authors suggest a new method for calculation of  $E_m$  in multi-layer soils, different from IEEE Std 80-2000 method.

The idea of this paper is to propose a simplified method of accounting for a two-layer soil structure based on the value of the mesh voltage  $E_m$  in applying the computational procedure of the standard [1] and determining the equivalent resistivity of the soil, given in [2].

## II. MESH VOLTAGE

The equation for mesh voltage [1] is:

$$E_m = \frac{\rho \cdot K_m \cdot K_i \cdot I_G}{L_m} = K_G \cdot I_G \quad (2)$$

$I_G$  - ground fault current, A;  
 $K_G$ , V/A

$K_m, K_i, L_m$  - according to equations (81) to (91) from [1];

$\rho$  - Soil resistivity,  $\Omega \cdot m$ .

$K_m$  - Spacing factor for mesh voltage, simplified method

$K_i$  - Correction factor for grid geometry, simplified method

$L_m$  - Effective length of  $L_C + L_R$  for mesh voltage, m;

$L_R$  - Total length of ground rods, m

$L_C$  - Total length of grid conductor, m

## III. EQUIVALENT SOIL RESISTIVITY IN A TWO-LAYER SOIL STRUCTURE

In order to account for the influence of the soil structure, it is necessary to calculate the equivalent resistivity  $\rho_e$ .

The approximation of the horizontally stratified medium with homogeneous earth is accomplished using the following commonly used formula [2,4]:

$$\rho_e = \frac{D}{\frac{1}{\rho_n} \left( D - \sum_{i=1}^{n-1} h_i \right) + \sum_{i=1}^{n-1} \frac{h_i}{\rho_i}} \quad (3)$$

Where  $h_i$  is the thickness of the  $i$ -th layer and  $D$  is the penetration depth that depends on the grounding system dimensions and  $\rho_i$  is the resistivity of the  $i$ -th layer. According to [2, 4] the recommended values of  $D$  are between 30 m and 50 m. The Eq. 3 for a two-layer soil is:

$$\rho_{e1,2} = \frac{D}{\frac{1}{\rho_2}(D - h_1) + \frac{h_1}{\rho_1}} \quad (4)$$

#### IV. CALCULATION PROCEDURE FOR MESH VOLTAGE

$K_G$  has been determined for grounding grids with a square or rectangular shape. It is used as indicated in [1]: S for a square grid and R for a rectangular grid. The number after the letter indicates the number of cells in the grid. Because in practice a grounding grid has a large number of meshes, the following kinds of grids are tested from S16 to S256 and from R16 to R256. It is assumed for most of the cases that  $\rho_1=100 \Omega m$ .  $K$ , which depends on the ratio between  $\rho_1$  and  $\rho_2$ , has different values, shown in Table 1. The depth of the grid  $h = 0,5$  and 1 m.

The following table represents the studied cases, which cover 720 situations of grounding grids without rods and different ratios between  $\rho_1$  and  $\rho_2$ . To allow comparison between the situations when  $E_m$  is calculated by using just one layer of soil ( $\rho_1$ ) and the suggested simplified method using equivalent resistivity  $\rho_{e1,2}$  (Eq. 3), there is "Case for comparison" in Table 1.

TABLE I  
STUDIED CASES

Grounding grids with a square shape without ground rods S16, S64, S144, S256 $h_1=0,7m$				
Sizes, m	K	$\rho_1/\rho_2$	Case for comparison	h,m
50x50	$\pm 0,33$	1/10	$\rho_{ekv} = \rho_1$	0,5
	$\pm 0,82$	1/5		
100x100	+0,67	1/2		1,0
	-0,9	2		
200x200		10		
		20		
Grounding grids with a rectangular shape without ground rods R16, R64, R144, R256 $h_1=0,7m$				
Sizes, m	K	$\rho_1/\rho_2$	Case for comparison	h,m
50x100	$\pm 0,33$	1/10	$\rho_{ekv} = \rho_1$	0,5
	$\pm 0,82$	1/5		
100x200	+0,67	1/2		1,0
	-0,9	2		
200x400		10		
		20		

\* For  $K = -0,9$   $\rho_l = 1000 \Omega m$ ;  $K = -0,82$   $\rho_l = 500 \Omega m$  and for other values of  $K$   $\rho_l = 100 \Omega m$

#### A. Results for $K_G$ for Grounding Grids with a Square or Rectangular Shape at Different Sizes and K:

For all cases in Fig.1 to Fig.7:

- 1 -  $K_G$  is obtained with equivalent resistivity  $\rho_{e1,2}$  (Eq. 4);
- 2 -  $K_G$  is obtained with equivalent resistivity  $\rho_{ekv} = \rho_1$ .

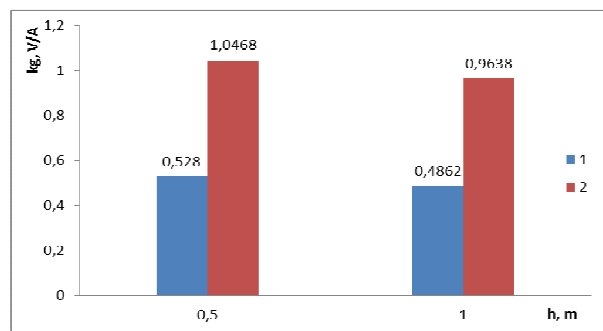


Fig.1.  $K_G$  versus  $h$  for  $S64$  100x100;  $K = -0,33$

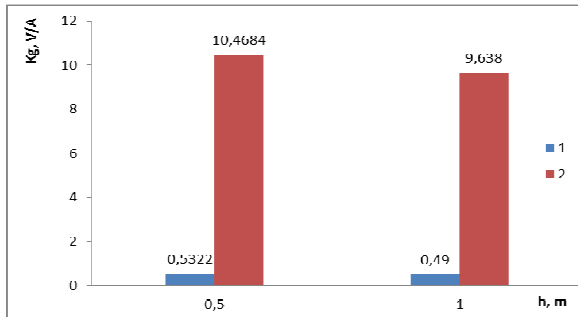


Fig.2.  $K_G$  versus  $h$  for  $S64$  100x100,  $K = -0,9$

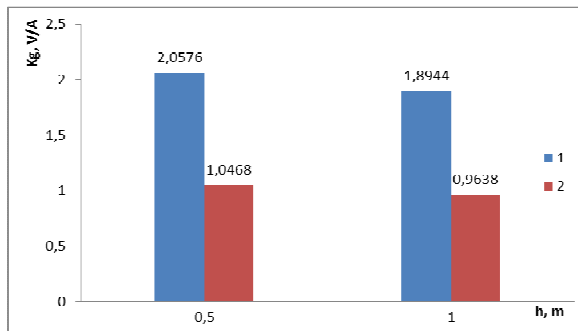


Fig.3.  $K_G$  versus  $h$  for  $S64$  100x100,  $K = +0,33$

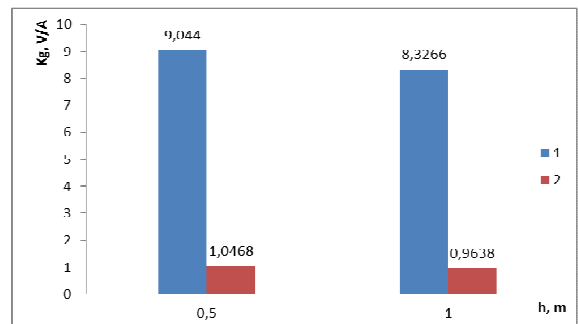


Fig.4.  $K_G$  versus  $h$  for  $S64$  100x100,  $K = +0,82$

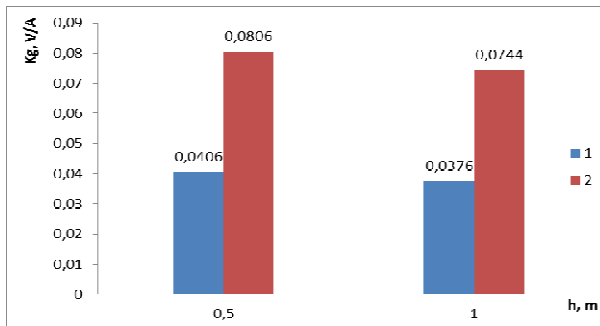


Fig.5.  $K_G$  versus  $h$  for R64 100x200;  $K = -0, 33$

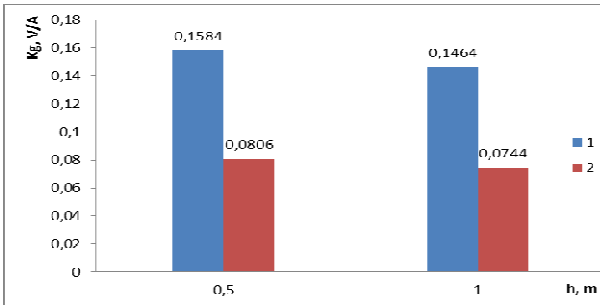


Fig.6.  $K_G$  versus  $h$  for R64 100x200;  $K = +0, 33$

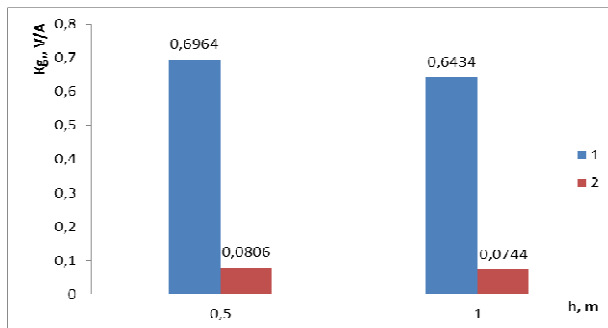


Fig.7.  $K_G$  versus  $h$  for R64 100x200;  $K = +0, 82$

#### B. Results for $K_G$ when the Grid is in the First Layer ( $\rho_1$ ) at Depth $h = 0,5$ m and $\rho_1 > \rho_2$ .

Table 2 and Fig. 8, Fig. 9 present the results for  $K_G$  when the grid is in the **first layer** ( $\rho_1$ ) at a depth  $h = 0,5$  m. For S64 100x100 m and R64 100x200  $\rho_1 > \rho_2$ ;  $\rho_1 / \rho_2 = 2; 10; 20$  and **negative K**:

$\rho_{ekv1}$  at  $K = -0,33$  ( $\rho_1 = 100\Omega.m$ ;  $\rho_2 = 50\Omega.m$ );  
 $\rho_{ekv2}$  at  $K = -0,82$  ( $\rho_1 = 500\Omega.m$ ;  $\rho_2 = 50\Omega.m$ );  
 $\rho_{ekv3}$  at  $K = -0,9$  ( $\rho_1 = 1000\Omega.m$ ;  $\rho_2 = 50\Omega.m$ );  $\rho_1 = 100\Omega.m$

#### C. Results for $K_G$ when the Grid is in the First Layer ( $\rho_1$ ) at Depth $h = 0,5$ m and $\rho_1 < \rho_2$ .

Table 3, Fig.8 and Fig. 9 present the results for  $K_G$  when the grid is in the **first layer** ( $\rho_1$ ) at depth  $h = 0,5$  m. For S64 100x100 m and R64 100x200  $\rho_1 < \rho_2$ ;  $\rho_1 / \rho_2 = 1/2; 1/5; 1/10$  and **positive K**:

$\rho_{ekv1}$  at  $K = +0,33$  ( $\rho_1 = 100\Omega.m$ ;  $\rho_2 = 200\Omega.m$ );

$\rho_{ekv2}$  at  $K = +0,67$  ( $\rho_1 = 100\Omega.m$ ;  $\rho_2 = 500\Omega.m$ );  
 $\rho_{ekv3}$  at  $K = +0,82$  ( $\rho_1 = 100\Omega.m$ ;  $\rho_2 = 1000\Omega.m$ );  
 $\rho_1 = 100\Omega.m$

TABLE 2  
 $K_G$  FOR GRID IN THE FIRST LAYER ( $\rho_1$ )  $\rho_1 > \rho_2$

$\rho_{ekv}$	$K$	$\rho_1 / \rho_2$	S64	R64
$\rho_{ekv1}$	-0,33	2	0,528	0,0406
$\rho_{ekv2}$	-0,82	10	0,5318	0,041
$\rho_{ekv3}$	-0,90	20	0,5322	0,041
$\rho_1 = \rho_2 = 100\Omega.m$	0	1	1,0468	0,0806

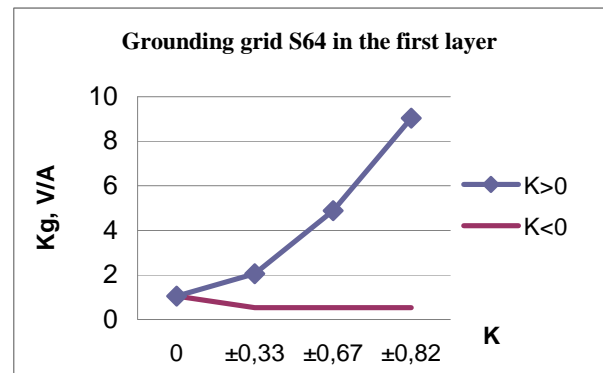


Fig.8.  $K_G$  versus  $K$  for S64 100x100

TABLE 3  
 $K_G$  FOR GRID IN THE FIRST LAYER ( $\rho_1$ )  $\rho_1 < \rho_2$

$\rho_{ekv}$	$K$	$\rho_1 / \rho_2$	S64	R64
$\rho_{ekv1}$	+0,33	1/2	2,0576	0,1584
$\rho_{ekv2}$	+0,67	1/5	4,8918	0,3768
$\rho_{ekv3}$	+0,82	1/10	9,044	0,6964
$\rho_1 = \rho_2 = 100\Omega.m$	0	1	1,0468	0,0806

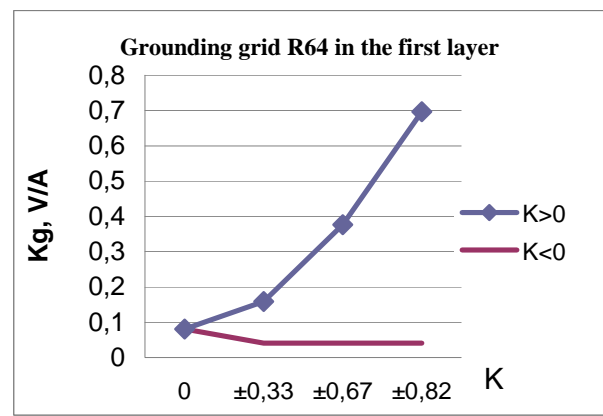


Fig.9.  $K_G$  versus  $K$  for R64 100x200

#### D. Results for $K_G$ when the Grid is in the Second Layer ( $\rho_2$ ) at Depth $h = 1,0$ m and $\rho_1 > \rho_2$

Table 4 and Fig. 9, Fig.10 present the results for  $K_G$  when the grid is in the **second layer** ( $\rho_2$ ) at depth  $h = 1,0$  m. For

S64 100x100 m and R64 100x200  $\rho_1 > \rho_2$ ;  $\rho_1/\rho_2 = 2; 10; 20$  and **negative K** (the values are the same as in B).

TABLE 4  
 $K_G$  FOR GRID IN THE SECOND LAYER ( $\rho_2$ )  $\rho_1 > \rho_2$

$\rho_{ekv}$	K	$\rho_1/\rho_2$	S64	R64
$\rho_{ekv1}$	- 0,33	2	0,4862	0,0376
$\rho_{ekv2}$	- 0,82	10	0,4896	0,0378
$\rho_{ekv3}$	- 0,90	20	0,4890	0,0378
$\rho_1 = \rho_2 = 100 \Omega \cdot m$	0	1	0,9638	0,0744

**E. Results for  $K_G$  when the Grid is in the Second Layer ( $\rho_2$ ) at Depth  $h = 1,0$  m and  $\rho_1 < \rho_2$**

Table 5 and Fig. 10, Fig.11 presents the result for  $K_G$  when the grid is in the **second layer** ( $\rho_2$ ) at a depth  $h = 1,0$  m. For S64 100x100 m and R64 100x200  $\rho_1 < \rho_2$ ;  $\rho_1/\rho_2 = 1/2; 1/5; 1/10$  and **positive K** (the values are the same as in C).

TABLE 5  
 $K_G$  FOR GRID IN THE SECOND LAYER ( $\rho_2$ )  $\rho_1 < \rho_2$

$\rho_{ekv}$	K	$\rho_1/\rho_2$	S64	R64
$\rho_{ekv1}$	+ 0,33	1/2	1,8944	0,1464
$\rho_{ekv2}$	+ 0,67	1/5	4,5038	0,348
$\rho_{ekv3}$	+ 0,82	1/10	8,3266	0,6434
$\rho_1 = \rho_2 = 100 \Omega \cdot m$	0	1	0,9638	0,0744

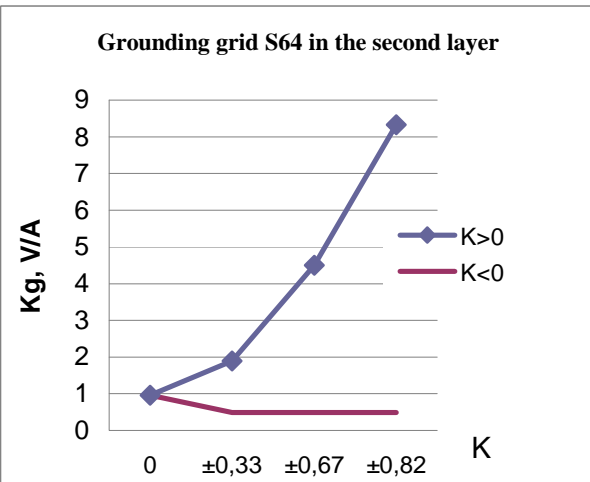


Fig.10. KG versus K for S64 100x100

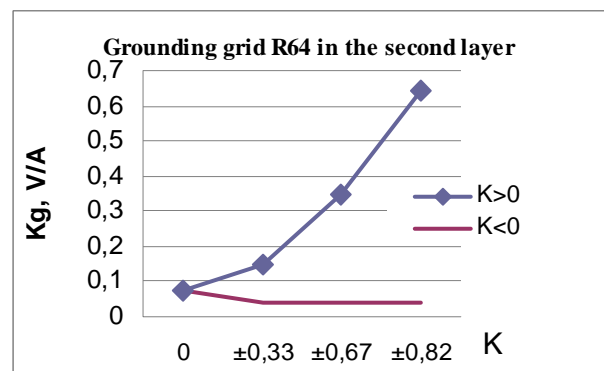


Fig.11.  $K_G$  versus K for R64 100x200

## I. CONCLUSION

1. The method and the computer program of the paper are confirmed using the discussion in F [1] about the values of the resistance of the grid for negative and positive K.
2. The results obtained at negative K showed that the value of  $K_G$  for the cases using  $\rho_{ekv}$  can be up to 20 times lower than the case of calculation with  $\rho_1$ . It leads to resizing and higher costs.
3. For positive K the value of  $K_G$  can be up to 2 times larger than the case of calculation with  $\rho_1$ . It means that the values obtained for  $E_m$  will be lower than the real ones, which affects electrical safety.
4. If the grid is either in the first layer or in the second layer at negative K, the range of change of  $K_G$  calculated without  $\rho_{ekv}$  (with  $\rho_1$ ) is less than the one at positive K.
5. For a two-layer soil it is convenient to use the suggested simple way to calculate the equivalent resistivity and  $E_m$ .

## ACKNOWLEDGEMENT

The carried out research is realized in the frames of the project, financed from the state budget "Investigation of processes in secondary circuits for control and protection" in TU-Varna.

## REFERENCES

- [1] IEEE Std 80- 2000, IEEE Guide for safety in AC Substation Grounding
- [2] S. Vujevic, P. Sarajevic, D. Lovric, "Time-harmonic analysis of grounding system in horizontally stratified multilayer medium", Electric Power Systems Research vol. 83 pp. 28– 34, 2012, www.elsevier.com/locate/epsr
- [3] J. Nahman, I. Paunovic, "Mesh voltages at earthing grids buried in multi-layer soil", Electric Power Systems Research vol. 80 pp. 556– 561, 2010, www.elsevier.com/locate/epsr
- [4] A.I. Jacobs, Reduction of the multilayer electrical structure of the earth to an equivalent two layers in the calculation of complex grounding systems, Electrical Technology (USSR) 3 (1970) 65–74.
- [5] Yordanova, M., B. Dimitrov. Potential characteristics of single and group earthing devices, iCEST 2010, 23-26 June, 2010, Ohrid, Macedonia.

# Design, Construction, Calibration and Use of A New Type of Electromagnetic Brake

Miroslav Bjekic<sup>1</sup>, Milos Bozic<sup>1</sup>, Marko Rosic<sup>1</sup>, Marko Popovic<sup>1</sup>, Dragisa Petkovic<sup>2</sup>

**Abstract –** The paper presents a new type of electromagnetic brake, designed at the Laboratory of electrical machines, drives, and control at the Faculty of technical sciences in Cacak, Serbia. In laboratory testing, the brake is designed to be an adjustable load for an electric motor. Procedure of design and construction is described. Calibration of the brake and measuring apparatus are described in detail. The most important electromechanical parameters are identified. The authors describe the procedure for its use as a controlled load of induction motors up to 7.5 kW of power, in order to determine the energy efficiency class.

**Keywords –** Electromagnetic brake, Design, Construction, Calibration.

## I. INTRODUCTION

This paper presents the procedure of design, construction and calibration of new type of electromagnetic brake. The brake is made as controlled load for electrical motors up to 7.5kW.

## II. DESIGN AND CONSTRUCTION

The brake has ferromagnetic disc with 8 ferromagnetic poles. Each pole has 690 winds of Cu wire (diameter of 0.95 mm). All conductors are in serial connection. Coils are powered with direct current. The direction of current should provide N-S poles cyclic. Brakes frame has two bearings, and they carry the shaft drive with disc. Between disc and poles is 0,8mm air gap. On the other side, the disc is attached to the motor shaft with footer.

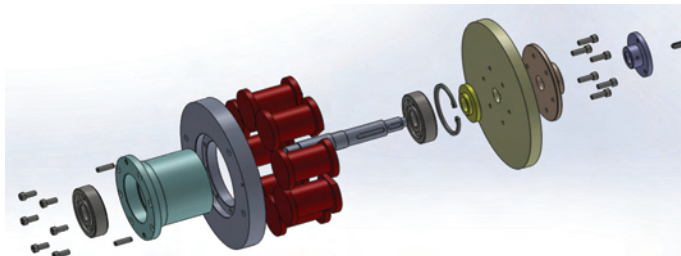


Fig. 1. Parts of electromagnetic brake

Work principle: motor rotates disc. Disc is a part of magnetic circuit, also disc moves in a magnetic field. In the disc is induced emf and the current witch creates a braking torque.

<sup>1</sup>Miroslav Bjekic, Milos Bozic, Marko Rosic, Marko Popovic are with the Faculty of Technical Sciences at University of Kragujevac, 65 Svetog Save 65, Cacak 32000, Serbia, E-mail: [mbjekic@gmail.com](mailto:mbjekic@gmail.com)

<sup>2</sup>Dragisa Petkovic is with the Masinsko-saobracajna skola, Dr Dragise Misovica, Cacak 32000, Serbia.

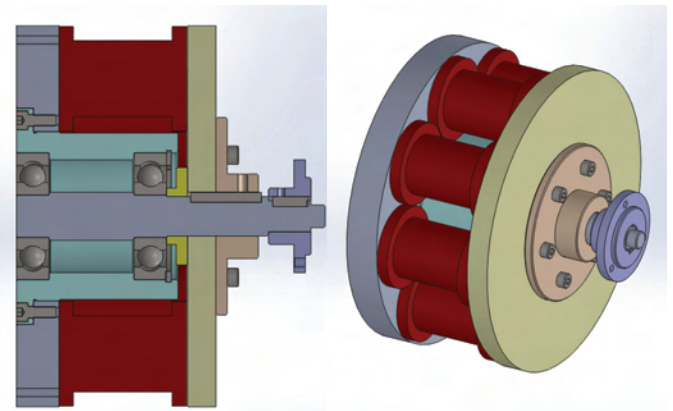


Fig. 2. Cross section and complete electromagnetic brake

During design, special attention was paid to the calculation of the axial electromagnetic force. This brakes construction is different from the standard brakes and it creates an unwanted axial force with which poles attract rotating disc [1]. The construction does not contain poles on both sides, and does not have two rotating discs, so the axial forces are not mutually canceled.

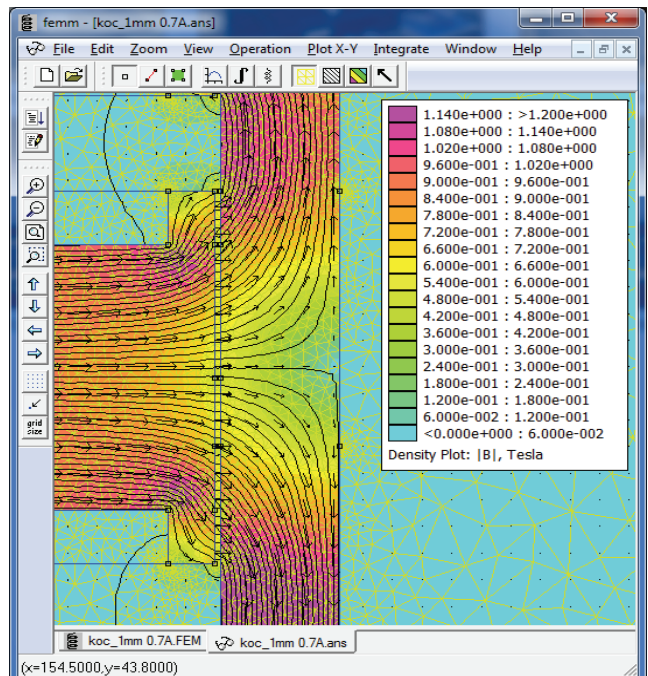


Fig. 3. Result of FEM simulation

For checking of construction parameters, FEM simulation was also performed. Figure 3. shows the approximate

distribution of the magnetic field in described magnetic system. For values of excitation current of 0.7 A (maximum current in calibration procedure) the axial force of  $8 \cdot 2.1 = 16.8 \text{ kN}$  was achieved.

### III. CALIBRATION

Induction motor 2.2 kW, with voltage of 380V was first connected to the brake. Modified equipment and software to determine the energy efficiency class of three-phase induction motors [2] was used. The motor was first in regime no load. Braking current was gradually increased for different values of the terminal voltage up to 7 A. In doing so, important parameters of electric motor are measured, and from them are directly calculated electromagnetic power and torque. Motors load is gradually increased until it stops.

Figures 4 and 5 show the results of measurements. From the figure can be observed, that the value of the breakdown torque achieved with brake was more than 70 Nm. A maximum power which is motor achieved is over 6 kW.

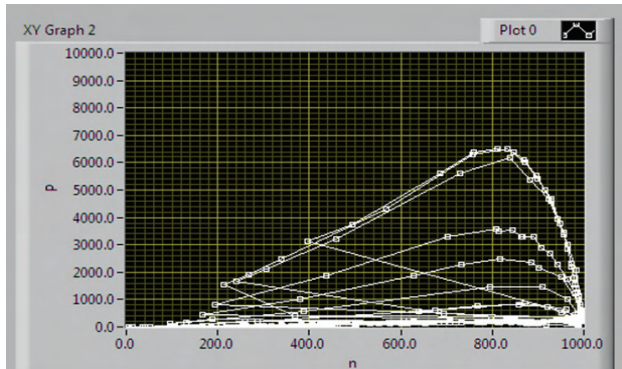


Fig. 4.  $P=f(n)$ ,  $I_k=0-7\text{A}$

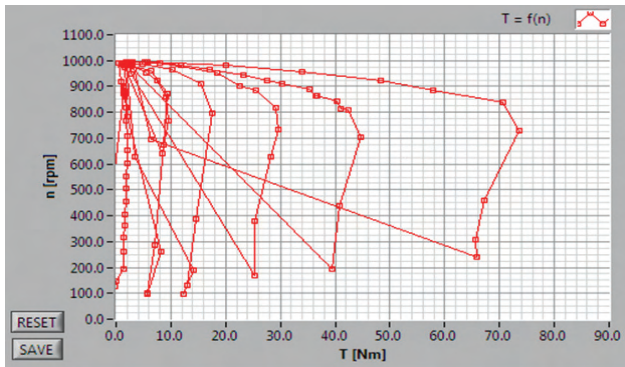


Fig. 5.  $n=f(T)$ ,  $U=50-400 \text{ V}$ ,  $I_k=0-7\text{A}$

However, for the calibration of brake DC motor was used. It has possibility of easier adjustment of mechanical characteristics: with voltage changing and decreasing the excitation current. Two DC motors were selected with powers 1.5 kW and 4.4 kW.

Several measurements were performed with different values of excitation current (up to a maximum nominal value), supply voltage (20V to 120V) and brakes current value from

0.2 A to 0.7 A. The results of the measurement are shown in the graph in Figure 8.



Fig. 6. DC motor1  $P=1500 \text{ kW}$



Fig. 7. DC motor2  $P=4400 \text{ kW}$

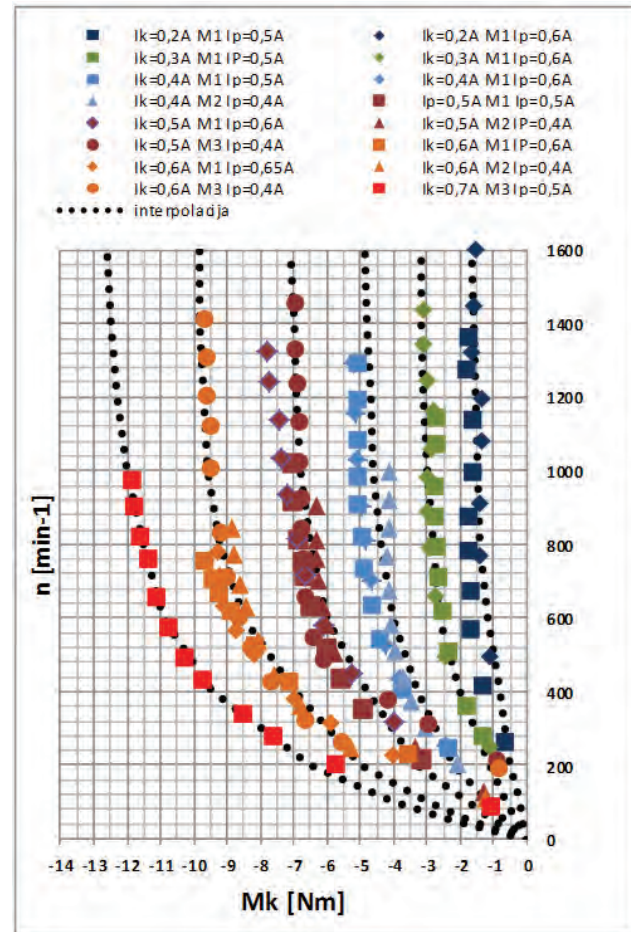


Fig. 8. Results of calibration with two DC motors

Motor 2 was adjusted two times for brake testing. That was the reason why these results are specifically separated: **mot2** i **mot3**.

Presented values are with accordance with expected values. Between the measured values the curve was drawn and its discrete numerical values are shown in the Table I.

TABLE I  
BRAKING TORQUE VALUES

n [min <sup>-1</sup> ]	M <sub>k</sub> [Nm] for I <sub>p</sub> =0,2-0,7A					
	0,2	0,3	0,4	0,5	0,6	0,7
0	0	0	0	0	0	0
50	0,12	0,35	0,71	1,06	1,76	2,35
100	0,2	0,6	1,2	1,8	3	4
200	0,5	1,1	2,2	3,3	5	6,5
400	0,8	2	3,3	4,8	7	9,45
600	1,2	2,6	4	6	8,5	10,9
800	1,4	2,8	4,4	6,5	9,2	11,5
1000	1,5	3	4,6	6,8	9,6	12
1200	1,55	3,1	4,7	6,9	9,7	12,3
1400	1,6	3,15	4,8	7	9,8	12,5
1600	1,65	3,2	4,85	7,1	9,8	12,6

Shown values, hereafter, will be used to determine the analytical expression of the braking electromagnetic torque as function of braking current and speed.

#### IV. DETERMINATION OF THE ANALYTICAL EXPRESSION OF THE BRAKING TORQUE

Here was used the MATLAB program and its application **cftool** with interpolation function (1).

$$M_k(n) = A \cdot e^{(B \cdot n)} + C \cdot e^{(D \cdot n)} \quad (1)$$

With this interpolation function dependence  $M(I_k)=f(n)$  can be presented efficiently and with few variables.

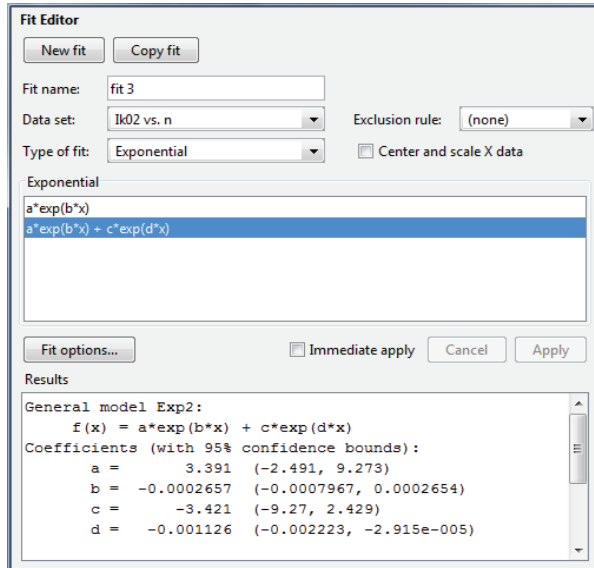


Fig. 9. Calculated coefficients A, B, C and D to obtain the interpolation function  $M=f(n)$  for  $I_k=0,2$  A

Figure 9 shows an example of calculated parameters for braking current  $I_k=0,2$  A.

Coefficients A, B, C and D were obtained for six values of braking current (0,2; 0,3; 0,4; 0,5 i 0,6 A).

Thereafter was made a new interpolation of interpolating coefficients with cubic polynomial (2):

$$y = p_1 \cdot I_k^3 + p_2 \cdot I_k^2 + p_3 \cdot I_k + p_4 \quad (2)$$

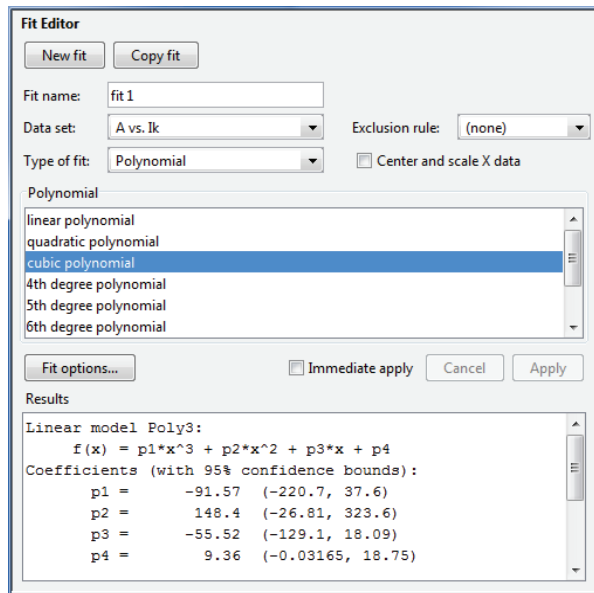


Fig. 10. Calculated coefficients of interpolation polynomial for determination of coefficient A

All results are presented in matrix form, suitable for programming:

$$\begin{bmatrix} A_1 & B_1 & C_1 & D_1 \\ A_2 & B_2 & C_2 & D_2 \\ A_3 & B_3 & C_3 & D_3 \\ A_4 & B_4 & C_4 & D_4 \end{bmatrix} = \begin{bmatrix} 91,57 & 0,0093 & 86,41 & 0,0452 \\ 148,40 & -0,1440 & -141,20 & 0,0672 \\ -55,52 & 0,0074 & 52,78 & -0,0358 \\ 9,36 & -0,0012 & -9,09 & 0,0037 \end{bmatrix} \quad (3)$$

$$A = A_1 \cdot I_k^3 + A_2 \cdot I_k^2 + A_3 \cdot I_k + A_4 \quad (4)$$

$$B = B_1 \cdot I_k^3 + B_2 \cdot I_k^2 + B_3 \cdot I_k + B_4 \quad (5)$$

$$C = C_1 \cdot I_k^3 + C_2 \cdot I_k^2 + C_3 \cdot I_k + C_4 \quad (6)$$

$$D = D_1 \cdot I_k^3 + D_2 \cdot I_k^2 + D_3 \cdot I_k + D_4 \quad (7)$$

The obtained results are shown in Figure 11. The figure shows set of analytical functions of electromagnetic braking torque as function of speed n and braking current  $I_k$ . Speed and braking current at some point define the braking electromagnetic torque at that point.

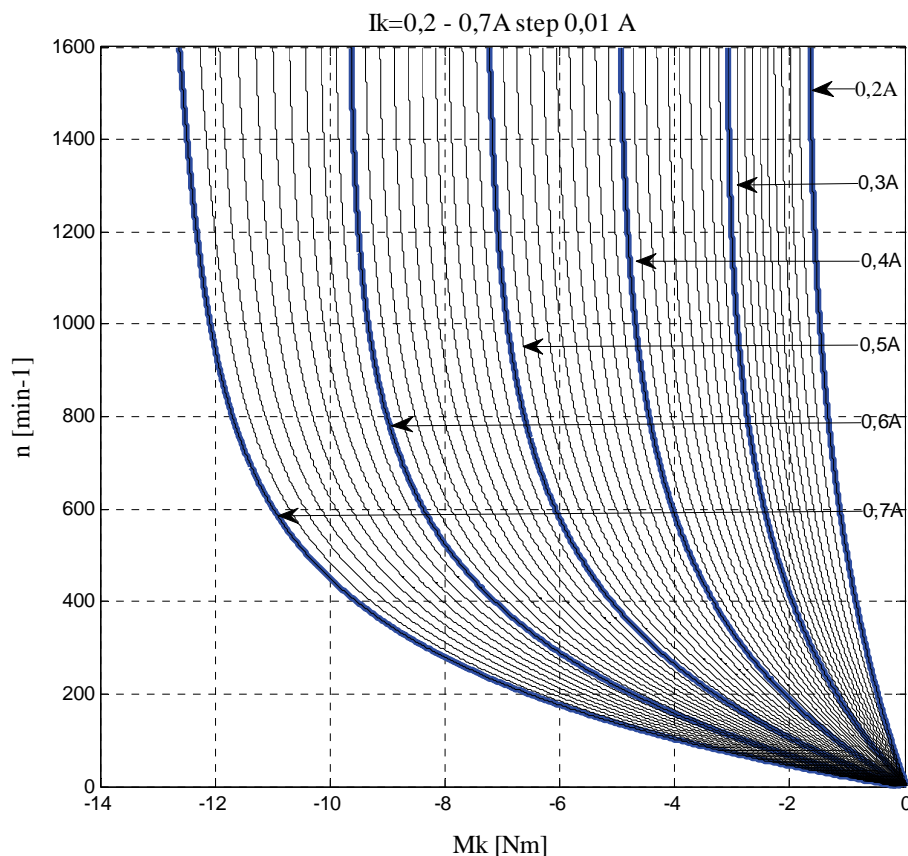


Fig. 11. Set of analytical functions that describes electromagnetic torque for speed range of 0-1600 min<sup>-1</sup> and braking currents from 0.2 A to 0.7A

## V. FUTURE STEPS

With described procedure it is possible to calculate the braking torque using the derived analytical expressions.

This means that the motor load (torque) can be determined, at any moment, if current values of only two parameters are known: speed of rotation and braking current.

The aim of further research can be introduced in this way: First, predefine motor load type: gravitational (constant load), fan or some other (variable load). Then, using feedback and new derived expression of required torque, braking current will be calculated considering the speed. By applying this current to the brake, motor will get the appropriate load.

## VI. CONCLUSION

This paper describes the process of design, construction and calibration of electromagnetic brake. The analytical expression of braking torque was derived, considering speed of rotation and braking current.

## ACKNOWLEDGEMENT

These results are part of the project financed by the Ministry of Education, Science and Technological Development of Serbia (TR33016).

## REFERENCES

- [1] [http://www.telmausa.com/TELMATECHWEB/DOC/PDF/Oc44\\_2071%20AC50-55.pdf](http://www.telmausa.com/TELMATECHWEB/DOC/PDF/Oc44_2071%20AC50-55.pdf)
- [2] M. Božić, M. Rosić, B. Koprivica, M. Bjekić, S. Antić, "Efficiency classes of three-phase, cage-induction motors (IE-code) software", INDEL2012, IX Symposium Industrial Electronics, INDEL 2012, pp 87-91, November 1-3, Banja Luka, Bosna i Hercegovina, 2012.
- [3] N. Pavlović "Proračun elektromagnetske kočnice za ispitivanje visokobrzinskih motora", INFOTEH-Jahorina Vol 11, 2012.
- [4] <http://www.stromaginc.com/PDF/eddycurrent.pdf>

# Energy Capability of Metal-Oxide Surge Arresters in Electric Power Lines 20 kV

Margreta Vasileva<sup>1</sup> and Marinela Yordanova<sup>2</sup>

**Abstract –** Practical experience indicates that the overloading of metal-oxide surge arresters (MOSAs) is due to peak value of lightning current, many consecutive lightning strokes or short-circuits. As a result of this breakdown of resistors occurs or surface discharges. In order MOSAs to be able to operate properly, their energy capability has to be higher than the expected energy loading at the moment of operation. The paper presents research results about protective operation and energy capability of metal-oxide surge arresters (MOSA) under influences of different lighting strokes and thermal loading of MOSA. The models give the emitted in MOSA energy needed to receive the heat field of MOSA.

**Keywords –** zinc-oxide varistor, metal-oxide surge arresters, energy capability, thermal replace scheme

## I. INTRODUCTION

The energy capability has been connected with the thermal load in the moment, when metal-oxyde surge arresters (MOSA) work. The operation of MOSA has been investigated under the influence of atmospheric excess voltages. An adiabatic thermal process has been considered. The absorption energy from MOSA has been received by mathematical model in Matlab.

The paper presents research results about protective operation and energy capability of metal-oxide surge arresters (MOSA) under influences of different lighting strokes and thermal loading of MOSA.

The researched problems have been resolved by electrical- thermal analogy. The received results are based on the substitute scheme with thermal capacitances, thermal strengthes and thermal fluxes.

The differential equations have been resolved by the method of the potential knots.

## II. MODELS OF LIGHTNING AND INDUCED SURGE WAVES

The shape of lightning and induced surge waves is

<sup>1</sup>Margreta Vasileva is with Technical University of Varna, Department of Electric Power Engineering, Studentska 1, Varna, 9010, Bulgaria, m.vasileva@tu-varna.bg

<sup>2</sup>Marinela Yordanova is with Technical University of Varna, Department of Electric Power Engineering, Studentska 1, Varna, 9010, Bulgaria, mary\_2000@abv.bg

aperiodic. The created model of lightning is shown in Fig. 1.

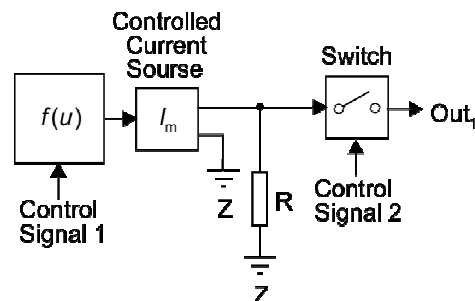


Fig. 1 Block lightning

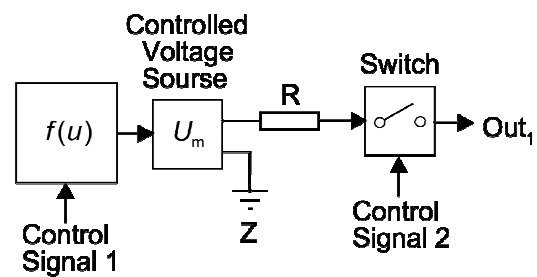


Fig. 2 Block induced overvoltages

The model in Fig. 1 is for single lightning. When there are N numbers of discharges the model consists of N number of that block.

The induced waves are modeled as a source of voltage with arbitrary shape and amplitude- Fig. 2.

Simulation Model of 20 kV grid is presented in [1]. It can be used to study wave processes.

The investigation has been done using the method of trapezoids for solving of the differential equations system. The program ode23t is used.

## III. INVESTIGATION OF THE INFLUENCE OF THE LIGHTNING CURRENT AMPLITUDE ON THE BEHAVIOR OF MOVO

The processes under examination are connected with operation of the MOSA in electrical power line 20 kV under single lightning stroke over a phase in the first interpole distance of line. The lightning stroke is with amplitude value of the current  $I_M$  and shape 1/10  $\mu$ s.

Fig. 3 illustrates the results for the impact of the lightning current 130 kA (probability of occurrence of lightning with this current is 1 %), and Fig. 4 - for  $I_M= 20$  kA (probability of occurrence - 75 %) [1].

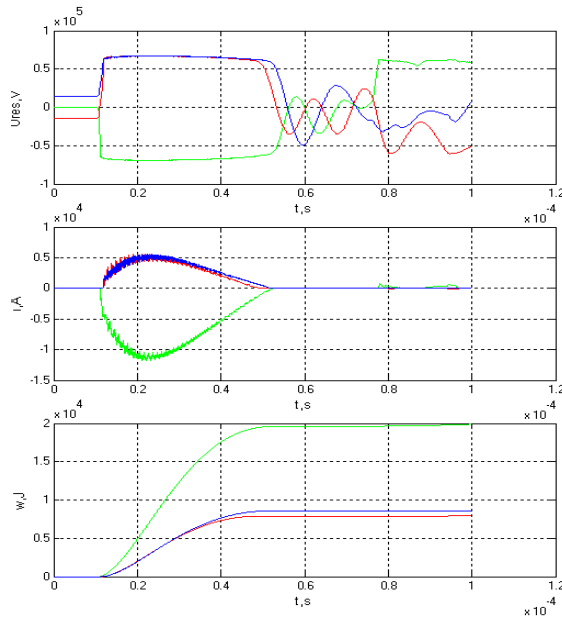


Fig. 3 Residual voltages, currents and energy, emitted in MOSA at  $I_M=130$  kA

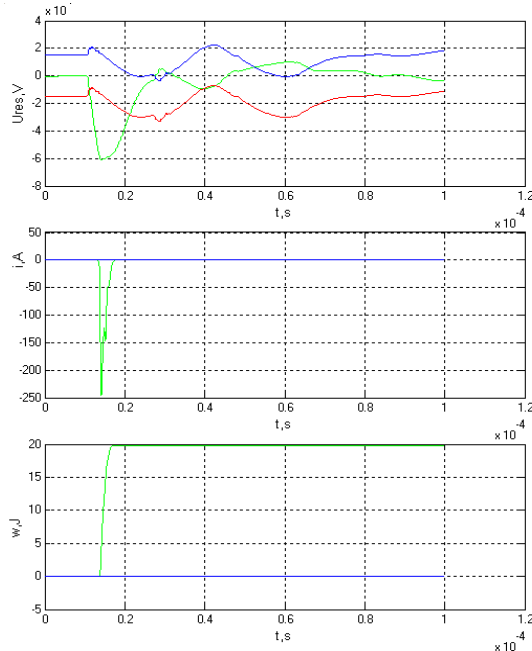


Fig. 4 Residual voltages, currents and energy, emitted in MOSA at  $I_M=20$  kA

#### IV. INVESTIGATION OF THE OPERATION OF MOSA UNDER INFLUENCE OF THE LIGHTNING STROKE WITH TWO CONSECUTIVE DISCHARGES AND INDUCED OVERVOLTAGES

The research is done for the same electrical power line 20 kV under lightning stroke with first discharge current

amplitude 80 kA and the second - 40 kA. The pause between them is 80  $\mu$ s.

Residual voltages, currents in MOSA and energy, emitted in MOSA are shown in fig. 5.

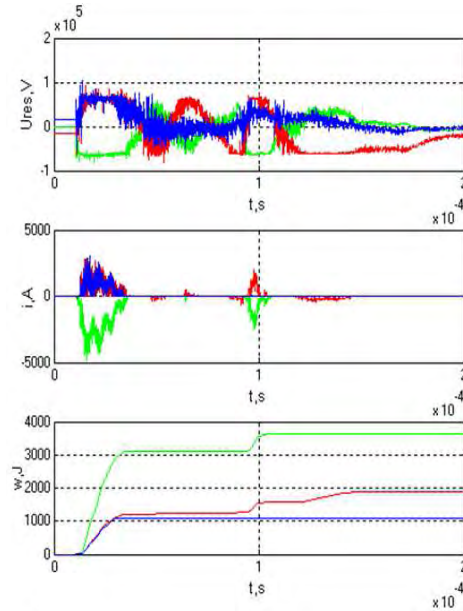


Fig. 5 Residual voltages , currents and energy, emitted in MOSA at double lightning

Fig. 6 and fig. 7 show the results in case of induced overvoltages for power line 20 kV whit amplitude 900 kV and 200 kV. Induced overvoltages with this amplitudes in Power line-20 kV occurred respectively 0,1 and 7 times per year for 30 hours lightning activity per year.

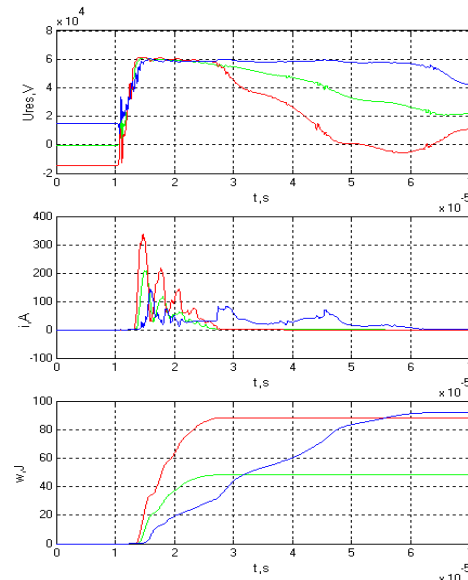


Fig. 6 Residual voltages , currents and energy, emitted in MOSA at induced overvoltages whit amplitude 200 kV

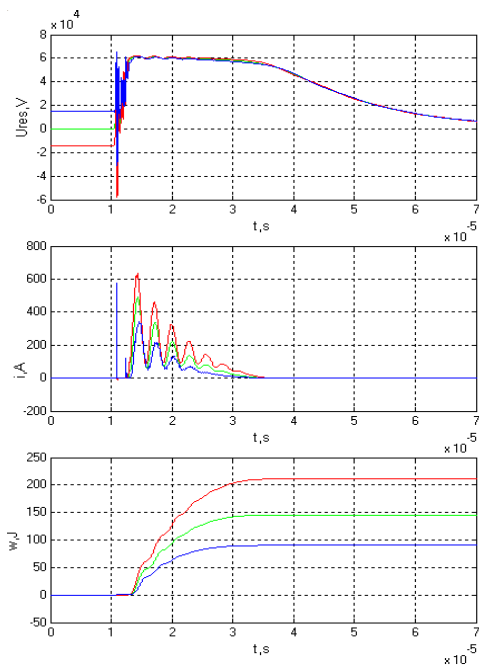


Fig. 7 Residual voltages , currents and energy, emitted in MOSA at induced overvoltages whit amplitude 900 kV

The analysis of the results shows that MOSAs limit overvoltages up to their protection level and retain energy sustainability.

Developed models for studying the behavior of MOVO in the grid can be used for their choice, taking into account the configuration of the system and its participating elements at different shape and duration of surges. They are also used for the next research – thermal loading of MOSA. The models give the emitted in MOSA energy needed to receive the heat field of MOSA.

## V. INVESTIGATION OF THE THERMAL LOADING OF THE MOSA AT THE OPERATION MODE

The thermal replace scheme in fig. 8 used electrical-thermal analogy for theoretical research over the heat loading. An adiabatic thermal process has been considered. The absorption energy from MOSA has been received by mathematical model in program Matlab [2],[3]. The differential equations have been resolved by the node potential method.

The following cases are investigated:

- Normal operation in electric power line 20 kV,  $I=1.10^{-4}$   
A. For the case the heat transfer to the ambient air is taken into account and the ambient temperature is  $T_0=45^\circ C$ .
- Fault situation – one phase short-circuit and transient overvoltage  $U=\sqrt{2} \cdot 24$  kV,  $I=0.0015$  A,  $t=10$  s.
- Single lightning stroke 130 kA, 1/10  $\mu$ s
- Single lightning stroke 100 kA, 10/350  $\mu$ s;
- Double lightning stroke 1/10  $\mu$ s, 80 kA and 40kA with the pause 80  $\mu$ s;

- Single lightning stroke 4/10  $\mu$ s, 100 kA – testing case.

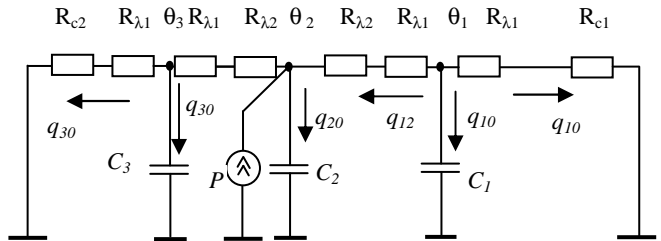


Fig. 8 Thermal replace scheme

$R_{c1}, R_{c2}$  – heat resistance of convection.,  $R_{\lambda2}$ , W/m.K – heat conduction resistance of MOSA;  $R_{\lambda1}$ , W/m.K – heat conduction resistance of silicone rubber housing ;  $C_2$ , J/K – heat capacity of MOSA;  $C_1$ ,  $C_3$ , J/K – heat capacity of silicone rubber housing;  $\theta_1, \theta_2, \theta_3$ , K- temperature change according to the ambient temperature;  $q_{ij}$ , W- thermal fluxes [4], [5].

MOSA is type MWK 24 with: height  $H=320$  mm and diameter  $d=47$  mm and number of blocks  $n=4$ . The housing is from silicone rubber.

The results for the temperature change in the work process are shown in Fig. 9 to Fig. 11.

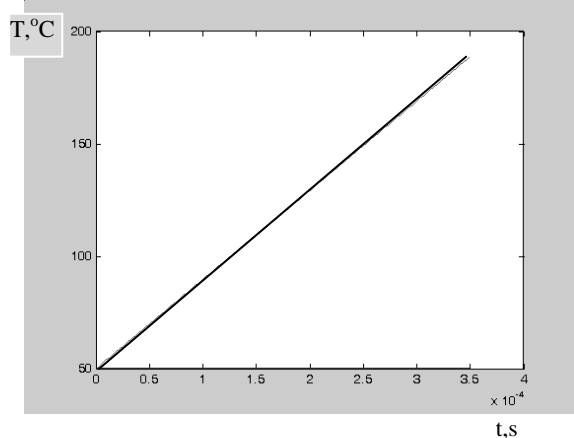


Fig. 9 Single lightning stroke  
100 kA, 10/350  $\mu$ s

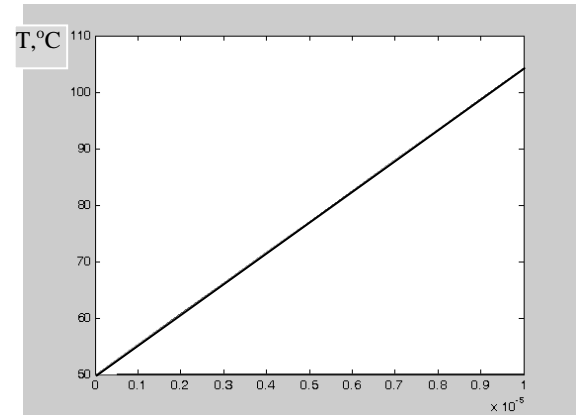


Fig. 10 Single lightning stroke  
4/10  $\mu$ s, 100 kA

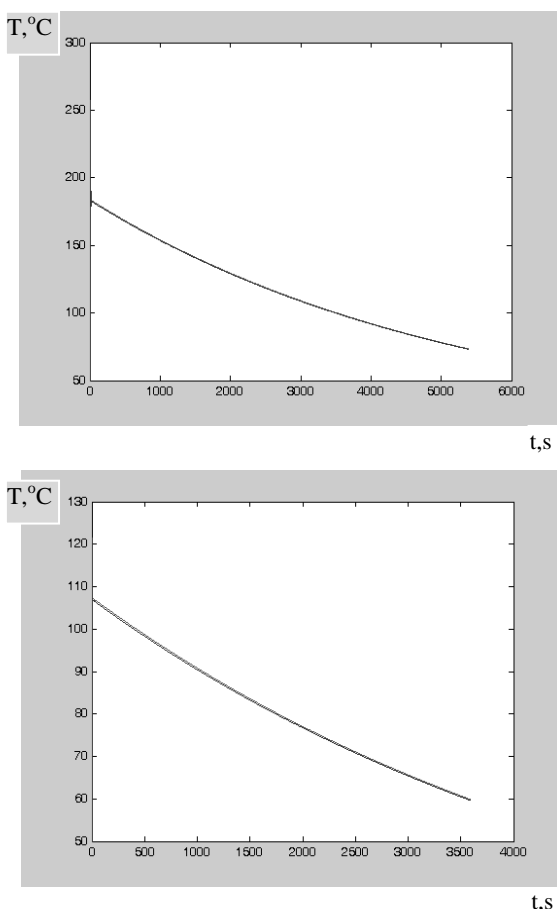


Fig. 11 Cooling below the operating voltage after MOVO's operation

## VI. CONCLUSION

The analysis of the results shows that MOSAs limit overvoltages up to their protection level and retain energy sustainability.

Metal oxide blocks overheating during normal operation of the power line 20 kV is about 5 K, which indicates favorable thermal load conditions.

## ACKNOWLEDGEMENT

The carried out research is realized in the frames of the project, financed from the state budget "Investigation of processes in secondary circuits for control and protection" in TU-Vara.

In cases of transient overvoltage, single lightning stroke 80 kA, 1/10 µs, double lightning stroke 1/10 µs, 80 kA, 40kA with the pause 80 µs temperatures are established in the range of 51 to 54 °C for the most adverse environmental conditions - 45 °C.

Most severe in terms of thermal load are conditions obtained by the influence of lightning off 100 kA, 10/350 µs (Fig. 9) and 4/10 µs, 100 kA (Fig. 10). MOVO temperatures reach values close to the limiting of material.

It is necessary up to 60-90 minutes to receive cooling of MOSAs under rate voltage for the most severe case of thermal loading. If there is another lightning stroke during the cooling process the destruction of MOSAs will happen

The proper choice of MOSAs according to energy loading ensures favorable thermal conditions. The most severe thermal modes are with the least probability, but destruction probability is very high.

## REFERENCES

- [1] Vassileva M., Limiting of overvoltages in electrical power networks 20 kV, Technical university of Varna, Bulgaria, PhD Thesis, 2004.
- [2] Yordanova M., M. Vassileva, Research over energy capability of metal-oxyde surge arresters in electric power lines 20 kV, Energy forum 2006, Varna, Bulgaria, pp. 114-118.
- [3] Petit A., D. Xuan, Jean G, An experimental method to determine the elektro-thermal model parameters of metal oxide surge arresters, IEEE Transactions on Power Delivery, vol.6, № 2, April 1991, pp. 715-721.
- [4] [http://www.zinc.org/info/zinc\\_oxide\\_properties](http://www.zinc.org/info/zinc_oxide_properties)
- [5] <http://lib.semi.ac.cn:8080/tsh/dzzy/wsqq/selected%20papers/HIGH%20TEMPERATURE/41-778.pdf>

# Model-experiment comparative analysis of roof type photovoltaic generator

Bohos Aprahamian<sup>1</sup> and Milena Goranova<sup>2</sup>

**Abstract –** The object of the presented study is a roof type photovoltaic generator delivering energy to the electricity grid through an inverter. A model-experiment comparative analysis of the roof type photovoltaic generator is proposed. The model is made during the design of the generator using the PVsyst software, and the experimental data are recorded by the system for one year.

The purpose of the comparison is to examine the factors influencing the accuracy of the model and specifying measures for its improvement.

**Keywords –** Roof type PV generator, PVsyst software, model, experiment.

## I. INTRODUCTION

A comparative analysis of the data obtained both from the model and the experiment conducted on photovoltaic generators is proposed. These are of roof type, built with modules from two different technologies.

The data from the model are obtained using the PVsyst software [9] in designing the generators. The experimental data are year-round operation of the system PV-generator - converter.

The aim of the study was to identify the factors influencing the errors in the models and approaches to correct the design of the system. Also, the comparison of the data from the models with the experiments should complement the studied literature [1,2,4,5,6].

## II. ANALYSIS

The wiring diagram of the experimentally investigated PV generators is shown in Figure 1. The two generators have the following main characteristics:

### A. Main characteristics of a PV generator, built with Sanyo HIT-205NHE5 modules (Figure 1.A.)

Characteristics of the modules:

- module type: Sanyo HIT-205NHE5 (Hybrid type);  $U_{oc}=50,3V$ ;  $I_{sc}=5,54A$ ;  $U_{mpp}=40,7V$ ;  $I_{mpp}=5,1A$ ;  $P_{mpp}=205Wp$ ;
- total number of modules 60.

Characteristics of the inverters:

- inverter type: SMA Sunny Boy SB 1100; DC Power: 1,23kWp; AC Power: 110 kW;
- total number of inverters 10.

Arrangement of the strings:

- total number of strings 10;
- number of modules in each string 6;
- number of strings attached to each inverter 1.

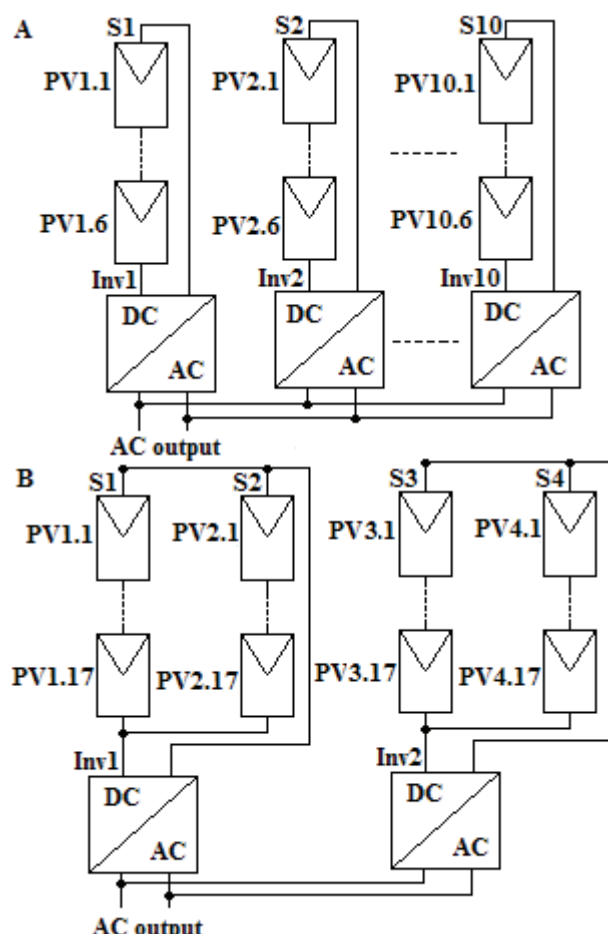


Figure 1. Architecture of the investigated PV generators.

### B. Main characteristics of a PV generator, built with Suntech STP180S-24/AC modules (Figure 1.B.)

Characteristics of the modules:

- module type: Suntech STP180S-24/AC (Monocrystalline type);  $U_{oc} = 44,8V$ ;  $I_{sc} = 5,3A$ ;  $U_{mpp} = 36V$ ;  $I_{mpp} = 5A$ ;  $P_{mpp} = 180Wp$ ;
- total number of modules 68.

Characteristics of the inverters:

<sup>1</sup> Bohos Aprahamian, Assoc. Professor, Technical University of Varna, Bulgaria, e-mail: bohos@abv.bg

<sup>2</sup> Milena Goranova, PhD student, Technical University of Varna, Bulgaria, e-mail: milenagoranova@email.bg

- inverter type: SMA Sunny Boy SB 5000 TL HC Multi-String; DC Power: 6,12 kWp; AC Power: 5,00 kW;
- total number of inverters 2.

Arrangement of the strings:

- total number of strings 4;
- number of modules in each string 17;
- number of strings attached to each inverter 2.

All modules are directed to the south (azimuth angle: 180 deg), at an angle of 30° (tilt angle: 30 deg).

The installation is stationary made on sloping roof, the angle at which you are unable to change.

Geographical coordinates of the analyzed PV system are: latitude - 43,12; longitude - 27,55; altitude - 20 m.

The factors subject to correction during the building of the models are as follows: Mismatch losses, Correction factor NOCT, Correction factor Albedo, Ohmic losses in the conductors.

The mismatch losses factor reflects on the performance discrepancy between the modules connected in series in the string. These losses are usually minimized by selection of components of the same characteristics, such as within the range of a few percent.

The Albedo factor describes the part of the global radiation which reaches the PV module surface due to the ground reflection of some parts of the direct or diffuse radiation.

The Ohmic losses in the conductors ( $R \cdot I^2$ ) are dependent on their diameter and length. As initial condition of the project maximum loss of 3% of this type was set.

The Nominal Operating Collector Temperature (NOCT) factor describes the temperature attained by the PV modules without back coverage under the standard operating conditions defined as: irradiance –  $E_N = 800 \text{ W/m}^2$ ; ambient temperature –  $T_{amb} = 20^\circ\text{C}$ ; wind velocity – 1 m/s.

The model is based on the fundamental equations proposed by a number of references [1,5,6,7].

The I-V curve of a module can be described using a five-parameter model [3,], mathematically representing the I-V curve data of a module, using the following five parameters:  $V_{oc}$ ,  $I_{sc}$ ,  $R_s$ ,  $R_p$ , and  $ekT$  [3,4]:

$$I = I_{sc} \left[ \frac{I_{sc} - \frac{U_{oc}}{R_p}}{\exp(ekT \cdot U_{oc}) - 1} \right] + \left\{ \exp[ekT(U + R_s I)] - 1 \right\} - \frac{(U + R_s I)}{R_p} \quad (1)$$

where:  $I$ , A – module output current;  $U$ , V – module voltage;  $I_{sc}$ , A – short circuit module current;  $U_{oc}$ , V – open circuit module voltage;  $R_s$ ,  $\Omega$  – module series resistance;  $R_p$ ,  $\Omega$  – module parallel resistance;  $ekT = q/nkT$ ;  $q$ , C – the electron charge;  $n$ , unitless – ideality factor per cell;  $k$ , Joule/K – Boltzmann's constant;  $T$ , K – temperature.

The five-parameter model was fitted to the corrected NOCT data obtained from each I-V curve run.

With the measured ambient temperature  $T_{amb}$  and NOCT the cell-temperature  $T_j$  can be approximately calculated. Then

follows the calculation of the cell temperature, depending on the irradiance and the ambient temperature.

$$T_j(E_{eff}, T_{amb}) = T_{amb} + (NOCT - T_{amb|N}) \frac{E_{eff}}{E_N} \quad (2)$$

where:  $T_j$ , K – junction-temperature;  $E_{eff}$ , phox – effective irradiance;  $T_{amb|N}$  –  $20^\circ\text{C}$  ambient temperature for NOCT;  $E_N$  – irradiance.

The comparative analysis is shown in Table 1, Table 2, Figure 2, Figure 3. The following indications are used:

- Invertor data – experimental data obtained by the inverters.
- Model data 1 – data obtained from the PVSyst model, build during the design of the system.
- Model data 2 – data obtained from the PVSyst model, after correction of the considered factors.
- Error – the resulting error in the comparison between Invertor data and Model data 1 (2), in %.

All figures show the average received electricity by month.

In Table 1, the results for modules of type Sanyo HIT-205NHE5 are presented. The average error in the Model data 1 amounted to 8,6%, and after the correction of the model is reduced to 4,6%. The comparison is given graphically in Figure 2.

Similarly the Table 2 shows the values for Suntech STP180S-24/AC. After the correction of the model the error decreased from 13,6% to 5,7%.

Table 3 provides a comparison between the factors and their influence on the resulting error. In the final column "All factors" are selected all the values of the correction factors, which give a minimum error.

### III. CONCLUSIONS

The obtained results show that the error in the initial model is significantly higher in the winter.

To obtain the most accurate results from the PVSyst model it is necessary to make corrections to the discussed factors in the following way:

- The correction of the Ohmic losses requires to point that due to the low transmission power the losses in the cables in the winter are smaller. The correction of this factor in the model should define losses less than 2%.
- The correction of the Albedo factor should comply with the recommended values for the season [8,9].
- Because the PV generators are for relatively low power, the mismatch losses are minimized by selecting the modules according to their characteristics. This is reflected in the corrected model, where they are reduced to 1%.
- The Nominal Operating Cell Temperature (NOCT) correction factor is corrected by reporting his value every month according to the average ambient temperature. Recommended values proposed in [2,4] are used.

The PVSyst model should be calculated separately for each month, which increases the accuracy of the obtained results.

**TABLE 1**  
COMPARATIVE ANALYSIS OF A PV GENERATOR, REALIZED WITH SANYO HIT-205NHE5 (HYBRID TYPE) MODULES

	Inverter data	Model data 1	Error %	Model data 2	Error %
	kWh			kWh	
Jan 13	330,06	280,5	17,7%	300,4	9,9%
Feb 13	550,2	450,8	22,0%	480,6	14,5%
Mar 13	1070,23	1000,3	7,0%	1040,5	2,9%
Apr 12	1410,53	1370,1	3,0%	1370,7	2,9%
May 12	1220,92	1230,2	-0,8%	1230,7	-0,8%
Jun 12	1890,31	1930,4	-2,1%	1920,4	-1,6%
Jul 12	2100,07	2180	-3,7%	2190,2	-4,1%
Aug 12	1900,22	1810,2	5,0%	1820,1	4,4%
Sep 12	1500,51	1440,7	4,2%	1450,4	3,5%
Oct 12	1170,48	1010,4	15,8%	1050,8	11,4%
Nov 12	560,4	550,1	1,9%	570,4	-1,8%
Dec 12	320,18	240,5	33,1%	280,7	14,1%
	Average :	8,6%		Average :	4,6%

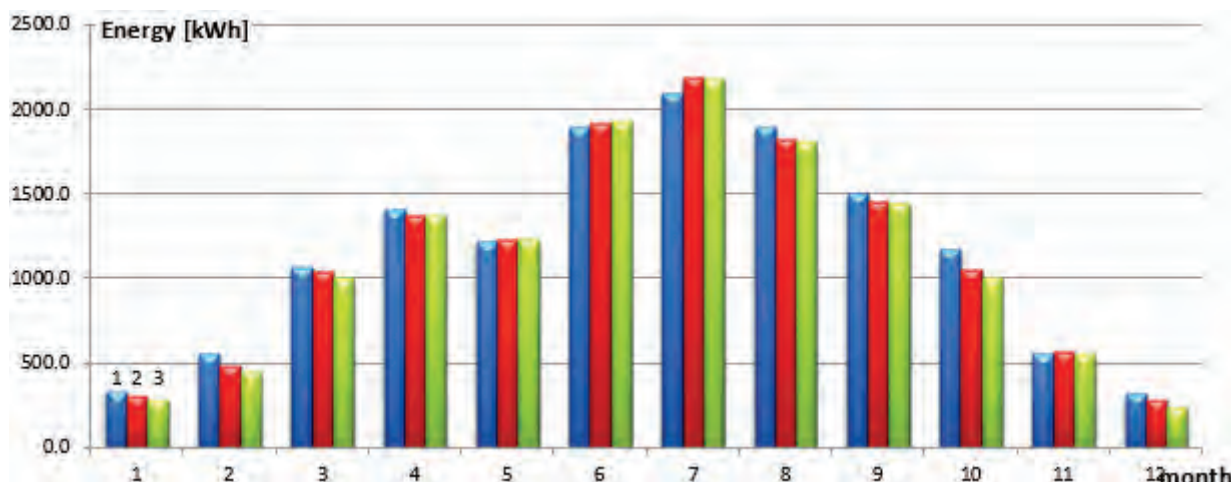


Figure 2. Comparative analysis of a PV generator, realized with Sanyo HIT-205NHE5 (Hybrid type) modules.

1 – Inverter data; 2 – Model data 2; 3 – Model data 1.

**TABLE 2**  
COMPARATIVE ANALYSIS OF A PV GENERATOR, REALIZED WITH SUNTECH STP180S-24/AC (MONOCRYSTALLINE TYPE) MODULES

	Inverter data	Model data 1	Error %	Model data 2	Error %
	kWh			kWh	
Jan 13	408,2	300,0	36,1%	350,1	16,6%
Feb 13	620,1	456,0	36,0%	540,0	14,8%
Mar 13	1106,1	936,0	18,2%	968,0	14,3%
Apr 12	1428,1	1348,0	5,9%	1412,0	1,1%
May 12	1228,1	1252,0	-1,9%	1248,2	-1,6%
Jun 12	1868,2	1914,0	-2,4%	1900,1	-1,7%
Jul 12	2060,1	2160,0	-4,6%	1998,1	3,1%
Aug 12	1912,1	1814,0	5,4%	1896,0	0,8%
Sep 12	1560,1	1444,0	8,0%	1508,0	3,5%
Oct 12	1240,1	1034,0	19,9%	1182,2	4,9%
Nov 12	596,1	568,0	4,9%	576,0	3,5%
Dec 12	340,0	260,0	30,8%	310,2	9,6%
	Average :	13,0%		Average :	5,7%

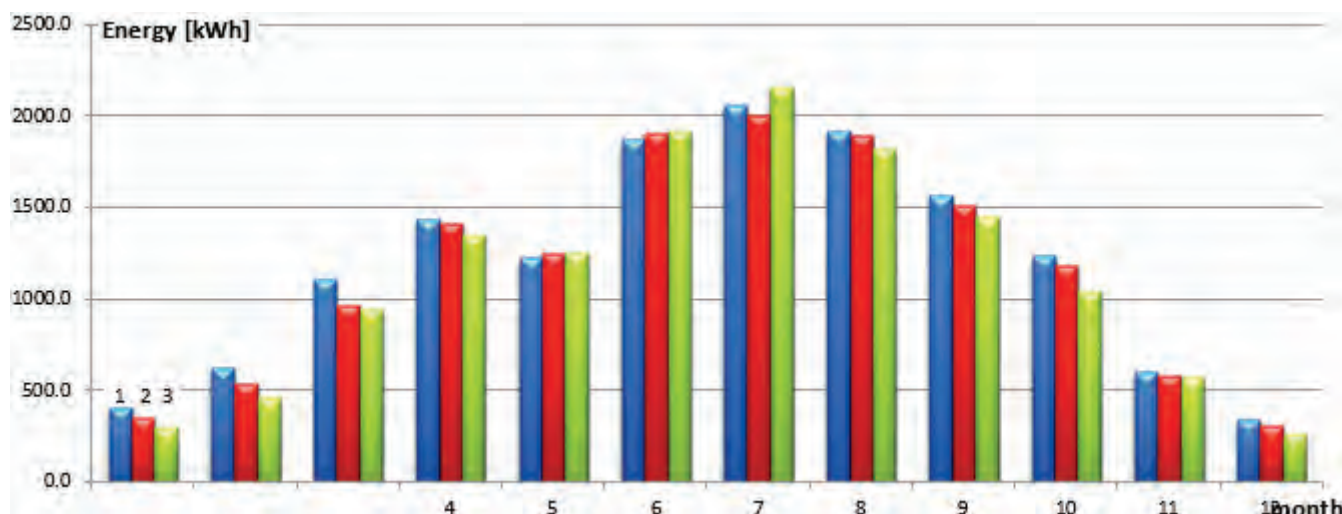


Figure 3. Comparative analysis of a PV generator, realized with Suntech STP180S-24/AC (Monocrystalline type) modules.  
1 – Inverter data; 2 – Model data 2; 3 – Model data 1.

TABLE 3  
INFLUANCE OF THE CONSIDERED FACTORS ON THE ERROR DURING THE CORRECTION OF THE MODEL

	Inverter data	Model data 1	Model data 2				All factors
			Factors kWh, %	Albedo	NOCT	Ohmic Losses	
January							
HIP	330.1	280.5	290.2 13,7%	280.6 17,6%	280.6 17,6%	290.2 13,7%	300.4 9,9%
MONO	408.2	300.0	310 31,7%	304 34,3%	304 34,3%	310 31,7%	350.06 16,6%
June							
HIP	1890.3	1930.4	1930.5 -2,1%	1950.0 -3,1%	1930.4 -2,1%	1930.0 -2,1%	1920.4 -1,6%
MONO	1868.2	1914.0	1920 -2,7%	1940 -3,7%	1928 -3,1%	1924 -2,9%	1900.1 -1,7%

#### ACKNOWLEDGEMENT

This research is realized in the frames of the project BG051PO001-3.3.06-0005, Program ‘Human Resources Development’.

#### REFERENCES

- [1] King D. L, W. E. Boyson, J. A. Kratochvil “Photovoltaic Array Performance Model” Sandia National Laboratories 2003
- [2] Krauter S., A. Preiss “Comparison Of Module Temperature Measurement Methods” 34th IEEE Photovoltaic Specialists Conference, 8-11 Juni 2009, Philadelphia, Pennsylvania (USA)
- [3] Lehman P.A., C.E. Chamberlin, “Field measurements of flat-plate module performance in Humboldt County, California”, Nineteenth IEEE PVSC, New Orleans, LA 1987
- [4] Reis A.M., N.T. Coleman, M.W. Marshall, P.A. Lehman, and C.E. Chamberlin, “Comparison of PV Module Performance Before and After 11-Years of Field Exposure”. Proceedings of the 29th IEEE Photovoltaics Specialists Conference New Orleans, Louisiana May, 2002
- [5] Tayyan A. “An Empirical model for Generating the IV Characteristics for a Photovoltaic System” Al-Aqsa Univ., 10 (S.E.) p. 214-221 2006.
- [6] Thevenard D. “Review And Recommendations For Improving The Modelling Of Building Integrated Photovoltaic Systems” Ninth International IBPSA Conference Montréal, Canada August 15-18, p1221-1228, 2005.
- [7] Wagner A. “Peak-power and internal series resistance measurement under natural ambient conditions”. EuroSun 2000 Copenhagen June 19-22, 2000
- [8] <https://eosweb.larc.nasa.gov/>
- [9] <http://www.pvsyst.com/en/>

# Renewable Energy Sources and Tariffng of Electrical Power

Silvija Letskovska<sup>1</sup> and Kamen Seymenliyski<sup>1</sup>

**Abstract – The goal of this work is the brief description of Bulgarian Energy System and the possibility the consumer to use renewable energy system using appropriated software.**

**Key words - energy system, renewable energy, PV-system.**

## I. INTRODUCTION.

The common rules for price forming for the industry are valid in determining the price of electrical energy. It is necessary to take in mind the specific particularities of energy production as well as these of the consumers of electrical energy. The main particularity of the electrical energy is the electrical energy is the limited possibility of keeping and charging. It must be consumed in the moment of its production following strong system rules for supporting of energy balance. In the time of production, transport, transformation and consumption of electrical energy the laws, methods and principles of electro technique are in fact. All economical statistical, political and social aspects and methods used in the energetic serve for more effective and correct applying.

Every deviation from them destroys normal function of the energy system. In this connection – the base task of different system for price forming in energetic is regulating using economical methods the balance between production and consuming. In Bulgaria work many thermal electrical centrals, with dive more than 80% of the necessary electrical energy. In the future this percent will increase permanently.

The bigger part in these centrals have high technical minimum – 70 to 75% from nominal power. In the same time parameter  $\beta$  in the energy system is very low:

$$\beta = P_{min} / P_{max} = 0.58 \div 0.60 \quad (1)$$

where:  $P_{min}$  – minimum loads;  $P_{max}$  – maximum loads.

This leads to difficultness in the work of electrical centrals in night minimum loads of the system. To be excluded, arised as a result of high operating difficultness and connected with them significant economical losses is necessary to act in two main direction [1, 2].

In the first place – to reach methods for increasing of night loads of the consumers of the electrical energy, and in the second place – to decrease the maximum loads of energy system or to search for cheap fast acting generating sources.

<sup>1</sup>Silvija Letskovska - Burgas Free University, San Stefano 62, 8000 Burgas, Bulgaria, E-mail: silvia@bfu.bg

<sup>1</sup>Kamen Seimenliyski -Burgas Free University, San Stefano 62, 8000 Burgas, Bulgaria, E-mail: kdimitrov@bfu.bg

Excluding of these problems is getting mainly using: introducing in the energy system of flexible production powers based on small renewable system (SRS), introduction in exploitation of pump-accumulating hydro electrical centrals (like PAHEC Chaira); regulating of consumption with economic methods, for supporting of the energy balance of the country with comparable constant load diagram.

The other trend in the last years is a seasoning transfer of high energy flows to the big sea truistic complexes. It due to intensive building of houses which are used only seasoning. For example, in the last several years only in complex Sunny Beach are connected about 70 new transformers stations and as result the installation power has been increasing with over 30%. In the summer truistic season the consumption of electrical energy only in the complex is significant higher (about 120 MW) compared with this of whole Stara Zagora region (about 80 MW). Burgas region (about 370 MW) during summer season consumes more than Jambol, Sliven and Stara Zagora regions taken together.

The distance of the consumers of the electric energy from the centrals influences significantly on the volume of losses. As a result of this the consumers situated close to the electric centrals (connected in the generated voltage) are in better situation. The consumers far way, consuming energy via several steps of transformation, increased losses for the transfer and transformation.

Power factor (on a practice – cosines  $\varphi$  of the consumers) also influences significantly in the transfer and transformation of the electrical energy.

Due to, that the electrical energy can not to be stored but must be immediately to be consumed, consumers, producers and distributors use different capital investments for unit of used energy. For consumer, which work only night time, do not require building of additional generation powers and are favourable for the system.

After performing not in the better way privatization of the electrical distributing companies the price of electrical energy is changed several time with the goal reaching of normatively declared in the privatization contracts of these companies profit. That leaded to disproportion, due to retardation of the price, respectively and the profit of the Common System operator, production powers, producers of the primary energy resources and etc.

Acting at the moment methods for determining price of electrical energy defined by State Commission for Energy and Water regulation tolerates some known possibilities for subjectivity and unambiguous interpretation of output information, as well as and using of prognostic data, which can be manipulated. It reacts and for price of the energy from renewable system.

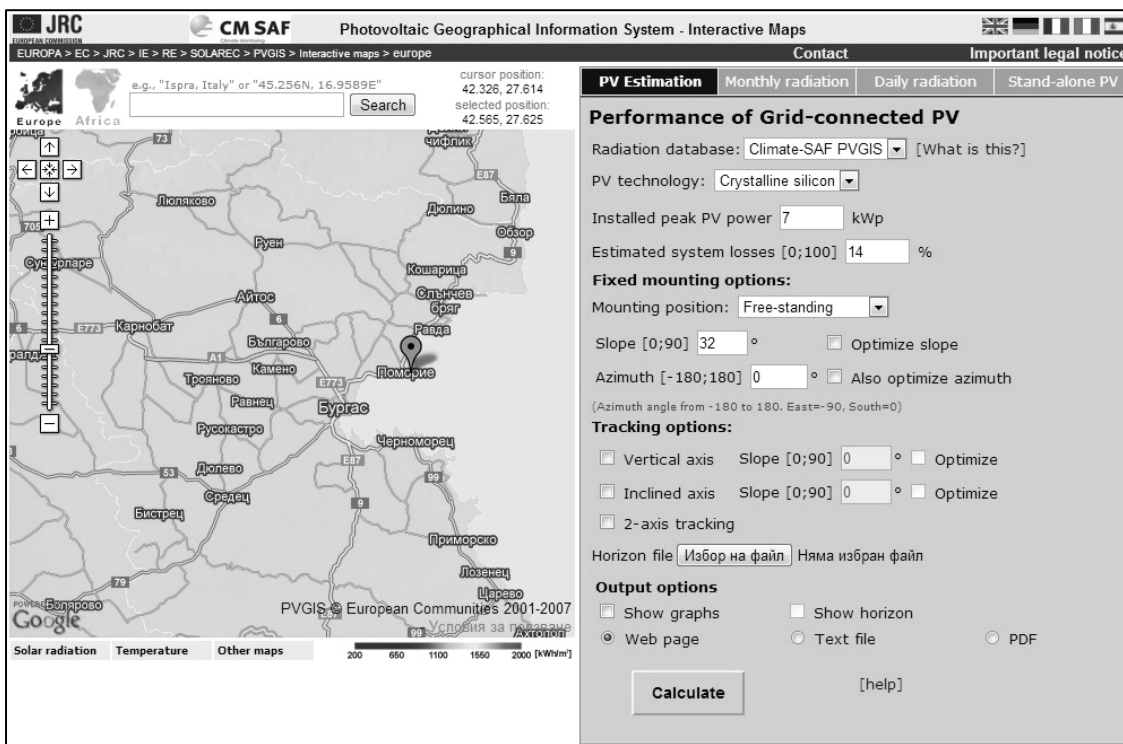


Fig. 1. Sun-energy odit of Pomorie.

With their connection into the networks of electrical distributing companies, with goal selling of electrical energy, the additional taxes are counted, which additionally make them expensive.

All these problems increases the actuality of building and connecting of renewable system for domestic consumption.

In this connection is important to investigate how much is economically favourably to build small renewable system based on photovoltaic panels in the truistic regions in Bulgaria.

As an example in this aspect is the town of Pomorie. It is served by the electrical distributing network, owing of EVN – Bulgaria and it has a number of problems of objective and subjective character. The territory of Pomorie town is occupied chiefly by houses - type multifamily homes, populated usually from one to four families. Average every one of these houses has roof space in the range of 100–300 m<sup>2</sup>.

The average usage of electrical energy for one family, data's from EVN is 115 lv in month. These data are on the base of the consumption of the average – statistical four members family. The consumption of the electrical energy is distributed as follows: 75% for heating; 15% for electrical appliances; 10% - for lighting [3].

Thus, if the initial calculation is done, oven these are the data for the price of electrical energy without transfer taxis and another elements, with form it, the next will appear:

- With price of one kW electrical energy 0.19 lv – average price for 1 kW, the quantity of the used energy for month will be 605 kW;
- Annually for one four members family is such average monthly consumption will be 7260 KWh, which will

form the price about 1400 lv. This means that the daily consumption is about 20 kWh.

## II. BUILDING OF AUTONOMOUS RENEWABLE ENERGY PV-SYSTEM ON THE TERRITORY OF POMORIE TOWN

Assessable potential of sun energy determines after calculating of several base factors: irregular distribution of energy resources of sun energy during the separated seasons of the year; physical – geographic particularities of the territory; limitations in building and exploitation of sun system in the specific territories, as nature reservations, military objects and etc.

Average annual quantity of sun shining for Bulgaria is about 2150 hours and average annual recourse sun radiation – 1517 kWh/m<sup>2</sup>.

As available annual potential for absorbing can be shown approximately 390 ktoe (As official source for evaluation of sun energy potential is used project of the program PHARE BG9307-03-01-L001 – «Technical and economical estimation of Renewable Energy in Bulgaria ». In the base of the project are data from the Institute for meteorology and hydrology in BAS, taken from all 119 molestations in Bulgaria for the period over 30 years).

After the analyse of data base zoning is done for sun potential and Bulgaria is divided of three regions depending on the intensity of sun shining.

Pomorie town is situated in the third region – South-East and South West region, in which is situated and southern cost. Average annual duration of sun shining in this region is from 500 h to 1750 kWh/m<sup>2</sup>.

With the help of Photovoltaic Geographical Information System (PVGIS) giving the coordinates of Pomorie town sun-energy audit was done on its territory (Fig. 1).

PVGIS is WEB-based system for science investigations, demonstrations and geographical evaluation of sun energy resource in the range of integrated ruling of distributed generation of an energy [4].

PVGIS combines data from laboratory investigation, monitoring and testing with geographical know ledges, for analysing technical, ecological and social-economical factors of producing electrical energy from sun energy [4].

With the help of PVGIS the calculation are performed, taking in mind the influence of different parameters which would create losses in functioning of one PV-system (temperature, corner reflection, conductors, invertors and etc.).

From the received result can be accepted, that on the territory of Pomorie town insiste favourable conditions for producing of electrical energy using building PV-systems, as well as building of tracking system is not economically (Fig. 2).

Fixed system: inclination=33°, orientation=0°				
Month	$E_d$	$E_m$	$H_d$	$H_m$
Jan	0.00	0	2.29	71.0
Feb	0.00	0	2.86	80.0
Mar	0.00	0	3.84	119
Apr	0.00	0	4.79	144
May	0.00	0	5.48	170
Jun	0.00	0	5.54	166
Jul	0.00	0	5.83	181
Aug	0.00	0	5.65	175
Sep	0.00	0	4.87	146
Oct	0.00	0	3.94	122
Nov	0.00	0	2.49	74.8
Dec	0.00	0	2.01	62.2
<b>Yearly average</b>	<b>0</b>	<b>0</b>	<b>4.14</b>	<b>126</b>
<b>Total for year</b>		<b>0</b>		<b>1510</b>

Fig. 2. The calculation with PVGIS.

Legend:  $E_g$  - Average daily electricity production from the given system (kWh);  $E_m$  - Average monthly electricity production from the given system (kWh);  $H_g$  - Average daily sum of global irradiation per square meter received by the modules of the given system ( $\text{kWh/m}^2$ );  $H_m$  - Average sum of global irradiation per square meter received by the modules of the given system.

#### PVGIS estimated of solar electricity generation

The point of chose has insufficient data to calculate the relative efficiency of the PV modules.

The result shown the See the map of relative efficiency for regions with valid data.

Location:  $42^{\circ}33'52''$  North,  $27^{\circ}38'59''$  East.

Elevation: 0m a.s.l, Solar radiation database used: PVGIS-classic; Nominal power of the PV system: 0.0kW (crystalline silicon); Estimated losses due to temperature: 8% (generic value for areas without temperature information or for PV module); Estimated loss due to angular reflectance effects: 3%.

Other losses (cables, inverter etc.): 15%. Combined PV system losses: 21.1%.

The technologies for producing of photovoltaic panels develop and improved with very high rate. The variation for increasing of coefficient of useful work (efficiency).

During the last years the price of the panels for square meter sensitively drops, in the same time increases output power, in keeping and decreasing of panel sizes. In the present moment on the market offers:

- Single crystal silicon panels (efficiency 13÷18%) with power from several to 300 Wp;
- Polycrystalline silicon photovoltaic panels with low efficiency (10÷14%) and low productivity in temperatures higher 250C. They strongly are influenced by the angle of sun radiation. They have application in building of photovoltaic systems for facade of building and roods of houses;
- Amorphous silicon panels (with lowest efficiency – less 11%), which are not so influenced by high temperatures and more effective in cloudy weather. The other advantage of thin type of panels is the possibility for producing of big variety of products – thin film photovoltaic modules, flexible photovoltaic modules for glasses, solar chargers for laptops, GSM and etc.

In the moment on the market has high number of producers which give different prices and technologies. Available separated as panels, invertors, controllers, batteries as well as finished system and performances [5-7].

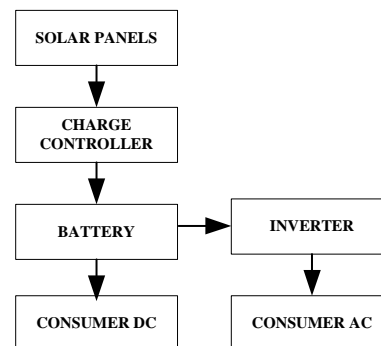


Fig. 3. PV-system - example variant.

On Fig. 3 is shown of an example variant of building of photovoltaic system on the root space for multifamily house on the territory of Pomorie town with power 5000 W. The choice of such system with lowest economical parameters the results are obtained shown on Fig. 4. The parameters (coordinates, power, losses and ets.) are given in PVGIS. The final results shows that the system will produce average annual about 6230 kWh.

Fixed system: inclination=32°, orientation=0°				
Month	$E_d$	$E_m$	$H_d$	$H_m$
Jan	9.19	285	2.25	69.6
Feb	12.60	352	3.13	87.8
Mar	15.80	489	4.06	126
Apr	19.10	573	5.08	152
May	23.20	718	6.32	196
Jun	23.20	696	6.47	194
Jul	23.90	742	6.73	208
Aug	23.80	737	6.67	207
Sep	19.40	583	5.32	160
Oct	14.40	445	3.80	118
Nov	10.80	325	2.72	81.7
Dec	9.11	282	2.24	69.4
<b>Yearly average</b>	<b>17.1</b>	<b>519</b>	<b>4.57</b>	<b>139</b>
<b>Total for year</b>	<b>6230</b>		<b>1670</b>	

Fig. 4. PV-system with lowest economical parameters.

Location: 42°34'16" North, 27°36'41" East.

Elevation: 2m a.s.l,

Solar radiation database used: PVGIS-CMSAF.

Nominal power of the PVsystem:5.0 kW (crystalline silicon); Estimated losses due to temperature and low irradiance: 10.4% (using local ambient temperature).

Other losses (cables, inverter etc.): 14%. Combined PV system losses:25.2%.

In Table I the prices of the chosen system are given and in Table II – produced energy and cost price of the produced electrical energy for the period of exploitation up to 25 years.

TABLE I  
PRICES OF THE CHOSEN SYSTEM

Prices of the system elements				
Type of element	Number	Price pcs (lv.)	Total (lv.)	
1 Single crystal PV module 175 Wp	10	525	5250	
2 Charge controller 12/24V, 50A	2	360	720	
3 Inverter 2/1500W, 230V/50Hz	2	670	1340	
4 Battery 12V, 100Ah	8	350	2800	
5. Other expenses (construction, wiring, documentation)	1	1000	1000	
Total value			11110	

TABLE II  
PRICES OF KWH

PV-system 5000W	Period of exploitation (years)					
	5	10	15	20	25	Remark
Produced energy (kWh)	31150	60000	88000	104000	118000	Calculated losses from amortization
Price kWh (lv.)	0.353	0.23	0.188	0.184	0.186	

## CONCLUSION

In so chosen object for investigation – multifamily house in Pomorie town and after calculations on the base of price and conditions, comparable with these of EVN at the moment, the accepted results are the base for next conclusions:

- If the proposed for building PV-system is used over ten years the price of one kWh will appear to be comparable with the price of one kWh electrical energy from EVN. In this moment 88000 kWh from EVN have price about 16720 lv;
- The proposed variant for building of PV-system with choice of firm for delivery and mounting will insure full recreation of the capital for nine years work of the system with present prices of the EVN. After these years the expenses will be only for the maintenance of the system.

## REFERENCES

- [1] K. Seymenliyski, S. Letskovska, P. Rahnev, The efficiency of tariff policy in Bulgarian energy system, Jubilee Conference – Ten years of the establishment of a National Military Institute, Veliko Tarnovo, 2012.
- [2] K. Seymenliyski, St. Mollova, P. Rahnev, state of the tariff policy in power system in Bulgaria, ubilee Conference - Ten years of the establishment of a National Military Institute, Veliko Tarnovo, 2012.
- [3] <http://www.evn.bg/Medii>
- [4] <http://re.jrc.ec.europa.eu/pvgrid/>
- [5] <http://www.motto-engineering.eu>
- [6] <http://solarenterprise.bg>
- [7] <http://elektronikabg.com>

# Experimental Verification of Algorithm for Indirect Domestic Load Recognition

Konstantin Gerasimov<sup>1</sup>, Yulian Rangelov<sup>2</sup> and Nikolay Nikolaev<sup>3</sup>

**Abstract –** The paper presents experimental verification of the efficiency of a developed by the authors algorithm for indirect domestic load recognition. For this purpose was developed a utility which measures instantaneous values of current and voltage at the household's feed in cable. The obtained data is then recorded and processed by software which implements the recognition algorithm. The output of the algorithm is information about the individual electrical consumption of the particular domestic appliances. The experimental results show that the algorithm successfully recognizes the more powerful consumers which form about 80% of a household electrical consumption.

**Keywords –** appliances, fuzzy logic, energy consumption, indirect load recognition.

## I. INTRODUCTION

During the last decade there is a big emphasis on not only the industrial, but on the domestic the energy efficiency as well. The fast developing economies consume more and more energy. The main sources of energy are still the fossil fuels. At the same time EC has set long-term goals which guarantee the gradual shift from this non-ecological production towards technologies based on renewable energy sources.

The plans for development of the electric power sector are that big part of the electrical energy for domestic needs should be covered by own photovoltaic, wind or other installations. Along with this it is necessary to increase not only the energy efficiency of the domestic appliances but also the efficiency of their use. The practice shows that a major problem for the domestic consumers is identification of the energy consumption of the separate appliances. Knowing this information each user can be educated to understand the impact of his energy consumer behavior and thus start improving the efficiency of use of the electrical appliances and making savings. For this purpose, during the last years there are many investigations aimed at creating tools which are capable of recognizing the switched on in a household domestic electrical appliances.

In this context, the authors have developed a new algorithm for indirect recognition of the switched on electrical appliances in a domestic household electric network. The

algorithm detects the deviation of the power at the main feed in cable of the household and by means of signal processing and a controller based on fuzzy logic determines which appliance has been switched. The algorithm itself is described in details in [1, 2]. Its efficiency has been verified by a computer simulation reproducing the energy consumption behavior of a household.

This paper aims at presenting an experimental verification of the efficiency of the algorithm for indirect recognition of the switched on domestic appliances. For this purpose was developed a measurement tool and it was used to record real processes of commutations of domestic appliances in random order. The obtained data is then recorded and processed by software which implements the recognition algorithm. The experimental data shows promising results.

The article is organized as follows: section II presents some details of the developed tool for measurement of current and voltage, as well as brief description of the algorithm itself. Section III presents the obtained experimental results. The main conclusions are drawn in section IV.

## II. ALGORITHM

### A. Measurement device

The measurement device is implemented on a microcontroller development kit Cerebot MX4cK with 8 MHz 32-bit processor of Microchip and 32KB SRAM memory chip. The sampling frequency of current and voltage is about 1.8 kHz. The analog-digital converter of the voltage sensor is 8-bit, while the current sensor is 12-bit. The measurement device is shown in Fig. 1. By means of USB 2.0 serial interface the data is transferred in real time to a computer, equipped with software which records it.

### B. Computer Algorithm for Indirect Load Recognition

The structural diagram of the algorithm for indirect domestic load recognition is shown in Fig. 2. The input data is the measurement of the instantaneous values of the current and the voltage.

The block for control of signal processing detects the occurrence of event – switching on or off of an electric appliance. For this purpose, the input of the block is the instantaneous value of the current. After that follows the calculation of its mean value. During normal regime of operation (i.e. there is no switching of electric appliance) the mean value of the current oscillates around zero. At the moment of commutation is observed a short peak value. This peak value is differentiated and filters by the next block. In order to operate correctly, the relay block accepts the absolute

<sup>1</sup>Konstantin Gerasimov is with Department "Electric Power Engineering" at Technical University of Varna, Studentska str. 1, Varna 9010, Bulgaria, E-mail: kkgerasimov@tu-varna.bg

<sup>2</sup>Yulian Rangelov is with Department "Electric Power Engineering" at Technical University of Varna, Studentska str. 1, Varna 9010, Bulgaria, E-mail: y.rangelov@tu-varna.bg

<sup>3</sup>Nikolay Nikolaev is with Department "Electric Power Engineering" at Technical University of Varna, Studentska str. 1, Varna 9010, Bulgaria, E-mail: n.nikolaev@tu-varna.bg

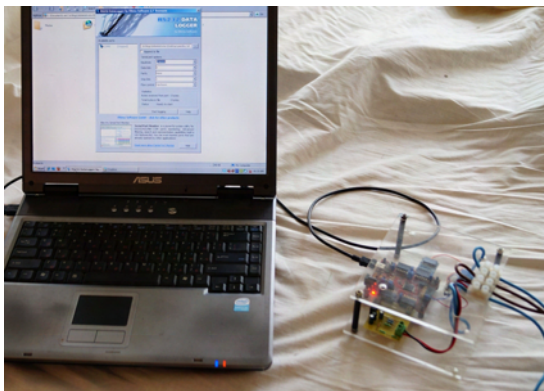


Fig. 1. Indirect load recognition algorithm structure diagram

value of the filtered signal. When an electric appliance is switched on or off is observed a sudden increase of this signal and when it reaches a preset threshold, the relay starts working. The obtained from the relay increasing front activates the block which produces an impulse signal with a fixed duration of 0.2 seconds.

The purpose of this block for compensation of the voltage magnitude is to correct the amplitude of the measured voltage when it is different from the nominal for the network. This is due to the fact that power consumption of the electrical appliances with heating elements (active resistance) follows a quadratic law of deviation, depending on the voltage.

The inputs of the block for signal processing are the

instantaneous value of the current and the corrected magnitude of the voltage. By multiplying these two values is obtained the normalized power, and after a consequent calculation of the mean values is obtained the normalized value of the active power. In order to differentiate the moment of commutation of any electrical appliance from the steady state of operation, the normalized active power is passed through a transfer function with parameters shown in Fig. 2.

When from the control block enters a rectangular impulse with duration of exactly 0.2 seconds, a logical Switch switches over to a position which takes as input the output of the aforementioned transfer function. At this state the integrator starts working. After 0,2 seconds, when the impulse changes from 1 to 0, the integrator is restarted and the logical switch is returned into position "switched off". At the output is obtained an impulse with a particular maximal value, according to which appliance is switched on or off.

To the Sample/Hold block are passed the impulses obtained from the block for signal processing. Apart from that, the S/H block is controlled by the control block. This configuration produces at the output of this block a short impulse with magnitude equal to the maximal value of the impulse obtained from the block for signal processing.

The operation of the Fuzzy logic controller is obviously based on the logic of the fuzzy sets. For each particular appliance is set a participation function corresponding to switching on and another participation function corresponding to the switching off of this appliance. According to what value enters at the input of the Fuzzy logic controller, at the

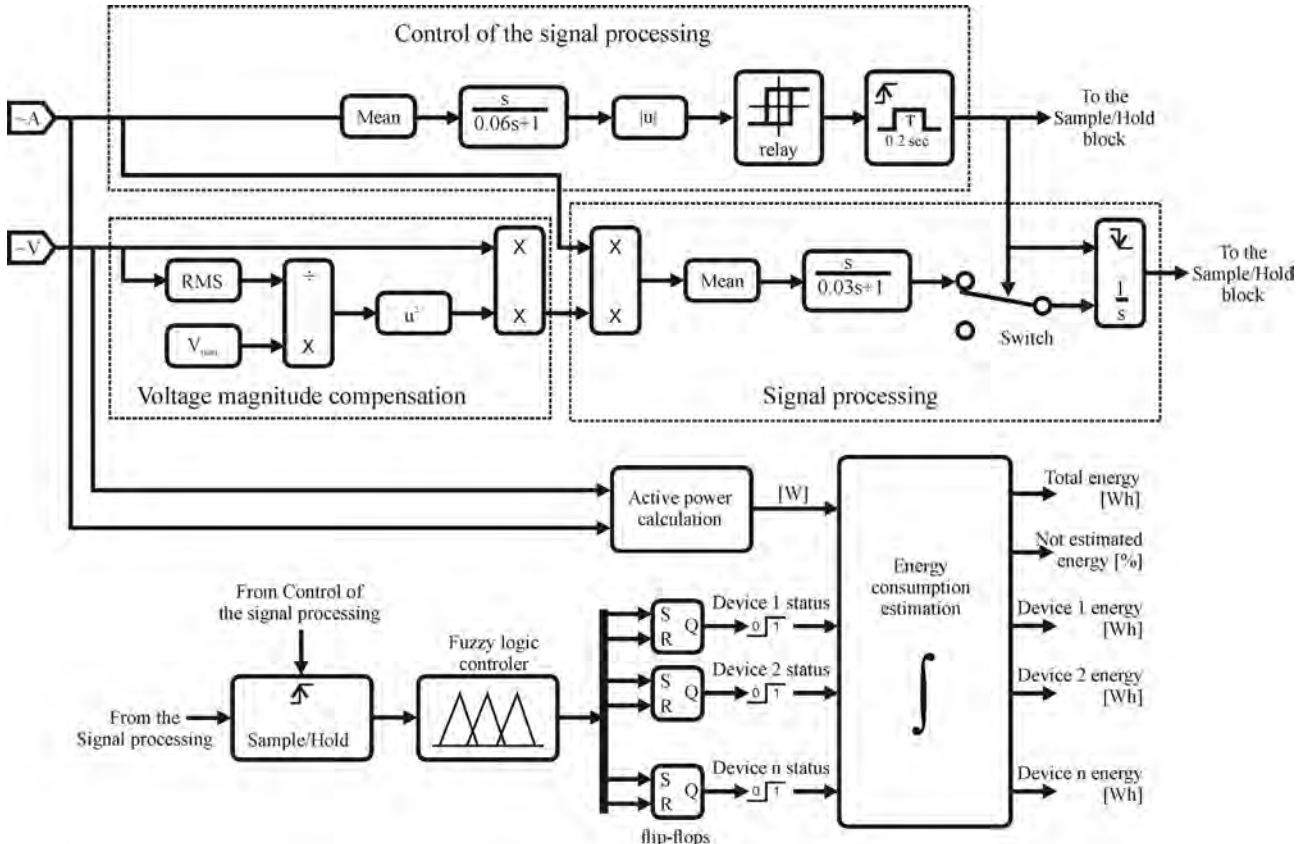


Fig. 2. Indirect load recognition algorithm structure diagram

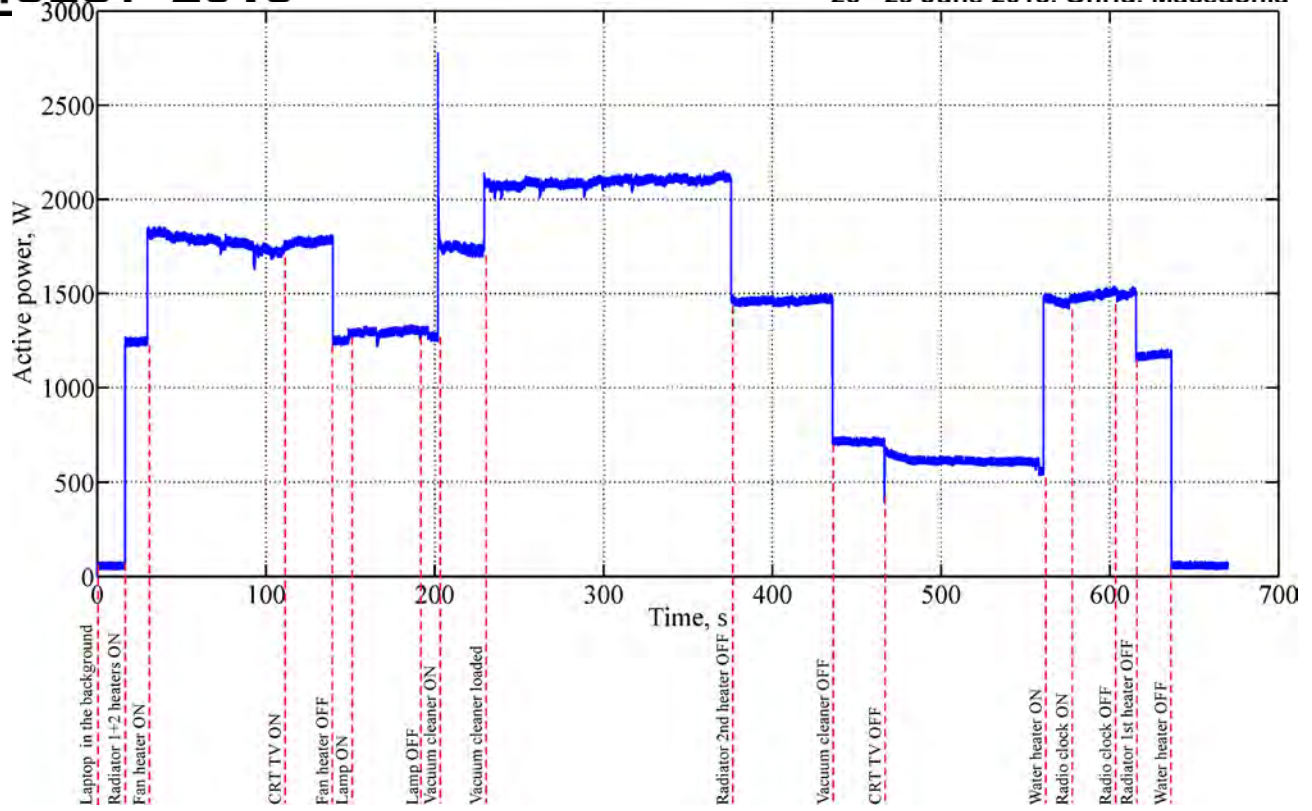


Fig. 3. Calculated active power

particular moment 1 appears at only one of the outputs. As already mentioned, for each appliance there are two outputs – for switching on and for switching off. These outputs, two by two, are passed to a corresponding RS trigger (separate one for each electrical appliance). At the trigger output of the corresponding appliance appears 1 if it is switched on, and respectively 0 if it is switched off.

When information about the states of all appliances is available, then data about their consumption can be accumulated. For a particular period of time the individual consumption of each electrical appliance can be determined the following integral:

$$E_{device} = \int_0^{\text{end of period}} \left[ state \cdot \left( \frac{V_{rms}}{V_{nom}} \right)^2 \cdot P_{nom} \right] \cdot dt \quad (1)$$

### III. EXPERIMENTAL VERIFICATION

In order to test the algorithm was created a scenario of switching on and off of the following electrical appliances: radiator (with two heaters), CRT television, vacuum cleaner, laptop, water heater, lamp, fan heater and a radio-clock. In Fig. 3 is shown the graphics of the calculated active power which passes through the main feed in cable. In the figure are shown also the instances of switching on and off of the electrical appliances. It should be noted that at the beginning both radiator's heaters are switched on and the laptop is switched on during the whole measurement. For the normal operation of the algorithm is necessary that for each heater, as well as for their combination, there is a participation function and a corresponding state output. Though, the information

about the consumed electric power has to be accumulated separately for each heater.

The experiment shows that the algorithm is capable of recognizing the radiator, the vacuum cleaner, the fan heater and the water heater. The rest of the appliances cannot be detected by the control block and the signal processing because the implemented analogue-digital converter is not sensitive enough to the small values of the current.

Fig. 4 shows the outputs of the algorithm, presenting the states of the recognized electrical appliances. It is seen that moments of switching on and off coincide with the corresponding ones from Fig. 3.

Table I presents information about the consumed by the recognized by the algorithm electrical appliances power during the experiment. The energy which they have consumed amounts for about 80 % of the total energy. The other 20 % is respectively consumed by the unrecognized electrical appliances.

TABLE I  
ENERGY CONSUMPTION ESTIMATION

Radiator 1 <sup>st</sup> heater	74.74 Wh
Radiator 2 <sup>nd</sup> heater	52.21 Wh
Fan heater	21.92 Wh
Vacuum cleaner	36.41 Wh
Water heater	19.69 Wh
Total energy consumed	255.2 Wh
Not estimated energy	20.55 % of the total

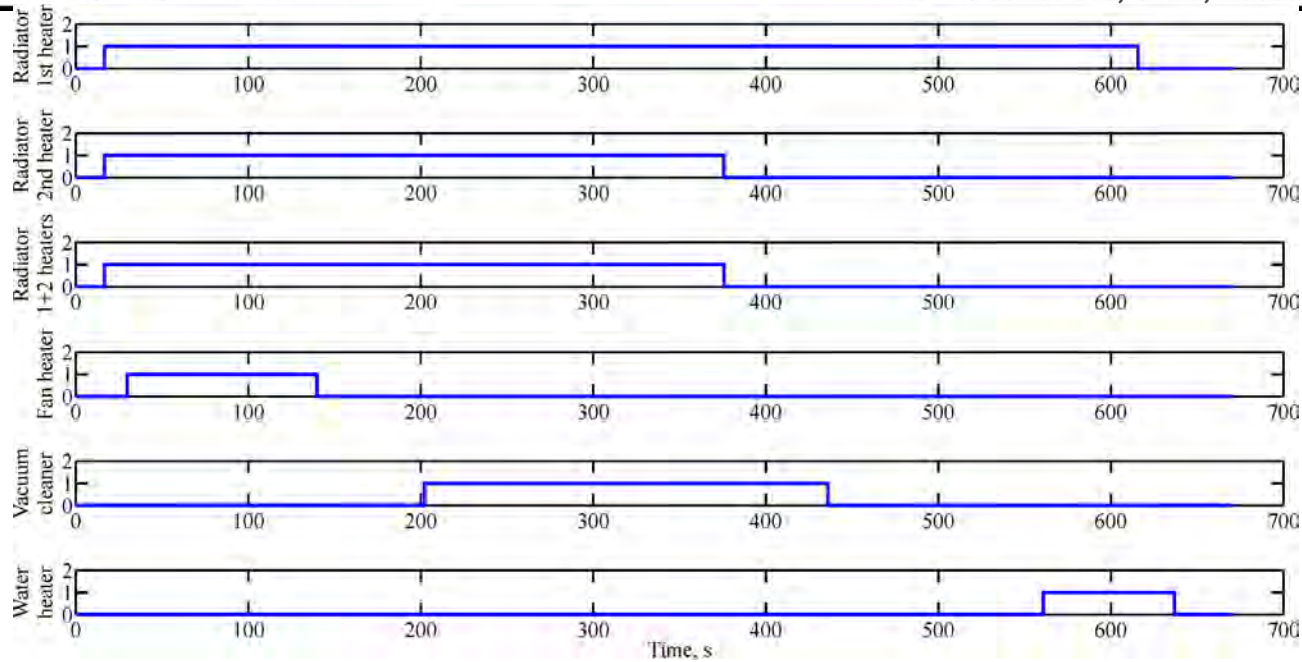


Fig. 4. Device status

#### IV. CONCLUSION

The conducted experimental study with real data from measurements show that the developed algorithm for indirect recognition of the electrical appliances switched on in a domestic household is capable of identifying the source of consumption of about 80 % of the consumed electrical energy.

Future improvements should be done in direction of use of analogue-digital converter with higher accuracy, as well as improvements in the control block. Thus the influence of the measurement noise will be decreased and the capabilities for recognition of lower-power consumers will be improved.

#### ACKNOWLEDGEMENT

This paper is prepared in the frames of Project MU03/164 - "Intelligent systems for energy management and control of consumer expenses", Ministry of Education Youth and Science, Bulgarian National Science Fund.

#### REFERENCES

- [1] N. Nikolaev, Y. Rangelov, A. Marinov "Algorithm for indirect load recognition in domestic power consumption", International conference PCIM 2013, Nuremberg, Germany (accepted for presentation).
- [2] N. Nikolaev, Y. Rangelov, V. Valchev, A. Marinov "Technique for indirect analysis of domestic power consumers based on power pattern recognition for smart energy metering", International conference MiPro 2013, Opatija, Croatia (accepted for presentation).

# Functionalities Extension of the NASAVR Software For Small-Signal Stability of Electric Power Systems

Julian Rangelov<sup>1</sup> Konstantin Gerasimov<sup>2</sup> Yoncho Kamenov<sup>3</sup> and Krum Gerasimov<sup>4</sup>

**Abstract –** This paper presents the functionalities extension of the NASAVR software tool for calculation of optimal settings of automatic voltage regulators and power system stabilizers of synchronous generators. The software tool was developed for NEK EAD (the National Electric Company of Bulgaria) by a team of experts from Technical University of Varna, headed by Prof. Dr.Sc. Eng Math. Krum Kostov Gerasimov.

**Keywords –** Electric power systems, synchronous generator, small-signal stability, automatic voltage regulators, power system stabilizers.

## I. INTRODUCTION

In May 2013 the electric power system (EPS) of Bulgaria, owned then by the National Electric Company (NEK EAD) of Bulgaria, became a full member of the Union for the Coordination of the Transmission of Electricity (UCTE) as part of the second synchronous zone. After the resynchronization between the first and the second synchronous zones in October 2004, the EPS of Bulgaria operates synchronously with UCTE. The primary obligation of the Bulgarian EPS is maintaining highly efficient and quality synchronous operation with UCTE. Therefore certain criteria had to be fulfilled such as: maintaining the system frequency within narrow limits, damping low-frequency local and inter-area electromechanical oscillations and their corresponding power oscillations. A number of measures for improving the quality of the synchronous operations were made during the preparation process before the interconnection of the Bulgarian EPS to UCTE. One of the most important measures was the rehabilitation of the electric power plants. The automatic voltage regulators (AVR) were modernized with new ones, equipped with power system stabilizers (PSS). The interconnection of the Bulgarian EPS with the UCTE and the negotiations for interconnection of Turkey afterwards, required the extension of the simulation model. Table I presents the model size before (old model) and after (new model) the interconnection of Turkey.

<sup>1</sup>Yulian Rangelov is Chief Assistant Professor at Department "Electric Power Engineering", Technical University of Varna, Studentska Str. 1, Varna 9010, Bulgaria, E-mail: y.rangelov@tu-varna.bg

<sup>2</sup>Konstantin Gerasimov is Assistant Professor at Department "Electric Power Engineering", Technical University of Varna, Studentska Str. 1, Varna 9010, Bulgaria, E-mail: kkgerasimov@tu-varna.bg

<sup>3</sup>Yoncho Kamenov is Associate Professor at Department "Electric Power Engineering", Technical University of Varna, Studentska Str. 1, Varna 9010, Bulgaria, E-mail: j.kamenov@tu-varna.bg

<sup>4</sup>Krum Gerasimov is Professor at Department "Electric Power Engineering", Technical University of Varna, Studentska Str. 1, Varna 9010, Bulgaria, E-mail: k.gerasimov@tu-varna.bg

Meanwhile, NEK started using the PSS®E software for solving power flow and time-domain simulations.

TABLE I  
SIMULATION MODEL SIZE

Elements	Old model	New model
Buses	1056	5176
Generators	352	1633
AVR	218	954
PSS	27	124
Transformers	441	1495
Lines	1042	5749
Loads	916	3255

This paper briefly introduces the basic principles of the NASAVR software tool and the functionalities of the new version. The presented examples illustrate the main software features.

## II. NASAVR PRODUCT PRESENTATION

### A. General overview

The development of the software tool for calculation of the parameters of systems for automatic voltage regulation and power system stabilizers NASAVR [2] was contracted by NEK EAD to a team of experts from Technical University of Varna, headed by Prof. Dr. Sc. Eng Math. Krum Kostov Gerasimov, and has been successfully implemented at NEK EAD.

Fig. 1 presents its generalized structures.

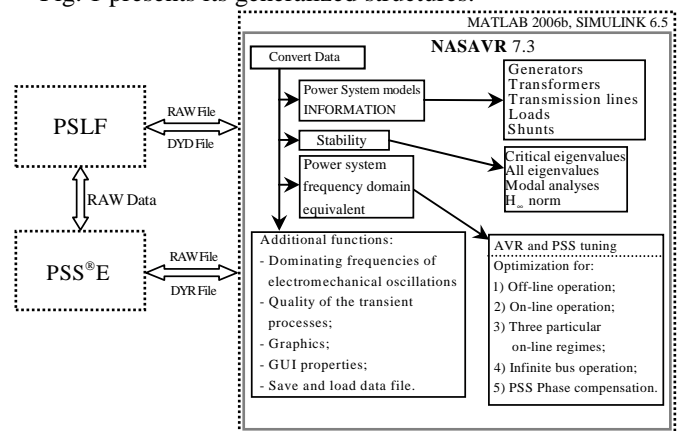


Fig. 1. General structure of the software tool  
NASAVER ver. 7.3

In the first version of NASAVR are implemented the following features:

- Import of raw data for the analyzed EPS from the database of the software GE PSLF 13.2;
- Systematic representation of the data for the analyzed EPS according to element type, its operation condition

- (switched on or off), its type of modeling in NASAVR, or according to the available inputs in the EPS;
- Assessment of the small-signal stability of the analyzed steady state and identification of the dominant frequencies in the electromechanical oscillations;
  - Calculation of the critical eigenvalues of the EPS under small disturbances;
  - Application of standard or accelerated procedure for calculation of eigenvalues or eigenvectors;
  - Assessment of the quality of the transient processes in EPS under small disturbances, based on the eigenvalues;
  - Frequency equivalence of the EPS by aggregation of its detailed mathematical description in the frequency domain in respect to the buses of the generators which are going to be tuned;
  - Determination of the AVR and PSS settings in respect to the criteria for preservation of the small-signal stability and the quality of the transient processes for one or three operating regimes at the same time;
  - Calculation of the frequency and step response of the synchronous generators in order to evaluate the quality of the transient processes;
  - Capability to account for the influence of real deviations of load and voltage at the buses of the analyzed generator at the process of optimization of AVR and PSS parameters.

#### *B. Import of input data from other programs (PSLF 16.04 and PSS®E 30.2)*

In order to make NASAVR more flexible, its source code was altered so that it can import data from the latest versions of the programs for power flow and dynamic stability analysis PSLF 16.04 and PSS®E 30.2. This was very important since most of the data exchanged in international projects is in PSS®E format. NASAVR recognizes the data format and reads it without the use of intermediate conversion software. This significantly speeds up the procedure for extraction of the necessary data from files reaching 50 000 lines of code.

#### *C. Expansion of the model database*

Another advantage of NASAVR is the variety of models implemented in it. As part of the modernization of power plants in the Bulgarian EPS were installed new AVR and PSS systems of different manufacturers like ABB, SIEMENS, ASLTOM and VATECH. This required the update of the model database. It should be noted that NASAVR works with mathematical descriptions linearized around a certain operating point and this means that direct implementation of the regulating systems models cannot be implemented directly but require linearization. Everything is based on standardized models [4], taking into account some specific features of the models in PSLF and PSS®E [5,6].

The latest version of NASAVR is capable of recognizing the following models:

#### *Generator models for an EPS model, created in:*

- *PSLF*: gencls, genrou, gensal;
- *PSS®E*: gencls, genroe, genrou, gensae, gensal.

#### *Excitation system models for an EPS model, created in:*

- *PSLF*: esac2a, esac3a, esac7b, exac1, exac1a, exac2, exac3, exac3a, exac4, exac6a, exac8b, exbbc, exdc1, exdc2, exdc2a, exdc4, exeli, exst1, exst2, exst2a, exst3, exst3a, exst4b, ieeet1, rexs, sexs, esdc1a, esdc2a, esdc3a, esst5b, esst6b, esst7b, exeli2;

- *PSS®E*: esac1a, esac2a, esac3a, esac4a, esac5a, esac6a, esac8b, esdc1a, esdc2a, esst1a, esst2a, esst3a, esst4b, ex2000, exac1, exac1a, exac2, exac3, exac4, exbas, exdc2, exeli, expic1, exst1, exst2, exst2a, exst3, ieeet1, ieeet2, ieeet3, ieeet4, ieeet5, ieeex1, ieeex2, ieeex3, ieeex4, ieet1a, ieet1b, ieet5a, ieex2a, sexs, urst5t, bbsex1, celin, emac1t, esurry, iwoex, urhidt.

#### *PSS models for an EPS model, created in:*

- *PSLF*: ieeest, pss2a, wsccst, pss2b, pssh;
- *PSS®E*: iee2st, ieeest, pss2a, ptist1, ptist3, st2cut, stab1, stab2a, stab3, stab4, ivost, stabni, ostb2t, ostb5t.

Additionally are model PSS of the following manufacturers: Elektrosila (Russia), kmu-siemens, gec alstom. also, there are models of pss type pss4b [8], mreck4 and mpss1a.

#### *Turbine and turbine governors models:*

- *PSLF*: gast, hygov, ieeeg1, ieeeg3, tgov1, tgov3;
- *PSS®E*: gast, hygov, ieeeg1, ieeeg3, tgov1, tgov3.

Totally, the latest version of NASAVR implements 123 models, compared to the 20 models at the initial version of the software.

#### *D. New features*

Thanks to the years of scientific research of the team which developed the software and the gained experience since its implementation, an expansion of the software features as well was made possible. Hereby are presented briefly only the most important one, concerning the analysis of the EPS small-signal stability and the determination of optimal settings of the AVR and PSS. These are:

- Optimization of the parameters of PSS by application of methods for phase compensation by momentum and by voltage in order to improve the damping of the low-frequency inter-area oscillations;

- Grouping of the synchronous units according to the phases of the oscillations they participate in and calculation of their damping degree;

- Capability to calculate the frequency response of a synchronous unit for input control and disturbing signals for all regime parameters;

- Generalized assessment of the quality of the transient processes of the analyzed generator or of the EPS as a whole by calculation of the  $H_\infty$  norm of the transfer matrix from the input signals to the mechanical speeds of the rotors [1,3,7];

- Incorporation of module which simulates measurement noise (available in practice) and of an algorithm for assessment its gain and influence when it passes through the regulating and stabilizing utilities;

- The calculated new settings of the AVR and PSS can be tested for 30 different operating points, chosen in advance in respect to the generator's load diagram.

### III. TEST AND IMPLEMENTATION OF NASAVR

In order to concentrate the attention on a specified synchronous unit during the analysis, the general mathematical model can be reordered into the structure shown in Fig. 2.

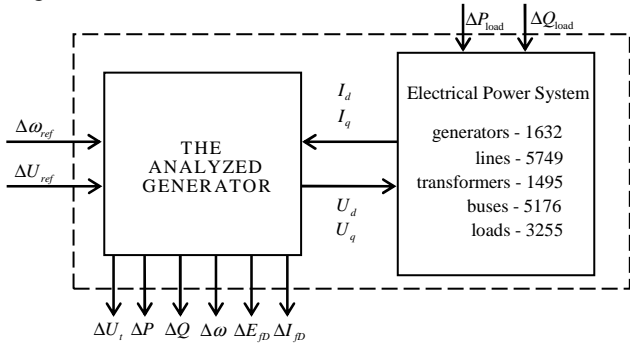


Fig. 2. Block diagram of the mathematical model, used for analysis of a specified synchronous unit

For verification of the composed model is used a recorded step response of the generator output active power, for a step change of reference of the automatic voltage regulator (Fig. 4). The composed mathematical model is the used to simulate the step response for the same conditions and for the corresponding operating state before the disturbance (Fig. 3). It is clearly seen that practically, at the initial stages of the transient process, there is overlapping of the times and magnitudes. At the next stages also practically there is no significant deviation of the main component. There are some deviations in the other components which are caused by a disturbing signal. Because it is accidental in nature, it cannot be reproduced exactly at the simulation and hence the deviations.

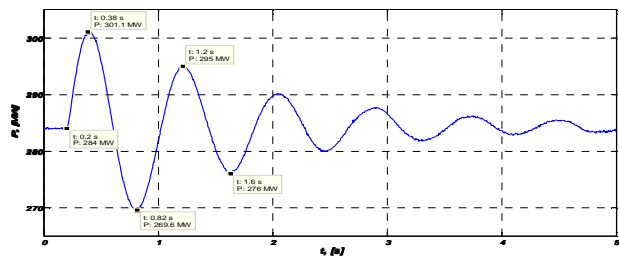


Fig. 3. Step response of the generator output active power, calculated with the developed simulation model, for a step change of +3% of  $U_{ref}$  and with PSS switched off

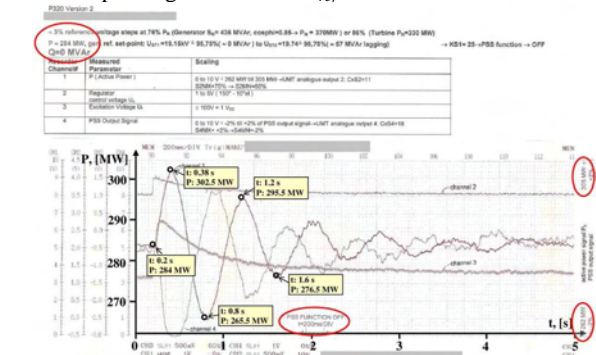


Fig. 4. Recorded step response of the generator output active power, for a step change of +3% of  $U_{ref}$  and with PSS switched off

In Fig. 5 is shown the  $H_\infty$  norm of the transfer matrix of the interconnected system generator-EPS. The generator is loaded with 213 MW active power and with 17.15 MVA reactive power. At its buses is measured voltage of 15.55 kV (this operating state is valid for all the results shown in figures from Fig. 5 to Fig. 9). One can clearly differentiate the influence of PSS on the local frequencies of oscillation (around 1Hz), when it is switched on. Also, appropriate settings of the PSS [7] could make it damp inter-area oscillations as well (see the red curve around 0,1Hz). Inappropriate settings though could amplify them (compare the blue curve around 0,1Hz in respect to the red and green ones).

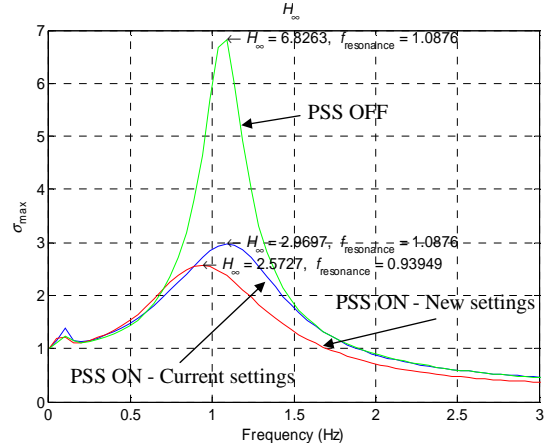


Fig. 5.  $H_\infty$  norm of the transfer matrix from  $\Delta U_{ref}$  to all output parameters of the generator

The frequency response from a disturbance in the voltage regulator reference  $\Delta U_{ref}$  to the deviations of the bus voltage ( $\Delta U$ ), active power ( $\Delta P$ ) and rotor speed ( $\Delta \omega$ ) gives information about the influence of the PSS settings to the synchronous unit.

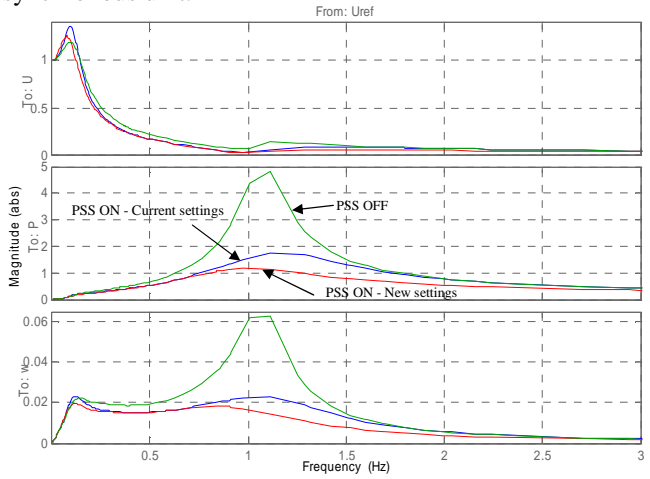


Fig. 8. Frequency response for a disturbance in the voltage regulator reference  $\Delta U_{ref}$  and the outputs  $\Delta U$ ,  $\Delta P$  and  $\Delta \omega$

The decreased more than twice  $H_\infty$  norm for the case when PSS is enabled (see Fig. 5) means improved quality of the transient processes. As confirmation of this fact are shown the results from the step responses of the analyzed generator (Fig. 9). It can be clearly seen, that the measurement noise of the voltage regulator output ( $\Delta E_{fd}$ ) is not passed through to the generator's output regime parameters ( $\Delta U$ ,  $\Delta P$ ,  $\Delta \omega$ ).

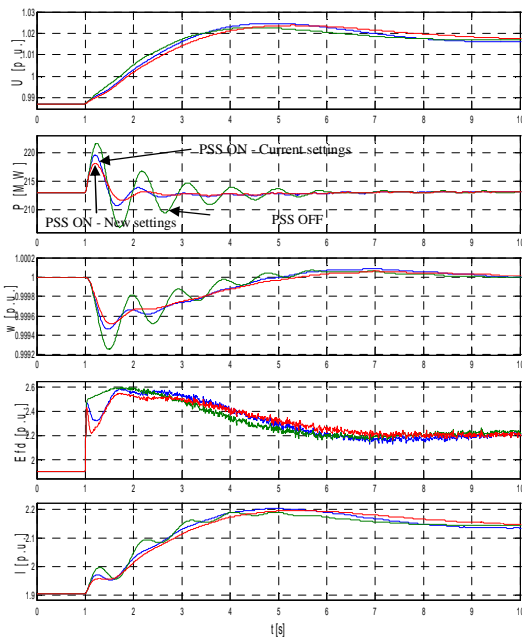


Fig. 9. Step response (with noise) of  $\Delta U$ ,  $\Delta P$ ,  $\Delta \omega$ ,  $\Delta E_{fd}$  and  $\Delta I_f$  for a step change of  $\Delta U_{ref} = +3\%$

Due to the dynamic structure of the EPS and its operating state, it is necessary that calculated appropriate settings should be checked by a variance of calculation for many enough (30) operating points of the analyzed synchronous generator, from different zones of its load diagram (as shown in Fig. 10)

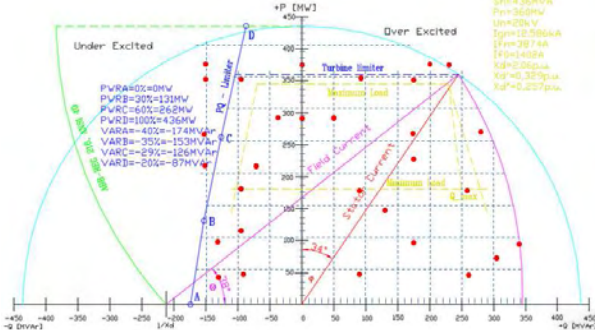


Fig. 10. Example load diagram with specified operating points

The results from the calculated chosen possible operating points, in the form of step responses for the same conditions as the ones from Fig. 9, are shown in Fig. 11.

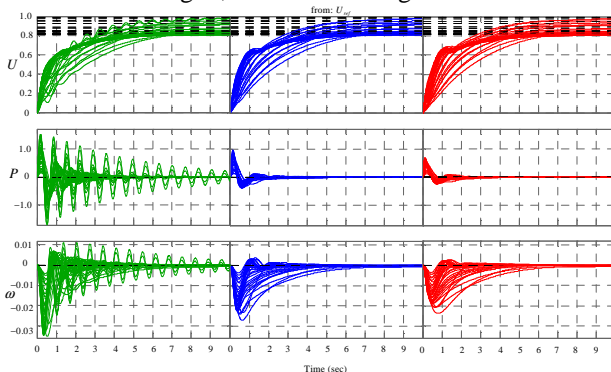


Fig. 11. Family of step response, based on the different operating points from the load diagram of the generator

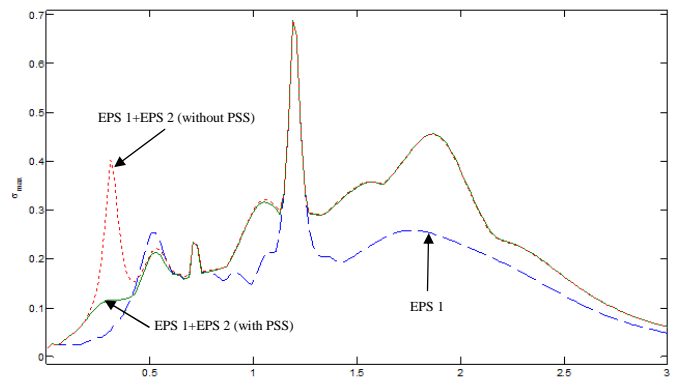


Fig. 12. Maximal singular values of the transfer matrix of two EPS and their interconnection

#### IV. CONCLUSION

The presented software tool NASAVR for calculation of the parameters of automatic voltage regulators and power system stabilizers of synchronous generators enable the user to conduct thorough analysis of the small-signal stability of large electric power systems. Proof of its build qualities are the finalized successfully projects for calculation of appropriate PSS settings in main Bulgarian power plants. Also, the team, which developed the software, participated in the calculation of the PSS settings in 5 Turkish power plants regarding the interconnection of the Turkish EPS to the interconnected European EPS ENTSO-E.

#### REFERENCES

- [1] Gerasimov K. K., Rangelov Y. E., A. M. Vrangov, Y. L. Kamenov. Usage of singular numbers in evaluation of the control of synchronous generators in the power system, Acta Universitatis Pontica Euxinus, Constanta, Romania, 2005, Vol.4, №1, pp.90-94.
- [2] Gerasimov, K., Y. Rangelov, Ch. Ivanov, Y. Kamenov. MATLAB Based Software for AVR and PSS Tuning. Acta Universitatis Pontica Euxinus, Constanta, Romania, Vol. II, №2, 2005, pp. 145-150.
- [3] Petkov P., M. Konstantinov, *Robust Control Systems*, ABC Tehnika, 2002. (in Bulgarian) ISBN: 9548873516
- [4] IEEE Recommended Practice for Excitation System Models for Power System Stability Studies. IEEE Power Engineering Society. IEEE Std 421.5™-2005
- [5] PSS/E™ 30. USERS MANUAL. Shaw Power Technologies, Inc.™ 2004.
- [6] PSLF User's Manual. General Electric International, Inc.
- [7] Rangelov, Y., K. Gerasimov, J. Kamenov, Kr. Gerasimov. Influence of the settings of PSS2A and 2B input filters over the damping of low-frequency power oscillations. *Proc. of ICEST 2011, Niš, Serbia, June 29 - July 1, 2011, Volume 3*, pp.977-980, ISBN: 978-8661250330
- [8] IEEE Tutorial Course Power System Stabilization Via Excitation Control. the IEEE Power Engineering Society General Meeting. Tampa, Florida, June 2007.

# Mechanical Design of High Voltage Overhead Transmission Lines With Thermal-Resistant Aluminum Alloy Conductors Considering the Heating From The Electrical Current

Yoncho Kamenov<sup>1</sup>, Yulian Rangelov<sup>2</sup> and Angel Vrangov<sup>3</sup>

**Abstract –** This paper considers the mechanical design of overhead transmission lines, taking into account the influence of the linear expansion of super thermal-resistant conductors due to the flowing continuous current. The paper presents results for the super thermal-resistant conductor sag at different maximum tensions and different conductor temperatures for a 110 kV overhead transmission line.

**Keywords –** Overhead transmission lines, super thermal-resistant conductors, mechanical design, continuous current.

## I. INTRODUCTION

The high-voltage overhead transmission lines are the backbone of the electric power systems. Their total length accounts for tens of thousands of kilometers. Building new power lines is a priority of each transmission system operator. On the other hand, engineers are looking for solutions to increase the power capability of the existing lines, since building new lines in private properties is extremely slow and complicated process. One of the possible solutions is the substitution of the old conductors with new ones, which have doubled transmission capacity by increasing the operation temperature from 70-90°C up to 210°C.

Fig. 1 shows the dependence of the conductor sag from the working temperature [5]. The coefficient of linear expansion  $\alpha$  of the classical aluminum-steel conductors (ACSR) is about  $19 \cdot 10^{-6} \text{ }^{\circ}\text{C}^{-1}$ . The super thermal-resistant conductors ZTACIR, which are studied in the paper, are made of aluminum-zirconium alloy, and are reinforced with nickel-iron alloy core (invar). They have  $\alpha=15,8 \cdot 10^{-6} \text{ }^{\circ}\text{C}^{-1}$ , determined mainly by the linear expansion of the invar core [2]. Another important property when heating combined conductors is the so called knee point (stress transfer point) [3,5]. When the conductor is heated above the knee point temperature, the resulting linear expansion coefficient decreases to the value of linear expansion of the invar core – about  $\alpha=3,5 \cdot 10^{-6} \text{ }^{\circ}\text{C}^{-1}$ . For ACSR and ZTACIR conductors this point is within the range

80-100 °C. The other two conductor types shown in Fig. 1 are designed to allow the different metals of the combined conductor to expand and shrink independently from each other. They are in turn more expensive and require special mounting hardware. However, due to their advantages they have found application in Europe [6,7].

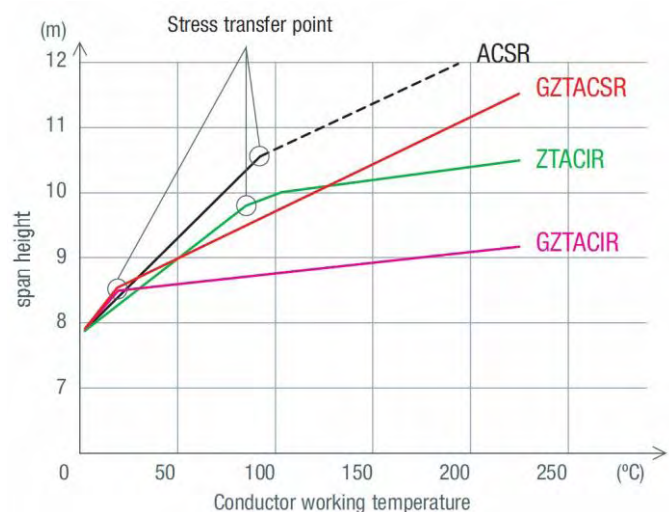


Fig. 1. Temperature dependence of the conductor sag

## II. METHODOLOGY

The design process of overhead transmission lines can be conditionally divided in a few stages, two of which are briefly explained in the following section.

### A. Evaluation of the Input Data

First of all, it is necessary to know the climate region where the line will be built. For example, the climate regions in Bulgaria are five, classified depending on the degree of conductor icing. Another important factors are the max wind speed when there is no ice on the conductor, the max wind speed when the conductor is iced, max air temperature (40 °C for Bulgaria), min temperature (-30 °C), average annual temperature, temperature when conductor icing begins (-5°C) and air temperature at max wind speed (15°C).

Second of all, the mechanical properties of the conductors should be determined – cross-section, weight, modulus of

<sup>1</sup>Yoncho Kamenov is with Department "Electric Power Engineering" at Technical University of Varna, Studentska str. 1, Varna 9010, Bulgaria, E-mail: [j.kamenov@tu-varna.bg](mailto:j.kamenov@tu-varna.bg)

<sup>2</sup>Yulian Rangelov is with Department "Electric Power Engineering" at Technical University of Varna, Studentska str. 1, Varna 9010, Bulgaria, E-mail: [y.rangelov@tu-varna.bg](mailto:y.rangelov@tu-varna.bg)

<sup>3</sup>Angel Vrangov is with Department "Electric Power Engineering" at Technical University of Varna, Studentska str. 1, Varna 9010, Bulgaria, E-mail: [a.vrangov@tu-varna.bg](mailto:a.vrangov@tu-varna.bg)

elasticity, thermal coefficient of linear expansion  $\alpha$ ,  $^{\circ}\text{C}^{-1}$  and tensile strength –  $\sigma_o$ .

Based on the climate conditions and the mechanical specifications of the conductor, the so called specific loads of the conductors  $\gamma$  are evaluated. The loads are namely:  $\gamma_1$  – load due to the conductor own weight;  $\gamma_2$  – load due to the ice shell on the conductors;  $\gamma_3 = \gamma_1 + \gamma_2$  – load due to the weight of the conductor and the weight of the ice;  $\gamma_4$  – load from the max wind speed  $V_{\max}$ , acting on non-iced conductor;  $\gamma_5$  – load from the wind acting on iced conductor, with max wind speed designated as  $V_n$ ;  $\gamma_6$  – load resulting from the conductor's own weight plus the load from the max wind speed;  $\gamma_7$  – load resulting from the load of the iced conductor plus the pressure from the  $V_n$  wind speed.

According to the Bulgarian regulations [1] the highest allowable tension of the conductors is evaluated as percentage of the conductors rated tensile strength. For overhead transmission lines and conductor cross-section above 95 mm<sup>2</sup>, the allowable tension is 45 % from the rated value, when calculated for max conductor mechanical loading or for min temperature. In case the conductors are substituted with different type, the allowable tension must reconcile with the tensions initially evaluated for the power line.

#### *B. Evaluation of the Maximum Mechanical Loading and the Maximum Sag of the Conductors*

As it is known, the mechanical design of the conductors of overhead transmission lines is based on the theory of flexible and non-elastic fibers (catenary). The characteristic of the actually used conductors do not completely match the characteristics of the flexible and non-elastic fibers, but for practical computations the difference is considered insignificant. Based on this theory, an equation for the conductor position between two electric poles can be derived. For simplicity, the following is assumed: - the points where the both ends of the conductor are mounted are considered to be still, while the conductors are articulated to that points; - the conductors are uniformly loaded along the whole length. Under the stress of the loads the conductors "hang" like homogeneous heavy flexible fiber (catenary); - the flexible fibers are subject to tensile force only; - the shape of the span curve of the conductor do not depend on the length of the interpole distance.

For overhead transmission lines up to 400 kV and interpole distance up to 500 m, the hyperbolic equation can be simplified assuming that the conductor span curve is parabolic. Then the equation is the following:

$$y = \frac{\gamma \cdot x^2}{2 \cdot \sigma_o}, \quad (1)$$

where  $\sigma_o$  is the mechanical tension of the conductor at the point with the deepest sag within a horizontal interpole.

If  $x$  from the latter equation is substituted with the distance between one of the poles and the deepest sag point for horizontal interpole, the maximum conductor sag can be evaluated as follows:

$$f = \frac{\gamma \cdot l^2}{8 \cdot \sigma_o}, \quad (2)$$

where  $l$  is the interpole distance.

The length of the conductor between the two poles is:

$$L = l + \frac{\gamma^2 \cdot l^3}{24 \cdot \sigma_o^2}. \quad (3)$$

When changing the atmospheric conditions it is assumed that the state of the conductor is changed in steps. First, the air temperature is changed from  $t_m$  to  $t_n$ , which causes a change of the conductor length from  $L_m$  to  $L_{ln}$ . Immediately after that, the mechanical load of the conductor changes along with the conductor length from  $L_{ln}$  to  $L_n$ . After some slight simplifications the formula for the conductor length becomes as follow:

$$L_n = L_m \left[ 1 + \alpha(t_n - t_m) + \beta(\sigma_n - \sigma_m) \right]. \quad (4)$$

Based on (3) and (4) the following equation for changing the conductor operation conditions from " $m$ " to " $n$ " is derived [3,9,10]:

$$\sigma_n - \frac{\gamma_n^2 \cdot l^2 \cdot E}{24 \cdot \sigma_n^2} = \sigma_m - \frac{\gamma_m^2 \cdot l^2 \cdot E}{24 \cdot \sigma_m^2} - \alpha \cdot E \cdot (t_n - t_m) \quad (5)$$

The maximum mechanical tension  $\sigma_{max}$  is determined among the following two operation conditions: №1.1 maximum load operation ( $\sigma_{\gamma 7}$ ,  $\gamma_7$  and  $t=-5^{\circ}\text{C}$ ) or №1.2 min temperature operation ( $\sigma_{min}$ ,  $\gamma_1$  and  $t=-30^{\circ}\text{C}$ ). The deepest conductor sag is determined among the following conditions: №2.1 iced conductors at no wind ( $\sigma_{\gamma 3}$ ,  $\gamma_3$  and  $t=-5^{\circ}\text{C}$ ) or №2.2 min temperature operation ( $\sigma_{\gamma 1}$ ,  $\gamma_1$  and  $t=40^{\circ}\text{C}$ ). There exist a critical interpole distance  $l_{kp}$  and a critical temperature  $t_{kp}$ , such that the max tension  $\sigma_{max}$  and the max conductor sag are equal for the both operation conditions. This fact makes it easy to determine the necessary design operation conditions.

### III. EXPERIMENTAL RESULTS

Different input data is used to obtain full picture of the deviation of the max conductor sag when designing overhead transmission lines with ZTACIR Ø19,04 mm conductors [5,8]. Different data combinations are obtained by varying the climate region (the ice thickness around the conductor) and the max tension of the conductor  $\sigma_{max}$ . The max tension  $\sigma_{max}$  values are selected according to the possibility for their realization when either a new line is designed or the aluminum-steel conductors of an existing line are changed with super thermal-resistant conductors ZTACIR Ø19,04 mm. In addition, the mechanical stress on the electric poles must not exceed the stress before the line reconstruction. Such conductor substitutions were realized for reconstruction of existing overhead lines in north-eastern Bulgaria [4].

The following parameters are assumed for the presented computations: max wind speed 35 m/s; max wind speed when

the conductors are iced 17,5 m/s; ice density 900 kg/m<sup>3</sup>; altitude 250 m; active height of the pole 16 m (max conductor sag 9,5 m).

The computations were made considering conductor temperature not exceeding the max allowable operation temperature of the super thermal-resistant conductors ZTACIR. Therefore, the variable coefficient of linear expansion  $\alpha$  (knee effect) is accounted.

The tables below present results for:

$l_{kp}$  – critical interpole distance;

$l_r$  – dimensioning interpole distance (the distance for which the max allowed conductor sag is observed);

$t_{kp}$  – critical temperature;

$\Delta f_{210-15}$  – the difference of the conductor sag at temperature 210 °C and 15 °C;

$\Delta f_{210-40}$  - the difference of the conductor sag at temperature 210 °C and 40 °C.

The tables present the deviations  $\Delta f_{210-15}$  and  $\Delta f_{210-40}$ , to determine the order of sag change due to heating from the continuous operation current, compared to the sag determined for the dimensioning temperatures in Bulgaria (15°C when two overhead lines intersect or the max air temperature).

The sag deviations are calculated for three different interpole distances – 200 m, 250 m and distance approximately equal to the dimensioning distance.

TABLE I  
CONDUCTOR SAG DEVIATION AT  $\sigma_{max}=75$  MPa

$l$ , m		Climate region			
		II	III	IV	I sp.
	$l_{kp}$ , m	98	68	51	31
	$l_r$ , m	261	226	197	155
	$t_{kp}$ , °C	26	35	41	49
200	$\Delta f_{210-15}, m$	1,84	1,48	1,17	0,75
	$\Delta f_{210-40}, m$	1,34	1,09	0,87	0,56
250	$\Delta f_{210-15}, m$	1,94	1,52	1,19	0,75
	$\Delta f_{210-40}, m$	1,43	1,13	0,89	0,56
$\approx l_r$	$\Delta f_{210-15}, m$	1,95	1,51	1,17	0,74
	$\Delta f_{210-40}, m$	1,44	1,12	0,87	0,55

TABLE II  
CONDUCTOR SAG DEVIATION AT  $\sigma_{max}=95$  MPa

$l$ , m		Climate region			
		II	III	IV	I sp.
	$l_{kp}$ , m	124	87	64	39
	$l_r$ , m	298	255	222	174
	$t_{kp}$ , °C	35	46	54	63
200	$\Delta f_{210-15}, m$	2,15	1,83	1,48	0,95
	$\Delta f_{210-40}, m$	1,57	1,34	1,09	0,71
250	$\Delta f_{210-15}, m$	2,32	1,89	1,50	0,95
	$\Delta f_{210-40}, m$	1,70	1,40	1,11	0,71
$\approx l_r$	$\Delta f_{210-15}, m$	2,43	1,90	1,49	0,95
	$\Delta f_{210-40}, m$	1,79	1,41	1,10	0,71

TABLE III  
CONDUCTOR SAG DEVIATION AT  $\sigma_{max}=125$  MPa

$l$ , m		Climate region			
		II	III	IV	I sp.
	$l_{kp}$ , m	163	114	84	52
	$l_r$ , m	346	294	255	200
	$t_{kp}$ , °C	48	63	73	85
200	$\Delta f_{210-15}, m$	2,32	2,25	1,94	1,27
	$\Delta f_{210-40}, m$	1,77	1,65	1,42	0,94
250	$\Delta f_{210-15}, m$	2,69	2,41	1,98	1,27
	$\Delta f_{210-40}, m$	2,00	1,77	1,46	0,95
$\approx l_r$	$\Delta f_{210-15}, m$	3,10	2,49	1,98	1,27
	$\Delta f_{210-40}, m$	2,29	1,84	1,46	0,94

TABLE IV  
CONDUCTOR SAG DEVIATION AT  $\sigma_{max}=150$  MPa

$l$ , m		Climate region			
		II	III	IV	I sp.
	$l_{kp}$ , m	196	137	101	62
	$l_r$ , m	381	324	280	220
	$t_{kp}$ , °C	60	77	89	103
200	$\Delta f_{210-15}, m$	2,13	2,30	2,26	1,58
	$\Delta f_{210-40}, m$	1,72	1,78	1,67	1,16
250	$\Delta f_{210-15}, m$	2,67	2,69	2,38	1,55
	$\Delta f_{210-40}, m$	2,07	2,01	1,75	1,15
$\approx l_r$	$\Delta f_{210-15}, m$	3,54	2,95	2,41	1,57
	$\Delta f_{210-40}, m$	2,63	2,17	1,77	1,16

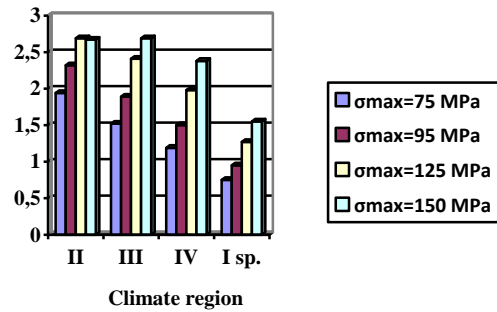


Fig. 2. Sag deviation  $\Delta f_{210-15}$  at  $l=250$  m

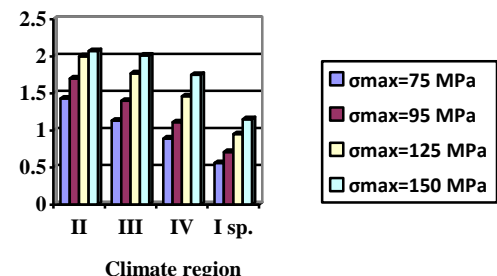


Fig. 3. Sag deviation  $\Delta f_{210-40}$  at  $l=250$  m

From the results it is found that:

- The critical temperature in the most cases is higher than the max air temperature in Bulgaria (40 °C), which means that if the conductor heating from the flowing current is not accounted the max sag condition is №2.1 (iced conductors without wind);
- $\Delta f_{210-15}$  and  $\Delta f_{210-40}$  deviate within a wide range (from half up to more than three meters), which compared to the max allowed sag (9,5 m) is a significant deviation;
- $\Delta f_{210-15}$  approaches values above 3 m, which means that the insulation distance between two intersecting overhead lines could be violated (according to [1] the insulation distance is between 3 m and 5,50 m);
- At constant dimensioning interpole distance the deviations  $\Delta f$  do not change significantly (up to 1 m) with the change of the max tension;
- At nonviolent climate conditions (it corresponds to increased initial tension of the conductors at no load from ice or wind) the calculated deviations are higher ( $\Delta f$ ).

#### IV. CONCLUSIONS

Based on the obtained results, the following conclusions can be drawn:

1. Due to the significant sag deviations of the super thermal-resistant conductors, the heating from the flowing electrical current should be accounted when calculating the distance from the conductor to the ground (or to other facilities being crossed by the line);
2. When crossing existing overhead lines, accounting the additional sag due to the heating from the electrical current is determining;
3. Due to the different sag deviations for the different air temperatures and climate regions, each case should be considered individually rather than in a typical way.

#### REFERENCES

- [1] Наредба №3 за устройството на електрическите уредби и електропроводните линии, Обн., ДВ, бр. 90 от 13.10.2004 г. и 91 от 14.10.2004 г., 2004.
- [2] Nishikawa, T. Y. Takak, M. Sanai, S. Kitamura, K. Nakama and T. Kariya, "Development of high strength invar alloy wire for high voltage overhead power transmission line.,," 2010.
- [3] leenders, l. "Upgrading overhead lines with high temperature, low sag conductors.,," Faculteit elektrotechniek, 2007.
- [4] Rangelov, Y. "Comparative analysis of power losses in overhead power lines for high voltage, for different parameters of the aluminum wires" in *iCEST, Proceedings of papers*, Nis, Serbia, 2011.
- [5] Deangeli prodotti, "Compact conductors in aluminium zirconium alloy having a high thermal limit," Product Catalog.
- [6] Zamora, I. A. Mazón. R. Criado. C. Alonso and J. R. Saenz, "Uprating using high-temperature electrical conductors.,," 2012.
- [7] Geary, R., T. Condon, T. Kavanagh, O. armstrong & J. Doyle. Introduction of high temperature low sag conductors to the Irish transmission grid. 21, rue d'artois, f-75008 paris. B2-104. Cigre 2012

- [8] Gianfranco Civili. Massimiliano handel. New types of conductors for overhead lines with high thermal resistance, which increase the current transmission capacity and limit the thermal expansion at high current intensity. De angeli prodotti s.p.a, bulk power system dynamics and control - vi, august 22-27, 2004, Cortina D'ampezzo, Italy

- [9] Генков, Х. В. Захарiev. Механична част на електрически мрежи, София: ТУ-София, 1993.

- [10] Edris, a. High-temperature, low-sag transmission conductors. Final report, june 2002. Palo alto, California, USA

# Optimization of Electric Resistance Furnace Using Backtracking Algorithm

Borislav Dimitrov<sup>1</sup>, Marinela Yordanova<sup>2</sup> and Hristo Nenov<sup>3</sup>

**Abstract –** The optimization algorithm "backtracking" belongs to the group of the dynamic optimization algorithms. In the paper the application of the backtracking for optimization of electric resistance furnace is presented for different objective functions. The results of the optimization procedure are processed by algorithms used in the graph theory. The application of different functions has been studied for implementation in the computational procedures.

**Keywords –** Algorithm "Backtracking", Optimization, Electric Resistance Furnaces, Energy Efficiency.

## I. INTRODUCTION

Electric resistance furnaces (ERF) for industrial applications are powerful consumers of electric energy and their optimization according to different objective functions is an important task. Fig.1.A shows the electric resistance furnace's typical construction. The most often applied objective function at optimization is minimum loss of energy, but also the other as minimal mass, volume and price find application. The mathematical description of the functions has been proposed in [2, 3]. It has been applied in this investigation of algorithm "backtracking" [7, 9] for optimization of ERF.

The aim of the paper is to investigate the possibility to apply the algorithm "backtracking" for electric furnaces optimization. The object of the research has been real furnace equipment, subject to reconstruction in order to reduce energy losses. The results are proposed for a particular furnace which insulation is designed with the algorithm under discussion.

## II. APPLYING ALGORITHM "BACKTRACKING" FOR OPTIMIZATION OF ERF

The principle of the algorithm backtracking [7, 9] consists in stepping solution of the problem. At each step the current solution expands the possible extensions. In case that the obtained results do not meet said requirements, the algorithm returns to the previous step and continues on an adjacent branch of the tree.

The search continues to find a solution, or to establish that the problem is unsolvable for the input conditions. The last statement can be reached by examining all possibilities. A recursive algorithm [1, 6, 7] is used - listing 1.

Listing. 1:

```
void try (step i){  
if (i>n) { // check received decision }  
else { // implement a solution in all possible ways }  
for (k=1; k<=n; k++)  
if (condition k is acceptable){ candidate registration;  
try (i+1) // recursive call to the function remove registration;  
}  
}
```

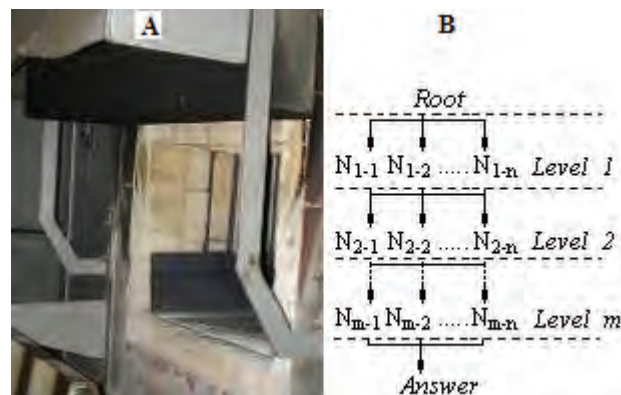


Fig.1. A–Typical construction of high temperature ERF; B–graphic interpretation of the algorithm "backtracking"

The application of the backtracking algorithm for optimal design of the ERF is illustrated by the tree structure shown in fig.1.B. The root of the tree contains the initial conditions for solving the problem. The number of levels (m) and the nodes (n) are defined by the objective function, respectively, the needed equations and database from the heat-insulating and fireproof materials. The following sequence is adopted:

- **Root** (Fig.1.B) – The input data: characteristics of the heated detail, temperature and heating time, the objective function of the optimization and other. Since the optimization procedure is directed to the heat-insulation of the furnace the database of fireproof and heat-insulating materials is necessary. Their main heat characteristics are:  $\lambda$  - thermal conductivity coefficient through the insulation; c - specific heat capacity; j - density;  $\tau_{\max}$  - maximum temperature.

- **Level (1, 2 ... m).** Each level contains an equation or computational procedure of pre-accepted methodology [4], which is calculated consistently. The number of levels is determined by the number of equations to be calculated. Moreover computing the relevant level has to determine the number of possible nodes that meet the requirements. They are marked as perspective (1, true, etc.) and passing to the next level going through. The others have no future (0). For example: the first level has a database of fireproof materials used in the first layer of insulation. Each node (N<sub>1-1</sub>, N<sub>1-2</sub> .. etc.) contains one material. Those materials responding to specific requirement are marked.

<sup>1</sup> eng. Borislav Dimitrov PhD, Assoc. Professor, Technical University of Varna, e-mail: bdimitrov@processmodelig.org

<sup>2</sup> eng. Marinela Yordanova PhD, Assoc. Professor, Technical University of Varna, e-mail: m.yordanova@tu-varna.bg

<sup>3</sup> eng. Hristo Nenov PhD

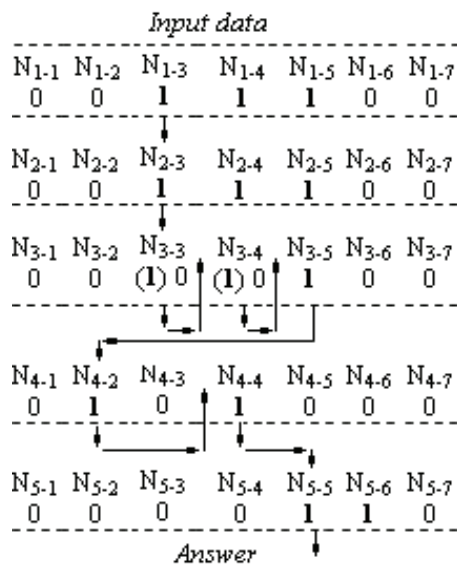


Fig. 2. Graphical representation of the algorithm "backtracking" in solving a specific optimization problem

- **Conditions.** Each of the levels contains limit conditions in accordance with the equation that determine the perceptiveness of the nodes. The conditions may be limits for overheating at rated current, contact resistance, contact force, etc.

- It passes to the second level through the first perspective node of the first level (eg, N<sub>1-2</sub>). By sequentially scanning nodes N<sub>2-1</sub> N<sub>2-n</sub> possible decisions, meeting the required conditions for this level, are searched for. If there are any, they are marked as perspective and through them it continues to the next level. If there is not perspective decision of the second level according the data in the node of the first level (N<sub>1-2</sub>), the algorithm returns to the first level. In this case N<sub>1-2</sub> is marked as a non-perspective and the calculation starts from the next perspective node. An example is shown in Figure 2: transition from level 3 to 4 via nodes N<sub>3-3</sub> and N<sub>3-4</sub> is impossible and they are marked as no perspective, i.e. the heat insulation materials are rejected as inappropriate to the restrictive conditions. Finally, transition is from node N<sub>3-5</sub>.

- The same sequence repeats up to final decision. The marked nodes contain the values of each of the levels, i.e. those are the decisions of each of the equations in the realization of the task. Computing can continue in the presence of marked but not explored nodes in different levels. This allows finding more than one decision.

The basic equations for design of the thermal insulation are composed on the base of the replacing scheme of Figure 3.

The accumulated energy in each layer (i-th) of the furnace walls:

$$(1) \quad Q_{erf} = c_i \cdot m_i \cdot (\tau_i - \tau_o)$$

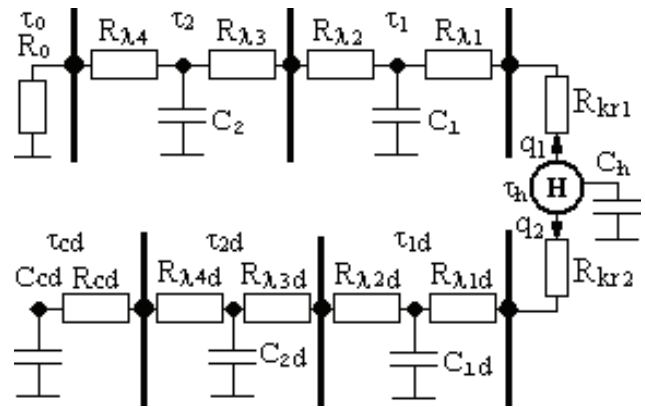


Fig.3. Replacing scheme used for the modeling of the thermal processes in the complex furnace-heated detail

The accumulated energy in the heated detail:

$$(2) \quad Q_d = c_{id} \cdot m_{id} \cdot (\tau_{id} - \tau_o)$$

Where the consecutive coefficients in layers are labeled with index i: c<sub>i</sub> (id) – specific heat of the furnace (the load); m<sub>i (id)</sub> – mass of the furnace (the load); τ<sub>i (id)</sub> – temperature in the furnace (the load); τ<sub>0</sub> – temperature of the ambient (initial temperature).

The total losses Q<sub>l</sub> are determined by the amount of the accumulated energy in the furnace walls and the losses to the environment Q<sub>o</sub>:

$$(3) \quad Q_l = Q_{erf} + Q_o$$

System of equations describing the transient heat process is composed from the replacing scheme as follows:

$$(4) \quad \begin{cases} q = \frac{\tau_h - \tau_1}{R_{kr1} + R_{\lambda 1}} + \frac{\tau_h - \tau_{1d}}{R_{kr2} + R_{\lambda 1d}} \\ C_1 \frac{d\tau_1}{dt} + \frac{\tau_1 - \tau_2}{R_{\lambda 2} + R_{\lambda 3}} = \frac{\tau_h - \tau_1}{R_{kr1} + R_{\lambda 1}} \\ C_{1d} \frac{d\tau_{1d}}{dt} + \frac{\tau_{1d} - \tau_{2d}}{R_{\lambda 2d} + R_{\lambda 3d}} = \frac{\tau_h - \tau_1}{R_{kr2} + R_{\lambda 1d}} \end{cases}$$

Computational procedure is implemented in Matlab, based on numerical methods of Runge-Kutta [4, 5, 10]. For receiving the transient process of heating of the researched furnace ode45, ode23, ode15s are used. This procedure is carried out in one of the levels (in the example N<sub>4</sub>). The differential equations giving the transient heat process are in the following system:

$$\begin{aligned}
 (5) \quad & C_1 \frac{d\tau_1}{dt} = - \left( \frac{1}{R_{kr1} + R_{\lambda 1} + R_{kr2} + R_{\lambda 1d}} \right) \cdot \tau_1 + \\
 & + \frac{q_1}{1 + \left( \frac{R_{kr1} + R_{\lambda 1}}{R_{kr2} + R_{\lambda 1d}} \right)} \\
 & C_2 \frac{d\tau_2}{dt} = \left( \frac{1}{R_{\lambda 2} + R_{\lambda 3}} \right) \cdot \tau_1 - \\
 & - \left( \frac{1}{R_{\lambda 2} + R_{\lambda 3}} + \frac{1}{R_{\lambda 4} + R_0} \right) \cdot \tau_2 \\
 & C_{1d} \frac{d\tau_{1d}}{dt} = \left( \frac{1}{R_{kr1} + R_{\lambda 1} + R_{kr2} + R_{\lambda 1d}} \right) \cdot \tau_{1d} \\
 & + \frac{q}{1 + \left( \frac{R_{kr2} + R_{\lambda 1d}}{R_{kr1} + R_{\lambda 1}} \right)} \\
 & C_{2d} \frac{d\tau_{2d}}{dt} = \left( \frac{1}{R_{\lambda 2d} + R_{32d}} \right) \cdot \theta_{d1} - \left( \frac{1}{R_{\lambda 4d} + R_{\lambda cd}} \right) \cdot \tau_{d2}
 \end{aligned}$$

The symbols in Figure 3 and those of systems of equations (4) and (5) are following:

$R_{\lambda 1+4}$  - resistances of the conductive heat transfer through the walls of the furnace. They conduct the heat flow of the losses  $q_1$  - form the chamber of the furnace to the outside environment.

$R_0$ ,  $R_{kr1}$ ,  $R_{kr2}$  - resistances of convection and radiation, respectively from the housing of the ERF towards the outside environment and from the heater H towards the surface of the heat insulation layer and the heated thermal load (detail).

$R_{\lambda 1+4d}$ ,  $R_{cd}$  - resistances of the conductive heat transfer in the heated thermal load. The useful heat flow  $q_2$  is conducted through them.

$C_1$ ,  $C_2$ ,  $C_{1d}$ ,  $C_{2d}$ ,  $C_{cd}$ ,  $C_h$  - heat capacity, respectively of the two layers of the furnace and the two layers and the center of the heated thermal load and the heater.

$\tau_h$ ,  $\tau_1$ ,  $\tau_2$ ,  $\tau_0$ ,  $\tau_{1d}$ ,  $\tau_{2d}$ ,  $\tau_{cd}$  - temperatures, respectively: of the heater; of the two layers of the furnace; the outside environment; the two layers and the center of the heated thermal load. The temperatures are given as initial values and they are determined each iteration of the computing procedure. Only the temperature of the outside environment  $\tau_0$  is excluded from this rule - it is set as constant. In this way a constraint from third order is set.

### III. PROCESSING RESULTS WITH GRAPH THEORY

The optimization procedure allows numerous results to be processed. The nodes, marked as promising, represent directed

graphs, an example of which is shown in Figure 4. This allows using algorithms to work with graphs.

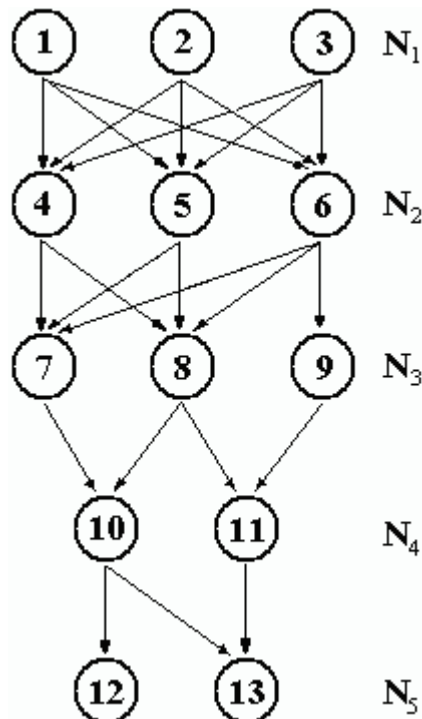


Fig.4. Oriented graph, consisting of optimization data of ERF.

To solve the optimization problem in question algorithm "BFS - Breath-First-Search" is used. Processing begins from the top vertex - i, i.e. in the specific task of level  $N_1$ , node 1 and all of its immediate neighbors are reviewed.

Then it proceeds to further search - search in the width of each of its neighbors. Generally, according to the graph theory BFS algorithm requires passing through all the nodes in this manner - i.e. sequential selection (random) of starting vertex until all nodes of the graph are not searched.

In this particular task it should always start from node of level  $N_1$ , because it makes no sense to start working on another part of the results. BSF function uses the adjacency matrix of A (Fig. 2).

The function used with C / C++ syntax is given in listing 2 [1, 6, 7]. Further studies have been made on the application of algorithms "DFS - Depth-First-Search" and Dijkstra's algorithm for finding minimum paths in a graph.

#### Listing 2:

```

#define MAXN 300
unsigned n; //counting the nodes of graph
unsigned v=1; //starting node for searching
void BSF (unsigned i){ //the function is called with BSF (v-1)
    unsigned k, j, p, queue[MAXN], currentVert, LevelVertex,
    queueEnd;
    for (k=0; k<n; k++)
        queue [k] = 0;
    for (k=0; k<n; k++)
        used [k] = 0 ;
    queue [0] = i ;
    ...
}

```

```

used [i] = 1 ;
currentVert = 0 ;
levelVertex = 1 ;
queueEnd = 1 ;
while ( currentVert < queueEnd ) {
for ( p = currentVert; p < levelVertex; p++ ) {
printf ("%ou", queue[p] + 1)
currentVert ++ ;
for ( j=0; j<n; j++ )
if( A[queue[p][j] && !used[j] ) {
queue [queueEnd++] = j ;
used[j] = 1 ;
}
printf ("\n");
levelVertex = queueEnd ;
}

```

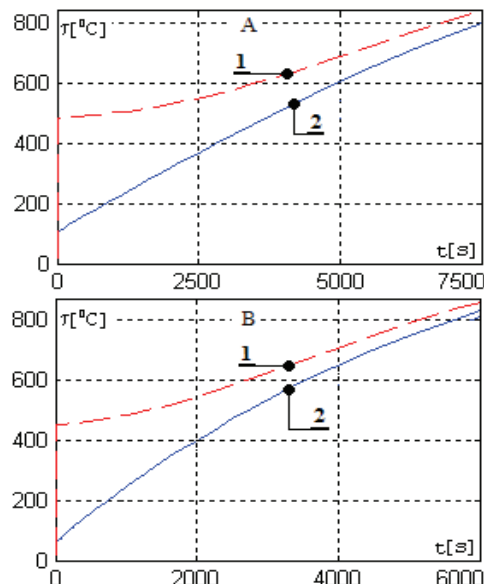


*Fig.5. Transient process of heating of ERF before (A) and after reconstruction of insulation (B) dimensioned with the proposed optimization procedure. 1 - temperature of the heater, 2 - the surface temperature of the load.*

Experimental studies have been made for the reconstructing middle- temperature ERF with installed capacity of 120kW. The reconstruction consists of replacement of heat-insulation. The new layer of the insulation is designed with the exposed procedure with the objective function - minimal losses. Fig. 5 shows the results before reconstruction. The operating temperature of 800°C of the surface of heated load (Figure 2) is achieved in approximately 7500 sec (2h). After designing of the furnace with the proposed optimization procedure (fig.5.B) at the same installed capacity, operating temperature is reached approximately 5500 sec. due to reduced losses. The furnace consumes about 34 kW/ h less per cycle. The example shown in Figure 5 is optimized with objective function- minimum losses, but the described methodology is applicable with objective functions- minimum mass, volume and price. In those cases the database must contain and price lists of materials. For practical purposes complete software for design of electro-thermal equipment is designed.

#### IV. CONCLUSION

The optimization algorithm „backtracking” and the processing results with *BFS – Breath-First-Search* can be applied for optimization of ERF. The correct work of algorithm requires large database for fire- proof and heat-insulating materials.

#### ACKNOWLEDGEMENT

This paper is developed in the frames of project “Improving energy efficiency and optimization of electro technological processes and devices”, № MY03/163 financed by the National Science Fund.

#### REFERENCES

- [1] L. Ameral, *Algorithms and Data Structures in C + +.*, Sofia 2001.
- [2] B. Dimitrov, Hr. Tahirilov, G. Nikolov, “Study and analysis of optimization approaches for insulation of an industrial grade furnace with electrical resistance heaters” XLVII International scientific conference on information, communication and energy systems and technologies, ICEST 2012, Veliko Tarnovo 2012.
- [3] B. Dimitrov B., Hr. Tahirilov, A. Marinov, “Improving energy efficiency of industrial grade furnaces with electrical resistance heaters and comparative model-experiment analysis” XLVII International scientific conference on information, communication and energy systems and technologies, ICEST 2012, Veliko Tarnovo, 2012.
- [4] B. Dimitrov, “Analysis of the calculation process, a mathematical model of the electric resistance”. Magazine Electrical and Electronics E + E, no.11-12, pp 78-83, 2006
- [5] B. Dimitrov, Hr. Tahirilov, “Comparison of numerical methods for solving transient resistance in the electric furnace”. Magazine Electrical and Electronics E + E, no. 5-6, pp 26-31, 2005.
- [6] J.Liberty , *C++ Unleashed* Sams, 1999.
- [7] P. Nakov, P. Dobrikov, *Programming C++ algorithms*, Sofia 2003.
- [8] Hr. Tahirilov, B. Dimitrov, *Design, modeling and optimization of electric resistance furnaces*, TU-Varna 2009.
- [9] Floudas C., P. Pardalos, *Encyclopedia of optimization*, Springer 2009.
- [10] Hahn B., D. Valentine, *Essential Matlab for Engineers and Scientists*, Elsevier 2010.

# Heat-accumulation system powered by photovoltaic modules

Milena Goranova<sup>1</sup> and Bohos Aprahamian<sup>2</sup>

**Abstract –** In this study a heating system working with Glauber's salt as heat-accumulation material is proposed. That is powered by renewable source - roof type photovoltaic (PV) generator. A design methodology for the system: PV generator - low temperature printed circuit board (PCB) heater - container with heat-accumulation material is proposed. A direct link between the generator and the heaters is used, since the characteristics of the system allow maximum use of the source. A complete laboratory experimental model, used for space heating, is presented.

**Keywords** – heat-accumulation, Glauber's salt, photovoltaic, PCB heater, Phase Change Materials - PCMs.

## I. INTRODUCTION

The properties of the materials with low melting temperature (so called Phase Change Materials - PCMs) and their application in the heating (or cooling) systems are a subject of concern in many research papers and patents [1, 2, 6, 7, 8, 9, 10]. The proposed systems in these sources are mainly based on direct use of solar radiation. Under the solar radiation impact the PCM reaches his melting temperature and some amount of heat is accumulated in it. Giving her through the night is used for space heating. Thus is used to build the passive houses (or so called solar houses) and new technologies for heating and insulation have been developed. The studied heating systems are designed and built for the construction of the buildings, as part of the premises. PCM is subjected to sunlight or a complex system of heat exchangers is used. This approach complicates the use of such systems in existing buildings which are not in accordance with the modern requirements for use of renewable energy. The aim of the paper is to propose a heating system operating through photovoltaic (PV) generator and low temperature printed circuit board (PCB) heaters. In this way the heating of PCM's heat storage material is not using solar radiation, but the electric power from a PV generator. Thus allows the use of the heating systems in existing buildings, without having their full reconstruction.

## II. ANALYSIS

To solve the task is designed, constructed and experimentally studied heat storage system with the following key elements:

- Steel, hermetically sealed containers with a parallelepiped shape (Figure 1., position 1) in which is placed the used PCM. In this case it is sodium sulfate decahydrate (Glauber's salt -  $\text{Na}_2\text{SO}_4 \cdot 10\text{H}_2\text{O}$ ).
- Flat, low PCB heaters located on the widest part of the container.
- Among these, a heat-conducting electrically insulating material is used, which is not shown in the figure.
- Roof type PV generators (Figure 2), with different structure and wiring scheme.

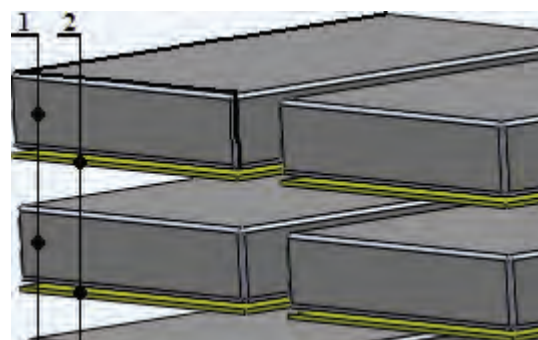


Figure 1. Construction of the heat storage system; 1 - containers with Glauber's salt; 2 - PCB heaters.

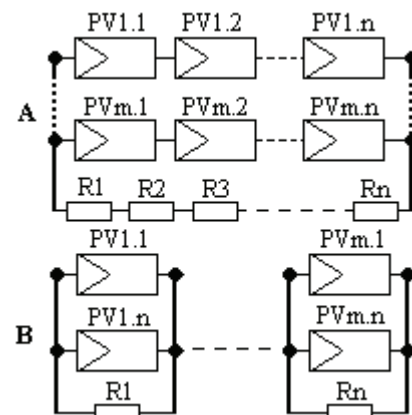


Figure 2. Wiring diagrams of the PV generators and heaters.

The direct connection between the heater and generator allows not to use converter, the goal is to obtain a low-cost system with fast payback. This requires the complex of parameters of the PV-PCB system to be dimensioned so as to ensure the maximum voltage and current, respectively, the maximum temperature of the heater with full power of the generator.

The steps in the design of the system are related to the dimensioning of his main three parts.

<sup>1</sup> Milena Goranova, PhD student, Technical University of Varna, Bulgaria, e-mail: milenagoranova@email.bg

<sup>2</sup> Bohos Aprahamian, Assoc. Professor, Technical University of Varna, Bulgaria, e-mail: bohos@abv.bg

### A. Basic equations in the design of the heat storage system

The thermal energy stored in the Glauber's salt is determined by its specific heat capacity  $c_g$ , its mass  $m_g$  and its initial  $\tau_o$  and final  $\tau_n$  temperatures :

$$Q_{Gsalt} = c_g \cdot m_g (\tau_n - \tau_o) = C_g \cdot \theta \quad (1)$$

where:

$C_g$  - heat capacity;  $\theta$  - temperature difference.

The heat storage system is effective when it reaches full melting of the salt.

This allows storage of the latent heat  $c_{gl}$  of the molten salt.

The stored energy  $Q_{Gsalt2}$  in the melting process is expressed by the equation (2):

$$Q_{Gsalt2} = C_g \cdot \theta + m_g \cdot c_{gl} \quad (2)$$

The energy  $Q_{Gsalt2}$ , the heating time  $t_n$  and the installed power of the heaters  $P_n$  are bound by the equation:

$$P_n = \frac{Q_{Gsalt2}}{t_n} \quad (3)$$

The needed energy  $Q_{Gsalt2}$  have to comply with the volume of heated space.

The heating time  $t_n$  is averaged over time to daylight for a specific location.

The main characteristics of the Glauber's salt applied for determination of the parameters of the heating system are shown in Table 1.

TABLE I

MAIN CHARACTERISTICS OF THE GLAUBER'S SALT -  $\text{Na}_2\text{SO}_4 \cdot 10\text{H}_2\text{O}$

Molar mass	322,2 g/mol
Density	1,464 g/cm <sup>3</sup>
Melting point	32,38 oC
Heat of fusion	254 kJ/kg 377 MJ/m <sup>3</sup>
Thermal conductivity	0.544 W/m.K

### B. Design of the PCB heaters

In the designing of the system we must take into account that the room is heated and during the melting period of the salt, through the heat transfer from the surface of the containers.

Both processes require enough installed capacity, which determines the total power of the heaters.

In this case, as an initial approximation, the resulting output of equation (3) is doubled.

The designing of the heaters was made according to [3.5] which deals with direct connection in the system PV generator – foil PCB heater.

The maximum temperature of the heater is 70oC to correspond to the temperature range of the systems with direct solar heating.

### C. Designing of the PV generator

In the experimentally studied model, the generator is roof type, filled with modules of several architectures: mono-and polycrystalline, thin film.

The basic equations necessary for designing the PV generator are as follows [4]:

Minimum nominal voltage:

$$U_{\min(\tau T)} = U_{\text{mpp(stc)}} + (T_u \cdot (\tau_T - \tau_{STC})) \quad (4)$$

where:

$\tau_T$  – temperature for calculations (module's temperature);

$\tau_{STC}$  – temperature of the module under standard testing conditions (25oC);

$U_{\text{mpp(stc)}}$  – voltage at maximum power for standard testing conditions;

$T_u$  – temperature coefficient of the voltage.

Maximum nominal voltage:

$$U_{\max(\tau T)} = U_{\text{mpp(stc)}} + (T_u \cdot (\tau_T - \tau_{STC})) \quad (5)$$

Maximum nominal current

$$I_{\max(\tau T)} = I_{\text{mpp(stc)}} + (T_i \cdot (\tau_T - \tau_{STC})) \quad (6)$$

where:

$I_{\text{mpp(stc)}}$  – nominal current at standard testing conditions;

$T_i$  – temperature coefficient of the current.

The described equations are specifying the structure of the generator: the number of series-connected modules in the string (PV1.1, PV1.2 ... PV1.n) and the number of strings in parallel.

Depending on the characteristics of the system it is possible that all the heaters can be connected in series (Figure 2. A) or each can be fed separately (Figure 2. B).

## III. EXPERIMENTAL DATA

The experiments were conducted using experimental model applied to heat the living space. The measurements were made during the winter season 2012-2013 at ambient temperature - 10C to +50C.

Figure 3 shows the process of heating of the salt, as measured by a thermocouple placed in the container. The experimental model reaches the temperature of the salt melt for approximately 2 hours. The melting process continued for 5 hours at a maximum power of the PV generator. After the complete melting of the salt the temperature should increase. In this the molten salt is overheated, but as this process takes

place in the late hours of the day at a small power of the generator, the overheating is not dangerous.

The cooling process of the molten salt is shown in Figure 4, graph 1. In order to compare, the same figure shows a typical cooling curve of material, in which no phase transition is reached, for example, water.

Figure 5 shows a record of the received power for several days. The group of curves in the sector 1 indicates days, which give a complete fusion of the salt. In curve 2 the resulting capacity is insufficient and the heating system works inefficiently.

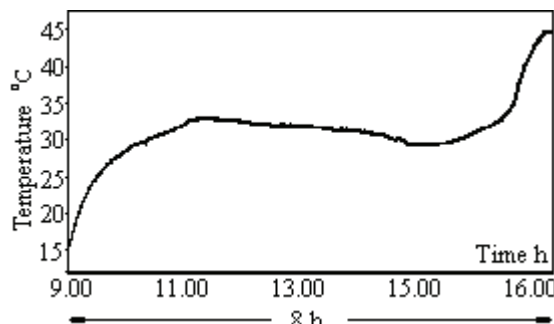


Figure 3. Transient heating process of the salt

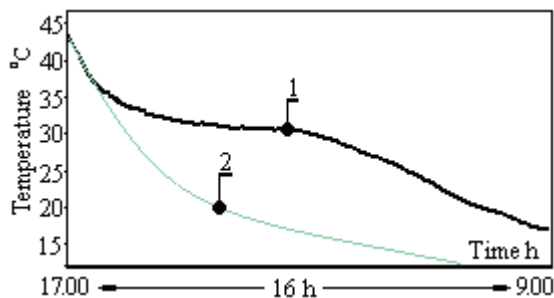


Figure 4. Transient cooling process:  
1 - Glauber's salt; 2 - water.

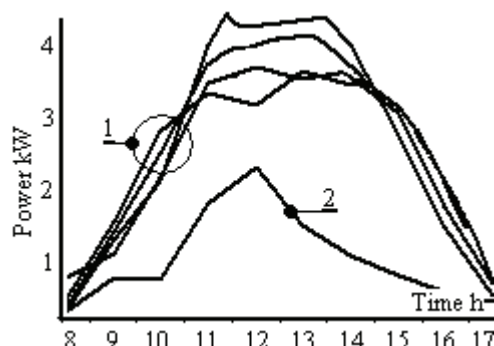


Figure 5. Power of the installed PV generator as a function of time of day

Figure 6 presents photo taken with IR camera of the heating system. The following positions are indicated: 1 - metal containers with Glauber's salt, 2 - PCB heater placed between the containers, 3 - electrically insulating, thermally conductive mica. The proposed construction allows uniform heating of the salt and achievement of the smelting process in the whole volume.

This is confirmed by the photo of Figure 7. A - temperature distribution on the surface of a heater placed on the containers.

The geometrical dimensions of the system container - heater are analyzed by the finite element method and simulation procedure.

Additional experiments were performed with a container in a cylindrical form and cylindrical (round) heaters, completely immersed in the salt.

The result is shown in Figure 6. B - during the heating the temperature is greatly unevenly distributed.

The volume around the heater overheats and melts, the remainder is cold, which is due to the low thermal conductivity of the salt.

#### IV. CONCLUSION

The studied heating system should reach full melting of the salt (Figure 3), in which the energy is accumulated according to equation (2).

As a result of the phase transition is obtained the cooling curve (Figure 4, graph 1), wherein the heating process is more efficient compared to the materials without a phase transition (Figure 4, graph 2).

The fundamental equations (1) - (6), and the studies in [3,5] allow the system PCB heater - PV generator to be designed so as to provide the desired temperature control of the heating.

The direct connection of the heaters and the generator without using converter reduces the investment cost and is shortening the repayment of the system.

On the other hand a converter would be useful as a voltage-adding power system through which shortages of power of the PV generator can be compensated (Figure 5, graph 2). The choice of using it complies with the specific requirements.

The system operates in a more stable connection to the scheme on Figure 1.B. as it is less dependent on the shading, contamination of the modules, changing the resistance of the heating element during the operation, etc.

The problem with this circuit is linked to the difficult wiring and therefore is used as a priority the scheme of Figure 1. A.

The proposed design ensures uniform heating of salt by uniform field across the PCB heater – Figure 7. A. Furthermore, the containers of parallelepiped shape can be mounted on the walls of the room without the loss of the space therein. The cylindrical structure of Figure 7. B. is not recommended.

#### ACKNOWLEDGEMENT

This research is realized in the frames of the project BG051PO001-3.3.06-0005, Program ‘Human Resources Development’

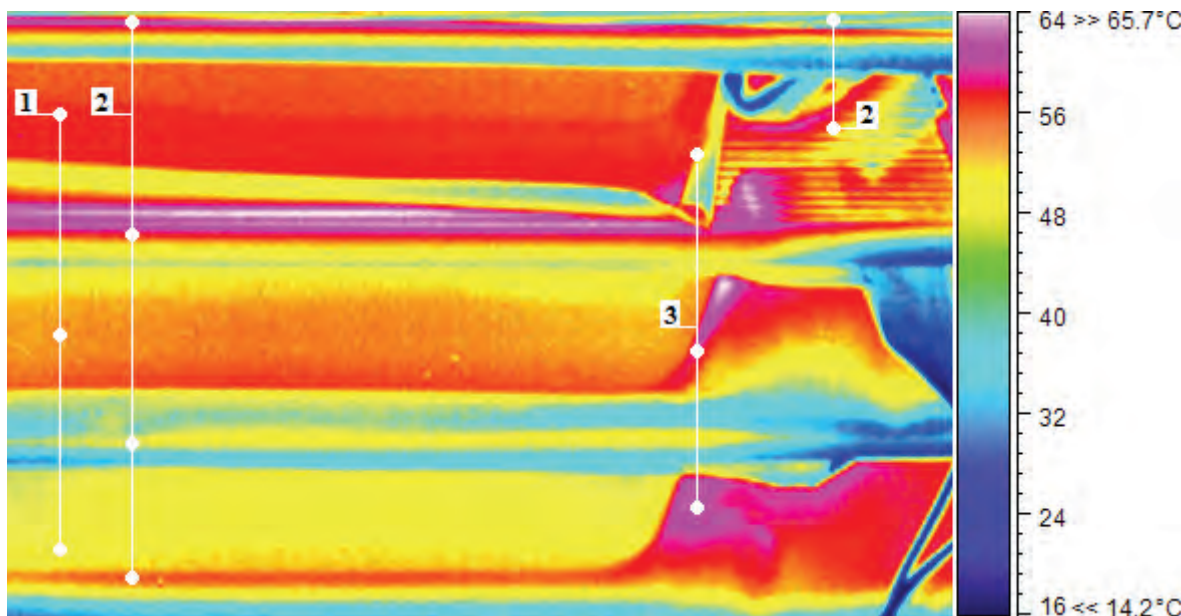


Figure 6. Photo of the heat storage system made with IR camera:  
1 - containers with Glauber's salt, 2 - flat PCB heater, 3 - electrical insulation.

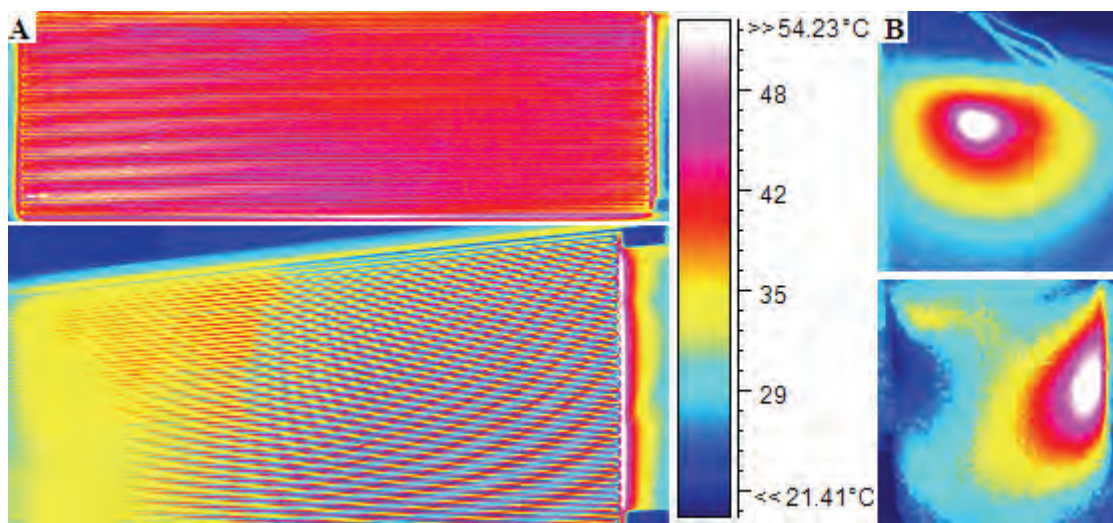


Figure 7. Photos with IR camera of: A - the temperature distribution on the surface of the PCB heating elements;  
B - cylindrical container with Glauber's salt, heated with cartridge heater.

## REFERENCES

- [1] Bruno F. Using phase change materials (pcms) for space heating and cooling in buildings. EcoLibrium 2005 pages 26-31.
- [2] Chadwick, Duane G. and Sherwood, Kim H., "Design Considerations in the Use of Glauber Salt for Energy Storage" (1981). Reports.Paper 566.
- [3] Dimitrov B., Hr. Tahirilov Autonomous PV heating system with foil heaters. ICEST 2010, Ohrid, Macedonia pages 891-895
- [4] Dimitrov B., Hr. Tahirilov Optimal distribution of PV modules according to dynamic optimization methods. ICEST 2010 Conference, Ohrid, Macedonia pages 887-891
- [5] Dimitrov. B., Valchev V. Investigation of a low-temperature chamber with foil heaters, powered by photovoltaic modules. "Електротехника и електроника Е+Е" 5-6 2011, стр. 8-14.

- [6] Sharma A, V. Tyagi b, C Chen, D. Buddhi, Review on thermal energy storage with phase change materials and applications. Renewable and Sustainable Energy Reviews 13 (2009) 318–345
- [7] Rozanna, D, Salmiah A, Chuah, T G, Medyan R, Thomas Choong S Y, Sa'ari M. A study on thermal characteristics of phase change material (PCM) in gypsum board for building application. Journal of Oil Palm Research Vol.17 2005, p.41-46
- [8] Farid M., Khudhair A., Razack S., Hallaj S. A review on phase change energy storage: materials and applications. Energy Conversion and Management 45, 2004, p.1597–1615
- [9] Fernández I., C.J. Renedo, S. Pérez, J. Carcedo, M. Mañana. Advances in phase change materials for thermal solar power plants Quality. International Conference on Renewable Energies and Power Quality, ICREPQ'11, 2010
- [10] [http://digitalcommons.usu.edu/water\\_rep/566](http://digitalcommons.usu.edu/water_rep/566)

# Model Study of the Processes In Current Instrument Transformers For The Purposes of Relay Protection

Krum Gerasimov<sup>1</sup>, Mediha Hamza<sup>2</sup>, Margreta Vasileva<sup>3</sup>, and Anton Filipov<sup>4</sup>

**Abstract – Model Study of the Processes In Current Instrument Transformers (CIT) is presented in various literary sources. Model of the Current Instrument Transformers is developed in MATLAB. Problem in using of this model is that the required parameters are not catalog. The purpose of this paper is to determine the parameters needed for modelling of CIT in MATLAB based on the known catalog parameters and made measurements.**

**Keywords – Current Instrument Transformers (CIT), Model, power systems, relay protection.**

## I. INTRODUCTION

Normal operation of the equipment in power systems depends on the proper functioning of the control circuits and protection. It is essential to measure the regime parameters for relay protection, automation, commercial metering and others. There are different technical solutions for measuring of regime parameters. The most widespread are Current Instrument Transformers (CIT) in Bulgaria.

They are devices with nonlinear characteristics and to provide the required accuracy of the measurements has strict rules for their selection. From the work of instrument transformers depends not only the accuracy of measurements, but also the reliability and proper operation of relay protection and automation. The model of Current Instrument Transformer must accurately reflects the relationship between the primary and secondary current

Model Study of the Processes In Current Instrument Transformers is presented in various literary sources [1], [2].

Model of the Current Instrument Transformers is developed in MATLAB. Problem in using of this model is that there are not the required parameters in the catalogs of CIT.

The purpose of this paper is to determine the parameters needed for modeling of CIT in MATLAB based on the known catalog parameters and made measurements.

<sup>1</sup>Krum Gerasimov is with the Faculty of Electrical Power Engineering at Technical University of Varna, 1 Studentska, Varna 9000, Bulgaria, E-mail: k.gerasimov@tu-varna.bg.

<sup>2</sup>Mediha Hamza is with the Faculty of Electrical Power Engineering at Technical University of Varna, 1 Studentska, Varna 9000, Bulgaria, E-mail: mediha.hamza@tu-varna.bg.

<sup>3</sup>Margreta Vasileva is with the Faculty of Electrical Power Engineering at Technical University of Varna, 1 Studentska, Varna 9000, Bulgaria, E-mail: m.vasileva@tu-varna.bg.

<sup>4</sup>Anton Filipov is with the Faculty of Electrical Power Engineering at Technical University of Varna, 1 Studentska, Varna 9000, Bulgaria, E-mail: filipov@tu-varna.bg.

## II. PREPARATION OF THE INFORMATION FOR THE MODEL

The paper is designed in two sections. The first section relates to the preparation of the information for the model based on the known catalog parameters and measurements. The second section presents the results of the model study of a particular CIT.

Catalogue information about CIT are nominal currents of primary and secondary coil ( $I_{1n}$ ,  $I_{2n}$ ) nominal voltage ( $U_n$ ), nominal secondary power ( $S_{2n}$ ), accuracy class, and the coefficients of dynamic and thermal sustainability.

CIT model in MATLAB requires a knowledge of: nominal power ( $S_n$ ), VA; nominal frequency  $f_n$ , Hz; primary and secondary winding voltages ( $U_1$ ,  $U_2$ ), V; active resistance ( $R_1$ ,  $R_2$ ) and inductance ( $L_1$ ,  $L_2$ ) of the primary and secondary winding, pu; active component of magnetization resistance ( $R_m$ ), pu and magnetization characteristic  $i_\mu^*(n)=f(\Psi^*(n))$ .

Algorithm to determine the required input parameters of CIT is as follows:

1) Determination of the nominal power  $S_n$

$$S_n = S_{2n}, \text{ VA} \quad (1)$$

2) Determination of the nominal frequency  $f_n$

$$f_n = 50\text{Hz} \quad (2)$$

3) Determination of  $U_2$  and  $U_1$

$$U_2 = \frac{S_{2n}}{I_{2n}}, \text{ V} \quad U_1 = \frac{U_2}{K_{CIT}}, \text{ V} \quad (3)$$

$$K_{CIT} = \frac{I_{1n}}{I_{2n}}, \text{ V} - \text{ coefficient of transformation}$$

4) Determination of R and L of the windings [3]

The active resistance  $R_2$  is determined by the experience of a short circuit when supplied with DC voltage and short circuit impedance  $Z_k$ , when supplied with power frequency voltage.

$$Z_{k^*(n)} = \frac{Z_k}{Z_{b2}} \quad Z_{b2} = Z_{2n} \frac{Z_{2n}}{Z_{2n}^2} \quad (4)$$

$$R_{2win^*(n)} = \frac{R_{2win}}{Z_{b2}} \quad R_{2win^*(n)} = \frac{R_{2win}}{Z_{b2}}$$

$$Z_{2win^{*(n)}} = \frac{\sqrt{Z_{k^{*(n)}}^2 - 4R_{2win^{*(n)}}^2}}{2}$$

$$X_{1win^{*(n)}} = X_{2win^{*(n)}} = L_{1win^{*(n)}} = L_{2win^{*(n)}}$$

5) Determination of  $R_m$

$$R_{m^{*(n)}} = \frac{100}{\text{accuracy class}} \quad (5)$$

6) Determination of magnetization characteristic

$$I_{\mu^{*(n)}} = f(\psi_{*(n)}) \quad (6)$$

The magnetization characteristic most frequently is asked in the form  $B = f(H)$  ( $B$ -magnetic induction;  $H$ -magnetic field).

The following dependencies are used to obtain the required description of the model:

$$i_{\mu^{*(n)}} = \frac{l_m}{w_1 I_{ln}} \cdot H \quad (7)$$

$$\psi_{*(n)} = \frac{w_1 S}{\psi_{b1}} \cdot B \quad \psi_{b1} = \frac{\sqrt{2U_1}}{\omega} \quad (8)$$

$l_m$  - average length of the magnetic line, m;  $W_1, W_2$  - number of turns of the primary and secondary windings;  $S$  - cross section of the magnetic core,  $m^2$ ;  $\omega$  - frequency, rad.

### III. RESULTS OF THE MODEL STUDY OF A PARTICULAR CIT

The following cases are investigated: normal operation; switching the breaker  $Q1$  at 0.02 seconds from the beginning of the simulation (the presence of the aperiodic component); three phase short-circuit (current is shown for one of the faulty phase); open secondary winding.

Change of the regime parameters is shown for the investigated cases: primary and secondary current; magnetic flux, magnetizing current; coefficient of transformation and voltage of the secondary winding. FIG. 2 shows the results obtained for normal operation. These results confirm the adequacy of the model.

The results for the other examined situations are shown in FIG. 3 - Fig. 5.

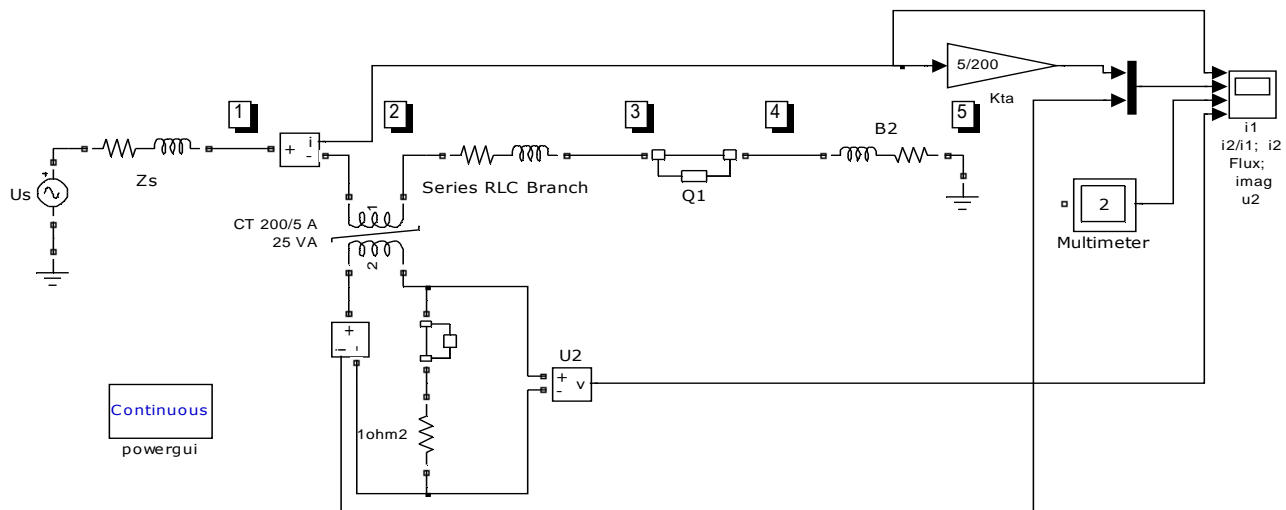


Fig. 1. Shows the model of research CIT, type TKC 200/5.

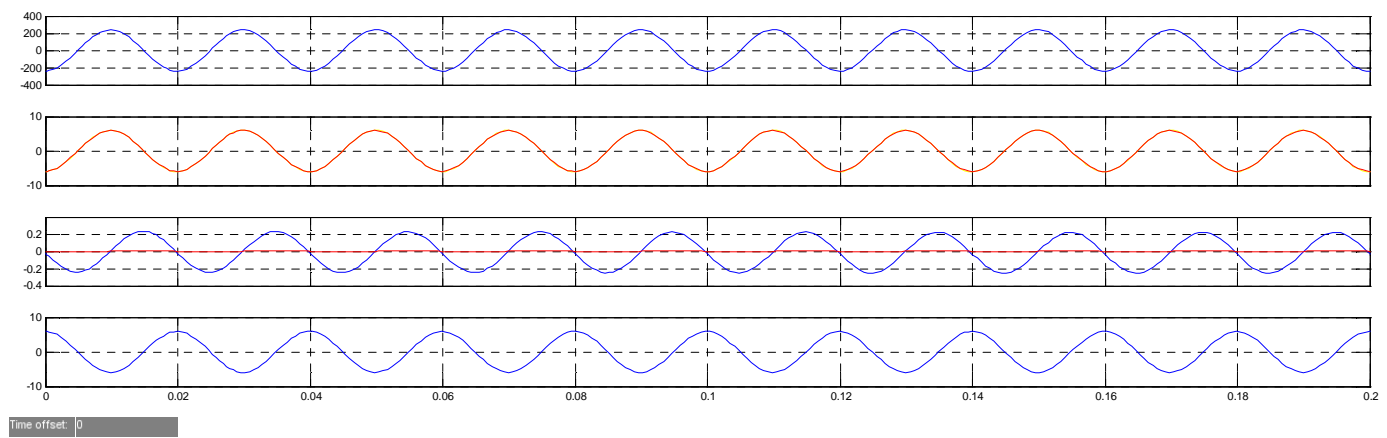


Fig. 2 Primary current (a); coefficient of transformation and secondary current (b); magnetic flux and magnetizing current (c); voltage of the secondary winding (d) for normal operation.

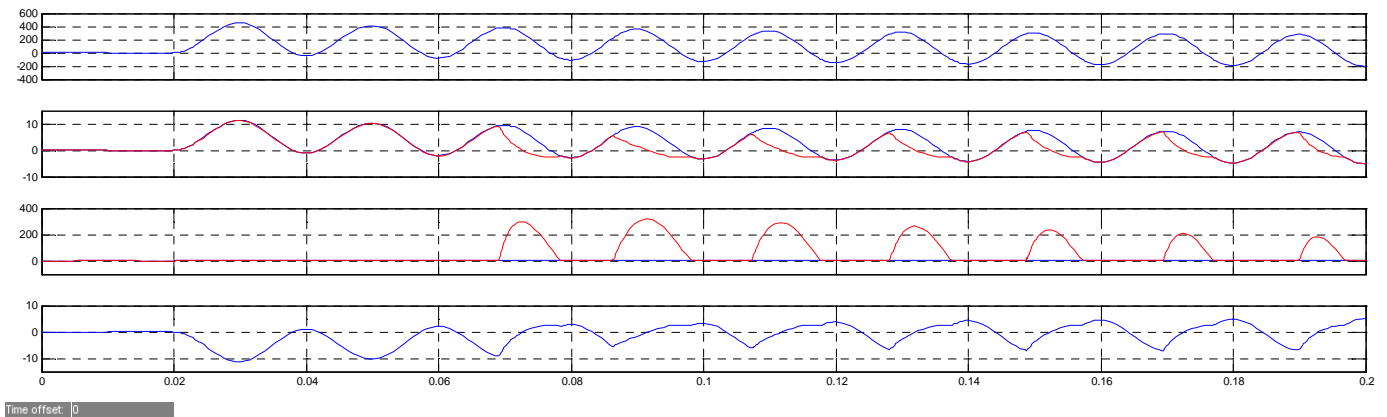


Fig. 3 Primary current (a); coefficient of transformation and secondary current (b); magnetic flux and magnetizing current (c); voltage of the secondary winding (d) on the presence of the aperiodic component.

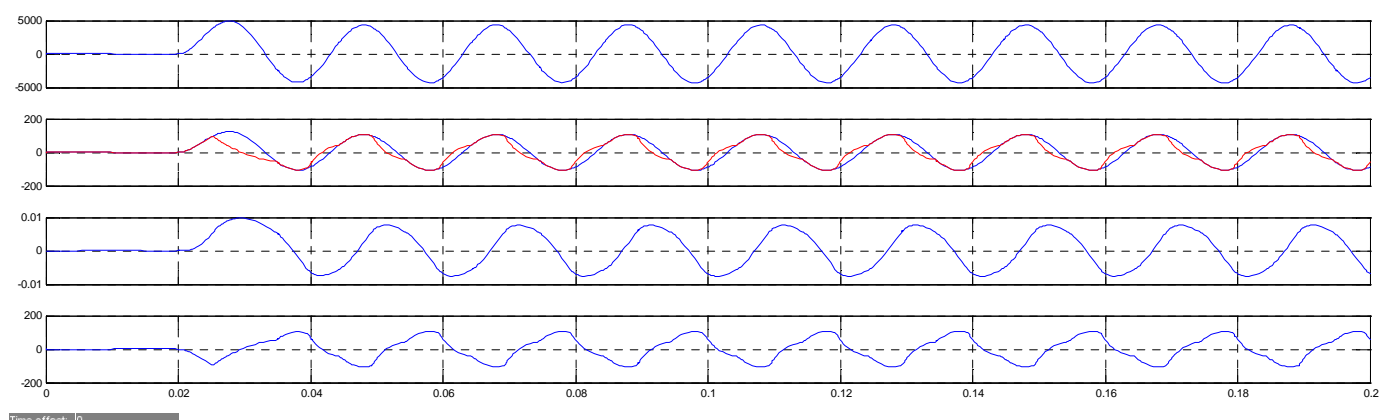


Fig. 4 Primary current (a); coefficient of transformation and secondary current (b); magnetic flux and magnetizing current (c); voltage of the secondary winding (d) on two phase short-circuit.

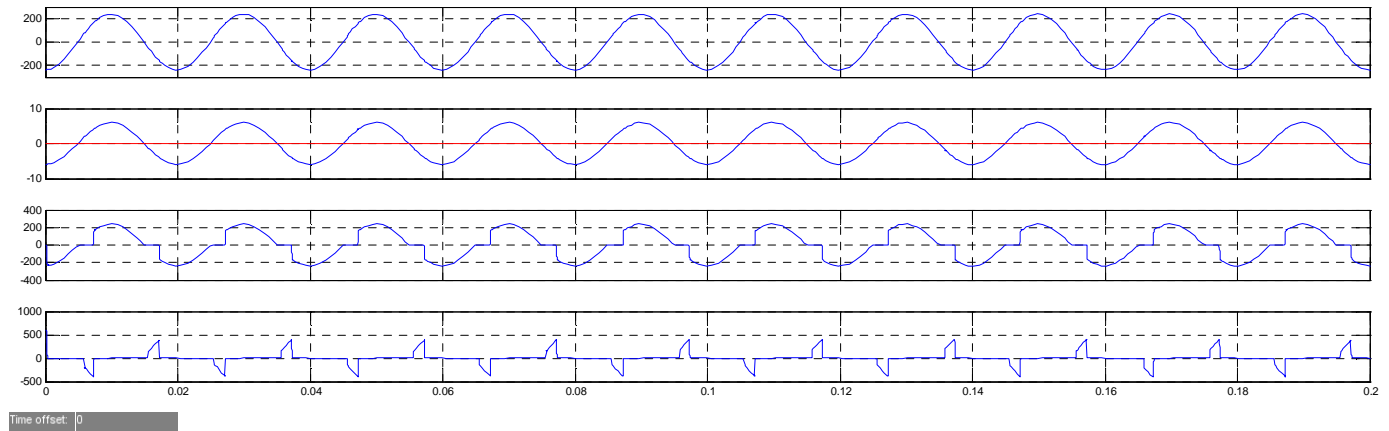


Fig.5 Primary current (a); coefficient of transformation and secondary current (b); magnetic flux and magnetizing current (c); voltage of the secondary winding (d) on open secondary winding.

#### IV. CONCLUSION

Based on the Model Investigation can be the following conclusions:

- 1) With the information available from catalogs and measurements can be obtained detailed model of CIT.
- 2) The adequacy of the created model are confirmed for the study regime parameters (Fig. 2 – Fig. 5).
- 3) Due to the presence of the aperiodic component can not obtain an accurate transformation of the current (Fig. 3).

The developed CIT model allows making a number of researches related to their work in different types of short-circuit for the purpose of relay protection.

#### REFERENCES

- [1] К. Герасимов, М. Василева, „Изчисляване на преходни режими в измервателни токови трансформатори”, сп. „Енергетика” бр.7, с. 34-37, 2006.
- [2] С. Минчев, „Математическо моделиране на измервателни трансформатори за електроенергийната система”, Дисертация, София, 2003.
- [3] К. Герасимов, Й. Каменов, „Моделиране в електроенергийните системи”, Варна, 2006.

#### ACKNOWLEDGEMENT

The carried out research is realized in the frames of the project, financed from the state budget “Investigation of processes in secondary circuits for control and protection”.

# Design of Photovoltaic plant for research purposes in University of Transport – Sofia

Ivan Milenov<sup>1</sup> and Vasil Dimitrov<sup>2</sup>

**Abstract –** The utilization of renewable energy sources is a means of achieving sustainable energy development. It minimizes the adverse impacts on the environment. In this paper, the use of solar energy is proposed. Different types of photovoltaic are widely used for direct conversion of the energy of sunlight into electricity.

**Keywords –** Photovoltaic System, Energy Efficiency.

## I. INTRODUCTION

The Sun is the largest fully renewable source of electricity production. The technology for direct conversion of sunlight into electricity is called photovoltaic (PV). It has rapidly developed in recent years. Photovoltaic systems are more widely used in civilian areas since the beginning of the 21<sup>st</sup> century. They offer environmentally friendly electricity production and reduce environmental pollution with the use of traditional methods for energy production [1, 2, 3]. The Solar PV system is a very reliable and clean source of electricity that can suit a wide range of applications such as residence, industry, agriculture, livestock, etc.

The basic components of the photovoltaic system are the PV modules. They change the solar energy into DC power that can be converted into AC power by an inverter. Then the power can be connected to the grid or used for AC load (appliances). Therefore, the photovoltaic systems could be divided into grid-connected systems, off-grid systems and hybrid systems.

The Solar PV systems include also many other components that should be selected according to the type of system, site location and applications. Backup batteries store unused at the moment electricity in order to supply electrical appliances when there is a demand. The solar charge controller regulates the voltage and the current coming from the PV panels and going to the battery. It prevents from battery overcharging and prolongs the battery life.

The Balance of system equipment (BOS) includes mounting systems and wiring systems used to integrate the solar modules into the structural and electrical systems of the building. The wiring systems include disconnects for the DC and AC sides of the inverter, ground-fault protection, and overcurrent protection for the solar modules. Meters providing indication of system performance could be also included in

the installation. Some meters can indicate energy usage.

The aim of this paper is to design a grid-connected PV system for converting solar energy into electricity using solar modules mounted on the roof of the building. Produced power will serve the domestic use of the laboratory “Renewable energy sources” in the “University of Transport” – Sofia. The design and construction of this PV installation will create possibilities of research and experiments by PhD students and teachers, as well as laboratory exercises with students in the programs of “Power Engineering and Electrical Equipment” and “Electric Vehicles”.

## II. SOLAR PV SYSTEM SIZING

The designs of a PV system include the determination of the size and orient the PV array to provide the expected electrical power and energy as well as selection of the other components of the solar installation.

### A. Determine power consumption demands

This solar PV system will be mainly used for experimental research and training of students. The selected power is 3 kW, because such solar plants are widely used in residential PV power systems. Lighting of the laboratory and the corridors of the building as well as computers and other low-power consumers will be the load of the system.

### B. Determine the PV modules output power

PV systems produce power in proportion to the intensity of sunlight striking the solar array surface. The intensity of light on a surface varies throughout a day, as well as day to day, so the actual output of a solar power system can vary substantially.

Most PV systems produce 55-to-110 Watts per square meter of array area. This is based on a variety of different technologies and the varying efficiency of different PV products. We dispose 32 solar modules Kaneka HB105, which will be installed on the roof. They are ideal for large-scale PV plants and open-space installations. They offer a higher initial power and achieve excellent efficiency in diffuse light. These modules generate energy even in low irradiation and are suitable for grid-connected systems and for heavy snow loads up to 2,400 Pa (2.4 kN/m<sup>2</sup>). Their technical data is given in Table 1 [6].

Solar modules produce DC electricity. The DC output of solar modules is rated by manufacturers under Standard Test Conditions (STC). These conditions are easily recreated in a factory, and allow for consistent comparisons of products, but need to be modified to estimate output under common outdoor

<sup>1</sup>Ivan Milenov is with Faculty of Communications and Electrical Equipment at the Todor Kableshkov University of Transport-Sofia, 158 Geo Milev Str., Sofia 1574, Bulgaria, E-mail: milenov55@abv.bg.

<sup>2</sup>Vasil Dimitrov is with Faculty of Communications and Electrical Equipment at the Todor Kableshkov University of Transport-Sofia, 158 Geo Milev Str., Sofia 1574, Bulgaria, E-mail: vdimitroff@abv.bg

TABLE I  
TECHNICAL DATA OF THE SOLAR MODULES KANEKA HB105

STC Power $P_{STC}$ ( $P_{max}$ )	105 Wp
STC Nominal Voltage $U_{mpp}$	53,5 V
STC Nominal Current	1,96 A
STC Open circuit voltage $U_{oc}$	71,0 V
STC Short circuit current $I_{sc}$	2,40 A
Power tolerance	+10%...-5%
Nominal Operating Cell Temperature (NOCT)	44°C
Ambient temperature (from ... to)	-25...60 °C
Temperature coefficient of $I_{sc}$	+0,1%/K
Temperature coefficient of $I_{sc}$	-0,248V/K
Temperature coefficient of $P_{max}$	-0,33%/K
Dimensions: 1210/1008/40 mm; Weight	18,0 kg

operating conditions. STC conditions are: solar cell temperature = 25°C; solar irradiance (intensity) = 1000 W/m<sup>2</sup> (often referred to as peak sunlight intensity, comparable to clear summer noon time intensity); and solar spectrum as filtered by passing through 1,5 thickness of atmosphere (Air mass AM=1,5). The modules Kaneka HB105 have a production tolerance of -5/+10% of the rating. It would be better to use the low end of the power output spectrum as a starting point (for example, 95 W for a "100-Watt module").

The module output power reduces as the module temperature increases [4]. When operating on a roof, a solar module will heat up substantially, reaching inner temperatures of 50-75°C. For crystalline modules, a typical temperature reduction factor ( $K_t$ ) is 89% in the middle of a spring or fall day, under full sunlight conditions.

Dirt and dust can accumulate on the solar module surface, blocking some of the sunlight and reducing the output. If the solar panels are regularly cleaned, a typical annual dust reduction factor ( $K_d$ ) to use is 90%.

The maximum power output of the total PV array is always less than the sum of the maximum output of the individual modules. This difference is a result of slight inconsistencies in performance from one module to the next and is called module mismatch and amounts to at least a 2% loss in system power. Power is also lost to resistance in the system wiring. These losses should be kept to a minimum but it is difficult to keep these losses below 3% for the system. A reasonable reduction factor for these losses ( $K_l$ ) is 95%.

The DC power generated by the solar module must be converted into AC power using an inverter, which could be connected to the electric power system. Some power is lost in the conversion process, and there are additional losses in the wires from the rooftop array down to the inverter. Modern inverters commonly used in residential PV power systems have peak efficiencies of 92-94% indicated by their manufacturers, but these again are measured under well-controlled factory conditions. Actual field conditions usually result in overall DC-to-AC conversion efficiencies  $\eta_{inv}$  of about 88-92%, with 90% a reasonable compromise.

So the module output has to be reduced by production tolerance ( $K_{pt}$ ), heat ( $K_{tc}$ ), dust ( $K_d$ ), AC conversion ( $\eta_{inv}$ ), wiring and other losses ( $K_l$ ). Therefore, the coefficient of the reduction  $K_{red}$  may be calculated by Eq. 1:

$$K_{red} = K_{pt} \cdot K_{tc} \cdot K_d \cdot \eta_{inv} \cdot K_l \quad (1)$$

After the calculation, the value of the  $K_{red}$  is 0,65.



Fig. 1. Roof mounted solar PV panels

So the rated power  $P_{STC}$  of one module  $P^I$  should be reduced by  $K_{red}$  and could be calculated by Eq. 2:

$$P^I = K_{red} \cdot P_{STC} = 0,65 \cdot P_{STC} \quad (2)$$

Therefore, the solar plant output power could be determined by Eq. 3:

$$P = n \cdot P^I = 32 \cdot 0,65 \cdot 105W = 2186W \approx 2,19kW \quad (3)$$

where n=32 is the number of the modules.

The PV array will be mounted above and parallel to the roof surface with a standoff of several centimeters for cooling purposes (Fig. 1) [8]. During the course of a day, the angle of sunlight striking the solar module will change, which will affect the power output. The output from the modules will rise from zero gradually during dawn hours, and increase with the sun angle to its peak output at midday, and then gradually decrease into the afternoon and back down to zero at night. While this variation is due in part to the changing intensity of the sun, the changing sun angle (relative to the modules) also has an effect. The pitch of the roof will affect the sun angle on the module surface, as well as the orientation of the roof.

If the module surface on a 32°-pitch roof faces due South in Sofia, the array will give the greatest output (correction factor  $K_o$  of 1.00). The South-West facing roof at a little bigger pitch would reduce the annual energy by 95% approximately (correction factor  $K_o$  of 0.95).

Annual energy production depends of the duration of solar radiation during different months of the year. According to the weather station the maximum sunshine throughout the year in Sofia is  $t_s=1993$  h [9, 10]. Thus the energy produced by the solar plant for 1 year may be calculated by Eq. 4:

$$E_y = P \cdot K_o \cdot t_s = 2,19kW \cdot 0,95 \cdot 1993 = 4146,5kWh \quad (4)$$

Dividing the total energy per year by 365 the average value of the produced solar energy for 1 day may be obtained:

$$E_d = 4146,5kWh / 365 \approx 11,4kWh \quad (5)$$

This energy will be sufficient to power the system load.

#### C. Inverter

The input rating of the inverter should never be lower than the total power of the load. The inverter must have the same nominal voltage as the battery. An IBC ServeMaster 3300MV inverter will be used in the solar installation. Its technical data is given in the Table 2 [7]. These inverters are innovative and ideal for small and medium photovoltaic systems. They are suitable for outdoor installation. Two individual DC inputs with separate MPP trackers are available. Maximum power point tracking (MPPT) is a technique that inverters use to get the maximum possible power from the solar PV panels. MPP trackers compensate for potential performance loss in partial shade or in the case of varying module alignments. The inverters are made by ride-through technology and tolerate voltage fluctuations that frequently occur in grids. They have very low standby and night consumption (8W and 0,2W respectively). A useful added benefit is the communications interface for system monitoring.

#### D. Battery

The battery type recommended for usage in the solar PV system is the deep cycle battery. The deep cycle battery is specifically designed in order to be discharged to low energy level and rapid recharged or cycle charged and discharged day after day for years. The battery should be large enough to store sufficient energy to power the load at nightfall and cloudy days.

The number of batteries depends on the inverter voltage.

8 pcs lead-acid 24-V batteries or 60 pcs lithium-ion cells will be used [5]. When they are fully charged, the voltage of the inverter input will be 202V approximately.

TABLE II  
TECHNICAL DATA OF THE INVERTER IBC SERVEMASTER 3300MV

Nominal DC power ( $P_{DC}$ )	3,6 kW
Nominal AC power ( $P_{AC}$ )	3,3 VA
Nominal input voltage ( $U_{DC}$ )	310 V
MPP-voltage	180-350 V
Max DC voltage – individual/parallel	450/410V
Output voltage range ( $U_{AC}$ )	230V $\pm$ 15%
AC frequency range ( $f$ )	(50 $\pm$ 5)Hz
Nominal DC current	5,8 A
Max DC current $I_{DC}$ (2 DC inputs)	2x10 A
Nominal AC current	14,5 A
Max. AC current	15,5 A
Max. efficiency / Euro efficiency	94,2/93,4%
Power factor at >20% load	0,97
Max THD (total harmonic distortion)	5
Max night consumption	0,2 W
Dimensions: 618/434/182 mm; Weight	20,0 kg
Interfaces	RS-485 modem

#### E. Solar charge controller

The charge controller limits the rate at which electric current is added to or drawn from electric batteries. It prevents from overcharging and may prevent against overvoltage, which can reduce battery performance or lifespan, and may pose a safety risk. It may also prevent completely draining ("deep discharging") a battery, or perform controlled discharges, depending on the battery technology, to protect battery life. Some controllers have a "PWM" mode. Pulse Width Modulation (PWM) is often used as one method of float charging. The controller constantly checks the state of the battery to determine the pulses frequency.

The selected solar charge controller has to match the voltage of PV array and batteries. The solar charge controller must also have enough capacity to handle the current from PV array. Thus the selection of the charge controller depends on PV panel configuration. The PV modules will be connected in series 4 and 8 parallel (4x8 configuration). According to standard practice, the sizing of solar charge controller is to take the short circuit current ( $I_{sc}$ ) of the PV array multiplied by 1.3. So the solar charge controller should be rated 26A at 200V or greater.

The scheme of the designed solar PV system is shown in Fig. 1. Measuring, safety and protective equipment are not represented, but they are also appropriately selected.

### III. EXPERIMENTAL RESEARCH

The conduct of research and training of the students require appropriate measuring equipment. Many ammeters, voltmeters and wattmeters are necessary. The efficiency of the solar PV system will be examined by them. The influence of the sun angle and radiation on the produced electricity, as well as the load changes on the AC voltage could be also studied.

Energy consumption meter will be used to indicate recuperated energy.

Using communication interface of the inverter the values of the all-important parameters could be exported to a computer and traced in real time:  $U_{DC}$ ,  $I_{DC}$ ,  $P_{DC}$ ,  $U_{AC}$ ,  $I_{AC}$ ,  $P_{AC}$ ,  $f$ ,  $t$  °C, Electricity (day, week, month, and year, as well as total).

The device status and faults could be displayed.

### IV. CONCLUSION

In this paper the design of a solar PV plant is made. This system will be used for research and training of the students. It will also reduce electricity costs. Produced energy will power the lighting and other low-voltage consumers.

The construction of the laboratory "Renewable energy sources" in the 'University of Transport' – Sofia will improve the quality of students education in this promising field. Possibilities of research will increase. The lecturers and PhD students will have the opportunity to set examinations on the solar PV system.

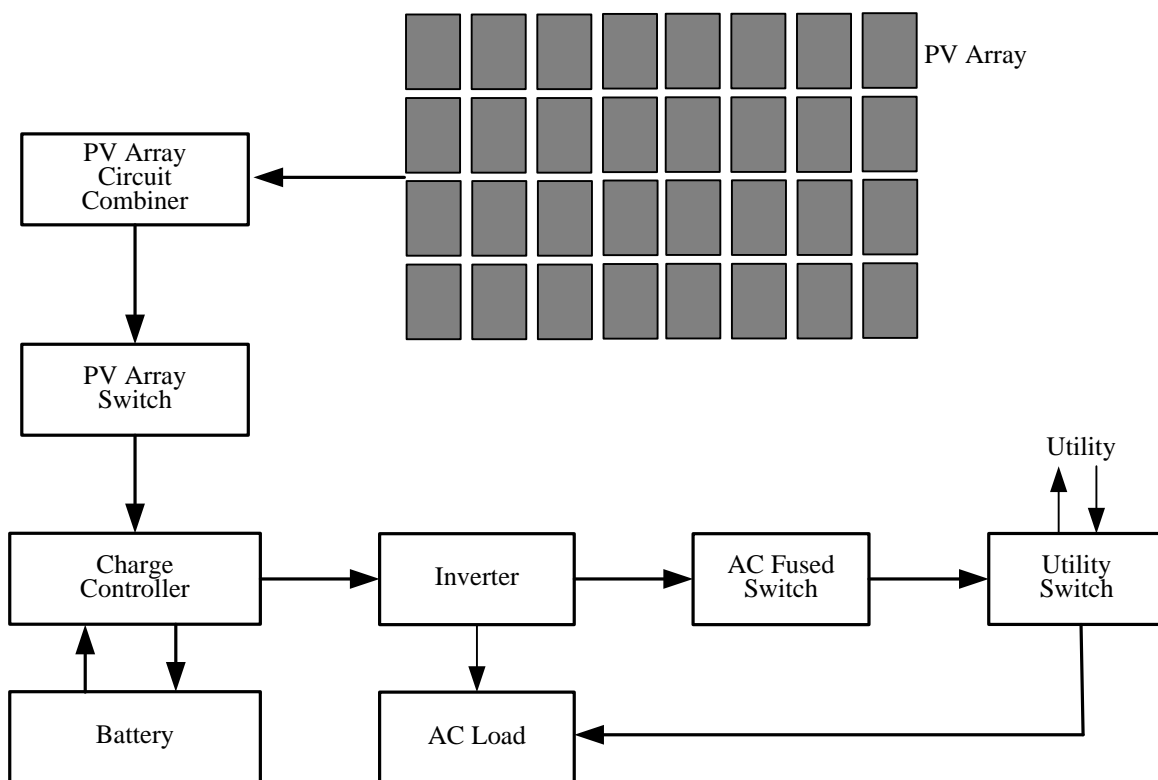


Fig. 2. Principle of operation of the designed solar PV system

## REFERENCES

- [1] Ю.Д. Сибиков, М.Ю. Сибиков, „Нетрадиционные и възобновляемые источники энергии“, Учебное пособие, Москва, Издательство КноРус, ISBN: 978-5-406-00378-0, 2010 г.
- [2] И. Евтимов, Р. Иванов, Г. Попов, „Възобновяеми енергийни източници“, Учебник, Русе, Издателство ПРИМАКС, ISBN: 978-954-8675-39-0, 2013 г.
- [3] Bent Soeser, „Renewable energy, Conversion, Transmission, and Storage“, Academic Press, ISBN 978-0-12-374262-9, 2007.
- [4] Aldo Vieira da Rosa, “Fundamentals of Renewable Energy Processes”, Second Edition, ISBN: 978-0-12-374639-9, 2009.
- [5] П. Пенев и др., “Използване на литиево-йонни елементи за изграждане на автономни захранващи източници и мерки за безопасност при експлоатацията им”, Научни трудове на РУ”Ангел Кънчев”, т.47, серия 9, 2008 г.
- [6] <http://bgsolar.com/>
- [7] <http://3k-solar.bg/>
- [8] [http://www.energy.ca.gov/reports/2001-09-04\\_500-01-020.PDF](http://www.energy.ca.gov/reports/2001-09-04_500-01-020.PDF)
- [9] <http://solargis.info/>
- [10] <http://www.emde-solar.com>

# Vector Analysis and Comparative Valuation of Precise and Approximate Non-Linear Models of Discrete Regulator with Reducing Input AC Voltage

Emil Panov<sup>1</sup>, Emil Barudov<sup>2</sup> and Stefan Barudov<sup>3</sup>

**Abstract –** The discrete regulation of AC voltages is used in many cases. Most often, it is achieved by power electronic converters, based on a transformer (autotransformer) and switching by the means of controllable semiconductor switches.

The present work is dedicated to the vector analysis and to the vector measurements in an autotransformer discrete voltage regulator, replaced by precise and approximate non-linear models with changing input voltage and commutation angle of the semiconductor switches.

**Keywords –** vector analysis, vector measurements, voltage regulator, semiconductor switch, thyristor

## I. INTRODUCTION

In Fig.1 the equivalent circuit of an autotransformer discrete AC voltage regulator (ADACVR) with four terminals and four controllable semiconductor switches (CSS) is shown. The equivalent circuit corresponds to the approximate model as the losses in the autotransformer core are not considered, the semiconductor switches are accepted for ideal and the RC groups, which shunt the thyristors in the semiconductor switches, are not taken into account. The adopted control algorithm is connected with switching at random moment as the commutation is always performed between two neighbouring semiconductor switches [1,2].

The feeding with control pulses is suspended to the thyristor switch, which will be turned off (the switch remains conductive until the natural commutation of the thyristors inside it), and the other switch starts to be fed with control pulses.

The equivalent circuit of the precise model and its mathematical description are presented in details in literature [3,4].

The aim of the current work is the comparative research into the loading (the semiconductor switches, the autotransformer windings) by vector analysis and vector measurements of the quantities during the commutation process at different character of the load – R, RL and RC and different commutation angles.

<sup>1</sup>Emil Panov (Assoc. Prof., PhD, Eng.) is with the Electrical Faculty at the Technical University of Varna, 1 Studentska str., Varna 9010, Bulgaria, e-mail: eipanov@yahoo.com.

<sup>2</sup>Emil Barudov (Assist. Prof., Eng.) is with the Electrical Faculty at the Technical University of Varna, 1 Studentska str., Varna 9010, Bulgaria, e-mail: ugl@abv.bg.

<sup>3</sup>Stefan Barudov (Prof., DSc, Eng.) is with the Engineering Faculty at the Naval Academy “N. Vaptsarov” Varna, 73 Vasil Drumev str., Varna 9026, Bulgaria e-mail: sbarudov@abv.bg.

## II. ANALYSIS

In this paper a vector analysis at low values of the input voltage of ADACVR is conducted. In this case, the switch K<sub>4</sub> is turned off and the switch K<sub>3</sub> is switched on (Fig.1).

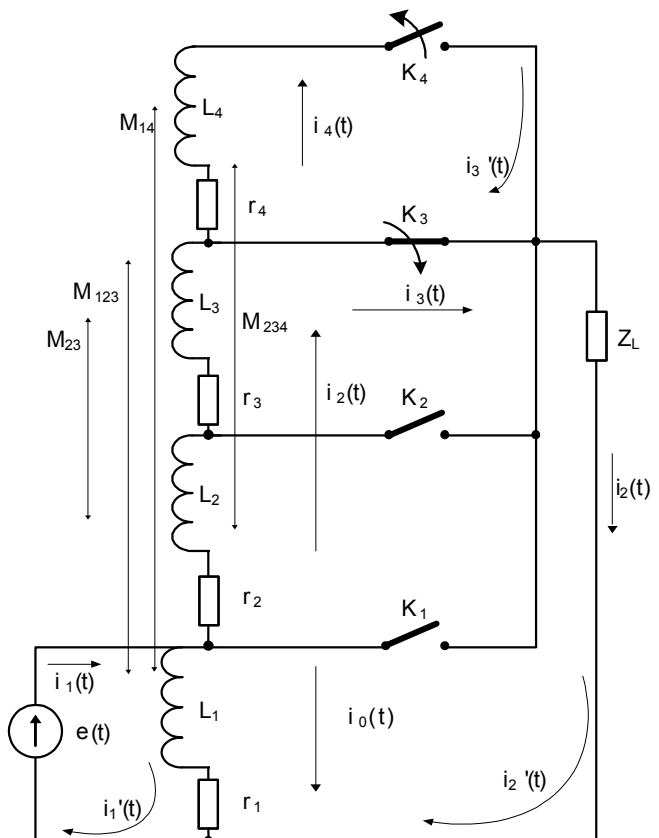
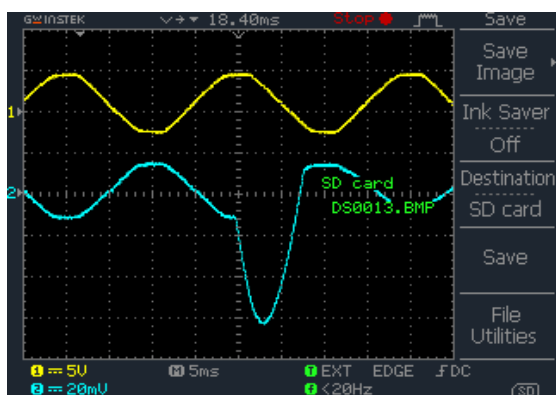
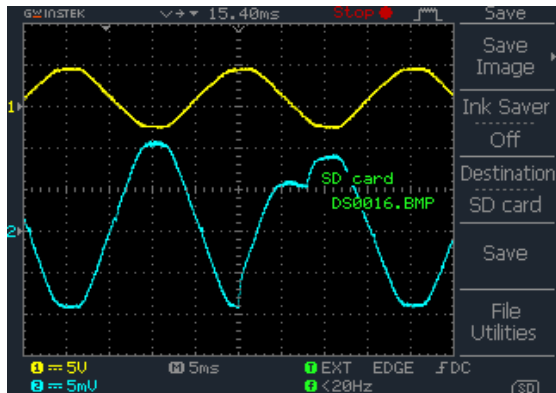


Fig.1. Equivalent circuit of an ADACVR with four CSS at input voltage change.

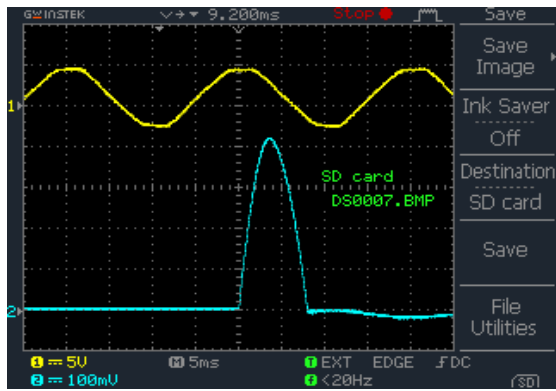
At the same time, at certain angles  $\varphi$  of the commutation process, it is possible  $r_4$  and  $L_4$  (Fig.1) to be connected in short circuit through two thyristors, one from the switch K<sub>4</sub> and one from the switch K<sub>3</sub> respectively, for the time until the natural commutation of the switch K<sub>4</sub> occurs. This mode assumes an overload regime of the fourth section of the autotransformer and the two connected in series thyristors from the switches K<sub>4</sub> and K<sub>3</sub>, when they are triggered.



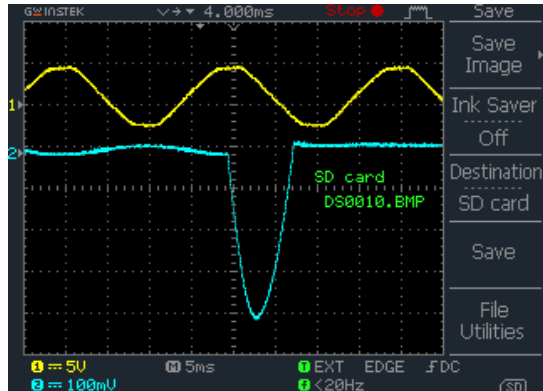
a) Oscillogram of the input current  $i_1(t)$  at  $\varphi=270^0$ .



b) Oscillogram of the output current  $i_2(t)$  at  $\varphi=270^0$ .

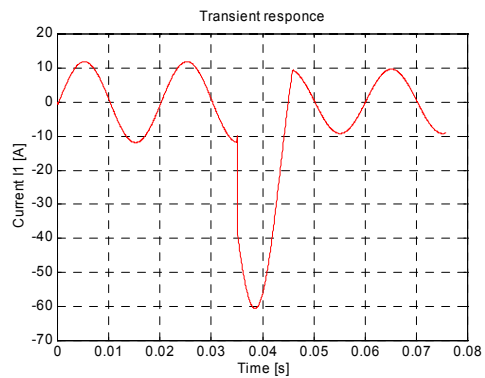


c) Oscillogram of the current through switch  $K_3$  -  $i_3(t)$  at  $\varphi=270^0$ .

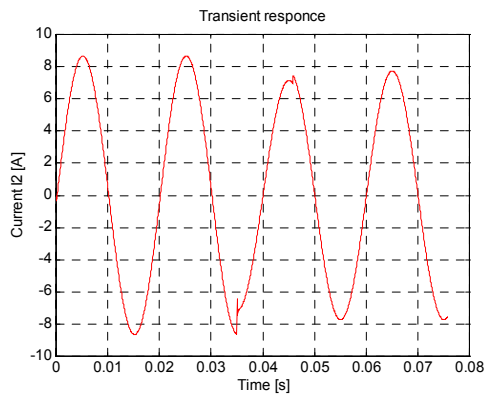


d) Oscillogram of the current through switch  $K_4$  -  $i_4(t)$  at  $\varphi=270^0$ .

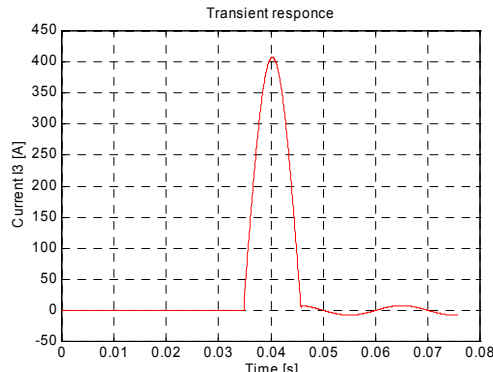
Fig.2. Experimental oscillograms of the currents of the ADACVR for R load and commutation angle  $\varphi=270^0$ .



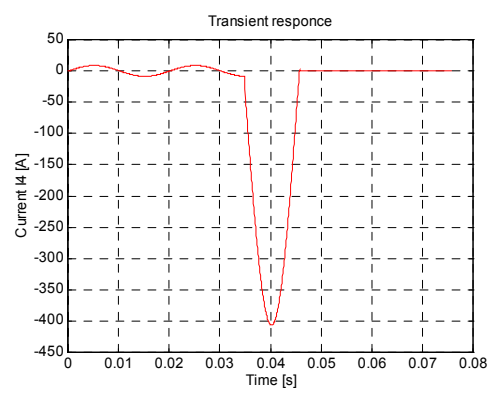
a) Simulation of the input current  $i_1(t)$  at  $\varphi=270^0$ .



b) Simulation of the output current  $i_2(t)$  at  $\varphi=270^0$ .

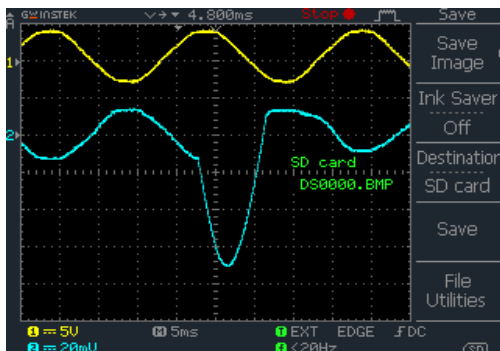


c) Simulation of the current through switch  $K_3$  -  $i_3(t)$  at  $\varphi=270^0$ .

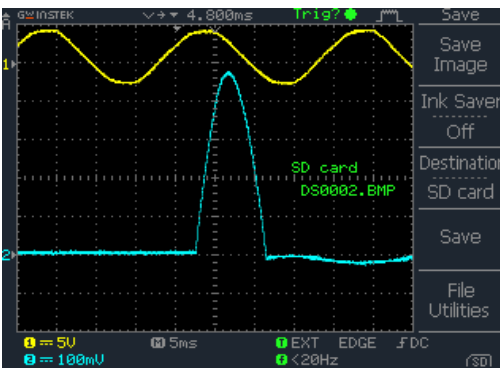


d) Simulation of the current through switch  $K_4$  -  $i_4(t)$  at  $\varphi=270^0$ .

Fig.3. Computer simulation of the currents of the ADACVR for R load and commutation angle  $\varphi=270^0$ .

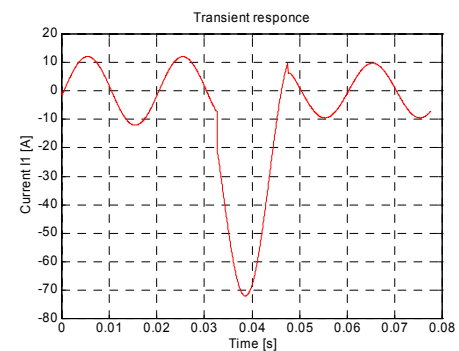


a) Oscillogram of the input current  $i_1(t)$  at  $\varphi=225^0$

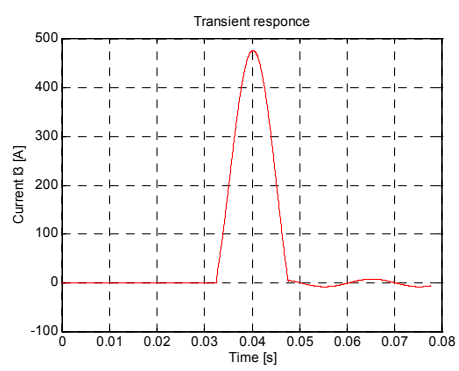


b) Oscillogram of the current through switch  $K_3 - i_3(t)$  at  $\varphi=225^0$ .

Fig.4. Experimental oscillograms of the currents of the ADACVR for RL load and commutation angle  $\varphi=225^0$ .

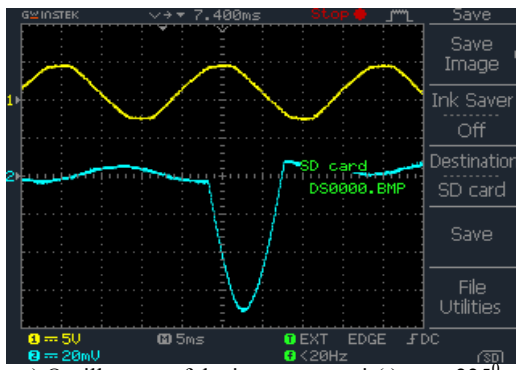


a) Simulation of the input current  $i_1(t)$  at  $\varphi=225^0$ .

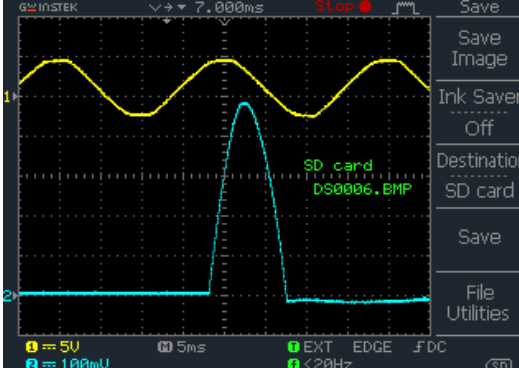


b) Simulation of the current through switch  $K_3 - i_3(t)$  at  $\varphi=225^0$ .

Fig.5. Computer simulation of the currents of the ADACVR for RL load and commutation angle  $\varphi=225^0$ .

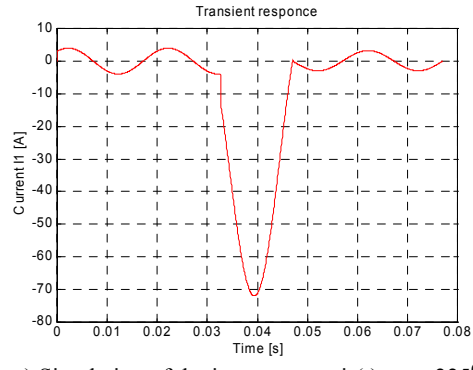


a) Oscillogram of the input current  $i_1(t)$  at  $\varphi=225^0$ .

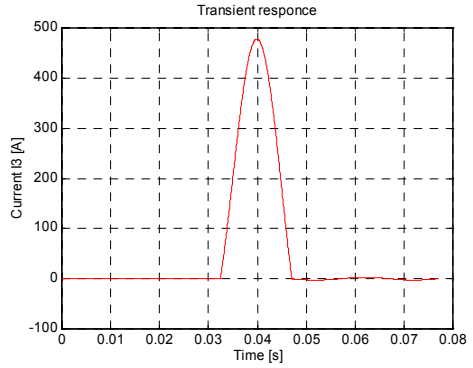


b) Oscillogram of the current through switch  $K_3 - i_3(t)$  at  $\varphi=225^0$ .

Fig.6. Experimental oscillograms of the currents of the ADACVR for RC load and commutation angle  $\varphi=225^0$ .



a) Simulation of the input current  $i_1(t)$  at  $\varphi=225^0$ .



b) Simulation of the current through switch  $K_3 - i_3(t)$  at  $\varphi=225^0$ .

Fig.7. Computer simulation of the currents of the ADACVR for RC load and commutation angle  $\varphi=225^0$ .

In case of an active load (R-load) and commutation angle  $\varphi=270^\circ$ , the results from the experimental oscillograms and the computer simulations with the programme AVTO in MATLAB integrated environment, are presented in Fig.2 and Fig.3. When we have RL and RC loads, the development of the commutation process can be followed in Fig.4 and Fig.5, Fig.6 and Fig.7 respectively. The experimental oscillograms and simulations are taken at commutation angle  $\varphi=225^\circ$ .

The received experimental data for a concrete regime (closed switch  $K_4$  and opened switch  $K_3$ ) are shown in Table 1. The analytical data in the table are very close to those from the analysis of the precise model [4,5,6]. The numerical values from the simulations with the approximate model of the voltage regulator differ with average deviation 0,9% (minimum deviation 0,07% and maximum deviation 2,83%) from those, received by a simulation with the precise model.

Table 1

<b>Load</b>	<b>Experimental data</b>			<b>Computer simulations</b>		
	I <sub>1</sub>	I <sub>2</sub>	U <sub>2</sub>	I <sub>1</sub>	I <sub>2</sub>	U <sub>2</sub>
	A	A	V	A	A	V
<b>R</b>	8,45	6,16	219	8,3965	6,1205	218,6
<b>RL</b>	9,75	7,03	219,9	8,5181	6,2016	217,8
<b>RC</b>	2,85	2,15	220,3	2,8034	2,1421	222,6

- Note: The loads for the experiments and the simulations, shown in the table, are as follows:

*R load* - 35,7Ω;

*RL load* - R-35,7Ω, L-1,76H (connected in parallel);

*RC load* - R-61,78Ω, C-38,09μF (connected in series).

In Table 2 the vector quantities of the currents and the voltages of the autotransformer discrete regulator from the equivalent circuit in Fig.1 are presented.

Table 2

<b>Load</b>	<b>Results from vector measurements</b>		
	$\dot{I}_1$	$\dot{I}_2$	$\dot{U}_2$
	A	A	V
<b>R</b>	$8,45e^{-j0,08}$	$6,16e^{-j0,06}$	219
<b>RL</b>	$9,75e^{-j0,14}$	$7,03e^{-j0,12}$	$219,9e^{j0,06}$
<b>RC</b>	$2,85e^{j0,89}$	$2,15e^{j0,92}$	$219e^{-j0,01}$

### III. CONCLUSION

A vector analysis and vector measurements of the quantities, referred to the commutation and the regimes in a power semiconductor converter with discrete regulation of the input AC voltage magnitude to the joined consumers have been conducted. A precise and approximate (with certain simplifications) models have been examined at different angles for the commutation process and for different loads.

Both results – from the experiments and from the computer simulations, show a very good match of the obtained results.

A programme AVTO in MATLAB is developed, and it allows visualization of the computer simulations as well as examination of the discrete AC voltage regulator with different loads and parameters of the commutation processes.

### ACKNOWLEDGEMENT

The presented results in the current paper are obtained under working at project NP1/2013 of the Technical University of Varna, Bulgaria, funded by the National Budget of Republic of Bulgaria.

### REFERENCES

- [1] Harlow James H., Transformers. The Electric Power Engineering Handbook. Ed. L.L. Grigsby Boca Raton: CRC Press LLC, 2001.
- [2] Fernando S., Power Electronics Handbook – voltage regulators. (Third Edition), 2011, Sónia Ferreira Pinto.
- [3] Barudov E., Panov E., Barudov S., Analysis of Electrical Processes in Alternating Voltage Control Systems. Journal of International Scientific Publication: Materials, Methods & Technologies, 2010, Vol. 4, Part 1, pp.154÷182, ISSN 1313-2539.
- [4] Barudov E., Panov E., Barudov S., Exploration of Precise Non-Linear Model of Discrete Autotransformer Step-Voltage AC Regulator with Semiconductor Commutators. Annual of TU-Varna, 2007, Bulgaria, ISSN: 1311-896X, pp.3÷10.
- [5] Barudov E., Panov E., Barudov S., Analysis of Electrical Processes in a Discrete Alternating Voltage Regulator with Active-Capacitive Load. International Scientific and Technical Conference “Electrical Power Engineering 2010”, ISBN 978-954-20-0497-4, pp.332÷341.
- [6] Barudov E., Panov E., Barudov S., Analysis of Electrical Processes in a Discrete Alternating Voltage Regulator with Active-Inductive Load. Annual of TU-Varna, 2010, Bulgaria, ISSN: 1311-896X, pp. 30÷36.

# LED Technology in public lighting installations – facts or fiction

Andrej Djuretic<sup>1</sup>, Nebojsa Arsic<sup>2</sup> and Mile Petrovic<sup>3</sup>

**Abstract** – This paper deals with constant attempts to present LEDs as miraculous sources globally and to clear the way for their domination on the global lighting market. Although it must be emphasized that LED technology really represents future of the artificial lighting, still these sources are not so powerful (especially when it comes to outdoor lighting) comparing to conventional HID sources, especially High Pressure Sodium lamps.

**Keywords** – LED and HID sources, system efficacy, ballast and driver efficiency, optical and thermal efficiency, mesopic vision, scotopic/ photopic ratio.

## I. INTRODUCTION [1]

The first LED ("Light Emitting Diode") was discovered in 1906. when H. J. Round reported electroluminescence as phenomenon using a crystal of silicon carbide and crystal detector. In the next 50 years nothing significant happened in this area, not until serious researches begun in semiconductor technology. In 1962. GE company introduces first red LED with efficacy 0.1 lm/W and in 1965. first yellow LED as well. In 1976. the first colour control concept was implemented by Jerry Laidman from Sound Chamber company (light intensity of each LED was controlled by using Pulse Width Modulation technique). The first commercial LEDs were commonly used as replacements for incandescent and neon indicator lamps, but real breakthrough with efficiency and light output came through in 1990's. The first high-brightness blue LED was demonstrated by Shuji Nakamura of Nichia Corporation in 1994 and was based on InGaN. Finally, in 1997. Nichia company introduces the first white LED by coating blue LED with yellow phosphor (yellow light combined with blue light produces light that appears white). To conclude, from the middle of the last century to 2007., LED efficiency increased around 1000 times (from 0.1 lm/W to 100 lm/W for Nichia cold white LED with colour temperature cca. 4500K). Today in 2013., LED efficacy is still increasing, it has already reached 150 lm/W and it's getting closer to fascinating value of 200 lm/W, which would put LEDs in front of all other light sources (Low and High pressure sodium, Metal-halide,

Fluorescent, Incandescent, Halogen, Xenon lamps, etc...).

## II. SYSTEM EFFICACY

Looking at the brochures of many different manufacturers (even some well known), one might think that luminaires with LED sources can replace HID (High Intensity Discharge) luminaires of even 3-5 times higher power? Very often it can be read that energy savings with LEDs reach 50% and sometimes even up to 80%. Needless to say, none of these brochures provides any information about lighting level – will it stay the same while power is decreasing? In Table 1 [2,3,4,5,6] values of luminous flux for some well known types of LED chips are obtained:

TABLE 1  
LUMINOUS FLUX OF MOST COMMONLY USED LEDs

Company	Type	CCR	Min. flux [lm] 25°C /350mA	Max. current [mA]
CREE	XP-G2	Cool White (5000-8300)K	147	1500
		Neutral white (3700-5300)K		
CREE	XP-G2	Warm white (2600-3700)K	129	1500
		Ultra White (5000-10000)K		
CREE	XP-E2	White (5000-5700)K	124	1000
		Warm white (2600-3700)K		
OSRAM	Golden Dragon Plus	Ultral White 6500K	116	1000
		White 5600K		
OSRAM	Golden Dragon Plus	Warm white (2500-4800)K	85	1000
		Ultra White (5700-6500)K		
OSRAM	OSLON SSL 80	Neutral White (4000-5000)K	115	1000
		Warm white (2700-4000)K		
OSRAM	OSLON SSL 80	Cool White 5650K	135	1000
		Neutral white 4100K		
LUMILEDS	Rebel ES	Warm white 3500K	103	1000

<sup>1</sup>Andrej Djuretic is marketing manager in the luminaire factory Minel-Schreder, Tosin Bunar 51, 11080 Zemun-Belgrade, Serbia, E-mail: a.djuretic@minel-schreder.rs.

<sup>2</sup>Nebojsa Arsic is at the Faculty of Technical Sciences University of Pristina – Kosovska mitrovica, Kneza Milosa 7, 38220 Kosovska Mitrovica, Serbia. E-mail: nebojsa.arsic@pr.ac.rs.

<sup>3</sup>Mile Petrovic is at the Faculty of Technical Sciences University of Pristina – Kosovska mitrovica, Kneza Milosa 7, 38220 Kosovska Mitrovica, Serbia. E-mail: mile.petrovic@pr.ac.rs.

These data are taken from manufacturers technical brochures for 2013. and it can be seen that luminous flux per chip doesn't exceed 147lm in case of cool white LEDs (colour temperature in 5000-8300K range). According to manufacturer technical brochure [2], these values are calculated in the laboratory conditions for PN junction temperature of 25°C and forward current of 350 mA. Usually, in public lighting installations (especially in urban areas) it is most common thing to use light sources of warm or neutral white colour. If, for example, XP-G2 chips produced by Cree company are taken into account, it can be seen from Table 1 that luminous flux of neutral white LED (3700-5300)K is 138 lm. However, this flux is valid only for PN junction temperature of 25°C, while in reality these temperatures are much higher and can go up to 150°C –usually we take this temperature is 85°C. Before going any further, let us define luminous efficacy, which is a measure of how well a light source produces visible light. It is the ratio of luminous flux to total power consumed by the light source [lm/W]. According to the Figure 1 [2], at this temperature system efficacy decreases for cca. 16.5 % (from cca 116% at 25°C to cca. 98.5% at 85°C).

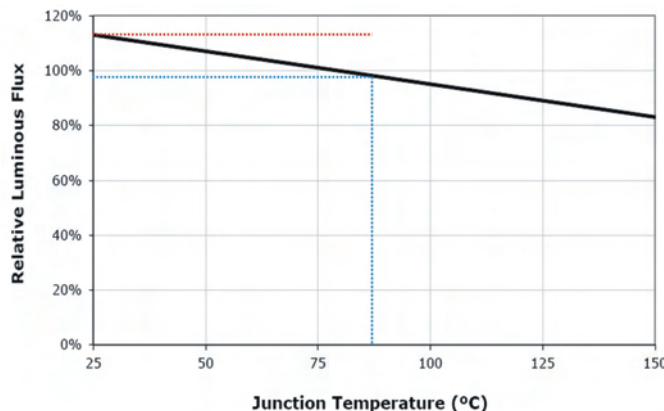


Fig. 1. Relative Flux vs. junction temperature ( $I_F = 350\text{mA}$ )

Based on value determined from curve above, real luminous flux at junction temperature of 85°C should be cca. 115 lm. However, although values of luminous flux can be determined from the curve in manufacturer technical brochure, these values are also given in table 2 shown below [2]. This value of 122 lm is higher than previous one and represents decrease of cca.12%. Since the idea of this paper is to prove that LEDs are not so efficient sources as it can be heard everywhere, less harsh value (the one that favors LEDs) of 122 lm is taken into calculations. Since power of single LED is cca. 1W (without driver losses), efficacy of single LED is 122 lm/W at 85°C, which represents thermal efficiency of 88%!

TABLE 2  
LUMINOUS FLUX CHARACTERISTICS OF CREE XP-G2 LEDs

Colour	CCT range		Base order codes Min. Luminous Flux @350 mA		
	Min.	Max.	Group	Flux [lm] @85°C	Flux [lm] @25°C
Cool White	5000K	8300K	R3	122	138
			R4	130	147
			R5	139	158
Outdoor white	3200K	5300K	R2	114	129
			R3	122	138
			R4	130	147
Neutral white	3700K	5300K	Q5	107	121
			R2	114	129
			R3	122	138

Efficacy of one luminaire with LED sources is not just a question of LED efficacy, but it is also affected by efficiency of LED drivers and efficiency (transmission coefficient) of lenses (collimators) and glass protector as well. If we take the most common (and the best at the same time) case where only LED chips are placed on PCB (Printed Circuit Board) without any electronic device (so called "passive PCB"), and all other necessary electronic devices are gathered and incorporated into "driver", efficiency of such driver (power supply constant current source) is often over 90%!

Figure 2 [7] shows typical electrical circuit and some of the most popular drivers that can be found on the market:

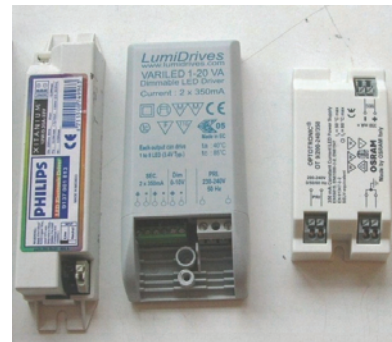
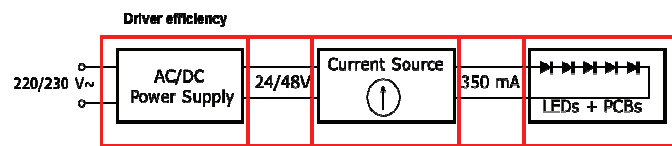


Fig. 2. Typical LED circuit and the most popular drivers on the market

Unlike conventional HID sources (most commonly High pressure sodium and Metal halide lamps) Led optical system usually doesn't contain reflector (although lately there are more such solutions (e.g. Hella Germany) where each diode has its own reflector – still very expensive solutions), but the light distribution control is done by using optical lenses (collimators) and glass protectors. Efficiency of collimators is usually around 85- 92% and by incorporating losses due to Fresnel reflection (cca. 8%), it can be assumed that LED optical system efficiency is approximately 80%!

After taking into account all aforementioned factors, it can be concluded that real light efficacy of one high quality LED luminaire (excellent thermal dissipation in luminaire and high quality LED chips, collimators and driver) is (Figure 3 [7]) :

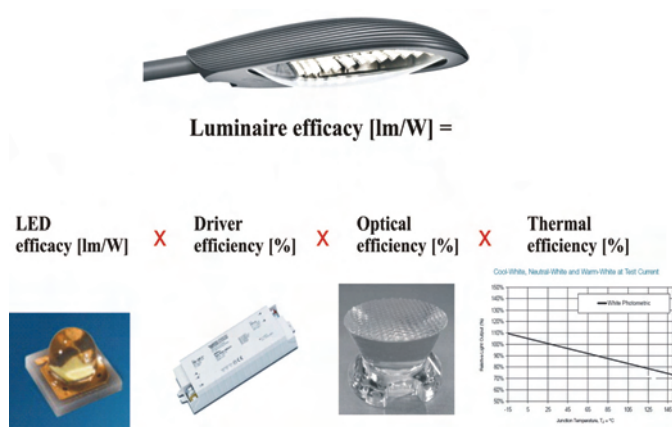


Fig. 3. Luminaire efficacy [lm/W]

In this particular case, system efficacy of one LED luminaire with Cree XP-G2 LED (and, for example, with Philips Xitanium driver and Carclo lenses used by Schreder, world known belgian luminaire manufacturer) is:

**LED system efficacy =**

**LED efficacy x driver efficiency x optical efficiency x thermal efficiency**

$$\begin{aligned}
 &= 122 \text{ lm/W} \times 90\% \times 80\% \times 88\% \\
 &= \boxed{77 \text{ lm/W}}
 \end{aligned} \tag{1}$$

Now when we established efficacy of one quality LED luminaire, comparison should be made with other sources that are most commonly used in public lighting installations – above all High Pressure Sodium lamps. It is important to mention that metal halide sources are also present in public lighting installations, but to a much lesser extent. Luminous efficacy of quality light source (e.g., lamp type NAV-T, manufactured by OSRAM [8]) is 94 lm/W 70W lamp power and 132 lm/W for 250W lamp power. Let's assume that for limitation of the amount of current in an electric circuit (so called stabilisation) magnetic ballast is used (still prevailing control gear in public lighting installations) and that average efficiency of quality magnetic ballast is over 85% (e.g.,

Philips BSN family [9]). Assuming that optical efficiency of quality system (luminaire) is approximately 82% (reflector + protector), it can be calculated that approximate luminous efficacy of quality HID luminaire with High Pressure sodium lamp is cca. 90 lm/W. This assumption is based on 10 years experience in lighting industry whereas these values are common knowledge and standard parameters for HID systems calculations (before LEDs came, HID sources prevailed for many years). Efficacy of one luminaire used in public lighting installation depends on optical efficiency, luminous efficacy of the light source and utilisation efficiency (utilisation coefficient – part of the luminous flux that reaches desired work plane, i.e. roadway that needs to be illuminated – Figure 4 [7]).

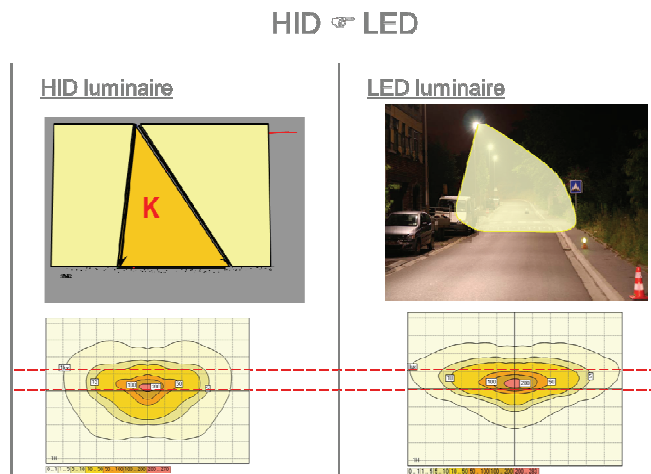


Fig. 4. Utilisation efficiency HID vs. LED

It can be assumed that average utilisation efficiency of one quality HID luminaire with HPS lamp is approximately 45% (value that can be often found in well-known manufacturers technical brochures and calculation softwares [7]). If we assume that utilisation coefficient for LED system is 70% (much effective light distribution control, due to LED source geometry light is emitted only in lower half-plane), we will have the following case (Figure 5 [7]):

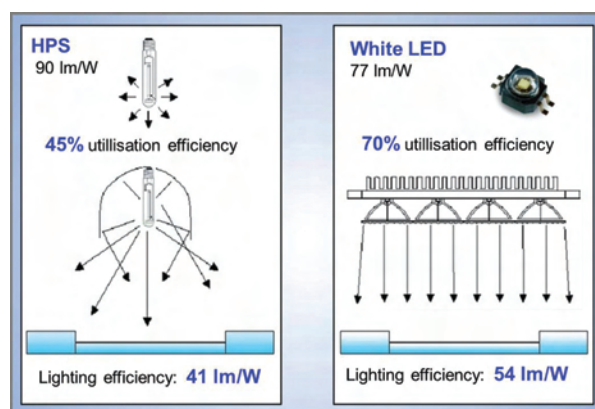


Fig. 5. Utilisation efficiency - HID vs. LED in real situation

And finally, Figure 6 [7] shows trends in increase of luminous efficiency from the middle of the twentieth century up to year 2013. with expected value of 160 lm/W.

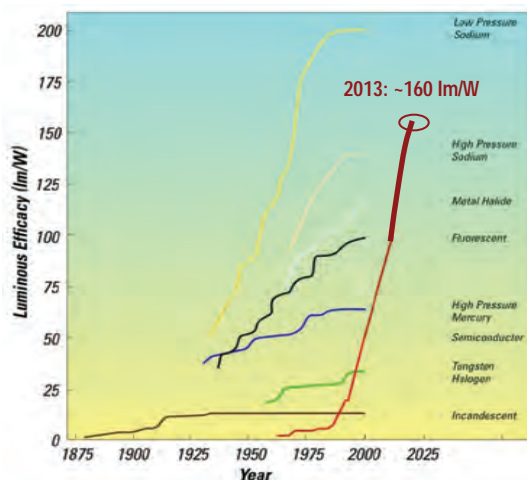


Fig. 6. Efficacy trends in LED industry

### III. CONCLUSION

Although previous analysis is not highly accurate (certain assumptions and approximations were made), it can be concluded with great certainty that **LED sources are not significantly more efficient than high pressure sodium lamps!**

According to analysis LED sources are approximately 25% more efficient, but that doesn't justify replacement of HID luminaires with LED luminaires of much lesser power (definitely not 50% or 80% energy savings). Usually customers are not sufficiently technically educated and don't realize that energy savings are only valid if we succeed to maintain same lighting level after replacement. It means that, if we want to keep same lighting conditions on the roadway (same lighting class – luminance level  $L_{av}$ , overall and longitudinal uniformity, threshold increment  $TI$  according to relevant international recommendations), replacement can be done only in 1.25:1 ratio! Since this is not the case and a lot of money has been invested in LED technology, recently there is a trend of lowering required lighting level (international recommendations given by CIE or CEN organisation) so that it becomes easier for LED lamps to achieve required level (Lighting class M3 or less). In that case, instead of high HPS powers (70, 100, 150, 250 and 400W), it will be possible to achieve desired lighting levels with LED luminaires of desired power (by simply determining the number of individual LED chips that we need).

It is also important to mention that if this analysis had been done 5 years ago, it would go in favor of HID sources since efficacy of LEDs increased cca. 40% in meantime. Also, analysis was conducted for high quality lighting equipment (well-known world manufacturers such as Philips, Schreder,

Cree and Osram), results would also go in favor of HID luminaires in case of LED equipment of lesser quality.

If we look at the Figure 6, it is clear that LED still didn't reach its peak and if this trend continues, it can be expected that until 2020. they globally reach magic value of 200 lm/W! While others are still trying, Cree company broke this efficacy barrier 2 years ago and they are announcing new record with New XLamp MK-R [10].

### ACKNOWLEDGEMENT

This paper was done in the framework of research on the project TR 35026, which was funded by Ministry of Education, Science and Technological Development of Republic of Serbia.

### REFERENCES

- [1] A. Djuretic, ""Solid state" lighting – new trends in the lighting technology", Serbian Lighting Society (DOS), Annual meeting 2007.
- [2] <http://www.cree.com/led-components-and-modules/products/xlamp/discrete-directional/xlamp-xpg2>
- [3] <http://www.cree.com/led-components-and-modules/products/xlamp/discrete-directional/xlamp-xpe2>
- [4] [http://www.osram-os.com/osram\\_os/en/products/product-promotions/led-for-automotive,-industry-and-consumer-applications/golden-dragon/index.jsp](http://www.osram-os.com/osram_os/en/products/product-promotions/led-for-automotive,-industry-and-consumer-applications/golden-dragon/index.jsp)
- [5] <http://catalog.osram-os.com/catalogue/catalogue.do?favOid=00000002000339de06680023&act=showBookmark>
- [6] <http://www.philipslumileds.com/products/luxeon-rebel/luxeon-rebel-white>
- [7] Schreder Photometry days 2010., Internal PPT presentation
- [8] [http://www.osram.com/osram\\_com/products/lamps/high-intensity-discharge-lamps/high-pressure-sodium-vapor-lamps/index.jsp](http://www.osram.com/osram_com/products/lamps/high-intensity-discharge-lamps/high-pressure-sodium-vapor-lamps/index.jsp)
- [9] [http://www.ecat.lighting.philips.com/l/lighting-electronics/hid/hid-electromagnetic/hid-basic-semi-parallel-ballasts-for-son-cdm-mh-lamps/913710104750\\_eu/](http://www.ecat.lighting.philips.com/l/lighting-electronics/hid/hid-electromagnetic/hid-basic-semi-parallel-ballasts-for-son-cdm-mh-lamps/913710104750_eu/)
- [10] <http://www.cree.com/news-and-events/cree-news/press-releases/2012/december/mkr-intro>

# Daily Load Curves for Different Months of Commercial Load Excluding Craft Stores and Shops

Lidija Korunovic<sup>1</sup> and Marko Vuckovic<sup>2</sup>

**Abstract** – Averaged chronological daily load curves for different months of the year, relating to the load class - commercial load excluding craft stores and shops, are presented and analysed in the paper. These curves are the result of procession of data measured by over two hundred and fifty energy meters installed at low voltage consumers. Daily load curves of working days, Saturdays and Sundays for months that belong to different seasons are mutually compared and compared with previously published results for load class of shops.

**Keywords** – Daily Load Curve, Low Voltage Consumer, Commercial Load.

## I. INTRODUCTION

The knowledge of load characteristics is the base for both exploitation and planning of distribution networks and electric power system. Therefore, it is very important to have reliable information about the load curves. The curves depend on many factors such as load composition, tariffs, influence of seasons, i.e. weather conditions, life habits, economic standard of living and the usage of central heating. Thus, it is not easy to determine statistically reliable load curves, especially at low voltage, because stochastic load variations significantly influence on the shape of load curves on this voltage level. Furthermore, it is expensive to perform measurements at large number of low voltage consumers and technically difficult to transmit and storage large amounts of data.

One of the papers that deal with load curves at low voltage is [1]. This paper presents the methodology for load curve determining on the basis of questionnaires completed by low voltage consumers. However, load curves obtained in this way can be used only for rough estimation, when it is not possible to perform numerous measurements at low voltage consumers. The results of such measurements performed during two years at low voltage consumers that belong to residential, commercial and industrial load class are presented in [2].

However, numerous measurements in long time periods with the possibility to storage huge number of data at one location became the reality with the usage of up to date energy meters and systems for remote energy meter reading. Such meters and the system are installed in electric power

<sup>1</sup>Lidija Korunovic is with the Faculty of Electronic Engineering, University of Nis, Aleksandra Medvedeva 14, 18000 Nis, Serbia, E-mail: lidija.korunovic@elfak.ni.ac.rs.

<sup>2</sup>Marko Vuckovic is with electric power distribution company „Jugoistok“ Nis, 46a Bul. Z. Djindjica, Nis 18000, Serbia.

distribution company „Jugoistok“ Nis. Thus, data measured by nearly seven thousands energy meters in the area of town Nis are collected. On the basis of the data regarding time period longer than two years statistically reliable daily load curves of two seasons and several load classes are obtained [3]. Therefore, these curves are very applicable. For example, the curves are implemented in the software for energy loss calculation in low voltage distribution network of town Nis, they are used for load factor and loss factor determining of different load classes at low voltage [4], while typical seasonal load duration curves are presented in [5].

This paper is continuation of the research which first results regarding the curves of two seasons and different load classes are presented in [3]. Thus, the paper presents the results of the analysis of daily load curves in different months of one load class at low voltage - commercial load excluding craft stores and shops. The load class includes offices, but also some households that are signed in as commercial load only due to the privilege not to pay a fee for the national television. Tariffs for the commercial load (at low voltage) excluding craft stores and shops and the households are the same. Data for the curves presented in this paper are collected from 259 energy meters using the system for remote energy meter reading. Since the consumers that belong to the same load class have similar load structure, the number of over two hundred and fifty consumers is large enough to form typical, averaged chronological daily load curves. Totally number of measurements of real power performed by these meters installed at commercial load excluding craft stores and shops is even 10 149 556.

In order to process such number of data and to form averaged chronological daily load curves of working day, Saturday and Sunday for every month of concerned time period, adequate computer program is made [6]. Firstly, this program sorts the data that correspond to working day, Saturday and Sunday of every month of concerned time period. After that, it sorts the data in 15 min long time periods of the day (24 hours), i.e. in 96 time periods. Then, the program averages the data and chronological load curves with 96 points for working day, Saturday and Sunday, for every month are formed.

This paper presents and/or describes daily load curves for working day, Saturday and Sunday of different months of one year. Curves of months in winter and summer season and intermediate period are analysed separately and the differences are quantified. The curves of typical month of winter season regarding working day, Saturday and Sunday are mutually compared and compared with corresponding curves of typical summer month. The results are compared with the results of the analysis regarding daily load curves of different months of shops [6, 7].

## II. CURVES OF MONTHS IN WINTER SEASON

According to electric power system of Serbia, winter season begins on October 15<sup>th</sup> when distant heating starts and summer season begins on April 15<sup>th</sup> when the heating stops. Therefore, months in winter season are: November, December, January, February and March, while summer months are: May, June, July, August and September. Since October and April do not fully belong to winter or summer season, in this paper they are called months of intermediate period.

Fig. 1 presents averaged daily load curves of working day of four months in winter season - November, March, January and February. The curve of December is missed because it is very close to the curve of March and it will be difficult to distinguish it. The curve of November is the lowest one that indicates that the usage of electricity for heating was limited in concerned month. On the other hand, the highest curve is the curve of February that is higher than the curve of January in significant period of the day. It can be explained by the influence of holidays in January when the offices do not work that effects the result of averaging.

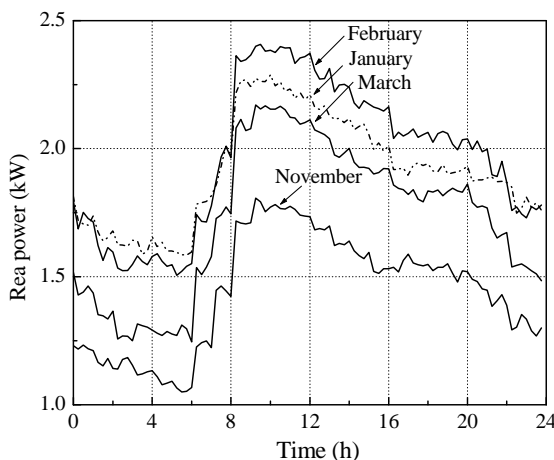


Fig. 1. Averaged daily load curves of working day in November, January, February and March.

The shape of all curves from Fig. 1 is similar. After the midnight the load decreases slowly to the minimum load that is around six o'clock in the morning. The minimum load of the curves is in the range from 1.05 kW in November to 1.58 kW in January. After that, the load increases in three steps approximately every hour that indicates the beginning of the work of certain consumer groups. The pick load of all curves appears at almost same time, in the period from 9:15 am to 10 am. It is 2.41, 2.29, 2.17 and 1.81 kW for the curves of February, January, March and November, respectively. Around 11 am all the curves start to decrease slowly by approximately 4 pm, it can be said they are almost constant from 4 pm to 7 pm or 8 pm, and after that the curves continue to decrease by 6 am.

Although the curves of months in winter season have similar shape, they differ from each other significantly. Thus, maximum deviation of the curve of November from the curve

of February is even 25.6 % and in all points it is greater than 22.4 %. The deviation of the curve of March from the curve of February is also significant - maximum deviation is 19.7 % and in 81 (of 96) points it is greater than 10 %. Only deviations of the curve of January from the highest curve are less than 10 %, i.e. these are up to 8 %. Therefore, is recommendable to use daily load curves of working days in certain months instead of one representative curve for all working days in winter season.

## III. CURVES OF MONTHS IN SUMMER SEASON

Four averaged daily load curves of months in summer season are presented in Fig. 2. The curve of July is not presented because it is between the curves of June and May that are close to each other, and therefore it will not be notable. The shapes of the curves in winter and summer season are similar, but the latter are significantly lower. Thus, the curve of June has the highest pick and it is 1.51 kW, while minimum load of the curves is in the range from 0.72 to 0.84 kW. In general, curves in summer season decrease after the midnight, increase in three steps after 6 o'clock in the morning, they have the pick load during working hours, and start to decrease rapidly in the afternoon, from 3 pm and in the evening, from 9 pm, when the groups of load devices of concerned load class turn off.

The curves of June and May cross each other several times, but the curve of June is the highest one in time period from 9 am to 4 pm. It is due to the large influence of air-conditioners used for cooling in summer months, particularly the hottest ones. The curve of September is the lowest one along almost whole its length due to limited usage of air-conditioners in September. This curve deviates up to 17.9 % from the curve of June. In 81 points the deviations are greater than 10 % that regard to be large. Therefore, for correct distribution network analyses, daily load curves for proper months should be used.

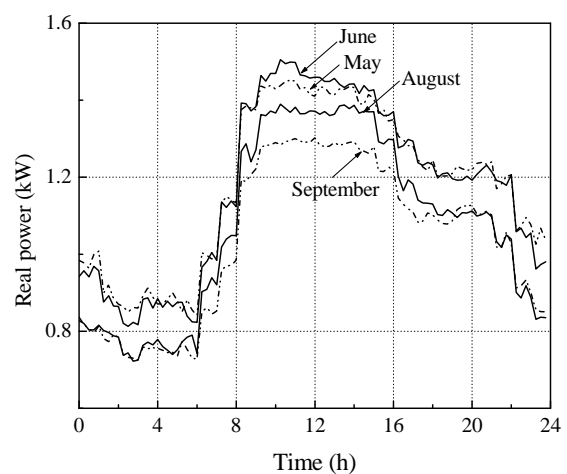


Fig. 2. Averaged daily load curves of working day in May, June, August and September.

#### IV. CURVES IN INTERMEDIATE PERIOD

Two curves of months in intermediate period, April and October, are presented in Fig. 3. The same figure presents the mean curve obtained by averaging these two curves. The curves are similar and have the similar shapes as the curves in winter season. However, they are significantly lower than the curves of cold winter months due to partial use of electricity for heating in intermediate period. Maximum load of April's and October's curves appears around 9:30 am. It is 1.59 kW and 1.51 kW, respectively, and the latter load is only 5 % less than the former one. Minimum load of both curves is almost the same, approximately 0.9 kW, and appears at 6 am.

Maximum deviation of October's curve from April's curve is above 10 %, it is 12.3%. However, the usage of mean curve instead of two curves of months in intermediate period can be treated as correct enough, because the maximum deviation of the curves of April and October from mean curve is 6.6 %, and in only 14 points it is greater than 5 %.

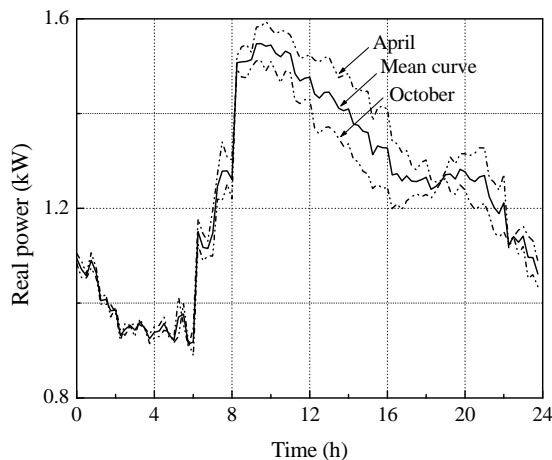


Fig. 3. Averaged daily load curves of working day in April and October and mean curve.

#### V. LOAD CURVES OF WEEKEND DAYS

For comparison, Fig. 4 presents averaged daily load curves of working day, Saturday and Sunday for winter month with highest load, February, and for summer month with lowest load, September. The curves of Saturday in February differs notable from working day curve in February in almost all day periods, except early morning hours and late at night, indicating that some of the offices do not work during Saturdays. The maximum deviation of Saturday load curve from working day curve is 11.7 % and in more than half of the points, deviations are greater than 5 % that regards to be considerable.

The curve of Sunday in February is considerably low in comparison with the curves of working day and Saturday. It varies in relatively narrow range, from 1.34 kW to 1.89 kW. Sunday daily load curve deviates from working day's and Saturday's curve very much, up to 32.4 % and 28.6 %, respectively, while in almost all points these deviations are greater than 5 %.

Pick load in September working day is 1.30 kW and it is almost twice smaller than the pick of February working day curve. September Sunday's curve is the lowest curve from Fig. 4 and its minimum (0.63 kW) is nearly four times smaller than the pick in February working day. Comparison of the curves in September yields that deviations of Saturday curve from the curve of working day are up to 18.5 %, while the curve of Sunday deviates from working day and Saturday load curves even more, maximum deviations are greater than 30 %. Similar deviations of Saturday and Sunday daily load curves from corresponding working day curves are obtained for other months of the year. Therefore, it is recommendable to consider load curves during weekend days separately, in both winter and summer season.

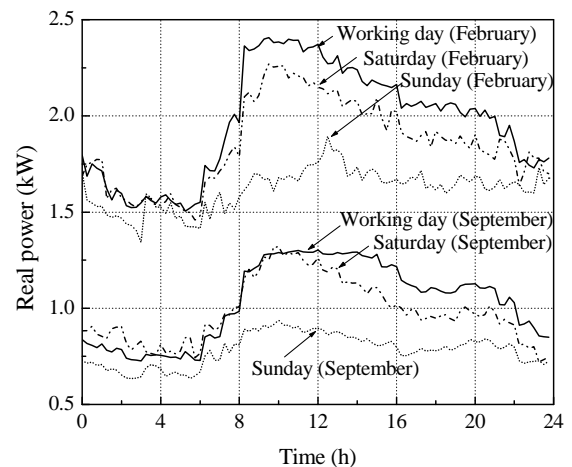


Fig. 4. Averaged daily load curves of working day, Saturday and Sunday in February and September.

Furthermore, the analyses of the curves of weekend days, Saturday and Sunday, regarding all months in winter season, all months in summer season and two months in intermediate period are performed separately. It is found that maximum deviation of the lowest Saturday's curve in winter season (of November) from the highest Saturday's curve in the same season (of February) is 37.7 % that is even greater than deviation found for corresponding curves of working days. Notable deviations are also found for lowest Saturday's curve of summer season (of September) from the highest Saturday's curve of the same season (of June). These are up to 21.8 % and greater than 10 % in approximately 70 % of points (68 points). On the other hand, Saturday's curves of April and October can be represented by mean curve, since all deviations are less than 10 % and in almost two thirds of points deviations are less than 5 %. It regards to be small.

Similar conclusions are drawn for Sunday curves. It is found that all deviations of the lowest curve in winter season from the highest curve in the same season are greater than 30 % (maximum deviation is even 42.6 %), that deviations of the lowest curve in summer season from the highest curve in summer season are greater than 10 % in all points (maximum deviation is 26.9 %), while the curves of intermediate period deviates less than 5 % in almost all points from the mean curve.

## VI. COMPARISON WITH THE RESULTS FOR SHOPS

This section deals with the comparison of some characteristics of daily load curves of commercial load excluding craft stores and shops considered in the paper with previously published curves of the load class of shops. Working day curves of different months of shops are depicted in [6], while [7] mostly deals with the analysis of Saturday's and Sunday's load curves of the same load class. The main difference between the curves presented in this paper and the curves of shops is that the first ones are significantly higher. For example, pick of working day daily load curve in February is 2.41 kW, but the pick of the highest curve among working day curves in winter months is almost two times smaller (1.33 kW). Also, for working day in September, the maximum load of the curve is 1.51 kW, but minimum load of the lowest curve of working day for shops is nearly two times smaller, 0.72 kW. On the other hand, maximum to minimum ratio of most of daily load curves for both load classes is around two. Further comparison of the curves of these load classes will be the subject of some other paper.

Maximum deviation between curves of working day in different months of winter season, presented in this paper, is 25.6 %, and it is almost the same as corresponding deviation found for shops. Maximum deviation for both weekend days, Saturday and Sunday, in months of winter season is around 40% for commercial load excluding craft stores and shops. It is also large for shops, but given in pu, 0.4pu and 0.44pu, since the curves of Saturday in [7] are normalized with maximum load among all Saturday's curves in months of winter season and Sunday's curves are normalized with maximum load among all Sunday's curves in winter months.

Smaller deviations of the curves are found in this paper for the months in summer season: 17.9 % for working day curves, 21.8 % for Saturday's curves and 26.9 % for Sunday's curves. Corresponding deviations are very large for shops: 0.27 pu, 0.51 pu and 0.48 pu, respectively (1 pu is maximum load in summer season of the highest curve among the curves of working day, of Saturday, and of Sunday, respectively).

For commercial load excluding craft stores and shops, maximum deviation of the curves of October's and April's working day from mean curve is relatively small, 6.6 %. Corresponding deviation for shops is 0.12 pu, where 1 pu is maximum load of October's and April's curve. October's and April's curves of Saturday and Sunday deviate from corresponding mean curves of commercial load excluding craft stores and shops up to 8.4 %. These deviations for shops are large [7]. They are given in pu, 0.32 pu and 0.41 pu, since the curves are normalized with maximum load of October's and April's curve, separately for Saturday and for Sunday.

## VII. CONCLUSION

The analysis of averaged working day curves for different months in winter season of commercial load excluding craft stores and shops showed that the load in cold winter month, February, is around two times higher than the load in the month of summer season with the lowest load. This month is September due to limited usage of air-conditioners. Saturday's

and Sunday's load curves in all months significantly differ from corresponding curves of working days.

Deviations between the curves of working day in the months of winter season are greater than 20 %, and corresponding deviations between the curves of Saturday and Sunday are also significant. For summer months, deviations are greater than 10 % in most of the points for working day and Saturday and in all points for Sunday. On the other hand, deviations of October's and April's curve from the mean curve are relatively small and in most of the points are less than 5 %.

Regarding all mentioned facts, for correct analysis of distribution networks, it is recommendable to use load curves of particular months of winter and summer season, for working day, Saturday and Sunday. It regards both commercial load excluding craft stores and shops, and the load class of shops. For the load class concerned in this paper, mean curve can be used instead of October's and April's load curves. Further research will include the analysis of curves of different load classes from several years, the influence on weather conditions on the shape of the curves, maximum load, minimum load and energy consumption, and load forecasting.

## ACKNOWLEDGEMENT

The work presented here was supported by the Serbian Ministry of Education and Science (projects III44004 and III44006).

## REFERENCES

- [1] Lj. Geric, P. Konjovic, P. Djapic and M. Sindjelic, "Modeling of Residential Load Shapes Using Method of Questionnaire", XXXVIII konferencija ETRAN-a, Conference Proceedings, vol. I, pp. 251-252, Nis, Yugoslavia, 1994. (in Serbian)
- [2] J. A. Jardini, C. M. V. Tahan, M. R. Gouvea, S. U. Ahn, F. M. Figueiredo, "Daily Load Profiles for Residential, Commercial and Industrial Low Voltage Consumers", IEEE Trans. on Power Delivery, vol. 15, no. 1, pp. 375-380, 2000.
- [3] L. Korunovic, M. Stojanovic, D. Tasic, L. Stoimenov and A. Krstic, "Analysis of load diagrams at low voltage of distribution network of Nis", VII Conference on Electricity Distribution in Serbia and Montenegro, R-6.02, Vrnjacka Banja, Serbia, 2010. (in Serbian)
- [4] L. Korunovic, M. Stojanovic, M. Vučkovic, D. Tasic and A. Krstic, "Faktor opterećenja i faktor gubitaka različitim kategorijama potrošnje na niskom naponu", 30. savetovanje Cigre Srbija, Conference Proceedings, R C6 13, Zlatibor, Srbija, 2011. (in Serbian)
- [5] L. Korunović, M. Vučković, M. Stojanović and D. Tasić, "The Analysis of Typical Seasonal Load Duration Curves of Low Voltage Consumers", iCEST 2011, Conference Proceedings, vol. 2, pp. 469-472, Niš, Srbija, 2011.
- [6] M. Vuckovic, "Averaged Daily Load Curves of Different Months of Shops in Wide Consumption Category", 4th IEEESTEC Student's Projects Conference, Conference Proceedings, pp. 19-21, Niš, Srbija, 2011. (in Serbian)
- [7] L. Korunović and M. Vučković, "The Analysis of Averaged Chronological Daily Load Curves for Different Months of Shops", SAUM 2012, Conference Proceedings, pp. 410-413, Niš, Serbia, 2012.

# Electromagnetic field analysis on salient poles synchronous motor in 3D

Blagoja Arapinoski<sup>1</sup>, Mirka Popnikolova Radevska<sup>1</sup>, Milan Cundev<sup>2</sup>, Vesna Ceselkoska<sup>1</sup>

*Abstract – This paper presents a methodology for numerical determinations and complex nonlinear analysis of electromagnetic field, of a three phase salient poles synchronous motor in 3D domains. The motor is mathematically modeled and calculated with nonlinear and iterative calculation using Finite Element Method. This method is very efficient for an accurate electromagnetic field solution. The program package is used for performing automatic generation of finite elements mesh. After defining material construction, loading and excitation in both motor windings, the distribution of electromagnetic field in 3D motor domains is generated, the air gap flux and distributions of the flux density at the middle line of air gap is determinate.*

**Keywords – three phase salient poles synchronous motor, finite element method, electromagnetic field in 3D.**

## I. INTRODUCTION

The three phase solid salient poles synchronous motor is rated following data: nominal power 2.5 kW, nominal voltage 240V, current of excitation 5.5A, voltage winding of excitation 30V, power factor 0.97, frequency 50Hz and nominal speed 1500rpm.

Finite elements method is proven tool for analyzing electromagnetic phenomena in electrical machines and devices. This method enables to enter “inside the machine” and to evaluate exactly magnetic quantities such as air gap flux or flux density in any part of the electrical motor.

## II. MODELLING OF SYNCHRONOUS MOTOR WITH FINITE ELEMENT METHOD

Design and modeling of three phase solid salient synchronous motor used program package for fully automatic design and modeling on model geometry based on solving the empirical equations based on his calculation by classical theory, using parts of the modern theory [1].

In the case considered three-dimensional nonlinear magnetic fields as expressed by the following system of equations:

$$\begin{aligned} rot H &= J, \quad div B = 0, \\ B &= \mu H, \quad rot A = B \end{aligned} \quad (1)$$

In this case the magnetic field is described by partial differential equation in vector form, for magnetic field

<sup>1</sup>Blagoja Arapinoski, Mirka Popnikolova Radevska, and Vesna Ceselkoska are with the Faculty of Technical sciences at University of Bitola, st. Ivo Lola Ribar nn, Bitola 7000, Macedonia.

<sup>2</sup>Milan Cundev is with the Faculty of Electrical engineering and information technologies, Skopje, Macedonia.

distribution in 3D domain:

$$rot(v(B)rot(A)) = J(x, y, z) \quad (2)$$

Equation 2, developed in differential form in 3D, takes the form of Poisson-equation:

$$\frac{\partial}{\partial x} \left[ v(B) \frac{\partial A}{\partial x} \right] + \frac{\partial}{\partial y} \left[ v(B) \frac{\partial A}{\partial y} \right] + \frac{\partial}{\partial z} \left[ v(B) \frac{\partial A}{\partial z} \right] = -J(x, y, z)$$

This equation can-not be solved analytically because the characteristic of magnetization is nonlinear. The solution is obtained by reduction of its system of partial differential equations which are solved using a computer. Automatic computer design is performed in several stages, in addition, the most important accurate definition of input data and motor geometry.

The stator is outer lamination stack where the three phase windings reside. Stator core is made from magnetic material with characteristics of magnetization given on Fig. 1 a), and rotor core is made from solid iron with magnetic characteristic given on Fig. 1.b.

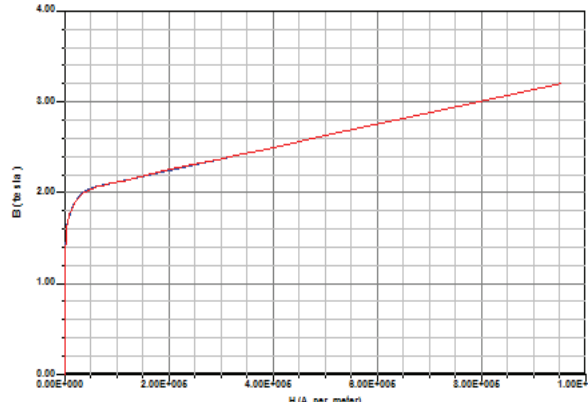


Fig.1.a. Magnetic characteristic of stator

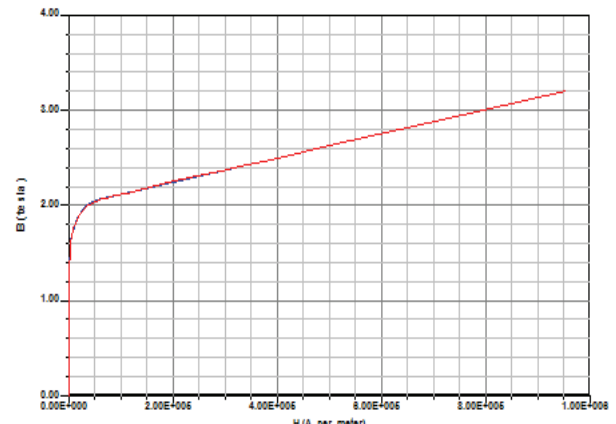


Fig.1.b. Magnetic characteristic of rotor

The stator is equipped with a three phase winding that has a sinusoidal spatial distribution. Step of winding is reduced and is  $y=11/12$ , while the rotor coil is performed as concentric. Part of motor geometry with windings is shown on Fig. 2.

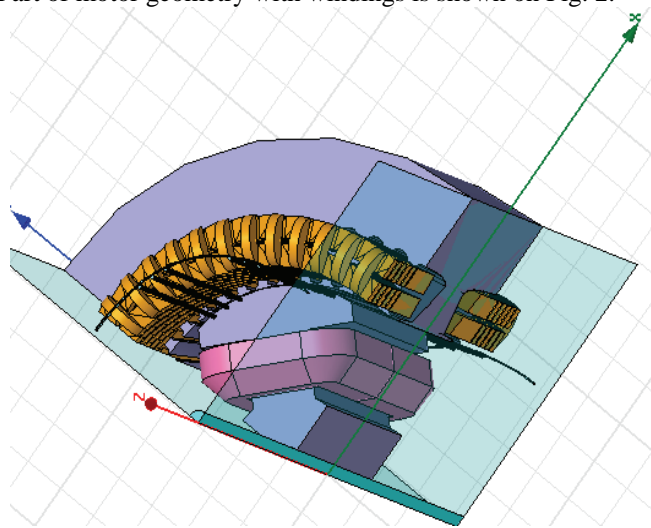


Fig.2. Part of motor geometry with windings

### III. DEFINING THE NECESSARY VARIABLES

To obtain the magnetic field distribution and intensity of magnetic field in the overall 3D synchronous motor domain, have a need for additional input the current densities and conductivity or magnetic voltages in both motor windings.

In order program to be able to solve the problem boundary conditions on the border areas must be defined. For analyzed three phase synchronous motor Dirichlet boundary conditions are used. On Fig. 3D motor model is presented and from figure very well see whole 3D geometry, stator core with three phase winding and rotor core with concentric windings.

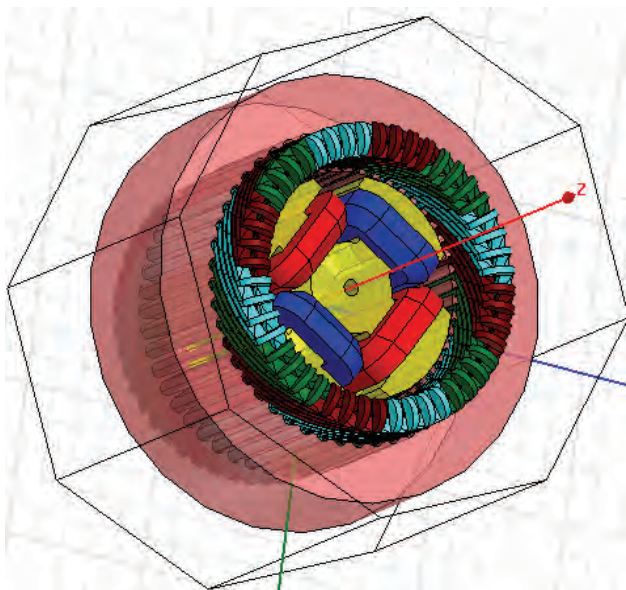


Fig.3. Three phase synchronous silent pole motor, 3D model

Mesh of finite elements is presented which is derived fully automatically and is consisted of 483205 Tetrahedron and is presented on Fig.4.

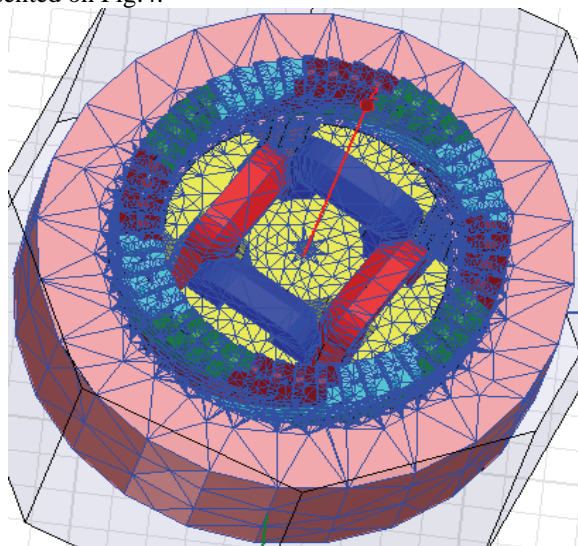


Fig.4. 3D Finite element mesh

To get more accurate computations in some regions the mesh density is increased, especially in the air gap on interface between two different materials, there mesh of finite elements is densest. The exact solution is obtained over 60 successive iterations that take place in 4 phases, during eight hours. The time required to resolve depends on the mesh density of finite elements and the specified accuracy of the results. In this analysis precision of the results is of the order  $10^{-6}$ .

### IV. ELECTROMAGNETIC CHARACTERISTICS IN 3D DOMAINS OF THREE PHASE SYNCHRONOUS MOTOR

By solving a number of nonlinear equations and iterative procedure leads to the final distribution of the magnetic flux density in overall 3D synchronous motor domain. Magnetic flux density in overall 3D motor domains when both windings are energized with rated currents is presented on Fig. 5.

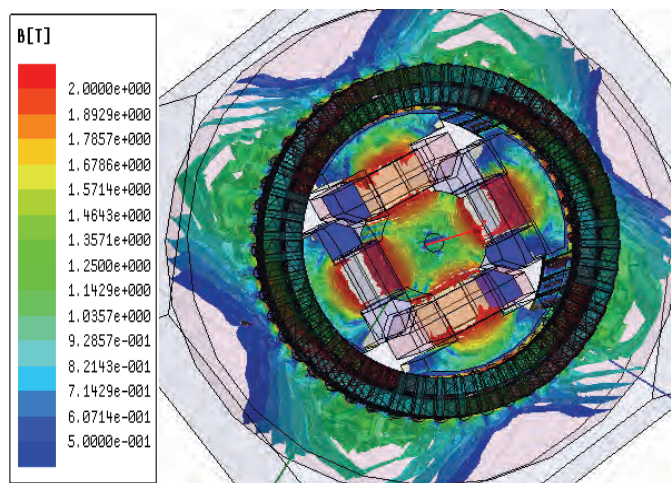


Fig.5. The magnetic flux density in overall 3D motor domains

Because data on the value of magnetic flux density in air gap is one of the most important here can be determinate and average value is 0.65T. Direction of the vector of the magnetic flux density is presented on Fig.6.

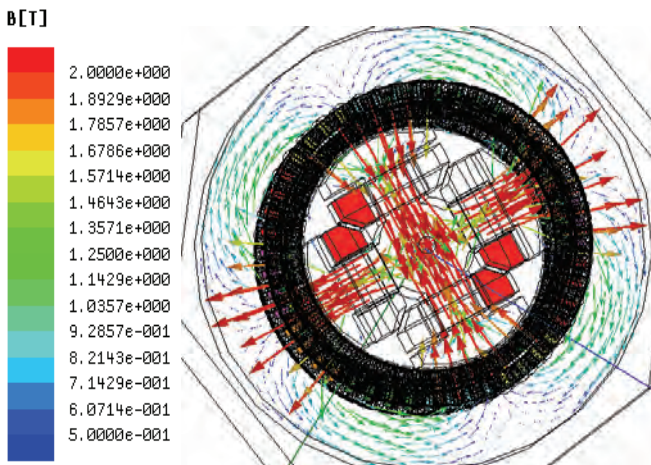


Fig.6. Direction of the vector of the magnetic flux density in 3D.

The further analysis of the motor is carried out with its electromagnetic characteristics, which are going to be determined from the values for the magnetic vector potential  $\mathbf{A}$  and its components in each node of the motor domain. First, the flux density is calculated by using the results of the FEM magnetic field calculation, applying them in Maxwell equation  $\mathbf{B} = \text{rot} \mathbf{A}$  and solving it numerically by PC-based program.

Having the distribution of the of the magnetic vector potential in the whole investigated domain of the motor, from the magnetic field calculation, the air-gap flux is determined:

$$\Phi_{\delta} = \sum \int \text{rot} \mathbf{A} ds = \oint \mathbf{A} dr = \sum \int \mathbf{B} ds = \iint (\mathbf{B} \cdot \mathbf{n}) ds \quad (4)$$

The characteristic of the air-gap flux linkage along one pole pitch for different constant rotor angular positions at various current loads and constant excitation current is presented in Fig.7

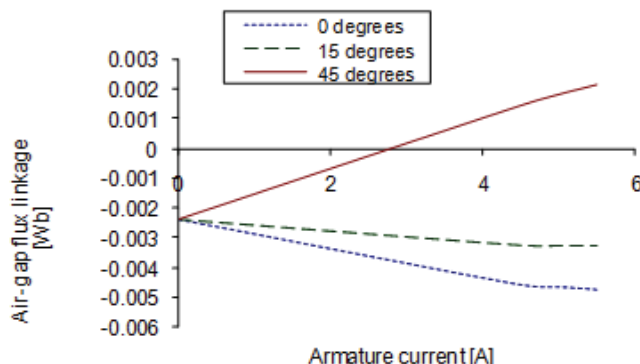


Fig.7 - Air-gap flux linkage characteristics versus different armature currents at constant excitation and various rotor positions

The air-gap flux linkage in dependence of the rotor position at constant excitation and different armature currents are presented in Fig.8.

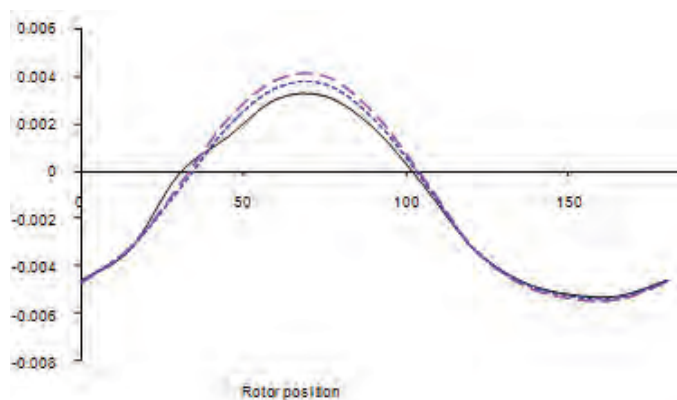


Fig.8. Air-gap flux linkage characteristics versus rotor positions for different armature currents at constant excitation

## V. CONCLUSION

In this paper is presented mathematical modeling of three phase synchronous motor, computation of the magnetic field distribution and the magnetic field intensity, by nonlinear iterative numerical method.

For this purpose is significant that the calculations are based as the most suitable Finite element method in 3D motor domains. This contemporary method enables exact magnetic quantities such as air gap flux or flux density distribution to be evaluated in any part of the machine. On the basis of the analyses of spatial distribution of the flux density in each part of the machine, one can "discover" the week points in magnetic core as well.

## REFERENCES

- [1] Mirka Popnikolova Radevska, Blagoja Arapinoski, *Computation of solid salient poles synchronous motor electromagnetic characteristic*, 10<sup>th</sup> international conference of applied electromagnetic IIEC 2011, Nis, Serbia, September, 2011.
- [2] B. Arapinoski, M. Popnikolova Radevska, "Electromagnetic and thermal analysis of power distribution transformer with FEM" IEST 2010, Ohrid, R.Macedonia 2010.
- [3] M. Popnikolova-Radevska, M. Cundev, L.Petkovska, "From Macroelements to Finite Elements Generation for Electrical Machines Field Analyses", ISEF International Symposium on Electromagnetic Fields in Electrical Engineering, Thessaloniki, Greece, 1995, p.p. 346-349.
- [4] B. Arapinoski, M. Popnikolova Radevska, D. Vidanovski "FEM Computation of ANORAD Synchronous Brushless linear motor" ELMA 2008, Sofia – Bulgaria.
- [5] M. Popnikolova Radevska: "Calculation of Electromechanical Characteristics on Overband Magnetic Separator with Finite Elements", IEST 2006, p.p. 367-370, Sofia, Bulgaria 2006.
- [6] M. Cundev, L. Petkovska, M. Popnikolova-Radevska, "An Analyses of Electrical Machines Synchronous Type Based on 3D-FEM" ICEMA International Conference on Electrical Machines and Applications, Harbin, China, September 1996, p.p. 29-32.

**This Page Intentionally Left Blank**

# Numerical analysis and calculation of parameters of Three-Phase Induction Motor with Double Squirrel Cage

Blagoja Arapinoski<sup>1</sup>, Milan Cundev<sup>2</sup>, and Mirka Popnikolova Radevska<sup>1</sup>

**Abstract –** This paper deals with modelling of three dimensional magnetic field and both numerical computations and analysis of parameters of three phase induction motor with double squirrel cage. The accuracy with which the electromagnetic quantities are computed in a great rate is dependent on the precision of calculations of electromagnetic field distribution in the machine. The 3D – Finite Element Method is very efficient for an accurate electromagnetic field solution and in this research is applied.

**Keywords –** Three-Phase induction motor with double squirrel cage, FEM 3D, electromagnetic analysis.

## I. INTRODUCTION

Three-phase induction motor with double cage is the most common application in regimes with frequent switching, in which the initial torque value should be greater. In this paper will be presented a modern way of obtaining three-dimensional magnetic field, and some operating characteristics of three-phase asynchronous motor with double cage rotor. Software which has been applied to obtain the distribution of the electromagnetic field in 3D motor domain uses the famous and powerful finite element method. The three-phase induction motor with double cage has the following rated data:  $P_n = 3.5kW$ ,  $U_n = 240V$ ,  $f = 50Hz$ ,  $2p = 4$ ,  $\cos \varphi = 0.85$ ,  $\eta = 84\%$ , and  $\Delta$  winding connection.

From the main linkage flux results, the motor inductance and the electromagnetic torque are determined numerically, and their characteristics for various load and rotor angular positions are presented.

## II. GEOMETRY OF THE CONSIDERED PROBLEM

The subject of the research is three phase asynchronous motor with double squirrel cage. As compared to the construction of the stator coil, the coil is identical to the standard three-phase asynchronous motors, in this case magnetic circuit of the stator is laminated and has 48 slots, they set a two-layered three-phase distributed coil with winding shortened step  $y = 11/12$ . The difference in this type of motor is in the rotor circuit, which are set two interconnected cages made of material with different conductance. Complete geometry of three-phase induction motor with double cage in 3D domain is presented on Figure 1.

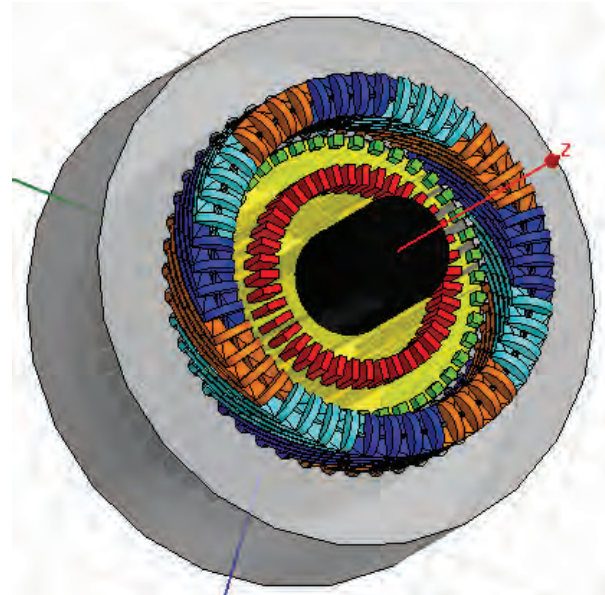


Fig. 1. Geometry of model in 3D domain.

The upper cage is known as start cage (used to run the electric motor when sliding is equal to 1), and is made of phosphor bronze alloy that has a lower conductivity compared to the bottom cage.

The bottom cage is made of copper and has the role of the working cage when the speed of the rotor has a large enough value that scrolling is close to nominal. Currents redistribution from the top in the bottom cage is completely automatic and is dependent on the rotor speed and load.

## III. MATHEMATICAL MODEL AND EQUIVALENT REPLACEMENT SCHEME

The theory of asynchronous motors with double cage can be traced to the theory of three-phase three-winding transformers. That means double cages asynchronous motors can be considered as three separate electrical circuits that are magnetically coupled. The circuit indicated by I, represents the stator and circuit II, and III, representing the upper and lower cage rotor respectively. Each of these circuits respond appropriately active resistance  $R_I, R_{II}, R_{III}$  and inductance, respectively corresponding total inductive winding resistance  $X_I, X_{II}, X_{III}$ .

In asynchronous motors with double cage rotor, when the load changes, and changes in engine speed and thus the frequency of the current in the rotor-conductors, which causes a change of inductance and resistance in the rotor circuit. This phenomenon can be expressed mathematically in a way that

<sup>1</sup>Blagoja Arapinoski and Mirka Popnikolova Radevska are with the Faculty of Technical sciences at University of Bitola, st. Ivo Lola Ribar nn, Bitola 7000, Macedonia.

<sup>2</sup>Milan Cundev is with the Faculty of Electrical engineering and information technologies, Skopje, Macedonia.

the active component of the resistance of the rotor circuit is divided by sliding  $s$ , or simply if the rotor circuit of the upper and bottom cage add extra value to the active resistance  $R \frac{1-s}{s}$ . In that case we can write the following expressions:

$$\begin{aligned}\bar{U}_2' &= \bar{I}_2' R_2' \frac{1-s}{s} \\ \bar{U}_3' &= \bar{I}_3' R_3' \frac{1-s}{s}\end{aligned}\quad (1)$$

Voltage equations for this type of motor received form given by:

$$\begin{aligned}\bar{U}_1 &= \bar{I}_1(R_1 + jX_{\sigma 1}) - \bar{I}_2'\left(R_2' + jX_{\sigma 2}'\right) - j\bar{I}_3'X_{\sigma 3} - \bar{I}_2' R_2 \frac{1-s}{s} \\ \bar{U}_1 &= \bar{I}_1(R_1 + jX_{\sigma 1}) - \bar{I}_3'\left(R_3' + jX_{\sigma 3}\right) - j\bar{I}_2'X_{\sigma 2}' - \bar{I}_3' R_3 \frac{1-s}{s}\end{aligned}\quad (2)$$

Based on the previous expressions can be compiled equivalent electric scheme of asynchronous motor with double cage and is given on Figure 2.

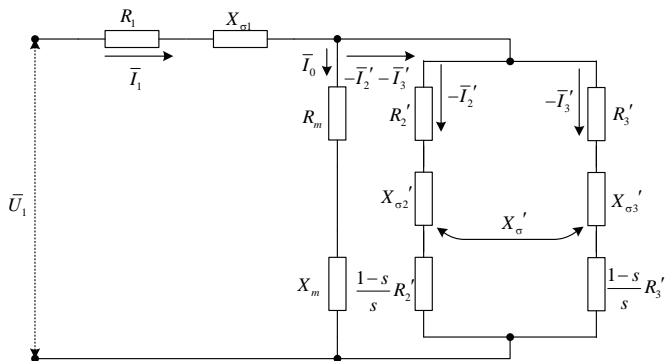


Fig. 2. Asynchronous motor with double cage - equivalent electric scheme.

#### IV. FINITE ELEMENT METHOD IN 3D FOR CALCULATION OF THE MAGNETIC FIELD

For performing the analysis a three dimensional numerical calculation of the magnetic vector potential and flux density in a three dimensional domain of the three-phase induction motor with double cage is required. For that purpose the above mentioned computer program based on 3D Finite Element Method has been used[1]-[8]. The numerical calculation is based on the Poisons' equation for magnetic field distribution in three dimensional domain:

$$rot(v(B) \cdot rot A) = J(x, y, z) \quad (3)$$

To realize a numerical solution of the equation (3) it is necessary to carry out a proper mathematical modeling of the machine. The 3D finite element mesh of three-phase induction motor with double cage is generated with 397994 elements and is performed fully automatically [1]. Then magnetic flux distribution can be plotted and this is presented on Fig.3 for excitation winding are energized with rated currents.

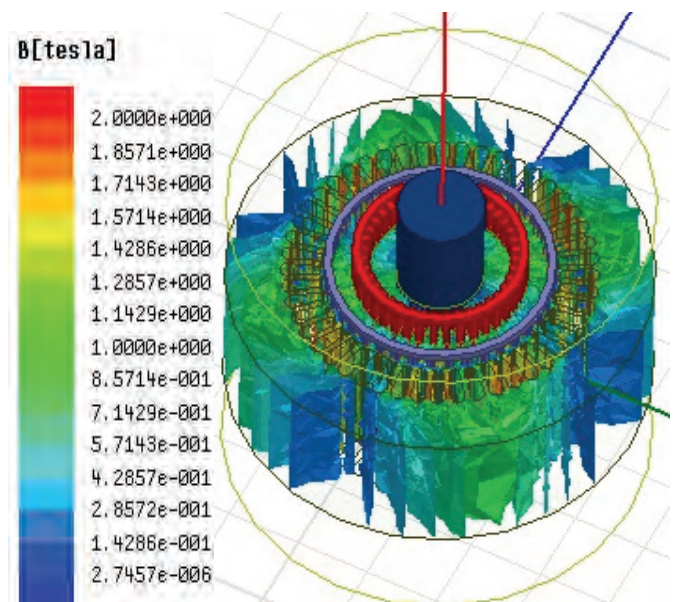


Fig. 3. Magnetic field distribution in 3D motor domain

By using the procedure for numerical differentiation, the distribution of the magnetic flux density at the middle line of the air-gap in three-phase induction motor with double cage is determinate,[8]. The characteristics of the magnetic flux density in dependence of the rotor position at different armature currents are presented in Figure 4.

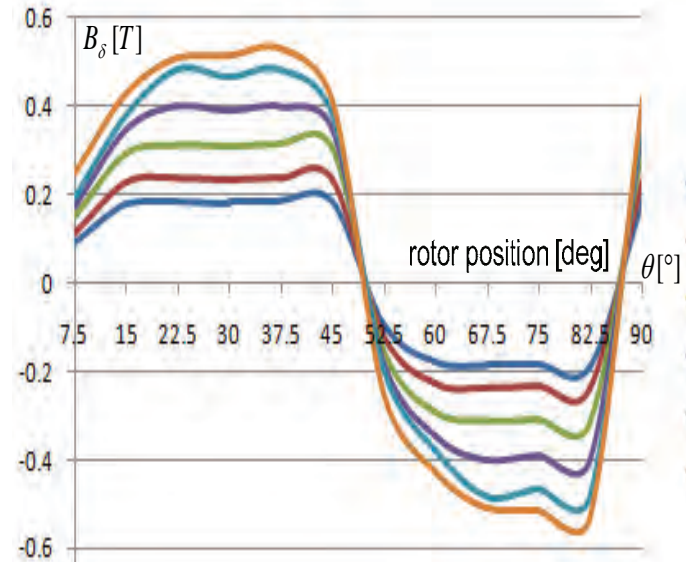


Fig. 4. Characteristic of the magnetic flux density

Having the distribution of the magnetic vector potential in the whole investigate domain of the three phase asynchronous motor with double cage, the main flux in the air gap is determinate as well as leakage flux in the stator and rotor windings, and is going to be determined starting from the equation:

$$\Phi_s = \sum \int rot A ds = \oint A dr = \sum \int B ds = \iint_s (B \cdot n) ds \quad (4)$$

Then result is:

$$\Psi_{\delta} = w \iint_S (\mathbf{B} \cdot \mathbf{n}) ds = w \iint_S \left( \frac{\partial A_z}{\partial x} - \frac{\partial A_x}{\partial z} \right) dz dx \quad (5)$$

In the differentials replaced with differences and integrals with sums, for determining  $\Psi_{\delta}$ , the relation is as follows:

$$\Psi_{\delta} = w \cdot L \sum_{i=1}^{N_x} \Delta A_{zi} = w \cdot L (A_{zNx} - A_{z1}) \quad (6)$$

The air-gap flux linkage  $\Psi_{\delta}$  for different constant rotor angular positions is presented on Figure 5.

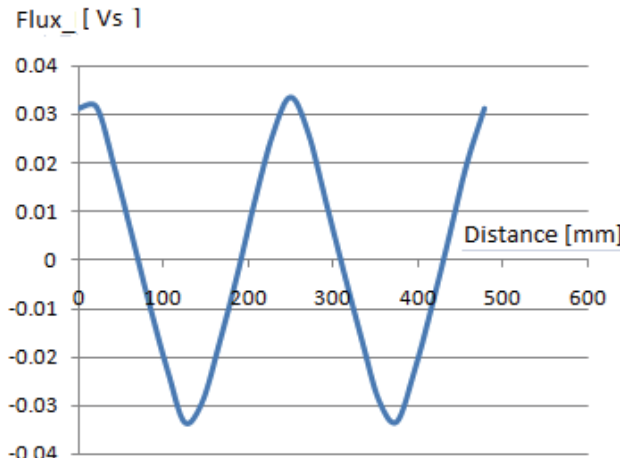


Fig.5. Air-gap flux linkage characteristics

## V. CALCULATION OF ELECTROMECHANICAL CHARACTERISTICS

The knowledge of electromagnetic torque characteristics is very important matter for analysis and performance of electrical motors. In this paper the energy concept for numerical calculation of electromagnetic torque is applied and for three phase asynchronous double cage motor will be calculated by the change of the magnetic system co-energy at virtual angular displacement of rotor for different currents in the stator and rotor bars.

The static electromagnetic torque is effected by the variation of magnetic field energy in the air-gap, at virtual displacement of the rotor.

The torque characteristic of the three phase asynchronous motor with double cage as a function of angular position of the rotor at rated load is given on the Figure 6.

The reliability of the calculated value of torque in this simulation analysis is confirmed, it is shown by the fact that the calculated value and the characteristic shape is identical to that obtained in experimental research done in the laboratory.

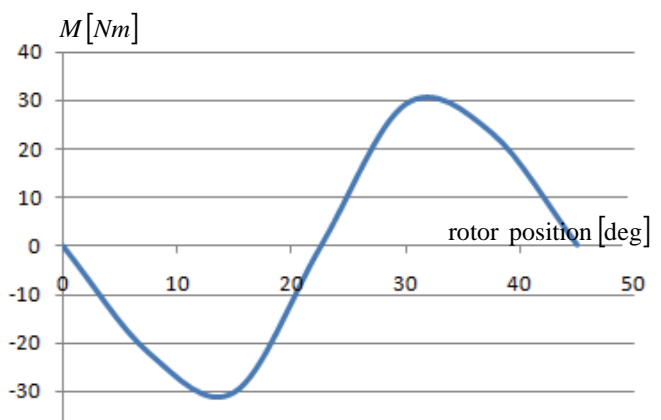


Fig.6. Torque characteristic of the three phase asynchronous motor with double cage as a function of angular position of the rotor

## VI. CONCLUSION

In this paper are presented some of the results obtained in an extensive research that aims to contribute to improving the performance of three phase asynchronous motor with double squirrel cage rotor. Applied software which made simulation analysis is based on the finite element method implemented in three-dimensional domain. This contemporary method enables exact magnetic quantities such as air gap flux or flux density distribution to be evaluated in any part of the motor. The results of the field computations after they are used for calculations of electromechanical characteristics, as the static and dynamic torque.

## REFERENCES

- [1] B.Arapinoski, M.Radevska, V. Ceselkoska and M.Cundev], "Modeling of Three Dimensional Magnetic Field in Three-Phase Induction Motor with Double Squirrel Cage " TEM Journal 2013.
- [2] Mirka Popnikolova Radevska, Blagoja Arapinoski, Computation of solid salient poles synchronous motor electromagnetic characteristic, 10<sup>th</sup> international conference of applied electromagnetic IIEC 2011, Nis, Serbia, September, 2011.
- [3] B. Arapinoski, M. Popnikolova Radevska, "Electromagnetic and thermal analysis of power distribution transformer with FEM" ICEST 2010, Ohrid, R.Macedonia 2010.
- [4] M. Popnikolova-Radevska, M. Cundev, L.Petkovska, "From Macroelements to Finite Elements Generation for Electrical Machines Field Analyses", ISEF International Symposium on Electromagnetic Fields in Electrical Engineering, Thessaloniki, Greece, 1995, p.p. 346-349.
- [5] B. Arapinoski, M. Popnikolova Radevska, D. Vidanovski "FEM Computation of ANORAD Synchronous Brushless linear motor" ELMA 2008, Sofia – Bulgaria.
- [6] M. Popnikolova Radevska: "Calculation of Electromechanical Characteristics on Overband Magnetic Separator with Finite Elements", ICEST 2006, p.p. 367-370, Sofia, Bulgaria 2006.  
M. Cundev, L. Petkovska, M. Popnikolova-Radevska, "An Analyses of Electrical Machines Synchronous Type Based on 3D-FEM " ICEMA International Conference on Electrical Machines and Applications, Harbin, China, September 1996, p.p. 29-32.

**This Page Intentionally Left Blank**

---

---

## Poster 10 - Control Systems

---

---



# Development of a system for power supply monitoring and autonomous ignition of gasoline generator

Goran Goranov<sup>1</sup> and Iskren Kandov<sup>2</sup>

**Abstract:** This paper describes system that monitors the presence on the electrical power supply and assures autonomous work of petrol aggregate.

**Keywords-component:** aggregate, power supply monitoring, autonomous power.

## I. INTRODUCTION

The development of a system for monitoring of the supply pressure is necessary in the cases when the process of the work of a given facility or a machine does not have to be interrupted, because of the voltage's interruptions in the power supply network. These kind of systems are used in the medicine, in the military technics and in some higher levels of computational machines.

The uninterruptible power supply (UPS) based systems for emergency power supply can not always provide alternative power supply for a long time [1]. The reasons for that are the type of the batteries and the batteries's capacity (li-ion, ni-mh, etc.).

The usage of the alternative power supply systems based on a petrol or a diesel engine is appropriate in these cases when the work process allows interruption of the power supply for a short time. The interruption time is determined by the type of the aggregate and the needed time for establishing of the direct current (DC). The estimation time can be critical in the cases when medical or computer equipment are supplied [2]. Even more, it is a well known fact that the diesel aggregates, which also provide and higher power supply (over 10 000 W) are more expensive than the petrol aggregates. This makes the diesel aggregates applicable for lower consumptions [3].

In order to avoid the power supply interruptions, even for milliseconds, and also to generate alternative energy, composite power supply systems are used. These systems contain of a set of other systems: a system for managing and monitoring of the supply pressure, a UPS system and a petrol aggregate for generating the electricity.

In the current report a development of a system for monitoring of the supply pressure of the electrical power supply is provided. In the cases of the supply pressure's absence an autonomous ignition of a petrol aggregate is initiated. As a result a constant electrical power is provided. The development meets the requirements of the ProHost LTD company, which is a hosting service provider in the bulgarian market. This investigation is applied in the cases of support of

the constant electrical power for the company's server room facilities.

## II. THE CONTROL SYSTEM DEVELOPMENT

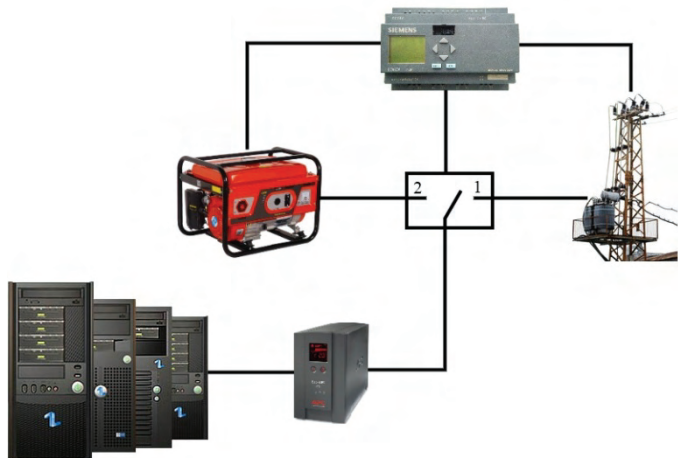


Fig.1 Network of power

The purpose of the control system is to monitor the presence on the electrical power supply and to provide alternative power for indefinite time in the cases when the power supply is not available. On the Fig.1 is shown simplified scheme of an example solution for the case of uninterrupted power supply.

The system can be also used to control and switch the power supply from the network and the electrical power that comes from the petrol aggregate. If electrical power is available, the on-line UPS transfers the electrical power to the server room. If the electrical power from the network is not available, the control system sends signal to the petrol engine to start working. The server room is powered by the UPS's battery, for the time which is needed to the network to establish baseline voltage. The control system switches the power supply from the network to the power that comes from the aggregate. The electrical power that is generated from a petrol aggregate is used to ensure the electrical power to the server's room and also to charge the UPS's battery. In the case when the on-line UPS is used there is no interruption of the power to the server room. This is not the case when the offline UPS (5ms) is used.

On the Figure 2 is shows a block diagram of the developed control system. The control system is based on a programmable logic controller (PLC) Siemens LOGO!12/24RC.

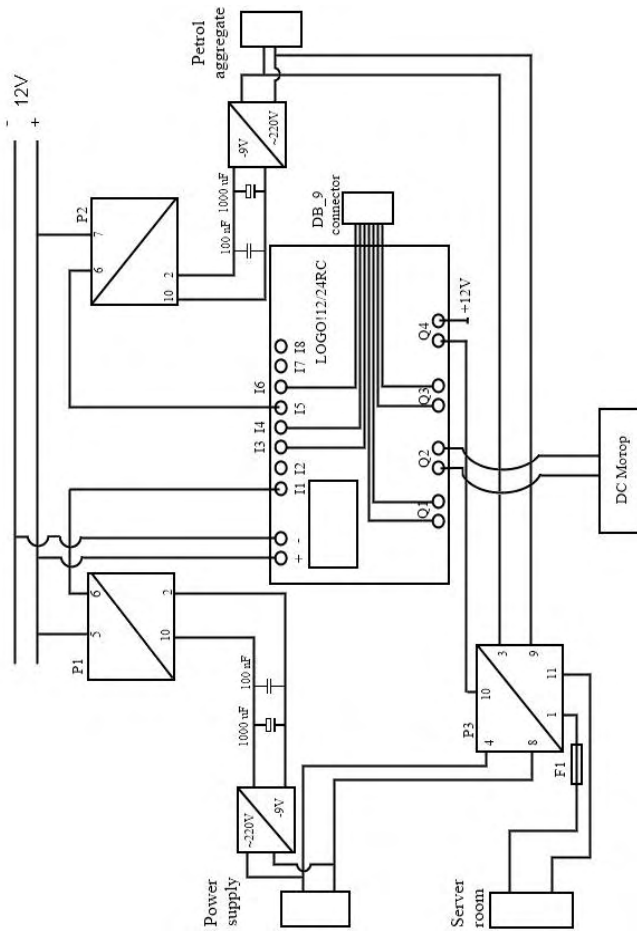


Fig.2 Block diagram of ignition sistem.

This controller possesses the necessary resources for the implementation [4, 5]:

- Sufficient number of physical inputs and outputs;
- Relay outputs - galvanically isolated with maximum current of 10A;
- The controller has two inputs which can be configured as analog inputs;
- Integrated electrically erasable programmable read-only memory (EEPROM)

The main blocks of the system, which are shown on the Figure 2 are:

- Sensors for monitoring of the presence of the power supply build from a transformer, a filter group and a relay;
- Contactor for switching power to the server room;
- Logical control unit for process management, based on the programmable logic controller (PLC);
- DC motor which controls the position of the choke ignition engine.

The aggregate has a manual choke, which requires the development of connecting rod mechanism for moving the position of the choke shown in Figure 3.

To determine the position of the choke are used three pieces of sensors connected to the inputs of the PLC (I3, I4 and I6).

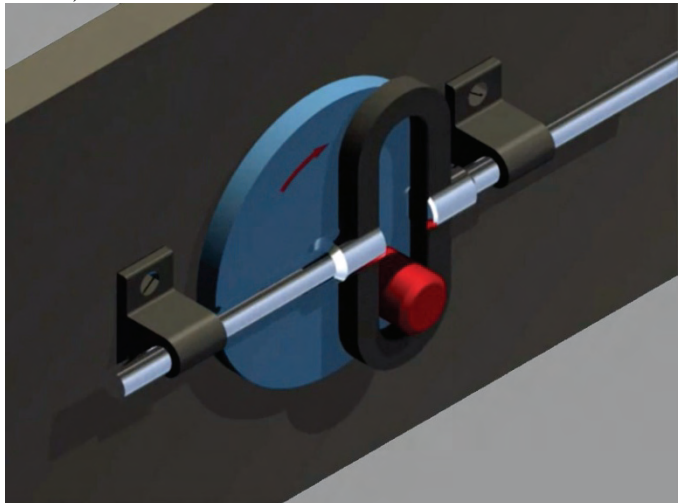


Fig.3 The crutch mechanism

Each of the sensors is attached in a specific position, this guarantees correct positioning of the choke for task execution that has been given. The sensor changes to a state of logical '1' in the case when the choke reaches a specific position. This is used to cancel the transfer of controlling signal to the motor. The developed program of LOGO! FBD [6] is based on function block diagram (FBD) and implements the following algorithm:

- If there is voltage in the network it is transferred to the input of the on-line UPS, and the output of the UPS powers the server room.
- If there is no power, the UPS powers the server room from battery source.
- The system detects that there is no power supply and initiates a process for starting the aggregate.
- After detecting the presence of the output voltage of the generator, the control system switches the input relay from position '1' to position '2'. The voltage from the generator is transmitted to the server room through the UPS.
- If there is any voltage from the electrical network, the control system waits specified time and sends a turn off signal to the petrol aggregate to switch the input relay from position '2' to position '1'.
- When igniting signal is sent to the electromotor, it starts to move slowly the choke of the petrol generator in two stages. First time to the half of its move in order to ignite and second time to the final position to the established conditions.

### III. DEVELOPMENT AND REALIZATION OF THE PROGRAMMING PART.

The development of the program carried out by the controller is achieved with the programming product LOGO!Soft Comfort v 6.1. This is a specialized software

product, which provides a user-friendly panel and a numerous opportunities.

Basics moments from the program development are:

- *In case of power down:*

When there is no power supply in the electrical network the sensor monitoring its presence and send a signal to the input I1 of the controller. To make sure that the power it's not just a disturbance, a check that the signal from the sensor is available for 20 sec is done. The program implementation of this fragment is as follows: the sensor signal which is transferred to the input I1 of the controller is also transferred to the timer with a relative on delay. The timer constant is set to 20 seconds. This timer guarantees a logical '1' as a value of its output when the value is available at its input for at least 20 seconds (Figure 4). The moment when the input I1 receives a signal a dialog window appears and notifies that there is no power supply in the network and that a process for igniting the aggregate was started.

- *Positioning and moving the choke:*

In order to achieve a smooth changing of the position of the choke the time of the transferred signal, the inertia of the motor should be taken in mind. A pulse width modulation is used. The time of the pulses for working and pausing is very carefully chosen. The smooth movement of the motor is required in order to make a proper assessment on its position.

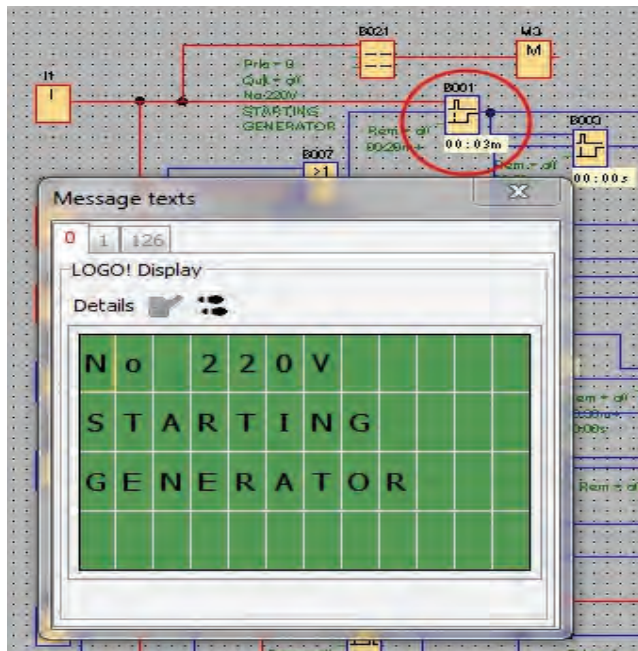


Fig.4 Ignition and move the choke

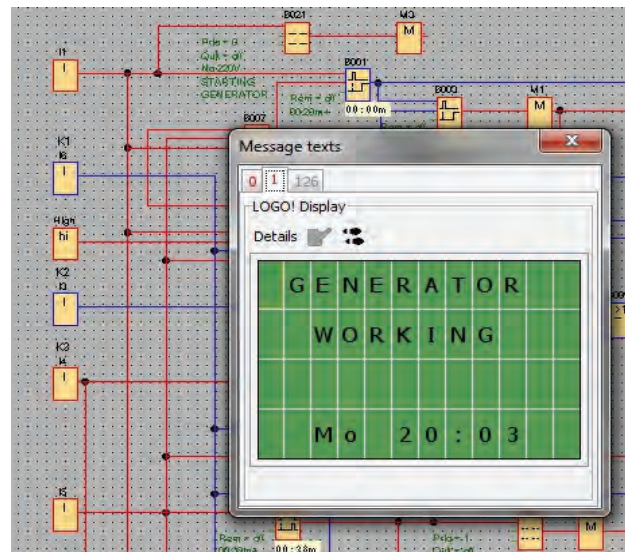


Fig.5 Stable output voltage- 220V, after ignition

To determine the position of the motor, there are 3 sensors connected to the corresponding outputs of the controller (I2, I3 and I4). In the beginning the motor is always in position '1', ( $I2 = '1'$ ) and when it reaches position '2' a signal is sent to the input (I3) from sensor 3 which stops the movement of the motor. Since the DC motor has a large momentum the time for sending control pulse is very little. To that time is also added and the time for commutation of the relay output of the controller and the time for treatment of the signal.

- *Conditions for work of the generator:*

In order to monitor the work of the generator the following conditions must be observed.

There must be no power supply in the network. The sensor monitoring for a voltage presence must be established in state '1' ( $I1 = 1$ ). The choke must be in state '3' – at the input (I4) of the controller there should be condition of logical '1'. The sensor monitoring for a voltage presence from the generator must be in state of logical '1' ( $I5 = '1'$ ), which means that the aggregate has managed to start and at its output a DC is generated with constant frequency. The counter which monitors the number of unsuccessful ignitions must show 0 – its purpose is to monitor how many times the generator has started. If there is a technical problem or lack of fuel and the generator fails to start more than 5 times the system cancels the process of igniting and on the display of the controller is shown that there were 5 unsuccessful ignites. If the aggregate has managed to start and therefore generates output voltage, the signal from the sensor monitoring for presence of output power resets the counter. In order to guarantee the correct work of the system there are algorithms and check for the correct execution of the program.

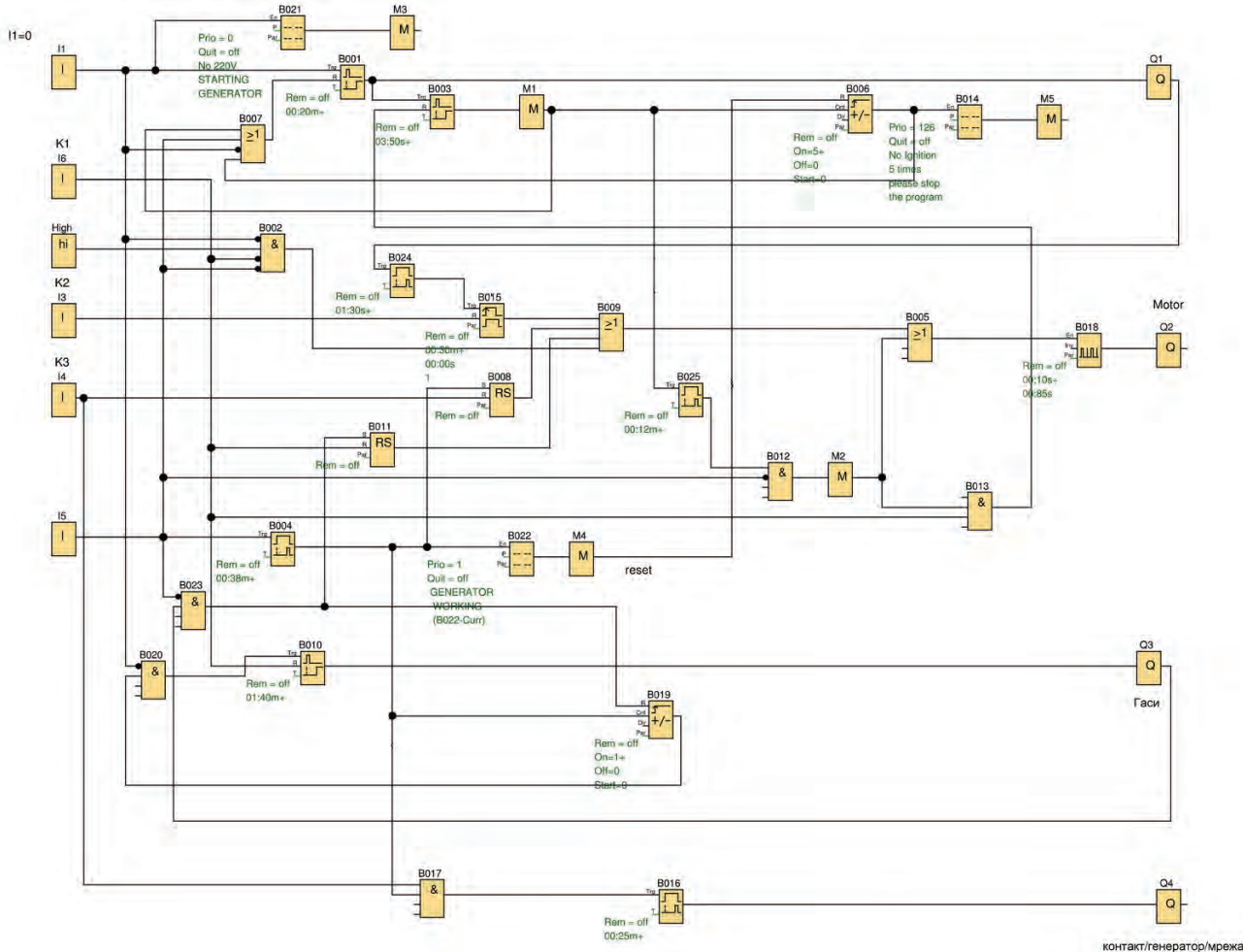


Fig.6. Block diagram of the program

There is a check that ensures that when the system first starts the choke will be in position '1' i.e. I2='1'. There is also a check for the state of all counters used in the scheme. This check resets all counters when the system first starts. There is a protection from a short circuit in the load which guarantees that when a short circuit is present the system will not start the process of igniting. For this implementation a 10A fast-acting fuse is used. Its signal is transferred to the input I7 of the controller. If by some reason there is a short circuit in the load, the control system indicates this on the monitor and permits the ignition of the aggregate. The full program in FBD, on which PLC's work is based, is shown on Figure 6. Additionally there is a possibility at input I8 to monitor the fuel levels. At critical levels there is a logical '1' at the input and the system displays a message on the monitor: "No fuel".

#### IV. CONCLUSION

There are autonomous ignition aggregate systems on the market, but they are too expensive. The system

we proposed in this article covers the sectors from low and middle business classes where autonomous aggregate is wanted but not affordable. The system is adaptive and successful to use with aggregates with different power levels and having automatic choke. Of course with bigger loads the power fragment must be recalculated.

## REFERENCES

- [1] Kevin McCarthy, Victor Avelar, "Comparing UPS System Design Configurations" Revision 3, EDG2 Inc. Schneider Electric.
  - [2] S. Maniktala, "Switching power supply A to Z" USA Elsavier INC, 2006.
  - [3] Erceg, G., Tesnjak,S. "Starting of diesel electrical aggregate loaded with an induction motor ". Proceedings of the 24th annual conference of the IEEE, Industrial Electronics Society, 1998. Iecon '98, pp. 673 - 678 vol.2.
  - [4] Hugh Jack, „Automating Manufacturing Systems with PLCs” 2003.
  - [5] Siemens AG, "LOGO!", manuale edition 2004, A5E00228550-01.
  - [6] Siemens AG, "LOGO Soft Confort!", Documentation 1999.

# Bondsim Modeling and Simulation of Chaos in Cascade Connected Nonlinear Electrical Systems

Bojana M. Zlatkovic<sup>1</sup> and Biljana Samardzic<sup>2</sup>

**Abstract –** The system consisting of several cascade connected electrical circuits is presented in this paper. In consideration to the systems structure and the fact that the tunnel diodes have nonlinear characteristics, one of the properties of this system is the possibility of the chaos appearance. The use of Bondsim tools, simplifying the modeling and simulation of cascade connected electrical circuits, is presented in this paper, too. The Bondsim library enables direct drawing of the Matlab/Simulink block diagrams from the bond graphs.

**Keywords –** Cascade systems, Chaos, Bifurcation, Bond graphs, Bondsim library.

## I. INTRODUCTION

The appearance of chaos was discerned in practically realized cascade systems before the exact theory of chaos had appeared. In the cascade systems, at great amplifications and the presence of certain nonlinearity, the existence of some motion was noticed. These motions are known as deterministic chaos, and they could not be classified as classically defined motions. As it is well known, deterministic chaos originates as a consequence of bifurcation in nonlinear system at certain values of parameters, [1, 2]. In this case those are system amplifications.

The chaotic motion was analyzed for discrete nonlinear systems firstly, i.e., for the iterative processes of the following type:

$$\mathbf{x}_{k+1} = f(r, \mathbf{x}_k) \quad (1)$$

where  $r$  is the control parameter,  $\mathbf{x}_k$  is the state vector. At certain value of parameter  $r$ , bifurcation appears. If that parameter becomes large enough, chaotic motion (depending on function  $f$ ) appears. In the case of Eq. (1) the discrete system is analyzed, where  $k$  is discrete time. In this case iteration is running through time.

The theory of deterministic chaos, developed for these systems, can be applied to the cascade connected systems, too, [3, 4]. In this case the iteration is spacious, i.e., each cascade in system presents iteration. While in the case of Eq. (1), iteration repeats in the same system, in the cascade system, the passing of the signal through the line of the cascade connected nonlinear subsystems, of the same structure, presents the iterative process. In that way the same theory,

<sup>1</sup>Bojana M. Zlatkovic is with the Faculty of Occupational Safety at University of Nis, Carnojevica 10a, 18000 Nis, Serbia, E-mail: [bojana.zlatkovic@open.telekom.rs](mailto:bojana.zlatkovic@open.telekom.rs)

<sup>2</sup>Biljana Samardzic is with the Faculty of Science and Mathematics at University of Nis, Visegradska 33, 18000 Nis, Serbia.

developed for the systems given by Eq. (1), can be applied to the cascade-connected systems analysis.

The trajectories in the cascade connected continuous systems can be very complex, because, besides the iterative processes appearing during the signal passing through the cascades, each system has its own dynamics, which presents more complex case than the system given by Eq. (1).

There are different approaches for deriving mathematical models of cascade connected systems. The one of them is using bond graphs [5-8]. The fundamental advantage of this modeling is that it is based on the central physics concept - energy. Bond graph consists of components which exchange energy or power using connections called bonds. The power is product of two variables: the effort  $e$  and the flow  $f$ . The effort (for example: voltage, force, pressure, etc.) and the flow (for example: current, velocity, volume flow rate, etc.) are generalization of similar phenomenon of physics. Therefore, the second advantage is that bond graphs can be used for the different types of systems (electrical, mechanical, hydraulic systems, etc.) and for their combinations (electro - mechanical, mechanical - hydraulic systems, etc.). The third advantage is that complex systems can be divided into simple elements using bond graphs. Bond graphs give the complete description of dynamical systems and the state space equations can be derived easily.

However, there is no need for deriving the state space equations from bond graphs if the Matlab/Simulink library called Bondsim is used, [9 - 12]. This library enables direct drawing of the Simulink block diagrams from the bond graphs and direct modeling and simulation of chaotic dynamic of cascade connected systems.

## II. BONDSIM – SIMULINK LIBRARY

Bondsim - Simulink library contains elements (blocks) which were derived from bond graph elements based on the knowledge of the causality and the appropriate functional relations between inputs and outputs. The elements of this library and their application are described in detail in [9 - 12], while the method for the direct transformation of causal bond graph models into the block diagrams (Fakri transformation) is described in [13].

Obtaining the simulation models in the form of block diagrams is done directly from bond graph models. Explicitly written equations are not necessary because the use of Bondsim elements realizes the constitutive relations of the bond graph elements and junctions. Fakri transformation is convenient for direct application of Bondsim elements to optimize Simulink blocks. Using the Bondsim library a visually more distinct simulation model is obtained and it enables simpler manipulation of elements of the simulation

model. The application of Bondsim library retained the computational as well as the topological structure of the system.

Matlab/Simulink package enables derivation of new elements in the form of blocks. In Section 3 the example of cascade connected electrical circuits is given where the nonlinear element - tunnel diode appears. Bondsim element of tunnel diode is created using the Simulink block Subsystem, i.e., by creating and masking it.

Current – voltage characteristic of tunnel diode is given in Fig. 1. From this characteristic can be seen that the voltage – effort is input and the current – flow is output of tunnel diode. Causal Bond graph element of tunnel diode noted as TD is given in Table I.

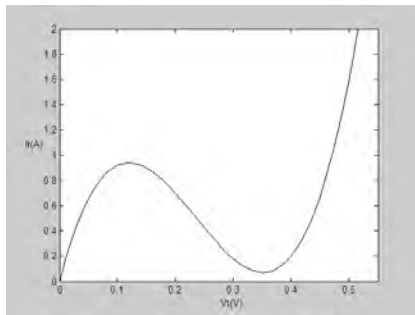


Fig. 1. Current – voltage characteristic of tunnel diode

Using interpolation the next tunnel diode function, i.e., constitutive relation of the TD bond graph element is obtained:

$$I_t = f(V_t) = 140V_t^3 - 99V_t^2 + 17.7V_t \quad (2)$$

The equivalent function blocks, Table I, are derived using the knowledge of causality and relation between input and output of bond graph element TD, Eq. (2). Finally, the Bondsim element of tunnel diode TD is formed using Simulink masking option, Table I, which Dialog box is given in Fig. 2. This Dialog box does not require inserting of parameters. It only gives information about input and output of TD element.

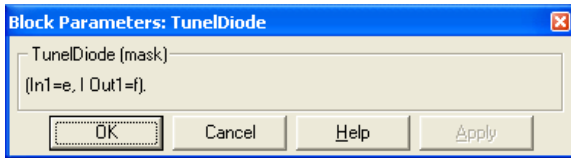


Fig. 2. The Dialog box of TD Bondsim element

TABLE I  
BOND GRAPH AND BONDSIM ELEMENT OF TUNNEL DIODE

Bond graph element	
Bondsim element	
Equivalent functional blocks	

### III. CHAOS MODELLING

In Fig. 3 the system consisting of 30 cascade connected electrical circuits is given. Each cascade has one nonlinear element, tunnel diode.

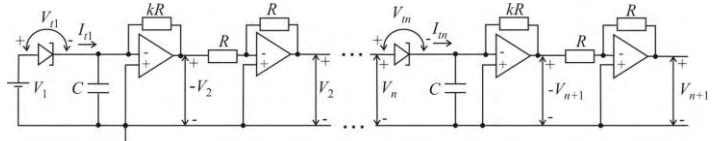


Fig. 3. System of 30 cascade connected electrical circuits

For the cascade systems of interest is to consider the following cases:

- The chaotic motion appearing as a result of the complex oscillations in system;
- The chaotic change of quasi steady states in some subsystems.

The second case will be considered further in the paper.

In the quasi steady state all capacitors are open circuits. Therefore, in the case of the quasi steady state, the system shown in Fig. 3 is transformed into the electrical system presented in Fig. 4.

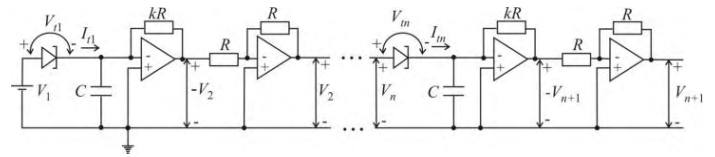


Fig. 4. System of 30 cascade connected electrical circuits in the case of the quasi steady state

For each cascade in Fig. 4 the next relations hold:

$$\begin{aligned} V_{ti,s} &= V_{i,s} \\ V_{i+1,s} &= k \cdot R \cdot I_{ti,s} \\ V_{i+1,s} &= k \cdot R \cdot f(V_{i,s}) \\ i &= 1, \dots, 30 \end{aligned} \quad (3)$$

where  $i$  is the order of the cascade and  $k$  is the control parameter on which value the existence of bifurcation and chaos depends. This equation presents the iterative process of type (1). The iteration is spacious.

Following the energy flow of system in Fig. 4 the bond graph model of one cascade is derived easily and given in Fig. 5.

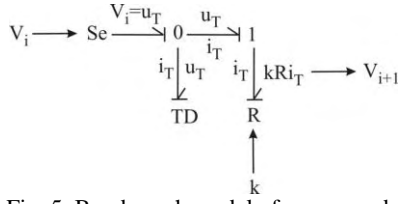


Fig. 5. Bond graph model of one cascade

Using the rules for direct transformation of bond graph models into Bondsims models, [10 - 13], Bondsims model of one cascade is obtained and given in Fig. 6.

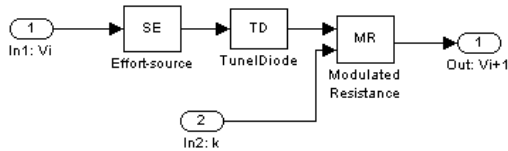


Fig. 6. Bondsims model of one cascade

Selecting the Bondsims model in Fig. 6 and checking the Simulink option Create subsystem the Simulink block Subsystem of one cascade is formed, Fig. 7.

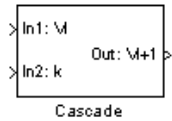


Fig. 7. Simulink block Subsystem of one cascade

Bondsims model of system of 30 cascade connected electrical circuits in the case of the quasi steady state, Fig. 8, is obtained connecting 30 Subsystems given in Fig. 7.

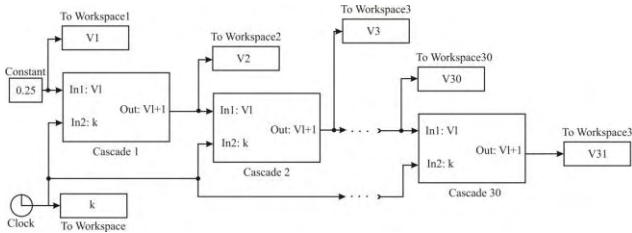


Fig. 8. Bondsims model of system given in Fig. 4

Results of simulation of the oscillatory and chaotic dynamic of cascade systems for  $R=1\Omega$  and input voltage  $V_1=0.25V$  are shown in Fig. 9. Fig. 9a shows bifurcation diagram, i.e., dependency of the voltages of the cascades  $V_{i,s}$  ( $i=1,\dots,31$ ) in the steady state on the parameter  $r$ . It can be noted that for a

small values of the parameter  $r$ , the most of cascades have the same output. The first bifurcation appears for  $r_1=0.2287$ , the next one for  $r_2=0.2897$ , and for  $r_3=0.32$  chaos appears in cascade system.

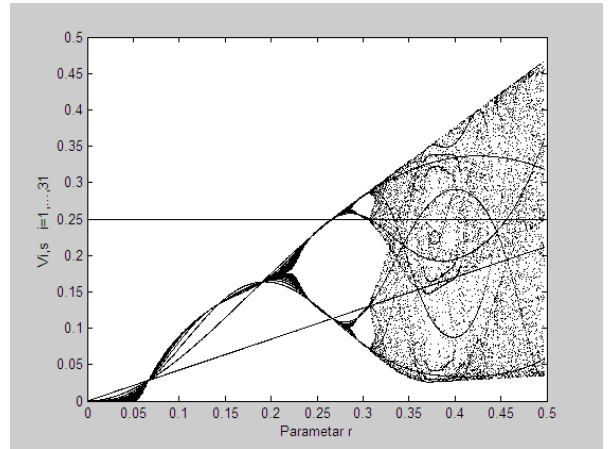


Fig. 9a. Bifurcation diagram

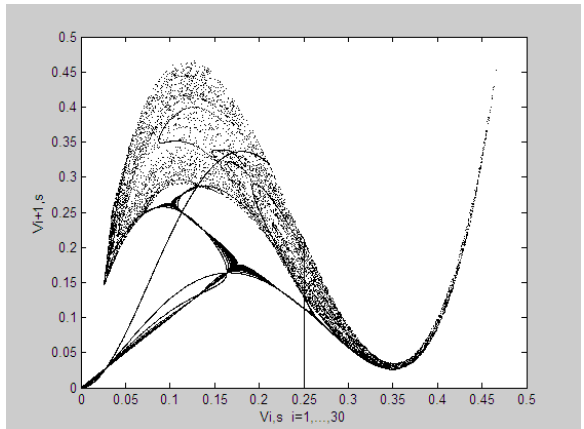


Fig. 9b. Dependency of the output of the  $(i+1)$ -th and the  $i$ -th cascade on the parameter  $k$

Fig. 9b shows the phase portrait  $(V_{i,s}, V_{i+1,s}), i=1,\dots,30$  in function of control parameter  $r$ . This diagram enabled the analysis of relations between the inputs and outputs of particular pairs of cascades in function of parameter  $r$ . Also, it enables the determination of optimal value of parameter  $r$  for the project of cascade systems.

These results are identical with ones given in [4] which were obtained using classical way of modeling, writing M-file in Matlab/Simulink package.

#### IV. CONCLUSION

In cascade systems, the signal passing through the line of cascade connected nonlinear subsystems, of the same structure, presents the iterative process. The trajectories in cascade connected continual systems can be very complex because, besides the iterative process which appears during the passing of the signal through cascades, each system has its own dynamic. For small values of parameter  $k$ , the outputs of all cascades are nearly same. At great amplification the

oscillation appear in the beginning cascades which can cause the appearance of bifurcation and chaos in the next cascades.

Using the nonlinear Bondsim elements a visually more distinct simulation model is obtained and it enables simpler manipulation of nonlinear elements of the simulation model. The application of Bondsim library retained the computational as well as the topological structure of the system. The simple application of proposed method is illustrated using a concrete example of modeling and simulation.

## REFERENCES

- [1] F. C. Moon, *Chaotic and fractal dynamics, An introduction for Applied scientists and engineers*, INC, John Wiley & Sons, 1992.
- [2] K. T. Alligood, T. D. Sauer, J. A. Yorke, *Chaos, An introduction to dynamical systems*, Springer, 1997.
- [3] B. Dankovic, M. Stankovic, B. Vidojkovic, "Simulation of Convergent, Oscillatory and Chaotic Dynamics of Cascade Systems", Proc. of 7th Symposium of Mathematics and its Applications, pp. 101-106, Timisoara, Romania, 1997.
- [4] B. Vidojković, B. Danković, B. M. Vidojković, "On the Bifurcation Appearance at Nonlinear Cascade Connected Systems", Proc. TELSIKS 2003, 6<sup>th</sup> International Conference on Telecommunications in Modern Satellite, Cable and Broadcasting Services, vol. 2, pp. 805 – 808, Nis, Serbia and Montenegro, 2003.
- [5] P. J. Gawthrop, L. Smith, *Metamodelling: Bond graphs and dynamic systems*, London, Prentice Hall International, 1996.
- [6] J. U. Thoma, *Simulation by bond graphs: Introduction to a graphical method*, Berlin, Springer-Verlag, 1990.
- [7] J. Thoma, B. Ould Bouamama, *Modelling and simulation in thermal and chemical engineering: A bond graph approach*, Berlin, Springer, 2000.
- [8] J. Thoma, *Introduction to bondgraphs and their applications*, Oxford, Pergamon press, 1975.
- [9] B. Vidojkovic, D. Antic, B. Dankovic, "Bondsim-Simulink tools for bond graph modelling and simulation", Proc. 7th Symposium of Mathematics and its Applications, pp. 243-248, Timisoara, Romania, 1997.
- [10] ] D. Antić, B. Vidojković, "Obtaining System Block Diagrams based on Bond Graph Models and Application of Bondsim Tools", International Journal of Modelling and Simulation, 21(4), pp. 257-262, 2001.
- [11] D. Antic, V. Nikolic, *Contribution to the conversion of Bond graph models into state space equations and block diagram simulation models*, Budapest, Monographical booklets in Applied & Computer mathematics, 2002.
- [12] D. Antic, B. Vidojkovic, V. Nikolic, "Obtaining the Bondsim simulation model from bond graph models with deriveate causality", Proc. 7<sup>th</sup> Symposium on Theoretical and Applied Mechanics, pp. 257-268, Struga, Macedonia, 2000.
- [13] A. Fakri, F. Rocaries, A. Carriere, "A simple method for the conversion of bond graph models in representation by block diagrams", International Conference on Bond Graph Modeling and Simulation (ICBGM'97), pp. 15-19, Phoenix, USA, 1997.

# Further results on integer and non-integer order PID control of robotic system

Mihailo Lazarević<sup>1</sup>, Srećko Batalov<sup>1</sup>, Milan Cajić<sup>2</sup> and Petar Mandić<sup>1</sup>

**Abstract** –This paper presents the new algorithms of integer and fractional order PID control based on genetic algorithms in the position control of a 3 DOF's robotic system driven by DC motors. Also, we propose a robust fractional-order  $PD^\alpha$  sliding mode control of a given robotic system.

**Keywords** –Fractional PID controller, control, robot, DC motor, optimal settings

## I. INTRODUCTION

Fractional calculus (FC) is a mathematical topic with more than 300 years old history, but its application to physics and engineering has been reported only in the recent years. The fractional integro-differential operators are a generalization of integration and derivation to non-integer order (fractional) operators, [1],[2]. As we know, due to its functional simplicity and performance robustness, the PID controllers are still used for many industrial applications. On the other hand, fractional calculus has the potential to accomplish what integer-order calculus cannot. In most cases, our objective of using fractional calculus is to apply the fractional order controller to enhance the system control performance i.e. better disturbance rejection ratios and less sensitivity to plant parameter variations compared to the traditional controllers. The fractional  $PI^\beta D^\alpha$  controller,[2] the CRONE controllers, [3] and the fractional lead-lag compensator,[4] are some of the well-known fractional order controllers. Three definitions are generally used for the fractional differintegral. First is the Grunwald definition, [2] suitable for numerical calculation given as:

$$^{GL}D_a^\alpha f(t) = \lim_{h \rightarrow 0} \frac{1}{h^\alpha} \sum_{j=0}^{\lfloor (t-a)/h \rfloor} (-1)^j \binom{\alpha}{j} f(t-jh), \quad (1)$$

where  $a, t$  are the limits of operator and  $[x]$  means the integer part of  $x$ . The left Riemann-Liouville (RL) definition of fractional derivative is given by

$$^{RL}D_t^\alpha f(t) = \frac{1}{\Gamma(n-\alpha)} \frac{d^n}{dt^n} \int_a^t \frac{f(\tau)}{(t-\tau)^{\alpha-n+1}} d\tau, \quad (2)$$

for  $(n-1 \leq \alpha < n)$  where  $\Gamma(\cdot)$  is the well known Euler's gamma function.

<sup>1</sup>Mihailo Lazarević is with the Faculty of Mechanical Eng. at University of Belgrade, Kraljice Marije 16, Belgrade 11032, Serbia, E-mail: mlazarevic@mas.bg.ac.rs

<sup>2</sup>Milan Cajić is with the Mathematical Institute SANU, University of Belgrade, Kneza Mihaila 36, Belgrade 11001, Serbia

$$_a^{RL}D_t^{-\alpha} f(t) = \frac{1}{\Gamma(\alpha)} \int_a^t \frac{f(\tau)}{(t-\tau)^{1-\alpha}} d\tau, \quad (2)$$

Also, there is another definition of left fractional derivative introduced by Caputo, [1],[2] as follows:

$$_a^C D_t^\alpha f(t) = \frac{1}{\Gamma(n-\alpha)} \int_a^t \frac{f^{(n)}(\tau)}{(t-\tau)^{\alpha-n+1}} d\tau, \quad n-1 < \alpha < n, \quad (3)$$

Caputo and Riemann-Liouville formulation coincide when the initial conditions are zero. In this paper, we suggest and obtain a new optimal algorithms of fractional order PID control based on genetic algorithms (GA) [5] in the control of robotic system driven by DC motors. GA is a stochastic global adaptive search optimization technique based on the mechanisms of natural selection. The objective of this work is to find out optimal settings based on genetic algorithms for a integer and fractional  $PI^\beta D^\alpha$  controller in order to fulfill different design specifications for the closed-loop system, taking advantage of the fractional orders,  $\alpha$  and  $\beta$ . Also, a sliding-mode controller (SMC) is a powerful tool to robustly control incompletely modeled or uncertain systems [6] which has many attractive features such as fast response, good transient response and asymptotic stability. However, an SMC has some disadvantages related to well-known chattering in the system due to the discontinuous control action are neglected high order control plant dynamics, actuator dynamics, sensor noise, etc. Recently, a fractional-order sliding mode control technique by Monje et al. [7] has been successfully applied for a robot manipulator. In this paper, we suggest and obtain a chattering-free fractional  $PD^\alpha$  sliding-mode controller in the control of a robotic system driven by DC motors.

## II. MAIN RESULTS: NON-INTEGER CONTROL OF A ROBOTIC SYSTEM WITH DC MOTORS

### A. Model of robotic system with DC motors

Here, we are interested in GA based fractional PID control of a robotic system (RS) with DC motors. RS is considered as an open linkage consisting of  $n+1$  rigid bodies  $[V_i]$  interconnected by  $n$  one-degree-of-freedom joints formed kinematical pairs of the fifth class, where the RS possesses  $n$  degrees of freedom,  $(q) = (q^1, q^2, \dots, q^n)^T$ . Specially, the Rodriguez' method,[8], is proposed for modelling kinematics and dynamics of the RS. The geometry of the system has been defined by unit vectors  $\vec{e}_i$ ,  $i = 1, 2, \dots, j, \dots, n$  as well as vectors

$\bar{\rho}_i$  and  $\bar{\rho}_{ii}$  and the parameters  $\xi_i, \bar{\xi}_i = 1 - \xi_i$  denote parameters for recognizing joints,  $\xi_i = 1 - \text{prismatic}, 0 - \text{revolute}$ . Here, equations of motion of the RS can be expressed in the identical covariant form as follows

$$\sum_{\alpha=1}^n a_{\alpha i}(q) \ddot{q}^\alpha + \sum_{\alpha=1}^n \sum_{\beta=1}^n \Gamma_{\alpha \beta, i}(q) \dot{q}^\alpha \dot{q}^\beta = Q_i \quad i = 1, 2, \dots, n. \quad (4)$$

where coefficients  $a_{\alpha \beta}$  are covariant coordinates of basic metric tensor  $[a_{\alpha \beta}] \in R^{n \times n}$  and  $\Gamma_{\alpha \beta, \gamma} \quad \alpha, \beta, \gamma = 1, 2, \dots, n$  presents Christoffel symbols of first kind and  $Q_i$  generalized forces.

Here, it is used RS with 3 DOF's ,Fig. 1, driven by 3 DC motors.

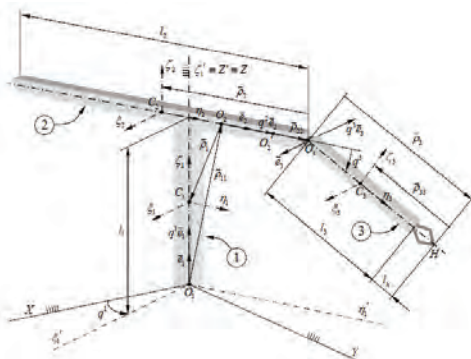


Fig.1 Robotic system with 3 DOF's

The next equation describes the given circuit of DC motor

$$R_i i_i(t) + L_i \frac{di_i(t)}{dt} + ems_i(t) = u_{vi}(t), \quad i = 1, 2, 3 \quad (5)$$

where  $R_i, L_i, i_i$  and  $u_{vi}$  are respectively resistance, inductivity, electrical current and voltage. Electromotive force is  $ems_i(t) = k_e dq_m / dt$  where  $k_e = \text{const}$  and  $q_m(t)$  is generalized coordinate of a DC motor as well as  $N_i$  than is  $q_{mi}(t) = N_i q_i(t), \quad i = 1, 2, 3, \quad N_i$  degree of reduction. It is assumed that  $Q_i^u(t) = N_i k_m i_i(t)$  where  $k_m = \text{const}$  is the torque constant. If the equation of RS is combined with (6) next equation can be written and taking into assumption that  $L \approx 0$  we obtain

$$R [N K_m]^{-1} (A(q) \ddot{q} + C(q, \dot{q}) + K_e N \dot{q} = u_v(t), \quad (6)$$

or in state space,  $x_p = [q_1 \ q_2 \ q_3]^T, x_v = [\dot{q}_1 \ \dot{q}_2 \ \dot{q}_3]^T$ , as follows:

$$\dot{x} = \begin{bmatrix} \dot{x}_p \\ \dot{x}_v \end{bmatrix} = \begin{bmatrix} x_v \\ -A^{-1}(x_p)(C(x) + Fx_v) \end{bmatrix} + \begin{bmatrix} 0_{3 \times 3} \\ -A^{-1}(x_p) \end{bmatrix} \tau(t) \quad (7)$$

$$y = h(x) = x_p \quad (8)$$

where are  $F = N K_m R^{-1} K_e N, \quad \tau = N K_m R^{-1} u_v$   $\quad (9)$

## B. GA-based optimal fractional PID control

### B.1 Fractional order PID controller- $PI^\beta D^\alpha$

Fractional order PID controller (FOPID) is the generalization of a standard (integer-order) PID (IOPID) controller, whereas

its output is a linear combination of the input and the fractional integer/derivative of the input. Recently, published results of FOPIID [2], [4], [9] indicate that the use of a FOPIID controller can improve both the stability and performance robustness of feedback control systems. However, FOPIID itself is an infinite dimensional linear filter and the tuning rules of FOPIID controllers are much more complex in compared classical PID controllers. Unlike conventional PID controller, there is no systematic and rigor design or tuning method existing for FOPIID controller. The time equation of the FOPIID controller is given by:

$$u(t) = K_p e(t) + K_d \frac{d}{dt}^\alpha e(t) + K_i \frac{1}{s^\beta} e(t) \quad (10)$$

For practical digital realization, the derivative part in s-domain has to be complemented by the first order filter

$$G_{FOPIID}(s) = K_p \left( 1 + \frac{1}{s^\beta T_i} + \frac{T_d s^\alpha}{(T_d / N)s + 1} \right), \quad (11)$$

The parameters are: gain  $K_p, K_d, K_i$ , noninteger order of derivative  $\alpha$  and integrator  $\beta$ , as well as the integral time constant,  $T_i = K_p / K_i$ , and the derivative  $T_d = K_d / K_p$ .

### B.2 Optimal tuning FOPIID using GA

In this paper, we propose using GA for determine the optimal parameters fractional order PID controllers. In real coding implementation, each chromosome is encoded as a vector of real numbers, of the same lengths as the solution vector. According to control objectives, five parameters  $K_p, K_d, K_i, \alpha, \beta$  are required to be designed in these settings. Next, optimality criterion which involves besides steady state error  $e$ , i.e IAE, integral of absolute magnitude of the error, overshoot  $P_o$ , as well as settling time  $T_s$  is introduced

$$J = |P_o| + T_s + \int |e| dt \rightarrow \min \quad (12)$$

All the GA parameters are arranged as follows: population size:  $N = 100$ ; crossover probability:  $p_c = 0.75$ ; mutation probability:  $p_m = p_{m0} \min(1, l/g)$ ,  $p_{m0} = 0.1$  -initial mutation probability,  $l = 25$  - generation threshold,  $g$  - current number of generation, generation gap  $gr = 0.35$ . Remainder stochastic sampling with replacement as selection method is used.

### C. Simulations and discussion

Both the FOPIID and the IOPID controllers are designed based on the proposed GA. Here, vector has the FOPIID parameters the ranges of FOPIID parameters are selected as

$$K_p \in [10, 200], \quad K_i \in [0, 100], \quad K_d \in [10, 200], \quad \alpha \in (0.2, 1], \quad \beta \in [0, 1], \quad (13)$$

TABLE I  
THE OPTIMAL PARAMETERS OF THE FOPIID,IOPID  
CONTROLLER BASED ON GA

controller	$K_p$	$K_i$	$K_d$	$\beta$	$\alpha$	$J_{opt}$
PID	1.	199	2	24	-	0.98651
	2.	212	2	26	-	0.84875
	3.	246	1	28	-	0.68718
FOPIID	1.	199	2	24	0.020	0.965
	2.	212	2	26	0.145	0.933
	3.	246	1	28	0.135	0.72954
						0.56187

In Table 1. they are presented the optimal parameters of the FOPID as well as IOPID controller using GA.

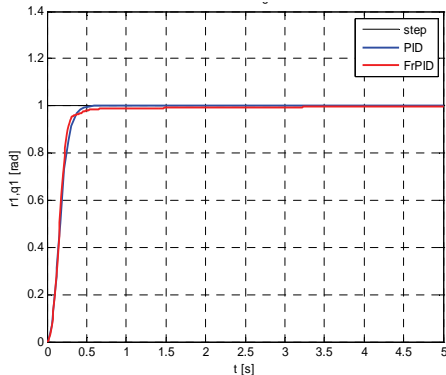


Fig. 2. The step responses of the  $q_1(t)$ [rad]

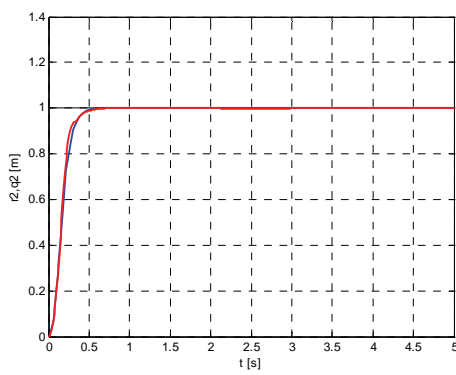


Fig. 3 The step responses of the  $q_2(t)$ [m]

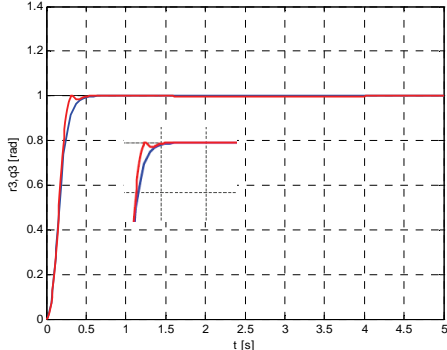


Fig. 4 The step responses of the  $q_3(t)$ [rad]

In simulations they are compared step responses of these two optimal FOPID/IOPID controllers, presented in Figs.2-4. As can be seen from the Figs.2-4 and Table1, better performance for robot control can be achieved using FOPID.

#### D. Chattering-free sliding mode controller design based on the fractional order $PD^\alpha$ sliding surface

Also, we suggested chattering-free fractional  $PD^\alpha$  sliding-mode controller in the control of a RS driven by DC motors. It is well-known that the sliding-mode control is used to obtain high-performance robust control nonsensitive to disturbances and parameter variations. For a nonlinear MIMO system represented in a so-called normal form

$$\dot{x} = f(x) + G(x)u \quad (15)$$

one general sliding mode control law is, [10]

$$u = -[\Lambda G(x)]^{-1} \Lambda [f(x) - \dot{x}_d] - [\Lambda G(x)]^{-1} Q \text{sgn}(s) \quad (16)$$

consisting of a continuous and discontinuous control part where switching surfaces  $s$  are defined as  $s = \Lambda(x - x_d)$ ,  $x_d$  being the vector of the desired states and the  $Q$  positive definite diagonal matrix. The elements of the matrix  $\Lambda$  are chosen so that the  $i$ -th component of the sliding hypersurface has the structure

$$s_i = \left( \frac{d}{dt} + \lambda_i \right)^{(n_i-1)} (x_i - x_{di}), \quad i = 1, 2, \dots, n \quad (17)$$

where  $r_i$  is the order of the  $i$ -th subsystem and  $\lambda_i > 0$ . More generally, considering Eq. (14) as a nominal (known) plant dynamics, we can write

$$\dot{x} = f(x) + \tilde{f}(x) + [G(x) + \tilde{G}(x)]u \quad (18)$$

where  $\tilde{f}(x)$  and  $\tilde{G}(x)$  represent uncertainties or unknown plant dynamics. Using the Lyapunov method one may conclude

$$\dot{s} = -PQ \text{sgn}(s) + (P - I)\Lambda[\dot{x}_d - f(x)] + \Lambda\tilde{f}(x) \quad (19)$$

where  $P := \Lambda(\tilde{G} + \tilde{G})(\Lambda G)^{-1}$ . Regardless whether  $\tilde{G} \neq 0$  and/or  $\tilde{f} \neq 0$ , with an appropriate choice of  $Q$ , we can obtain  $s^T \dot{s} < 0$  for  $\|s\| > 0$ , and this result indicates that the error vector defined by the difference  $x - x_d$  is attracted by the subspace characterized by  $s = 0$  and moves toward the origin according to what is prescribed by  $s = 0$ , [10]. In most cases, this leads to good results but there are some disadvantages such as a *chattering* phenomenon. We suggested the application of the fractional sliding surface in order to decrease output signal oscillations. In this paper, it can be shown that, without a special tuning of  $Q$  for the perturbed plant case, model uncertainties can be successfully compensated using just the fractional order sliding surface and the values of  $Q$  suitable for the nominal plant. For a 3-DOF RS, a conventional sliding manifold is of the first order  $PD$  structure  $s_i = d\tilde{x}_i/dt + \lambda_i \tilde{x}_i$ ,  $i = 1, 2, 3$  where  $\tilde{x}_i = x_i - x_{id}$  and here we propose a fractional  $PD^\alpha$  structure as follows:

$$s_i = d^\alpha \tilde{x}_i / dt^\alpha + \lambda_i \tilde{x}_i, \quad i = 1, 2, 3 \quad (20)$$

#### Simulation results for the position control based on fractional $PD^\alpha$ sliding-mode control

Some experimental simulations were undertaken for  $\alpha = 0.7, 0.8, 0.9, 0.95, 0.99$ , and we have found that the best results are obtained with  $\alpha = 0.95$ , and the matrix  $Q_{\text{nom}} = \text{diag}[5, 5, 5]$  as well as  $\lambda = (5, 2.5, 2.5)^T$ . To verify the robustness of the proposed fractional sliding/mode control we have applied the next parameters variation as follows:

$$\frac{\Delta m_i}{m_i}, i = 1, 2, 3 \sim 9.5\%, \quad \frac{\Delta K_i}{K_i} \sim 10\%, \quad \frac{\Delta J_i}{J_i} \sim 15\% \quad (21)$$

The simulation results are depicted in Figs.5 to 8, where the black lines ( $h(t)$ ) are the desired trajectories. In particular, we present the comparison results for the second coordinate  $q_2$  responses with the  $PD$  and fractional  $PD^\alpha$  cases with all other conditions being the same, for the nominal object, Fig.6 and the perturbed object, Fig.8.

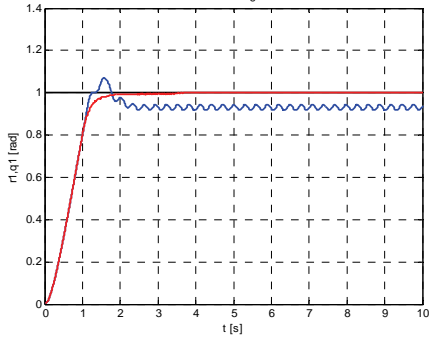


Fig.5. Stabilizing using the sliding mode control  $PD$  and the fractional  $PD^\alpha$  - nominal case,  $q_1(t)[\text{rad}]$

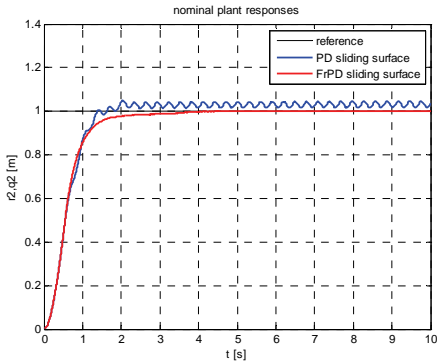


Fig.6. Stabilizing using the sliding mode control  $PD$  and the fractional  $PD^\alpha$  - nominal case,  $q_2(t)[\text{m}]$

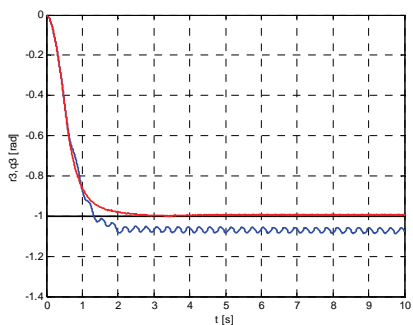


Fig.7. Stabilizing using the sliding mode control  $PD$  and the fractional  $PD^\alpha$  - nominal case,  $q_3(t)[\text{rad}]$

### Perturbed case:(only $q_2$ )

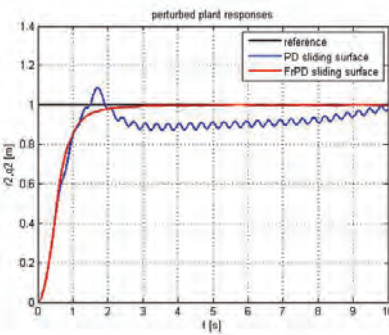


Fig. 8. Stabilizing using the sliding mode control  $PD$  and the fractional  $PD^\alpha$  - perturbed case

### III. CONCLUSION

From previous comparison we conclude that the optimal FOPID controller gives better performance for robot control as compared to optimal IOPID controller method. Also, it is shown that a sliding mode control with the fractional sliding surface is more robust to parameter perturbations and, what is most important to emphasize, the output oscillations are almost completely attenuated and the overall quality of the transient response is much better.

### ACKNOWLEDGEMENT

This research is partially supported by the Serbian Ministry of Education, Science and Technological Development under the number TR 35006.

### REFERENCES

- [1] P.K.B.,Oldham, J.Spanier, *The Fractional Calculus: Theory and Applications of Differentiation and Integration to Arbitrary Order*, Academic Press, New York, NY, USA, 1974.
- [2] I. Podlubny, *Fractional Differential Equations*. Academic Press, San Diego,1999.
- [3] A. Oustaloup, *La Commande CRONE*, Hermes, Paris,1991.
- [4] C.A.Monje,V. Feliu, “The fractional-order lead compensator”, In: IEEE International Conference on Computational Cybernetics. Vienna, Austria, August 30-September 1, 2004.
- [5] R.Haupt, and S.E. Haupt, *Practical Genetic Algorithms*, Wiley-IEEE, New York,2004.
- [6] S.C.,Edwards,S.K., Spurgeon, *Sliding mode control theory and applications*, Taylor & Fran., NewYork, 1998.
- [7] C.A Monje,et al.: *Fractional-order Systems and Controls*, Springer - Verlag, London, 2010.
- [8] M.Lazarević, “Optimal control of redundant robots in human-like fashion:general considerations”. FME Trans. Fac. of Mech. Eng., Univ.of Belgrade, Belgrade, vol.33no.2,pp. 53-64,2005.
- [9] M.P.Lazarević, Lj Bucanović, S. Batalov, “Optimal Fractional Order PID Control Of Expansion Turbine In The Air Production Cryogenic Liquid”, FDA2012, Nanjing, May 2012.
- [10] O.EMehmet.,C. Kasnakoglu, *A fractional adaptation law for sliding mode control*, Int. J. Adapt. Control Signal Process., John Wiley & Sons. 2008.

# Investigating the behaviour of the welding manipulator tip

Svetlana Gerganova-Savova

**Abstract – The most important element of the welding robot is the powering and moving of the manipulator units. This is why, upon designing the system for positioning of the welding head, it is necessary that the input parameters are specified.**

**Keywords – Roots, Process, Welding robot.**

## I. INTRODUCTION

The systems for robot controls calculate the trajectory of movement of the weld nozzle by interpolation; they produce signals for execution of commands and control the movement by taking into account the specific parameters of the manipulator. They set the static and dynamic accuracy, as the width of the arc weld differs – from 5 mm in the automotive industry to 30 mm in the ship-building industry [3]. The most important element of the welding robot is the powering and moving of the manipulator units. The speed of motion, depending on the type of welding, may start from a millimeter per second. This is why, upon designing the system for positioning of the welding head, it is necessary that the input parameters are specified. Such a system is displayed on the diagram [2].

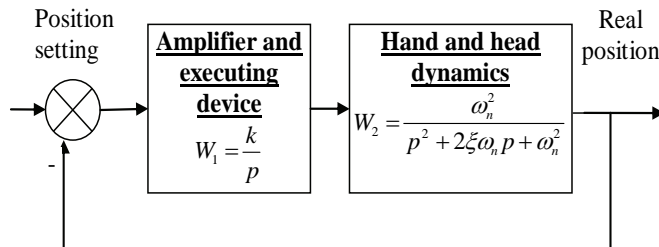


Fig. 1. The system

The dynamics of the hand and the head of the welding manipulator is described as follows:

$$W_2 = \frac{\omega_n^2}{p^2 + 2\xi\omega_n p + \omega_n^2} \quad (1)$$

Svetlana Gerganova-Savova is with the Automation of Manufacturing Department, College in the Structure of the Technical University of Varna, 1 Studentska, Varna 9010, Bulgaria, E-mail: gerganova-savova@lycos.com.

The amplifier and executing device is described as follows:

$$W_1 = \frac{k}{p} \quad (2)$$

For an open system:

$$W_{oc} = \frac{k\omega_n^2}{p^3 + 2\xi\omega_n p^2 + \omega_n^2 p} \quad (3)$$

on- systems deviation frequency,  $\xi=0.2$

The combined transient function of a closed system is:

$$W_{sc} = \frac{k\omega_n^2}{p^3 + 2\xi\omega_n p^2 + \omega_n^2 p + k\omega_n^2} \quad (4)$$

The researches on the threshold of stability [1] show  $k_{rp}=0.4\omega_n$ , where the recommended ratio for the system is:  $0.1 < k/\omega_n < 0.3$  [2].

When the ration  $k/\omega_n$  is at its lowest value, where  $k=1$ ,  $\omega_n=10$ , the roots are:

$$p_{1,2} = -1.4842 \pm 9.7332i$$

$$p_3 = -1.0316$$

The process is slow, the transient response is:  $t_p \approx 5\text{sec}$ , as shown on Figure 2.

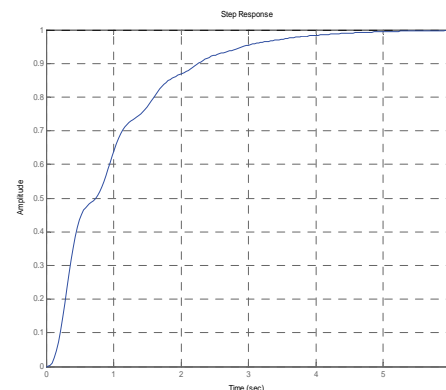


Fig. 2. The process

The same ratio, but with higher  $k=10$ , leads to the transient response, as shown on Figure 3.

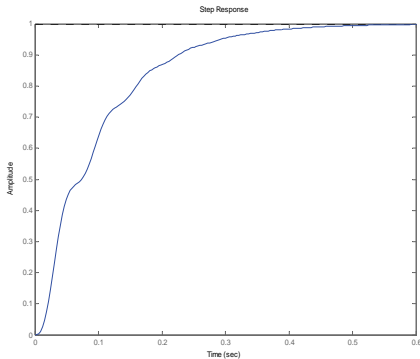


Fig. 3. The process

The result is a faster process. In both cases the transient response features a nice curve. The two real components have close to each other values.

The test for stability by frequency criterion in the middle of the recommended interval  $k/\omega_n = 0.2$  ( $k=2$ ;  $\omega_n=10$ ) is shown on figure 4. The system is stable and has a good stability margin:  $\Delta L \approx 10dB$ ,  $\Delta\varphi \approx 80^\circ$ .

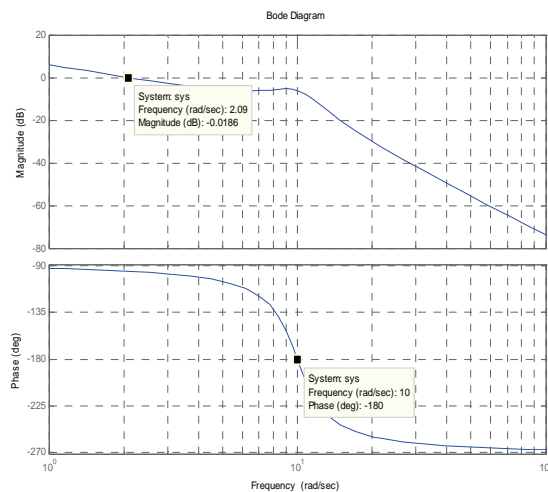


Fig. 4. The test for stability

The roots of the closed system in this case are:

$$p_{1,2} = -0.9584 \pm j 9.7513$$

$$p_3 = -2.0832$$

The imaginary part is tenfold bigger than the real one.

By  $\Delta = \pm 3\%$ , the transient response is 2.2, according to the formula  $t_p \approx \frac{4}{\xi\omega_n} \approx 2 \text{ sec}$ , which could also be seen on figure 5. It is recommended that the time value at the first peak in these processes is 1 [2].

The transient function has the form of an oscillating process, monotonous without overregulation. Here the deviation of the complex component with frequency  $\omega_n\sqrt{1-\xi^2}$  is added to the a-periodic component. This corresponds to a faster moderating oscillating component in comparison to a slower moderating exponential component of the real parameter, which is close to the imaginary axis. With the decrease of the imaginary component the amplitude is increased and the frequency of deviations is reduced – the process becomes oscillating with overregulation. The real root should correspond to the real component of the complex root, at the most 2-3 times bigger than the latter, then being a monotonous process, where the periodic component can be observed.

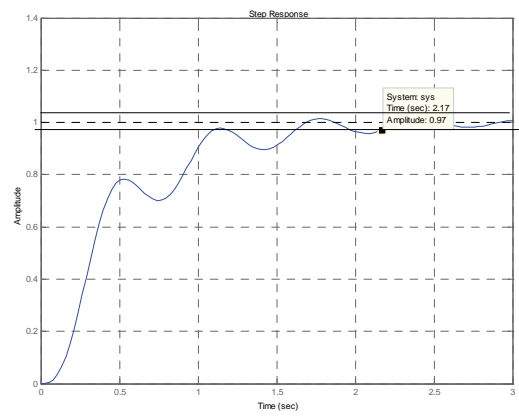


Fig. 5. The transient response

If the ratio stays the same, but there is a change in parameters:  $k=20$  at  $\omega_n=100$ , the result is displayed on figure 6.

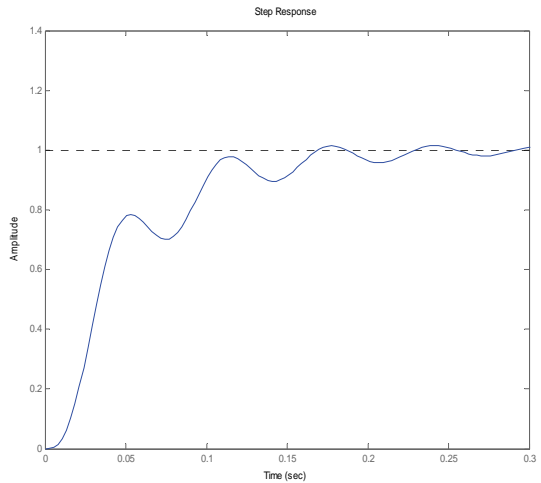


Fig. 6. The transient response

The process becomes faster, the amplification coefficient is increased, but its curve is still the same: oscillating monotonous, without overregulation.

If the ratio at the upper limits  $k/\omega_n=0.3$  ( $k=3$ ,  $\omega_n=10$ ) is changed, the roots become:

$$p_{1,2} = -0.4565 + 9.8475i$$

$$p_3 = -3.0870,$$

and the transient response is presented on figure 7.

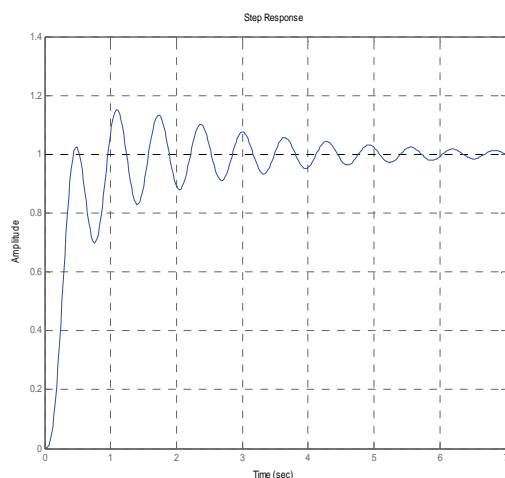


Fig. 7. The transient response

The process here becomes oscillating with overregulation of approx. 18%, which for real processes is up to 1 mm for a welding seam of 5mm width, and up to 6 mm for a welding seam of 30mm width, taking into account that a diagram of a stabilized power supply is reviewed.

The test for stability by frequency criterion (in the lowest value, middle of the recommended interval, at the upper limits) is shown on figure 8.

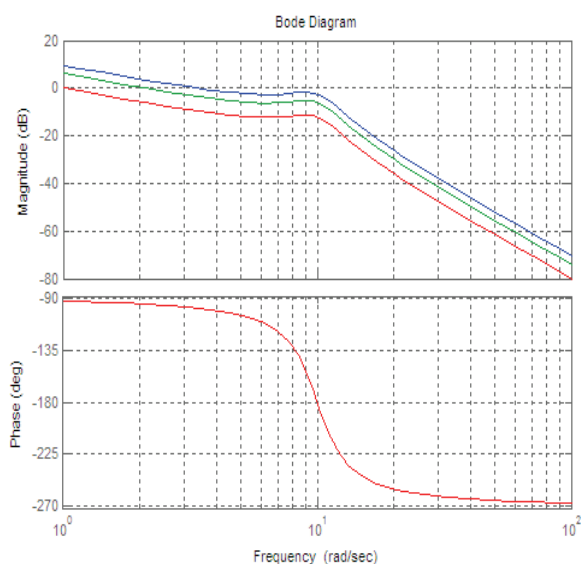


Fig. 8. The test for stability

By the simulation tests from the system at figure 1 a transient response is achieved, which is closest to the aperiodic one at values of  $k/\omega_n=0.1$ . With the ratio growth the oscillating character becomes even clearer – the real component of the complex roots decreases, i.e. the oscillation indicator increases (the ratio imaginary to real component of the dominant root). The influence of the real root weakens – it distances from the imaginary axis.

## REFERENCES

- [1] Gene Franklin, J. David Powell, Abbas Emami-Naeini, Feedback Control of Dynamic Systems, Pearson Education Inc., New Jersey, 2006.
- [2] Richard Dorf, Robert Bishop, Modern Control Systems, 2008.
- [3] <http://info-svarka.ru/oborudovanie/svarochnye-protsessy-kak-obekty-avtomaticheskogo-upravleniya>

**This Page Intentionally Left Blank**

# Neuro-Genetic Algorithm for Non-Destructive Food Quality Determination

Tanya Titova<sup>1</sup>, Veselin Nachev<sup>2</sup>, Chavdar Damyanov<sup>3</sup> and Nanko Bozukov<sup>4</sup>

**Abstract –** Hybrid neuro-genetic networks are a subclass of neural networks combining random-search methods with adaptive optimization with the direct analogy of natural selection and genetics in biological systems.

The paper tries to improve the efficiency of automated classifiers in the systems for automated quality determination and sorting via hybrid structures.

**Keywords –** Artificial Neural Network, Genetic Algorithm, Neuro-Genetic Algorithm, Food Quality.

## I. INTRODUCTION

Recent years have witnessed an increasing proliferation of information processing technologies based on the combination of methods belonging to different spheres of science and technology. There are many examples of experimental research which successfully integrate neural networks with methods pertaining to wavelet transform theory, genetic programming, fuzzy logic, etc [6,7].

The paper concentrates on the problems related to the improvement of neural network efficiency through hybrid structures featuring genetic algorithms.

## II. NEURAL NETWORKS

Artificial neural networks (ANN) have been thoroughly studied and tested for various applications. Nevertheless, there arise some problems that remain to be solved, which is challenging to ongoing research. One of these problems has to do with the determination of suitable network dimensionality and topology [5,8].

The design of a neural network (NN) is a complex task due to the fact that in most cases it is very difficult to find an optimal dimensionality (Fig. 1).

The methods for determining network architecture are subdivided into statistical and dynamic. Dynamic methods are commonly used since they can readily supply the network with an optimum dimensionality. These methods resort to

<sup>1</sup>Tanya Titova, Department Automation and Control Systems University of Food Technologies, 26 Maritsa Blvd, Plovdiv, 4002 Bulgaria, e-mail: t\_titova@abv.bg

<sup>2</sup>Veselin Nachev, Department Automation and Control Systems University of Food Technologies, 26 Maritsa Blvd, Plovdiv, 4002 Bulgaria, e-mail: v\_nachevbg@yahoo.com

<sup>3</sup>Chavdar Damyanov, Department Automation and Control Systems University of Food Technologies, 26 Maritsa Blvd, Plovdiv, 4002 Bulgaria, e-mail: chavdam@yahoo.com

<sup>4</sup>Nanko Bozukov, Department "Informatics and Statistics" at University of Food Technologies - Plovdiv, 26 Maritsa Blvd, Plovdiv 4002, Bulgaria, e-mail: bozukovnanko@abv.bg.

constructive (“growing”) or destructive (“pruning”) techniques or combinations.

According to the constructive method, a small neural network is set up and more neurons and connections are subsequently added until a balance is reached. The major drawback here is that the neural network in its final form is more complex than desired or needed.

The destructive method starts with a fully connected neural network (weights and neurons). Afterwards, the network is gradually reduced via a specific algorithm until the proper network structure is obtained. The basic problem lies in the complexity of the initial network and connection weight setup as well as in the assessment of their relative impact on the target function. It is also very difficult to find an evaluation function and network reduction rules on the basis of which the algorithm will be able to generate a sufficiently small network [2,6].

Evolutionary artificial neural networks (EANN) are being increasingly studied and applied. They are a subtype of ANNs

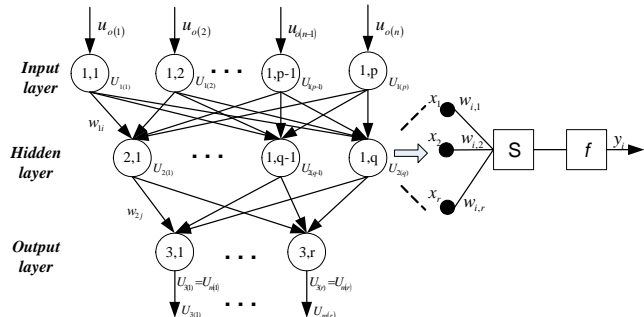


Fig.1. Typical Structure of Neural Networks

constituting hybrid structures which use an evolutionary strategy. Evolutionary algorithms can be applied to the optimization of neural systems so that various problems can be solved, such as connection weight determination, training, architecture synthesis, feature selection, connection with initialization weights, solution that ends the ANN training, etc. EANNs may also be adapted to an environment with recurring changes in the conditions, such as composition, sample size, number of classes, etc.

In essence, the problem is defined thus: if there are  $H$ -number neurons in the hidden layer, then there are  $O(2^{H^2})$  network typologies. With a calculation complexity of this kind, it is expedient to look for a suboptimal solution using efficient heuristic algorithms.

Genetic algorithms (GA) are widely applied as such. They are a combination of heuristic rules and stochastic search algorithms, which some authors believe to be the only possible means of finding an optimal solution.

### III. GENETIC ALGORITHMS

Genetic algorithms (GA) are based on a stochastic method for global search and optimization which imitates the evolution of living organisms delineated by Charles Darwin in his "On the Origin of Species by means of Natural Selection". For the most part, these algorithms feature operators which select the individuals (solutions) to reproduce themselves and generate new individuals on the basis of those that have already been selected and determine the composition of the population for the next generation. Crossover and mutation operators are the most important ones participating in this procedure. GAs belong to the group of evolutionary algorithms.

Evolutionary algorithms make use of the three basic principles of natural evolution as described by Darwin: natural selection, variety of individuals and reproduction, maintained via the differences between prior and subsequent generations. In the 1960s, these three characteristics of natural evolution inspired a number of researchers to come up with independent stochastic search methods:

- *Evolutionary programming*
- *Evolution strategies*
- *Genetic algorithms*.

All three methods work with a range of individuals. The selection principle is applied by means of a criterion evaluating the proximity between the individual and the solution desired. The most adaptable individuals proceed to the next generation [5].

The huge variety of problems, not only engineering ones but also problems belonging to other spheres of knowledge, necessitates the application of algorithms of a different type, with different characteristics and configuration. This necessity is responsible for the multitude of different evolutionary algorithms and the great number of researchers working on them.

The GA principle holds as follows:

1. An initial set of combinations (populations) is randomly selected  $I_0 = \{i_1, i_2, \dots, i_s\}$  and it is postulated that

$$f^* = \max(f(i) \mid i \in I_0), \quad k := 0$$

2. Until the ending criterion (specific time or number of generations) is fulfilled, the following is carried out:

2.1. Selection of parents  $i_1$  and  $i_2$  from the population  $I_k$  - selection operator. Proportionate selection (roulette wheel selection) is used. The probability for a  $k$ -step solution  $i$  being a parent is:

$$P(i - \text{selected}) = f(i) / \sum_{i=1}^{I_k} f(i), \quad i \in I_k$$

2.2. Constructing  $i^l$  on the basis of  $i_1$  and  $i_2$  - crossing-over operator. The operator is performed with a  $P_c$  probability and for a random point of separation (Fig. 2). If the operator is not realized (with a  $1 - P_c$  probability), the offspring takes after its parents.



Fig. 2. Tentative diagram of a crossing-over operator.

2.3. Modification of  $i^l$  - mutation operator.

The operator is realized with a  $P_m$  user-defined probability.

2.4. If  $f^* < f(i^l)$ , then  $f^* := f(i^l)$ .

2.5. Population renewal ( $k := k + 1$ ).

### IV. NEURO-GENETIC ALGORITHMS

Neuro-genetic algorithms make use of the combination of an artificial neural network (ANN) and genetic algorithms (GA) to optimize the NN parameters. When the parameter values of a NN are initially entered, they are not usually optimal. That is why GAs are used to determine the weights of the network, suitable training parameters or reduce the size of the training sample by opting for the most significant features and network structure. The network structure to a great extent determines the network efficiency and the problems which it will be able to solve. We know that in order to determine non-linearly separable classes, the network must have at least one layer between inputs and outputs but the determination of the number and size of the hidden layers is commonly defined on the basis of expertise. The number of the input variables accounts for the dimensionality of the neural network. To avoid the problems with its re-training and improve its work, the number of the input variables should be smaller. A GA can optimize the inputs by generating proper network architecture for a specified data range. The preliminary processing of the data is also essential for discovering information and eliminating improper or undesirable features. Many researchers are highly interested in the transformation and selection of a subset of features. Hence, it is vital to optimize the structure of ANNs [1,3,4].

The flowchart of the hybrid neuro-genetic approach is shown in Fig. 3. It has been applied to potato classification.

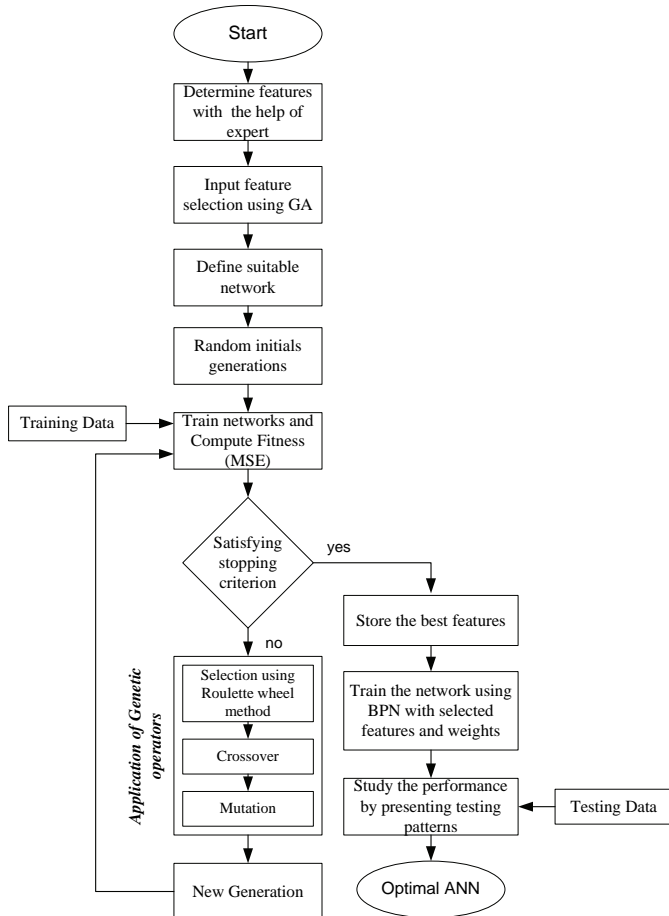


Fig. 3. Hybrid Neuro-Genetic Algorithm

The results demonstrate that this approach is likely to enhance precision compared to the results obtained from classification using only a NN and backpropagation.

The hybrid neuro-genetic algorithm holds as follows:

1. The features are determined with the help of experts.
2. Initialization of count=0, fitness=0, number of cycles
3. Generation of an initial population. The individual's chromosome is formulated as a sequence of genes, each of which is encrypted at the input.
4. Design of a proper network (input, hidden and output layers)
5. Determination of the weight for each connection.
6. NN training with backpropagation.
7. Finding the accumulated error and the value of the fitness function. Genotypes are evaluated on the basis of a fitness function.
8. If the preceding fitness function is smaller than the current fitness value, the current function is kept.
9. count = count +1
10. The selection: the two parents are selected by means of the roulette wheel principle, i.e. randomly.
11. The genetic operations of crossover, mutation and reproduction generate new characteristics (and new weights are applied for each connection).
12. If (the number of cycles <= count), then point 4.
13. The NN is trained with the features selected.
14. The NN is tested with the testing sample.

## V. EXPERIMENTS AND RESULTS

### A. Materials

Potatoes are classified on the basis of the presence and degree of damage of the tubers (internal and external defects, diseases, genetic anomaly, injuries, etc.). The expert classifies each tuber into one of the following classes - D<sub>1</sub> (1<sup>st</sup> quality), D<sub>2</sub> (2<sup>nd</sup> quality) и D<sub>3</sub> (3<sup>rd</sup> quality). Each realization U[n] of the light transmission coefficient consists of L=25 values, registered by the longitudinal scanning of the tuber. The U[n] function possesses almost complete spectrophotometric information about the product and is invariant to disturbances and product thickness.

The reference evaluation and classification of the potato tubers was carried out with the help of the methodology outlined in [2]. It is worth pointing out that the recognition algorithm does not diagnose the disease of the infected potato but identifies only the presence of a defect in the tissue. As a result of scanning, signals are received which are proportional to the optical densities of transmission OD<sub>T</sub> and reflection OD<sub>R</sub>. The signals have different shapes depending on the respective wavelength, the shape and size of the tubers, the presence and location of the defects.

### B. Experimental

In a MATLAB environment, various structures of neural networks were tested experimentally. As shown in Fig. 3, for the realization a feature selection algorithm was used. Therefore, the feature vector is represented by a feature bit mask fig.p where N refers to the initial set of features while the possible solutions in this case amount to  $2^N - 1$ .

TABLE I  
FEATURE VECTOR ENCODING

FEATURES	S1	S2	S3	S4	...	SN
FEATURE BIT MASK (CHROMOSOMES)	0	1	1	0	...	1

The other basic elements of the algorithm are realized via training modules which are presented in the most generalized fashion by the following pseudocode:

#### Learning program fragment:

```

% Create a neural network
net = feedforwardnet(n);
net.layers{1}.transferFcn = 'tansig';
net.layers{2}.transferFcn = 'logsig';
% Configure the neural network for this dataset
net = configure(net, inputs, targets); view(net)
% Create handle to the MSE_TEST function, that calculates MSE
h = @(x) mse_test(x, net, inputs, targets,B,instances)
% Set of Parameters of Genetic Algorithms
ga_opts = gaoptimset('TolFun', 1e-20,'display','iter','Generations',1000);
% Running the genetic algorithm with desired options
[x_ga_opt, err_ga] = ga(h,(n*n+n+3*n+3),ga_opts);
Fitness function:
function mse_calc = mse_test(x, net, inputs,
targets,B,instances)
net = setwb(net, x');
y = net(inputs);
  
```

```
% Calculating the mean squared error
length(y);
mse_calc = sum(sum((y-targets).^2))/length(y);
end
```

### C. Calculation errors

Total (resultant) error is determined by the formula:

$$e_0 = \frac{100}{m} \sum_{i=1}^N \left( \sum_{k=1}^N m_{ik} - m_{ii} \right), \%$$

or  $e_0 = 1 - (\sum_{i=1}^N m_{ii}) / m = 1 - Acc.$

where:  $m = \sum_{k=1}^N m_k^c$  is the total number of objects in the training sample. The total error can also be calculated by the equivalent formula:

$$e_0 = \sum_{i=1}^N e_i P(D_i),$$

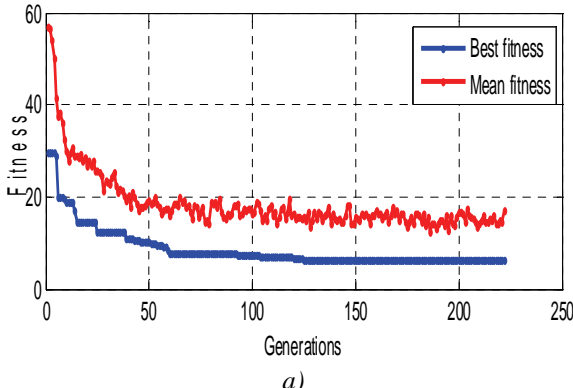
where  $P(D_i) = m_i^c / m$ , ( $i = 1, 2, \dots, N$ ) are the a priori probabilities of distribution of the objects of the respective classes  $i$ . According to the rule:  $\sum_{i=1}^N P(D_i) = 1$ , because the features  $S \in D_i$  form a complete group of incompatible events.

After the training the performance of the algorithm, and more precisely its accuracy, is evaluated using a control (test) sample. The resulting error of the test is shown in table of errors, which in the particular case of Table II .

TABLE II  
RESULTS OF THE CLASSIFICATION

GENERAL ERROR E, %	MULTIPLAYER PERCEPTRON NETWORKS	NN WITH GA OPTIMIZATION	NN WITH GA OPTIMIZATION AND FEATURE SELECTION
TRAIN SET	6,58	6,73	6,82
TEST SET	9,58	7,60	6,47

These are trends in a NN genetic training by using the primary feature space and feature selection (Fig. 4.).



a)

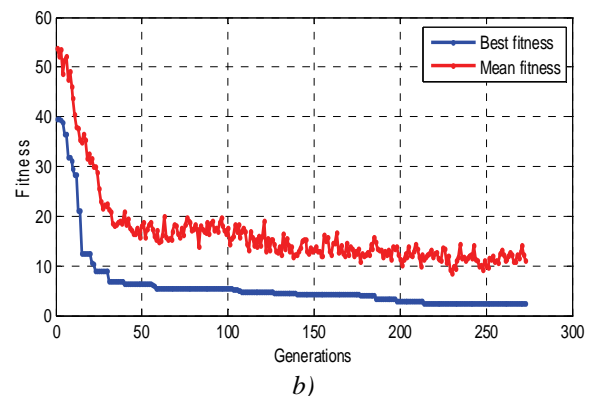


Fig. 4. Trends in a NN genetic training by using the primary feature space a) and feature selection b)

## VI. CONCLUSION

Experimentally, it was proven possible to adapt the genetic algorithms and Neural Networks in hybrid structure to spectral image recognition methods related to potato quality evaluation and classification problems.

The results in Table 2 demonstrate the advantages of hybrid neural-genetic algorithms for classification to Multilayer Perceptron Networks and structural genetic algorithm to optimize neural network architecture.

## REFERENCES

- [1] Admuthe L. S., S. D. Apte, Neuro-Genetic Cost Optimization Model: Application of Textile Spinning Process, International Journal of Computer Theory and Engineering, Vol. 1, No. 4, 441-444, October 2009
- [2] Damyanov C., Non-destructive Quality Evaluation in Automatic Sorting Systems, UFT Academic Publishing House, Plovdiv, p.360, 2006
- [3] Petridis V., Paterakis E., Kehagias "A hybrid neural-genetic multimodel parameter estimation algorithm" IEEE Trans. on neural networks, vol.9 no.5 1998
- [4] Shanthi D., Dr.G.Sahoo, Dr.N.Saravanan. Input Feature Selection using Hybrid Neuro-Genetic Approach in the Diagnosis of Stroke Disease, IJCSNS International Journal of Computer Science and Network Security, Vol.8 No.12, 99-107, December 2008
- [5] Siddique, M.N.H.; Tokhi, M.O, Training neural networks: backpropagation vs. genetic algorithms, International Joint Conference on Neural Networks, Vol. 4, p. 2673 – 2678, 2001
- [6] Titova T., V. Nachev A structural genetic algorithm to optimize neural network architecture, "Food Science Engineering and Technology 2007" Scientific Works of the UFT - Plovdiv, Volume LIV, St. 3, 101-107, 19-20.10. 2007
- [7] Titova T., V. Nachev, Ch. Damyanov. Application of Genetic Algorithms for Neural Networks Trainings, International Conference Automatics and Informatics' 07, II-9-II-12, October 3 – 6, 2007, Sofia
- [8] Wang W. J., Tang X. C., Li W. C., A variable structure neural networks model and its applications, IEEE TENCON, Vol. 2:5, p. 799-802, 1993

# 11DoF inertial system for dynamics analysis of moving objects

Rosen Miletiev<sup>1</sup>, Emil Iontchev<sup>2</sup>, Ivaylo Simeonov<sup>3</sup>, Rumen Yordanov<sup>4</sup>

**Abstract** - The current paper proposed 11 DoF system based on 3-axis accelerometer, 3-axis gyroscope, 3-axis magnetometer, barometer and GPS receiver to calculate the dynamic response of the moving device and to solve the navigation tasks by combination of the IMU and GPS systems. Also GSM/GPRS modem is built-in to send the inertial and navigation data via GPRS connection to remote server to meet the real-time requirements. The experimental data are accomplished to represent the system possibilities to read, store and send the inertial and navigation data.

**Keywords** - inertial navigation, IMU system

## I. INTRODUCTION

The dynamics analysis and localization of the moving objects define the necessity of the information and communication system with maximum number of degrees of freedom. MEMS technology allows production of small, cheap and low power consumption devices which may measure the linear and angular accelerations and may be used in different commercial applications [1]. Unfortunately the low-cost MEMS devices need of algorithms for compensation of their disadvantages, such as GPS-IMU system integration [2] to reduce the numerical integration errors, barometer – accelerometer combination [3] to reduce the dependency of the accelerometer data over the inclination or combined algorithms for calculation of the heading angle in the compass system [4].

The current paper proposed 11 DoF system based on 3-axis accelerometer, 3-axis gyroscope, 3-axis magnetometer, barometer and GPS receiver to calculate the dynamic response of the moving device and to solve the navigation tasks by combination of the IMU and GPS systems. The existing IMU measurement systems are combined only with a GPS receiver [5] and some of them also have build-in GSM modem, but the sampling frequency is much lower [6]. The sampling frequency in these systems varies from 20Hz [5] to 84Hz [7] while the proposed system read the inertial and navigation data

<sup>1</sup>Rosen Miletiev is with the Faculty of Telecommunications at Technical University of Sofia, 8 Kl. Ohridski Blvd, Sofia 1000, Bulgaria. E-mail: [miletiev@tu-sofia.bg](mailto:miletiev@tu-sofia.bg)

<sup>2</sup>Emil Iontchev is with the Higher School of Transport “T. Kableshkov” 158 Geo Milev Street, Sofia 1574, Bulgaria, E-mail: [e\\_iontchev@yahoo.com](mailto:e_iontchev@yahoo.com)

<sup>3</sup>Ivaylo Simeonov is with the Faculty of Computer Systems and Control at Technical University of Sofia, 8 Kl. Ohridski Blvd, Sofia 1000, Bulgaria, E-mail: [ivosim@abv.bg](mailto:ivosim@abv.bg)

<sup>4</sup>Rumen Yordanov is with the Faculty of Electronic Engineering and Technologies at Technical University of Sofia, 8 Kl. Ohridski Blvd, Sofia 1000, Bulgaria, E-mail: [yordanov@tu-sofia.bg](mailto:yordanov@tu-sofia.bg)

with sampling frequency of 100Hz to minimize the integration errors. It is shown that the proposed system is capable to send the inertial and navigation data to database server in real-time situations and the navigation error may be reduced to increase the inertial navigation accuracy.

## II. SYSTEM DESCRIPTION

The system block diagram is shown at Figure 1. It consists of the following main blocks used in the experiments:

- IMU system – 9DoF system, consists of 3D linear accelerometer, 3D gyroscope and 3D magnetometer, which are integrated in the single IMU unit, produced by Atmel. One of the supported IMU systems is 9DoF Atmel Inertial One ATAVRSBIN1 board, which contains:
  - InvenSense three-axis MEMS gyroscope (ITG-3200)
  - Bosch Sensortec three-axis MEMS accelerometer (BMA150)
  - AKM three-axis electronic compass (AK8975)
  - Temperature sensing through ITG-3200 or BMA150.
 The second supported IMU system is Atmel Inertial Two ATAVRSBIN2 board which contains:
  - InvenSense three-axis MEMS gyroscope (IMU-3000<sup>TM</sup>)
  - Kionix® three-axis MEMS accelerometer (KXTF9)
  - Honeywell three-axis electronic compass (HMC5883)
  - Temperature sensing through IMU-3000.
 The microcontroller read the data from the IMU system via CH0 channel of I<sup>2</sup>C multiplexer.
- MEMS barometer based on the Atmel ATAVRSBPR1 board, which contains the high precision Bosch Sensortec digital pressure sensor (BMP085) with a temperature control and correction of the barometric data. The microcontroller read the data from the barometric board via CH1 channel of I<sup>2</sup>C multiplexer.
- I<sup>2</sup>C multiplexer based on PCA9540, which is 1-of-2 bi-directional translating multiplexer, controlled via the I<sup>2</sup>C bus. The SCL/SDA upstream pair fans out to two SCx/SDx downstream pairs or channels. The I<sup>2</sup>C multiplexer allows connecting two identical boards to the system expansion slots to increase the reliability for some critical applications such as unmanned devices.
- Micro SD card – The additional flash memory up to 2GB is used to record the inertial, navigation, magnetic, temperature and barometric data. The microcontroller read/write the data from/to the micro SD card via SPI interface (MSSP1 module).
- GPS receiver – The navigation data are obtained by the GPS/GNSS module (LEA 6S) produces by Swiss-based

ublox. This module has been designed for low power consumption, low costs and UART, USB and DDC ( $I^2C$  compliant) interfaces. The GPS receiver is capable to update the navigation data up to 10Hz.

- GSM/GPRS modem is used to send the navigation and inertial data to the database server at a real-time. It is based on the quadband GSM (LEON G100) produced by the same company due to the simple integration of u-blox GPS and A-GPS and quad-band GSM/GPRS, class 10.
- Microcontroller – The 8-bit high performance RISC PIC18 microcontroller is used to read the navigation and inertial data and to control the external devices according to their position. The PIC18 microcontrollers are optimized for C programming and have advanced peripherals (SPI/ $I^2C$ ™, UARTs, PWMs, 10-bit ADC, etc.).

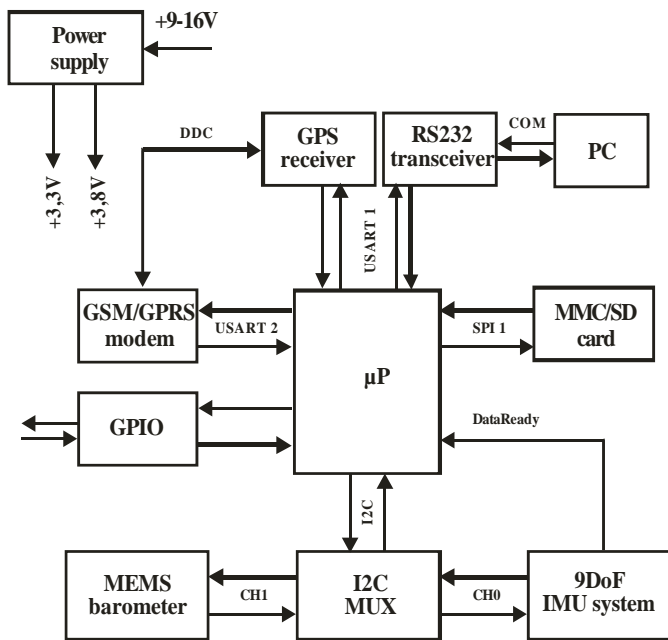


Figure 1. System block diagram

One of the system specific features is fastened with the  $I^2C$  multiplexer, so the reading algorithm had to be capable to switch between the both  $I^2C$  channels.

The data acquisition algorithm is shown at Figure 2. It consists of 10 frames with time duration of 10ms, so the 10 frames form 100ms duration data block. This data block contains of:

- NMEA 0183 RMC message (maximum 80 bytes);
- NMEA 0183 GGA message (maximum 80 bytes);
- 10 measurements of the 3-axis linear accelerometer (60 bytes);
- 10 measurements of the 3-axis gyroscope (60 bytes);
- 5 measurements of the 3-axis magnetometer (30 bytes) multiplexed with 5 temperature measurements from accelerometer and gyroscope (30 bytes);
- 1 barometer measurement and 1 temperature measurement of the barometer temperature for temperature corrections of the pressure.

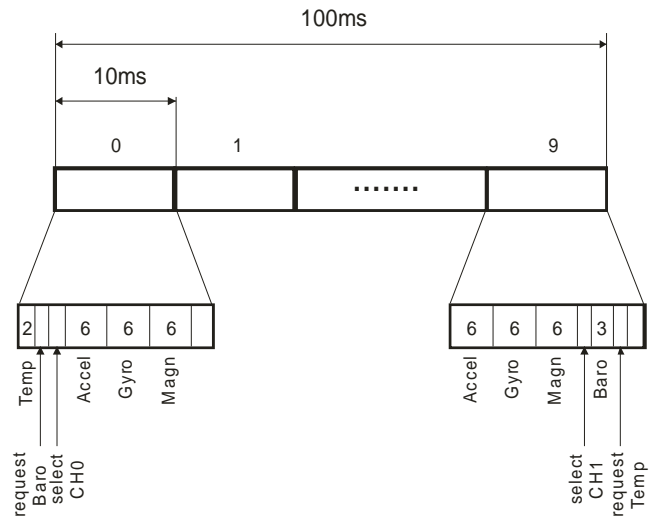


Figure 2. Data acquisition algorithm

The data acquisition algorithm is agreed with the time conversion requirements of the barometer. The temperature measurement requires 4.5ms delay while the ultra high resolution pressure measurement – at least 25.5ms. The establishment of the corrected temperature and pressure data are accomplished on the basis of the barometer calibration EEPROM values and Bosch BMP085 Barometer Floating Point Pressure Calculations.

### III. EXPERIMENTAL DATA AND ANALYSIS

An experimental test of the system is accomplished to test the ability of read, store and send the inertial and navigation data to the remote server. The data are recorded to the local system FLASH memory (micro SD card with capacity of 2GB) and after that the data are processed using MATLAB routine. The orientation of the IMU axes in relation to the vehicle axes is shown at Figure 3.

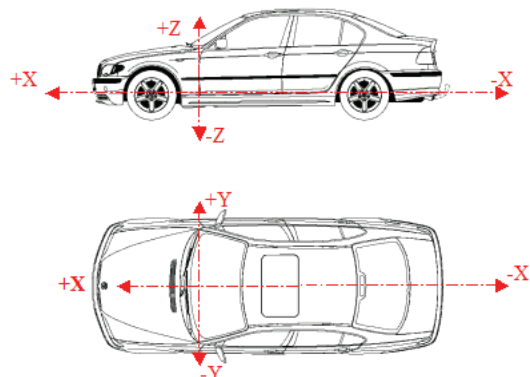


Figure 3. IMU axes orientation

The results are shown at the following figures:  
 Figure 4. X,Y,Z accelerometer data respectively;  
 Figure 5. Atmospheric pressure graph;  
 Figure 6. X,Y,Z gyroscope data respectively;  
 Figure 7. Altitude graph (GPS data);  
 Figure 8. X,Y,Z magnetometer data respectively;  
 Figure 9. Driving track (latitude/longitude)

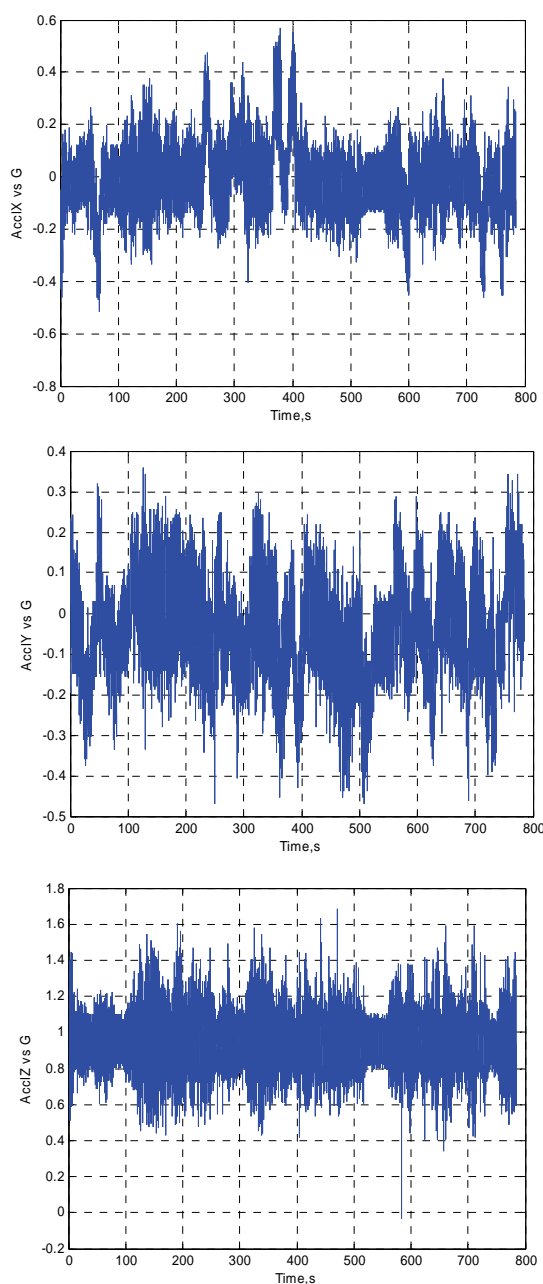


Figure 4. X,Y,Z Accelerometer data

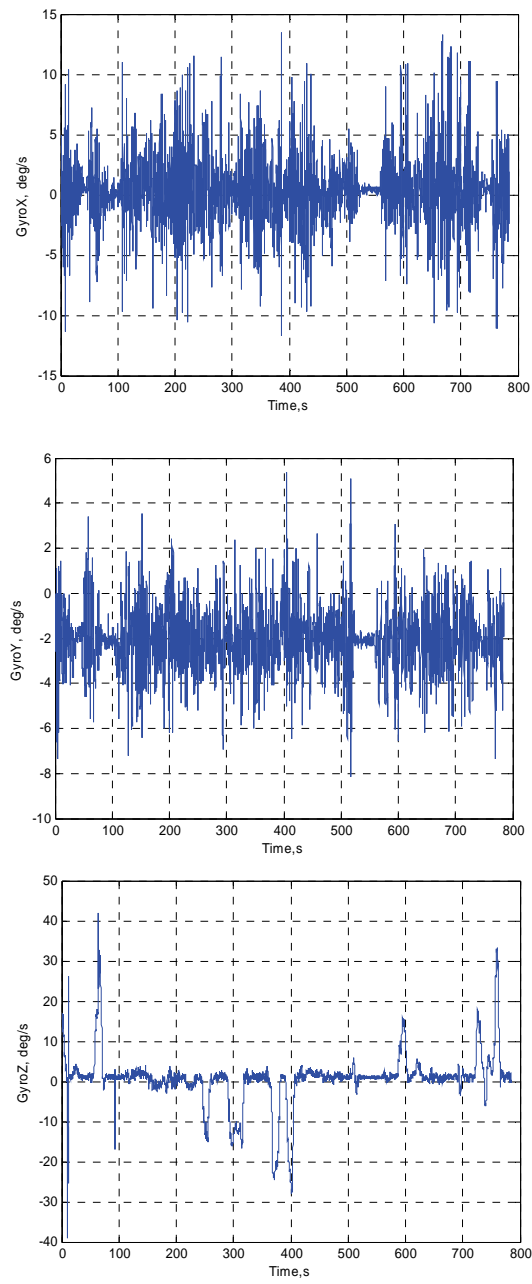


Figure 6. X,Y,Z gyroscope data

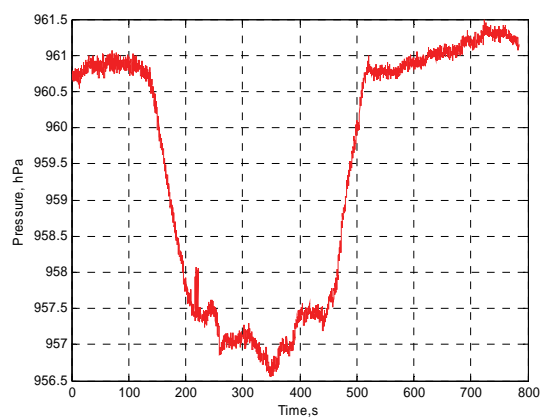


Figure 5. Barometer data

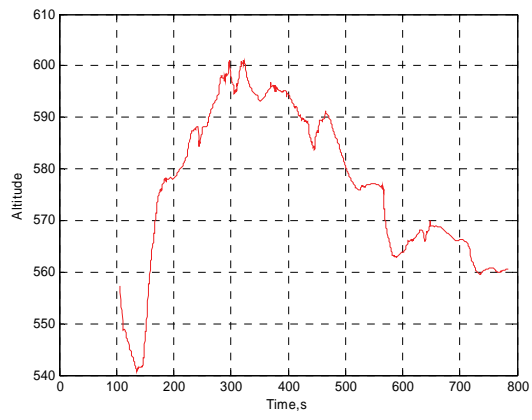


Figure 7. Altitude graph

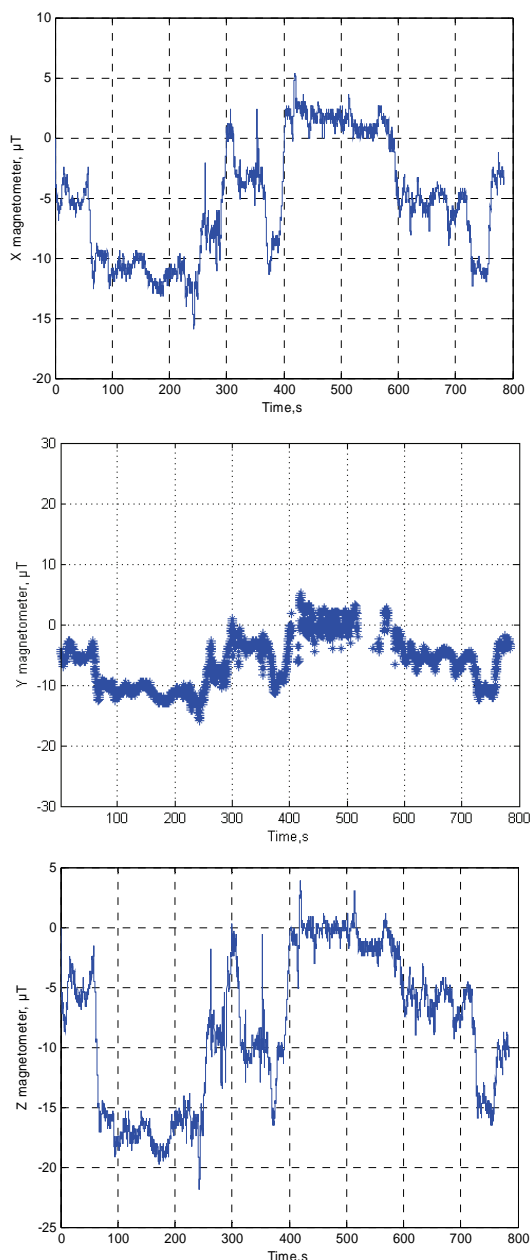


Figure 8. X,Y,Z magnetometer data

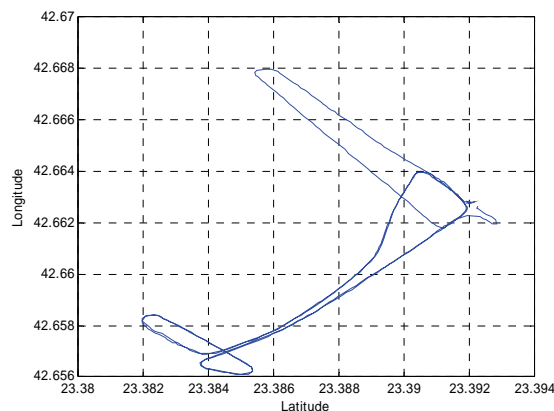


Figure 9. Driving track

The shown graphic data proof the system ability to read all linear and angular accelerations, atmospheric pressure and GPS data and all chip temperature sensors (temperature graphs are not shown). The MEMS sensor information may be used for localization purposes when GPS signal is lost or is not available.

#### IV. CONCLUSIONS

The current paper discusses the 11DoF IMU system which is capable to all inertial and navigation data to solve the navigation tasks by combination of the IMU and GPS systems.

The design of this system is inspired by the need of a high speed IMU system which is capable to store locally and send data to remote server. The existing systems are distinguished with the first or second feature while the proposed system combines the both ones. The system may be used for inertial navigation based on the EKF (Extended Kalman filter) due to the high sampling frequency and small integration errors, gyro stabilized platforms, platform control due to the PWM interface, MVEDR (Motor Vehicle Event Data Recorder) systems or crash monitor for aircrafts, trains or cars.

#### ACKNOWLEDGEMENT

This paper was prepared and supported by the National Fund under contract number No.DTK02/2-2009.

#### REFERENCES

- [1]. Stephen Beeby, Graham Ensell, Michael Kraft, Neil White, MEMS Mechanical Sensors, Artech House, Inc., 2004
- [2]. Mohinder S. Grewal, Lawrence R. Weill, Angus P. Andrews, Global positioning systems, inertial navigation and integration, John Wiley & Sons., Inc., 2007
- [3]. Jussi Collin, G. Lachapelle, Jani Käppi, MEMS-IMU for Personal Positioning in a Vehicle – A Gyro-Free Approach, GPS 2002 Conference (Session C3a), Portland, OR, 24-27 September, U.S. Institute of Navigation
- [4]. www.st.com, AN3192, Application note, Using LSM303DLH for a tilt compensated electronic compass, Doc ID 17353 Rev 1, August 2010
- [5]. Pifu Zhang, Jason Gu, Evangelos E. Milios, and Peter Huynh, Navigation with IMU/GPS/Digital Compass with Unscented Kalman Filter, Proceedings of the IEEE International Conference on Mechatronics & Automation Niagara Falls, Canada, July 2005
- [6]. Luu Manh Ha, Tran Duc Tan, Chu Duc Trinh, Nguyen Thang Long, Nguyen Dinh Duc, INS/GPS Navigation for Land Applications via GSM/GPRS Network, Proceeding of 2nd Integrated Circuits and Devices in Vietnam (ICDV2011). ISBN: 978-4-88552-258-1, pp.30-55
- [7]. Salah Sukkarieh, Eduardo M. Nebot, and Hugh F. Durrant-Whyte, A High Integrity IMU/GPS Navigation Loop for Autonomous Land Vehicle Applications, IEEE TRANSACTIONS ON ROBOTICS AND AUTOMATION, Vol. 15, No. 3, June 1999

# Principles and Methods of Data Models Creation Within Automated Control Systems

Zoya Hubenova<sup>1</sup>, Antonio Andonov<sup>2</sup>, Vladimir Gergov<sup>2</sup>

**Abstract –** The article addresses the problems of automating the decision making process and management of multifunctional complex (technical) objects taking into account the man – operator's availability and the informative provision of its activities. The following is referred to: the principles of analysis and synthesis of information models and the factors that influence the quality of performance of the control systems. Algorithmic method is proposed to form a pattern reflecting the key action of the operator in emergency conditions.

**Keywords –** automated systems, informational model, man – operator.

## I. TOPICALITY

The contemporary methods of complex objects control, transmitting and processing information, and the central control systems of technological processes represent complex man – machine facilities. Within these both technical appliances and staff actions are unified. The efficiency of such systems depends on the man – operator's and technics' coordination.

In this paper, the automatized control system (ACS) is examined as an aggregate of technical means and the man – operator (MO). Its main features are stability, controllability, and observability which define the system's quality. The systems stability is determined by the controllability, i.e. the aptitude for reducing the controlled object to a state previously given by means of control influence. It is also determined by the possibility of observing the controlled objects' state. Both properties controllability and observability are related to each other, i.e. the system is fully controllable if and only if the connected system is also observable and vice versa. Within the ACS there is a process of information compressing and processing while information is either being lost or distorted inevitably, [1, 2, 9].

The availability of the MO within the ACS justifies the necessity of increasing the control system efficiency on the account of heuristic capabilities inherent to the human factor in unexpected and poor formulated situations. The human activity is reduced to perception and assessment the information, making and implementing decisions, [4], the MO's availability enhances the system ability to adapt during operations under unexpected situations. Another peculiarity of its work is the reciprocal action with the information objects

and the influence exerted upon the objects through a remote control, not the interaction with the real objects. One of the main factors, exerting influence on both the quality of MO's activity and therefore the system as a whole, is the *information security* of its activity.

The information model (IM), in its capacity of the most important compound of the information security, represents particular organizational cumulative information at the ACS operator's disposal, [3, 5, 10]. The state information is usually a combination of information models of the interacting objects which are perceived through information display means. The information model is defined as organized, according to a set of rules, image of the labor ways and means, the system "man-machine" (SMM), external environment, and ways to influence them. Following the model, the operator captures the image of the object, its state at any point in time and makes a decision. The information model combines two fields: sensor (sensitive), consisting of signaling devices, i.e. devices, indicators, audible signals, screens, etc., and sensorimotor, consisting of controls, i.e. knobs, levers, buttons, cutoffs, switches, and more. The information model sensing field includes all signals perceived by the operator directly from the machine.

The means of information display are part of the MO's working place meant to form the IM [6]. Thus, the information model is considered as a set of objects (phenomena, processes) data presented to the MO. The operator perceived the direct information visually (over 90%) and in acoustic way by means of information display ways and means.

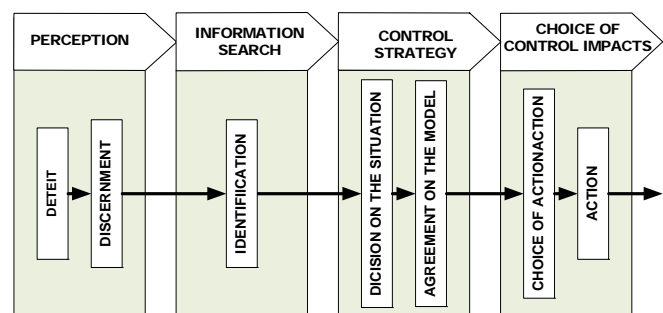


Fig. 1. Information reception by the MO within ACS.

The IM perception process, as a result of which the image of subject forms, occurs by means of information included in the *conceptual model* formed within the MO's memory. The model is a set of MO's ideas about goals and objectives of the labor activity and conditions of the ways of work, the SMM, external environment and means of influence.

The activity information security influence upon the MO's performance is determined firstly by the integrity and completeness of the IM, secondly by the organization of

<sup>1</sup>Space Research and Technology Institute – BAS, Acad G. Bonchev Str., Bl. 1, 1113 Sofia, Bulgaria, E-mail: [zhubenova@space.bas.bg](mailto:zhubenova@space.bas.bg)

<sup>2</sup>University of Transport Todor Kableshkov, 158 Geo Milev str., 1574 Sofia, Bulgaria, E-mail: [andonov@vtu.bg](mailto:andonov@vtu.bg), [gergov@vtu.bg](mailto:gergov@vtu.bg)

means that convey information to the MO, and finally by the quality of the conceptual model. The IM could be described from morphological (structure of the studied system), functional (application), and organizational point of view, [9]. Basic concepts of morphological descriptions are the composition and the volume. Having considered the specifics of IM as an abstract linguistic system, its morphological and organizational descriptions might be merged. In order to establish a functional description of the IM, it is necessary to analyze the basic principles of receiving and processing information from the MO to the ACS.

## II. PRINCIPLES OF OPTIMAL ORGANIZATION OF THE IM.

The man's paradigm as a section of information processing is based on the general laws of control processes within living and non-living systems: the equivalent unit paradigm is based on the MO's specific actions depending on its personal characteristics and information security of its activities; the IM paradigm are not limited to the MO's interaction with the object, rather with its IM; the operational paradigm reflects the MO's adaptability to the conditions and the means necessary for its activities in accordance with its task previously assigned.

Having unified these paradigms, we are allowed to form the general principles of analysis and synthesis of the IM.

*Target compatibility principle:* non-discrepancy of the objectives of the man and entire ergatic system (ES) and, therefore, MO's ways of interaction (material, energy and information resources by means of which the man implements its activity) with the entire system. The realization of this principle implies assessment of the IM in terms of man's conformity and complexity of the problem being solved [7].

Possible formalization can be done by assuming that  $S_i^g$  is one of the target functions of the ES ( $i \in N$ , where  $N$  is the number of activities functions being considered) and  $S_j^c$  is one of the target functions concerning the entire ES. Then the principle of target compatibility will be determined by:

$$(\forall i \in N)(\exists j \in M)(S_i^g \cap S_j^c \neq \emptyset) \quad (1)$$

This principle can be refined further. Firstly, by means of identifying the need to link the indicators of the quality of the business resources and the quality of human activity itself enabled by these means.

$$\begin{aligned} (\forall y_{ij} : i \in N_j, j \in L)(\exists f_{ij} : K^j = \\ = f_{ij}(y_{ij}, y_{kj} = i \text{ dem}), \end{aligned} \quad (2)$$

where  $y_{ij}$  is a quality indicator of the  $j^{\text{th}}$  mean of activity in terms of the  $i^{\text{th}}$  property;  $N_j$  is the set of relevant properties of the  $j^{\text{th}}$  mean;  $L$  is the set of means of activity;  $K^j$  is quality of the operator's activity through the  $j^{\text{th}}$  mean;  $f_{ij}$  is function of the quality of the activities carried out by the operator in terms of the  $j^{\text{th}}$  mean in terms of the  $i^{\text{th}}$  property.

Secondly, it is necessary to perform a possibility to explicitly include the quality indicator in terms of the  $j^{\text{th}}$  activity mean of the ES quality indicator.

$$\begin{aligned} \bar{Y} &= \{ \bar{y}_1, \bar{y}_2, \dots, \bar{y}_j, \dots, \bar{y}_l, \bar{x}_1, \bar{x}_2, \dots, \bar{x}_k, \dots, \bar{x}_m \} \\ \bar{Y}_j &= \{ y_{1j}, y_{2j}, \dots, y_{ij}, \dots, y_{nj} \} \quad (3) \\ \bar{X}_k &= \{ x_{1k}, x_{2k}, \dots, x_{ik}, \dots, x_{rk} \}, \end{aligned}$$

where  $Y^-$  is the ES quality indicator;  $y_i$  are quality indicator of the ES  $j^{\text{th}}$  component related to the MO's means of activity;  $L$  is a set of the ES elements related to the manufacture ways and means;  $N_j$  is a set of  $j^{\text{th}}$  mean properties under consideration ( $j=L^-$ );  $X^-$  is the quality indicator of the ES  $k^{\text{th}}$  compound that is not related to the manufacture ways and means;  $R_k$  is a set of ES elements which are not related to the MO's activity manufacture ways and means  $k=M^-$ .

Implementing this principle provides development of indicators for selecting the most rational option as regards the MO's ways of activity as well as optimization within the entire system in order to synthesize the whole set of means of MO's information security.

*Optimality principle:* it determines possible approaches toward IM optimization, both in terms of the best solution from many possible and in the sense of bringing IM into an optimum condition. Among the entire possible set ( $T$ ) of IM, each element of which is distinguished by a certain quality indicator vector  $Y_{\langle m \rangle}(T_j)$ , the optimal  $T^{\text{opt}}$  is this one which is distinguished by such vector  $Y_{\langle m \rangle}(T^{\text{opt}})$  so that the last vector component is less than the relevant component of another arbitrary vector  $Y_{\langle m \rangle}(T' \in T)$ , i.e.

$$Y_{\langle m \rangle}(T_i \in T) = \{ y_1(T_i), y_2(T_i), \dots, y_i(T_i), \dots, y_{\langle m \rangle}(T_i) \} \quad (4)$$

$$Y_i(T^{\text{opt}}) \geq Y(T'), [i = \overline{1, M}] \quad (5)$$

Implementing this principle defines the possible approaches toward IM optimisation, i.e. the best option selection among the other possible as well as putting IM into its optimal condition.

Particular principles characterizing the specific requirements that the IM should meet and determining the man's role into the automated system are following:

1) Principle of minimum operating effort – the MO has to perform the work required and this part of work that cannot be performed by the system at that.

2) Principle of maximum mutual understanding - the system provides maximum support to the MO, i.e. the information provided should not require / allow interpretation and recoding.

3) Principle of minimum volume of user RAM - the person is required to memorize as little as possible.

4) Principle of maximum control done by MO – the operator must be able to control the sequence of work and if necessary, modify it.

5) Principle of optimal load – an allocation of functions is recommended such that the operator, in accordance with the rate of incoming data, either does not run short of sensors (loss of activity) or is not in excess of sensors (missing signals).

6) Principle of responsibility – the MO is assigned a number of important functions, even if full automation is available.

### III. ALGORITHMIC MODELS MEANT TO DESIGN THE IM.

The algorithmic methods allow for forming patterns reflecting the operator's algorithm of action taking into account the peculiarities of work under a variety of conditions, [4, 8]. Such conditions may be rosters, emergency conditions, etc. The operator's activity is a set of several activities  $A = \{Act_i\}$ , where  $Act_i$  is the  $i^{th}$  activity so that each activity could be considered as a set of precedents  $P_{ij}$ , i.e. consecutive actions taken to work out problems.

The informational volume included in the model and the rules of its organization must comply with the control process objectives and methods. Physically, the IM is implemented by means of the display information devices, while the most significant feature of the MO's activity with the IM is the need of information consistency obtained through the control and measurement devices and the monitors, both between as well as the real controllable objects. Indeed, the overall MO's activity is built upon the basis of information compliance.

An exemplary organizational chart of the MO's activity is shown in Fig. 2, while the informational interaction between the operator and the machine is generally divided into the following stages.

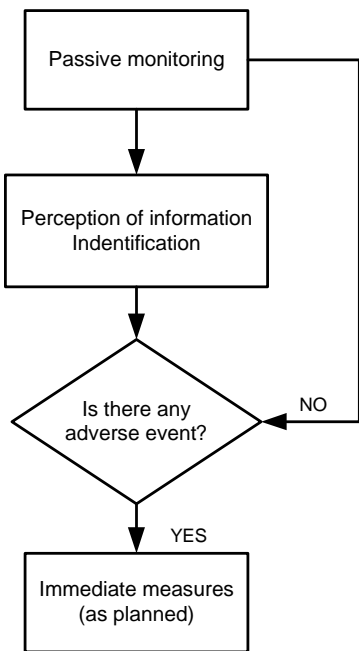


Fig.2. Structural scheme of human activity operator.

1) Information perception. It is a process including following qualitatively different operations: a process, including the following qualitatively different operations: the detection of the object by perception during close monitoring of the production process, or instrumentation monitoring reflecting the parameters of the current processes, selection

individual signs within the objects rising to the operator's challenges, introduction with individual signs and the very object of perception. The perception is carried out by means of sense organs from which point it is transmitted to the central nervous system.

2) Processing of the information obtained, i.e. assessment, analysis, and summary on the basis of previously defined or set up criteria and assessments. The assessment is made based on a comparison between the data model and the designed within the operator internal conceptual model of the situation (the control system) and leads to making a decision. The conceptual model is a product of understanding the operator's situation considering the forthcoming task. Unlike the IM, it refers to internal man's psychological – mental abilities and the operator's ways and means of action. Thus, the operator's decisions are influenced not only by the external information but also the internal one.

3) Implementation of the decision taken by means of the actuators. In the EU, this is the control through which changes to the current processes are implemented in case of control devices influence.

### VI. CONCLUSION.

Within the ACS the operator performs a wide spectrum of functions through utilizing a variety of technical ways and means. The main problem of the human – machine optimization is the agreement between psychological, psychophysiological, anthropometrical, and physiological characteristics and abilities, and the technical properties of the means of automation, the environmental parameters and the staff working place. Moreover, the information models should commonly meet the following five quality criteria:

1. Degree of adequacy of the generated indexing alongside the actual state and behavior of the object. The expertise methods are estimated (digital images).
2. Reliability of reproducing and reading the information. The error probability and the error size during measurements and necessary information adoption is estimated.
3. Time required for observing the information field and making a decision – the input-output characteristics are estimated.
4. Correspondence between the spatial components of the system (controls) and the optimal location in the workspace – spatial characteristics.
5. Speed (intensity) of information flows reproduction as well as IM informativeness and intensity (informativeness = intensity per unit area).

### REFERENCES

- [1] Гечов П., Хубенова З., Попов В., Изследване на човека като управляваща система в среда на виртуална реалност, FIFTH SCIENTIFIC CONFERENCE with International Participation Dedicated to the 40th Anniversary of the Space Research Institute and the 30th Anniversary of the First Bulgarian Astronaut's Mission SPACE, ECOLOGY, NANOTECHNOLOGY, SAFETY, 2009 г., р. 96.

- [2]. Венда В.Ф., Системы гибридного интелекта: Эволюция, психология, информатика, М., Машиностроение, 1999, 448 с.
- [3]. Горский Ю. М. Информационные аспекты управления и моделирования, М., Наука, 1978
- [4]. Craik, KJW (1948). Theory of the human operator in control systems: II. Man as an element in a control system. *British Journal of Psychology* , 38 (3), 142-148.
- [5]. Getsov P., W., Popov, K., Stoianov, The Men as a Control System parametrical model, 30 years organised space investigations in Bulgaria, SRI-BAS, Sofia, pp. 259-261, 2000
- [6]. Human-Computer Interaction and Operators' Performance: Optimizing Work Design with Activity Theory edited by Gregory Z. Bedny, Waldemar Karwowski, CPC Press, 2010
- [7]. Peter H. Lindsay , Donald A. Norman, Human Information Processing, by Academic Press Inc.,U.S, 1972
- [8]. Thomas B. Sheridan, William R. Ferrell, Men-Machine Systems: Information, Control and Decision Models of Human Performance, Hardcover, 2002
- [9]. Salvendy Gavriel (Editor), Handbook of Human Factors and Ergonomics, Purdue University, 2006, Canada.
- [10]. Ye.B. Tsoi, M.G. Grif, A.V. Dubrovskikh. Design and estimation of education quality in engineering education // Proceedings of the International Conference on Engineering Education, Prague, Czech, 1999

# Bond Graph Modelling and Simulation of the 3D Crane System Using Dymola

Dragan Antić<sup>1</sup>, Dragana Trajković<sup>2</sup>, Saša Nikolić<sup>1</sup>, Staniša Perić<sup>1</sup> and Marko Milojković<sup>1</sup>

**Abstract – An application of Bond graph technique for modelling and simulation of the industrial three-dimensional (3D) crane system is presented in this paper. First, the description of considered system is given, and after that the total bond graph model is determined. In addition, several simulations, for concrete values of parameters, in Dymola are performed. Finally, the simulation results are compared with already developed one, and it is verified that obtained bond graph model determines system dynamics adequately.**

**Keywords – Bond graph, 3D crane, Dymola, Modelling and simulation.**

## I. INTRODUCTION

The concept of bond graphs was first developed by Paynter [1]. The main idea was further developed by Karnopp and Rosenberg [2, 3]. The fundamental advantage of bond graphs is in central physics concept-energy (bond graph consists of components which exchange energy using connections; these connectors represent bonds). The effort (voltage, force, pressure, etc.) and the flow (current, velocity, volume, flow rate, etc.) are generalization of similar phenomena in physics. The factors which characterize the effort and flow have different interpretations in different physical domains (mechanical, electrical, hydraulic, thermal, chemical systems). Obtained model can be successfully tested in software package *Dymola* which is adjusted for simulation purposes.

*Dymola* is a commercial modelling and simulation environment based on the open *Modelica* modelling language (an object-oriented, declarative, multi-domain modelling language for component-oriented modelling of complex systems). The *BondLib* library, firstly presented by *Cellier* in 2003, is designed as a graphical library for modelling physical systems using the bond graph metaphor. This library contains the basic elements for analog electronic circuits, translational and rotational mechanical systems, hydraulic and thermal systems.

It is already proven in many papers that bond graph technique can be successfully used as a modelling tool for various types of process [4-10]. In [11, 12] we used bond graph method for modelling of submersible pumps in water industry. The obtained model is used as an object for the control design based on orthogonal polynomials.

In this paper we present the process of modelling and

<sup>1</sup>Dragan Antić, Saša Nikolić, Staniša Perić, Marko Milojković are with the Faculty of Electronic Engineering at University of Niš, A. Medvedeva, 18000 Niš, Rep. of Serbia, E-mails: {dragan.antic, sasa.s.nikolic, stanisa.peric, marko.miljkovic}@elfak.ni.ac.rs.

<sup>2</sup>Dragana Trajković is with the Faculty of Mechanical Engineering at University of Niš, A. Medvedeva, 18000 Niš, Rep. of Serbia, E-mail: dragana.trajkovic@masfak.ni.ac.rs.

simulation of three-dimensional laboratory model of industrial crane. In addition, the simulation of obtained model is performed using *Dymola* and simulation results are presented and discussed. In order to verify the effectiveness of obtained bond graph model, the simulation results are compared with already existing one and it is proved that this model fully describes the 3D industrial crane system dynamics. In future work, obtained model can be used as a plant for design of some control algorithms based on advanced control method.

## II. 3D CRANE SYSTEM DESCRIPTION

Three-dimensional laboratory model of industrial crane (see Fig. 1), made by Inteco [13], is a highly non-linear electromechanical system having a complex dynamic behaviour and creating challenging control problems. It consists of a payload hanging on a pendulum-like lift-line wound by a motor mounted on a cart. The payload is lifted and lowered in the  $z$  direction. Both the rail and the cart are capable of horizontal motion in the  $x$  direction. The cart is capable of horizontal motion along the rail in the  $y$  direction. Therefore the payload attached to the end of the lift-line can move freely in three dimensions. The 3D crane is driven by three DC motors.



Fig. 1. The 3D crane system manufactured by Inteco

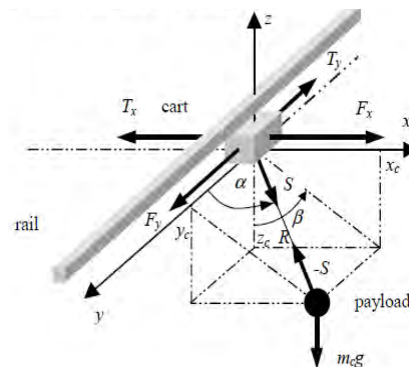


Fig. 2. Free body diagram of the 3D crane system

There are five identical encoders measuring five state variables:  $x_w$  represents the distance of the rail with the cart from the centre of the construction frame;  $y_w$  is the distance of the cart from the centre of the rail;  $R$  denotes the length of the lift-line;  $\alpha$  represents the angle between the  $y$  axis and the lift-line;  $\beta$  is the angle between the negative direction on the  $z$  axis and the projection of the lift-line onto the  $xz$  plane. The schematic representation of the 3D crane system is shown in Fig. 2.

The relationships that describe a given system are [14]:

$$\mu_1 = \frac{m_c}{m_w}, \quad \mu_2 = \frac{m_c}{m_w + m_s}, \quad (1)$$

$$u_1 = \frac{F_x}{m_w}, \quad u_2 = \frac{F_y}{m_w + m_s}, \quad u_3 = \frac{F_R}{m_c}, \quad (2)$$

$$T_1 = \frac{T_x}{m_w}, \quad T_2 = \frac{T_y}{m_w + m_s}, \quad T_3 = \frac{T_R}{m_c}, \quad (3)$$

$$N_1 = u_1 - T_1, \quad N_2 = u_2 - T_2, \quad N_3 = u_3 - T_3, \quad (4)$$

where  $m_c$ ,  $m_w$ ,  $m_s$  - mass of the payload, cart and moving rail, respectively,  $x_c$ ,  $y_c$ ,  $z_c$  - coordinates of the payload,  $S$  - reaction force in the lift-line acting on the cart,  $F_x$  - force driving the rail with cart,  $F_y$  - force driving the cart along the rail,  $F_R$  - force controlling the length of the lift-line and  $T_x$ ,  $T_y$ , - friction forces.

The load position is described by the following equations:

$$x_c = x_w + R \cos \alpha, \quad (5)$$

$$y_c = y_w + R \sin \alpha \sin \beta, \quad (6)$$

$$z_c = -R \sin \alpha \cos \beta, \quad (7)$$

$$R^2 = (y_c - y_w)^2 + z_c^2 + (x_c - x_w)^2. \quad (8)$$

Crane dynamics is described by:

$$m_c \ddot{x}_c = -S_x, \quad m_c \ddot{y}_c = -S_y, \quad m_c \ddot{z}_c = -S_z - m_c g. \quad (9)$$

where  $S_x$ ,  $S_y$ ,  $S_z$  are components of the force i.e.:

$$S_x = S \cos \alpha, \quad S_y = S \sin \alpha \sin \beta, \quad S_z = -S \sin \alpha \cos \beta. \quad (10)$$

The first two DC motors control the position of the cart and the last one controls the length of the lift-line. If the flag is set to 1 and the encoder detects range over sizing, the corresponding DC motor is switched off. If the flag is set to 0 the motion continues in spite of the range limit exceeded in the encoder register.

### III. BOND GRAPH MODEL OF THREE-DIMENSIONAL INDUSTRIAL CRANE

The basics elements, used in bond graph model of 3D crane system, are: the resistor  $R$  (dissipative element), the capacitor

$C$ , the inductor  $I$  (energy storage element), the modulated transformer  $MTF$ , the gyrator  $GY$  (conservative element), the effort and flow sources (energy source elements). There are also junction structure elements: 0-junction and 1-junction. The 0-junction is a flow balance junction or a common junction. It has a single effort on all its bonds and the algebraic sum flows is null. The 1-junction is an effort balance junction or a common flow junction. It has a single flow on all its bonds and the algebraic sum of effort is null. The effort source  $Se$  in  $z$  axis enters effort, i.e. force of gravity  $mg$ , while flow sources  $Sf$  from DC motors in  $x$ ,  $y$ ,  $z$  axis enters flows-velocity as a starting information in the process. DC motors are included individually. Junction with the identical flow  $1a$  presents the port with the same velocity and sum of forces gravity, inertial force from payload and velocity from DC motor. The first derivative of positions  $z_c$ ,  $y_c$ ,  $x_c$  represents the corresponding velocities  $\dot{z}_c$ ,  $\dot{y}_c$ ,  $\dot{x}_c$  of the payload. Junction  $1d$  is a sum of inertia of the cart and friction forces  $R$ :  $Tx$ . Junction  $0a$  is defined as a sum of velocities in functions of variables-string radius  $\dot{R}$  and angular velocity  $\dot{\alpha}$ , where the output force from  $0a$  is input in junction  $1d$  while output bond is inertia of payload. Junction  $1f$ ,  $1g$  and  $1h$  defines the velocities  $\dot{\alpha}$ ,  $\dot{\beta}$  and  $\dot{R}$ . Junction  $0a$ ,  $0b$ ,  $0c$  and  $1a$ ,  $1b$ ,  $1c$  are defined with the following equations:

$$0a : \dot{x}_c = \dot{x}_w + \dot{R} \cos \alpha - R \dot{\alpha} \sin \alpha, \quad (11)$$

$$0b : \dot{y}_c = \dot{y}_w + \dot{R} \sin \alpha \sin \beta + R \dot{\alpha} \cos \alpha \sin \beta + R \dot{\beta} \sin \alpha \cos \beta, \quad (12)$$

$$0c : \dot{z}_c = -\dot{R} \sin \alpha \cos \beta - R \dot{\alpha} \cos \alpha \cos \beta + R \dot{\beta} \sin \alpha \sin \beta, \quad (13)$$

$$1a : m_c \ddot{x}_c = -m_c g - R \sin \alpha \cos \beta + Sf_{DCmotor}, \quad (14)$$

$$1d : m_w \ddot{x}_w = Sf_{DCmotor} - T_x + S \cos \alpha, \quad (15)$$

$$1c : (m_w + m_s) \ddot{x}_w = Sf_{DCmotor} - T_y + S \sin \alpha \sin \beta. \quad (16)$$

Bond graph model of the DC motor (see Fig. 3) consists of two 1-junctions, two  $R$  and two  $I$  elements. There exists commonly junction  $1s$  and  $1t$  with the identical flow contains for four bonds. A PIDs controller for the positions, voltages and limiters are connected to motors. The main problem is reflected in causality and it is avoided using acausal bond graph. To derive the total acausal bond graph, there is need to create two kinds of connector class:  $e$ -connector,  $f$ -connector to establish acausal bond, where: the  $Se$ -element stands for the voltage and forces source; the seven  $I$ -elements represent the moment of inertia derived from the mass and the magnetic energy and the kinetic energies of the rotor and the load from DC motor; the six  $R$ -elements enable the friction and the dissipative energy in the electrical circuit; the  $GY$ -element depicts the electro-mechanical coupling; the  $MTF$ -element is associated to the power conserving rotation into translation velocities. The total acausal bond graph of the 3D crane system is illustrated in Fig. 4. It is based on the system equations (5)-(10). Model is described by three unknown coordinates of the two angular velocities.

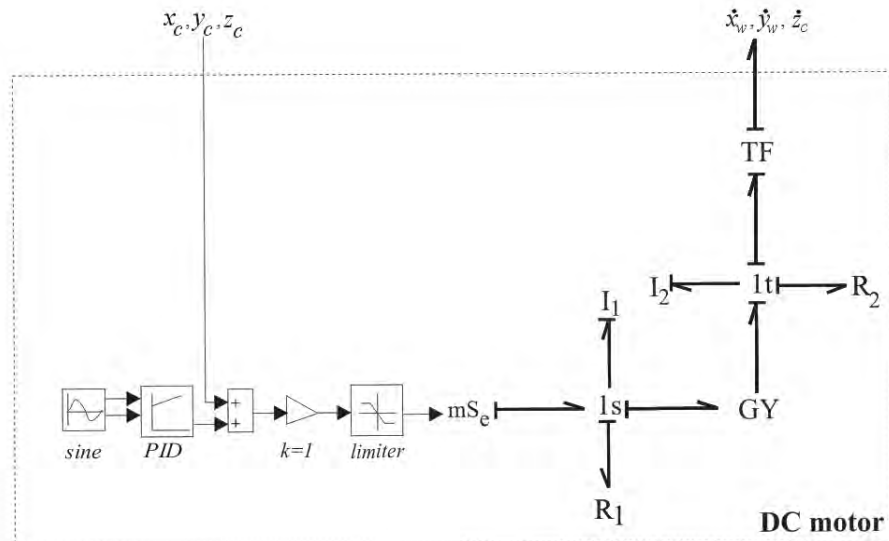


Fig. 3. Bond graph model of the DC motor

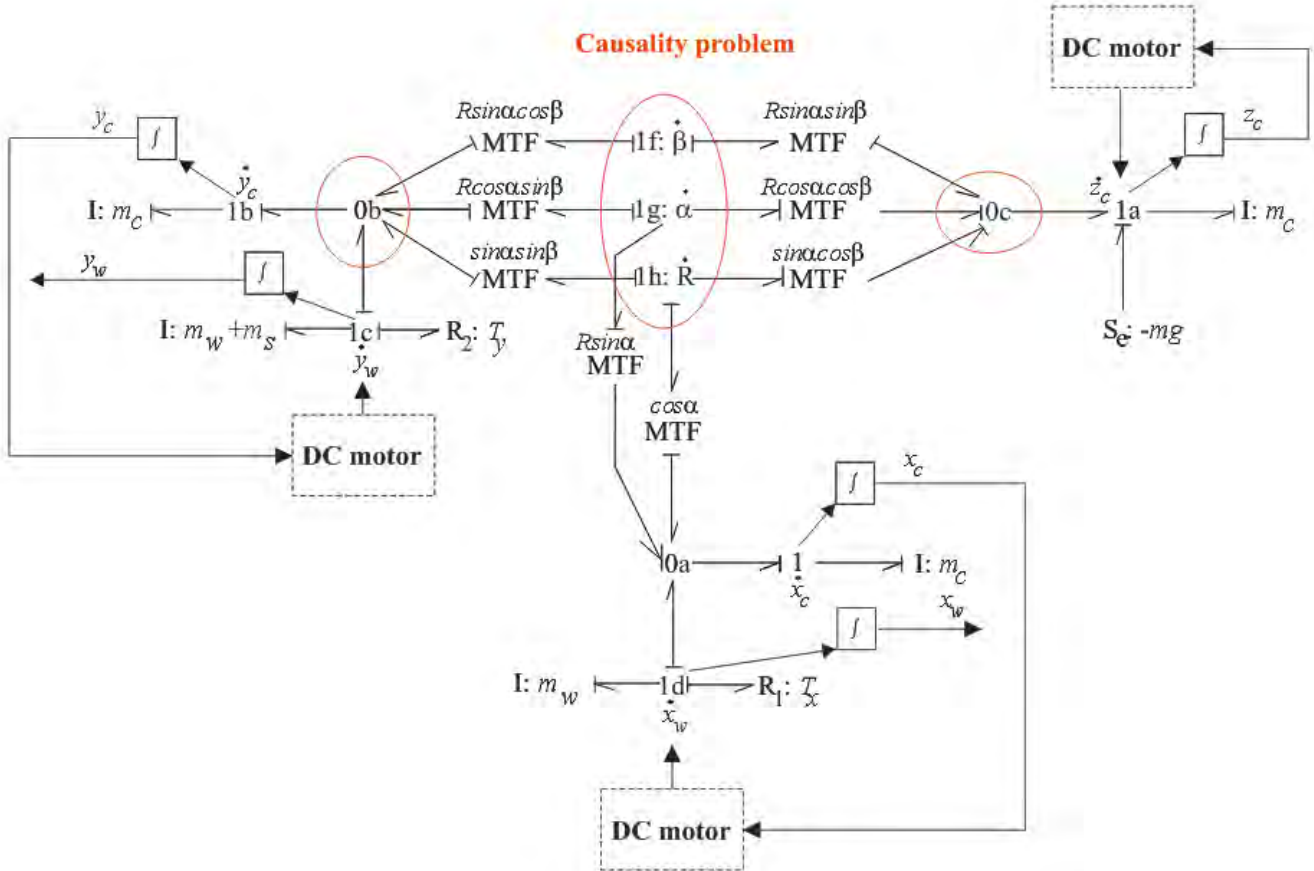


Fig. 4. Acausal bond graph model of the 3D crane system

#### IV. SIMULATION RESULTS

In order to verify the efficiency of proposed method for modelling of 3D crane system and validity of obtained model, we performed the several simulations in *Dymola*. The

considered parameters of simulation are:  $\alpha=10^\circ$ ,  $\beta=30^\circ$ ,  $m_c=0.35\text{kg}$ ,  $m_w=0.8\text{kg}$ ,  $m_s=0.5\text{kg}$ ,  $T_x=0.235\text{Nm}$ . The parameters used for the DC motor are:  $L=0.02\text{H}$ ;  $R_1=4\Omega$ ;  $R_2=2.5\text{Nm/s}$ ;  $J=0.2\text{kgm}^2$ . Simulation time is  $t=0.02\text{s}$ .

In Fig. 5, position responses for  $x$ ,  $y$  and  $z$ -axis are presented. These simulation results are compared with

simulation results presented in [13]. It can be noticed that obtained results (dashed lines) are very close to the existing one (solid line), which proves that bond graph model fully determines system dynamics. This is useful for student

exercises where they can implement their control algorithm based on different models. Also, in some application the bond graph model is more suitable for controller design than conventional one, obtained in other graphic tool environment.

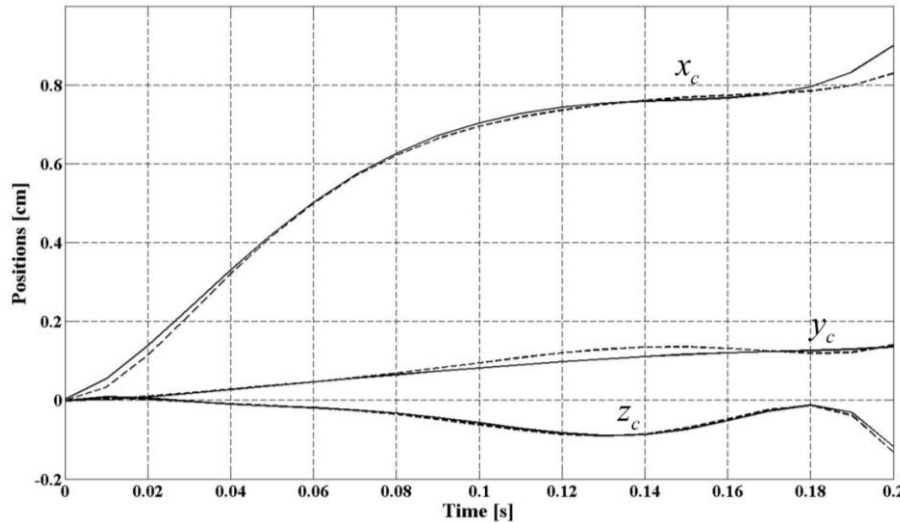


Fig. 5. Position responses for  $x$ ,  $y$ , and  $z$ -axis

## V. CONCLUSION

In this paper we presented the bond graph technique applied in modelling of three-dimensional (3D) laboratory crane system. First, the complete mathematical background of considered system is given. After that, the complete process of bond graph modelling is described and corresponding bond graph models are presented. Finally, the bond graph model of 3D crane system is tested through simulations in *Dymola* and obtained results are compared with already existing one. It is proved that bond graph model fully determined the 3D crane system dynamics. In future work, this model can be used as a plant for controller design.

## ACKNOWLEDGEMENT

This paper was realized as a part of the projects TR 35005, III 43007 and III 44006 financed by the Ministry of Education, Science and Technological Development of the Republic of Serbia.

## REFERENCES

- [1] H. M. Paynter, *Analysis and Design of Engineering Systems*, M.I.T. Press, Cambridge, 1961.
- [2] R. C. Rosenberg, D. C. Karnopp, *Introduction to Physical System Dynamics*, McGraw-Hill Book Co., New York, 1983.
- [3] D. C. Karnopp, D. L. Margolis and R. C. Rosenberg, *System Dynamics: A Unified Approach*, John Wiley & Sons, New York, 1990.
- [4] O.K. Bouamama, K. Medjaher, M. Bayart, A. K. Samantaray, and B. Conrard, "Fault Detection and Isolation of Smart Actuators Using Bond Graphs and External Models", *Control Engineering Practice*, vol. 13, no. 2, pp. 159-175, 2005.
- [5] H.B. Pacejka, "Modelling Complex Vehicle Systems Using Bond Graphs", *Journal of the Franklin Institute*, vol. 319, no. 1, pp. 67-81, 1985.
- [6] P.J. Mosterman, R. Kapadia, and G. Biswas, "Using Bond Graphs for Diagnosis of Dynamic Physical Systems", in *Proceedings of the 5th International Workshop on Principles of Diagnosis*, pp. 81-85, 1995.
- [7] C. Sueur and G. Dauphin-Tanguy, "Bond-graph Approach for Structural Analysis of MIMO Linear Systems", *Journal of the Franklin Institute*, vol. 328, no. 1, pp. 55-70, 1991.
- [8] E. Sosnovsky and B. Forget, "Bond Graphs for Spatial Kinetics Analysis of Nuclear Reactors", *Annals of Nuclear Energy*, vol. 56, pp. 208-226, 2013.
- [9] S.V. Ragavan, M. Shanmugavel, B. Shirinzadeh and V. Ganapathy, "Unified Modelling Framework for UAVs using Bond Graphs", in *12th International Conference on Intelligent Systems Design and Applications (ISDA)*, pp. 21-27, 2012.
- [10] D. Trajković, V. Nikolić, D. Antić and B. Danković, "Analyzing, Modelling and Simulation of the Cascade Connected Transporters in Tire Industry Using Signal and Bond Graphs", *Machine Dynamics Problems*, vol. 29, no. 3, pp. 91-106, 2005.
- [11] D. Trajković, V. Nikolić, D. Antić, S. Nikolić and S. Perić, "Application of the Hybrid Bond Graphs and Orthogonal Rational Filters for Sag Voltage Effect Reduction", *Electronics and Electrical Engineering*, in press.
- [12] D. Trajković, V. Nikolić, S. Nikolić, S. Perić and M. Milojković, "Modeling and Simulation of Pump Station Using Bond Graphs", *XI International Conference on Systems, Automatic Control and Measurements, SAUM 2012*, pp. 455-458, 2012.
- [13] Inteco, 3D Crane System-User's Manual, Available at [www.inteco.com.pl](http://www.inteco.com.pl), 2008.
- [14] Z. Jovanović, D. Antić, Z. Stajić, M. Milošević, S. Nikolić and S. Perić, "Genetic Algorithms Applied in Parameters Determination of the 3D Crane Model", *Facta Universitatis, Series: Automatic Control and Robotics*, vol. 10, no. 1, pp. 19-27, 2011.

# Identification of Dynamic Processes with Artificial Neural Networks

Jordan Badev<sup>1</sup> and Ivan Maslinkov<sup>2</sup>

**Abstract —** In this writing are studied the options for application of Artificial Neural Networks (ANN) in dynamic processes modelling, and mainly in identification and modelling of cases that conventionally are expressed with differential (difference) equations. Special attention has been paid to models identification that is further transformed into ANN training to experimental results of the actual physical model.

**Keywords —** Dynamic Processes Modelling, Artificial Neural Networks, Recursive Perceptron, Discrete AR Models

## I. INTRODUCTION

In A basic approach in designing automation systems is the modelling of separate elements and/or the entire structure of the signal network for process values control. The end results of automation greatly depend on the type and quality of the models employed. The engineering of models that are relevant to the physical processes is done at the beginning of the design stage and is known as identification. Most often subject to identification is the physical process to be controlled, the so called Object of Control. As it is known, ANN in terms of calculation are “heavy” models, since they require computing resources greater than those necessary for other types of analytical models, however they have certain advantages – teach method similar to that of the human beings, solution supply guaranteed, input data noise resistance, “firm” structures (parallel structures) suitable for non-linear and MIMO models, etc. With the massive employment of high capacity computing equipment in the design, the ANN shortcomings are practically insignificant.

For the dynamic control static and dynamic models are used. The output values with static models depend only on the input current values, while with the dynamic models they depend both on current and prior input values. In this writing, for the purpose of clarity, only SISO models are studied, the results, however, being in the greater part relevant for the MIMO models.

It is known and proven that the straight ANN of definite number of neurons in the hidden layers are universal approximators of static functions (models) [1]. The aim of the present writing is to explore the ANN capabilities for dynamic processes modelling.

## II. MODELLING OF DYNAMIC PROCESSES WITH ARTIFICIAL NEURAL NETWORKS

Since the experimental data identification problems are discrete in their nature, herein discrete models and methods are studied.

If the discrete object input signal is  $u(k)$  and the discrete object response is  $y(k)$ , then the general equation that is the discrete image of the continuous differential equation may be presented as:

$$y(k) + a_1 * y(k-1) + a_2 * y(k-2) + \dots + a_n * y(k-n) = b_1 u(k-1) + b_2 u(k-2) + \dots + b_m u(k-m) \quad (1)$$

where  $n \geq m$ .

Without losing totality, it is studied the type where the values of  $u(k)$  and  $y(k)$  participate in a linear way, i.e. it is easy to model an expression with these values but of non-linear type. Often in identification these values are called regressors and they are assumed to be known values (measurable).

The finding of an object relevant model of the above type means to determine the coefficients

$$[a_1, a_2, \dots, a_n, b_1, b_2, \dots, b_m] \quad (2)$$

so that when calculating the response  $y(k)$  by the expression (model) above given for  $k \geq n$ , the difference with the measured value  $y_o(k)$  to be minimal, i.e.  $e(k) = y_o(k) - y(k) \approx 0$ .

That problem is easy to solve provided that the necessary experiments are conducted with the object; it is far more difficult if the model is non-linear to the regressors.

If we assume that through ANN processes in the object could be modelled (the dependency  $y_o(k) = f(u(k))$ ), the process of selecting a relevant model can be presented as the chart in Fig.1.

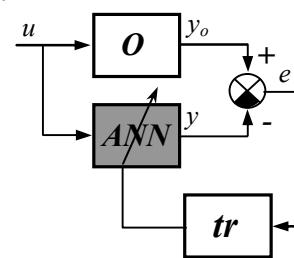


Fig.1 Problem of the identification whit ANN

<sup>1</sup>Jordan Badev, D-r, Assistant in the Engineering Faculty of the University of Food Technologies, bul. Mariza 26, Plovdiv, 4000, Bulgaria, E-mail: [j\\_badev@abv.bg](mailto:j_badev@abv.bg)

<sup>2</sup>Ivan Maslinkov, D-r, Ass. Prof. in the Engineering Faculty of the University of Food Technologies, bul. Mariza 26, Plovdiv, 4000, Bulgaria, E-mail: [imm@uft-plovdiv.bg](mailto:imm@uft-plovdiv.bg)

In this figure:

*O* - object of identification (control);

*ANN* - Neural network;

*r* - ANN training algorithm.

It is seen in the chart that: the object output coincides with the ANN output, i.e.  $y(k)$ ; the process of finding the coefficients Eq.(2) is transformed into a training process of the network with the object's input-output data [ $u(k)$ ,  $y_o(k)$ ]; the identification pattern is one and the same for identification of static, dynamic, linear, non-linear etc. models.

The model type is determined by the ANN model and parameters, and the input-output data for training.

The very nature of dynamic models supposes the use of more complex than the strait ANN structures, namely the ANN recurrent structures [2]. Characteristic of these structures is modelling of earlier (following) values of the quantities through unitary elements ( $z^{-1}$ ), for retaining the information in one stroke (discretization period -  $T_0$ ).

For example: Eq.(1) could be presented with the structure in Fig.2.

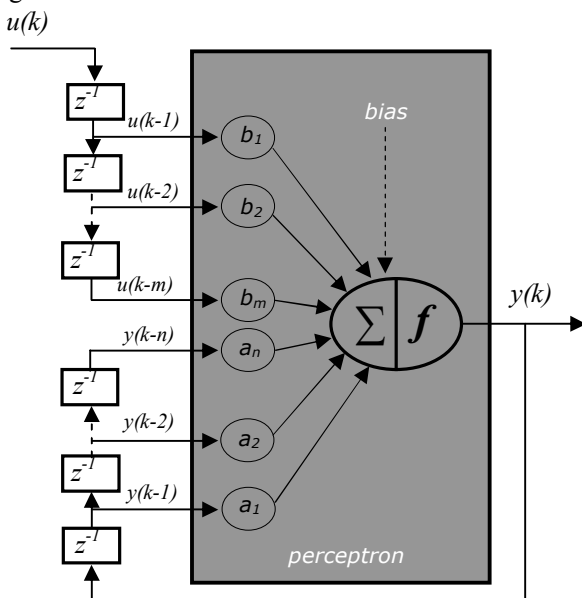


Fig.2 Linear ARX model

Obviously the chart in the grey (big) square is a linear perceptron that is a unitary structure building the ANN. It is so because Eq.(1) is of the autoregression type (AR). In this case it is evident that coefficients in Eq.(1) coincide with the connection weights at the perceptron input, so it is natural that the process of finding the coefficient Eq.(2) be transformed into an ANN training process.

With more complex equations the chart shall contain a greater number of and/or with non-linear perceptrons, possibly distributed in different layers (multilayer), in which case there is no congruence between connection weights and coefficients and the obtained model is of the "black box" type, namely ANN.

It is not hard to present the models in the space state.

If is written the following for this type SISO models in general:

$$\begin{aligned} x(k+1) &= f_1(x(k), u(k)) \\ y(k) &= f_2(x(k)) \end{aligned} \quad (3)$$

In this model  $x(k)$  is  $n$ -dimensional vector and the neural model is demonstrated with the chart in fig. 3

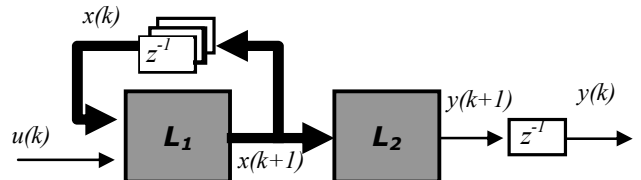


Fig.3 Neural model in the space state.

In this figure the blocks  $L_1$  and  $L_2$  perform respectively the functions  $f_1$  and  $f_2$  that generally can be implemented by a certain number and type of perceptrons distributed in two layers.

If it is a linear object, the functions are linear, and so are the perceptron activating functions in the two layers. This is the case applicable for the AR models, most widely used in practice. Here the required computing capacity is minimal and the training process is the fastest. In many cases the non-linear models are modelled with only the first,  $L_1$  neural layer non-linear.

### III. EXPERIMENTAL DATA AND RESULTS

The identification of actual physical objects is frequently done by experimental transient characteristics that contain the basic information of the static and dynamic properties, and therefore are used for objective evaluation of the control quality. The models are relevant if they produce one and the same response to various input signals.

In this writing, for better flexibility is haven used data simulated with known discrete transfer function (TF) -  $W(z)$ . The validation of the neural model is through visual comparison between the model response and the neural model response.

The sufficient ANN for modelling linear models is a single-layer linear neuron (one linear neuron) of one output and inputs depending on the model's order – Fig. 2. The training process is up to the level of the mean square difference (MSE) between the network output  $1*10^{-10}$ , by the Levenberg-Marquardt recursion (*trainlm*).

Training set is known with: the response values  $y(k)$ ; the amplitude of input signal  $u_{tr}(k)$ ; is the measuring period  $T_0$ .  $u_{test}$  is the testing of neural model input signal.

In this writing, through ANN have been modelled TF of a periodic second order object -Eq.4 and fifth-order oscillatory object – Eq.5.

$$W(s) = \frac{0.003121 * z^{-1} + 0.001 * z^{-2}}{1 - 1.01 * z^{-1} + 0.08208 * z^{-2}} \quad (4)$$

$$t(0)=0; t(end)=4 \text{ sec.}; T_0=0.05 \text{ sec.}$$

The ANN is taught with  $u_{tr}=1/k$ , for 5 epochs and the following difference is achieved  $MSE=4.25*10^{-12}$ .

The test results with  $u_{test}=1(t)=u_{tr}$  are given in Fig.4.

The test results with  $u_{test}=1.2*I(t)$  are given in Fig.5.

The test results with  $u_{test}=5*\sin(t)$  are given in Fig.6.

In all graphs:

- 1** - object response (TC);
- 2** - neural model response.

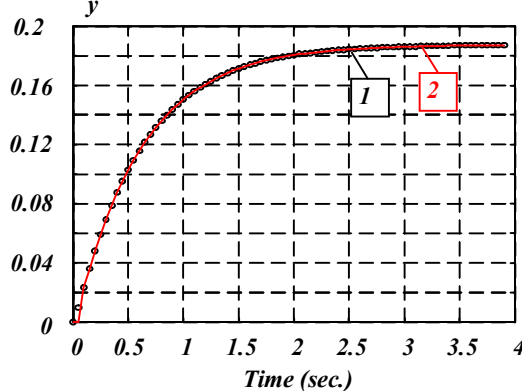


Fig.4 Response with  $u_{test}=u_{tr}=1(t)$

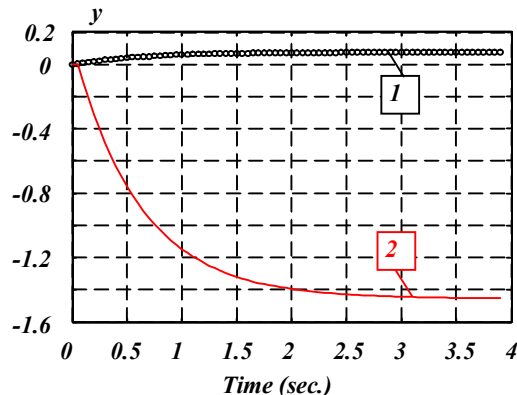


Fig.5 Response with  $u_{test}=1.2*I(t)$

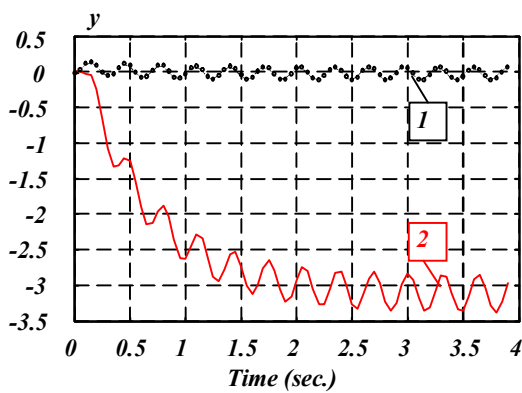


Fig.6 Response with  $u_{test}=5*\sin(t)$

In fig.7 the response of the ANN that is taught and tested with the same ramp input, i.e.  $u_{tr}=1*t=u_{test}$ .

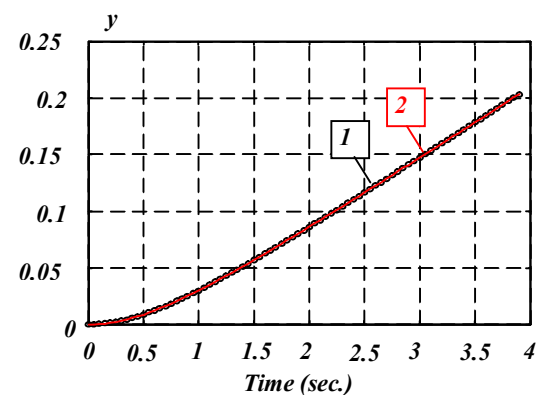


Fig.7 Response with  $u_{tr}=u_{test}=t$

The oscillatory object is modeled by TF - Eq.(5).

$$W(s) = \frac{0.02056 * z^{-1} + 0.07613 * z^{-2} + 0.0177z^{-3}}{1 - 2.662 * z^{-1} + 2.417 * z^{-2} - 0.7408z^{-3}} \quad (5)$$

$t(0)=0$ ;  $t(end)=160$  sec.;  $T_0=1$  sec.

The ANN is taught with  $u_{tr}=5*I(t)$  for 3 epochs and a difference of  $MSE=4.25*10^{-10}$  is achieved.

The test results with  $u_{test}=5*I(t)=u_{tr}$  are given in Fig.8.

The test results with  $u_{test}=1.2*I(t)$  are given in Fig.9.

The test results with  $u_{test}=5*\sin(t)$  are given in Fig.10.

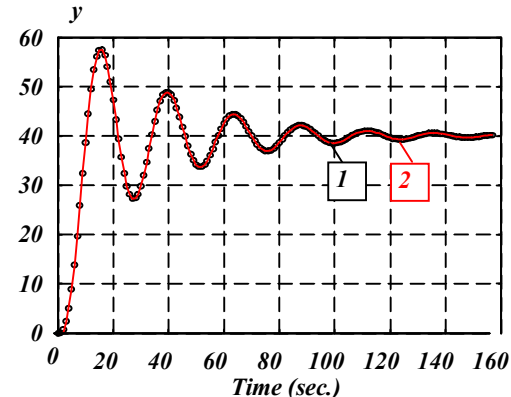


Fig.8 Response with  $u_{tr}=u_{test}=5*I(t)$

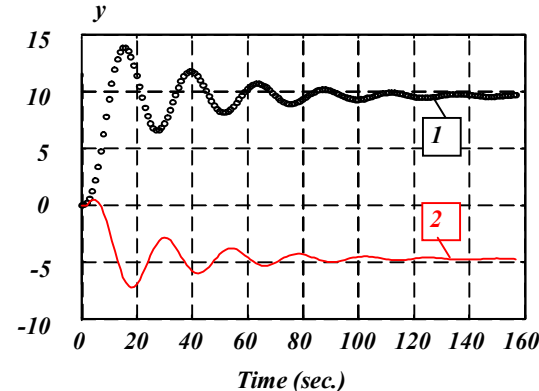


Fig.9 Response with  $u_{test}=1.2*I(t)$

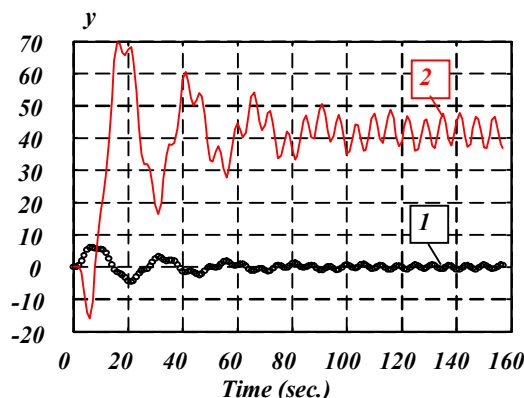


Fig.10 Response with  $u_{test}=5*\sin(t)$

Applying the same method, it has been performed training and testing of other neural models intended for modelling other functions, the results of which are skipped herein, since they are similar.

#### IV. CONCLUSIONS AND RECOMMENDATIONS.

All results lead to the following major conclusions:

- 1) Through recursive ANN it is possible to model linear dynamic functions of random order only for the input signal with which they have been taught - Figs. 4, 7 and 8.
- 2) The input training signal may be of arbitrary type (step, ramp, sinusoidal, etc.) - Figs. 4, 7 and 8.

3) For linear objects, relevant neural models may be obtained also for input signals different from the amplitude training step ones, provided that the ANN is taught by the standard response characteristic, and the amplitude  $\Delta u$  is accounted separately as a static amplification coefficient of object, i.e.

if for  $u=I(t)$ , the ANN response is  $y(t)$ , then for  $u=\Delta u * I(t)$ , the neural model response is  $y(t)=\Delta u * y(t)$

4) ANN with single layer of neurons are preferred with modelling linear dynamic functions due to greater accuracy and faster teaching.

5) With non-linear functions it is preferable to use double-layer structures of first layer non-linear neurons, and one linear in the second layer.

6) With ANN taught by the classical method (back-propagation; Levenberg-Marquardt, etc.) dynamic functions of input signal different from the training one can not be modelled – Figs. 5, 6, 9 and 10. This is explained with the fact that networks store their inputs. They find one of the possible solutions.

7) Taking into account the above examples and the arguments, obviously with ANN modelling we must consider the fact that the “black box” models have inaccessible state variables (unknown underlying structure), which to some extent limits their application.

#### REFERENCES

- [1] K. Hornik, M. Stinchcombe, H. M&White, Multilayer feedforward networks are universal approximators (Discussion paper 88-45), San Diego, CA, Department of economics, University of California, 1988.
- [21] S. Haykin, Neural Networks (sec.edition), Prentice Hall, Pearson education, 1999.

# AGV Guidance System Simulation with Lego Mindstorm NXT and RobotC

Violeta Kostova<sup>1</sup>, Ramona Markoska<sup>2</sup> and Mitko Kostov<sup>3</sup>

**Abstract –** The paper gives an analysis of automated guided vehicles navigation systems. A simulation of guidance is presented by using LEGO Mindstorm NXT package. On the basis of theoretical studies and experience, a robot is programmed in the programming language RobotC in order to demonstrate the functionality of real AGV vehicle-forklift.

**Keywords –** automated guided vehicles, navigation, LEGO NXT, robotics, RobotC.

## I. INTRODUCTION

Productivity and flexibility are the primary goal of today's automation technology, what can be achieved only in a fully integrated production environment. The high demands in the production often cause chaotic situations in warehouses. Human mistakes negatively affect the safety in a production environment, efficiency and quality of products. These disadvantages are reduced by introduction of automated guided vehicles (AGV).

Automated guided vehicles are among the fastest growing classes of equipment in the material handling industry. They are battery-powered, unmanned vehicles with programming capabilities for path selection and positioning. They are capable of responding to frequently changing transport schemes, and they can be integrated into fully automated intelligent control systems. The aim is to improve efficiency in material transfer and increase production, which results AGV to be used in production lines of modern manufacturing plants.

Integrated intelligent computers allow automated guided vehicles to safely operate at higher speeds while transferring the products. Precise movements and rotation allows management in narrow space. They can significantly reduce the need for human resources to carry goods in a manufacturing plant. An unmanned AGV vehicle uses optical path for fast and safe movement in warehouses. It is remotely driven vehicle that can perform operations like picking up load, transferring it through a set of predefined paths and its delivery to the specified locations.

Introduction of unmanned vehicles in the warehouses has a big effect on safety. With help of sensors, automated guided

vehicles can detect objects in its path. Automation eliminates or solves the problem of traffic congestion and reduces the possibility of accidents.

This paper presents the results of simulation of navigation and operating of automated guided vehicles. A robot is designed to demonstrate the functionality of the AGV vehicle. Based on theoretical studies and experiences, the robot is programmed to demonstrate the functionality of real-forklift AGV vehicle.

The paper is organized as follows. After the introduction section and the explanation of the need of these vehicles to improve safety in the production environment, efficiency and quality of production, the second section reviews the types of AGV vehicles navigation and guidance. The third section describes the hardware and software platform that are used in simulations presented in the fourth section. The fifth section concludes the paper.

## II. VEHICLE NAVIGATION

Navigation and guidance systems of AGV vehicles evolved a lot from the moment they emerged up to date. There are two basic principles for AGV navigation – following a fixed path/route and free navigation. AGV navigation with fixed route is the oldest type of navigation. It is used today, but most of AGV systems are with free navigation, which allows flexibility and easier maintenance. Some of the most important technologies of navigation based on these two principles include: (i) Wired guide: wires are embedded in the floor and they are detected to determine the vehicle's position relative to the wire. (ii) Inertial guide: gyroscopes and wheel odometers are used (for measuring the traveled distance) in order to conduct very precise guidance. Magnets placed in the floor at regular intervals are used to reset. (iii) Laser guide: a rotating laser transmitter-receiver is installed in the vehicle. The navigation is based on the emitted and reflected laser beams. The angle and distance of movement of the vehicle are calculated and compared to parameters in preset network. As a result, the AGV vehicle can find its location.

### A. Fixed path (wire guidance)

This type of guidance was the main way in development of AGV industry in 1970's. AGV vehicles that follow a fixed path have a fixed route sensor on the underside of the vehicle, which detects the path in the ground surface. The sensor role is to detect a path, and to guide the vehicle just over the path. If the path is turning, the sensor detects the absence of path, returns a feedback to the vehicle control, which guides the vehicle to the right path. The role of the sensor in conjunction with the control and steering system is to keep the AGV vehicle on the path.

<sup>1</sup>Violeta Kostova is with the Faculty of Technical Sciences, Ivo Lola Ribar bb, 7000 Bitola, Macedonia, E-mail: kost.violeta@gmail.com.

<sup>2</sup>Ramona Markoska is with the Faculty of Technical Sciences, Ivo Lola Ribar bb, 7000 Bitola, Macedonia, E-mail: ramona.markoska@uklo.edu.mk.

<sup>3</sup>Mitko Kostov is with the Faculty of Technical Sciences, Ivo Lola Ribar bb, 7000 Bitola, Macedonia, E-mail: mitko.kostov@uklo.edu.mk.

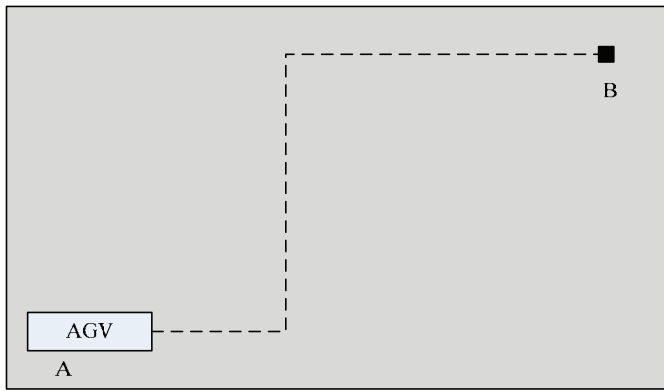


Fig. 1. Fixed path of an AGV vehicle.

The main characteristics of an AGV system with fixed path (Fig. 1) are: the paths of the AGV are well marked on the floor, continuous and fixed, but they still can be changed. Different types of marking the paths are used, but systems with inductive guidance and systems with optical guidance can be distinguished.

This is a simple method of navigation that requires a very simple resources. But the main drawback is that AGV vehicle can only follow the line, and thus its operations are very limited. In addition, the vehicle does not know its current position in the track. Further issue of strategies based on following route is cost and time required to set tracks. In some cases there is a need several AGV paths to intersect with each other, which can confuse the sensor for following the path. These strategies are also non-flexible in a case of need for new investment and it takes time to modify the path of the vehicle. The vehicles are also highly dependent on the track - if they lost contact with the track, they can no longer operate. This condition may occur due to corrupt or obscure track, but can also occur in case AGV vehicle too quickly accessing a turning point.

#### B. Free navigation (non-wire guidance)

In the 1980's non-wire guidance is introduced. It does not suffer from the above problems and it is based on localization of AGV vehicle. Localization differs from following a line because it tries to specify the position and orientation of the vehicle in relation to the environment rather than making small adjustments in its movement. AGV vehicle is not limited to movement along a fixed path, but rather any position in the environment is permitted (Fig. 2).

The laser and inertial navigation are examples of this kind of navigation. They provide increased accuracy and flexibility of the system. When it is necessary to make adjustments to the path, there is no need to change the infrastructure, thus there is no slowdown in production and transport process.

For navigating in unrestricted open space, wireless AGV systems at any moment have to know vehicles' position and always to be able to determine the path to the end point, without the benefits of systems with fixed paths.

AGV systems with free navigation have a map of the area in which the AGV functions, which is placed in the memory of microcomputers in the vehicle, as well as more fixed

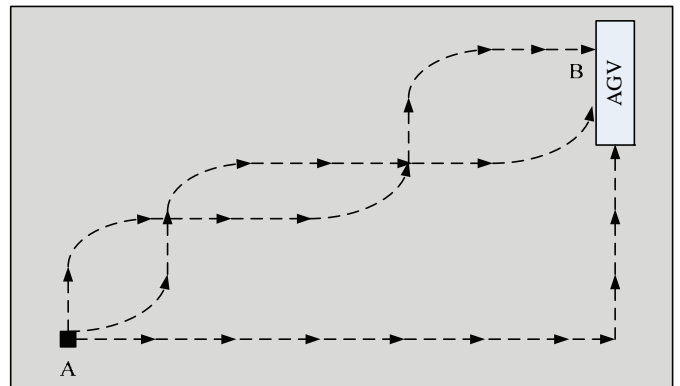


Fig. 2. Free paths of an AGV vehicles.

reference points in the working area of the AGV, which can always be detected by the vehicle.

The vehicles also have planned routes. During the movement of the vehicle, the microcomputer measures the traveled distance, direction and angle of turning of the vehicle.

Decoders placed on the wheels provide data for the traveled path and the change of direction. This technology allows independent movement of the vehicle, but due to errors in measuring the actual position of the vehicle differs from the calculated position. Correction of the position of the vehicle is done by external reference points.

### III. DESCRIPTION OF THE HARDWARE AND SOFTWARE SIMULATION PLATFORM

Lego Mindstorm NXT 2.0 package contains hardware and software which can be used to construct small programmable robots that can be easily adapted to different needs. The package includes a programmable 32-bit ARM7 microcontroller that can be programmed to perform various operations, 256KB Flash and 64 KB RAM memory, a set of sensors, motors and Lego-blocks for constructing mechanical systems.

Designed robots can be programmed in different programming platforms: LabView, Matlab, Robolab, C, C++, Visual Basic, Java, RobotC, etc.

From a communication point of view, the controller has a USB port for loading a program from computer. For this purpose bluetooth connection can be used. In addition, the controller has four inputs and three output ports. The four input ports can be used for attaching different sensors: color sensor, touch sensor, light sensor, ultrasonic sensor (to detect objects at a distance), sound sensor, etc. The three output ports are used for attaching of three servo motors, labeled A, B and C. Bluetooth wireless communication allows robot to communicate and cooperate with other NXT microcontrollers, receive orders from computers, smart phones and other bluetooth devices.

### IV. DESCRIPTION MODEL

For the simulation purposes, AGV-forklift vehicle that uses wire guidance is constructed (Fig. 3). Lego Mindstorm NXT



Fig. 3. The vecible that was used for the simulation.

2.0 package is used, since it allows easily and fast to construct robots and mechanical systems, which can then be programmed to perform different operations.

The vehicle communicates (takes orders) with a communication center and according to the received commands it transports load from one workstation (A, B, C and D) to another. The stations in the polygon are connected by tracks, as it is illustrated in Fig. 4. The communication with the communication center is simulated by using bluetooth connection with a smart mobile phone that runs the operating system Android. The idea is by sending different data through the phone, to give a certain command to the vehicle to perform some operation.

The block diagram of the algorithm for vehicle operating is given in Fig. 5. At the beginning, the vehicle is in listening mode. When the vehicle receives data through bluetooth, it checks if data is 0, 1 or 2, and afterwards it stops (for received data 0) or performs sequences belonging to the respective scenario (Scenario 1 or Scenario 2 for received data 1 or 2, respectively). According to Scenario 1, the vehicle (from the workstation A) is sent to the station B, where it takes load and transfer the load to station C by following a path. According to Scenario 2, the vehicle is sent to the station C (by following a path), there it takes load and transfer the load to the station D.

The functionality of the vehicle in terms of navigation and interaction with the environment is made possible by incorporating several different types of sensors. The light sensor is located on the bottom of the vehicle and used for detection of the different intensity of the color of the line compared to the surface, which allows the vehicle to be able to follow this line. Ultrasonic sensor is located in the front of the vehicle in order to detect objects ahead.

For the simulation of the vehicle activities, a program code is written in the programming language RobotC.

The block diagrams of Scenarios 1 and 2 are illustrated in Fig. 6, while the source code of the simulation program written in RobotC is completely given in [11]. According to the program, the vehicle listens to a command and if there is command 1 or 2, it moves and follows the navigation track by using the light sensor, while in the same time the ultrasonic sensor checks if the vehicle reached the target, i.e. it moves until the criterion for detection the station is satisfied to load or unload. Once the station is detected,



Fig. 4. The polygon for operating of the AGV vecible.

depending on the scenario, the vehicle loads or unloads the load.

By applying the made model and the software solution, a number of simulations are performed. It is concluded that this platform, besides simplicity and low cost, is quite enough for studying and simulating all aspects of a modern production and the need of automatic guided vehicles. The communication capabilities of the NXT controller and the ability to connect and exchange information with other vehicles give possibility in future studies to analyze the concepts of cooperative action of a group of vehicles to perform the same task by using different evolutionary algorithms and other modern concepts which are being studied today in intelligent systems.

## V. CONCLUSION

The possibilities of AGV vehicles are enhanced with the ability to send and receive data through data communication. This flexibility of AGV vehicles, as a result of remote communication, allows them to interact with other autonomous vehicles and be capable of various operations. A continuous coordination between vehicles contributes to efficiency and savings in finance.

The paper analyzes the automatic guided vehicles navigation. A robot is designed in order to demonstrate the functionality of a typical model of AGV vehicle - forklift. On the basis of theoretical studies and experiences, the AGV robot is programmed to demonstrate the functionality of the operation of real AGV vehicle. A software solution is developed according to which the vehicle performs a specific task and it is concluded that this platform can be successfully used for simulation of processes involving automatic guided vehicles.

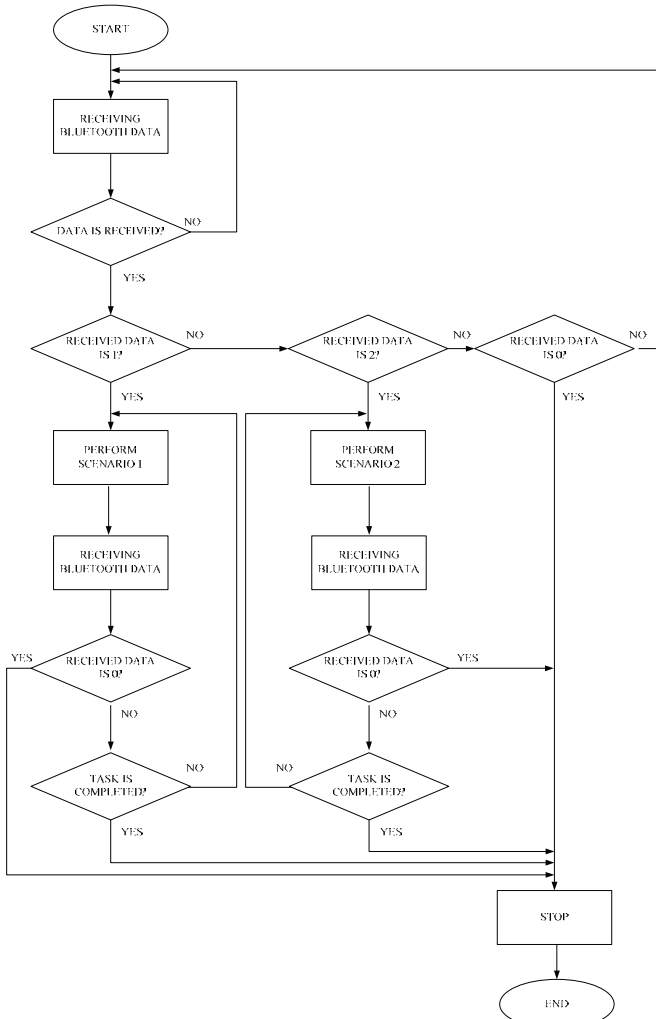


Fig. 5. Bloch-diagram of the software solution.

## REFERENCES

- [1] T. Tsumura "Survey of autonomous guided vehicles in Japanese factory", Proceedings of the IEEE International Conference on Robotics and Automation, pages 1329-1334, San Francisco, CA, April 1986.
- [2] I. J. Cox and G.T. Wilfong, editors, "Autonomous Robot Vehicles", Springer-Verlag, USA, 1990.
- [3] H. K. Shivanand, M. M. Benal, V. Koti, Flexible Manufacturing System, New Age International Limited, Publishers, 2006.
- [4] S. Butdee, A. Subsoman, F. Vignat, P.K.D.V. Yarlagadda, "Control and path prediction of an Automate Guided Vehicle", Journal of Achievements in Materials and Manufacturing Engineering, Dec. 2008.

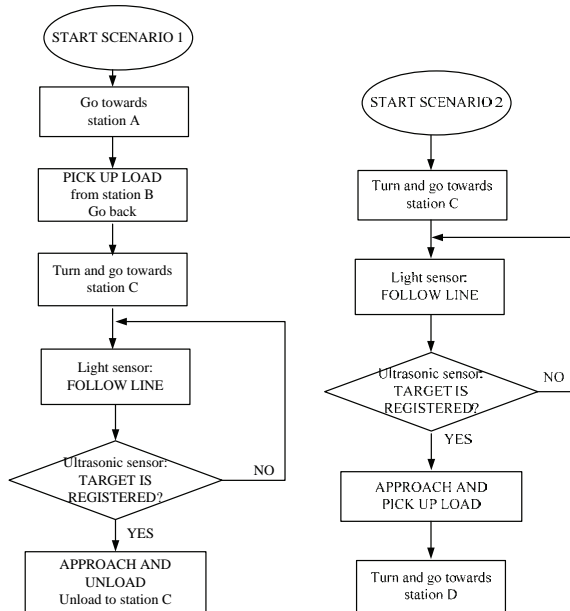


Fig. 6. The two scenarios of operating the AGV vehicle.

- [5] Atul Tiwari, "Scheduling of Automated Guided Vehicles in Flexible Manufacturing Systems environment", 2010.
- [6] Rajeev K. Piyare, Member, IAEENG, and Ravinesh Singh, "Wireless Control of an Automated Guided Vehicle", Proc. of Int. Conf. of Engineers and Computer Sc., Hong Kong, 2011.
- [7] Axel Hoff, Holger Vogelsang, Uwe Brinkschulte, Oliver Hammerschmidt, "Simulation and Visualization of Automated Guided Vehicle Systems in a Real Production Environment".
- [8] Ryan G. Rosandich, Richard R. Lindeke, Jeff Berg, "Developing an Automatic Guided Vehicle for Small to Medium Sized Enterprises".
- [9] Axel Hoff, Holger Vogelsang, Uwe Brinkschulte, Oliver Hammerschmidt, "Simulation and visualization of Automated Guided Vehicle Systems in a Real Production Environment".
- [10] Dinis Fernandes, Luís Farrolas, Pedro Brito, Pedro Lima, "Progresses on the Design of Small Flexible Automated Guided Vehicles".
- [11] Violeta Kostova, "Industrial application of automated guided vehicles" (MSc thesis), Faculty of Technical Sciences Bitola, 2012.
- [12] Markoska, R., "RobotC programming", (teaching materials). International project for Development of Regional Interdisciplinary Mechatronics Studies, TEMPUS DRIMS, 2012.

---

---

## Poster 11 - Engineering Education

---

---



# Teaching FPGA-Based CPU Cores and Microcontrollers

Valentina Rankovska

**Abstract –** A methodology for teaching FPGA-based CPU cores and microcontrollers from the very first stages is presented in the paper. There are many difficulties for the students connected with the FPGA and CPU hardware and software complexity. Concrete steps, tools and examples are suggested to achieve better results in teaching.

**Keywords –** Field-Programmable Gate Arrays (FPGA), CPU (Central Processing Unit) Cores design, Microcontrollers, Teaching methodology.

## I. INTRODUCTION

In the second half of the PLD (Programmable Logic Devices)-Based Circuits Design course the students have to study implementation of the complex programmable logic arrays to develop embedded systems. They are already familiar with the architecture, features, operation, building blocks modes, etc. of the conventional microcontrollers. This is an actual problem because of the gradual involving of those innovative devices into the scope of digital and microprocessor circuits with the respective advantages [1]. The use of FPGAs also allows the students to study the operation of the microprocessors form the inside, especially when they try to make it themselves [6], [7], [8], [9].

On the other hand it is very difficult for the students to use them, because of the following reasons:

- The architecture complexity of the FPGA integrated circuits in comparison to the conventional ones;
- The more complex digital and microprocessor devices design technology where completely new stages and tools are used together with the traditional ones;
- Related with the previous point – new and considerably more complex integrated development environments with a quite many features and possibilities;
- The fact that the enormous logic capacity and the possibility for using a great variety of IP (Intellectual Property) cores allow building into one chip designs with great circuit complexity and multidisciplinary nature;
- Except the upper featured objective preconditions – also the lack of students' motivation especially in the present economic conditions, etc.

The aim of the present work is to suggest a methodology for teaching/ study of a CPU (Central Processor Unit) core and peripherals design with simple operation for educational and research purposes.

## II. PRELIMINARY KNOWLEDGE AND SKILLS OF THE STUDENTS

Preliminary knowledge and skills form from previous courses, connected with:

- Digital elements, devices and basic circuits;
- Architecture and operational principles of a hypothetical microprocessor, microcontroller, embedded system;
- Architecture, building blocks and operational principles of conventional general purpose microcontrollers;
- Assembler and high level programming languages.

Before to begin studying CPU cores design in the current course the students are also familiar with:

- Architecture, features and resources of the Field-Programmable Gate Arrays;
- Stages, hardware and software tools used to design digital circuits in FPGAs;
- Hardware description languages such as VHDL, Verilog, AHDL, etc. (Currently VHDL is used.)

Having in mind the difficulties for the students featured before, they have to be supplied with enough data and documentation:

- FPGA and development boards documentation – handbooks, user manuals, tutorials, example projects, which are useful in studying the features of the programmable logic and development boards;
- Integrated development environment documentation including tutorials helping to study the design sequence;
- Documentation and tutorials concerning the hardware description language used (VHDL);
- Architecture and features of IP cores – CPU and peripherals, which could be used freely for educational purposes;
- Links to Internet resources like:
  - Companies producing programmable logic and hardware and software development tools;
  - Sites of similar university courses, where often variety of useful information could be found: lecture presentations, labs, course and final projects, etc.
  - Projects and forum sites concerning the subjects, etc.

Except supplying with documentation the requirements to the students connected with the stated labs and projects problems have to be extremely clear and detailed.

All this is achieved to a greater degree by the means of e-learning, part of which is the Moodle course for the discipline [4].

Valentina Rankovska is with the Faculty of Electrotechnics and Electronics at Technical University of Gabrovo, 4 H. Dimitar str., Gabrovo 5300, Bulgaria, E-mail: rankovska@tugab.bg.

### III. TEACHING METHODOLOGY IN DESIGNING FPGA-BASED CPU CORES AND PERIPHERALS

FPGAs of Altera are used in the learning process together with the free version of the software - Quartus II Web Edition and development boards TREX C1 and DE2-70 with FPGA Cyclone and Cyclone II respectively.

There are two possible design approaches, which can be used with the full version of Quartus II:

- **Flat compilation flow with no design partitions** – the entire design is compiled together; it is applied for small and not too complex designs. The software performs the defined logic and placement optimizations on the whole design. This approach is easy to implement and is the only one possible with the free version of Quartus II. It is not convenient for large designs as the compilation time increases considerably.

- **Incremental compilation with design partitions** - the design is split into partitions, on which different designers can work independently. This can simplify the design process and reduce compilation time. It is preferable in large and complex designs.

The first approach is used in the laboratory classes as on one hand it is free and on the other hand it is easier to implement with the comparatively simple students' projects.

The CPU core design is a complicated and quite difficult process. That is why the students wouldn't be able to acquire the design of a core for a real application for the short time of the course. And also the course is not dedicated only to microprocessor systems design, but to more general object.

We must have in mind that during the Microprocessor Circuits course (held in the previous semester) they have studied the architecture and the operation of a hypothetical microprocessor on the level of building blocks. That is why it is necessary to pass through the following stages in studying the design of microprocessors and microcontrollers in order to be easier for the students:

#### **1. Embedded system design using software module for its generation and library components, defined from the designer (student):**

- Studying the library features and resources of the software module for system-on-a-programmable chip synthesis SOPC Builder (included in Quartus II);
- Studying the architecture, features and configuring options for the three versions of the software core Nios II of Altera;
- Designing an embedded system based on Nios II with reduced set of peripherals.

#### **2. Design of a CPU core with simple set of operations and peripherals:**

- Planning the CPU core architecture with a reduced set of operations;
- Designing definite blocks of the CPU core, beginning with the Arithmetic-Logic Unit (ALU);
- Expanding the microprocessor core to achieve a working variant for learning purposes;
- Designing memory blocks and peripherals with reduced complexity;

- Joining together and testing the operation of the CPU core and the peripheral blocks.

#### **3. Analysis and study of a ready CPU core functionalities with simple architecture**

Different design approaches are used at the different teaching stages. Firstly the students learn to develop digital projects by inputting the design using Block/ Symbol Editor and library components of Quartus II (they synthesize the circuit (circuits) in a form of a block/functional diagram). The approach is used in the first stage. The modeling in the second stage is performed in VHDL.

It must be noticed here that software development tools for the student processor are not created having in mind the defined course purposes and the limited course workload.

#### **Developing an embedded system using library components**

The software module SOPC Builder is used for system in a chip generation. A microprocessor circuit, based on Altera's software processor Nios II is developed (Fig. 1) [3].

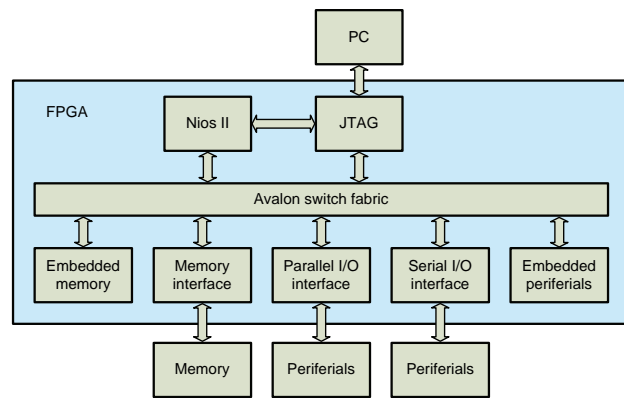


Fig. 1. SOPC based on Nios II and DE2-70

SOPC Builder enables to define and generate entire system in a programmable chip in an easy way. The designed system could be based on a processor or not and if there is a processor in it, it may be Nios II or other. The module connects together the components of the system automatically. For that purpose it makes the routing and (if it is necessary) generates interconnect logic. That is why it is very suitable for the lowest level of learning.

The GUI (Graphical User Interface) of SOPC Builder with library components added is shown in Fig. 2.

It was mentioned that at this stage the students are already familiar with a hardwired conventional microcontroller from the Microprocessor Circuits course. Now they have the opportunity to design their own microcontroller with flexible reconfigurable architecture and to test it. And moreover – on one hand they do not need still to examine the inside structure of the used blocks and on the other hand they may configure them according to the assignment in the laboratory class.

#### **Design of a CPU core and peripherals**

- *Planning of a CPU core architecture*

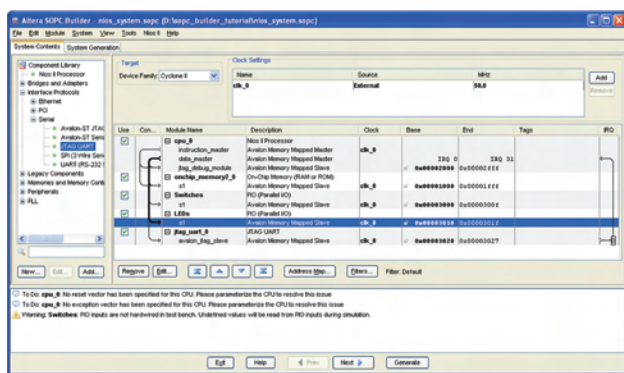


Fig. 2. Components of SOPC system based on Nios II

It is a considerably complicated stage which is difficult for the students at most degree. That is because till the moment they have studied a ready submitted structure and an operation of a microprocessor and a microcontroller without explaining the reasons for being that. So the processes passing in the blocks and the ways of their interaction are still hidden for the students.

At the CPU core design, although it is not obvious, the process begins not from the mechanical “collecting” of blocks building its architecture (though at the end it will look like a known one), but from the answers of the following general questions:

- What kind of operations have to perform the designed processor;
- How it will access the various types of memory blocks, etc.

A functional diagram of a general purpose microprocessor is shown in Fig. 3 [7].

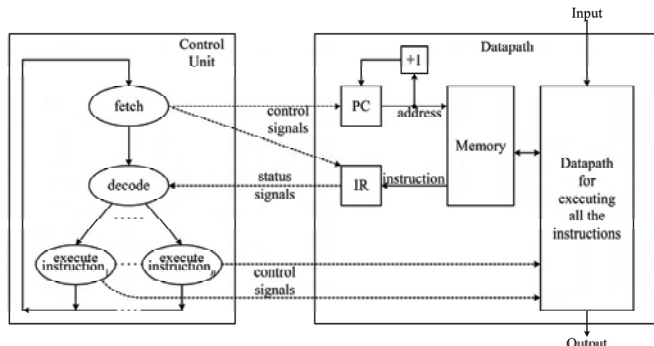


Fig. 3. Functional circuit of a general purpose CPU

After defining the instruction set the ways of their decoding and execution have to be determined. Several questions must be answered: how many and what kind of operations must be able to execute the processor; what will be the mnemonic code of the instructions; what operation code will be assigned to each instruction and what will be their length.

After that the design of the executable unit follows. A datapath has to be made on this step, so the following questions have to be answered: what kind of operation unit we need; how many registers; how will they be organized; how

will be connected the two units – the control and the executable ones.

At creating the datapath we have to determine how the processor will fetch and execute the instructions from the program memory. In this connection there are additional operations and registers, for instance the program counter (PC), the instruction register (IR), etc.

The control unit cyclic pass through three major steps, called usually instruction cycle: 1) instruction fetch; 2) instruction decoding and 3) execution. Every step is executed during one state of the state machine.

The simplest variant of a completely synchronous programmable logic-based device is a RISC processor with a two-stage pipelined execution of the instructions.

#### • Arithmetic-Logic Unit

We use a minimum number of instructions executed by the ALU for the example training processor – addition, subtraction, increment, decrement, logic AND, OR, NOT and accumulator output. Hence three bits are enough for the operation codes (S). Two general purpose registers are used – A and B. The operands are 4-bits long in order to implement the project using the 18 switches of the development board. We have to input the operands and the machine code of the instruction tested. The process, in which body the instructions are modeled (in VHDL), is the following:

```
PROCESS(S, A, B)
BEGIN
    CASE S IS
        WHEN "000" => F <= A;
        WHEN "001" => F <= A AND B;
        WHEN "010" => F <= A OR B;
        WHEN "011" => F <= NOT A;
        WHEN "100" => F <= A + B;
        WHEN "101" => F <= A - B;
        WHEN "110" => F <= A + 1;
        WHEN OTHERS => F <= A - 1;
    END CASE;
END PROCESS;
```

The students perform a functional simulation to test all the operations and for that purpose they first make a vector waveform file. Practically the design is tested on the DE2-70 development board. A test of the “adding” operation is shown in Fig. 4.

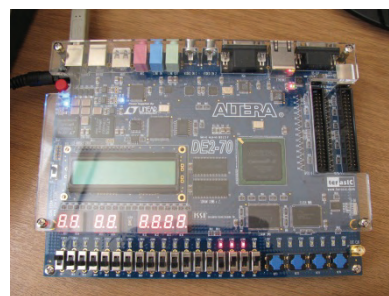


Fig. 4. Testing the instruction for addition of two register operands

After that additional blocks and features have to be added at the development process, such as: interrupt management block; reset control block; ways to access the memory blocks, including pointer and data registers, instructions, status flags,

etc. It is also necessary to organize the pipelined execution of the instructions.

These problems are quite complicated to be performed in the laboratory classes and further more - for the part of the semester. That is why the students have to be supplied not only with detailed directions for completing the tasks but also with additional information like ready models of similar blocks. They will have the opportunity and the task to analyze and modify them and also to make course and final projects.

- *Program and Data memory*

The FPGAs Cyclone II include embedded memory consisting of columns of M4K blocks that can be configured to provide various memory functions such as RAM, first-in first-out (FIFO) buffers, and ROM. M4K memory blocks provide over 1 Mbit of RAM at up to 250-MHz operation. It is not enough volume for the most real applications but it is enough for the designed simple processor.

The M4K blocks which are used as a program memory, are initialized in advance with the operation codes of the instructions of the example test program. For that purpose the embedded in Quartus II memory editor is used.

#### **Analysis and study of a ready CPU core functionalities with simple architecture**

The study of a ready software core for a real application is an extremely complicated process, even if it is simple. It is a stage which could be applied in activities like extracurricular unaided work or team-based work at the end of the course, practices, course and final projects. For that purpose it is convenient to use free software core with a comparatively simple functions [2], [5].

## IV. CONCLUSION

A methodology for teaching FPGA-based CPU cores and microcontrollers from the very first stages is presented in the paper.

There are many circumstances which make difficult for the students to study the microprocessor and microcontroller development using programmable logic. The suggested approach includes step by step beginning with simple problems design of two kinds of microprocessor systems with

minimum functionalities – using library components and modeling a system with VHDL.

The future work addresses enlarging the e-learning means, like animations, multimedia, etc.

Also an archive of custom (students) library components and projects will be made, which will be accessible for the next-year students as useful examples – to learn and expand.

## ACKNOWLEDGEMENT

The present work is partially supported by the Science Research Fund at the Ministry of Education, Youth and Science.

## REFERENCES

- [1] V. Rankovska, H. Karailiev. "Digital Devices and Systems Design using Field-Programmable Gate Arrays", «E+E», no.1-2, pp. 8-15, 2011. (in Bulgarian)
- [2] V. Rankovska, "Microprocessor Cores for Complex Programmable Logic Arrays", Unitech'11, Conference Proceedings, vol. 1, pp. I-186 – I-191, Gabrovo, Bulgaria, 2011, (in Bulgarian)
- [3] V. Rankovska, "FPGA (Field Programmable Gate Arrays) – based System-on-a-Programmable-Chip Development for Educational Purposes", iCEST 2012, Conference Proceedings, vol. 2, pp. 489-492, Sofia, Bulgaria, 2012.
- [4] umis.tugab.bg/moodle/
- [5] www.opencores.org
- [6] V. Sklyarov, I. Sklyarova, "Multimedia Tools for Teaching Reconfigurable Systems", MoMM2006 Conference Proceedings, pp. 211-220, Yogyakarta, Indonesia, 2006.
- [7] Enoch O. Hwang, "Digital Logic and Microprocessor Design With VHDL", La Sierra University, Riverside, 2005.
- [8] Thomas Weng, Yi Zhu and Chung-Kuan Cheng, "Digital Design and Programmable Logic Boards: Do Students Actually Learn More?", 38th ASEE/IEEE Frontiers in Education, Conference Proceedings, Saratoga Springs, NY, 2008.
- [9] Joaquín Olivares, José Manuel Palomares, José Manuel Soto and Juan Carlos Gámez, "Teaching Microprocessors Design Using FPGAs", IEEE EDUCON Education Engineering, Conference Proceedings, pp. 1189-1193, Madrid, Spain, 2010.

# Interactive Learning Module Implementing "Divide and Search" Procedure in Convolutional Encoders Analysis

Adriana Borodzhieva<sup>1</sup>, Galia Marinova<sup>2</sup> and Tzvetomir Vassilev<sup>3</sup>

**Abstract –** This paper addresses a simulation study of convolutional encoders and decoders in presence of noise. An Interactive Learning Module with graphical user interface is implemented using MATLAB and GUIDE. The paper describes the layout and the functionality of the Interactive Learning Module with graphical user interface implementing “Divide and Search” procedure in convolutional encoders’ analysis.

The Interactive Learning Module will be used in the teaching the course “Coding in Telecommunications Systems”, included as optional in the curriculum of specialty “Telecommunication Systems” for Bachelor degree.

**Keywords –** Convolutional encoding and decoding, MATLAB, GUIDE, simulation.

## I. INTRODUCTION

Numerous existing interactive program modules only allow encoding and decoding of binary sequences using convolutional encoders/decoders [9, 10], but they do not keep a database of all valid combinations of polynomial generators and the corresponding value of the parameter *free distance*, and a database of the *best convolutional encoders*, the encoders with maximum free distance defining the corrective capabilities of the encoders.

For example, the e-learning interactive course “Channel coding and decoding” [9] is organized in 3 parts: lecture-based course, exercises and dynamic simulations. The main objectives of this tool are: explaining through illustrations the realization of the encoder, the decoding process, error detection and correction, performances of the codes.

Based on authors work on convolutional encoders during the last several years, an Interactive Learning Module, which integrates processes “divide” and “search” to find candidates for the *best encoders* and appropriate learning content, is developed in order to assist students in learning the topic of convolutional encoders analysis. The Interactive Learning Module described in the paper is a part of a software system for convolutional encoding/decoding. It is based on a set of MATLAB tools developed and tested previously [6, 7, 8]. A special Graphical User Interface (GUI) is realized to facilitate

<sup>1</sup>Adriana Borodzhieva is with the Faculty of Electrical Engineering, Electronics and Automation at Ruse University, 8 Studentska Str., Ruse 7017, Bulgaria, e-mail: aborodjieva@ecs.uni-ruse.bg.

<sup>2</sup>Galia Marinova is with the Telecommunications Faculty, Technical University of Sofia, 8 Kl. Ohridski Blvd., Sofia 1000, Bulgaria, e-mail: gim@tu-sofia.bg.

<sup>3</sup>Tzvetomir Vassilev is with the Faculty of Natural Sciences and Education at Ruse University, 8 Studentska Str., Ruse 7017, Bulgaria, e-mail: TVassilev@uni-ruse.bg.

interactivity and learning process.

The learning content in the Interactive Learning Module covers subjects from communication circuit architecture to illustrations on the choice of connections between the adders and the register’s flip-flops in the convolutional encoder’s structure influencing the characteristics of the code, and changes in the choice of connections creating different codes. The connections are not selected and changed randomly. The problem of selecting connections giving optimal distance properties is complex and generally unsolvable, but for any value of the constraint length of the code less than 20, the best codes are found [1, 2, 3, 4, 5]. The Interactive Learning Module is intended for simulation study of convolutional encoders and decoders in presence of noise.

The Interactive Learning Module is implemented using MATLAB and GUIDE (Graphical User Interface Development Environment). First the software system for convolutional encoding is described briefly, then the GUI developed and finally the Interactive Learning Module functionality.

## II. SOFTWARE SYSTEM FOR CONVOLUTIONAL ENCODING AND INTERACTIVE LEARNING MODULE IMPLEMENTING “DIVIDE AND SEARCH” PROCEDURE

### A. Software system for convolutional encoding

Using the computational and graphical environment MATLAB and its extensions Communications Toolbox and Symbolic Math Toolboxes [11] a software system for simulation study of convolutional encoders and decoders in the presence of noise is implemented. The system integrates four modules: Module 1: “Divide and search”, Module 2: “Convolutional encoding and decoding”, Module 3: “Determining the performance of convolutional encoders”, and Module 4: “Simulation study of cascaded convolutional encoders” (Fig. 1).

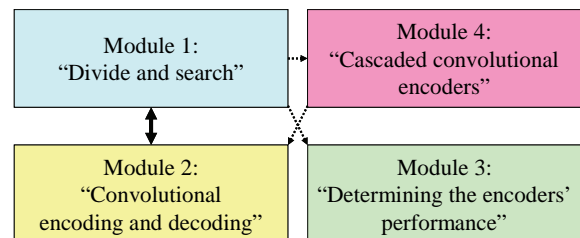


Fig. 1. Architecture of the system implemented and connectivity of the four modules of the system

The first module performs “Divide and search” procedure involving the processes “dividing” the combinations of generator polynomials into valid and non-valid, and “searching” the valid combinations to find the encoders, *candidates for the best encoders*.

### B. Layout and Functionality of GUI

The layout of the Interactive Learning Module with GUI is presented in Fig. 2. The layout is organized in 5 panels:

- Panel 1: Convolutional encoders;
- Panel 2: 4 push-buttons giving information about Module 1;
- Panel 3: Parameters of the studied group of convolutional encoders;
- Panel 4: Run;
- Panel 5: Visualization of the databases.

These five panels in the layout with the push-buttons and pop-up menus are described in details further.

Pressing the “Info” push-button (Fig. 2, panel 2) the architecture of the system implemented is shown in a separate graphics window, as the connection of the four modules of the system are given, as well as information about the use of Module 1: “Divide and search” (Fig. 1).

Below a “Convolutional encoders” panel (Fig. 2, panel 1) with two push-buttons and two pop-up menus is located. It supports learning content on the topics of digital communication systems and convolutional encoders.

The “Convolutional encoders” panel (Fig. 2, panel 1) allows students to learn some basic concepts in the theory of convolutional codes. When pushing the first push-button

(“What is DCS?”) the structure of the functional diagram of a digital communication system (DCS) is shown in a separate graphics window where the blocks “channel coding” (in the transmitter) and “channel decoding” (in the receiver) in a digital communication system are marked in blue, and they are subject of the study using the implemented application.

When pushing the second push-button (“What is it?”) the structure of a convolutional encoder and a brief explanation of its principle of operation are shown in a graphical window.

From the “Description” pop-up menu a representation model (connections vectors, polynomial generators, state diagram, tree diagram, trellis diagram) of a convolutional encoder is chosen from six possible options. The model selected is displayed in a separate graphical window. Fig. 3 illustrates the selection of connections vectors option) and information relevant to the representation model of the encoder for the simplest convolutional encoder with constraint length  $L = 3$  and number of generator polynomials  $n = 2$ , with generators 111 and 101, respectively is given in details.

From the “Applications” pop-up menu (Fig. 2, panel 1) one of seven proposed applications of the convolutional encoders in the field of telecommunications is chosen. It aims to inspire students on the subject studied. For each of the selected options for learning content on convolutional encoders’ applications in telecommunications (coding in a channel with error grouping, channel coding in wireless communications, encoding in control channels in GSM, encoding in control channels in IS-54, parameters of encoders, used in GSM and IS-95, history of space exploration, global satellite systems for personal communications) is displayed in a separate graphics window.

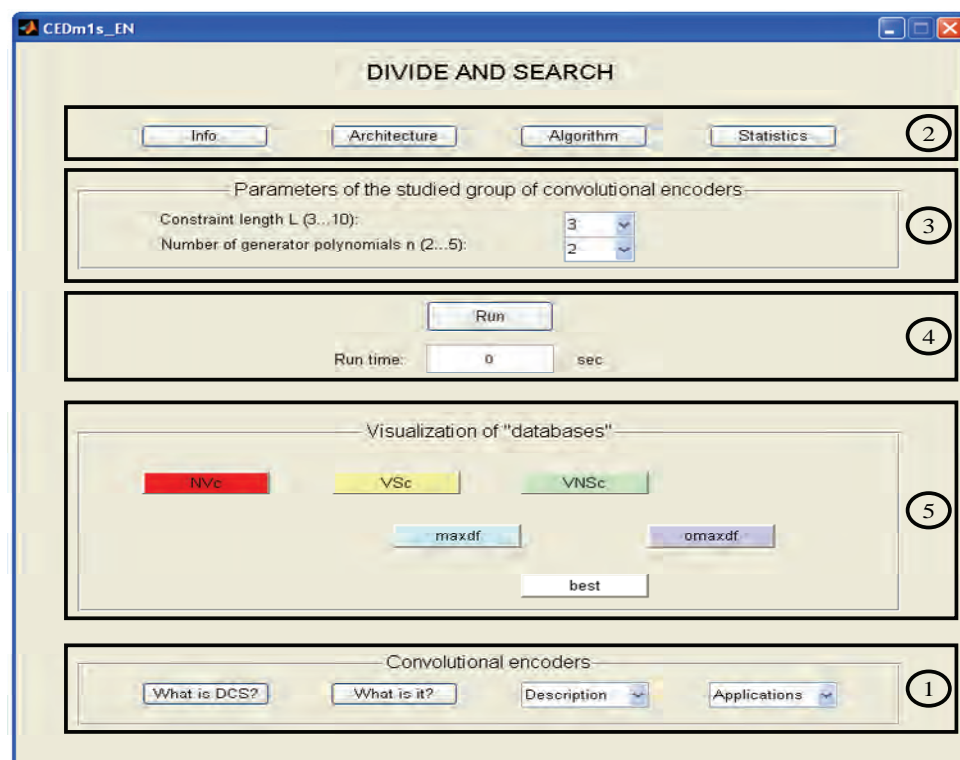


Fig. 2. Layout of the Interactive Learning Module with GUI

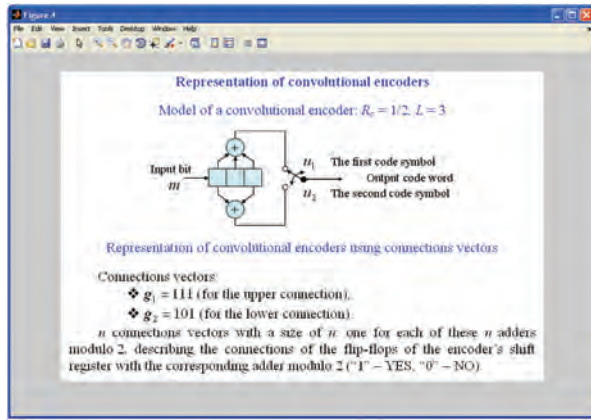


Fig. 3. Learning content on the representation model of a convolutional encoder using connections vectors

### C. Functionality of the Interactive Learning Module

Pressing the “Architecture” push-button the architecture of Module 1: “Divide and search” is displayed in a separate graphics window (Fig. 4), the third improved version [7].

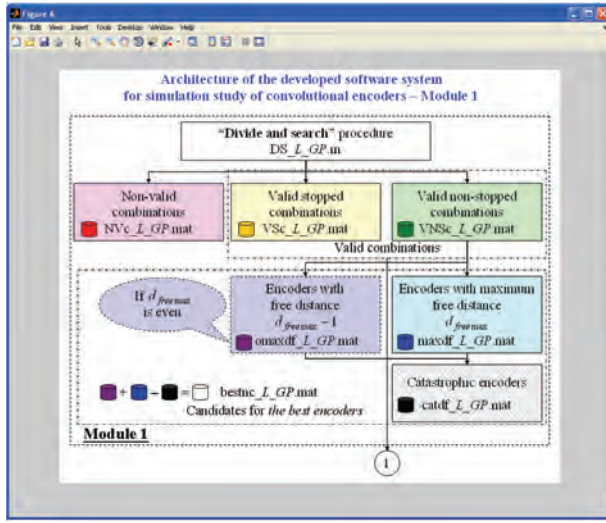


Fig. 4. Architecture of Module 1: “Divide and search” when pressing the “Architecture” push-button

The blocks of the architecture in Fig. 4 are described below. After passing through all possible combinations of polynomial generators, they are divided into two groups:

1) non-valid combinations, stored in the database NVC<sub>L</sub>\_GP.mat and not examined;

2) valid combinations divided into two subgroups: valid stopped combinations, stored in the database VSc<sub>L</sub>\_GP.mat, for which the simulation is terminated after a fixed time (100 s) in an attempt to determine their *free distance* and valid non-stopped combinations, stored in the database VNSe<sub>L</sub>\_GP.mat, for which the simulation of the “divide and search” procedure has completed successfully, as their *free distance* is determined. From all valid non-stopped combinations in a separate database maxdf<sub>L</sub>\_GP.mat the combinations with a maximum value of the parameter *free*

*distance d<sub>free max</sub>* are stored. If *d<sub>free max</sub>* is even the database omaxdf<sub>L</sub>\_GP.mat is generated where the encoders with *free distance d<sub>free max</sub> - 1* are kept. These two databases form the database best<sub>L</sub>\_GP.mat, which stores all possible *candidates for the best encoders*. The databases VNSe<sub>L</sub>\_GP.mat, maxdf<sub>L</sub>\_GP.mat, omaxdf<sub>L</sub>\_GP.mat and best<sub>L</sub>\_GP.mat are modified respectively into the databases VNSe<sub>L</sub>\_GP\_df.mat, maxdf<sub>L</sub>\_GP\_df.mat, omaxdf<sub>L</sub>\_GP\_df.mat and best<sub>L</sub>\_GP\_df.mat, containing information about the corresponding value of the parameter *free distance*.

After testing the candidates for the best encoders using Module 2 of the system all catastrophic encoders that allow catastrophic spreading of errors during the decoding process are stored in the database catdf<sub>L</sub>\_GP.mat. After eliminating the catastrophic encoders from the database best<sub>L</sub>\_GP.mat the database bestnc<sub>L</sub>\_GP.mat containing the encoders that actually have the chance to be the best is formed [7].

Module 1 was tested for the following cases:  $L=3$  and  $GP=2 \div 5$ ,  $L=4$  and  $GP=2 \div 5$ ,  $L=5$  and  $GP=2 \div 5$ ,  $L=6$  and  $GP=2 \div 3$ ,  $L=7$  and  $GP=2 \div 3$ ,  $L=8$  and  $GP=2 \div 3$ ,  $L=9$  and  $GP=2$ ,  $L=10$  and  $GP=2$ . Using the mathematical models developed for cascaded convolutional encoders [8], “Divide and search” procedure is implemented for convolutional encoders with two registers and three generator polynomials used as internal encoder in the structure of the cascaded convolutional encoder, for the cases  $L=[2 \ 2]$  and  $GP=3$ ,  $L=[3 \ 3]$  and  $GP=3$ .

The results of the simulation study are summarized in the table that is displayed in a separate graphics window when clicking on the “Statistics” push-button (Fig. 5).

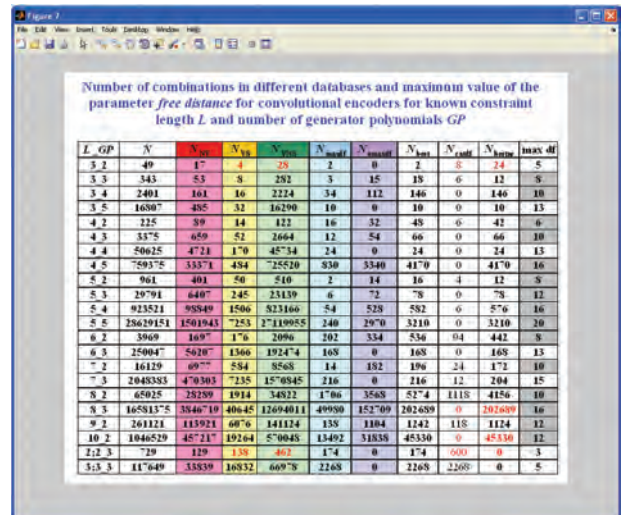


Fig. 5. Analysis of convolutional encoders when pressing the “Statistics” push-button

In the “Parameters of the studied group of convolutional encoders” panel the user is able to choose from a pop-up menu the value of the constraint length  $L$  (3 to 10) and the number of generator polynomials  $n$  (2 to 5) of the encoder. These lists of options could be extended to other possible values. Pressing the “Run” push-button (Fig. 2, panel 4) a

dialog box “Selection?” is shown (Fig. 6) with the following message: “The use of embedded databases is recommended, since in some cases the simulation takes too long time! Do you want to follow the procedure “Divide and search?””.

If the user selects “No”, the data from running “Divide and search” procedure embedded in the developed application is loaded and the user can use it “for granted” when working with other system’s modules. If the user wants to continue to test the performance of the procedure he/she may need to be armed with great patience. The run time for the procedure is shown in seconds, when performing the “Divide and search” procedure. Otherwise the corresponding field is blank. For example, the simulation time for testing the group of convolutional encoders with  $L = 3$ ,  $GP = 2$  is 417.5930 sec.



Fig. 6. Dialog box “Selection?” when pressing the “Run” push-button

In the “Visualization of databases” button-group (Fig. 2, panel 5) there are six push-buttons: NVc, VSc, VNSc, maxdf, omaxdf and best. When pressing one of them the diagram of the algorithm implemented in the script DS\_L\_GP.m (only when  $L = 3$ ,  $GP = 2$ ) is given in a graphical window (Fig. 7) and the content of the corresponding database is visualized in the Variable Editor (Fig. 8) where the first two columns are the decimal generators (Fig. 8, block 1), and the third column (if available) is the value of the *free distance* (Fig. 8, block 2). The best encoders with maximum free distance are shown in Fig. 8, block 3.

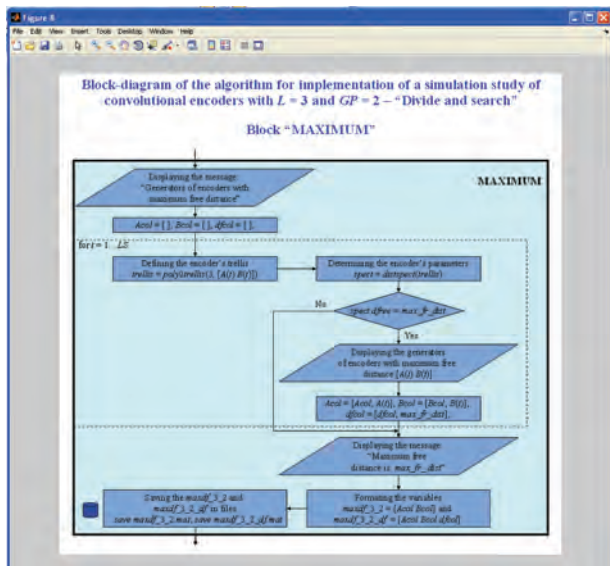


Fig. 7. Block-diagram of the algorithm implemented in “Divide and search” procedure – block “Maximum” when pressing the “maxdf” push-button

Fig. 8. Variable Editor for the variables VNSc\_3\_2 and VNSc\_3\_2\_df when pressing the “VNSc” push-button

### III. CONCLUSION

The Interactive Learning Module will be used in teaching the course “Coding in Telecommunications Systems”, included as optional in the curriculum of the specialty “Telecommunication Systems” for the Bachelor degree. Future work plans to develop similar applications covering other codes studied in this course: linear, cyclic, BCH-codes, Reed-Solomon codes and turbo-codes.

### REFERENCES

- [1] R. E. Blahut, “Theory and Practice of Error Control Codes”, Addison-Wesley Pub. Co., 1983.
- [2] S. J. Curry, “Selection of Convolutional Codes Having Large Free Distance”, PhD dissertation, University of California, Los Angeles, 1971.
- [3] K. J. Larsen, “Short Convolutional Codes with Maximal Free Distance for Rates 1/2, 1/3, and 1/4”, IEEE Transactions on Information Theory, vol. IT19, no 3, 1973, pp. 371 – 372.
- [4] J. P. Odenwalder, “Optimal Decoding of Convolutional Codes”, PhD dissertation, University of California, Los Angeles, 1970.
- [5] B. Sklar, “Digital Communications: Fundamentals and Applications”, New Jersey, Prentice Hall, 1988.
- [6] A. Borodzhieva, “Software Instruments for Investigating Convolutional Encoding and Decoding Processes Applied in Communication Systems”, International Symposium for Design and Technology of Electronic Packaging, 14th Edition, SIITME 2008, Predeal, Romania, Conference proceedings, pp.135 – 139.
- [7] A. Borodzhieva, “Software System for Convolutional Encoders Investigation Using MATLAB and Communication Toolbox”, Advanced Aspects of Theoretical Electrical Engineering, Sozopol ’09, Regular papers, Part 2, pp. 117 – 123.
- [8] A. Borodzhieva, “Simulation Investigation of Cascaded Convolutional Encoders Using MATLAB and Communication Toolbox. Advanced Aspects of Theoretical Electrical Engineering, Sozopol ’09, Regular papers, Part 2, pp. 108 – 116.
- [9] F. Nouvel, “Channel Coding and Decoding: an E-Learning Inter-Active Course”, Proc. of Int. Conf. on Information and Communication Technologies: From Theory to Applications, 2004, pp. 113 – 117.
- [10] R. Tervo, “Digital Communications”, <http://www.ee.unb.ca/cgi-bin/tervo/viterbi.pl>
- [11] MathWorks website, [www.mathworks.com](http://www.mathworks.com)

# GUI for Properties Measurement of Medical Images

Veska Georgieva<sup>1</sup> and Olga Valchkova<sup>2</sup>

**Abstract –** In the paper is presented software for measurement of some statistic properties, which can be used by analyses of medical image objects and its graphic user interface (GUI). It works in the MATLAB environment and uses IMAGE TOOLBOXES defined functions. The investigated properties can be obtained on the base of shape measurements and pixel value measurements of the images. The GUI proposes also an interactive option to choose region of interest (ROI) in the processed image and some parameters of the applied methods.

The presented GUI is suitable to engineering education for studying of this processing. The proposed GUI can be applied also to real medical images attempt to make diagnostic more precise.

Some experimental results are presented, obtained by computer simulation in MATLAB Environment.

**Keywords –** Medical images, Analyse of medical objects, Shape measurement, Pixel value measurement, and Graphic user interface.

## I. INTRODUCTION

The medical imaging technologies exploit the interaction between the human anatomy and the output of emissive materials or emissions devices. These emissions are then used to obtain pictures of human anatomy. The most popular technologies are ultrasound (US), X-rays, Computed tomography (CT) and Magnetic resonance imaging (MRI). These images provide important anatomical information to physicians and specialist upon which can be made diagnoses. In order for pathology or any tissue for that matter to be visible in a medical image there must be obtain some information about statistic properties of the specific objects in the analyzed regions[1].

The paper presents an application and GUI for measurement of set of properties of MRI images. In clinical practice, MRI is used to distinguish pathologic tissue from normal tissue. MRI provides detailed images of the body in any plane. It provides much greater contrast between the different soft tissues of the body than CT does, making it especially useful in neurological (brain), musculoskeletal, cardiovascular, and ontological imaging. The GUI can be applied also to different medical modalities images.

The image analyses functions include: Calculation of histograms for detailed visual analysis, computing of shape measurements such as area, bounding box (as the smallest rectangle containing region), center of mass of the selected

region, based on location and intensity value, perimeter and orientation of the selected object and the distance between different points in the medical objects [2]. In this case are used fast algorithms to compute the true Euclidean distance transform, especially in the 2-D case [3]. The orientation is the angle in degree between the X-axis and the major axis of the ellipse that has the same second-moments as the region.

The software is created in MATLAB 7.12 environment by using IMAGE PROCESSING TOOLBOX.

The graphic user interface consists of checkboxes, buttons, edit boxes, pop-up controls, which make it easy to use. Users enter or choose input data in a single form, because input information changes and visualizations are easier and faster in this way. The processed image can be saved on the disk and so can be used to another processing or its visualization.

## II. GUI FOR PROPERTIES MEASUREMENT OF MEDICAL IMAGES

The proposed GUI for properties measurement of medical images is presented on Fig.1. It is divided in several areas, where the user applies different settings, concerning image analyzing functions and theirs parameters.

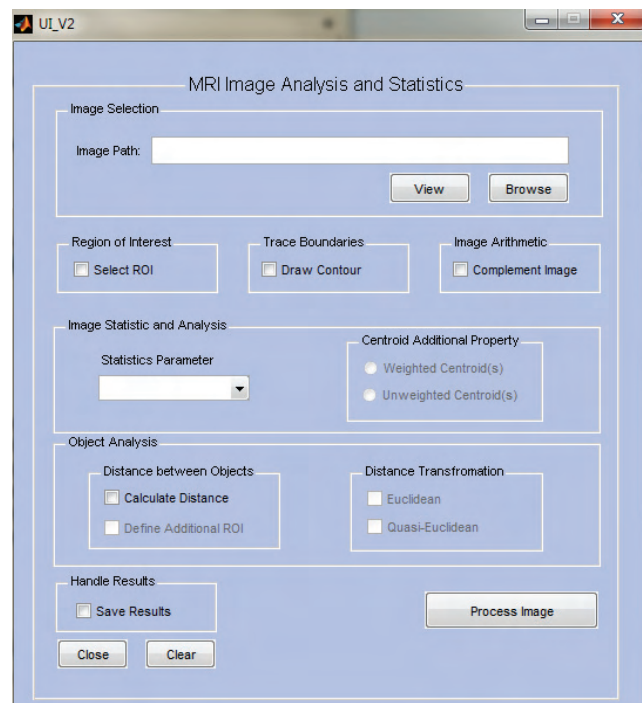


Fig.1. GUI for properties measurements of medical images

The area “Image Selection” is for entering an image file name with an image file extension. The user can navigate among the folders in the work folder and choose image by

<sup>1</sup>Veska Georgieva is with the Faculty of Telecommunications at Technical University of Sofia, 8 Kl. Ohridski Blvd, Sofia 1000, Bulgaria, E-mail: [vesg@tu-sofia.bg](mailto:vesg@tu-sofia.bg)

<sup>2</sup>Olga Valchkova is with the Faculty of German Engineering Education and Industrial Management at TU of Sofia, 8 Kl. Ohridski Blvd, Sofia 1000, Bulgaria, E-mail: [ovaltschkova@gmail.com](mailto:ovaltschkova@gmail.com)

using “Browse” button and view the image by using “View” button.



Fig. 2. Area “Image Selection”

The user can choose some functions such as region of interest (ROI), contour of the selected objects and (or) complement of image. With the last function the dark areas of the image become lighter and light areas become darker. They are not obligatory for image statistic and analysis, but they can give more visual information for the investigations.

The area “Image Statistic and Analyses” is shown on Fig. 3. The user can select different statistic shape properties from the medical object such as bounding box, standard deviation, perimeter, area, orientation, computing of partial histogram and the centroid. For more precisely investigation can be selected also the type of the center of mass of the selected ROI. The computed histogram is presented in graphical mode.

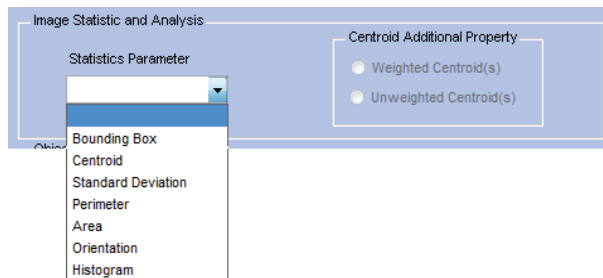


Fig. 3. Area “Image Statistic and Analysis”

The next area “Object Analysis” is shown on Fig.4. It can be used by computing a distance between two or more objects in the image. In this case are used fast algorithms to compute the true Euclidean or (and) Quasi- Euclidean distance transform. They can be selected respectively from the Checkboxes.

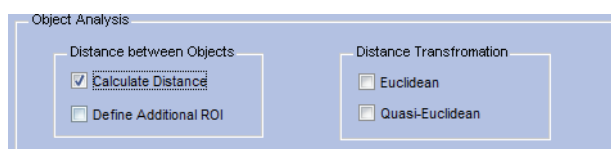


Fig. 4. Area “Object Analysis”

The obtained results can be saved on HDD in image files in ‘jpg’ format by selecting the check- box “Save Results” in area “Handle Results”. They can be used by more detailed statistic processing and analyzing.

After choosing all input information the procedure of processing begins, when the user clicks on button “Process Image”. Then the final result is shown – original image, and the obtained result-images. When button “Close” is pressed the program can be closed. Message about a mistake “Invalid

Image Path” or a warning message such as “Please specify the Image Path” can be obtained by simulation.

### III. TASKS CARRIED OUT FROM THE MAIN PROGRAM

The basic algorithm that works behind is shown in Fig.5.

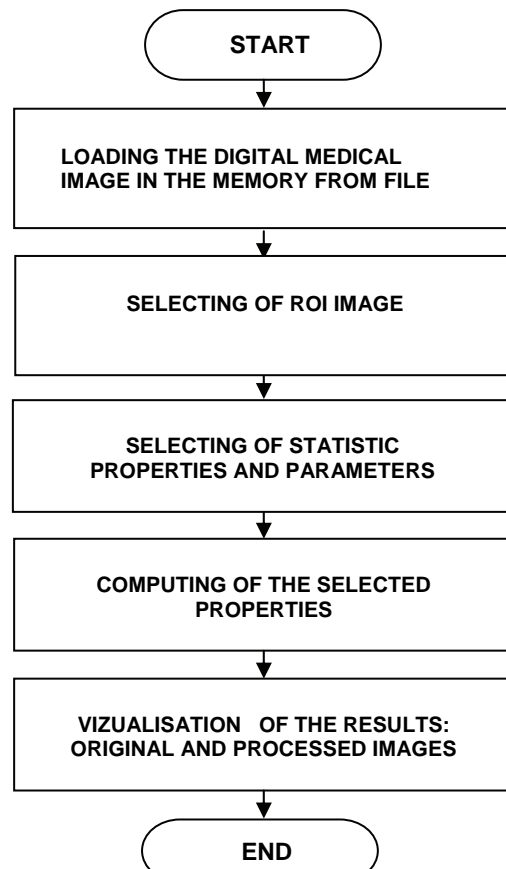


Fig. 5. Block diagram of the basic algorithm

By acting of component from GUI can be implemented a callback-function from the main program. Every graphic component can be treated to object. Every object can be referred to handle. The objects referred a complex of attributes, which can be manipulated from the software. The multifarious attributes can be leaved for using in MATLAB environment, such as “Enabled”, “Value”, “Visible”, “On”, “Off” etc. [4]. Every attribute can be enabling in the presence of corresponding handle or reference to the object. Every graphic component can be reiterated to a cycle of events for the MATLAB environment by initialization of the graphic application. It submits addresses of the callback- functions, associated to a given event, which are important. By its identification can be called out a corresponding callback- function. One of the important tasks that the main program has is input data validation. The execution is canceled if an error concerned with wrong information occurs. Another essential purpose of the main program is presenting the input

information in appropriate data structures. It is necessary for the next steps in the processing strategy, in this step the processing is made with appropriate input data.

Some results from simulation, which illustrate the working of the program, are presented in the next figures below.

In Fig.6 is shown the original MRI image of size 512x256 pixels with brain tumor.

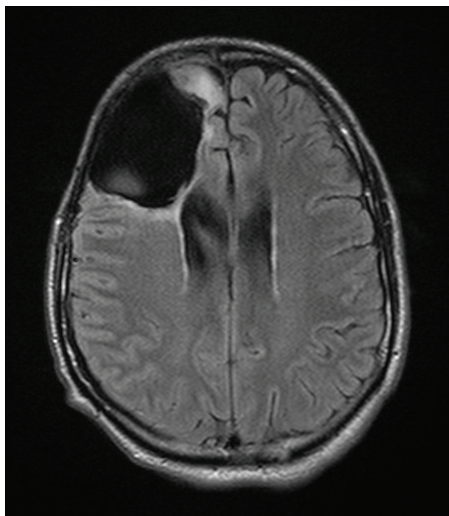


Fig. 6. Original MRI image

In Fig.7 are presented selected ROI image of size 120x100 pixels and its modification, made by complement of the original ROI image.

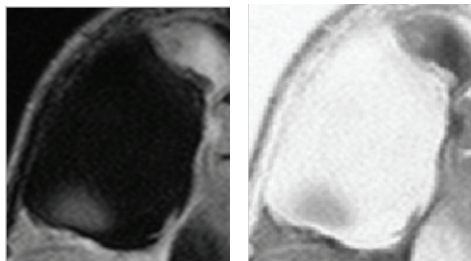


Fig. 7. Selected original ROI image and its modification

In the next figures are presented the results obtained by computing of some statistic properties of the investigated objects. In Fig. 8 are displayed exterior object boundaries (colored inside).



Fig. 8. Exterior object boundaries in ROI image

In Fig. 9 is shown the computed histogram of the selected ROI image.

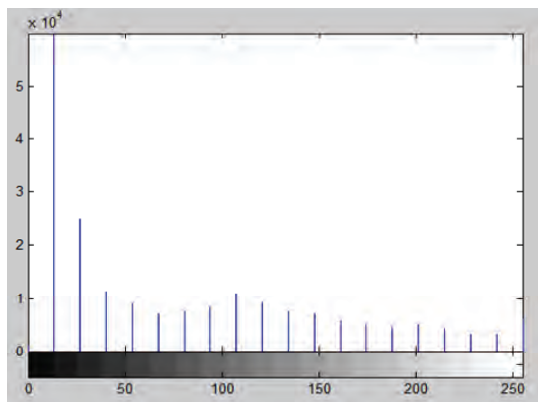


Fig. 9. The histogram of selected ROI image

Fig. 10 illustrates the axes and the orientation of the corresponding ellipses of some objects and weighted centroids in the investigated region in order to obtain information of their position detection.

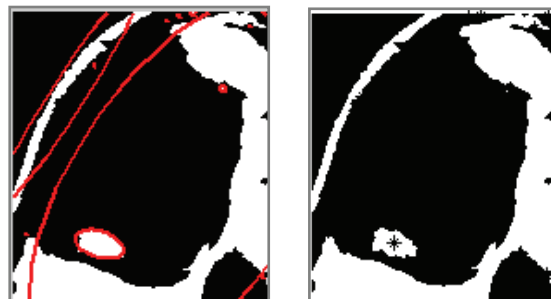


Fig. 10. Orientation of the corresponding ellipses and centroids of some objects

In Fig. 11 are shown 4 selected points (P1, P2, P3 and P4) from the investigated objects and the graphic of the computed Euclidean distance.

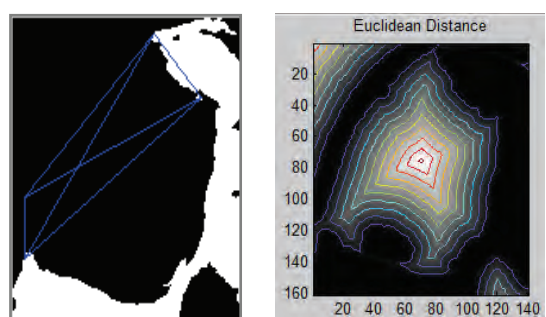


Fig. 11. Selected points and graphic of their Euclidean distances

In Table 1 are presented the Euclidean distances between the selected points, which are calculated by the program.

TABLE I  
EUCLIDEAN DISTANCES BETWEEN THE SELECTED POINTS

Points	P1	P2	P3	P4
P1	0	33	143.67	138.05
P2	33	0	117.52	120.30
P3	143.67	117.52	0	44.69
P4	138.05	120.30	44.69	0

#### IV. CONCLUSION

In this paper is presented a GUI for measurement of set of statistic properties, which can be used by analyses of medical image objects. It uses MATLAB defined function and works in MATLAB 7.12 environment. The processing can be used to analyze objects as organs and tumors by using of shape measurement and pixel measurement algorithms. The GUI can be used in engineering education for studying this process. It can be used also in real time to provide important anatomical information in medical images to physicians and specialist upon which can be made diagnoses of different diseases. Some results can be used for future application in 3D visualization.

#### REFERENCES

- [1] M. Smith, A. Docef, "Transforms in telemedicine applications", Kluwer Academic Publishers, 1999.
- [2] H. Mallot, Datenanalyse mit Matlab: Mathematische Grundlagen, Eberhard Universität Tübingen, 2011
- [3] W. Pratt, "Digital Image Processing", John Wiley & Sons Inc., 2001.
- [4] MATLAB User's Guide. Accessed at: [www.mathwork.com](http://www.mathwork.com)

# Realization of flying shear for laboratory experiments

Božić Miloš<sup>1</sup>, Nebojša Mitrović<sup>2</sup> and Marko Rosić<sup>1</sup>

**Abstract –** In industry automatic lines, it is all about shorter production time. It would be the best for some automatic lines, to do cutting or drilling on moving parts without stopping. This type of machine is commonly called “machine on the fly”. This paper presents realization of one type of machine known as a parallel “flying shear” for laboratory experiments. Main components of the system are PLC controller, AC servo drive and variable frequency drive. It would be used for testing of different algorithms and for educational purposes.

**Keywords –** flying shear; PLC; variable frequency drive; servo drive.

## I. INTRODUCTION

The flying shear is a common industrial application for cutting a product into smaller lengths, without stopping the line, this means that the main production process is not interrupted, and so machine's productivity is maximized. The cutting tool is typically mounted on a carriage that moves either parallel to the product flow or at an angle across the product flow. The flying shear drive accelerates the carriage to synchronize with the line speed. While they are synchronized the cut is done. After that the carriage decelerates and returns to start position ready to cut again. There are also many other similar applications where a carriage must be synchronized at line speed. The most of these applications can also be accommodated using the flying shear application software.

A couple of examples are:

A machine extrudes plastic pipes that must be supplied to the customer in pre-cut lengths. The extrusion process requires the extruder to run at a continuous speed to maintain the quality of the product. The pipe is uniform along its length and provided the length is within a set tolerance then the pipe is fit for sale. The flying shear is used to cut the product cyclically.

Linear flying shears are used in a variety of applications ranging from cutting material on the fly, filling bottles as they are moving on a conveyor, to forming soft material in a mold while being transferred along the process. This particular overview describes the flying shear (cutting) application, but can be used for any process that requires speed matching to a given axis. Linear flying shear applications can be used to solve both random in-feed and constant feed applications. This application controls the linear axis of the saw to ensure

<sup>1</sup>Miloš Božić and Marko Rosić is with the Faculty of Technical sciences at University Kragujevac, Svetog Save 65, Cacak 32000, Serbia, e-mail: milos.bozic@ftn.kg.ac.rs.

<sup>2</sup>Nebojša Mitrović is with the Faculty of Electronic Engineering, Aleksandra Medvedeva 14, 18000 Nis, Serbia, e-mail: nebojsa.mitrovic@elfak.ni.ac.rs

accurate cutting as well as a digital output for providing control of the cutting mechanism [1]–[5].

## II. PARALLEL FLYING SHEAR

With parallel flying shears, the carriage travels in the same direction as the material. In the example shown below a shear is used to cut through a material, while the carriage and the material are synchronized. The shear would then be raised and would return to the start position ready to repeat the cycle. The parallel mode is best suited to applications where the tool operates instantaneously across the whole material width at the same time, such as a punch tool or a shear.

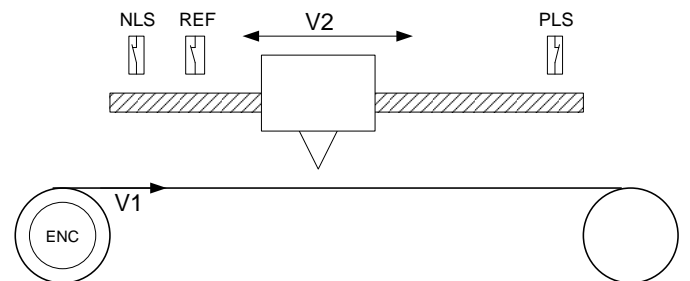


Fig. 1. Flying shear concept

Components shown in Fig. 1. above are:

- NLS – negative limit switch
- PLS – positive limit switch
- REF – reference switch
- $V_1$  – conveyor speed
- $V_2$  – carriage speed
- ENC – master encoder

## III. ALGORITHM

Algorithm for flying shear application can be divided into three steps [6].

1. Homing
2. Synchronization
3. Specific operation (cutting, printing, gluing...)
4. Back to start position

Homing is process wherein the system is seeking for reference point or home. Homing can be done in many different ways, using the reference switch, using limits switches, with encoder, or with some mechanical barrier. When the system is referenced, next step in the algorithm can start.

Synchronization is process wherein linear axis with carriage is pretending to synchronize its moving with conveyor. When the speed of the carriage becomes equal to speed of conveyor, these two axes are synchronized. During synchronized moving some specific operation can be done. After specific operation is done carriage on linear axis go back to start position and wait for next move.

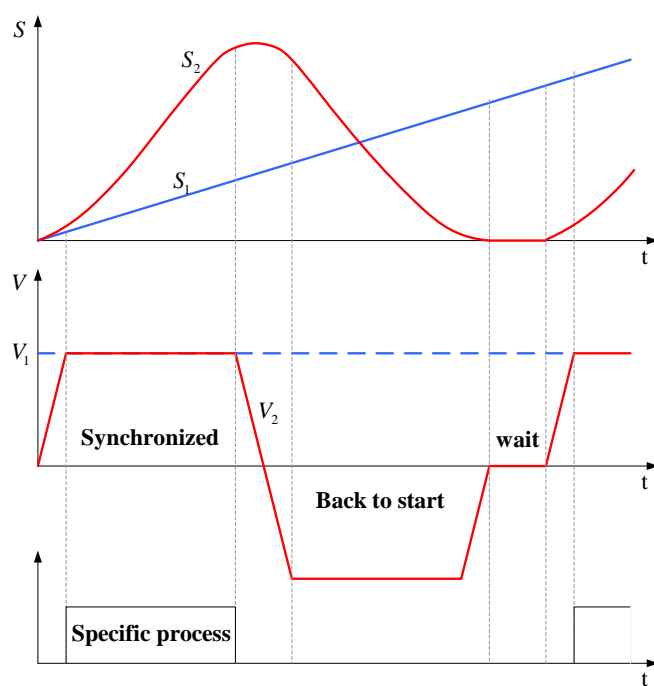


Fig. 2. Timing sequence

There are two different types of work regime of linear axis. It can be: continuous and discontinues. When carriage goes back to a start position also called wait position it is discontinues regime, and when there is no time for back to wait position it is continuous regime.

#### IV. COMPONENTS OF THE SYSTEM

The main components of the system are presented on Fig. 3:

- Programmable logic controller
- Servo drive
- Variable frequency drive
- Servo motor
- Master encoder
- Induction motor

##### A. Programmable logic controller

Programmable logic controller (PLC) used for this application is Schneider Electric Modicon M238. This controller offers high performance at low cost with efficient embedded features dedicated to simple axis motion control

(high speed counting up to 100kHz, high speed pulse train and pulse width outputs). Embedded CANopen master allows easy and adaptable architectures for development flexibility. There are two serial lines for HMI connection or peripherals devices [7].

##### B. Servo AC drive

Motion servo drive used for this application is Schneider Electric Lexium32M. This motion servo drive enables different work regimes: speed, position, torque and electronic gear. For a use of this application, servo is working in electronic gear regime. Electronic gear regime represents the operation in which two independent axes can be synchronized. The work way is based on getting impulses from the master encoder directly into a pulse train input (PTI) on motion servo drive. The basic thing which should be set is ratio between impulses from encoders. The purpose is to get good ratio between the speeds [8].

##### C. Variable frequency drives

Variable frequency drive (VFD) used for this application is Schneider Electric Altivar 312. This frequency drive represents standard industrial convertor. He has CANopen port, so the wiring is minimized. All commands and reference of speed are being setup through CANopen communication [9].

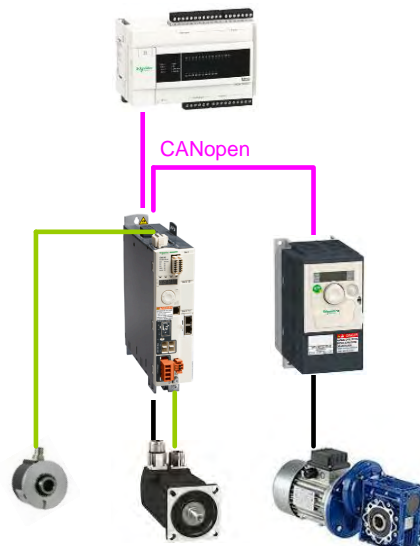


Fig. 3. Connection diagram

Master encoder is classical industrial incremental encoder with 1024 pulses per turn. He has two phases A and B. Based on the pulses number from encoder length of the cutting peace is tracked. Also, the instantaneous speed of line is calculated.

#### V. REALIZATION OF ALGORITHM IN CODESYS

PLC controller used in this project is in accordance with standard 61131-3. The main part of algorithm is created using

higher abstraction language sequential functional chart (SFC). Steps inside SFC program are created using functional block diagram (FB). Using this type of programming created program looks like algorithm [10][11].

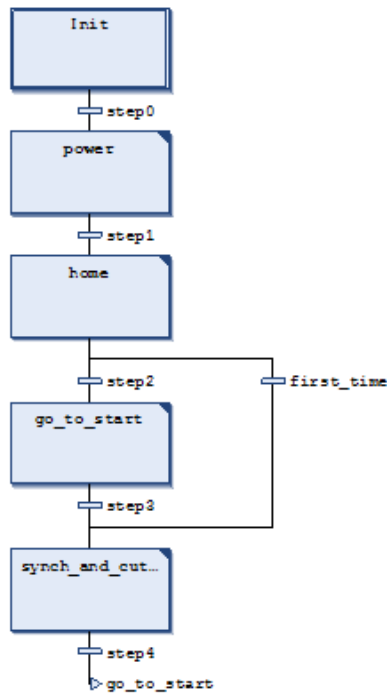


Fig. 4. SFC program

In the SFC program next steps can be noticed:

**Init** – in this step the starting initialization of the system is done.

**Power** – during this step the energetic part of VFD and motion servo drive are enabled. Also, if there is a need for device resetting it can be done in this step.

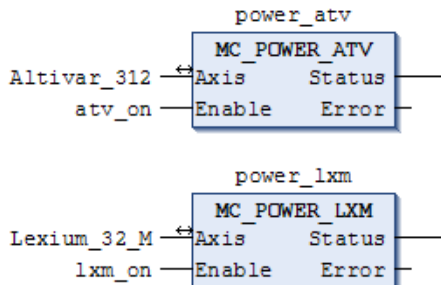


Fig. 5. Powering VFD and motion servo drive

**Home** – this is the step in which system is seeking for reference – zero point. Method used for homing is method with limith switch without reference switch. During this operation linear axis is moving until stepping on the switch. In that moment linear axis is stopping and returns for couple

encoders pulses. That is reference or home position. The next Fig. 6. shows layout of function block for homing. As it can be seen on block the following parameters like: homing mode, homing speed, number of pulses for returning, has to be entered.

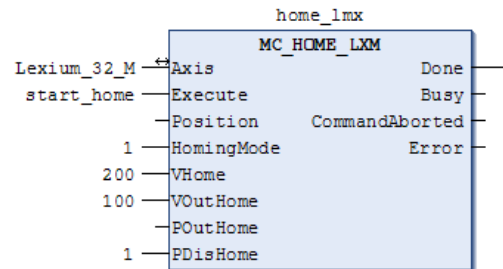


Fig. 6. Function block for homing

**Synch\_and\_cutting** – in this step synchronization of axes is in progress. When the axes synchronization is done, specific operation during synchronized movement can be preceded. After the operation is done, axes are ending their work in synchronization and linear axis goes back to reference point. Function block for synchronization of axes is GearIn. This block needs parameters like numerator and denominator to be entered. And with them the ratio of speeds is achieved. Function block GearOut is used, for desynchronization.

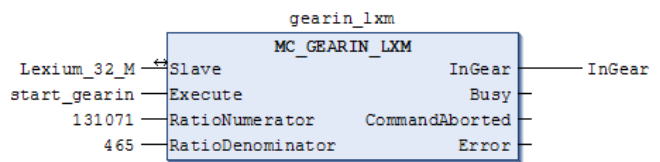


Fig. 7. . Function block GearIn

**Go\_to\_start** – during this step carriage returns to its start position. This step is very different from homing step. Reference point is known so there is no need to seek limit switch, and carriage is sent to start point with functional block MOVEABSOLUTE.

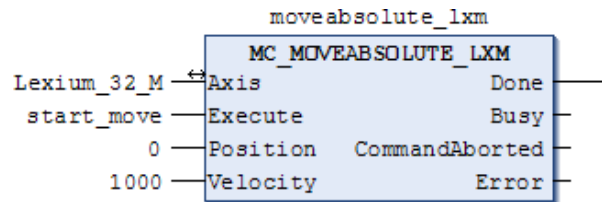


Fig. 8. . Function block move absolute

After return to start position, cycle start again from go\_to\_start point in program.

For this application, graphical user interface in Codesys visualization is also developed. In that way the user can enter parameters like speed of the line, length of the peace etc.

Beside entered parameters user can monitor current values of variables like position of carriage, speed of line.

## VI. EXPERIMENTAL RESULTS

In this PLC controller object called trace can be added. His function is to show some variables in form of time diagram. On next figure position and speed of servo axis is shown.

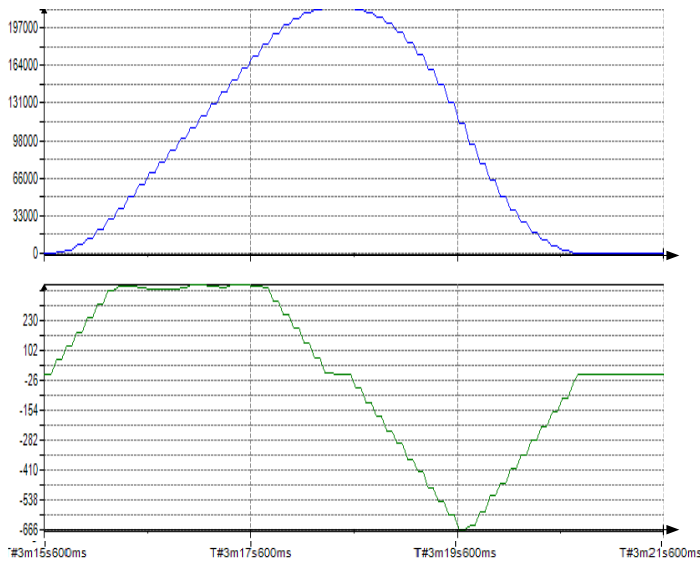


Fig. 9. Position and speed of servo axis

## VII. CONCLUSION

In this paper is presented the realization of flying shear application intended for laboratory and educational purposes. It has parallel structure.

Using this laboratory model many different algorithms can be developed. Here is presented a simple application with PLC. More advanced applications require motion controller. By using the motion controllers possibilities are much higher. Function block like flying shear is also available.

This application model is very practical for students work. It allows them to change parameters and test model of flying shear in safe laboratory environment. From this model students can adopt a different knowledge's, like:

- Setting up variable frequency drive;
- Setting up motion servo drive;
- Programing of PLC using standardized Codesys software package
- Creating of different control algorithm

Future steps will be improvement of dynamical features on mechanical part of system. Also the real motion controller will be used.

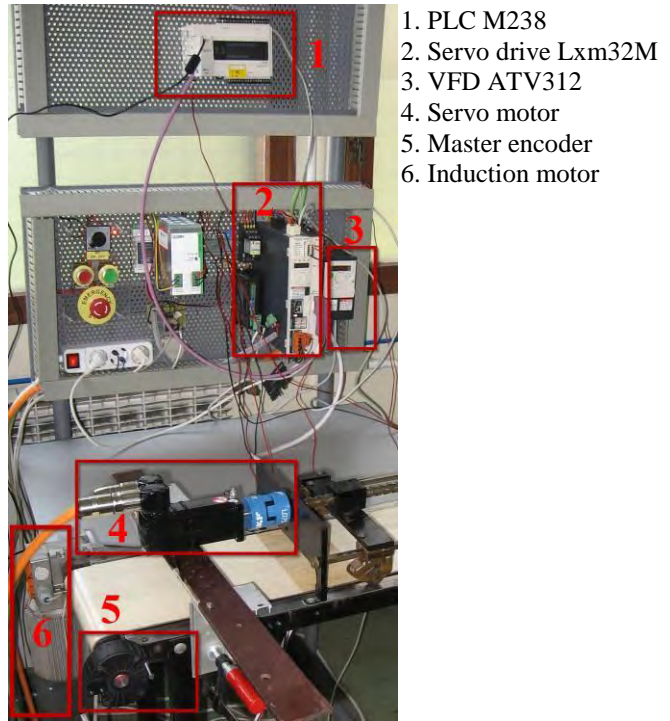


Fig. 10. Flying shear system in mechatronic laboratory

## REFERENCES

- [1] Controller for Flying Operation (Flying Saws, Shears, Punchers etc.), Motrona GmbH, [http://www.motrona.com/cutter\\_control\\_1.html](http://www.motrona.com/cutter_control_1.html), april 2013
- [2] Linear flying shear Yaskawa, [http://www.yaskawa.com/site/\\_industries.nsf/applicationDoc/appflyingshear.html](http://www.yaskawa.com/site/_industries.nsf/applicationDoc/appflyingshear.html), april 2013
- [3] Emerson Industrial automation, <http://www.emersonindustrial.com/en-EN/controltechniques/products/industryolutions/flyingshear/Pages/flyingshear.aspx>, april 2013
- [4] Baldor motion, <http://www.baldormotion.com/support/supportme/downloads/docslib/AN00116-003-%20Flying%20shear.pdf>, april 2013
- [5] Flying Shear Position Control, <http://www.control.com/thread/1265720499>, discussion forum, april 2013
- [6] Motion tutorials, <http://www.galilmc.com/learning/tutorials.php>, april 2013
- [7] Logic controller modicon M238, manual, <http://www.schneider-electric.com/download/>, march 2013
- [8] Motion servo drive Lexium32, manual, <http://www.schneider-electric.com/download/>, march 2013
- [9] Variable frequency drive ATV312, manual, <http://www.schneider-electric.com/download/>, march 2013
- [10] 3S-Smart Software Solutions, Codesys manual, [www.codesys.com/support-training/self-help/codesys-manual.html](http://www.codesys.com/support-training/self-help/codesys-manual.html), april 2013
- [11] Motion Control, PLCopen organization, [www.plcopen.org/](http://www.plcopen.org/), april 2013

# Curricula Innovation of the Study Program in Environmental Protection Engineering

Tale Geramitcioski<sup>1</sup>, Vangelce Mitrevski<sup>2</sup>, Ilios Vilos<sup>3</sup> and Pece Mitrevski<sup>4</sup>

**Abstract –** The academic program for undergraduate studies - Engineering for environmental protection, is designed as a highly interdisciplinary and multidisciplinary study program. It consists of several educational research fields from the engineering vocation and is formed by study units that make the interdisciplinarity of the program. A special problem of the transition countries, such as the unequal economic growth and the need for plausible development, imperatively impose the need for educated professionals who will be ready and educated in such a way to solve the accumulated complex problems in the area of engineering for environment protection.

**Keywords –** Study program, Curriculum, Engineering, Environmental protection.

## I. INTRODUCTION

The academic program of undergraduate studies - the first cycle (Bologna), Engineering for environmental protection is designed as a highly interdisciplinary and multidisciplinary study program. The program of undergraduate studies of engineering for environmental protection consists of educational research fields from the engineering vocation and is formed by study units that with the intersection of several disciplines make the interdisciplinary of the program. In the realization of the program the curriculum areas of environmental protection, machinery, energy, electrical engineering, management, construction and basic scientific disciplines of mathematics, chemistry, physics and other sciences that form the basis of multidisciplinary engineering study program for environment protection are studied.

The universal phenomenon of global warming, acid rains, the effect of greenhouse, ozone holes, extinction and the vanish of a complete range of plants and animals, changed conditions of life, destruction of the natural resources and

<sup>1</sup>Tale Geramitcioski is with the Department of Mechanical Engineering, Faculty of Technical Sciences at the "St. Kliment Ohridski" University of Bitola, Ivo Lola Ribar b.b., Bitola 7000, Republic of Macedonia, E-mail: tale.geramitcioski@uklo.edu.mk.

<sup>2</sup>Vangelce Mitrevski is with the Department of Mechanical Engineering, Faculty of Technical Sciences at the "St. Kliment Ohridski" University of Bitola, Ivo Lola Ribar b.b., Bitola 7000, Republic of Macedonia, E-mail: vangelce.mitrevski@uklo.edu.mk.

<sup>3</sup>Ilios Vilos is with the Department of Traffic and Transport Engineering, Faculty of Technical Sciences at the "St. Kliment Ohridski" University of Bitola, Ivo Lola Ribar b.b., Bitola 7000, Republic of Macedonia, E-mail: vilos.ilios@uklo.edu.mk.

<sup>4</sup>Pece Mitrevski is with the Department of Computer Science and Engineering, Faculty of Technical Sciences at the "St. Kliment Ohridski" University of Bitola, Ivo Lola Ribar b.b., Bitola 7000, Republic of Macedonia, E-mail: pece.mitrevski@uklo.edu.mk.

riches at a global and local national level grew into one of the most important world issues and factors in the future sustainable development of the human civilization.

A special problem of the transition countries (such as the Republic of Macedonia) as the unequal economic growth, the need for plausible development, imperatively impose the need for educated professionals who in the commercial and industrial systems, public enterprises and state institutions will be ready and educated in such a way to solve the accumulated complex problems in the area of engineering for environment protection.

The interdisciplinarity of the study program of the engineering for environment protection is the one which is the result of technical and engineering knowledge, provides an opportunity to educate engineers for the environmental protection who will be able to solve the accumulated issues in the system of environmental protection, and also in other industrial and commercial systems in the Republic and outside its borders.

Engineering for environment protection program that was created as a response to the needs of the industry, economy and the institutions that are facing with the problems relating to environmental protection and which need engineers with interdisciplinary knowledge in the field of engineering for environment protection.

## II. SUBJECT AND OBJECTIVES OF THE STUDY PROGRAM

The subject of the study program is to educate students about the profession engineer for environment protection in accordance to the needs and development of the country and very complex engineering problems in the environment, which in direction of society development must be resolved. The study program of engineering for environment protection is designed in such a way that it provides the acquisition of competencies, knowledge, and skills that are socially justified and useful. The Faculty of Technical Sciences defines the basic tasks and goals so as to educate highly competent personnel in the field of technology and engineering. The subject of the study program of engineering for environment protection is fully in line with the basic tasks and goals of the Faculty of Technical Sciences in Bitola.

With the implementation of Curriculum Thus designed, engineers for the protection of the environment which own competence in European and worldwide frames are educated. The aim of the study program is achieving competence and academic knowledge and skills in the engineering field of environmental protection. It includes among other developing innovative engineering capabilities for consideration of ecological problems, the ability for critical and analytical

thinking, to develop the characteristics of teamwork, cooperation, communication skills and subduing specific practical skills needed for an optimum professional work.

The aim of the study program is to mold an expert who owns a sufficient necessary knowledge of the basic scientific disciplines (mathematics, physics, chemistry, mechanics, thermodynamics) to create a clear picture of the processes unfolding in the industrial systems and the environment, as well as knowledge and skills from traditional engineering disciplines mechanical engineering, energy, processing systems, programming and applied scientific disciplines such as waste and hazardous substances management, environmental projects, assessments, managing and reducing the threat and risk over the environment.

One of the specific purposes, which is consistent with the goals of educating professionals at the Faculty of Technical Sciences, is developing a level of knowledge and awareness among students about the need for permanent education (Life Long Learning – 3L), especially in the areas of plausible development and environmental protection.

The aim of the study program also is educating professionals in the domain of the teamwork, as well as developing the abilities and skills for announcing and displaying the results to the professional and general public.

### III. STRUCTURE OF THE STUDY PROGRAM

The title of the study program for undergraduate studies - the first cycle is Engineering for environment protection. As a result of the processes of learning knowledge , skills and competencies are acquired that enable students to use their knowledge to solve problems that arise in the profession, the practice of research, by using theoretical technical literature and enables the continuation of post graduate studies (Second cycle). Following the needs of the economy of our country and the adoption of the new law for high education, new curricula are organized into two cycles:

1. Bologna first cycle with a duration of eight (8) semesters (four academic years) and

2. Bologna second cycle with a duration of two (2) semesters (one academic year).

At the undergraduate studies - Bologna first cycle, which last for four academic years there is one study group: Engineering for environmental protection.

In the course of study, students are given the opportunity, according to their own aspirations and desires, in addition to the compulsory subjects, elect a number of optional subjects.

The compulsory as well as the optional subjects, are defined on the basis of dominant identified problems of the environmental protection in our country, the region and globally, and also on the basis of experience and similar study programs in the EU and the countries worldwide. The structure of the studies is organized such that the first six semesters have common subjects for the three modules, which then constitute a ground for subduing the professional disciplines in the seventh and eighth semester, as well as during the second cycle of the study. From the seventh semester students can choose one of the three modules. Thus, the students are offered a broad opportunity to build

themselves as specialists in more specialized areas, with an opportunity to choose many vocational subjects from one or more areas.

Therefore, in order to provide a greater flexibility of the study program, during the academic years, in addition to the compulsory subjects, optional subjects are also projected. The optional subjects are chosen from groups of enclosed subjects, but the students have an opportunity, according to their own aspirations and desires, but in accordance with the teachers, to choose one of the subjects from the Faculty of Technical Sciences, St. "Kliment Ohridski" University or from another University in the country or abroad. At the same time certain conditions that are prescribed for attending the classes of the optional subject should be fulfilled.

The ratio of European points that are received about certain types of subjects is in accordance with the existing legal norms in the Republic of Macedonia and the University St. Kliment Ohridski "- Bitola. Each subject brings a certain number of European credits (ECTS), and for the completion (graduation) of the first cycle, it is necessary to achieve the minimum 240 European credits. For the completion (graduation) of the second cycle, it is necessary to achieve the total of 300 European credits.

### IV. QUALIFICATIONS AND COMPETENCIES OF GRADUATE STUDENTS

Students at the end of the study of the first cycle (with completion of all exams including the eighth semester),i.e., after the accomplishing the required minimum of 240 European points, they graduate and gain a degree "Bachelor of University Engineer of Engineering for Environment Protection" or "Bachelor of Science in Environment Protection Engineering". Students at the end of the study of the second cycle (with completion of all exams including the tenth semester), i.e., after the accomplishing the required minimum of 300 European points, graduate and gain a degree "Master of Engineering in Environment Protection" or "Master of Science in Environment Protection Engineering".

Graduates from the first and second cycle of engineering in environment protection are competent, qualified and competitive to solve the real problems from the practice, as well as to continue their education, provided that they are determined to do it. Competencies primarily include: developing an ability for critical thinking, an ability to analyze problems, synthesize solutions, prediction and evaluation of the behavior of the chosen solution with a clear image of which are good and which are bad sides to the foresaid.

When it comes to the specific abilities of the students, by adopting the study program, the student acquires fundamental knowledge and understanding the disciplines of the technical and engineering professions, as well as the ability to solve specific problems with implementation of scientific methods and procedures. Given the interdisciplinary nature of engineering study program for environmental protection, it is especially important the ability to connect to and overview of the fundamental and technical disciplines, the holistic approach and knowledge of the basic expertise and skills from

different areas and their utilization. The graduate students of the first cycle of university studies in engineering for the environment protection are capable, in an appropriate manner, to design, and project and present results and activities out of the engineering practice. During the study, emphasis will be placed on much more intensive usage of modern information technologies and tools. Graduates of the first cycle are competent to apply their knowledge into practice and monitor news in the profession, solve problems at all levels and collaborate with local social and international institutions and organizations. Students are able to project, organize, manage in the field of environmental protection. During the study, the student acquires the ability to make experiments independently, interpret and statistically process results, as well as to formulate and convey concrete, realistic and applicable conclusions.

Graduates in engineering for environmental protection – Associate degree (second cycle), are able to define and present the results of the work in an appropriate manner with a very intensive use of information and communication technologies.

Graduates of the second cycle own also additional competencies, unlike students from undergraduate studies, to apply the knowledge into practice and monitoring the implementation of innovations in the profession. Students are qualified to project, organize and manage the environmental protection. In the course of study, students acquire the ability to independently plan and implement an experimental statistical processing of results, as well as formulation and adoption of appropriate conclusions. Graduates (First and Second cycle), from engineering for environmental protection also gain competencies so as how to keep using the resources of the Republic of Macedonia in accordance with the fundamental principles of plausible development. During the study program, students in particular nurture and develop the ability for team work and development of professional ethics.

## V. MOBILITY OF THE STUDENTS

The mobility of the students is provided through the Agreement of academic, scientific and technical cooperation with Fakultet Tehnickih Nauka (Faculty of Technical Sciences) at the University of Novi Sad, Serbia.

## VI. PLAUSIBILITY OF CURRICULA

If Macedonia wants to keep pace with the changes in the environment, its aim is to have well educated engineers for environmental protection - professionals. The purpose of the study programs is creating a basis for competitive model in the education of engineers for environmental protection in line with internationally recognized norms and standards.

Potential students will be informed about the new opportunities and offer by the Faculty using printed brochures and the website of the Faculty ([www.tfb.edu.mk](http://www.tfb.edu.mk)). The study programs allow update, using the European system for transferring points (ECTS), optional subjects, with which is achieved education on many levels. Starting from the first

cycle which lasts for four years and the second cycle lasting a year, the proposed program is designed so that it can easily fit in the system of higher education  $4 + 1 = 5$ , which opens the possibility for the third cycle (doctoral studies) for a period of three years (six semesters). The Mechanical Engineering Department will respond to the changing demands of national, regional and international level.

## VII. FUNDING OF THE STUDY PROGRAMS (CURRICULA)

The financing of the study programs will be according to the criteria for financing curricula by the Ministry of Education and Science of the Republic of Macedonia, and in accordance with the positive legal solutions in this area.

## VIII. CONCLUSION

Serial concept of pre-gradual and post-gradual study via Bologna Declaration looks simple, but it's quite difficult to work out its contents and program:

- It is necessary to distinguish goals of separate stages of education (3-2-3) in connection with different profile of the graduates.
- We have to find proper mechanisms and criteria for assessing quality of education in separate stages.
- Implementation of structured education will demand creation of new curricula and to expand the programs in some subjects.
- In connection with the fact that graduates acquire a wide range of comprehensive knowledge, it will be possible for the universities to concentrate on scientific education.
- Mutual relations of educational programs mentioned above will allow students to have maximal mobility, i.e. transfers between different institutions.
- It is necessary to economize in the education process through approximation curricula of technical departments in the first semesters of education. This is a necessary premise for introducing parallel education in foreign language and for implementation of distance learning elements.

## REFERENCES

- [1] Anwar, S., Favier, P. & Ravalitera, G., An International Collaboration in Engineering Project Design and Curriculum Development: A Case Study. In International Conference on Engineering Education ICEE'1999, Ostrava (Czech Rep.). VSB-TUO, 1999, paper 123, 5 p. ISSN 1562-3580.
- [2] Badiru, Adedeji B. and Herschel J. Baxi, "Industrial Engineering Education for the 21st Century," Industrial Engineering, Vol. 26, No. 7, July 1994, pp. 66-68.
- [3] Bakker, R.M., Geraedts, H.G.M. & van Schenk Brill, D., 1999, A Model for Education in Innovative Engineering, WESIC Conf. Newport: 103-110.
- [4] Geramitcioski, T., "Engineering Education in the Republic of Macedonia – Current State, Perspectives and Development" (in

- Macedonian), ENGINEERING, UDK 62, ISSN 1409-5564, pp. 24-30, 2006.
- [5] Hernant, K., "Engineering Education and Quality Assurance in Europe – After the Bologna Declaration", Engineering Design in Engineering Education, Tokyo, 2004
- [6] Kaminsky, D., Zamarsky, V., Role of Technical University in the Development of Innovation Process. In International Conference on Engineering Education ICEE'2000. Taipei (Taiwan) : National Chiao Tung University, 2000, Paper , 5 p. ISSN 1562-3580
- [7] Landryova, L. & Farana, R., Improving Quality Assurance Co-Operation with European Union Universities. In International Conference on Engineering Education ICEE'2000. Taipei (Taiwan): National Chiao Tung University, 2000, Paper MC5-4, 6 p. ISSN 1562-3580
- [8] Smutny, L. & Vitecek, A., Accreditation of study branches pre-gradual and post-gradual studies on Mechanical Engineering faculties of Czech Republic. In International Conference on Engineering Education ICEE'2000. Taipei (Taiwan): National Chiao Tung University, 2000, Paper WA8-2, 7 p. ISSN 1562-3580.
- [9] Swearengen, J. C. et al, "Globalization and the Undergraduate Manufacturing Engineering Curriculum," Journal of Engineering Education, April 2002, Vol. 94, No. 2, pp. 255-261.

# English for specific purposes on Cloud Platform

Danica Milosevic<sup>1</sup> and Borivoje Milosevic<sup>2</sup>

**Abstract** – This paper discusses the applications of CLOUD services applied to English for specific purposes electronic-learning. Electronics learning (e-learning) is a very broad term that includes all methods and techniques for teaching with the help of computers and the Internet.

**Keywords** – ESP, Cloud, Services.

## I. INTRODUCTION

English for Specific Purposes - ESP is a relatively new discipline within Applied Linguistics that bids a new learner-centered approach to English language teaching whose methodology is based on the specific needs of the learner. Several of the vocational language projects make use of a full-fledged virtual English for specific purposes learning environment. These projects have been created with funding supplied by EU grant programs, including Lingua, Leonardo, and Socrates. These projects, can be implemented in Moodle and make extensive use of new media and collaborative tools. This also incorporates language e-portfolios. Interesting projects in this area also include BeCult and Online VoCAL/Weblingua [10], both of which have richly developed tools and media. Creating effective electronic tools for language learning frequently requires large data sets containing extensive examples of actual human language use. Collections of authentic language in spoken and written forms provide developers the means to enrich their applications with real world examples. As the Internet continues to expand exponentially, the vast "CLOUD" of Web pages created provides a nearly inexhaustible and continuously updated language bank, particularly in English. The issue remains, however, how to make practical use of large amounts of data for English for Specific Purposes learning, given storage and data processing demands. In fact, one may ask 'What is the difference between the ESP and General English approach?' Hutchinson et al. answer this quite simply, "in theory nothing, in practice a great deal". English for Specific Purposes (ESP) is known as a learner-centered approach to teaching English as a foreign or second language. It meets the needs of (mostly) adult learners who need to learn a foreign language for use in their specific fields, such as science, technology, medicine, leisure, and academic learning.

Kennedy and Bolitho [11] point out that ESP is based on "an investigation of the purposes of the learner and the set of communicative needs arising from these purposes", figure 1.



Fig. 1. ESP environment

ESP concentrates more on language in context than on teaching grammar and language structures. It covers subjects varying from accounting or computer science to tourism and business management. The ESP focal point is that English is not taught as a subject separated from the students real world (or wishes); instead, it is integrated into a subject matter area important to the learners.

Absolute Characteristics of English for Specific Purposes are:

1. ESP is defined to meet specific needs of the learners
2. ESP makes use of underlying methodology and activities of the discipline it serves
3. ESP is centered on the language appropriate to these activities in terms of grammar, lexis, register, study skills, discourse and genre.

Variable Characteristics of English for Specific Purposes are:

1. ESP may be related to or designed for specific disciplines
2. ESP may use, in specific teaching situations, a different methodology from that of General English
3. ESP is likely to be designed for adult learners, either at a tertiary level institution or in a professional work situation. It could, however, be for learners at secondary school level.
4. ESP is generally designed for intermediate or advanced students.
5. Most ESP courses assume some basic knowledge of the language systems

ESP are offered by different educationalists and we can identify three types of ESP :

1. English as a restricted language;
2. English for academic and occupational purposes;
3. English with specific topics.

<sup>1</sup>Danica Milosevic is with the Technical College University of Nis, A. Medvedeva 20, Nis 18000, Serbia, E-mail: danicamil@yahoo.com.

<sup>2</sup>Borivoje Milosevic is with the Technical College University of Nis, A. Medvedeva 20, Nis 18000, Serbia, E-mail: borivojemilosevic@yahoo.com.

But, ESP tree looks like in the figure 2.

Algorithm that shows the basic level in the development of ESP learning based on one of the platforms can be seen in figure 3.

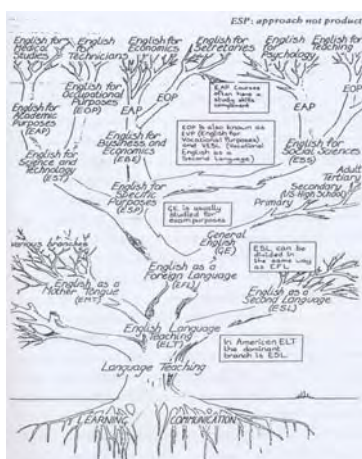


Fig. 2. ESP tree

ESP is a relatively new discipline within Applied Linguistics that bids a new learner-centered approach to English language teaching whose methodology is based on the

## II. EXPOSITION

The twenty first century marked pedagogy knowledge so that learning is not a process of "receiving knowledge" but an active process in which the student contextualizes and builds knowledge mastering ESP learning strategies, there is a need to be in an electronic learning pedagogical application of these elements. Popular name Liens. 2.0 marked the transition from HTML to XML and emergence of other tools that enable the organization of social interaction in a group on the Internet, even when it comes to very large groups of people. Thus, at the beginning of the twenty first century, electronic learning enables and promotes the active role of students in the process of teaching, group learning and delivery of multimedia materials on different platforms (computer, mobile phone ...).

In this modern age, many new technologies are being introduced every day and make human life easier. Web-based technologies today have a major contribution to reducing the routine work that users have to invest in order to obtain the required information. They introduced online education services for a range of different courses, based on the Internet platform. Widespread use [10] of XML for encoding corpora and text collections is moving towards a resolution of this problem. XML has become the *de facto* standard for encoding of language corpora. XML recommends itself because of its platform independence, extensibility, and widespread acceptance by software companies and researchers. Standardizing text encoding in XML greatly facilitates data interchange. Since structural and semantic information about a text is separated from its presentation in XML, the same encoded text can be displayed in multiple ways, using CSS style sheets or XSLT transformations. With the advent of XML as the preferred system for representation of corpus resources, existing tools have been modified to work with XML, while new applications have been created that are designed to be XML ready. The Linguist's Toolbox, for example, now features export to XML. The text searching software, Xaira, designed to be used with the British National Corpus, has been re-written as a general purposes XML search engine with full Unicode support. The Unicode editor CLaRK has been designed specifically to work with XML. Language archives can now be submitted to OLAC (Open Language Archives Community) by uploading a single XML file containing the necessary metadata information about the resource. Tools for the semi-automatic annotation of corpus data are being developed, such as @nnotate from the University of Saarland. DepAnn is a treebank creation tool, which uses Tiger-XML, the accepted standard for treebank encoding. EULIA, from the University of the Basque Country, provides a graphical Web interface for editing annotated corpora. These kinds of tools will become increasingly important as language data sets increase in size, since manually annotating texts to create treebanks is a slow and expensive process.

However, new platform - Cloud computing is essentially a highly flexible, cost-effective," user friendly" checked platform, whose main task is delivery and providing business or consumer IT services over the Internet. Resources Cloud systems are evolving very rapidly, along with all processes,

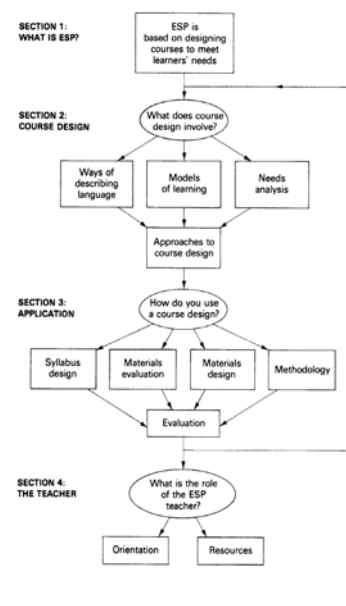


Fig. 3. Outline of a learning centred approach to ESP

specific needs of the learner. Defined to meet the specific needs of the learners, ESP makes use of methodology and the activities of the discipline it serves by focusing on the language appropriate to these activities. So, ESP has become such an important ( somme might say the most important ) part of the English language teaching.

applications, and services obtained through "on demand", regardless of the user's location or device within a broadband Internet network. They represent a large pool of easily usable and accessible virtualized resources (such as hardware, development platforms and / or services). These resources can be dynamically reconfigured to adapt scale load, which also achieves the optimal utilization of resources. Cloud computing customers can use one or more Cloud computing services based on their business needs. There are many ways to approach clients of Cloud computing through various forms of hardware devices such as PDAs, mobile phones, standard computers, portable computers, and software applications such as Web browsers etc.

Cloud Computing [12] is a task that has been encapsulated in a way that it can be automated and supplied to the clients in a consistent and constant way. Any component can be considered as a service, from entities closest to hardware such as the storage space or the computational time, to software components aimed at authenticating a user or to manage the mailing, the management of a data base or the monitoring of the use of the system resources.

Both the public and private cloud models are now in use. Available to anyone with the Internet, the public models include Infrastructure as a Service (IaaS), Software as a Service (SaaS) Cloud as IBM LotusLive, Platform as a Service (PaaS) Cloud as IBM Computing on demand, and security and data protection as a service (SDPaaS) Cloud for example, such as IBM in Management service.

*IaaS* is the lowest layer in a network environment. The user may request the provision of standard services, including computing power and resources for memorizing data. It sets these resources in the virtual environment and thus provides the necessary computing power and resources, regardless of the strength of their devices.

*PaaS* is a higher level of abstraction. It serves to secure the development environment, testing environment, servers platforms and other services, where users can develop applications based on the Internet as well as other server services.

*SaaS* is a software distribution model, designed for delivery to Web\_, whom users can post and access via Internet hosting. SaaS providers are seeking to build information for the entire network infrastructure, software, hardware, operating platform and are responsible for implementation of all service, maintenance and other services.

ESP learning based on Cloud technology is a subset of Cloud Computing applied to the field of education. What is the future for the development of technology and e-learning infrastructure. ESP based training Cloud\_u has all the necessary resources, such as hardware and software to enhance traditional learning infrastructure [14], figure 4.

Since educational materials for ESP - learning systems are virtualised in Cloud servers, these materials are made available for the use of students and other educational

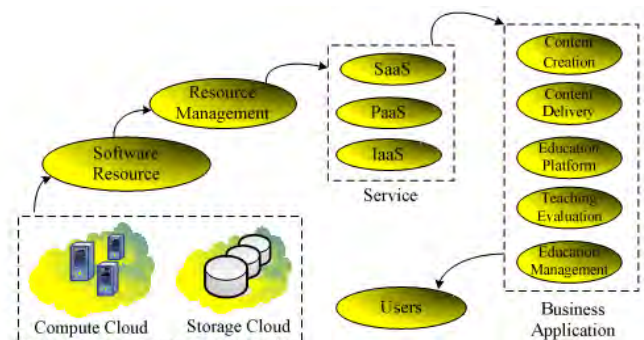


Fig. 4. Architecture of ESP- learning cloud

institutions and businesses. There are two important Cloud environments for students and other users which offer a wide array of services for ESP- learning: Virtual (Virtual Learning Environment - VLE) and personal (Personal Learning Environment - PLE).

PLE offers users a wide range of services, some of which are:

- 1) The user can edit their own learning objectives in its own system for ESP-learning.
- 2) The user can operate the system for ESP-learning across the organization and learning materials and have control over all processes in the system.
- 3) The user can interact in the learning process with other users in the same system for ESP-learning.

For users there are many advantages of using this system:

- Lower costs, users of the system for ESP-learning do not need to have a high-performance computers to run their applications. They safely run with Cloud platforms and services are paid on a pay-as-you-go basis. Fixed monthly costs are low because Cloud computing networks are taking advantage by bringing large numbers - millions of users, and the low cost of functioning at information centers, which are managed from another location.
- No up-front investment in IT, which is particularly attractive to small and medium education institutions, enterprises and newly founded companies, and since the applications are processed on a Cloud platform, client machines can create problems in their work.
- Since the applications for ESP-learning are centered on the powerful Cloud servers, the software automatically updates with Cloud sources. No need to install and maintain servers, managed superstructure or care about whether the software is compatible with the hardware.
- No need for license management applications.
- Students and other users have numerous advantages using Cloud\_a for ESP-learning. Can run on-line courses, attend on-line exams, receive feedback from professors and instructors, and send their projects and specific assignments to be

assessed. The system can easily adapt to the needs of more users or additional services - or it can reduce the activity when seasonal demand for services drops.

- If any of the fonts and format documents do not open properly on other devices, users of Cloud systems do not have to worry about this problem because such documents are now open directly to the cloud system. Therefore, there is the ability to access documents and features from any machine instead of attachment to a particular device.
- The system can be expanded, and does not have to be purchased, which is beneficial to some companies that are still developing.

Outrank the teachers are great and will mention only:

- They are preparing online offers for student testing, practicing and creating better resources for students through the content management, access to tests and their preparation, access to the content of students' homework, projects that the students have done. Also, they send feedback and communicate with students through on-line forums.

### III. CONCLUSION

Cloud computing represents a new platform that can be used as the concept of e-learning purposes, based on earlier models of distributed services, which have been created in the last decade and allow easy access to the network, at the request of the user, set the Shared Resource. Cloud Computing has found a large number of applications: computing in the form of services (utility computing), the software in the form of services (software-as-a-service), network resources, servers, hard disk space, services on demand (on-demand services), systems of electronic learning (e-learning), other applications and services that can be rapidly provided to users on the use and with minimal intervention or action by the provider. Advantages of these solutions in e-learning are indisputable both for users and for teachers who are preparing courses.

### REFERENCES

- [1] [www.microsoftsrbs.rs/.../Elektronsko\\_ucenje.pdf](http://www.microsoftsrbs.rs/.../Elektronsko_ucenje.pdf)
- [2] Blinco K., Mason J., McLean N., Wilson S., "Trends and Issues in E-learning Infrastructure Development", Prepared on behalf of DEST (Australia) and JISC-CETIS (UK), Version 2, 19 July 2004.
- [3] Barik N., Karforma S., "Risks and remedies in E-learning system", International Journal of Network Security & Its Applications (IJNSA), Vol.4, No.1, January 2012
- [4] [http://images.google.com/images?hl=sl&source=hp&q=cloud+computing&gbv=2&aq=f&aq=g10&aql=&oq=&gs\\_rfai=](http://images.google.com/images?hl=sl&source=hp&q=cloud+computing&gbv=2&aq=f&aq=g10&aql=&oq=&gs_rfai=)
- [5] Kumar G., Chelikani A., "Analysis of security issues in cloud based E-learning", 2011., MAGI23, University of Boracs, Sweden
- [6] Madan D., Pant A., Kumar S., Arora A., "E-learning based on Cloud Computing", International Journal of Advanced Research in Computer Science and Software Engineering, Volume 2, Issue 2, February 2012.
- [7] Rajam S., Cortez R., Vazhenin A., Bhalla S., "E-Learning Computational Cloud (eLC2): Web Services Platform to Enhance Task Collaboration", 2010., IEEE/WIC/ACM International Conference on Web Intelligence and Intelligent Agent Technology, University of Aizu, Fukushima, Japan
- [8] Masud A. H., Huang X., "An E-learning System Architecture based on Cloud Computing", World Academy of Science, Engineering and Technology 62, 2012.
- [9] Mohammed Mizel Tahir, ENGLISH FOR SPECIFIC PURPOSES (ESP) AND SYLLABUS DESIGN By: MA. ELT Methodology
- [10] Robert Godwin-Jones, EMERGING TECHNOLOGIES OF ELASTIC CLOUDS AND TREEBANKS: NEW OPPORTUNITIES FOR CONTENT -BASED AND DATA-DRIVEN LANGUAGE LEARNING, Language Learning & Technology Vol.12, No.1, February 2008, pp. 12-18
- [11] Kennedy, C. & Bolitho, R. (1984) English for Specific Purposes. London: Macmillan.
- [12] A. Fernández, D. Peralta, F. Herrera, and J.M. Benítez, An Overview of E-Learning in Cloud Computing, Dept. of Computer Science and Artificial Intelligence, CITIC-UGR (Research Center on Information and Communications Technology). University of Granada,
- [13] Borivoje Milošević, Slobodan Obradović, E LEARNING BASED ON CLOUD PLATFORMS, YU INFO, 2013, Kopaonik, Serbia.
- [14] Svetlana Kim, Su-Mi Song and Yong-Ik Yoon, Smart Learning Services Based on Smart Cloud Computing, Department of Multimedia Science, Sookmyung Women's University, Chungpa-Dong 2-Ga, Yongsan-Gu 140-742, Seoul, Korea
- [15] Sedayao, J. Implementing and operating an internet scale distributed application using service oriented architecture principles and cloud computing infrastructure. In Proceedings of the 10th International Conference on Information Integration and Web-Based Applications & Services, iiWAS2008, Linz, Austria, 24–26 November 2008; pp. 417-421.
- [16] DeCoufle B., The impact of cloud computing in schools, The Datacenter Journal, <http://datacenterjournal.com/content/view/3032/40/>, July 2009
- [17] Creeger M., CTO Roundtable: Cloud Computing Communications of the ACM, vol. 52, no. 8, august 2009, pp. 50-56
- [18] Sonia Carmen Munteanu, English for Science and Technology: Technical texts for academic purposes, Summary of PhD Thesis
- [19] Halliday M.A.K. Spoken and written language. Oxford: Oxford University Press.
- [20] Bruce, I., 'Cognitive genre structure in Methods sections of research articles: A corpus study', Journal of English for Academic Purposes, vol. 7, pp. 38-54.
- [21] Bloor, M. & Bloor, T., Languages for specific purposes: practice and theory, Centre for Language and Communication Studies Occasional Papers, 19, Dublin: Trinity College, Centre for Language and Communication Studies.
- [22] Lee, E. & Brasseur, Visualizing Technical Information: A cultural Critique, New York: Baywood Publishing Company.
- [23] Orr, Th., English for Science and Technology: profiles and perspectives, Fukushima: Center for language research, University of Aizu.
- [24] Swales, J. M., Genre Analysis – English in Academic and Research Settings, Cambridge: Cambridge University Press.

# Online simulation of nonlinearity limitations in a single mode optical fiber

Kalin Dimitrov<sup>1</sup> and Lidia Jordanova<sup>2</sup>

**Abstract –** This paper considers the calculations of the basic limitations in the transmission of digital signals in a single mode optical fiber. We have used formulae and dependencies adapted for distance (online) application. We have considered the basic problems and advantages of client-server architecture design of optical communication lines. We have also considered possible application in small companies and online distance learning.

**Keywords –** fiber optics, nonlinear effects, distance learning

## I. INTRODUCTION

An optical fiber communication system aims at transmitting the maximum number of bits per second over the maximum possible distance with the fewest errors. Among the major transmission media for long distance communication, we can consider single mode optical fibers, which have very few losses and wide-bandwidth. System performance is essentially affected by fiber attenuation, dispersions and nonlinearities.

It is very difficult to evaluate the performance of optical fiber communication systems by applying only analytical techniques. It is important to use computer aided techniques in such cases, in order to study the performance of these systems [1].

Many of the programs require essential calculating power, whose installation for the users is not always justified. Another problem is the necessity to issue new program versions or correct old ones, which is due to the development of calculation algorithms.

Nowadays, the programs which are adapted for distance application and use client-server technology are becoming more and more important. The application of such programs is a step forward towards the wider introduction of the so-called cloud technologies [2]. Generally, this gives one the opportunity to use software applications provided in the form of web services, while at the same time one basically counts on the access to the hardware and system resources of the data centers offering these services.

In the contemporary optical communication systems, the technology wavelength-division multiplex (WDM) is used more and more often. This technology makes it possible to increase the transport capacity by using multiple wavelengths. Considering the constant boosting of information flows, this technology will tend to be used more often in the future. Not

<sup>1</sup>Kalin Dimitrov is with the Faculty of Telecommunications at Technical University of Sofia, 8 Kl. Ohridski Blvd, Sofia 1000, Bulgaria, E-mail: kld@tu-sofia.bg.

<sup>2</sup>Lidia Jordanova is with the Faculty of Telecommunications at Technical University of Sofia, 8 Kl. Ohridski Blvd, Sofia 1000, Bulgaria, E-mail: jordanova@tu-sofia.bg.

only will it be applied for long haul but also for metro and shorter lines.

In WDM systems, the greatest challenge is to achieve simultaneously smaller channel separation as well as higher bit rates of the optical carrier with the aim to increase transmission capacity. At a certain point these goals become contradictory, because of dispersion and nonlinear effects in the single mode optical fiber [3-5].

Of course, for such lines it is necessary to train many people for design and exploitation [6-8].

## II. LIMITATIONS

### A. Attenuation

Modern optical fibers have low attenuation coefficients (about 0.2 dB/km) but if the optical signals are carried at a long distance, they must be amplified at every 80 to 120 km. Erbium-doped fiber amplifier are used very often. When the power of the transmitted signal turns out to be higher than a predefined threshold level, some nonlinear effects can appear in the optical fiber thus causing noise and distortion.

### B. Dispersion

Chromatic dispersion and polarization mode dispersion (PMD) are the two main sources of dispersion in the single-mode optical fibers. The first one is due to frequency dependence of the fiber refractive index. The spectral components of the transmitted pulse travel at different velocities and arrive at the fiber end at different times, thus causing some pulse broadening. PMD takes place when the fiber core is not perfectly circular, which causes the two polarizations of light to travel at different velocity. The different arrival times of the two polarizations will cause the pulse to broaden in a similar way as the chromatic dispersion.

### C. Nonlinear effects

There are two types of nonlinear effects in the optical fibers: scattering effects and Kerr effects. Stimulated Raman scattering (SRS) and stimulated Brillouin scattering (SBS) are associated with the first type. They are due to non-elastic interaction between a pump wave and the fiber core. Kerr effects occur because of the dependence of the refractive index on the power density inside the fiber core. Three types of Kerr effects are considered to be important for modern optical communications: four-wave mixing (FWM), self-phase modulation (SPM) and cross-phase modulation (XPM).

### III. ONLINE CALCULATIONS

#### A. Choice of platform and implementation

In this section we have considered the open-source client-server option. We use Apache, PHP and MySQL. The advantages in comparison with Matlab®, for example, are that it is not necessary to pay license fees, and the fact that they are relatively widespread (because they are used for the distribution of classic web pages). The application of these environments makes possible the relatively easy integration of the results in open systems for e-learning such as Moodle. The main disadvantage is that to date there are relatively few specialized papers on simulations suitable for training or calculations in telecommunications.

Considering the above-mentioned facts, we have created a PHP script to calculate the restrictions and suitable web pages for data input and output (fig. 1).

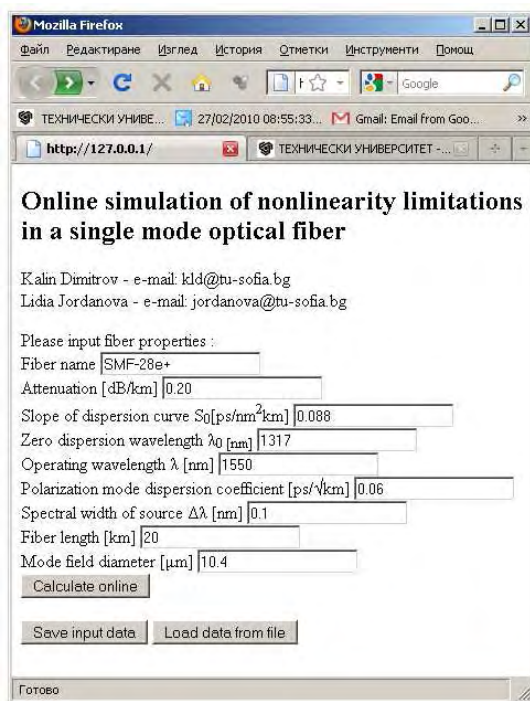


Fig. 1. Page view with the input data for SMF 28e+, Corning® fiber.

#### B. Example calculation

In the numerical tests we have used the data for the current single mode fibers of the company Corning - SMF 28, SMF 28e and SMF 28e+. We have used formulas from our previous papers [5,9,10].

Some of the results for SMF 28e+ are:

- Pulse spread due to chr. dispersion  $\Delta t_{ch} = 37.99 \text{ ps}$ ;
- Pulse spread due to PMD  $\Delta t_{PMD} = 0.9 \text{ ps}$ ;

- Maximum NRZ bit rate limited by dispersion  $BR=9.09 \text{ Gbps}$ ;
- Effective area  $A_{eff} = 84.95 \mu\text{m}^2$ ;
- Effective length of fiber  $L_{eff.} = 13.07 \text{ km}$ ;
- Stimulated Brillouin Scattering power threshold  $P_{th}(SBS) = 4.36 \text{ dBm}$ ;
- Stimulated Raman Scattering power threshold  $P_{th}(SRS) = 0.17 \text{ dBm}$ ;
- Nonlinear propagation threshold  $\gamma = 1.53 \times 10^{-3}$ .

### IV. CONCLUSION

We have developed an open source environment for calculation of the restrictions resulting from nonlinearities and dispersion effects in single-mode optical fibers. This paper is suitable for integration into e-learning systems. It is also adequate for general use and upgrading while complying with the main principles of open source.

### ACKNOWLEDGEMENT

The research described in this paper is supported by the Bulgarian National Science Fund under contract No ДДВУ 02/74/2010.

### REFERENCES

- [1] L.N. Binh, *Optical Fiber Communication Systems. Theory and Practice with Matlab and Simulink Models*, CRC Press, 2010.
- [2] D. Angeli, E. Masala, "A cost-effective cloud computing framework for accelerating multimedia communication simulations", J. Parallel Distrib. Comput., vol.72, pp. 1373–1385, 2012.
- [3] P. Agrawal, *Nonlinear fiber optics*, Academic Press, 2001.
- [4] J. Bel Hadj Tahar, Theoretical and Simulation Approaches for Studying Compensation Strategies of Nonlinear Effects Digital Lightwave Links Using DWDM Technology, Journal of Computer Science 3 (11), pp.887-893, Science Publications, 2007.
- [5] L. Jordanova, D. Dobrev, Fiber Nonlinearity Limitations in WDM CATV Systems, ICEST Conference, pp.279-282, Ohrid, 2007.
- [6] Q. Zhang, GUI based computer modeling and design platform to promote interactive learning in fiber optic communications, Conference on Frontiers in Education - FECS , pp. S3H-14-S3H-19, 2007.
- [7] S.H. Saeid Al-Bazzaz, Simulation of Single Mode Fiber Optics and Optical Communication Components Using VC++, IJCSNS International Journal of Computer Science and Network Security, vol.8, N.2, pp.300-308, 2008
- [8] S.H. Saeid, Computer Simulation and Performance Evaluation of Single Mode Fiber Optics, Proceedings of The World Congress on Engineering, pp.1007-1012, 2012.
- [9] L. Jordanova, D. Dobrev, Influence of dispersion and non-linear effects in optical fiber on the parameters of CATV system, ICEST Conference, pp.199-202, Bitola, 2004.
- [10] L. Jordanova, D. Dobrev, Fiber Nonlinearity Limitations in WDM CATV Systems, ICEST Conference, vol. 1, pp. 16-19, Nis, 2008.

## AUTHOR INDEX

### **A**

Acevski N.,337  
 Agatonovic M.,425, 429  
 Aleksandrov A., 651  
 Aleksandrova M., 663,  
 691  
 Altimirski E.,191, 417,  
 421  
 Anastoska J. M., 547  
 Anchev N.,219  
 Andonov A., 503, 817  
 Angelevska S.,313, 347  
 Angelevski Z.,313,347  
 Angelov K.,403  
 Angelov N.,603  
 Angelova K.,371  
 Antić D., 821  
 Antonov P.,145  
 Aprahamian B., 735, 759  
 Arapinoski B., 783, 787  
 Arsić N.,149, 775  
 Asenov O.,495  
 Atamian D., 103  
 Atanasković A., 53, 65  
 Atanasov I.,531  
 Atanasovski B.,219  
 Atanassov A., 671

### **B**

Badev J., 825  
 Bahtovski A.,571  
 Barudov E., 771  
 Barudov S., 677, 771  
 Batalov S., 801  
 Bekiarski A.,467  
 Bekov E., 567  
 Bjekic M., 727  
 Bjurström J.,359  
 Blau K., 53  
 Bogdanović N.,367  
 Bonev B.,407  
 Borisova L., 671  
 Borodzhieva A., 839  
 Bozic M., 727  
 Bozukov N.,623, 809  
 Branović I., 515  
 Brodić D.,161,165, 619

### **C**

Cajić M., 801  
 Causevski A.,317  
 Ceselkoska V., 783  
 Cherneva G.,501  
 Cholakova I., 659  
 Cirić D.,125,129  
 Crnisanin A., 607  
 Cundev M., 783, 787

### **D**

Damyanov C., 809

Denić D.,379,383

Denishev K., 691  
 Despotović V., 619  
 Dimitreska C.,313  
 Dimitrijević A.,245  
 Dimitrijević B., 107  
 Dimitrijević T., 69, 73  
 Dimitrov B.,615, 755  
 Dimitrov D.,183,329  
 Dimitrov K.,133,137,859  
 Dimitrov M. N.,647  
 Dimitrov V.,371, 475,  
 767

Dimitrova E.,479  
 Dimitrova R., 723  
 Dimkina E.,501  
 Dimova R.,463, 475  
 Dimovski T.,223  
 Djokic I.,611  
 Djorđević G., 99  
 Djordjević N.,535  
 Djorić A., 53, 65  
 Djošić D., 79, 83  
 Djuretic A., 775  
 Dobrev D., 61  
 Dobrev R.,531  
 Dojčinović N., 597  
 Dončov N., 73,429  
 Donevski A.,175  
 Drača D., 483

Draganov I.,161,165  
 Draganov N.,651,655  
 Draganov V.,371  
 Draganova T., 651  
 Dutsolova Y., 691  
 Dzhudzhev B., 705, 709

### **F**

Fehér A.,433  
 Filipov A., 763  
 Fillyov K.,291  
 Fustik V.,183

### **G**

Gadjeva E.,303,307  
 Gajić D.,261  
 Ganev Z.,399,409  
 Gavrilovska L., 87  
 Gechev M.,403  
 Gega V.,215  
 Genova K.,179, 254, 555  
 Georgiev Y., 659  
 Georgieva T.,455  
 Georgieva V.,581, 843  
 Geramitcioski T.,393, 851  
 Gerasimov K., 743, 747,  
 763  
 Gerganova S. S. 805  
 Gergov V., 817  
 Gjorgijevski J.,333

Goranov G., 793  
 Goranova M., 735, 759  
 Gordana J.,341  
 Gospodinova E., 705  
 Grancharova N.,577  
 Gueorguieff L.,145  
 Guliashki V.,179, 253,  
 555  
 Gusev M.,111, 175, 211,  
 219, 227, 277,571  
 Guseva A.,227  
 Gushev P.,227

### **H**

Hamza M., 763  
 Hristoski I.,207  
 Hristov A.,281  
 Hubenova Z., 817  
 Hut I., 597

### **I**

Iliev A.,183,329  
 Iliev F.,503  
 Iliev I.,413  
 Ilieva D.,585  
 Iontchev E.,117, 813  
 Ivancheva V., 705, 709  
 Ivanov P.,169  
 Ivanova M.,677

### **J**

Jajac N.,241  
 Jakšić B., 487  
 Janevski T., 95,111  
 Janković M.,125,129  
 Janković S.,515  
 Jankulovski J.,547  
 Jocić A.,383  
 Joković J., 69, 73, 597  
 Jordanova L., 61, 859  
 Jovanovic G.,235  
 Jovanović M.,257  
 Jovković S., 633

### **K**

Kachulkova S., 705, 709  
 Kajan E., 607  
 Kaloyanov N.,417  
 Kamenov Y., 747,751  
 Kandov I., 793  
 Karadzhov Ts.,685  
 Karailiev V., 717  
 Katardjiev I.,359  
 Kenov R.,117  
 Kimovski D.,281  
 Kirilov L.,179, 253, 555  
 Kiryakova D., 671  
 Kitanov S., 95  
 Kiteva R. N.,183, 329  
 Kjurchievska D.,641

Koceski S.,269, 355

Kocev T.,223  
 Kolev G.,691  
 Kolev N., 37  
 Koleva P., 495  
 Kontrec N., 83  
 Korsemov C., 555  
 Korunovic L., 779  
 Kosanovic M., 91  
 Kostadinova S.,463  
 Kostov M., 829  
 Kostova V., 829  
 Kotevski A.,519  
 Kountchev R.,169  
 Kovačević M.,265  
 Kovachev Y.,389  
 Kovacheva M.,287, 667  
 Kukulovska M., 87  
 Kuzmanov I.,313, 347,  
 519

### **L**

Laskov L., 61  
 Lazarević M., 801  
 Lazic L., 611  
 Letskovska S., 675, 695,  
 739  
 Lozanovska A., 563, 637  
 Lukić J.,383

### **M**

Malecic A.,321  
 Maleš I. N., 53, 65  
 Mandić P., 801  
 Manolova A.,169  
 Marićić S., 79  
 Marinova G., 839  
 Markoska R., 829  
 Markova V.,371  
 Marković A., 487  
 Marovac U.,607  
 Maslinkov I., 825  
 Mašović D.,149,153  
 Mihajlović V.,265  
 Mihov G.,687  
 Mijakovska S.,593  
 Mijić M., 149,153  
 Mikarovski G., 519  
 Miladic S.,459  
 Milenov I., 767  
 Miletiev R.,117, 295, 813  
 Milev D.,133,137  
 Milijic M.,425  
 Milivojević D., 165, 619  
 Milivojević Z.,141, 505,  
 589  
 Miljković G.,379, 383  
 Milojković M., 821  
 Miloš B., 847

Milosavljević A., 245,  
265  
Milosavljević D.,141  
Milosevic B., 633, 855  
Milosevic D., 855  
Milošević N., 107  
Milovanović B., 65,  
69,429  
Milovanović E.,199  
Milovanović I.,199, 425,  
429  
Mirčevski S.,361  
Mircheski B., 637,563  
Mironov R.,121  
Mitić D.,235  
Mitrev R.,351  
Mitrevska C.,393  
Mitrevski P.,207, 215,  
223, 273, 393, 543, 547,  
851  
Mitrevski V.,393, 851  
Mitrović N., 847  
Mitsev Ts., 37,389  
Mladenović S., 515  
Moreira M.,359  
Musa S. M., 187,299,375

**N**

Nachev V., 623, 809  
Nagy S.,433  
Naka N.,539  
Nakamatsu K., 23  
Necov B.,455  
Nedelchev M., 42,413  
Nedelkoska J.,625, 629  
Nedelkovski I., 563, 593,  
637  
Nenov H.,615, 755  
Nenova M.,509  
Neshov N.,159,161  
Nešić N.,367, 713  
Nikolaev N.,325, 743  
Nikolić G.,231  
Nikolić S., 821  
Nikolić T.,199, 232, 235  
Nikolić Z.,107  
Nikolov G.,471  
Nikolova P. S.,317

**O**

Obradovic S., 633  
Oliver D.,187  
Oliver J. D., 299, 375

**P**

Pacheco C., 49  
Pacheco J., 49  
Panagiev O., 34, 45  
Panajotović A.,483  
Pandiev I.,287, 295, 681  
Panić S., 83  
Panov E., 771  
Panov S.,269, 355

Pantić A.,125  
Parachkevov D., 695  
Pargovski J., 563  
Pavlov M., 619  
Pavlovic A., 611  
Pavlović Š. D.,149, 153  
Peeva K.,467  
Pejović M., 713  
Pejović M.,367  
Pencheva E.,527, 531  
Perić M., 79  
Perić S., 821  
Pešović U., 57  
Petkovic D., 727  
Petković M., 99  
Petrov P.,351, 581  
Petrović B.,231  
Petrović M., 775  
Petrovski J., 539  
Plamenov V.,417  
Pleshkova S.,467  
Pljaskovic A., 607, 611  
Popnikolova R. M., 783,  
787  
Popovic M., 727  
Poulkov V., 495  
Predic B.,241  
Prisaganec M.,273

**R**

Radmanović M.,249  
Radoyska P.,291  
Rahnev P., 671, 675, 695  
Rajković M.,141  
Rančić D.,245, 265,535  
Randić S., 57  
Rangelov Y., 743, 747,  
751  
Rankovska V., 717, 835  
Reis A. D., 49  
Ribeiro C., 49  
Ristov S.,175, 211, 219,  
227, 277  
Rosic M., 727, 847

**S**

Sabev H.,685  
Sadiku M. O.,187, 299,  
375  
Samardzic B., 797  
Savoska S., 539, 625, 629  
Sekulović N., 483  
Seymenliyski K., 695,  
739  
Shayib M. A.,375  
Shoshkov Ts.,295, 687  
Shotova M.,471  
Simeonov I.,117, 813  
Simeonov P.,421  
Simić M.,379,383  
Simić V., 487  
Simjanoska M.,277  
Slavov V., 709

Smiljaković V., 57, 699  
Spalević P., 83,487  
Spasova K. E.,543  
Spirov R.,577  
Stamenković M.,129  
Stamenković N., 83  
Stanchev O.,567  
Stanislavljevic K.,195  
Stanković R.,261  
Stankovic V.,195  
Stankovic Z.,425,429  
Stefanović Č., 79, 83  
Stefanović D., 79  
Stefanović M., 79, 483,  
633  
Stevic D.,597  
Stoianov N.,191  
Stoianov P.,491  
Stoimenov E.,295  
Stojanović D.,203,241  
Stojanović N.,203  
Stojanović V.,505  
Stojčev M.,91, 199, 231,  
235  
Stojkoska E.,337  
Stojković I., 619  
Stošović S., 107

**T**

Takov T.,659  
Taleska E., 625,629  
Tasić V.,165,619  
Tembely M, 187  
Titova T., 623, 809  
Todorova M.,523, 551,  
559  
Todorović Z., 487  
Todosijević D.,257  
Toshev H., 555  
Trajković D., 821  
Trajkovik V.,183  
Trifonova T.,371, 475  
Trpezanovski Lj.,333  
Tsankov B., 103

**V**

Valchev V.,471, 567  
Valcheva D.,551  
Valchkova O., 843  
Valkov G.,307  
Varangov A., 751  
Vasić B., 99  
Vasileva M., 723, 731,  
763  
Vasiljević M., 515  
Vassilev Tz., 839  
Veiga H., 49  
Velchev Y.,133,137  
Veličković Z.,589  
Velkoski G.,211,277  
Veselinovska B.,111  
Vesković S., 515  
Vichev P.,417

Vidanovski D.,361

Vilos I., 851

Vuckovic M., 779

**Y**

Yakimov P.,667  
Yantchev V.,359  
Yordanov R., 813  
Yordanova M., 723, 731,  
755

**Z**

Zdravković N., 99  
Zhivkov P.,179  
Zivanović D.,379  
Zivanovic Z., 699  
Zlatkovic B., 797